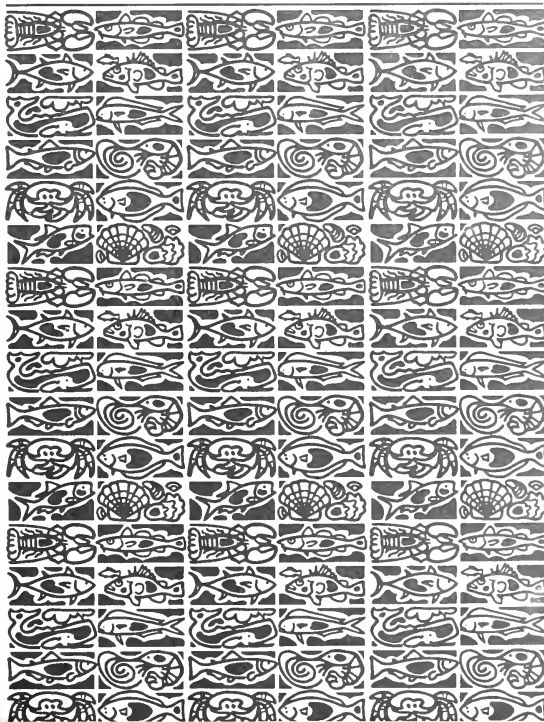




U.S. Department
of Commerce

Volume 103
Number 1
January 2005

Fishery Bulletin



**U.S. Department
of Commerce**

Donald L. Evans
Secretary

**National Oceanic
and Atmospheric
Administration**

Vice Admiral
Conrad C. Lautenbacher Jr.,
USN (ret.)

Under Secretary for
Oceans and Atmosphere

**National Marine
Fisheries Service**

William T. Hogarth
Assistant Administrator
for Fisheries



The *Fishery Bulletin* (ISSN 0090-0656) is published quarterly by the Scientific Publications Office, National Marine Fisheries Service, NOAA, 7600 Sand Point Way NE, BIN C15700, Seattle, WA 98115-0070. Periodicals postage is paid at Seattle, WA, and at additional mailing offices. POSTMASTER: Send address changes for subscriptions to *Fishery Bulletin*, Superintendent of Documents, Attn: Chief, Mail List Branch, Mail Stop SSOM, Washington, DC 20402-9373.

Although the contents of this publication have not been copyrighted and may be reprinted entirely, reference to source is appreciated.

The Secretary of Commerce has determined that the publication of this periodical is necessary according to law for the transaction of public business of this Department. Use of funds for printing of this periodical has been approved by the Director of the Office of Management and Budget.

For sale by the Superintendent of Documents, U.S. Government Printing Office, Washington, DC 20402. Subscription price per year: \$55.00 domestic and \$68.75 foreign. Cost per single issue: \$28.00 domestic and \$35.00 foreign. See back for order form.

Fishery Bulletin

Scientific Editor
Norman Bartoo, PhD

Associate Editor
Sarah Shoffler

National Marine Fisheries Service, NOAA
8604 La Jolla Shores Drive
La Jolla, California 92037

Managing Editor
Sharyn Matriotti

National Marine Fisheries Service
Scientific Publications Office
7600 Sand Point Way NE, BIN C15700
Seattle, Washington 98115-0070

Editorial Committee

Harlyn O. Halvorson, PhD	University of Massachusetts, Boston
Ronald W. Hardy, PhD	University of Idaho, Hagerman
Richard D. Methot, PhD	National Marine Fisheries Service
Theodore W. Pietsch, PhD	University of Washington, Seattle
Joseph E. Powers, PhD	National Marine Fisheries Service
Harald Rosenthal, PhD	Universitat Kiel, Germany
Fredric M. Serchuk, PhD	National Marine Fisheries Service
George Watters, PhD	National Marine Fisheries Service

***Fishery Bulletin* web site: www.fishbull.noaa.gov**

The *Fishery Bulletin* carries original research reports and technical notes on investigations in fishery science, engineering, and economics. It began as the Bulletin of the United States Fish Commission in 1881; it became the Bulletin of the Bureau of Fisheries in 1904 and the *Fishery Bulletin of the Fish and Wildlife Service* in 1941. Separates were issued as documents through volume 46; the last document was No. 1103. Beginning with volume 47 in 1931 and continuing through volume 62 in 1963, each separate appeared as a numbered bulletin. A new system began in 1963 with volume 63 in which papers are bound together in a single issue of the bulletin. Beginning with volume 70, number 1, January 1972, the *Fishery Bulletin* became a periodical, issued quarterly. In this form, it is available by subscription from the Superintendent of Documents, U.S. Government Printing Office, Washington, DC 20402. It is also available free in limited numbers to libraries, research institutions, State and Federal agencies, and in exchange for other scientific publications.

U.S. Department
of Commerce
Seattle, Washington

Volume 103
Number 1
January 2005

Fishery Bulletin

Contents

Articles

- 1-14 **Bochenek, Eleanor A., Eric N. Powell, Allison J. Bonner, and Sarah E. Banta**
An assessment of scup (*Stenotomus chrysops*) and black sea bass (*Centropristis striata*) discards in the directed otter trawl fisheries in the Mid-Atlantic Bight
- 15-22 **Cooper, Daniel W., Katherine E. Pearson, and Donald R. Gunderson**
Fecundity of shortspine thornyhead (*Sebastolobus alascanus*) and longspine thornyhead (*S. altivelis*) (Scorpaenidae) from the northeastern Pacific Ocean, determined by stereological and gravimetric techniques
- 23-33 **DeMartini, Edward E., Marti L. McCracken, Robert B. Moffitt, and Jerry A. Wetherall**
Relative pleopod length as an indicator of size at sexual maturity in slipper (*Scyllarides squammosus*) and spiny Hawaiian (*Panulirus marginatus*) lobsters
- 34-51 **Fisher, Joseph P., and William G. Pearcy**
Seasonal changes in growth of coho salmon (*Oncorhynchus kisutch*) off Oregon and Washington and concurrent changes in the spacing of scale circuli
- 52-62 **Groeneveld, Johan C., Jimmy P. Khanyile, and David S. Schoeman**
Escapement of the Cape rock lobster (*Jasus lalandii*) through the mesh and entrance of commercial traps
- 63-70 **Grusha, Donna S., and Mark R. Patterson**
Quantification of drag and lift imposed by pop-up satellite archival tags and estimation of the metabolic cost to cownose rays (*Rhinoptera bonasus*)
- 71-83 **Harvey, Chris J.**
Effects of El Niño events on energy demand and egg production of rockfish (Scorpaenidae: *Sebastes*): a bioenergetics approach

The conclusions and opinions expressed in *Fishery Bulletin* are solely those of the authors and do not represent the official position of the National Marine Fisheries Service (NOAA) or any other agency or institution.

The National Marine Fisheries Service (NMFS) does not approve, recommend, or endorse any proprietary product or proprietary material mentioned in this publication. No reference shall be made to NMFS, in any advertising or sales promotion which would indicate or imply that NMFS approves, recommends, or endorses any proprietary product or proprietary material mentioned herein, or which has as its purpose an intent to cause directly or indirectly the advertised product to be used or purchased because of this NMFS publication.

- 84–96 Horodysky, Andrij Z., and John E. Graves
Application of pop-up satellite archival tag technology to estimate postrelease survival of white marlin (*Tetrapturus albidus*) caught on circle and straight-shank (“J”) hooks in the western North Atlantic recreational fishery
- 97–107 Kerr, Lisa A., Allen H. Andrews, Kristen Munk, Kenneth H. Coale, Brian R. Frantz, Gregor M. Cailliet, and Thomas A. Brown
Age validation of quillback (*Sebastes maliger*) using bomb radiocarbon
- 108–129 Marancik, Katrin E., Lisa M. Clough, and Jonathan A. Hare
Cross-shelf and seasonal variation in larval fish assemblages on the southeast United States continental shelf off the coast of Georgia
- 130–141 O’Farrell, Michael R., and Ralph J. Larson
Year-class formation in Pacific herring (*Clupea pallasii*) estimated from spawning-date distributions of juveniles in San Francisco Bay, California
- 142–152 Parker, Denise M., William J. Cooke, and George H. Balazs
Diet of oceanic loggerhead sea turtles (*Caretta caretta*) in the central North Pacific
- 153–160 Roberson, Nancy E., Daniel K. Kimura, Donald R. Gunderson, and Allen M. Shimada
Indirect validation of the age-reading method for Pacific cod (*Gadus macrocephalus*) using otoliths from marked and recaptured fish
- 161–168 Sulikowski, James A., Jeff Kneebone, Scott Elzey, Joe Jurek, Patrick D. Danley, W. Huntting Howell, and Paul C. W. Tsang
Age and growth estimates of the thorny skate (*Amblyraja radiata*) in the western Gulf of Maine
- 169–182 Tracey, Sean R., and Jeremy M. Lyle
Age validation, growth modeling, and mortality estimates for striped trumpeter (*Latris lineata*) from southeastern Australia: making the most of patchy data
- 183–194 Trnski, Thomas, Amanda C. Hay, and D. Stewart Fielder
Larval development of estuary perch (*Macquaria colonorum*) and Australian bass (*M. novemaculeata*) (Perciformes: Percichthyidae), and comments on their life history
- 195–206 Venerus, Leonardo A., Laura Machinandiarena, Martin D. Ehrlich, and Ana M. Parma
Early life history of the Argentine sandperch *Pseudoperca semifasciata* (Pinguipedidae) off northern Patagonia
- 207–218 Wilson, Matthew T., Annette L. Brown, and Kathryn L. Mier
Geographic variation among age-0 walleye pollock (*Theragra chalcogramma*): evidence of mesoscale variation in nursery quality?

Note

- 219–226 Markaida, Unai, Joshua J. C. Rosenthal, and William F. Gilly
Tagging studies on the jumbo squid (*Dosidicus gigas*) in the Gulf of California, Mexico

Abstract—This study was undertaken to re-assess the level of scup (*Stenotomus chrysops*) discards by weight and to evaluate the effect of various codend mesh sizes on the level of scup discards in the winter-trawl scup fishery. Scup discards were high in directed scup tows regardless of codend mesh—typically one to five times the weight of landings. The weight of scup discards in the present study did not differ significantly from that recorded in scup-targeted tows in the NMFS observer database. Most discards were required as such by the 22.86 cm TL (total length) fish-size limit for catches. Mesh sizes ≤ 12.7 cm, including the current legal mesh size (11.43 cm) did not adequately filter out scup smaller than 22.86 cm. The median length of scup discards was about 19.83 cm TL. Lowering the legal size for scup from 22.86 to 19.83 cm TL would greatly reduce discard mortality. Scup discards were a small fraction (0.4%) of black sea bass (*Centropristis striata*) landings in black-sea-bass-targeted tows. The black sea bass fishery is currently regulated under the small-mesh fishery gear-restricted area plan in which fishing is prohibited in some areas to reduce scup mortality. Our study found no evidence to support the efficacy of this management approach. The expectations that discarding would increase disproportionately as the trip limit (limit [in kilograms] on catch for a species) was reached towards the end of the trip and that discards would increase when the trip limit was reduced from 4536 kg to 454 kg at the end of the directed fishing season were not supported. Trip limits did not significantly affect discard mortality.

Manuscript submitted 6 January 2003 to the Scientific Editor's Office.

Manuscript approved for publication 7 September by the Scientific Editor.

Fish. Bull. 103:1–14 (2005).

An assessment of scup (*Stenotomus chrysops*) and black sea bass (*Centropristis striata*) discards in the directed otter trawl fisheries in the Mid-Atlantic Bight

Eleanor A. Bochenek

Eric N. Powell

Allison J. Bonner

Sarah E. Banta

Haskin Shellfish Research Laboratory
Rutgers, The State University of New Jersey
6959 Miller Ave.
Port Norris, New Jersey 08349-3167

E-mail address (for E. A. Bochenek), bochenek@hsl.rutgers.edu

Because of regulations, market factors, and other reasons, both commercial and recreational fishermen discard some of their catch. Discards are considered one of the principal sources of mortality for many fish species, including those of significant commercial and recreational fisheries (Howell and Langdon, 1987; Glass et al., 1999; Suuronen et al., 1996).

The Sustainable Fisheries Act (SFA), governing U.S. fisheries management in federal waters, states that "conservation and management measures shall minimize bycatch." Much has been written about the environmental impact of discarding (Mooney-Seus, 1999; Alverson, 1999; Kennelly, 1999). Discard mortality reduces population size by limiting the number of individuals that can reach maturity and spawn. Because EEZ (Exclusive Economic Zone) fisheries must be managed at B_{msy} (biomass at maximum sustainable yield) under SFA guidelines and discards must be included in estimates of the TAC (total allowable catch), discard mortality also reduces total allowable landings. Therefore, discarding is not just an environmental problem; it is a problem that affects all aspects of fisheries.

A recreational and commercial fishery for scup (*Stenotomus chrysops*) occurs in the Mid-Atlantic Bight

(the portion of the U.S. Atlantic coast extending from Cape Hatteras to Cape Cod) and New England regions where scup are caught south and offshore in the winter and north and inshore in the summer (NEFSC¹). In 1996, the legal size for commercially caught scup was raised to 22.86 cm total length (TL), more or less coincidently with the establishment of a legal codend mesh size of 11.43 cm to reduce discard mortality (MAFMC, 1996). Discarding is considered to be an important cause of mortality for this important commercial and recreational species (NEFSC²). Kennelly (1999) reported large amounts of scup

¹ NEFSC (Northeast Fisheries Science Center). 2002. SARC 35. 35th Northeast regional stock assessment workshop (35th SAW). Stock assessment review committee (SARC) consensus summary of assessments. Northeast Fisheries Science Center Reference Document 02-14, 259 p. Northeast Fisheries Science Center, NMFS, NOAA, 166 Water St., Woods Hole, MA 02543.

² NEFSC (Northeast Fisheries Science Center). 2000. SARC 31. 31st Northeast regional stock assessment workshop (31st SAW). Stock assessment review committee (SARC) consensus summary of assessments. Northeast Fisheries Science Center Reference Document 00-15, 409 p. Northeast Fisheries Science Center, NMFS, NOAA, 166 Water St., Woods Hole, MA 02543.

discards from demersal trawlers operating in certain areas and depths in the Mid-Atlantic Bight. High numbers of scup discards occur in the directed scup fishery (Powell et al., 2004). It is generally believed that one of the keys to effective management of scup is to reduce discard mortality (NEFSC²; NEFSC¹). Fisheries managers attempt to control discard mortality using a number of management measures, but principally through mesh regulations and time or area closures.

Analysis of NMFS observer data by Powell et al.³ indicated that scup comprised 65% of the total catch in scup-targeted tows, but that the discards-to-landings ratio for scup in these tows was 1.05. Somewhat more than half of the scup taken in scup-targeted tows were subsequently discarded. However, this analysis was based on relatively few observations; many of the tows used codends with mesh sizes below the current legal mesh size of 11.43 cm. As a consequence, applicability of the NMFS observer data to the present-day scup fishery is unclear. The objective of the present study was to obtain additional observations in the directed scup fishery to re-assess the level of discards by weight and to evaluate the effect of simple variations in codend mesh size on the level of scup discards.

Data analysis focused on scup. However, we also analyzed black sea bass (*Centropomus striata*) catches using the same methods as those for scup. Black sea bass were included because one management option is to require a common codend mesh size for the two species. The present legal mesh size for black sea bass is 10.16 cm and the minimum size of black sea bass that can be harvested is 27.94 cm TL. Commonality would simplify fishing methods because the two species are often targeted on the same trip.

Methods

Description of data

This study was undertaken during the 2001 winter scup trawl fishery in the Mid-Atlantic Bight. The legal trip limit for scup was 4536 kg from 1 January through 24 January. After 24 January until the close of the season in late February, the legal trip limit for scup was lowered to 454 kg. An experimental fishing permit was obtained from NMFS 1) to allow the vessels to fish in the GRAs (gear-restricted areas), implemented to reduce scup discards in the *Loligo* squid, (*Loligo pealeii*), silver hake (*Merluccius bilinearis*), and black sea bass fisheries, 2) to allow the use of codends with meshes less than the legal 11.43-cm mesh, and 3) to allow commercial vessels

to retain an additional 1361 kg of scup per trip to help defray study costs.

The four vessels participating in this study used the following codends: 1) the legal-size (11.43-cm) mesh codend; 2) a composite codend with 30 meshes of 10.16-cm mesh at the very end of the bag followed by 45 meshes of 11.43-cm mesh; and 3) codends with some meshes ≥ 12.7 cm (including codends with or without a composite design). Two tows with codends of smaller mesh size (between 6.35 and 10.16 cm) were also observed and these tows were included in data tabulations for completeness. The composite codend was designed as a mechanism to reduce large catches of small scup when abundant scup are encountered but was also designed to retain black sea bass and scup when abundance was low. Captains usually had two of the codends onboard the vessel during a fishing trip and were asked to fish the codends in an ABBA sequence (i.e., first tow with codend A, second tow with codend B, third tow with codend B, next tow with codend A, and so forth). These tows typically lasted no longer than one hour. Otherwise, the captain operated his boat using normal fishing practices, including selecting where and when to fish.

The catch from each tow was sorted to species and weighed. Fork lengths (FL) were obtained for a minimum of fifty scup discarded followed by a minimum of fifty scup landed. If time permitted, length-frequency information was collected for black sea bass and discarded individuals were measured. Because some regulations use TL, FL was converted when necessary to TL with the following equation: $TL(\text{cm}) = 1.14FL(\text{cm}) - 0.44$ (Hamer⁴ in MAFMC [1996]).

Catch data obtained from this study of the winter 2001 scup fishery were compared to scup-targeted tows from the NMFS observer database for 1997 through mid-2000 (Powell et al.³). NMFS observer program methodology is detailed in the Northeast Fisheries Science Center Fisheries Observer Program Manual (NEFSC⁵). Mesh size reported in the NMFS observer database included an array of small-mesh codends less than present-day legal size, as well as the legal mesh size of 11.43 cm.

A depth was assigned for each tow as the mean of the depths of net deployment and retrieval. Swept area of the tow could not be calculated directly because door or wing spread were not recorded by us, nor were these metrics available in NMFS observed tows. A surrogate for true swept area was obtained as "the average of the recorded headrope and sweep lengths" multiplied

³ Powell, E. N., E. A. Bochenek, S. E. Banta, and A. J. Bonner. 2000. Scup bycatch in the small-mesh fisheries of the Mid-Atlantic. Final Report, National Fisheries Institute Scientific Monitoring Committee, 74 p. Haskin Shellfish Research Laboratory, Rutgers University, 6959 Millers Ave., Port Norris, NJ 08349.

⁴ Hamer, P. E. 1979. Studies of the scup, *Stenotomus chrysops*, in the Middle Atlantic Bight. N.J. Div. Fish. Game and Shellfish, misc. rep. no. 5M, 14 p. New Jersey Department of Environmental Protection, New Jersey Division of Fish and Wildlife, Division of Marine Fisheries, Nacote Creek Research Station, PO Box 418, Port Republic, NJ 08241.

⁵ NEFSC (Northeast Fisheries Science Center). 2001. Fisheries observer program manual, 217 p. Northeast Fisheries Science Center, NMFS, NOAA, 166 Water St., Woods Hole, MA 02583.

by "the recorded tow time and speed." CPUE was then calculated by using estimated swept area as the effort term. Scope was calculated as "tow wire out" divided by "average water depth." For geographic location, each tow was assigned to a 10-minute square area (10-minute latitude and longitude) (Powell et al.³).

For some analyses, data from the present study's winter 2001 fishery and the NMFS observer database were assigned to categories by codend mesh size: the legal codend with 11.43-cm mesh; a composite codend with 10.16-cm mesh followed by 11.43-cm mesh; codends with meshes less than 6.35 cm; codends with meshes between 6.35 cm and 10.16 cm; and codends having some meshes greater than or equal to 12.7 cm. Gear type was assigned to either a millionaire or large-mesh box net based on the net styles used in our study and interpretations of NMFS observer-recorded net descriptions by knowledgeable fishermen.

Statistical analysis

Catch was evaluated by using the ratio of scup discards to landings, total catch of all species, total discards of all species, total scup discards, total scup landings, and a comparison of whether the catch of scup per tow was above or below the median for all tows in the study. In addition, we examined the influence of fishing decisions on discards 1) by distinguishing tows where scup discards exceeded scup landings from tows where landings exceeded discards and 2) by distinguishing between the scup catch of tows taken in the first and last half of the trip. For the latter, we also analyzed tows by their fractional position in the trip (whether a tow occurred at the start of a trip, $1/4$, $1/2$, $3/4$, or at the end of the trip). This approach yielded results equivalent to the simpler assignment of tows to the first and last half of the trip. Only the results of the simpler analysis are presented. Finally, we evaluated the impact of fishing decisions on the length frequencies of scup caught. ANOVAs were run by using ranked raw variables with class variables that defined fishing practice (mesh size, gear, scope, effort), time, and catch. The variable time was used to allocate tows to three categories:

- 1 Those trips from the present study taken from 1 to 24 January 2001 with a legal trip limit of 4536 kg of scup;
- 2 Those trips from the present study taken after 24 January 2001, with a legal trip limit of 454 kg of scup; and
- 3 Those scup trips taken in 1997–2000 from the NMFS observer reports.

Length frequencies were analyzed by ANOVA by using the 25th, 50th, and 75th percentiles and the mean as descriptive variables. In initial analyses, the interaction terms between mesh size or time and the other independent variables were included. Interaction terms were not significant more frequently than expected by chance and, accordingly, were not included in our results. Significant

differences identified by the ANOVA were further investigated by using Tukey's studentized range test and, for covariates, by Spearman's rank correlation.

Results

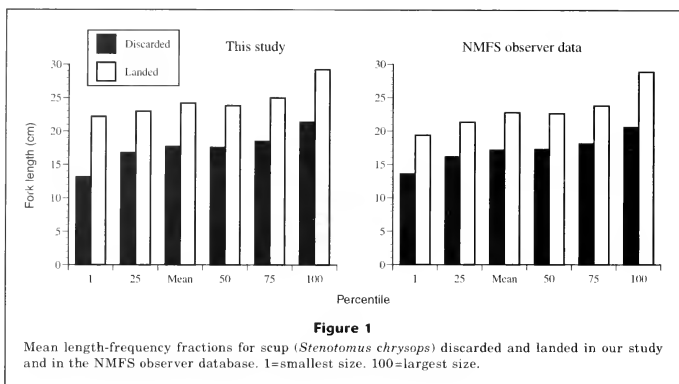
Catch statistics—scup

Ten trips were taken during our study and 62 tows were successfully completed; 39 tows targeted scup and 12 tows targeted black sea bass (Table 1). For the remaining tows, the captain targeted *Loligo* squid as part of the normal fishing process and used a much smaller codend mesh size. These *Loligo*-targeted tows were excluded from further analyses. However, frequent changes in target species emphasize the need for tow rather than trip-aggregated data in discard analyses (Powell et al., 2004) because multiple targets within trips commonly occur in Mid-Atlantic Bight fisheries.

The majority of tows were taken in NMFS statistical area 622. Scup-targeted tows occurred primarily during daylight and at depths ranging from about 73.2 to 137.2 m in our study and from 54.9 to 109.7 m in the NMFS observer data set. A few tows from both the NMFS observer database and our study were deleted from the analysis because the catch was released overboard rather than brought onboard. Bycatch estimates from these tows were assumed to be inaccurate in comparison to other tows. This phenomenon occurs sporadically in many fisheries (e.g., Roel et al., 2000). In our study, six scup-targeted tows were disregarded for this reason. All four participating boats had at least one trip where one tow was released overboard. Observers reported that the net was so full of fish, primarily scup, in these tows that it could not be brought on deck. The catch for one black-sea-bass-targeted tow was released overboard. In addition, tows in which no discards were recorded were not analyzed. Generally, such tows occurred when the observer was asleep or sea conditions were too dangerous to collect data from the tow. Such tows did not occur in our study but did occur sporadically in the NMFS observer database. Regardless of the reason, we assumed that any tow without recorded discards represented incomplete sampling and, consequently, we discarded that tow from further analysis (Powell et al.³). Differences in the tabulated number of observed tows and the number of observed tows analyzed reflect the number of tows excluded from the analyses for these two reasons.

Length frequency—scup

The length frequencies of landings and discards were consistently significantly different (often $P \leq 0.0001$) (Fig. 1). The mean size of discarded scup was 17.7 cm and ranged from 13.2 to 21.4 cm in our study. Fifty percent of the scup discarded fell between 16.8 cm (25th percentile) and 18.5 cm (75th percentile). In contrast, the average size of scup landed was 24.2 cm and ranged from 22.2 to 29.2 cm. Fifty percent of the scup landed

**Table 1**

Synopsis of scup and black-sea-bass-targeted tows by study, gear, and codend mesh size, including those tows where the catch was released overboard.

Scup-targeted tows

Study	Gear	6.35–10.16 cm mesh	11.43-cm mesh	10.16+11.43 cm composite	≥12.7 cm	Totals
This study	Millionaire net	2	3	0	0	5
	Large box net	0	14	19	7	40
Totals		2	17	19	7	45

Study	Gear	<6.35-cm mesh	6.35–10.16 cm mesh	11.43-cm mesh	Unknown	Totals
NMFS	Millionaire net	9	5	3	0	17
	Large box bet	5	4	2	7	18
Totals		14	9	5	7	35

Black-sea-bass-targeted tows

Study	Gear	6.35–10.16 cm mesh	11.43-cm mesh	10.16+11.43 cm composite	Totals
This study	Millionaire net	0	0	0	0
	Large box net	0	3	9	12
Totals		0	3	9	12

Study	Gear	<6.35-cm mesh	6.35–10.16 cm mesh	11.43-cm mesh	Unknown	Totals
NMFS	Millionaire net	0	0	0	0	0
	Large box net	0	6	0	0	6
Totals		0	6	0	0	6

fell between 22.9 cm (25th percentile) and 25.0 cm (75th percentile). For the NMFS observer data, the mean size of scup discards was 17.2 cm and ranged from 13.6 to 20.6 cm. Fifty percent of the scup discarded fell between 16.2 cm (25th percentile) and 18.2 cm (75th percentile). For scup landed, the mean size was 22.8 cm and ranged from 19.4 to 28.9 cm. Fifty percent of the scup landed fell between 21.3 cm (25th percentile) and 23.8 cm (75th percentile).

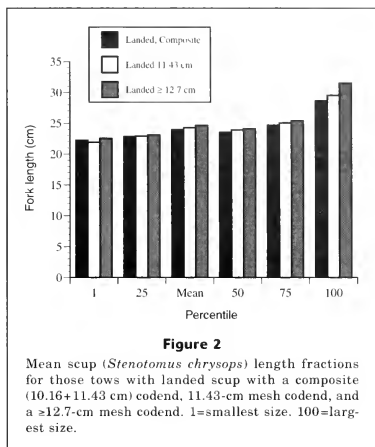
Codend and gear

Vessels participating in this study and in the NMFS observer program used either millionaire or box nets (Table 1). More tows were made with the box net in both data sets (Table 1). Most tows in our study were made with the composite and 11.43-cm codends because comparison of these two codends was one focus of our study. Most scup-targeted tows in the NMFS observer database were made with codends ≤ 10.16 cm mesh (Table 1).

Codend mesh size did not have a significant effect on catch length frequencies when data from our study and the NMFS observer data were analyzed separately or combined. We deleted codends with the smallest meshes (meshes ≤ 10.16 cm) and re-analyzed the data for the remaining larger codend meshes. Again, catch length frequencies were not significantly different for any of the codend mesh sizes. Finally, we considered the landed and discarded scup separately. For landings, codend mesh size had a moderately significant effect on median length ($P=0.0220$) and a stronger significant effect on mean length ($P=0.0062$). Codends with some meshes ≥ 12.7 cm caught more of the landed size fraction than the composite and slightly more than the 11.43-cm mesh codend; however, the actual difference in mean length between the three mesh-size groups was small, approximately one cm (Fig. 2).

The efficiency of the codend may change with the amount of fish caught such that selectivity declines with high catches. Accordingly, scup catches were divided into two groups: those above and those below the median catch for all tows. For catches above the median, codend mesh size had a significant effect ($P=0.0441$) on the 25th percentile of size for scup discarded in our study. The 25th percentile size was largest for codends with some meshes ≥ 12.7 cm and smallest for the composite codend. For landed scup, the 25th percentile sizes were about 22.0 cm regardless of codend mesh size. No significant differences existed between codend mesh sizes for scup length frequency in tows with catches below the median.

We examined the composition of the catch by weight. Codend mesh size had a limited effect on the ratio of scup discarded to landed, the total catch and total discards of all species, and total scup landed and discarded. Scup discards were greater with codends having some meshes ≥ 12.7 cm ($P=0.0211$). More scup were landed from these tows as well ($P=0.0034$) and therefore this codend style may contribute to a greater catch rate (Table 2). Very likely, this trend in increased



catch is produced by the small number of tows ($n=7$) in this mesh size category rather than a real improvement in net performance.

No significant gear effects existed for any of the length-frequency fractions in the combined data set (our study and NMFS observer study). The only significant effect of scope ($P=0.0175$) was on total scup discarded in our study. This effect was not present in the NMFS observer data set.

Discards-to-landings ratio

Of the 62 tows completed in our study, 39 targeted scup. The NMFS observer program, from 1997–mid 2000, included 35 scup-targeted tows (Table 3). Overall, mean catch per tow for scup-targeted tows was 972.6 kg in our study and 945.3 kg for NMFS observed tows. In our study, the discards-to-landings ratio for all species combined ranged from 1.77 with the composite codend to 2.91 with a codend with some meshes ≥ 12.7 cm. In the NMFS observer data set, the discards-to-landings ratio for all species combined in scup-targeted tows ranged from 0.47 with codends having meshes of 6.35–10.16 cm to 3.43 with codends with meshes of 11.43 cm (Table 2). The mean discards-to-landings ratio for scup ranged from 1.1 for the NMFS database to 2.4 for our study (Table 3). Ratios varied from a low of 0.35 to a high of 5.72 among the various gear and mesh-size combinations (Table 4).

We analyzed cases where scup discards exceeded or were less than landings. When our data and the NMFS observer data were combined, the 25th ($P=0.0219$), 50th

Table 2

Mean weight (in kilograms) of scup discarded, scup landed, total discards of all species, total catch of all species, and total discards-to-landings ratio of all species per tow by codend mesh size for this study and the NMFS observer data.

Study	Codend	Scup discarded	Scup landed	Total discards	Total catch	Total discards-to-landings ratio	Total number of tows
This study	Composite	659.7	329.3	1078.1	1686.0	1.77	16
This study	11.43 cm	607.8	210.7	1060.2	1437.7	2.81	14
This study	≥12.70 cm	1020.7	404.9	1973.4	2652.8	2.91	7
NMFS	<6.35 cm	615.5	493.4	949.1	1530.1	1.63	14
NMFS	6.35–10.16 cm	230.5	510.5	321.1	999.2	0.47	9
NMFS	11.43 cm	535.2	260.0	1015.7	1311.6	3.43	5

Table 3

Mean catch and landings per tow for scup and black sea bass-targeted tows.

Scup						
Study	Tow type	Total no. of tows	Mean catch (kg)	Mean landed (kg)	Mean discarded (kg)	Ratio of scup discards to landings
This study	Target	39	972.6	286.3	686.3	2.40
NMFS	Target	35	945.3	461.3	484.0	1.05
Black sea bass						
Study	Tow type	Total no. of tows	Mean catch (kg)	Mean landed (kg)	Mean discarded (kg)	Ratio of black sea bass discards to landings
This study	Target	10	365.0	278.7	86.3	0.31
NMFS	Target	6	171.9	170.1	1.8	0.01

($P=0.0085$), and 75th ($P=0.0038$) percentile sizes and the mean length ($P=0.0001$) were significantly lower for tows in which most scup were discarded (Fig. 3). When the data sets were analyzed separately, our study found that the 50th ($P=0.0133$) and 75th ($P=0.0040$) percentile sizes and the mean length ($P=0.0338$) were significantly lower for tows where discards exceeded landings. Not surprisingly, when fishermen caught larger scup, fewer scup were discarded. In the NMFS observer data set, no significant size effects were found for any of the percentile fractions.

When the discards and landings were analyzed separately, the lengths of fish discarded did not differ between tows for which discards exceeded landings and tows for which landings exceeded discards. However, for the landed fish, the 50th ($P=0.0034$) and 75th ($P=0.0018$) percentile sizes and the mean length ($P=0.0033$) were larger for tows where landings exceeded discards (Fig. 4). Discards decline when larger scup are proportionately more abundant in the catch.

We examined the influence of total catch (all species combined) on the length-frequencies of scup in tows

where scup landings exceeded or did not exceed scup discards. For those tows with total catches below the median catch, a significant effect was noted for the median ($P=0.0039$), the 75th percentile ($P=0.0006$), and the mean ($P=0.0288$) length of scup. In those tows where total catch weight was relatively low, the median, mean, and 75th percentile lengths were larger in tows where scup landings exceeded discards. No significant effects on the length-frequency distribution of scup were observed for total catches that were above the median. The analysis identifies a strong trend towards the landing of larger-size scup in tows yielding total catches below the median for all tows.

Both landings and discards were affected in those tows in which total catch fell below the median. For landed scup, the median ($P=0.0062$), the 75th percentile ($P=0.0051$), and the mean ($P=0.0113$) length were higher in tows with total catches below the median when scup landings exceeded discards. For those scup that were discarded from tows with total catches below the median, a significant size effect was observed for the 75th percentile ($P=0.0265$). Discarded scup were larger in

Table 4

Synopsis of catch and landings data (kg) by study, gear, and codend mesh size for scup-targeted tows in our study and those in the NMFS observer database.

Gear	Mesh size	Total scup/tow	Scup landed	Scup discarded	Ratio of scup discards to landings	Number of tows
This study						
Large box	10.16+11.43 cm composite	1332.3	519.3	813.0	1.57	9
	11.43 cm	1572.8	431.6	1141.2	2.64	5
	≥12.70 cm	2609.7	624.1	1985.6	3.18	2
Millionaire	6.35–10.16 cm	32.7	16.3	16.3	1.00	1
	10.16+11.43 cm composite	547.5	85.0	462.5	5.44	7
	11.43 cm	399.5	88.1	311.5	3.54	9
Unknown	≥12.70 cm	951.9	317.2	634.8	2.00	5
		636.8	94.8	542.0	5.72	1
NMFS						
Large box	<6.35 cm	1076.7	196.0	880.8	4.49	5
	6.35–10.16 cm	20.8	3.4	17.4	5.12	4
	11.43 cm	176.9	131.5	45.4	0.35	2
Unknown		988.2	477.6	510.6	1.07	7
Millionaire	<6.35 cm	1126.6	658.6	468.1	0.71	9
	6.35–10.16cm	1317.1	916.2	401.0	0.44	5
	11.43 cm	1207.3	345.5	861.8	2.49	3

Table 5

Total discards and total catch of all fish species (in kg) and scup discarded and landed (in kg) for only those tows characterized by having more or less discards of scup than the median catch per tow.

Study	More or less discards	Scup discarded	Scup landed	Total discards	Total catch	Total number of tows
This study	Less	145.4	355.6	565.4	1027.5	11
This study	More	898.9	259.0	1451.6	1982.3	28
NMFS	Less	235.1	521.1	426.3	1058.3	20
NMFS	More	815.9	381.5	1242.8	1761.5	15

these tows, reflecting the overall larger size of the scup catch in tows where total catch was relatively low.

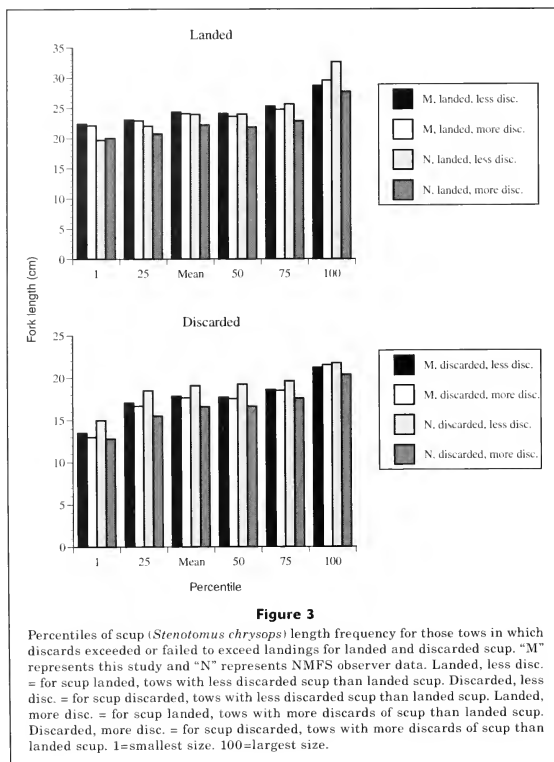
Finally, for tows in which scup discards exceeded landings, total catch of all species and total discards of all species were also high. This trend was significant for total catch ($P=0.0273$) and total discards ($P=0.0038$) in our study (Table 5) and for total discards ($P=0.0017$) and total catch ($P=0.0112$) in the NMFS observer data set (Table 5). Therefore, scup discards tended to increase with respect to landings as total catch increased.

Time and effort

For our study, effort significantly affected the 25th ($P=0.0247$) and 50th ($P=0.0466$) percentiles of the size-frequency distribution of discards. The size frequencies

for landings were not similarly affected. In both former cases, the 25th and 50th percentile sizes were larger when effort was less (shorter tows). No significant effects were observed in the NMFS observer data set. Because the length frequency of the entire catch did not change significantly, this is likely an effect of processing onboard the boat.

Given trip limits, one might anticipate discards to increase in tows made at the end of the trip. We examined the amount of scup caught either in the first half of the tows or in the last half of the tows on each trip. For this study, more scup were landed ($P=0.0008$) and discarded ($P=0.0001$) in tows that occurred during the last half of the trip. Total catch and total discards were unaffected. For the NMFS observer data set, more scup were landed ($P=0.0001$) and discarded ($P=0.0001$)



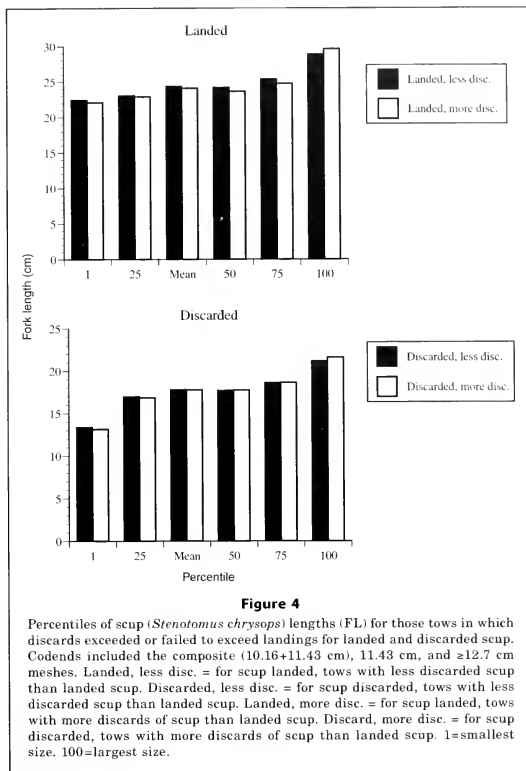
and the total catch of all species ($P=0.0195$) and total discards of all species ($P=0.0004$) were higher in tows taken during the last half of the trip (Table 6). More scup being landed and discarded in the last half of the trip indicates that captains learn where to fish for scup during the trip and CPUE rises as a consequence. No evidence exists that discards increased with respect to landings during the trip.

We anticipated that reduction of the trip limit from 4536 kg to 454 kg on 24 January would influence the total weight of discards. Time did influence total weight of scup discards ($P=0.0056$) in our study. More discards per tow occurred on trips taken prior to 24 January, likely because of the larger trip limit (weight

limit per species for each trip) for the 1–24 January period. With a larger trip limit, more scup can be caught per tow and therefore more scup will be discarded. The discards-to-landings ratio, however, was not significantly affected—indicating that captains controlled total scup catch in proportion to the landing limit.

The present study versus the NMFS observer study

We compared trends in our data with those in the NMFS observer data. The subset of directed scup tows in the two data sets rarely disagreed, despite the disparity in codend mesh sizes reported (Table 1).

**Table 6**

Mean weight (in kg) of scup discarded and landed and the total of all fish species landed and discarded per tow for scup-targeted tows in the first half of the trip and the second half of the trip.

Study	First half or second half of trip	Scup discarded	Scup landed	Total discards	Total catch	Total number of tows
This study	First	253.3	125.2	970.2	1279.7	22
This study	Second	1246.8	494.7	1501.2	2273.8	17
NMFS	First	43.2	23.2	463.0	670.3	19
NMFS	Second	1007.5	981.5	1148.3	2178.3	16

Table 7

Mean weight (in kg) of black sea bass discarded, black sea bass landed, total discards of all species, total catch of all species, and total discards-to-landings ratio of all species per tow by codend mesh size and gear for this study and the NMFS observer data.

Study	Gear	Codend	Black sea bass discarded	Black sea bass landed	Total discards	Total catch	Total discards to landings	Ratio of Total number of tows
This study	Large box	10.16+11.43 cm composite	119.2	366.7	845.6	1306.9	1.83	7
This study	Large box	11.43 cm	5.0	25.9	1201.8	1250.3	24.78	2
This study	Millionaire	11.43 cm	18.6	168.3	368.1	683.8	1.17	1
NMFS	Large box	6.35–10.16 cm	1.8	170.1	23.7	224.2	0.12	6

Catch statistics—black sea bass

During the winter scup season, black sea bass are legally caught with 10.16-cm mesh codends in offshore waters. A boat captain often will target scup and black sea bass on the same trip, but will use different mesh codends. A total of 12 black-sea-bass-targeted tows were observed in our study and 6 black-sea-bass-targeted tows were documented in the NMFS observer data set (Table 1).

Length frequency—black sea bass

Black sea bass length-frequency distributions were highly significantly different (often $P=0.0001$) between those fish landed and those discarded. The mean size of discarded black sea bass from our study was 22.9 cm and ranged from 18.4 to 25.4 cm. Fifty percent of the black sea bass discarded fell between 22.1 cm (25th percentile) and 24.3 cm (75th percentile). In contrast, the mean size of landed black sea bass was 31.1 cm and ranged from 25.4 to 40.9 cm. For black sea bass landed, fifty percent of the fish were found between 28.6 cm (25th percentile) and 33.3 cm (75th percentile). For the NMFS observer data, the mean size of black sea bass discarded was 23.4 cm and ranged from 20.7 to 27.0 cm. Fifty percent of the black sea bass discarded fell between 22.3 cm (25th percentile) and 24.7 cm (75th percentile). The mean size of landed black sea bass was 28.5 cm and ranged from 24.5 to 34.0 cm. For landed black sea bass, fifty percent fell between 25.0 cm (25th percentile) and 31.5 cm (75th percentile).

Codend and gear

Nine tows were made with the composite codend and three tows were made with the 11.43-cm legal mesh codend in our study. For the NMFS observer data, all six targeted tows fell into the 6.35–10.16 cm mesh-size group that included the legal mesh size of 10.16 cm (Table 1).

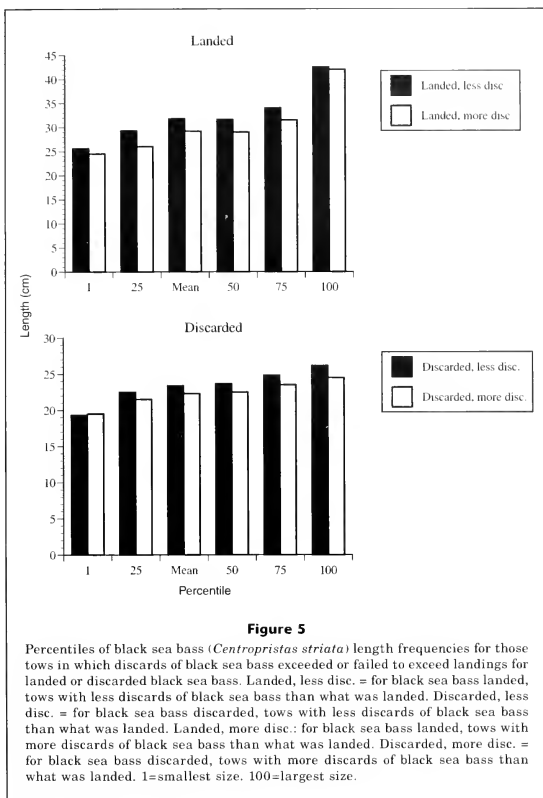
We found no significant effects of codend mesh size on the percentile length-frequency fractions of black sea bass. We considered landed and discarded black sea

bass separately for those tows with total catches above and below the median and, once again, no significant codend mesh-size effects were observed. The total number of tows, however, was small. A significant codend mesh-size effect ($P=0.0389$) was observed for black sea bass landed. Landings were higher with the larger mesh codends (composite 10.16+11.43 cm codend and the 11.43-cm codend) rather than with the ≤ 10.16 -cm mesh codend (Table 7). The small number of total tows with the larger codend mesh sizes (10.16+11.43 cm and the 11.43 cm) is probably responsible for this difference in landings rather than differences in net performance. Gear effects (net types) were not determined because only the box net was used.

Discards-to-landings ratio

Total mean catch per tow was 365 kg and total mean landings per tow was 279 kg for the 10 tows in our study. For the six directed tows in the NMFS observer data, average total catch was 172 kg and average total landings were 170 kg (Table 3). In black-sea-bass-targeted tows, the black sea bass catch comprised 34.2% of the total catch. The discards-to-landings ratio for black sea bass was 0.230. Relatively few black sea bass were discarded. Scup comprised 0.9% of the total catch in black sea bass targeted tows. Less than one percent (0.4%) of the scup catch in black-sea-bass-targeted tows was discarded.

We analyzed cases where black sea bass discards exceeded or were less than landings in tows where total catch (all species combined) was above or below the median. For total catches above the median, a significant size effect was noted for the median length ($P=0.0040$), the 75th percentile size ($P=0.0007$), and the mean length ($P=0.0026$). Larger fish were present in tows where discarding was lower (Fig. 5). No significant effects on the size distribution of black sea bass were observed in tows with total catches below the median. We further divided the catches above the median into discards and landings. For those black sea bass that were landed from tows with total catches above the median, a significant size effect was observed for the 25th ($P=0.0199$), the



50th ($P=0.0280$), and the 75th ($P=0.0090$) percentile size fractions and the mean length ($P=0.0133$). The size of landed black sea bass was larger in tows where discarding was low (Fig. 5).

Time and effort

Because of trip limits, discards could increase in tows taken near the end of a trip. Therefore, we compared the catch of black sea bass in the first and the last half of the tows. The quantity caught and the length-frequency

percentiles were not significantly different between the first and last half of the tows. In contrast, for scup trips, discards and landings tended to be higher in tows made in the last half of the trip.

Effort significantly affected the 25th ($P=0.0010$), 50th ($P=0.0003$), and 75th percentile ($P=0.0153$) size fractions of black sea bass for the combined data sets (NMFS study and our study). In these cases, higher effort was associated with more smaller fish. When the two data sets were analyzed independently, most of the effort effects were no longer present.

Discussion

Scup

The type of net (gear) and the size of codend mesh had only a minor effect on the length frequencies of scup caught. Although variations in codend mesh size normally influence catch in other studies (Hastie, 1996; Petrakis and Stergiou, 1997; Stergiou et al., 1997; Broadhurst et al., 1999), a wide range in codend mesh sizes produced similar results for scup. Codends with some meshes ≥ 12.7 cm appeared to catch more of the size classes of fish chosen for landing than the composite codend and just slightly more than the legal 11.43-cm mesh codend; therefore the ≥ 12.7 -cm mesh codend may reduce discards. The actual difference in scup lengths between the three codends was only about one cm. In terms of kilograms caught, more scup were caught in tows with the larger codend mesh. Landings increased, but so did discards, so that the discards-to-landings ratio remained unchanged. This finding indicates that the small upward bias in sizes caught did not significantly reduce total catch. In general, the smaller mesh codends (6.35–10.16 cm) and the composite codend (10.16+11.43 cm) performed similarly to the current legal mesh design (11.43 cm). Overall, discards of scup remained high regardless of the type of gear (nets) and codends used.

In our study, more larger scup were caught in longer tows. When a boat encounters a large school of scup, the mean length of the catch tended to be smaller. In addition, the larger-size scup tended to be caught more often in those tows with total catches below the median. This trend is probably a biological effect, but an effect of mesh size or gear cannot be excluded. Most populations contain relatively few larger fish and, therefore, more smaller individuals. Morse⁶ (in Steimle et al., 1999) noted that scup schools are size-structured. When larger scup are less common in schools, then schools with these larger individuals most likely would be smaller and more effort would be required to achieve the same catch of these individuals. The same result would occur if larger scup tended to be on the outside or above smaller scup in schools. Little is known about scup behavior. However, any spatial size structure in the population could promote a direct relationship between effort and the mean length of fish caught and an inverse relationship between total catch (all species) and mean length of fish caught.

As an alternative explanation for the lower catch rate of larger individuals, clogging of the codend may occur when catch rates are high and, as a consequence, size-selectivity would decline. Different codend mesh sizes do not seem to affect the number of discarded scup as much as one might anticipate because codends clog dur-

ing the interception of large schools. Accordingly, lower CPUE could produce greater size selectivity resulting in increased mean length when catches are relatively low. However, the trends observed in length frequency with effort and total catch were not significantly influenced by codend mesh size. Accordingly, the observed trend is likely a direct consequence of fishing on size-structured populations.

In general, more scup were landed and discarded in the last half of a trip. This finding indicates that the captain learns where to fish for scup by the second half of the trip and CPUE increases as a consequence. We had expected an increase in discards as the trip limit was reached towards the end of the trip. However, no effect of trip limits on the total weight of discards could be discerned in our data set or the NMFS observer data set.

More scup were discarded per tow in tows observed during the first half of the 2001 season, namely 1–24 January, than in the second half of the season, 25 January–February, but the discards-to-landings ratio did not vary for either half of the season. The fact that the ratio did not differ indicates that more scup are discarded per tow when fishermen are allowed a larger trip limit (4536 kg). The higher discards of scup per tow during the first half of the season are likely due to the increased total catch per tow that might be anticipated when allowable landings are higher. Accordingly, captains are able to reduce catch rate and, thus, discards when landing limits are low.

We compared the NMFS observer database to our observer data. Despite a substantial variation in the distribution of codend mesh sizes between the two data sets, the discards-to-landings ratio was not significantly different. Concerns raised by the high discards-to-landings ratio observed in the NMFS observer data were supported by our study. The discards-to-landings ratio for the directed scup fishery consistently exceeded 1.0.

In summary, the objective of our study was to evaluate the effect of codend mesh size on the amount of scup discards and to identify mechanisms to reduce scup discards. Although we observed a number of trends in discards in our study, neither the current legal mesh nor any of the experimental codends seem to adequately filter out scup smaller than 22.86 cm. Neither did trip limits seem to influence the total weight of scup discards. In fact, the only consistent trends produced by variations in effort and total catch seem most likely due to biological effects not easily controlled for by the captain of a fish vessel. Overall, the total weight of discards seems to be primarily a function of the regulated size limit, abetted by the tendency for smaller fish to be captured when encounter rates are high. The present study found that the length of the median discards was about 17.78 cm FL (19.83 cm TL based upon a conversion factor of Hamer⁴ [in MAFMC, 1996]). O'Brien et al. (1993) and NEFSC (1993) reported that 50% of both male and female scup reach maturity at 15.49 cm FL (17.27 cm TL). Therefore, lowering the scup minimum size limit to 17.78 cm FL (19.83 cm TL) would greatly

⁶ Morse, W. W. 1978. Biological and fisheries data on scup, *Stenotomus chrysops* (Linnaeus). NMFS, NEFSC, Sandy Hook Lab. tech. ser. rep. no. 12, 41 p. James J. Howard Marine Sciences Laboratory, Northeast Fisheries Science Center, 74 Magruder Rd., Sandy Hook, NJ 07732.

reduce scup discards, yet permit the majority of scup to attain sexual maturity. Kilograms discarded might be reduced by more than half. Fishermen would reach their trip limit sooner and thus stop fishing earlier. As a result, fishing mortality rate even on larger scup would be reduced. This single change would reduce discards more than any change in net or codend design tested to date and would not result in any increase in fishing-induced mortality for scup.

Black sea bass

Estimates of discards of black sea bass are low in the black-sea-bass-targeted fishery, based on the few observed tows in our study and data from the NMFS observer database. Regardless of which codends were used, the same size fractions of black sea bass were caught. The composite codend (10.16+11.43 cm mesh) caught more black sea bass than were landed. Discards was also higher. As with scup, mesh size and gear type had minor effects on the size frequency, the discards-to-landings ratio, and the kilograms of black sea bass caught. The majority of tows where black sea bass were caught had ratios of black sea bass discarded to landed of less than 0.3, indicating that few discards occur in this fishery. In contrast, most of the scup tows were characterized by discards-to-landings ratios greater than one. The differences in discards-to-landings ratios between black sea bass and scup may be due to a combination of biological factors controlling the average size of scup in the larger schools and to regulatory factors that do not match well with the size range of scup in schools.

Unlike scup, black sea bass size frequencies and total weight caught were similar in tows taken during the first and last half of the trip. Trip limits are in effect for both black sea bass and scup. The difference between the two species in the distribution of catch through the time course of the trip may be the result of biological effects in that the schooling of scup would tend to produce higher catches during the middle or latter part of the trip as the captain finds schools of fish.

Powell et al.³ showed that black sea bass and scup are caught simultaneously more frequently than expected by chance in tows in the Atlantic mackerel (*Scomber scombrus*), *Loligo* squid, scup, and silver hake fisheries and suggested that they should be regulated together. Our analysis also showed this pattern in that the two species were frequently caught in the same tows (39 out of 40 scup-targeted tows and seven out of 10 black-sea-bass-targeted tows caught both scup and black sea bass). In addition, Shepherd and Terceiro (1994), Musick et al., (1985), and Musick and Mercer (1977) also found that both scup and black sea bass were caught in the same tow. Use of a common codend mesh size regulation for both fisheries may prove useful. The failure to find significant differences between mesh sizes suggests that the 10.16+11.43 cm composite bag might be a reasonable choice for both fisheries. However, scup discards were a small fraction of black sea bass landings in black-sea-bass-targeted tows (0.4%)—very small in comparison to

the percentage in scup-targeted tows. This finding indicates that there is considerable discrimination between the two species at the level of the fishery. The black sea bass fishery is currently regulated under the small-mesh fishery GRA plan in which fishing is prohibited in some areas to reduce scup mortality. This investigation finds no evidence to support the efficacy of this management approach. Scup discards do not appear to be an important attribute of the black sea bass fishery.

Conclusions

Because fishermen catch both scup and black sea bass in the same tow and because the current regulations require fishermen to use an 11.43-cm mesh codend when targeting scup, and, a 10.16-cm mesh codend when targeting black sea bass, two different codend mesh sizes are used on the same trip. The composite codend was designed to retain the smaller black sea bass catches and some scup when catch rates are low but permits more scup to escape at higher catch rates. The composite codend (10.16+11.43 cm mesh) performed as well as the other codends used in our study, including the 11.43-cm legal-size codend. The composite codend with 10.16-cm mesh followed by the 11.43-cm or 12.7-cm mesh codends should be further evaluated on both black sea bass and scup-directed tows. If this composite codend works equally as well as the legal 11.43-cm mesh codend currently in place for scup (and the data presented here suggest that it does), consideration should be given to using this codend because it permits the retention of smaller black sea bass without negatively influencing scup. This change would eliminate the need to carry two codends onboard and thus would reduce overall trip costs without impacting the number of scup discards. However, neither codend successfully addresses the need to significantly reduce scup discarding in the scup-directed fishery.

Codends with some 12.7-cm meshes tended to reduce discards by reducing the catchability of smaller scup, but the trends were often not significant, possibly due to the small sample size, but possibly also because nets were clogged by schools of smaller-size scup. The data indicate that further studies with 12.7-cm or greater mesh composites may identify codend configurations that will produce fewer discards. DeAlteris and La Valley (1999) have documented that scup can survive capture in a trawl net and subsequent escapement. Therefore, optimizing codend mesh size could reduce discard mortality.

Larger scup were caught in tows where the total catch weight was low. Large catches tended to accompany the interception of scup schools. These large catches can clog the nets and thus reduce size selection even at larger mesh sizes. Alternatively, larger scup may not be associated with smaller scup in schools. We cannot discriminate between the two explanations. Regardless of the reason, the tendency of the largest catches to contain proportionately more smaller fish will likely minimize the positive influence of net management in

reducing scup discards. Rather, the tendency of the largest catches to contain proportionately more smaller fish suggests that fisheries managers may want to lower the legal-size limit for scup from 22.86 cm to 17.78 cm FL. The median size of scup discards in our study was 17.78 cm FL. Setting the size limit at 17.78 cm FL (19.83 cm TL) would greatly reduce discards and thus overall discard mortality. This management change would likely have a much greater effect in reducing scup discards than any other single management measure directed at gear modification or area closure and would not endanger the stock (most discarded scup fail to survive); thus, any approach significantly reducing discards must significantly increase overall survival of the population.

Acknowledgments

We would like to thank the National Fisheries Institute, Scientific Monitoring Committee, for providing support for this project. We also thank the captain and crew for the use of the four commercial fishing vessels from Cape May that cooperated in the project. Without their assistance, this project would not have been possible. We also thank NMFS-NEFSC for providing the NMFS observer data used in our analysis.

Literature cited

- Alverson, D. L.
1999. Some observations on the science of bycatch. MTS (Marine Technology Society) Journal 33(2):6-12.
- Broadhurst, M. K., S. J. Kennelly, and S. Eayrs.
1999. Flow-related effects in prawn-trawl codends: potential for increasing the escape of unwanted fish through square-mesh panels. Fish. Bull. 97:1-8.
- DeAlteris, J., and K. J. La Valley.
1999. Physiological response of scup, *Stenotomus chrysops*, to a simulated trawl capture and escape event. MTS Journal 33(2):25-34.
- Glass, C. W., B. Sano, H. O. Milliken, G. D. Morris, and H. A. Carr.
1999. Bycatch reduction in Massachusetts inshore squid (*Loligo pealei*) trawl fisheries. MTS Journal 33(2):35-41.
- Hastie, L. C.
1996. Estimation of trawl codend selectivity for squid (*Loligo forbesi*), based on Scottish research vessel survey data. ICES J Mar Sci 53:741-744.
- Howell, W. H., and R. Langdon.
1987. Commercial trawler discards of four flounder species in the Gulf of Maine. North Am. J. Fish Manag. 7:6-117.
- Kennelly, S. J.
1999. Areas, depths and times of high discard rates of scup, *Stenotomus chrysops*, during demersal fish trawling off the northeastern United States. Fish. Bull. 97:185-192.
- MAFMC (Mid-Atlantic Fishery Management Council).
1996. Amendment 8 to the summer flounder, scup, and black sea bass fishery management plan: fishery management plan and final environmental impact statement for the scup fishery. January 1996, 353 p. Mid-Atlantic Fishery Management Council, Dover, DE.
- Mooney-Seus, M.
1999. Formula for bycatch reduction. MTS Journal 33(2):3-5.
- Musick, J. A., J. A. Colvocoresses, and E. J. Foell.
1985. Seasonality and the distribution, availability and composition of fish assemblages in Chesapeake Bight. In Fish community ecology in estuaries and coastal lagoons: towards an ecosystem integration (A. Y. Arancibia, ed.), p. 451-474. OR(R) UNAM (Universidad Nacional Autonoma de Mexico) Press, Mexico. [ISBN 9688376183.]
- Musick, J. A., and L. P. Mercer.
1977. Seasonal distribution of black sea bass, *Centropristis striata*, in the Mid-Atlantic Bight with comments on the ecology and fisheries of the species. Trans. Am. Fish. Soc. 106:12-25.
- NEFSC (Northeast Fisheries Science Center).
1993. Status of the fishery resources off the Northeastern United States. NOAA Tech. Mem. NMFS-F/NEC-101, 140 p.
- O'Brien, L., J. Burnett, and R. K. Mayo.
1993. Maturation of nineteen species of finfish off the northeast coast of the United States, 1985-1990. NOAA Tech. Rep. NMFS 113, 66 p.
- Petrakis, G., and K. I. Stergiou.
1997. Size selectivity of diamond and square mesh codends for four commercial Mediterranean fish species. ICES J Mar Sci. 54:13-23.
- Powell, E. N., A. J. Bonner, B. Muller, and E. A. Bochenek.
2004. Assessment of the effectiveness of scup bycatch-reduction regulations in the *Loligo* squid fishery. J. Environ. Manag. 71:155-167.
- Roel, B. A., K. L. Cochran, and J. J. Field.
2000. Investigation into the declining trend in Chokka squid *Loligo vulgaris reynaudii* catches made by South African trawlers. S. Afr. J. Mar. Sci. 22:212-135.
- Shepherd, G. R., and M. Terceiro.
1994. The summer flounder, scup and black sea bass fishery of the Middle Atlantic Bight and southern New England waters. NOAA Tech. Rept. NMFS 122, 13 p.
- Steimle, F. W., C. A. Zetlin, P. L. Berrien, D. L. Johnson, and S. Chang.
1999. Essential fish habitat source document: scup, *Stenotomus chrysops*, life history and habitat characteristics. NOAA Tech. Mem. NMFS-NE-149, 48 p.
- Stergiou, K. I., C.-Y. Politou, E. D. Christou, and G. Petrakis.
1997. Selectivity experiments in the NE Mediterranean: the effect of trawl codend mesh size on species diversity and discards. ICES J Mar Sci 34:774-786.
- Suuronen, P., J. A. Perez-Comas, L. Lehtonen, and V. Tschernij.
1996. Size-related mortality of herring (*Clupea harengus* L.) escaping through a rigid sorting grid and trawl codend meshes. ICES J Mar Sci 53:691-700.

Abstract—Fecundity was estimated for shortspine thornyhead (*Sebastes alascanus*) and longspine thornyhead (*S. altivelis*) from the northeastern Pacific Ocean. Fecundity was not significantly different between shortspine thornyhead off Alaska and the West Coast of the United States and is described by $0.0544 \times FL^{3.978}$, where FL = fish fork length (cm). Fecundity was estimated for longspine thornyhead off the West Coast of the United States and is described by $0.8890 \times FL^{3.249}$. Contrary to expectations for batch spawners, fecundity estimates for each species were not lower for fish collected during the spawning season compared to those collected prior to the spawning season. Stereological and gravimetric fecundity estimation techniques for shortspine thornyhead provided similar results. The stereological method enabled the estimation of fecundity for samples collected earlier in ovarian development; however it could not be used for fecundity estimation in larger fish.

Fecundity of shortspine thornyhead (*Sebastes alascanus*) and longspine thornyhead (*S. altivelis*) (Scorpaenidae) from the northeastern Pacific Ocean, determined by stereological and gravimetric techniques*

Daniel W. Cooper

Katherine E. Pearson

Donald R. Gunderson

School of Aquatic and Fishery Sciences

University of Washington

1122 NE Boat Street

Seattle, Washington 98105.

Present address (for D. W. Cooper, contact author): Alaska Fisheries Science Center, F/AKCZ
7600 Sand Point Way NE
Seattle, Washington 98115-0700.

E-mail address (for D. W. Cooper) dan.cooper@noaa.gov

Shortspine thornyhead (*Sebastes alascanus*) is distributed from the Bering Sea to Baja California (Orr et al., 2000). Longspine thornyhead (*S. altivelis*) is distributed from the Gulf of Alaska to Baja California (Orr et al., 2000), and a few specimens have recently been collected in the eastern Bering Sea (Hoff and Britt, 2003). Both species are commercially important (Piner and Methot, 2001; Gaichas and Ianneli, 2003) and inhabit deep waters over the continental shelf and slope. Both shortspine and longspine thornyhead are determinate spawners (Wakefield, 1990; Pearson and Gunderson, 2003), and spawn pelagic, gelatinous egg masses (Pearcy, 1962; Best, 1964; Wakefield, 1990; Wakefield and Smith, 1990). Shortspine thornyhead spawn between April and July in Alaska, and between December and May along the West Coast of the United States, whereas longspine spawn between January and April along the West Coast (Pearson and Gunderson, 2003).

Annual fecundity is used as a measure of reproductive output in fishery population models and life history studies. Accurate annual fecundity estimates require identifying oocytes to be spawned in the current spawning season. For iteroparous spawners, developing oocytes are often

distinguished from reserve oocytes by diameter or yolk presence (Macer, 1974). Collection date for samples is important. If samples are collected too early in oocyte development, some developing oocytes will be indistinguishable from reserve oocytes, and fecundity will be underestimated.

In shortspine thornyhead, oocyte stages 4–8 are maturing to be spawned in the current spawning season, whereas oocyte stages 1–3 are reserve oocytes to be spawned in future spawning seasons (Pearson and Gunderson, 2003). Early vitellogenic oocytes (stage 4) overlap in size with late perinucleus (stage 3) reserve oocytes (Pearson and Gunderson, 2003). Late vitellogenic oocytes (stage 5) are easily distinguished from reserve oocytes. In whole oocytes, neither oocyte size nor appearance can be relied on to distinguish stage-3 and early stage-4 oocytes; however stage-3 and stage-4 oocytes can be visually distinguished from histological samples (Pearson and Gunderson, 2003). Emerson et al. (1990) developed a stereological method to estimate fecundity

Manuscript submitted 15 July 2003 to the Scientific Editor's Office.

Manuscript approved for publication 20 September 2003 by the Scientific Editor.

Fish. Bull. 103:15–22 (2005).

* Contribution 929 from the Joint Institute for the Study of the Atmosphere and Ocean (JISAO), 4909 25th Ave NE, Seattle, WA.

from histological sections. Unlike gravimetric methods (e.g., Hunter et al., 1992) where whole oocytes are used to estimate fecundity, stereological methods do not rely on oocyte diameter or other proxies for vitellogenesis. A collection of shortspine thornyhead ovaries from Alaska contained few specimens considered suitable for a gravimetric fecundity method because too few of the specimens contained all developing oocytes in stage 5 or beyond. However, enough samples were suitable for the stereological method.

This study provides a fecundity estimate based on stereological and gravimetric techniques for shortspine thornyhead off Alaska. Benefits and limitations of the stereological method in this case are discussed. A gravimetric technique is also used to estimate fecundity for longspine thornyhead and shortspine thornyhead from samples off the West Coast of the United States. In addition, we examine the hypothesis that thornyheads are batch spawners, and that fecundity consequently declines over the course of the spawning season (Wakefield, 1990).

Materials and methods

Ovaries were collected from a large geographic area in Alaska, including the Gulf of Alaska, the Aleutian Islands, and the Bering Sea. National Marine Fisheries Service (NMFS) observers aboard commercial fishing vessels collected ovaries from April through June 2000. Length and somatic weight (ovaries and stomach contents removed) (± 5 g) were recorded at sea. Ovaries were excised and placed in 10% formalin solution buffered with sodium bicarbonate.

Ovaries from shortspine thornyhead and longspine thornyhead were also collected during the 1999 NMFS West Coast trawl survey. Samples were collected between Northern California and Washington (34°57'N lat, 121°33'W long. to 48°04' lat, 125°58'W long.). Length and somatic weight (± 2 g) were recorded at sea.

Additional West Coast longspine and shortspine thornyhead ovaries were collected from commercial fishing vessels by the Oregon Department of Fish and Wildlife in Astoria. Ovaries were collected off Oregon and Washington from February through May 2000, during December 2000, and during January 2001. After shipment to the NMFS Alaska Fisheries Science Center in Seattle, length, somatic weight (± 2 g), and ovary weight (± 0.001 g) were recorded. Ovaries were excised and placed in 10% formalin buffered with sodium bicarbonate.

A cross section was removed from one ovarian lobe (middle or middle posterior region) for histological processing. When a whole cross section was too large to fit on a microscope slide, a wedge was cut from the cross section that included both the ovarian wall and the center of the ovary. Samples were processed through a dehydration series, embedded in paraffin, and sectioned at 4 μ m. Slides were stained with hematoxylin and eosin.

Gravimetric fecundity estimation

Histological ovary sections were examined at 100 \times magnification to select samples for the gravimetric method. Oocytes were identified to one of eight developmental stages as described by Pearson and Gunderson (2003). To differentiate between oocytes to be spawned in the current year and reserve oocytes for future years, only ovaries with all maturing oocytes in stage-5 (late vitellogenesis) and beyond were used. By definition, yolk fills more than 50% of the cytoplasm within stage-5 oocytes, and the dark yolk made it easy to distinguish these oocytes. Stage-4 oocytes would also be spawned in the current year but overlapped significantly in size with nonmature stage-3 oocytes, and early stage-4 oocytes did not always have enough yolk (0–50%) to differentiate them from stage-3 oocytes with the gravimetric method. Specimens containing any stage-4 oocytes were omitted as a result. Ovaries with stage-8 oocytes were also omitted because the increased amount of gelatinous material which surrounds the oocytes in *Sebastolobus* could not be contained within the ovaries during subsampling.

Ovaries were weighed (± 0.001 g) after they had been stored in formalin. Subsamples were cut from the ovaries and weighed (± 0.001 g). For smaller ovaries, an entire cross section was taken. For larger ovaries, a pie-piece-shaped wedge was cut from the cross section to ensure a representative sample of outer ovarian wall. When cut correctly, a wedge starting at the center of the cross section would have the same weight ratio of ovarian wall to wedge subsample as the original cross section. Subsamples usually contained approximately 1000 oocytes (mean=1133), but this number varied according to stage of development and the amount of gelatinous material in the ovary (range: 108–3711).

Gelatinous material could not be subsampled by cutting at room temperature; therefore ovaries were briefly frozen before subsampling. This procedure enabled the gelatinous material to be cut, and also made it easier to obtain a representative sample of the ovarian wall. Initially, parts of three ovaries were frozen, and no effects of the freezing were detected with a light microscope. Only samples for gravimetric fecundity estimates were briefly frozen.

No difference in oocyte density was found among the different regions of the ovaries (see "Results" section); however, gravimetric subsamples were still taken randomly along the length of the ovaries to minimize potential bias from any location.

The oocytes in the subsamples were counted under a stereomicroscope, and fecundity was estimated by

$$Fec = \frac{W}{w} N,$$

where Fec = estimated fecundity;
 W = total ovary weight;
 w = subsample weight; and
 n = number of oocytes in the subsample.

Stereological fecundity estimation

The majority of oocytes within an ovary were found to be at the same developmental stage; however development was not completely synchronous. Some ovaries containing stage-5 and -6 oocytes (late vitellogenesis to migratory nucleus) also contained a few stage-4 oocytes, which although unsuitable for fecundity estimation with the gravimetric method, could be used with the stereological method described by Emerson et al. (1990). Fecundity was estimated from ten of these samples by using the stereological method to complete the shortspine thornyhead collection from Alaska.

Fecundity was estimated per unit of volume and then multiplied by the volume of both ovaries. The formula used to estimate fecundity per unit of volume is

$$N_v = \frac{k N_a^{3/2}}{\beta V_i^{3/2}}$$

where N_v = the number of oocytes per unit of volume;

k = an oocyte size correction coefficient;

β = an oocyte shape correction coefficient;

N_a = the average number of vitellogenic oocytes per unit of area; and

V_i = the average fractional volume of vitellogenic oocytes per unit of area.

The method for estimating the parameter k is given in Emerson et al. (1990) and the parameter k was estimated for six shortspine thornyhead samples. The resulting k values had a small range (1.0088–1.022), and a small standard deviation (0.0066), and a mean k value of 1.017 was used for all samples as a result. β was calculated by using the method given in Weibel and Gomez (1962). The β parameter was calculated from one shortspine thornyhead sample (53 oocytes) to be 1.565.

Exact volume of sample ovaries was impossible to determine because portions of the ovaries had already been removed for histological study (Pearson and Gunderson, 2003). Volume was estimated by dividing whole ovary weight by an average density of 1.052 g/mL. This was the average density from six samples (SD=0.0297) estimated by water displacement in a graduated cylinder.

Values for N_a and V_i were estimated by using a simplified Weibel grid for particulate structures (Weibel et al., 1966) instead of a Weibel multipurpose grid. A square containing 13 rows of 13 points was created and printed out on a clear acetate sheet. This overlay was taped to the front of a monitor. A video camera mounted to a stereomicroscope sent the image of the histology section to the computer monitor. The number of vitellogenic oocytes per grid and the number of points falling on vitellogenic oocytes were recorded and used to estimate N_a and V_i , respectively. The Weibel grid was used at 25 \times magnification, and 50 \times magnifica-

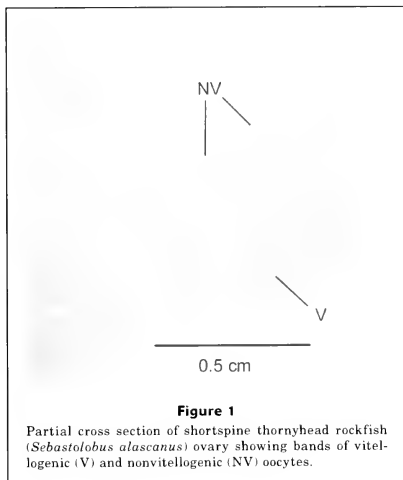


Figure 1
Partial cross section of shortspine thornyhead rockfish (*Sebastolobus alascanus*) ovary showing bands of vitellogenic (V) and nonvitellogenic (NV) oocytes.

tion was used to help distinguish borderline vitellogenic oocytes.

A sampling grid was placed under the ovary histological section. The corner of the Weibel grid was aligned with corners of the sampling grid in order to systematically sample the ovary cross section. Two histological sections were sampled per ovary.

The number of Weibel grid counts per ovary depended on the size of the ovary cross section. An average of 55.9 (range: 29–103) Weibel grid counts were taken per ovary. This number was greater than the average number of Weibel grid counts used by Emerson et al. (1990), but the extra counts were made because shortspine thornyhead vitellogenic oocytes develop on peduncles (Erickson and Pikitch, 1993; Pearson and Gunderson 2003) and are distributed in a band around the central part of the ovary (Fig. 1). Because the vitellogenic oocytes are not uniformly distributed, the Weibel grid was applied systematically at more points across the entire ovary, and the counts were averaged. Because the whole cross section could not be systematically sampled and averaged, cross sections of larger fish were not used for stereological estimates.

Statistical methods

Length-fecundity relationships were estimated by using the following equation:

$$Fec = aL^b,$$

Table 1
Fecundity estimates (number of oocytes) by ovary location and method.

Species	Stereological method				Gravimetric method			
	Sample location in ovary				Sample location in ovary			
	Mid	Posterior	Anterior	CV	Mid	Posterior	Anterior	CV
Shortspine	122,180	87,504	111,758	0.166	131,934	110,456	111,425	0.103
Shortspine	313,131	257,378	304,348	0.103	269,453	230,992	257,427	0.078
Shortspine	184,802	199,572	203,014	0.049				
Shortspine	474,432		458,877	0.024				
Longspine	38,061	26,179	28,424	0.204	38,968	33,207	33,653	0.091
Longspine	36,152	23,127	19,411	0.335				
			Mean CV	0.147			Mean CV	0.091

where Fec = estimated fecundity;

l = fork length; and

parameters a and b were estimated by nonlinear regression with SPSS software (version 11.0, SPSS Inc., Chicago, IL).

Weight-fecundity relationships were estimated by using the following equation

$$Fec = m(Wt_{somatic})^b + b1,$$

where Fec = estimated fecundity;

$Wt_{somatic}$ = somatic weight; and

m and $b1$ were estimated by using linear regression in EXCEL (Microsoft, Redmond, WA).

Reduction in variance F tests (Quinn and Deriso, 1999) were used to compare fecundity relationships between areas, studies, and before and during spawning season.

Results

Ovary location differences

We tested for difference in oocyte density between middle, posterior, and anterior sections of six ovary pairs with the stereological method (ovaries from the migratory nucleus to late hydration phase) and did not find a significant difference in ovary location (two-way ANOVA, $P=0.148$) (Table 1).

Stereological method versus gravimetric method

The gravimetric method and the stereological method provided similar results. For shortspine thornyhead, the average ratio of gravimetric to stereological estimates for ten pairs of data was 0.993 (Table 2), and a plot of

the gravimetric versus stereological estimates showed that they follow a 1:1 trend line (Fig. 2). The gravimetric method gave a somewhat lower coefficient of variation than the stereological method, based on multiple samples of the same ovaries (Table 1). An F test (Quinn and Deriso, 1999) did not show a significant difference ($P=0.84$) between the gravimetric ($n=16$) and stereological ($n=10$) methods in the length-fecundity relationships obtained for Alaskan shortspine thornyhead, and the data were therefore combined (Fig. 3).

Shortspine thornyhead

Shortspine thornyheads from Alaska ($n=26$) and the West Coast ($n=30$) had similar fecundity at length (Fig. 3). An F test did not indicate fecundity at length for the two areas was significantly different ($P=0.53$); therefore the data were combined to obtain the relationships (Figs. 3 and 4):

$$Fec = 0.0544(\text{Fork Length}(cm))^{3.978} \quad (r^2=0.792, n=56)$$

$$Fec = 0.223(Wt_{somatic}(g)) - 63.079 \quad (r^2=0.781, n=53).$$

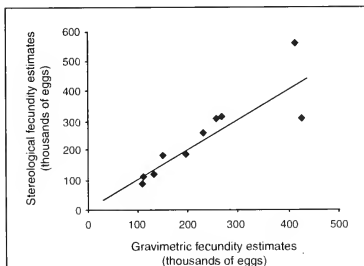
A majority of the shortspine thornyhead fecundity at length data points obtained in this study fell below the regression line reported by Miller (1985) (Fig. 3). The raw data from Miller (1985) were not published; therefore no statistical test was possible.

The data were also separated into months preceding the start of spawning and those after the start of spawning (Pearson and Gunderson, 2003) to look for evidence of batch spawning. Shortspine collected between October and November were grouped as specimens before the start of spawning. Shortspine collected from April through June in Alaska and from March through May off the West Coast were grouped as specimens after the start of spawning. Fish collected after spawning had begun ($n=41$) did not show a significant

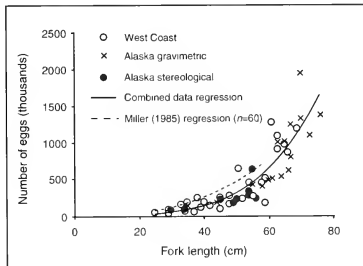
Table 2

Paired fecundity estimates (number of oocytes) by method and by section of the ovary (middle, posterior, anterior) where oocyte samples were taken.

Specimen	Position in the ovary	Gravimetric	Stereological	Ratio of gravimetric to stereological
Shortspine 1	Middle	150,448	184,853	0.814
Shortspine 2	Middle	195,356	187,037	1.044
Shortspine 3	Middle	427,717	307,771	1.390
Shortspine 4	Middle	414,594	561,258	0.739
Shortspine 5	Middle	131,934	122,180	1.080
	Posterior	110,456	87,504	1.262
	Anterior	111,425	111,758	0.997
Shortspine 6	Middle	269,453	313,131	0.861
	Posterior	230,992	257,378	0.897
	Anterior	257,427	304,348	0.846
				Mean ratio 0.993

**Figure 2**

Plot of gravimetric versus stereological fecundity estimates for ten shortspine thornyhead rockfish (*Sebastolobus alascanus*) data pairs. Line = 1:1 ratio.

**Figure 3**

Shortspine thornyhead (*Sebastolobus alascanus*) fecundity-at-length estimates by location and method, and regression of combined data (our study) and by regression of data from Miller's study (1985).

decrease in fecundity at length when compared to fish collected before spawning had begun ($n=11$) (F test, $P=0.71$) (Fig. 5).

Longspine thornyhead

Longspine thornyhead fecundity data conformed more closely to a linear regression on somatic weight (Fig. 6):

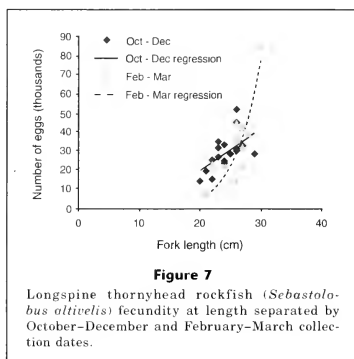
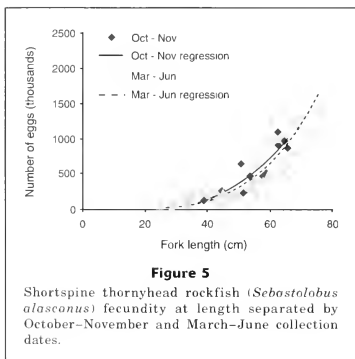
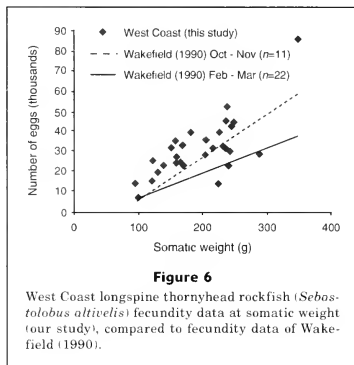
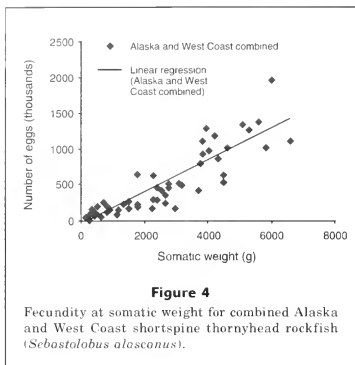
$$Fec = 183.81(Wt_{somatic}(g)) - 4617 \quad (r^2 = 0.536, n = 29)$$

than to a nonlinear regression on length (Fig. 7):

$$Fec = 0.8890(Fork\ Length(cm))^{3.249} \quad (r^2 = 0.442, n = 29).$$

A majority of the predicted fecundity values at somatic weight were higher than those derived from Wakefield's (1990) regression line on somatic weight (Fig. 6), but Wakefield's (1990) raw data were not published.

Wakefield (1990) estimated spawning to begin in February and created separate fecundity-at-weight relationships for fish collected in October–November and in February–March. He noted a decline in fecundity as the spawning season progressed but did not test this fecundity difference for statistical significance. Similar groupings (October–December, $n=17$; and February–March, $n=11$) in our study did show a statistically significant difference in fecundity as the spawning season progressed (F test, $P=0.004$) (Fig. 7); however, the



regression lines intersected, and the February–March group was not lower than the October–December group. The February–March group did have lower fecundity than the October–December group for lengths smaller than 27 cm; however the sample size was very small. No significant difference existed between the two groups when the single, large fecundity observation late in the spawning season was ignored ($P=0.34$).

Discussion

Emerson et al. (1990) cited the ability to distinguish borderline vitellogenic oocytes from nonvitellogenic

oocytes as an advantage of the stereological method, and this was a clear benefit in our study. The stereological method allowed us to differentiate between vitellogenic and nonvitellogenic oocytes at an earlier stage of ovary development than was possible with the gravimetric method. However, the use of ovaries in earlier stages of development increases the potential magnitude of fecundity overestimates due to atresia. Atresia, or the resorption of oocytes, is a potential source of error for fecundity estimates (Hunter et al., 1992). Although atretic oocytes can be identified with the stereological method, oocytes that are destined for atresia will be counted, causing fecundity to be overestimated. The amount of atresia will determine the magnitude of this overestimate. Samples

collected at later ovarian development stages would avoid this potential error (Tuene et al., 2002).

Because of a nonrandom distribution of vitellogenic and nonvitellogenic oocytes in the ovary, it was necessary to average Weibel grid counts over an entire ovary cross section. Larger ovaries that did not fit on a single slide could not be used, so that fecundity of larger fish had to be determined with the gravimetric method. This was a major limitation because few fish greater than 60 cm had ovaries small enough to be suitable for the stereological method. This limitation, however, might not apply to fish species with vitellogenic oocytes randomly distributed throughout the ovary.

The number of Weibel grid counts required was larger in our study than in Emerson et al. (1990), and the extra counts increased the amount of time involved with computation of fecundity estimates. In addition to the time required to prepare histological sections, the time to obtain stereological estimates took approximately twice as long as those obtained with the gravimetric method. Our estimates of shortspine thornyhead fecundity at length (Fig. 3) appeared lower than the regression published by Miller (1985), but our longspine thornyhead fecundity estimates were higher than those published by Wakefield (1990) (Fig. 6). Several potential explanations exist for the differences. Temporal or geographic differences in fecundity could exist. Samples from different decades were used in the two studies, and Wakefield (1990) used longspine samples taken from off Point Sur, California, whereas we used samples collected off Oregon and Washington. However, the differences may also be explained by methodological differences between authors, including different criteria to include oocytes in fecundity estimates, and differences in the ovarian development of samples. Relatively small sample sizes from our study and from Wakefield (1990) may add uncertainty to these fecundity estimates. The length range of samples could also affect comparisons for shortspine thornyhead fecundity. The fecundity estimates from Miller (1985) did not include any fish greater than 60 cm, whereas we used fish approaching 80 cm.

Wakefield (1990) grouped fecundity data by date, that is to say before the start of spawning and after the start of spawning. His data indicated a decline in fecundity after spawning begins, which he attributed to batch spawning. Similar temporal groupings in our study did not necessarily show a decrease in fecundity that was indicative of batch spawning in longspine or shortspine thornyhead. An important caveat regarding these comparisons is that the combination of small sample sizes and high variability in fecundity at length would cause only large differences in fecundity to be detected. However, the sample sizes used for comparison before and during spawning season (shortspine thornyhead $n=11, 41$) (longspine thornyhead $n=17, 11$) were close to the sample sizes Wakefield (1990) used as evidence for batch spawning ($n=11, 22$). Larger sample sizes for both species would help answer the question of whether these are batch-spawning species. Pearson and Gunderson (2003) did not find any hydrated oocytes

or postovulatory follicles co-occurring with vitellogenic oocytes in histological sections of either species used in our study. They concluded that batch spawning does not occur from off Northern California to Alaska for shortspine thornyhead, and from off Northern California to Washington for longspine thornyhead, and the results of the present study support this conclusion.

Ovaries are often opportunistically collected during commercial fishing seasons or scheduled fisheries surveys and may not provide oocyte samples from the optimum time of year for estimating fecundity with gravimetric techniques. Nevertheless, the stereological technique enabled us to make fecundity estimates for a greater number of the available samples. The technique could be used in similar instances where the logistics of sampling require collections to be made earlier than the optimal date for gravimetric estimates.

Acknowledgments

Dave Douglas of the Oregon Department of Fish and Wildlife collected many samples, as did numerous NMFS RACE and REFM division scientists and the following NMFS observers: C. Colway, A. Hayward, W. Mitchell, E. White, N. Spang, K. Redslob, M. Waters, and D. Tran. We thank Frank Morado, Lisa Appesland, and Dan Nichol of the NMFS Alaska Fisheries Science Center (AFSC) for use of equipment and equipment instruction. We also thank Marcus Duke of the UW SAFS for creating a Weibel grid. Jim Ianelli and Rebecca Reuter of the NMFS Alaska Fisheries Science Center provided quantitative assistance. Cathy Schwartz of the UW SAFS assisted with the figures and tables. We thank two anonymous reviewers for providing useful comments. This research was supported by the Joint Institute for the Study of the Atmosphere and Ocean (JISAO) under NOAA cooperative agreement no. NA17RJ1232.

Literature cited

- Best, E. A.
1964. Spawning of longspine channel rockfish, *Sebastolobus altivelis* Gilbert. Calif. Fish Game 50:265-267.
- Emerson L. S., M. G. Walker, and P. R. Witthames.
1990. A stereological method for estimating fish fecundity. J. Fish Biol. 36:721-730.
- Erickson, D. L., and E. K. Pikitch.
1993. A histological description of shortspine thornyhead, *Sebastolobus alascanus*, ovaries: structures associated with the production of gelatinous egg masses. Environ. Biol. Fishes 36:273-282.
- Gaichas, S., and J. N. Ianelli.
2003. Assessment of thornyheads (*Sebastolobus* spp.) in the Gulf of Alaska. In Stock assessment and fishery evaluation report for the groundfish resources of the Gulf of Alaska, p. 659-698. North Pacific Fishery Management Council, Anchorage, AK.
- Hoff, G. R., and L. L. Britt.
2003. The 2002 eastern Bering Sea upper continental slope

- survey of groundfish and invertebrate resources. NOAA Tech. Memo. NMFS-AFSC-141, 261 p.
- Hunter, J. R., B. J. Macewicz, N. C. Lo, and C. A. Kimbrell.
1992. Fecundity, spawning, and maturity of female Dover sole, *Microstomus pacificus*, with an evaluation of assumptions and precision. Fish. Bull. 90:101-128.
- Macer, C. T.
1974. The reproductive biology of the horse mackerel *Trachurus trachurus* (L.) in the North Sea and English Channel. J. Fish Biol. 6:415-438.
- Miller, P. P.
1985. Life history study of the shortspine thornyhead, *Sebastolobus alascanus*, at Cape Ommaney, southeastern Alaska. M.S. thesis, 76 p. Univ. of Alaska, Juneau, AK.
- Orr, J. W., M. A. Brown, and D. C. Baker.
2000. Guide to rockfishes (Scorpaenidae) of the genera *Sebastes*, *Sebastolobus*, and *Adelosebastes* of the Northeast Pacific Ocean, 2nd ed. NOAA Tech. Memo. NMFS-AFSC-117, 48 p.
- Pearcy, W. G.
1962. Egg masses and early developmental stages of the scorpaenid fish, *Sebastolobus*. J. Fish. Res. Board Can. 19:1169-1173.
- Pearson, K. E., and D. R. Gundersen.
2003. Reproductive biology and ecology of shortspine thornyhead rockfish, *Sebastolobus alascanus*, and longspine thornyhead rockfish, *S. altivelis*, from the northeastern Pacific Ocean. Environ. Biol. Fishes 67:11-136.
- Piner, K., and R. Methot.
2001. Stock assessment and fishery evaluation report of shortspine thornyhead off the Pacific West Coast of the United States 2001. In Status of the Pacific coast groundfish fishery through 2001 and acceptable biological catches for 2002. Pacific Fishery Management Council, Portland, OR.
- Quinn, T. J., and R. B. Deriso.
1999. Quantitative fish dynamics, 542 p. Oxford Univ. Press, New York, NY.
- Tuene, S., A. C. Gundersen, W. Emblem, I. Fossen, J. Boje, P. Steingrund, and L. H. Ofstad.
2002. Maturation and occurrence of atresia in oocytes of Greenland halibut (*Reinhardtius hippoglossoides* W.) in the waters of East Greenland, Faroe Islands and Hatton Bank. In Reproduction of West-Nordic Greenland halibut: studies reflecting on maturity, fecundity, spawning, and TEP (A. C. Gundersen, ed.), p. 39-69. TemaNord 2002:519.
- Wakefield, W. W.
1990. Patterns in the distribution of demersal fishes on the upper continental slope off central California with studies on the role of ontogenetic vertical migration in particle flux. Ph.D. diss., 281 p. Univ. California, San Diego, CA.
- Wakefield, W. W., and K. L. Smith Jr.
1990. Ontogenetic vertical migration in *Sebastolobus altivelis* as a mechanism for transport of particulate organic matter at continental slope depths. Limnol. Oceanogr. 35:1314-1328.
- Weibel, E. R., and D. M. Gomez.
1962. A principle for counting tissue structures on random sections. J. Appl. Physiol. 17:343-348.
- Weibel, E. R., G. S. Kistler, and W. Scherle.
1966. Practical stereological methods for morphometric cytology. J. Cell Biol. 30:22-38.

Abstract—Body size at gonadal maturity is described for females of the slipper lobster (*Scyllarides squammosus*) (Scyllaridae) and the endemic Hawaiian spiny lobster (*Panulirus marginatus*) (Palinuridae) based on microscopic examination of histological preparations of ovaries. These data are used to validate several morphological metrics (relative exopodite length, ovigerous condition) of functional sexual maturity. Relative exopodite length ("pleopod length") produced consistent estimates of size at maturity when evaluated with a newly derived statistical application for estimating size at the morphometric maturation point (MMP) for the population, identified as the midpoint of a sigmoid function spanning the estimated boundaries of overlap between the largest immature and smallest adult animals. Estimates of the MMP were related to matched (same-year) characterizations of sexual maturity based on ovigerous condition—a more conventional measure of functional maturity previously used to characterize maturity for the two lobster species. Both measures of functional maturity were similar for the respective species and were within 5% and 2% of one another for slipper and spiny lobster, respectively. The precision observed for two shipboard collection series of pleopod-length data indicated that the method is reliable and not dependent on specialized expertise. Precision of maturity estimates for *S. squammosus* with the pleopod-length metric was similar to that for *P. marginatus* with any of the other measures (including conventional evidence of ovigerous condition) and greatly exceeded the precision of estimates for *S. squammosus* based on ovigerous condition alone. The two measures of functional maturity averaged within 8% of the estimated size at gonadal maturity for the respective species. Appendage-to-body size proportions, such as the pleopod length metric, hold great promise, particularly for species of slipper lobsters like *S. squammosus* for which there exist no other reliable conventional morphological measures of sexual maturity. Morphometric proportions also should be included among the factors evaluated when assessing size at sexual maturity in spiny lobster stocks; previously, these proportions have been obtained routinely only for brachyuran crabs within the Crustacea.

Manuscript submitted 2 September 2003 to the Scientific Editor's Office.

Manuscript approved for publication 26 August 2004 by the Scientific Editor.

Fish. Bull. 103:23–33 (2005).

Relative pleopod length as an indicator of size at sexual maturity in slipper (*Scyllarides squammosus*) and spiny Hawaiian (*Panulirus marginatus*) lobsters

Edward E. DeMartini

Marti L. McCracken

Robert B. Moffitt

Jerry A. Wetherall

Pacific Islands Fisheries Science Center
National Marine Fisheries Service, NOAA

2570 Dole Street
Honolulu, Hawaii 96822-2396

E-mail address (for E. E. DeMartini) edward.demartini@noaa.gov

Estimates of body size and age at sexual maturity provide key information for stock assessments and hence for managing sustainable fisheries. Characterizations of size at maturity are relatively straightforward in lobsters and most other crustaceans. One presently accepted standard is to regress percentage mature against classes of some body size metric and to fit a logistic model to predict the size class in which 50% of the population is mature. A necessary prerequisite is accurate data on the maturation state of individuals. In spiny lobsters of the family Palinuridae, female maturation is usually deduced from "berried" (ovigerous) condition (Groeneveld and Melville-Smith, 1994), the presence of external morphological indicators such as changes in the number of pleopod setae (Gregory and Labisky, 1981; Montgomery, 1992), relative lengths of abdominal and thoracic segments (Jayakody, 1989), or proportional lengths of segments of walking or egg-bearing appendages at the pubertal molt (George and Morgan, 1979; Grey, 1979; Junio, 1987; Plaut, 1993; Evans et al., 1995; Hogarth and Barratt, 1996; Minagawa and Higuchi, 1997). A major complication arises, however, when the percentage mature within size classes cannot be accurately described. Such is the case for *Scyllarides squammosus*, a species of slipper lobster (family Scyllaridae) that prior to closure of the fishery in 2000

had become an increasingly important target of the Northwestern Hawaiian Island (NWHI) commercial trap fishery. In *S. squammosus*, unberried but mature females are indistinguishable, based on gross external morphology, from immature females. In this species, the additional variance introduced by combining falsely classified "immature" with truly immature females inflates requisite sample sizes enough (given the sampling effort feasible on annual research surveys) to prevent characterization of possible changes in size at maturity with data pooled from less than several surveys. Combining unberried adults with true immature individuals also introduces an overestimation bias (DeMartini et al., 2003).

To date only one study has provided a description of the use of a morphological measure of maturity in a slipper lobster (Hossain, 1978). Morphology-based maturity measures have been described for numerous spiny lobsters of the genus *Panulirus*, but such measures for the endemic Hawaiian spiny lobster (*Panulirus marginatus*) have not been fully described (Prescott, 1984).

Our objectives are to describe the development and use of an external body metric for accurately and precisely characterizing body size at morphological (functional) sexual maturity in female *Scyllarides squammosus*. We likewise use this external metric

to estimate size at maturity of females of the Hawaiian spiny lobster, for which functional maturity can be accurately described by using a combination of other, more apparent external features. We also estimate body size at gonadal maturity by microscopic examination of histological preparations of ovaries of each species and use these results to validate the functional maturity characterizations. We contrast the benefits of the different approaches for estimating functional maturity in these two lobsters and discuss the potential importance of applying efficient measures of maturation for managing the NWHI lobster fishery.

Materials and methods

Specimen collection

A research vessel was used to set and retrieve lobster traps. All specimens of spiny lobster used in this study were taken from Necker Bank surrounding Necker Island (23°34'N, 164°42'W), NWHI. All the slipper lobsters used were taken from Maro Bank, located about 600 km to the northwest of Necker at 25°25'N, 170°35'W. Lobsters were caught from bank terraces at median depths of 15 fm (slipper lobsters, Maro) and 17 fm (spiny lobsters, Necker) with molded plastic (Fathoms Plus[®], San Diego, CA) traps baited with 1 kg of mackerel (*Scomber japonicus*) and left for a standard (overnight) soak.

Shipboard processing

All specimens were processed alive within minutes of trap retrieval. Tail width (TW), as defined for slipper lobster by DeMartini and Williams (2001) and for Hawaiian spiny lobster by DeMartini et al. (2003), was measured with 0.1 mm accuracy. Berried females were scored by egg-development stage with a gross visual proxy (brooded eggs noted as either orange or brown in color to the unaided eye). Female spiny lobsters were scored by the presence or absence and by condition ("smooth"=unused, "rough"=partly used) of spermatophoric (sperm) mass (Matthews, 1951; Berry and Heydorn, 1970) on the sternum. Female *S. squammosus* in almost all cases lack a sperm mass and the presence-absence of this feature provides no useful information. In 1998–2000, ovaries were dissected from a maximum of two living specimens for each 1-mm TW class of the two species and fixed in 10% (sea water buffered) formalin for subsequent histological analyses. Egg-bearing "tails" (abdominal segments) were flash-frozen at -20 C.

During 1997–99, pleopods of each species were measured aboard ship to evaluate measurement accuracy under field conditions. Maxima of 10 live individuals per 1-mm TW class of each species were measured as described below. Two independent measurements of each specimen were made by each of two measurers (one inexperienced and one experienced). In 2000–01, pleopods for a larger series of morphometrics were simi-

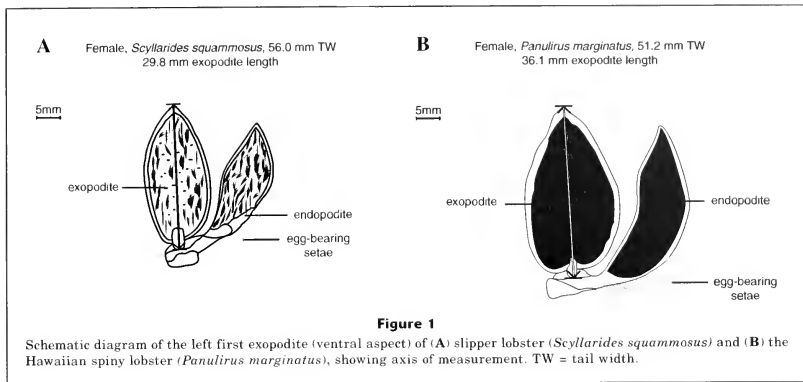
larly measured aboard ship to evaluate production-scale numbers (500–1000 specimens per species on each cruise) based on a single measurement per specimen taken by one measurer.

Laboratory measurements

Beginning with specimens collected in 2000, the lengths of exopodites on first pleopods were measured for a representative sample of berried and unberried tails of each species, after the tails were thawed overnight in a refrigerator at 3 C. Preliminary observations indicated that the first pleopod was disproportionately large in berried females; measurements of the first pleopod of all (berried and unberried) females moreover were the most precise, i.e. the measurements were more likely to be obtained again—probably because the first pleopod was the easiest to measure. The straightline distance between base and tip of exopodite on the first pleopod (exopodite length=EL) was measured with dial calipers to 0.01 mm. An analogous measurement of exopodite width (EW) was taken perpendicular to the EL axis at the structure's widest point. The left exopodite in ventral aspect (Fig. 1) was routinely measured because the ventral aspect was easier to measure for live animals aboard ship. Measurements of the right exopodite (of the same specimen) in dorsal aspect were taken for a range of body sizes to evaluate the possible influence of aspect (dorsal vs. ventral) or body side (left vs. right) on the measurement that was taken. Replicate measurements (independent, with calipers reset to zero between measurements) were used to assess inter-measurer and inherent measurement error. Formalized ovaries were weighed (blotted damp-dry) to the nearest 0.01 g after fixation for at least a month.

Histological validation

Fixed ovary specimens of each species were dehydrated, imbedded, and sectioned by using standard techniques, and were stained with hematoxylin and counter-stained with eosin to differentiate protein and yolk materials within oocytes. Histological slides were viewed under a compound microscope at 150 \times magnification. For each specimen, the diameters (average of major and minor axis) were measured for 10 oocytes (randomly chosen) within the largest size class of oocytes present. The median diameter was used to characterize oocyte size for that specimen; the median diameter based on 10 measurements yielded CVs (100% \times standard error/mean) <10% (DeMartini et al., 2003). Developmental staging followed Minagawa (1997) and Minagawa and Sano (1997): females were scored as mature 1) if unberried in developing or ripe ovarian stages II and III, respectively; 2) if berried in ripe and redeveloping stages IV and V, respectively; or 3) if recently spent (stage VI) with heavily setose pleopods (*P. marginatus* only). Inactive females in stage I were scored as immature. A gonad index, calculated as $GI = (OW \times 10^5 / TW^3)$, where OW = ovary weight in g, was used to complement his-

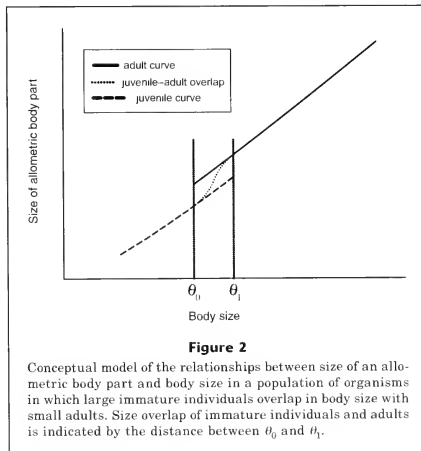


tological scores in assessing gonadal maturity (Minagawa and Sano, 1997). Gonadal maturity was used as a means of validating, as well as referencing, estimates of size at functional maturity (Ennis, 1984).

Statistical analyses

Data for EL and EW (as response variables) and TW (regressor) for the same specimen were first plotted for all specimens of each species. Preliminary evaluations of these data (both raw and log-transformed) with least-squares linear regression (REG procedure; SAS vers. 8, SAS Institute, Inc., Cary, NC) indicated allometric relationships for which double-log functions provided approximate fits. Identification of join points by iteration based on minimizing the total residual sums of squares of pairs of joined regression equations (Somerton, 1980), however, resulted in linear spline fits that, although significant, had obviously nonrandom residuals. Simple linear fits with log-log plots, however, were useful for selecting the most appropriate metric: the regressions of EW on TW, qualitatively similar to those for EL regressed on TW, had consistently lower r^2 values, likely because pleopod width was more difficult to measure than pleopod length. The EL metric was therefore chosen for all further analyses.

Because lobsters, like most biological populations, are composed of individuals that differ in the size at which first maturity occurs, we fitted a curve to the EL-TW relation that included a sigmoid segment bridging the region between the estimated sizes of the smallest adults (θ_0) and the largest immature individuals (θ_1) (Fig. 2). The curve was fitted by using iterative reweighted least



squares (S-Plus 6 for Windows, Insightful Corporation, Seattle, WA; Ratkowsky, 1983) with appropriate weights to standardize the variance (Appendix). The morphometric maturation point, hereafter referred to as the MMP, was estimated at the inflection ($(\theta_0 + \theta_1)/2$) of the sigmoid segment of the curve. This inflexion point represents the body size at which we expect 50% of the lobsters to become sexually mature (median size at attainment of

maturity). Confidence bounds on the MMP were estimated by using the studentized bootstrap method (Davison and Hinkley, 1997) with 1000 iterations.

In order to characterize median body size at gonadal maturity, the percentage mature per 5-mm TW class, deduced from viewing histological preparations of ovaries, was fitted to the conventional (2-parameter) logistic model,

$$P_x = 100 / \{1 + \exp[-a(TW - b)]\},$$

where P_x = percent mature at TW = x ;
 a and b are unknown constants; and
 TW = tail width in mm.

To similarly estimate median size at maturity based on gross external characteristics, the percentage mature per 5-mm TW class was fitted to a 3-parameter logistic model for *Scyllarides squammosus* and to the conventional 2-parameter logistic for *Panulirus marginatus*. For *S. squammosus*, percentage maturity per 5-mm TW class was estimated by fitting the 3-parameter logistic equation,

$$P_x = 100a / \{1 + \exp[(4b/a)(c - TW)]\},$$

where a = the asymptotic proportion berried;
 b = the slope of the logistic function at the inflection point; and
 $c = TW_{50}$ is the tail width at the inflection point (size at 50% of asymptote).

This function has been fully described for estimating percentage maturity based on incidence of ovigerous females in *S. squammosus*; the extra parameter is needed to fit an asymptote to the sigmoidal function at a value less than 100% (DeMartini et al., 2002). Parameters of the various models were estimated by using the maximum-likelihood nonlinear curve fitting procedure SAS NLIN; all nonlinear regressions were weighted by the square root of sample sizes.

The body size at which 50% of the population was estimated as mature (hereafter referred to as TW_{50}) was compared for 1) TW_{50} based on the relative incidence of berried individuals within the female population (both species), adjusted for the co-presence of a sperm mass (*P. marginatus* only), 2) TW_{50} estimated from histological evidence (both species), and 3) the MMP of the allometric EL-to-TW relation (both species). Estimates were compared graphically among methods for each species.

Analyses of pleopod-based maturity followed a series of evaluations of pleopod characteristics used to identify a standardized metric. Measurement aspect (dorsal, ventral) and side (right, left) were compared within individuals by using paired t -tests. A randomized complete block (RCB) ANOVA (SAS PROC ANOVA), with specimen as the blocking factor, was used to evaluate the effects of measurer and measurement venue (at sea versus ashore) on the mean measurement bias and precision (CVs) of pleopod measurements.

Results

Pleopod characteristics

Measurement error, and effect of side of lobster and aspect (ventral versus dorsal) on measurements Inherent measurement error averaged 0.23 mm and 0.16 mm (1.0% and 0.4%) for slipper and Hawaiian spiny lobster, respectively, based on two independent measurements by the same measurer. Exopodites of left-side pleopods averaged 3% and 2% shorter than exopodites of right-side pleopods for the two respective species (paired t -test; both $P < 0.001$; Table 1). Exopodites of first left pleopods were 4% and 2% longer in ventral aspect for slipper and spiny lobster, respectively, (RCB ANOVA; both $P < 0.001$; Table 1).

Measurement venue A matched (same-specimen) series of measurements made aboard ship versus in the laboratory (all by the same measurer) indicated a systematic difference in left pleopod length (ship > lab; RCB ANOVA; both $P = 0.001$) for slipper lobster and spiny lobster (Table 1). For each species, however, the mean difference between venues was trivial (0.2–0.4 mm or 0.6–1.4%). Differences between ship and laboratory were detectable despite the consistently lower precision provided by shipboard measurements (shipboard CVs were 47% and 39% larger for slipper and spiny lobster, respectively; RCB ANOVA: both $P < 0.001$; Table 1). Absolute differences between shipboard and lab CVs were small for the respective species (0.2% and 0.7%; Table 1).

Measurer effects An extensive series of shipboard inter-measurer comparisons between pleopod length measurements taken by one experienced (A) and a second inexperienced (B) measurer indicated trivial systematic differences between measurers (0.2%; RCB ANOVA; $P = 0.25$). Precision also was unaffected by measurer ($P = 0.31$; Table 1).

Standardized metric It follows from the above that the best measure available for use was the length (in ventral aspect) of the left first exopodite. This metric was used in all quantitative comparisons among maturity assessment methods and is recommended for future applications with these species.

Estimated sizes at functional maturity

Slipper lobster Pleopod-to-TW relations for *S. squammosus* did not differ meaningfully between 2000 and 2001 (ANCOVA; accept H_0 : slopes equal, $P = 0.11$; intercepts only 0.5% different) and both years' data were pooled for further analyses. The estimated MMP (95% CI) for the TW at which 50% of the female *S. squammosus* exhibit a disproportionately long first left exopodite was 47.6 mm (45.1–49.4 mm; Fig. 3). Estimated median body size at functional maturity based on presence or absence of berried eggs, using the same series of 2000–01 specimens, was 55.5 (52.7–58.3) mm TW (Fig. 4).

Table 1

Results of tests of potential effects of various criterion variables on the accuracy (bias of delta-bars) and precision (CVs of deltas) for measured lengths of first pleopod exopodites for slipper lobster (*Scyllarides squammosus*) and Hawaiian spiny lobster (*Panulirus marginatus*) caught from Necker Bank, Hawaii. Delta-bar = mean paired-difference; samples sizes are *n* paired observations.

Variable	Criterion	Test statistic	Delta-bar	<i>P</i>	<i>n</i>
Slipper lobster					
Body side (left vs. right)	accuracy	paired <i>t</i> = -4.0	0.9 mm	0.001	74
Measurement aspect (ventral vs. dorsal)	accuracy	RCB Anova <i>F</i> _{1,62} = 202.7	0.9 mm	0.001	63
Measurement venue (shipboard vs. lab)	accuracy	RCB Anova <i>F</i> _{1,62} = 23.6	0.4 mm	0.001	63
Measurement venue (shipboard vs. lab)	precision	RCB Anova <i>F</i> _{1,62} = 21.6	0.7 %	0.001	63
Measurer (A vs. B)	accuracy	RCB Anova <i>F</i> _{1,62} = 21.3	0.3 mm	0.001	63
Measurer (A vs. B)	precision	RCB Anova <i>F</i> _{1,62} = 1.54	0.2 %	0.22	63
Spiny lobster					
Body side (left vs. right)	accuracy	paired <i>t</i> = -5.7	0.7 mm	0.001	135
Measurement aspect (ventral vs. dorsal)	accuracy	RCB Anova <i>F</i> _{1,32} = 31.7	0.7 mm	0.001	33
Measurement venue (shipboard vs. lab)	accuracy	RCB Anova <i>F</i> _{1,87} = 11.62	0.2 mm	0.001	88
Measurement venue (shipboard vs. lab)	precision	RCB Anova <i>F</i> _{1,87} = 11.74	0.4 %	0.001	88
Measurer (A vs. B)	accuracy	RCB Anova <i>F</i> _{1,87} = 1.37	<0.1 mm	0.25	88
Measurer (A vs. B)	precision	RCB Anova <i>F</i> _{1,87} = 1.04	<0.2 %	0.31	88

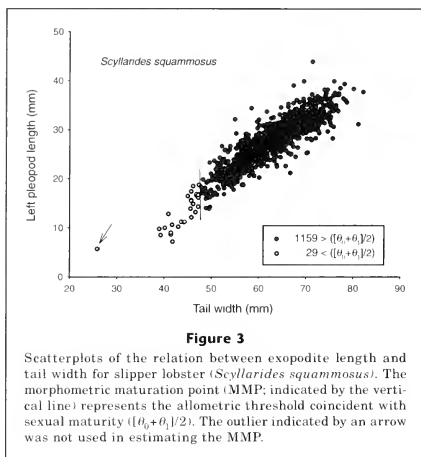
Spiny lobster Year effects on pleopod-to-TW relations for *P. marginatus* were likewise insignificant (ANCOVA, accept H_0 ; slopes equal, $P > 0.67$; intercepts only 0.2% different) and data for both years were pooled for further analyses. The MMP for the TW at which 50% of the *P. marginatus* females exhibit a disproportionately long pleopod was 36.4 mm (34.1–38.0 mm; Fig. 5). Figure 6 illustrates the corresponding estimate of median size at functional maturity, 35.4 (33.7–37.1) mm TW, based on the combined criteria of sperm mass and berried egg presence, for *P. marginatus*.

Estimated sizes at physiological maturity

Gonadal maturity determined from microscopic staging of histological ovary preparations indicated maturation stages ranging from oögonial to fully vitellogenic (Table 2; Minagawa and Sano, 1997) for the females of each species. For both species, gonad indices (GIs) and

median oocyte diameters generally increased over the cycle of development even though berried specimens exhibited lower GIs and oocyte sizes than unberried adults of the respective species (Table 2). The ovaries of mature females contained a preponderance of fully yolkeo oocytes whose average minimum diameter (following dehydration and staining) was 0.24 mm and 0.30 mm for *S. squammosus* and *P. marginatus*, respectively. The maximum observed diameter of fully yolkeo oocytes was 0.60 mm (in *S. squammosus*) and 0.58 mm (*P. marginatus*).

The proportions of observed immature individuals ranged from 32% to 38% of total female specimens (depending on species) and were sufficient to construct logistic curves relating percentage gonadal maturity to body size for each species. Estimated median TWs at gonadal maturity were 51.1 (48.6–53.5) mm and 40.5 (37.9–43.1) mm TW for *S. squammosus* (Fig. 4) and *P. marginatus* (Fig. 6), respectively.

**Table 2**

Stages of ovarian development in 197 slipper lobster (*Scyllarides squammosus*) and 122 Hawaiian spiny lobster (*Panulirus marginatus*) caught from Necker Bank, Hawaii. There were no stage-VI *S. squammosus*.

Ovarian stage	Characteristics of ovaries and oocytes	Gonad index mean \pm SD (range)	n	Most advanced oocyte substage (median diameter)
Slipper lobster				
I (inactive)	oogonia and previtellogenic oocytes conspicuous; ovary white	0.43 \pm 0.25 (0.02–1.08)	60	preyolk platelet (0.18 mm)
II–III (developing and ripe)	unberried; developing moderately to fully vitellogenic oocytes; ovary pale orange to orange	1.63 \pm 1.45 (0.25–5.47)	75	prematuration or maturation (0.28 mm)
IV–V (ripe and redeveloping)	berried; developed fully yolked oocytes; ovary dark orange	1.12 \pm 0.66 (0.15–3.30)	62	maturation (0.26 mm)
Spiny lobster				
I (inactive)	oogonia and previtellogenic oocytes; ovary white	0.85 \pm 0.67 (0.16–2.59)	30	preyolk platelet (0.12)
II–III (developing and ripe)	unberried; developing moderately to fully vitellogenic oocytes; ovary pale orange to orange	14.03 \pm 4.46 (3.32–22.69)	42	prematuration or maturation (0.49)
IV–V (ripe and redeveloping)	berried; developed fully yolked oocytes; ovary dark orange	5.84 \pm 4.31 (0.56–17.06)	47	maturation (0.30)
VI (spent)	residual unspawned mature oocytes; ovulation traces	14.85 \pm 6.38 (7.5–18.9)	3	yolk platelet but atretic (0.48)

Discussion

Properties of the EL-TW model

In order to determine morphometric maturity, we first attempted to use a method developed by Watters and Hobday (1998). With this method splines were used to model the relationship between the morphometric character and body size; then the morphometric size at which the second derivative of the fitted curve is maximal is computed. At first this technique is alluring in that it makes no allometric or other assumption as to the shape of the relationship between the morphometric character and body size. It instead assumes that maturation corresponds to the maximum of the second derivative. This assumption is likely invalid even if we assume that the relationship between the morphometric character and body size changes abruptly at maturation for each individual (as at the pubertal molt in crustaceans) because individuals in the population mature at different sizes. When we applied the Watters and Hobday method, the resulting body size estimate appeared to characterize the minimum, not the median, size at attainment of sexual maturity in the population and was clearly inappropriate for our needs. Our method generated fitted splines that were comfortably similar in shape to the parametric logistic (sigmoidal function) models that we used to estimate maturation with berried and histological criteria.

The magnitude of the difference between the sizes at maturity estimated by our and the Watters and Hobday (1998) model should vary in proportion to the magnitude of the difference between the minimum (θ_0) and median ($[(\theta_0 + \theta_1)/2]$) body sizes at maturity and therefore be case-dependent. In our slipper lobster case, the θ_0 and θ_1 estimates differed by about 6.6 mm; hence, the two model estimates differed by about $6.6/2 = 3.3$ mm or approximately 7% of the $[(\theta_0 + \theta_1)/2]$ median. Because other cases certainly include those in which immature and adult sizes overlap even more greatly, we suggest that our more general and accurate model be adopted.

Functional versus physiological measures of maturity

Morphological features can provide adequate if imperfect measures of functional sexual maturity, as can physiological evidence for gonadal maturity (Ennis, 1984). Morphological features such as ovigerous condition can underestimate the incidence of mature individuals, but the degree to which they do so depends on numerous factors including species and population. Physiological metrics in some cases can provide more accurate estimators of both body size and age at maturity because they reveal the reproductive readiness of individuals at the time of collection. Individual body size and age at maturity can be decoupled from functional maturity metrics in Crustacea, however. For example, some crustaceans like majid crabs exhibit determinate growth following a terminal, pubertal molt (Hartnoll, 1982). For such species, size at attainment of sexual maturity is synonymous

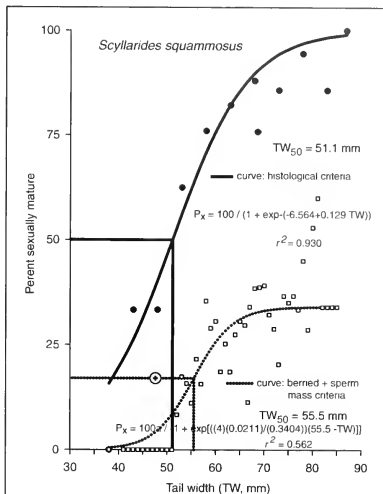
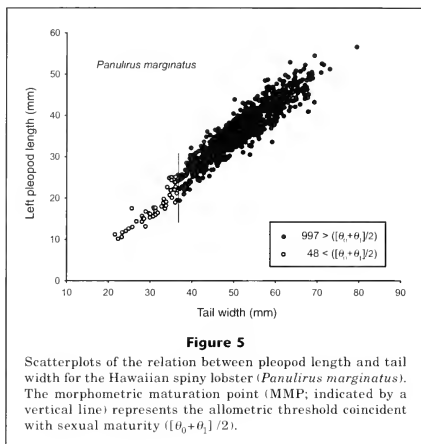


Figure 4

Scatterplots and fitted curves of the relations between body size (tail width, TW) and percent sexual maturity based on functional maturity gauged by presence-absence of berried condition (dotted curve), overlaid on gonadal maturation gauged by microscopic examination of ovaries (dark-line curve); the pleopod length-based morphometric maturation point (MPP) estimate of size at functional maturity is indicated by the large circle with cross-hairs (⊕), for slipper lobster (*Scyllarides squammosus*). A 3-parameter logistic equation was necessary to fit the dotted curve; a 2-parameter logistic was sufficient to fit the dark-line curve (see text).

with the median body size of adults. These two attributes are not synonymous for lobsters with indeterminate growth. It is further obvious that the pleopods and other allometric body parts of Crustacea like lobsters reflect an array of gonadal maturities ranging from developing immature to fully mature, which can be problematic because some or many females might abort and resorb developing gonadal eggs after the pubertal molt (Aiken and Waddy, 1980) or may not become inseminated (Heydorn, 1969). By attributing maturity to specimens that either have not matured physiologically or that will not reproduce although capable of doing so, appendage-to-body proportions can underestimate the age at maturity in Crustacea. The degree of underestimation should be proportional to the incidence of gonadal resorption during the intermolt period following the pubertal molt,

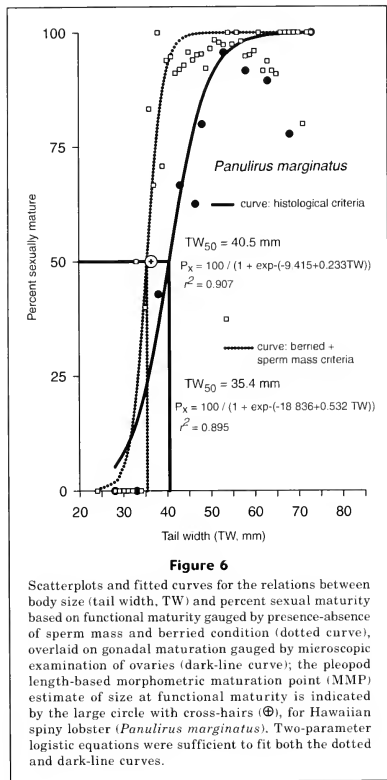


as well as the duration of the intermolt. These specific topics deserve future study.

The above caveats notwithstanding, it is helpful to compare estimates of body sizes at sexual maturity based on various morphological and physiological evidence and to ascertain the degree of agreement among the estimates (Fernandez-Vergaz et al., 2000). The estimate of MMP (47.6 mm) indicated by the pleopod length-to-TW relation for *S. squammosus*, for example, was about 16% smaller than the median size at maturity (55.5 \pm 1.35 SE) mm) estimated by using simple presence-absence of berried eggs for the same series of specimens. The latter estimate, however, is imprecise and an overestimate. The long-term mean TW at 50% maturity based on berried condition for the period from 1986 to 2001, indistinguishable among component years, was 50.0 \pm 0.83 mm, more precise than the single-year estimate although still biased high (DeMartini et al., 2002). If this 50.0 value is used for reference, the pleopod length-based estimate of the MMP falls within <5% of the long-term mean. For *P. marginatus*, the analogous MMP = 36.4 mm value was within 3% of the estimated median size at maturity (35.4 mm) based on the combined criteria of berried eggs and sperm mass presence. All the various estimates of functional maturity for the two species were within 2.0–12.6% (mean=7.9%) of the best respective estimate of gonadal maturity. These close similarities, despite the inherent biases of the two methods, indicate that maturity metrics such as relative pleopod length can provide highly satisfactory proxies of true functional maturity that are closely related to gonadal maturity in certain cases.

Pleopod length as a maturity metric

In some Crustacea (once again, not lobsters, as far as is known), allometries are not fixed at the pubertal molt; and, in a minority of these, allometric growth is seasonally cyclic and allometries disappear when mature instars molt during nonreproductive periods (Hartnoll, 1974, 1982). And body proportions may not be strong predictors of sexual maturity for clawed lobsters (Comeau and Savoie, 2002). In many, if not most, decapods such as spiny lobsters (e.g., George and Morgan, 1979; Groeneveld and Melville-Smith, 1994), however, relative appendage-to-body sizes, as well as obvious morphological criteria such as the presence of berried eggs and a sperm mass, indicate functional sexual maturity. Body part allometries in some cases can be better predictors of maturity than more obvious characters like berried eggs. An incomplete measure such as percentage berried, exemplified by the slipper lobster (*S. squammosus*) in the present study, can falsely fail to detect reproductively inactive adult females. Appendage-to-body size proportions thus have one major advantage over other morphometrics in that they permit reproductively inactive adult females to be correctly classified as mature. This advantage is relatively unimportant in other species like *P. marginatus* for which additional gross morphological indicators such as the presence-absence of a sperm mass complement the information provided by berried condition. Even so, proportional appendage lengths can be used in such cases as another fairly inexpensive and independent measure that could contribute to a multivariate assessment of maturity,



unconstrained by a conspicuous but perhaps inaccurate feature like berried condition.

Management implications

Estimates of body size at sexual maturity can provide key information to various stock assessment models, but only if the estimates are accurate and sufficiently precise. For the slipper lobster (*S. squammosus*), DeMartini et al. (2002) have shown that estimates made by using percent berried as the lone maturity criterion, the only morphological metric previously available, are both inaccurate and imprecise. The inability to distinguish

truly immature from mature, but reproductively inactive, females generates an inflated "immature" class, and the estimates of median size at sexual maturity thus obtained with logistic equation fits are biased high. Variances of median-size estimates based on sample sizes available on single research surveys are often so large that 3-parameter logistic applications (necessary to scale maturity to 100%) fail to converge, and reliable individual-year estimates are impossible (DeMartini et al., 2002). Unfortunately, the temporal dynamics of targeting species by fishermen in the NWHI trap fishery and the rapid phenotypic responses in fecundity and maturation size to harvesting, fluctuating natural productivity, and changing population densities that have been observed in *P. marginatus* (DeMartini et al., 2003), require that size at maturity be re-estimated at short (one-to-several-year) intervals for this species at least and possibly for *S. squammosus* as well.

The accurate and precise estimates of median body size at sexual maturity made possible by using the pleopod length metric enable such yearly re-evaluations for *S. squammosus* and provide a second reliable and independent estimator for *P. marginatus*. Our successful applications for a scyllarid as well as a palinurid, together with prior observations for numerous other spiny lobster species, indicate that easily measured appendage length-to-body size relations are generally suitable for assessing functional sexual maturity in lobsters and other decapods. We recommend that these relations be explored for other commercially exploited crustacean stocks and wherever possible routinely applied to provide cost-effective and timely information on size at maturity for stock assessments. Managers responsible for the assessment of lobster and other crustacean stocks will then have a more complete toolbox of methods generally available for assessing the size at maturity and harvestability of stocks, particularly for species like *S. squammosus* in which conventional morphological measures are inadequate.

Acknowledgments

We thank D. Yamaguchi for assistance with Figure 1 and G. DiNardo and J. Polovina for constructive criticisms of the manuscript.

Literature cited

- Aiken, D. E., and S. L. Waddy.
1980. Reproductive biology. In *The biology and management of lobsters, vol. I, physiology and behavior* (J. S. Cobb and B. F. Phillips, eds.), p. 215–276. Academic Press, New York, NY.
- Berry, P. F., and A. E. F. Heydorn.
1970. A comparison of the spermatophoric masses and mechanisms of fertilization in Southern African spiny lobsters (Palinuridae). *S. Afr. Assoc. Mar. Biol. Res., Oceanogr. Res. Inst. Invest. Rep.* 25, 18 p.

- Comeau, M., and F. Savoie.
2002. Maturity and reproductive cycle of the female American lobster, *Homarus americanus*, in the southern Gulf of St. Lawrence, Canada. *J. Crust. Biol.* 22:762-774.
- Davison, A. C., and D. V. Hinkley.
1997. Bootstrap methods and their application, 582 p. Cambridge University Press, New York, NY.
- DeMartini, E. E., G. T. DiNardo, and H. A. Williams.
2003. Temporal changes in population density, fecundity and egg size of the Hawaiian spiny lobster, *Panulirus marginatus*, at Necker Bank, Northwestern Hawaiian Islands. *Fish. Bull.* 101:22-31.
- DeMartini, E. E., P. Kleiber, and G. T. DiNardo.
2002. Comprehensive (1986-2001) characterization of size at sexual maturity for Hawaiian spiny lobster (*Panulirus marginatus*) and slipper lobster (*Scyllarides squammosus*) in the Northwestern Hawaiian Islands. NOAA Tech Memo NMFS-SWFSC-344, 12 p.
- DeMartini, E. E., and H. A. Williams.
2001. Fecundity and egg size of *Scyllarides squammosus* (Decapoda: Scyllaridae) at Maro Reef, Northwestern Hawaiian Islands. *J. Crust. Biol.* 21:891-896.
- Ennis, G. P.
1984. Comparison of physiological and functional size-at-maturity relationships in two Newfoundland populations of lobsters *Homarus americanus*. *Fish. Bull.* 82:244-249.
- Evans, C. R., A. P. M. Lockwood, A. J. Evans, and E. Free.
1995. Field studies of the reproductive biology of the spiny lobster *Panulirus argus* (Latreille) and *P. guttatus* (Latreille) at Bermuda. *J. Shellfish Res.* 14:371-381.
- Fernandez-Vergaz, V., L. J. Lopez Abellan, and E. Balguerias.
2000. Morphometric, functional and sexual maturity of the deep-sea red crab *Chaceon affinis* inhabiting Canary Island waters: chronology of maturation. *Mar. Ecol. Prog. Ser.* 204:169-178.
- George, R. W., and G. R. Morgan.
1979. Linear growth stages in the rock lobster (*Panulirus versicolor*) as a method for determining size at first physical maturity. *Rap. P.-V. Reun. Cons. Int. Explor. Mer* 175:182-185.
- Gregory, D. R. Jr., and R. F. Labisky.
1981. Ovigerous setae as an indicator of reproductive maturity in the spiny lobster, *Panulirus argus* (Latreille). *Northeast Gulf Sci.* 4:109-113.
- Grey, K. A.
1979. Estimates of the size at first maturity of the western rock lobster, *Panulirus cygnus*, using secondary sexual characteristics. *Aust. J. Mar. Freshw. Res.* 30:785-791.
- Groeneveld, J. C., and R. Melville-Smith.
1994. Size at onset of sexual maturity in the south coast rock lobster, *Panulirus gilchristi* (Decapoda: Palinuridae). *S. Afr. J. Mar. Sci.* 14:219-233.
- Hartnoll, R. G.
1974. Variation in growth pattern between some secondary sexual characters in crabs (Decapoda: Brachyura). *Crustaceana* 27:131-136.
1982. Growth. In *The Biology of Crustacea*, vol. I, embryology, morphology, and genetics (D. E. Bliss, ed.), p. 111-196. Academic Press, London.
- Heydorn, A. E. F.
1969. The rock lobster of the South African west coast *Jasus lalandii* (H. Milne-Edwards). 2. Population studies, behavior, reproduction, moulting, growth and migration. *S. Afr. Div. Sea Fish. Invest. Rep.* 7:1-52.
- Hogarth, P. J., and L. A. Barratt.
1996. Size distribution, maturity and fecundity of the spiny lobster *Panulirus penicillatus* (Oliver 1791) in the Red Sea. *Trop. Zool.* 9:399-408.
- Hossain, M. A.
1978. Appearance and development of sexual characters of sand lobster *Thenus orientalis* (Lund) (Decapoda: Scyllaridae) from the Bay of Bengal. *Bangladesh. J. Zool.* 6:31-42.
- Jayakody, D. S.
1989. Size at onset of sexual maturity and onset of spawning in female *Panulirus homarus* (Crustacea: Decapoda: Palinuridae) in Sri Lanka. *Mar. Ecol. Prog. Ser.* 57:83-87.
- Junio, M. A. R.
1987. Some aspects of the reproduction of *Panulirus penicillatus* (Decapoda: Palinuridae). *Bull. Mar. Sci.* 41:242-252.
- Mathews, D. C.
1951. The origin, development, and nature of the spermatophoric mass of the spiny lobster, *Panulirus penicillatus* (Oliver). *Pac. Sci.* 5:359-371.
- Minagawa, M.
1997. Reproductive cycle and size-dependent spawning of female spiny lobsters (*Panulirus japonicus*) off Oshima Island, Tokyo, Japan. *Mar. Freshw. Res.* 48:869-874.
- Minagawa, M., and S. Higuchi.
1997. Analysis of size, gonadal maturation, and functional maturity in the spiny lobster *Panulirus japonicus* (Decapoda: Palinuridae). *J. Crust. Biol.* 17:70-80.
- Minagawa, M., and M. Sano.
1997. Oogenesis and ovarian development cycle of the spiny lobster *Panulirus japonicus* (Decapoda: Palinuridae). *Mar. Freshw. Res.* 48:875-887.
- Montgomery, S. S.
1992. Sizes at first maturity and at onset of breeding in female *Jasus verreauxi* (Decapoda: Palinuridae) from New South Wales waters, Australia. *Aust. J. Mar. Freshw. Res.* 43:1373-1379.
- Plant, I.
1993. Sexual maturity, reproductive season and fecundity of the spiny lobster *Panulirus penicillatus* from the Gulf of Eilat (Aqaba), Red Sea. *Aust. J. Mar. Freshw. Res.* 44:527-535.
- Prescott, J. H.
1984. Determination of size at maturity in the Hawaiian spiny lobster *Panulirus marginatus*, from changes in relative growth. *Proc. Res. Inv. NWHI-SEEA GRANT-MR-84-01*, p. 345. Univ. Hawaii, Honolulu, HI.
- Ratkowsky, D. A.
1983. Nonlinear regression modeling: a unified practical approach, 276 p. Marcel Dekker, New York, NY.
- Somerton, D. A.
1980. A computer technique for estimating the size of sexual maturity in crabs. *Can. J. Fish. Aquat. Sci.* 37:1488-1494.
- Watters, G., and A. J. Hobday.
1998. A new method for estimating the morphometric size at maturity of crabs. *Can. J. Fish. Aquat. Sci.* 55:704-714.

Appendix

Method for estimation of maturation with pleopod metrics

To model the allometry we used the power function $Y = \alpha X^\beta$ and assumed multiplicative error. The logarithmic transformation of this function leads to a linear regression model. Specifically, we defined $\ln(Y) = f_1(X) + \varepsilon_1$, where $f_1(X) = \alpha_1 + \beta_1 \ln(X)$ and $\alpha_1 = \ln(\delta_1)$, as the allometric relationship for juvenile lobsters and $\ln(Y) = f_2(X) + \varepsilon_2$, where $f_2(X) = \alpha_2 + \beta_2 \ln(X)$ and $\alpha_2 = \ln(\delta_2)$, as the allometric relationship for adult lobsters. The errors, ε_1 and ε_2 , were assumed to be independent and normally distributed with mean 0 and variance σ_1^2 and σ_2^2 , respectively. We assumed that maturation occurred over a range of tail widths. Dividing the domain of x into four intervals, we defined the probability that a lobster with observed tail width x was mature (m) as

$$P(m|x) = \begin{cases} 0 & x < \theta_0 \\ \frac{x - \theta_0}{\theta_1 - \theta_0} \exp\left(-\gamma \left(\frac{\theta_0 + \theta_1 - 2x}{\theta_1 - \theta_0}\right)\right) & \theta_0 \leq x < \frac{\theta_0 + \theta_1}{2} \\ 1 - \frac{\theta_1 - x}{\theta_1 - \theta_0} \exp\left(-\gamma \left(\frac{2x - (\theta_0 + \theta_1)}{\theta_1 - \theta_0}\right)\right) & \frac{\theta_0 + \theta_1}{2} \leq x < \theta_1 \\ 1 & x \geq \theta_1 \end{cases} \quad (1)$$

When $\gamma = 0$, $P(m|x)$ increases linearly from 0 to 1 over the interval $[\theta_0, \theta_1]$. For $\gamma > 0$, the curves are sigmoidal, symmetrical, and the rate that the probability changes with respect to tail width is bell shaped (the sigmoidal curve first accelerates, then decelerates). The point of inflection, $(\theta_0 + \theta_1)/2$, is the tail width at which 50% of the lobsters are expected to be mature. For both species, we assumed that $\gamma \geq 0$.

Defining the allometry model and the probability of maturity as above, we expressed the model relating pleopod length to tail width as $\ln(Y) = f_1(X)(1 - P(m|x)) + f_2(X)P(m|x) + \varepsilon$, where ε are independent normal variates with mean 0 and covariance V_m .

Assuming (x_i, y_i) $i = 1, \dots, n$ independent paired observations and $\sigma^2 = \sigma_1^2 = \sigma_2^2$, $V_m = I\sigma^2 + M$, where I is the $(n \times n)$ identity matrix, M is the diagonal matrix $M_{ii} = \Delta^2(x_i)P(m_i|x_i)(1 - P(m_i|x_i))$, and $\Delta(x_i) = f_2(x_i) - f_1(x_i)$. Hence, we have a weighted least squares problem with weights

$$w_i = \begin{cases} 1 & \text{if } x_i \leq \theta_0 \text{ or } x_i \geq \theta_1 \\ \frac{\sigma^2}{(\sigma^2 + M_{ii})} & \text{if } \theta_0 < x_i < \theta_1. \end{cases} \quad (2)$$

To fit the model, we defined $\alpha_3 = \alpha_2 - \alpha_1$ and $\beta_3 = \beta_2 - \beta_1$ and expressed the model as $\ln(Y) = f_3(X)P(m|x) + f_1(X) + \varepsilon$, where $f_3(X) = \alpha_3 + \beta_3 \ln(X)$. To ensure that the curve in the transition range was monotonically increasing (if $\beta_3 > 0$), θ_0 was bounded such that $\theta_0 \geq \exp(-\alpha_3/\beta_3)$, and if $\beta_3 < 0$, θ_1 was bounded such that $\theta_1 \leq \exp(-\alpha_3/\beta_3)$. The curve was fitted by using iteratively reweighted least squares. The weights were recomputed at each iteration.

While fitting the lobster data to the specified model, we observed that one or more of the parameters involved in defining the sigmoidal curve departed from linear behavior. Under these circumstances, the confidence interval derived by assuming the asymptotic properties of maximum likelihood estimates may be invalid (Ratkowsky, 1983). Therefore, we computed approximate 95% confidence intervals for the point of inflection using the bootstrap method. Specifically, we used case resampling with 1000 bootstrap replications. Confidence intervals were derived by using the studentized bootstrap confidence limits (Davison and Hinkley, 1997).

Abstract—In this study we present new information on seasonal variation in absolute growth rate in length of coho salmon (*Oncorhynchus kisutch*) in the ocean off Oregon and Washington, and relate these changes in growth rate to concurrent changes in the spacing of scale circuli. Average spacing of scale circuli and average rate of circulus formation were significantly and positively correlated with average growth rate among groups of juvenile and maturing coho salmon and thus could provide estimates of growth between age groups and seasons. Regression analyses indicated that the spacing of circuli was proportional to the scale growth rate raised to the 0.4–0.6 power. Seasonal changes in the spacing of scale circuli reflected seasonal changes in apparent growth rates of fish. Spacing of circuli at the scale margin was greatest during the spring and early summer, decreased during the summer, and was lowest in winter or early spring. Changes over time in length of fish caught during research cruises indicated that the average growth rate of juvenile coho salmon between June and September was about 1.3 mm/d and then decreased during the fall and winter to about 0.6 mm/d. Average growth rate of maturing fish was about 2 mm/d between May and June, then decreased to about 1 mm/d between June and September. Average apparent growth rates of groups of maturing coded-wire-tagged coho salmon caught in the ocean hook-and-line fisheries also decreased between June and September. Our results indicate that seasonal change in the spacing of scale circuli is a useful indicator of seasonal change in growth rate of coho salmon in the ocean.

Seasonal changes in growth of coho salmon (*Oncorhynchus kisutch*) off Oregon and Washington and concurrent changes in the spacing of scale circuli

Joseph P. Fisher

William G. Pearcy

College of Oceanic and Atmospheric Sciences
Oregon State University
104 Ocean Admin. Building
Corvallis, Oregon 97331-5503

E-mail address (for J. P. Fisher): jfisher@coas.oregonstate.edu

Large interannual and decadal variations occur in the abundance and productivity of North Pacific salmonids. These fluctuations, which affect harvestable biomass, are influenced by survival rates, ages at maturity, and somatic growth (Beamish and Bouillon, 1993; Mantua et al., 1997; Hare et al. 1999; Pypser et al., 1999; Hobday and Boehlert, 2001).

The growth of smolts after ocean entry—growth that is critical to production—is also thought to be an important determinant of their survival. As for juvenile and larval fishes in general, size-selective mortality may occur (Miller et al., 1988; Bailey and Houde, 1989; Litvak and Leggett, 1992; Sogard, 1997) with the result that faster growing salmonids experience less mortality from predators than slower growing salmonids (Parker, 1971; Bax, 1983; Fisher and Pearcy, 1988; Holtby et al., 1990; Jaenicke et al., 1994; Willette, 1996, 2001). This size-selective mortality may explain much of the interannual variability in survival of juvenile salmonids and the subsequent abundance of different year classes. However, other investigators have not found a strong relationship between growth of juvenile salmon and mortality (Fisher and Pearcy, 1988; Mathews and Ishida, 1989; Blackburn, 1990).

Intercirculus spacing of scales has been used to estimate early ocean

growth rate of juvenile salmon and has been linked to differential survival rates. For example, Healey (1982) used the spacing of the first five circuli to demonstrate intensive size-selective mortality in juvenile chum salmon (*Oncorhynchus keta*) as they migrated offshore. Holtby et al. (1990) correlated early ocean growth, based on intercirculus spacing, with marine survival of age 1+ coho (*O. kisutch*) smolts. The spacing of early ocean circuli from the scales of maturing Atlantic salmon (*Salmo salar*) has been used to estimate juvenile growth rates, which are correlated with survival and age at maturity, and to identify stocks (Friedland et al., 1993; Friedland and Haas, 1996; Friedland and Reddin, 2000; Friedland et al., 2000).

Correlation between circulus spacing and growth rate was reported by Fisher and Pearcy (1990) for age 0,0 coho smolts reared for 60 days in salt water tanks. In addition, positive correlations between the spacing of scale circuli and fish growth rate have been observed for rainbow trout (*O. mykiss*) (Bhatia, 1932), and sockeye salmon (*O. nerka*) (Fukuwaka and Kaeriyama, 1997), and between the spacing of circuli and feeding ration and growth for sockeye salmon (Bilton and Robins, 1971; Bilton, 1975). Bigelow and White (1996) were able to manipulate the spacing of scale circuli of cutthroat trout (*O. clarkii*)

Table 1
Main sources of coho salmon data used in this study.

Source	Numbers of fish	Scale samples
CWT maturing fish caught in the Oregon ocean sport and troll fisheries 1982–92 (see Table 2)	687	687
Maturing coho salmon caught in the ocean during research cruises		
1981–85	1391	352
1998–2002	714	236
Juvenile fish caught in the ocean during research cruises		
1981–85		1798
1998–2002	3684	1052
CWT maturing coho salmon caught in the sport and troll ocean fisheries (all catch areas) and released between northern Oregon and northern Washington ¹	149,718	—

¹ FL data in the Pacific States Marine Fisheries Commission, Regional Mark Information System online CWT database <http://www.rmis.org/>. [Accessed 1 April 2003.]

in the hatchery by varying the feeding levels: the group that was fed the most also grew the most and had the most widely spaced scale circuli. Positive correlations between circulus spacing and growth also have been observed for nonsalmonid fishes including *Tilapia* (Doyle et al., 1987; Matriccia et al., 1989; Talbot and Doyle, 1992), and walleye (*Stizostedion vitreum*) (Glenn and Mathias, 1985).

Circulus spacing is potentially useful for comparing ocean growth rates of salmon in the ocean. Spacing of the first few ocean scale circuli may indicate relative growth rates of juvenile fish immediately after ocean entry. However, in order for spacing of scale circuli to be a practical indicator of fish growth rate, the relationship between the two must be consistent and significant. The relationship between circulus spacing and fish or scale growth rate is determined by the relative rates of growth and circulus formation. If circuli (like tree rings) are formed at a constant rate, then there would be a directly proportional relationship between spacing and growth rate (e.g., a doubling of growth rate would result in a doubling of spacing). Conversely, if the rates at which circuli are formed are directly proportional to growth rates (e.g., a doubling of growth rate would result in a doubling of circulus formation rate), then the spacing of circuli would be constant. Our earlier study of growth rate, circulus formation, and circulus spacing among 82 individually marked juvenile coho salmon growing for a period of 63 days in saltwater tanks indicated that neither of these two extremes is the case, but that both circulus formation rate and circulus spacing are positively correlated with fish growth rate (Fisher and Pearcy, 1990).

Our main objectives in this study are to further assess the reliability of circulus spacing as an indicator of growth rate in FL of coho salmon in the ocean, to investigate how growth of coho salmon changes seasonally, and to compare any seasonal changes in growth rate with seasonal changes in the spacing of scale cir-

culi. If circulus spacing is a reliable indicator of growth rate, then seasonal changes in growth rate should be tracked by changes in the spacing of circuli laid down at the scale margin. We investigated relationships between scale growth rate, fish growth rate, circulus spacing, and circulus formation rate for coded-wire-tagged (CWT) adult coho salmon collected in the ocean fisheries in years when ocean growth varied widely, including year classes affected by the 1982–83 El Niño, and for juvenile and maturing coho salmon caught in the ocean off Oregon and Washington in research cruises 1981–85 and 1998–2002.

Materials and methods

Scale and FL data

Fish fork length (FL) and scale data from a variety of sources were used in this study (Table 1). During research cruises on the Oregon and Washington coastal shelf we collected juvenile and maturing coho salmon in the upper 20–40 m of the water column with purse seines from 1981–85 (Pearcy and Fisher, 1988, 1990) and with a rope trawl from 1998–2002 (Emmett and Brodeur, 2000). Scales samples were removed from the fish from an area equivalent to area "A" described in Scarnnechia (1979). When scales were not available from area "A," we took scales from between areas "A" and "B" in Scarnnechia (1979). (See also Clutter and Whitesel, 1956). We also examined scales from the same area from 687 maturing CWT Columbia River and northern coastal Oregon coho salmon caught in the Oregon ocean fisheries between 1982 and 1992.

Changes over time in FLs of maturing coho salmon caught in research nets and of CWT hatchery coho salmon originating between northern Oregon and northern Washington and caught in the ocean fisheries be-

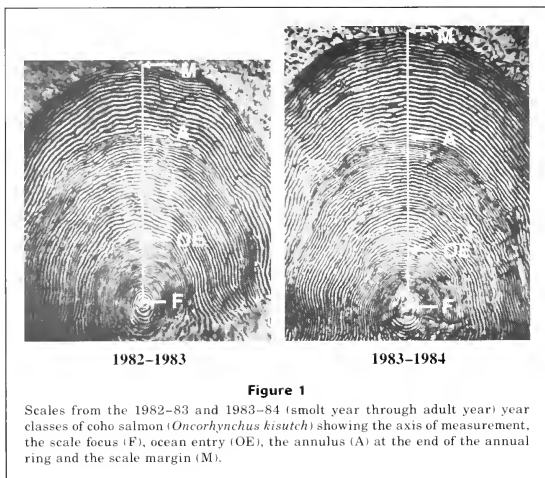


Figure 1

Scales from the 1982-83 and 1983-84 (smolt year through adult year) year classes of coho salmon (*Oncorhynchus kisutch*) showing the axis of measurement, the scale focus (F), ocean entry (OE), the annulus (A) at the end of the annual ring and the scale margin (M).

tween 1975 and 2002 were used to estimate growth rates of maturing fish (Table 1).

Scale measurements

We measured the distances (mm) along the anterior-posterior scale axis from the focus (F) to the last circulus of the freshwater zone (ocean entry, OE), to the outside edge of the winter annual ring (the "winter annulus," A) when present, and to the margin (M), and also determined the total numbers and average spacing of circuli in the ocean growth zone (Fig. 1). For certain scale samples we also determined the spacing of every circulus in the ocean growth zone of the scales or of the last few circuli at the scale margin.

Measurements of scales from juvenile fish caught during research cruises 1981-85 were taken from images projected by a microfiche reader at a magnification of about 88 \times and measurements of scales from all other fish were acquired with image analysis software (Optimas, vers. 5.1, Optimas, Inc., Seattle, WA, and Image-Pro Discovery, vers. 4.5, Media Cybernetics, Silver Spring, MD) by using a CCD camera coupled to a Leica compound microscope. All measurements were calibrated from images of a stage micrometer.

Circulus spacing and formation rate versus growth rate

We used correlation and regression analyses to relate average circulus spacing and formation rate to average

scale and fish growth rate among year classes of juvenile coho salmon during their first four or five months in the ocean and among groups of maturing CWT coho salmon during their entire ocean life (Table 2). We described the relationships between the scale characteristics and growth rate as power functions by using natural log (ln) transformed variables in linear regressions. Geometric mean (GM) regression (Ricker, 1973, 1992; Sokal and Rohlf, 1995) was used to relate the ln-transformed variables because they were subject to both natural variability and measurement error and because our purpose in the present study was to describe the functional relationships between the variables and not to predict one from the other.

For each fish, rates of scale growth, fish growth, and circulus formation in the ocean were estimated as $(SR - SR_{OE})/\Delta t$, $(FL - FL_{OE})/\Delta t$, and $CIRC/\Delta t$, respectively, where SR = scale radius at capture, SR_{OE} = scale radius at ocean entry (F to OE in Fig. 1), FL = fork length at capture, FL_{OE} = estimated fork length at ocean entry, $CIRC$ = the total number of circuli in the ocean growth zone of the scale, and Δt = estimated days between ocean entry and capture. Average spacing of circuli was calculated as $(SR_{LAST} - SR_{OE})/CIRC$, where SR_{LAST} = the scale radius to the last circulus before the scale margin.

For juvenile fish, FL_{OE} was estimated by using the Fraser-Lee back-calculation method (Ricker, 1992) and the intercept from the FL - SR regression for ocean-caught juvenile fish (34.16 mm, Fig. 2). However, be-

cause of allometry in the FL-SR relationships of juvenile and maturing fish (Fig. 2), which a ln-ln transformation of the data failed adequately to correct, the Fraser-Lee method was not used to estimate FL_{OE} of the maturing fish caught in the ocean. Instead, FL_{OE} of maturing fish was estimated by direct substitution of (SR_{OE}) into the GM regression relationship between FL and SR for juvenile coho salmon caught in the ocean 1981-85 and 1998-2001 (gray regression line, Fig. 2).

For juvenile fish caught in August or September, Δt was estimated as the capture date minus 25 May, a date near the peak of coho salmon smolt migration in the Columbia River estuary (Dawley et al., 1985a). Because we used a single date of ocean entry for all fish, errors in estimated growth rates of some individual juvenile coho salmon probably were quite large; the timing of ocean entry of fish can vary by as much as two months. However, for the correlation and regression analyses we used growth rates averaged by year class, which were probably quite accurate, if the average date of ocean entry of the fish in the samples is assumed to be similar across years. In the Columbia River, the major source of juvenile coho salmon on the Oregon and Washington coasts, ocean entry was concentrated between late April and early June and the timing of ocean entry varied little between years (Dawley et al., 1985a).

Dates of ocean entry of the maturing CWT Sandy and Cowlitz hatchery coho salmon (Table 2) were estimated from the hatchery release dates and the rates of downstream migrations of these fish observed during extensive sampling of migrating smolts at rkm 75 in the upper Columbia River estuary (Dawley et al., 1985b). To estimate dates of ocean entry of the Fall Creek hatchery fish, for which data on downstream migration were lacking, we assumed that smolts migrated to the ocean from the different release sites at the same average rate of downstream migration as that of Cowlitz Hatchery fish released in late April (5.7 km/d).

Potential errors in estimated growth rates of maturing CWT coho salmon caused by inaccurately estimating size of fish at ocean entry, or date of ocean entry, were proportionally very small when compared to the total amount or duration of ocean growth. At a typical SR_{OE} of around 0.7 mm, the 95% prediction limits for FL from the SR-FL regression of juvenile fish (Fig. 2) are about ± 31 mm. An error in size at OE of 15-30 mm would only be 2-10% of the estimated total growth in FL in the ocean of the maturing fish (320 mm-610 mm). Similarly, an error in estimated date of ocean entry of 30 days would equal only about 6-10% of the total time that the fish was in the ocean (336-535 d). Errors for the group-averaged data used in our correlation and regression analyses were probably much lower.

Seasonal changes in spacing of circuli

To investigate whether circulus spacing and growth rate were correlated seasonally, we first described the patterns of seasonally changing circulus spacing of juvenile and maturing coho salmon in the ocean and

Table 2

Nine year classes of juvenile coho salmon caught in research nets in August or September and 17 groups of CWT maturing coho salmon caught in the Oregon ocean fisheries used in the correlation and regression analyses of scale characteristics and growth rate. CWT maturing fish were from three hatcheries (Fall Creek "F" on the northern Oregon coast and Sandy "S" and Cowlitz "C" in the lower Columbia River basin) and were released from hatcheries during three periods.

Capture year	Hatcheries	Numbers of fish
CWT maturing fish released late April or early May (days 119-127)		
1982	F, S	11, 15
1983	F, S, C	34, 17, 51
1984	S, C	52, 35
1985	S, C	12, 26
1986	S	67
1987	S	94
1989	S	57
1990	S	18
CWT maturing fish released in March (days 74-76)		
1984	F	31
1985	F	21
CWT maturing fish released in late May or early June (days 151-157)		
1991	S	30
1992	S	77
Juvenile fish		
1981	—	99
1982	—	95
1983	—	81
1984	—	88
1998	—	13
1999	—	60
2000	—	75
2001	—	67
2002	—	123

then compared these patterns of changing circulus spacing to changing fish growth rates. Because the widths of the pre-annulus and postannulus scale zones and the numbers of circuli in each zone varied greatly among individual fish and among groups of fish, we described circulus spacing in each of 25 equally spaced intervals between OE and the annulus and in each of 25 equally spaced intervals between the annulus and the scale margin, rather than on a circulus by circulus basis. Specifically, the pre-annulus and postannulus ocean zones of scales were each divided into 25 equal intervals, and the radial distance from OE to the upper bounds of each of the intervals was determined. Next, the numbers of ocean circuli between OE and the upper bounds of each of the 50 intervals were interpolated. For example, if a boundary fell 25% of the distance

between the 38th and 39th ocean circulus, the circulus number 38.25 was assigned to that boundary. We calculated the circulus spacing in each interval as $\Delta\text{mm}/\Delta\text{circ}$, where Δmm = the width in mm of the interval, and Δcirc = the difference between the interpolated circulus numbers at the upper and lower bounds of the interval. The circulus spacing in each of the 50 intervals was averaged across all the scales from the fish in a group. This produced a profile of the average spacing of circuli at 50 different positions in relation to *OE* (lower bound of interval 1), the annulus (upper bound of interval 25) and the scale margin (upper bound of interval 50). Finally, the group-average circulus spacing in each of the 50 intervals was plotted against the group-average radial distance from *OE* to the upper bounds of each of the 50 intervals. For juvenile fish caught in trawls in September 1999–2002, circulus spacing was described at 25 intervals in relation to *OE* (lower bound of interval 1) and the scale margin (upper bound of interval 25).

Seasonal changes in the spacing of circuli at the growing edge of the scale may reflect similar seasonal changes in the growth rate of the juvenile and maturing coho salmon. To investigate this possible correlation, we measured the spacing of the last two circulus pairs at the scale margin of juvenile fish caught in early and late summer in 1982 and 1999 through 2002 and of maturing fish caught in research nets 1981–83 and 2000–2002 and in the ocean fisheries 1982–92 (Table 1). Mean spacing of the last two circulus pairs was summarized by cruise for the fish caught in research nets, and by 10-day catch intervals for the fish caught in the ocean fisheries. The seasonal trends in spacing at the scale margin were then compared with the seasonal trend in apparent growth rates of fish.

Seasonal changes in fish growth rate

Seasonal trends in growth rates of juvenile and maturing coho salmon caught in research cruises 1981–83 and 1998–2002 were estimated from the changes between cruises in average FL. We also estimated average growth rates (pooled across years) of juvenile and adult coho salmon during different seasons by fitting regressions to the FL versus catch date data.

Changing stock composition of the juvenile (Teel et al., 2003) or maturing coho salmon caught in research nets over the course of the summer could potentially have a strong effect, independent of growth, on the size distributions of fish caught at different times. Therefore, changes over time in average FLs of mixed stocks of fish, such as in our research collections, may not accurately indicate actual fish growth rates.

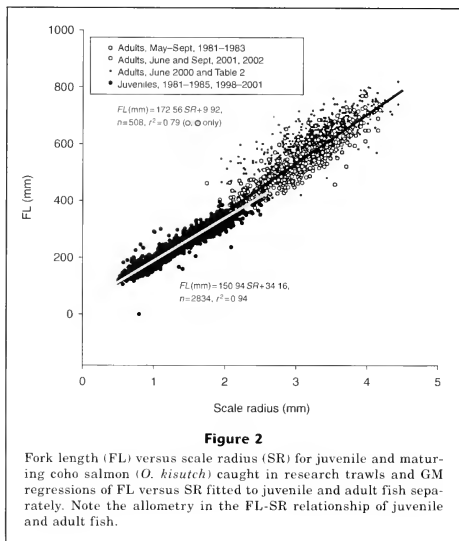


Figure 2

Fork length (FL) versus scale radius (SR) for juvenile and maturing coho salmon (*O. kisutch*) caught in research trawls and GM regressions of FL versus SR fitted to juvenile and adult fish separately. Note the allometry in the FL-SR relationship of juvenile and adult fish.

Because of the potential for error when inferring seasonal changes in growth rate from changes over time in average FLs of mixed stocks of fish, we also examined temporal changes in FL of maturing CWT coho salmon of known origin caught in the ocean hook-and-line fisheries (sport and troll fisheries). Using data available from the Pacific States Marine Fisheries Commission¹ we investigated changes over the summer in FLs of maturing CWT coho salmon originating from six areas (north Oregon coast, lower Columbia River basin–Oregon, lower Columbia River basin–Washington, Willapa Bay basin, Grays Harbor basin, and the northwest Washington coast). Because the date that a smolt is released from a hatchery (e.g., March vs. June) could affect its size the following year, we also grouped the fish by release periods of 25–46 days duration. Data were available on FLs of maturing CWT fish from 1975–2002. For each group in each year we calculated the average FL of CWT fish at 10-day intervals in the hook-and-line fisheries (sport and troll fisheries) pooled for all catch areas between California and Alaska. Data were discarded when there were fewer than 5 fish mea-

¹ Regional Mark Information System CWT database (<http://www.rmis.org>). [Accessed on: 1 April 2003.]

Table 3

Summary statistics of average estimated fish growth rate, average estimated scale growth rate, average estimated rate of circulus formation, and average circulus spacing between ocean entry and late summer for nine year classes of juvenile coho salmon and during the entire ocean growth period for the 17 groups of CWT maturing coho salmon (see Table 2).

Statistic	Average fish growth rate (mm/d)	Average scale growth rate (mm/d)	Average circulus formation rate (circuli/d)	Average circulus spacing (mm)
Juvenile fish, n=9				
Grand average	1.33	0.0087	0.188	0.0460
Minimum	1.18	0.0080	0.175	0.0428
Maximum	1.52	0.0101	0.202	0.0494
SD	0.10	0.0007	0.008	0.0023
CV	7.6%	8.3%	4.1%	4.9%
Maturing fish, n=17				
Grand average	1.11	0.0060	0.131	0.0463
Minimum	0.94	0.0048	0.110	0.0426
Maximum	1.23	0.0066	0.144	0.0511
SD	0.07	0.0005	0.009	0.0020
CV	6.7%	8.1%	6.8%	4.4%

sured in any 10-day catch period. The average FLs were averaged across all years of data, yielding grand-average FLs for each 10-day catch period. The grand average FL for each 10-day catch interval comprised 1–27 years of data, but those periods with fewer than 5 years of data were discarded. In all, FLs from 149,718 fish were used in the analysis. Grand average FLs and the apparent growth rates in FL between each 10-day catch period were plotted against date and compared with the seasonal changes in circulus spacing at the scale margin of the fish in our scale sample.

Results

Growth and scale statistics for juvenile and maturing fish

Average growth rates and circulus formation rates were greater for juvenile fish during their first ocean summer than for maturing fish during their entire ocean life probably because maturing fish experience slow growth in the winter (Table 3). During their first summer in the ocean, juvenile fish grew an average of 1.33 mm/d and formed circuli at the rate of 0.188/d (one every 5.3 days); whereas, during their entire ocean life maturing fish grew an average of 1.11 mm/d and formed circuli at the rate of 0.131/d (one every 7.6 days). The highest average growth rate (1.52 mm/d) among the eight year classes of juvenile coho salmon was about 28% higher than the lowest average growth rate (1.18 mm/d). The percentage range in growth rate of maturing fish was similar (31%). Average spacing of circuli was similar for both juvenile and maturing coho salmon (0.0460 mm vs. 0.0463 mm), probably because scales from the maturing

fish contained both more narrowly spaced circuli formed during the winter and more widely spaced circuli formed during the second ocean summer (see below). The variation among groups in average circulus spacing (CV=4.9% and 4.4%) was lower than the variation in fish or scale growth rates (CV=6.7% to 8.3%), although estimation error may have increased the coefficients of variation of the growth rates.

Correlations between scale characteristics and growth rate

Circulus spacing was strongly correlated ($r=0.89$ and 0.82 , respectively) with scale and fish growth rates among the nine year classes of juvenile coho salmon (Table 4). Circulus spacing was also significantly correlated with scale and fish growth rates among the 17 groups of maturing fish, but the correlations were weaker ($r=0.57$ and 0.55 , respectively) than those for the juvenile fish. Conversely, correlations between the rate of circulus formation and the scale and fish growth rates were slightly higher for the maturing fish ($r=0.85$ and 0.75 , respectively) than for the juvenile fish ($r=0.76$ and 0.81 , respectively). These results suggest that when growth is averaged over several seasons, during which growth rate varies greatly and may even cease for varying periods of time, differences in growth among year classes or groups may be reflected more clearly by differences in the numbers of circuli laid down on the scale than by differences in the average spacing of circuli.

Although the average spacing of circuli and the average rate at which circuli form were both correlated with scale and fish growth rates, they were not correlated with each other (Table 4). This finding indicates that

circulus spacing and circulus formation rate are independent indicators of growth rate—both tending to increase with increasing growth rate but not necessarily together in the same fish or in the same group or year class. At least when averaged over periods of months or more than a year, differences in average growth rate may be expressed by differences in average spacing of circuli, differences in average rate of circulus formation, or differences in both.

Regressions of circulus spacing and formation rate on growth rate

We expressed average spacing of circuli and rates of circulus formation as power functions of the scale growth rates, equivalent to linear regressions of ln-ln transformed data. These regressions are shown in Figures 3 and 4 for year classes of juvenile fish and groups of maturing fish, respectively. Because scale growth rate and fish growth rate were very strongly correlated (Table 4), we show only the regressions with scale growth rate.

Change in average spacing of circuli and in average rate at which circuli form was proportionally smaller than the change in average scale growth rate. Average spacing of circuli was proportional to the average scale growth rate raised to the 0.6 power (juvenile fish, Fig. 3A) or the 0.5 power (maturing fish, Fig. 4A). If these relationships hold over a wider range of scale growth rate and circulus spacing, then a doubling of scale growth rate would be associated with only a 1.5-fold ($2^{0.6}$) or 1.4-fold ($2^{0.5}$) increase in circulus spacing. Similarly, average rate of circulus formation was proportional to the average scale growth rate raised to the 0.5 power (juvenile fish, Fig. 3B) or the 0.8 power (maturing fish, Fig. 4B).

Seasonal changes in circulus spacing and fish growth rate

Seasonal changes in average circulus spacing were consistent among the different year classes and release times of CWT coho salmon (Fig. 5, A–E). During the first year in the ocean, average spacing of scale circuli increased rapidly after OE (usually in May) to average peak values of about 0.050 mm–0.055 mm, then gradually decreased to average minimum values of about 0.031 mm–0.040 mm in the annual ring. By late September 1999–2002, spacing at the margin of scales from juvenile fish had decreased from peak values (Fig. 5E), indicating that the gradual decrease in spacing of circuli which forms the annual ring begins as early as the late summer of the first ocean year. For some year classes (e.g., 82–83, 85–86, 90–91, 91–92) the annual ring was a distinct narrow zone of very closely spaced circuli (Fig. 5, A and C), whereas in other years the annual ring was broad and subtle, with more widely spaced circuli (e.g., 83–84, 86–87, and 84–85 for the March released fish; Fig. 5, A and B).

After the annulus (black dots, Fig. 5), the spacing of circuli increased sharply to peak values of about

Table 4

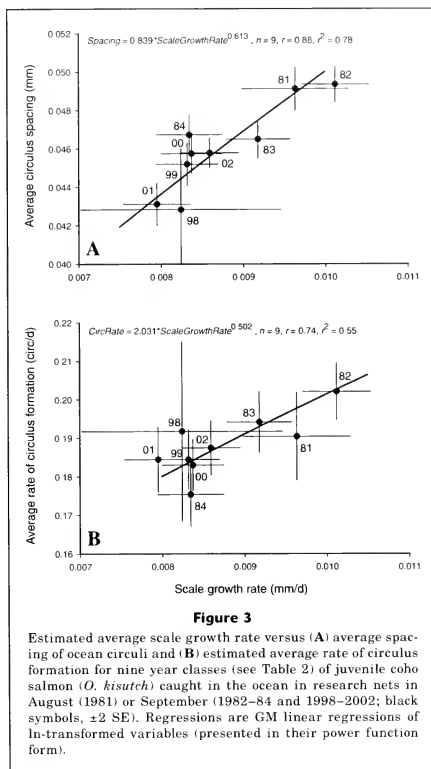
Correlations (r) between average circulus spacing (mm), average estimated scale growth rate (mm/d), average estimated fish growth rate (mm/d), and average estimated circulus formation rate (circuli/d) between ocean entry and late summer for nine year classes of juvenile coho salmon and during the entire ocean growth period for 17 groups of CWT maturing coho salmon (see Table 2). All correlations were significant ($P < 0.05$), except where noted ("n.s").

Comparison	Juvenile fish	Maturing fish
	r	r
Circulus spacing vs. scale growth rate	0.89	0.57
Circulus spacing vs. fish growth rate	0.82	0.55
Circulus spacing vs. circulus formation rate	0.38, n.s.	0.05, n.s.
Scale growth rate vs. fish growth rate	0.97	0.91
Scale growth rate vs. circulus formation rate	0.76	0.85
Fish growth rate vs. circulus formation rate	0.81	0.75

0.055 mm–0.060 mm and remained high for a variable distance. Compared to the peak spacing, spacing of circuli at the scale margin was relatively high for maturing fish caught in late June or July 1982, 1984, 1985, 1986, 1987, 1991, and 2000, whereas, spacing at the scale margin was quite low compared to the peak spacing for fish caught in July 1983, 1989, 1990, and 1992 (Fig. 5, A, C, and D). Spacing at the scale margin was very low among unmarked maturing fish caught in late September 2001 (Fig. 5D).

Compared to the large interseasonal variation in spacing of circuli in the pre- and postannulus zones, from about 0.03 mm in the annual ring to about 0.06 mm for the most widely spaced circuli, interannual variation the peak and minimum spacing of circuli was quite small. The peak spacing of circuli was similar among year classes, even when total growth differed greatly (e.g., the 82–83 vs. the 81–82 and 83–84 year classes, Fig. 5A). The unusually small postannulus scale growth of fish caught during a strong El Niño in July 1983 (Fig. 5A) was characterized by a much narrower region of widely spaced circuli and more closely spaced circuli at the scale margin than in other years.

In general, pre-annulus scale growth was greatest for the fish released in March (Fig. 5B), was slightly less for the fish released in late April or early May (Fig. 5A), and was smallest for the fish released in late May or early June (Fig. 5C). These data indicate that date of release may strongly affect the amount of growth at-

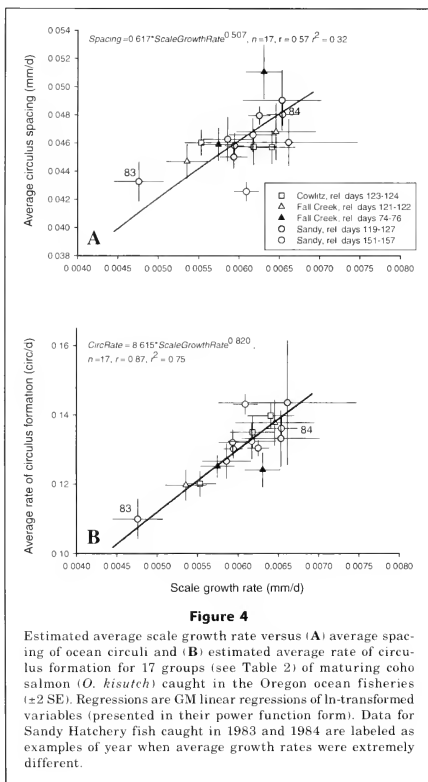


tained by juvenile coho salmon during their first summer, fall, and winter in the ocean.

Do the seasonal changes in circulus spacing in the ocean growth zones of scales coincide with similar seasonal changes in growth rates of juvenile and maturing coho salmon? In Figure 6 we plotted the average lengths of juvenile and maturing coho salmon from all research cruises 1981–2002 and the average apparent growth rates of coho salmon during different seasons (dashed lines). Apparent average growth rate of juvenile coho salmon between June and September was 1.30 mm/d, about twice the apparent growth rate of 0.64 mm/d between September and the following May. Apparent

growth rates of maturing fish between late May and late June was very rapid (2.11 mm/d), about twice as great as the apparent growth rate of maturing fish later between June and September (1.01 mm/d).

In a general sense, this pattern of changing apparent growth rate over time in the ocean corresponds well to the pattern of changing circulus spacing seen in Figure 5, A–E. The rapid growth of juvenile coho salmon between June and September occurs during a period when the spacing of circuli generally is high (Fig. 5E). When maturing fish were caught in the ocean fisheries in late June and in July and August a zone of widely spaced circuli already was present on the scales (Fig. 5,



A–C), indicating that these widely spaced circuli were produced earlier during the period of apparently rapid growth in the spring and early summer (Fig. 6). Circulus spacing at the scale margin was already declining in July among maturing fish in some years (Fig. 5A), and was clearly lower among maturing fish caught in August or September (Fig. 5, B and D) indicating that these more narrowly spaced circuli were produced sometime during the apparently slower growth of maturing fish between late June and September (Fig. 6). Finally, the low spacing of circuli in the annual ring occurs sometime between late September of the first year and

mid-May of the second year, which was also the period of lowest apparent growth rate (Fig. 6).

The pattern of changing circulus spacing at the scale margin is most clearly seen when average spacing of the outer two circulus pairs is plotted against the average Julian day of capture (Fig. 7, A and B). Among juvenile fish caught in research nets, the average spacing of the circuli at the scale margin was narrower in September than in June (Fig. 7A, see also Fig. 5E). We lack sufficient FL data from mid and late summer to determine whether or not a decrease in the average growth rate of juvenile fish was associated with the observed

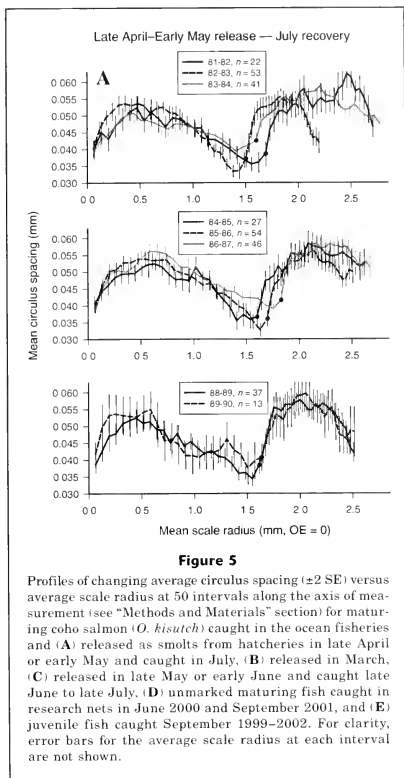


Figure 5

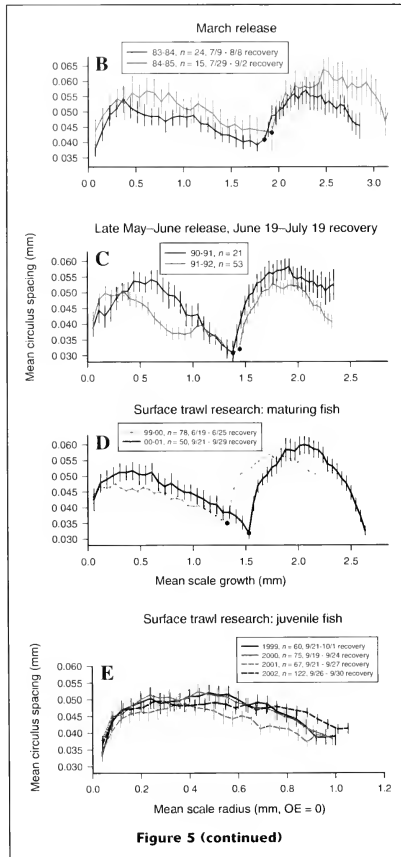
Profiles of changing average circulus spacing (\pm SE) versus average scale radius at 50 intervals along the axis of measurement (see "Methods and Materials" section) for maturing coho salmon (*O. kisutch*) caught in the ocean fisheries and (A) released as smolts from hatcheries in late April or early May and caught in July, (B) released in March, (C) released in late May or early June and caught late June to late July, (D) unmarked maturing fish caught in research nets in June 2000 and September 2001, and (E) juvenile fish caught September 1999–2002. For clarity, error bars for the average scale radius at each interval are not shown.

decrease in spacing of circuli at the scale margin in September.

Among maturing fish, average spacing of the last two circulus pairs at the scale margin decreased greatly between the spring through early summer period and early fall (Fig. 7B). The decrease in circulus spacing at the scale margin during the summer occurred for both maturing fish of mixed stocks caught in research nets (gray and white symbols) and for CWT fish of known stocks caught in the ocean sport and troll fisheries (black symbols). The decrease also was very consistent among year classes; 11 of the 12 year-class groups

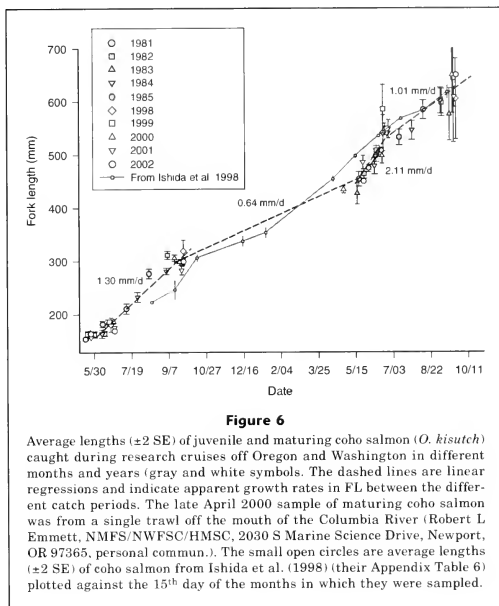
(grouped by release period and pooled across hatcheries) of Table 2 showed significant negative correlations between spacing at the margin and date of capture ($P < 0.05$, $r = -0.40$ to -0.59). In September the average circulus spacing at the scale margin was about as low as the average circulus spacing in the annual ring (about 0.035 mm).

The decrease in spacing of circuli at the scale margin over the summer mirrors a similar decrease over the summer in apparent growth rates in FL of maturing fish caught in research nets (Fig. 7C). The apparent growth rates of maturing coho salmon were usually



higher between the May and June research cruises (2–3 mm FL/d) than between cruises later in the summer (0.5–1.5 mm FL/d)(Fig. 7C, see also Fig. 6). The concurrent decreases in spacing of circuli at the scale margin and in apparent growth rate of coho salmon in the ocean is consistent with the hypothesis that seasonal changes in scale circulus spacing reflect seasonal changes in fish growth rate.

Additional evidence for decreasing growth rate of maturing coho salmon over the course of the summer comes from FLs of CWT fish in the hook-and-line fisheries (sport and troll fisheries). Generally, apparent growth rates in FL of maturing coho salmon originating from northern coastal Oregon streams and from both the Oregon and Washington sides of the Columbia river basin were highest from late May to mid-June and



decreased greatly by mid-August (Fig. 8, A and B). For three periods, 20 May–29 June, 29 June–8 August, and 8 August–27 September, median apparent growth rates were 1.43 mm/d ($n=19$), 0.64 mm/d ($n=24$), and 0.24 mm/d ($n=27$), respectively.

Growth rates of fish from coastal Washington rivers also decreased over the summer, but the decrease was not as great as for the Oregon and Columbia River fish, and the apparent growth rates of the Washington fish were higher at comparable times during the summer (Fig. 9, A and B). The apparent growth rates of Gray Harbor basin fish were over 2 mm/d from late June to mid-July and remained comparatively high (about 1.0 mm/d) into late October (Fig. 9B). Washington fish generally were not caught in the fisheries until mid- or late June, about a month after the first catches of the Oregon and Columbia River fish. For three periods 19 June–29 July, 29 July–7 September, and 7 September–27 October, median apparent growth rates of the coastal Washington fish were 1.23 mm/d ($n=13$), 0.92 mm/d ($n=16$), and 1.06 mm/d ($n=9$), respectively.

The growth data for CWT fish from the sport and troll fisheries, especially those for the coastal Oregon

and Columbia River stocks, were consistent with the growth data from the mixed stock catches of coho salmon in research nets off Oregon and Washington in that both data sets indicated a substantial decrease in growth rate (FL) of maturing coho salmon between the May–June period and the August–September period. The decreases over the summer in circulus spacing at the scale margin (Fig. 7B) and in apparent growth rates of maturing CWT coho salmon of known origin (Fig. 8B) is further evidence that scale circulus spacing and fish growth rate are correlated seasonally.

Discussion

Our data indicate that the seasonal cycle of changing ocean circulus spacing on scales of juvenile and adult coho salmon mirrors a similar seasonal cycle in the growth rate of these fish. We lack direct data for coho salmon collected between late September of the first calendar year of ocean residence and mid-May of the second calendar year, but growth rate during part of the fall and winter may be as low as 0.5mm/d

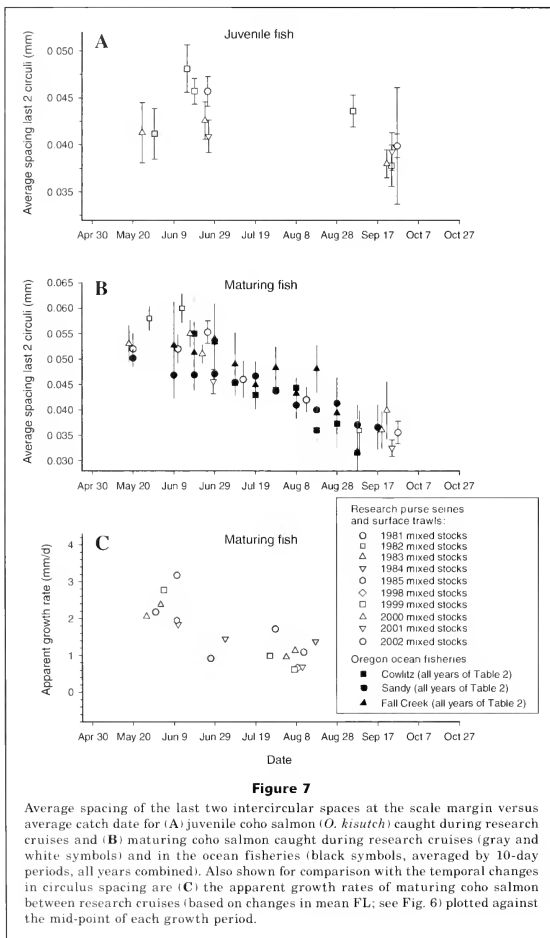
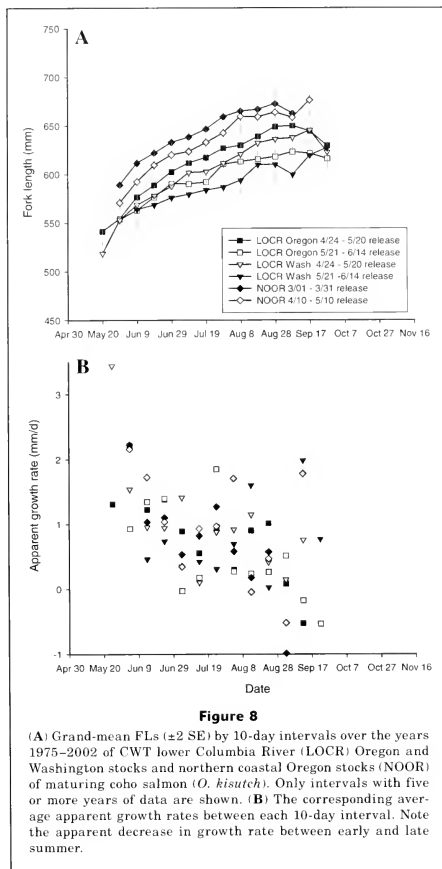


Figure 7

Average spacing of the last two intercirculi at the scale margin versus average catch date for (A) juvenile coho salmon (*O. kisutch*) caught during research cruises and (B) maturing coho salmon caught during research cruises (gray and white symbols) and in the ocean fisheries (black symbols, averaged by 10-day periods, all years combined). Also shown for comparison with the temporal changes in circuli spacing are (C) the apparent growth rates of maturing coho salmon between research cruises (based on changes in mean FL; see Fig. 6) plotted against the mid-point of each growth period.

based on data in Ishida et al. (1998). Therefore, the roughly twofold range in spacing of circuli in the ocean growth zone of scales from maturing fish that we found probably represents about a fourfold range in fish growth

rate in the ocean (from about 0.5 mm/d in the winter to 2.1mm/d in the spring and early summer). Thus, changes in the spacing of scale circuli are relatively small when compared to the corresponding changes in fish growth



rate. However, the large seasonal changes in growth rate of coho salmon in the ocean are readily detectable from the changes in circulus spacing on the scale.

In June 2001, 2002, and 2003 average spacing of the last two circulus pairs at the scale margin was positively correlated ($P < 0.01$) with plasma IGF-I (insulin-like growth factor-I) concentrations from juvenile fish caught in the ocean in research nets ($n = 119, 163,$ and 206 and

$r = 0.52, 0.52,$ and 0.59 in 2001, 2002, and 2003, respectively) (Beckman² and Fisher, unpubl. data). Because plasma IGF-I levels have been shown to be positively

² Beckman, B. 2004. Unpubl. data. Integrative Fish Biology Program, Northwest Fisheries Science Center, National Marine Fisheries Service, 2725 Montlake Boulevard East, Seattle, Washington 98112.

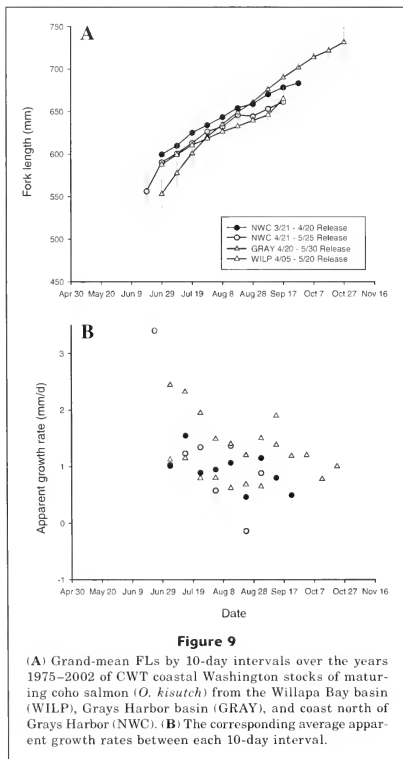
correlated with instantaneous growth rates (in length) of juvenile coho salmon (Beckman et al., 2004), the finding that plasma IGF-I is also correlated with the spacing of circuli at the scale margin of juvenile coho salmon is further evidence that circulus spacing and growth rate are positively related for coho salmon.

Our data suggest that growth rate in FL of maturing coho salmon is usually highest between early or mid-April and late June. This is a period of increasing photoperiod and often rising sea-surface temperature (SST) at 50°N in the northeastern Pacific Ocean, but is well before the maximum SST in late August (Fig. 10). Both increased day length and temperature stimulate growth in salmonids (Brett, 1979; Björnsson, 1997). The

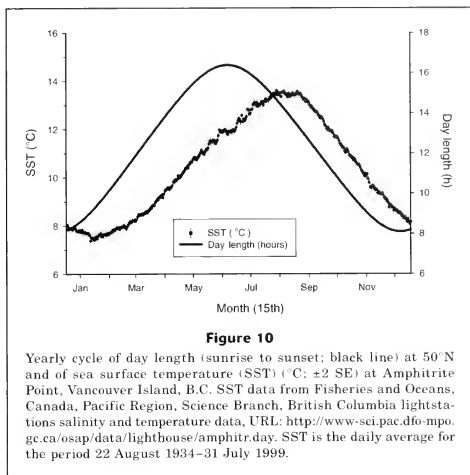
decreases in apparent growth rate in length of maturing coho salmon after the summer solstice could be associated with a number of factors. One possibility is that there is a shift during the summer away from skeletal growth to growth in weight (with a resultant increase in condition) or to gonadal development. Data in Ishida et al. (1998) for coho salmon caught in research nets in the North Pacific tend to support this proposition (their Appendix Table 6). Their data indicate that the rate of growth in FL of maturing coho salmon decreased from 1.45 mm/d between April and May to 0.49 mm/d between July and August. (See also Fig. 6, present study). Over the same time period the condition index (weight (g) × (10⁷/FL[mm])³) of the fish they sampled increased from 113.3 to 143.8, an increase of 27%. Thus, skeletal growth slowed over the summer, but the condition of the fish increased.

In contrast to growth rates of Columbia River coho salmon, which decreased greatly between early and late summer, and were quite low (≤ 0.5 mm/d) by August and September, the growth rates of fish from the Grays Harbor basin, although also declining during the summer, remained high well into September and early October (~0.7–1.4 mm/d), allowing the Grays Harbor fish to attain a significantly larger final average FL. Several factors may result in these differing growth patterns of maturing fish from the two groups. Many of the fish from the Columbia River are early spawners, and peak spawning occurs from late October to early November, whereas the Grays Harbor fish are mainly late spawners, and peak spawning occurs from mid-November to late-December (Weitkamp et al., 1995). Because of their later spawning the Grays Harbor fish may shift from somatic to gonadal growth later in the summer or fall than do the earlier spawners from the Columbia River. Maturing coho salmon from the Grays Harbor drainage also have a much more northerly distribution than do maturing fish from the Columbia River (Weitkamp and Neely, 2002) and, therefore, the two groups encounter very different ocean conditions (e.g., temperature, salinity, prey fields, prey distributions, and potential competitors for food) while feeding in coastal waters. The different environmental conditions experienced by the Columbia River and Grays Harbor fish may also contribute to their differing temporal growth patterns.

Because of the poor conditions for growth of fish associated with the 1983 El Niño, adult coho salmon in 1983 were exceptionally small off Oregon and were in poor condition (Pearcy et al., 1985; Johnson, 1988). Our scale analysis indicates that the small size of fish in 1983 was largely due to a failure of growth of maturing fish after formation of the winter annulus. Although the average scale radius between OE and the winter annulus was slightly smaller for the 1982–83 year class than for other year classes, the average scale radius between the winter annulus and the scale margin, representing the growth of maturing fish in spring and early summer, was



(A) Grand-mean FLs by 10-day intervals over the years 1975–2002 of CWT coastal Washington stocks of maturing coho salmon (*O. kisutch*) from the Willapa Bay basin (WILP), Grays Harbor basin (GRAY), and coast north of Grays Harbor (NWC). (B) The corresponding average apparent growth rates between each 10-day interval.



exceptionally low for this year class (Fig. 5A). Circulus spacing revealed two notable trends. First, in 1983 the maximum spacing of circuli following the winter annulus was only very slightly lower than in other years, which indicates that spring growth in FL of maturing fish in 1983 was not unusually low. Perhaps maturing coho salmon continued to grow in length in spring 1983, when photoperiod was increasing rapidly, despite low food availability. Björnsson (1997) found that changes in photoperiod may possibly control the level of pituitary growth hormone (GH), which strongly stimulates skeletal growth in salmonids and that increased levels of GH can induce growth in length even during starvation. Second, the spacing of circuli at the scale margin for fish caught in July 1983 was unusually low, similar to the spacing at the scale margin from fish caught in August of most years. This finding indicates very slow growth rates for maturing fish by July 1983. Length data¹ for maturing CWT coho salmon from the Oregon side of the Columbia River basin caught in the ocean sport and troll fisheries indicated that between June and September 1983 the average length of fish changed very little, which would indicate that somatic growth ceased during the summer.

Our results confirm the utility of circulus spacing as an indicator of growth rate in FL of coho salmon in the ocean. Correlations between average circulus spacing and estimated average growth rates of groups of fish were significant and positive (Table 4), even

when growth was measured over long intervals of time (four to five months for juveniles, and over a year for maturing coho salmon), and even when the estimates of growth rate were subject to error. In addition, our data indicate large seasonal changes in growth rate in FL of coho salmon in the coastal ocean off Oregon and Washington, a result also suggested by data in Ishida et al. (1998) for coho salmon in the North Pacific (see Fig. 6), and these seasonal changes in growth rate appear to be tracked by seasonal changes in spacing of scale circuli.

Acknowledgments

We thank all personnel from the Estuarine and Ocean Ecology Division of the National Marine Fisheries Service and from Oregon State University who participated either in the research cruises or in processing samples from those cruises. We also thank Lisa Borgerson of the Oregon Department of Fish and Wildlife for supplying scales from coho salmon caught in the ocean fisheries, and the captains and crews of the FV *Sea Eagle*, FV *Ocean Harvester*, FV *Frosti* and the RV *Ricker* for their expert assistance during the cruises. Ric Brodeur and Edmundo Casillas provided helpful comments on an earlier version of this paper. This study was funded by the Bonneville Power Administration through a grant to the National Marine Fisheries Service and from NMFS to Oregon State University.

Literature cited

- Bailey, K. M., and E. D. Houde.
1989. Predation on eggs and larvae of marine fishes and the problem of recruitment. *Adv. Mar. Biol.* 25:1-83.
- Bax, N. J.
1983. Early marine mortality of marked juvenile chum salmon (*Oncorhynchus keta*) released in Hood Canal, Puget Sound, Washington, in 1980. *Can. J. Fish. Aquat. Sci.* 40:426-435.
- Beamish, R. J., and D. R. Bouillon.
1993. Pacific salmon production trends in relation to climate. *Can. J. Fish. Aquat. Sci.* 50:1002-1016.
- Beckman, B. R., W. Fairgrieve, and K. A. Cooper,
C. V. W. Mahnken, and R. J. Beamish.
2004. Evaluation of endocrine indices of growth in individual post-smolt coho salmon. *Trans. Am. Fish. Soc.* 133:1057-1067.
- Bhatia, D.
1932. Factors involved in the production of annual zones on the scales of the rainbow trout (*Salmo irideus*). II. *J. Exp. Biol.* 9:6-11.
- Bigelow, P. E., and R. G. White.
1996. Evaluation of growth interruption as a means of manipulating scale patterns for mass-marking hatchery trout. *N. Am. J. Fish. Manag.* 16:142-153.
- Bilton, H. T.
1975. Factors influencing the formation of scale characters. *Int. North Pac. Fish. Comm. Bull.* 32:102-108.
- Bilton, H. T., and G. L. Robins.
1971. Effects of feeding level on circuli formation on scales of young sockeye salmon (*Oncorhynchus nerka*). *J. Fish. Res. Board Can.* 28:861-868.
- Bjornsson, B. T.
1997. The biology of salmon growth hormone: from daylight to dominance. *Fish. Physiol. Biochem.* 17:9-24.
- Blackbourn, D. J.
1990. Comparison of release size and environmental data with the marine survival rates of some wild and enhanced stocks of pink and chum salmon in British Columbia and Washington state. In *Proceedings 14th northeast Pacific pink and chum salmon workshop* (P. A. Knudsen, ed.), p. 82-87. Washington Dept. Fish., Olympia, WA.
- Brett, J. R.
1979. Environmental factors and growth. In *Fish physiology*, vol. 8, Bioenergetics and growth (W. S. Hoar, D. J. Randall, and J. R. Brett, eds.), p. 599-675. Academic Press, New York, NY.
- Clutter, R. L., and L. E. Whitesel.
1956. Collection and interpretation of sockeye salmon scales. *Int. Pac. Salmon Fish. Comm. Bull.* 9, 159 p.
- Dawley, E. M., R. D. Ledgerwood, and A. Jensen.
1985a. Beach and purse seine sampling of juvenile salmonids in the Columbia River estuary and ocean plume, 1977-1983. Volume I: Procedures, sampling effort, and catch data. NOAA Tech. Memo. NMFS F/NWC-74. i-x, 397 p.
- 1985b. Beach and purse seine sampling of juvenile salmonids in the Columbia River estuary and ocean plume, 1977-1983. Volume II: Data on marked recoveries. NOAA Tech. Memo. NMFS F/NWC-75. i-vii, 260 p.
- Doyle, R. W., A. J. Talbot, and R. R. Nicholas.
1987. Statistical interrelation of length, growth, and scale circulus spacing: appraisal of a growth rate estimator for fish. *Can. J. Fish. Aquat. Sci.* 44:1520-1528.
- Emmett, R. L., and R. D. Brodeur.
2000. Recent changes in the pelagic nekton community off Oregon and Washington in relation to some physical oceanographic conditions. *North Pacific Anad. Fish. Comm. Bull.* 2:11-20.
- Fisher, J. P., and W. G. Pearcy.
1988. Growth of juvenile coho salmon (*Oncorhynchus kisutch*) in the ocean off Oregon and Washington, USA, in years of differing coastal upwelling. *Can. J. Fish. Aquat. Sci.* 45:1036-1044.
1990. Spacing of scale circuli versus growth rate in young coho salmon. *Fish. Bull.* 88:637-643.
- Friedland, K. D., and R. E. Haas.
1996. Marine post-smolt growth and age at maturity of Atlantic salmon. *J. Fish Biol.* 48:1-15.
- Friedland, K. D., L. P. Hansen, D. A. Dunkley, and J. C. MacLean.
2000. Linkage between ocean climate, post-smolt growth, and survival of Atlantic salmon (*Salmo salar* L.) in the North Sea area. *ICES Journal of Marine Science.* 57:419-429.
- Friedland, K. D., and D. G. Reddin.
2000. Growth patterns of Labrador Sea Atlantic salmon post-smolts and the temporal scale of recruitment synchrony for North American salmon stocks. *Can. J. Fish. Aquat. Sci.* 57:1181-1189.
- Friedland, K. D., D. G. Reddin, and J. F. Kocik.
1993. Marine survival of North American and European Atlantic salmon: effects of growth and environment. *ICES J. Mar. Sci.* 50:481-492.
- Fukuwaka, M., and M. Kaeriyama.
1997. Scale analyses to estimate somatic growth in sockeye salmon, *Oncorhynchus nerka*. *Can. J. Fish. Aquat. Sci.* 54:631-636.
- Glenn, C. L., and J. A. Mathias.
1985. Circuli development on body scales of young pond-reared walleye (*Stizostedion bitreum*). *Can. J. Zool.* 63:912-915.
- Hare, S. R., N. J. Mantua, and R. C. Francis.
1999. Inverse production regimes: Alaska and West Coast Pacific salmon. *Fisheries* 24:6-15.
- Healey, M. C.
1982. Timing and relative intensity of size-selective mortality of juvenile chum salmon (*Oncorhynchus keta*) during early sea life. *Can. J. Fish. Aquat. Sci.* 39:952-957.
- Hobday, A. J., and G. W. Boehlert.
2001. The role of coastal ocean variation in spatial and temporal patterns in survival and size of coho salmon (*Oncorhynchus kisutch*). *Can. J. Fish. Aquat. Sci.* 58:2021-2036.
- Holtby, L. B., B. C. Andersen, and R. K. Kadawaki.
1990. Importance of smolt size and early ocean growth to interannual variability in marine survival of coho salmon (*Oncorhynchus kisutch*). *Can. J. Fish. Aquat. Sci.* 47:2181-2194.
- Ishida, Y., S. Ito, Y. Ueno, and J. Sakai.
1998. Seasonal growth patterns of Pacific salmon (*Oncorhynchus* spp.) in offshore waters of the North Pacific Ocean. *N. Pac. Anad. Fish. Comm. Bull.* 1:66-80.
- Jaenicke, H. W., M. J. Jaenicke, and G. T. Oliver.
1994. Predicting northern southeast Alaska pink salmon returns by early marine scale growth, p. 97-110. North-

- east Pacific pink and chum salmon workshop, Alaska Sea Grant Prog., Alaska Univ., Fairbanks, AK.
- Johnson, S. L.
1988. The effects of the 1983 El Niño on Oregon's coho (*Oncorhynchus kisutch*) and chinook (*O. tshawytscha*) salmon. *Fish. Res.* 6:105-123.
- Litvak, M. K., and W. C. Leggett.
1992. Age and size-selective predation on larval fishes: the bigger-is-better hypothesis revisited. *Mar. Ecol. Prog. Ser.* 81:13-24.
- Mathews, S. B., and Y. Ishida.
1989. Survival, ocean growth and ocean distribution of differentially timed releases of hatchery coho salmon (*Oncorhynchus kisutch*). *Can. J. Fish. Aquat. Sci.* 46:1216-1226.
- Matria, T. A. J. Talbot and R. W. Doyle.
1989. Instantaneous growth rate of tilapia genotypes in undisturbed aquaculture systems. I. "Red" and "grey" morphs in Indonesia. *Aquaculture* 77:295-306.
- Mantua, N. J., S. R. Hare, Zhang, Y., J. M. Wallace and F. C. Francis.
1997. A Pacific interdecadal climate oscillation with impacts on salmon production. *Bull. Am. Meteorol. Soc.* 78:1069-1080.
- Miller, T. J., L. B. Crowder, J. A. Rice, and E. A. Marschall.
1988. Larval size and recruitment mechanisms in fishes: toward a conceptual framework. *Can. J. Fish. Aquat. Sci.* 45:1657-1670.
- Parker, R. R.
1971. Size selective predation among juvenile salmonid fishes in a British Columbia inlet. *J. Fish. Res. Board Can.* 28:1503-1510.
- Pearcy, W., J. Fisher, R. Brodeur, and S. Johnson.
1985. Effects of the 1983 El Niño on coastal nekton off Oregon and Washington. In *El Niño North, Niño effects in the eastern subarctic Pacific Ocean*, p. 188-204. Washington Sea Grant Program, Univ. Washington, Seattle, WA.
- Pearcy, W. G., and J. P. Fisher.
1988. Migrations of coho salmon, *Oncorhynchus kisutch*, during their first summer in the ocean. *Fish. Bull.* 86:173-195.
1990. Distribution and abundance of juvenile salmonids off Oregon and Washington, 1981-1985. NOAA Tech. Rep. NMFS 93, 83 p.
- Pyper, B. J., R. M. Peterman, M. F. Lapointe, and C. J. Walters.
1999. Patterns of covariation in length and age at maturity of British Columbia and Alaska sockeye salmon (*Oncorhynchus nerka*) stocks. *Can. J. Aquat. Sci.* 56:1046-1057.
- Ricker, W. E.
1973. Linear regressions in fishery research. *J. Fish. Res. Board Can.* 30:409-434.
1992. Back-calculation of fish lengths based on proportionality between scale and length increments. *Can. J. Fish. Aquat. Sci.* 49:1018-1026.
- Scarnecchia, D. L.
1979. Variation of scale characteristics of coho salmon with sampling location on the body. *Prog. Fish-Cult.* 41:132-135.
- Sogard, S. M.
1997. Size-selective mortality in the juvenile stage of teleost fishes: a review. *Bull. Mar. Sci.* 60:1129-1157.
- Sokal, R. R., and F. J. Rohlf
1995. *Biometry. The principles and practice of statistics in biological research*, 3rd ed., 887 p. W. H. Freeman and Company, New York, NY.
- Talbot, A. J., and R. W. Doyle.
1992. Statistical interrelation of length, growth, and scale circulus spacing: use of ossification to detect nongrowing fish. *Can. J. Fish. Aquat. Sci.* 49:701-707.
- Teel, D. J., D. M. Van Doornik, D. R. Kuligowski, and W. S. Grant.
2003. Genetic analysis of juvenile coho salmon (*Oncorhynchus kisutch*) off Oregon and Washington reveals few Columbia River wild fish. *Fish. Bull.* 101:640-652.
- Weitkamp, L., and K. Neely.
2002. Coho salmon (*Oncorhynchus kisutch*) ocean migration patterns: insight from marine coded-wire tag recoveries. *Can. J. Fish. Aquat. Sci.* 59:1100-1115.
- Weitkamp, L. A., T. C. Wainwright, G. J. Bryant, G. B. Milner, D. J. Teel, R. G. Kope, and R. S. Waples.
1995. Status review of coho salmon from Washington, Oregon, and California. NOAA Tech. Memo. NMFS-NWFSC-24, 258 p.
- Willette, T. M.
1996. Impacts of the Exxon Valdez oil spill on the migration, growth, and survival of juvenile pink salmon in Prince William Sound. *Am. Fish. Soc. Symp.* 18:533-550.
2001. Foraging behaviour of juvenile pink salmon (*Oncorhynchus gorbuscha*) and size-dependent predations risk. *Fish. Oceanogr.* 10(Suppl. 1):110-131.

Abstract—Metal-framed traps covered with polyethylene mesh used in the fishery for the South African Cape rock lobster (*Jasus lalandii*) incidentally capture large numbers of undersize (<75 mm CL) specimens. Air-exposure, handling, and release procedures affect captured rock lobsters and reduce the productivity of the stock, which is heavily fished. Optimally, traps should retain legal-size rock lobsters and allow sublegal animals to escape before traps are hauled. Escapement, based on lobster morphometric measurements, through meshes of 62 mm, 75 mm, and 100 mm was investigated theoretically under controlled conditions in an aquarium, and during field trials. SELECT models were used to model escapement, wherever appropriate. Size-selectivity curves based on the logistic model fitted the aquarium and field data better than asymmetrical Richards curves. The lobster length at 50% retention (L_{50}) on the escapement curve for 100-mm mesh in the aquarium (75.5 mm CL) approximated the minimum legal size (75 mm CL); however estimates of L_{50} increased to 77.4 mm in field trials where trap-entrances were sealed, and to 82.2 mm where trap-entrances were open. Therefore, rock lobsters that cannot escape through the mesh of sealed field traps do so through the trap entrance of open traps. By contrast, the wider selection range and lower L_{25} of field, compared to aquarium, trials ($SR=8.2$ mm vs. 2.6 mm; $L_{25}=73.4$ mm vs. 74.1 mm), indicate that small lobsters that should be able to escape from 100-mm mesh traps do not always do so. Escapement from 62-mm mesh traps with open entrance funnels increased by 40–60% over sealed traps. The findings of this study with a known size distribution, are related to those of a recent indirect (comparative) study for the same species, and implications for trap surveys, commercial catch rates, and ghost fishing are discussed.

Manuscript submitted 20 March 2003 to the Scientific Editor.

Manuscript approved for publication 1 July 2003 by the Scientific Editor.

Fish Bull. 103:52–62 (2005).

Escapement of the Cape rock lobster (*Jasus lalandii*) through the mesh and entrance of commercial traps

Johan C. Groeneveld

Marine and Coastal Management
5th floor Foretrust Building
Martin Hamerschlacht Street, Foreshore
Cape Town, South Africa
E-mail address: Jgroenev@deat.gov.za

Jimmy P. Khanyile

National Research Foundation
P.O. Box 2600
Pretoria 0001, South Africa

David S. Schoeman

Department of Zoology
University of Port Elizabeth
Port Elizabeth 6031, South Africa

The traps used in lobster and crab fisheries are a versatile fishing gear that can be modified to target specific species and size ranges through choice of design and bait (Miller, 1990). Selection by traps of only the desired size classes reduces sorting time and may increase the catch rates of legal-size animals (Fogarty and Borden, 1980; Everson et al., 1992; Rosa-Pacheco and Ramirez-Rodriguez, 1996). Capture, sorting and release procedures have furthermore been implicated in accidental and stress-induced mortalities (Brown and Caputi, 1983; 1985; Hunt et al., 1986), as well as in sublethal injuries, such as limb loss (legs or antennae), which may retard somatic growth (Davis, 1981; Brown and Caputi, 1985). Air exposure, even over short periods, can induce behavioral changes such as reduced responsiveness to threatening stimuli (Vermeer, 1987) and lead to higher predation risk among released animals (Brown and Caputi, 1983). Furthermore, displacement from home reefs disrupts feeding behavior and can affect growth increments (Brown and Caputi, 1985). Managers of many crustacean trap fisheries have responded to these problems by introducing escape vents of various sizes and shapes (Krouse, 1989;

Miller, 1990; Everson et al., 1992; Arana and Ziller, 1994; Rosa-Pacheco and Ramirez-Rodriguez, 1996; Treble et al., 1998; Schoeman et al., 2002a), because they successfully allow undersize specimens to escape (Arana and Ziller, 1994; Treble et al. 1998).

In fisheries management, size selectivity curves are important for estimates of incidental mortality, recruitment in yield-per-recruit analysis, and age- and length-based population models (Millar and Fryer, 1999). Notably, size selectivity can be used to evaluate the minimum legal size (MLS) and the effects of changing escape vent or mesh size regulations on the future productivity of the resource (Treble et al., 1998).

Most selectivity studies on which mesh- or escape vent size are based are comparative (indirect), implying that the size distribution of the population is unknown and that variants of the same gear type are fished simultaneously (Millar and Fryer, 1999). Results from indirect studies can, however, be influenced by trap soak times, trap saturation effects (Miller, 1990), seasonal size and sex-specific patterns in catchability (Pollock and Beyers, 1979), and by differences in morphometric ratios of subpopulations (Fogarty and Borden,

1980; Maynard et al., 1987). These disadvantages are offset by the convenience with which indirect studies measure selectivity under operational conditions. Far fewer direct studies, in which the size distribution of the fished population is known (Millar and Fryer, 1999), have been published, and those that have been published have included several laboratory studies where the escape of crustaceans from traps was monitored (Krouse and Thomas, 1975; Krouse, 1978; Everson et al., 1992). Direct studies do not recreate true commercial conditions, but rather provide a contact-selectivity curve (or retention curve) that quantifies the difference in length distribution between the catch and the population of fish coming in contact with the gear (Millar and Fryer, 1999). This information is useful as a benchmark against which operational, seasonal, and spatial selectivity patterns can be measured.

Commercial fishing for the South African Cape rock lobster (*Jasus lalandii*) originated in the late nineteenth century and reached its pinnacle in the 1950s, when nearly 11,000 tons were landed annually (Pollock, 1986). However, since then catches have declined markedly, especially during the 1990s, when annual catch restrictions based on the assumption of decreased population strength, reduced the yield to 2000–3000 tons per year (Pollock et al., 2000). In response to these operational changes, several recent modifications have been made to the regulations governing gear used in the fishery (Schoeman et al., 2002b). The changes most pertinent to this study took place in 1984, when mesh size was increased from 62 to 100 mm (stretched) to reduce the relative catch of undersize *J. lalandii* (Schoeman et al., 2002b), and during the early 1990s, when the minimum size limit was reduced from its historic level of 89 mm carapace length (CL) to 75 mm CL (Cockcroft and Payne, 1999; Pollock et al., 2000). Despite these two measures, the proportion of the commercial catch <75 mm CL that has to be released remains around 35–40% (MCM¹). At present, the biomass of the *J. lalandii* resource that is larger than the minimum legal size is estimated at about 6% of its pristine value, whereas the spawning biomass (of mature female rock lobsters) is estimated to be 21% (Johnston, 1998). Consequently, it is clear that the resource is heavily depleted and that there is little scope for wasted production through unnecessary damage to undersize lobsters (Schoeman et al., 2002a).

Most studies on trap selectivity of *J. lalandii* (Newman and Pollock, 1969; Crous, 1976; Pollock and Beyers, 1979) predate the changes to mesh and minimum legal size described above and did not provide selectivity curves. In the only recent study, Schoeman et al. (2002a) used the SELECT (Share Each Length class's Catch Total) method (Millar, 1992; Millar and Walsh, 1992) to investigate the selectivity properties of vari-

ous modifications to commercial and research traps in comparison with the standard 100-mm stretched mesh trap design. This study was indirect, in that it simulated commercial fishing and compared catch rates in other traps to those made with a small-mesh (62 mm, stretched) trap, which acted as a control.

Several processes are involved in the selectivity of traps: namely the attraction of rock lobsters by bait; their ability to enter traps through trap openings of various sizes, shapes, and localities within the trap; their behavior in and around traps; their escapement through the trap opening and their escapement through mesh openings or escape vents (Miller, 1990). The present study focuses on escapement of captured *J. lalandii* through the mesh of stretched mesh traps and through trap entrances. The aims are to investigate the relationships between CL and other morphometric measures for male rock lobsters in order to use these relationships to estimate theoretical escapement curves for any given mesh size; to compare these curves to observed escapement rates through selected meshes in the aquarium; and to extend these comparisons to field conditions. The overall aim is to determine the optimum mesh characteristics that maximize efficiency in targeting legal-size male *J. lalandii*.

Material and methods

Mesh size of lobster traps

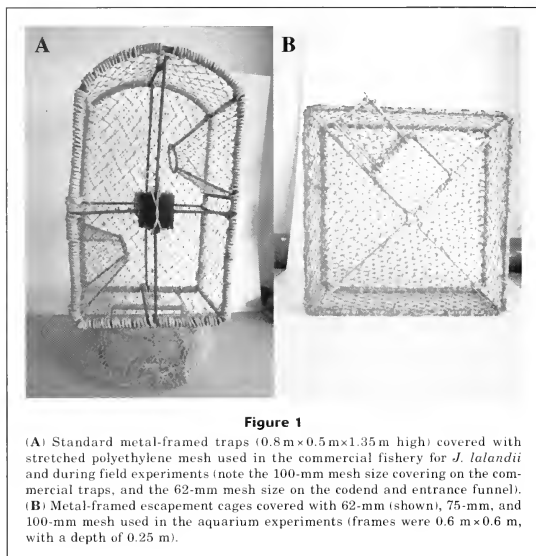
Mesh size is defined as the measurement from inside of knot to inside of knot when the net is stretched in the direction of the long diagonal of the meshes, i.e., lengthwise of the net. Netting is made of polyethylene. Commercial rock lobster traps (Fig. 1) are covered with 100-mm stretched mesh (or 50-mm bars, also measured from the insides of knots), which are stretched in such a manner over the metal frame that the openings are square.

Morphometric variables measured

Following manual trials that involved fitting lobster carapaces of different sizes through an adjustable square hole, three carapace dimensions were identified as likely to play a role in regulating escapement. These were the following: 1) carapace width (CW), measured laterally, across the widest point of the carapace; 2) carapace depth (CD), measured dorsoventrally, extending from the highest point of the dorsal carapace surface to the lowest point on the ventral surface of the thoracic plate; and 3) carapace base (CB), measured ventrally, between the distal edges of the second segment of the last walking legs, with the legs folded flush against the carapace.

Each of these dimensions was measured (± 1 mm) for each of 169 male rock lobsters caught in research traps deployed off the Cape Peninsula between 1999 and 2002. Corresponding data regarding carapace length

¹ MCM (Marine and Coastal Management). 2002. Unpubl. data. MCM, Martin Hamerschelacht St., Cape Town, South Africa.



(CL), measured mid-dorsally from the posterior edge of the carapace to the anterior tip of the rostral spine, were also collected. This was done because CL is the dimension most frequently mentioned in legislation pertaining to this species (Schoeman et al., 2002b) and has therefore been the focus of most size-based studies (Newman and Pollock, 1969; Pollock and Beyers, 1979; Schoeman et al., 2002a). Relationships between the CL and each of CW, CD, and CB were explored by using simple least-squares regression analyses.

Theoretical calculations of escapement

In order to investigate morphological characteristics that physically limit escapement through meshes of various dimensions as a function of CL, digital photographs were taken of the posterior cross section of 46 male carapaces (tail removed) covering a range of sizes between 40 mm CL and 106 mm CL. Using standard graphics software, we superimposed a square on each image to represent a square of polyethylene mesh, similar to that used in a South African rock lobster trap.

This simulated mesh was orientated so that its base was parallel with the carapace base of the lobster under consideration. It was then proportioned so that each of its sides was equal in length to the corresponding CB.

Once this procedure had been completed, the simulated mesh square was rotated and resized so that we could determine the dimensions of the smallest square through which each lobster could pass. This measure was designated the "critical mesh size" for that image.

Critical mesh size was related to CL by using simple linear regression analysis. In this way, the theoretically appropriate mesh aperture required to target all lobster larger than a given size could be predicted from the minimum CL of the target group (for convenience, this CL will be designated the "critical CL").

Aquarium trials

Having addressed the matter of whether or not lobsters theoretically should be able to escape a mesh of given dimensions, the next question to be posed is whether or not they can do so under ideal (laboratory) conditions? For these purposes, three stretched mesh sizes were considered: 1) 62 mm, which coincides with the mesh size used in the commercial fishery prior to 1984 and also with the mesh currently used on traps deployed in the Fishery Independent Monitoring Survey (FIMS) (Schoeman et al., 2002a); 2) 100 mm, which corresponds with the mesh currently used on commercial traps for *J. lalandii*; and 3) 75 mm, which was used to provide

information on selectivity for meshes of intermediate aperture dimensions.

Each of these experimental meshes was used to construct an escapement cage by stretching the mesh over a mild-steel frame in order to present square escape apertures of varying dimensions, as determined by the size of the mesh used (Fig. 1). These cages were deployed in an aquarium tank measuring 1.8 m × 1.8 m and having a depth of 1.5 m. Fresh sea water was continuously supplied to this tank by a through-flow system that regulating water temperature between 12° and 16°C, well within the natural temperature range of *J. lalandii* (Heydorn, 1969).

For each mesh size, male rock lobsters of various carapace lengths (373 lobsters measuring 34–91 mm CL for 62-mm mesh; 351 lobsters measuring 34–75 mm CL for 75-mm mesh; and 142 lobsters measuring 70–91 mm CL for 100-mm mesh) were collected live from the sea and transported to the experimental aquarium tank. Care was taken to ensure that approximately equal numbers of lobsters were available for each 2-mm size-class within the respective size ranges, although fewer lobsters tended to be available in size classes towards the ends of the frequency distributions.

Once at the aquarium, lobsters were placed inside the experimental cages in groups of up to 20 and left for 30 minutes. Individuals that did not escape during this period were gently pushed towards the mesh openings, encouraging escapement, where this was possible. Subsequently, the CL frequency distributions were determined both for those lobsters that escaped the mesh as well as those that were retained. Several replicate escapement experiments were conducted for each mesh size, but because the experimental cages were too small to hold large numbers of lobsters, replicate selection curves could not be computed. Instead, all data were pooled for each mesh size for further analyses.

Field trials

The final question to be posed is whether or not lobsters do escape from traps when afforded the opportunity to do so under field conditions? To address this problem, field trials were undertaken off the Western Cape Peninsula during monthly sampling sessions conducted by the research vessel *Sardinops* in July 2000 and from December 2001 to March 2002—a total of five distinct sampling surveys.

Four categories of standard rock lobster traps (Fig. 1) were employed: 1) 62-mm stretched mesh, with entrance funnels open; 2) 62-mm stretched mesh, with entrance funnels blocked by a fine-mesh insert; 3) 100-mm stretched mesh, with entrance funnels open; and 4) 100-mm stretched mesh, with entrance funnels blocked.

Duplicate bottom long-lines consisting of 10 traps each were prepared, of which six were normal commercial traps, and the remaining four were experimental traps, and these 10 traps were spread in haphazard order along the line, excluding the end traps. Into each trap was placed a sample of approximately 40 male rock

lobsters, each of which had been measured (CL) and marked by cutting a notch in its uropod. In this way, it was possible to distinguish between lobsters that had been placed in the trap and those that had entered the trap of their own accord.

Experimental traps were deployed without bait, in order to limit their ability to attract lobsters and also to remove one of the prime incentives that captive lobsters might have to remain in a trap, even when it could escape. These trap lines were soaked overnight and on their retrieval, each remaining lobster was re-measured (CL) and inspected to identify specimens that had entered the traps voluntarily. Eight replicates were completed for each of the four categories of traps.

Construction of selectivity curves

The contact-selection curves (*sensu* Millar and Fryer, 1999) for the meshes used in the laboratory and field trials were modeled by using the SELECT method (Millar and Walsh, 1992) as applied to covered codend experiments (Millar and Fryer, 1999). We felt that this approach was warranted because we collected data with respect to lobsters in both a “codend” (those retained in the traps) and a “cover” (those that escaped, but for which data were available by inference).

The logistic and Richards formulations of the general selectivity curve were fitted by using Excel (Microsoft, Redmond, WA) routines (Tokai²). These two selectivity functions were chosen because of their relative simplicity, their broad use over a range of different fisheries, and the availability of estimation routines for their parameters (Millar and Fryer, 1999).

The Richards curve has the equation

$$r(l) = \left(\frac{\exp(a+bl)}{1+\exp(a+bl)} \right)^\delta,$$

where $r(l)$ is the probability that an individual of length l attempting to pass through a mesh of given size will be retained by it (Millar and Fryer, 1999); and a , b , and δ are constants. The logistic curve is the special case of this formulation, where $\delta=1$.

According to these models, the lobster length at 50% retention (L_{50}) and the selection range ($SR=L_{75}-L_{25}$) are defined as follows:

$$L_{50} = \frac{\ln\left(\frac{0.5^\delta}{1-0.5^\delta}\right) - a}{b},$$

$$\text{simplicly to } L_{50} = -\frac{a}{b} \text{ when } \delta = 1, \text{ and}$$

² Tokai, T. 2002. Personal commun. Department of Marine Science and Technology, Tokyo University of Fisheries, Konan Minatoku, Tokyo 108, Japan.

$$SR = \frac{\ln\left(\frac{0.75^\delta}{1-0.75^\delta}\right) - \ln\left(\frac{0.25^\delta}{1-0.25^\delta}\right)}{b}$$

$$\text{simplifying to } SR = \frac{2\ln(3)}{b}, \text{ when } \delta = 1.$$

All calculations were made on the basis of 2-mm-CL size classes covering the entire size range for each frequency distribution. The 2-mm-CL size classes were used to ensure consistency across models, and also to balance data resolution against the number of size classes expected to have either zero catch or zero escapement (Millar and Fryer, 1999). Wherever necessary, hypothesis tests were conducted in accordance with the recommendations of Millar and Walsh (1992) and Millar and Fryer (1999).

Results

Morphometric relationships

Least-squares regression analysis indicated highly significant linear relationships between CL and each of the other morphometric variables measured (Fig. 2). In each case, at least 97% of the variability in the predictor variable was explained by CL, indicating a high degree of correlation among predictors. Nevertheless, for any given CL, CB was consistently the largest variable measured, whereas CD was the smallest. Furthermore, CB increased more rapidly in response to increasing CL than either CW or CD (ANCOVA: $F=115.165$; $df=2, 167$; $P<0.001$). We therefore concluded that CB would likely be the morphometric variable that limits escapement through stretched square meshes.

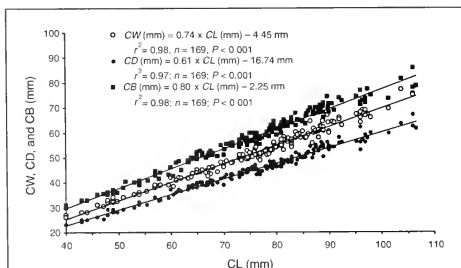


Figure 2

Individual linear relationships between carapace length (CL) and each of carapace width (CW), carapace depth (CD), and carapace base (CB) for *J. lalandii*.

Theoretical calculation of escapement

The mesh size that appeared (on the basis of visual inspection) to limit escapement was expressed as a function of CL with a simple, linear, least-squares regression model (Fig. 3). This relationship was highly significant and explained 99% of the variability in critical mesh size.

Using inverse prediction methods (Zar, 1999), we calculated the critical CL (mean \pm 95% confidence interval) from the regression model illustrated in Figure 3 for any mesh size. For 62-mm mesh, the critical CL is estimated at 43.8 (± 4.12) mm; for the 75-mm mesh the estimate is 52.3 (± 4.15) mm; whereas for the 100-mm mesh it is 68.7 (± 4.12) mm. Given the implicit assumption that lobsters smaller than the critical CL can escape, but that larger lobsters are retained, the mean critical CL can be used as an estimate of L_{50} .

Aquarium trials

No lobsters larger than 48 mm CL escaped the 62-mm mesh traps in the aquarium and none smaller than 44 mm CL were retained. This finding resulted in an extremely steep selection curve with a narrow SR (Fig. 4; Table 1). For the 75-mm mesh, no lobsters larger than 61 mm CL escaped and no lobsters smaller than 54 mm CL were retained. This finding resulted in a slightly more gentle selection curve, but with a reasonably tight SR (Fig. 4, Table 1). Similarly, for the 100-mm mesh, no lobsters larger than 79 mm CL escaped and no lobsters smaller than 74 mm CL were retained. This finding resulted in a selection curve that closely resembled that for the 75-mm mesh, except that the curve shifted a few size categories to the right (Fig. 4; Table 1).

For all meshes, the symmetrical logistic model was selected in preference to the asymmetrical Richards model (Table 1), and in all cases the selected model fitted the data reasonably well (Fig. 4). It should, however, be noted that all hypothesis tests were conducted by using the deviance residuals and their degrees of freedom for all size classes sampled. This was necessary because the very tight selection curves (especially for the 62-mm mesh) resulted in relatively small numbers of size classes in which retention probability was neither zero nor one.

The above results indicate that L_{50} -estimates for each mesh size are substantially larger than the corresponding estimates of critical CL from the theoretical escapement model. In fact, assuming that the asymptotic standard errors provided in Table 1 could be converted to 95% confidence intervals by a multiplication factor of two, only the confidence intervals for these statistics from the 62 mm mesh would overlap. By contrast, confidence intervals for the critical CL are well below those for the L_{50} for both the 75 mm mesh and the 100-mm mesh. This impression is confirmed by inspecting the probabilities of

Table 1

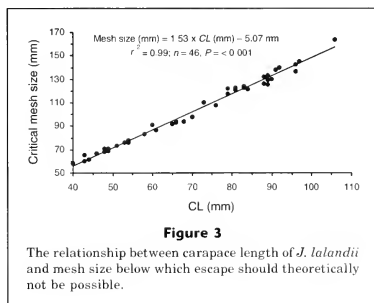
Statistics from SELECT analysis for the aquarium escapement trials. Values in parentheses are asymptotic standard errors *sensu* Millar (1993). These standard errors are provided only for the best model fits for each of the various categories of data. Note that all hypothesis tests were conducted by using deviance residuals for the full model and their degrees of freedom (see text for explanation).

	62-mm mesh		75-mm mesh		100-mm mesh	
	Logistic	Richards	Logistic	Richards	Logistic	Richards
<i>a</i>	-76.479 (23.159)	-351.538	-58.217 (10.079)	-400.075	-64.101 (11.655)	-41.224
<i>b</i> (/mm)	1.649 (0.500)	7.463	0.991 (0.173)	6.589	0.849 (0.155)	0.615
δ		6.567		13.173		0.010
<i>L</i> ₅₀ (mm)	46.389 (0.309)	46.493	58.717 (0.302)	59.333	75.459 (0.376)	75.144
<i>SR</i> (mm)	1.333 (0.404)	0.989	2.216 (0.386)	2.200	2.587 (0.471)	2.567
Selection factor	0.75		0.78		0.76	
<i>H</i> ₀ : data have binomial distribution (i.e., data are not overdispersed)						
Deviance	0.802	0.209	1.984	1.092	8.675	6.435
df	27	26	19	18	12	11
<i>P</i> -value	1	1	0.999	0.728	0.730	0.843
<i>H</i> ₀ : $\delta=1$						
Deviance	0.593		0.892		2.240	
df	1		1		1	
<i>P</i> -value	0.441		0.345		0.134	

retention, $r(t)$, by each mesh size of a lobster at its corresponding mean critical CL. For the 62-mm mesh this probability is 0.014 (0.926 at the upper 95% confidence limit for the critical CL); for the 75-mm mesh it is 0.002 (0.096 at the upper 95% confidence limit for the critical CL); and for the 100-mm mesh it is 0.003 (0.099 at the upper 95% confidence limit for the critical CL).

Field trials

Escapement from traps with 62-mm mesh was highly variable both for the traps with entrance funnels left open, as well as for those with entrance funnels that were sealed, but was surprisingly high for the latter (Fig. 5). Furthermore, it is clear that the relationship between proportion of lobsters retained and CL was not logistic, as it was for the larger mesh sizes (Figs. 5 and 6). Instead, simple, least squares regression analysis indicated linear relationships between these variables both for traps with open entrance funnels as well as for those with entrance funnels closed (Fig. 5). There was no difference between the slopes ($t=1.138$; $df=10$; $P=0.282$; common slope=0.795/mm), although their intercepts did differ significantly ($t=14.079$; $df=11$; $P<0.001$).



No lobsters smaller than 62 mm CL were retained in the 100-mm mesh traps with open entrances, and no upper size limit was reached beyond which escapement was completely eliminated. By contrast, when the entrance funnels to the traps were sealed, no lobsters smaller than 64 mm CL were retained and no lobsters

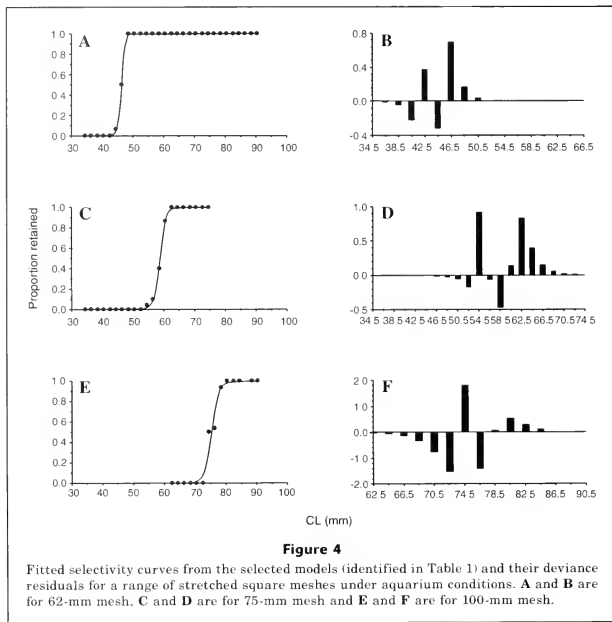


Figure 4

Fitted selectivity curves from the selected models (identified in Table 1) and their deviance residuals for a range of stretched square meshes under aquarium conditions. A and B are for 62-mm mesh. C and D are for 75-mm mesh and E and F are for 100-mm mesh.

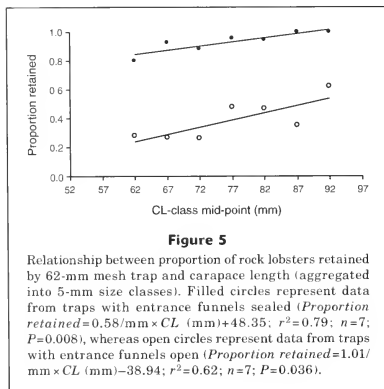


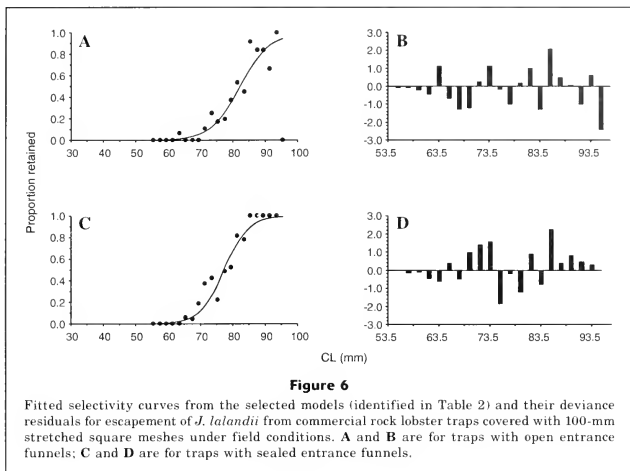
Figure 5

Relationship between proportion of rock lobsters retained by 62-mm mesh trap and carapace length (aggregated into 5-mm size classes). Filled circles represent data from traps with entrance funnels sealed ($Proportion\ retained = 0.58/mm \times CL\ (mm) + 48.35$; $r^2 = 0.79$; $n = 7$; $P = 0.008$), whereas open circles represent data from traps with entrance funnels open ($Proportion\ retained = 1.01/mm \times CL\ (mm) - 38.94$; $r^2 = 0.62$; $n = 7$; $P = 0.036$).

larger than 84 mm CL escaped. This resulted in contact selectivity curves for which estimates of both L_{50} and SR decreased when captive lobsters were denied the opportunity to escape through the entrance funnels (Fig. 6; Table 2). This finding indicates that considerable numbers of lobsters of all sizes can escape commercial traps by the entrance funnels.

Irrespective of whether the entrance funnels of the traps was sealed, the symmetrical logistic model was selected in preference to the asymmetrical Richards model (Table 2), and the selected model fitted the data reasonably well (Fig. 6; Table 2), although not as well as the models fitted to the aquarium data (Fig. 4; Table 1).

In comparison with the selectivity curves from the aquarium trials with 100-mm mesh, the corresponding curves from field trials indicated that greater numbers of larger lobsters are retained in practice than under laboratory conditions (Figs. 4 and 6). This finding indicates that some lobsters are retained in commercial traps, even though they can escape, which goes some way to explaining the more "scattered" fit of the logistic model compared to the field data.



Discussion

This study focuses on escapement of Cape rock lobster (*J. lalandii*) through mesh openings, and on escapement through the trap entrance of commercial traps. Three questions were initially posed, namely: through what mesh size, in theory, can a lobster of given CL escape; are lobsters physically able to escape through this theoretical mesh size, or are there other factors such as orientation and mobility of lobster appendages that prevent escapement; and what proportion of sublegal and legal size lobsters escape through the mesh and trap entrance of commercial traps? In brief, the results showed a weak leak between theoretical values and the ability of the lobsters to escape.

Carapace base (CB) was isolated as the dimension most likely to limit escapement through stretched square meshes. This dimension superceded carapace width and depth, which have been more widely assumed to be the limiting factors to escapement of lobsters (Treble et al., 1998), mainly because our measurement included the width of the last pair of walking legs, folded flush against the carapace. Experimenting with lobster carapaces and an adjustable square hole showed that the joints of these appendages protrude ventrolaterally from the carapace, and the orientation and limited mobility of these appendages would prevent the lobster from escaping. Nevertheless, our theoretical escapement model included all three measurements in the underlying computer simulations to determine the appropriate

mesh aperture required to target all lobsters larger than a given size.

The theoretical escapement model produced surprisingly small values of "critical CL" for all three mesh sizes in comparison with the corresponding selectivity curves from the aquarium experiment. This result implies that many rock lobsters that should theoretically not have been able to escape, did so in the aquarium trials. We therefore concluded that the theoretical model was weak and that the mechanics of escapement appear to be more complex than can be shown by simple measurements of the carapace dimensions and may rely also on the orientation of lobsters during escapement (Stasko, 1975).

Selectivity curves developed from aquarium data indicated that an 85-mm-CL lobster should not have been able to escape a 100-mm mesh trap. However, field data indicated that escapement from 100-mm mesh traps with sealed trap openings exceeded 10%. Thus, rock lobsters that should not have been able to escape, according to aquarium experiments, did escape under field conditions. This result was expected, because the mesh of traps used in the commercial fishery (and field experiments) is often unevenly stretched across the metal trap-frame, and therefore some openings lose their square dimensions. This unevenness in the stretch of the mesh was clearly illustrated by a random sample of 40 knot-to-knot aperture measurements from four 100-mm mesh commercial traps, which had diagonal dimensions significantly larger than the 70.71 mm predicted

by Pythagoras's theorem ($t=4.470$; $df=39$; $P<<0.001$). In addition, repairs to torn meshes often leave openings that are somewhat larger than 100 mm and that are not square (Groeneveld, personal. observ.). The wider *SR* of the selectivity curve for field data compared to the tight *SR* of the aquarium curves supports this "unevenly stretched mesh" hypothesis.

Paradoxically, a 70-mm-CL lobster, which has a 1% chance of being retained by a 100 mm mesh in the laboratory has an 11% probability of being retained by a trap with the same mesh in the field (even when its entrances are sealed). Thus, some rock lobsters that should, and could have escaped through the 100 mm mesh of the field traps did not. Schoeman et al. (2002a) suggested that small rock lobsters that can escape do not always do so because they use the trap as a refuge against predators. Alternatively, overnight soak times (as used in the field trials) may be too short for all the small rock lobsters to escape. The probability of

escape is much reduced during hauling because captive specimens are then pressed into a tight mass within the fine-mesh (62-mm) codend of the trap.

No escapement from sealed 62-mm mesh traps was expected during field trials, based on the aquarium L_{50} of 46.4 (± 0.3) mm and the size range of lobsters used in the field (60 mm–95 mm CL). Nevertheless, small losses (0–18%, depending on lobster size; see Fig. 5) did occur. Only two explanations are possible, namely: 1) that lobsters still managed to escaped through the mesh of the sealed 62-mm traps, despite precautions taken to ensure that the meshes of these traps were undamaged and that trap openings were properly sealed; and 2) that some individuals sustained injuries during exposure and handling, and subsequently were cannibalized by the healthy rock lobsters in the traps. This second conclusion is supported by the presence of shell fragments observed in traps after their retrieval. Because these regressions had the same positive slopes, it seems likely that smaller rock lobsters would be more susceptible to injury and cannibalism than larger animals, and their susceptibility holds irrespective of whether the trap entrance is sealed or not.

Escapement from 62-mm mesh traps with open entrance funnels increased by 40–60% compared to escapement from traps with sealed traps (Fig. 5). This finding has significant implications for the FIMS, which relies on catches made by 62-mm mesh traps and is conducted annually as a measure of the relative abundance of the *J. lalandii* resource. During a survey, it is assumed that all the Cape rock lobsters that are captured are retained and that trap-selection is uniform across all the size classes of these lobsters (Johnston, 1998). It appears that neither of these two assumptions can be met: significant escapement does occur through the trap entrance and there is a greater retention of larger specimens than smaller specimens.

When the trap entrance was left open in the 100-mm mesh field trials, L_{50} increased to 82.3 mm (from 77.4 mm in sealed traps), thus indicating that captive Cape rock lobsters can and do use the trap entrance of commercial traps to escape. The open traps also have a wider *SR* of 10.1 mm (compared to 8.2 mm in sealed traps), and therefore animals with a CL of >87 mm ($L_{75}=87.3$ mm), which are very unlikely to be able to get through the mesh apertures, will still be able to use the trap entrance to exit. The presence of this escape vent implies that there is little danger of ghost-fishing when using this trap type and that Cape rock lobsters of all sizes should be able to vacate the trap once the bait has been consumed. From a commercial viewpoint, however, the problem of leaving traps in the water for too long is that legal-size specimens, which cannot fit through the mesh, will escape through the entrance, thus decreasing catch rates considerably.

The aquarium result ($L_{50}=75.1$ mm) is considered the most accurate direct measurement of the selectivity of 100-mm square mesh for *J. lalandii*, because care was taken to ensure that the mesh was stretched

Table 2

Statistics from SELECT analysis for the field escapement trials. Values in parentheses are asymptotic standard errors *sensu* Millar (1993). These standard errors are provided only for the best model fits for each of the various categories of data. Note that all hypothesis tests were conducted by using deviance residuals for the full model and their degrees of freedom (see text for explanation).

	100-mm mesh		100-mm mesh	
	Trap-entrance open		Trap-entrance sealed	
	Logistic	Richards	Logistic	Richards
<i>a</i>	-17.856 (2.460)	-14.299	-20.801 (2.437)	-51.967
<i>b</i> (mm)	0.217 (0.031)	0.181	0.2686 (0.031)	0.626
δ		0.641		4.238
L_{50} (mm)	82.274 (0.379)	82.222	77.444 (0.379)	78.458
<i>SR</i> (mm)	10.124 (0.498)	10.809	8.181 (0.498)	7.997
Selection factor	0.82		0.77	
H_0 : data have binomial distribution (i.e., data are not overdispersed)				
Deviance	21.593	21.257	18.698	15.807
df	19	18	17	16
<i>P</i> -value	0.305	0.267	0.346	0.467
H_0 : $\delta = 1$				
Deviance	0.336		2.891	
df	1		1	
<i>P</i> -value	0.562		0.090	

evenly with square openings across the metal trap-frame and because we made sure that all lobsters that could escape, did, resulting in a tight SR of 2.6 mm. This L_{50} is remarkably close to the present MLS of 75 mm CL for the commercial fishery, especially considering that 100-mm mesh was first used when the MLS was 89 mm CL, and that the commercial mesh size remained at 100 mm despite the 14 mm CL reduction in MLS during the early 1990s (Schoeman et al., 2002b). The L_{50} obtained from the field trials with sealed trap openings (77.4 mm) was also close to the present MLS.

In a recent indirect study (i.e., where the size composition of a population was unknown) Schoeman et al. (2002a) found L_{50} to be 79.2 mm ($SR=11.1$ mm) under commercial operational conditions. The increase in L_{50} (above the 75.1 mm and 77.4 mm found in the direct aquarium and field studies, respectively) is the result of the trap entrances of commercial traps remaining open, so that rock lobsters that are too large to fit through the mesh can still escape through the entrance. In the present direct study, this factor increased the L_{50} from 77.5 mm (sealed entrance) to 82.2 mm (open entrance) for 100-mm mesh. Thus, one conclusion of the indirect study, namely that the South African fishery for *J. lalandii* is unusual in that standard commercial traps are covered with mesh having an aperture considerably wider ($L_{50}=79.2$ mm CL) than that required to retain Cape rock lobsters of the current MLS (Schoeman et al., 2002a), must now be seen in a different light. The selectivity of the 100-mm stretched mesh itself now appears not to be wider than that which is currently required (based on the direct results). Rather, the indirectly determined L_{50} appears to have been inflated by the numbers of larger lobsters that were able to escape through the trap entrance.

Direct studies of the escapement of crustaceans from pots (Krouse and Thomas, 1975; Krouse, 1978; Everson et al., 1992) have often been criticized because these studies themselves may affect the behavior of the animals and do not include the dynamics of the processes of entry and escapement (Xu and Millar, 1993; Treble et al., 1998). We recognize these weaknesses, but felt that direct studies remain useful because they can be used to set a theoretical benchmark against which the results of indirect studies can be tested, especially if the trap selectivity of the latter depends on area and season. Various insights were gained from the present study, particularly because it closely followed an indirect study of trap selectivity for *J. lalandii* (Schoeman et al., 2002a). In conclusion, this study of escapement of *J. lalandii* through square meshes showed 1) that 100-mm mesh size is, theoretically, near optimal for the fishery; 2) that many Cape rock lobsters that are able to escape through the mesh do not do so; 3) that the rock lobsters that are shown theoretically to be unable to escape through the mesh of commercial traps, often can do so; and 4) that specimens too large to escape through the mesh can escape through the trap entrance.

Acknowledgments

This study would not have been possible without the funding and infrastructure provided by Marine and Coastal Management (Department of Environmental Affairs and Tourism, South Africa). In particular, we would like to thank our colleagues, Steven McCue, Neil van den Heever, and Danie van Zyl for technical support. We are also grateful to the skipper and crew of the research vessel *Sardinops*, which was used to conduct the field trials. J.P.K. received financial assistance from the Fridtjof Nansen and NORAD, and would like to thank his supervisors, Anders Ferno and Geir Blom, at the University of Bergen in Norway, for their assistance with an earlier draft of this manuscript. D.S.S. thanks the University of Port Elizabeth for support in terms of finance and infrastructure. Finally, the constructive comments of three anonymous referees are acknowledged; these aided substantially in clarifying certain parts of the original manuscript.

Literature cited

- Arana, P. E., and S. V. Ziller.
1994. Modelling the selectivity of traps in the capture of spiny lobster (*Jasus frontalis*), in the Juan Fernandez archipelago (Chile). *Investigación pesq.*, Santiago 38:1-21.
- Brown, R. S., and N. Caputi.
1983. Factors affecting the recapture of undersize western rock lobster *Panulirus cygnus* George returned by fishermen to the sea. *Fish. Res.* 2:103-128.
1985. Factors affecting the growth of undersize western rock lobster, *Panulirus cygnus* George, returned by fishermen to the sea. *Fish. Bull.* 83:567-574.
- Cockcroft, A. C., and A. I. L. Payne.
1999. A cautious fisheries management policy in South Africa: the fisheries for rock lobster. *Mar. Policy* 23(6):587-600.
- Crous, H. B.
1976. A comparison of the efficiency of escape gaps and deck grid sorters for the selection of legal-sized rock lobsters *Jasus lalandii*. *Fish. Bull. S. Afr.* 8:5-12.
- Davis, G. E.
1981. Effects of injuries on spiny lobster, *Panulirus argus*, and implications for fishery management. *Fish. Bull.* 78:979-984.
- Everson, A. R., R. A. Skillman, and J. J. Polovina.
1992. Evaluation of rectangular and circular escape vents in the northwestern Hawaiian Islands lobster fishery. *N. Am. J. Fish. Manag.* 12:161-171.
- Fogarty, M. J., and V. D. Borden.
1980. Effects of trap-venting on gear selectivity in the inshore Rhode Island American lobster, *Homarus americanus*, fishery. *Fish. Bull.* 77:925-933.
- Heydorn, A. E. F.
1969. The rock lobster of the South African west coast *Jasus lalandii* (H. Milne-Edwards): 2. Population studies, behaviour, reproduction, moulting, growth and migration. *Invest. Rep. Div. Sea Fish. S. Afr.* 71, 52 p.
- Hunt, J. H., W. G. Lyons, and F. S. Kennedy.
1986. Effects of exposure and confinement on spiny

- lobsters, *Panulirus argus*, used as attractants in the Florida trap fishery. Fish. Bull. 84:69-76.
- Johnston, S. J.
1998. The development of an operational management procedure for the South African west coast rock lobster fishery. Ph.D. diss., 370 p. Univ. Cape Town, Cape Town, South Africa.
- Krouse, J. S.
1978. Effectiveness of escape vent shape in traps for catching legal-sized lobster, *Homarus americanus*, and harvestable-sized crabs, *Cancer borealis* and *Cancer irroratus*. Fish. Bull. 76:425-432.
1989. Performance and selectivity of trap fisheries for crustaceans. In Marine invertebrate fisheries: their assessment and management (J. F. Caddy, ed.), p. 307-325. Wiley, New York, NY.
- Krouse, J. S., and J. C. Thomas.
1975. Effects of trap-selectivity and some lobster population parameters on size composition of the American lobster, *Homarus americanus* catch along the Maine coast. Fish. Bull. 73:862-871.
- Maynard, D. R., N. Branch, Y. Chiasson, and G. Y. Conan.
1987. Comparison of three lobster (*Homarus americanus*) trap escape mechanisms and application of a theoretical retention curve for these devices in the southern Gulf of St. Lawrence lobster fishery. Canadian Atlantic Fisheries Scientific Advisory Committee, Research Document, 87/87, 34 p.
- Millar, R. B.
1992. Estimating the size-selectivity of fishing gear by conditioning on the total catch. J. Am. Stat. Assoc. 87: 962-968.
1993. Analysis of trawl selectivity studies (addendum): implementation in SAS. Fish. Res. 17:373-377.
- Millar, R. B., and R. J. Fryer.
1999. Estimating the size-selection curves of towed gears, traps, nets and hooks. Revs. Fish Biol. Fish. 9:89-116.
- Millar, R. B., and S. J. Walsh.
1992. Analysis of trawl selectivity studies with an application to trouser trawls. Fish. Res. 13:205-220.
- Miller, R. J.
1990. Effectiveness of crab and lobster traps. Can. J. Fish. Aquat. Sci. 47:1228-1251.
- Newman, G. G., and D. E. Pollock.
1969. The efficiency of rock lobster fishing gear. S. Afr. Shipp. News Fish. Ind. Rev. 24(6):79-81.
- Pollock, D. E.
1986. Review of the fishery for and biology of the Cape rock lobster *Jasus lalandii* with notes on larval recruitment. Can. J. Fish. Aquat. Sci. 43(11):2107-2117.
- Pollock, D. E., and C. J. de B. Beyers.
1979. Trap selectivity and seasonal catchability of rock lobster *Jasus lalandii* at Robben Island sanctuary, near Cape Town. Fish. Bull. S. Afr. 12:75-77.
- Pollock, D. E., A. C. Cockcroft, J. C. Groeneveld, and D. S. Schoeman.
2000. The commercial fisheries for *Jasus* and *Palinurus* species in the south-east Atlantic and south-west Indian oceans. In Spiny lobsters: fisheries and culture (B. F. Phillips and J. Kittaka, eds.), p. 105-120. Blackwell Science, UK.
- Rosa-Pacheco, R. D. L., and M. Ramirez-Rodriguez.
1996. Escape vents in traps for the fishery of the California spiny lobster, *Panulirus interruptus*, in Baja California Sur, Mexico. Cienc. Mar., Baja Calif., Mex. 22:235-243.
- Schoeman, D. S., A. C. Cockcroft, D. L. Van Zyl, and P. C. Goosen.
2002a. Trap selectivity and the effects of altering gear design in the South African rock lobster *Jasus lalandii* commercial fishery. S. Afr. J. Mar. Sci. 24:37-48.
- 2002b. Changes to regulations and the gear used in the South African commercial fishery for *Jasus lalandii*. S. Afr. J. Mar. Sci. 24:365-370.
- Stasko, A. B.
1975. Modified lobster traps for catching crabs and keeping lobsters out. J. Fish. Res. Board Can. 32(12): 2515-2520.
- Treble, R. J., R. B. Millar, and T. I. Walker.
1998. Size-selectivity of lobster pots with escape-gaps: application of the SELECT method to the southern rock lobster (*Jasus edwardsii*) fishery in Victoria, Australia. Fish. Res. 34:289-305.
- Vermeer, G. K.
1987. Effects of air exposure on desiccation rate, hemolymph chemistry, and escape behaviour of the spiny lobster, *Panulirus argus*. Fish. Bull. 85:45-51.
- Xu, X., and R. B. Millar.
1993. Estimation of trap selectivity for male snow crab (*Chionoecetes opilio*) using the SELECT modeling approach with unequal sampling effort. Can. J. Fish. Aquat. Sci. 50:2485-2490.
- Zar, J. H.
1999. Biostatistical analysis, 663 p. Prentice-Hall, Inc., Englewood Cliffs, NJ.

Abstract—The recent development of the pop-up satellite archival tag (PSAT) has allowed the collection of information on a tagged animal, such as geolocation, pressure (depth), and ambient water temperature. The success of early studies, where PSATs were used on pelagic fishes, has spurred increasing interest in the use of these tags on a large variety of species and age groups. However, some species and age groups may not be suitable candidates for carrying a PSAT because of the relatively large size of the tag and the consequent energy cost to the study animal. We examined potential energetic costs to carrying a tag for the cownose ray (*Rhinoptera bonasus*). Two forces act on an animal tagged with a PSAT: lift from the PSATs buoyancy and drag as the tag is moved through the water column. In a freshwater flume, a spring scale measured the total force exerted by a PSAT at flume velocities from 0.00 to 0.60 m/s. By measuring the angle of deflection of the PSAT at each velocity, we separated total force into its constituent forces—lift and drag. The power required to carry a PSAT horizontally through the water was then calculated from the drag force and velocity. Using published metabolic rates, we calculated the power for a ray of a given size to swim at a specified velocity (i.e., its swimming power). For each velocity, the power required to carry a PSAT was compared to the swimming power expressed as a percentage, %TAX (Tag Altered eXertion). A %TAX greater than 5% was felt to be energetically significant. Our analysis indicated that a ray larger than 14.8 kg can carry a PSAT without exceeding this criterion. This method of estimating swimming power can be applied to other species and would allow a researcher to decide the suitability of a given study animal for tagging with a PSAT.

Manuscript submitted 21 May 2003
to the Scientific Editor's Office.

Manuscript approved for publication
13 July 2004 by the Scientific Editor.

Fish. Bull. 103:63–70 (2005).

Quantification of drag and lift imposed by pop-up satellite archival tags and estimation of the metabolic cost to cownose rays (*Rhinoptera bonasus*)*

Donna S. Grusha

Mark R. Patterson

Virginia Institute of Marine Science

College of William and Mary

P.O. Box 1346

Gloucester Point, Virginia 23062-1346

E-mail address (for D. S. Grusha): dsg@vims.edu

The pop-up satellite archival tag (PSAT) was developed in the late 1990s primarily for the tracking of large pelagic fish (Arnold and Dewar, 2001; Gunn and Block, 2001). This electronic tag is attached to a large fish, collects data on the environment of the fish for a preprogrammed period, and then detaches from the fish by corrosion of a release pin. A float on the tag carries the tag to the surface of the water where the PSAT begins transmitting the archived environmental data. The pop-up location is determined by the Argos satellites that in turn transmit the data to a relay station. The earliest uses of these tags have been on large pelagic fishes such as Atlantic bluefin tuna (*Thunnus thynnus*) (Block et al., 1998; Lutcavage et al., 1999) and blue marlin (*Makaira nigricans*) (Graves et al., 2002). In the early tuna studies, PSATs were used to investigate geographic range and possible stock structure. Graves et al. (2002) used the tags to assess postrelease survival of blue marlin from the recreational fishery. Over their short history, the PSATs have been improved to collect even more data than the original models and currently record light levels, temperature, and pressure readings. The light levels are used to estimate geolocation and the pressure readings are converted to depth measurements. Combined with the temperature readings, the depth measurements can provide detailed information about the study animal's swimming behavior. Experiences with the first-generation tags led to the

development of various fail-safe features (Arnold and Dewar, 2001). Both premature detachment (made evident by the tag floating at the surface) or lack of vertical movement (i.e., constant depth, which indicates probable death of the animal) initiate early transmission of archived data. Should the tag be carried to an extreme depth where water pressure might physically crush the tag, release mechanisms, both software-based and mechanical, have been developed to free the tag from the animal.

PSATs were developed to supplement the tracking data that could be acquired through acoustic tagging and archival tagging. Acoustic tagging is most useful for studying fine-scale movement and habitat use and for collecting physiological data (Arnold and Dewar, 2001; Gunn and Block, 2001). However, its use is limited by the need for labor-intensive, real-time tracking from a research vessel or the availability of fixed listening stations. Dagorn et al. (2001) described clear interactions between some of the yellowfin tuna (*Thunnus albacares*) being tracked and the research vessel—a violation of the assumption that the tracking operation does not alter the behavior of the fish. Archival tags also collect both environmental and physiological data but

* Contribution 2629 from the Virginia Institute of Marine Science, College of William and Mary, Gloucester Point, VA 23062.

over much longer time scales (sometimes years) and across ocean-basin geographic scales (Arnold and Dewar, 2001; Gunn and Block, 2001). These tags can provide information on both seasonal behavior and migration routes. Although data collection is fishery-independent, data retrieval is dependent on the recapture of the fish by fishermen and on the recognition and return of the archival tag. PSATs are a merger of archival and satellite telemetry technology. Because PSATs are attached externally, only environmental data can be collected. The tags can be programmed to gather data for a predetermined duration and then to disengage and transmit data at a determined time. The major advantage of this tag is that both data acquisition and retrieval are fishery-independent and the researcher knows when to expect to receive data. However, data retrieval is limited by data compression required to compensate for low data transfer rates to the Argos satellites, finite battery life, and relatively high transmission errors (Arnold and Dewar, 2001; Gunn and Block, 2001). PSATs provide accurate endpoint locations based on Doppler shifts of successive transmissions during a single satellite pass. However, geolocation throughout the tagging duration is based on light levels that estimate dawn and dusk. By determining time of local noon and day length, longitude and latitude can be calculated. According to Hill and Braun (2001), even with optimal geolocation analysis, the expected variability in longitude is a constant 0.32° but the expected variability in latitude will never be less than 0.7° . The relationship between day length and latitude is strongest at high latitudes and at the time of the solstices but weakens near the equator and becomes nearly indeterminate at the equinoxes (Sibert et al., 2003).

An implicit assumption in using these tags is that while the fish tows the tag, the tag does not affect the study animal's behavior or survival. This is a reasonable assumption for large pelagic fishes and is supported by theoretical estimates of the energetic cost of towing a PSAT (Kerstetter, 2002); however, the actual energy cost to a given fish has not previously been quantified. The success of early studies on pelagic fishes has spurred increasing interest in using these tags on a large variety of species and age groups. As studies are undertaken with PSATs, a logical extension is to pose the question: "At what point does the energy cost of carrying a PSAT negatively affect a study animal?" Blaylock (1990) addressed a similar question regarding the impact of sonic transmitters on the swimming behavior of cownose rays (*Rhinoptera bonasus*). In his study, he videotaped cownose rays for ten-minute intervals before and after attachment of a mock transmitter. Energy expenditure was estimated by counting wingbeats per second before and after attachment of the transmitter. He concluded that in the short term a transmitter-tow ratio mass ratio of less than 0.03 had no statistically significant effect on ray swimming behavior.

In this study, the impact of a PSAT on a study animal is evaluated in terms of the forces that the PSAT exerts on the animal, specifically lift (i.e., buoyancy)

and drag. Lift and drag are both vector quantities; lift acts in the vertical direction and drag, as measured in this study, acts in the horizontal direction. These vector components are additive to give the total force acting on the attachment site of a PSAT. At a recent tagging workshop associated with the Pelagic Fisheries Research Program,¹ the problem of premature release of some PSATs from the research animal was cited as a common difficulty. Premature release may be attributed to a number of potential failures of either the tag itself or the attachment device. Possible sources for this problem cited at this workshop include detachment of the anchor from the study animal, failure of the tether between the PSAT and the anchor, failure of the release pin on the PSAT, and failure of the release software itself. The magnitude of the total force acting on the attachment site chronically may provide some insight into whether anchor failure is a possible source for this problem.

Drag as an isolated force is the product of four defining factors:

$$F_D = \frac{1}{2} \rho S U^2 C_D, \quad (1)$$

where F_D = force due to drag (in newtons, N);

ρ = density (kg/m^3) of the fluid through which the object is moving;

S = projected surface area (m^2) of the object;

U = relative velocity (m/s) between the object and the fluid; and

C_D = drag coefficient (dimensionless) which is largely dependent upon the shape of the object.

Furthermore, the power required to pull the tag through the water can also be related to drag mathematically:

$$P = F_D U = \frac{1}{2} \rho S U^3 C_D, \quad (2)$$

where P = power (in watts, W).

Of particular note in these relationships, drag is proportional to velocity squared and power is related to velocity cubed provided that all other factors are constant. For example, as velocity is doubled, drag increases by a factor of four, whereas power increases by a factor of eight. The characteristic of the tag that most affects drag in this relationship is its projected surface area which, in turn, is defined by its size and shape. The projected surface area of the PSAT changes as the tag is pulled through the water at different velocities and in turn changes the drag coefficient at each velocity. On the other hand, lift is determined by the buoyancy of the tag. The dry weight of the tag is not a factor in either of these relationships under steady flow con-

¹ Pelagic Fisheries Research Program. 2002. PFRP PI Meeting, December 4–6, 2002. University of Hawaii at Manoa, 1000 Pope Rd., MSB 312, Honolulu, HI 96822. <http://www.soest.hawaii.edu/PFRP/meetings.html>. [Accessed 16 June 2004.]

ditions. The weight of the tag is one important during accelerations and decelerations. During acceleration, the mass of the tag positively affects the magnitude of two separate forces that add to the hydrodynamic drag, and likewise during deceleration, these extra forces develop on the attachment point that could cause tag loss.

The motivation for this study is to determine the feasibility of tagging cownose rays (*R. bonasus*) with PSATs to study their fall migration. By quantifying the forces that act upon an animal when a PSAT is attached, and using published metabolic rates, we can estimate the energetic cost for the ray to carry a PSAT. Moreover, this type of analysis can be used to determine the minimum size of ray suitable for tagging. Considering the wide variety of user-determined modifications that can be implemented in applying these tags, this experiment is intentionally designed to isolate the PSAT from other variables. In this way, these results can be applied to a broad range of applications so that each user can decide the manner in which a specific modification of the tag is likely to affect the forces of lift and drag.

Methods

Drag was measured on two brands of PSAT. One tag was manufactured by Wildlife Computers, Inc. (Model PAT, 16150 NE 85th St #226, Redmond, WA 98052) and the other was a mock tag made by Microwave Telemetry, Inc. (Model PTT-100, 10280 Old Columbia Road, Suite 260, Columbia, MD 21046) weighted to simulate a functional tag. The two tags are very similar in size and shape (Fig. 1). The Wildlife Computer PAT has a body length of 180 mm (not including the antenna) and a dry weight of 75 g and the Microwave Telemetry PTT is 175 mm long and weighs 68 g. Measurements were obtained in a 22,700-liter freshwater recirculating flume 24 meters in length located at the Virginia Institute of Marine Science. A 30-g spring scale was used to measure force and was suspended above the flume. A 1.25-cm low-friction Delrin rod was suspended approximately 55 cm below the water surface by a metal bracket and placed directly below the spring scale. A 90-cm length of 0.46-mm diameter (20-lb test) monofilament line connected the tag to the spring

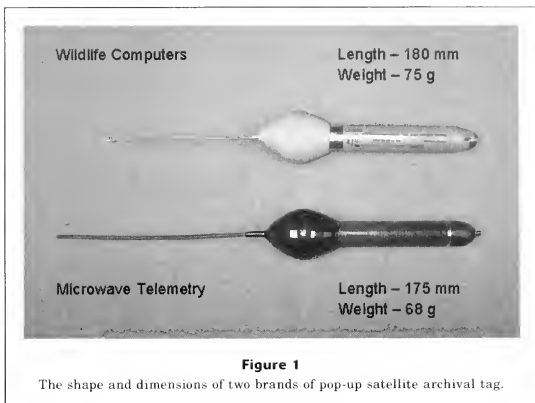


Figure 1
The shape and dimensions of two brands of pop-up satellite archival tag.

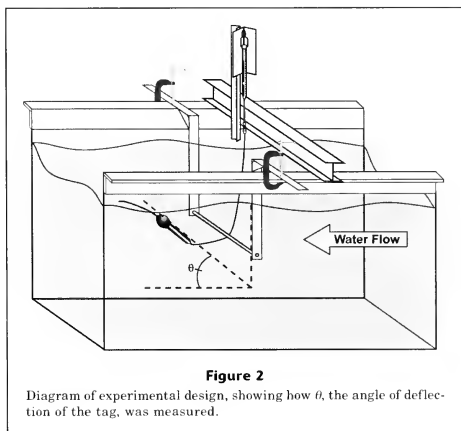


Figure 2
Diagram of experimental design, showing how θ , the angle of deflection of the tag, was measured.

scale by loops tied at either end. One loop was threaded through the release pin in order to lasso the tag. The other loop was then attached to the clip on the spring scale and the tag was passed under the Delrin rod so that it floated to the other side (Fig. 2). The depth of the Delrin rod and the length of the monofilament were selected so that the tag was completely immersed in the water throughout the experiment and so that it floated within

Table 1

Spring scale measurements, angle of deflection, summary of forces exerted and power required for two brands of PSAT over flume velocities from 0.00 m/s to 0.60 m/s. The spring scale measurements include the range over a 5-minute period. The angle of deflection was measured from the horizontal. Total force, lift, and drag (in newtons, N) were calculated from Equations 3, 4, and 5, respectively. Power (in watts, W) was calculated as the product of flume velocity and drag.

PSAT	Flume velocity (m/s)	Spring scale measurement (g)	θ ($^{\circ}$)	Total force (N)	Lift (N)	Drag (N)	Power (W)
Wildlife Computers	0.00	6.50 \pm 0.25	90.0	0.064	0.064	0.000	0.000
	0.15	7.50 \pm 0.25	76.5	0.074	0.072	0.017	0.003
	0.30	10.50 \pm 0.25	42.0	0.103	0.069	0.076	0.023
	0.45	15.0 \pm 0.5	40.0	0.147	0.094	0.113	0.051
	0.60	19.0 \pm 1.0	31.5	0.186	0.097	0.159	0.095
Microwave Telemetry	0.00	11.75 \pm 0.25	90.0	0.115	0.115	0.000	0.000
	0.15	12.25 \pm 0.25	75.5	0.120	0.116	0.030	0.004
	0.30	13.50 \pm 0.25	61.5	0.132	0.116	0.063	0.019
	0.45	16.0 \pm 0.5	42.5	0.157	0.106	0.116	0.052
	0.60	21.5 \pm 1.0	41.5	0.211	0.140	0.159	0.095

the central portion of the flume. Prior to the experiment, the monofilament line was attached to the spring scale and the spring scale was then set at zero so that the weight of the monofilament line was excluded from the subsequent measurements. The flume temperature was measured at 20°C. Measurements were taken on each tag at flume velocities of 0.0, 0.15, 0.30, 0.45, and 0.60 m/s, the maximum velocity of the flume. At each flume velocity, the flume flow was allowed to equilibrate for 10 minutes. Then spring scale measurements were observed over a period of five minutes and the mid-point measurement and its range were recorded. The raw measurement was then converted to total force, F_T (N):

$$F_T = (\text{raw measurement (g)})(1\text{kg}/1000\text{g})(9.8\text{m/s}^2). \quad (3)$$

In addition, a digital photo was taken of each tag at each velocity from the side of the flume in order to measure the angle of deflection (θ) as measured upward from horizontal. Accordingly, the total force (F_T) could then be separated into its component forces, lift (F_L) and drag (F_D):

$$F_L = \sin \theta F_T, \quad (4)$$

$$F_D = \cos \theta F_T. \quad (5)$$

Results

The spring scale measurement for the Wildlife Computers PAT increased from 6.50 g at 0.00 m/s to 19.0 g at 0.60 m/s and the Microwave Telemetry PTT increased from 11.75 g to 21.5 g over the same flume velocity increase (Table 1). Because of increasing turbulence

in the flume at the two higher flume velocities, the range of the spring scale measurements also increased. The total force exerted by the Wildlife Computers PAT increased from 0.064 N to 0.186 N as the flume velocity was increased (Table 1). Similarly, the drag and calculated power required to pull the tag through the water column at the highest velocity was 0.159 N and 0.095 W, respectively. The lift of this PSAT also increased, but not continuously, from 0.064 N to 0.097 N. The forces exerted by the Microwave Telemetry PTT were very similar but had higher lift values. The total force increased from 0.115 N to 0.211 N, the drag increased to 0.159 N and the power required to pull this PSAT was 0.095 W at the highest velocity. The lift increased from 0.115 N to 0.140 N but again not in a continuous manner. Force-velocity curves for both PSATs were very similar (Fig. 3). Lift was relatively constant for each tag, although at different magnitudes. Total force and drag both increased over the range of flume velocities and roughly paralleled each other between 0.30 m/s and 0.60 m/s.

Discussion

Considered alone, the power required to pull a given PSAT at a particular velocity has little relevance, but when considered in the context of an animal's usual energy expenditure to swim at that velocity, it can be expressed as %TAX (Tag Altered eXertion), defined as the increase in energy required by the animal to pull the PSAT at the specified velocity, normalized by the routine or active metabolic rate (see below). In his biotelemetry studies, Blaylock (1992) measured mean routine swimming speeds between 0.20 m/s and 0.29 m/s in cownose rays. Maximum swimming speeds for cownose rays have

not been measured; however, with visual observation, Smith (1980) reported witnessing several undisturbed schools of cownose rays swimming near the surface at ~4–5 knots (2.06–2.57 m/s). Using data reported in first sightings during spring migration of cownose rays along the South Atlantic Bight, Smith estimated migration speeds as high as 12.5 nautical miles per day. Assuming the rays migrated continuously, that rate would require a swimming speed of 0.27 m/s; if they were actively migrating 50% of the time, they would have to swim at 0.54 m/s.

Published metabolic rates can be used to estimate the energy required for an animal to swim at various speeds. When information is not available on a study species, a suitable proxy species can be used. In the example of the cownose ray, no data are currently available regarding metabolic rates; however, DuPreez et al. (1988) published metabolic rates for the bull ray (*Myliobatis* [= *Myliobatus*] *aquila*) over a range of temperatures. *Myliobatis aquila* is a good proxy species for *R. bonasus* because the two species are morphologically similar, similar in size, and both inhabit temperate to subtropical coastal waters. Because the flume measurements were obtained at 20°C and this is also a typical mid-range temperature for either species, the equations for metabolic rates at this temperature will be used (Eq. 6, a–c). Metabolic rates are expressed as a set of three equations that yield the standard metabolic rate (SMR), the routine metabolic rate (RMR), and the active metabolic rate (AMR).

$$\text{SMR} \log_{10} R = 2.86 - 0.32 \times \log_{10} (M \times 1000), \quad (6a)$$

$$\text{RMR} \log_{10} R = 2.79 - 0.27 \times \log_{10} (M \times 1000), \quad (6b)$$

$$\text{AMR} \log_{10} R = 2.74 - 0.22 \times \log_{10} (M \times 1000), \quad (6c)$$

where M = mass (kg) of the ray (DuPreez et al.'s 1988 equations have been modified so as to express M in MKS units); and R = metabolic rate (mg O_2 /(kg × h)).

Using the size of an average female cownose ray of 15.5 kg (Smith, 1980) and solving for R , the SMR, RMR and AMR are estimated as 33.0, 45.6, and 65.8 mg O_2 /(kg × h) respectively. These rates can then be used to estimate swimming power at routine and active swimming speeds:

$$SP_{MR} = (?MR - SMR) \times (1W/kg) / (256mg O_2 / (kg \times h)) \times M, \quad (7)$$

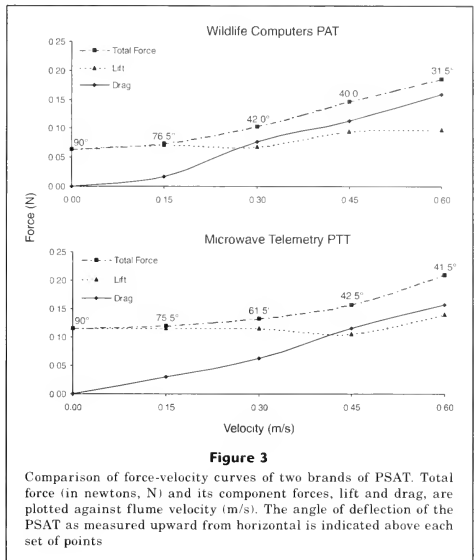


Figure 3

Comparison of force-velocity curves of two brands of PSAT. Total force (in newtons, N) and its component forces, lift and drag, are plotted against flume velocity (m/s). The angle of deflection of the PSAT as measured upward from horizontal is indicated above each set of points

where SP_{MR} = swimming power (W) for RMR or AMR.

Making the appropriate substitutions into Equation 7 yields $SP_{RMR} = 0.76$ W and $SP_{AMR} = 1.99$ W. Drag can then be expressed as %TAX:

$$\%TAX = (P / SP_{MR}) \times 100. \quad (8)$$

For swimming speeds of 0.15 m/s and 0.30 m/s, SP_{RMR} is used, and for swimming speeds of 0.45 m/s and 0.60 m/s, SP_{AMR} is used (Table 2).

Although lift has not been considered in the above analysis, it is an important component of the total force affecting a study animal. As a chronically applied force acting against the anchor site where the PSAT attaches, this total force may contribute to premature release of the PSAT from the study animal. Moreover, for animals where diving behavior is important for survival (e.g., diving for prey or diving to escape predators) lift becomes an additional tax on the animal's energy resources. Using total force as an approximation of the force to be overcome by the animal when diving, we can estimate the total power required to dive as *Total force as %TAX* (Table 2).

We propose that an increase in energy requirement, %TAX, of <5% will not negatively impact a study ani-

Table 2

Metabolic cost to a 15.5 kg cownose ray carrying a PSAT at various velocities expressed as %TAX. Drag and total force are the forces created by the PSAT to be overcome by the swimming ray. Power and total power are the rates of energy expenditure required to overcome these forces. *Drag as %TAX* and *Total force as %TAX* are the increases in energy expenditures, normalized by the routine or active metabolic rate (speed dependent—see text), required to carry the PSAT at a given velocity. Drag, power, and *Drag as %TAX* apply to a ray swimming in the horizontal plane. Total force, total power, and *Total force as %TAX* account for the buoyancy of the PSAT and apply when the ray is diving.

PSAT	Flume velocity (m/s)	Drag (N)	Power (W)	Drag as %TAX	Total force (N)	Total power (W)	Total force as %TAX
Wildlife Computers	0.00	0.000	0.000	0.00	0.064	0.000	0.00
	0.15	0.017	0.003	0.34	0.074	0.011	1.44
	0.30	0.076	0.023	3.01	0.103	0.031	4.05
	0.45	0.113	0.051	2.55	0.147	0.066	3.33
	0.60	0.159	0.095	4.80	0.186	0.112	5.63
Microwave Telemetry	0.00	0.000	0.000	0.00	0.115	0.000	0.00
	0.15	0.030	0.004	0.59	0.120	0.018	2.36
	0.30	0.063	0.019	2.46	0.132	0.040	5.20
	0.45	0.116	0.052	2.62	0.157	0.071	3.55
	0.60	0.159	0.095	4.77	0.211	0.126	6.37

mal that has adequate food resources in nature; higher loads are felt to be energetically significant. In this example using a 15.5-kg cownose ray, the *Drag as %TAX* is within acceptable parameters; however, at 0.60 m/s the *Total force as %TAX* begins to exceed these guidelines. At this point, a researcher would have to consider whether diving behavior at this speed would be a significant factor in the animal's survival.

Another application of this information would be to determine the minimum reasonable size for a study animal of a particular species. Blaylock (1990) attempted to address this issue for cownose rays by considering the transmitter-to-ray mass ratio using dry weights. The advantage of using metabolic rates is that it identifies subtler but significant increases in energy requirement to carry a PSAT. In his study, Blaylock examined two age groups, a 0+ age group that had an average weight of 1.8 kg and a 1+ age group that ranged in size between 4.3 kg and 7.8 kg. He concluded that the 0+ age group was negatively impacted by the sonic tag but that the 1+ age group was not effected. A PSAT is physically smaller than the sonic tags used in his experiment; in addition, it is attached to the animal at the nose-end of the tag so that it is carried with the long axis of the tag parallel to the long axis of the animal (Blaylock's sonic tags were attached so that the long axis of the tag was carried perpendicular to the long axis of the animal). Both these factors—smaller physical size and nose-end orientation in space—decrease the projected surface area of the tag. As an example, consider the metabolic cost of carrying a Wildlife Computers PAT to each of these sizes (1.8, 4.3, and 7.8 kg) of cownose ray (Table 3). For the 1.8-kg ray, only the exertion of carrying the PSAT at 0.15 m/s horizontally was associ-

ated with a %TAX of <5%; higher swimming speeds or downward diving markedly increased the %TAX. It is obvious why short-term effects of carrying a sonic tag were evident. For the 4.3-kg ray, all swimming speeds greater than 0.15 m/s, whether horizontal or diving, required increased energy expenditures of >5%. For the 7.8-kg ray, %TAX was acceptable at 0.15 m/s, marginal to slightly elevated for mid-range speeds, and was clearly excessive at high speed. According to this analysis, rays of these size classes would not be good candidates for carrying a PSAT. As determined in this study, the smallest cownose ray that ought to be considered for PSAT tracking would be 14.8 kg. *Drag as %TAX* is $\leq 5\%$ for all speeds and only slightly >5% for *Total force as %TAX* at 0.60 m/s. Because prolonged high speed diving behavior is not likely a factor in this ray's ability to survive, the minor elevation of %TAX for diving at 0.60 m/s can be disregarded.

When applying this type of analysis to other species that predominantly swim at speeds greater than 0.60 m/s, several caveats make unwise the extrapolation of these data to higher velocities. Referring back to the equations describing drag and power, Equation 1 and Equation 2, respectively, drag is proportional to velocity squared and power is proportional to velocity cubed provided that all other factors are constant. However, in examining Figure 3, as velocity increases from 0.00 m/s to 0.60 m/s, all other factors are not constant. Specifically, the angle of deflection, θ , decreases from 90° at 0.00 m/s to as low as 31.5° at 0.60 m/s. First, the projected surface area, S , over which water flows decreases as velocity increases. Second, the orientation (effective shape) of the object also effectively changes as velocity increases. Hence the drag co-efficient, C_D

Table 3

Metabolic costs to various sizes of cownose ray to carry a Wildlife Computers PSAT expressed as %TAX. Drag as %TAX is the increase in energy expenditure, normalized by the routine or active metabolic rate (speed dependent—see text), required by the ray to carry the PSAT while swimming in the horizontal plane. Total force as %TAX accounts for the buoyancy of the PSAT and applies when the ray is diving.

Weight of ray (kg)	Drag as %TAX				Total force as %TAX			
	Swimming velocity (m/s)				Swimming velocity (m/s)			
	0.15	0.30	0.45	0.60	0.15	0.30	0.45	0.60
1.8	2.39	21.32	18.53	34.84	10.25	28.69	24.19	40.86
4.3	1.05	9.32	8.06	15.16	4.48	12.58	10.53	17.78
7.8	0.62	5.50	4.70	8.84	2.65	7.41	6.41	10.37
14.8	0.35	3.15	2.66	5.00	1.51	4.24	3.48	5.87

also changes. At some velocity greater than 0.60 m/s, θ will approach 0°, and at that point S and C_D would remain constant for higher velocities. After that velocity is reached, then for higher velocities, drag would increase proportionately to the square of velocity and power would increase proportionately to the cube of velocity. In other words, between 0.00 m/s and 0.60 m/s, the changes in S and C_D mask the parabolic relationship of drag with velocity. Because the velocity at which S and C_D become constant is not known, extrapolations far beyond the maximum velocity for which drag was measured would be risky.

The effect of the changing values of S and C_D is evident in this data set. For example in Table 1, as velocity doubles from 0.30 m/s to 0.60 m/s, drag increases by only 2.09 and 2.52 for the Wildlife Computers PAT and the Microwave Telemetry PTT-100, respectively, rather than by a factor of four. Similarly, power increases by 4.13 and 5.00 for the two PSATs and not by a factor of eight. For both these tags, θ decreases with increasing velocity resulting in a smaller value for S and a different value for C_D .

By examining the forces exerted by a PSAT at various velocities, insights regarding the impact of these forces on a study animal can be gained. The combined forces of lift and drag act chronically on the anchor site of the PSAT. Although this study does not specifically address attachment methods, the forces of lift and drag exerted by a PSAT are not negligible and cannot be ignored when evaluating an attachment technique. A PSAT also imposes an energetic cost to the study animal. If that energy cost compromises the animal's behavior or survival, the information gained from the tag is not representative of an untagged animal. By estimating the energetic cost to an intended study animal, a researcher can make a more informed decision regarding the suitability of the animal for this type of tagging. Although direct extrapolation to higher swimming speeds is not possible with our data, the principles outlined in this study can be applied to faster swimming species such as tunas and billfishes that are frequently tagged.

Acknowledgments

We would like to thank T. Nelson, S. Wilson, W. Reiser and R. Gammisch for their assistance in running and setting up the flume, T. Mathes for his enthusiastic support, and R. Brill, D. Kerstetter, and J. Hoeng for helpful discussions. Financial support was provided by NOAA Office of Sea Grant.

Literature cited

- Arnold, G., and H. Dewar
2001. Electronic tags in marine fisheries research: a 30-year perspective. In *Electronic tagging and tracking in marine fisheries* (J. R. Sibert and J. L. Nielsen, eds.), p. 7–64. Kluwer Academic Publishers, Dordrecht, The Netherlands.
- Blaylock, R. A.
1990. Effects of external biotelemetry transmitters on behavior of the cownose ray *Rhinoptera bonasus* (Mitchell 1815). *J. Exp. Mar. Biol. Ecol.* 141:213–220.
1992. Distribution, abundance, and behavior of the cownose ray, *Rhinoptera bonasus* (Mitchell 1815), in lower Chesapeake Bay. Ph.D. diss., 129 p. College of William and Mary, Williamsburg, VA.
- Block, B. A., H. Dewar, C. Farwell, and E. D. Prince.
1998. A new satellite technology for tracking the movement of Atlantic bluefin tuna. *Proc. Natl. Acad. Sci.* 95:9384–9389.
- Dagorn, L., E. Josse, and P. Bach.
2001. Association of yellowfin tuna (*Thunnus albacares*) with tracking vessels during ultrasonic telemetry experiments. *Fish. Bull.* 99:40–48.
- DuPreez, H. H., A. McLachlan, and J. F. K. Marais.
1988. Oxygen consumption of two nearshore marine elasmobranchs, *Rhinobatos annulatus* (Muller & Henle, 1841) and *Myliobatus aquila* (Linnaeus, 1758). *Comp. Biochem. Physiol.* 89A:283–294.
- Graves, J. E., B. E. Luckhurst, and E. D. Prince.
2002. An evaluation of pop-up satellite tags for estimating post-release survival of blue marlin. *Fish. Bull.* 100:134–142.

- Gunn, J., and B. Block.
2001. Advances in acoustic, archival, and satellite tagging of tunas. In *Tuna: physiology, ecology, and evolution* (B. A. Block and E. D. Stevens, eds.), p. 167-224. Academic Press, San Diego, CA.
- Hill, R. D., and M. J. Braun.
2001. Geolocation by light level—the next step: latitude. In *Electronic tagging and tracking in marine fisheries* (J. R. Sibert and J. L. Nielsen, eds.), p. 315-330. Kluwer Academic Publishers, Dordrecht, The Netherlands.
- Kerstetter, D. W.
2002. Use of pop-up satellite tag technology to estimate survival of blue marlin (*Makaira nigricans*) released from pelagic longline gear. M.S. thesis, 109 p. College of William and Mary, Williamsburg, VA.
- Lutcavage, M. E., R. W. Brill, G. B. Skomal, B. Chase, and P. Howey.
1999. Results of pop-up satellite tagging of spawning size class fish in the Gulf of Maine: Do North Atlantic bluefin tuna spawn in the mid-Atlantic? *Can. J. Fish. Aquat. Sci.* 56:173-177.
- Sibert, J. R., M. K. Musyl, and R. W. Brill.
2003. Horizontal movements of bigeye tuna (*Thunnus obesus*) near Hawaii determined by Kalman filter analysis of archival tagging data. *Fish. Oceanogr.* 12: 141-151.
- Smith, J. W.
1980. The life history of the cownose ray, *Rhinoptera bonasus* (Mitchill 1815), in lower Chesapeake Bay, with notes on the management of the species. M.A. thesis, 151 p. College of William and Mary, Williamsburg, VA.

Abstract—Fish bioenergetics models estimate relationships between energy budgets and environmental and physiological variables. This study presents a generic rockfish (*Sebastes*) bioenergetics model and estimates energy consumption by northern California blue rockfish (*S. mystinus*) under average (baseline) and El Niño conditions. Compared to males, female *S. mystinus* required more energy because they were larger and had greater reproductive costs. When El Niño conditions (warmer temperatures; lower growth, condition, and fecundity) were experienced every 3–7 years, energy consumption decreased on an individual and a per-recruit basis in relation to baseline conditions, but the decrease was minor (<4% at the individual scale, <7% at the per-recruit scale) compared to decreases in female egg production (12–19% at the individual scale, 15–23% at the per-recruit scale). When mortality in per-recruit models was increased by adding fishing, energy consumption in El Niño models grew more similar to that seen in the baseline model. However, egg production decreased significantly—an effect exacerbated by the frequency of El Niño events. Sensitivity analyses showed that energy consumption estimates were most sensitive to respiration parameters, energy density, and female fecundity, and that estimated consumption increased as parameter uncertainty increased. This model provides a means of understanding rockfish trophic ecology in the context of community structure and environmental change by synthesizing metabolic, demographic, and environmental information. Future research should focus on acquiring such information so that models like the bioenergetics model can be used to estimate the effect of climate change, community shifts, and different harvesting strategies on rockfish energy demands.

Manuscript submitted 20 October 2003
to the Scientific Editor's Office.

Manuscript approved for publication
2 August 2004 by the Scientific Editor.
Fish. Bull. 103:71–83 (2005).

Effects of El Niño events on energy demand and egg production of rockfish (*Scorpaenidae: Sebastes*): a bioenergetics approach

Chris J. Harvey

Northwest Fisheries Science Center
National Marine Fisheries Service
2725 Montlake Blvd. E
Seattle, Washington 98112
E-mail address: Chris.Harvey@noaa.gov

Over 90 species of rockfish (*Sebastes* spp.) are found in kelp beds, rocky reefs, pelagic habitats, and continental shelf and slope zones of the temperate and subarctic North Pacific; these species feed on a range of organisms, from zooplankton to fish (Love et al., 2002). Although they are a key component of groundfish fisheries on the U.S. Pacific Coast, many rockfish have declined considerably in recent decades, owing to overfishing and climate-induced downturns in production (Parker et al., 2000). Conservation efforts, ranging from coast-wide fishery closures to establishment of marine reserves, have been enacted in order to rehabilitate rockfish stocks. The efficacy of such actions depends in part on the dynamics of the communities in which rockfish exist. Key among these dynamics are trophic interactions, as influenced by abiotic factors and rockfish population structure.

Although rockfish are widely distributed and important to the ecology, fisheries, and conservation efforts of the Pacific Coast, little is known about their trophic dynamics. For example, of the 65 rockfish species that live along the North American West Coast, quantitative diet data are available for only 15 species (Murie, 1995). Better information on the food habits and energetics of both juvenile and adult rockfish would facilitate a greater understanding of the role they play in their communities, and how their role is affected by external forces. This is particularly true given observations that environmental variation can have strong effects on rockfish growth and condition (Lenarz et al., 1995; Woodbury, 1999).

Fish bioenergetics models relate the energy consumption, growth, and energy allocation patterns of fishes to environmental and physiological variables such as temperature, food quality, body size, and reproductive status (Kitchell et al., 1977). These models, founded in thermodynamic laws of mass and energy balance, can successfully predict patterns of energy demands by fish (Madenjian et al., 2000). At the scale of the individual fish, bioenergetics models can estimate effects of a fish on its community (in terms of the amount of prey it consumes) and effects of the environment on the fish, such as how changes in temperature or food availability influence energy consumption and growth (Rice et al., 1983). When coupled to population models, bioenergetics models can predict prey-predator supply-demand relationships (Negus, 1995) and determine how different fishery management policies will affect prey resources in the community from which the targeted fish is extracted (Kitchell et al., 1997; Essington et al., 2002; Schindler et al., 2002). Thus, these models may facilitate a more community- or ecosystem-level approach to rockfish management.

In this study, I develop a generic *Sebastes* bioenergetics model. My first objective is to detail the parameters and the sensitivity analysis of the model, thereby offering a synthesis of what is known about *Sebastes* energetic physiology and identifying parameters for which greater information is desirable. The second goal is to present a simple application of the model: an estimation of the effects of

El Niño related environmental changes on the energy demands of blue rockfish (*S. mystinus*) under unfished and fished conditions. Two relevant characteristics of El Niño events in U.S. West Coast waters are elevated temperatures and reductions in growth rates and reproductive condition of *Sebastes* (Lenarz et al., 1995; VenTresca et al., 1995; Woodbury, 1999). The bioenergetics approach can incorporate these changes and can therefore help to characterize the role of rockfish as consumers in a dynamic environment.

Methods

Model structure

I followed the basic structure of bioenergetics models established for other fishes (e.g., Kitchell et al., 1977; Hewett and Johnson, 1992), in which energy intake (consumption) equals all energy outputs (respiration, wastes, growth, and reproduction). The basic model equation is

$$C = (R + A + S) + (F + U) + (\Delta B + G), \quad (1)$$

where C = consumption, R = respiration, A = active metabolism, S = specific dynamic action (digestive costs), F = egestion, U = excretion, ΔB = somatic growth, and G = gonad production. The respiration and active metabolism portions of Equation 1 take the form

$$R = RA \times W^{RB} \times f(T) \times ACT, \quad (2)$$

where RA and RB are constants that describe the allometric respiration function, W is wet biomass, $f(T)$ is a temperature dependence function, and ACT is an activity multiplier (Kitchell et al., 1977). The function $f(T)$ (Kitchell et al., 1977) is a hump-shaped function that requires estimates of optimal (RTO) and maximum (RTM) temperatures for respiration, and a Q_{10} (RQ).

The terms S , U , and F all scale to total consumption (Kitchell et al., 1977). One can thus think of them as a general energy loss term

$$Loss = (S + U) \times (C - F) + F. \quad (3)$$

Model parameters

Although parameters are derived from studies of many rockfish species, I developed the present model to describe energetic dynamics of *S. mystinus*, for which a considerable literature exists regarding diet and responses to climate variability (e.g., Hallacher and Roberts, 1985; Bodkin et al., 1987; Hobson and Chess, 1988; Lenarz et al., 1995; VenTresca et al., 1995).

Respiration parameter estimates came from studies of other *Sebastes* species or related scorpaenid fishes (Table 1). For RTM , I used published estimates for *S. thompsoni* and *S. schlegeli* (Ouchi, 1977; Tsuchida and Setoguma, 1997), and assumed that RTO would be 5°C

Table 1

Parameter values for the generic *Sebastes* bioenergetics model.

Parameter	Description	Value
RA	Intercept of the allometric respiration function	0.0143
RB	Slope for allometric respiration function	-0.2485
RQ	Slope for temperature dependence of respiration (Q_{10})	2
ACT	Multiplier for active metabolism	1
RTO	Optimum temperature for respiration	23°C
RTM	Maximum temperature for respiration	28°C
SDA	Specific dynamic action coefficient	0.163
EA	Egestion coefficient	0.104
UA	Excretion coefficient	0.068
ED	Energy density (somatic tissue) of wet mass	6,120 J/g
GED	Energy density (female gonadal tissue) of wet mass	8,627 J/g
GA	Coefficient of the female length-fecundity relationship	1.559
GB	Exponent of the female length-fecundity relationship	3.179
GSI_{max}	Maximum male gonadosomatic index	0.008

cooler. The resulting RTO was similar to upper temperatures at which juvenile *S. diploproa* experienced zero growth while feeding (Boehlert, 1981). RQ was based on low-temperature Q_{10} values in several scorpaenid respiration studies (Boehlert et al. 1991; Yang et al., 1992; Kita et al., 1996; Vetter and Lynn, 1997). RA , the oxygen consumption rate for a 1-g fish at RTO , was derived from data for nongestating *S. schlegeli* (Boehlert et al., 1991). RB , which describes the allometric scaling of respiration, was also derived from data for nongestating *S. schlegeli* spanning a range of roughly 0.7 to 1.9 kg body mass (Boehlert et al., 1991). Respiration terms were converted to energy units by an oxycealoric correction (13.56 J/mg O_2), and then to biomass by assuming that rockfish energy density (ED) = 6,120 J/g wet mass (Perez, 1994).

The ACT multiplier was assumed to equal 1. This assumption is best justified in cases where routine respiration rates were used to determine parameters for the model. Boehlert et al. (1991) stated that *S. schlegeli* in their analysis were generally inactive, which implies that rates derived from their data represent resting

metabolism. I chose to keep *ACT* at 1, however, because I could find no data describing a reasonable activity multiplier. Thus, *Sebastes* model outputs may underestimate energy consumption under conditions in which individuals are especially active.

I obtained growth (ΔB in Eq. 1) terms using von Bertalanffy length-at-age curves and data for length-to-mass conversions for *S. mystinus* as summarized by Love et al. (2002). Because female *S. mystinus* are larger at age than males, growth was modeled with sex-specific von Bertalanffy curves with the difference equation method of Gulland (1983). Digestion and waste terms *S*, *F*, and *U* were derived from previous teleost models (Hewett and Johnson, 1992).

I estimated gonad production (*G*) with gonadosomatic indexes (GSI) and size-fecundity relationships (females only), assuming that female and male *S. mystinus* mature equally over the range of lengths observed by Wyllie-Echeverria (1987), and reproduce once annually. For males, I assumed that gonads have the same ED as somatic tissue; for females, I assumed that gonadal energy density (*GED*) = 8,627 J/g, which was the average of gonadal energy density at the onset of embryogenesis for *S. flavidus* and *S. jordani* (MacFarlane and Norton, 1999). Estimated maximum female GSI was based on a fecundity-length relationship:

$$\text{fecundity} = GA \times TL^{GB}, \quad (4)$$

where *GA* and *GB* were taken from a generic rockfish length-fecundity relationship (Love et al., 2002) and *TL* is total length in cm. Fecundity was converted to biomass units by assuming that each egg weighed 0.0003 g, which I derived from Love et al. (1990) by dividing the mean maximum female gonad weight by the estimated fecundity of modal mature females for several species. For mature males, I assumed a constant maximum GSI based on data for other species (Love et al., 1990). Post-spawning GSI was assumed to be 10% of the maximum for each sex, as with other rockfish (Love et al., 1990). The *G* terms were the difference between the maximum and minimum GSIs for each sex, expressed as mass (and, in females, adjusted by multiplying by *GED/ED*).

Rockfish are viviparous, and developing larvae may receive energy from both yolk and maternal sources (Love et al., 2002). During gestation in a laboratory, female *S. schlegelii* consumed 35% to 117% more oxygen than nongestating fish of similar size (Boehlert et al., 1991). To account for the possibility that blue rockfish may also be matrotrophically viviparous, I increased female respiration by 50% during the gestation period (assumed to be 45 days per year based on gestation times of other species [Boehlert et al., 1991]).

Model application: effects of El Niño on blue rockfish energy consumption

To examine the effects of El Niño on *S. mystinus* energy consumption, I created two model conditions: a baseline model and an El Niño model that estimated *S. mystinus*

Table 2

Changes in the *S. mystinus* bioenergetics model that were implemented in El Niño scenarios in relation to the baseline model.

Variable	Change
Temperature	Increased 1.5°C in El Niño years ¹
Growth (length increment)	Decreased 17.5% in El Niño years ¹
Female condition factor	Decreased 10% in El Niño years; decreased 5% the year following an El Niño ²
Male condition factor	Decreased 7.5% in El Niño years; decreased 5% the year following an El Niño ²
Fecundity	Decreased 67% in El Niño years ²

¹ Source: Lenarz et al., 1995.

² Source: VenTresca et al., 1995.

energy demands, in megajoules (MJ), required for necessary growth, reproduction, and related metabolic costs. I used MJ rather than prey biomass as the currency because quantitative, seasonal diet data for *S. mystinus* in northern California were available for average years (Hobson and Chess 1988) but not for El Niño years. During the 1982–83 El Niño, Lea et al. (1999) found that central Californian *S. mystinus* consumed large numbers of the pelagic crab *Neuroncodes planipes*, which is typically found south of Point Conception during average years. During the same time period, *S. mystinus* ate few tunicates or scyphozoans (Lea et al., 1999), which were the predominate prey of *S. mystinus* in average years (Hobson and Chess, 1988). These findings suggest a major shift in *S. mystinus* prey composition during El Niño events.

The baseline model simulates energy consumption of northern California *S. mystinus* from age 0 to age 30, based on quarterly growth estimates from sex-specific von Bertalanffy curves (Love et al., 2002) and seasonal temperature data from Hobson and Chess (1988). Mature females released larvae in the fourth quarter of each year, and mature males released gametes in the third quarter (Wyllie-Echeverria, 1987). Energy consumption for both sexes from ages 0 to 30 was expressed at two scales: for the 30-year life span of an individual; and on a per-recruit basis (under the assumption that there was no fishing mortality and that the natural mortality rate [*M*] was 0.2, applied in quarterly time steps).

The El Niño model was similar to the baseline model, except an El Niño occurred every three to seven years. During these years there were changes in temperature, growth, condition, and fecundity (Table 2). Temperature increases in El Niño years were similar to temperature anomalies in northern California waters during major El Niño events from 1957 to 1993 (Lenarz et al., 1995). Changes in growth (in terms of length increment), con-

dition (the ratio of actual to expected weight, based on length-weight relationships), and fecundity were based on empirical measures of *S. mystinus* during El Niño years (Lenarz et al., 1995; VenTresca et al., 1995). As in the baseline model, I expressed energy consumption by both sexes at individual and per-recruit scales.

Finally, I ran simulations at the per-recruit scale in which the total mortality rate (Z) was increased by adding a fishing-induced mortality rate (F) in increments of 0.05 to M ; fishing mortality was imposed on fish greater than 20 cm, the size at which *S. mystinus* enters fisheries in California waters (Laidig et al., 2003). The range of Z examined was 0.2 (natural mortality only) to 1.0 (a heavily overfished condition). These simulations were run under baseline conditions and El Niño conditions to determine if there was any interaction between El Niño effects and Z .

Sensitivity analysis

To measure sensitivity of the *Sebastes* bioenergetics model to different parameters, I used a Monte Carlo error analysis method (Bartell et al., 1986). In this method, parameters are drawn randomly from normal distributions with means equal to parameter estimates (Table 1) and with a coefficient of variation (CV) of either 2%, 10%, or 20%. Cases where randomly drawn RTO was greater than RTM were discarded. Female and male models were run 1000 times for each of the three CVs. Individual simulations ran to age 30 at 0.25-year increments; seasonal temperatures were those used in the baseline model. Parameter influence on 30-year cumulative consumption estimates was judged according to the parameters' relative partial sums of squares (RPSS), which quantify the influence of a parameter after all other parameters have been accounted for. RPSS for all parameters were calculated with SYSTAT (version 10.2, SYSTAT Software Inc., Richmond, CA). Additionally, means and standard deviations of consumption estimates from RPSS analyses were calculated to capture the range of energy consumption possible over the lifetime of female and male *S. mystinus*.

Results

Northern California *S. mystinus* baseline energy demands

Baseline energetic demands of northern California *S. mystinus* were a function of size, sex, and the scale of calculation (i.e., individual versus per recruit). As size increased, more energy was allocated to respiration, elimination of wastes, and reproduction, and steadily less energy was allocated to growth (Fig. 1). At the individual scale, females consumed more than males at all ages. The sexes diverged markedly as fish matured (beginning at age 3 for females, age 4 for males), and continued to diverge as fish approached asymptotic sizes (Fig. 2A). The disparity was related to sex-based differences in growth rate, maximum size, GSI, and

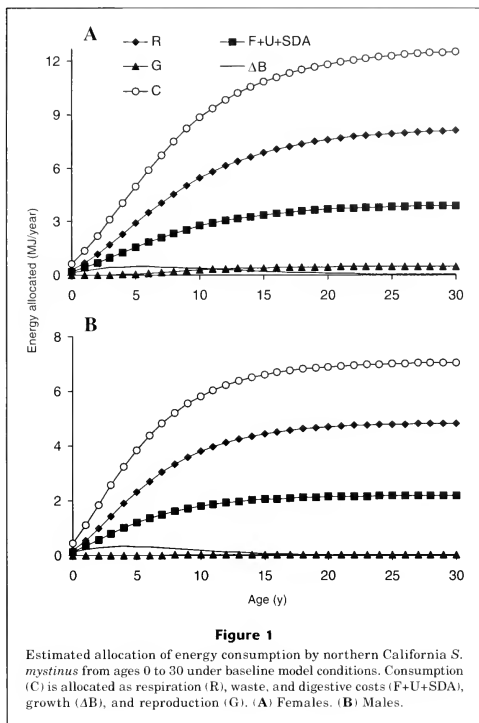
the increased respiration of gestating females. Cumulative consumption through age 30 was 285.0 MJ for individual females, and 174.6 MJ for individual males. Assuming a prey energy density of 1500 J/g (given *S. mystinus* diets [Hobson and Chess, 1988] and prey-density measurements of the same or related prey species [Paine and Vadas, 1969; Thayer et al., 1973; Foy and Norcross, 1999]), this energy density equates to a long-term average energy consumption rate of 2.7% body mass per day for females and 2.8% body mass per day for males.

Females also had greater requirements than males at the per-recruit scale, although mortality gradually lessened the contribution of older age classes (Fig. 2B), nullifying some of the disparity between the sexes at the individual scale. Cumulative female and male per-recruit energy consumption was 20.7 MJ and 14.8 MJ, respectively. Per-recruit energy consumption, the product of age-specific consumption rate and relative fish abundance, peaked at ages 4–6, indicating that those age groups have the greatest potential to affect their prey species.

Effects of El Niño on *S. mystinus* energetics

El Niño events changed *S. mystinus* energy consumption compared to that in the baseline model, but the direction and magnitude of change were dependent on sex, age, scale of calculation (individual vs. per recruit), and the number and frequency of El Niño events experienced by a given cohort. To demonstrate this change, I modeled growth of two cohorts that experienced El Niño regimes of moderate or high intensity. The first cohort ("cohort A") experienced five El Niño events by age 30, whereas the second cohort ("cohort B") experienced eight El Niño events (Figs. 3 and 4).

At the scale of individual fish, cohorts A and B experienced lower energy consumption in El Niño events, particularly among females. During El Niño years, which first occurred at age 3 for cohort A and at age 1 for cohort B, consumption by females was always lower than the baseline value (Fig. 3A). In immature females, the disparity was 7–10% lower than the baseline value and was 12–13% lower for mature females. These reductions in consumption were a function of lower growth rates, poor condition factor, and reduced fecundity during El Niño years. In contrast, consumption by males during El Niño years was 4–9% lower than the baseline value among immature individuals, but was roughly equal to the baseline value for mature individuals (Fig. 3B), in part because males did not experience drastic changes in reproductive condition during El Niño years. Both sexes experienced years when energy consumption was greater than the baseline value, particularly two years after an El Niño event when the somatic condition factor returned to normal and greater-than-average growth for that age occurred. By age 30, sizes of fish in both El Niño models were close to the asymptotic maxima and were therefore similar to baseline sizes (Table 3). Cumulative 30-year energy consumption values were

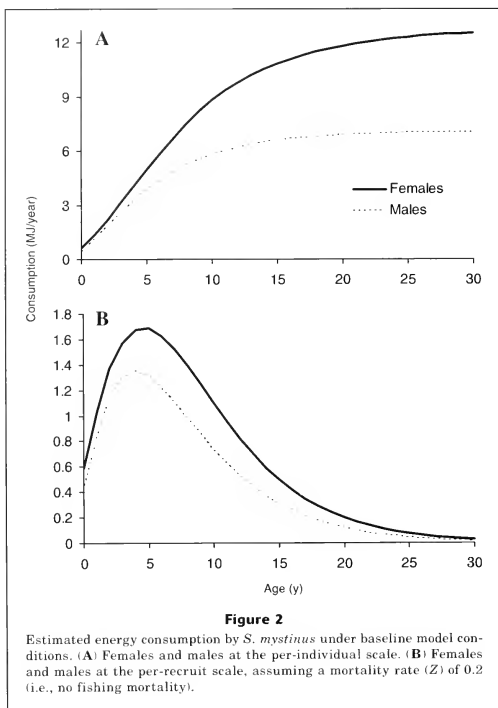


also similar in all models and in both sexes, despite the declines experienced by females.

Repeated exposure to El Niño also affected reproduction by *S. mystinus*. Both sexes experienced delays in maturation as a result of slowed growth rates during El Niño events, and the delay was related to the number of El Niño years experienced at young ages. In the baseline model, 50% maturity was reached at age 6 for both sexes. In cohort A, 50% maturity was reached at age 6 by females, but at age 7 by males. Under the more arduous conditions of cohort B, both sexes reached 50% maturity at age 7. The effect of delayed maturation in terms of energy consumption should be greatest in females because of their greater investments in reproduction, although this was not especially noticeable at the scale of cumulative consumption per individual

(Table 3). A further effect of El Niño events occurred in female egg production. The dramatic reduction in fecundity during El Niño years over the course of an individual female's life caused cumulative egg production in cohort A to be only 87.9% of the baseline level, and cohort B female egg production was only 81.3% of the baseline level (Fig. 3C).

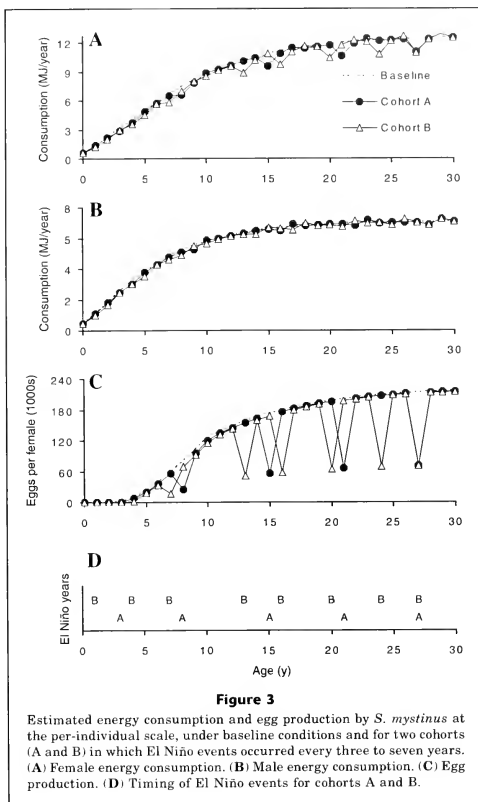
More pronounced El Niño effects occurred at the per-recruit scale. El Niño conditions reduced per-recruit energy consumption in both sexes in contrast to baseline conditions (Fig. 4, A and B). Incorporating mortality lowered the contribution of older age groups, where individual consumption was highest (Fig. 3, A and B), thereby magnifying the El Niño effects on young fish. The negative effects on young age classes were exacerbated in females by slowed maturation and reduced

**Table 3**

Final weights and cumulative energy consumptions for female and male *S. mystinus* from bioenergetics models run under baseline and El Niño conditions. All values are taken from the end of the 30th year. Cohort-A and cohort-B individuals experienced five and eight El Niño events, respectively (see Figs. 3 and 4).

Model	Final weight (g)		Total consumption (MJ)	
	Females	Males	Females	Males
Baseline	1,134.3	617.2	285.0	174.6
Cohort A	1,129.4	616.5	278.1	173.3
Cohort B	1,126.8	616.1	273.6	172.1

fecundity (due to slower growth), resulting in lower per-recruit consumption to meet reproductive costs. Thirty-year cumulative per-recruit energy consumption was 20.0 MJ for cohort-A females (3.2% lower than the baseline value), and 19.4 MJ for cohort-B females (6.3% less than the baseline value). Cumulative per-recruit consumption by cohort-A males was 14.5 MJ (1.9% lower than baseline), whereas cohort-B males consumed 14.2 MJ (4.4% less than the baseline level). The reduction of cumulative egg production was also more drastic at the per-recruit scale: cohort-A females produced 15% fewer eggs than the baseline level, whereas cohort-B females produced 23% fewer eggs at the per-recruit scale (Fig. 4C). These reductions in egg production were related to smaller size, lower fecundity in El Niño years, delayed maturation, and accumulative mortality, all of which allowed fewer females to reach maturity.

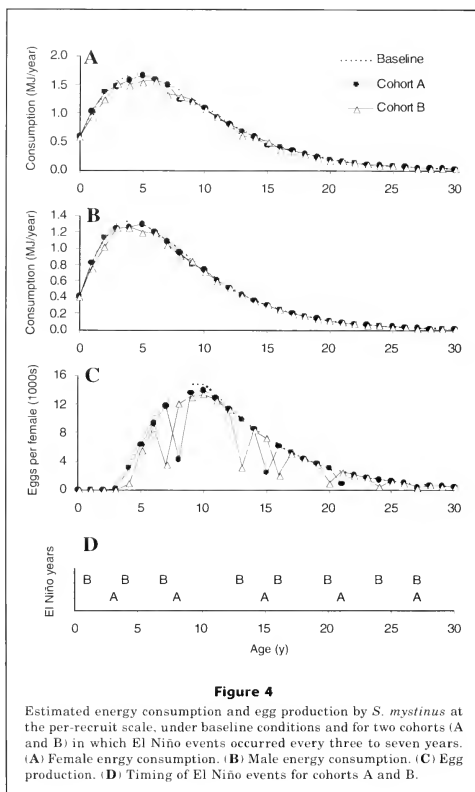


Effects of El Niño on fished cohorts

Adding fishing mortality to the total mortality rate applied in the per-recruit simulations caused changes in the total energy consumption and egg production of *S. mystinus* experiencing repeated El Niño events, in contrast to the baseline state. Under both El Niño regimes, per-recruit consumption by both sexes increased slowly as Z increased until it was nearly identical to the baseline level for cohort A (Fig. 5A) or exceeded the baseline for cohort B (Fig. 5B). The reason for this is that the slower growth experienced during El Niño years meant

that fish reached 200 mm (the size of recruitment into the fishery) later and therefore were not as rapidly subjected to fishing mortality as baseline fish. This extra period of feeding prior to reaching 200 mm was sufficient to equal or exceed the per-recruit energy consumption level in the baseline model.

In contrast, increased Z caused strong declines in egg production, and that effect was exacerbated by the frequency of El Niño years, as demonstrated by the steeper decline in cohort B (Fig. 5B). Delayed maturation caused by El Niño meant that many females were removed by fishing before they were able to reproduce;



furthermore, those that escaped fishing had lower fecundities because of their smaller size and reduced egg production because of the number of El Niño years experienced.

Sensitivity analysis

Based on the RPSS analysis, sensitivity of rockfish bioenergetics models to parameter variation was a function of sex, size, and the CV of the parameter set. When $CV = 2\%$, the model was most sensitive to respiration

parameters in Equation 2 (particularly RB , RQ , and RTO) and to ED , although the rank order varied slightly by sex (Fig. 6, A and B). The sum of the $RPSS_{CV=2\%}$ for all parameters was >0.99 for both the male and female models. This result implies that energy consumption responded linearly to parameter variation because summed RPSS values scale from 0 to 1, with 1 implying a linear response to parameter perturbation (Bartell et al., 1986). When CV increased to 10%, the rank order of parameter sensitivity changed slightly, although respiration parameters and ED remained most important

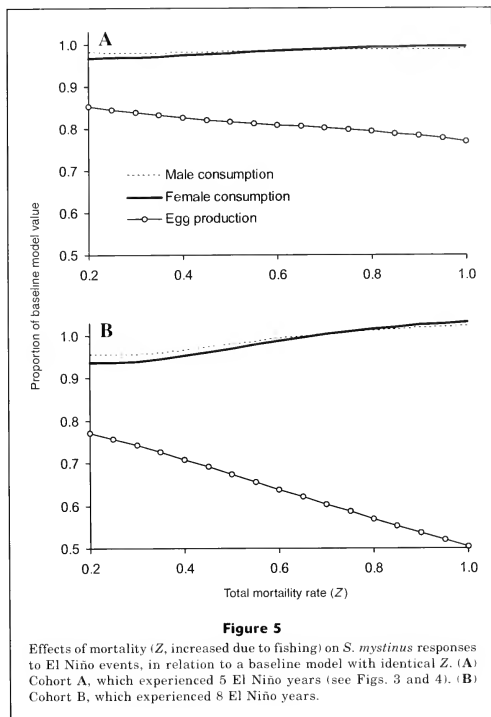
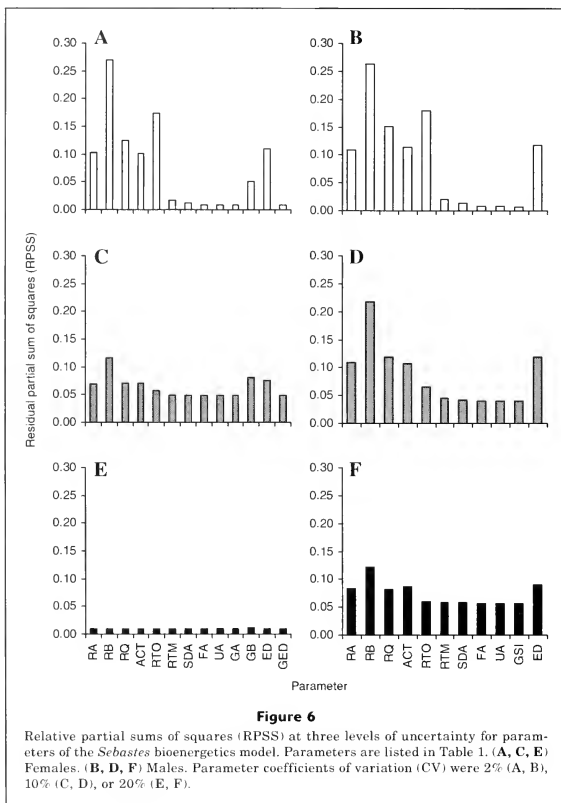


(Fig. 6, C and D). $RPSS_{CV=10\%}$ values declined to 0.84 and 0.94 for females and males, respectively, indicating a greater degree of nonlinearity in response to parameter variation. Finally, when CV increased to 20%, there were major changes in parameter rank order and RPSS, especially for females (Fig. 6E). All female parameters essentially had equal weight, and $RPSS_{CV=20\%}$ dropped dramatically to 0.14, indicating a nonlinear response to parameter variation. Males experienced slight changes in parameter rank order at CV = 20% (Fig. 6F) and increasingly nonlinear behavior related to parameter variation ($RPSS_{CV=20\%} = 0.81$). Because the major difference in the models for the two sexes is the reproductive terms (i.e., Eq. 4 for females vs. the simple GSI calculation for males), the GA or GB terms (or both) appear

to be the cause of poor female model performance at high parameter uncertainty. Also, because GA and GB should only affect female energy budgets as the females mature, model sensitivity to those parameters is likely size dependent.

Energy consumption estimates generated in RPSS analyses were consistently greater than estimates generated by the baseline deterministic model, which used the parameter values from Table 1. Mean consumption estimates and standard deviations increased as the parameter CV increased (Table 4). This effect was more pronounced in females than in males, especially when parameter CV=20%. At that level of parameter uncertainty, male and especially female consumption estimates had very large standard deviations.



Discussion

According to the generic rockfish bioenergetics model, repeated exposure to El Niño conditions lowered the growth, maturation rate, and reproductive level of *S. mystinus*. This happened at both the individual and per-recruit scales; the latter may be most relevant when placing a cohort of fish into a community context because younger age groups have the greatest potential energy demand when mortality is accounted for. In El Niño years, increased temperatures caused respiration rates

of both sexes to increase in contrast to respiration rate in the baseline model, whereas lower growth rates and poor fecundity reduced energy demands. In the long term, these rates equated to a net decrease in energy consumption, which was more pronounced in females than in males because of the higher growth rate and reproductive investment for females. Ironically, adding mortality through fishing pressure lessened the effect of El Niño on *S. mystinus* consumption in contrast to baseline conditions, but that was because rockfish in the El Niño models took longer to reach sizes vulnerable to

Table 4

Energy consumption estimates for *S. mystinus* by a deterministic baseline model (parameters given in Table 1) and simulations run for relative partial sums of squares (RPSS) analysis. Estimates from the RPSS analysis were determined at three levels of parameter uncertainty, with parameter coefficients of variation (CV) equal to 2, 10, or 20%.

Model	Estimated energy consumption (MJ; mean \pm SD)	
	Females	Males
Baseline	285.0	174.6
CV = 2%	286.0 \pm 16.1	175.3 \pm 10.1
CV = 10%	314.3 \pm 102.8	183.9 \pm 57.6
CV = 20%	515.1 \pm 1131.4	209.0 \pm 131.7

fishing. However, the El Niño models may have overestimated per-recruit consumption because I did not add in direct El Niño related mortality; natural mortality may actually increase during El Niño years, as suggested by anecdotal mass mortality events affecting *S. mystinus* during the 1982–83 El Niño (Bodkin et al., 1987).

More dramatic than the effect of El Niño on energy consumption was the effect on egg production. Individual and per-recruit lifetime fecundity dropped (by roughly 12–19% and 15–23%, respectively) in the El Niño models—an effect that was even more drastic as fishing pressure increased. These declines were disproportionate in comparison to changes in long-term energy consumption, which declined by <4% at the individual scale and <7% at the per-recruit scale under even an arduous El Niño regime; and compared to changes in the size of age-30 individuals, which were essentially equal in the baseline and El Niño models. In other words, under a long-term climate regime with El Niño events, total energy demand of females is similar to a baseline regime, and lifetime gross conversion efficiency (growth/consumption) increases, but the conversion efficiency of consumption into reproduction is constrained considerably. That constraint is due largely to delayed maturity, poorer overall fecundity (particularly in El Niño years), and, at the per-recruit scale, the culling effect of natural and fishing mortality.

Of course, the implications from the models for *S. mystinus* must be viewed as hypotheses based on a generic *Sebastes* model. Although the ability of the bioenergetics approach to synthesize demographic, physiological, and environmental data makes it a powerful tool for characterizing dynamic linkages between fish, prey communities, and climate, use of this approach for studies of *Sebastes* will require additional empirical data. A rich body of information exists for some parameters, such as growth rate, fecundity, and depth distribution (Love et al., 1990; Love et al., 2002). However, many

relevant data are lacking, notably diet data. Because of seasonal changes in temperature and reproductive state, rockfish energetics are also seasonal. Seasonal diet changes have been observed in several (largely inshore) species (Love and Ebeling, 1978; Hallacher and Roberts, 1985; Hobson and Chess, 1988; Murie, 1995). Diets may also change with fish size (Love and Ebeling, 1978; Murie, 1995). Data that capture the trophic ontogeny of different species would allow a better depiction of how energy consumptive patterns of a population change with demographics, particularly given the disproportionate demands of younger age classes (Fig. 4). When possible, diet data should be based on weight or volume so that estimates of energy requirements can be readily converted into masses of prey consumed.

Properly incorporating environmental variability will require information not just on temperature variability, but on how rockfish growth, reproduction, and diet vary under different climate regimes. As discussed previously, El Niño and Pacific Decadal Oscillation events have been shown to affect growth, fecundity, and recruitment success of some well-studied species of rockfish. Little information is available on how these factors are affected by La Niña events, however. Furthermore, climate variability may lead to markedly different prey communities (Brodeur and Pearcy, 1992; Lea et al., 1999), resulting in diet shifts about which we currently have little information for most rockfish. Because *S. mystinus* maintained relatively high energy demand during El Niño years, despite slower growth rates and lower fecundity, the prey quality and quantity during such events is clearly important.

Ultimately, these models can be expanded to the population level to place rockfish in the context of their communities. This approach can elucidate how factors such as fishing, environmental variability, and recruitment variability influence the role of rockfish as predators on specific prey taxa, as has been done in bioenergetics models for other predators (Kitchell et al., 1997; Essington et al., 2002; Schindler et al., 2002). Because energy budgets are influenced by fish size and reproductive state, expanding to the population level will require size- or age-structured population models, such as those used in many rockfish stock assessments (e.g., Pacific Fishery Management Council, 2000). Most *Sebastes* stock assessments to date are for species that live in shelf or slope habitats, whereas the species whose food habits and basic energetic information are best known are inshore species. Therefore, a key part of producing useful bioenergetics analysis at the population level will be to prioritize populations or species assemblages for which bioenergetics models might be most useful, and to identify which type of information (population structure or basic biology and ecology) is lacking.

Finally, the generic model parameters in this study required information from several species. Interspecies parameter borrowing has been criticized (Ney, 1993), and the results from such models deserve careful appraisal. The sensitivity analysis demonstrates the importance of this issue: with increasing parameter uncertainty,

the model not only became less reliable (i.e., RPSS decreased, especially for females), but also projected higher energy consumption rates. However, the sensitivity analysis points specifically to the parameters (respiration, energy density, female fecundity) that are most influential and deserve attention in laboratory studies. Additional work is required to better characterize *ACT*, the activity multiplier, particularly for *Sebastes* species that are more pelagically oriented. In many bioenergetics models, consumption is a parameter, such that growth, not consumption, can be the model output. Although studies of energy consumption by juvenile black rockfish (*S. melanops*) have been undertaken (Boehlert and Yoklavich, 1983), more effort is needed in this area.

Conclusion

Although there are limitations to realizing the potential of bioenergetics models in the study of rockfish ecology, those limitations do not overshadow the value of using available information to produce general heuristic models to examine important questions. Such questions include how climate variability affects rockfish consumption patterns, reproduction, and predation rates on different prey taxa; how size-selective fishing may influence rockfish consumption patterns; and how rockfish energy demands compare with available prey resources in regions where population rebuilding efforts are proposed or under way. When ultimately coupled with population models, the bioenergetics approach offers a means to clarify the role that rockfish play in their communities.

Acknowledgments

Suggestions from Phil Levin, Nick Tolimieri, Daniel Schindler, Rich Zabel, Jim Kitchell, Steve Bartell, Kevin Piner, Tina Wyllie-Echeverria, and two anonymous reviewers greatly improved this manuscript.

Literature cited

Bartell, S. M., J. E. Breck, R. H. Gardner, and A. L. Brenkert.
1986. Individual parameter perturbation and error analysis of fish bioenergetics models. *Can. J. Fish. Aquat. Sci.* 43:160-168.

Boehlert, G. W.
1981. The role of temperature and photoperiod in the ontogenetic migration of prejuvenile *Sebastes diploproa* (Pisces: scorpaenidae). *Calif. Fish. Game* 67:164-175.

Boehlert, G. W., and M. M. Yoklavich.
1983. Effects of temperature, ration, and fish size on growth of juvenile black rockfish, *Sebastes melanops*. *Environ. Biol. Fishes* 8:17-28.

Boehlert, G. W., M. Kuskari, and J. Yamada.
1991. Oxygen consumption of gestating female *Sebastes schlegelii*: estimating the reproductive costs of livebearing. *Environ. Biol. Fishes* 30:81-89.

Bodkin, J. L., G. R. VanBlaricom, and R. J. Jameson.
1987. Mortalities of kelp-forest fishes associated with large oceanic waves off central California, 1982-1983. *Environ. Biol. Fishes* 18:73-76.

Broder, R. D., and W. G. Pearcy.
1992. Effects of environmental variability on trophic interactions and food web structure in a pelagic upwelling system. *Mar. Ecol. Prog. Ser.* 84:101-119.

Essington, T. E., D. E. Schindler, R. J. Olson, J. F. Kitchell, C. Boggs, and R. Hilborn.
2002. Alternative fisheries and the predation rate of yellowfin tuna in the eastern Pacific Ocean. *Ecol. Appl.* 12:724-734.

Foy, R. J., and B. L. Norcross.
1999. Spatial and temporal variability in the diet of juvenile Pacific herring (*Clupea pallasii*) in Prince William Sound, Alaska. *Can. J. Zool.* 77:697-706.

Gulland, J. A.
1983. Fish stock assessment, 223 p. John Wiley and Sons, New York, NY.

Hallacher, L. E., and D. A. Roberts.
1985. Differential utilization of space and food by the inshore rockfishes (Scorpaenidae: *Sebastes*) of Carmel Bay, California. *Environ. Biol. Fishes* 12:91-110.

Hewett, S. W., and B. L. Johnson.
1992. Fish bioenergetics model 2, 79 p. Univ. Wisconsin Sea Grant Inst., Madison, WI.

Hobson, E. S., and J. R. Chess.
1988. Trophic relations of the blue rockfish, *Sebastes mystinus*, in a coastal upwelling system off northern California. *Fish. Bull.* 86:715-743.

Kita, J., S. Tsuchida, and T. Setoguma.
1996. Temperature preference and tolerance, and oxygen consumption of the marbled rockfish, *Sebastes marmoratus*. *Mar. Biol.* 125:467-471.

Kitchell, J. F., D. E. Schindler, R. Ogutu-Ohwayo, and P. N. Reinthal.
1997. The Nile perch in Lake Victoria: interactions between predation and fisheries. *Ecol. Appl.* 7:653-664.

Kitchell, J. F., D. J. Stewart, and D. Weininger.
1977. Applications of a bioenergetics model to yellow perch (*Perca flavescens*) and walleye (*Stizostedion vitreum vitreum*). *J. Fish. Res. Board Can.* 34:1922-1935.

Laidig, T. E., Pearson, D. E., and L. L. Sinclair.
2003. Age and growth of blue rockfish (*S. mystinus*) from central and northern California. *Fish. Bull.* 101:800-808.

Lea, R. N., R. D. McAllister, and D. A. VenTresca.
1999. Biological aspects of nearshore rockfishes of the genus *Sebastes* from central California with notes on ecologically related sport fishes. *Calif. Dep. Fish Game Fish Bull.* 177, 109 p.

Lernarz, W. H., D. A. VenTresca, W. M. Graham, F. B. Schwing, and F. Chavez.
1995. Explorations of El Niño events and associated biological population dynamics off central California. *Calif. Coop. Oceanic Fish. Invest. Rep.* 36:106-119.

Love, M. S., and A. W. Ebeling.
1978. Food and habitat of three switch-feeding fishes in the kelp forests off Santa Barbara, California. *Fish. Bull.* 76:257-271.

Love, M. S., P. Morris, M. McCrae, and R. Collins.
1990. Life history aspects of 19 rockfish species (Scorpaenidae: *Sebastes*) from the Southern California Bight. *NOAA Tech. Rep. NMFS* 87, 38 p.

- Love, M. S., M. Yoklavich, and L. Thorsteinson.
2002. The rockfishes of the northeast Pacific, 405 p.
Univ. California Press, Berkeley, CA.
- MacFarlane, R. B., and E. C. Norton.
1999. Nutritional dynamics during embryonic development in the viviparous genus *Sebastes* and their application to the assessment of reproductive success. *Fish. Bull.* 97:273-281.
- Madenjian, C. P., D. V. O'Connor, and D. A. Nortrup.
2000. A new approach toward evaluation of fish bioenergetics models. *Can. J. Fish. Aquat. Sci.* 57:1025-1032.
- Murie, D. J.
1995. Comparative feeding ecology of two sympatric rockfish congeners, *Sebastes caurinus* (copper rockfish) and *S. maliger* (quillback rockfish). *Mar. Biol.* 124:341-353.
- Negus, M. T.
1995. Bioenergetics modeling as a salmonine management tool applied to Minnesota waters of Lake Superior. *N. Am. J. Fish. Manag.* 15:60-78.
- Ney, J. J.
1993. Bioenergetic modeling today: growing pains on the cutting edge. *Trans. Am. Fish. Soc.* 122:736-748.
- Ouchi, K.
1977. Temperature tolerance of young rockfish, *Sebastes thompsoni* (Jordan et Hubbs). *Bull. Jap. Sea Reg. Fish. Res. Lab.* 28:1-8.
- Pacific Fishery Management Council.
2000. Status of the Pacific coast groundfish fishery through 2000 and recommended biological catches for 2001: stock assessment and fishery evaluation. Pacific Fishery Management Council, Portland, OR.
- Paine, R. T., and R. L. Vadas.
1969. Calorific values of benthic marine algae and their postulated relation to invertebrate food preference. *Mar. Biol.* 4:79-86.
- Parker, S. J., S. A. Berkeley, J. T. Golden, D. R. Gunderson, J. Heifetz, M. A. Hixon, R. Larson, B. M. Leaman, M. S. Love, J. A. Musick, V. M. O'Connell, S. Ralston, H. J. Weeks, and M. M. Yoklavich.
2000. Management of Pacific rockfish. *Fisheries* 25: 22-29.
- Perez, M. A.
1994. Calorimetry measurements of energy value of some Alaskan fishes and squids. NOAA Tech. Memo. NMFS-AFSC-32. 32 p.
- Rice, J. A., J. E. Breck, S. M. Bartell, and J. F. Kitchell.
1983. Evaluating the constraints of temperature, activity, and consumption on growth of largemouth bass. *Environ. Biol. Fishes* 9:263-275.
- Schindler, D. E., T. E. Essington, J. F. Kitchell, C. Boggs, and R. Hilborn.
2002. Sharks and tunas: fisheries impacts on predators with contrasting life histories. *Ecol. Appl.* 12:735-748.
- Thayer, G. W., W. E. Schaaf, J. W. Angelovic, and M. W. LaCroix.
1973. Caloric measurements of some estuarine organisms. *Fish. Bull.* 71:289-296.
- Tsuchida, S., and T. Setoguma.
1997. Temperature responses of young Schlegel's black rockfish *Sebastes schlegelii*. *Nippon Suisan Gakk.* 63:317-325.
- VenTresca, D. A., R. H. Parrish, J. L. Houk, M. L. Gingras, S. D. Short, and N. L. Crane.
1995. El Niño effects on the somatic and reproductive condition of blue rockfish, *Sebastes mystinus*. *Cal. Coop. Oceanic Fish. Invest. Rep.* 36:167-174.
- Vetter, R. D., and E. A. Lynn.
1997. Bathymetric demography, enzyme activity patterns, and bioenergetics of deep-living scorpaenid fishes (genera *Sebastes* and *Sebastolobus*): paradigms revisited. *Mar. Ecol. Prog. Ser.* 155:173-188.
- Woodbury, D.
1999. Reduction of growth in otoliths of widow and yellowtail rockfish (*Sebastes entomelas* and *S. flavidus*) during the 1983 El Niño. *Fish. Bull.* 97:680-689.
- Wyllie-Echeverria, T.
1987. Thirty-four species of California rockfishes: maturity and seasonality of reproduction. *Fish. Bull.* 85: 229-250.
- Yang, T.-H., N. C. Lai, J. B. Graham, and G. N. Somero.
1992. Respiratory, blood, and heart enzymatic adaptations of *Sebastolobus alascanus* (Scorpaenidae; Teleostei) to the oxygen minimum zone: a comparative study. *Biol. Bull.* 183:490-499.

Abstract—Short-duration (5- or 10-day) deployments of pop-up satellite archival tags were used to estimate survival of white marlin (*Tetrapturus albidus*) released from the western North Atlantic recreational fishery. Forty-one tags, each recording temperature, pressure, and light level readings approximately every two minutes for 5-day tags ($n=5$) or four minutes for 10-day tags ($n=36$), were attached to white marlin caught with dead baits rigged on straight-shank ("J") hooks ($n=21$) or circle hooks ($n=20$) in offshore waters of the U.S. Mid-Atlantic region, the Dominican Republic, Mexico, and Venezuela. Forty tags (97.8%) transmitted data to the satellites of the Argos system, and 33 tags (82.5%) transmitted data consistent with survival of tagged animals over the deployment duration. Approximately 61% (range: 19–95%) of all archived data were successfully recovered from each tag. Survival was significantly ($P<0.01$) higher for white marlin caught on circle hooks (100%) than for those caught on straight-shank ("J") hooks (65%). Time-to-death ranged from 10 minutes to 64 hours following release for the seven documented mortalities, and five animals died within the first six hours after release. These results indicate that a simple change in hook type can significantly increase the survival of white marlin released from recreational fishing gear.

Application of pop-up satellite archival tag technology to estimate postrelease survival of white marlin (*Tetrapturus albidus*) caught on circle and straight-shank ("J") hooks in the western North Atlantic recreational fishery*

Andrij Z. Horodysky

John E. Graves

Virginia Institute of Marine Science
College of William and Mary
Route 1208 Greate Rd.
Gloucester Point, Virginia 23062

E-mail address (for J. E. Graves, contact author): graves@vims.edu

Atlantic white marlin (*Tetrapturus albidus* Poey, 1860) are targeted by a directed recreational fishery and occur as incidental bycatch in commercial fisheries throughout the warm pelagic waters of the Atlantic Ocean. Total reported recreational and commercial landings of white marlin peaked at 4911 metric tons (t) in the mid-1960s, declined steadily during the next 15 years, and have since fluctuated without trend between 1000 and 2000 t despite substantial increases in fishing effort (ICCAT, 2003). Recent population assessments conducted by the Standing Committee for Research and Statistics (SCRS) of the International Commission for the Conservation of Atlantic Tunas (ICCAT) indicate that the Atlantic-wide white marlin stock is currently at historically low levels and has been severely overexploited for over three decades (ICCAT, 2003). In the 2002 white marlin assessment, the 2001 biomass was estimated to be less than 12% of that required for maximum sustainable yield (MSY) under the continuity case (ICCAT, 2003). Current harvest is estimated to be more than eight times the replacement yield (ICCAT, 2003).

In response to the overfished status of white marlin, ICCAT has adopted binding international recommendations to decrease overall Atlantic landings of this species by 67% from 1996 or 1999 levels (whichever is greater) through the release of all live white marlin from commercial pelagic longline and purse-seine gears (ICCAT, 2001). How-

ever, even these dramatic reductions may be ineffective in rebuilding the white marlin stock. Goodyear (2000) estimated that a 60% decrease from 1999 fishing mortality levels would be required to halt the reduction of Atlantic blue marlin (*Makaira nigricans*). Because white marlin experience higher levels of fishing-induced mortality, it is expected that the reduction in mortality required to stabilize this stock will be even greater.

Management measures within the United States, established by the Atlantic Billfish Fishery Management Plan (FMP) (NMFS, 1988) and subsequent Amendment 1 (NMFS, 1999), have also been implemented to reduce white marlin fishing mortality. U.S. commercial fishermen have been prohibited from landing or possessing all Atlantic istiophorids since 1988. Dead discards of white marlin from the U.S. commercial pelagic longline fishery peaked at 107 t in 1989, and have decreased to 40–60 t over the last several years (White Marlin Status Review Team¹). Management

* Contribution 2610 from the Virginia Institute of Marine Science, College of William and Mary, Gloucester Point, VA 23062.

¹ White Marlin Status Review Team. 2002. Atlantic white marlin status review document, 49 p. Report to the National Marine Fisheries Service, Southeast Regional Office, September 3, 2002. www.nmfs.gov/prot_res/readingrm/Candidate_Plus/white_marlin/whm_status_review.pdf

measures for U.S. recreational anglers include a minimum size of 66 inches lower jaw fork length (NMFS, 1999) and mandatory reporting of landed billfishes (NMFS, 2003). White marlin landings by U.S. recreational anglers ranged between 40 and 110 t from 1960 to the mid-1980s (Goodyear and Prince, 2003) and have decreased to about 2 t in recent years. At present, over 99% of the 4000–8000 white marlin estimated to be caught annually by U.S. recreational fishermen are released (Goodyear and Prince, 2003).

The benefit of current management measures that rely on the release of white marlin cannot be evaluated because levels of postrelease survival are not known for this species. Recapture rates of billfishes tagged with conventional tags are very low (0.4–1.83%; Prince et al., 2003; Ortiz et al., 2003), which may result from high postrelease mortality, tag shedding, or a failure to report recaptures (Bayley and Prince, 1994; Jones and Prince, 1998). Little acoustic tracking has been conducted on white marlin (Skomal and Chase, 2002; $n=2$ tracks), but similar work on other istiophorid species indicates relatively high postrelease survival for periods ranging from a few hours to a few days for fish released from recreational fisheries (e.g., sailfish: Jolley and Irby, 1979; blue marlin: Holland et al., 1990; Block et al., 1992; black marlin: Pepperell and Davis, 1999). However, data from acoustic tracking studies bear limitations and biases that preclude their use in estimating billfish postrelease survival (Pepperell and Davis, 1999; Graves et al., 2002). In the absence of better data, all recreationally released billfishes have been assumed to survive (Peel, 1995), and estimates of white marlin postrelease mortality are currently not incorporated into ICCAT landing statistics or assessments (White Marlin Status Review Team, 2002).

Developments in pop-up satellite archival tag (PSAT) technology have greatly improved scientific understanding of the behavior, movements and postrelease survival of highly migratory marine fishes, including bluefin tuna (Block et al., 2001), swordfish (Sedberry and Loferer, 2001), white sharks (Boustany et al., 2002), blue marlin (Graves et al., 2002; Kerstetter et al., 2003), black marlin (Gunn et al., 2003), and striped marlin (Domeier et al., 2003). To estimate the postrelease survival of billfishes, researchers have used PSAT deployment durations ranging from five days to seven months (Graves et al., 2002; Domeier et al., 2003; Kerstetter et al., 2003). Goodyear (2002) cautioned that longer duration deployments increase the potential for tag shedding, tag malfunction, and data corruption, and may bias postrelease survival estimates by including additional sources of mortality other than the capture event. Graves et al. (2002) considered five days to be an appropriate window to detect mortality in blue marlin released from recreational gear in offshore waters of Bermuda, citing recaptures of blue marlin tagged with conventional tags within five days of the initial tagging event as evidence that some istiophorids may recover sufficiently to resume feeding shortly after capture.

Survival estimates for other istiophorid species released from recreational fishing gear may not be applicable to white marlin. One reason may involve body size: recreationally caught blue marlin and striped marlin are generally larger than white marlin. Inter- and intra-specific differences in body size may affect feeding behavior, fight time, handling time, as well as postrelease recovery (Kieffer, 2000). Another reason may involve the different angling techniques used to catch certain istiophorid species. Blue marlin often hook themselves in the mouth and head while aggressively pursuing high speed trolled lures (Graves et al., 2002). In contrast, as white and striped marlin approach a specific baitfish in the trolling spread, many anglers free-spool (i.e., “drop-back”) rigged natural baits to feeding marlin to imitate stunned baitfish (Mather et al., 1975). This process increases the probability that straight-shank (“J”) hooks rigged with natural baits will damage vital internal areas such as the gills, esophagus, and stomach (Prince et al., 2002a). Recently, several studies have documented a reduction in hook-induced trauma associated with the use of circle hooks in fisheries targeting estuarine and pelagic fishes (Lucy and Studholme, 2002). However, there is little research specifically comparing levels of postrelease survival of pelagic fishes caught on circle and straight-shank (“J”) hooks. Prince et al. (2002a) and Skomal et al. (2002) examined hooking locations and injuries in sailfish and bluefin tuna caught on both hook types but lacked postrelease survival data from study animals. Domeier et al. (2003) did not detect a significant difference between striped marlin caught on circle and straight-shank (“J”) hooks, although the authors did observe significantly decreased rates of deep-hooking and tissue trauma with circle hooks compared to straight-shank (“J”) hooks.

We used data recovered from PSATs to estimate the survival of 41 white marlin caught on circle and straight-shank (“J”) hooks in the recreational fishery and released in the western North Atlantic Ocean during 2002–2003. In addition, differences in hooking locations and hook-induced trauma for white marlin caught on circle and straight-shank (“J”) hooks were assessed.

Methods

Tags

The Microwave Telemetry, Inc. (Columbia, MD) PTT-100 HR model PSAT tag was used in our study. This tag is slightly buoyant, measures 35 cm by 4 cm, and weighs <70 grams. The body of the tag contains a lithium composite battery, a microprocessor, a pressure sensor, a temperature gauge, and a transmitter, all housed within a black resin-filled carbon fiber tube. Flotation is provided by a spherical resin bulb embedded with buoyant glass beads. This tag model is programmed to record and archive a continuous series of temperature,

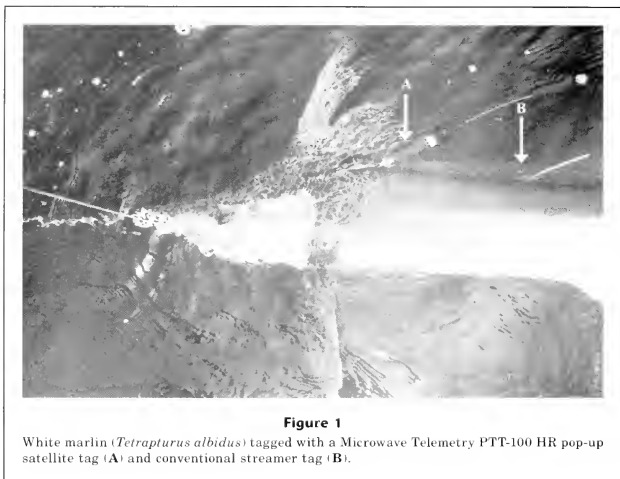


Figure 1

White marlin (*Tetrapturus albidus*) tagged with a Microwave Telemetry PTT-100 HR pop-up satellite tag (A) and conventional streamer tag (B).

light, and pressure (depth) measurements, and can withstand pressure equivalent to a depth of 3000 m. Tags programmed to disengage after five days ($n=5$) recorded measurements approximately every two minutes, whereas tags programmed to disengage after ten days ($n=35$) recorded measurements about every four minutes. Additionally, both 5-day and 10-day tag models transmitted archived and real-time surface temperature, pressure, and light level readings to orbiting satellites of the Argos system for 7–10 days following release from the study animals.

PSATs were attached to white marlin by an assembly composed of 16 cm of 400-pound test Momoi® brand (Momoi Fishing Co., Ako City, Japan) monofilament fishing line attached to a large hydroscopic, surgical-grade nylon intramuscular tag anchor according to the method of Graves et al. (2002). Anchors were implanted with 10-cm stainless steel applicators attached to 0.3-m, 1-m, or 2-m tagging poles (the length of the tagging pole varied depending on the distance from a boat's gunwhales to the water) and were inserted approximately 9 cm deep into an area about 10 cm posterior to the origin of the dorsal fin and 5 cm ventral to the base of the dorsal fin (Fig. 1). In this region, the nylon anchor has an opportunity to pass through and potentially interlock with pterygiophores supporting the dorsal fin well above the coelomic cavity (Prince et al., 2002b; Graves et al., 2002). When possible, a conventional tag was also implanted posterior to the PSAT.

Deployment

White marlin were tagged in the offshore waters of the U.S. Mid-Atlantic Bight, the Dominican Republic, Mexico, and Venezuela (Table 1). These locations were chosen for vessel availability and seasonal concentrations of white marlin. All tagging operations were conducted on private or charter recreational fishing vessels targeting billfishes and tunas. White marlin were caught on 20–40 lb class sportfishing tackle and fought in a manner consistent with typical recreational fishing practice (G. Harvey, personal commun.²). The first 41 white marlin caught and successfully positioned boatside were tagged. Fish were not brought to the boat until they were sufficiently quiet to facilitate optimal tag placement. When possible, crew members positioned white marlin for tagging by holding them by the bill and dorsal fin in the water alongside the boat, a technique often used when controlling a billfish to remove hooks. On boats with high gunwhales that prohibited holding the captured fish by the bill, the marlin were “leadere” to the boat’s side and moved into position for tagging when calm. Six hooked white marlin escaped prior to tagging because frayed leaders broke or hooks slipped during this process. Hooks were removed when feasible;

² Harvey, G. 2002. Personal commun. Guy Harvey Enterprises, 4350 Oakes Rd. Suite 518, Davie, FL 33314.

Table 1
Summary of white marlin (*Tetrapturus albidus*) tagging locations during 2002–2003.

Location	Dates of tagging	Tag deployment duration (in days)	Number of tags deployed
Mid-Atlantic Coast	2002: 18–22 Aug, 5–21 Sep	10	11
	2003: 22 Aug	10	1
Punta Cana, Dominican Republic	2002: 15–19 May	5	5
Isla Mujeres, Mexico	2003: 10–12 June	10	3
La Guaira, Venezuela	2002: 23–25 Nov	10	6
	2003: 12–13 Sep 1 Oct	10	15

otherwise, they were left in the fish and the leader was cut as close to the animal as possible prior to release. Both practices are common in the recreational billfish fishery. After capture and positioning alongside tagging vessels, six white marlin were observed to have lost color, and were lethargic and unable to maintain vertical position in the water. These fish were resuscitated alongside the moving boat for 1–5 minutes prior to release—also a common practice in the recreational fishery.

Gear type, fight time, handling time, fight behavior, hooking location, overall fish condition, estimated weight, and GPS coordinates of the release location were recorded for each tagged white marlin. Fight time was defined as the interval from the time the fish was hooked to the time it was “leadered” alongside the boat prior to tagging. Handling time included tagging and resuscitation, if applicable. In accordance with Prince et al. (2002a), straight-shank (“J”) hooks were defined as those with a point parallel to the main hook shaft, whereas circle hooks were defined as having a point perpendicular to the main hook shaft. All circle and straight-shank (“J”) hooks were rigged with dead ballyhoo (*Hemiramphus brasiliensis*) bait. Size 7/0 Mustad straight-shank (“J”) hooks (models 9175 and 7731) were rigged with the hook exiting the ventral surface of the ballyhoo. Two models of circle hooks were employed in this study: Mustad Demon Fine Wire (model C39952BL, size 7/0; 5° offset, $n=9$) and Eagle Claw Circle Sea (L2004EL, sizes 7/0–9/0; non-offset, $n=11$). All circle hooks were rigged so that they pointed upwards from the head of the ballyhoo (see Prince et al., 2002a). The rigging designations and fishing techniques unique to each hook type were maintained in our study to reflect the usual application of circle and straight-shank (“J”) hooks in the white marlin recreational fishery. Other than these differences, all handling, tagging, and recording methods were the same for both treatments.

Hooking locations were pooled into two categories: jaw, externally visible (including all lip-hooked, foul-hooked, and bill-entangled white marlin) and deep, not externally visible (including all white marlin hooked in the palate, gills, esophagus, and everted stomachs). Bleeding was recorded as present or absent, and the

general location of bleeding was recorded when it was possible to identify the source.

Data analysis

Survival of released white marlin was determined from two distinct lines of evidence provided by the satellite tags: net movement, and water temperature and depth profiles. Time series of water temperature and depth measurements taken about every 2 minutes (5-day tags) or 4 minutes (10-day tags) were used to discriminate surviving from moribund animals. Net movement was determined as a minimum straight line distance traveled between the coordinates of the initial tagging event and the coordinates of the first reliable satellite contact with the detached tag (inferred to be the location of tag pop-up) derived from Argos location codes 1, 2, or 3 for the first or second day of transmission. In cases where tags did not report more precise location codes, an average of all location code 0 readings for the first day of transmission was used as a proxy for the location of the tag pop-up. To determine the directions (and magnitudes) of observed surface currents in areas where fish were tagged, GPS coordinates (Argos location codes of 1, 2, or 3, or a daily mean of location code 0, for tags lacking these) were plotted for the 7–10 days that the tags were floating at the surface and transmitting data to satellites. Maps, tracks, and distances were generated by using MATLAB (version 6.5, release 13.1, Mathworks Inc, Natick, MA).

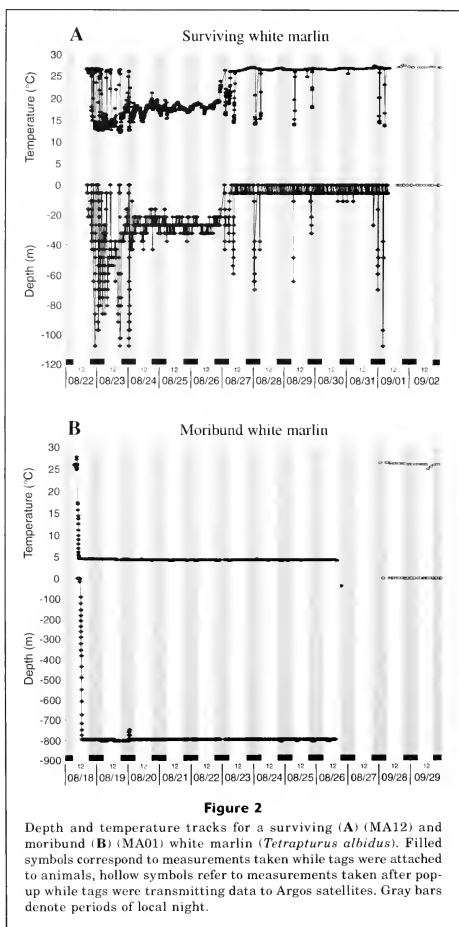
Cochran-Mantel-Haenszel (CMH) tests were used to address the effect of circle and straight-shank (“J”) hooks on survival, hooking location, and the degree of hook-induced trauma. A Yates correction for small sample size was applied when expected cell values were less than 5 (Agresti, 1990). The effects of fight time and total handling time on survival were assessed with Wilcoxon-Mann-Whitney exact tests, with the null hypothesis that there was no difference between surviving and moribund white marlin. All statistical analyses were conducted by using SAS (version 8, SAS Institute, Cary, NC). The lone nonreporting tag observed in our study was excluded from all subsequent analyses.

We conducted bootstrapping simulations to examine the effect of sample size on the 95% confidence intervals of the release mortality estimates using software developed by Goodyear (2002). Distributions of estimates were based on 10,000 simulations with an underlying release mortality equivalent to that observed for straight-shank ("J") hooks for experiments containing 10–200 tags and no sources of error (e.g., no premature release of tags, no tagging-induced mortality, and no natural mortality).

Results

Forty-one white marlin were tagged in four geographic locations during 2002–2003 (Table 1). Information for each fish is summarized in Table 2. Fight times were fairly typical for this fishery (mean: 15.8 min, range: 3–83 min), although two animals required more than 30 minutes before they were sufficiently calm at boathside for tag placement. Overall, forty tags (97.6%) transmitted data to the satellites of the Argos system and of these, thirty-seven tags remained attached to study animals for the full five- or ten-day duration. One five-day tag was released prematurely from a surviving white marlin after 2.5 days, presumably because it had not been attached securely. This individual showed behavior similar to other surviving white marlin while the tag was attached and was presumed to have survived for the purposes of our study. Additionally, two 10-day tags attached to moribund white marlin disengaged from the carcasses prior to the expected date after an extended amount of time at a constant depth and temperature on the seafloor. Approximately 61% of data (range: 19–95%) were successfully transmitted from reporting tags.

Overall, 33 of 40 tags (82.5%) returned data that indicated the survival of tagged animals throughout the duration of tag deployment. Surviving white marlin exhibited daily variations in water temperature and depth data while carrying PSATs (Fig. 2A). The net movement of surviving animals could not be explained by the speed or direction of current patterns alone over the course of the tag deployment (Table 2, Fig. 3A). In contrast, moribund white marlin (Fig. 2B) sank to the seafloor (237–1307 m) and to constant water temperatures (3.7–12.5°C), where they remained until the tags disengaged and floated to the surface not far from the initial tagging location (Fig. 3B). Five of the seven moribund white marlin died within the first six hours of release;



four of these five animals died within the first hour (Table 2).

The two white marlin that experienced the longest fight times (46 and 83 min) died more than 24 hours following their release. White marlin VZ03-11 had a

Table 2

Summary information for tagged white marlin (*Tetrapturus albidus*) released from recreational fishing gear in the western North Atlantic Ocean. Total fight time is defined as the interval between the time that the fish was hooked and the time that it was brought to the side of the boat prior to tagging. Handling time included tagging and resuscitation, where applicable. "D/N" refers to deep, not externally visible hooking locations, "foul" refers to a white marlin hooked in the dorsal musculature. Tail-wrapped fish are denoted with the symbol "^T", resuscitated marlin are denoted with the symbol "^R".

Tag number	Estimated weight (kg)	Fight time (minutes)	Handling time (minutes)	Hook type	Location of hook in or on fish	Bleeding (Yes/No)	Fate (living or dead)	Movement (nmi/km direction)
DR02-01	23	19	1	"J"	D/N	N	L	23/43 NW
DR02-02	20	29	1	"J"	D/N	N	L	39/72 NW
DR02-03	20	29	1	"J"	D/N	Y	L	33/61 NE
DR02-04	25	83	1	"J"	D/N	Y	D	—
DR02-05	20	6	1	"J"	D/N	N	L	60/111 SE
MA01	18	7	1	"J"	D/N	Y	D	—
MA02	20	24	1	"J"	jaw	N	L	63/117 S
MA03	18	9	1	"J"	D/N	Y	L	51/94 S
MA05	20	17	1	"J"	D/N	Y	L	24/44 S
MA06	18	7	1	"J"	D/N	Y	D	—
MA07	20	7	1	"J"	jaw	Y	D	—
MA08 ^{T, R}	25	17	2	"J"	jaw	N	D	—
MA09	23	9	1	"J"	jaw	N	L	103/191 NE
MA10	23	13	1	"J"	jaw	Y	L	102/189 SE
MA11 ^T	27	16	1	"J"	jaw	N	L	260/482 SE
MA12 ^R	23	11	1	"J"	jaw	N	L	59/109 SE
VZ02-01	27	8	1	circle	jaw	N	L	118/219 NW
VZ02-02	23	12	1	circle	jaw	N	L	80/148 NE
VZ02-03 ^{T, R}	20	4	2	circle	jaw	N	L	69/128 NW
VZ02-04	18	9	1	circle	jaw	N	L	63/117 NE
VZ02-05	20	7	1	circle	jaw	N	L	67/124 N
VZ02-06	23	9	1	circle	jaw	N	L	98/181 NW
MX03-01 ^T	27	15	1	circle	jaw	N	L	172/319 NW
MX03-02	18	14	1	circle	jaw	N	L	422/782 NW
MX03-03 ^{T, R}	23	21	5	circle	jaw	N	L	211/391 NW
VZ03-01	20	3	1	circle	jaw	N	L	85/157 NE
VZ03-02	30	6	1	circle	jaw	N	L	127/235 NE
VZ03-03	23	12	1	circle	jaw	N	L	16/30 N
VZ03-04	27	10	1	circle	jaw	Y	L	114/211 NE
VZ03-05	34	23	1	circle	jaw	N	L	40/74 W
VZ03-06	23	9	1	circle	jaw	N	L	49/91 NE
VZ03-07	23	15	1	circle	jaw	N	L	23/43 NE
VZ03-08	23	7	1	circle	jaw	N	L	39/72 NE
VZ03-09 ^T	23	10	1	circle	jaw	N	L	127/235 NE
VZ03-10 ^{T, R}	23	28	2	"J"	jaw	N	L	81/150 NE
VZ03-11 ^{T, R}	23	46	3	"J"	foul	N	D	—
VZ03-12	18	23	1	"J"	jaw	N	L	19/35 NW
VZ03-13	16	17	1	"J"	D/N	Y	D	—
VZ03-14	20	14	1	circle	jaw	N	L	131/243 NW
VZ03-15	20	8	1	circle	jaw	N	L	128/237 NE

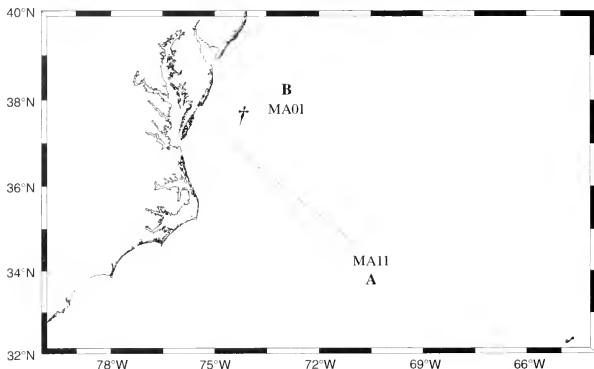


Figure 3

Minimum straight line distances traveled by a surviving white marlin (*Tetrapturus albidus*) (solid line) (A) and the drifting track of a transmitting tag (dotted line) in offshore waters of the U.S. Mid-Atlantic Bight. The cross (B) denotes a moribund white marlin that sank to the seafloor shortly after it was released, illustrating that dead fish did not travel far from the initial tagging coordinates.

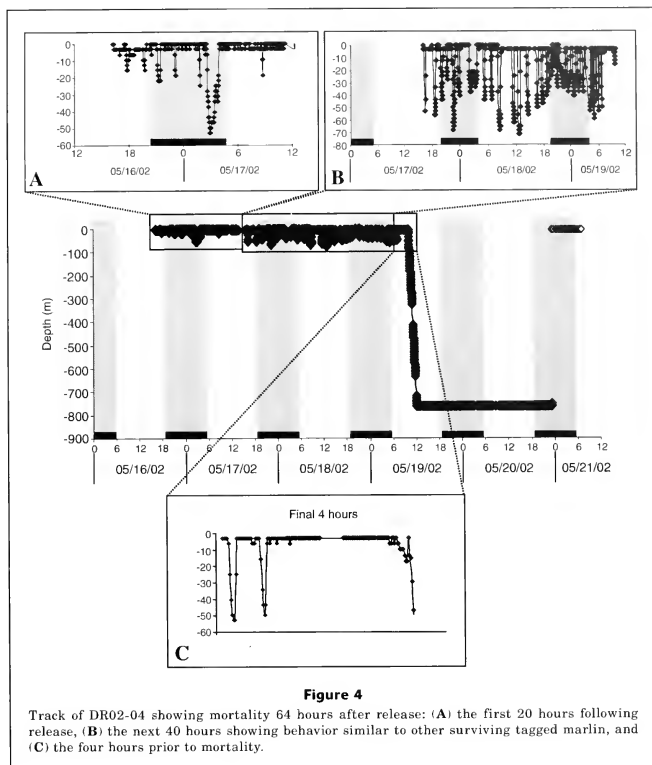
fight time of 46 minutes and died 27 hours after tagging, and DR02-04 had a fight time of 83 minutes and died 64 hours after tagging (Fig. 4). There was no significant difference in fight time ($Z=0.4996$, $P=0.62$) between surviving and moribund white marlin, largely due to the large range of fight times for moribund animals. Handling times ranged from 1 to 5 minutes per fish.

Hook type had a highly significant effect on the postrelease survival of white marlin (Fig. 5). Fish caught on circle hooks experienced significantly higher survival (20 of 20; 100%) than those caught on straight-shank ("J") hooks (13 of 20; 65%) (Yates's corrected CMH $\chi^2=7.386$, $P<0.007$). There were also highly significant differences in hooking locations and hook-induced trauma between hook types (Fig. 5). Odds ratios revealed that white marlin caught on straight-shank ("J") hooks were 41 times more likely to be hooked deeply (Yates's corrected CMH $\chi^2=11.48$, $P<0.001$) and over 15 times more likely to sustain hook-induced tissue trauma resulting in bleeding (CMH $\chi^2=8.3$, $P<0.005$) than fish caught on circle hooks. Of the white marlin caught on straight-shank ("J") hooks, half were hooked in deep locations, and 70% of these fish were bleeding. Four of the seven observed mortalities were those of deep-hooked and bleeding fish. Overall, 56% of bleeding, 40% of deep-hooked, and 57% of deep-hooked and bleeding white marlin perished following release. In contrast, all white marlin caught on circle hooks were hooked in the jaw, and bleeding was evident only in a single animal in which the hook point exited the edge

of the eye socket but did not damage the eye. Additionally, 20% (8 of 40) of the white marlin in our study became entangled in the line during the fight and were "leadered" to the boat tail-first, a condition known as "tailwrapped" (Holts and Bedford, 1990). This phenomenon was equally distributed with respect to hook type. Five tailwrapped white marlin required resuscitation, and two tailwrapped white marlin hooked in the jaw with straight-shank ("J") hooks died.

With the model developed by Goodyear (2002), the results of 10,000 simulated experiments at an underlying true mortality rate of 35% indicated that approximate 95% confidence intervals for mortality estimates for an experiment deploying 20 tags on white marlin caught on straight-shank ("J") hooks range from 15% to 59% in the absence of confounding factors. A dramatic increase in sample size would be required to improve the precision of mortality estimates (Fig 6). Doubling the sample size ($n=40$) would decrease the 95% confidence intervals to about $\pm 15\%$ of the true value and quadrupling the number of tags ($n=80$ PSATs) would reduce confidence intervals to about $\pm 10\%$ of the true value. More than 200 PSATs would have to be deployed to lower the confidence intervals to $\pm 5\%$ of the true value.

The net displacement of released white marlin was variable among individuals and across locations and was used as an independent line of evidence to assess survival. Surviving white marlin demonstrated movement patterns that cannot be explained by surface currents alone. Distances and directions of displacement are summarized in Table 2. White marlin tagged with



10-day PSATs moved an average of 101 (± 84) nautical miles (nmi) or 188 km (± 155) and those tagged with 5-day PSATs moved an average of 38.8 nmi (± 15.6) or 72 km (± 29).

Discussion

The results of this study clearly indicate that hook type significantly affects the survival of white marlin released from recreational fishing gear. White marlin caught on circle hooks were much more likely to survive release from recreational fisheries than those caught on straight-shank ("J") hooks. These results concur with

previous research across a broad range of fishes caught by diverse recreational fishing techniques (Muoneke and Childress, 1994; Diggles and Ernst, 1997; Lukacovic and Uphoff, 2002; Malchoff et al., 2002; Skomal et al., 2002; Zimmerman and Bochenek, 2002). However, the results of our study differ with those of Domeier et al. (2003), who noted differences in deep-hooking and bleeding between striped marlin caught on circle hooks and those caught on "J" hooks but did not detect a significant difference in mortality between hook types. Differences between the two studies may result from a disparity in body size between the two species, specific bait types (white marlin were caught on dead baits in the present study, Domeier et al. [2003] used live baits),

or sampling error (or a combination of these factors). It should be noted that Domeier et al. (2003) and the crew of the present study both used non-offset and 5° offset circle hooks.

The survival rate observed for white marlin caught on straight-shank ("J") hooks in our study (65%) is slightly lower than that reported for other istiophorid species (blue marlin 89%, Graves et al., 2002; striped marlin 71%, Domeier et al., 2003) caught on this type of hook. Differences in the recreational fishing practices for these species may account for the variation in levels of istiophorid postrelease survival. In recreational fisheries that target striped marlin and white marlin, longer drop-back durations with natural baits rigged on "J" hooks increase the probability of deep-hooking and internal damage, which influence mortality. The postrelease mortality rates of white marlin and striped

marlin from drop-back fisheries are similar and are notably higher than that of blue marlin caught on high-speed trolled baits.

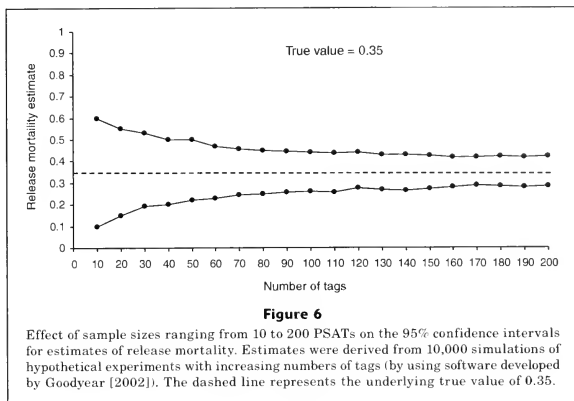
The results of our study also agree with previous research documenting increased deep-hooking and tissue trauma associated with the use of straight-shank ("J") hooks. In contrast to circle hooks, "J" hooks are over 20 times more likely to cause bleeding in sailfish (Prince et al., 2002a), five times more likely to cause bleeding in striped marlin (Domeier et al., 2003), and 15 times more likely to cause bleeding in white marlin (present study). Slightly more than half of the bleeding white marlin and less than half of the deep-hooked fish caught on "J" hooks died in our study. Observations of rusted hooks encapsulated in the viscera of otherwise healthy istiophorids (Prince et al., 2002a) have indicated that wounds resulting from deep-hooking are not necessarily lethal. Furthermore, the results of the present study also indicate that jaw hooking locations are not exclusively nonlethal. Straight-shank ("J") hooks can cause lacerations to vital organs such as the eye, brain, pharynx, esophagus, and stomach before detaching from the initial hooking location and rehooking in regions that are typically considered less lethal, such as the jaw and bill (Prince et al., 2002a). These internal injuries are difficult to record without additional handling and internal examination and confound relationships between hooking location and mortality in the absence of other predictors. Regardless, the significantly higher survival rate for white marlin caught on circle hooks, coupled with reduced rates of deep-hooking and tissue trauma, indicate that this terminal gear may decrease postrelease mortality rates in drop-back fisheries that currently use "J" hooks.

None of the white marlin caught on circle hooks in this study were hooked deeply. Despite documenting significantly lower deep-hooking rates with circle hooks, previous studies have nonetheless observed that both non-offset and offset circle hooks may occasionally hook fish deeply (Prince et al., 2002a; Skomal et al. 2002). This is especially true of severely offset (e.g., 15°) circle hooks, which are highly associated with increased levels of deep hooking and which may mitigate any conservation benefits associated with the use of this terminal gear (Prince et al., 2002a).

Resuscitation of exhausted istiophorids is a common practice in the recreational fishery. Five white marlin that were tailwrapped and unable to ram-ventilate during the fight were resuscitated in our study. For example, white marlin MX03-03 was tailwrapped for the final seven minutes of the 21-minute fight and appeared to be severely exhausted at boatside. This fish was unable to regulate its position in the water when the PSAT was implanted, and required the longest resuscitation of any white marlin in this study (~5 min.). After release, a diver confirmed that this marlin regained color and actively swam away upon reaching cooler water at a depth of about 20 m (G. Harvey²). Depth and temperature data showed that this fish survived for the entire 10-day tag deployment duration. Failure

Hook type	Hook location	Bleeding	Fate	
"J" hook 20	Jaw, ext. visible 10 (50%)	No 8 (80%)	Live 6 Dead 2	
		Yes 2 (20%)	Live 1 Dead 1	
	Deep, not ext. visible 10 (50%)	No 3 (30%)	Live 3 Dead 0	
		Yes 7 (70%)	Live 3 Dead 4	
	Circle hook 20	Jaw, ext. visible 20 (100%)	No 19 (95%)	Live 19 Dead 0
			Yes 1 (5%)	Live 1 Dead 0
Deep, not ext. visible 0		No n/a	Live n/a Dead n/a	
		Yes n/a	Live n/a Dead n/a	

Figure 5
Effects of circle and straight-shank ("J") hooks on hooking location, trauma, and fate. Ext. = externally. n/a = not applicable.



to revive any of the exhausted or tailwrapped white marlin in this study would have biased the mortality estimate upwards if any of these animals perished as a result of exhaustion.

It is unlikely that trauma induced by boatside handling or tagging contributed to the difference between the mortality of white marlin caught on circle hooks and those caught on "J" hooks. Holts and Bedford (1990) and Domeier et al. (2003) suggested that striped marlin in their studies may have died as a result of striking the tagging vessel rather than from hook-induced injury. We observed only one white marlin (DR02-01) strike the side of a tagging vessel; this fish survived and exhibited behavior similar to other healthy white marlin for the full five-day tag deployment duration.

The implications for stomach eversion on billfish survival are unclear because of fairly few observations in studies assessing survival. Stomach eversion appears to be a natural behavioral mechanism by which undesired food items and remnants may be expelled, and stomachs quickly retracted (Holts and Bedford, 1990). In addition, the generally weakened condition of some marlin with everted stomachs indicates that this condition may occur in response to stress (Holts and Bedford, 1990; Pepperell and Davis, 1999). A striped marlin with an everted stomach tracked by Holts and Bedford (1990) survived, whereas a black marlin with an everted stomach tracked by Pepperell and Davis (1999) and a white marlin in this condition tagged by Kerstetter et al. (2004) were both attacked by sharks and died. In the present study, two white marlin (DR02-03 and MA01) everted their stomachs during the fight. White marlin DR02-03 showed behavior consistent with survival until the tag was prematurely released after 2.5 days. In contrast, white marlin MA01 was hooked

in its everted stomach and bled profusely during the fight. Depth data recovered from the PSAT attached to this animal indicated that it died less than 10 minutes after release. The survival of some istiophorids with everted stomachs supports the release of fish in this condition; however, without further observations of animals in this condition, the relevance of stomach eversion in predicting mortality of released billfishes remains uncertain.

The majority of mortalities observed in our study occurred within the first six hours of release; however two mortalities (DR02-04 and VZ03-13) occurred more than 24 hours after tagging. Insights into the behavior of VZ03-13 prior to mortality are compromised by large sections of missing data; however, it should be noted that the final four hours prior to death were associated with surface waters. Likewise, white marlin DR02-04 (Fig. 3A) spent the majority of the first day almost entirely within nearsurface waters following release. Similar prolonged surface associations have been documented in blue marlin (Block et al., 1992) and striped marlin (Brill et al., 1993)—a behavioral pattern that has been attributed to that of a badly injured fish (Brill et al., 1993). White marlin DR02-04 resumed diving behavior similar to that observed in healthy tagged fish (Fig. 3B) after 20 hours, indicating possible recovery from catch-and-release procedures. This white marlin again returned to the surface for four hours prior to its death 64 hours after release.

The two white marlin that had the longest fight times in our study, DR02-04 and VZ03-11 (83 and 46 min, respectively), may have experienced delayed postrelease mortality associated with physiological stress, such as intracellular acidosis following exhaustive exercise (Wood et al., 1983) or haemodilution (Bourke et al.,

1987). These mortalities appear to have occurred too soon to have been caused by infection (Bourke et al., 1987) and too late to have been caused by lactic acidosis. Postexertion recovery in istiophorid billfishes is poorly studied, but Skomal and Chase (2002) reported significant perturbations in blood chemistry, including elevation in blood cortisol levels in bluefin tuna (*Thunnus thynnus*), yellowfin tuna (*Thunnus albacares*), and white marlin exposed to prolonged angling bouts (mean=46 min). Acoustic tracks of these animals revealed recovery periods characterized by limited diving behavior for two hours or less after release. The death of white marlin DR02-04 after apparent recovery (Fig. 3C) may be the result of natural mortality, another capture event, or delayed mortality associated with release from recreational fishing gear. Mortality associated with the trauma induced by retained fishing hooks need not be immediate. Blue sharks with fishing hooks embedded in the esophagus or perforating the gastric wall have been found to experience systemic debilitating disease that may affect survival over longer time intervals (Borucinska et al., 2001, 2002).

We also cannot discount predation as a possible cause of mortality for any of the white marlin that died in our study. Acoustic tagging studies have described predation on tagged and released sailfish (Jolley and Irby, 1979), blue marlin (Block et al., 1992) and black marlin (Pepperell and Davis, 1999) by sharks. Recently, Kerstetter et al. (2004) observed results consistent with scavenging and predation on PSAT-tagged white marlin and opah (*Lampris guttatus*) by sharks. Both Block et al. (1992) and Kerstetter et al. (2004) documented attacks on tagged marlin that exhibited prolonged surface associations—the same pattern shown by DR02-04 immediately following its release and prior to mortality.

One tag (MA04) in our study failed to transmit data and was eliminated from all analyses. In previous PSAT studies demonstrating billfish survival, mortalities of tagged istiophorids were not directly observed (Graves et al., 2002; Kerstetter et al., 2003), and the authors conservatively regarded nonreporting tags to be evidence of mortality. The early tag models used in these studies may have failed to transmit data because moribund animals were located at depths that exceeded the tolerance limit (650 m) of the tags or because of other factors, including tag malfunction, mechanical damage (Graves et al., 2002; Kerstetter et al., 2003) or tag ingestion (Kerstetter et al., 2004), or a combination of these factors. Other authors, using newer models of PSATs rated to withstand pressure equivalent to a depth of 3000 m, have clearly documented several mortalities and have chosen to eliminate nonreporting tags from their analyses (Domeier et al., 2003, present study). Treating nonreporting tags as mortalities will bias mortality estimates upwards if tags fail to report for reasons other than catch-and-release-induced mortality (Goodyear, 2002).

Relatively small sample sizes and fairly limited spatial coverage in the present study precluded the use of these data to infer Atlantic-wide estimates of postrelease mortality rates for white marlin. Given the need to ac-

count for geographical differences in body sizes of white marlin, fishing gears, drop-back durations, angler skill level, habitat variables, predator densities, and locations, the sample size needed to generate an accurate estimate of postrelease mortality for the entire Atlantic recreational sportfishery could easily require more than a thousand tags (Goodyear, 2002). Results of simulated experiments suggest that if the true underlying J-hook mortality rate is 35%, more than 200 PSATs would have to be deployed on white marlin caught on this terminal tackle to reduce the 95% confidence intervals to $\pm 5\%$ of the true value. The cost of such an experiment (~\$1 million for tags alone) is presently prohibitive, particularly considering that these estimates are derived under the assumption of ideal conditions (no premature releases, no tag-induced mortality, and no natural mortality) (Goodyear, 2002). The presence of any confounding factors would increase the necessary sample size and the total cost of such an experiment (Goodyear, 2002).

Despite a relatively small sample size, the present study clearly demonstrates the importance of hook type for the postrelease survival of white marlin. Our results indicate that a highly significant proportion of released white marlin caught on straight-shank ("J") hooks perish and that these hooks are significantly more likely to hook fish deeply and cause internal damage. In contrast, the survival rate of all white marlin caught on circle hooks indicates that a simple change in terminal tackle can significantly reduce postrelease fishing mortality in the recreational fishery.

Acknowledgments

The authors would like to thank Captains Mike Adkins (*South Jersey Champion*), O. B. O'Bryan (*Sea-D*), Jimmy Grant (*Vintage*), Gene Hawn (*Ocean Fifty Seven*), Ryan Higgins (*Caliente*), Ken Neill (*Healthy Grin*), Steve Richardson (*Backlash*), Rod Ryan (*White Witch*), and Rom Whittaker (*Release*), as well as their crews, for their skill in finding white marlin and for their patience with us as we deployed PSATs. We thank Phil Goodyear for kindly providing the bootstrapping software for simulations, Eric Prince (NMFS) for suggestions regarding bait rigging techniques, Paul Howey and Lissa Werbos (Microwave Telemetry, Inc) for technical assistance with the tags, Lorraine Brasseur (VIMS) for assistance with MATLAB programming, Robert Diaz (VIMS) for advice with statistical methods, and David Kerstetter (VIMS) for helpful comments on this manuscript. We gratefully acknowledge the logistical support of Guy Harvey, Dick Weber, and John Wendkos. This project was funded by the National Marine Fisheries Service and Marine Ventures, Inc.

Literature cited

- Agresti, A.
1990. Categorical data analysis, 558 p. John Wiley and Sons, Inc., New York, NY.

- Bayley, R. E., and E. D. Prince.
1994. A review of the tag release and recapture files for Istiophoridae from the Southeast Fisheries Science Center's Cooperative Gamefish Tagging Program. Int. Comm. Cons. Atl. Tunas (ICCAT) Coll. Vol. Sci. Pap. Vol. 41:527-548.
- Block, B. A., D. T. Booth, and F. G. Carey.
1992. Depth and temperature of the blue marlin, *Makaira nigricans*, observed by acoustic telemetry. Mar. Biol. 114:175-183.
- Block, B. A., H. Dewar, S. B. Blackwell, T. D. Williams, E. D. Prince, C. J. Farwell, A. Boustany, S. L. H. Teo, A. Seitz, A. Walli, and D. Fudge.
2001. Migratory movements, depth preferences, and thermal biology of Atlantic bluefin tuna. Science 293 (5533):1310-1314.
- Brill, R. W., D. B. Holts, R. K. C. Chang, S. Sullivan, H. Dewar, and F. G. Carey.
1993. Vertical and horizontal movements of striped marlin (*Tetrapturus audax*) near the Hawaiian Islands, determined by ultrasonic telemetry, with simultaneous measurement of oceanic currents. Mar. Biol. 117: 567-574.
- Borucinska, J., N. Kohler, L. Natanson, and G. Skomal.
2002. Pathology associated with retained fishing hooks in blue sharks (*Prionace glauca*) with implications for their conservation. J. Fish Disease 25(9):515-521.
- Borucinska, J., J. Martin, and G. Skomal.
2001. Peritonitis and pericarditis associated with gastric perforation by a retained fishing hook in a blue shark (*Prionace glauca*) (Linnaeus, 1758). J. Aquat. Animal Health 13:347-254.
- Bourke, R. E., J. Brock, and R. M. Nakamura.
1987. A study of delayed capture mortality syndrome in skipjack tuna, *Katsuwonus pelamis* (L.). J. Fish Disease 10:275-287.
- Boustany, A. M., S. F. Davis, P. Pyle, S. D. Anderson, B. J. LeBoef, and B. A. Block.
2002. Satellite tagging: expanded niche for white sharks. Nature 412(6867):35-36.
- Diggles, B. K., and I. Ernst.
1997. Hooking mortality of two species of shallow-water reef fish caught by recreational angling methods. Mar. Freshw. Res. 48(6):479-483.
- Domeier, M. L., H. Dewar, and N. Nasby-Lucas.
2003. Mortality rate of striped marlin (*Tetrapturus audax*) caught with recreational tackle. Mar. Freshw. Res. 54(4):435-445.
- Goodyear, C. P.
2000. Biomass projections for Atlantic blue marlin: potential benefits of fishing mortality reductions. ICCAT (Int. Comm. Conserv. Atl. Tunas) Coll. Vol. Sci. Pap. 52:1502-1506.
2002. Factors affecting robust estimates of the catch-and-release mortality using pop-up tag technology. In Catch and release in marine recreational fisheries (J. A. Lucy and A. Studholme, eds.), p. 172-179. Am. Fish. Soc. Symp. 30, Bethesda, MD.
- Goodyear, C. P., and E. Prince.
2003. U.S. recreational harvest of white marlin. ICCAT (Int. Comm. Conserv. Atl. Tunas) Coll. Vol. Sci. Pap. 55:624-632.
- Graves, J. E., B. E. Luchhurst, and E. D. Prince.
2002. An evaluation of pop-up satellite tags for estimating postrelease survival of blue marlin (*Makaira nigricans*) from a recreational fishery. Fish. Bull. 100:134-142.
- Gunn, J. S., T. A. Patterson, and J. G. Pepperell.
2003. Short-term movement and behavior of black marlin *Makaira indica* in the Coral Sea as determined through a pop-up satellite archival tagging experiment. Mar. Freshw. Res. 54:509-513.
- Holts, D., and D. Bedford.
1990. Activity patterns of striped marlin in the southern California Bight. In Planning the future of billfishes (R. H. Stroud, ed.), p. 81-93. National Coalition for Marine Conservation Inc., Savannah, GA.
- Holland, K., R. Brill, and R. K. C. Chang.
1990. Horizontal and vertical movements of Pacific blue marlin captured and released using sportfishing gear. Fish. Bull. 88:397-402.
- ICCAT (International Commission for the Conservation of Atlantic Tunas).
2001. Report of the fourth ICCAT billfish workshop. Int. Comm. Cons. Atl. Tunas (ICCAT) Coll. Vol. Sci. Pap. 53:1-22.
2003. Report of the 2002 white marlin stock assessment meeting. Int. Comm. Cons. Atl. Tunas (ICCAT) Coll. Vol. Sci. Pap. 55(2): 350-452.
- Jolley, J. W., and E. W. Irby.
1979. Survival of tagged and released Atlantic sailfish (*Istiophorus platyterus*: Istiophoridae) determined with acoustic telemetry. Bull. Mar. Sci. 29:155-169.
- Jones, C. D., and E. D. Prince.
1998. The cooperative tagging center mark-recapture database for Istiophoridae (1954-1995) with an analysis of the west Atlantic ICCAT billfish tagging program. Int. Comm. Cons. Atl. Tunas (ICCAT) Coll. Vol. Sci. Pap. Vol. 47:311-322.
- Kerstetter, D. W., B. E. Luchhurst, E. D. Prince, and J. E. Graves.
2003. Use of pop-up satellite archival tags to demonstrate survival of blue marlin (*Makaira nigricans*) released from pelagic longline gear. Fish. Bull. 101:939-948.
- Kerstetter, D. W., J. J. Polovina, and J. E. Graves.
2004. Evidence of shark predation and scavenging on fishes equipped with pop-up satellite archival tags. Fish. Bull. 102:750-756.
- Kieffer, J. D.
2000. Limits to exhaustive exercise in fish. Comp. Biochem. Physiol. A. 126:161-179.
- Lucy, J. A. and A. L. Studholme, editors.
2002. Catch and release in marine recreational fisheries. Am. Fish. Soc. Symp. 30, Bethesda, MD, 250 p.
- Lukacovic, R., and J. H. Uphoff.
2002. Hook location, fish size, and season as factors influencing catch-and-release mortality of striped bass caught with bait in Chesapeake Bay. Extended abstract. In Catch and release in marine recreational fisheries (J. A. Lucy and A. Studholme, eds.) p. 97-100. Am. Fish. Soc. Symp. 30, Bethesda, MD.
- Malchoff, M. H., J. Gearhart, J. Lucy, and P. J. Sullivan.
2002. The influence of hook type, hook wound location, and other variables associated with post catch-and-release mortality in the US summer flounder recreational fishery. Extended abstract. In Catch and release in marine recreational fisheries (J. A. Lucy and A. Studholme, eds.), p. 101-105. Am. Fish. Soc. Symp. 30, Bethesda, MD.
- Mather, F. J. III, H. L. Clark, and J. M. Mason Jr.
1975. Synopsis of the biology of the white marlin *Tetrapturus albidus* Poey (1861). In Proceedings of the International Billfish Symposium Kailua-Kona, Hawaii, 9-12

- August 1972. Part 3: Species Synopses (R. S. Shomura and F. Williams, eds.), p. 55-94. NOAA Tech. Rep. NMFS SSRF-675.
- Muoneke M. I., and W. M. Childress.
1994. Hooking mortality: a review for recreational fisheries. *Rev. Fish. Sci.* 2(2):123-156.
- NMFS. (National Marine Fisheries Service.)
1988. The Atlantic billfish fishery management plan. NOAA-NMFS-F/SF-Highly Migratory Species Division, Silver Spring, MD.
1999. Amendment 1 to the Atlantic billfish fishery management plan. NOAA-NMFS-F/SF-Highly Migratory Species Division, NMFS, Silver Spring, MD.
2003. Final rule: Atlantic highly migratory species: monitoring of recreational landings. 50 F.R. 711-715.
- Ortiz, M., E. D. Prince, J. E. Serafy, D. B. Holts, K. B. Davy, J. G. Pepperell, M. B. Lowry, and J. C. Holdsworth.
2003. Global overview of the major constituent-based billfish tagging programs and their results since 1954. *Mar. Freshw. Res.* 54(4):489-507.
- Peel, E.
1995. No place to hide: highly migratory fish in the Atlantic Ocean, 125 p. Center for Marine Conservation, Washington, D.C.
- Pepperell, J. G., and T. L. O. Davis.
1999. Post-release behavior of black marlin (*Makaira indica*) caught and released using sportfishing gear off the Great Barrier Reef (Australia). *Mar. Biol.* 135:369-380.
- Prince, E. D., M. Ortiz, and A. Venizelos.
2002a. A comparison of circle hook and "J" hook performance in recreational catch-and-release fisheries for billfish. *In* Catch and release in marine recreational fisheries (J. A. Lucy and A. Studholme, eds.), p. 66-79. *Am. Fish. Soc. Symp.* 30, Bethesda, MD.
- Prince, E. D., M. Ortiz, A. Venizelos, and D. S. Rosenthal.
2002b. In-water conventional tagging techniques developed by the cooperative tagging center for large, highly migratory species. *In* Catch and release in marine recreational fisheries (J. A. Lucy and A. Studholme, eds.), p. 155-171. *Am. Fish. Soc. Symp.* 30, Bethesda, MD.
- Prince, E. D., C. Rivero, J. E. Serafy, C. Porch, G. P. Scott, and K. B. Davy.
2003. An update of the tag release and recapture files for Atlantic white marlin. *Int. Comm. Cons. Atl. Tunas (ICCAT) Coll. Vol. Sci. Pap. Vol.* 55(2):578-593.
- Sedberry, G. R., and J. K. Loeffer.
2001. Satellite telemetry tracking of swordfish, *Xiphias gladius*, off the eastern United States. *Mar. Biol.* 139:355-360.
- Skomal, G. B., and B. C. Chase.
2002. The physiological effects of angling on post-release survivorship in tunas, sharks, and marlin. Extended abstract. *In* Catch and release in marine recreational fisheries (J. A. Lucy and A. Studholme, eds.), p. 135-138. *Am. Fish. Soc. Symp.* 30, Bethesda, MD.
- Skomal, G. B., B. C. Chase, and E. D. Prince.
2002. A comparison of circle and straight hook performance in recreational fisheries for juvenile Atlantic bluefin tuna. *In* Catch and release in marine recreational fisheries (J. A. Lucy and A. Studholme, eds.), p. 57-65. *Am. Fish. Soc. Symp.* 30, Bethesda, MD.
- Zimmerman, S. R., and E. A. Bochenek.
2002. Evaluation of the effectiveness of circle hooks in New Jersey's recreational summer flounder fishery. Extended abstract. *In* Catch and release in marine recreational fisheries (J. A. Lucy and A. Studholme, eds.), p. 106-109. *Am. Fish. Soc. Symp.* 30, Bethesda, MD.
- Wood, C. M., J. D. Turner, and M. S. Graham.
1983. Why do fish die after severe exercise? *J. Fish. Biol.* 22:189-201.

Abstract—Rockfishes (*Sebastes* spp.) support one of the most economically important fisheries of the Pacific Northwest and it is essential for sustainable management that age estimation procedures be validated for these species. Atmospheric testing of thermonuclear devices during the 1950s and 1960s created a global radiocarbon (^{14}C) signal in the ocean environment that scientists have identified as a useful tracer and chronological marker in natural systems. In this study, we first demonstrated that fewer samples are necessary for age validation using the bomb-generated ^{14}C signal by emphasizing the utility of the time-specific marker created by the initial rise of bomb- ^{14}C . Second, the bomb-generated ^{14}C signal retained in fish otoliths was used to validate the age and age estimation method of the quillback rockfish (*Sebastes maliger*) in the waters of southeast Alaska. Radiocarbon values from the first year's growth of quillback rockfish otoliths were plotted against estimated birth year to produce a ^{14}C time series spanning 1950 to 1985. The initial rise in bomb- ^{14}C from prebomb levels ($\sim -90\%$) occurred in 1959 (± 1 year) and ^{14}C levels rose relatively rapidly to peak $\Delta^{14}\text{C}$ values in 1967 ($+105.4\%$) and subsequently declined through the end of the time series in 1985 ($+15.4\%$). The agreement between the year of initial rise of ^{14}C levels from the quillback rockfish time series and the chronology determined for the waters of southeast Alaska from yelloweye rockfish (*S. ruberrimus*) otoliths validated the aging method for the quillback rockfish. The concordance of the entire quillback rockfish ^{14}C time series with the yelloweye rockfish time series demonstrated the effectiveness of this age validation technique, confirmed the longevity of the quillback rockfish up to a minimum of 43 years, and strongly confirms higher age estimates of up to 90 years.

Age validation of quillback rockfish (*Sebastes maliger*) using bomb radiocarbon

Lisa A. Kerr

Allen H. Andrews

Moss Landing Marine Laboratories

California State University

8272 Moss Landing Road

Moss Landing, California 95039

Present address (for L. A. Kerr): Chesapeake Biological Laboratory

University of Maryland Center

for Environmental Science

P.O. Box 38,

Solomons, Maryland 20688

E-mail address (for L. A. Kerr, contact author): kerr@ci.umces.edu

Kristen Munk

Alaska Department of Fish and Game

Division of Commercial Fisheries

1255 W. 8th Street

Juneau, Alaska 99801

Kenneth H. Coale

Moss Landing Marine Laboratories

California State University

8272 Moss Landing Road

Moss Landing, California 95039

Brian R. Frantz

Center for Accelerator Mass Spectrometry

Lawrence Livermore National Laboratory

7000 East Avenue

Livermore, California 94551

Gregor M. Cailliet

Moss Landing Marine Laboratories

California State University

8272 Moss Landing Road

Moss Landing, California 95039

Thomas A. Brown

Center for Accelerator Mass Spectrometry

Lawrence Livermore National Laboratory

7000 East Avenue

Livermore, California 94551

Rockfishes (*Sebastes* spp.) comprise one of the most commercially important fisheries in the northeast Pacific Ocean. Some rockfish species possess life history characteristics, such as long life, slow growth, late age at maturity, low natural mortality, and variable juvenile recruitment success, all of which make them particularly vulnerable to overfishing (Adams, 1980; Archibald et al., 1981; Leaman and Beamish, 1984; Cailliet et al., 2001.). Rockfish population biomass and size composition have declined to very low levels today in part because of continued high exploitation rates (Love et al., 2002). Prevention of further population declines is a management imperative. Sustain-

able management of marine fisheries requires accurate life history information, of which validated age and growth characteristics can be one of the most important aspects.

Underestimated age can lead to inflated estimates of total allowable catch for a fishery that is unsustainable at that level of exploitation (Beamish and McFarlane, 1983; Campana, 2001). For example, underestimated longevity and improper management allowed overfishing that accelerated the decline of the Pacific ocean perch (*Sebastes alutus*) of the northeastern Pacific Ocean (Beamish, 1979; Archibald et al., 1983). Reliable estimates of age are also essential for understanding life history traits,

Manuscript submitted 11 April 2003
to the Scientific Editor's Office.

Manuscript approved for publication
24 August 2004 by the Scientific Editor.

Fish. Bull. 103:97–107 (2005).

such as age at maturity, rate of growth, longevity, and reproduction frequency (Beamish and McFarlane, 1983). For production (large-scale) aging purposes, age validation is especially important because it provides a standardized basis for ongoing aging efforts to identify strong and weak cohorts (Campana, 2001).

The most common method of age estimation of bony fishes is counting growth zones in their calcified inner ear bones, or otoliths (Chilton and Beamish, 1982; Beamish and McFarlane, 1987). A pair of translucent and opaque growth zones is often assumed to represent one year of growth (Williams and Bedford, 1974). By counting growth zones an estimate of fish age is possible; however, growth patterns are not easily discernible for all species. Age interpretations in long-lived species can be particularly difficult and subjective because of the compression of growth zones within the otolith (Munk, 2001). Therefore, it is necessary to validate the periodicity of growth zones in otoliths with an independent and objective method. Despite the importance of accurate age estimates for understanding and managing fish populations, validated age and growth characteristics are often not available (Beamish and McFarlane, 1983; Campana, 2001). Traditional age validation techniques, such as captive rearing, mark-recapture, and tag-recapture, can be difficult or impractical for long-lived and deep-dwelling fishes.

An alternative technique to traditional age validation methods uses radiocarbon (^{14}C) produced by the atmospheric testing of thermonuclear devices in the 1950s and 1960s as a time-specific marker (Kalish, 1993). This established method of validating otolith-derived age estimates of fishes involves relating the discrete temporal variation of ^{14}C recorded in otoliths to an established ^{14}C chronology. Otoliths are closed systems, accreting calcium carbonate throughout the life of the fish and this calcium carbonate is conserved through time. The measurement of bomb-produced ^{14}C in otoliths of fishes is considered one of the best objective means to validate otolith-based age estimates in long-lived fishes (Campana, 2001).

This technique is most reliable for fishes that inhabit the surface mixed layer of the ocean, at least during a portion of their life history. Uncertainty regarding mixing rate at depth and limited data on the ^{14}C signal in deeper waters make it difficult to use this technique for organisms that live below the mixed layer throughout their lives (Kalish, 1995, 2001). Studies indicate that the main source of carbon (70–90%) for otoliths is from dissolved inorganic carbon (DIC) in seawater and that the remainder (10–30%) is dietary (Kalish, 1991; Farrell and Campana, 1996; Schwarz et al., 1998). An understanding of the life history of the fish (in particular diet, movement, and habitat) and the regional oceanography of the area are integral for interpreting otolith ^{14}C data. One caveat of this technique is that it must use otoliths with birth dates, including the period of initial increase in ^{14}C (mid-1950s to mid-1960s; Kalish, 1995). Consequently, this technique is well suited for age validation of long-lived species or species for

which there is an archived otolith collection with birth years that span this period. The application of bomb ^{14}C for age validation of long-lived species is advantageous, in that it provides a minimum longevity and verifies the periodicity of growth zones in otoliths with only a small amount of material and with a high degree of precision (Kalish, 1993; Campana, 2001). However, the high cost of ^{14}C analysis (~\$400–\$500 per sample) has been a limiting factor in the widespread application of this technique.

The quillback rockfish (*Sebastes maliger*) is a commercially important rockfish that represents a portion (~8%) of the demersal shelf rockfish assemblage landings in the Gulf of Alaska (O'Connell et al.¹). Species within the demersal shelf group are considered long-lived, late maturing, and sedentary as adults, making them highly susceptible to fishing pressure (O'Connell et al.¹). Estimated exploitation rates are low; once exploited beyond a sustainable level, recovery is slow (Leaman and Beamish, 1984; Francis, 1985; O'Connell et al.¹). Longevity estimates for the quillback rockfish are wide ranging, from 15 to 90 years (38 years, Barker, 1979; 55 years, Richards and Cass, 1986; 15 years, Reilly et al.²; 76 years, Yamanaka and Kronland, 1997; >32 years, Casillas et al., 1998; 90 years, Munk, 2001), and no age validation has been performed for this species to date.

Quillback rockfish are found associated with rocky substrate in relatively shallow continental shelf waters (9 to 146 m)—their abundance decreasing with increasing depth below 73 m (Kramer and O'Connell, 1995). As juveniles, quillback rockfish inhabit nearshore benthic habitat. Tagging studies confirmed that they do not demonstrate migratory behavior and are residents in their shallow-water habitat (Matthews, 1990). Because 1) most longevity estimates indicate that some present-day adult quillback rockfish were born in the prebomb era, 2) quillback rockfish in the juvenile stage are found in the ocean mixed layer, and 3) a suitable ^{14}C time series exists for the waters off southeast Alaska (previously determined from yelloweye rockfish [*S. ruberrimus*] otoliths [Kerr et al., 2004]), the quillback rockfish is an ideal candidate for ^{14}C age validation.

The objectives of our study were 1) to develop a method for determining the minimum number of samples required for bomb ^{14}C age validation to minimize cost, 2) to validate both age and age estimation methods of the quillback rockfish by measuring ^{14}C in aged otoliths and to compare the timing of the initial rise in ^{14}C with

¹ O'Connell, V. M., D. W. Carlile, and C. Brylinsky. 2002. Demersal shelf rockfish assessment for 2002. Stock assessment and fishery evaluation report for the groundfish resources of the Gulf of Alaska, 36 p. North Pacific Fishery Management Council (NPFMC), P.O. Box 103136, Anchorage AK 99510.

² Reilly, P. N., D. Wilson-Vandenberg, R. N. Lea, C. Wilson, and M. Sullivan. 1994. Recreational angler's guide to the common nearshore fishes of Northern and Central California. California Department of Fish and Game, Marine Resources Leaflet, 57 p. Calif. Dep. Fish and Game, 20 Lower Ragsdale Drive, Suite 100, Monterey, CA 93940.

the chronology determined for the waters of southeast Alaska (i.e., yelloweye rockfish), and 3) to analyze ^{14}C in aged quillback rockfish otoliths, spanning the pre- to postbomb era, in order to examine the complete ^{14}C time series and demonstrate the effectiveness of using the timing of the initial rise in ^{14}C as an age validation method.

Materials and methods

Sample size assessment

Because of the considerable cost of accelerator mass spectrometry (AMS) analyses, the minimum number of ^{14}C samples required to validate the aging method of the quillback rockfish was mathematically determined from a previously determined yelloweye rockfish otolith ^{14}C time series for the waters of southeast Alaska (Kerr et al., 2004). To assess minimum sample size, estimated years of initial rise in ^{14}C levels (and associated errors) were determined for different numbers of data points ($n=3, 5, 7, 9,$ and 11) subsampled from the bomb-rise region of the yelloweye rockfish data set. The estimated years of initial rise from each subsample set were then compared to the initial year of rise and error determined from all bomb-rise yelloweye rockfish ^{14}C samples ($n=23$). Because the error associated with the yelloweye rockfish bomb-rise data set is limited by the uncertainty associated with age estimates for yelloweye rockfish, a maximum error of ± 2 years for fish with birth years during the bomb rise (1956 to 1971; Kerr et al., 2004) was our precision criterion for defining the minimum number of quillback rockfish otolith samples.

Twenty-three yelloweye rockfish otolith ^{14}C values with birth years from 1956 to 1971 were divided into data sets of 3, 5, 7, 9, and 11 data points. A stratified sampling approach was applied by creating bomb ^{14}C linear regressions from repeated selection of 3, 5, 7, 9, and 11 data points at uniform intervals from 1956 to 1971. Random selection of data points was not practical because it is established that the careful choice of sample year during the rapid rise in ^{14}C is required for this technique (Baker and Wilson, 2001). The year of initial rise in ^{14}C , and associated error, was determined from the bomb ^{14}C regressions. The year of initial ^{14}C rise was calculated with the following formula:

$$x = (y - b)/m,$$

where x = year of initial rise in ^{14}C values;

y = average prebomb ^{14}C value;

m = slope of the line; and

b = y -intercept.

The error associated with the year of initial rise in ^{14}C values (σ_x) was calculated by using the delta method (treating b as a scalar; Wang et al., 1975):

$$\sigma_x = \sigma_y / \sigma_m,$$

where σ_y = error associated with average prebomb ^{14}C value

σ_m = error associated with the slope of the line.

Radiocarbon analysis

Sagittal otoliths of quillback rockfish were collected from a random subsampling of catches from commercial long-line fishing vessels in the coastal waters off southeast Alaska by the Alaska Department of Fish and Game (ADFG), Juneau, AK in 2000 (Fig. 1). A single otolith from a pair taken from each fish was aged by using the break-and-burn method developed by researchers at the Mark, Tag, and Age Laboratory, ADFG in Juneau, AK, and the corresponding intact otolith was analyzed for ^{14}C . Whole and broken-and-burned otoliths were stored dry in paper envelopes. Year of capture, estimated final age, assigned year class, readability code, and reader identification information were archived and provided by ADFG for each sample.

Fifteen quillback rockfish otoliths, with estimated birth years ranging from the prebomb 1950s to the postbomb mid-1980s were selected for ^{14}C analysis. The core of each otolith, which constitutes the first year of growth, was analyzed for ^{14}C . From life history information, it is known that the core was formed while the fish inhabited the ocean mixed layer during its early growth stage (Yoklavich et al., 1996). To determine the average length and width, and minimum depth of the core, whole and broken-and-burned otoliths from adult quillback rockfish were examined under a Leica[®] dissecting microscope with an attached Spot RT[®] video camera and were measured using Image Pro Plus[®] image analysis software (version 4.1 for Windows, Media Cybernetics, Silver Spring, MD). Cores were extracted with a milling machine with a 1.6-mm (1/16") diameter end mill. To minimize the extraction of material deposited after the first year of growth, length, width, and depth parameters of the otolith core were used to guide coring. Because the first year of growth in quillback rockfish otoliths is clearly visible from the distal surface of the otolith we were able to visually correct for individual variability in otolith core size. The core (first year of growth in the otolith) was reduced to powder, collected, and weighed to the nearest 0.1 mg.

For ^{14}C analysis, otolith calcium carbonate (CaCO_3) was converted to pure carbon in the form of graphite (Vogel et al., 1984, 1987) and measured for ^{14}C content by using AMS at the Center for Accelerator Mass Spectrometry, Lawrence Livermore National Laboratory. The ^{14}C values were reported as $\Delta^{14}\text{C}$ (Stuvier and Polach, 1977).

The ^{14}C values measured in quillback rockfish otolith cores were plotted with respect to corresponding birth years assessed from break-and-burn age estimates, taking into consideration the potential variation of the age estimate (coefficient of variation=2.6%, rounded to the nearest whole number; Chang, 1982). The ^{14}C time series for the waters of southeast Alaska established from the otoliths of the age-validated yelloweye rockfish

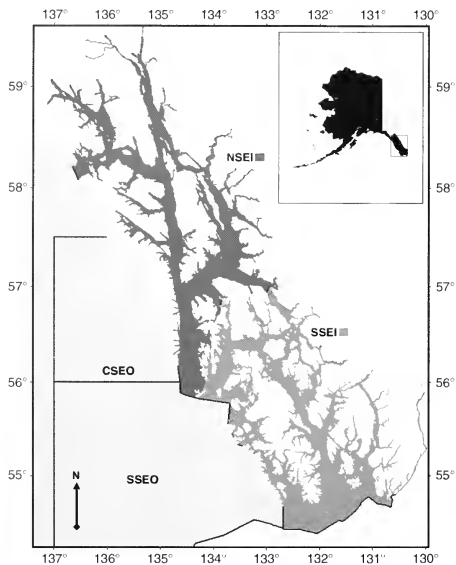


Figure 1

Map of southeast Alaska with regions where quillback rockfish (*Sebastes maliger*) used for otolith radiocarbon analyses were captured. Quillback rockfish were collected from random subsampling of catches from commercial longline fishing vessels in the coastal waters off southeast Alaska (CSEO: Central Southeast Offshore (outside), SSEI: Southern Southeast Inshore, SSEO: Southern Southeast Offshore, and NSEI Northern Southeast Inshore (inside)) by the Alaska Department of Fish and Game, Juneau, AK, in 2000. Note that the specific geographic location for individual fish during the first year of life is unknown; however, life history information indicates that quillback rockfish are not migratory and exhibit residential behavior in shallow-water habitat. Hence, the general location of the fish collected and used in this study may be useful in a broad context.

($n=43$) was used for temporal calibration of the quillback rockfish record (Andrews et al., 2002; Kerr et al., 2004). The level of concordance between the years of initial rise in ^{14}C in the two time series was the basis for validating the otolith-based age estimates of the quillback rockfish. The degree of agreement between the ^{14}C time series, spanning the pre- to postbomb era, for the quillback and yelloweye rockfishes was examined to demonstrate the effectiveness of determining the year of initial rise in ^{14}C as an age validation method, and whether the entire time series for the quillback provided

any further information relevant to age validation. To do this, the yelloweye rockfish ^{14}C time series was divided into three intervals (prebomb, bomb rise, and postbomb) and fitted with confidence intervals. The prebomb era ^{14}C values (1950–57) were fitted with an average (± 2 SD); the bomb rise (1959–71) and postbomb era values (1966–85) were fitted with a linear regression and corresponding 95% prediction intervals. A qualitative comparison of the quillback rockfish ^{14}C record was made with other existing marine records: two Hawaiian Islands coral records—Oahu (Toggweiler et al., 1991)

Table 1

Range of the year of calculated initial rise in radiocarbon and the associated range of error calculated for bomb radiocarbon regressions. Each regression comprised varying numbers of yelloweye rockfish radiocarbon data points ($n=3, 5, 7, 9,$ and 11) and was compared to the year of initial ^{14}C rise and error was determined from all bomb-rise yelloweye rockfish ^{14}C samples ($n=23$, last row) to determine the minimum number of quillback rockfish otolith samples sufficient to achieve the desired degree of precision (± 2 years).

Number of data points in regression	Number of regressions	Range of the year of calculated initial rise in ^{14}C	Error range (\pm years)
3	8	1954.1–1960.3	0.8–6.8
5	5	1956.0–1959.4	1.3–2.9
7	4	1956.5–1957.9	1.0–2.5
9	3	1957.1–1957.3	0.9–1.8
11	2	1957.0–1957.8	1.2–1.5
23	1	1957.3	n/a

and Kona (Druffel et al., 2001)—and two otolith-based northern hemisphere ^{14}C records—for northwest Atlantic haddock (Campana, 1997) and the Barents Sea Arcto-Norwegian cod (Kalish et al., 2001).

Results

Sample size assessment

The estimated years of initial rise in ^{14}C calculated for the bomb- ^{14}C regressions, composed of 3, 5, 7, 9, and 11 yelloweye rockfish data points spanning 1956 to 1971, converged towards the calculated year for all 23 data points as the number of samples comprising the regressions increased (Table 1). In parallel, the errors associated with the estimated years of initial rise in ^{14}C decreased as the number of ^{14}C samples increased (Table 1). The degree of precision within the quillback rockfish record was limited by the uncertainty associated with age estimates for yelloweye rockfish (a maximum error of ± 2 years based on growth zone counts for fish with birth years from 1956 to 1971; Kerr et al., 2004). Examination of the error (years) associated with the year of initial rise in ^{14}C for the number of data points comprising each regression in relation to our ± 2 year criterion indicated that a sample size of nine data points resulted in error values that ranged below 2 years (Table 1). Therefore, it was concluded that nine ^{14}C samples spanning 1956–71 would be sufficient to provide a suitable degree of precision in the quillback rockfish record. In addition, a limited number of samples, in this case 4, were required to establish an average prebomb level for the intercept year.

Radiocarbon analysis

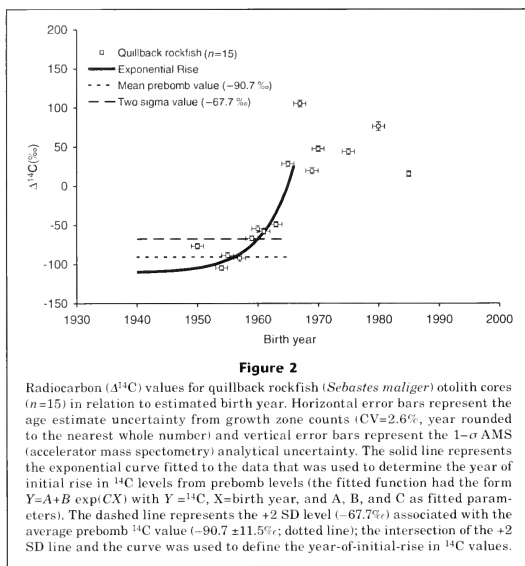
The ^{14}C measured in 15 previously aged quillback rockfish otoliths with presumed birth years from 1950 to 1985 varied considerably over time (Table 2). Otoliths

Table 2

Summary of fish and otolith data from quillback rockfish collected off the coast of southeast Alaska. Resolved age is the final age estimate given by Alaska Department of Fish and Game. Birth year is the collection year (2000) minus the resolved age. Age error is the uncertainty associated with the age estimate (CV=2.6%; year rounded to the nearest whole number). Radiocarbon values in the otolith cores of yelloweye rockfish are expressed as $\Delta^{14}\text{C}$ with the AMS analytical uncertainty.

Resolved age (years)	Birth year (\pm age error)	$\Delta^{14}\text{C}$ (‰)
50	1950 ± 1	-76.9 ± 3.3
46	1954 ± 1	-104.8 ± 3.2
45	1955 ± 1	-89.0 ± 4.0
43	1957 ± 1	-92.2 ± 3.8
41	1959 ± 1	-66.9 ± 3.3
40	1960 ± 1	-54.7 ± 4.2
39	1961 ± 1	-57.8 ± 3.7
37	1963 ± 1	-49.1 ± 3.3
35	1965 ± 1	28.2 ± 3.7
33	1967 ± 1	105.4 ± 4.2
31	1969 ± 1	19.4 ± 4.0
30	1970 ± 1	47.5 ± 3.6
25	1975 ± 1	43.9 ± 4.0
20	1980 ± 1	76.3 ± 5.5
15	1985 ± 0	15.4 ± 3.7

from quillback rockfish with birth years 1950–57 contained prebomb ^{14}C levels. Although there was more variation in these prebomb values than expected from ^{14}C uncertainties, the level was relatively consistent over time, averaging $-90.7 (\pm 11.5)\text{‰}$ (mean \pm SD). A sharp rise in otolith ^{14}C values was evident in 1959 (± 1 year);



this sample was the first to have a ^{14}C value ($-66.9 \pm 3.3\%$) that was above prebomb radiocarbon levels with a $+2$ SD criteria (upper limit of -67.7%). This first indication of a rise in ^{14}C related to the rise of the bomb was in agreement with the exponential fit of the quillback rockfish ^{14}C times series (Fig. 2). The ^{14}C record for quillback rockfish otoliths peaked in 1967 with a maximum ^{14}C concentration of $+105.4 (\pm 4)\%$. This peak was followed by a generally declining, but inconsistent, trend in ^{14}C values to 1985 (last birth year sampled).

The ^{14}C values measured in quillback rockfish otoliths plotted against estimated birth years produced a characteristic increasing and decreasing curve representative of bomb-generated ^{14}C changes over time (Fig. 3). The quillback rockfish ^{14}C record was synchronous with a ^{14}C time series for southeast Alaskan waters determined from yelloweye rockfish otoliths (Kerr et al., 2004); the average prebomb ^{14}C values for the quillback rockfish were in close agreement with the average yelloweye rockfish prebomb levels ($-102.2 \pm 9.3\%$ [mean \pm SD]). The year of initial rise in the quillback and yelloweye rockfish records (1959 [± 1 year] cf. 1958 [± 2 years]) and peak in ^{14}C values (1967 cf. 1966) for these two species coincided within one year, a period encompassed within the uncertainty associated

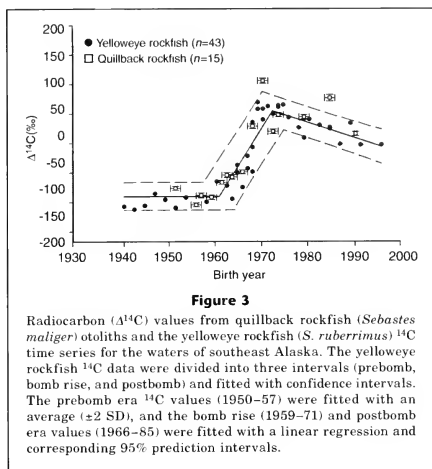
with break-and-burn age estimates. Furthermore, the postbomb decline in quillback rockfish ^{14}C values was similar to that of the yelloweye rockfish. In addition, thirteen of the fifteen quillback rockfish ^{14}C values fell within the confidence intervals of the yelloweye rockfish ^{14}C curve (Fig. 3).

The comparison of the quillback rockfish ^{14}C record with that for Hawaiian Islands corals (Toggweiler et al., 1991; Druffel et al., 2001) and two otolith-based northern hemisphere ^{14}C chronologies (northwest Atlantic haddock [Campana, 1997] and Barents Sea Arcto-Norwegian cod [Kalish et al., 2001]) revealed similarities in the year of initial rise and rate of rise of ^{14}C values, and differences in the pre- and postbomb eras that can be explained by regional oceanographic effects (Fig. 4).

Discussion

Sample size assessment

Although the ^{14}C technique has great potential for validating the age of many long-lived fishes, one of the main disadvantages has been the high cost of AMS ^{14}C analyses. By providing a means of defining the



minimum number of samples required to achieve the desired degree of precision, the present study takes a step toward reducing the number of prescribed samples, (i.e., 20–30 otoliths; Campana, 2001), effectively making age validation more affordable.

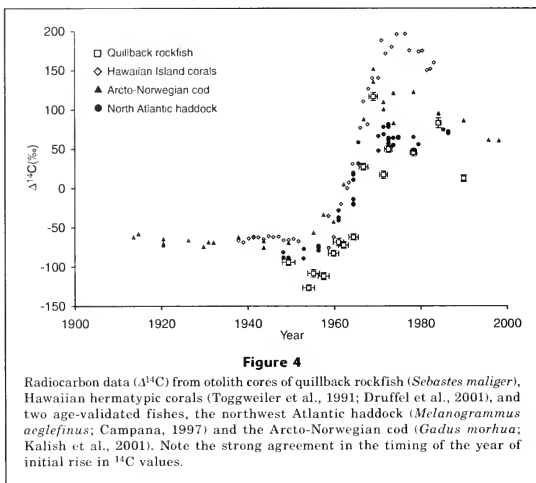
To determine the number of samples necessary for an age validation study, an assessment of the degree of precision is required. The degree of precision may be defined by the level of variation in the chronology or the uncertainty associated with age estimates. It can also be dependent on the estimated longevity of the fish and the resolution of age that is sufficient for the purposes of the study. For example, a resolution of ± 5 years may be sufficient for a species estimated to live 100 years, but would not be satisfactory for a species estimated to live 20 years. The higher degree of precision, the greater the cost will be for a study. However, a maximum precision can be attained at a minimum cost by taking into consideration the precision of the ^{14}C time series, the error associated with age estimates, and the age resolution necessary to accomplish the goals of the study.

In our study, the ± 2 -year variation of the yelloweye rockfish ^{14}C time series limited the precision to which the age of the quillback rockfish could be determined through comparison. Stratified sampling of nine quillback rockfish ^{14}C values between 1956 and 1971 revealed an average year of initial rise in ^{14}C of 1959 (± 1 year) that was in close agreement with the year of initial rise determined for the yelloweye rockfish time series. Thus, given the unique circumstances for this

species, we have quantitatively reduced the number of samples required for age validation to 9 (given that some sampling or additional information is used to establish prebomb levels). It can also be envisioned that ^{14}C analysis of a single fish otolith could establish a minimum longevity for a species if the ^{14}C levels measured in the otolith core of an adult fish with a known capture year were consistent with established prebomb ^{14}C levels for the regional waters in which that fish spent its first year. This exercise illustrates the necessity of defining precision on a species-by-species basis prior to beginning a ^{14}C study. Despite the high cost of AMS analyses, the overall project cost may be lower and of shorter duration than traditional age validation studies because of the relatively short time required to prepare and process the minimum number of otoliths. Currently, the ^{14}C technique is considered one of the most effective methods for age validation of long-lived fishes (Campana, 2001) and as costs are minimized, future application of the bomb ^{14}C age-validation technique of marine fishes should increase.

Radiocarbon analysis

To interpret radiocarbon values recorded in marine organisms it is essential to put them in the context of the regional oceanography. The Alaska coastal current, driven by wind stress and enriched with freshwater runoff, is the driving force behind the coastal dynamics off southeast Alaska (Royer, 1982). The coastal environment off southeast Alaska is characterized by significant



downwelling, high wind stress, eddies, and storm activity, resulting in a high degree of mixing. The rapid rise and early peak recorded in quillback rockfish otoliths, followed by a postbomb decline, indicated rapid ocean-atmosphere gas exchange in the shelf waters off southeast Alaska. Shallow continental shelf waters, such as the environment inhabited by juvenile quillback rockfish, have a thin mixed layer and relatively long surface residence time, resulting in a relatively fast response and build up of bomb- ^{14}C from the atmospheric signal. In addition, low prebomb ^{14}C values in the quillback rockfish record may indicate the influence of upwelled ^{14}C -depleted waters on southeast Alaskan coastal surface waters. This is expected because surface waters sampled off the Alaskan Peninsula (GEOSECS; Ostlund and Stuvier, 1980) in 1973 had low ^{14}C values (+62‰) in relation to the subtropical Pacific (Oahu coral, +174.5‰ in 1973, Toggweiler et al., 1991), indicating the influence of upwelled ^{14}C -depleted waters.

A comparison of the ^{14}C time series determined from quillback rockfish otoliths to the established ^{14}C time series exhibited synchronicity with the global rise in radiocarbon. The quillback rockfish record and high latitude northern hemisphere records from Arcto-Norwegian cod and haddock exhibited nearly identical years of initial rise and rates of ^{14}C increase. Note that there are differences among these records in the prebomb and peak ^{14}C levels attained and the behavior of bomb- ^{14}C after the peak, but it is irrelevant to the utility of the technique as an age validation tool. The quillback rockfish record

was also temporally similar to a Hawaiian Island corals record (Oahu, Toggweiler et al., 1991; Hawaii, Druffel et al., 2001), both increasing rapidly from the late 1950s. However, as expected, the corals had higher prebomb levels (-50‰ cf. -90‰), a later peak (1971 cf. 1967) at a higher value (174‰ cf. 105‰), and the indication of a more rapid decline in the postbomb years. These differences are indicative of the different oceanographic influences on the subtropical waters (e.g., lesser relative influence of upwelled, ^{14}C -depleted, deep water).

Possible sources of error in the quillback rockfish ^{14}C record are the specific location of each fish during its first year of growth, possible inaccuracies in the method of extracting the core, age estimate uncertainty, and variable oceanographic conditions during the year of otolith formation. The unknown geographic location of individual fish during the first year of life is a potential source of ^{14}C variation. Although juvenile quillback rockfish occupy relatively limited regions, factors such as local bathymetry, coastal upwelling, and freshwater input are likely to impact the ^{14}C content of the local waters. Two of the quillback otolith samples (birth years 1967 and 1980) had considerably higher (-50‰) ^{14}C values when compared to the highest yelloweye rockfish value for that same year. These elevated ^{14}C values may indicate that the individuals resided in different water masses. The variability of otolith ^{14}C values from regional effects is evident in the observed $\pm 11.5\%$ (1 SD) associated with prebomb values, a higher variability than expected from the analytical uncertain-

ties of the AMS ^{14}C measurements ($\sim\pm 3\text{--}4\%$). Elevated ^{14}C levels have also been recorded in otoliths of the black drum (*Pogonias cromis*), known to reside in estuaries during the juvenile stage (Campana and Jones, 1998); these elevated values are attributed to the rapid exchange of atmospheric ^{14}C in the well-mixed estuarine environment and the influence of river input. Quillback rockfish are known to inhabit more nearshore waters than those inhabited by yelloweye rockfish (Love et al., 2002), which could explain the elevated ^{14}C levels.

The core-extraction method was designed to limit the inclusion of more recently formed material (older than age 1); however, the inclusion of some of this material may have inadvertently occurred, perhaps introducing error to the quillback rockfish ^{14}C record. This kind of error could alter the ^{14}C value from the actual core year value depending on the time of otolith formation in relation to the bomb ^{14}C signal. A small addition of material with ^{14}C content different from the core material, however, may not produce a significant change in the timing of the initial rise and the shape of the rise. We feel that in most cases this would lead to an underaging of the fish and provide us with a minimum age estimate.

Perhaps the most significant potential source of error is the uncertainty associated with age estimation methods (coefficient of variation=2.6%). Growth zone counting error could have contributed to variation in the quillback rockfish record; however, the otoliths used in our study were chosen specifically to provide clearly definable growth zones and the highest rank in age-estimate confidence. The samples chosen were best-case examples of precise age determinations.

Short-term regional-scale changes in oceanographic conditions, such as upwelling events, may have affected ^{14}C levels at the time of otolith formation. The variation in postbomb measurements exemplifies this factor.

Considering the discussions above and the similar biology, ecology, and distribution of the two rockfish species, we believe that the use of the yelloweye rockfish ^{14}C time-series (Kerr et al., 2004) as a means of temporal calibration for the quillback rockfish record is well supported. The year of initial rise in ^{14}C for quillback rockfish otoliths (1959 [± 1 year]) is in agreement with the yelloweye rockfish record (1958 [± 2 years]); this finding validates the age estimates of the quillback rockfish and the accuracy of the break-and-burn age estimation method. In addition, the concordance of the quillback time series (1950 to 1985) provides further support for the age validation. Note that the ^{14}C levels, timing of the peak, and the subsequent decline were similar between species. In addition, all but two of the quillback rockfish ^{14}C values (sample years 1967 and 1980) fell within the confidence intervals for the yelloweye rockfish ^{14}C curve, further supporting the concordance of the two rockfish records. If there had been consistent underaging or overaging of quillback rockfish otoliths, this discrepancy would have resulted in a chronology that was not in phase with the yelloweye rockfish time series (Campana et al., 2002).

This application of the bomb- ^{14}C technique has confirmed the longevity of quillback rockfish to a minimum of 43 (± 1) years. This minimum age estimate is based on the last individual fish sample (estimated birth year of 1957 from growth zone counting) to have prebomb levels, immediately preceding the significant rise in ^{14}C levels observed in 1959 (± 1) year. These findings effectively refute previous longevity estimates less than 43 years (Barker, 1979; Reilly et al.²). In addition, it is reasonable to assume that the annual growth pattern continues throughout life; hence, these findings strongly support longevity estimates exceeding 43 years and ranging up to 90 years (Richards and Cass, 1986; Yamanaka and Kronland, 1997; Casillas et al., 1998; Munk, 2001).

Conclusions

It is our intention to not only validate the age and age estimation method for the quillback rockfish, but to determine the most effective number of samples for age validation with bomb radiocarbon. From our results, it appears that the concordance of the full ^{14}C time series is not entirely necessary for validating the age of fish, and perhaps of any other organism. Because the evolution and magnitude of the bomb- ^{14}C rise from the pre-bomb to postbomb era is subject to variations due to the specific oceanography of the region, the ^{14}C time series are in fact regional and are not universally applicable to all validation studies. The agreement of the entire ^{14}C time series does not provide additional information relevant to age validation. Hence, we propose that the year-of-initial-rise method be considered an effective ^{14}C age validation approach. This method both reduces the number of samples required for age validation and effectively precludes the perceived need to establish a pre- to postbomb ^{14}C reference time series for every region of the world's oceans. Because the year of initial rise in ^{14}C levels in surface waters is well defined (1958 [± 2 years]), it should be treated as a time-specific marker for organisms that inhabit the mixed layer of the oceans for some or all of their life cycle.

Acknowledgments

We thank the Alaska Department of Fish and Game for providing aged otolith samples. This article was supported in part by the National Sea Grant College Program of the U.S. Department of Commerce's National Oceanic and Atmospheric Administration under NOAA Grant no. NA06RG0142, project number R/F-190, through the California Sea Grant College Program, and in part by the California State Resources Agency. This work was performed, in part, under the auspices of the U.S. Department of Energy by University of California, Lawrence Livermore National Laboratory under contract no. W-7405-Eng-48. This research was also funded in part by the Pacific States Marine Fisheries Commission, Earl H. and Ethel M. Myers Oceanographic

and Marine Biological Trust, Packard Foundation, and Project AWARE.

Literature cited

- Adams, P. B.
1980. Life history patterns in marine fishes and their consequences for fisheries management. *Fish. Bull.* 78:1-12.
- Andrews, A. H., G. M. Cailliet, K. H. Coale, K. M. Munk, M. M. Mahoney, and V. M. O'Connell.
2002. Radiometric age validation of the yelloweye rockfish (*Sebastes ruberrimus*) from southeastern Alaska. *Mar. Freshw. Res.* 53:139-146.
- Archibald, C. P., D. Fournier, and B. M. Leaman.
1983. Reconstruction of stock history and development of rehabilitation strategies for Pacific ocean perch in Queen Charlotte Sound, Canada. *N. Am. J. Fish. Manag.* 3:283-294.
- Archibald, C. P., W. Shaw, and B. M. Leaman.
1981. Growth and mortality estimates of rockfish (Scorpaenidae) from B.C. coastal waters, 1977-1979. *Can. Tec. Rep. Fish. Aquat. Sci.* 1048, 57 p.
- Baker, M. S., and C. A. Wilson.
2000. Use of bomb radiocarbon to validate otolith section ages of red snapper *Lutjanus campechanus* from the northern Gulf of Mexico. *Limnol. Oceanogr.* 46(7):1819-1824.
- Barker, M. W.
1979. Population and fishery dynamics of recreationally exploited marine bottomfishes of northern Puget Sound. Ph.D. diss., 135 p. Univ. Wash., Seattle, WA.
- Beamish, R. J.
1979. New information on the longevity of Pacific ocean perch (*Sebastes alutus*). *J. Fish. Res. Board Can.* 36:1395-1400.
- Beamish, R. J., and G. A. McFarlane.
1983. The forgotten requirement for age validation in fisheries biology. *Trans. Am. Fish. Soc.* 112:735-743.
1987. Current trends in age determination methodology. In *The age and growth of fish* (R. C. Summerfelt and G. E. Hall, eds.), p. 15-42. The Iowa State Univ. Press, Ames, IA.
- Cailliet, G. M., A. H. Andrews, E. J. Burton, D. L. Watters, D. E. Kline, and L. A. Ferry-Graham.
2001. Age determination and validation studies of marine fishes: do deep-dwellers live longer? *Exp. Gerontol.* 36:739-764.
- Campana, S. E.
1997. Use of radiocarbon from nuclear fallout as a dated marker in the otoliths of haddock *Melanogrammus aeglefinus*. *Mar. Ecol. Prog. Ser.* 150:49-56.
2001. Accuracy, precision and quality control in age determination, including a review of the use and abuse of age validation methods. *J. Fish Biol.* 59:197-242.
- Campana, S. E., and C. M. Jones.
1998. Radiocarbon from nuclear testing applied to age validation of black drum, *Pogonias cromis*. *Fish. Bull.* 96:185-192.
- Campana, S. E., L. J. Natanson, and S. Myklevold.
2002. Bomb dating and age determination of large pelagic sharks. *Can. J. Fish. Aquat. Sci.* 59:450-455.
- Casillas, E., L. Crockett, Y. DeReynier, J. Glock, M. Helvey, B. Meyer, C. Schmitt, M. Yoklavich, A. Bailey, B. Chao, B. Johnson, and T. Pepperell.
1998. Essential fish habitat West Coast groundfish appendix, 778 p. NMFS, Montlake, Seattle, WA.
- Chang, W. Y. B.
1982. A statistical method for evaluating reproducibility of age determination. *Can. J. Fish. Aquat. Sci.* 39:1208-1210.
- Chilton, D. E., and R. J. Beamish.
1982. Age determination methods for fishes studied by the groundfish program at the Pacific biological station. *Can. Spec. Publ. Fish. Aquat. Sci.* 60, 102 p.
- Druffel, E. R. M., S. Griffin, T. P. Guilderson, M. Kashgarian, J. Southon, and D. P. Schrag.
2001. Changes in subtropical North Pacific radiocarbon and correlation with climate variability. *Radiocarbon* 43(1):15-25.
- Farrell, J., and S. E. Campana.
1996. Regulation of calcium and strontium deposition on the otoliths of juvenile tilapia, *Oreochromis niloticus*. *Comp. Biochem. Physiol.* 115A:103-109.
- Francis, R. C.
1985. Fisheries research and its application to west coast groundfish management. In *Proceedings of the conference on fisheries management: issues and options* (T. Frady ed.), p. 285-304. Alaska Sea Grant Report. 85-2, Univ. Alaska, Fairbanks, AK.
- Kalish, J. M.
1991. ^{13}C and ^{15}O isotopic disequilibria in fish otoliths: metabolic and kinetic effects. *Mar. Ecol. Prog. Ser.* 75:191-203.
1993. Pre- and post-bomb radiocarbon in fish otoliths. *Earth Planet. Sci. Lett.* 114:549-554.
1995. Radiocarbon and fish biology. In *Recent developments in fish otolith research* (D. H. Secor, J. M. Dean, and S. E. Campana, eds.), p. 637-653. Univ. South Carolina Press, Columbia, SC.
2001. Use of the bomb radiocarbon chronometer to validate fish age. Final Report FRDC Project 93/109, 384 p. Fisheries Research and Development Corporation, Canberra, Australia.
- Kalish, J. M., R. Nydal, K. H. Nedreaas, G. S. Burr, and G. L. Eide.
2001. A time history of pre- and post-bomb radiocarbon in the Barents Sea derived from Arcto-Norwegian cod otoliths. *Radiocarbon* 43(2B):843-855.
- Kerr, L. A., A. H. Andrews, B. R. Frantz, K. H. Coale, T. A. Brown, and G. M. Cailliet.
2004. Radiocarbon in otoliths of yelloweye rockfish (*Sebastes ruberrimus*): a reference time series for the waters of southeast Alaska. *Can. J. Fish. Aquat. Sci.* 61:443-451.
- Kramer, D. E., and V. M. O'Connell.
1995. Guide to northeast Pacific rockfishes: genera *Sebastes* and *Sebastes*. Alaska Sea Grant Advisory Bulletin 25, 78 p. Univ. Alaska, Fairbanks, AK.
- Leaman, B. M., and R. J. Beamish.
1984. Ecological and management implications of longevity in some northeast Pacific groundfishes. *Int. North Pac. Fish. Comm. Bull.* 42:85-97.
- Love, M. S., M. Yoklavich, and L. Thorsteinson.
2002. The rockfishes of the Northeast Pacific, 404 p. Univ. California Press, Berkeley, CA.
- Matthews, K. R.
1990. An experimental study of the habitat prefer-

- ences and movement patterns of copper, quillback, and brown rockfishes (*Sebastes* spp.). *Environ. Biol. Fishes* 29:161-178.
- Munk, K. M.
2001. Maximum ages of groundfishes in waters off Alaska and British Columbia and considerations of age determination. *Alaska Fish. Res. Bull.* 8(1):12-21.
- Ostlund, H. G., and M. Stuiver.
1980. GEOSECS Pacific Radiocarbon. *Radiocarbon* 22(1):25-53.
- Richards, L. J., and A. J. Cass.
1986. The British Columbia inshore rockfish fishery: Stock assessment and fleet dynamics of an unrestricted fishery, p. 299-308. *In* Proceedings of the international rockfish symposium, Lowell Wakefield fisheries symposium, Anchorage, Alaska, October 20-22, 1986. Alaska Sea Grant Report 87-2.
- Royer, T. C.
1982. Coastal fresh water discharge in the northeast Pacific. *J. Geophys. Res.* 87(C3):2017-2021
- Schwarcz, H. P., Y. Gao, S. Campana, D. Browne, M. Knyf, and U. Brand.
1998. Stable carbon isotope variations in otoliths of Atlantic cod (*Gadus morhua*). *Can. J. Fish. Aquat. Sci.* 55:1798-1806.
- Stuiver, M., and H. A. Polach.
1977. Discussion: reporting of ^{14}C data. *Radiocarbon* 19(3):355-363.
- Toggweiler, J. R., K. Dixon, and W. S. Broecker.
1991. The Peru upwelling and the ventilation of the South Pacific thermocline. *J. Geophys. Res.* 96:20467-20497.
- Vogel, J. S., D. E. Nelson, and J. R. Southon.
1987. ^{14}C background levels in an accelerator mass spectrometry system. *Radiocarbon* 29(3):323-333.
- Vogel, J. S., J. R. Southon, D. E. Nelson, and T. A. Brown.
1984. Performance of catalytically condensed carbon for use in accelerator mass spectrometry. *Nucl. Instr. Methods B5:289-293.*
- Wang, C. H., D. L. Willis, and W. D. Loveland.
1975. Radiotracer methodology in the biological, environmental, and physical sciences, 480 p. Prentice Hall, Englewood Cliffs, NJ.
- Williams, T., and B. C. Bedford.
1974. The use of otoliths for age determination. *In* The ageing of fish. Proceedings of an international symposium (T. B. Bagenal, ed.), p. 114-123. Unwin Brothers Limited, Surrey, England.
- Yamanaka, K. L., and A. R. Kronlund.
1997. Inshore rockfish stock assessment for the west coast of Canada in 1996 and recommended yields for 1997. *Can. Tech. Rep. Fish. Aquat. Sci.* 2175, 80 p.
- Yoklavich, M. M., V. J. Loeb, M. Nishimoto, and B. Daly.
1996. Nearshore assemblages of larval rockfishes and their physical environment off central California during an extended El Niño event, 1991-1993. *Fish. Bull.* 94:766-782.

Abstract—Seasonal and cross-shelf patterns were investigated in larval fish assemblages on the continental shelf off the coast of Georgia. The influence of environmental factors on larval distributions also was examined, and larval transport processes on the shelf were considered. Ichthyoplankton and environmental data were collected approximately every other month from spring 2000 to winter 2002. Ten stations were repeatedly sampled along a 110-km cross-shelf transect, including four stations in the vicinity of Gray's Reef National Marine Sanctuary. Correspondence analysis (CA) on untransformed community data identified two seasonal (warm weather [spring, summer, and fall] and winter) and three cross-shelf larval assemblages (inner-, mid-, and outer-shelf). Five environmental factors (temperature, salinity, density, depth of the water column, and stratification) were related to larval cross-shelf distribution. Specifically, increased water column stratification was associated with the outer-shelf assemblage in spring, summer, and fall. The inner shelf assemblage was associated with generally lower temperatures and lower salinities in the spring and summer and higher salinities in the winter. The three cross-shelf regions indicated by the three assemblages coincided with the location of three primary water masses on the shelf. However, taxa occurring together within an assemblage were transported to different parts of the shelf; thus, transport across the continental shelf off the coast of Georgia cannot be explained solely by two-dimensional physical factors.

Cross-shelf and seasonal variation in larval fish assemblages on the southeast United States continental shelf off the coast of Georgia

Katrin E. Marancik

Department of Biology
East Carolina University
East Fifth Street
Greenville, North Carolina 27858
Present address: Center for Coastal Fisheries and Habitat Research
NOAA Beaufort Laboratory
101 Pivers Island Road
Beaufort, North Carolina 28516
E-mail address: Katey.Marancik@noaa.gov

Lisa M. Clough

Department of Biology
East Carolina University
East Fifth Street
Greenville, North Carolina 27858

Jonathan A. Hare

Center for Coastal Fisheries and Habitat Research
NOAA Beaufort Laboratory
101 Pivers Island Road
Beaufort, North Carolina 28516

The study of larval fish assemblages provides information on community structure, spawning, and larval transport. Larval fish assemblages are groups of larvae with similar temporal and spatial distributions (Cowen et al., 1993). Larval distribution patterns are initially determined by spawning time and location; larvae of species with similar spawning patterns are initially in the same larval assemblage (Rakocinski et al., 1996). Physical forcing and larval behavior then modify the structure of larval assemblages and ultimately determine the outcome of larval transport (Cowen et al., 1993; Smith et al., 1999; Hare et al., 2001).

Marine protected areas (MPAs) are portions of the marine environment designated to "provide lasting protection for part or all of the natural and cultural resources therein" (Federal Register, 2000). A number of specific conservation objectives are encom-

passed by this definition, such as protecting small areas with historical significance or aesthetic quality, or protecting much larger areas to enhance fisheries through increases in spawning stock biomass and the supply of recruits to surrounding areas (Crowder et al., 2000). However, whether an MPA provides recruits to other areas is difficult to quantify and involves determining the fate of larvae and juveniles spawned in a protected area (Stephenson, 1999; Warner et al., 2000).

MPAs are under consideration as a fisheries management tool on the southeast United States continental shelf (Plan Development Team, 1990), and larval assemblage studies would provide useful information regarding spawning and larval transport. Although substantial larval fish research has been conducted on the southeast U.S. continental shelf, no studies have examined the dynamics

of larval fish assemblages in this area. For example, during the *RV Dolphin* cruises, the Marine Resources Monitoring, Assessment, and Prediction (MARMAP) cruises, and the Southeast Area Monitoring and Assessment Program (SEAMAP) cruises, ichthyoplankton surveys were conducted on the southeast United States continental shelf. From these surveys, spawning time was defined for a large group of species (Fahay, 1975), and the temporal and spatial distribution of larvae were described for a few select species (Kendall and Walford, 1979; Collins and Stender, 1987; 1989; Smith et al., 1994) and for multiple taxa, but mostly at the family level (Powles and Stender, 1976). Similarly, other programs (e.g., the South Atlantic Bight Recruitment Experiment) examined spawning and larval transport of "estuarine-dependent" species such as Atlantic menhaden (e.g., Judy and Lewis, 1983; Hoss et al., 1997; Hare et al., 1999; Checkley et al., 1999), but results for the entire suite of species sampled were not reported. For studies where the broader community of larval fish on the southeast U.S. shelf was addressed, the structure and dynamics of larval assemblages were not defined (Powell and Robbins, 1994, 1998; Govoni and Spach, 1999; Powell et al., 2000).

The purpose of this study was to examine larval fish assemblages on the continental shelf off the coast of Georgia, USA. This region of the continental shelf was targeted because of 1) the nature of the broad shallow shelf, 2) the location of Gray's Reef National Marine Sanctuary 20 km from shore, and 3) the location of several proposed deepwater MPAs (70–200 m water depth) in the region. Temporal and spatial patterns in larval distributions were described to explain spawning and larval transport processes on the continental shelf off the coast of Georgia, and the implications for MPAs in the region were addressed.

Materials and methods

Study site

The southeast United States continental shelf extends from West Palm Beach, Florida, to Cape Hatteras, North Carolina. Moving north from West Palm Beach (15 km), the shelf widens to Georgia (200 km) and then narrows to Cape Hatteras (35 km). Physical forcing by the Gulf Stream, which is part of the North Atlantic Western Boundary Current system, varies along the shelf. As the Gulf Stream flows northward along the shelf edge, it meanders, and cyclonic frontal eddies form in meander troughs (Lee et al., 1991). Meanders and frontal eddies grow in dimension from just north of the Straits of Florida (27°N latitude) to St. Augustine, Florida (30°N latitude), and then decrease from St. Augustine to just south of Charleston, South Carolina (32°N latitude). Meanders and frontal eddies grow in dimension again downstream of the Charleston Bump (32–33°N latitude), and then decrease again from Cape Fear, North Carolina (33°N latitude), to Cape Hatteras, North Carolina (36°N latitude).

Table 1

Year, month, and season of ichthyoplankton sampling and number of stations sampled in the Georgia Bight region of the southeast United States continental shelf.

Year	Month	Season	Number of stations
2000	April	spring	4
2000	August	summer	8
2000	October	fall	7
2001	January	winter	8
2001	March	winter	8
2001	May	spring	7
2001	June	summer	7
2001	August	summer	10
2001	October	fall	8
2002	February	winter	10

In addition to along-shelf variation in geophysical structure and Gulf Stream forcing, the southeast United States continental shelf can be divided into three cross-shelf zones based on physical circulation dynamics (Boicourt et al., 1998). Circulation on the inner-shelf (0–20 m water depth) is influenced by tidal currents, river inflow, and wind (Atkinson and Menzel, 1985; Pietrafesa et al., 1985a). Wind-driven flow predominates on the mid-shelf (20–40 m water depth) and there is only minor Gulf Stream and tidal influence (Atkinson and Menzel, 1985). Flow on the outer-shelf (40–75 m water depth) is dominated by the passage of Gulf Stream frontal eddies and upwelling at the shelf break (Pietrafesa et al., 1985b).

Inner and mid-shelf physical processes are relatively more important off the coast of Georgia compared to other segments of the southeast United States continental shelf (Boicourt et al., 1998). The continental shelf off the coast of Georgia is the area of diminishing meanders and eddies from St. Augustine, Florida, to Charleston, South Carolina. Tidal range and freshwater inflow is greatest in the Georgia portion of the southeast shelf (Atkinson and Menzel, 1985). Further, because the shelf is widest off the coast of Georgia (approximately 200 km), the Gulf Stream is less influential on mid- and inner-shelf dynamics compared to the rest of the southeast United States continental shelf (Lee et al., 1991).

Collection of larval fish and CTD data

Ichthyoplankton sampling was conducted approximately every other month from April 2000 through February 2002 (Table 1). A maximum of ten stations, approximately 18.5 km apart, were sampled during each cruise. Stations were missed on some cruises owing to weather and equipment failure. The transect was 110 km long and spanned 10 to 50 m water depth (Fig. 1). Four sta-

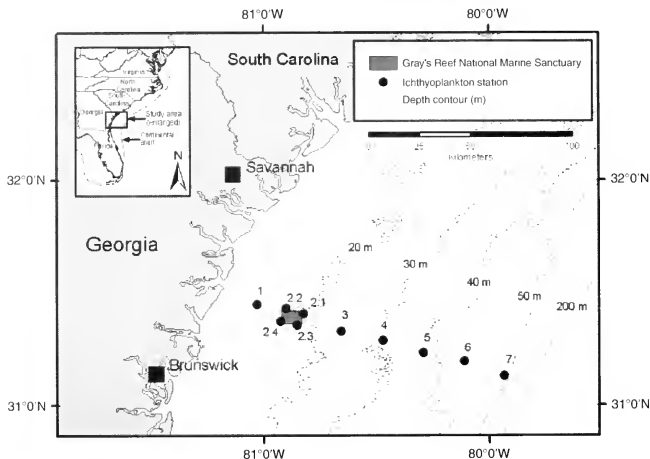


Figure 1

Map of the study area and the cross-shelf transect used for sampling larval abundance and environmental data bimonthly from April 2000 to February 2002 (see Table 1). Four stations (stations 2.1–2.4) were located around Gray's Reef National Marine Sanctuary.

tions were placed immediately adjacent to the four sides of Gray's Reef National Marine Sanctuary. At each station, temperature, salinity, density, and water depth were measured from the water's surface to one meter above the bottom with a Seabird conductivity-temperature-depth (CTD probe (SBE19, Seabird Electronics, Inc., Bellevue, WA). Ichthyoplankton was collected at each station with a five-minute single oblique net tow to within one meter of the bottom. For all but one cruise (August 2000), a 61-cm paired bongo frame fitted with 333- μm or 505- μm mesh nets was used. During the remaining cruise, a 1-m ichthyoplankton sled with 333- μm mesh net was used because of the smaller size of the research vessel. A flow meter (General Oceanica) was used to measure the volume of water filtered.

A gear comparison study, conducted during October 2000, showed that ichthyoplankton samples collected with the two gear types (61-cm bongo versus 1-m² ichthyoplankton sled) were similar. An analysis of variance (ANOVA) on the mean larval concentration revealed no significant differences between the two gear types (one-way ANOVA: $F=0.489$; $df=1$; $P>0.5$). Also, an analysis of similarities (ANOSIM, Clarke and Warwick, 2001) determined that the community structure varied more within than between gear types (ANOSIM: $R=-0.11$; $S=77.57$). Similarly, preliminary analysis of the effect

of gear selectivity due to mesh size indicated that the larval communities collected by 333- μm mesh and by 505- μm mesh nets were similar. Thus, data from all cruises were combined in the subsequent analyses (see Marancik, 2003, for more details).

Preparation of ichthyoplankton data

All ichthyoplankton samples were sorted and larval fish were identified to the lowest possible taxonomic level by using previously published descriptions (e.g., Fahay, 1983; Johnson and Keener, 1984; Richards, 2001) and descriptions developed as part of this study. Identification to species was not easy given the diversity of species along the southeast United States continental shelf (see Kendall and Matarese, 1994), yet every effort was made to identify larvae to species-level (46.3% to species, 27.4% to genus, 6.7% unidentified). Larval concentrations were calculated as number of larvae/100 m³.

Two data sets were used for statistical analyses, differing in the inclusion of rare taxa. Rare taxa pose a problem in community analyses. Some rare taxa occur because of transport anomalies (Cowen et al., 1993), and their inclusion in data analyses can confound the definition of larval assemblages. However, rare taxa can also be indicative of consistent, but low larval abun-

Table 2

Taxa collected during two years of sampling (April 2000–February 2002) constituting one or ten percent of any one sample from the continental shelf off the coast of Georgia and included in the analyses. The taxonomic codes used in the figures of this article are also shown. Taxa included in the one percent and ten percent data sets are marked by an "X." Also indicated are the seasonal assemblage (warm weather [WA] and winter [WI]) and larval assemblage (I=inner-shelf, M=mid-shelf, O=outer-shelf) in which larvae were collected (based on correspondence analyses).

Family	Species	Taxonomic code	Included in 1% data set	Included in 10% data set	Season	Assemblage
Muraenidae	<i>Gymnothorax</i> sp.		X		WA/WI	I/O
Ophichthidae	<i>Ophichthus</i> sp.		X		WA/WI	M/O
	<i>Myrophis punctatus</i>	Mpun	X	X	WI	M
Clupeidae	<i>Brevoortia tyrannus</i>	Btyr	X	X	WI	M
	<i>Etrumeus teres</i>		X		WI	O
	<i>Opisthonema oglinum</i>	Oogl	X	X	WA	I/O
Engraulidae	<i>Anchoa hepsetus</i>	Ahep	X	X	WA	I/M
	<i>Engraulis eurystole</i>		X		WA	O
Gonostomatidae	<i>Cyclothone</i> spp.		X		WA	O
Phosichthyidae	<i>Vinciguerria nimbaria</i>		X		WA	O
Paralepididae	<i>Lestidium atlanticum</i>		X		WI	O
Myctophidae	<i>Diaphus</i> spp.		X		WA/WI	M/O
	<i>Lepidophanes</i> spp.		X		WA	O
	<i>Ceratoscopelus maderensis</i>		X		WA/WI	M/O
	<i>Ceratoscopelus warmingii</i>		X		WI	M
	<i>Electrona risso</i>		X		WI	O
	<i>Hygophum hygemi</i>		X		WI	O
	<i>Hygophum reinhardtii</i>		X		WA	O
	<i>Lampadena urophaos</i>		X		WA	M
	<i>Myctophum affini</i>		X		WA	O
	<i>Myctophum selenops</i>		X		WA	O
Bregmacerotidae	<i>Bregmaceros atlanticus</i>		X		WA	O
	<i>Bregmaceros cantori</i>		X		WA/WI	I/O
	<i>Bregmaceros houdei</i>		X		WA/WI	M
Gadidae	<i>Urophycis</i> sp.		X		WI	M
Ophidiidae	<i>Ophidion antiphodus/holbrooki</i>		X		WA/WI	I/M
	<i>Ophidion josephi</i>		X		WA/WI	I/O
	<i>Ophidion marginatum</i>	Omar	X	X	WA	M
	<i>Ophidion selenops</i>		X		WA	M
	<i>Otophidium omostigmum</i>	Oomo	X	X	WA/WI	M
Holocentridae	Holocentridae		X		WA	O
Syngnathidae	<i>Hippocampus</i> sp.		X		WA	I
	<i>Syngnathus fuscus/louisianae</i>		X		WA	I
	<i>Syngnathus louisianae</i>		X		WA	I
Scorpaenidae	Scorpaenidae		X		WA/WI	M/O

continued

dance (Leis, 1989); excluding these taxa could remove data useful in defining larval assemblages. Thus, two taxa inclusion data sets were selected. The first data set comprised taxa that made up greater than one percent abundance at any one station, and the second data set included those taxa that made up at least 10 percent abundance at any one station (Table 2).

The data sets were further truncated by eliminating, with a few exceptions, all taxa not identified to genus or species level. Priacanthidae, Scaridae, Scorpaenidae, and Epinephalinae were included because, despite potential inclusion of multiple species, these larvae represent some of the only reef taxa collected, and larval assemblage data including these taxa would be useful

Table 2 (continued)

Family	Species	Taxonomic code	Included in 1% dataset	Included in 10% dataset	Season	Assemblage
Serranidae	Epinephalinae		X		WA/WI	M/O
	Serraninae		X		WA/WI	M/O
	<i>Diplectrum</i> spp.		X		WA/WI	I/M/O
	<i>Hemanthias vivanus</i>		X		WA	O
	<i>Serraniculus pumilio</i>		X		WA	M
Priacanthidae	Priacanthidae		X		WA	M/O
Pomatomidae	<i>Pomatomus saltatrix</i>		X		WA	O
Carangidae	<i>Elagatus bipinnulata</i>		X		WA	M/O
Coryphaenidae	<i>Coryphaena hippurus</i>		X		WA	I/O
Lutjanidae	<i>Lutjanus</i> sp.		X		WA	O
	<i>Rhomboplites aurorubens</i>		X		WA	O
Sparidae	<i>Lagodon rhomboides</i>	Lrho	X	X	WI	I
Sciaenidae	<i>Bairdiella chrysur</i>		X		WA	I
	<i>Cynoscion nothus</i>		X		WA	I/M
	<i>Cynoscion regalis</i>		X		WA	I
	<i>Larimus fasciatus</i>		X		WA	I/M
	<i>Leiostomus xanthurus</i>	Lxan	X	X	WI	I/M
	<i>Menticirrhus americanus</i>	Mame	X	X	WA	I
	<i>Micropogonias undulatus</i>	Mund	X	X	WA/WI	I/M
	<i>Pogonias cromis</i>		X		WA	I
	<i>Sciaenops ocellatus</i>		X		WA	I
	Pomacentridae	<i>Abudefduf</i> sp.		X		WA
<i>Chromis</i> spp.			X		WA	O
Mugilidae	<i>Mugil curema</i>		X		WI	M
Labridae	<i>Halichoeres</i> sp.		X		WA/WI	M
	<i>Xyrichthys</i> spp.	Xyr	X	X	WA	M/O
Scaridae	Scaridae		X		WA/WI	I/M/O
Dactyloscopidae	Dactyloscopidae type 1 (<i>D. moorei</i>)		X		WA	I
	Dactyloscopidae type 2		X		WA	M
	Dactyloscopidae type 3		X		WA/WI	O
Callionymidae	<i>Diplogrammus pauciradiatus</i>	Dpau	X	X	WA/WI	M
Scombridae	<i>Euthynnus alletteratus</i>		X		WA	O
	<i>Scomberomorus cavalla</i>		X		WA	O
	<i>Scomberomorus maculatus</i>		X		WA	I
	<i>Auxis rochei</i>	Aroc	X	X	WA	O
	<i>Scomber japonicus</i>		X		WA/WI	M/O
Stromateidae	<i>Ariomma</i> sp.		X		WA/WI	M/O
Bothidae	<i>Bothus ocellatus/robinsi</i>	Boce	X	X	WA/WI	M/O
Paralichthyidae	<i>Cyclopsetta</i> sp.		X		WA/WI	M/O
	<i>Engyphrys</i> spp.		X		WA	O
	<i>Syacium</i> spp.		X		WA	M/O
	<i>Paralichthys albigata/lethostigma</i>		X		WI	O
	<i>Citharichthys arctifrons</i>		X		WI	I
	<i>Citharichthys cornutus</i>		X		WA	O
	<i>Citharichthys gymnorhinus</i>		X		WA/WI	I/M/O
	<i>Citharichthys spilopterus</i>	Cspi	X	X	WI	M
	<i>Etropus crossotus</i>	Ecro	X	X	WA	M
	<i>Hippoglossina oblongatta</i>		X		WA	M
<i>Paralichthys lethostigma</i>		X		WI	M	
Soleidae	<i>Trinectes maculatus</i>		X		WA	I
Balistidae	<i>Monacanthus hispidus</i>		X		WA	O

Table 3

Mean values for each station (station 2 is the average of stations 2.1–2.4) of the sixteen environmental variables used in canonical correspondence analysis to determine which environmental variables were most significantly linked to the larvae of the Georgia Bight. Temperature, salinity, and density gradients are horizontal gradients based on the difference between adjacent stations. Stratification of the water column was calculated by using Simpson's stratification parameter and is a measure of vertical change in density.

Environmental variables	Code	Station						
		1	2	3	4	5	6	7
Depth (m)	DEP	12.44	18.51	23.15	33.05	37.03	41.48	45.94
Average temperature (°C)	AVGTEM	19.51	20.76	21.67	22.33	21.97	22.73	23.10
Temperature gradient (°C)	TEMGRAD	-0.29	-0.67	-1.10	-0.82	-0.52	-1.33	-0.59
Average salinity	AVGSAL	34.78	35.70	36.11	36.32	36.35	36.30	36.24
Salinity gradient	SALGRAD	-0.88	-1.13	-0.56	-0.25	0.03	0.12	0.19
Average density (kg/m ³)	AVGDEN	24.56	24.97	25.04	25.05	25.18	24.92	24.79
Density gradient (kg/m ³)	DENGRAD	-0.64	-0.74	-0.18	0.01	0.16	0.44	0.31
Stratification	STRAT	3.10	1.47	3.37	6.19	13.41	42.41	98.44

for managing reef fish on the southeast United States continental shelf (see Powell and Robbins, 1994; 1998). Serraninae were also included because the majority of these larvae are likely one type: *Serranus subligarius*. In contrast, larvae identified to some genera were excluded because there are multiple species common in the area within each genus, and each species likely has different larval distributions: *Etropus* spp. (3 species), *Prionotus* spp. (14 species), *Sphoeroides* spp. (11 species), *Symphurus* spp., (22 species), and *Syngnathus* spp. (10 species). In summary, 86 taxa were included in the one percent data set, and 16 taxa were included in the ten percent data set (Table 2).

Preparation of environmental data

Season, water mass, and eight environmental variables (mostly derived from temperature and salinity data) were chosen in an attempt to explain variation in the ichthyoplankton data (Table 3). For subsequent use in multivariate analyses, all environmental variables were standardized to a mean of zero and a standard deviation of one.

CTD data were processed with the manufacturer's software (Seasave vers. 5.3, Seabird Electronics, Inc., Bellevue, WA) and averaged into 0.5-m bins. Two parameters were derived to describe each hydrographic variable (salinity, temperature, density): an average value through the entire water column and a horizontal gradient value (calculated as the difference in value between the two adjacent stations). Vertical stratification was estimated by using Simpson's stratification parameter (Simpson and James, 1986):

$$\Phi = 1/h \int_{-h}^0 (\bar{\rho} - \rho)gzdz,$$

where h = water column depth;

$\bar{\rho}$ = average water column density;

ρ = water density;

g = acceleration due to gravity; and

z = depth.

The stratification parameter, Φ (joules/m³), is a measure of the resistance of water to mixing; higher numbers signify higher resistance to mixing.

Temperature and salinity data were further used to define water masses on the continental shelf off the coast of Georgia. Pietrafesa et al. (1994) defined four water masses on the southeast U.S. continental shelf: Georgia Bight Water, Carolina Capes Water, Virginia Coastal Water, and Gulf Stream Water. However, temperature data collected on the continental shelf off the coast of Georgia exhibited greater seasonal variability (10–29°C) than reported by Pietrafesa et al. (1994; 14–29°C). As a result, water mass definitions for our study, although based largely on the definitions of Pietrafesa et al. (1994), reflect the greater range of temperature and reflect the natural breaks in temperature, salinity, and stratification data. Specifically, two water masses (inner-shelf water and mid-shelf water) and two mixes (inner-shelf–mid-shelf mixed water and mid-shelf–Gulf Stream mixed water) were defined (Fig. 2). Inner-shelf water was characterized by salinities <35 ppt and seasonally variable temperatures. This water mass was found during winter and spring and was distributed inside the 20-m isobath (Fig. 3). Mid-shelf water, with salinities >36 (Fig. 2), was typically well mixed vertically (Simpson's stratification parameter value <10). Mid-shelf water was found year round over large sections of the shelf, particularly in the fall (Fig. 3). A mixture between inner-shelf and mid-shelf water was defined with salinities between 35 and 36 (Fig. 2). A mixture was also defined

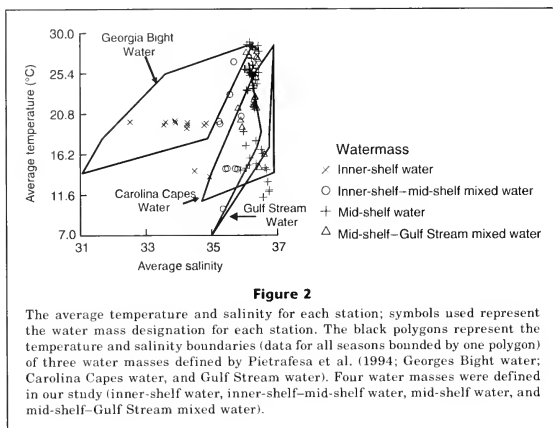


Figure 2

The average temperature and salinity for each station; symbols used represent the water mass designation for each station. The black polygons represent the temperature and salinity boundaries (data for all seasons bounded by one polygon) of three water masses defined by Pietrafesa et al. (1994; Georges Bight water; Carolina Capes water, and Gulf Stream water). Four water masses were defined in our study (inner-shelf water, inner-shelf-mid-shelf water, mid-shelf water, and mid-shelf-Gulf Stream mixed water).

as mid-shelf water and Gulf Stream water (Fig. 2). Gulf Stream water was not encountered, but its temperature and salinity properties are well documented (Churchill et al., 1993; Pietrafesa et al., 1994). Mid-shelf-Gulf Stream mixed water was highly stratified (Simpson's stratification parameter value >10), with warm highly saline water intruding on the surface during fall, winter, and spring and cool highly saline water intruding at depth during summer. Mid-shelf-Gulf Stream mixed water was encountered on most cruises and was found farthest offshore (Fig. 3).

Cruises were assigned to one of four seasons (Table 1) based on wind and temperature regimes. Although Blanton et al. (1985) identified five seasons for the southeast United States based on wind regimes (Spring [March-May], summer [June-July], transition [August], autumn [September-October], and winter [November-February]), the temperature data collected in our study supported classifying both August cruises as summer and the March cruise as winter.

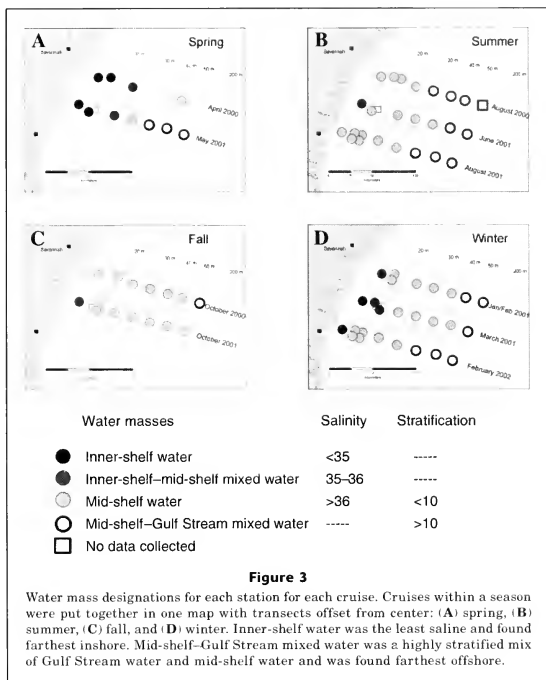
Data analyses

Multivariate analyses were used to define larval assemblages and to explore the factors that influence distribution of larval assemblages on the continental shelf off the coast of Georgia. Multivariate analyses arrange sites and species along environmental gradients creating a low dimensional map (an ordination). Analyses can be conducted for samples where the distance between points in the ordination represents the similarity of species abundance between samples. Analyses also can be conducted for species where the distance between

points in the ordination represents the similarity in the sample distribution between species. Ordinations, then, can be analyzed in two ways: with regard to proximity and dimensionality. Points that occur in close proximity can be considered similar based on similar composition. Points that occur on the same dimension define gradients in the data.

The effects of data transformation (untransformed, square root transformed, and fourth root transformed) and species inclusions (1% and 10% data sets) on the ordination of community and environmental data by two multivariate ordination techniques, multidimensional scaling and correspondence analysis (CA), were compared to determine which method was more effective at analyzing the larval fish data collected on the continental shelf off the coast of Georgia (Marancik, 2003). Overall, the two analytical methods produced similar ordinations and were robust to the inclusion of rare species and to the type of data transformation.

Correspondence analysis on untransformed larval fish concentration data was used to define larval assemblages in relation to season and the entire two-year data set. One of the strengths of CA is that it allows one to plot analyses of species and station data simultaneously on one ordination, thereby, allowing immediate comparisons between those stations that occur in close proximity in ordination space and those taxa that influence that proximity. Eigenvalues are a measure of the importance of each CA dimension (ter Braak and Smilauer, 2002). Thus, the dimensions needed to describe patterns in the data can be determined by an abrupt drop in the magnitude of eigenvalues from one dimension to the next.



Canonical correspondence analysis (CCA), which incorporates environmental variables by aligning species and station data along environmental gradients, was used to explore the relationship between larval assemblages and the environment. The species-environment correlation is a measure of the strength of the relation between the species data and the environmental data for each CCA dimension (ter Braak and Smilauer, 2002). The product of the species-environment correlation and the eigenvalue can be used to describe the variance in the data. CA and CCA were performed by using the statistical package CANOCO (Ter Braak, 1988).

Multivariate analyses were used to determine which fish species spawn on the continental shelf off the coast of Georgia, to examine what environmental factors influence larval distribution, and to explore the physical factors affecting the transport of larvae spawned on the shelf. Specifically, six objectives were addressed:

- 1) cross-shelf patterns in the larval fish community;
- 2) larval assemblages associated with cross-shelf patterns in the larval fish community;
- 3) the relation among cross-shelf patterns in the larval fish community, larval assemblages, and environmental variables;
- 4) the relation between water mass and larval assemblages;
- 5) seasonal patterns in the larval fish community and larval assemblages; and
- 6) the relation between seasonal larval assemblages and environmental variables.

In addition to addressing the six specific objectives, the implications for larval transport were considered. By comparing the distributions of specific taxa to the patterns discerned by addressing the objectives above, some insights were gained into larval transport processes. The distribution of taxa representative of each larval assemblage was examined for patterns through space and time. Mechanisms driving larval transport were then explored by linking these patterns to water mass and other environmental variables.

Results

Two dimensions were sufficient to explain the majority of the variance in the larval concentration data (Table 4). The winter data eigenvalues indicated the relevance of a third dimension; yet, inspection of three dimensions did not define any patterns not indicated by the first two dimensions. Thus, two dimensions were analyzed for each season in both the CA and CCA analyses.

Cross-shelf patterns in the larval fish community

A cross-shelf pattern in the larval community was observed. In spring, summer, and fall, the inshore stations (stations 1–3) were in close proximity, forming an inner-shelf station group in the ordination resulting from the CA (Fig. 4). Along the same dimension (axis) as the inner-shelf station was a mid-shelf station group of stations 3–6 (stations 2.1–2.4 were also included in this group in spring, summer, and winter). An outer-shelf group composed of offshore stations (stations 5–7) was distributed along a nearly perpendicular dimension, and the mid-shelf group was at the intersection of the two dimensions (Fig. 4). Analysis of the one-percent species data set revealed an identical pattern for each season (not shown).

The winter station ordination resulted in a less distinct cross-shelf pattern (Fig. 4D). In January 2001, stations 1, 2, 3, and 6 were in the inner-shelf group; whereas, stations 4 and 7 from the same cruise were in the mid-shelf group, and station 5 was in the outer-shelf group. Some of this blurring of the cross-shelf pattern in the ordination may be explained by a lower total catch, giving the taxa found across the shelf (*Brevoortia tyrannus* and *Leiostomus xanthurus*) more influence over the data. In addition, most of the variance was explained by the first dimension (Table 4), meaning that the separation of the outer-shelf group (stations 5 and 6) from the mid- and inner-shelf groups is based on a weak relationship among the stations.

Larval assemblages associated with cross-shelf patterns in the larval fish community

Three larval assemblages were defined that corresponded to the three station groups (Fig. 5). The inner-shelf assemblage was composed of species that spawn in coastal and estuarine habitats. Larvae in this assemblage were distributed within the 20-m isobath and confined largely to stations classified as inner-shelf (Fig. 6). The inner-shelf assemblage was primarily represented by *Menticirrhus americanus* during spring, summer, and fall, and by *Micropogonius undulatus* and *Lagodon rhomboides* during winter (Table 5). Taxa included in the mid-shelf assemblage were generally found between the 20- and 40-m isobaths. Some mid-shelf taxa, however, were found across the shelf (stations 1–7) and a large percentage of the larvae occurring in each region were mid-shelf taxa (Fig. 6). The outer-shelf assemblage comprised offshore or deepwater spawned taxa and was

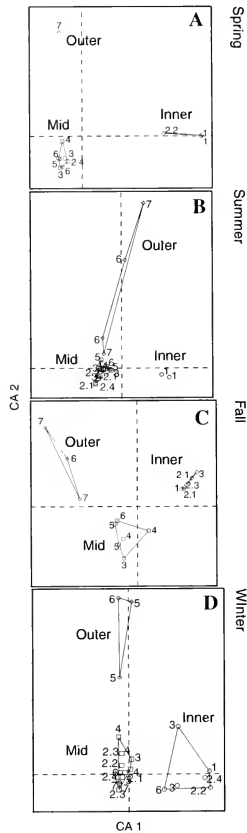


Figure 4

Correspondence analysis ordinations (portraying the first and second dimension scores) of the larval fish community data showing station groups in each season (A) spring, (B) summer, (C) fall, and (D) winter. Three cross-shelf station groups were identified within each season. Solid lines enclose the boundary of each station group with three or more stations. Station groups comprising one or two stations are not enclosed by a solid line. Each station group is labeled and portrayed with a different symbol. The dashed lines intersect at the origin of the plot. Analyses were conducted with larval concentration data only. Data from each cruise within a season are shown together.

Table 4

Eigenvalues and species-environment correlations (r^2) for each axis analyzed (correspondence analysis [CA] and canonical correspondence analysis [CAA]) by season and the entire year. A sharp drop in the eigenvalue marks the axes that explain most of the data. Species and environment correlations represent the strength of the relation between the species data and the environmental data for each axis within each season. Values of zero denote no relation; values of one denote a perfect relation. The product of the species-environment correlation and the eigenvalue explains the variance in the data for CCA. Eigenvalues alone explain the variance in the data for CA.

Season	CA axis				CCA axis			
	1	2	3	4	1	2	3	4
Spring								
Eigenvalue	0.932	0.674	0.348	0.107	0.89	0.631	0.329	0.068
r^2					0.98	0.969	0.969	0.796
Summer								
Eigenvalue	0.792	0.621	0.537	0.292	0.703	0.564	0.409	0.159
r^2					0.959	0.959	0.889	0.799
Fall								
Eigenvalue	0.738	0.544	0.273	0.106	0.707	0.443	0.228	0.053
r^2					0.983	0.909	0.935	0.946
Winter								
Eigenvalue	0.526	0.287	0.197	0.165	0.42	0.104	0.059	0.041
r^2					0.894	0.665	0.645	0.496
Year								
Eigenvalue	0.937	0.788	0.607	0.54	0.773	0.61	0.319	0.276
r^2					0.923	0.899	0.8	0.735

Table 5

Three cross-shelf larval assemblages (inner-shelf, mid-shelf, and outer-shelf) were persistent in the Georgia Bight with seasonal changes in membership. Shown are the assemblages from the ten-percent data set. "Bothus ocellatus/robinsi" means *B. ocellatus* and *B. robinsi* or one of either of them.

Season	Inner	Mid	Outer
Spring	<i>Menticirrhus americanus</i>	<i>Diplogrammus pauciradiatus</i> <i>Ophidion omostignum</i> <i>Bothus ocellatus/robinsi</i> <i>Xyrichthys</i> spp. <i>Micropogonias undulatus</i> <i>Etropus crossotus</i> <i>Anchoa hepsetus</i>	<i>Auxis rochei</i> <i>Opisthonema oglinum</i>
Summer	<i>M. americanus</i> <i>O. oglinum</i>	<i>D. pauciradiatus</i> <i>O. omostignum</i> <i>Ophidion marginatum</i> <i>Xyrichthys</i> spp. <i>E. crossotus</i> <i>M. undulatus</i> <i>A. hepsetus</i>	<i>A. rochei</i> <i>B. ocellatus/robinsi</i>
Fall	<i>M. americanus</i> <i>A. hepsetus</i> <i>O. marginatum</i> <i>Leiostomus xanthurus</i>	<i>D. pauciradiatus</i> <i>M. undulatus</i> <i>E. crossotus</i> <i>O. omostignum</i>	<i>Xyrichthys</i> spp. <i>B. ocellatus/robinsi</i>
Winter	<i>M. undulatus</i> <i>L. rhomboides</i>	<i>B. tyrannus</i> <i>M. punctatus</i> <i>C. spilopterus</i> <i>D. pauciradiatus</i> <i>O. omostignum</i> <i>L. xanthurus</i>	<i>B. ocellatus/robinsi</i>

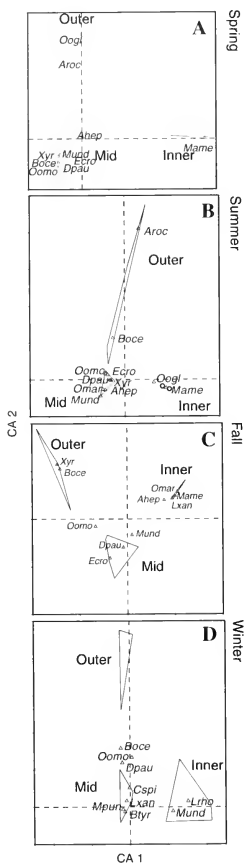


Figure 5

Correspondence analysis (CA) ordinations (portraying the first and second dimension scores) of the larval fish community data showing species in each season: (A) spring, (B) summer, (C) fall, and (D) winter. A larval fish assemblage was associated with each cross-shelf station group. Each station group is outlined and labeled as in Figure 4. The dashed lines intersect at the origin of the plot. Analyses were conducted by using larval concentration data only. Refer to table 2 for definitions of larval taxa codes. Three larval fish assemblages were defined based on species association with station groups (see table 5).

found primarily at outer-shelf stations (Fig. 6). *Auxis rochei* and *Bothus ocellatus/robinsi* (where the slash (/) means "*B. ocellatus* and *B. robinsi*" or one of these species) represented the outer-shelf assemblage (Table 5).

The region of the shelf with the highest species richness depended on the inclusion of rare taxa and season. With the exception of fall, species richness was highest in the mid-shelf group when only abundant taxa were included in analyses (Table 5, Fig. 7A). When rare taxa were included (the 1% data set), species richness was highest in the mid-shelf group during spring and summer and highest in the outer-shelf group during fall and winter (Fig. 7B).

Relationship among cross-shelf patterns in the larval fish community, larval assemblages, and environmental variables

Five environmental variables were correlated to the cross-shelf pattern in station groups and larval assemblages. Water density, salinity, temperature, depth, and stratification of the water column had a significant relation to the structure of larval assemblages and the grouping of stations in the CCA ($P < 0.05$ for each variable, Monte Carlo permutation test; Table 6). The species-environment correlation for the first two axes of the ordination was greater than 0.79, indicating a strong association between the environment and larval assemblages (Table 6). Although the portrayal of station groups and larval assemblages in ordination space was not identical when environmental data were included (compare Figs. 4 and 5 to 8), the cross-shelf pattern in station groups and larval assemblages was maintained (Fig. 8).

The first CCA dimension, in all seasons, was most highly influenced by the depth, temperature, salinity, and density of the water (Fig. 8). In spring, summer, and winter, the mid- and outer-shelf stations were aligned along CCA 1 and separated from the inner-shelf stations along this gradient (Fig. 8). Similarly, in fall, the three station groups were arranged separately along this gradient with the mid-shelf groups intermediate to the inner- and outer-shelf stations. Thus, the separation between inner-shelf and mid- and outer-shelf stations is related to a gradient in depth, temperature, salinity, and density.

The second dimension separated outer-shelf stations from inner- and mid-shelf station groups. In spring and summer, the second dimension (CCA 2) was clearly influenced by stratification (Fig. 8). The outer-shelf stations experienced a higher degree of stratification, separating them from the inner- and mid-shelf stations. During fall and winter, stratification still impacted the second dimension, but less dramatically. In summary, outer-shelf stations were distinguished from mid- and inner-shelf stations by increased stratification of the water.

Relation between larval assemblages and water mass distributions

When hydrographic variables were combined to define water mass, a possible explanation for the cross-shelf

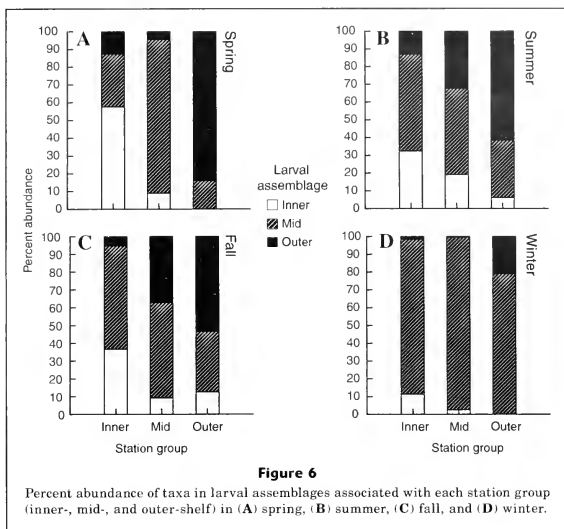


Figure 6

Percent abundance of taxa in larval assemblages associated with each station group (inner-, mid-, and outer-shelf) in (A) spring, (B) summer, (C) fall, and (D) winter.

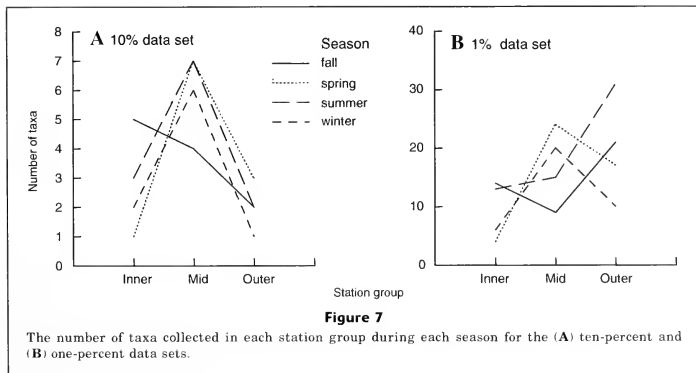


Figure 7

The number of taxa collected in each station group during each season for the (A) ten-percent and (B) one-percent data sets.

pattern in the larval community was revealed. Physical data delineated four water masses (Fig. 3). Larval fish assemblages differentiated only three of these water masses. Stations associated with inner-shelf water (the

inshoremost water mass) and mid-shelf–Gulf Stream mixed water (the offshoremost water mass) formed distinct groups in the ordination of larval community data (Fig. 9). Stations associated with mid-shelf water also

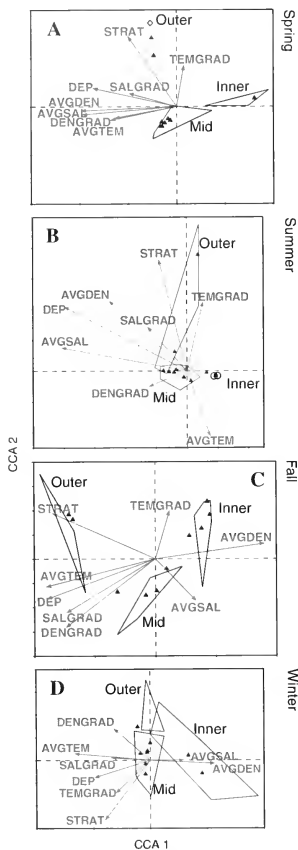


Figure 8

Canonical correspondence analysis (CCA) ordinations (portraying the first and second dimension scores) of the larval fish community data showing the correlations between environmental variables, species, and station groups: (A) spring, (B) summer, (C) fall, and (D) winter. The solid triangles mark the location of taxa (as in Fig. 5), and the polygons surround the three cross-shelf station groups (as in Fig. 4). The arrows depict the gradient of each environmental variable. The dashed lines intersect at the origin of the plot. Analyses were conducted with both larval and environmental data. Refer to Table 3 for definitions of environmental variable codes.

Table 6

The P values from a Monte Carlo permutation test on the environmental variables for each season. Significant values ($P < 0.05$) are shown in bold font. See Table 3 for definitions of variable codes.

Variable code	Season			
	Spring	Summer	Fall	Winter
AVGDEN	0.002	0.01	0.34	0.494
AVGSAL	0.002	0.022	0.016	0.004
AVGTEM	0.152	0.1	0.04	0.016
DENGGRAD	0.836	0.076	0.466	0.958
SALGRAD	0.456	0.086	0.78	0.634
TEMGRAD	0.074	0.076	0.38	0.574
DEP	0.468	0.002	0.002	0.68
STRAT	0.036	0.014	0.012	0.504

formed distinct groups. The fourth water mass, inner-shelf–mid-shelf mixed water overlapped with either inner-shelf or mid-shelf water depending on season. In summary, the cross-shelf distribution and assemblages of water masses coincided with the three cross-shelf regions described: inner-shelf, mid-shelf, and outer-shelf characterized by inner-shelf water, mid-shelf water, and mid-shelf–Gulf Stream mixed water, respectively.

Seasonal patterns in the cross-shelf distributions of the larval fish community

The ten percent data set revealed two distinct seasonal station groups (Fig. 10). The winter stations occurred in close proximity and were separate from stations sampled during the rest of the seasons (Fig. 10A). However, inner-shelf stations sampled during fall overlapped with the winter stations because of the presence of winter and fall spawning species (*L. xanthurus* and *M. undulatus*). There was also overlap of the winter and the warm weather outer-shelf stations (Fig. 10, A and B).

Similarly, the ten percent data set revealed two seasonal assemblages in the larval community data (Fig. 10, C and D). The warm weather assemblage comprised taxa associated with the warm weather station group and were collected during spring, summer, and fall. The winter assemblage was associated with the winter station group and comprised taxa collected during winter. Taxa from the warm weather inner- and mid-shelf assemblages were different from those representing the winter inner- and mid-shelf assemblages (Table 5). The outer-shelf assemblage, however, was less seasonally distinct, represented by *Bothus ocellatus/robinsi* in summer, fall, and winter and by *Auxis rochei* in spring, summer, and fall (Table 5).

Relation between seasonal larval assemblages and environmental variables

The seasonal pattern in the larval concentration data described above was maintained when constrained by environmental variables in the CCA. The community data clearly showed a seasonal influence on the first dimension in ordination space; winter taxa were separate from taxa collected during the rest of the seasons. This seasonal pattern was also reflected in the environmental data (Fig. 11). Salinity, density, temperature, depth, and stratification of the water column were again the most significant environmental variables for explaining variance in the species data ($P < 0.05$, Monte Carlo permutation test, Table 6). The warm weather stations and taxa coincided with higher water temperature, lower density, and a lower density gradient. In addition, the cross-shelf pattern evident in the second and third dimensions of the full larval concentration data (Fig. 10, A and B) appeared to correlate with depth of the water column, the degree of stratification in the water column, and salinity (Fig. 11).

Implications for larval transport

The structure of larval assemblages was linked to water mass distributions and the cross-shelf zonation of physical circulation processes. Three cross-shelf zones of physical dynamics have been defined previously (Atkinson and Menzel, 1985; Pietrafesa et al., 1985a, 1985b; Lee et al., 1991; Boicourt et al., 1998). Three analogous cross-shelf zones were delineated in the larval community data. The cross-shelf larval assemblages were linked to three water masses with cross-shelf structure, and to the physical-chemical characteristics of the region (temperature, salinity, density, and stratification of the water column). The three cross-shelf zones identified previously in terms of physical dynamics coincided with the station groups and larval assemblages identified in our study. Thus, larval distribution and physical properties of the ocean are linked and indicate a strong influence of physical properties and processes on the distribution of larval fish on the southeast United States continental shelf.

Retention on the inner-shelf was a clear larval transport pattern identified in the analyses. *Menticirrhus americanus* represents the inner-shelf group (Table 5) and were always found inshore of the 20-m isobath in inner-shelf water, in inner-shelf-mid-shelf mixed water, or in mid-shelf water, (Fig. 12). Spawning likely occurs on the inner-shelf (Cowan and Shaw, 1988), and larvae are retained in the inner-shelf region.

The analyses also demonstrated that transport from offshore onto the shelf is limited on the continental shelf off the coast of Georgia. *Ceratoscopelus maderensis* and *Auxis rochei* were found only at offshore stations (Fig. 13), representing the outer-shelf group (Table 5) and the mid-shelf-Gulf Stream mixed water mass. The presence of *C. maderensis* identified transport of a mesopelagic fish to waters inshore of the shelf break; how-

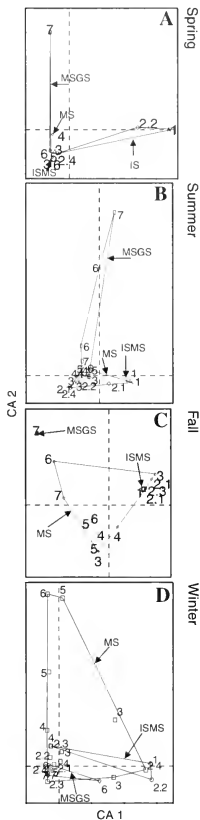


Figure 9

Correspondence analysis (CA) ordinations (portraying the first and second dimension scores) of the larval fish community data showing the full ten-percent data set: (A) spring, (B) summer, (C) fall, and (D) winter. The points represent stations classified by water mass. Solid lines enclose the boundary of each station group with three or more stations. Station groups comprising one or two stations are not enclosed by a solid line. Each station group is labeled and portrayed with a different symbol. Stations with inner-shelf water are labeled with IS (inner-shelf), inner-shelf-mid-shelf mixed water with ISMS, mid-shelf water with MS, and mid-shelf-Gulf Stream mixed water with MSGS. The dashed lines intersect at the origin of the plot. Analyses were conducted using larval data only.

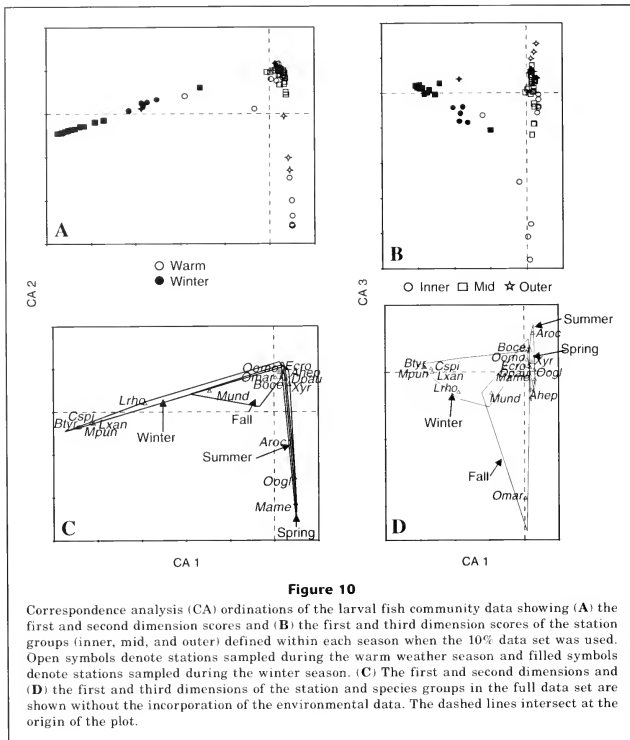


Figure 10

Correspondence analysis (CA) ordinations of the larval fish community data showing (A) the first and second dimension scores and (B) the first and third dimension scores of the station groups (inner, mid, and outer) defined within each season when the 10% data set was used. Open symbols denote stations sampled during the warm weather season and filled symbols denote stations sampled during the winter season. (C) The first and second dimensions and (D) the first and third dimensions of the station and species groups in the full data set are shown without the incorporation of the environmental data. The dashed lines intersect at the origin of the plot.

ever, the rarity of this species on the continental shelf off the coast of Georgia provides evidence for relatively limited onshore transport from off the shelf. Powell and Robins (1994, 1998) and Govoni and Spach (1999) also collected tropical and deepwater taxa inshore of the shelf break. The presence of these taxa was likely due to frequent but variable exchange of larvae across the Gulf Stream front (Govoni and Spach, 1999). Less is known about spawning of *A. rochei* but the species' larval distribution represents restriction to offshore waters (always collected offshore of the 40-m isobath).

During winter, when *B. tyrannus* was found across the shelf (Fig. 14), *Bothus ocellatus/robinsi* was collected only on the outer part of the shelf (Fig. 14). Both *B. tyrannus* and *B. ocellatus/robinsi* likely spawn on the

outer shelf. However, unlike *B. tyrannus*, *Bothus ocellatus/robinsi* was never collected inshore of station 3 (the boundary between the inner- and mid-shelf zones), indicating that the two taxa may experience different transport pathways or different seasonal spawning patterns (see "Discussion" section).

Discussion

Three cross-shelf regions were defined on the continental shelf off the coast of Georgia based on the distribution and abundance of larval fish: inner-shelf, mid-shelf, and outer-shelf. Each region was dominated by a distinct group of species (i.e., larval assemblage). The inner-shelf

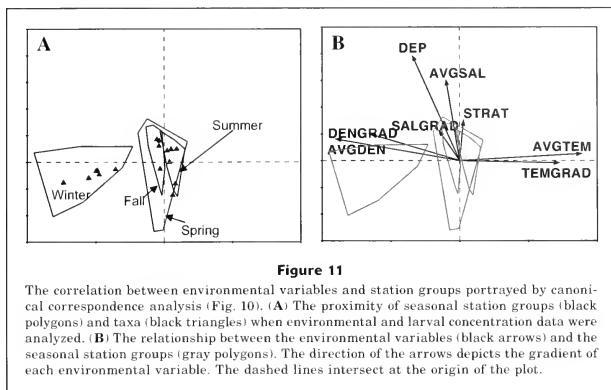


Figure 11

The correlation between environmental variables and station groups portrayed by canonical correspondence analysis (Fig. 10). (A) The proximity of seasonal station groups (black polygons) and taxa (black triangles) when environmental and larval concentration data were analyzed. (B) The relationship between the environmental variables (black arrows) and the seasonal station groups (gray polygons). The direction of the arrows depicts the gradient of each environmental variable. The dashed lines intersect at the origin of the plot.

region was defined inshore of the 20-m isobath (Figs. 4, 5, 12). The inner-shelf larval assemblage was the least diverse taxonomically (Table 2, Fig. 7B), and most taxa in the assemblage were nearshore or estuarine spawning species (e.g., *Cynoscion regalis*, *Menticirrhus americanus*, Table 2). Gradients in salinity and density were associated with the separation of the inner-shelf region but the direction of the gradient varied among seasons; in the spring and summer the inner-shelf region was characterized by lower salinity and density, whereas in the fall and winter, the inner-shelf region was characterized by higher salinities and densities (Fig. 8). The restricted inshore distribution of the assemblage indicated mechanisms of larval retention in the inner-shelf zone.

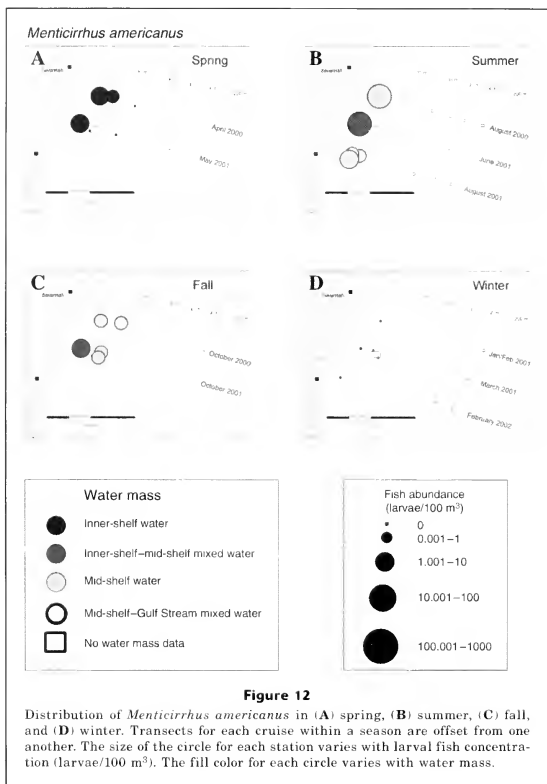
The mid-shelf region was defined between the 20- and 40-m isobaths (Figs. 4, 5, 12). The mid-shelf larval assemblage was distributed over the widest area (Figs. 4, 5, 12) and species in the assemblage were found in all three regions defined (Fig. 6). The mid-shelf region and larval assemblage were related to the average environmental parameters encountered on the shelf (Fig. 8), which varied seasonally. The broad distribution of the assemblage indicated either broad spawning distributions of member species or mechanism of larval transport to both the inner- and outer-shelf regions.

The outer-shelf region was defined as the area offshore from the 40-m isobath (Figs. 4, 5, 12). The outer-shelf region was related to increased stratification of the water column, which was likely a result of Gulf Stream waters mixing onshore. These periodic intrusions would help explain the higher species richness of rare taxa found on the outer-shelf during fall and winter (Fig. 7B). Taxa in the outer-shelf assemblage were either spawned on the outer-shelf (e.g., *Hemanthias vivanus*), spawned offshore of the shelf break and trans-

ported onto the shelf (e.g., *Ceratoscopelus maderensis*), or spawned south of the study area and transported onto the shelf (e.g., *Abudefduf* sp.). Most outer-shelf taxa, however, were restricted to outer-shelf stations indicating limited onshore exchange between the outer- and mid-shelf regions.

Larval assemblages on the continental shelf off the coast of Georgia are derived from a combination of spawning distributions and larval transport; *Brevoortia tyrannus* and *Bothus ocellatus/robinsi* provide an example. *Brevoortia tyrannus* spawn in water temperatures between 16° and 23°C during winter (Checkley et al. 1999); these temperatures were experienced in the mid- and outer-shelf regions during winter. *Bothus ocellatus/robinsi* adults also occur on the mid- and outer-shelf of the continental shelf off the coast of Georgia (Gutierrez, 1967). Thus, during winter the spawning distribution of these two species are likely similar. The larval distributions, however, are different: *B. tyrannus* larvae were collected in all three regions of the shelf during winter, whereas *B. ocellatus/robinsi* were collected on the mid- and outer-shelf (Fig. 14). The vertical distributions of the two species also are different. *B. tyrannus* larvae occur higher in the water column than do *B. ocellatus/robinsi* (Hare and Govoni¹). The observed differences in horizontal distribution could result from the differences in vertical distributions. Alternatively, the distributional differences could result from physiological differences that allow *B. tyrannus* larvae to survive cooler inshore waters or could result from seasonal cross-shelf spawning patterns that result

¹ Hare, J. A., and J. J. Govoni. 2004. In review. Vertical distribution and the outcome of larval fish transport along the southeast US continental shelf during winter.



in *B. tyrannus* spawning inshore during the fall. This example demonstrates that there are multiple mechanisms or pathways that affect the transport of larval fish, and that each species may be subject to different transport regimes. Therefore, to understand larval transport, many factors, including physical forcing mechanisms, the horizontal and vertical distributions of larvae, seasonal patterns, and the physiology of a species, need to be considered.

Temporal larval assemblages were defined in addition to the spatial assemblages. Larvae clearly separated into two seasonal spawning groups: winter and

warm seasons (Fig. 10). The winter assemblage was associated with cool, denser water, whereas the warm water assemblage was associated with warmer, less dense water (Fig. 11). The cross-shelf structure in larval assemblages was still evident in the two seasonal assemblages, but there was overlap in the winter and warm-weather outer-shelf assemblages (Fig. 10). This overlap occurred in waters with the least seasonal variability in temperature and salinity and likely results from year-round spawning by species in the outer-shelf assemblage or year-round supply of larvae to the outer-shelf region by the Gulf Stream.

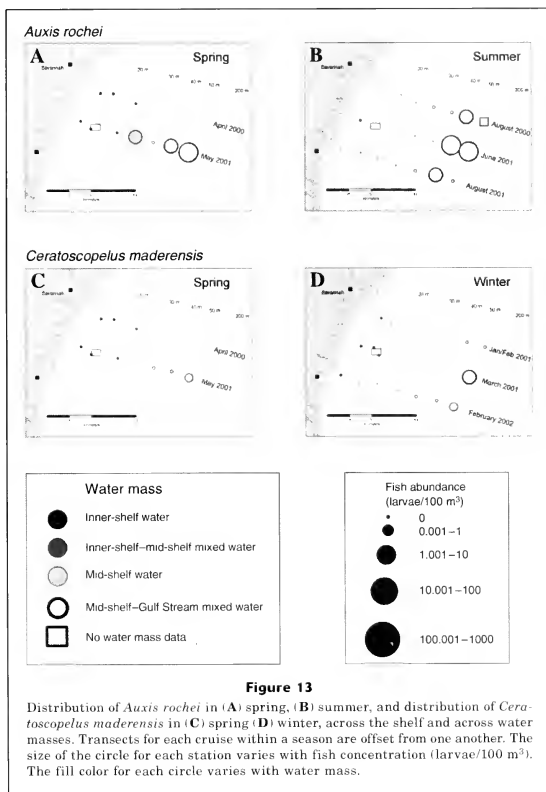


Figure 13

Distribution of *Auxis rochei* in (A) spring, (B) summer, and distribution of *Ceratoscopelus maderensis* in (C) spring (D) winter, across the shelf and across water masses. Transects for each cruise within a season are offset from one another. The size of the circle for each station varies with fish concentration (larvae/100 m³). The fill color for each circle varies with water mass.

Winter-spawning species that use estuaries are frequently grouped together as “estuarine-dependent” taxa (*sensu* Warlen and Burke, 1990). However, Hare and Govoni¹ found that vertical distributions of these winter taxa are different. In addition, our study demonstrated that the horizontal distributions of these species are distinct: *Lagadon rhomboides* and *Micropogonias undulatus* were members of the inner-shelf assemblage and *Leiostomus xanthurus*, *Myrophis punctatus*, and *Brevoortia tyrannus* were members of the mid-shelf assemblage. These findings imply that often grouped “estuarine-dependent” species have different spawning

locations or experience different larval transport processes (or both) and may not reflect a single group.

The definition of three regions based on larval fish distributions is consistent with the division of the shelf into three cross-shelf zones based on physical dynamics. The inner-shelf (0–20 m) is dominated by freshwater discharge, tides, and winds; the mid-shelf (20–40 m) is influenced by wind and tides; and the outer-shelf (40–75 m) is affected by the Gulf Stream and wind (Atkinson and Menzel, 1985; Pietrafesa et al., 1985a, 1985b; Lee et al., 1991; Boicourt et al., 1998). Thus, the physical dynamics of the shelf appear to be closely linked to spa-

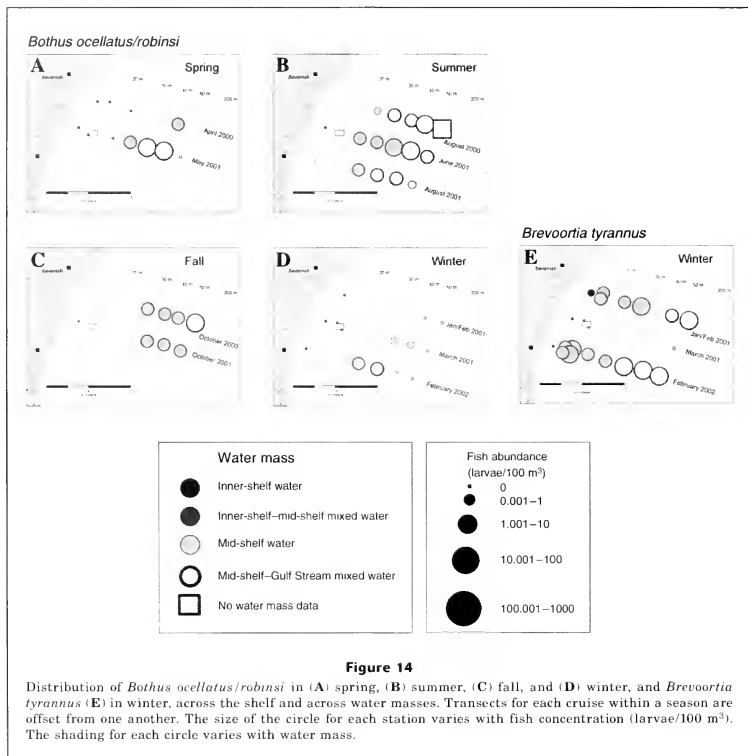


Figure 14

Distribution of *Bothus ocellatus/robinsi* in (A) spring, (B) summer, (C) fall, and (D) winter, and *Brevoortia tyrannus* (E) in winter, across the shelf and across water masses. Transects for each cruise within a season are offset from one another. The size of the circle for each station varies with fish concentration (larvae/100 m³). The shading for each circle varies with water mass.

tial patterns in the distribution of larval fish. Further physiochemical characteristics of the environment (e.g., temperature, salinity, water masses) are highly associated with the structure of larval assemblages (Tables 4, 6, Fig. 9), again indicating a strong link between physical dynamics and larval distribution. However, patterns in spawning and behaviorally modified vertical distributions also have an influence on larval distributions and thus a simple two-dimensional passive model will not adequately explain the distribution of larval fish on the continental shelf off the coast of Georgia.

The three regions defined in our study have important implications for the consideration of MPAs on the southeast United States shelf. The described cross-shelf

zones (inner-, mid-, or outer-shelf) provide information needed to protect spawning habitat of specific species (e.g., *Rhomboplites aurorubens* spawns on the outer-shelf; Table 2). Conversely, the species included in an area under consideration for protection can also be derived (e.g., Gray's Reef National Marine Sanctuary potentially protects species spawning at the interface between the inner- and mid-shelf, Table 2). Further, spawning location information can be derived for several species protected under the South Atlantic Fisheries Management Council's coastal migratory pelagics management plan (e.g., *Rachycentron canadum*, *Scomberomorus cavalla*, *Scomberomorus maculatus*, or *Coryphaena hippurus*, Table 2), but individuals of

these species range so widely (Sutter et al., 1991), only very large MPAs would afford protection from fishing (Parrish 1999, Beck and Odaya 2001). Unfortunately, many species in the snapper-grouper complex, a more sedentary group of species of particular importance in the southeast United States, were not collected. Either these taxa do not spawn on the continental shelf off the coast of Georgia and their larvae are rarely transported into the area, or snapper-grouper spawning on the continental shelf off the coast of Georgia is at a very low level and larvae are quite rare.

Another aspect of MPAs designed for fisheries management is production of individuals in the MPA and their supply to surrounding areas; larval transport is a major mechanism of supply. On the continental shelf off the coast of Georgia, larval assemblages suggest that the supply of larvae from the south (by the Gulf Stream) and even between cross-shelf zones is limited. Members of the outer-shelf assemblage rarely occurred on the mid- and inner-shelf, and members of the inner-shelf assemblage rarely occurred on the mid- and outer-shelf. Thus, larvae spawned on the inner-shelf and to a lesser degree on the mid-shelf likely remain on the continental shelf off the coast of Georgia and appear to be subject to local retention. MPAs in the region, therefore, could provide a local benefit by supplying recruits to nonprotected areas on the continental shelf off the coast of Georgia.

Acknowledgments

We would like to thank all who helped with sample collections, sorting, and analyses: G. Bohne, R. Bohne, C. Bonn, J. Burke, M. Burton, B. Degan, M. Duncan, J. Govoni, M. Greene, E. Jugovich, S. Lem, J. Loefer, R. Mays, R. McNatt, A. Powell, R. Rogers, S. Shoffler, S. Varnam, H. Walsh, and T. Zimanski. We appreciate the hard work and dedication of the officers and crew of the NOAA Ship *Ferrel*, NOAA Ship *Jane Yarn*, NOAA Ship *Oregon II*, and RV *Cape Fear*. Frank Hernandez provided invaluable help with the CTD processing and stratification calculations. We would also like to thank J. Johnson, S. Norton, A. Powell, F. Hernandez, E. Williams, P. Marraro, W. Richards, and an anonymous reviewer for their comments on previous drafts. Most of all, we thank Gray's Reef National Marine Sanctuary and the National Marine Sanctuary Office for funding the project.

Literature cited

- Atkinson, L. P., and D. W. Menzel.
1995. Introduction: Oceanography of the southeast United States continental shelf. In *Oceanography of the southeastern U.S. continental shelf* (L. P. Atkinson, D. W. Menzel, and K. A. Bush, eds.), p 1-9. Am Geophysical Union, Washington, D. C.
- Beck, M. W., and M. Odaya.
2001. Ecoregional planning in marine environments: identifying priority sites for conservation in the northern Gulf of Mexico. *Aquat. Conserv.*: 11:235-242
- Blanton, J. O., F. B. Schwing, A. H. Weber, L. J. Pietrafesa, and D. W. Hayes.
1985. Wind stress climatology in the south Atlantic Bight. In *Oceanography of the Southeastern U.S. continental shelf* (L. P. Atkinson, D. W. Menzel, and K. A. Bush, eds.), p. 10-22. American Geophysical Union, Washington, D.C.
- Boicourt, W. C., W. J. Wiseman Jr., A. Valle-Levinson, and L. P. Atkinson.
1998. Chapter 6. Continental shelf of the southeastern United States and the Gulf of Mexico: in the shadow of the western boundary current. In *The sea*, vol. 11 (A. R. Robinson and K. H. Brink, eds.), p. 135-182. John Wiley and Sons, Inc., New York, NY.
- Checkley, Jr., D. M., P. B. Ortner, F. E. Werner, L. R. Settle, and S. R. Cumming.
1999. Spawning habitat of the Atlantic menhaden in Onslow Bay, North Carolina. *Fish. Oceanogr.* 8:22-36.
- Churchill, J. H., E. R. Levine, D. N. Connors, and P. C. Cornillon.
1993. Mixing of shelf, slope and Gulf Stream water over the continental slope of the Middle Atlantic Bight. *Deep-Sea Res.* 40:1063-1085.
- Clarke, K. R., and R. M. Warwick.
2001. Change in marine communities: an approach to statistical analysis and interpretation. PRIMER-E, 2nd ed., 144 p. Plymouth Marine Laboratory, Plymouth, Cornwall, UK.
- Collins, M. R., and B. W. Stender.
1987. Larval king mackerel (*Scomberomorus cavalla*), Spanish mackerel (*S. maculatus*), and bluefish (*Pomatomus saltatrix*) off the southeast coast of the United States, 1973-1980. *Bull. Mar. Sci.* 41:822-834.
1987. Larval striped mullet (*Mugil cephalus*) and white mullet (*Mugil curema*) off the southeastern United States. *Bull. Mar. Sci.* 45:580-589.
- Cowan, J. H., and R. F. Shaw.
1988. The distribution, abundance, and transport of larval sciaenids collected during winter and early spring from the continental shelf waters off west Louisiana. *Fish. Bull.* 86:129-142.
- Cowen, R. K., J. A. Hare, and M. P. Fahay.
1993. Beyond hydrography: can physical processes explain larval fish assemblages within the Middle Atlantic Bight? *Bull. Mar. Sci.* 53:567-587.
- Crowder, L. B., S. J. Lyman, W. F. Figueira, and J. Priddy.
2000. Source-sink population dynamics and the problem of siting marine reserves. *Bull. Mar. Sci.* 66:799-820.
- Fahay, M. P.
1975. An annotated list of larval and juvenile fishes captured with surface-towed meter net in the South Atlantic Bight during four RV *Dolphin* cruises between May 1967 and February 1968. NOAA/NMFS Technical Report SSRF 685, 39 p.
1983. Guide to the early stages of marine fishes occurring in the western North Atlantic Ocean, Cape Hatteras to the southern Scotian Shelf. *Northwest Atl. Fish. Sci.* 4:1-423.
- Federal Register.
2000. Presidential documents. Executive Order 13158 of

- May 26, 2000. Volume 65, number 105, May 31 2000. U.S. Government Printing Office, Washington, D.C.
- Govoni, J. J., and H. L. Spach.
1999. Exchange and flux of larval fishes across the western Gulf Stream front south of Cape Hatteras, USA, in winter. *Fish. Oceanogr.* 8(suppl. 2):77-92.
- Gutierrez, E. J.
1967. Field guide to the flatfishes of the family Bothidae in the Western North Atlantic, 47 p. United States Department of the Interior, Washington, D.C.
- Hare, J. A., J. A. Quinlan, F. E. Werner, B. O. Blanton, J. J. Govoni, R. B. Forward, L. R. Settle, and D. E. Hoss.
1999. Larval transport during winter in the SABRE study area: results of a coupled vertical larval behavior-three-dimensional circulation model. *Fish. Oceanogr.* 8:57-76.
- Hare, J. A., M. P. Fahay, and R. K. Cowen.
2001. Springtime ichthyoplankton of the Slope Sea: larval assemblages, relation to hydrography and implications for larval transport. *Fish. Oceanogr.* 10:164-192.
- Hoss, D. E., H. L. Spach, L. R. Settle, J. A. Hare, and E. H. Laban.
1997. The growth and behaviour of two species of clupeid larvae and how it affects their oceanic transport. In *Ichthyoplankton ecology* (A. J. Geffen, J. M. Fives, J. E. Thorpe, eds.), 22 p. Fisheries Society of the British Isles, Galway, Ireland.
- Johnson, G. D., and P. Keener.
1984. Aid to the identification of American grouper larvae. *Bull. Mar. Sci.* 34:106-134.
- Judy, M. H., and R. M. Lewis.
1983. Distribution of eggs and larvae of Atlantic menhaden, *Brevoortia tyrannus* along the Atlantic coast of the United States. U. S. National Marine Fisheries Service, Special Scientific Report—Fisheries 774, 23 p.
- Kendall, A. W., Jr., and A. C. Materese.
1994. Status of early life history descriptions of marine teleosts. *Fish. Bull.* 92:725-36.
- Kendall, A. W., Jr., and L. A. Walford.
1979. Sources and distribution of bluefish, *Pomatomus saltatrix*, larvae and juveniles off the east coast of the United States. *Fish. Bull.* 77:213-27.
- Lee, T. N., J. A. Yoder, and L. P. Atkinson.
1991. Gulf Stream frontal edge influence on productivity of the southeast U.S. continental shelf. *J. Geophys. Res.* 96:22191-2205.
- Leis, J. M.
1989. Larval biology of butterflyfishes (Pisces, Chaetodontidae): what do we really know? *Environ. Biol. Fishes* 25:87-100.
- Marancik, K. E.
2003. Larval fish assemblages of the Georgia Bight. M.S. thesis, 149 p. East Carolina Univ., Greenville, NC.
- Parrish, R.
1999. Marine reserves for fisheries management: why not. *CalCOFI Rep.* 40:77-6
- Pietrafesa, L. J., J. O. Blanton, J. D. Wang, V. Kourafalou, T. L. Lee, and K. A. Bush.
1985a. The tidal regime in the South Atlantic Bight. In *Oceanography of the southeastern U.S. continental shelf* (L. P. Atkinson, D. W. Menzel, K. A. Bush, eds.), p. 63-6. American Geophysical Union, Washington, D.C.
- Pietrafesa, L. J., G. S. Janowitz, and P. A. Wittman.
1985b. Physical oceanographic processes in the Carolina Capes. In *Oceanography of the southeastern U.S. continental shelf* (L. P. Atkinson, D. W. Menzel, K. A. Bush, eds.), p. 23-32. American Geophysical Union, Washington, D.C.
- Pietrafesa, L. J., J. M. Morrison, M. P. McCann, J. Churchill, E. Bohm, and R. W. Houghton.
1994. Water mass linkages between the Middle and South Atlantic Bights. *Deep-Sea Res.* II 41:365-89.
- Plan Development Team.
1990. The potential of marine fishery reserves for reef fish management in the U.S. southern Atlantic. NOAA Tech. Memo. NMFS-SEFC-261, 40 p.
- Powell, A. B., D. G. Lindquist, and J. A. Hare.
2000. Larval and pelagic juvenile fishes collected with three types of gear in Gulf Stream and shelf waters in Onslow Bay, North Carolina, and comments on ichthyoplankton distribution and hydrography. *Fish. Bull.* 98:427-38.
- Powell, A. B., and R. E. Robbins.
1994. Abundance and distribution of ichthyoplankton along an inshore-offshore transect in Onslow Bay, North Carolina. NOAA Tech. Report NMFS 120, 28 p.
1998. Ichthyoplankton adjacent to live-bottom habitats in Onslow Bay, North Carolina. NOAA Tech. Report NMFS 133, 32 p.
- Powles, H., and B. W. Stender.
1976. Observations on composition, seasonality and distribution of ichthyoplankton from MARMAP cruises in the South Atlantic Bight in 1973. South Carolina Marine Resources Center, Technical Report Series Number 11, Charleston, SC.
- Rakocinski, C. F., J. Lyczkowski-Shultz, and S. L. Richardson.
1996. Ichthyoplankton assemblage structure in Mississippi Sound as revealed by canonical correspondence analysis. *Estuar. Coast. Shelf Sci.* 43:237-57.
- Richards, W. J. (ed.).
2001. Preliminary guide to the identification of the early life history stages of fishes of the Western Central Atlantic. (<http://www4.cookman.edu/noaa/>). [Accessed 12 May 2004.]
- Simpson, J. H., and I. D. James.
1986. Coastal and estuarine fronts. In *Baroclinic processes on continental shelves* (C. N. K. Moores, ed.), p. 63-93. American Geophysical Union, Washington, D.C.
- Smith, W., P. Berrien, and T. Potthoff.
1994. Spawning patterns of bluefish, *Pomatomus saltatrix* in the northeast continental shelf ecosystem. *Bull. Mar. Sci.* 54:8-6.
- Smith, K. A., M. T. Gibbs, J. H. Middleton, and I. M. Suthers.
1999. Short term variability in larval fish assemblages of the Sydney shelf: tracers of hydrographic variability. *Mar. Ecol. Prog. Ser.* 178:1-5.
- Stephenson, R. L.
1999. Stock complexity in fisheries management: A perspective of emerging issues related to population sub-units. *Fish. Res.* 43:247-249.
- Sutter, F. C., III, R. I. Williams, and M. F. Godcharles.
1991. Movement patterns and stock affinities of king mackerel in the southeast United States. *Fish. Bull.* 89:315-324.
- ter Braak, C. F. J.
1985. CANOCO—a FORTRAN program for canonical community ordination by correspondence analysis, principal components analysis and redundancy analysis. Technical Report: LWA-88-02. Groep Landbouw-wiskunde, Wageningen, The Netherlands.

- ter Braak, C. F. J., and P. Smlauer.
2002. CANOCO Reference manual and CanoDraw for Windows User's guide: software for canonical community ordination (vers. 4.5), 500 p. Microcomputer Power Ithaca, New York, NY.
- Warlen, S. M., and J. S. Burke.
1990. Immigration of larvae of fall/winter spawning marine fishes into a North Carolina estuary. *Estuaries* 13:453-61.
- Warner, R. R., S. E. Swearer, and J. E. Caselle.
2000. Larval accumulation and retention: Implications for the design of marine reserves and essential fish habitat. *Bull. Mar. Sci.* 66:821-830.

Abstract—Inter and intra-annual variation in year-class strength was analyzed for San Francisco Bay Pacific herring (*Clupea pallasii*) by using otoliths of juveniles. Juvenile herring were collected from March through June in 1999 and 2000 and otoliths from subsamples of these collections were aged by daily otolith increment analysis. The composition of the year classes in 1999 and 2000 were determined by back-calculating the birth date distribution for surviving juvenile herring. In 2000, 729% more juveniles were captured than in 1999, even though an estimated 12% fewer eggs were spawned in 2000. Spawning-date distributions show that survival for the 2000 year class was exceptionally good for a short (approximately 1 month) period of spawning, resulting in a large abundance of juvenile recruits. Analysis of age at size shows that growth rate increased significantly as the spawning season progressed both in 1999 and 2000. However, only in 2000 were the bulk of surviving juveniles a product of the fast growth period. In the two years examined, year-class strength was not predicted by the estimated number of eggs spawned, but rather appeared to depend on survival of eggs or larvae (or both) through the juvenile stage. Fast growth through the larval stage may have little effect on year-class strength if mortality during the egg stage is high and few larvae are available.

Year-class formation in Pacific herring (*Clupea pallasii*) estimated from spawning-date distributions of juveniles in San Francisco Bay, California

Michael R. O'Farrell

Ralph J. Larson

Department of Biology
San Francisco State University
1600 Holloway Avenue
San Francisco, CA 94132

Present address (for M. R. O'Farrell, contact author): Department of Wildlife,
Fish and Conservation Biology
University of California, Davis
One Shields Avenue
Davis, California 95616

E-mail address (for M. R. O'Farrell): mrofarrell@ucdavis.edu

Both biological and physical sources of mortality have been suggested as important in determining year-class strength in fish populations. Food limitation at first feeding (Hjort, 1914; Cushing, 1975; Lasker, 1975; Cushing, 1996), larval retention (Iles and Sinclair, 1982; Sinclair and Iles, 1985), a juvenile critical period (Bollens et al., 1992; Thorisson, 1994), as well as predation and environmental conditions may ultimately affect recruitment. Egg development time and larval growth rate have the capacity to adjust the relative impacts of these mortality sources on individual propagules by modifying stage duration (Houde, 1989; Yoklavich and Bailey, 1990).

Juvenile fishes can be used to assess both inter- and intra-annual variation in egg and larval survival. Interannual variation in year-class strength is often inferred from measures of juvenile abundance (e.g., Baxter et al., 1999). In addition, when the total number of eggs spawned is known, juvenile abundance can be used to assess overall variation in egg and larval survival. Intra-annual variation in egg and larval survival can be estimated from the birth-date distribution of surviving juveniles, as determined from otolith daily increment analysis. Particularly when data on actual spawning-date distri-

butions are available, the birth date distribution of survivors can be used to identify periods of spawning that contributed differentially to juvenile recruitment (Methot, 1983; Rice et al., 1987; Yoklavich and Bailey, 1990; Moksness and Fossum, 1992; Fox, 1997; Takahashi et al., 1999).

Recruitment of juvenile Pacific herring (*Clupea pallasii*) varies interannually by over an order of magnitude in San Francisco Bay (Baxter et al., 1999) and is the culmination of several processes. Schools of adult herring enter San Francisco Bay in discrete batches during the fall and winter. These schools shoal and deposit eggs and milt during spawning events that often correspond to the quarter moon phase. Spawning events can vary in duration from approximately one day to one week, and simultaneous events may occur at different spawning sites throughout the bay. Herring lay adhesive eggs intertidally and subtidally on rocks, algae, aquatic plants, pier pilings, and other substrates (Alderice and Velsen, 1971; Hay, 1985). Eggs can experience extremely high mortality due to predation (McGurk, 1986; Bishop and Green, 2001), suboptimal temperature and salinity conditions (Alderice and Velsen, 1971; Griffin et al., 1998), as well as reduced hatching and developmental abnormalities associated with certain substrate se-

lection (Vines et al., 2000). Larvae hatch from eggs after an incubation period, and the San Francisco Bay estuary can serve as a larval nursery area until after metamorphosis into the juvenile stage (Hay, 1985).

Our objectives were 1) to identify periods in the spawning season that lead to successful (or unsuccessful) juvenile recruitment and 2) to evaluate larval and juvenile growth variation for two herring year classes. We used otoliths of juvenile herring from the 1999 and 2000 year classes to back-calculate spawning-date distributions and determine spawning times that lead to successful recruitment. Distributions of spawning were obtained from management surveys. Growth was then evaluated to determine its role in year-class formation.

Methods

Surveys

All information on adult herring spawning events and juvenile herring specimens were obtained from ongoing monitoring and management surveys conducted by the California Department of Fish and Game (CDFG).

Data on timing, location, and magnitude of herring spawning events for the 1998–99 and 1999–2000 spawning seasons were obtained from the herring spawn survey conducted by the California Department of Fish and Game (CDFG). The survey is conducted from November through March throughout central San Francisco Bay, the area of most herring spawning (Watters et al., 2004). The central bay region is searched for herring spawning on a daily basis from a small boat, and the entire spawning region is covered at least once per week. Eggs are located visually at low tide and by rake in shallow subtidal areas. When a spawning area is located, the number of eggs per square meter is measured from a subsample of the spawning area and is expanded to an estimate of total eggs spawned (for spawning survey method details, see Spratt, 1981; Watters et al., 2004). At the end of the 1998–99 and 1999–2000 spawning seasons, information on date, location, spawning area, average eggs/m², total eggs, and the spawning biomass estimate was provided for the purpose of this study (Watters¹).

Juvenile (age-0) herring were sampled monthly from 30 stations in San Francisco Bay aboard the RV *Longfin* as part of CDFG's Bay/Delta Division's Bay study (Fig. 1). Each station was visited once a month and juvenile herring were retained from catches during the months of April–June 1999 and March–June 2000. Stations were sampled by mid-water trawl with a 3.7-m² mouth and 1.3-cm mesh codend, towed against the current, for 12 minutes. Volume of water filtered was calculated by using a flowmeter and was used to calculate

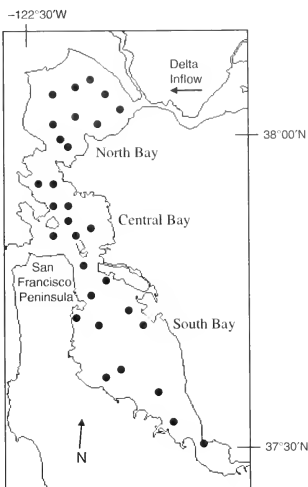


Figure 1
Midwater trawl sampling stations in San Francisco Bay.

catch per unit of effort (CPUE) for each station. Juvenile herring were measured onboard, sorted from the catch, kept on ice, and transported to the laboratory, where they were frozen. Relative recruitment in each year was calculated by summing the CPUE at each station for the months of March–June in 1999 and 2000.

Otolith preparation and analysis

Frozen juvenile herring, separated by date and station, were thawed in batches and all fish were re-measured for standard length to the nearest mm. If the catch was small at a particular station (less than approximately 10 individuals), all specimens from that station were reserved for otolith analysis. If the catch was large, a subsample of the measured catch was reserved for otolith analysis. Subsampling consisted of randomly selecting at least two specimens from each 1-mm length bin in the catch.

Both sagittal otoliths were extracted from each fish, cleaned with fresh water, and transferred to a microscope slide where they were allowed to dry. When completely dry, both otoliths were mounted on the slide, convex side up, with clear nail polish.

Otoliths were read with a compound microscope. Because otoliths were too thick to allow sufficient light transmission for increment reading, all otoliths were

¹ Watters, D. 2000. Personal commun. Calif. Dep. Fish and Game, 411 Burgess Dr., Menlo Park, CA 94025.

ground with 2000 grit sandpaper. Otoliths were alternately ground and examined under the microscope at 100 \times to ensure that the section was thin enough to allow sufficient light transmission, yet not over-ground so that the edges of the otolith were lost.

Daily increment deposition in herring begins at yolk sac absorption, corresponding with the first heavy ring near the nucleus (Geffen, 1982; McGurk, 1984a; McGurk, 1987; Moksness and Weststad, 1989). This heavy ring was located in all herring examined and increment counts were initiated there. Increment counts were made at 1000 \times (with an oil immersion objective) and 400 \times (without oil immersion) magnification along the axis of maximum resolution. All increments were counted from the first heavy ring until the last ring on the edge of the otolith.

Several days after the first reading, the same reader performed a reading on the second otolith. If the two increment counts differed by more than a value of 7, a third reading was conducted at a later date on the highest quality otolith. If the three increment counts differed from each other by more than a value of 7, otolith data from that fish were not used in further analyses. Where two readings differed by 7 or fewer increments, the final increment number for each fish was determined by averaging the two increment counts.

Daily otolith increment deposition has been demonstrated in Pacific herring larvae reared in captivity (McGurk, 1984a; Moksness and Weststad, 1989) and in the field (McGurk, 1987). In our study, otolith increments were assumed to be deposited daily and the validity of this assumption is treated in the "Results" and "Discussion" sections. Precision of otolith increment counts was determined by computing the average percent error for each otolith examined (Beamish and Fournier, 1981).

Spawning-date distributions

Spawning-date distributions were constructed from specimens retained for otolith analysis in 1999 and 2000. Distributions were calculated 1) by adding a constant of 14 days to the otolith increment count and 2) by subtracting that value (otolith increments+14) from the Julian date of capture. Because Pacific herring begin daily increment deposition at yolk sac absorption, the constant of 14 days was added to the increment value to account for egg incubation and the yolk sac larval period. Taylor (1971) reported a 9-day egg incubation period for a British Columbia Pacific herring stock between 13.4°C and 13.8°C. For San Francisco Bay spawned herring, Griffin et al. (1998) found developmental rate to be influenced by salinity; the greatest hatching rate occurred 10 days after fertilization at a salinity of 14 ppt. Yolk sac absorption occurs in Pacific herring 4–7 days after hatching (McGurk, 1987; Griffin et al., 2004, and references therein). The final value of 14 days for egg incubation and yolk sac absorption used in our study was determined 1) from laboratory-derived values reported for British Columbia (Taylor, 1971; McGurk, 1987) and

San Francisco Bay (Griffin et al., 1998) herring populations and 2) by visually matching back-calculated spawning-date distributions with the observed spawning-date distribution from the CDFG spawn-deposition survey.

The back-calculated spawning-date distributions determined from specimens used for otolith analysis were extrapolated to include as many herring as possible caught in the juvenile surveys of 1999 and 2000. Length-frequency distributions were converted to spawning-date distributions by using age-length keys. Separate age-length keys were constructed for each survey in both 1999 and 2000. In some cases, the monthly survey was split into two legs separated by several days. When the monthly survey was split into legs, separate age-length keys were constructed for each leg.

It was not possible to fit all herring caught between the months of March and June into age-length keys because some samples were inadvertently discarded after measurement in the field. If the range of lengths in the discarded samples extended beyond the sizes of samples aged, a complete age-length key could not be constructed. To avoid ascribing a possibly inaccurate age to a fish outside the size range of the age-length key, those fish were not included in the spawning-date distribution. Table 1 displays the number of herring caught in each leg, the number of otoliths used to construct the age-length key for that survey leg, and the total number and proportion of juveniles caught that are represented in the spawning-date distribution. The number of juveniles caught was greater than the number of juveniles in the spawning-date distribution for all but one survey leg. This discrepancy was due to discarded fish (in the field) with lengths not within the range of the age-length key constructed from the subsampled individuals.

Mortality estimate corrections are often superimposed upon spawning-date or hatching-date distributions to account for different size juveniles captured (Methot, 1983). Presumably a larger juvenile is older, and thus has been exposed to mortality factors for a longer period of time than has a smaller juvenile. The lack of a correction for juvenile mortality can lead to an underrepresentation of larger juveniles in the distribution. Because of the noncontinuous mid-water trawl sampling schedule, mortality rates could not be estimated from the data used in our study. As a result, mortality corrections were calculated by using an instantaneous mortality rate value of 0.016/d, corresponding to the greater of two mortality rates calculated from juvenile Pacific herring in Prince William Sound, Alaska (Stokesbury et al., 2002).

Spawning-date distributions were corrected for mortality by calculating abundance at 100 days (N_{100}). For fishes aged at less than 100 days:

$$N_{100} = N_a e^{-0.016(100-a)}, \quad (1)$$

where a is the age of the fish in days.

Table 1

Summary of the catch, number of *Clupea pallasii* otoliths examined from the catch, number and percent available for use in the spawning-date distributions, and catch per unit of effort (CPUE) for the midwater trawl survey in 1999 and 2000. Σ CPUE represents summed CPUE for all stations in each survey leg. Juveniles were not used in analysis if they were inadvertently discarded in the field and if a complete age-length key could not be constructed.

Survey dates	Area surveyed	Juveniles caught	Otoliths examined	Used in analysis	Percent used	Σ CPUE
1999						
Mar 99	entire bay	0	0	0	0	0
21 Apr 99	central and north	41	0	0	0%	1653
26–28 Apr 99	south and north	66	53	60	91%	2360
18–19 May 99	north	19	4	2	11%	771
24–27 May 99	north, central, and south	280	251	273	98%	12,856
9–10 Jun 99	north and central	91	25	45	49%	3457
15 Jun 99	south	61	0	0	0%	2551
Total		558	333	380	68%	23,648
2000						
8–9 Mar 00	north and central	11	0	0	0%	637
13–14 Mar 00	south	7	7	6	86%	294
4–5 Apr 00	north	25	25	25	100%	1053
10–11 Apr 00	central and south	302	115	284	94%	14,712
10 May 00	north	898	77	740	82%	38,270
22–24 May 00	central and south	2244	77	2237	100%	102,516
6–7 Jun 00	central and south	569	74	569	100%	25,352
13 Jun 00	north	13	0	0	0%	539
Total		4069	375	3861	95%	183,373

For fishes aged greater than 100 days:

$$N_{100} = \frac{N_0}{e^{-0.015(a-100)}} \quad (2)$$

Combining the results of Equations 1 and 2 produced the mortality-corrected spawning-date distributions.

Growth

To evaluate correlates of both inter- and intra-annual variation in survival to the juvenile stage, we wanted to compare growth rates of herring up to the juvenile stage. However, because it was apparent that growth rates may have differed for specimens spawned at different times of the year, either a linear or nonlinear growth curve fitted to size-at-age data would be erroneous (O'Farrell, 2001). Larger (older) and smaller (younger) individuals would have experienced different growth histories; therefore a plot of size versus age for any sample of fish would not reflect the growth history of any one cohort. Furthermore, consecutive samples rarely contained individuals from any given cohort because older juveniles appeared to leave San Francisco Bay. Finally, we did not have data on size at age of larvae; therefore growth curves would be incomplete.

Instead, we used age at size to compare growth within and between years. To do this, we computed the num-

Table 2

Summary statistics and distribution of juvenile *Clupea harengus* lengths within the 40–50 mm size bin for sampling events where size-at-age data were used. Other sampling events were not included in growth analyses because they did not contain juvenile herring between the sizes of 40 mm and 50 mm.

Survey leg	n	Mean (mm)	SD (mm)
26–27 Apr 99	15	43.80	2.54
24–27 May 99	162	45.02	2.63
9 Jun 99	10	42.20	2.82
5 Apr 00	16	46.25	3.00
10–11 Apr 00	23	46.43	2.94
10 May 00	9	43.67	3.04
22–24 May 00	36	44.81	3.19
6–7 Jun 00	36	46.56	2.82

ber of otolith increments (days after yolk sac absorption) present in fish between 40 mm and 50 mm standard length. This size group was chosen to analyze growth because it was well represented in both in the 1998–99 and 1999–2000 spawning seasons. The mean and stan-

standard deviation of the length distribution within the 40–50 mm bin for each sampling event is provided in Table 2. Thus, the amount of time (measured by otolith increments) needed for fish to grow to the 40 mm–50 mm size group was used to compare growth. Differences in age at length were evaluated and compared with observed variation in juvenile abundance.

Results

Egg and juvenile abundance

Both the magnitude and timing of estimated egg deposition differed little between the 1998–99 and 1999–2000 spawning seasons (Fig. 2). Total egg deposition was estimated to be 9.66×10^{11} eggs for 1998–1999 and 8.59×10^{11} eggs for 1999–2000 (Watters²). Peak egg deposition in both spawning years occurred in January (Fig. 2).

Abundance of juvenile herring resulting from these two spawning seasons differed greatly. The cumulative estimated relative recruitment ($\Sigma CPUE$) of juvenile herring was 7.75 times greater in 2000 than 1999 (Table 1).

General patterns of juvenile herring distribution were similar in 1999 and 2000. Juvenile herring recruited to the sampling gear in March and April and were widely

distributed throughout the bay (Fig. 3). Peak abundances occurred in May for both 1999 and 2000, and juveniles were caught throughout the study area. By June, abundances decreased and herring became more concentrated in the central Bay region, presumably aggregating in this area prior to exiting San Francisco Bay for the coastal ocean (Fig. 3).

Spawning-date distributions

The temporal distribution of successful spawning-dates differed between the 1999 and 2000 year classes (Fig. 4, A and B). In 1999, the earliest spawning-date that resulted in juvenile recruitment was 30 November 1998. The greatest numbers of juvenile recruits were a product of the middle of the spawning season, from approximately early January 1999 though early February 1999, and the highest recruitment occurred from spawnings between 10 January and 14 January 1999 (Fig. 4A). An additional spike of recruitment was observed from spawning events at the end of the season (early March). The period of highest recruitment came at the same time as the highest spawning intensity. Spawning events early in the spawning season (November–December) appeared to produce few juveniles (Fig. 4A).

In 2000, juveniles recruited from much earlier spawning events. Back-calculated spawning dates indicated that spawning may have occurred as early as 13 October 1999 (Fig. 4B). Both the March 2000 and April 2000 juvenile surveys contained herring with back-calculated spawning dates that ranged from mid to late October, indicating that a spawning event occurred extremely early in the spawning season and was undetected by the spawn-deposition survey (which commences in November). Although early spawnings appeared to produce some recruitment success, a near lack of success was noted for many of the mid-season spawnings that occurred from mid-November through mid-January 2000 (Fig. 4B). This period of poor survival was then followed by the period of highest recruitment; spawning dates ranged from mid-January to early March and peak recruitment resulted from February spawning (Fig. 4B).

Juvenile mortality corrections superimposed upon the spawning-date distributions had little effect on the general results. An instantaneous juvenile mortality rate of 0.016/d produced minor adjustments on the percent recruitment resulting from particular spawning periods in both years (Fig. 4, A and B). This mortality correction did not alter the general spawning periods that resulted in juvenile recruitment. Increasing the instantaneous juvenile mortality rate to 0.05/d (O'Farrell, unpubl. data) also had negligible effects on the general results of the spawning-date distributions.

Data for both 1999 and 2000 are not totally complete. The spawning-date distribution for 1999 was based on a total of 380 herring, whereas 558 herring were caught between the months of March and June. Similarly, the 2000 spawning-date distribution was based on a total of 3861 herring, whereas 4069 herring were caught during the same months (Table 1). Fish were omitted from

² Watters, D. 2000. Unpubl. data. Calif. Dep of Fish and Game, 411 Burgess Dr., Menlo Park, CA 94025.

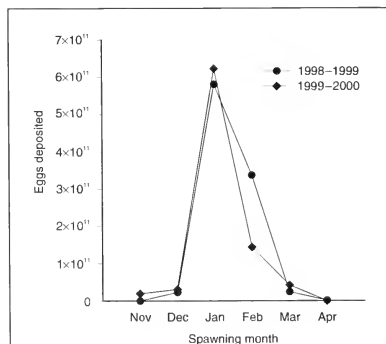
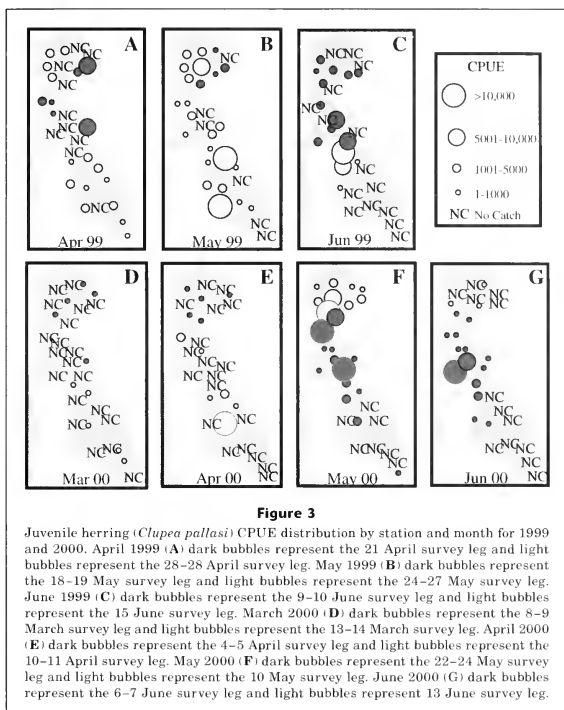


Figure 2

Total egg deposition by Pacific herring (*Clupea pallasii*), summed by spawning month for the 1998–99 and 1999–2000 spawning seasons. Data provided by the California Department of Fish and Game, Menlo Park.



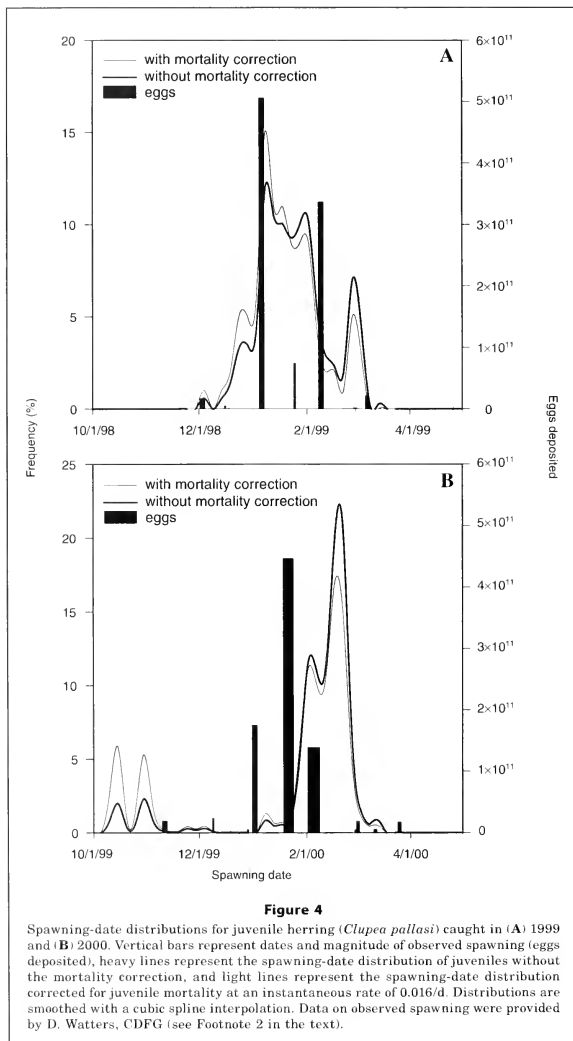
the spawning-date distribution because some samples were discarded and otoliths were unavailable. Because of evidence for intrayear growth-rate variation, other age-at-length data were not used to infer spawning dates for these fish. The standard length data for the fish not included in this analysis were used for all other analyses in our study.

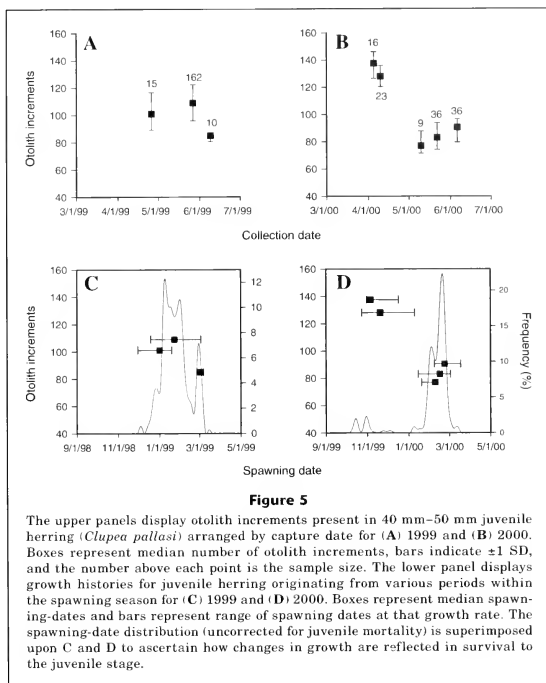
Precision of multiple otolith readings was calculated for all otoliths examined. Average percent error (Beamish and Fournier, 1981) was 3.60% in 1999 and 1.64% in 2000, indicating that aging precision was less than 4 days for 100-day old herring in both years.

Growth

Different patterns of age at length (40–50 mm) were observed in 1999 and 2000. In 1999, specimens between

40 mm and 50 mm were captured in three survey legs. A significant decrease in the number of otolith increments for juveniles 40 mm–50 mm standard length was detected in 1999 (Fig. 5A; Kruskal-Wallis test; $H=27.93$, $P<0.0001$). Nonparametric multiple comparisons indicated that there was a nonsignificant difference in otolith increment counts for herring caught in the April 1999 and the May 1999 surveys, but herring from these surveys had significantly higher median otolith increment counts than those from the June 1999 survey. In this later survey, juvenile herring were caught that were a product of spawning events occurring late in the spawning season. Figure 5C displays the median and range of spawning dates of the specimens aged for Figure 5A. Juvenile herring that were a product of spawning between 27 February 1999 and 7 March 1999 reached a 40–50 mm size range significantly faster than





specimens recruiting from earlier spawning periods. The period of greatest recruitment occurred during the slower growth period in 1999 (Fig. 5C).

In 2000, 40 mm–50 mm juvenile herring were caught in five survey legs conducted during three months (April, May, and June). The data are displayed by survey leg; pooling the data by month, however, does not change the result. Median increment counts differed significantly for the 2000 surveys (Fig. 5B; $H=76.39$, $P<0.0001$). Otolith increment counts for 40 mm–50 mm specimens did not differ for the 5 April 2000 and 10–11 April 2000 surveys. However, the age at length for these surveys was significantly greater than for the three later survey legs (10 May 2000, 22–24 May 2000, and 6 June 2000), which did not significantly differ from each other. Herring caught in the three later surveys grew significantly faster than herring caught in the two earlier surveys. The significant decrease in age at length indicates that juvenile herring that were a product of spawning be-

tween 15 January 2000 and 18 March 2000 grew faster than specimens recruiting from earlier spawning events. The majority of juvenile recruits in 2000 were a product of the fast growth period (Fig. 5D).

Accuracy of growth-rate estimates determined from growth increments on otoliths

The above analyses depended upon the assumption that increments were deposited daily in the otoliths examined. Two lines of evidence point to the validity of this assumption. First, back-calculated spawning-dates generally agreed with the known spawning season of San Francisco Bay herring, and several peaks in back-calculated spawning dates match known spawning events quite closely (Fig. 4, A and B).

Second, juvenile growth rates appear to be high enough for daily growth (McGurk, 1984b). Clear length-frequency modes were visible for three sampling events

in 2000. Assuming linear growth between these time periods, the advancement of these length-frequency modes resulted in growth rates of 0.75 mm/d (Fig. 6, arrow in A), 0.83 mm/d (arrow in B), and 0.64 mm/d (arrow in C). McGurk (1984b) demonstrated daily increment deposition in herring if the larval growth rate exceeded 0.36 mm/d. Our data did not allow us to estimate growth rates of larvae; however, the estimated juvenile growth rates presented above are much greater than necessary for daily increment deposition.

Discussion

Catches of juvenile herring were much greater in 2000 than in 1999. Between the months of March and June 2000, cumulative CPUE was more than seven times greater than during the same period in 1999, yet an estimated 12% more eggs were deposited during the

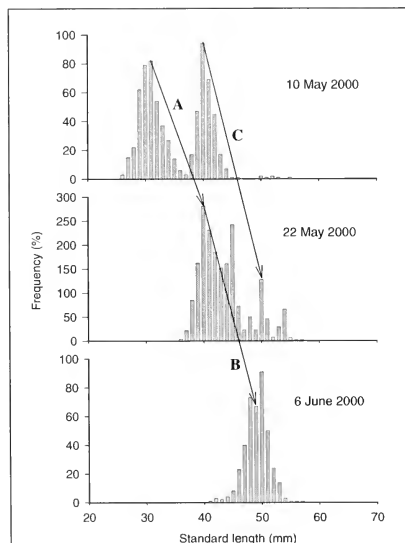


Figure 6

Length frequencies for juvenile herring (*Clupea pallasii*) captured on 10 May 2000, 22 May 2000, and 6 June 2000. Arrows represent the estimated propagation of length modes through time. Linear growth rates, calculated from each trajectory, are as follows: A=0.75 mm/d; trajectory B=0.83 mm/d; and C=0.64 mm/d.

1988–99 spawning season. Because observed differences in recruitment between 1999 and 2000 far exceeded differences in the total eggs spawned, differential survivorship during the egg or larval stages (or both) must be responsible for disparate year-class strengths.

The spawning-date distributions presented for 1999 and 2000 did not contain all herring caught by the mid-water trawl survey between the months of March and June. Because they could not be accurately assigned ages with an age-length key (Table 1), 178 herring were omitted from the distribution in 1999. Most specimens omitted from this distribution were caught in the early April 1999 and late June 1999 survey legs. As a result, the spawning-date distribution likely underestimated the recruitment from very early and very late season spawnings. In 2000, 208 specimens, from a variety of survey legs, were omitted from the spawning-date distribution (Table 1). Because a large number of herring were caught in 2000, it is unlikely that these omissions would significantly change the shape of the spawning-date distribution. The loss of data in this case does not change the overall result of large year-class-strength variation.

The noncontinuous sampling schedule for juveniles may have resulted in either an underestimation or overestimation of CPUE and thus year-class strength. In several months, the mid-water trawl survey was conducted over two legs separated by several days (Table 1, Fig. 3). This noncontinuous sampling could have produced error in our estimates because aggregations of juveniles, through movement between areas, could conceivably have escaped detection by trawls (resulting in CPUE underestimation) or have been sampled twice in the same month (resulting in CPUE overestimation). However, O'Farrell (2001) showed that dispersal of herring from a successful spawning event could occur through much of San Francisco Bay. Therefore, we do not believe that aggregations of juveniles were completely missed by the mid-water trawl survey. The degree to which aggregations of juveniles were sampled more than once in a sampling month is not known.

Variation in age estimates undoubtedly produced back-calculated spawning-dates that did not match exactly with true spawning dates. Yet, for some spawning events, very good matches between back-calculated and reported spawning events indicate that the age estimations were accurate for many of the cohorts examined (O'Farrell, 2001). Other cohorts that did not match as well with reported spawnings may be the result of 1) a spawning event undetected by the spawn-deposition study, 2) a small, "spot" spawning that did not qualify as a true spawning event for the spawn-deposition study, or 3) very slow or fast growth through a portion of the larval life history that interrupted daily increment deposition (McGurk, 1984b, 1987).

Increased survival did not occur throughout the entire 2000 spawning season. Instead, periods of good survival and poor survival were present, yet the

periods of good survival in 2000 led to a much stronger year class than that of 1999. Detecting a "match" of favorable conditions that led to recruitment success was not possible in our study because of the myriad factors that can determine recruitment success. Rather than attempting to explain the observed survival differences with specific mechanisms, we suggest what may possibly contribute to the observed patterns.

Larval survival

The degree to which larval survival depends upon biotic or abiotic factors is difficult to estimate. Fox (2001) presented data showing that year-class strength in the Blackwater stock of Atlantic herring (*Clupea harengus* L.) was determined by survival after the egg stage. However, it is not clear whether variation in survival was due to density-dependent or environmental factors. A recent study has shown that salinity can affect larval survival after hatching in San Francisco Bay herring (Griffin et al., 2004). Here, the salinity during embryonic development was a factor in yolksac larval survival in different salinity treatments. Regardless of the form of mortality operating on larvae, small changes in larval growth rate can lead to large changes in levels of recruitment (Houde, 1987). Faster larval growth results in shorter larval stage duration and thus decreased exposure to the characteristically high mortality of the larval stage. Age at size for herring in this study decreased significantly as the spawning season progressed both in 1999 and 2000. From this finding, we infer that positive changes in growth rate occurred during the spring and summer. Seasonal positive shifts in growth have also been observed in Pacific herring populations in Prince William Sound, Alaska, between the months of June and October (Stokesbury et al., 1999).

In 1999, the greatest number of recruits came from mid to late-season spawning events. The late February to early March spike in recruitment (Fig. 4A) may be partially explained by within-year growth variation. This group of survivors appeared to be derived from a relatively small number of eggs. Recruits from that spawning period grew significantly faster than recruits from earlier spawning events. The largest spawning events of the 1998–99 spawning season produced recruits that grew slower than the recruits spawned in early March and thus may have experienced lower relative survival.

Within-year growth rate variation also partially explains the 2000 year class. The 2000 year class was dominated by late season recruitment, primarily from spawning in February 2000. Herring from spawning events occurring between late October 1999 and mid-January 2000 had a significantly higher median age at length than herring produced from subsequent spawning times. This slow growth may in part explain the near lack of recruitment from the two highest magnitude spawns occurring from 1 to 3 Jan 2000 and from 19 to 24 Jan 2000. However, age at length decreased (and thus growth rate increased) for spawning events occurring from late January 2000 to early March 2000.

The timing of the growth rate switch (from slow to fast) coincided closely with the spawning period producing the greatest amount of recruitment. The general trend of high levels of recruitment from late season spawning events indicates that increased growth rate played a role in the good survival during this period. However, recruitment from very early spawning events and the small number of recruits resulting from late March 2000 spawning was not explained solely by this within-year growth variation.

Egg mortality

Variation in mortality during the egg stage may also affect recruitment in San Francisco Bay herring. Fertilization, embryonic development, and hatching success of Pacific herring are strongly tied to environmental conditions (Alderdice and Velsen, 1971; Griffin et al., 1998). The optimal range for fertilization and development of the San Francisco Bay population is between 12 ppt and 24 ppt, and both percent fertilization and percent hatching is maximized at 16 ppt (Griffin et al., 1998). The herring spawning season in San Francisco Bay is a time of rapidly changing salinities. High salinities generally persist through the fall months. In winter, rapid decreases in salinity due to freshwater from the San Joaquin–Sacramento Delta, storm drain runoff and local creek purges (Oda³) are common, yet the magnitude varies between years (Conomos et al., 1985). In the two years examined, salinity during the winter spawning season varied both above and below the optimum range determined by Griffin et al. (1998). These salinity fluctuations could have a large effect on the supply of larvae into the San Francisco Bay system.

Mortality during the egg stage can be exceedingly high in Pacific herring due to predation and other biotic interactions (Alderdice and Velsen, 1971; McGurk, 1986; Rooper et al., 1999; Bishop and Green, 2001). As a result, egg incubation time may have a significant effect upon eventual recruitment. The length of times of egg incubation and the yolksac larval stage were combined in our study and the combined period was given a constant value of 14 days. In actuality, egg incubation time (Taylor, 1971; McGurk, 1987) and embryonic development (Alderdice and Velsen, 1971; Griffin et al., 1998) are strongly linked to environmental factors and likely have a significant effect upon recruitment before growth rates can determine survival. Analysis of egg incubation and yolksac larval duration for separate cohorts was not performed in our study. It may, however, play a large role in larval abundance.

Conclusion

The 1999 and 2000 spawning-date distributions indicate that year classes can be shaped by periods of good and

³ Oda, K. 2000. Personal commun. Calif. Dep. Fish and Game, 411 Burgess Dr., Menlo Park, CA 94025.

poor survival lasting shorter than the duration of the spawning season, yet longer than the duration of an individual spawning event. The distributions indicated that variation in survivorship was not only a function of individual spawn success. Rather, periods of good and poor survivorship in 1999 and 2000 were of longer duration than one spawning event. The period of exceptionally good survival that led to the majority of the strong 2000 year class was approximately one month in duration and incorporated several spawning events. Yet this window of good survival was much shorter than the entire 2000 spawning season. Variation in survivorship between individual spawnings may be less important in shaping the year class than survivorship variation on a longer time scale.

Visual examination of the spawning-date distribution superimposed upon juvenile age at length indicate that faster growth had a positive effect on recruitment in 2000, and a negligible effect in 1999. For larval growth to affect recruitment, larvae must be available from hatching eggs. Year-class strength variation in Pacific herring could depend upon both egg and larval survival.

The timing of peak herring spawning in San Francisco Bay may be a tradeoff between maximizing larval growth rates and spawning when hydrographic conditions are optimal for embryonic development. In the two years examined, growth rate increased with the progression of the spawning season. It follows that the herring population could maximize recruitment by spawning later so that larvae grow faster. However, because delta outflow is generally high in February and March on account of winter storms, late season spawning may expose eggs to low salinities and thus decreased hatching rates. Peak spawning may occur in January as a trade off between growth-rate and egg-hatching success.

Acknowledgments

This research would not have been possible without the extensive cooperation of the California Department of Fish and Game Belmont and Stockton offices. In particular, we would like to thank Diana Waters, Ken Oda, Sara Peterson, Kathy Hieb, Kevin Fleming, Tom Greiner, Suzanne Deleon, and the entire crew of the RV *Longfin*. Stephen Bollens, Steven Obrebski, Ken Oda, and three anonymous reviewers provided very helpful comments on various drafts of this manuscript.

Literature cited

- Alderdice, D. F., and F. P. J. Velsen.
1971. Some effects of salinity and temperature on early development of Pacific herring (*Clupea harengus pallasi*). J. Fish. Res. Board Can. 28:1545-1562.
- Baxter, R., K. Hieb, S. DeLeon, K. Fleming, and J. Orsi.
1999. Report on the 1980-1995 fish, shrimp and crab sampling in the San Francisco estuary. Technical Report 63, California Department of Fish and Game, Stockton, CA.
- Beamish, R. J., and D. A. Fournier.
1981. A method for comparing the precision of a set of age determinations. Can. J. Fish. Aquat. Sci. 38:982-983.
- Bishop, M. A., and P. G. Green.
2001. Predation on Pacific herring (*Clupea pallasi*) spawn by birds in Prince William Sound, Alaska. Fish. Oceanogr. 10(suppl. 1):149-158.
- Bollens, S. M., B. W. Frost, H. R. Schwanager, C. S. Davis, K. J. Way, and M. C. Landsteiner.
1992. Seasonal plankton cycles in a temperate fjord and comments on the match-mismatch hypothesis. J. Plankton Res. 14:1279-1305.
- Conomos, T. J., R. E. Smith, and J. W. Gartner.
1985. Environmental setting of San Francisco Bay. Hydrobiologia 129:1-12.
- Cushing, D. H.
1975. Marine ecology and fisheries. Cambridge Univ. Press, Cambridge, UK.
1996. Toward a science of recruitment in fish populations. Excell. Ecol. 7, 175 p.
- Fogarty, M. J., M. P. Sissenwine, and E. B. Cohen.
1991. Recruitment variability and the dynamics of exploited marine populations. Trends Ecol. Evol. 6: 241-246
- Fox, C. J.
2001. Recent trends in stock-recruitment of Blackwater herring (*Clupea harengus* L.) in relation to larval production. ICES J. Mar. Sci. 58:750-762.
- Fox, D. A.
1997. Otolith increment analysis and the application toward understanding recruitment variation in Pacific hake (*Merluccius productus*) within Dabob Bay, WA. M.S. thesis, 73 p. Univ. Washington, Seattle, WA.
- Geffen, A. J.
1982. Otolith ring deposition in relation to growth rate in herring (*Clupea harengus*) and Turbot (*Scophthalmus maximus*) larvae. Mar. Biol. 71:317-326.
- Griffin, F. J., M. R. Brenner, H. M. Brown, E. H. Smith, C. A. Vines, and G. N. Cherr.
2004. Survival of Pacific herring larvae is a function of external salinity. In Early life history of fishes in the San Francisco Estuary and watershed (F. Feyrer, L. R. Brown, R. L. Brown, and J. J. Orsi, eds.), p. 37-46. Am. Fish. Soc. Symp. 39, Bethesda, MD.
- Griffin, F. J., M. C. Pillai, C. A. Vines, J. Kaaria, T. Hibbard-Robbins, R. Yanagimachi, and G. N. Cherr.
1998. Effects of salinity on sperm motility, fertilization, and development in the Pacific herring, *Clupea pallasi*. Biol. Bull. 194:25-35.
- Hay, D. E.
1985. Reproductive biology of Pacific herring (*Clupea harengus pallasi*). Can. J. Fish. Aquat. Sci. 42(suppl. 1):111-126.
- Hjort, J.
1914. Fluctuations in the great fisheries of northern Europe viewed in light of biological research. Rapp. P.V. Reun. Cons. Int. Explor. Mer 20:1-228.
- Houde, E. D.
1987. Fish early life dynamics and recruitment variability. Am. Fish. Soc. Symp. 2:17-29.
1989. Sublethals and episodes in the early life of fishes. J. Fish Biol. 35(suppl. A):29-38.

- Iles, T. D. and M. Sinclair.
1982. Atlantic herring: stock discreteness and abundance. *Science* 215(5):627-633.
- Lasker, R.
1975. Field criteria for survival of anchovy larvae: the relation between inshore chlorophyll maximum layers and successful first feeding. *Fish. Bull.* 73:453-462.
- McGurk, M. D.
1984a. Ring deposition in the otoliths of larval Pacific herring, *Clupea harengus pallasii*. *Fish. Bull.* 82: 113-120.
1984b. Effects of delayed feeding and temperature on the age of irreversible starvation and on the rates of growth and mortality of Pacific herring larvae. *Mar. Biol.* 84:13-26.
1986. Natural mortality rates of marine pelagic fish eggs and larvae: role of spatial patchiness. *Mar. Ecol. Prog. Ser.* 34:227-242.
1987. Age and growth of Pacific herring based on length-frequency analysis and otolith ring number. *Env. Biol. Fish.* 20(1):33-47.
- Methot, R. D., Jr.
1983. Seasonal variation in survival of larval northern anchovy, *Engraulis mordax*, estimated from the age distribution of juveniles. *Fish. Bull.* 81:741-750.
- Moksness, E., and P. Fossum.
1992. Daily growth rate and hatching-date distribution of Norwegian spring-spawning herring (*Clupea harengus* L.). *ICES J. Mar. Sci.* 49:217-221.
- Moksness, E., and V. Westestad.
1989. Ageing and back-calculating growth rates of Pacific herring, *Clupea pallasii*, larvae by reading daily otolith increments. *Fish. Bull.* 87(3):509-513.
- O'Farrell, M. R.
2001. Year class formation of Pacific herring in San Francisco Bay. M.A. thesis, 73 p. San Francisco State Univ., San Francisco, CA.
- Rice, J. A., L. B. Crowder, and M.E. Holey.
1987. Exploration of mechanisms regulating larval survival in Lake Michigan bloater: a recruitment analysis based on characteristics of individual larvae. *Trans. Am. Fish. Soc.* 116:703-718.
- Rooper, C. N., L. J. Haldorson, and T. J. Quinn II.
1999. Habitat factors controlling Pacific herring (*Clupea pallasii*) egg loss in Prince William Sound, Alaska. *Can. J. Fish. Aquat. Sci.* 56:1133-1142.
- Sinclair, M., and T. D. Iles.
1985. Atlantic herring (*Clupea harengus*) distribution in the Gulf of Maine-Scotian Shelf area in relation to oceanographic features. *Can. J. Fish. Aquat. Sci.* 42:880-887.
- Spratt, J. D.
1981. Status of the Pacific herring, *Clupea harengus pallasii*, resource in California 1972 to 1980. *Cal. Dep. Fish and Game, Fish. Bull.* 171, 107 p.
- Stokesbury, K. D. E., R. L. Foy, and B. L. Norcross.
1999. Spatial and temporal variability in juvenile Pacific herring, *Clupea pallasii*, growth in Prince William Sound, Alaska. *Environ. Biol. Fish.* 56:409-418.
- Stokesbury, K. D. E., J. Kirsch E. V. Patrick, and B. L. Norcross.
2002. Natural mortality estimates of juvenile Pacific herring (*Clupea pallasii*) in Prince William Sound, Alaska. *Can. J. Fish. Aquat. Sci.* 59:416-423.
- Takahashi, I., K. Azuma, H. Hiroyuki, and F. Shinji.
1999. Different mortality in larval stage of Ayu *Plecoglossus altivelis* by birth dates in the Shimanto estuary and adjacent coastal waters. *Fish. Sci.* 65(2):206-210.
- Taylor, F. H. C.
1971. Variation in hatching success in Pacific herring (*Clupea pallasii*) eggs with water depth, temperature, salinity, and egg mass thickness. *Rapp. P.-V. Reun. Cons. Perm. Int. Explor. Mer* 160:128-136.
- Thorisson, K.
1994. Is metamorphosis a critical interval in the early-life of marine fishes? *Environ. Biol. Fish.* 40:23-36.
- Vines, C. A., T. Robbins, F. J. Griffin, and G. N. Cherr.
2000. The effects of diffusible creosote-derived compounds on development in Pacific herring (*Clupea pallasii*). *Aquat. Toxicol.* (NY) 51:225-239.
- Watters, D. L., H. M. Brown, F. J. Griffin, E. J. Larson, and G. N. Cherr.
2004. Pacific herring *Clupea pallasii* spawning grounds in San Francisco Bay: 1973 to 2000. *In* Early life history of fishes in the San Francisco Estuary and watershed (F. Feyrer, L. R. Brown, R. L. Brown, and J. J. Orsi, eds.), p. 3-14. *Am. Fish. Soc. Symp.* 39, Bethesda, MD.
- Yoklavich, M. M., and K. M. Bailey.
1990. Hatching period, growth and survival of young wall-eye pollock *Theragra chalcogramma* as determined from otolith analysis. *Mar. Ecol. Prog. Ser.* 64:13-23.

Abstract—Diet analysis of 52 loggerhead sea turtles (*Caretta caretta*) collected as bycatch from 1990 to 1992 in the high-seas driftnet fishery operating between lat. 29.5°N and 43°N and between long. 150°E and 154°W demonstrated that these turtles fed predominately at the surface; few deeper water prey items were present in their stomachs. The turtles ranged in size from 13.5 to 74.0 cm curved carapace length. Whole turtles ($n=10$) and excised stomachs ($n=42$) were frozen and transported to a laboratory for analysis of major faunal components. Neustonic species accounted for four of the five most common prey taxa. The most common prey items were *Janthina* spp. (Gastropoda); *Carinaria cithara* Benson 1835 (Heteropoda); a chondrophore, *Veleva veleva* (Hydrodia); *Lepas* spp. (Cirripedia), *Planes* spp. (Decapoda: Grapsidae), and pyrosomas (*Pyrosoma* spp.).

Diet of oceanic loggerhead sea turtles (*Caretta caretta*) in the central North Pacific

Denise M. Parker

Joint Institute for Marine and Atmospheric Research
8604 La Jolla Shores Drive
La Jolla, California 92037
Present address: Northwest Fisheries Science Center
National Marine Fisheries Service, NOAA
Newport, Oregon 97365-5275

E-mail address: Denise.Parker@noaa.gov

William J. Cooke

AECOS, Inc.
970 N. Kalaheo Avenue, Suite C311
Kailua, Hawaii 96734

George H. Balazs

Pacific Islands Fisheries Science Center, Honolulu Laboratory
National Marine Fisheries Service
2570 Dole Street
Honolulu, Hawaii 96822-2396

Loggerhead sea turtles are circum-global, inhabiting temperate, subtropical, and tropical waters of the Atlantic, Pacific, and Indian Oceans. In the Pacific, loggerhead sea turtles have been found in nearshore waters of China, Taiwan, Japan, Australia, and New Zealand and are seen in offshore waters of Washington, California, and northwestern Mexico (Dodd, 1988; Pitman, 1990). Nesting in the North Pacific Ocean occurs in Japan; there is no known nesting in the eastern North Pacific (Márquez and Villanueva, 1982; Frazier, 1985; Bartlett, 1989). Trans-Pacific migrations of juveniles have been documented from mitochondrial DNA analyses of individuals found feeding off Baja California. Bowen et al. (1995) identified these Baja sea turtles as originating from Japanese rookeries, although a small percentage come from Australia. Recent research indicates that all loggerhead sea turtles found in the oceanic realm of the central North Pacific Ocean are of Japanese stock (Dutton et al., 1998). Tagging studies in Japan and the Eastern Pacific also demonstrate transpacific migrations of loggerhead sea turtles between the

east and west Pacific (Balazs, 1989; Resendiz et al., 1998; Uchida and Teruya¹).

Recent oceanic satellite tracking studies of loggerhead sea turtles indicate that they are active in their oceanic movements. These turtles follow subtropical fronts as they travel toward Japan from east to west across the Pacific Ocean, often swimming against weak geostrophic currents (Polovina et al., 2000; Polovina et al., 2004). One hypothesis discussed in Polovina et al. (2000; 2004) suggests that this species obtains prey items from the subtropical fronts along which they travel. A sharp gradient in surface chlorophyll is observed along the main frontal area where these turtles are commonly encountered. This frontal area, the transition zone chlorophyll front

¹ Uchida, S., and H. Teruya. 1991. A) Transpacific migration of a tagged loggerhead, *Caretta caretta*. B) Tag-return result of loggerhead released from Okinawa Islands, Japan. In International symposium on sea turtles '88 in Japan (I. Uchida, ed.), p. 169–182. Himeji City Aquarium, Tegarayama 440 Nishinobusue, Himeji-shi, Hyogo 670, Japan.

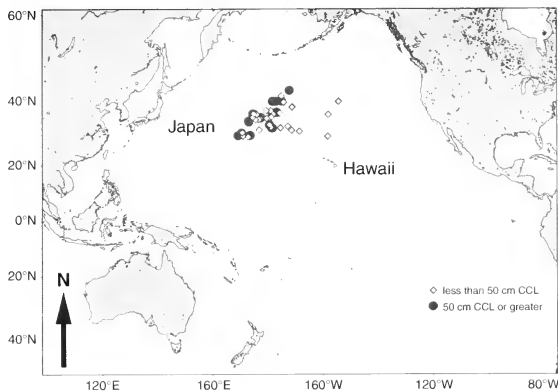


Figure 1

Distribution of loggerhead sea turtles (*Caretta caretta*) incidentally captured in the international high seas driftnet fishery in the central North Pacific Ocean. Turtles smaller than 50 cm curved carapace length (CCL) are shown as open diamonds and those larger than 50 cm CCL are shown as black circles.

(TZCF), is an area of concentrated phytoplankton that also collects and attracts a variety of neustonic and oceanic organisms—many of which may be potential prey times, as well as predators, of oceanic-stage loggerhead sea turtles in the Pacific. Polovina et al. (2000, 2004) have suggested that the turtles are foraging along the TZCF.

The duration of the juvenile oceanic stage for loggerhead sea turtles in the Pacific is currently unknown. In the Atlantic, juvenile turtles inhabit the oceanic zone for approximately 10 years (Bjorndal et al., 2000). Based on growth analyses (Zug et al., 1995; Chaloupka, 1998), it is probable that this sea turtle from the Pacific can have a similar extended oceanic stage, which in some cases may last until sexual maturity (30+ years).

Understanding the diets of sea turtles is important for their conservation. Foraging studies have been done with oceanic-stage turtles in the Atlantic (Van Nierop and den Hartog, 1984). However, there is a paucity of information regarding the foraging ecology of oceanic-stage loggerhead sea turtles in the Pacific. Such information can help identify important food resources and foraging areas necessary for guiding decisions regarding the management of endangered sea turtle populations (Bjorndal, 1999). The objective of the present study is to determine the diet composition of loggerhead sea turtles from the central North Pacific Ocean and to discuss the possibility of interactions between these turtles and commercial fisheries that may occur as a result of the foraging behavior of these sea turtles.

Method

National Marine Fisheries Service (NMFS) observers between 1990 and 1992 obtained 52 dead loggerhead sea turtles. These specimens were taken as bycatch in the international high-seas driftnet fishery, which targeted squid and albacore (Wetherall et al., 1993). NMFS observers recorded capture position and sea surface temperature aboard commercial driftnet vessels. Samples were collected between latitude 29.5°N and 43°N and longitude 150°E and 154°W (Fig. 1). A total of 10 whole specimens and 42 excised stomachs were frozen and transported to a Honolulu laboratory for analysis. Stomachs were removed from whole specimens and all stomachs were examined from anterior to posterior. Gross observations of stomach contents were made and the contents were sorted to the lowest identifiable taxonomic level by using a dissecting microscope. Major fauna were identified, quantified by volume, and the percent contribution (to stomach contents) of each major organism was calculated (Forbes, 1999). Presence of jellyfish or other jellies were identified by presence of tentacles, nematocysts, and whole or partial individuals. *Planes* spp. were identified from descriptions of Spivak and Bas (1999). Frequency of occurrence of major components was calculated by dividing the number of stomachs in which the prey item occurred by the total number of turtle stomachs examined. Percent sample volume was calculated for all prey items by summing the total volume of each prey item and dividing it by the total volume of all

prey collected. Summing the total volume of each prey item and dividing it by the total stomach volume for those samples, where the prey item was present, yielded the mean percent volume. Regression analysis was done to determine if any correlation existed between sea surface temperature, sample volume, and size of turtle.

Results

Loggerhead sea turtles collected in our study were found widely distributed over the central North Pacific Ocean and there was no apparent difference in distribution

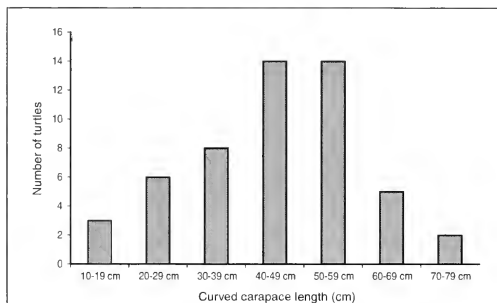


Figure 2

Size distribution for the 52 loggerhead sea turtles (*Caretta caretta*) obtained as samples in the high-seas driftnet fishery. Sizes were grouped into 10-cm size classes.

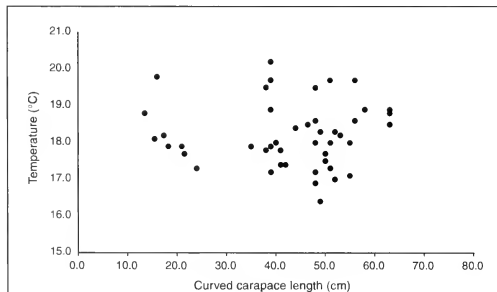


Figure 3

Relationship between curved carapace length (CCL, cm) of loggerhead sea turtles (*Caretta caretta*) and sea surface temperature (SST, $n=52$).

between size classes (Fig. 1). The turtle specimens ranged from 13.5 cm to 74.0 cm curved carapace length (CCL, Fig. 2); the mean was 44.8 [± 14.5] cm CCL. Figure 2 shows the distribution of turtles in each 10-cm size class. Sea surface temperatures in the area of capture ranged from 16° to 20°C. There was no correlation between size of turtle and sea surface temperature in the area of capture ($F=0.58$, $r^2=0.01$, Fig. 3).

All 52 stomachs examined contained prey items; the level of fill varied from 6 mL to 1262 mL. Items found in the anterior portion of the stomach were the most identifiable and contents varied between turtles. Unidentifiable remains were located mainly in the posterior end of the stomach or the intestines if a whole gastrointestinal tract was analyzed. Only one of the samples analyzed included an entire gastrointestinal tract.

A taxonomic listing of diet items identified for the loggerhead sea turtles of the central North Pacific is shown in Table 1 along with frequency of occurrence and mean percent sample volume of each prey item. The six most common (frequent) prey items were identified. These included *Janthina* spp., which occurred in 75% of samples, and *Planes* spp., which occurred in 56% of samples. *Lepas* spp. occurred in 52% of the samples, and *Carinaria cithara* was found in 50% of samples. *Velevella velevella*, was found in 25% of the samples, and pyrosomas were found in 21% of samples (Table 1). Other common food items found in stomachs were fish eggs (25% of stomachs), salps, amphipods (46% of stomachs), small fish, and plastic items (35% of stomachs, Table 1). Some plastic items included small plastic beads, thin plastic sheets, polypropylene line, and even a small plastic fish, which had been an individual soy sauce container. Although *Velevella*, pyrosomas, and salps were represented as prey items in our samples, other types of jellies may not have been well represented because their soft bodies may dissolve more quickly in stomach acids. It is also possible that unidentified jellies may comprise the unidentified remains, which occurred in 71% of stomachs and comprised 13.8% of total sample volume; however, a portion of the unidentified remains were likely masticated portions of identified prey items. Table 2 shows the mean percent prey item volumes for the six most common prey items. The six most common prey items can be ranked from largest to smallest mean volumes in

Table 1

Percent occurrence and percentage of total sample volume (volume of prey for all stomachs combined) for prey items (listed to lowest taxonomic order) found in loggerhead sea turtles (*Caretta caretta*, $n=52$ turtles).

Prey group	Occurrence (%)	Percent volume (%)
<i>Carinaria cithara</i> Benson 1835	50.0	43.8
<i>Janthina</i> spp. (includes <i>J. janthina</i> and <i>J. prolongata</i> = <i>J. globosa</i>)	75.0	14.4
<i>Lepas</i> spp. (includes <i>L. anserifera</i> Linnaeus 1767 and <i>L. anatifera</i> Linnaeus 1758)	51.9	6.7
<i>Veleva veleva</i> Linnaeus 1758 (by-the-wind-sailor)	25.0	10.6
<i>Planes</i> spp. Dana 1852	55.8	1.2
<i>Pyrosoma</i> spp.	21.0	3.4
Fish eggs (<i>Hirundichthys speculiger</i> and unidentified spp.)	25.0	1.9
Cephalopoda (squid and octopus fragments and paralarvae)	21.2	0.5
Debris (plastic, styrofoam, paper, rubber, polypropylene, etc.)	34.6	0.3
Debris (wood, bird feathers)	11.5	<0.1
Salpidae	13.5	0.5
Family Sternoptychidae (hatchetfish)	7.7	0.1
<i>Electrona</i> sp.—Myctophidae	1.9	0.1
Gammaridea and Hyperidea amphipods	46.2	<0.1
Thecosomate pteropods	13.5	<0.1
<i>Cavolinia globulosa</i> (Gray 1850)	11.5	<0.1
POLYCHAETA (polychaete worms)—Alciopidae	5.8	<0.1
ISOPODA	3.8	<0.1
MYSIDACEA—mysid	3.8	<0.1
<i>Creseis</i> sp.	1.9	<0.1
PHAEOPHYTA (brown algae)— <i>Cystoseira</i> sp.	1.9	<0.1
EUPHAUSIACEA—euphausiid	1.9	<0.1
Unidentified tunicate spp.	13.5	1.0
Unidentified jellies	13.5	0.5
Unidentified crustaceans	5.8	0.5
Unidentified remains	71.2	13.8

the following order: 1) *Carinaria cithara*, 2) *Pyrosoma* spp., 3) *Janthina* spp., 4) *Veleva veleva*, 5) *Lepas* spp., and 6) *Planes* spp.

Mean sample volume was 370.2 [± 319.4] mL. Size of loggerhead sea turtles did not influence the volume of prey items for turtle sizes 35–70+ cm ($F=0.11$, $r^2=0.05$). However, the smaller turtles did have smaller volumes of prey items present in their stomachs, because all turtles 13–34 cm had less than 80 mL total stomach volume (Fig. 4). The size of the turtle did not appear to be a factor in the type of prey ingested. The one exception may be *Veleva veleva*. Turtles smaller than 30 cm CCL in our sample did not ingest this prey item, albeit sample size for less than 30-cm turtles was relatively small compared to the number of 40- and 50-cm size class turtles (Fig. 2); therefore, this apparent trend may not be the case for the general population.

Of the six most common prey items, *Carinaria cithara* had the highest percent sample volume, 43.8% of total sample volume. In general, percent volumes of *C. cithara* were high; 20 of the 27 turtle stomachs

Table 2

Mean percent volume and percent volume ranges for the six most frequently observed prey items found in driftnet captured loggerhead sea turtles (*Caretta caretta*).

Prey item	Mean percent volume	Standard deviation (\pm)	Range
<i>Janthina</i> spp.	30.7%	34.8%	1–97%
<i>Carinaria cithara</i>	52.8%	33.1%	1–98%
<i>Lepas</i> spp.	19.1%	24.7%	1–99%
<i>Veleva veleva</i>	22.7%	29.4%	1–84%
<i>Planes</i> spp.	5.6%	10.1%	1–38%
<i>Pyrosoma</i> spp.	44.7%	33.7%	1–88%

had percent volumes greater than 30% with this prey item and a number of stomachs had percent volumes greater than 90%. *Janthina* spp. had the next highest

percent sample volume at 14.4%. The percent volume of *Janthina* was generally high; 15 of 37 turtle stomachs had greater than 30% volume of this species. Only 4 of the 13 stomachs with *Velella velella* had greater than 30% sample volume; yet *Velella* made up almost 11% of total sample volume, and one of the stomach samples was almost entirely filled (84% volume) with *Velella* prey. In the samples that contained pyrosomas, this prey item often comprised a high percent of the total gut content—up to 88% stomach volume—and 7 out of 11 stomachs had greater than 30% stomach volume of pyrosomas. *Planes* spp. comprised more than 30% of stomach volume in only 2 of the 29 stomachs containing this species. *Lepas* spp. often occurred in very high percent volumes (up to 99% of total gut content in one sample), although only 6 of 21 stomachs had percent volumes greater than 30% for *Lepas*.

Discussion

Prey items

Loggerhead sea turtles in North Pacific oceanic habitats are opportunistic feeders that ingest items floating at or near the surface. Availability of prey in the oceanic realm is generally characterized as patchy. This means that the majority of the ocean contains little to no forage, but in some areas high densities of prey can be found. This unpredictability of prey availability likely contributes to the opportunistic feeding behavior of the loggerhead sea turtle. The TZCF, an area of convergence created within the subtropical frontal zone by cooler denser water masses converging and sinking below warmer lighter water masses (Roden, 1991), may serve to help concentrate different prey items. Prey items such as *Velella* can often concentrate in large numbers in such areas (Evans, 1986). All size classes of this sea turtle

collected in our study were found between 16° and 21°C (Fig. 3), which typically are the temperatures that define the subtropical frontal zone and TZCF (Roden, 1991). Eighty-three percent of prey items that were recorded were found floating on the surface or were found on floating objects and would also likely be concentrated at convergent fronts such as the TZCF, driven there by the currents and winds (Polovina, et al., 2000; Polovina et al., 2004). It is suggested that this concentration of prey, along the convergent fronts, may be aggregating the loggerhead sea turtles traveling along this area, which are likely foraging on the increased densities of prey (Polovina et al., 2003a). Turtles in our study smaller than 30-cm CCL had very low volumes of prey in their stomachs. It is unknown whether the paucity of prey items in these turtle stomachs was related to the individual's size, e.g. they were physically not able to capture or ingest certain types of prey items, or perhaps to a lack of experience in foraging due to youth, given that turtles in this size range were determined to be between 1 and 4 years of age by Zug et al. (1995), or to other mitigating factors.

Another indication that loggerhead sea turtles are opportunistic feeders is the presence of oceanic, mesopelagic fish as prey items. The total number of fish (lanternfish and hatchfish) in the samples was low (only 0.1 % of total stomach volume). These species of fish tend to stay below the photic zone usually at depths greater than 300 m during the day and migrate up near the surface at night. Lanternfish make diel vertical migrations where they reach maximum densities at 100 m at night. During nightly movements some species can also come directly to the surface (Hulley, 1990). Some species of hatchfish also make diel vertical migrations, which would bring them to within 100 m of the surface at night (Weitzman, 1986; Froese and Pauly, 2003). Because of the low numbers, it is likely that loggerhead sea turtles ingest only dead or debilitated fish rather than actively hunt and chase such species. The presence of these species also indicates that the turtles may be feeding at night when they would be more likely to encounter the fish during their diel movement. Another prey item exhibiting diel vertical migration is the pyrosomas. Pyrosomas, which are a part of Pacific leatherback sea turtle diets (Davenport and Balazs, 1991), were also present in loggerhead sea turtle stomach samples. Pyrosomas are colonial tunicates comprising individual zooids embedded in the walls of a gelatinous tube. These colonies can become quite large (some greater than 4 meters in length) and tend to drift with ocean currents and accumulate along frontal zones which make them accessible to the sea turtle that forages opportunistically. In at least one species (*P. atlanticum*) has been recorded to stay below 300 m during the

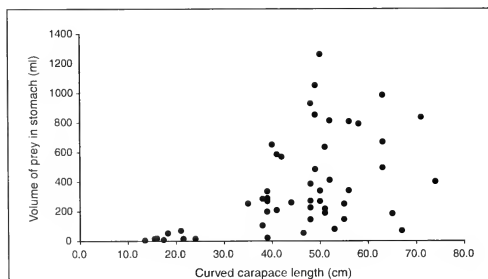


Figure 4

Relationship between curved carapace length (CCL, cm) of loggerheads (*Caretta caretta*) and stomach volume (mL, n=52)

day and move up near the surface at night (Andersen and Sardou, 1994); this activity again may indicate active night foraging by the loggerhead sea turtle.

Loggerhead sea turtles may feed by swallowing floating prey whole and also by biting whole prey (or portions off a whole prey) found on large floating objects. A commonly ingested prey item, *Veleva veleva*, known as "by-the-wind-sailor" (Eldredge and Devaney, 1977), typically was found intact. *Janthina* spp., predatory gastropods whose main prey item is *Veleva veleva*, were also frequently found whole in stomachs. Small *Janthina* spp. have been observed directly on *Veleva*, and it has been hypothesized that *Janthina* use *Veleva* to settle on and use the *Veleva* as floatation until they become too large for the host (Bayer, 1963). This behavior may be a reason why whole *Janthina* and *Veleva* were often found together in stomach samples. *Janthina* spp. had been previously noted as a prey item of loggerhead sea turtles in the Azores and South Africa (Dodd, 1988) but was first identified as a prey item in the Pacific Ocean in a preliminary unpublished report by Cooke in 1992—data that are included in the present study. The high frequency of occurrence of *Veleva veleva* and whole *Janthina* spp. support the hypothesis that loggerhead sea turtles will feed on the surface, swallowing their prey whole. Distribution of *Veleva veleva* is patchy; densities range from $<1/1000\text{ m}^3$ to $1000/1000\text{ m}^3$ and densities of *Janthina* spp. are considerably less than those of *Veleva*. When optimum combinations of prevailing winds and currents converge, densities of *Veleva veleva* have been observed to be in concentrations upward of $10,000/1000\text{ m}^3$, forming patches so large and dense they have been likened to oil tanker sludge by mariners (Evans, 1986; Parker, personal observ.). It is possible that the one turtle that had a stomach volume of 84% *Veleva* found one of these patches on which to feed. *Veleva veleva* was the one common prey item that was not found in stomachs of turtles less than 30-cm CCL. Because *Veleva* were commonly swallowed whole, it is possible that an average size *Veleva*, which range from 5 to 10 cm (Evans, 1986), might have been too large for a 13–29 cm CCL turtle to swallow whole.

The epibiotic oceanic crabs and the gooseneck barnacles (*Lepas* spp.) usually occur on floating objects; *Planes* sometimes even rides on *Veleva* (Chace, 1951). *Planes* spp. also have been observed and collected from the tail area of loggerhead sea turtle themselves (Dav-enport, 1994; NMFS observers³). Although approximately 80% of stomach samples with *Planes* spp. contained whole crabs, which were identified as *P. cyaneus*, there

were also numerous masticated crabs and pieces of crabs. These pieces could have been *P. marinus* because whole specimens are necessary to identify *Planes* spp. (Spivak and Bas, 1999); therefore the lowest taxonomic identification for this study was limited to *Planes* spp. Densities of *Planes* spp. and *Lepas* spp. are not well documented but are likely limited by the amount of substrate on which they can settle or on the amount of floating objects available. Natural drifting objects such as tree logs or pumice from volcanic eruptions have been documented since the nineteenth century (Kew, 1893, cited in Jokiel, 1990). The "floating islands," as they have been called, continue to be important for transporting organisms, from corals to reef fish across the oceans (Jokiel, 1990). Man-made objects also supply substrate and habitat on which different organisms can settle. Buoys and logs that wash ashore often have *Lepas* spp. attached to them, some with *Lepas* spp. covering 100% of the area that was underwater (Parker, personal observ.). Although the frequency of occurrence of *Planes* spp. in stomach samples was high, the percent sample volume of *Planes* was relatively low (1.2% total volume) and the mean volume of *Planes* found was also low (5.6%, Table 2), indicating that this prey was either taken opportunistically or accidentally. It is not known whether the *Planes* were ingested along with other prey items or were actually grazed from larger floating objects. In contrast, *Lepas* spp. often occurred in very high percent volumes, indicating that the turtles were actively grazing these prey. The constant presence of *Lepas* spp. in samples strongly supports the hypothesis that loggerhead sea turtles feed not only by swallowing prey whole, but also by biting prey off larger floating objects. Small chunks of Styrofoam were still attached to the bases of some *Lepas* specimens indicating that the turtle had bitten off some of the floating object itself while grazing on prey found on the floating debris.

Among other floating items that often occurred in the turtles' stomachs, one common element was fish eggs. Some of these fish eggs were identified as *Hirundichthys speculiger* or flying fish eggs. Amphipods were another common item but comprised a very small fraction of total gut content ($<1\%$), indicating that they were not a targeted prey item. Amphipods were possibly ingested incidentally as epiphytes on other items or as part of the gut contents of other prey items. The proportion of man-made drift debris in our sample was low in contrast to prior studies (Balazs, 1985; Allen, 1992; Bjorndal et al., 1994; Kamezaki, 1994; Tomas et al., 2002). Plastics and other man-made debris were commonly found, occurring in about 35% of stomachs, but they comprised a very small fraction of the total gut content ($<1\%$).

Loggerhead sea turtles also actively forage at deeper depths if high densities of prey items are present. An initial study of pelagic dive behavior of this species (Polovina et al., 2003) indicates that they regularly dive down to depths of 100 m and may also forage at those depths, which may account for the high frequency of occurrence and high total percent volume of

² Cooke, W. J. 1992. A taxonomic analysis of stomach contents from loggerhead turtles (*Caretta caretta*). AECOS report no. 697, 12 p. Prepared for NOAA, NMFS, Honolulu Laboratory, 2570 Dole Street, Honolulu, Hawaii 96822. [Available from AECOS, Inc., 45-939 Kamehameha Hwy., Rm. 104, Kaneohe, Hawaii 96744.]

³ NMFS (National Marine Fisheries Service) observers. 1997–2000. Personal commun. Pacific Islands Fisheries Science Center, 2570 Dole Street, Honolulu, HI 96822-2396.

the heteropod *Carinaria cithara*. Okutani (1961) first recorded sea turtles consuming *Carinaria* (including *Carinaria cithara*, Benson 1835), in the western North Pacific. Heteropods are found in the upper photic zone (within 100 m of the surface) but are not typically a neustonic or floating species. Recorded heteropod densities in the Pacific are variable (<1/1000 m³ to 150/1000 m³, Seapy, 1974, cited in Lalli and Gilmer, 1989). Although these densities seem very low, it is clear that in this area of the central North Pacific heteropods are numerous enough within diving depths of loggerhead sea turtles to make this an attractive prey item for the turtles.

Conclusion—Interactions with fisheries

The bycatch of nontargeted species in different fisheries has been an issue for many years (Wetherall et al., 1993; Wetherall, 1996; Gardner and Nichols, 2001; Suganuma⁴). Bycatch of sea turtles has also been an issue for the conservation management of most sea turtle species. Sea turtle mortalities have occurred in nearly all fisheries (gillnet, driftnet, trawl, and longline). During their transpacific migrations loggerhead sea turtles move through areas of multinational longline fishing (Lewison et al., 2004). Mortalities of sea turtles after longline fishery interactions have been estimated between 28% and 50% by both U.S. and Japanese researchers (Nishemura and Nakahigashi, 1990; Kleiber,⁵ McCracken⁶) and loggerhead sea turtles comprise a large percentage of the sea turtle interactions in longline fisheries, as high as 59% of sea turtles captured in the Hawaii-based longline fleet. The longline fishery as well as various other fisheries in the Pacific (Gardner and Nichols, 2001) have been implicated as part of the reason for recent declines in the loggerhead sea turtle populations both in Japan (Kamezaki and Matsui, 1997; Sato et al., 1997; Suganuma⁴) and also in Australia, and southern nesting areas (Limpus and Couper, 1994; Limpus and Reimer⁷). Research on feeding behavior may help with the mitigation of fisheries interactions.

Learning more about the life history of loggerhead sea turtles and understanding more about the movements, foraging behavior, and prey of these turtles are important for making well-informed management decisions because foraging behavior may change as seasons change and as these turtles move through different habitats (Bjorndal, 1997). Although our study indicates that these turtles forage mainly on floating or near-surface prey in the open ocean, studies in different areas show different feeding habits. The oceanic, near-surface feeding behavior of loggerhead sea turtles is likely one reason for the numerous longline fishery interactions in the central North Pacific. The recorded dive data for these turtles indicate that they spend a large percentage of their time near the surface—as much as 78% of their time is spent within 10 m of the surface (Polovina et al., 2003b). Juvenile loggerhead sea turtles are rarely found in the waters adjacent to Japan (Uchida, 1973); the juvenile turtles are thought to use the Kuroshiro Current to move out into the Pacific and the southern edge of the Subarctic Gyre during their eastward movement toward foraging grounds in the Eastern Pacific (Bowen et al., 1995). In the Atlantic, however, small neonate loggerhead sea turtles have been found associated with drifts of floating material, especially *Sargassum* rafts (Witherington, 2002), and although large, regular drifts of floating material are rare in the Pacific, small loggerhead sea turtles may also be associated with floatsam (Pitman, 1990).

Studies have indicated that foraging changes throughout the lifecycle of loggerhead sea turtles (van Nierop and den Hartog, 1984; Plotkin et al., 1993; Godley et al., 1997; Tomas et al., 2001). In the Pacific, oceanic immature turtles (present study) forage on different prey from that foraged by subadults in the pelagic and neritic areas off Baja California (Nichols et al., 2000; Peckham and Nichols, 2003; Seminoff et al., 2004), and adults in benthic neritic habitats, in turn, forage on different prey near Japan and China (Hitase et al., 2002). Japanese loggerhead sea turtles foraging in the Eastern Pacific target *Pleuroncodes planipes*, the pelagic red crab, which occurs year round off Baja California. These turtles interact with the artisanal fisheries in the area which are both pelagic and benthic fisheries (Gomez-Gutierrez and Sanchez-Ortiz, 1997; Bartlett, 1998; Gomez-Gutierrez et al., 2000; Peckham and Nichols, 2003). Loggerhead sea turtles have also been found on the Gulf of California side of Baja California, likely foraging on the large abundance of invertebrate fauna found there (Brusca, 1980), and these turtles face fishing pressure from the artisanal gillnet fishery in this area (Seminoff et al., 2004).

⁴ Suganuma, H. 2002. Population trends and mortality of Japanese loggerhead turtles, *Caretta caretta*, in Japan. In Proc. Western Pacific Sea Turtle Coop. Res. and Mgmt. Workshop (I. Kiman, ed.), p. 74–77. Western Pacific Regional Fishery Management Council, 1164 Bishop Street, Suite 1400, Honolulu, HI 96813.

⁵ Kleiber, P. 1995. Estimating annual takes and kills of sea turtles by the Hawaiian longline fishery, 1991–1997, from observer program and logbook data. Administrative report H-98-08, 21 p. Southwest Fisheries Science Center, Nat. Mar. Fish. Serv., NOAA, 2570 Dole St., Honolulu, HI 96822.

⁶ McCracken, M. L. 2000. Estimation of sea turtle take and mortality in the Hawaiian longline fisheries. Administrative report H-00-06, 29 p. Southwest Fisheries Science Center, Nat. Mar. Fish. Serv., NOAA, 2570 Dole St., Honolulu, HI 96822.

⁷ Limpus, C. J., and D. Reimer. 1994. The loggerhead turtle, *Caretta caretta*, in Queensland: a population in decline. In Proceedings of the Australian marine turtle conservation workshop (R. James, compiler), p. 39–59. Queensland Dep. Environ and Heritage and Aust. Nat. Conserv. Agency, GPO Box 787, Canberra ACT 2601, Australia.

Converting CCL to straight carapace length (SCL; using the conversion equation: $CCL = 1.388 + (1.053) SCL$, in Bjørndal et al., 2000), size classes found in our study ranged from 11.5 cm to 68.9 cm SCL with a mean of 41.2 [±12.4] cm SCL. The East Pacific recruits were slightly larger with means of 46.9–61.9 cm SCL (Seminoff et al., 2004). Most of these turtles were immature to subadult turtles, and only a few were adult-size turtles. According to Zug et al. (1995), the loggerhead sea turtles recruiting to the nearshore and neritic habitats of Baja California are likely 10 years of age or older, indicating that these turtles might spend as many as 10 years before arriving at their East Pacific foraging habitat. After returning to the West Pacific, satellite telemetry has found that adult loggerhead sea turtles also reside in both neritic and pelagic habitats (Baba et al., 1992, 1993; Kamezaki et al., 1997; Sakamoto et al., 1997) putting them at risk of interaction with nearshore gillnet fisheries as well as pelagic longline fisheries. Hitase et al. (2002) found a size difference between adults in neritic and oceanic habitats—the postnesting females that chose oceanic habitats were smaller (mainly <80.0 cm) than those that used neritic habitats for postnesting foraging—and also suggested that some adult turtles may not recruit to neritic areas near Japan and China. This may be evidence that some loggerhead sea turtles remain in the oceanic habitat their whole life cycle, returning nearshore only to mate or nest. In the Atlantic, juveniles as well as adults of this species can be found in neritic foraging habitats of the Gulf of Mexico, and these turtles can have interactions with coastal trawl and other coastal fisheries in the area (Plotkin et al., 1993). Juvenile turtles have also been observed and captured in areas along the eastern coast of the United States where they have been found feeding on benthic invertebrates (Burke et al., 1990; Epperly et al., 1990). Very small, neonate loggerhead sea turtles have been found associating with and foraging in *Sargassum* drifts while they are transported by the Gulf Stream into the mid-Atlantic (Witherington, 2002); therefore, the harvest of *Sargassum* or trawling through this area would affect these juveniles. There is some evidence that juvenile Atlantic loggerhead sea turtles may move between coastal and pelagic forage habitats, which would expose them to both coastal and pelagic fisheries (Witzell, 2002). In the Mediterranean, both juvenile and adult loggerhead sea turtles also have variety of foraging behaviors. In the eastern Mediterranean, postpelagic juveniles and adults forage mainly in neritic habitats on benthic prey items where they would interact with coastal trawl and other artisanal fisheries (Godley et al., 1997). In the western Mediterranean, juvenile turtles of this species forage in both pelagic as well as neritic habitats, where they are at risk of fishery interactions in many different fisheries including longline, trawling, and coastal fisheries (Tomas et al., 2001). Postpelagic juveniles in the Mediterranean may be recruits from the Atlantic Ocean or may come from the endemic Mediterranean population. Adult loggerhead sea turtles have been

noted to also move between the eastern and western basins of the Mediterranean in response to seasonal temperature changes (Bentivegna, 2002). During this migration between two benthic feeding areas, some of the turtles would spend extensive amounts of time in the pelagic habitat likely foraging on pelagic prey items. This intra-Mediterranean movement puts these turtles at risk of interactions with a multinational fishery contingent of pelagic as well as coastal fisheries (Bentivegna, 2002).

One possible way to mitigate increased fisheries interactions in the Pacific and other areas might be to identify specific loggerhead foraging areas for protection, such as the area around Baja California, Mexico. In the central North Pacific, our study (Fig. 1), as well as recent satellite tracking studies of juvenile and adult loggerhead sea turtles (Hitase et al., 2002; Parker et al., 2003; Polovina et al., 2004), has indicated that the area west of and around the Emperor seamounts, between 160° and 180°E might also be an important foraging habitat. Most of the turtles in our study were collected from this area (Fig. 1) and one juvenile spent 10 months west of the Emperor Seamounts, between 160° and 170°E, before its satellite transmitter stopped transmitting data (Parker et al., 2003). In this area, the southern edge of the Kuroshiro Extension Current forms numerous eddies that are semipermanent features throughout the year. Reduction of fishing effort or other fishery mitigation techniques in this area may greatly decrease the number of fisheries interactions that Pacific loggerhead sea turtles experience. International cooperation is needed in order to manage these foraging habitats. More studies also need to be done on the ecology of these turtles so that fishery interactions at all life stages can be addressed and so that a total picture of the life history of this species can be obtained.

Acknowledgments

We would like to acknowledge the hard work of all the NMFS fishery observers for obtaining the samples, Russ Miya and Bryan Winton for their help in the initial sorting, and Mike Seki and Kevin Landgraf for their help in identifying prey items. We would also like to acknowledge the review and comments of Alan Bolten, Jeffrey Seminoff, George Antonelis, Jerry Wetherall, Colin Limpus, Judith Kendig, Francine Fiust, Shawn Murakawa, and two anonymous reviewers.

Literature cited

- Allen, W.
1992. Loggerhead dies after ingesting marine debris. *Mar. Turtle Newsl.* 58:10.
- Andersen, V., and J. Sardou.
1994. *Pyrosoma atlanticum* (Tunicata, Thaliacea): diel migration and vertical distribution as a function of colony size. *J. Plankton Res.* 16(4):337–349.

- Baba, N., M. Miyota, H. Suganuma, and H. Tachikawa.
1992. Research on migratory routes of loggerhead turtles and green turtles by the Argos system. Report on commissioned project for data analysis by scientific observers aboard fishing vessels in 1991. Fish. Agency Jpn., Tokyo, p. 89-99. [In Japanese.]
1993. Research on migratory routes of loggerhead turtles and green turtles by the Argos system. Report on commissioned project for data analysis by scientific observers aboard fishing vessels in 1992. Fish. Agency of Jpn., Tokyo, p. 86-99. [In Japanese.]
- Balazs, G.
1989. New initiatives to study sea turtles in the eastern Pacific. *Mar. Turtle Newsl.* 47:19-21.
1985. Impact of ocean debris on marine turtles: entanglement and ingestion. In R.S. Shomura and H.O. Yoshida (eds.), Proceedings of the workshop on the fate and impact of marine debris, 26-29 November 1984, Honolulu, Hawaii, p. 387-429. NOAA Tech. Memo. NMFS, NOAA-TM-SWFC-54.
- Bartlett, G.
1989. Juvenile *Caretta* off Pacific coast of Baja California. *Not. Caguamas* 2:2-10.
- Bayer, F. M.
1963. Observations on pelagic mollusks associated with siphonophores *Veella* and *Physalia*. *B. Mar. Sci.* 13(3):454-466.
- Bentivegna, F.
2002. Intra-Mediterranean migrations of loggerhead sea turtles (*Caretta caretta*) monitored by satellite telemetry. *Mar. Biol.* 141: 795-800.
- Bjorndal, K. A.
1997. Foraging ecology and nutrition of sea turtles. In *The biology of sea turtles* (P. Lutz and J. Musick, eds.), p. 199-32. CRC Press, Boca Raton, FL.
1999. Priorities for research in foraging habitats. In *Research and management techniques for the conservation of sea turtles* (K. L. Eckert, K. A. Bjorndal, F. A. Abreu-Grobois, and M. Donnelly, eds.), p. 12-18. IUCN (International Union for the Conservation of Nature and Natural Resources)/SSC (Species Survival Commission), *Mar. Turtle Spec. Group Publ. No. 4*, Washington, DC.
- Bjorndal, K. A., A. B. Bolten, and C. J. Laguex.
1994. Ingestion of marine debris by juvenile sea turtles in coastal Florida habitats. *Mar. Pollut. Bull.* 28: 154-158.
- Bjorndal, K. A., A. B. Bolten, and H. R. Martins.
2000. Somatic growth model of juvenile loggerhead sea turtles *Caretta caretta*: duration of pelagic stage. *Mar. Ecol. Prog. Ser.* 202: 265-272.
- Bowen, B. W., F. A. Abreu-Grobois, G. H. Balazs, N. Kamezaki, C. J. Limpus and R. J. Ferl.
1995. Trans-Pacific migrations of the loggerhead turtle (*Caretta caretta*) demonstrated with mitochondrial DNA markers. *Proc. Natl. Acad. Sci.* 92: 3731-3734.
- Brusca, R. C.
1980. Intertidal invertebrates of the Gulf of California, 513 p. Univ. Arizona Press, Tucson, AZ.
- Burke, V. J., S. J. Morreale, and E. A. Standa.
1990. Comparisons of diet and growth of Kemp's Ridley and loggerhead turtles from the Northeastern U.S. In *Proceedings of the tenth annual workshop on sea turtle biology and conservation* (T. H. Richardson, J. I. Richardson, and M. Donnelly (comps.), p. 135. NOAA Tech. Memo NMFS-SEFC-278.
- Chace, F. A.
1951. The oceanic crabs of the genera *Planes* and *Pachygrapus*. *Proc. U.S. Natl. Mus.* 101:65-103.
- Chaloupka, M.
1998. Polyphasic growth in pelagic loggerhead sea turtles. *Copeia* 1998(2):516-518.
- Davenport, J.
1994. A cleaning association between the oceanic crab (*Planes minutus*) and the loggerhead sea turtle (*Caretta caretta*). *J. Mar. Biol. Assoc. UK* 74(3):735-737.
- Davenport, J., and G. H. Balazs.
1991. Fiery Bodies: Are pyrosomas an important component of the diet of leatherback turtles. *Brit. Herp. Soc.* 37:33-38.
- Dodd, C. K., Jr.
1988. Synopsis of the biological data on the loggerhead sea turtle *Caretta caretta* (Linnaeus 1758). U.S. Fish Wildl. Serv. Biol. Rep. 88(14), 110 p.
- Dutton, P. H., G. H. Balazs, and A. E. Dizon.
1998. Genetic stock identification of sea turtles caught in the Hawaii-based pelagic longline fishery. In *Proceedings of the seventeenth annual sea turtle symposium* (S. P. Epperly and J. Braun, compilers), p. 43. NOAA Tech. Memo. NMFS-SEFSC-415.
- Eldredge, L. G., and D. M. Devaney.
1977. Other hydrozoans. In *Reef and shore fauna of Hawaii*, Sec.1: Protozoa through Ctenophora. B. P. Bishop Mus. Spec. Publ. 64(1):105-107.
- Epperly, S. P., J. Braun, and A. Veishlow.
1990. Distribution and species composition of sea turtles in North Carolina. In *Proceedings of the tenth annual workshop on sea turtle biology and conservation* (T. H. Richardson, J. I. Richardson, and M. Donnelly (comps.), p. 95-96. NOAA Tech. Memo NMFS-SEFC-278.
- Evans, F.
1986. *Veella veella* (L.), the 'by-the-wind-sailor' in the North Pacific Ocean in 1985. *Mar. Obs.* 56(7): 196-200.
- Forbes, G. A.
1999. Diet sampling and diet component analysis. In *Research and management techniques for the conservation of sea turtles* (K. L. Eckert, K. A. Bjorndal, F. A. Abreu-Grobois, and M. Donnelly, eds.), p. 144-148. IUCN/SSC *Mar. Turtle Spec. Group Publ. no. 4*, Washington, D.C.
- Frazier, J.
1985. Misidentification of sea turtles in the East Pacific: *Caretta caretta* and *Lepidochelys olivacea*. *J. Herpetol.* 1:1-11.
- Froese, R., and D. Pauly, eds.
2003. FishBase. World Wide Web electronic publication. www.fishbase.org. [Accessed 6 March 2004.]
- Gardner, S. C., and W. J. Nichols.
2001. Assessment of sea turtle mortality rates in the Bahia Magdalena region, Baja, California Sur, Mexico. *Chel. Cons. Biol.* 4:197-199.
- Godley, B. J., S. M. Smith, P. F. Clark, and J. D. Taylor.
1997. Molluscan and crustacean items in the diet of the loggerhead turtle, *Caretta caretta* (Linnaeus, 1758) [Testudines: Cheloniidae] in the eastern Mediterranean. *J. Molluscan Stud.* 63:474-476.
- Gomez-Gutierrez, J., E. Dominguez-Hernandez, C. J. Robinson, and V. Arenas.
2000. Hydroacoustical evidence of autumn inshore residence of the pelagic red crab *Pluroncodes planipes* at Punta Eugenia, Baja California, Mexico. *Mar. Ecol. Prog. Ser.* 208:283-291.

- Gomez-Gutierrez, J., and C. A. Sanchez-Ortiz.
1997. Larval drift and population structure of the pelagic phase of *Pleuroncodes planipes* (Stimpson) (Crustacea: Galatheaidea) off the southwest coast of Baja California, Mexico. *B. Mar. Sci.* 61(2):305-325.
- Hitase, H., N. Takai, Y. Matsuzawa, W. Sakamoto, K. Omuta, K. Goto, N. Arai, and T. Fujiwara.
2002. Size-related differences in feeding habitat use of adult female loggerhead turtles *Caretta caretta* around Japan determined by stable isotope analyses and satellite telemetry. *Mar. Ecol. Prog. Ser.* 233: 273-281.
- Hulley, P. A.
1990. Myctophidae. In *Fishes of the Southern Ocean* (O. Gon and P. C. Heemstra, eds.), p. 146-178. J. L. B. Smith Institute of Ichthyology, Grahamstown, South Africa. [ref. 5182 from website FishBase: www.fishbase.org.]
- Jokiel, P. L.
1990. Long-distance dispersal by rafting: re-emergence of an old hypothesis. *Endeavour, New Series.* 14(2):66-73.
- Kamezaki, N.
1994. Review of quantitative data on plastic debris found in the intestine (sic) of the sea turtle. *Umigame News.* 22: 9-14. [In Japanese.]
- Kamezaki, N., and M. Matsui.
1997. A review of biological studies on sea turtles in Japan. *Jpn. J. Herpetol.* 17(1):16-32.
- Kamezaki, N., I. Miyawaki, H. Sugauma, K. Omuta, Y. Nakajima, K. Goto, K. Sato, Y. Matsuzawa, M. Samejima, M. Ishii, and T. Iwamoto.
1997. Post-nesting migration of Japanese loggerhead turtle, *Caretta caretta*. *Wildl. Conserv. Jpn.* 3:29-39. [In Japanese with English abstract.]
- Lalli, C. M., and R. W. Gilmer.
1989. Pelagic snails: the holoplanktonic gastropod mollusks, 259 p. Stanford Univ. Press, Stanford, CA.
- Lewison, R. L., S. A. Freeman, and L. D. Crowder.
2004. Quantifying the effects of fisheries on threatened species: the impact of pelagic longlines on loggerhead and leatherback sea turtles. *Ecol. Lett.* 7(3):221-231.
- Limpus, C. J., and P. Couper.
1994. Loggerheads: a species in decline. *Wildl. Aust.* 30:11-13.
- Márquez, M. R., and A. O. Villanueva.
1982. Situación actual y recomendaciones para el manejo de las tortugas marinas de la costa occidental de México, en especial la tortuga golfina *Lepidochelys olivacea*. *Cienc. Pesquera INP* 2:83-91.
- Nichols, W. J., A. Resendiz, and C. Mayoral-Russeau.
2000. Biology and conservation of loggerhead turtles in Baja California, Mexico. In *Proceedings of the nineteenth annual symposium on sea turtle biology and conservation* (H. J. Kalb and T. Wibbels, comps), p. 169-171. NOAA Tech. Memo. NMFS-SEFSC-443.
- Nishemura, W., and S. Nakahigashi.
1990. Incidental capture of sea turtles by Japanese research and training vessels: results of a questionnaire. *Mar. Turtle News.* 51:1-4.
- Okutani, T.
1961. Notes on the genus *Carinaria* (Heteropoda) from Japanese and adjacent waters. *Publs. Seto Mar. Biol. Lab.* 9:333-353.
- Parker, D. M., J. Polovina, G. H. Balazs, and E. Howell.
2003. The lost years: long-term movement of a maturing loggerhead turtle in the northern Pacific Ocean. In *Proceedings of the twenty-second annual symposium on sea turtle biology and conservation* (J. A. Seminoff, comp.), p. 294-296. NOAA Tech. Memo. NMFS-SEFSC-503.
- Peckham, H., and W. J. Nichols.
2003. Why did the turtle cross the ocean? Pelagic red crabs and loggerhead turtles along the Baja California coast. In *Proceedings of the twenty-second annual symposium on sea turtle biology and conservation* (J. A. Seminoff, comp.), p. 47. NOAA Tech. Memo. NMFS-SEFSC-503.
- Pitman, R. L.
1990. Pelagic distribution and biology of sea turtles in the Eastern Tropical Pacific. In *Proceedings of the tenth annual workshop on sea turtle biology and conservation* (T. H. Richardson, J. I. Richardson, and M. Donnelly, comps.), p. 143-148. 1. NOAA Tech. Memo. NMFS-SEFSC-278.
- Plotkin, P. T., M. K. Wicksten, and A. E. Amos.
1993. Feeding ecology of the loggerhead sea turtle *Caretta caretta* in the Northwestern Gulf of Mexico. *Mar. Biol.* 115:1-15.
- Polovina, J. J., G. H. Balazs, E. A. Howell, D. M. Parker, M. P. Seki, and P. H. Dutton.
2004. Forage and migration habitat of loggerhead (*Caretta caretta*) and olive ridley (*Lepidochelys olivacea*) sea turtles in the central North Pacific Ocean. *Fish. Oceanogr.* 13:36-51.
- Polovina, J. J., E. A. Howell, D. M. Parker, and G. H. Balazs.
2003. Dive depth distribution of loggerhead (*Caretta caretta*) and olive ridley (*Lepidochelys olivacea*) turtles in the central North Pacific Ocean: Might deep longline sets catch fewer turtles. *Fish. Bull.* 101: 189-193.
- Polovina, J. J., D. R. Kobayashi, D. M. Parker, M. P. Seki and G. H. Balazs.
2000. Turtles on the edge: movement of loggerhead turtles (*Caretta caretta*) along oceanic fronts spanning longline fishing grounds in the Central North Pacific, 1997-1998. *Fish. Oceanogr.* 9:71-82.
- Resendiz, A., B. Resendiz, W. J. Nichols, J. A. Seminoff, and N. Kamezaki.
1998. First confirmed east-west transpacific movement of a loggerhead sea turtle, *Caretta caretta*, released in Baja California, Mexico. *Pac. Sci.* 52(2):151-153.
- Roden, G. I.
1991. Subarctic-subtropical transition zone of the North Pacific: large-scale aspects and mesoscale structure. In *Biology, oceanography, and fisheries of the North Pacific Transition Zone and Subarctic Frontal Zone* (J. A. Wetherall, ed.), p. 1-38. NOAA Tech Rep. NMFS, SWFSC 105.
- Sakamoto, W., T. Bando, N. Arai, and N. Baba.
1997. Migration paths of adult female and male loggerhead turtles, *Caretta caretta*, determined through satellite telemetry. *Fisheries Sci.* 63:547-552.
- Sato, K., T. Bando, Y. Matsuzawa, H. Tanaka, W. Sakamoto, S. Minamikawa, and K. Goto.
1997. Decline of the loggerhead turtle, *Caretta caretta*, nesting on Senri beach in Minabe, Wakayama, Japan. *Chel. Conserv. Biol.* 2:600-603.
- Seminoff, J. A., A. Resendiz, B. Resendiz, and W. J. Nichols.
2004. Occurrence of loggerhead sea turtles (*Caretta caretta*) in the Gulf of California, Mexico: evidence of life-history variation in the Pacific Ocean. *Herpetol. Rev.* 35(1):24-27.
- Spivak, E. D., and C. C. Bas.
1999. First finding of the pelagic crab *Planes marinus* (Decapod: Grapsidae) in the Southwest Atlantic. *J. Crustacean Biol.* 19(1):72-26.

- Tomas, J., F. J. Aznar, and J. A. Raga.
2001. Feeding ecology of the loggerhead turtle *Caretta caretta* in the western Mediterranean. *J. Zool. Lond.* 255:525-532.
- Tomas, J., R. Guitart, R. Mateo, and J. A. Raga.
2002. Marine debris ingestion in loggerhead sea turtles, *Caretta caretta*, from the western Mediterranean. *Mar. Poll. Bull.* 44:221-216.
- Uchida, I.
1973. Pacific loggerhead turtle—pursuing its mysterious oceanic life. *Anima* 1(3):5-17. [In Japanese.]
- Weitzman, S. H.
1986. Sternoptychidae. In *Smith's sea fishes* (M. M. Smith and P. C. Heemstra, eds.), p. 253-259. Springer-Verlag, Berlin.
- Wetherall, J. A.
1996. Assessing impacts of Hawaiian longline fishing on Japanese loggerheads and Malaysian leatherbacks: some exploratory studies using TURTSIM. In *Status of marine turtles in the Pacific Ocean relevant to incidental take in the Hawaii-based pelagic longline fishery* (A. Bolten, J. A. Wetherall, G. H. Balazs, and S. G. Pooley, comps.), p. 57-75. NOAA Tech. Memo. NMFS-SWFSC-230.
- Wetherall, J. A., G. H. Balazs, R. A. Tokunaga, and M. Y. Y. Yong.
1993. Bycatch of marine turtles in North Pacific high-seas driftnet fishery and impacts on stock. In *INPFC symposium on biology, distribution, and stock assessment of species caught in the high seas driftnet fishery in the North Pacific Ocean, 53(III)* (J. Ito et al., eds.), p. 519-538. Int. N. Pac. Fish. Comm., Vancouver, Canada.
- Witherington, B. E.
2002. Ecology of neonate loggerhead turtles inhabiting lines of downwelling near a Gulf Stream front. *Mar. Biol.* 140:843-853.
- Witzell, W. N.
2002. Immature Atlantic loggerhead turtles (*Caretta caretta*): suggested changes to the life history model. *Herpetol. Rev.* 33:266-269.
- Van Nierop, M. M., and J. C. den Hartog.
1984. A study of the gut contents of five juvenile loggerhead turtles, *Caretta caretta* (Linnaeus) (Reptilia Cheloniidae), from the south-Eastern part of the North Atlantic Ocean, with emphasis on coelenterate identification. *Zool. Meded. Leiden* 59:35-54.
- Zug, G. R., G. H. Balazs, and J. A. Wetherall.
1995. Growth in juvenile loggerhead sea turtles (*Caretta caretta*) in the North Pacific pelagic habitat. *Copeia* 2:484-487.

Abstract—Two examples of indirect validation are described for age-reading methods of Pacific cod (*Gadus macrocephalus*). Aging criteria that exclude faint translucent zones (checks) in counts of annuli and criteria that include faint zones were both tested. Otoliths from marked and recaptured fish were used to back-calculate the length of each fish at the time of its release by using measurements of the area of annuli. Estimated fish size at time of release and actual observed fish size were similar, supporting the assumption that translucent zones are laid down on an annual basis. A second method for validating reading criteria used otolith age and von Bertalanffy parameters, estimated from the tagging data, to predict how much each fish grew in length after tagging. We found that otolith aging criteria applied to otoliths from tagged and recovered Pacific cod predicted quite accurately the growth increments that we observed in these specimens. These results provide further evidence that the current aging criteria are not underestimating the age of the fish and support our current interpretation of checks (i.e., as subannual marks). We expect these indirect validations to advance age determination for Pacific cod, which in turn would enhance development of stock assessment methods based on age structure for this species in the eastern Bering Sea.

Indirect validation of the age-reading method for Pacific cod (*Gadus macrocephalus*) using otoliths from marked and recaptured fish

Nancy E. Roberson

Daniel K. Kimura

National Marine Fisheries Service, NOAA
Alaska Fisheries Science Center
7600 Sand Point Way, NE
Seattle, Washington 98115

E-mail address (for N. E. Roberson): Nancy.Roberson@noaa.gov

Donald R. Gunderson

University of Washington
School of Aquatic and Fishery Sciences
1122 N.E. Boat Street
Seattle, Washington 98105

Allen M. Shimada

National Marine Fisheries Service, NOAA
Office of Research
1315 East-West Hwy
Silver Spring, Maryland 20910-3282

Pacific cod (*Gadus macrocephalus* Tilesius, 1810) is an important species in eastern Bering Sea commercial fisheries and is second only to walleye pollock (*Theragra chalcogramma*) in landings (Thompson and Dorn¹). It is also considered to be one of the most difficult of all commercially important Alaska groundfish species to age. Scientists from both Canada and the United States have experienced similar difficulties in finding an appropriate aging structure, which can be consistently interpreted to track large year classes of cod through time. Historically, scales and otoliths have been the two most common structures used for determining the ages of fish species. Unfortunately, age-readers employing these structures have experienced limited success in the case of Pacific cod (Kimura and Lyons, 1990).

The Pacific Biological Station in Canada stopped aging Pacific cod in 1978, after age estimates derived from scale readings began yielding

year classes that were inconsistent with length-frequency time series from field surveys (Westrheim and Shaw, 1982). The Alaska Fisheries Science Center's (AFSC) Resource Ecology and Fisheries Management (REFM) Division is responsible for stock assessment of Pacific cod in the Gulf of Alaska and eastern Bering Sea. The REFM Division's Age and Growth Program used scales for determining the age of Pacific cod from 1976 to the early 1980s. Thereafter, the program used the break-and-burn method with otoliths to age Pacific

¹ Thompson, G. G., and M. W. Dorn. 1999. Pacific cod. In Stock assessment and fishery evaluation report for the groundfish resources for the Bering Sea/Aleutian Islands regions (plan team for groundfish fisheries of the Bering Sea/Aleutian Islands), p. 151–205. North Pacific Fishery Management Council, 605 W. 4th Avenue Suite 306, Anchorage, AK 99501.

cod (Thompson and Methot²). In the otoliths of young Pacific cod (under 6 years), there is a tendency for sub-annual marks (also known as "checks") to be very dark and evenly spaced, making them difficult to distinguish from annuli. This confusion makes it difficult to age the species to an exact age.

From 1990 through 1992, the AFSC noticed that the average length at a specific age was smaller than it had been in previous years. The decrease was noticed in ages 1–6 but was especially dramatic in 1-, 2-, and 3-year-olds. It is generally theorized that the shift was the result of one of two scenarios: either the fish population experienced an actual decrease in length-at-age or the age readers were over-aging fish by counting marks other than annuli. Unable to pinpoint the reason for the shift and given the inherent difficulty of aging cod, production (large-scale) aging of Pacific cod was indefinitely suspended at the AFSC.

Pacific cod stock assessments in Alaska have since depended largely on length-frequency data alone to model population age structure because of the difficulties in obtaining age estimates (Thompson and Dorn³). However, the use of length-frequency data as proxies for age data can be problematic. If external factors such as ocean conditions affect somatic growth to such a degree that length-at-age within the population is highly variable, such as appears to be the case for Pacific cod, then the population becomes difficult to model. Otoliths, on the other hand, are permanent records of growth that are more independent of external factors.

Consequently, the Age and Growth Program initiated a new study in 1998 to re-examine the otolith aging structure for Pacific cod. This study used otoliths from tagged Alaska Pacific cod to validate aging criteria for otoliths.

Methods

Otoliths and length data were collected during a tagging study conducted by the AFSC. Between 1982 and 1990, 12,396 Pacific cod were tagged and released in the eastern Bering Sea during summer bottom-trawl surveys (See Shimada and Kimura, 1994). Fish were measured to the nearest 0.5 cm fork length, tagged with uniquely marked spaghetti tags, and set free. Over a period of 13 years, commercial fishing vessels recaptured 375 (3%) of the tagged fish and returned otoliths from 112 fish (106 of which were usable) (Table 1). More details on the tagging methods can be found in Shimada and Kimura (1994).

Otolith preparation

One sagittal otolith from each recaptured fish was selected for our study. We did not discriminate between left and right otoliths based on the results of Sakurai and Hukuda (1984) who were unable to detect any consistent differences between the weight and length of right and left Pacific cod otoliths.

Each otolith was cleaned and preserved in 95% ethanol. After having been preserved for approximately one month, a line was penciled across the otolith center from the dorsal apex to the ventral apex to ensure that the otoliths would later be sectioned at the core.

The otolith was then placed in a polyester mold and set in black resin (Technovit 3040, Energy Beam Sciences, Agawam, MA), forming a block of resin. A slow-speed saw was used to cut the blocks in half. This produced two smaller blocks, each with an exposed view of the otolith in the transverse plane and cut through the center. One of the two blocks was selected and glued (otolith side down) to a glass slide. The glass slide was mounted to a Hillquist thin section machine (Hillquist Inc., Fall City, WA) and the section was ground down to a thickness of 0.25 mm. A coverslip was permanently glued on the top of the section with marine-grade epoxy.

Sections were placed on a piece of black velvet (which added contrast) on the stage of a 50× dissecting microscope, and reflected light was used for illumination. The sections were viewed on a computer monitor by using a Cohu 6500 monochrome video camera, Integral Flashpoint 128 frame grabber and Optimas 6.5 imaging software (Media Cybernetics, Silver Spring, MD).

Age-reading criteria

Traditional qualitative aging criteria were used to distinguish annuli from checks. The criterion for identification as an annulus was a continuous translucent band that could be seen along the entire structure or as a ridge or groove on the structure (Secor et al., 1995). Checks (i.e., subannual marks) are translucent zones that appear very similar to annuli. They were determined primarily by the incompleteness of the zone around the entire section, by zone darkness, and by spacing between zones. When translucent zones could be classified as either annuli or additional subannual marks, they were classified as checks. Annuli, checks, and edges (the space between the last annulus and the edge of the otolith) were traced by using the Optimas 6.5 software package and measurements of their areas and major axis lengths were collected (Fig. 1). All otoliths were read blind; that is, information about fish length and date of capture (Table 1) was withheld from the reader to prevent bias.

When all the otoliths had been aged and measured, the age reader returned to each otolith section to estimate the area and length of the otolith when the fish was tagged. This was accomplished by following a two-step process. The first step was to approximate the location of the otolith cross-section that corresponded to

² Thompson, G. G., and R. D. Methot. 1993. Pacific cod. In Stock assessment and fishery evaluation report for the groundfish resources for the Bering Sea/Aleutian Islands regions as projected for 1994 (plan team for groundfish fisheries of the Bering Sea/Aleutian Islands), p. 2–28. North Pacific Fishery Management Council, 605 W. 4th Avenue Suite 306, Anchorage, AK 99501.

Table 1

Mark and recapture data for spaghetti-tagged Pacific cod (*Gadus macrocephalus*). L_1 = fork length at tagging (mm), L_2 = fork length at recapture (mm), d_1 = time at liberty (months), a_1 = age estimated from L_1 and d_1 , a_2 = age at recapture estimated by using the fish's otolith and age-reading criteria, and NR = not reported.

L_1	L_2	d_1	a_1	a_2	$a_1 - a_2$	L_1	L_2	d_1	a_1	a_2	$a_1 - a_2$
430	480	9	4	3	1	625	550	3	6.5	5	1.5
680	875	21	8	7	1	740	850	26	8	8	0
690	830	30	8	8	0	650	670	4	6	7	-1
590	500	4	6	7	-1	525	550	5	5	4	1
530	690	30	7	7	0	645	720	9	7	6	1
430	500	10	4	4	0	835	890	14	7	8	-1
600	620	8	6	7	-1	560	600	5	5	4	1
390	490	11	3.5	3	0.5	645	830	38	9	8	1
630	660	5	6.5	4	2.5	405	412	4	3.5	2	1.5
670	750	9	7	8	-1	460	550	8	4	3	1
630	850	49	9.5	10	-0.5	735	760	1	6	7	-1
590	650	7	6	6	0	620	650	1	5	6	-1
450	570	25	5	6	-1	545	550	4	4	6	-2
630	660	7	6.5	6	0.5	555	560	2	4	5	-1
440	525	14	4.5	5	-0.5	680	730	19	7.5	6	1.5
705	890	35	9	8	1	640	680	4	6.5	4	2.5
556	680	25	6	8	-2	730	730	6	7	7	0
480	540	7	5.5	3	2.5	540	655	12	5	5	0
620	660	2	5	9	-4	600	720	14	6	6	0
630	730	17	7	8	-1	540	700	17	5	6	-1
600	730	44	8.5	7	1.5	530	920	50	8	9	-1
630	623	1	5.5	6	-0.5	610	691	16	6	8	-2
702	760	11	7	8	-1	690	800	10	7	5	2
330	530	22	4	3	1	555	630	7	5	6	-1
540	706	20	6	5	1	790	NR	21	8	7	1
390	578	22	4.5	4	0.5	560	630	8	5	5	0
670	710	4	6	9	-3	520	550	2	4	4	0
820	825	2	6	8	-2	535	NR	18	5.5	6	-0.5
690	710	8	7	8	-1	460	530	7	4	3	1
725	850	17	7.5	6	1.5	590	930	93	12.5	15	-2.5
530	590	9	5	5	0	690	742	5	6.5	6	0.5
660	690	3	6	7	-1	720	770	8	7	9	-2
580	770	57	9.5	10	-0.5	870	924	7	7	8	-1
450	695	25	5	5	0	520	523	7	5	3	2
815	860	10	7	8	-1	470	530	6	4.5	3	1.5
540	670	22	6	7	-1	630	740	13	6.5	7	-0.5
740	670	7	7	6	1	510	630	13	5	6	-1
670	705	2	6	8	-2	650	720	13	7	6	1
650	640	0	6	7	-1	570	675	20	6	8	-2
710	860	19	8	7	1	690	660	20	7.5	8	-0.5
670	810	20	8	7	1	660	760	23	8	8	0
780	770	1	6	8	-2	690	750	7	7	7	0
810	850	7	7	8	-1	560	630	8	5	5	0
485	640	21	5.5	6	-0.5	530	700	7	5	7	-2
305	850	39	4.5	8	-3.5	600	620	10	5.5	4	1.5
695	710	9	7	6	1	595	970	50	8.5	9	-0.5
610	810	30	8	6	2	520	910	32	6.5	7	-0.5
660	820	30	9	7	2	540	800	30	6	7	-1
610	725	26	7	7	0	820	830	2	6	6	0
580	720	30	7.5	7	0.5	585	782	34	7.5	6	1.5
530	830	33	7	6	1	680	790	9	7	6	1
600	760	17	7	6	1	676	1080	70	11.5	11	0.5
515	730	26	6	5	1	585	590	0	4.5	5	-0.5

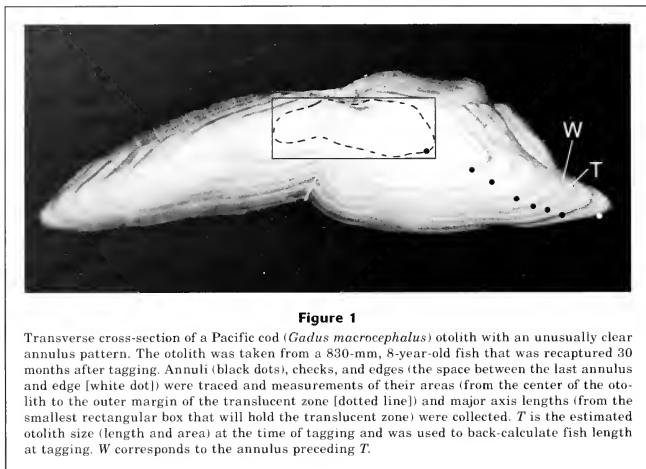


Figure 1

Transverse cross-section of a Pacific cod (*Gadus macrocephalus*) otolith with an unusually clear annulus pattern. The otolith was taken from a 830-mm, 8-year-old fish that was recaptured 30 months after tagging. Annuli (black dots), checks, and edges (the space between the last annulus and edge [white dot]) were traced and measurements of their areas (from the center of the otolith to the outer margin of the translucent zone [dotted line]) and major axis lengths (from the smallest rectangular box that will hold the translucent zone) were collected. *T* is the estimated otolith size (length and area) at the time of tagging and was used to back-calculate fish length at tagging. *W* corresponds to the annulus preceding *T*.

the time of tagging. The second step was calculating the area and length of that region, producing an estimated otolith size at the time of tagging.

First, to approximate the location of the otolith that corresponded to the time of tagging required the reader to know how long (years) the fish had been at liberty, after tagging. Using this knowledge and starting from the last annulus before the edge, the reader counted towards the center of the otolith, the number of years (as represented by annuli) that the fish had been at liberty. (In cases where the fish had been at liberty for less than one year before being caught again, the reader began at the edge rather than at the last annulus before the edge). Assuming that all annuli are laid down by late winter, the reader would end up on the annulus that preceded the summer of tagging. This annulus represents the size of the otolith just prior to tagging and for sake of further explanation, its area and length will be identified as *W* (Fig. 1). To complete the procedure, the reader needed only to measure the summer increment which followed *W*, divide it in half and add it to *W*. These calculations were assumed to reflect the size of the fish's otolith at time of tagging and were used as *O_t* values (the size of the otolith at tagging) to back-calculate fish size at initial capture.

Estimating fish length by using tagged fish and back-calculations

Annuli on tagged fish otoliths can be used to estimate the length of each fish at an earlier age. Smedstad

and Holm (1996) compared six different back-calculation formulae on tagged Atlantic cod (*Gadus morhua*) and found that the age-independent, nonlinear, body proportional (nbp) hypothesis worked the best. Pacific cod is a gadid closely related to the Atlantic cod; therefore we also used the nonlinear, body proportional formula

$$L_t = (O_t / O_c)^v L_c,$$

where L_t = the predicted fish length at tagging or desired age;

O_t = the size (either radius or area) of otolith at tagging;

O_c = the size of otolith at time of recapture;

v = the slope from the regression of $\ln(L)$ on $\ln(O)$; and

L_c = the fish length at recapture.

This analysis was performed by using two different measures of otolith size, the cross-sectional area and major axis (i.e., length) of otolith increments (Fig. 1).

Estimating growth increments in fish length from tagged fish

We can use tagged fish otolith ages to estimate how much each fish grew in length after tagging, in a manner similar to Fabens' equation (Ricker, 1975), using the von

Table 2

Results of regressing Ln fish length on Ln otolith area and Ln fish length on Ln otolith major axis by using tagged fish data. Fish length was measured in mm, otolith area in mm², and otolith major axis in mm, n=96.

	Coefficients	Standard error	t stat	P-value
Regression of Ln Fish length on Ln Otolith area				
Intercept	4.637299	0.117551	39.44929	2.75E-60
Slope (v)	0.65732	0.040471	16.24168	4.96E-29
Regression of Ln Fish length on Ln Otolith major axis				
Intercept	4.27009	0.229693	18.5904	3.01E-33
Slope (v)	1.012865	0.102305	9.900426	2.99E-16

Bertalanffy equation (Ricker, 1975). However, because we could estimate the age of fish at time of recapture, we were able to manipulate the von Bertalanffy equation to obtain the following equation:

$$L_2 - L_1 = L_{inf} \left[\left(e^{-K(L_2 - d - t_0)} \right) - \left(e^{-K(L_1 - t_0)} \right) \right],$$

where L_1 = length at tagging;

L_2 = length at recapture;

L_{inf} = maximum size;

K = growth rate;

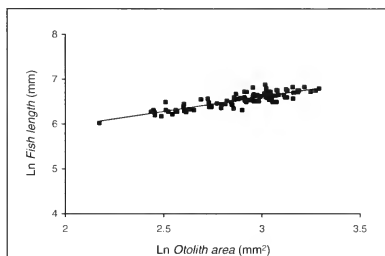
a_2 = estimated age at recovery determined from our otolith ages;

d = time at liberty; and

t_0 = age at length 0 mm.

Given von Bertalanffy parameters and age at recovery, a (fish) length increment for time after tagging can be predicted. Using published L_{inf} and K estimates from tagging data, $L_{inf} = 1043$ mm, $K = 0.222$ (Kimura et al., 1993), we estimated $L_2 - L_1$. One weakness in these estimates is that the growth parameters estimated by Kimura et al. (1993) were based on only positive growth increments (there were some instances where recaptured fish were smaller than they were at tagging, demonstrating negative growth increments).

A value for t_0 was estimated iteratively in the von Bertalanffy equation by using the subroutine Solver (Frontline Systems Inc., Incline Village, NE) from the Excel software package with the following parameter values: $K = 0.222$, $t = 1$ year old, $L_{inf} = 1043$ mm (Kimura et al., 1993), L_t = length at age one = 180 mm (from the 1977 year class [Foucher et al., 1984]). Because these von Bertalanffy parameters are not based on age determination, they provide an indirect method for validating aging criteria. In addition, ages determined by readers were scaled smaller (by 0.75) and larger (by 1.25) in order to simulate the results of younger and older aging criteria. Plots of observed and predicted growth increments should agree if the aging criteria for a_2 reflect the true age of fish.

**Figure 2**

Relationship between Ln fish length and Ln otolith area based on tagged and recaptured Pacific cod ($r^2=0.735$, $Y=4.6+0.66X$, $n=96$).

Results

Predicting fish length from tagged fish and back-calculations

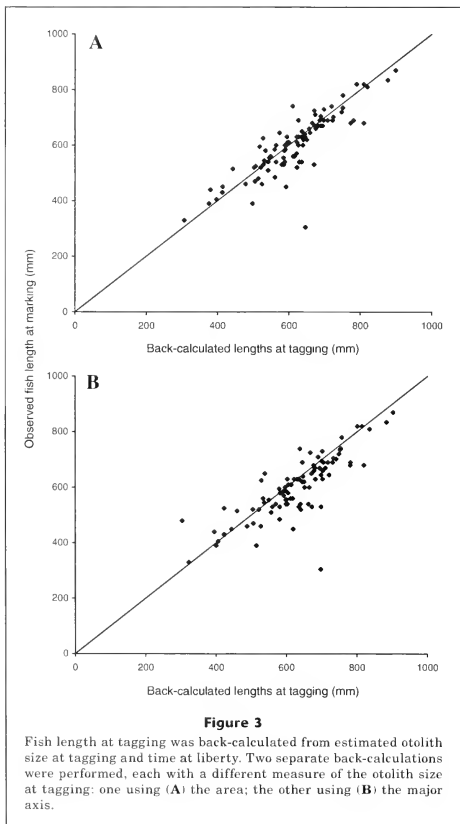
The parameter v used in all back-calculations in our study was estimated by using otolith area and again by using the major axis of the otolith (Fig. 1). Based on the slopes from the regression of Ln fish length on Ln otolith size (Table 2, [Fig. 2]), the coefficients should be $v=1.01$ for otolith length and $v=0.66$ for otolith areas.

Back-calculations were performed by using the otolith area and were repeated by using the major axis. Scatter plots of estimated and observed fish lengths were used to visually inspect how well back-calculation determines fish length (Fig. 3). Assuming that the residuals of the back-calculated length at tagging have independent chi-square distributions, an F -test indicates that back-calculations derived from otolith areas are significantly more accurate than back-calculations derived from the major axis ($P<0.05$). However, because we used the two

different methods on the same otoliths, the residuals were correlated and thus this result can be considered only approximate.

Predicting growth increments of fish length from tagged fish

Using the von Bertalanffy curve fitted with the data from the tagged fish sample, we estimated the value of t_0 to be 0.147.



The amount that each tagged fish grew after tagging was calculated three times by using fish age at recovery and the von Bertalanffy equation (Fig. 4). The calculated sums of squared deviations for the three sets of predicted values are as follows: 433,955 when fish age is scaled by 0.75, 419,477 when fish age is scaled by 1.0, and 761,545 when fish age is scaled by 1.25. The lowest sum of squared deviations accompanied ages that were scaled by 0.86. Assuming that the residuals of the estimated growth increments have independent chi-square distributions, an F -test indicates that residuals were significantly larger ($P < 0.05$) when ages were scaled 25% older and there was no significant difference ($P < 0.05$) between reader-determined ages and ages scaled 25% younger. The three sets of residuals came from the same otoliths and would be correlated; therefore, this result can be considered only approximate.

Another test of our reading criteria was performed through a more direct comparison: simply "aging" the tagged fish from estimated age at tagging (based on length), plus the time after tagging (Table 1). Out of 106 samples, 75% of these fish were within one year of the age that we had determined from otolith readings, and 94% were within two years. The average percent error (Beamish and Fournier, 1981) was 8.70, and the average deviation from tagged-based age was -0.075 . Results of a Z -test indicated that the average deviation was not significantly different from zero ($P = 0.724$) and indicated no bias in the age estimates.

Discussion

Beamish and McFarlane (1983) noted that "validating a method of age determination is as important in fishery biology as standardizing solutions or calibrating instruments are in other sciences." Age determination must reflect the actual age of each fish in order to be a useful tool for use in stock assessments. Although much effort has been devoted in the past to finding an appropriate aging structure for Pacific cod, particularly with dorsal fin rays (Beamish, 1981; Lai et al., 1987; Kimura and Lyons, 1990), scales and otoliths (Lai et al., 1987; Kimura and Lyons, 1990), a directly validated method of age determination has yet to be found (Westrheim, 1996). The otolith seems to be the most promising structure for production (large-scale) age reading of Pacific cod (Kimura and Lyons, 1990); however it is not without weaknesses (i.e., the faint patterns of some translucent zones can lead to low precision between readers and are a constant concern in regard to

under- or overestimated ages). The key difficulty of the cod otolith patterns is differentiating the translucent zones that are annual from the translucent zones that are checks, particularly in young fish. It is necessary to have validated criteria in order to confidently eliminate checks without under-aging the fish. In our study, we have given two examples of indirect validation for Pacific cod age determination by using otoliths from marked and recaptured fish.

In the first example, we used back-calculations to test our reading criteria, which exclude counting lighter translucent zones. Early in the study, we found a strong relationship between otolith size and fish length, which supported using back-calculations as a vehicle to test accuracy. Overall, using strong translucent zones to back-calculate fish length at tagging gave fairly accurate results. This finding supports the assumption that translucent zones are laid down on an annual basis.

An ancillary finding was that otolith area measurements provided more accurate estimates of fish length than otolith lengths. Although back-calculations are typically performed by using radial or diametral measurement, the more accurate estimates of fish length from otolith area measurements are not surprising in that otolith area is a more comprehensive measure of otolith three-dimensional growth.

A second indirect validation of reading criteria was possible by estimating how much each tagged fish grew (millimeters) between tagging and recapture by its estimated age at recovery and von Bertalanffy growth parameters (derived only from tagging data). When compared to the observed growth increments, we found that the results support our proposed aging criteria (which exclude lighter translucent zones) because these criteria give the best fit to growth increments based on the mark-recapture growth increments. Aging the fish older (by counting light translucent zones) or younger (counting less annuli by banding translucent zones together) increases the residual fit to the mark-recapture growth increments. Large growth increments of fish length were difficult to estimate (Fig. 4). A possible explanation is that the longer a fish remains at liberty, the more likely that the growth becomes asymptotic, making the relationship between the growth increment and time at liberty less exact.

The final test for reading criteria was performed through a more direct comparison: simply "aging" the tagged fish by its length-at-release plus its time at liberty after tagging and comparing that age to the otolith-based age at recovery. Dwyer et al. (2003) also used this method in their study of yellowtail flounder (*Limanda ferruginea*). Average deviation from tag-based age was -0.075 ; 75% of these fish were found to be within one year of our age according to otolith readings, and 94% were within two years. These results provide further evidence that the current criteria do not result in the underestimation of the age of the fish and support the practice of not counting checks.

We found that growth information residing in otoliths from tagged and recovered Pacific cod provided

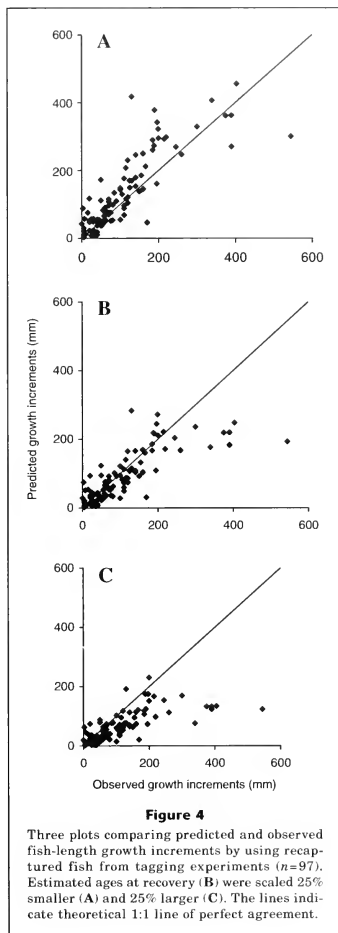


Figure 4

Three plots comparing predicted and observed fish-length growth increments by using recaptured fish from tagging experiments ($n=97$). Estimated ages at recovery (B) were scaled 25% smaller (A) and 25% larger (C). The lines indicate theoretical 1:1 line of perfect agreement.

significant information applicable to indirectly validating otolith aging criteria. Therefore, it seems that otoliths from other species that were tagged and recovered might be useful for indirect age validation as well. The

information provided in our study indicates that our aging criteria for Pacific cod are roughly correct and that errors are probably within plus or minus 1 or 2 years. However, the problem of the shift in length at age alluded to in the introduction is more difficult to elucidate. Analysis made during this study seems to indicate that both environmental growth factors and changes in otolith aging criteria could have played a role in this apparent shift.

Acknowledgments

This work was performed in partial fulfillment of the requirements for an M.S. degree at the School of Aquatic and Fishery Sciences at the University of Washington and was supported by the National Marine Fisheries Service. We would like to express our appreciation to those individuals who assisted in the tagging and recapture process and to the two anonymous reviewers for their helpful comments on the manuscript.

Literature cited

- Beamish, R. J.
1981. Use of sections of fin-rays to age walleye pollock, Pacific cod, albacore, and the importance of this method. *Trans. Am. Fish. Soc.* 110:287-299.
- Beamish, R. J., and D. A. Fournier.
1981. A method for comparing the precision of a set of age determinations. *Can. J. Fish. Aquat. Sci.* 38:982-983.
- Beamish, R. J., and G. A. McFarlane.
1983. The forgotten requirement for age validation in fisheries biology. *Trans. Am. Fish. Soc.* 112:735
- Dwyer, K. S., S. J. Walsh, and S. E. Campana.
2003. Age determination, validation and growth of Grand Bank yellowtail flounder (*Limanda ferruginea*). *ICES J. Mar. Sci.* 60:1123-1138.
- Foucher, R. P., R. G. Bakkala, and D. Fournier.
1984. Comparison of age frequency derived by length-frequency analysis and scale reading for Pacific cod in the North Pacific Ocean. *Int. North Pac. Fish. Comm. Bull.* 42:232-242.
- Kimura, D. K., and J. J. Lyons.
1990. Choosing a structure for the production aging of Pacific cod (*Gadus macrocephalus*). *Int. N. Pac. Fish. Comm. Bull.* 50:9-23.
- Kimura, D. K., A. M. Shimada, and S. A. Lowe.
1990. Estimating von Bertalanffy growth parameter of sablefish (*Anoplopoma fimbria*) and Pacific cod (*Gadus macrocephalus*) using tag-recapture data. *Fish. Bull.* 91:271-280.
- Lai, H. L., D. R. Gunderson, and L. L. Loh.
1987. Age determination of Pacific cod, *Gadus macrocephalus*, using five aging methods. *Fish. Bull.* 85:713-723.
- Ricker, W. E.
1975. Computation and interpretation of biological statistics of fish populations. *Bull. Fish. Res. Board Can.* 191, p. 382.
- Sakurai, Y., and S. Hukuda.
1984. The age and growth of the spawning Pacific cod in Mutsu Bay. *Sci. Rep. Aquat. Cen., Aomori Pref.* 3:9-14.
- Secor, D. H., J. M. Dean, and S. E. Campana (eds.).
1995. Recent developments in fish otolith research. Belle W. Baruch Institute for Marine Biology and Coastal Research., Univ. South Carolina Press, Columbia, SC.
- Shimada, A. M., and D. K. Kimura.
1994. Seasonal movements of Pacific cod, *Gadus macrocephalus*, in the eastern Bering Sea and adjacent waters based on tag-recapture data. *Fish. Bull.* 92:800-816.
- Smedstad, O. M., and J. C. Holm.
1996. Validation of back-calculation formulae for cod otoliths. *J. Fish Biol.* 49:973-985.
- Westrheim, S. J.
1996. On the Pacific cod (*Gadus macrocephalus*) in British Columbia waters, and a comparison with Pacific cod elsewhere, and Atlantic cod (*G. morhua*). *Can. Tech. Rep. Fish. Aquat. Sci.* 2092, 390 p.
- Westrheim, S. J., and W. Shaw.
1982. Progress report on validating age determination methods for Pacific cod (*Gadus macrocephalus*). *Can. Manuscr. Rep. Fish. Aquat. Sci.* 1670, 41 p.

Abstract—The northwest Atlantic population of thorny skates (*Amblyraja radiata*) inhabits an area that ranges from Greenland and Hudson Bay, Canada, to South Carolina. Despite such a wide range, very little is known about most aspects of the biology of this species. Recent stock assessment studies in the northeast United States indicate that the biomass of the thorny skate is below the threshold levels mandated by the Sustainable Fisheries Act. In order to gain insight into the life history of this skate, we estimated age and growth for thorny skates, using vertebral band counts from 224 individuals ranging in size from 29 to 105 cm total length (TL). Age bias plots and the coefficient of variation indicated that our aging method represents a nonbiased and precise approach for the age assessment of *A. radiata*. Marginal increments were significantly different between months (Kruskal-Wallis $P < 0.001$); a distinct trend of increasing monthly increment growth began in August. Age-at-length data were used to determine the von Bertalanffy growth parameters for this population: $L_{\infty} = 127$ cm (TL) and $k = 0.11$ for males; $L_{\infty} = 120$ cm (TL) and $k = 0.13$ for females. The oldest age estimates obtained for the thorny skate were 16 years for both males and females, which corresponded to total lengths of 103 cm and 105 cm, respectively.

Age and growth estimates of the thorny skate (*Amblyraja radiata*) in the western Gulf of Maine

James A. Sulikowski

Jeff Kneebone

Scott Elzey

Zoology Department, Spaulding Hall

46 College Road

University of New Hampshire

Durham, New Hampshire 03824

E-mail address (for J. A. Sulikowski, senior author):
jsulikow@hotmail.com

Joe Jurek

Yankee Fisherman's Cooperative

P.O. Box 2240

Seabrook, New Hampshire 03874

Patrick D. Danley

Department of Biology

University of Maryland

College Park, Maryland 20724

W. Huntington Howell

Zoology Department, Spaulding Hall

46 College Road

University of New Hampshire

Durham, New Hampshire 03824

Paul C.W. Tsang

Department of Animal and Nutritional Sciences

Kendall Hall

129 Main St.

University of New Hampshire

Durham, New Hampshire 03824.

The northeast skate complex consists of seven species endemic to the waters off the New England coast of the United States (New England Fisheries Management Council (NEFMC^{1,2}). In the past, these skates were generally discarded because of their low commercial value (NEFMC^{1,2}). More recently, the rapidly expanding markets for human consumption of skate wing and for use as lobster bait have made three of these species (winter skate [*Leucoraja ocellata*], little skate [*L. erinacea*], and thorny skate [*Amblyraja radiata*]) commercially more viable (Sosebee, 2000; NEFMC^{1,2}). Despite an increasing commercial importance, harvests for skate in the U.S. portion of the western north Atlantic remain unregulated and have the potential to over-exploit the stocks. Moreover, life history information is almost nonexistent for most of these elasmobranch fishes (Frisk, 2000 NEFMC^{1,2}).

The available information from the few skates that have been studied categorizes them as equilibrium strategists (K selected) because they reach sexual maturity at a late age, have a low fecundity, and are relatively long-lived (Holden 1977; Winemiller and Rose, 1992; Zeiner and Wolfe, 1993; Francis et al., 2001; Frisk et al., 2001; Sulikowski et al., 2003). These

characteristics, coupled with the practice of selective removal of large individuals, make these animals more likely to be over-exploited by commercial fisheries (Brander 1981; Hoenig and Gruber, 1990; Casey and Myers 1998; Dulvey et al., 2000; Frisk et al., 2001).

The thorny skate (*Amblyraja radiata*) is a cosmopolitan species found on both sides of the Atlantic ocean from Greenland and Iceland to the English Channel in the eastern Atlantic (Compagno et al., 1989) and from Greenland and Hudson Bay, Canada, to South Carolina, United States, in the western Atlantic (Robins and Ray, 1986; Collette and Klein, 2002). Along with this broad geographic range, marked differences in size exist for specimens captured in different regions of the Atlantic. For

Manuscript submitted 21 August 2003
to the Scientific Editor's Office.

Manuscript approved for publication
8 July 2004 by the Scientific Editor.

Fish. Bull. 103:161–168 (2005).

¹ NEFMC (New England Fishery Management Council). 2001. 2000 stock assessment and fishery evaluation (SAFE) report for the northeast skate complex. NEFMC, 50 Water Street, Mill 2 Newburyport, MA 01950.

² NEFMC (New England Fishery Management Council). 2003. Skate fisheries management plan. NEFMC, 50 Water Street, Mill 2 Newburyport, MA. 01950.

example, the thorny skate reaches total lengths of over 100 cm in the Gulf of Maine (Collette and Klein, 2002), whereas specimens captured off the Labrador coast do not reach total lengths >72 cm (Templeman, 1987). Although no directed fisheries for this species exists in the Gulf of Maine, this skate meets the minimum 1/4 pound-cut pectoral-fin size sought after by wing processors (Sosebee, 2000; NEFMC^{1,2}). Unfortunately, because landings are not reported by species, the proportion of thorny skates to the total wing market is unknown. Recent assessment studies in the northeast United States (NEFSC³) indicate that the biomass of thorny skates is declining, and is below threshold levels mandated by the Sustainable Fisheries Act (SFA; NMFS⁴). Thus, owing to the recent commercial interest in this species and the concomitant decline in population size, obtaining life history information for this species has become more important. In order to provide insight into the biology of this species and to determine the stock status (Simpfendorfer, 1993; Frisk et al., 2001), our objectives were to estimate age and growth rates of *A. radiata* based on banding patterns in vertebral centra from specimens collected in the western Gulf of Maine.

Materials and methods

Sampling

Thorny skates were captured by otter trawl in an approximate 900 square mile area centered at 42°50'N and 70°15'W in the Gulf of Maine between June 2001 and May 2002. These locations varied from 30 to 40 km off the coast of New Hampshire. Approximate depths at this location ranged between 100 and 120 m. This area was chosen for two reasons: 1) these waters support the vast majority of commercial fishing in New Hampshire and can be easily accessed during normal fishing operations; and 2) because of rolling closures within the Gulf of Maine, an experimental fishing permit was granted to us by the National Marine Fisheries Service (NMFS) to collect thorny skates in this location during the months of April, May, and June, when these waters are closed to commercial fishing. Although our sampling was conducted in a small portion of the species' range, the sizes of thorny rays collected corresponded to those collected during the NEFSC bottom trawl surveys conducted throughout the Gulf of Maine and Georges Bank (NEFMC¹; NEFSC³). From this information, it is unlikely that differences in other biological parameters exist.

Skates were maintained alive on board the vessel until arrival at the University of New Hampshire's Coastal

Marine Laboratory (CML). There, individual fish were euthanized (0.3g/L bath of MS222). Total length (TL in cm) was measured as a straight line distance from the tip of the rostrum to the end of the tail, and disc width (DW in cm) as a straight line distance between the tips of the widest portion of pectoral fins. Total wet weight (kg) was also recorded.

Preparation of vertebral samples

Vertebral samples, taken from above the abdominal cavity, were removed from 320 thorny skates (154 females and 166 males), labeled, and stored frozen. After having been thawed, three centra from each specimen were removed from the vertebral column, stripped of excess tissue and air dried. Large centra were cut sagittally with a DremelTM tool fitted with a mini saw attachment while held with a vice-like device. Smaller centra were sanded with a DremelTM tool to replicate a sagittal cut. Processed vertebrae were mounted horizontally on glass microscope slides and ground with successively finer-grit (no. 180, no. 400, no. 600) wet-dry sandpaper. Each vertebra was then remounted and the other side ground to produce a thin (300-micrometer) hourglass section.

Band counts

Vertebral sections were digitally photographed with a Canon Powershot S40 attached to a Leica S8PO dissecting microscope and reflected light. Magnification depended on the size of the section and varied from 4x to 12x (Fig. 1). A growth ring (band count) was defined as one opaque and translucent band pair that traversed the intermedialia and that clearly extended into the corpus calcareum (Casey et al., 1985; Brown and Gruber, 1988; Sulikowski et al., 2003). The birth mark (age zero) was defined as the first distinct mark distal to the focus that coincided with a change in the angle of the corpus calcareum (Casey et al., 1985; Wintner and Cliff, 1996; Sulikowski et al., 2003).

Precision and bias

Nonconsecutive band counts were made independently by two readers for each specimen used in the study without prior knowledge of the skate's length or of previous counts. A Tukey test was used to test for differences between ages. Age determination bias between readers was assessed through the use of an age-bias plot. This type of graph displays band counts of one reader against a second reader in reference to an equivalence line. Specifically, reader 2 is represented as mean age and 95% confidence intervals corresponding to each of the age classes estimated by reader 1 (Campana et al., 1995). Divergence from the equivalence line, where reader 1 = reader 2, would indicate a systematic difference between readers. Precision estimates of each reader were calculated by using the coefficient of variation (CV) as described by Chang (1982) and Campana et al. (1995).

³ NEFSC (Northeast Fisheries Science Center). 1999. 30th Northeast regional stock assessment workshop. NEFSC, 166 Water Street, Woods Hole, MA 02543-1026.

⁴ NMFS (National Marine Fisheries Service). 2002. Annual report to Congress on the status of U.S. fisheries 2001, 142 p. NMFS, NOAA, Silver Spring, MD 20910.

Marginal increment analyses

The annual periodicity of band pair formation was investigated using marginal increment analyses (MIA). Because the annuli in older adult specimens were compressed, marginal increments were calculated from randomly selected juvenile specimens (Simpfendorfer, 1993; Sulikowski et al., 2003). For MIA, the distance of the final opaque band and the penultimate opaque band, from the centrum edge, was measured with a compound microscope and optical micrometer. The marginal increment was calculated as the ratio of the distance between the final and penultimate bands (Branstetter and Musick, 1984; Caillet, 1990; Simpfendorfer, 1993; Simpfendorfer et al., 2000; Sulikowski et al., 2003). Average increments were plotted by month of capture to identify trends in band formation, and a Kruskal-Wallis one-way analysis of variance on ranks was used to test for differences in marginal increment by month (Simpfendorfer et al., 2000; Sulikowski et al., 2003).

Growth estimates

A von Bertalanffy growth function (VBGF) was fitted to the data with the following equation (von Bertalanffy, 1938):

$$L_t = L_\infty(1 - e^{-k(t-t_0)}),$$

where L_t = total length at time t (age in years);

L_∞ = theoretical asymptotic length;

k = Brody growth constant; and

t_0 = theoretical age at zero length.

The VBGF was calculated by using FISH-PARM, a computer program for parameter estimation of nonlinear models with Marquardt's (1963) algorithm for least-square estimation of nonlinear parameters (Prager et al., 1987).

Results

Morphological measurements

Out of the 320 specimens collected, a total of 224 were used for our study (Table 1). Males ($n=103$) ranged between 29 and 103 cm TL, 18–75 mm DW, and 0.125–10.5 kg body weight (data not shown), whereas females ($n=121$) ranged between 31 and 105 cm TL, 18–74 cm DW, and 0.170–11.4 kg body weight (data not shown). Total length, disk width, and body weight were strongly correlated in males, females, and when data from the sexes were combined (all coefficient of determination [r^2] values were greater than 0.87).

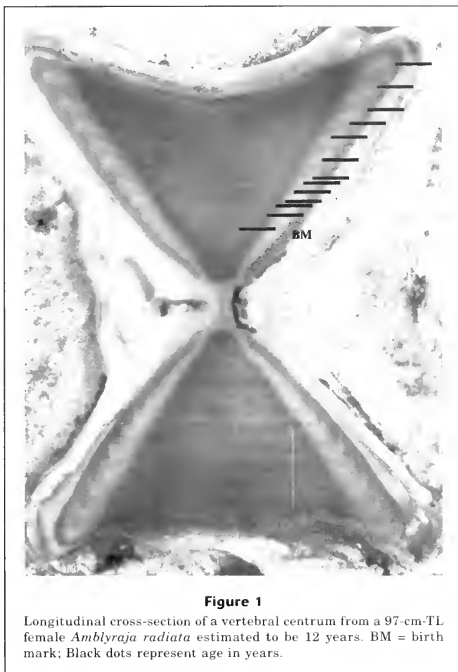


Figure 1

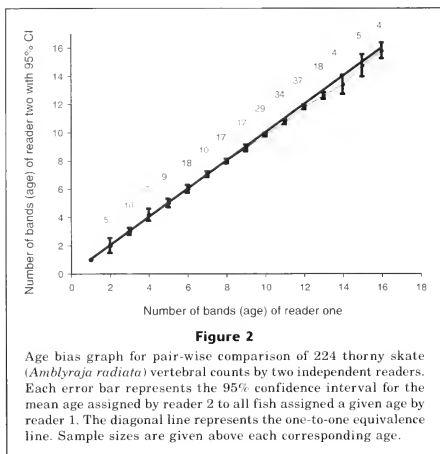
Longitudinal cross-section of a vertebral centrum from a 97-cm-TL female *Amblyraja radiata* estimated to be 12 years. BM = birth mark; Black dots represent age in years.

Vertebral analyses

Comparison of counts between two readers indicated no appreciable bias in the counting process (Fig. 2) and the coefficient of variation for all sampled vertebrae was 2.8%. This level of precision is considered acceptable (Campana, 2001) and counts generated by both readers were combined (averaged) for the analyses (Skomal and Natanson, 2003).

The relationship between TL and centrum diameter was linear ($r^2=0.93$; $P<0.05$) and there were no significant differences in this relationship (ANCOVA, $P<0.05$) between males and females. Because no significant difference existed between TL and centrum diameter between the sexes, these data were combined (Fig. 3).

A total of 120 skates (10 per month) were used for marginal increment analyses. Marginal increments were significantly different between months (Kruskal-Wallis $P<0.001$); there was a distinct trend of increasing

**Table 1**

Average total length (TL) and disc width (DW) at age for male and female thorny skates (*A. radiata*). Sizes are presented as mean \pm 1 SEM; sample sizes are given in parentheses.

Age (years)	Male TL (cm)	Female TL (cm)	Sexes combined	Male DW (cm)	Female DW (cm)	Sexes combined
2	33 (5) \pm 1		33 (5) \pm 1	23 \pm 1		2 \pm 1
3	37 (3) \pm 1	37 (7) \pm 1	37 (10) \pm 1	26 \pm 1	27 \pm 0	27 \pm 1
4	43 (5) \pm 1	42 (2) \pm 2	42 (7) \pm 1	29 \pm 0	29 \pm 1	29 \pm 1
5	48 (2) \pm 2	49 (7) \pm 2	48 (9) \pm 1	33 \pm 0	35 \pm 0	34 \pm 1
6	64 (1) \pm 1	54 (17) \pm 1	54 (18) \pm 1	44 \pm 0	39 \pm 2	39 \pm 2
7	69 (5) \pm 1	62 (5) \pm 3	64 (10) \pm 1	50 \pm 1	44 \pm 2	47 \pm 1
8	71 (6) \pm 1	73 (11) \pm 2	72 (17) \pm 2	52 \pm 1	53 \pm 2	53 \pm 1
9	78 (9) \pm 1	78 (8) \pm 2	78 (17) \pm 1	57 \pm 2	57 \pm 1	57 \pm 1
10	86 (14) \pm 1	82 (15) \pm 1	84 (29) \pm 1	63 \pm 2	60 \pm 1	61 \pm 1
11	88 (17) \pm 1	89 (17) \pm 1	89 (34) \pm 1	65 \pm 1	65 \pm 1	65 \pm 1
12	93 (18) \pm 1	92 (19) \pm 0	92 (37) \pm 1	68 \pm 1	66 \pm 1	67 \pm 1
13	99 (10) \pm 1	95 (8) \pm 1	97 (18) \pm 1	73 \pm 1	68 \pm 1	70 \pm 1
14	97 (3) \pm 3	98 (1) \pm 0	96 (4) \pm 2	70 \pm 2	70 \pm 0	70 \pm 1
15	102 (2) \pm 1	101 (3) \pm 0	101 (5) \pm 1	70 \pm 1	74 \pm 2	74 \pm 1
16	101 (3) \pm 2	105 (1) \pm 0	102 (4) \pm 2	75 \pm 1	70 \pm 1	75 \pm 1

monthly increment growth that peaked in July, followed by a large decline in August (Fig. 4). Based on this information, the increment analyses support the likelihood that a single opaque band may be formed annually on vertebral centra during August or September. The

marginal analysis was only conclusive for juvenile-size animals (skates \leq 80 cm TL). As thorny skates matured, their growth slowed dramatically and the band counts in older specimens became compressed, making it difficult to discern monthly changes in margin width.

Age and growth estimates

The von Bertalanffy growth curves (VBGC) fitted to total length-at-age data (Fig. 5) provided a reasonable fit with a low standard error for males, females, and both sexes combined (Table 2). Furthermore, the VBGC parameters for males, females, and the sexes combined were similar, and because no differences in age-at-size existed between males and females ($P > 0.05$ ANOVA), those data were combined (Fig. 5).

Discussion

Precision estimates, the relationship between TL and centrum diameter, and marginal increment analysis support the use of vertebral centra for age analyses of thorny skates captured in the Gulf of Maine (Conrath et al., 2002; Sulikowski et al., 2003). Furthermore, the 2.8% coefficient of variation indicates that our aging method represents a precise approach for the age assessment of *A. radiata* (Campana, 2001). Minimal width of the marginal increment for thorny skates captured in August and September (Fig. 4) supports the hypothesis of annual band formation in this species. Moreover, these results compare favorably to cycles in marginal increments (Sulikowski et al., 2003) and to annual vertebral band patterns in other skate species (Holden and Vince, 1973; Waring, 1984; Natanson, 1993; Zeiner and Wolfe, 1993; Walmsley-Hart et al., 1999; Francis et al., 2001). However, because the band counts of the largest and oldest animals in the population were compressed (too small for us to discern marginal increments from their widths), the marginal increment analysis included only juvenile skates that were ≤ 80 cm total length and the annular nature of the growth bands was verified for only those length groups. Nevertheless, we assumed that as the skates grew larger and older, the annual nature of growth ring deposition continued throughout their lifetime (Conrath et al., 2002).

During 42 sampling trips from June 2001 through May 2002 (approximately three trips per month), individuals < 30 cm TL were rarely captured. The lack of specimens in this size class and smaller size classes was most likely due to the mesh size of the commercial trawl nets. Trawl nets used by commercial fishermen in the Gulf of Maine are restricted to a 6½-inch diamond mesh-size opening, which facilitates the release of most fish below 30 cm TL.

Our estimates of L_{∞} exceed the largest specimens in our field collections for both females and males. Growth parameters estimated from the Gompertz and logistics equations also produced over-estimations of L_{∞} for the

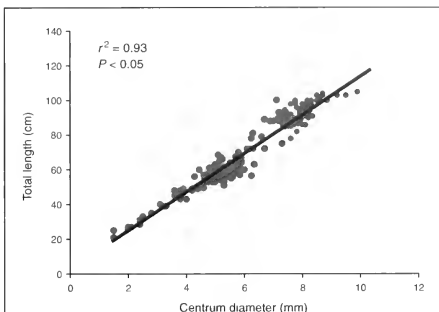


Figure 3
The relationship of total length (cm) to centrum diameter (mm) for combined sexes of thorny skate (*Amblyraja radiata*).

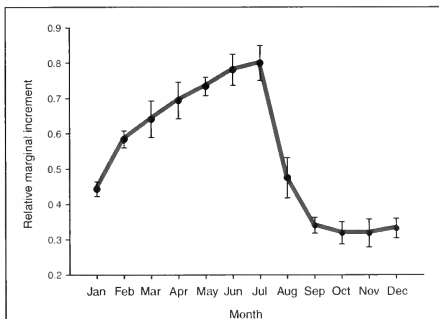


Figure 4
Mean monthly marginal increments of opaque bands for *Amblyraja radiata* from the Gulf of Maine. Marginal increments were calculated each month from 10 specimens whose centra contained less than 10 annuli. Error bars represent $1 \pm \text{SEM}$.

thorny skates in our study. Because the von Bertalanffy growth curve (VBGC) is most widely used and accepted in elasmobranch age and growth studies, we chose to use this function to fit our data. Over estimation of L_{∞} with the VBGC has been documented in most skate species studied to date (Table 3). Campana (2001) suggested that the smallest and largest specimens are the most influential in the estimation of growth. Moreover, both Walmsley-Hart et al. (1999) and Sulikowski et

al. (2003) suggested that rareness of large individuals was most likely responsible for their over estimation of L_{∞} . Similarly, in a study of the blue shark (*Prionace glauca*) in the northwest Atlantic, Skomal and Natanson (2003) suggested that earlier studies on the same species contained artificially inflated L_{∞} estimates and lower growth rates because of the lack of maximum-size fish. The rareness of large specimens in our study may have been due to these larger individuals being able to avoid the fishing gear or may indicate that mortality, natural or fishing induced, prevents them from attaining these lengths. Exploratory manipulation of our data indicated that inclusion of maximum observed sizes (i.e., thorny skates over 103 cm TL) produced divergent results with regard to von Bertalanffy parameters. For example, the addition of maximum-size fish, using 20 years as the maximum age (Templeman, 1984) and 105 cm as the maximum total length (from the present study), reduced the combined sex L_{∞} from 124 cm TL to 116 cm TL. However, the same effect was not documented when adding hatching size (age zero) fish (note: because no documented size for thorny skates exists within the Gulf of Maine, the authors used known hatching sizes for a similar congener species, the winter skate (*Leucoraja ocellata*). Be that as it may, the reasonable fit of the thorny skate data (Table 2) to the VBGC (Fig. 5) for *A. radiata*, along with a comparison with other batoid studies (Table 3), indicates that this is an appropriate model for this skate species.

Growth rates were similar for both sexes of thorny skate ($k=0.13$ for females and $k=0.11$ for males) and commensurate with other skate species of a similar size. The oldest age obtained for male and female thorny skates was 16 years (Table 1). These data are in agreement with the assumption that larger batoids, such as *A. radiata*, *R. pullopunctata* (Walmsley-Hart et al., 1999), and *L. ocellata* (Sulikowski et al., 2003) are longer lived and slower growing than smaller species. For instance, *R. erinacea*, which reaches a total length of 52 cm, has been aged to 8 years and found to have

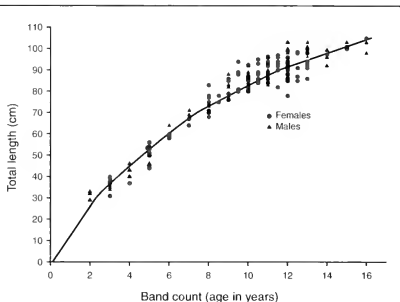


Figure 5

Von Bertalanffy growth curve generated from combined vertebral data for female and male thorny skates (*Amblyraja radiata*) from the western Gulf of Maine. Individual VBGC parameters are given in Table 2.

a corresponding k value of 0.352 (Johnson, 1979; Warner, 1984).

The reduction in biomass of the thorny skate below threshold levels mandated by the SFA necessitates the development of management measures to rebuild these stocks in accordance with the Magnuson-Stevens Fishery Conservation and Management Act. However, the development and implementation of a successful fisheries management plan for the species require in-depth analyses of appropriate biological information. Moreover, accurate stock assessment data for skates is difficult to collect in the northeast U.S. because individual species are rarely differentiated in landings information (NEFMC^{1,2}). As a result, fluctuations in stock size will continue to be difficult to detect and successful implementation of fisheries management plans will remain problematic. This article is the first in a series aimed at providing life history data for the management of thorny skates indigenous to the Gulf of Maine. The basic age and growth parameters for the thorny skate provided in the present study support the hypothesis that *A. radiata*, like other elasmobranchs, require conservative management because of their slow growth rate and susceptibility to over-exploitation (Brander, 1981; Kusher et al., 1992; Zeiner and Wolf, 1993; Frisk et al., 2001; Sulikowski et al., 2003).

Table 2

Calculated von Bertalanffy parameters for male, female, and combined sexes of *A. radiata*.

Parameter	Male	Female	Combined sexes
L_{∞} (cm TL)	127.00	120.00	124.00
K (year)	0.11	0.13	0.12
t_0 (year)	-0.37	-0.4	-0.35
r^2	0.96	0.92	0.94
SE	0.01	0.01	0.001
n	103.00	121.00	224.00

Acknowledgments

Collection of skates was conducted on the FV *Mystique Lady*. We thank Noel Carlson for maintenance of the fish at the U.N.H. Coastal Marine Laboratory and Matt Ayer for his help in digitizing the vertebrae samples. This

Table 3

Comparison of von Bertalanffy derived L_{∞} to the observed (total lengths L) for a number of skate species. L_{∞} (mm) = disk width.

Scientific name	Sex	L_{∞} (mm)	L observed (mm)	Max. age (yr)	Source
<i>Raja microocellata</i>	♀♂	1370 (TL)	875 ¹	9	Ryland and Ajayi, 1984
<i>Raja montagui</i>	♀♂	978 (TL)	710 ¹	7	Ryland and Ajayi, 1984
<i>Raja clavata</i>	♀	1047 (TL)	1392	7	Ryland and Ajayi, 1984
<i>Raja erinacea</i>	♀♂	527 (TL)	520	8	Waring, 1984
<i>Raja rhina</i>	♂	967 (TL)	1322	13	Zeiner and Wolf, 1993
<i>Raja rhina</i>	♀	1067 (TL)	1047	12	Zeiner and Wolf, 1993
<i>Raja wallacei</i>	♂	405 (DW)	512	15	Walmsley-Hart et al., 1999
<i>Raja wallacei</i>	♀	435 (DW)	571	15	Walmsley-Hart et al., 1999
<i>Raja pullopanctata</i>	♂	771 (DW)	696	18	Walmsley-Hart et al., 1999
<i>Raja pullopanctata</i>	♀	1327 (DW)	747	14	Walmsley-Hart et al., 1999
<i>Raja pullopanctata</i>	♀	1327 (DW)	747	14	Walmsley-Hart et al., 1999
<i>Dipturus nasutus</i>	♀♂	700 (TL)	913	9	Francis et al., 2001
<i>Dipturus innominatus</i>	♀♂	1330 (TL)	1505	24	Francis et al., 2001
<i>Leucoraja ocellata</i>	♀♂	1314 (TL)	936 ¹	19	Sulikowski et al., 2003
<i>Amblyraja radiata</i>	♀♂	1240 (TL)	1020 ¹	16	Present study

¹ Average of male and female observed TL.

project was supported by a Northeast Consortium grant (no. NA16FL1324) to PCWT, JAS, and PDD.

Literature cited

- Brander, K.
1981. Disappearance of common skate *Raja batis* from Irish Sea. *Nature* 290 (5801):48–49.
- Branstetter, S., and J. A. Musick.
1984. Age and growth estimates for the sand tiger in the northwestern Atlantic ocean. *Trans. Am. Fish. Soc.* 123:242–254.
- Brown, C. B., and S. H. Gruber.
1988. Age assessment of the lemon shark, *Negaprion brevirostris*, using tetracycline validated vertebral centra. *Copeia* 3:747–753.
- Casey, J. G., H. L. Pratt, and C. E. Stillwell.
1985. Age and growth of the sandbar shark (*Carcharhinus plumbeus*) from the western North Atlantic. *Can. J. Fish. Aquat. Sci.* 42(5):963–975.
- Casey, J. M., and R. A. Myers.
1998. Near extinction of a large widely distributed fish. *Science* 28:690–692.
- Cailliet, G. M.
1990. Elasmobranch age determination and verification: an updated review. In *Elasmobranchs as living resources: advances in the biology, ecology, systematics and the status of the fisheries* (L. Pratt Jr, S. H. Gruber, and T. Tanuchi (eds.)), p. 157–165. NOAA Tech. Report NMFS 90.
- Campana, S. E.
2001. Accuracy, precision and quality control in age determination including a review of the use and abuse of age validation methods. *J. Fish. Biol.* 59:197–242.
- Campana, S. E., M. C. Annand, and J. I. Mcmillan.
1995. Graphical and statistical methods for determining the consistency of age determinations. *Trans. Am. Fish. Soc.* 124:131–138.
- Chang, W. Y. B.
1982. A statistical method for evaluating the reproducibility of age determination. *Can. J. Fish. Aquat. Sci.* 39:1208–1210.
- Collette, B., and G. Klein-MacPhee, eds.
2002. *Bigelow and Schroeder's fishes of the Gulf of Maine*, 3rd ed., p. 62–66. Smithsonian Institution Press, Washington, D. C.
- Compagno, L. J. V., D. A. Ebert, and M. J. Smale.
1989. *Guide to the sharks and rays of southern Africa*, 158 p. New Holland (Publ.) Ltd., London.
- Conrath, C. L., J. Gelsleichter, and J. A. Musick.
2002. Age and growth of the smooth dogfish, *Mustelus canis*, in the northwest Atlantic. *Fish. Bull.* 100:674–682.
- Dulvey, N. K., J. D. MetCalfe, J. Glanville, M. G. Pawson, and J. D. Reynolds.
2000. Fishery stability, local extinctions, and shifts in community structure in skates. *Cons. Biol.* 14 (1): 283–293.
- Francis, M., C. O. Maolagain, and D. Stevens.
2001. Age, growth, and sexual maturity of two New Zealand endemic skates, *Dipturus nasutus* and *D. innominatus*. *N. Z. J. Mar. Freshw. Res.* 35:831–842.
- Frisk, M. G.
2000. Estimation and analysis of biological parameters in elasmobranch fishes and the population dynamics of the little skate *Raja erinacea*, thorny skate *R. radiata* and Barndoor skate *R. laevis*. M.S. thesis, 112 p. Center for Environmental Science, Univ. Maryland, Cambridge, MD.
- Frisk, M. G., T. J. Miller, and M. J. Fogarty.
2001. Estimation and analysis of biological parameters in elasmobranch fishes: a comparative life history study. *Can. J. Fish. Aquat. Sci.* 58(5):969–981.

- Hoenig, J., and S. H. Gruber.
1990. Life history patterns in the elasmobranchs: implications for fisheries management. In Elasmobranchs as living resources: advances in the biology, ecology, systematics and the status of the fisheries (H. L. Pratt Jr. S. H. Gruber, and T. Tanuchi, eds.), p. 1-16. NOAA Tech. Report, NMFS 90.
- Holden, M. J.
1977. Elasmobranchs. In Fish population dynamics (J. A. Gulland, ed.), p. 187-214. J. Wiley and Sons, London, England.
- Holden, M. J., and M. R. Vince.
1973. Age validation studies on the centra of *Raja clavata* using tetracycline. J. Cons. Int. Explor. Mer 35:13-17.
- Johnson, G. F.
1979. The biology of the little skate, *Raja erinacea*, in Block Island Sound, Rhode Island. Unpubl. M.A. thesis, 119 p. Univ. Rhode Island, Kingston, RI.
- Kusher, D. I., S. E. Smith, and G. M. Cailliet
1992. Validated age and growth of the leopard shark, *Triakis semifasciata*, with comments on reproduction. Environ. Biol. Fish. 35:187-203.
- Magnuson Fishery Conservation and Management Act.
1994. 16 U.S.C. 1801-1882 (1994), amended by Sustainable Fisheries Act, Pub. L. No. 104-297, 110 Stat. 3559 (1996).
- Marquardt, D. W.
1963. An algorithm for the least squares estimation of nonlinear parameters. J. Soc. Ind. Appl. Math. 2: 431-441.
- Natanson, L. J.
1993. Effect of temperature on band deposition in the little skate, *Raja erinacea*. Copeia 1993:199-206.
- Prager, M. H., S. B. Saila, and C. W. Recksiek.
1987. Fishparm: a microcomputer program for parameter estimation of nonlinear models in fishery science. Old Dominion University, Norfolk Virginia, Tech. Rep. (87-10):1-37.
- Robins, C. R., and G. C. Ray.
1986. A field guide to Atlantic coast fishes of North America, 354 p. Houghton Mifflin Co., Boston, MA.
- Ryland, J. S., and T. O Ajayi.
1984. Growth and population dynamics of three *Raja* species (Batoidei) in Carmarthen Bay, British Isles. J. Cons. Int. Explor. Mer 41:111-120.
- Simpfendorfer, C. A.
1993. Age and growth of the Australian sharpnose shark, *Rhizoprionodon taylori*, from north Queensland, Australia. Environ. Biol. Fish. 36(3):233-241.
2000. Age and growth of the whiskery shark, *Furgaleus macki*, from south-western Australia. Environ. Biol. Fish. 58:335-343.
- Skomal, G. B., and L. J. Natanson.
2003. Age and growth of the blue shark (*Prionace glauca*) in the North Atlantic Ocean. Fish. Bull. 101:627-639.
- Sosebee, K.
2000. Skates. Status of fishery resources off the north-eastern United States. NOAA Tech. Mem. NMFS-NE. 115:114-115.
- Sulikowski, J. A., M. D. Morin, S. H. Suk, and W. H. Howell.
2003. Age and growth of the winter skate, *Leucoraja ocellata*, in the Gulf of Maine. Fish. Bull. 101:405-413.
- Templeman, W.
1984. Migrations of thorny skate, *Raja radiata*, tagged in the Newfoundland area. J. Northw. Atl. Fish. Sci. 5(1):55-63.
1987. Differences in sexual maturity and related characteristics between populations of thorny skate *Raja radiata* in the northwest atlantic. J. Northw. Atl. Fish. Sci. 44 (1):155-168.
- Von Bertalanffy, L.
1938. A quantitative theory of organic growth (inquiries of growth laws II). Human Biology 10:181-183.
- Walmsley-Hart, S. A., W. H. H. Sauer, and C. D. Buxton.
1999. The biology of the skates *Raja wallacei* and *R. pullopunctata* (Batoidea: Rajidae) on the Agulhas Bank, South Africa. S. Afr. J. Mar. Sci. 21:165-179.
- Waring, G. T.
1984. Age, growth and mortality of the little skate off the northeast coast of the United States. Trans. Am. Fish. Soc. 113:314-321.
- Winemiller, K. O., and K. A. Rose.
1992. Patterns of life history diversification in North American fishes: implication for population regulation. Can. J. Fish. Aquat. Sci. 49:2196-2218.
- Wintner, S. P., and G. Cliff.
1996. Age and growth determination of the blacktip shark, *Carcharhinus limbatus*, from the east coast of South Africa. Fish. Bull. 94 (1):135-144.
- Zeiner, S. J., and P. G. Wolf.
1993. Growth characteristics and estimates of age at maturity of two species of skates (*Raja binoculata* and *Raja rhina*) from Monterey Bay, California. In Conservation biology of elasmobranchs (S. Branstetter, ed.), p. 87-90. NOAA Tech. Report NMFS 115.

Abstract—Age estimates for striped trumpeter (*Latris lineata*) from Tasmanian waters were produced by counting annuli on the transverse section of sagittal otoliths and were validated by comparison of growth with known-age individuals and modal progression of a strong recruitment pulse. Estimated ages ranged from one to 43 years; fast growth rates were observed for the first five years. Minimal sexual dimorphism was shown to exist between length, weight, and growth characteristics of striped trumpeter. Seasonal growth variability was strong in individuals up to at least age four, and growth rates peaked approximately one month after the observed peak in sea surface temperature. A modified two-phase von Bertalanffy growth function was fitted to the length-at-age data, and the transition between growth phases was linked to apparent changes in physiological and life history traits, including offshore movement as fish approach maturity. The two-phase curve was found to represent the mean length at age in the data better than the standard von Bertalanffy growth function. Total mortality was estimated by using catch curve analysis based on the standard and two-phase von Bertalanffy growth functions, and estimates of natural mortality were calculated by using two empirical models, one based on longevity and the other based on the parameters L_{∞} and k from both growth functions. The interactions between an inshore gillnet fishery targeting predominately juveniles and an offshore hook fishery targeting predominately adults highlight the need to use a precautionary approach when developing harvest strategies.

Age validation, growth modeling, and mortality estimates for striped trumpeter (*Latris lineata*) from southeastern Australia: making the most of patchy data

Sean R. Tracey

Jeremy M. Lyle

Marine Research Laboratories
Tasmanian Aquaculture and Fisheries Institute
Private Bag 49
Hobart 7001, Tasmania, Australia
E-mail address (for S.R. Tracey) stracey@utas.edu.au

Striped trumpeter (*Latris lineata*) are widely distributed around the temperate latitudes of southern Australia, New Zealand (Last et al., 1983), the Gough and Tristan Da Cunha Island groups in the southern Atlantic Ocean (Andrew et al., 1995), and the Amsterdam and St. Paul Island groups in the southern Indian Ocean (Duhamel, 1989). They are opportunistic carnivores associated with epibenthic communities over rocky reefs at moderate depths from 5 to 300 m along the continental shelf. The species can grow to a relatively large size, 1200 mm in total length and 25 kg in weight (Gomon et al., 1994). Spawning apparently occurs offshore, and females are highly fecund multiple-spawners (Furlani and Ruwald, 1999). Although there have been a number of ichthyoplankton surveys in Tasmanian waters, only a few striped trumpeter larvae have been collected, caught during the late austral winter through early spring months at near-shore (30–50 m) and shelf edge sites (~200 m) (Furlani and Ruwald, 1999). Larval rearing trials have shown that the presettlement phase is complex and extended; individuals can remain in this neritic-pelagic phase for up to 9 months after hatching before metamorphosis into the juvenile stage takes place (Morehead¹). As juveniles striped trumpeter settle on shallow rocky reefs.

In Tasmania striped trumpeter are taken commercially over inshore reefs (5 to 50 m), generally as a by-

catch of gillnetting, and are targeted with hook methods (handline, drop-line, longline, and trotline) on deeper reefs (80 to 300 m). Small, subadult individuals dominate inshore catches, whereas larger individuals are taken from offshore reefs. In recent years the combined annual commercial catch has been typically less than 100 metric tons (Lyle²). Striped trumpeter also attract significant interest from recreational fishermen, who use both hooks and gill nets. Furthermore, the aquaculture potential for this species is currently being assessed in Tasmania (Furlani and Ruwald, 1999; Cobcroft et al., 2001). Despite wide interest in this species, there is a general paucity of information on age, growth, and stock structure of wild populations.

Assessing the growth of a species is a fundamental part of fisheries population dynamics. Ever since Beverton and Holt (1957) introduced the von Bertalanffy growth model to fisheries research it has become ubiquitous in descriptions of the increase in size

Manuscript submitted 20 December 2003
to the Scientific Editor's Office.

Manuscript approved for publication
7 September 2004 by the Scientific Editor.
Fish. Bull. 103:169–182 (2005).

¹ Morehead, D. 2003. Personal commun. Tasmanian Aquaculture and Fisheries Institute, Univ. Tasmania, GPO Private Bag 49, Hobart, Tasmania, Australia 7001.

² Lyle, J. M. 2003. Tasmanian scalefish fishery—2002. Fishery assessment report of the Marine Research Laboratories, Tasmanian Aquaculture and Fisheries Institute, Tasmania. [Available from TAFI GPO Private Bag 49, Hobart, Tasmania, Australia 7001.]

of a species as a function of age. The parameters common to the von Bertalanffy growth function (VBGF) are used in stock assessment models such as empirical derivatives of natural mortality (Pauly, 1980) and assessments of yield per recruit and spawning stock biomass (Beverton and Holt, 1957). Despite the von Bertalanffy growth parameters being well established as cornerstones of many stock assessment models, several authors have highlighted limitations of the original derivation of the growth function to adequately represent growth of a population (Knight, 1968; Sainsbury, 1979; Roff, 1980; Schnute, 1981; Bayliff, et al, 1991; Hearn and Polacheck, 2003). This limitation becomes especially evident with limited or patchy data. The limitations of the von Bertalanffy growth function have created three scenarios: 1) use the VBGF and retain the use of the parameters to derive per-recruit estimates at the possible expense of physiological integrity; 2) derive or employ a model that is not based on the von Bertalanffy parameters (such as a linear or logistic model) or another polynomial function (for instance, the Gompertz equation [Schnute, 1981]) and in doing so the expediency of the von Bertalanffy parameters in stock assessments is compromised; 3), use or develop an extension of the von Bertalanffy equation with the caveat that, by introducing additional parameters, the problem of reduced parsimony by over parameterisation would need to be considered.

While investigating the life history characteristics of striped trumpeter, we became aware that the original description of the VBGF would not adequately represent growth of this species, in part because of the patchy data available for analysis.

This study aims to describe the age and growth of striped trumpeter from Tasmania. Seasonal growth oscillations are considered for the first four years by using actual length-at-age data from a strong cohort. We then employ and evaluate an extension of the VBGF that offers a better fit to the sample population of aged individuals and allows the flexibility of assigning representative growth and mortality parameters to different life phases of the population. Growth parameters derived from both the standard von Bertalanffy and extended von Bertalanffy models are used in our catch curve analyses, and the empirical models of Pauly (1980) and Hoenig (1983) are used to allow comparison of mortality estimates.

Materials and methods

Striped trumpeter were collected opportunistically from various sites off the east and southeast coasts of Tasmania from a variety of fisheries dependent and independent sources spanning the period 1990–2002 (Table 1). Inshore catches were predominately taken with gill nets ranging in mesh sizes from 64 to 150 mm. Offshore catches were taken by hook-and-line methods. Samples ranged from intact specimens, for which the full range of biological information was collected, to processed frames

Table 1

Composition of Tasmanian sampling data from 1990 through 2002 showing data from inshore gill net and offshore hook fisheries. Numbers in parentheses represent the number of individuals aged from each particular sampling regime.

Year	Gill net	Hook	Total
1990	—	45	45
1991	—	332	332
1992	—	126	126
1994	3	8	11
1995	228	12	240
1996	529	55	585
1997	193	2	195
1998	7	171	178
1999	205	902	1107
2000	—	91	91
2001	—	60	60
2002	—	97	99
Total	1165 (268)	1901 (508)	3069 (776)

from which length and, depending on condition of the body, sex and gonad weight were recorded. All specimens were measured for fork length (± 1 mm) and, where possible, total weight was recorded (± 1 gram). Otoliths were collected when possible. This *ad hoc* sampling approach created a temporally irregular data set.

Kolmogorov-Smirnov tests ($\alpha=0.05$) were used to determine whether significant differences existed between male and female length-frequency distributions or between length-frequency distributions by depth strata.

Analysis of residual sums of squares (Chen, 1992) was used to determine whether a significant difference existed between the sex-specific length-weight relationships that were fitted by minimizing the sum of square residuals and that are described by the power function

$$W = aL^b, \quad (1)$$

where W = whole weight (g);

L = fork length (mm); and

a and b = constants.

Sex ratios were compared for significant deviation from 1:1 by chi-square tests.

Aging technique

Sagittal otoliths were removed from 873 individuals and a subsample of 295 otoliths were individually weighed to the nearest milligram. One randomly selected otolith from each fish was embedded in clear polyester casting resin. A transverse section was taken through

the primordial region (width approximately 300 μm) and mounted on a microscope slide. A stereo dissecter microscope at 25 \times magnification was used to aid the interpretation of increments in the mounted sections. Increment measurements were made by using Leica IM^o image digitization and analysis software (Leica Microsystems, Wetzlar, Germany). All counts and increment measurements were made without knowledge of fish size, sex, or date at capture to avoid reader bias.

Position of the first annual increment was determined by testing the close correspondence of otolith microstructure and body size between known-age individuals reared from eggs in aquaria and wild-caught specimens. To ensure that growth in cultured individuals also reflected growth in wild specimens, a hypothesis of comparable growth was tested by fitting traditional VBGFs to the length-at-age data of 288 cultured individuals (maximum known age: 4 years) and 268 wild specimens (maximum otolith-derived age: 4 years). A likelihood ratio test (Kimura, 1980) was then used to test for significance. The VBGF model was in the form

$$L_t = L_\infty(1 - e^{-k(t-t_0)}) + \varepsilon \quad (2)$$

where L_t = length at age t ;

L_∞ = average asymptotic length;

k = a constant describing how rapidly L_∞ is achieved;

t_0 = the theoretical age where length equals zero; and

ε = independent normally distributed (0, σ^2) error term.

Modal progression of length frequencies from a strong cohort of juvenile fish was sampled over a three-year period (1995–97). This cohort provided an opportunity to validate annual periodicity in increment deposition. By applying an aging protocol based on position of the first increment and assuming that each opaque+translucent zonal pair represented one year of growth, this recruitment pulse could be tracked over seven years in age-frequency progression.

A random subsample of 335 otoliths was read a second time by the primary reader, and a second subsample of 46 otoliths by a second reader, both experienced in otolith interpretation. Precision was assessed by determining percentage agreement between repeated readings, age bias plots (Campana et al., 1994), and calculating the average percent error (APE) (Beamish and Fournier, 1981).

Growth modeling

The length-frequency progression of a strong and discrete cohort of fish indicated that striped trumpeter may be subject to seasonal growth variability. This variability was described by integrating a sinusoidal function (Pitcher and MacDonald, 1973; Haddon, 2001) into a standard VBGF and by applying this function to the actual weekly length-at-age data of individuals

sampled from the strong 1993 cohort over the period 1995 through 1997, where the model was described as

$$L_t = L_\infty \left(1 - e^{-C \cos\left(\frac{2\pi(t-S)}{52}\right) + k(t-t_0)} \right) + \varepsilon \quad (3)$$

where C = the magnitude of the oscillations above and below the nonseasonal growth curve of the sinusoidal cycle;

S = the starting point in weeks of the sinusoidal cycles; and

52 = the cycle period in weeks.

The timing of seasonal growth was compared with weekly average sea surface temperature (SST) on the southeast coast of Tasmania over the sampling period, calculated by using optimum interpolation (Reynolds et al., 2002) of raw remotely sensed data from the area (NOAA-CIRES³). A sine function was fitted to the weekly average SST by using least squares regression to compare the timing and phase of growth and temperature and test for a significant correlation.

All individuals aged were assigned a "decimal" age, where the decimal portion represented the proportion of the year between a nominal average date of spawning (1st October) and the date of capture. We assumed a nominal peak spawning date of 1 October based on an assessment of monthly averaged gonadosomatic index (Tracey, unpubl. data), which is consistent with that observed for wild-caught broodstock held under ambient conditions (Morehead¹).

Growth of the sampled population was initially described by using the standard von Bertalanffy growth function (Eq. 2). However, a preliminary visual assessment of the fit suggested it did not produce an adequate representation of the entire data set. In an attempt to find a model that better represented the data, the fit of the standard von Bertalanffy growth function (VBGF_s) was compared with an extension of the traditional von Bertalanffy growth model fitted by minimization of the sum of negative log-likelihood; normal distribution of the error term. The model chosen was similar to that used by Hearn and Polacheck (2003) and involved fitting a VBGF function either side of an age at transference, described as

$$L_t = \begin{cases} (L_{-1}(1 - e^{-k_1(t-t_{01})}) + \varepsilon & \text{for } t < t^\delta \\ (L^\delta + (L_{+2} - L^\delta)(1 - e^{-k_2(t-t_{02})}) + \varepsilon & \text{for } t \geq t^\delta \end{cases} \quad (4)$$

³ Data sourced from the NOAA-CIRES Climate Diagnostics Center, Boulder, CO 80305. <http://www.cdc.noaa.gov/>. [Accessed 15 Sep. 2002]

where $L_{\infty 1}$, k_1 , t_{01} = VBGF parameters applied to the first growth phase;

$L_{\infty 2}$, k_2 , t_{02} = VBGF parameters applied to the second growth phase;

L^b = length of transference from one growth phase to the next; and

t^b = age of transference from one growth phase to the next; calculated as,

$$t^b = t_{01} - \frac{1}{k_1} \ln \left(1 - \frac{L_t}{L_{\infty 1}} \right). \quad (5)$$

Having fitted Equation 4, we smoothed the discontinuity from the first growth stanza to the second, assuming normal distribution around the age at transference by integrating a normal probability cumulative distribution function (PDF) where the mean is equal to the age of transference (4.4 years) and where the standard deviation is arbitrarily set at 1.0. This model is referred to as the two-phase von Bertalanffy growth function (VBGF_{TP}) and is now represented as

$$L_t = \begin{cases} \left(1 - \int_{t-t_0}^{t^b} \frac{1}{\sigma\sqrt{2\pi}} e^{-\frac{(t-t_0)^2}{2\sigma^2}} \right) \left(L_{\infty 1} (1 - e^{-k_1(t-t_0)}) + \varepsilon \right) + \\ \left(\int_{t-t^b}^{t_{max}} \frac{1}{\sigma\sqrt{2\pi}} e^{-\frac{(t-t^b)^2}{2\sigma^2}} \right) \left(L^b + (L_{\infty 2} - L^b) (1 - e^{-k_2(t-t^b)}) + \varepsilon \right) \end{cases}, \quad (6)$$

where t_{max} = maximum age present in the sample; and

σ^2 = standard deviation of cumulative density function with mean t^b .

The model that best represented the data was judged on a combination of parsimony as determined by the Akaike information criterion (AIC) (Akaike, 1974), quality of fit by minimization of the negative log-likelihood value derived from each model, visual inspection of the residuals, and as an index of fit, the percent deviation of L_{∞} for each model from the maximum observed length (L_{max}).

The hypothesis of sexual dimorphism in growth was tested by using likelihood ratio tests (Kimura, 1980) for both the VBGF_S and VBGF_{TP} models fitted to the length-at-age data of all individuals whose sex had been determined.

Mortality estimation

Mortality estimates were calculated by using the parameters of both the VBGF_S and VBGF_{TP} functions. An estimate of instantaneous rate of total mortality (Z) for the offshore hook fishery was calculated for 1998 by applying a length converted catch curve analysis (LCCCA *sensu* Pauly, 1983) to the length-frequency data.

Estimates of instantaneous rate of natural mortality (M) were calculated by using two empirical equations. The first equation, derived by Pauly (1980), is described as

$$\log_{10} M = -0.0066 - 0.279 \log_{10} L_{\infty \gamma} + 0.6543 \log_{10} k_{\gamma} + 0.4634 \log_{10} T, \quad (7)$$

where $L_{\infty \gamma}$ and k_{γ} = parameters derived from the VBGF_S or from the second growth phase of the VBGF_{TP}; and

T = average annual sea surface temperature (°C) at the area of capture.

The mean annual sea surface temperature on the east coast of Tasmania in 1998 was estimated as 14°C (NOAA-CIRES⁵). The second equation used was the regression equation of Hoenig (1983):

$$\ln Z = 1.46 - 1.01 \ln t_{max}; \quad M-Z \text{ assuming } F=0, \quad (8)$$

where t_{max} = the maximum age for the species in years.

Estimates of fishing mortality (F) were calculated by subtracting natural mortality from total mortality.

Results

Males ranged in length from 203 mm to 815 mm ($n=504$) and females ranged from 269 mm to 950 mm ($n=565$). Length-frequency distributions did not differ significantly between sexes (Kolmogorov-Smirnov; $Z=0.91$ $P=0.38$).

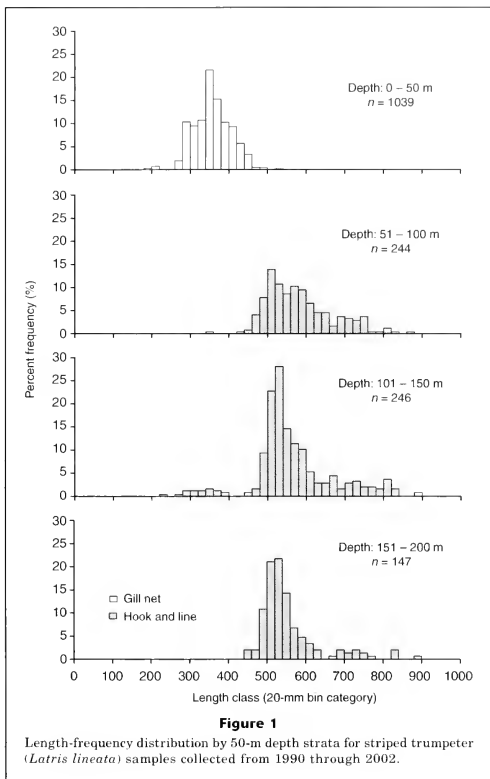
Pooling the length-frequency data of all individuals produced a bimodal frequency distribution. However, when grouped by depth (Fig. 1), the data revealed a significant depth-based stratification between the shallow (<50 m stratum) and the deeper strata (Kolmogorov-Smirnov; $Z=13.8$ $P<0.001$), occurring at around 450 mm in length.

Analysis of residual sums of squares indicated no significant difference between the sex-specific length-weight relationships ($F=0.02$ $df=2$ $P=0.10$); consequently a power regression was applied to the length-weight data of all individuals combined (Table 2).

The sex ratio of males to females (1.0:1.3) from the inshore net fishery showed a low level of significant difference from 1:1 ($\chi^2=3.88$ $P=0.049$ $n=232$), whereas, the ratio of males to females (1.0:1.1) caught from the offshore hook fishery did not show significant difference from 1:1 ($\chi^2=0.933$ $P=0.334$ $n=840$).

Age estimates

Age was successfully estimated for 776 (89%) individuals. Transverse otolith sections showed typical distinct alternate light and dark zone formations within the

**Table 2**

Predictive equations used to compare weight and length, otolith weight and age, and reader variability across age classes, for striped trumpeter (*Latris lineata*).

Dependent variable	Independent variable	n	Equation	r ²
Weight (W)	Fork length (L)	491	$W = 2 \times 10^{-5} \times L^{3.00}$	0.99
Otolith weight (OW)	Age (t)	295	$OW = 7.32 + (1.70 \times t)$	0.89
Primary reader, count 2 (P ₂)	Primary reader, count 1 (P ₁)	339	$P_2 = 0.05 + (0.99 \times P_1)$	0.99
Secondary reader, count 1 (S ₁)	Primary reader, count 1 (P ₁)	46	$S_1 = 0.27 + (0.97 \times P_1)$	0.97

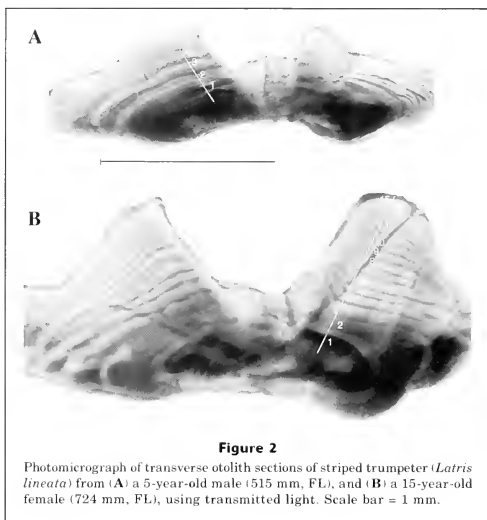


Figure 2

Photomicrograph of transverse otolith sections of striped trumpeter (*Latris lineata*) from (A) a 5-year-old male (515 mm, FL), and (B) a 15-year-old female (724 mm, FL), using transmitted light. Scale bar = 1 mm.

otolith matrix. Viewed under transmitted light the zones showed as dark (opaque) and light (translucent) (Fig. 2). A robust linear relationship existed between otolith mass and individual age (Table 2).

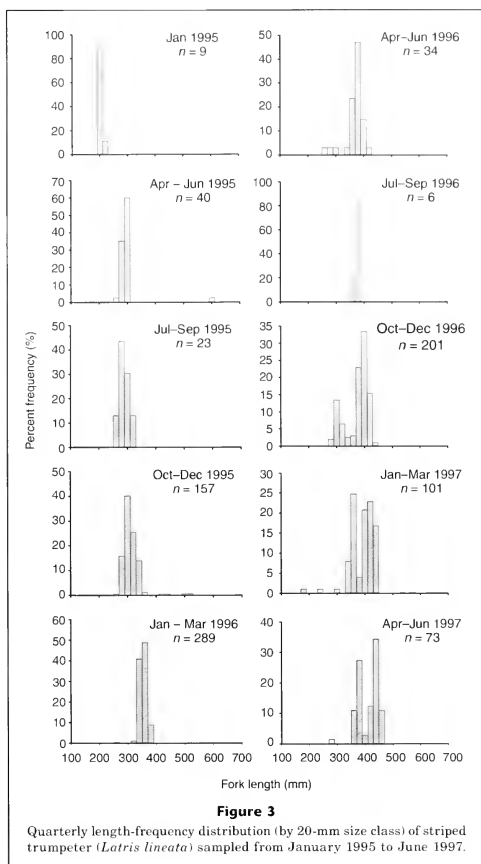
The core area of each section consisted of an opaque region. Immediately adjacent to this was a faint thin translucent zone followed by the first broad opaque annual increment. In some cases the transition from core to the first expected increment could not be discerned because of a continuation of the opaque region (the expected thin translucent zone was too faint to see). In such cases, increment measurements were required to ensure that the annulus was not overlooked. Mean increment radius (\pm SD) from the primordia to the first annulus was $491 \pm 63 \mu\text{m}$ ($n=122$); and the deposition of the second annulus occurred at a mean radius of $733 \pm 55 \mu\text{m}$ ($n=122$). The next four opaque and translucent zone pairs were relatively broad compared with subsequent zones that consistently narrowed as they approached the growing edge (Fig. 2).

To validate the first increment we compared somatic and otolith growth of wild individuals with that of individuals cultured under ambient conditions. Larval-rearing trials of striped trumpeter juveniles have produced mean lengths of 190 mm at 14 months and 261 mm at 24 months. The smallest individuals recorded from the wild in our study were 190–220 mm and were captured in January 1995. From the rearing trials it seemed

reasonable to assume that the wild-caught individuals of this size were between 1 and 2 years of age. If a birth date of 1 October is assumed, these individuals would have been about 16 months old and therefore were spawned in 1993. Viewing the sectioned otoliths of these small wild-caught individuals revealed only one increment within the margin, analogous to the increment composition of cultured individuals at a similar length.

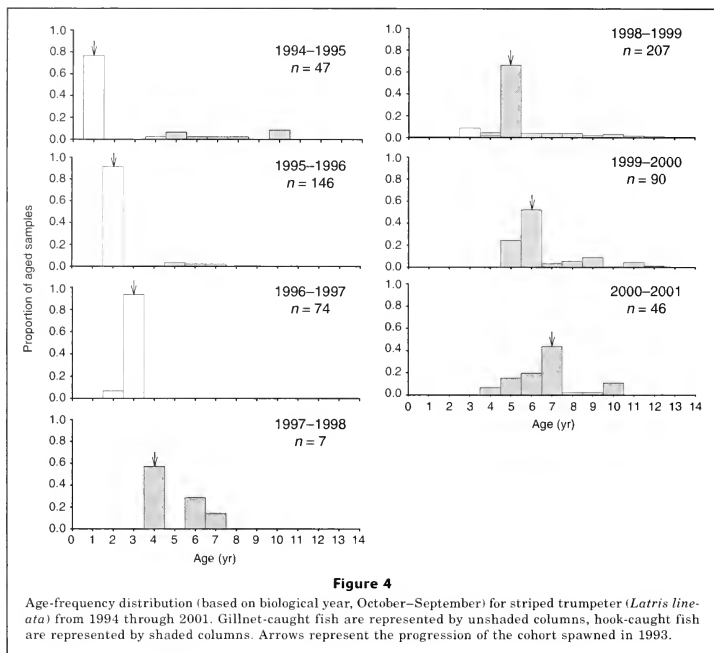
To test for comparable growth between wild and cultured individuals as a means to facilitate confident validation of the first increment deposition, von Bertalanffy growth curves were fitted to length-at-age data of both wild (based on otoliths) and cultured individuals (of known age) to age four. A likelihood ratio test indicated that wild-caught individuals increased in length slightly faster than those cultured to the same age ($\chi^2=5.3$ df=6 $P=0.51$); however, this trend was not significant ($F=4.4$ df=23 $P=0.04$).

Tracking length-frequency distributions (Fig. 3) from 1995 through 1997, from inshore gillnet samples, revealed progression of a strong cohort. Based on its size structure, the spawning year for this cohort was assumed to be 1993. A second cohort was evident in the last quarter of 1996, assumed to have been spawned in 1994. The progression of the cohort spawned in 1993 was clearly evident in the age structure of the samples over the period 1995–2001, proving useful in the valida-



tion of annual periodicity (Fig. 4). However, inferences about population age structure cannot be drawn from the age-frequency histograms because some sample sizes were low and there was discriminatory sampling (by gear type) over the period. For instance up to 1996-97 most of the aged samples were from inshore gillnet catches, whereas subsequent samples were derived primarily from hook catches.

Precision of repeated age estimation was high. Second readings by the primary reader were 79% in agreement with first readings, yielding an APE of 0.93%. Eighteen percent of second readings gave rise to a one-year difference and 3% of second readings differed by 2 years, and no significant tendency to overestimate or underestimate age was evident. An age bias plot did not differ significantly from 1:1 for the primary reader (Table 2).



Precision of the second reader's age estimates when compared with those of the primary reader were also satisfactory, yielding an APE of 1.59%, and no significant bias was revealed at any age class (Table 2).

The maximum observed ages for males and females were 29 and 43 years, respectively. From the available data, it is unclear whether apparent differences in longevity between the sexes are representative because very few individuals over the age of 25 were sampled. However, there was no significant difference in the age-frequency composition of the pooled samples based on sex (Kolmogorov-Smirnov; $Z=1.05$ $P=0.22$).

Growth modeling

The strong 1993 cohort allowed us to closely monitor the actual length at age of striped trumpeter. Average size increased from 190 mm (1.3 years) in January 1995 to 300 mm (2.1 years) by November 1996 (Fig. 3) and 420 mm (4.0 years) by November 1997. The seasonal VBGF

model indicated that the majority of observed growth in this cohort occurred between January and May (late austral summer through autumn) and that there was little growth apparent between June and December (Fig. 5). The sine wave representing seasonal fluctuations indicated that the peak growth rate occurred in May. Comparing this sine function with that derived for SST (Fig. 6), we identified a first-order serial correlation—the strongest correlation identified when a 34-day lag period was incorporated in the growth phase.

The parameters of the $VBGF_S$ and $VBGF_{TP}$ fitted to the aged individuals are presented in Table 3. The $VBGF_{TP}$ gave the more parsimonious fit to the pooled length-at-age data according to the deterministic AIC value and underestimated L_x in relation to L_{max} to a lesser extent than the $VBGF_S$ (Table 3), reflecting a better fit to the data in the older age classes. In conjunction with a visual assessment of residuals, it was apparent that the $VBGF_S$ underestimated length at age above 20 years (Fig. 7). The better fit by the $VBGF_{TP}$

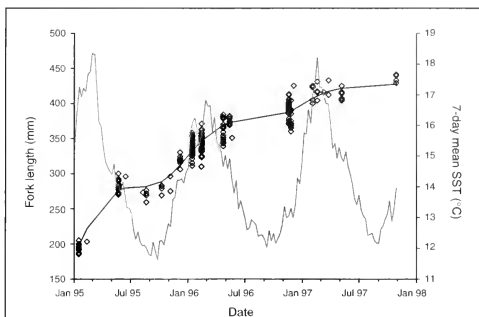


Figure 5

Length-at-age data (\diamond) of the 1993 striped trumpeter (*Latris lineata*) cohort fitted with a modified von Bertalanffy growth function to represent seasonal growth (black line), plotted against a 7-day average SST at the time of sampling (gray line).

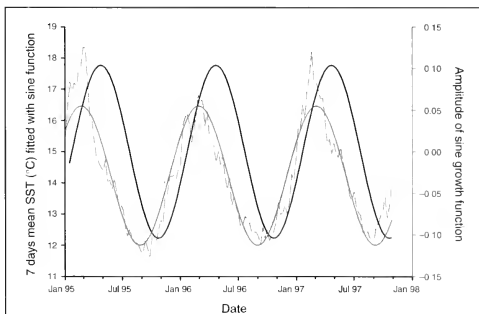


Figure 6

Seven-day mean SST (broken gray line) fitted with a sine wave (gray line) plotted against the sine function (black line) extracted from the seasonal von Bertalanffy growth function fitted in Figure 5.

supports the hypothesis that a more complex growth model was required for striped trumpeter.

The VBGF_{TP} was sensitive to the value *age at transference*. A profile of negative log likelihood for a range of age-at-transference values (Fig. 8) assisted in determining the correct absolute minima. The negative log-likelihood profile revealed a low minima range across age at transference from 3.5 to 4.6 years, which, however,

converged to a lowest value at age 4.4 years. Fitting the PDF to the growth curve substantially smoothed the point of transition, producing a curve that represented the data well. Setting an arbitrary standard deviation of 1.0 around the age at transference provided a normally distributed two-tailed range at transference (90 percent confidence adjusted for bias) from 1.3 to 7.8 years.

A likelihood ratio test (LRT) identified a slight significant difference between male and female VBGF_S growth curves ($\chi^2=13.20$ $df=3$ $P=0.04$), but there was no significant difference when the VBGF_{TP} was tested ($\chi^2=10.83$ $df=6$ $P=0.09$).

Mortality estimation

Ages 9–23 and 7–25 were included in the LCCCA regressions of the VBGF_S and the VBGF_{TP}, respectively, to

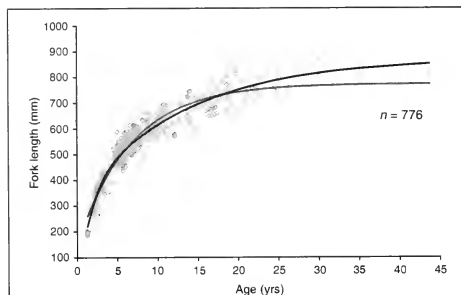


Figure 7

Pooled length-at-age data for striped trumpeter (*Latris lineata*). The black line represents the optimal two-phase von Bertalanffy growth function (VBGF_{TP}), with a mean age at transference of 4.4 years and a standard deviation equal to 1; the gray line represents the optimal standard von Bertalanffy growth function (VBGF_S).

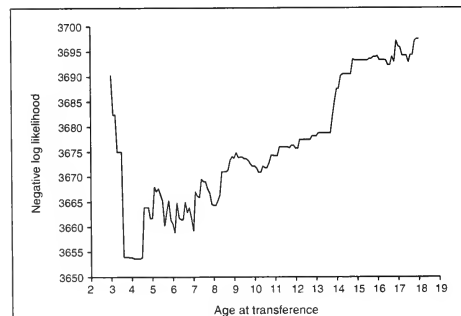


Figure 8

Negative log-likelihood profile plot of increasing age-at-transference values for striped trumpeter (*Latris lineata*).

estimate Z (Fig. 9). Individuals below these ranges were assumed, by their respective model, not to have fully recruited to the offshore fishery, and individuals over the age of 25 were excluded due to poor sample size. These age ranges effectively excluded the strong 1993 recruitment pulse from the regression, thereby avoiding the complication of including a known strong year class in the analysis.

Application of the VBGF_{TP} model resulted in lower estimates of Z and M (based on the Pauly equation), compared with those calculated by using the VBGF_S parameters (Table 4). The estimate of Z based on the Hoenig (1983) equation was assumed to be close to M because F is low for this species. The Hoenig M was very similar to the Pauly estimate when VBGF_{TP} parameters were used. In this case M was just below 0.1, indicating an annual natural mortality rate of about 9%. The VBGF_{TP} estimates indicate that F was slightly higher than M in the offshore fishery. By contrast, the standard VBGF_S parameters produced a substantially higher estimate of M (0.15) based on the Pauly equation than predicted by the Hoenig approximation, indicating an annual natural mortality rate of about 14%. Derived estimates of F with the VBGF_{TP} were slightly higher than M , whereas F in relation to M was variable for the VBGF_S, depending on the equation used to derive M .

Discussion

The present study represents the first report of age and growth of striped trumpeter. Despite having available a patchy data set, we were able to validate age and overcome the limitations of the von Bertalanffy equation to represent these data by the use of a robust growth model. Striped trumpeter are long lived, have a maximum age in excess of 40 years, and growth is particularly rapid up to age five, after which it slows dramatically.

The species has a complex early life history involving a long planktonic larval phase of around nine months (Morehead¹), an inshore juvenile phase, and then movement offshore into deepwater.

Gear selectivity (gill nets in the shallow and hook catches in the deeper waters) may have influenced the fish-size structure of our samples, especially when grouped by depth, although it is highly unlikely that the size differences could be completely attributed to gear type alone. For instance, small individuals (<400 mm) were occasionally taken by hooks in the deeper strata and individuals over 500 mm were taken by gill nets in less than 50 m. The commercial hook fishery

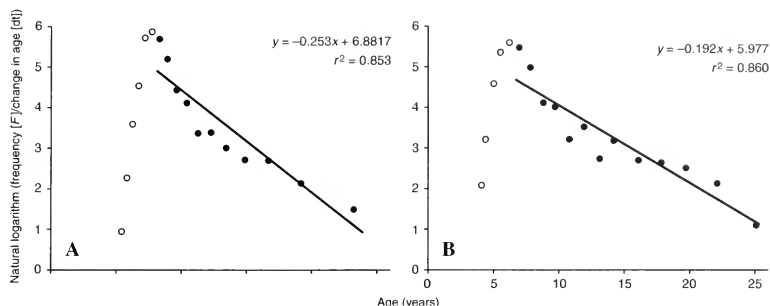


Figure 9

Length-converted catch curve analysis for striped trumpeter (*Latris lineata*) length and age data from 1998. (A) Age composition was based on the standard von Bertalanffy growth function (VBGF_S), (B) age composition was based on the second stanza of the two-phase von Bertalanffy growth function (VBGF_{TP}). Solid points were included in the respective linear regressions.

for striped trumpeter is largely restricted to depths of greater than 50 m, and despite considerable hook-fishing effort at shallower depths targeting other demersal reef species, notably the wrasses *Notolabrus fucicola* and *N. tetricus*, minimal catches of striped trumpeter are taken and those that are caught tend to be small in size (Lyle²). Rather, size structuring by depth is believed to reflect the movement of striped trumpeter offshore into deeper water as they grow and mature.

Seasonal growth was dramatic in young striped trumpeter (Fig. 5). This phenomenon is common in temperate species (Haddon, 2001; Jordan, 2001; McGarvey and Fowler, 2002), and has been linked to fluctuations in environmental factors, such as water temperature and oceanographic conditions, as well as biotic factors, such as seasonality in primary productivity (Harris et al., 1991; Jordan, 2001). Our study supports a correlation between water temperature and seasonal growth (Fig. 6); maximum growth was observed to take place consistently over a three-year period, approximately one month after the peak sea-surface temperatures.

Knowledge of growth and growth variability is essential to the understanding of a stock's population dynamics. To achieve an accurate assessment of these characteristics, several issues need to be addressed. Foremost, is a rigorous approach to the validation and precision testing of age estimates (Campana, 2001). In this study, a combination of age validation protocols outlined by Fowler and Doherty (1992) and Campana (2001) were subscribed to: 1) otoliths must display an internal structure of increments, (Fig. 3); 2) otoliths must grow throughout the lives of fish at a perceptible rate, which was confirmed by the otolith weight-at-age

Table 3

Parameter estimates derived from the two growth functions (standard von Bertalanffy growth function, [VBGF_S] and the two-phase von Bertalanffy growth function [VBGF_{TP}]) applied to the length-at-age data of striped trumpeter (*Latris lineata*) in Tasmania. Growth parameters are defined in the text, NOP = number of parameters in the model, AIC = Akaike information criterion, and L_{max} = the maximum length of all individuals included in the growth models.

		VBGF _S	VBGF _{TP}
Growth parameters	$L_{\infty 1}$	773.27	532.77
	k_1	0.15	0.43
	t_{01}	-1.46	0.03
	L^b	—	450.11
	$L_{\infty 2}$	—	871.59
	k_2	—	0.08
	t_{02}	—	3.49
	t^b	—	4.4
	σ^2 of t^b	—	1.0
Diagnostics	NOP	3.0	9.0
	-log likelihood	3759.98	3700.13
	AIC	5335.12	5211.30
	% deviation of $L_{\infty 2}$ from L_{max}	-13.7	-2.7

regression (Table 2); 3) the age of first increment formation must be determined; and 4) increment periodicity across the entire age range of interest must be veri-

Table 4

Estimates of instantaneous rates of total (Z), natural (M), and fishing (F) mortality for striped trumpeter (*Latris lineata*) determined with age-based catch curve analysis and the empirical equations of Hoenig (1983) and Pauly (1980). $VBGF_{TP}$ = estimates derived from the parameters of the two-phase von Bertalanffy growth function, $VBGF_S$ = estimates derived from the parameters of the standard von Bertalanffy growth function and LCCCA = length converted catch curve analysis.

Method	Z		M		F	
	$VBGF_S$	$VBGF_{TP}$	$VBGF_S$	$VBGF_{TP}$	$VBGF_S$	$VBGF_{TP}$
LCCCA	0.253	0.192	—	—	—	—
Hoenig	—	—	0.096	0.096	0.157	0.096
Pauly	—	—	0.151	0.092	0.102	0.100

fied. We used cultured individuals to determine which opaque or translucent zone represented the first growth increment, although the accuracy of age validation with cultured individuals has been questioned by Campana (2001). In our study, the close correspondence between the growth of cultured and wild fish over a period of several years gives us confidence in using this approach to validate first increment position. The slightly slower growth rate observed in cultured striped trumpeter can be attributed to jaw malformation—a phenomenon that has been shown to affect feeding ability (Cobcroft et al., 2001).

Modal progression of the 1993 cohort through time provided indirect validation for annual periodicity in increment formation up until age seven. Validation across all age classes was not possible in our study, although validation after the age of five years was significant. That is, validation was achieved past the average age at which fish moved offshore into deeper water, and past the age at which there was a significant reduction in growth rate.

The second consideration to address when studying animal growth is model selection. Akaike's information criterion is a standard method for model selection that provides an implementation of Occam's razor, in which parsimony or simplicity is balanced against goodness-of-fit (Forster, 2000). However, model selection should not rely on statistical fit alone; it should also provide a biologically sensible interpretation across the entire range of ages in the sampled population (Haddon, 2001). In the case of striped trumpeter, the standard von Bertalanffy function provided a poor representation of growth in older individuals, resulting in an unrealistically low L_{∞} . This problem was largely overcome by the application of a two-phase growth function. Similar to that used on large pelagics, such as *Thunnus maccoyii* (Bayliff et al., 1991; Hearn and Polacheck, 2003). In their application of the model, Hearn and Polacheck (2003) considered biological traits when discussing the justification for age at transference, namely the reduction in growth rate, and inshore to offshore migration. In the present study we have considered analogous traits to seed the age of transference for striped trumpeter.

In this species there is a marked transition in size structure between shallow and deeper reefs that occurs at around 450 mm or between 4 and 5 years (Fig. 8). In addition, a visual assessment of the length-at-age data highlighted a marked decrease in growth rate at a similar age.

Solving for the age at transference produced a point estimate that results in a sharp discontinuity in the growth curve; an observation that Hearn and Polacheck (2003) highlighted as biologically unrealistic. The range of low negative log likelihood values described by the age at transference profile is due to the patchiness of data around these ages, creating uncertainty in the model. We have assumed in this case that the converged value of 4.4 years is accurate and that the variability around this point is normally distributed with a standard deviation equal to one. By including the normal probability distribution function we have effectively created a smooth transition between growth phases. This function implies that age at transference has some level of inherent variability, which is likely to be more biologically plausible than knife-edge transition.

A further extension of the two-phase model was tested by applying the seasonal growth version of the VBGF (described in Eq. 3) to the first phase and a standard VBGF to the second phase, but was disregarded because of the effect of over parameterization on parsimony. However, this approach did highlight the flexibility of the two-phase model to allow for a more dynamic representation of population growth characteristics.

This study supports the assertion by Hearn and Polacheck (2003) that discontinuity in growth rate may be a more common phenomenon in fish than implied by growth models reported in the literature. Such a two-phase growth model, where age at transference coincides with the transition phase from one fishery to another, has proven useful. It allows separate growth parameters to be tracked to each fishery, and as such, provides a precursor to developing a more biologically robust production model with dynamic parameters at age and for fishing method.

The predictive regression developed by Pauly (1980) that estimates natural mortality is based on the direct

relationship between longevity (t_{max}) and the magnitude of the physiological growth parameters k and L_{∞} . As such, it would be reasonable to assume that if a good fit exists between length at age that the growth parameters, when employed in such an empirical model, would yield a natural mortality estimate approximately equal to that determined by a regression model that is based on t_{max} (Hoening, 1983). The two-phase growth function also provided a more conservative estimate of M than the standard von Bertalanffy model. Overestimates of M can lead to unrealistically high estimates of productivity and a potential yield that may in turn lead to overexploitation of a stock.

Protracted longevity, slow growth in later life, large body size, recruitment variability, and relatively low natural mortality once individuals reach adulthood are all characteristics typical of a K-selected species (where equilibrium is the biological strategy). Such species are often regarded as being susceptible to growth over-fishing and stock depletion (Booth and Buxton, 1997). For instance, increased fishing effort on the inshore fishery, as has been observed with the recruitment of strong cohorts, will affect subsequent recruitment to the offshore fishery and spawning stock. The current analysis indicates that fishing mortality is slightly higher than natural mortality and, in the absence of further strong recruitment, a decline in the stock size is likely if fishing pressure is not reduced.

Acknowledgments

The authors gratefully acknowledge Ray Murphy and Alan Jordan who collected many of the earlier samples and undertook preliminary examination of the otoliths. The assistance of the captain and crew of FRV *Challenger* in collecting samples is also thankfully acknowledged. Philippe Ziegler, Dirk Welsford, and Malcolm Haddon provided constructive criticism and ideas in terms of the analyses and reviewed the manuscript; Sarah Irvine and an anonymous reviewer provided constructive feedback on final versions of this manuscript.

Literature cited

- Akaike, H.
1974. A new look at the statistical model identification. Institute of Electrical and Electronic Engineers Transactions on Automatic Control, AC-19, p. 716-723. IEEE Control Systems Society, New York, NY.
- Andrew, T. G., T. Hecht, P. C. Heemstra, and J. R. E. Lutjeharms.
1995. Fishes of the Tristan Da Cunha group and Gough Island, South Atlantic Ocean. JLB Smith Institute of Ichthyology. Ichthyol. Bull. 63:1-41.
- Bayliff, W. H., I. Ishizuka, and R. B. Deriso.
1991. Growth, movement, and attrition of northern bluefin tuna, *Thunnus thynnus*, in the Pacific Ocean, as determined by tagging. Inter-Am. Trop. Tuna Comm. Bull. 20(1):1-94.
- Beamish, R. J., and D. A. Fournier.
1981. A method for comparing the precision of a set of age determinations. Can. J. Fish. Aquat. Sci. 38: 982-983.
- Beverton, R. J. H., and S. J. Holt.
1957. On the dynamics of exploited fish populations. U.K. Ministry of Agriculture and Fisheries, Fisheries Investigations (series 2), 19:1-533.
- Booth, A. J., and C. D. Buxton.
1997. Management of the panga *Pterogymnus laniarius* (Pisces: Sparidae), on the Agulhas Bank, South Africa using per-recruit models. Fish. Res. 32:1-11.
- Campana, S. E.
2001. Accuracy, precision and quality control in age determination, including a review of the use and abuse of age validation methods. J. Fish. Biol. 59:197-242.
- Campana, S. E., M. C. Annand, and J. I. Mcmillan.
1994. Graphical and statistical methods for determining the consistency of age determinations. Trans. Am. Fish. Soc. 124(1):131-138.
- Chen, Y. D. A., Jackson, and H. H. Harvey.
1992. A comparison of von Bertalanffy and polynomial functions in modelling fish growth data. Can. J. Fish. Aquat. Sci. 49:1228-1235.
- Cobcroft, J. M., P. M. Pankhurst, J. Sadler, and P. R. Hart.
2001. Jaw development and malformation in cultured striped trumpeter *Latris lineata*. Aquaculture 199:3-4: 267-282.
- Duhamel, G.
1989. Ichtyofaune des îles Saint-Paul et Amsterdam (Océan Indien sud). Mésogée. 49:21-47.
- Forster, M. R.
2000. Key concepts on model selection: performance and generalizability. J. Math. Psych. 44:205-231.
- Fowler, A. J., and P. J. Doherty.
1992. Validation of annual growth increments in the otoliths of two species of damselfish from the southern Great Barrier Reef. Aust. J. Mar. Freshw. Res. 43: 1057-1068.
- Furlani, D. M., and F. P. Ruwald
1999. Egg and larval development of laboratory-reared striped trumpeter *Latris lineata* (Forster in Bloch and Schneider 1801) (Percoidae: Latridiidae) from Tasmanian waters. N.Z. J. Mar. Freshw. Res. 33:16-83.
- Gomon, M. F., J. C. M. Glover, and R. H. Kuitert.
1994. The fishes of Australia's south coast, 992 p. The Flora and Fauna of South Australia Handbooks Committee. State Printers, Adelaide, South Australia, Australia.
- Haddon, M.
2001. Modelling and quantitative methods in fisheries. Chapman and Hall, Boca Raton, FL.
- Harris, G. P., F. B. Griffiths, L. A. Clementson, V. Lyne, and H. Van der Doe.
1991. Seasonal and interannual variability in physical processes, nutrient cycling and the structure of the food chain in Tasmanian shelf waters. J. Plankton Res. 13 (Suppl.):109-131.
- Hearn, W. S., and T. Polacheck.
2003. Estimating long-term growth-rate changes of southern bluefin tuna (*Thunnus maccoyii*) from two periods of tag-return data. Fish. Bull. 101:58-74.
- Hoening, J. M.
1983. Empirical use of longevity data to estimate mortality rates. Fish. Bull. 82:898-902.
- Jordan, A. R.
2001. Age, growth and spatial and interannual trends in age composition of jackass morwong, *Nemadactylus*

- macropterus*, in Tasmania. Aust. J. Mar. Freshw. Res. 52:651-660.
- Kimura, D. K.
1980. Likelihood methods for the von Bertalanffy growth curve. Fish. Bull. 77:765-776.
- Knight, W.
1968. Asymptotic growth: an example of nonsense disguised as mathematics. J. Fish. Res. Board Can. 25:1303-1307.
- Last, P. R., E. O. G. Scott, and F. H. Talbot.
1983. Fishes of Tasmania, 563 p. Tasmanian Fish-eries Development Authority, Hobart, Tasmania, Australia.
- McGarvey, R., and A. J. Fowler
2002. Seasonal growth of King George whiting (*Sillaginodes punctata*) estimated from length-at-age samples of the legal-size harvest. Fish. Bull. 100:545-558.
- Pauly, D.
1980. On the interrelationships between natural mortality, growth parameters, and mean environmental temperature in 175 fish stocks. J. Cons. Int. Explor. Mer 39(2):175-192.
1983. Length-converted catch curves: a powerful tool for fisheries research in the tropics (part 1). Fishbyte 1(2):9-13.
- Pitcher, T. J., and P. D. M. MacDonald.
1973. Two models for seasonal growth in fishes. J. Appl. Ecol. 10:559-606.
- Reynolds, R. W., N. A. Rayner, T. M. Smith, D. C. Stokes, and W. Wang.
2002. An improved in situ and satellite SST analysis for climate. J. Climate 15:1609-1625.
- Roff, D. A.
1980. A motion for the retirement of the von Bertalanffy function. Can. J. Fish. Aquat. Sci. 37:127-129.
- Sansbury, K. J.
1979. Effect of individual variability on the von Bertalanffy growth equation. Can. J. Fish. Aquat. Sci. 37: 241-247.
- Schnute, J.
1981. A versatile growth model with statistically stable parameters. Can. J. Fish. Aquat. Sci. 38:1128-1140.

Abstract—Morphological development of the larvae and small juveniles of estuary perch (*Macquaria colonorum*) (17 specimens, 4.8–13.5 mm body length) and Australian bass (*M. novemaculeata*) (38 specimens, 3.3–14.1 mm) (Family Percichthyidae) is described from channel-net and beach-seine collections of both species, and from reared larvae of *M. novemaculeata*. The larvae of both are characterized by having 24–25 myomeres, a large triangular gut (54–67% of BL) in postflexion larvae, small spines on the preopercle and interopercle, a smooth supraocular ridge, a small to moderate gap between the anus and the origin of the anal fin, and distinctive pigment patterns. The two species can be distinguished most easily by the different distribution of their melanophores. The adults spawn in estuaries and larvae are presumed to remain in estuaries before migrating to adult freshwater habitat. However, larvae of both species were collected as they entered a central New South Wales estuary from the ocean on flood tides; such transport may have consequences for the dispersal of larvae among estuaries. Larval morphology and published genetic evidence supports a reconsideration of the generic arrangement of the four species currently placed in the genus *Macquaria*.

Larval development of estuary perch (*Macquaria colonorum*) and Australian bass (*M. novemaculeata*) (Perciformes: Percichthyidae), and comments on their life history

Thomas Trnski

Amanda C. Hay

Ichthyology, Australian Museum
6 College Street
Sydney, New South Wales 2010, Australia

E-mail address (for T. Trnski, senior author): tomt@ausmus.gov.au

D. Stewart Fielder

New South Wales Fisheries
Port Stephens Fisheries Centre
Private Bag 1
Nelson Bay, New South Wales 2315, Australia

The Percichthyidae is a family of freshwater fishes restricted to Australia (8 genera, 17 species) and South America (2 genera, 7 species) (Johnson, 1984; Nelson, 1994; Allen et al., 2002; Paxton et al., in press). There is continuing debate regarding the monophyly of the family; several genera are variously allocated to separate families: *Gadopsis* is allocated to Gadopsidae (Allen et al., 2002; see Johnson, 1984 for a history of the systematic placement of the genus) and *Edelia*, *Nannatherina*, and *Nannoperca* are allocated to Nannopercidae (Allen et al., 2002). Other Australian genera of Percichthyidae include *Bostockia*, *Guyu*, *Maccullochella*, and *Macquaria* (Pusey and Kennard, 2001; Allen et al., 2002; Paxton et al., in press). The genera *Percalates* and *Plectroplites* were synonymized with *Macquaria*, based on morphological and biochemical characters (MacDonald, 1978), and although this arrangement was accepted by Paxton and Hanley (1989), Paxton et al. (in press), Eschmeyer (1998), Johnson (1984), and Nelson (1994) recognized both *Percalates* and *Plectroplites* as valid genera.

There are four described species in the genus *Macquaria*, all confined to southeastern Australia. *Macquaria ambigua* occurs naturally in freshwaters of the Murray-Darling river

system and has been translocated outside of its natural range (Kailola et al., 1993; Allen et al., 2002). There is genetic evidence for an additional undescribed freshwater species closely related to *M. ambigua* from central Australian drainages (Musyl and Keenan, 1992). *Macquaria australasica* is also confined to freshwater of the Murray-Darling river system, and an isolated population exists from the Shoalhaven and Hawkesbury Rivers, New South Wales (Allen et al., 2002) that may be a separate species (Dufty, 1986). The other two species (*M. colonorum* and *M. novemaculeata*) are catadromous and occur in coastal southeastern Australian drainages between southern Queensland and eastern South Australia (Paxton et al., in press). They are sympatric from northern New South Wales (NSW) to eastern Victoria. Adults of *M. novemaculeata* occur in freshwater, whereas *M. colonorum* prefers brackish water of estuaries (Williams, 1970). Both species migrate to estuarine areas to breed in winter (Allen et al., 2002). Both species are protected from commercial fishing but are highly prized by recreational fishermen (Harris and Rowland, 1996; Allen et al., 2002) and *M. novemaculeata* is an important aquaculture species.

Manuscript submitted 20 November 2003
to the Scientific Editor's Office.

Manuscript approved for publication
15 June 2004 by the Scientific Editor.
Fish. Bull. 103:183–194 (2005).

Of the 17 Australian percichthyids, larvae of only *Maccullochella macquariensis*, *M. peelii peelii*, and *Macquaria ambigua* have been described (Dakin and Kesteven, 1938; Lake, 1967; Brown and Neira, 1998). Larval and early juvenile development of the estuary perch (*Macquaria colonorum*) and the Australian bass (*Macquaria novemaculeata*) is described from specimens collected from the central and southern coast of NSW, and from reared larvae of the latter species obtained from brood stock from central NSW. This is the first description of the morphological development of the early life history of these two species.

Materials and methods

Morphological definitions, measurements, and abbreviations follow Neira et al. (1998) and Leis and Carson-Ewart (2000). Larvae and juveniles were examined and measured under a dissecting microscope at magnifications from 6 to 50 \times . Precision of the measurements varied with magnification but ranged from 0.02 to 0.16 mm. Where morphometric values are given as a percentage, they are as a proportion of body length (BL) unless otherwise indicated. All pigment described is external unless otherwise specified. The juveniles collected are in transition from larvae to juveniles because they retain some of their larval characters and squamation is incomplete; these are called "transitional juveniles" (Vigliola and Harmelin-Vivien, 2001). Illustrations were prepared with a Zeiss SR with an adjustable drawing tube.

Field-caught larvae were collected in a fixed 2-m² channel net with about 1-mm mesh in Swansea Channel, Lake Macquarie, central NSW. The net filtered surface waters to 1 m depth during night flood tides (Trnski, 2002). Small juveniles were collected in a 30-m beach seine dragged over sand, mud, and *Zostera* seagrass in the Clyde River, southern NSW. Reared larvae of *M. novemaculeata* were obtained from rearing tanks at the Port Stephens Fisheries Centre, an aquaculture research facility of NSW Fisheries. Brood stock came from the Williams River, central NSW. All specimens were initially fixed in 10% formalin and subsequently transferred to 70% ethanol.

Field-caught larvae were restricted to a narrow size range: 4.8–7.1 mm body length (BL) for *M. colonorum* ($n=12$), and 4.6–7.6 mm BL for *M. novemaculeata* ($n=15$). Juveniles of both species ranged from 10.3 to 13.5 ($n=5$) and from 10.1 to 14.1 mm BL ($n=5$), respectively. Reared larvae of *M. novemaculeata* were available to confirm the identification of the larvae and to extend the developmental series for this species to 3.3–10.2 mm BL ($n=18$).

All material examined is registered in the fish collection at the Australian Museum. Registration numbers of *M. colonorum* larvae are AMS I.20052-010, I.41690-005 to -008, I.41691-002, I.41692-001, I.41693-001; *M. novemaculeata* are AMS I.20052-012, I.27051-013, I.41561-001 to -008, I.41590-001, I.41641-001, I.41661-

001 and -002, I.41662-001, I.41668-001, I.41690-001 to -0004, I.41691-001, I.41694-001.

Identification

Field-caught larvae and juveniles were identified as percichthyids by using the characters in Brown and Neira (1998), particularly the combination of a relatively large gut, the small to moderate gap between the anus and origin of the anal fin prior to complete formation of the anal-fin, continuous dorsal fin, fin-ray, and vertebral counts, and head spination including small preopercular spines, a small interopercular spine, and a smooth supraopercular ridge. The larvae and juveniles described here were confirmed as being *Macquaria colonorum* and *M. novemaculeata* because of their coastal distribution and meristics; all other species in the family are restricted to freshwater. The overlap in meristics between *M. colonorum* and *M. novemaculeata* made separation of the species difficult. The availability of reared *M. novemaculeata* from positively identified adults determined the species allocations.

Results

Development of *Macquaria colonorum*

Adult meristic data Dorsal (D) IX–X, 8–11; Anal (A) III, 7–9; Pectoral (P₁) 12–16; Pelvic (P₂) 1, 5; Vertebrae 25
17 specimens: 4.8–7.1 and 10.3–13.5 mm BL

General morphology (Tables 1 and 2, Fig. 1) Larvae and transitional juveniles are moderately deep bodied (body depth, BD 30–35%). The body and head are laterally compressed. There are 24–25 myomeres (12–14 preanal and 11–13 postanal). The large, triangular gut is fully coiled in the smallest larva examined. The preanal length ranges from 60% to 67%. The conspicuous gas bladder located over the midgut is small to moderate in size but difficult to distinguish in transitional juveniles. The round to slightly elongate head is large (head length, HL 32–41%). The snout is slightly concave to straight. The snout is approximately the same length as the eye diameter but becomes shorter from 7 mm. The eye is round and moderate in size (27–32% of HL) in larvae but becomes moderate to large in transitional juveniles (32–36% of HL). The large mouth reaches to the middle of the pupil. Small canine teeth are present in both jaws in all larvae examined. The nasal pit closes shortly after settlement, by 12.5 mm.

Head spination is weak. Three short spines are present on the posterior preopercular border in the smallest larva examined; a fourth spine is present in some postflexion larvae from 6.3 mm and in all transitional juveniles. The spine at the angle of the preopercle is longest but remains shorter than the pupil diameter. A minute interopercular spine is present from 6.0 mm and persists in all transitional juveniles. A low, smooth

Table 1

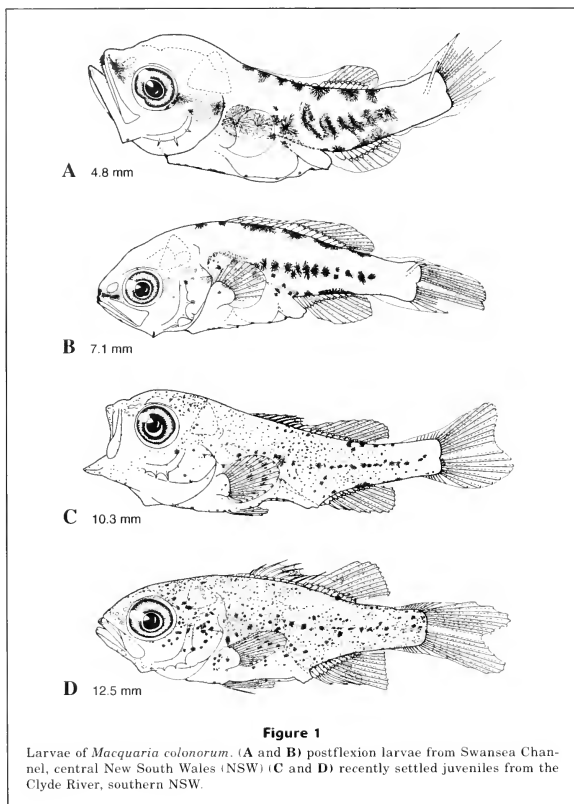
Morphometric data for *Macquaria colonorum* larvae from channel-net samples and juveniles from beach-seine samples. Measurements are in mm. VAFL = vent to anal-fin length.

Body length	Precanal length	Predorsal length	Body depth	Head length	Snout length	Eye diameter	VAFL
Flexion							
4.80	3.40	2.48	1.49	1.96	0.58	0.58	0.04
5.10	3.40	3.00	1.60	1.88	0.60	0.56	0
5.40	3.40	2.80	1.60	1.72	0.50	0.50	0
5.48	3.32	2.91	1.74	1.80	0.56	0.56	0
Postflexion							
5.73	3.49	2.80	1.99	2.08	0.56	0.60	0
5.98	3.68	3.24	1.99	2.04	0.60	0.60	0
6.00	3.72	2.60	1.92	2.00	0.50	0.60	0
6.31	3.98	2.57	2.16	2.20	0.60	0.68	0
6.60	4.00	3.00	2.20	2.40	0.64	0.64	0
6.81	4.15	3.07	2.16	2.32	0.66	0.66	0
7.00	4.32	3.32	2.08	2.24	0.60	0.72	0
7.10	4.36	2.91	2.32	2.28	0.60	0.72	0
Settled							
10.29	6.81	4.81	3.15	3.74	0.91	1.25	0
10.62	6.81	4.98	3.24	3.90	0.95	1.25	0
11.29	7.47	5.56	3.74	4.48	1.00	1.58	0
12.45	7.97	5.64	4.15	4.57	1.00	1.66	0
13.45	8.70	6.64	4.48	5.23	1.41	1.83	0

Table 2

Meristic data for *Macquaria colonorum* larvae and juveniles. () indicates only fin bases present, [] incipient rays or spines, |] ray transforming to a spine, d = damaged.

Body length	Dorsal	Anal	Pectoral	Pelvic	Caudal	Myomeres
Flexion						
4.80	(V), 9	(I), 8[1]			9+7[1]	14+11=25
5.10	d, (10)	(I), 9			[1]8+7[1]	13+11=24
5.40	d, (9)	(II), 9	[2]		9+8	13+12=25
5.48	(III), 9	(II), 8	3		9+8	12+12=25
Postflexion						
5.73	(IV), 11	(II), 8	5		9+8	13+12=25
5.98	(V), 10	(II), 8	2		9+8	13+12=25
6.00	(IV), 10	(II), 8	3		9+8	13+12=25
6.31	(IV) , 11	[II], 9	9	buds	9+8	13+12=25
6.60	IV, 11	II, 9	5	buds	9+8	13+12=25
6.81	VII, 11	II, 10	9	buds	9+8	13+12=25
7.00	VII, 11	II, 10	5 (d)	buds	9+8	12+13=25
7.10	VIII, 10	II I, 9	11[1]	buds	9+8	14+11=25
Settled						
10.29	VIII I, 10	II I, 8	15	I,5	7+9+8+6	13+12=25
10.62	VIII I, 10	II I, 8	13	I,5	7+9+8+4	12+13=25
11.29	IX, 10	III, 8	15	I,5	7+9+8+8	12+13=25
12.45	IX, 10	III, 8	14	I,5	12+9+8+7	12+13=25
13.45	IX, 10	III, 9	14	I,5	9+9+8+8	12+13=25



supraocular and supracleithral ridge form by the time notochord flexion is complete. A weak posttemporal ridge is present from 7 mm, and a small spine develops in transitional juveniles from 11.3 mm. A small spine develops on the supracleithrum from 10.6 mm. An opercular spine is present in transitional juveniles.

Dorsal-fin soft rays are ossified by the completion of notochord flexion, the posteriormost rays being the last to ossify. The pterygiophores of the spinous rays of the dorsal fin develop from posterior to anterior and begin to form during notochord flexion. Spines begin to ossify in postflexion larvae by 6.3 mm, and the full comple-

ment of dorsal-fin elements is present by 7.1 mm. All soft rays of the anal fin are ossified by the completion of notochord flexion, by which time 1-2 pterygiophores of the spinous rays are present. The first two anal-fin spines are ossified by 6.6 mm. The last spinous soft ray of the dorsal and the third spinous ray of the anal fin transforms from a soft ray after settlement and they are fully transformed by 11.3 mm. Incipient rays begin to form in the pectoral fin during notochord flexion, and the rays ossify from dorsal to ventral in postflexion larvae. A few pectoral-fin rays remain unossified at 7.1 mm and are fully ossified prior to settlement.

Pelvic-fin buds appear in postflexion larvae from 6.3 mm, but no elements have formed in the largest specimen; they are all ossified in the transitional juveniles. All primary caudal-fin rays are ossified by the end of notochord flexion. Procurent caudal rays are present in the transitional juveniles. Notochord flexion commences before 4.8 mm, and is complete by 5.7 mm. Scales have not begun to develop in the largest transitional juvenile examined (13.5 mm).

Pigment (Fig. 1, A–D) Larvae are moderately to heavily pigmented; melanophores are concentrated on the dorsal and ventral midlines, and midlateral surface of the trunk and tail. Small expanded melanophores are present at the tips of the upper and lower jaws, and there are one or two melanophores ventral to the nasal pit. Additional internal melanophores are present along the roof of the mouth, and posterior to the eye below the mid- and hindbrain. External melanophores may be present on the operculum in line with the eye. One or two melanophores are present on the ventral midline of the lower jaw, and there is one at the angle of the lower jaw.

Four to seven large, expanded melanophores are present along the dorsal midline of the trunk and tail, from the nape to just posterior to the dorsal-fin base. There are one or two melanophores on the nape and four or five along the dorsal-fin base. A series of large, expanded melanophores is present along the lateral midline of the trunk and tail, commencing at the gas bladder and extending to the posterior end of the dorsal and anal fins. In postflexion larvae, this series extends onto the anterior third of the caudal peduncle. Internal melanophores are present over the gas bladder, the mid- and hindgut, and may be present along the notochord. The external and internal pigment series thus give the impression of a line of heavy pigment from the tip of the snout, across the head and trunk, to the tail.

Small melanophores are present along the ventral midline of the gut; one melanophore on the isthmus immediately anterior to the cleithral symphysis, usually three (range: 2–4) melanophores between the cleithral symphysis and pelvic-fin base, and usually three (range: 1–4) melanophores between the pelvic-fin base and the anus. Expanded melanophores are present along the ventral midline of the tail, from above the anus to the posterior end of the anal-fin base. Between one and three melanophores occur along the anal-fin base. A small melanophore is occasionally present in early postflexion larvae at the base of ventral primary caudal-fin rays 1–2.

In transitional juveniles, the expanded melanophores are relatively smaller, and are most prominent midlaterally along the trunk and tail. The expanded melanophores along the dorsal and ventral midlines become small to absent during the juvenile stage. Additional expanded melanophores develop laterally on the head and body, and the dorsal and anal fins become pigmented. Small melanophores cover the head and body—coverage lightest ventrally on the head and gut. Three broad

vertical bands become apparent dorsally on the nape, below the center of the spinous dorsal fin and below the center of the soft dorsal fin by 13.5 mm.

Development of *Macquaria novemaculeata* larvae

Adult meristic data D VIII–X, 8–11; A III, 7–9; P₁ 12–16; P₂ 1, 5; Vertebrae 25; 38 specimens: 3.3–14.1 mm BL

Eggs and hatching Eggs are approximately 900 μ m in diameter and have multiple oil globules. Larvae are 3.3 mm SL at time of hatching.

General morphology (Tables 3 and 4, Fig. 2) Yolksac and early preflexion larvae are elongate (BD 15–18%), but in late preflexion and flexion larvae, body depth becomes moderate (BD 26–34%). Body depth of field-caught postflexion larvae ranges from 29% to 35%, and in transitional juveniles from 33% to 34%. Reared postflexion larvae and transitional juveniles are deeper than wild larvae, ranging from 32% to 44%, which is an artifact of the extremely full guts in the reared larvae. Body depth decreases abruptly posterior to the anus, although this becomes less marked with development. The head and body are laterally compressed. There are 25 myomeres (10–13 preanal+12–15 postanal). In general, there are 10–12 preanal myomeres in preflexion and flexion larvae, and 12–13 preanal myomeres in postflexion larvae and transitional juveniles. The gut is initially straight in yolksac larvae but is coiled by 3.9 mm. The gut is oval to triangular in shape; preanal length reaches 44–56% of BL in yolksac and preflexion larvae, 54–60% in flexion stage larvae, and 54–66% in postflexion larvae and transitional juveniles. The gut mass is large, particularly in reared postflexion larvae and transitional juveniles. The conspicuous gas bladder, which is located over the midgut, is moderate to large in size, except in the yolksac larvae where it is small and inconspicuous. The head is round and small in yolksac larvae (HL 15–16%), moderate in preflexion larvae (HL 22–31%), and becomes moderate to large in flexion (29–35%) and postflexion larvae and transitional juveniles (32–38%). The snout is always shorter than the eye diameter and is initially concave, but becomes convex to straight in postflexion larvae. The eye is moderate to large (27–36% of HL) but is relatively larger in yolksac larvae (42–45% of HL). The eye is initially unpigmented, but is fully pigmented by 3.6–3.8 mm, prior to the complete absorption of the yolk. The moderate mouth reaches to the middle of the pupil. Small canine teeth appear in both jaws in late preflexion larvae by 4.4 mm. The number of teeth increases with development. The nasal pit begins to close by 8.6 mm, and both nostrils are developed by 10.3 mm.

Head spination is weak. A small spine appears at the preopercular angle by the end of the preflexion stage. By the time notochord flexion is complete, there are three spines on the posterior preopercular border, and the spine at the angle is the longest. All spines are shorter than the pupil diameter. Additional spines

Table 3

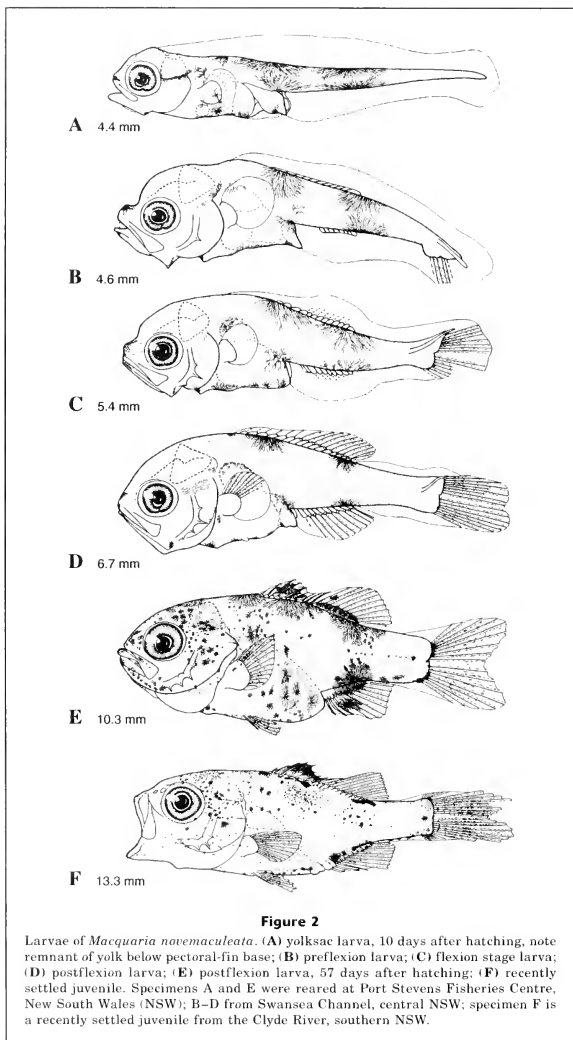
Morphometric data for *Macquaria novemaculeata* larvae from channel net samples and reared in aquaria (body length preceded by "R"), and juveniles from beach-seine samples. Measurements are in mm. VAFL = vent to anal-fin length.

Body length	Prenal length	Predorsal length	Body depth	Head length	Snout length	Eye diameter	VAFL
Yolksac							
R 3.32	1.48		0.52	0.53	0.16	0.24	
R 3.60	1.60		0.58	0.53	0.16	0.22	
Preflexion							
R 3.60	2.00		0.92	0.96	0.24	0.34	
R 3.80	2.00		1.00	1.04	0.30	0.38	
R 3.90	1.76		0.64	0.84	0.18	0.30	
R 4.20	2.00		0.64	0.93	0.20	0.33	
R 4.40	2.00		0.78	1.06	0.26	0.34	
4.57	2.36	2.16	1.20	1.40	0.28	0.40	0.22
Flexion							
5.00	2.72	2.40	1.52	1.48	0.32	0.48	0.12
5.14	2.90	2.32	1.48	1.76	0.44	0.48	0.10
R 5.31	2.84	2.60	1.40	1.60	0.48	0.56	0.20
5.39	2.74	2.66	1.58	1.60	0.40	0.48	0.12
R 5.39	2.90	2.66	1.36	1.56	0.40	0.56	0.20
5.47	2.80	2.74	1.60	1.72	0.44	0.48	0.12
R 5.47	3.00	2.60	1.56	1.76	0.52	0.60	0.12
5.70	3.40	2.92	1.96	2.00	0.52	0.56	0.06
5.90	3.32	2.90	1.80	1.88	0.52	0.56	0.04
Postflexion							
5.64	3.07	2.41	1.66	2.00	0.52	0.60	0.08
5.89	3.52	2.64	2.00	2.00	0.52	0.60	0.06
6.06	3.32	2.81	1.99	2.00	0.52	0.56	0.10
6.30	3.40	2.57	1.91	1.99	0.50	0.60	0.20
6.60	3.73	2.91	2.24	2.08	0.50	0.66	0
6.72	3.74	2.82	2.24	2.16	0.60	0.64	0.08
R 6.72	3.74	2.60	2.16	2.16	0.52	0.76	0.08
R 7.20	3.98	3.00	2.32	2.28	0.52	0.68	0.08
7.40	4.15	3.02	2.49	2.32	0.66	0.72	0
R 7.47	4.15	3.04	2.49	2.48	0.64	0.72	0.08
7.55	4.30	3.15	2.66	2.57	0.66	0.72	0
R 8.18	5.31	3.49	3.07	2.91	0.75	0.91	0
R 8.60	5.56	4.15	3.24	3.24	0.83	1.08	0
R 9.20	5.56	3.98	3.75	3.50	0.75	1.21	0
Settled							
10.13	6.64	4.81	3.49	3.65	0.83	1.33	0
R 10.20	6.64	4.57	3.74	3.74	0.83	1.33	0
R 10.30	6.64	4.57	3.99	3.82	1.05	1.33	0
11.62	7.55	5.56	3.82	4.23	1.00	1.49	0
11.62	7.55	5.47	3.98	4.39	1.07	1.49	0
13.28	8.30	5.98	4.56	4.98	1.41	1.66	0
14.10	8.63	6.47	4.65	5.15	1.41	1.74	0

Table 4

Meristic data of *Macquaria novemaculeata* larvae and juveniles. Body length preceded by "R" indicates larvae reared in aquarium. () indicates only fin bases present, [] incipient rays or spines, |] ray transforming to a spine.

Body length	Dorsal	Anal	Pectoral	Pelvic	Caudal	Myomeres
Yolksac						
R 3.32						10+15=25
R 3.60						11+14=25
Preflexion						
R 3.60						12+13=25
R 3.80						11+14=25
R 3.90						11+14=25
R 4.20						10+15=25
R 4.40						10+15=25
4.57	(9)	(8)			[2+3]	10+15=25
Flexion						
5.00	(VI), (6)	(8)			7+6	10+15=25
5.14	(VI), (8)	(9)			8+7	10+15=25
R 5.31	(III), (9)	(8)			[7+6]	12+13=25
5.39	(IV), [9]	(I, [9])			8+7	11+14=25
R 5.39	(III), (9)	(9)			6+6	12+13=25
5.47	(V), [8]	[I], [7]			[1]7+7[1]	11+14=25
R 5.47	(VI), [10]	(I, [8])1			[1]8+7[1]	12+13=25
5.70	VI, 10	(I, 8	6		9+8	13+13=26
5.90	[IV, 10	(I, 8	6		9+8	12+13=25
Postflexion						
5.64	VI, 10	(I, 9	5		9+8	10+15=25
5.89	[VI], 10	(I, 9	5		9+8	12+13=25
6.06	VI, 10	(I, 9	6		9+8	12+13=25
6.30	VI, 11	I, 9	6	buds	9+8	11+14=25
6.60	VI, 11	I, 9	8		9+8	12+13=25
6.72	VI, 11	I, 9	8	buds	9+8	12+13=25
R 6.72	VI, 10	I, 9	12	buds	9+8	12+13=25
R 7.20	VII, 11	II, 9	10	buds	9+8	12+13=25
7.40	VII, 11	II, 9	12	buds	9+8	13+12=25
R 7.47	VII, 11	II, 9	13	buds	9+8	12+13=25
7.55	VII, 11	II, 9	12	buds	9+8	12+13=25
R 8.18	VIII, 11	II, 9	13	I, 5	9+8	13+12=25
R 8.60	VIII, 11	II, 8	13	I, 5	9+8	13+12=25
R 9.20	IX, 10	III], 7	15	I, 5	9+8	13+12=25
Settled						
10.13	IX, 10	III], 8	14	I, 5	7+9+8+7	12+13=25
R 10.20	IX, 10	III], 8	14	I, 5	9+8	13+12=25
R 10.30	IX, 10	III], 8	14	I, 5	9+8	13+12=25
11.62	VIII (11),10	II (11), 8	14	I, 5	9+9+8+8	13+12=25
11.62	IX, 9	II (11), 8	14	I, 5	8+9+8+7	13+12=25
13.28	IX, 10	III, 8	14	I, 5	7+9+8+9	12+13=25
14.1	IX, 10	III, 8	14	I, 5	9+9+8+7	12+13=25



form as larvae develop; four or five spines are present in larvae and transitional juveniles from 7.5–8.2 mm. A minute spine (rarely two) develops on the anterior preopercular border from 9 mm; a third spine develops in transitional juveniles from 13.3 mm. A small interopercular spine develops by the time notochord flexion is complete. Low posttemporal and supraocular ridges, but no spines, develop during notochord flexion; they both become inconspicuous in postflexion larvae from 8.2 and 8.6 mm, respectively. An opercular spine is present from 8.6 mm. A small supracleithral spine is present in transitional juveniles from 10.1 mm.

The pterygiophores of all the soft rays and up to six of the pterygiophores of the first dorsal fin form during notochord flexion. Soft rays of the dorsal fin are ossified by the time notochord flexion is complete, whereas spinous rays ossify from posterior to anterior in late flexion and early postflexion larvae by 5.7–6.1 mm. The full complement of spines is present by 8.2 mm. Anal-fin pterygiophores form during notochord flexion, and all soft rays are ossified by the time notochord flexion is complete. Spinous rays of the anal fin begin to ossify in postflexion larvae by 6.3 mm, and all anal-fin elements are present by 7.2 mm. The last spinous ray of the dorsal fin and the third spinous ray of the anal fin transform from a soft ray between 7.6 and 9.2 mm. Pectoral-fin elements begin to ossify by the time notochord flexion is complete, and all rays are present in postflexion larvae by 7.5 mm. Pelvic-fin buds form in postflexion larvae by 6.7 mm, and all elements are ossified by 8.2 mm. Caudal-fin rays first appear in preflexion larvae from 4.6 mm, and all principal rays are ossified by the time notochord flexion is complete. Procurrent caudal rays are present in field-caught transitional juveniles. Notochord flexion commences between 4.6 and 5.0 mm, and is complete by 5.6–6.1 mm. There is a prominent gap between the anus and anal fin while the anal fin forms (vent to anal-fin length [VAFL] up to 5% of BL). The gap reduces in size as the anal fin develops, and it is absent by 7.6 mm. Scales have not developed in the largest specimen examined.

Pigment (Fig. 2, A–F) Larvae are moderately to heavily pigmented. An expanded melanophore is present on the tip of the snout and a small melanophore develops under the tip of the lower jaw in preflexion larvae from 3.6 mm. A second melanophore on the snout develops posterior to the first by the time notochord flexion is complete. A single melanophore is present at the angle of the lower jaw. A few small melanophores develop ventrally along the lower jaw in postflexion larvae from 7.2 mm. A series of internal melanophores underlie the mid- and hindbrain.

There are two very large expanded melanophores on the dorsal midline of the tail; the first is on the trunk centered over the hindgut, and the second is mid way along the tail. Once the dorsal fin forms they are centred under the middle of the spinous portion of the dorsal fin and under the posterior end of the soft dorsal fin, respectively. An additional smaller expanded

melanophore is present from 7.2 to 7.5 mm on the dorsal midline of the nape above the pectoral-fin base.

Two very large expanded melanophores occur ventrally, opposite the two large dorsal melanophores. The anteriormost of these melanophores reduces in prominence as larvae develop and is inconspicuous to absent by metamorphosis. Internal expanded melanophores over the gas bladder may have filaments that emerge externally, particularly in preflexion and flexion larvae. Internal melanophores along the notochord may be apparent on the caudal peduncle in postflexion larvae from 7 mm. There is an expanded melanophore on the midline of the isthmus, immediately anterior to the cleithral symphysis. A series of three to six small, expanded melanophores is present along the ventral midline of the gut. In postflexion larvae there is a bilaterally paired melanophore anterior to the pelvic-fin base, and two to four melanophores along the midline of the gut between the pelvic-fin base and the anus. A small contracted melanophore ventrally on the posterior margin of the caudal-fin base develops between 5.0 and 6.1 mm, and is located between ventral rays 1–5. This melanophore expands from 6.7 to 7.6 mm and spreads across up to four ray bases.

Pigment distribution spreads rapidly over most of the head from 7.2 to 7.5 mm, and laterally on the trunk, gut and tail from 8.2 mm. The expanded melanophores on the dorsal and ventral midlines of the trunk and tail remain large as the larvae develop; the posterior-most of these increases in intensity in reared larvae. The expanded melanophores on the dorsal and ventral midlines of the body become relatively smaller after settlement. By settlement, small melanophores develop on the membranes of the pectoral, pelvic, anal, and caudal fins, and the membrane of the spinous portion of the dorsal fin becomes heavily pigmented. After settlement, small melanophores cover most of the head and body, but the heaviest cover is seen dorsally. Three broad vertical bands become apparent dorsally on the nape, below the center of the spinous dorsal fin, and below the center of the soft dorsal fin in the largest specimen examined (14.1 mm).

Discussion

Adults of *M. colonorum* and *M. novemaculeata*, which have only minor morphological differences, such as the relative length of the snout, the profile of the head dorsally, postorbital head length, and gill-raker counts, are difficult to distinguish (Williams, 1970). None of these characters are useful for distinguishing larvae. The larvae of these two species could be positively identified only by comparison with reared larvae derived from positively identified brood stock.

Melanophore distribution is the most distinguishing character between the larvae of *M. colonorum* and *M. novemaculeata*. *Macquaria colonorum* has between four and seven expanded melanophores along the dorsal midline of the trunk and tail between 4.8 and 7.1 mm.

Macquaria novemaculeata has only two melanophores, and these are much larger; a third expanded melanophore develops on the nape from 7.2 mm. In addition, *M. novemaculeata* lacks a midlateral series of melanophores along the tail until settlement, and it is never as well developed as that in *M. colonorum*. On the other hand, *M. colonorum* has a prominent midlateral series until after settlement. One other morphological character that distinguishes the larvae is a snout length which is about equal to eye diameter in *M. colonorum* larvae until 7 mm, but snout length is always smaller than the eye diameter in *M. novemaculeata*.

Within the genus *Macquaria*, larval development of only *M. ambigua* has been described (Lake, 1967; Brown and Neira, 1998). There are several differences in the life history and development of the larvae of *M. ambigua* compared with *M. colonorum* and *M. novemaculeata*. *Macquaria ambigua* is restricted to freshwater, the eggs are large (3.3–4.2 mm in diameter, compared with 0.9 mm in reared *M. novemaculeata*) and the yolk sac in *M. ambigua* is large in small larvae and is not resorbed until the flexion stage (Brown and Neira, 1998). Compared with the larvae described in the present study, larvae of *M. ambigua* have more myomeres (24–28, but typically 26–27), and these larvae are relatively large by the time they complete notochord flexion (7.3 mm). They also lack an interopercular spine and supraocular ridge, and lack dorsal and lateral pigment on the tail until the postflexion stage.

Larvae of several other generalized percoid families are morphologically similar to *Macquaria*, including Latidae (Trnski et al., 2000), Microcanthidae (Walker et al., 2000a), Kyphosidae (Walker et al., 2000b), and some Apogonidae (Leis and Rennis, 2000). The latid genus *Lates* is morphologically most similar to the *Macquaria* larvae described in the present study but is tropical and does not have an overlapping distribution with *Macquaria*. *Lates* can be distinguished by the small size at notochord flexion (3.0–3.8 mm), dorsal and pectoral fin-ray counts when complete, and heavier melanophore distribution at a given size. Microcanthid and kyphosid larvae can be distinguished from coastal percichthyid larvae by the higher number of fin elements in the dorsal and anal fins, and the presence of supraclithral spines that are absent in larval percichthyids until the juvenile stage. Some deep-bodied apogonids resemble *Macquaria* larvae but can be distinguished by having separate spinous and soft dorsal fins and a large, conspicuous gas bladder.

Larvae of *M. colonorum* and *M. novemaculeata* were collected in Swansea Channel from July to August. This collection period coincides with adults of *M. novemaculeata* spawning from June to September in central New South Wales (Harris, 1986). *Macquaria colonorum* probably spawns at a similar time (McCarragher and McKenzie, 1986), and eggs have been collected from June to November in western Victoria (Newton, 1996). Adults of both species are thought to spawn in the middle reaches of estuaries at salinities above 8–10 g/kg (Harris, 1986; McCarragher, 1986), but *M. novemaculeata* will spawn in

waters up to 35 g/kg in culture (Battaglene and Sellosse, 1996). The optimal conditions for incubation and hatching of *M. novemaculeata* eggs are 18 ± 1 °C and salinity at 25 to 35‰ (van der Wal, 1985). Eggs are buoyant within this salinity range and hatch in 42 h at 18°C.

The presence of field-caught larvae of both species on incoming tides in Swansea Channel indicates that the larvae have spent some time in the ocean and that the eggs were potentially spawned in the ocean rather than in an estuary if they were not carried out to sea by outgoing tides. *Macquaria novemaculeata* adults move downstream into estuaries to spawn in water of suitable salinity. In low rainfall years, the spawning location is further upstream than in wet years, when spawning can occur in shallow coastal waters adjacent to estuaries (Searle¹). Mature *M. novemaculeata* adults can be found outside of estuaries in wet years (Williams 1970). This is verified by the collection of mature adults by trawl in July 1995 in 11–17 m of water off Newcastle, NSW (AMS L.37358-001). *Macquaria colonorum* adults have also been collected on the continental shelf (McCarragher and McKenzie, 1986). In addition, larvae can tolerate waters of marine salinity in culture, and late in their larval phase wild larvae can tolerate marine salinity as shown from our field collections. The presence of larvae and adults in continental shelf waters may provide two modes of dispersal among estuaries. Thus, these two species of *Macquaria* may not be confined to freshwater and estuarine conditions as often assumed (Harris and Rowland, 1996; Allen et al., 2002).

The smallest juveniles of *M. colonorum* and *M. novemaculeata* collected in the wild are from the Clyde River estuary, southern NSW. These range in size from 10 to 14 mm SL, and were collected among *Zostera* seagrass. They are morphologically similar to the largest pelagic larvae collected in the channel net in Swansea Channel. Based on the largest larvae and smallest juveniles, settlement occurs between 7.1 and 10.3 mm SL in *M. colonorum* and between 9.2 and 10.1 mm in *M. novemaculeata*. Transition to the juvenile stage is gradual, because scales are not present and juvenile pigmentation is still forming at about 15 mm. Juveniles of both species have been collected in estuarine waters until at least 100 mm SL (AMS fish collection). Juveniles of *M. novemaculeata* would be expected to migrate to freshwater because this is the nominal adult habitat (Williams, 1970), but the size at which this migration occurs is unclear.

The two species described in the present study were the only members of the genus *Percalates*, until this genus (along with *Plectroplites*) was synonymized with *Macquaria* by MacDonald (1978). Analyzing morphological and biochemical similarities of the three genera, MacDonald (1978) listed eight morphological differences that distinguished *Percalates* from *Macquaria* and *Plectroplites*. Protein electrophoresis similarities were stron-

¹ Searle, G. 2002. Personal commun. Searle Aquaculture, 255 School Rd, Palmers Island NSW 2463.

ger between *Pe.* (currently *Macquaria colonorum* and *Pe. (Macquaria) novemaculeata* (similarity coefficient 0.95), and *M. australasica* and *Pl. (Macquaria) ambigua* (0.71) than between the *Percalates* and *Macquaria* + *Plectroplites* (0.63) (MacDonald, 1978). The species of *Percalates* are euryhaline, whereas *Macquaria* and *Plectroplites* are strictly freshwater. This fact, combined with the difference in larval morphological features between *Macquaria ambigua* (Brown and Neira, 1998) and *M. colonorum* and *M. novemaculeata*, provides evidence that the genus *Macquaria* as defined by MacDonald may be polyphyletic. Recent phylogenetic analysis of the Percichthyidae with the use of molecular data indicates that *M. colonorum* and *M. novemaculeata* are more closely related to *Maccullochella* species than to *Macquaria (sensu stricto)* (Jerry et al., 2001). Molecular and larval evidence indicates the two catadromous species (*M. colonorum* and *M. novemaculeata*) belong in a genus separate from the freshwater species (*M. ambigua* and *M. australasica*).

Acknowledgments

Comments by Dave Johnson, Jeff Leis, and Tony Miskiewicz improved the manuscript. Sue Bullock illustrated the larvae from camera lucida sketches by TT. Glen Searle provided information on spawning habits that aided interpretation of larval distributions. Mark McGrouther provided access to specimens held in the Fish Collection at the Australian Museum (AMS). Larval collections in the field were supported by funds from Lake Macquarie City Council. Preparation of this paper was supported by a NSW Government Biodiversity Enhancement Grant to AMS, and by AMS.

Literature cited

- Allen, G. R., S. H. Midgley, and M. Allen.
2002. Field guide to the freshwater fishes of Australia, 394 p. Western Australian Museum, Perth, Western Australia, Australia.
- Battaglene, S. C., and P. M. Selosse.
1996. Hormone-induced ovulation and spawning of captive and wild broodfish of the catadromous Australian bass, *Macquaria novemaculeata* (Steindachner), (Percichthyidae). *Aquacult. Res.* 27:191-204.
- Brown, P., and F. J. Neira.
1998. Percichthyidae: basses, perches, cods. In *Larvae of temperate Australian fishes: laboratory guide for larval fish identification* (F. J. Neira, A. G. Miskiewicz and T. Trnski, eds.), p. 259-265. Univ. Western Australia Press, Perth, Western Australia, Australia.
- Dakin, J. W., and G. L. Kesteven.
1938. The Murray cod (*Maccullochella macquariensis* (Cuv. And Val.)). *Bull. New South Wales State Fish.* 1:1-18.
- Duffy, S.
1986. Genetic and morphological divergence between populations of macquarie perch (*Macquaria australasica*) east and west of the Great Dividing Range. Honours thesis, 43 p. Univ. New South Wales, Sydney, New South Wales, Australia.
- Eschmeyer, W. N. (ed.)
1998. *Catalog of fishes*, 2905 p. Special publication 1, Center for Biodiversity Research and Information, California Academy of Sciences, San Francisco, CA.
- Harris, J. H.
1986. Reproduction of the Australian bass, *Macquaria novemaculeata* (Perciformes: Percichthyidae) in the Sydney Basin. *Aust. J. Mar. Freshw. Res.* 37:209-235.
- Harris, J. H., and S. J. Rowland.
1996. Family Percichthyidae: Australian freshwater cods and basses. In *Freshwater fishes of south-eastern Australia* (R. M. McDowall, ed.), p. 150-163. Reed Books, Chatswood, New South Wales., Australia.
- Jerry, D. R., M. S. Elphinstone, and P. B. Baverstock.
2001. Phylogenetic relationships of Australian members of the family Percichthyidae inferred from mitochondrial 12s rRNA sequence data. *Molec. Phylogenetics Evol.* 18:335-347.
- Johnson, G. D.
1984. Percoidei: development and relationships. In *Ontogeny and systematics of fishes* (H. G. Moser, W. J. Richards, D. M. Cohen, M. P. Fahay, A. W. Kendall Jr., and S. L. Richardson, eds.), p. 464-498. Am. Soc. Ichthyol. Herpetol., Spec. Publ. 1.
- Kailola, P. J., M. J. Williams, P. C. Stewart, R. E. Reichelt, A. McNee, and C. Grieve.
1993. Australian fisheries resources, 422 p. Bureau of Resource Sciences, and Fisheries Research and Development Corporation, Canberra, New South Wales, Australia.
- Lake, J. S.
1967. Rearing experiments with five species of Australian Freshwater fishes. II. Morphogenesis and ontogeny. *Aust. J. Mar. Freshw. Res.* 18:155-173.
- Leis, J. M., and B. M. Carson-Ewart.
2000. The larvae of Indo-Pacific coastal fishes: an identification guide to marine fish larvae. *Fauna Malesiana Handbooks*, 2850 p. Brill, Leiden, The Netherlands.
- Leis, J. M., and D. S. Rennis.
2000. Apogonidae (cardinalfishes). In *The larvae of Indo-Pacific coastal fishes: an identification guide to marine fish larvae* (J. M. Leis and B. M. Carson-Ewart, eds.), p. 273-279. *Fauna Malesiana Handbooks* 2, Brill, Leiden, The Netherlands.
- McCarragher, D. B.
1986. Observations on the distribution, spawning, growth and diet of Australian bass (*Macquaria novemaculeata*) in Victorian waters. *Arthur Rylah Inst. Environ. Res. Tech. Rep. Ser.* 47.
- McCarragher, D. B., and J. A. McKenzie.
1986. Observations on the distribution, growth, spawning and diet of estuary perch (*Macquaria colonorum*) in Victorian waters. *Arthur Rylah Inst. Environ. Res. Tech. Rep. Ser.* 42.
- MacDonald, C. M.
1978. Morphological and biological systematics of Australian freshwater and estuarine percichthyid fishes. *Aust. J. Mar. Freshw. Res.* 29:667-698.
- Musyl, M. K., and C. P. Keenan.
1992. Population genetics and zoogeography of Australian freshwater golden perch, *Macquaria ambigua* (Richardson 1845) (Teleostei: Percichthyidae), and electrophoretic identification of a new species from the Lake Eyre Basin. *Aust. J. Mar. Freshw. Res.* 43:1585-1601.

- Neira, F. J., A. G. Miskiewicz, and T. Trnski.
1998. Larvae of temperate Australian fishes: laboratory guide for larval fish identification, 474 p. Univ. Western Australia Press, Perth, Western Australia, Australia.
- Nelson, J. S.
1994. Fishes of the world, 3rd ed., 600 p. John Wiley and Sons, New York, NY.
- Newton, G. M.
1996. Estuarine ichthyoplankton ecology in relation to hydrology and zooplankton dynamics in a salt-wedge estuary. *Mar. Freshw. Res.* 47:99-111.
- Paxton, J. R., and J. E. Hanley.
1989. Percichthyidae. In *Zoological catalogue of Australia*, vol. 7: Petromyzontidae to Carangidae (J. R. Paxton, D. F. Hoese, G. R. Allen, and J. E. Hanley (eds.)), p. 509-515. Australian Government Publishing Service, Canberra, New South Wales, Australia.
- Paxton, J. R., J. E. Hanley, D. J. Bray, and D. F. Hoese.
In press. Percichthyidae. In *Pisces (part 2)*, Mugilidae to Molidae. *Zoological catalogue of Australia*, vol. 7 (part 2) (D. F. Hoese, D. J. Bray, D. J., G. R. Allen, C. J. Allen, N. J. Cross, and J. R. Paxton, eds.). Australian Government Publishing Service, Canberra, New South Wales, Australia.
- Pusey, B. J., and M. J. Kennard.
2001. *Guyu wujalwujalensis*, a new genus and species (Pisces: Percichthyidae) from north-eastern Queensland, Australia. *Ichthyol. Explor. Freshw.* 12:17-28.
- Trnski, T.
2002. Behaviour of settlement-stage larvae of fishes with an estuarine juvenile phase: *in situ* observations in a warm-temperate estuary. *Mar. Ecol. Progr. Ser.* 242:205-214.
- Trnski, T., D. J. Russell, and J. M. Leis.
2000. Latidae (barramundi, sea basses). In *The larvae of Indo-Pacific coastal fishes: an identification guide to marine fish larvae* (J. M. Leis and B. M. Carson-Ewart, eds.), p. 313-316. Fauna Malesiana Handbooks 2, Brill, Leiden, The Netherlands.
- Van der Wal, E.
1985. Effects of temperature and salinity on the hatch rate and survival of Australian bass (*Macquaria novemaculeata*) eggs and yolk-sac larvae. *Aquaculture* 47:239-244.
- Vigliola, L., and M. Harmelin-Vivien.
2001. Post-settlement ontogeny in three Mediterranean reef fish species of the genus *Diplodus*. *Bull. Mar. Sci.* 68:271-286.
- Walker Jr, H. J., A. G. Miskiewicz, and F. J. Neira.
2000a. Microcanthidae (stripey). In *The larvae of Indo-Pacific coastal fishes: an identification guide to marine fish larvae* (J. M. Leis and B. M. Carson-Ewart, eds.), p. 470-473. Fauna Malesiana Handbooks 2, Brill, Leiden, The Netherlands.
- Walker Jr, H. J., F. J. Neira, A. G. Miskiewicz, and B. M. Carson-Ewart.
2000b. Kyphosidae (rudderfishes, sea chubs). In *The larvae of Indo-Pacific coastal fishes: an identification guide to marine fish larvae* (J. M. Leis and B. M. Carson-Ewart, eds.), p. 466-469. Fauna Malesiana Handbooks 2, Brill, Leiden, The Netherlands.
- Williams, N. J.
1970. A comparison of the two species of the genus *Percaletes* Ramsay and Ogilby (Percomorphi: Macquariidae), and their taxonomy. *State Fisheries Research Bulletin* 11, 60 p. Chief Secretary's Department, Sydney, New South Wales, Australia.

Abstract—The Argentine sandperch *Pseudoperca semifasciata* (Pinguipedidae) sustains an important commercial and recreational fishery in the northern Patagonian gulfs of Argentina. We describe the morphological features of larvae and posttransition juveniles of *P. semifasciata* and analyze the abundance and distribution of early life-history stages obtained from 19 research cruises conducted on the Argentine shelf between 1978 and 2001. *Pseudoperca semifasciata* larvae were distinguished from other larvae by the modal number of myomeres (between 36 and 38), their elongated body, the size of their gut, and by osteological features of the neuro- and branchiocranium. *Pseudoperca semifasciata* and *Pinguipes brasiliensis* (the other sympatric species of pinguipedid fishes) posttransition juveniles were distinguished by their head shape, pigmentation pattern, and by the number of spines of the dorsal fin (five in *P. semifasciata* and seven in *P. brasiliensis*). The abundance and distribution of *P. semifasciata* at early stages indicate the existence of at least three offshore reproductive grounds between 42–43°S, 43–44°S, and 44–45°S, and a delayed spawning pulse in the southern stocks.

Early life history of the Argentine sandperch *Pseudoperca semifasciata* (Pinguipedidae) off northern Patagonia

Leonardo A. Venerus

Centro Nacional Patagónico—Consejo Nacional de Investigaciones Científicas y Técnicas
Boulevard Brown s/n, (U9120ACV)
Puerto Madryn, Chubut, Argentina
E-mail address: leo@cenpat.edu.ar

Laura Machinandiarena

Martín D. Ehrlich

Instituto Nacional de Investigación y Desarrollo Pesquero
PO Box 175, (B7602HSA)
Mar del Plata, Buenos Aires, Argentina

Ana M. Parma

Centro Nacional Patagónico—Consejo Nacional de Investigaciones Científicas y Técnicas
Boulevard Brown s/n, (U9120ACV)
Puerto Madryn, Chubut, Argentina

The family Pinguipedidae (Osteichthyes, Perciformes) includes six genera and about 50 marine species and one freshwater species (Froese and Pauly, 2004). On the Argentine continental shelf this family is represented by two species, *Pseudoperca semifasciata* (Cuvier, 1829) and *Pinguipes brasiliensis* Cuvier, 1829.

The Argentine sandperch *P. semifasciata* is an important incidental catch in the bottom trawl and long-line commercial fisheries that target hake (*Merluccius hubbsi*) in the northern Patagonian coast off Argentina (Otero et al., 1982; Elias and Burgos, 1988; González, 1998). In recent years, the reported annual landings have oscillated between 1900 and 3780 metric tons (official statistics, SAGPYA-DNPYA¹). In northern Patagonia, *P. semifasciata* is also targeted by sport anglers and spear fishermen and represents a tourist attraction for recreational divers. It inhabits rocky and sandy bottoms, from 23°S in Brazil to 47°S in Argentina (Cousseau and Perrotta, 2000), mainly in coastal waters, although it has been found in depths of up to 100 m (Menezes and Figueiredo, 1985).

Very little is known about the ecology and behavior of *P. semifasciata*, and most of what is known is based on limited observations during underwater visual censuses on shallow reefs where adults concentrate (González, 1998). Previous studies have focused on morphological features (Herrera and Cousseau, 1996; Rosa and Rosa, 1997; Gosztonyi and Kuba²), age and growth (Elias and Burgos, 1988; Fulco, 1996; González, 1998), diet (Elias and Rajoy, 1992; González, 2002), and reproductive traits, including reproductive season, spawning modality, and age at first maturity (Macchi et al., 1995;

¹ SAGPYA-DNPYA. 2003. Capturas marítimas totales 1992–2002. Manuscript, 71 p. [Available from Secretaría de Agricultura, Ganadería y Pesca de la Nación. Dirección de Pesca y Acuicultura, Paseo Colón 982 P.B. Of. 59 – (C1063ACW) Buenos Aires, Argentina.] <http://www.sagpya.mecon.gov.ar> [Accessed July 2004].

² Gosztonyi, A. E., and L. Kuba. 1996. Atlas de huesos craneales y de la cintura escapular de peces costeros patagónicos. Inf. Téc. FPN 4, 29 p. [Available from CENPAT, Blvd. Brown s/n (U9120ACV), Puerto Madryn, Chubut, Argentina.]

Fulco, 1996; González, 1998). *Pseudoperca semifasciata* is a multiple spawner with low hatch fecundity and an extended reproductive season (Macchi et al., 1995; González, 1998). There is little information on the early life history of the species because only specimens >20–25 cm are found on reefs and the habitat of juveniles has not been described. In general, information about the early stages of pinguipedid fishes from the southwest Atlantic Ocean is scarce. De Cabo³ reported pinguipedid larvae from the Argentine shelf but did not identify the specimens to species level.

In the present study, we describe development of *P. semifasciata* from larvae to the posttransition juvenile stage (*sensu* Vigliola and Harmelin-Vivien, 2001) and analyze data on distribution and abundance on the northern Patagonian shelf. This information is needed to locate main reproductive and nursery grounds for the species.

³ De Cabo, L. 1988. Descripción de tres larvas de peces teleosteos del Mar Argentino: Mugiloididae, Ophidiidae (*Genypterus blacodes*) y Tripterygiidae (*Tripterygion cunninghami*). Unpubl. manuscript, 58 p. Facultad de Ciencias Exactas y Naturales, Universidad de Buenos Aires-INIDEP. [Available from INIDEP: P.O. Box 175 (B7602HSA) Buenos Aires, Argentina.]

Materials and methods

Fish larvae and posttransition juveniles were collected during 19 research cruises conducted by INIDEP (Instituto Nacional de Investigación y Desarrollo Pesquero) between 1978 and 2001. A total of 592 ichthyoplankton samples and 277 juvenile trawl samples were analyzed (Table 1).

Larvae

Ichthyoplankton was sampled by using Bongo, Nackthai, and PairOVET nets. The Bongo net was fitted with 300- μ m mesh and a flowmeter. The Nackthai sampler, a German modification of the Gulf V high-speed sampler (Nellen and Hempel, 1969), was fitted with a 400- μ m mesh net and a flowmeter. Both samplers were towed obliquely from bottom to surface. The PairOVET sampler, a Bongo-type version of the CalVET, was fitted with two 200- μ m mesh nets to sample fish eggs (Smith et al., 1985) and was towed vertically. Samples were fixed in a solution of 5% formalin to seawater. During most cruises, depths at which *P. semifasciata* were located were determined by a SCANMAR sensor mounted on the sampler.

Table 1

Research cruises in the Argentine Sea during 1978–2001. Only those cruises with at least one positive station containing larvae or posttransition juveniles of *Pseudoperca semifasciata* were included in the analysis. EH=RV Dr. Eduardo L. Holmberg; OB=RV *Capitán Oca Balda*; SM=RV *Shinkai Maru*.

Year	Cruise	Dates	No. of stations	Lat. S range	Long. W range
Ichthyoplankton surveys					
1978–79	SM-IX	26 Dec–07 Jan	28	42°27'–45°30'	61°58'–66°01'
1982	EH-05/82	19 Nov–03 Dec	65	35°55'–40°53'	54°45'–61°57'
1983	EH-01/83	14 Jan–26 Jan	43	38°30'–44°32'	58°00'–65°07'
1985	OB-02/85	25 Mar–04 Apr	30	44°41'–46°52'	65°05'–67°18'
1986	OB-01/86	20 Jan–03 Feb	40	41°34'–44°36'	61°27'–65°05'
	OB-07/86	09 Dec–22 Dec	43	43°01'–46°50'	62°40'–66°51'
1991	OB-07/91	01 Nov–11 Nov	35	35°49'–36°51'	56°03'–56°59'
1995	OB-14/95	05 Dec–18 Dec	75	41°16'–45°22'	60°00'–67°00'
1996	EH-17/96	12 Dec–21 Dec	18	42°29'–44°01'	62°03'–65°16'
1998	OB-10/98	07 Dec–20 Dec	87	42°21'–45°36'	61°00'–65°44'
1999	OB-09/99	11 Dec–17 Dec	15	43°21'–44°01'	62°59'–65°12'
2000	OB-14/00	09 Dec–21 Dec	27	43°19'–46°24'	63°37'–66°48'
2001	EH-01/01	06 Jan–29 Jan	28	43°19'–46°54'	62°12'–67°33'
	OB-02/01	12 Feb–25 Feb	40	42°54'–45°25'	62°30'–66°12'
	OB-13/01	10 Nov 13 Nov	18	42°21'–43°42'	61°55'–65°01'
Posttransition juvenile trawls					
1992	EH-02/92	02 Mar–21 Mar	45	42°04'–45°43'	62°45'–66°14'
1998	EH-04/98	01 Apr–10 Apr	41	43°18'–47°02'	63°51'–66°43'
1999	EH-04/99	20 May–31 May	56	43°10'–47°01'	63°51'–66°42'
2000	OB-05/00	01 Jun–20 Jun	112	43°45'–47°02'	61°53'–67°25'
2001	OB-02/01	12 Feb–25 Feb	23	42°54'–45°25'	62°30'–66°12'

A total of 68 preserved larvae, ranging in body length (BL) from 3.3 to 11.7 mm, were used to describe larval development. Terminology for morphometrics followed Neira et al. (1998). Additionally, head depth (HD) was defined as the maximum depth of the head. Preserved larvae were measured to the nearest 0.1 mm with an ocular micrometer fitted to a dissecting microscope, and their pigmentation pattern was recorded. Possible shrinkage was not considered in the measurements. Whenever possible, the number of vertebrae and numbers of dorsal, anal, caudal, pectoral, and pelvic fin rays were recorded. In addition, 14 larvae from 3.4 to 11.7 mm BL were cleared and stained following the methods of Potthoff (1984) and Taylor and Van Dyke (1985), and then examined for meristics and osteological features. Myomere and fin-ray counts and morphometric measurements were made on the left side of the body. Larval abundance was expressed as the number of larvae/10 m² of sea surface as recommended by Smith and Richardson (1977).

Posttransition juveniles

Posttransition juveniles were collected with a small bottom trawl called "Piloto," with the following features: 6 m total length, 6-m headrope and groundrope, 25-mm wing mesh size, 10-mm codend mesh size, 0.25-m² otter board surface and 12 kg weight, 10-m bridles and 0.80-m vertical opening. In Argentina, commercial fishing vessels use this gear for locating shrimp concentrations. Additionally, an epibenthic sampler (Rothlisberg and Percy, 1976) fitted with 1-mm mesh was used on one cruise (EH-02/92). We believe that individuals up to 12 cm total length were well represented in samples obtained with this gear.

A total of 27 posttransition juveniles, ranging from 22 to 83 mm body length (BL), were used to describe Argentine sandperch developmental stages. Samples were either frozen or fixed in 5% formalin to seawater solution. Measurements and degree of pigmentation were recorded after preservation.

Total length (TL), body length (=standard length), head length (HL), predorsal length (PDL), and preanal length (PAL) were measured to the nearest 1 mm. Head depth (HD), body depth (BD), and eye diameter (ED) were measured to the nearest 0.2 mm. Three juveniles between 22 and 33 mm BL were cleared and stained (Potthoff, 1984; Taylor and Van Dyke, 1985) and examined for meristics.

The density of posttransition juveniles, expressed as individuals/square nautical mile (nmi²), was estimated from swept area. The family Pinguipedidae includes two species (morphologically very similar as juveniles) that overlap in the Argentine Sea. Unfortunately, not all individuals caught during the cruises were examined by us; therefore, to avoid biases caused by identification errors, the posttransition juveniles of both species were considered as a group. Distributional centroids and ellipses were calculated by following the method of Kendall and Picquelle (1989), that is by weighting

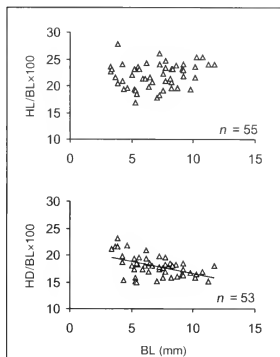


Figure 1

Relative head length (HL/BL × 100) and relative head depth (HD/BL × 100) against body length (BL) in *Pseudoperca semifasciata* larvae, regardless of the flexion stage of the notochord. Solid line represents a linear trend ($n=53$; $r^2=0.2576$; $P<0.001$).

each station by the density of juveniles caught. For this purpose each density value was standardized with respect to the maximum density observed for each survey season over all years.

Results

Description of larvae

General morphological features The larval body was elongate and relative BD was <25% in all stages of development (Table 2). The smallest larva collected (yolksac larva) was 3.3 mm BL. Its yolk sac was small and the single oil globule was located on the anterior part of the yolk mass. Notochord flexion began at 6 mm and was complete by 7–8 mm BL. As development proceeded, larvae became slightly deeper and laterally compressed. The head was small, with a rounded snout and no spines. The oblique mouth was open by the end of the yolksac larval stage. By 10 mm BL, premaxilla and dentary bones were covered with caniniform teeth. The premaxilla was an elongated bone with three processes on its dorsal margin—the first one perpendicular to the premaxilla. Relative head length remained constant, whereas relative head depth diminished during development (Fig. 1). The eyes were pigmented and their relative diameter decreased during the preflexion stage, and

Table 2

Body proportions of *Pseudoperca semifasciata* larvae, according to the flexion stage of the notochord. Mean (\pm SE), range and number of observations are shown in the table. BD=body depth; BL=body length; ED=eye diameter; HD=head depth; HL=head length; PAL=preanal length.

		BD/BL \times 100	HD/BL \times 100
Preflexion	3.3–7.1 mm BL; n=36:	16.4 \pm 3.1 (12.4–25.5) n=27	18.5 \pm 2.3 (14.8–23.1) n=25
Flexion	6.2–8.7 mm BL; n=8:	14.5 \pm 1.4 (12.2–16.1) n=5	17.1 \pm 1.2 (15.9–19.4) n=8
Postflexion	7.3–11.7 mm BL; n=20:	16.8 \pm 1.3 (14.3–19.5) n=20	17.4 \pm 1.4 (15.2–19.8) n=20
		PAL/BL \times 100	ED/BL \times 100
Preflexion		53.6 \pm 4.1 (45.0–62.5) n=29	7.8 \pm 1.1 (5.9–10.9) n=29
Flexion		52.0 \pm 2.2 (49.4–56.5) n=8	6.1 \pm 0.3 (5.6–6.5) n=8
Postflexion		52.5 \pm 2.7 (47.3–57.5) n=20	6.1 \pm 0.7 (4.9–7.6) n=20
		HL/BL \times 100	
Preflexion		21.2 \pm 2.4 (17.0–27.7) n=27	
Flexion		20.5 \pm 1.9 (18.2–24.2) n=8	
Postflexion		23.4 \pm 1.5 (19.3–26.0) n=20	

then remained constant (Fig. 2, A and B). The gut was initially straight but began to constrict at 4 mm BL and was loosely constricted throughout development (Fig. 3, A–C). It was moderate to long and extended to near the midpoint of the body, resulting in a relative preanal length of 0.45 to 0.62 BL.

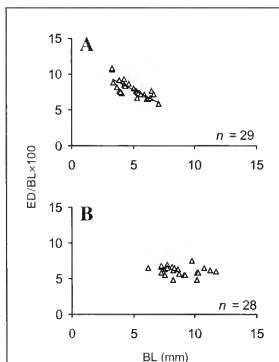


Figure 2

Relative eye diameter (ED/BL \times 100) against body length (BL) in *Pseudoperca semifasciata* larvae. (A) Preflexion larvae. Solid line represents a linear trend (n=29; $r^2=0.6228$; $P<0.001$). (B) Flexion and postflexion larvae.

Body pigmentation Argentine sandperch larvae were lightly pigmented during all stages of development (Fig. 3; A–C). The pigmentation on the ventral body surface, between the isthmus and the anus, consisted of small stellate melanophores. Several small melanophores were scattered on the lateral surface of the anterior part of the gut. A double row of minute melanophores along the ventral surface ended in a single melanophore at the constriction of the gut. Pigmentation along the lateral midline of the tail consisted of four to seven stellate melanophores.

In preflexion larvae (Fig. 3A), small spots were evident along the lower jaw and the ventral part of the head. Several small stellate melanophores were present on the dorsal surface of the gut. A few melanophores were scattered at the base of the pectoral fin bud.

Preflexion and flexion larvae (Fig. 3, A and B) showed a distinct pattern of 12 to 23 small postanal melanophores serially arranged, about one per myomere, along the ventral midline. A total of 11 to 18 melanophores, about one melanophore per anal fin pterygiophore, was observed in postflexion larvae (Fig. 3C). As flexion progressed (Fig. 3, B and C), the number of melanophores on the ventral part of the head and over the gut diminished.

Fins and meristic features Modes of preanal and postanal myomeres were 14 and 23, respectively. All specimens examined had 33–40 total myomeres (mode:36–38 myomeres). Vertebral column ossification started anteriorly. A total of 38–39 vertebrae were recorded in 10–12 mm BL postflexion larvae (n=2).

In yolksac larvae, finfold and pectoral buds were the first fin development distinguished. In preflexion and flexion larvae, the finfold was present and it was gradually lost as the true fins developed. The sequence of fin-ray formation, characterized by initial development of fin elements, was caudal (7–8 mm BL), then pectoral

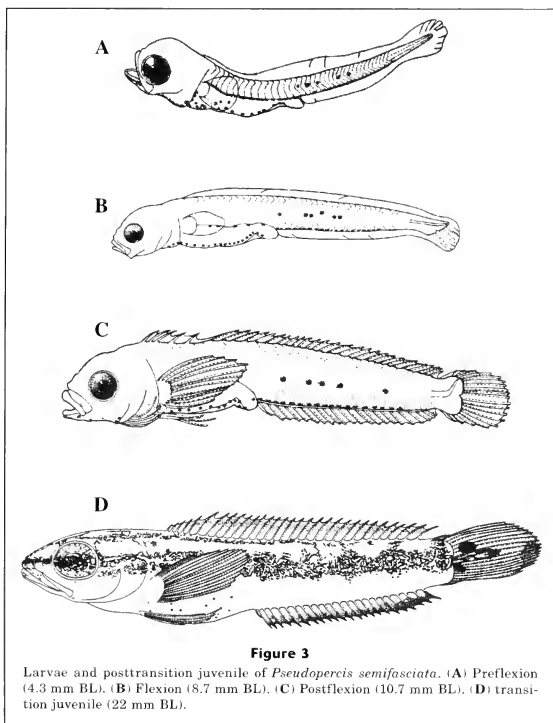


Figure 3
Larvae and posttransition juvenile of *Pseudoperca semifasciata*. (A) Preflexion (4.3 mm BL). (B) Flexion (8.7 mm BL). (C) Postflexion (10.7 mm BL). (D) transition juvenile (22 mm BL).

(9–10 mm BL), anal (9–10 mm BL), dorsal (9–10 mm BL), and pelvic (10–11 mm BL). Elements of the caudal fin began forming at flexion stage, and remaining fins at the postflexion stage. By 9–10 mm BL, dorsal (V+26–27) and anal (II+20–22) fin elements reached their full complement.

Description of posttransition juveniles

The posttransition juvenile stage was characterized by the acquisition of complete fin-ray complements and by morphological similarities with the adults (Table 3, Fig. 4). The transition from pelagic to benthic habitat in this species, i.e. settlement, probably occurred at about 20 mm BL because the smallest benthic juvenile of *Pseudoperca semifasciata* reported was 22 mm BL.

Table 3

Body proportions (mean [\pm SE] and range) of *Pseudoperca semifasciata* posttransition juveniles. BD=body depth; BL=body length; ED=eye diameter; HD=head depth; HL=head length; PAL=preanal length; PDL=predorsal length.

BD/BL \times 100	HD/BL \times 100
15.1 \pm 1.4 (12.7–19.3)	13.8 \pm 1.5 (11.9–19.3)
PAL/BL \times 100	ED/BL \times 100
41.7 \pm 2.2 (37.7 – 48.0)	8.4 \pm 1.1 (6.4–11.9)
HL/BL \times 100	PDL/BL \times 100
23.0 \pm 2.4 (17.6–31.6)	27.8 \pm 1.3 (25.7–30.2)

Individuals became more thick bodied as they developed. The body was elongate and relative body depth remained fairly constant throughout development. The snout was longer and rounded, and relative head length was moderate. The mouth was terminal, reaching to the middle of the eye, and had fleshy lips. Both jaws presented only caniniform teeth. Two opercular spines were also present in all specimens studied. Relative head depth decreased slightly during development, but not relative eye diameter. Gut length was moderate (PAL/BL 0.38–0.48), and the anus was situated near the midpoint of the body (Fig. 3D). Relative predorsal length (0.26–0.30) diminished during development.

The scales were ctenoid. Smaller posttransition juveniles (BL \pm 35 mm) retained some of the larval pigmentation pattern. Larger juveniles showed several dark vertical bars, not completely defined at this stage of development, and three horizontal stripes along the body (Fig. 3D). Vertical bars developed progressively from the caudal peduncle to the head. Two lateral stripes formed continuous bands along each side of the body, almost entirely above the midline. The upper stripe developed from the tip of the snout and the lower one began below the eye, both extending to the anterior caudal peduncle. Another stripe developed from the dorsal region of the head between the eyes and extended along the dorsal fin, joining the upper lateral stripe at the posterior third part of the body. In large posttransition juveniles (\geq 47 mm BL), the membrane of the dorsal fin was pigmented more densely between the spines than between the rays; there were also dark blotches on the membrane between the rays. Anal-fin membranes were more pigmented than those of the dorsal fin. The membranes of the pectoral, pelvic, and caudal fins, and the external border of the membranes of the dorsal fin, were yellow in frozen individuals. By 22 mm BL, the conspicuous

dark blotch observed in adult *P. semifasciata* on the base of the caudal fin upper lobe (Herrera and Cousseau, 1996) was already present (Fig. 3D). The pelvic fin was large and slightly shorter than the pectoral fin, whose margin was rounded.

Abundance and distribution

Larvae Larvae of Argentine sandperch occurred between 36°42'S and 46°30'S, mainly in coastal waters, in the vicinity of the 50-m isobath (Fig. 5). The southernmost limit where larvae were collected was within San Jorge Gulf, which was surveyed in late March (fall). Larvae were present in only 3.55% of the stations in densities that varied between two and 74 larvae/10 m² of sea surface (Table 4). Greater densities (>20 larvae/10 m² of sea surface) were obtained in December 1986, 1996, and 1999, off the coast between Engaño Bay and Isla Escondida. Positive stations formed scattered clumps along the whole distributional area of the species. Minimum and maximum depths sampled were 20 and 71 m, respectively. Water temperature at 10 m depth at positive stations varied between 12.3°C (March 1985) and 18.7°C (December 1999) (mean temperature [\pm SE]: 15.2°C [\pm 2.1°C]).

Posttransition juveniles Posttransition pinguipedid juveniles were found between 42°27'S and 43°37'S in February and March, and between 43°17'S and 44°58'S from April to June, primarily in the vicinity of the 50-m isobath (Fig. 6, A and B). The percentages of positive stations were 5.9% and 7.7% in summer and fall surveys, respectively. Maximum juvenile densities were 4410 individuals/nmi² in summer and 27,027 individuals/nmi² in fall (Table 5).

The grid of stations used during the summer and fall cruises overlapped (Fig. 6, A and B), covering the main area of concentration of *P. semifasciata* (Otero et al., 1982). Minimum and maximum depths were 54 and 74 m in summer surveys (mean depth [\pm SE]: 64.5 [\pm 10.0] m), and 34 and 79 m in fall surveys (mean depth [\pm SE]: 60.4 [\pm 13.7] m). The distributional ellipses calculated for summer and fall from the positive stations were small and widely separated. Maximum summer densities of posttransition pinguipedids were found southeast of Peninsula Valdés, whereas greatest fall densities were detected northeast of Camarones Bay (Fig. 6, A and B).

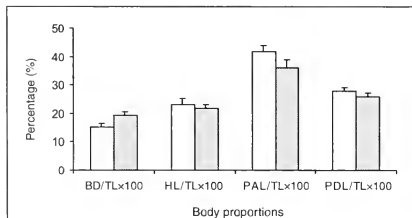


Figure 4

Comparisons between body proportions in posttransition juveniles (white bars) and adults (gray bars) of *Pseudoperca semifasciata*. Relative measures were taken with respect to total length (TL). Body depth (BD), head length (HL), preanal length (PAL), predorsal length (PDL). Proportions for adults were estimated from 99 individuals between <30 cm and 90 cm TL (González, 1998).

Discussion

Literature describing the early stages of species belonging to the family Pinguipedidae (formerly Mugiloididae) is scarce. The few available studies refer to the larval development of *Paraperca* spp. (Leis and Rennis, 1983; Watson et al., 1984; Houde et al., 1986; Neira, 1998; Leis and Rennis, 2000)

and *Prolatilus jugularis* (Vélez et al., 2003). Larval abundance and distribution have been studied for a few species of *Paraperca* (Houde et al., 1986; Gaughan et al., 1990; Neira et al., 1992) and, more recently, for *Prolatilus jugularis* (Vélez et al., 2003); no information is available for posttransition pinguipedid juveniles.

Larvae of *P. semifasciata* resembled the larvae of other pinguipedids in their gut size, meristics, and general pattern of pigmentation. They differed from *Paraperca* spp. and *P. jugularis* larvae in some relevant features:

- The head had no spines and was less rotund, rather moderate instead of large (HL ranged from 0.17 to 0.30 BL; mean HL/BL=0.22 [± 0.02]);
- The body was rather elongate instead of moderate (BD ranged from 0.12 to 0.26 BL; mean BD/BL=0.16 [± 0.03]);
- The notochord flexion occurred between 6.2 and 8.7 mm BL, at a relatively large size range compared to that for *Paraperca* spp. (3.7–4.8 mm BL) and to *P. jugularis* (5.7–6.9 mm BL). *Pseudoperca semifasciata* is a larger and more rotund species;
- The finfold was still present in preflexion and flexion larvae.

De Cabo³ described some osteological, meristic, and morphological characteristics of Argentine Sea pinguipedid larvae. Like De Cabo³ we found that the first cranial bones that appeared during larval development in *P. semifasciata* were the premaxilla, the dentary and the cleithrum. These structures were already ossified in 3.4 mm BL preflexion larvae. From the adult osteological descriptions by Herrera and Cousseau (1996) and Gosztanyi and Kuba,² we determined that the larvae studied were *P. semifasciata*. The only other sympatric species of Pinguipedidae in the Argentine shelf is the Brazilian sandperch (*Pinguipes brasilianus*), which shares several similarities in meristic counts with *P. semifasciata* (Rosa and Rosa, 1987; Herrera and Cousseau, 1996). However, some osteological features from the neuro- and branchiocranium are of great value for identification of larval stages of *P. semifasciata*. The two species could be distinguished by the placement of the first process of the premaxilla, which is perpendicular to the premaxilla in the Argentine sandperch, and back-inclined in the Brazilian sandperch, drawing an acute angle with the premaxilla (Herrera and Cousseau, 1996). The dentary in *P. semifasciata* has a quadrangulate anterior end and a margin almost straight, whereas the margin of the dentary in *P. brasilianus* is oblique (Herrera and Cousseau, 1996). In addition, the head and the teeth patch of the vomer are quadrangulate in *Pinguipes* and triangular in *Pseudoperca* (Herrera and Cousseau, 1996).

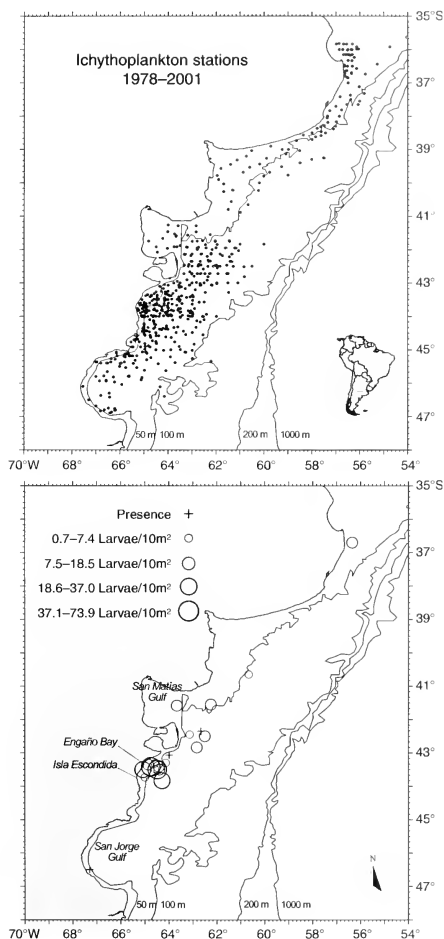


Figure 5

Distribution of ichthyoplankton stations (upper) and *Pseudoperca semifasciata* larvae (lower) in the Argentine Sea in the period 1978–2001. Dot diameter, classified into four categories, is proportional to larval abundance at each station (expressed as larvae/10 m² of sea surface).

Table 4

Positive stations for *Pseudoperis semifasciata* larvae in the Argentine Sea, during 1978–2001. Temperature values in parentheses indicate that only surface temperature was registered. W/d=missing data.

Cruise	Date	Sampler	Lat. S	Long. W	Abundance (larvae/10 m ² of sea surface)	Water temperature (at 10 m depth)	Depth (m)
SM-IX	28 Dec 1978	Bongo	42°27'	63°08'	7.36	w/d	70
EH-05/82	22 Nov 1982	Bongo	40°39'	60°40'	5.85	(12.8)	53
EH-01/83	21 Jan 1983	Bongo	43°44'	65°00'	4.82	16.7	52
OB-02/85	30 Mar 1985	Bongo	46°30'	67°18'	Presence	12.3	56
OB-07/86	20 Dec 1986	Nackthai	43°25'	64°45'	73.91	14.2	34
OB-07/86	20 Dec 1986	Nackthai	43°50'	64°17'	19.78	14.0	47
OB-01/86	22 Jan 1986	Nackthai	41°33'	62°15'	13.76	18.7	45
OB-01/86	22 Jan 1986	Nackthai	41°35'	63°40'	8.64	17.6	51
OB-07/91	02 Nov 1991	Nackthai	36°42'	56°21'	15.33	w/d	20
OB-14/95	12 Dec 1995	Pairovet	43°04'	63°59'	Presence	13.0	65
EH-17/96	15 Dec 1996	Nackthai	43°30'	65°05'	23.92	14.3	24
OB-10/98	10 Dec 1998	Nackthai	42°21'	62°40'	Presence	w/d	66
OB-09/99	12 Dec 1999	Nackthai	43°21'	64°52'	17.22	(14.6)	20
OB-09/99	12 Dec 1999	Nackthai	43°30'	64°29'	41.00	(21.0)	49
OB-14/00	11 Dec 2000	Bongo	43°19'	64°35'	1.81	(12.8)	37
OB-14/00	11 Dec 2000	Bongo	43°30'	64°24'	8.44	13.8	52
EH-01/01	26 Jan 2001	Bongo	43°29'	64°35'	2.51	15.9	47
OB-02/01	16 Feb 2001	Bongo	43°18'	64°08'	5.20	15.8	59
OB-13/01	10 Nov 2001	Bongo	42°30'	62°30'	9.30	w/d	71
OB-13/01	11 Nov 2001	Bongo	42°50'	62°55'	9.36	w/d	71
OB-13/01	13 Nov 2001	Bongo	43°25'	64°49'	7.99	w/d	38

The modal number of myomeres (36–38; $n=47$) in *P. semifasciata* larvae matched the number of vertebrae reported for adults (36–37; $n=50$) by González (1998). The dorsal and anal fin elements reached their full complement by 9–10 mm BL, whereas the caudal-, pelvic-, and pectoral-fin elements were still incomplete in the size range analyzed in this study (3.3 to 11.7 mm BL). *Pseudoperis semifasciata* and *P. brasilianus* post-transition juveniles differ in their head shape, pigmentation pattern, and in the number of spines of the dorsal fin. The snout is larger in the Brazilian sandperch and the dorsal profile of the head is less convexly shaped than in *P. semifasciata*. These head shape differences increased with size. In *P. brasilianus*, the lateral stripes were less conspicuous than in *P. semifasciata*, and the vertical bars appeared earlier in the development (seven vertical bars were present in ca. 50 mm BL individuals). Furthermore, vertical bars in *P. semifasciata* were more defined at the base of the dorsal fin, whereas they extended below the midline in *P. brasilianus*. *Pseudoperis semifasciata* had five dorsal-fin spines, and *P. brasilianus* had seven spines, both in the range reported by Herrera and Cousseau (1996).

Both the epibenthic sampler and the "Piloto" trawl used to collect juveniles sample the fauna from the bottom to approximately one meter above the bottom. The

fact that juveniles were caught in the lowest strata of the water column indicates that juveniles had settled to benthic habitat, even though the *P. semifasciata* post-transition juveniles still conserved some larval pigmentation, had not completely developed adult pigmentation pattern, and had already acquired morphological proportions similar to adults.

Even though the abundance and distribution data used in our study came from cruises that targeted other species, they provide satisfactory spatiotemporal coverage. This was particularly true for the ichthyoplankton surveys, which covered a great portion of the distributional area of *P. semifasciata* in the northern Patagonian shelf, mainly during the peak of the reproductive season (November–December). Among the Piloto positive stations ($n=20$), *P. brasilianus* was found by itself only at three stations. Also, *P. brasilianus* was far less abundant than *P. semifasciata* posttransition juveniles in the trawl samples. As a consequence, we consider that the abundance and distribution patterns of post-transition pinguipedid juveniles adequately reflect the abundance and distribution of *P. semifasciata* posttransition juveniles in the Argentine shelf.

The abundance and distribution of *P. semifasciata* larvae and posttransition juveniles indicate the presence of at least three main reproductive grounds, one

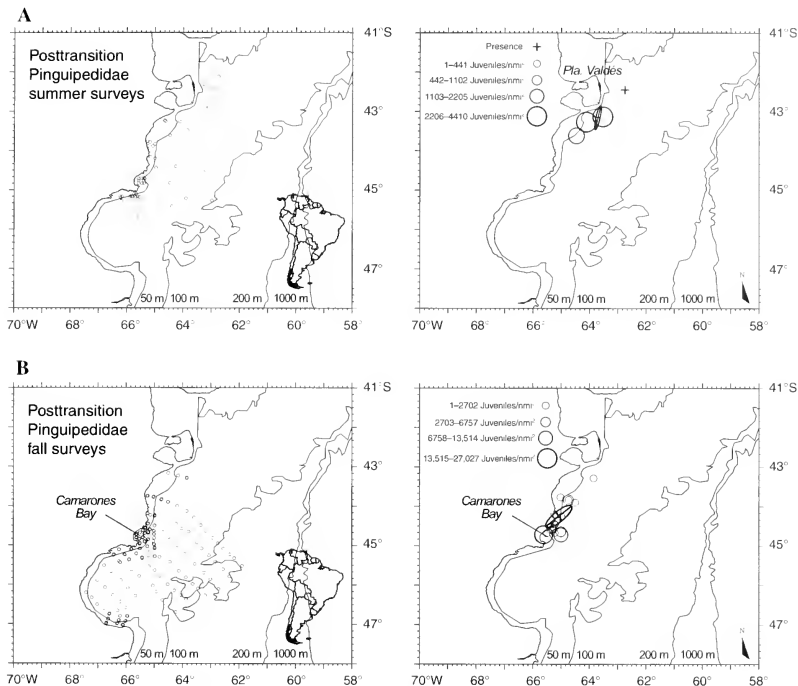


Figure 6

Distribution of "Piloto" or epibenthic sampler stations (left) and Pinguipedidae posttransition juveniles (right) in the Argentine Sea by season. (A) Summer surveys. (B) Fall surveys. Dot diameter, classified into four categories, is proportional to posttransition juvenile abundance at each station (expressed as no. of juveniles/nmi²).

located off Peninsula Valdés (42–43°S, 63°W), another off the coast between Engaño Bay and Isla Escondida (43–44°S, 64°W to the coast), and the third off northeastern Camarones Bay (44–45°S, 65°W to the coast). These areas are linked to a frontal zone, the Northern Patagonia frontal system, which is highly productive during the spring and summer and could offer retention mechanisms for larvae (Bogazzi et al., in press). In December 1978, Argentine sandperches of both sexes were observed running near Isla Escondida (Ehrlich, personal observ.). In addition, Elias and Burgos (1988) reported great concentrations of Argentine sandperches off Peninsula Valdés (42–44°S) between October and December, based on commercial fishery data for the period

1981–88. These reproductive grounds are consistent with the principal areas of summer concentration described by Otero et al. (1982). Furthermore, Elias and Burgos (1988) attributed the decline in yields and average size observed in January and February to the dispersal of postspawning individuals. However, initial results from an ongoing tag-recapture program in San José Gulf indicate that this species may have a high site fidelity and a limited dispersal (Venerus et al., 2003). In this case, the declines in yield and average size as the fishing season progresses could be a consequence of the fishing effort itself. Macchi et al. (1995) detected a decrease in the proportion of females in January, which also may imply an emigration from the reproductive sites.

Table 5

Positive stations for posttransition pinguipedids in the Argentine Sea, during 1992–2001. The "Species" column show the categories assigned in the survey reports. Underlined items in the "Abundance" column indicate that some or all of the specimens were preserved and at least one individual was correctly identified as *Pseudoperca semifasciata*. EBS= epibenthic sampler.

Cruise	Date	Season	Sampler	Lat. S	Long. W	Species	Abundance (individuals/nmi ²)	Depth (m)
EH-02/92	18 Mar 1992	Summer	EBS	42°27'	62°45'	<i>Pseudoperca</i>	Presence	71
OB-02/01	14 Feb 2001	Summer	Piloto trawl	43°08'	63°32'	Both	<u>4409.5</u>	74
OB-02/01	16 Feb 2001	Summer	Piloto trawl	43°16'	64°07'	Pinguipedidae	2572.2	59
OB-02/01	17 Feb 2001	Summer	Piloto trawl	43°37'	64°28'	Pinguipedidae	1286.1	54
EH-04/98	07 Apr 1998	Fall	Piloto trawl	44°40'	65°13'	<i>Pseudoperca</i>	1492.6	74
EH-04/98	07 Apr 1998	Fall	Piloto trawl	44°43'	65°00'	<i>Pseudoperca</i>	10,204.1	79
EH-04/98	07 Apr 1998	Fall	Piloto trawl	44°38'	65°01'	<i>Pseudoperca</i>	4761.9	78
EH-04/98	07 Apr 1998	Fall	Piloto trawl	44°34'	65°20'	<i>Pseudoperca</i>	3448.3	52
EH-04/98	07 Apr 1998	Fall	Piloto trawl	44°28'	65°14'	<i>Pseudoperca</i>	1587.3	61
EH-04/99	28 May 1999	Fall	Piloto trawl	44°12'	65°14'	<i>Pseudoperca</i>	<u>1449.3</u>	34
EH-04/99	28 May 1999	Fall	Piloto trawl	43°50'	64°44'	<i>Pinguipes</i>	1315.8	64
EH-04/99	29 May 1999	Fall	Piloto trawl	43°54'	64°30'	<i>Pinguipes</i>	1265.8	65
EH-04/99	29 May 1999	Fall	Piloto trawl	43°17'	63°51'	<i>Pseudoperca</i>	1250.0	73
OB-05/00	11 Jun 2000	Fall	Piloto trawl	44°27'	65°13'	<i>Pinguipes</i>	2631.6	64
OB-05/00	11 Jun 2000	Fall	Piloto trawl	44°34'	65°19'	<i>Pseudoperca</i>	<u>1250.0</u>	58
OB-05/00	11 Jun 2000	Fall	Piloto trawl	44°41'	65°31'	<i>Pseudoperca</i>	<u>1351.4</u>	43
OB-05/00	11 Jun 2000	Fall	Piloto trawl	44°43'	65°37'	Both	<u>27,027.0</u>	38
OB-05/00	15 Jun 2000	Fall	Piloto trawl	44°15'	64°59'	<i>Pinguipes</i>	1449.3	72
OB-05/00	18 Jun 2000	Fall	Piloto trawl	43°50'	64°44'	Both	<u>5194.8</u>	59
OB-05/00	18 Jun 2000	Fall	Piloto trawl	43°46'	65°01'	<i>Pseudoperca</i>	<u>1388.9</u>	52

The low number of positive stations in spite of the intense sampling conducted within the area of distribution of *P. semifasciata* suggests a reduced spawning site. Both the area off Península Valdés and the one near Isla Escondida have rocky bottoms, which complicates trawling operations. A few experienced captains were able to target *P. semifasciata* by trawling along sandy corridors between rocky outcrops off Península Valdés during the reproductive season (Eliás⁴). Likewise, where running Argentine sandperches were observed near Isla Escondida, trawling is possible only in one orientation (Ehrlich, personal observ.). This could indicate that spawning grounds are associated with rocky outcrops. Spawning associated with rocky reefs and the existence of chromatic sexual dimorphism is compatible with Macchi et al.'s (1995) and González's (1998) suggestions of a complex mating system involving sexual courtship.

Spawning activity of *P. semifasciata* in northern Patagonia (42–44°S) peaks in November and December (Eliás and Burgos, 1988; Macchi et al., 1995), and in October within San Matías Gulf (González, 1998). Maximum densities of larvae (>20 larvae/10 m² of sea surface) were found in December 1986, 1996, and 1999.

The temperature at 10 m depth at positive ichthyoplankton stations varied between 12.3°C and 18.7°C. Such a wide range of temperature reflects the wide latitudinal range in the distribution of *P. semifasciata* and the extended time period (November–March) in which larvae were collected.

Posttransition pinguipedid juveniles were mainly collected at depths between 60 and 65 m, in both seasons sampled (summer and fall). A total of seven *P. semifasciata* juveniles ranging in total length from 66 to 82 mm were collected in fall (June), near the northern coast of San Matías Gulf (40°58'S–41°00'S; 64°18'W–64°24'W), at 29–54 m depth, associated with rib mussel beds (*Aulacomia ater*) (González⁵). Our distributional data indicate that settlement and nursery grounds could be located near shore. The absence of posttransition juveniles off northeast of Camarones Bay during summer and their presence in the fall could be a consequence of a delayed spawning pulse in the southern stocks. Some independent observations support this hypothesis: 1) back-calculations of hatching date based on daily growth increments from 19 post-

⁴ Eliás, I. 2004. Personal commun. Centro Nacional Patagónico, Puerto Madryn, Chubut, Argentina.

⁵ González, R. A. C. 2004. Personal commun. Instituto de Biología Marina y Pesquera "Alc. Storni", San Antonio Oeste, Río Negro, Argentina.

transition juveniles collected in northeast Camarones Bay, between 43°50'S and 44°43'S, indicated birth dates between February and March (Venerus and Brown, 2003); 2) the collection of one *P. semifasciata* larva in San Jorge Gulf (46°30'S 67°18'W) on 30 March 1985; and 3) macroscopic observations of the ovaries from 24 mature females angled near Islas Blancas, Camarones Bay (ca. 44°46'S 65°38'W) on 26 and 27 January 2002, most of which (58.3%) were in the late developing stage ($n=4$) or in the gravid and running stage ($n=10$) (macroscopic maturation stages *sensu* González, 1998). This delayed spawning pulse in the southern stocks apparently follows the annual cycle of seawater warming on the Argentine shelf (Ciancio⁶). Similar delays have been reported for the Argentine hake (*Merluccius hubbsi*) (Pájaro and Macchi⁷; Machinandiarena et al.⁸).

Further investigations focused on the seasonal distribution of spawners are needed to confirm the existence of spawning aggregations indicated by the presence of larvae and posttransition juveniles. Mark-recapture and telemetry studies could be used to investigate the spatial dynamics of reproductive activity of this species in the Argentine Sea. Given the relative sedentary habits of adult Argentine sandperches, the use of reproductive refuges appear *a priori* to provide a suitable approach to protect this species.

Acknowledgments

We thank the crew and scientific staff on board for collecting the material. We also thank Atila Gosztonyi, Raúl González, and two anonymous reviewers for providing useful comments on the manuscript. L.A.V. was supported by a fellowship from Consejo Nacional de Investigaciones Científicas y Técnicas (CONICET).

Literature cited

- Bogazzi, E., A. Baldoni, A. Rivas, P. Martos, R. Reta, J. M. Orensanz, M. Lasta, and P. Dell'Arciprete.
In press. Spatial correspondence between areas of concentration of Patagonian scallop (*Zygochlamys patagonica*) and frontal systems in the Southwestern Atlantic. *Fish. Oceanograph.*
- ⁶ Ciancio, J. 2004. Unpubl. data. Centro Nacional Patagónico, Puerto Madryn, Chubut, Argentina.
- ⁷ Pájaro, M., and G. J. Macchi. 2001. Distribución espacial y estimación de la talla de primera maduración del stock patagónico de merluza (*Merluccius hubbsi*) en el período de puesta diciembre 2000-abril 2001. *INIDEP Inf. Téc. Int.* 100, 14 p. [Available from INIDEP: P.O. Box 175 (B7602HSA) Buenos Aires, Argentina.]
- ⁸ Machinandiarena, L., M. D. Ehrlich, D., Brown, M. Pájaro, and E. Leonarduzzi. 2004. Distribución y abundancia de huevos y larvas de merluza (*Merluccius hubbsi*) en el litoral norpatagónico. Período diciembre 2000 a marzo-abril 2001. *Inf. Téc. Int. DNI-INIDEP* 29, 16 p. [Available from INIDEP: P.O. Box 175 (B7602HSA) Buenos Aires, Argentina.]

- Cousseau, M. B., and R. G. Perrotta.
2000. Peces marinos de Argentina: Biología, distribución, pesca, 163 p. INIDEP. Mar del Plata, Buenos Aires, Argentina.
- Elias, I., and G. Burgos.
1988. Edad y crecimiento del "salmón de mar," *Pseudoperca semifasciata* (Cuvier, 1829) (Osteichthyes, Pinguipedidae) en aguas norpatagónicas argentinas. *Inv. Pesq.* 52:533-548.
- Elias, I., and C. R. Rajoy.
1992. Hábitos alimentarios del "salmon de mar" *Pseudoperca semifasciata* (Cuvier, 1829): Pinguipedidae en aguas norpatagónicas argentinas. *Rev. Biol. Mar.* 27:133-146.
- Froese, R., and D. Pauly (eds.)
2004. Fishbase. World wide web electronic publication. www.fishbase.org. [Accessed April 2004].
- Fulco, V. K.
1996. Aspectos ecológicos y pesqueros del "salmón de mar" *Pseudoperca semifasciata* (Cuvier, 1829) (Osteichthyes, Pinguipedidae) en aguas norpatagónicas. Licenciatura diss., 21 p. Facultad de Ciencias Naturales, Universidad Nacional de la Patagonia San Juan Bosco, Puerto Madryn, Chubut, Argentina.
- Gaughan, D. J., F. J. Neira, L. E. Beckley, and I. C. Potter.
1990. Composition, seasonality and distribution of ichthyoplankton in the lower Swan Estuary, south-western Australia. *Aust. J. Mar. Freshw. Res.* 41:529-543.
- González, R. A. C.
1998. Biología y explotación pesquera del salmón de mar *Pseudoperca semifasciata* (Cuvier, 1829) (Pinguipedidae) en el Golfo San Matías, Patagonia, Argentina. Ph.D. diss., 135 p. Universidad Nacional del Sur, Bahía Blanca, Buenos Aires, Argentina.
2002. Alimentación del salmón de mar *Pseudoperca semifasciata* (Cuvier, 1829) en el golfo San Matías. *IBMP-Serie Publicaciones* 1:14-21.
- Herrera, M., and M. B. Cousseau.
1996. Comparación del esqueleto óseo de dos especies de peces de la familia Pinguipedidae. *Nat. Patagon. (Cienc. Biol.)* 4:95-110.
- Houde, E. D., S. Almatar, J. C. Leak, and C. E. Dowd.
1986. Ichthyoplankton abundance and diversity in the Western Arabian Gulf. *Kuwait Bull. Mar. Sci.* 8:107-393.
- Kendall Jr., A. W., and S. J. Piquelle.
1989. Egg and larval distributions of walleye pollock *Theragra chalcogramma* in the Shelikof Strait, Gulf of Alaska. *Fish. Bull.* 88:133-154.
- Leis, J. M., and D. S. Rennis.
1983. The larvae of Indo-Pacific coral reef fishes, 269 p. New South Wales University Press, Sydney, Australia, and Univ. Hawaii Press, Honolulu, HI.
2000. Pinguipedidae—grubfishes, sandperches. *In The larvae of Indo-Pacific coastal fishes: an identification guide to marine fish larvae (Fauna Malesiana Handbooks 2)* (J. M. Leis and B. M. Carson-Ewart, eds.), p. 565-658. E. J. Brill, Leiden, The Netherlands.
- Macchi, G. J., I. Elias, and G. E. Burgos.
1995. Histological observations on the reproductive cycle of the Argentinean sandperch, *Pseudoperca semifasciata* (Osteichthyes, Pinguipedidae). *Sci. Mar.* 59: 119-127.
- Menezes, N. A., and J. L. Figureado.
1985. Manual de peixes marinhos do sudeste do Brasil.

- V. Teleostei (4), 105 p. Mus. Zool. Univ. São Paulo, Brazil.
- Neira, F. J.
1998. Pinguipedidae: sandperches, grubfishes. In Larvae of temperate Australian fishes: Laboratory guide for larval fish identification (F. J. Neira, A. G. Miskiewicz, and T. Trnski, eds.), p. 362-365. Univ. Western Australia Press, Nedlands, Western Australia, Australia.
- Neira, F. J., A. G. Miskiewicz, and T. Trnski. (eds.)
1998. Larvae of temperate Australian fishes. Laboratory guide for larval fish identification, 474 p. Univ. Western Australia Press, Nedlands, Western Australia.
- Neira, F. J., I. C. Potter, and J. S. Bradley.
1992. Seasonal and spatial changes in the larval fish fauna within a large temperate Australian estuary. Mar. Biol. 112:1-16.
- Nellen, W., and G. Hempel.
1969. Versuche zur Fangigkeit des "Hai" und des modifizierten Gulf-V-plankton-samplers "Nackthai". Meeresforsch. 20:141-154.
- Otero, H., S. J. Bezzi, M. Renzi, and G. Verazay.
1982. Atlas de los recursos pesqueros demersales del Mar Argentino, 248 p. Contrib. INIDEP 423, Mar del Plata, Buenos Aires.
- Potthoff, T.
1984. Clearing and staining techniques. In Ontogeny and systematics of fishes (G. Moser, W. J. Richards, D. M. Cohen, M. P. Fahay, A. W. Kendall, and S. L. Richardson, eds.), p. 35-37. Am. Soc. Ichthy. Herp., Spec. Publ. 1.
- Rosa, I. L., and R. S. Rosa.
1997. Systematic revision of the South American species of Pinguipedidae (Teleostei, Trachinoidei). Revta. Bras. Zool. 14:845-865.
- Rothlisberg, P. C., and W. G. Pearcy.
1976. An epibenthic sampler used to study the ontogeny of vertical migration of *Pandalus jordani* (Decapoda, Caridea). Fish. Bull. 74:994-998.
- Smith, P. E., and S. L. Richardson.
1977. Standard techniques for pelagic fish egg and larva surveys. FAO Fish. Tech. Paper 175, 100 p.
- Smith, P. E., W. C. Flery, and R. P. Hewitt.
1985. The CalCOFI vertical egg tow (CalVET) net. In An egg production method for estimating spawning biomass of pelagic fish: application to the northern anchovy (*Engraulis mordax*) (R. Lasker, ed.), p. 27-33. NOAA Tech. Rep. NMFS 36.
- Taylor, W. K. and G. C. Van Dyke.
1985. Revised procedures of staining and clearing small fishes and other vertebrates for bone and cartilage study. Cymbium 9:107-119.
- Vélez, J., W. Watson, and E. M. Sandknop.
2003. Larval development of the Pacific sandperch (*Protilus jugularis*) (Pisces: Pinguipedidae) from the Independencia Bight, Pisco, Peru. J. Mar. Biol. Assoc. UK 83:1137-1142.
- Venerus, L. A., and D. Brown.
2003. Análisis de la microestructura de otolitos *lapilli* en juveniles de edad 0 del salmón de mar, *Pseudoperca semifasciata*. Abstracts of the V Jornadas Nacionales de Ciencias del Mar, Instituto Nacional de Investigación y Desarrollo Pesquero and Universidad Nacional de Mar del Plata, 8-12 Dec. 2003, p. 181. Mar del Plata, Buenos Aires, Argentina.
- Venerus, L. A., A. M. Parma, and D. E. Galvan.
2003. Dinámica espacial del salmón de mar, *Pseudoperca semifasciata*, en los arrecifes rocosos del golfo San Jose, Argentina. Resultados iniciales de un programa de marcación. Abstracts of the XXIII Congreso de Ciencias del Mar, Sociedad Chilena de Ciencias del Mar, 5-8 May 2003, p. 152. Sociedad Chilena de Ciencias del Mar and Universidad de Magallanes, Punta Arenas, Chile.
- Vigliola, L., and M. Harmelin-Vivien.
2001. Post-settlement ontogeny in three Mediterranean reef fishes of the genus *Diplodus*. Bull. Mar. Sci. 68:271-286.
- Watson, W., A. C. Matarese, and E. G. Stevens.
1984. Trachinoidea: development and relationships. In Ontogeny and systematics of fishes (G. Moser, W. J. Richards, D. M. Cohen, M. P. Fahay, A. W. Kendall, and S. L. Richardson, eds.), p. 554-561. Am. Soc. Ichthyol. Herpet. Spec. Publ. 1.

Abstract—Nurseries play an important part in the production of marine fishes. Determining the relative importance of different nurseries in maintaining the parental population, however, can be difficult. In the western Gulf of Alaska, the Kodiak Island vicinity may be particularly well suited as a pollock nursery because of a prey-rich nearshore environment. Our objectives were 1) to examine age-0 pollock body condition, growth, and diet for evidence of a nearshore-shelf effect, and 2) to determine if variation in the potential prey field of zooplankton was associated with this effect. This was a pilot study that occurred in three bays and over the adjacent shelf off east Kodiak Island during 5–18 September 1993. Sampling occurred only during night at locations where echo sign indicated the presence of age-0 pollock. Echo sign was targeted to increase the chance of collecting fish given the limited vessel time. Fish condition was indicated by length-specific body weight. Growth rate indices were estimated for three different periods by using fish length-age data and daily otolith increment widths: 1) from hatching date to capture, 2) 1–5 d before capture, and 3) 6–10 d before capture. Fish diet was determined from gut content analysis. Considerable variation among areas was evident in zooplankton composition, and fish condition, growth, and diet. However, relatively high prey densities, as well as fish condition and growth rates indicated that Chiniak Bay was particularly well suited as a pollock nursery. Hatching-date distributions indicated that most of the age-0 walleye pollock from bays were spawned earlier than were those from the shelf. The benefit of being reared in nearshore areas is therefore realized more by individuals that were spawned early than by individuals spawned relatively late.

Geographic variation among age-0 walleye pollock (*Theragra chalcogramma*): evidence of mesoscale variation in nursery quality?*

Matthew T. Wilson

Annette L. Brown

Kathryn L. Mier

Alaska Fisheries Science Center
National Marine Fisheries Service, NOAA
7600 Sand Point Way, NE
Seattle, Washington 98115
E-mail address (for M. T. Wilson): matt.wilson@noaa.gov

The location of suitable fish nurseries has long been of interest to fishery scientists (Kendall and Duker, 1998). Such areas are a link in the chain of resources that sustain the productivity of a population and shape its evolution. Although the presence of juvenile fish in an area may indicate a nursery, relative importance among nursery areas ultimately depends on the number and reproductive fitness of reared individuals that contribute to the parental population. These qualities, however, are usually not measurable. Instead, we focus on measuring the size of juveniles, their body condition, diet, growth, and other characteristics that are accessible and relevant to fish survival. However, because these indices are not free of measurement error, it is advisable to consider more than one index (Suthers, 1998).

In the North Pacific Ocean, walleye pollock (*Theragra chalcogramma*) have adapted to the heterogeneity and productivity of coastal areas; they now support one of the world's most productive fisheries. Walleye pollock are a semidemersal gadid. Spawning typically occurs in mid-water during the spring at locations near, or over, the continental shelf (Kendall and Picquelle, 1989; Bailey et al., 1997). Fertilization is external. The eggs and larvae are pelagic, remaining in the plankton for ca. 4 months while they are dispersed over large areas. At 25–40 mm standard length (SL), larvae transform to juveniles (Brown et al., 2001) and become increasingly

nektonic. Juveniles are referred to as "age-0" when they are between transition and 12-months old (40–130 mm SL, Brodeur and Wilson, 1996a). They are zooplanktivorous, feeding mostly on copepods and euphausiids, but other taxa sometimes dominate their diet (Brodeur and Wilson, 1996a). Age-0 juveniles commonly occur in various habitats from nearshore to the outer continental shelf (Nakatani and Maeda, 1987; Sobolevskiy et al., 1992; Carlson, 1995; Natsume and Sasaki, 1995; Brodeur and Wilson, 1996a; Wilson, 2000). Occasionally, they are found farther offshore (Tang et al., 1995), but probably in small numbers (Brodeur et al., 1999; Shida et al., 1999).

The early life stages of walleye pollock have been extensively studied in the Gulf of Alaska (GOA) (Kendall et al., 1996). In the Gulf, young pollock are most abundant in the western region (Brodeur and Wilson, 1996a). This region is naturally divided into two areas by the Shelikof Sea Valley, which cuts through the shelf at ca. 156°N longitude (Fig. 1). To the east, the Kodiak vicinity includes the continental shelf around the Kodiak Island Archipelago. To the west, the lower Alaska Peninsula vicinity extends to Unimak Pass at the Peninsula's southwestern terminus. During the 1980s, age-0 abundance in the

Manuscript submitted 20 November 2003
to the Scientific Editor's Office.

Manuscript approved for publication
16 September 2004 by the Scientific Editor.
Fish. Bull. 103:207–218 (2005).

* Contribution FOCI-0417 to NOAA's Fisheries-Oceanography Coordinated Investigations, 7600 Sand Point Way NE, Seattle, WA 98115.

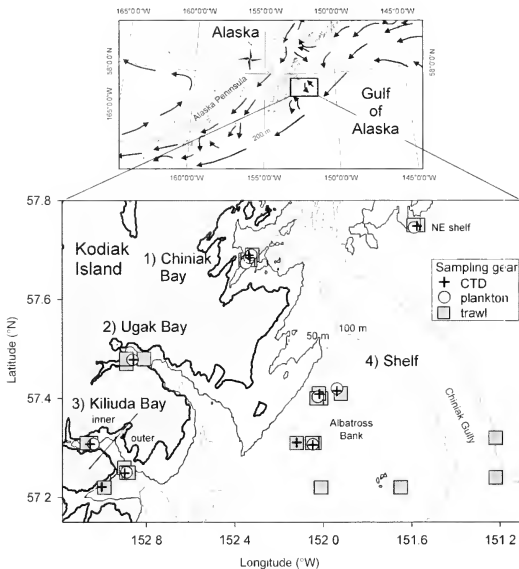


Figure 1

Location of sampling operations (CTD, plankton, and trawl) conducted during 5–18 September 1993, Kodiak Island, Alaska, to examine geographic variation among age-0 walleye pollock (*Theragra chalcogramma*). The ocean currents, shown as arrows on upper map, are adapted from Reed and Schumacher (1986).

Kodiak vicinity was related to the recruitment of pollock to the GOA fishery (Wilson, 2000). Furthermore, age-0 juveniles in this vicinity were large in comparison to those collected elsewhere (Wilson, 2000). The large size of the “Kodiak” juveniles may reflect faster growth (Bailey et al., 1996) due to a rich diet of euphausiids (Merati and Brodeur, 1996). In contrast, the diet of age-0 pollock along the Lower Peninsula was dominated by larvaceans (Merati and Brodeur, 1996). Interestingly, high densities of age-0 pollock were closer to shore in the Kodiak vicinity than along the Lower Peninsula where the shelf is relatively broad.

The apparent richness of the Kodiak Island vicinity may reflect its relative upstream position in the Alaska Coastal Current (ACC) (Fig. 1). Stabeno et al. (2004) integrated much research on the ACC to provide a comprehensive view of its importance in circulation over the GOA shelf. The ACC is wind driven and structured by seasonal influxes of fresh water. Flow is generally

southwestward over the shelf but there is considerable topographic influence. For example, landmasses at the northern entrance to Shelikof Strait (Kennedy-Stevenson Entrance) allow only about 70% of the ACC water to enter the Strait. The remaining 30% of the water flows south around the northeastern end of the Kodiak Archipelago. This bifurcation of flow occurs in an area of vigorous tidal mixing and localized upwelling, both of which contribute to increased biological productivity. Off the northeastern Archipelago, Stabeno et al. (2004) have shown that the ACC follows bathymetric contours into and out of sea valleys, thus, providing some across-shelf movement of water. Advection of water was found by Coyle et al. (1990) to be important in the enhancement of zooplankton in Auke Bay, which is in the eastern GOA. Less is known about the exchange of water and zooplankton between the bays and fjords of the western GOA and the adjacent shelf. Thus, the ACC probably helps enrich the waters off northeastern

Kodiak Island, but we do not yet understand how this actually affects walleye pollock in nearshore nurseries.

In this article, we present information from a pilot study to better understand the environmental basis for the apparent richness of the Kodiak Island vicinity as a pollock nursery. Our objectives were 1) to examine age-0 pollock size, body condition, growth, and diet for evidence of geographic effect (nearshore versus shelf), and 2) to determine if their potential prey field (i.e., zooplankton) was associated with this effect.

Materials and methods

This study was conducted as an ancillary project during a research cruise off east Kodiak Island, 5–18 September 1993 (Fig. 1). In this area, the shelf is about 50 nmi wide and has an offshore bank (Albatross Bank) crossed by deep gullies (Barnabas and Chiniak gullies) extending from the slope to the coast. Bays form the upper reaches of these troughs and receive seasonal influxes of freshwater (Rogers et al.¹). Over the shelf, net transport is southwestward (ca. 5 cm/s) (Stabeno et al., 1995). A boundary current, the Alaska Stream, exists farther offshore and flows rapidly to the southwest (Reed and Schumacher, 1986).

Sampling was conducted from the NOAA ship *Miller Freeman* (Fig. 1). Sampling occurred only at night to avoid complications of diel fish movement (Brodeur and Wilson, 1996b) and feeding patterns (Merati and Brodeur, 1996). A 38-kHz, Simrad-EK500 echo-sounder system was used to help guide our sampling to locations where age-0 pollock were likely present. The targeting of echo signs resulted in an irregular sample-location pattern and biased estimation of fish abundance; however, it focused our sampling at locations where age-0 pollock were likely present and thereby contributed to successful fish collections. Sampling was accomplished in four areas: Chiniak Bay, Ugak Bay, Kiliuda Bay, and over the adjacent shelf. All data analyses included these four areas as geographic strata; finer divisions (e.g., inner and outer Kiliuda Bay, and NE and Albatross Bank) were not possible given the available data and chosen analytical methods.

Age-0 pollock were obtained from the four areas with a bottom trawl and a midwater trawl (Wilson et al., 1996). The codend of each trawl was lined with a 3-mm mesh net. Towing speed averaged 4.5 k/h. Previous comparisons between these trawls indicated no significant difference with regard to estimation of age-0 pollock size or abundance (Brodeur and Wilson, 1996a; Wilson et al., 1996). Differences in the sampling effort

used to collect each sample were corrected by dividing the age-0 catch by the volume filtered. Volume filtered was estimated by multiplying the distance fished (meters traveled while at depth) by the mouth opening of the trawl (m^2) (Wilson, 2000). Thus, age-0 catches are reported as number of fish per m^3 .

Size composition of walleye pollock for each area was estimated by measuring the standard length (SL) of fresh age-0 pollock to the nearest millimeter. For large catches, a random subsample of about 300 individuals was used to represent the entire catch; otherwise, SL on every individual was measured. Length frequencies were expanded to the standardized catch estimates. Age-0 juveniles were clearly distinguishable from older pollock (<130 mm versus >150 mm SL) as indicated by Brodeur and Wilson (1996a). Random subsamples of age-0 pollock were also frozen at sea for subsequent determination of body condition, age, growth, and diet.

In the laboratory, length-specific weights of 776 age-0 pollock were used to examine area differences in body condition (Table 1). The fish were thawed within four months of collection. Excess water was blotted from each individual, and each specimen was measured to the nearest millimeter SL and weighed whole to the nearest 0.01 gram. Afterwards, each carcass was stored in 95% ethanol for eventual gut content analysis. Lengths and somatic weights, obtained from the subset of fish used in the gut analysis, were also analyzed to verify that geographic differences in condition were not dependent on whole versus somatic weight.

Growth rate was estimated for 128 individuals by using fish length and age data. Age, in days, was estimated as the number of daily increments visible in the microstructure of sagittal otoliths following Brown and Bailey (1992). Length-age relationships were examined for evidence of an area effect on growth rates integrated over the period from hatching to capture. We used these relationships to convert the length composition for each sample to a hatching-date distribution, and by summing across samples we then obtained area-specific hatching-date distributions.

To estimate growth rate realized near the point of capture we measured the width of recent daily otolith increments. Following Bailey (1989), we measured the width of the two outermost, nonoverlapping 5-increment bands on each of 97 sagittal otoliths. These widths were assumed to relate directly to body growth during the first (1–5 days) and second (6–10 days) 5-d periods before capture, and that the increments were deposited while individuals were near the point of capture. Thus, growth rate indices were obtained for three different periods: 1) hatching date to capture date, 2) 1–5 days before capture, and 3) 6–10 days before capture.

Gut content analysis was conducted on 300 individuals according to the method of Merati and Brodeur (1996) to determine feeding intensity and taxonomic composition of age-0 prey. No more than 15 fish per sample were examined. Each fish was measured (SL), blotted dry, and weighed immediately prior to dissection. Stomachs were excised between the esophagus and

¹ Rogers, D. E., D. J. Rabin, B. J. Rogers, K. J. Garrison, and M. E. Wangerin. 1979. Seasonal composition and food web relationships of marine organisms in the nearshore zone of Kodiak Island—including ichthyoplankton, meroplankton (shellfish), zooplankton, and fish. Annual rep. OCSEAP RU553, FRI-UW-7925, 291 p. Fish. Res. Inst., Univ. Washington, Seattle, WA.

Table 1

Number of age-0 walleye pollock (*Theragra chalcogramma*) collected near Kodiak Island, Alaska, September 1993, measured for standard length, and examined in the laboratory to estimate condition, growth, and the weight and taxonomic composition of stomach contents. Sample is the number of trawl hauls.

Location	Sample (n)	Laboratory examinations (no. of fish)							Evaluated for gut content weight and composition
		At-sea collections (no. of fish)		Condition		Growth			
		Caught	Measured for SL	whole ¹ wt.	somatic ² wt.	Age	Band width		
							1-5 ³	6-10 ⁴	
Chiniak Bay	7	1858	709	223	75	23	17	17	75
Ugak Bay	4	2506	773	218	91	28	12	12	91
Kiliuda Bay	7	562	279	165	66	41	33	33	66
Shelf	14	358	358	170	68	36	35	35	65
All combined	32	5284	2119	776	300	128	97	97	297

¹ Whole wet weights from thawed fish.

² Somatic wet weights from fish preserved in 95% ethanol after freezing at sea.

³ Collective width of daily otolith increments 1-5; numbering begins with the most peripheral increment.

⁴ Collective width of daily otolith increments 6-10.

pylorus. Gut contents were dissected from the specimens and weighed to the nearest 0.001 gram. Somatic weight represented whole wet weight minus the gut content weight. Three fish were omitted from further consideration because of apparent regurgitation. Taxonomic composition of age-0 diets was determined by counting the organisms in the gut after sorting them into broad taxonomic groups.

Zooplankton was collected by using a 1-m Tucker net (333- μ m mesh) to sample where age-0 pollock had been collected. The net was fished through acoustic echo layers believed to be age-0 pollock in order to characterize their immediate prey field. Potential prey items were sorted into broad taxonomic groups and enumerated at the Polish Plankton and Identification Center, Szecein, Poland.

Temperature and salinity profiles (near surface to 10 m off bottom) were obtained by using a Seabird SBE-911+ CTD system. Profile data were collected during deployment at a descent rate of ca. 0.5 m/s.

Statistically significant differences in age-0 condition, growth, and feeding intensity among geographic areas were detected with split-plot analysis of covariance (ANCOVA) and *post hoc* multiple comparison tests (Proc Mixed, SAS software, Littell et al., 1996). The covariates were fish length or age (days since hatching). Following Milliken and Johnson (2002), we first tested for covariate significance (H_0 : all slopes=0) and homogeneity of slopes (H_0 : equal slopes) to ensure appropriateness of the following reduced, common-slope model:

$$Y = \alpha + \beta x_{ij} + \text{Area}_i + \text{Sample}_j \{ \text{Area}_i \} + e_{ijk}$$

where Y = dependent variable;

α = intercept parameter;

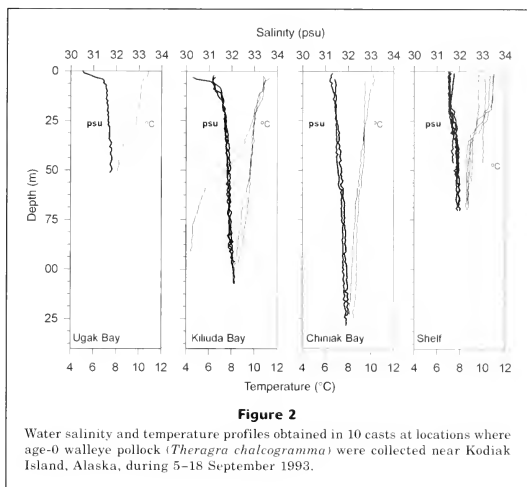
β = slope parameter;

x_{ij} = covariate for sample i and area j ; and

e_{ijk} = replicate error for sample i , area j , and fish k .

A split-plot design was necessary to account for the nesting of samples (trawl catches) within area, and individuals within sample. To avoid pseudoreplication, trawl catch was the sampling unit instead of individual fish. Area was a fixed effect; sample was a random effect. For body condition, lengths and weights were log_e-transformed according to the method of Paterson (1992); two points were omitted because of suspiciously low length-specific, whole-body weight. For feeding intensity, gut content weights (GCW) were fourth-root transformed (GCW^{0.25}) to linearize the GCW-length relationship and remove heteroscedasticity (Clarke and Warwick, 2001). Significance of *post hoc* pairwise differences was based on a Bonferroni-corrected, 0.05-level of significance. The standardized catch data were not incorporated into these tests; therefore the conclusions pertain to the samples not weighted by catch.

Nonmetric multidimensional scaling (NMS, PC-Ord, McCune and Mefford, 1999) was used to ordinate the diet and plankton samples according to taxonomic composition. Each diet sample represented the average numerical composition of the diet of all fish in the sample. This value was calculated by dividing the sum of all items within each taxonomic category by the number of fish in the sample. The ordinations, one for diet and another for plankton, were based on Bray-Curtis similarity coefficients of fourth root-transformed data. Differences among the four areas were statistically tested by using a two-way nested analysis of similarity



(ANOSIM, PRIMER, Clarke and Warwick, 2001) applied to the Bray-Curtis similarity matrices.

Results

Overall, salinity ranged from 30.3 to 33.0 ppt, and water temperature ranged from 4.4 to 11.3°C (Fig. 2). Shallow surface layers of relatively fresh water were evident from low near-surface salinities in Ugak Bay and in the inner part of Kiliuda Bay. This part of Kiliuda Bay was also well stratified thermally. Unfortunately, it was not possible to include inner Kiliuda Bay as a fifth area in subsequent statistical analyses because of insufficient sampling. Thermal stratification was also evident at shelf sampling locations.

A total of 5284 age-0 pollock were collected in 25 of the 32 successful trawl hauls (Table 1). These fish were absent only at the four most-offshore locations over Albatross Bank and Chiniak Gully (Fig. 3). In addition, no age-0 pollock were caught in shallow (<35-m depth) tows at locations on Albatross Bank; a dense and expansive school of capelin (*Mallotus villosus*) may have displaced them downward. Median age-0 density was 0.0006 fish/m³; the maximum (0.095 fish/m³) was found in Ugak Bay.

Standard lengths of 2119 age-0 pollock ranged from 25 to 121 mm SL (Table 1, Fig. 4). The fish in Chiniak Bay (91 mm SL), Ugak Bay (90 mm SL), and Kiliuda Bay (89 mm SL) all had a median SL that were larger

than the median length of fish collected over the shelf (71 mm SL). A surprising number of individuals <50 mm SL were collected in Ugak Bay and inner Kiliuda Bay.

Body condition, based on the reduced, common-slope ANCOVA model, varied among the four areas (Table 2). Because of this effect, area-specific equations were used to describe the length-weight relationship (Table 3, Fig. 5A). After accounting for differences in length, we found that fish from the shelf weighed less than the individuals collected in Chiniak Bay and Ugak Bay. Individuals from Kiliuda Bay were intermediate in weight, differing only from the Ugak Bay fish (Table 4). Similar conclusions from the somatic-weight data of fish used in the diet examinations indicated that gut-content weight was not responsible for the relatively low length-specific weights of fish from Kiliuda Bay and the shelf (Tables 2 and 4).

The fish age-length relationship also varied by area. The relationship was described by using a reduced, common-slope model (Table 2). The common slope was 0.78 mm/d (Table 3, Fig. 5B). Differences in line elevation, or age-specific length, indicated that fish from the shelf grew more slowly during the hatch-to-capture period than did the fish from Chiniak or Kiliuda bays (Table 4). Applying these equations to the length data resulted in hatching-date distributions that ranged from mid March to mid July (Fig. 6). The fish collected in Chiniak Bay (17 April), Kiliuda Bay (20 April), and Ugak Bay (25 April) all had earlier median hatching

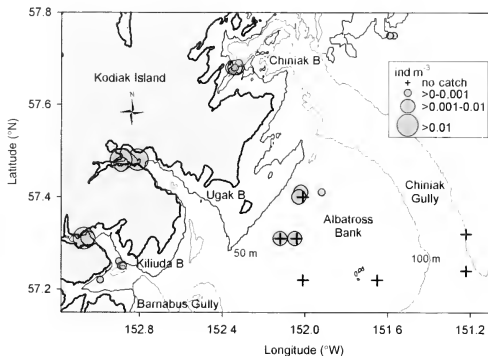


Figure 3

Geographic distribution of standardized catches (no. of individuals/m³) of age-0 walleye pollock (*Theragra chalcogramma*) collected in trawl hauls conducted near Kodiak Island during 5–18 September 1993.

dates in comparison to fish from the shelf (8 May). Interestingly, the hatching dates of the cohort of small individuals from Ugak Bay and inner Kiliuda Bay ranged from June to July.

Mean otolith increment width varied with area. It was not necessary to include fish length as a covariate (Table 2). For the 1–5 d precatch period, the large mean increment width associated with fish from Chiniak Bay (0.036-mm band width) was different from the means of

each other area (Table 4). The only other difference was between the Kiliuda Bay (0.026 mm) and shelf (0.030 mm) areas. The only difference for the 6–10 d precatch period was again between the Kiliuda Bay (0.029 mm) and shelf (0.036 mm) areas.

No area effect on gut content weight (GCW) was detected (Table 2). There was, however, a significant fish length effect (Fig. 5C), and this was incorporated in the final model (Table 3). After adjusting for length, area-specific mean GCW agreed in rank with area-specific fish weight (Table 4).

Differences in taxonomic composition of age-0 pollock diets resulted in a good separation of samples by area (Fig. 7A, ANOSIM, $R=0.533$, $P=0.001$). Each pair-wise comparison of areas resulted in a significant difference ($P<0.05$) (the one sample of small fish from Kiliuda Bay, and two samples from the shelf of fish with empty stomachs were omitted from the ANOSIM). The diet of fish from Ugak Bay and Kiliuda Bay were mostly crab larvae or copepods, depending on fish size (Table 5A). Over the shelf, fish diets comprised mostly euphausiids (74%). In contrast, fish from Chiniak Bay had a much more varied diet; no single prey category exceeded 40% of the items per stomach. Note the correspondence between the number of prey per fish (Table 5A) and mean gut-content weight (Table 4); both were lowest for fish from the shelf.

Differences in taxonomic composition also resulted in separation of the plankton samples by area (Fig. 7B, ANOSIM, $R=0.886$, $P=0.001$). Pair-wise comparisons indicated a difference between Chiniak Bay and the shelf ($R=0.813$, $P=0.029$). Ugak Bay was not included in the comparisons because only one sample was avail-

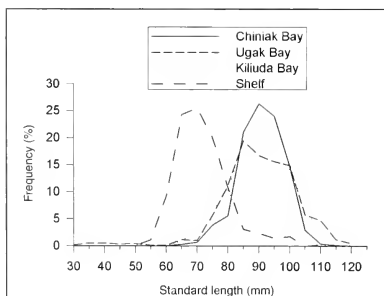


Figure 4

Size composition (mm SL) of age-0 walleye pollock (*Theragra chalcogramma*) by area from samples collected near Kodiak Island, 5–18 September 1993.

Table 2

Summary results of six ANCOVA tests of an area effect on six dependent variables obtained from laboratory analysis of age-0 pollock: body condition (whole or somatic weight), three indices of growth, and gut content weight. NDF and DDF are numerator and denominator degrees of freedom for the *F* test, respectively.

Dependent variable	H_0 : all slopes = 0	H_0 : equal slopes	Reduced model				
			Source	NDF	DDF	Type III <i>F</i>	<i>P</i> > <i>F</i>
Condition							
whole weight	<i>P</i> =0.0001	<i>P</i> =0.3340	Area	3	14.2	6.81	0.0045
			ln(SL)	1	769	105824	0.0001
somatic weight	<i>P</i> =0.0001	<i>P</i> =0.3115	Area	3	17.8	10.01	0.0004
			ln(SL)	1	294	31000	0.0001
Growth							
age-specific length	<i>P</i> =0.0001	<i>P</i> =0.4140	Area	3	4.3	14.43	0.0106
			Age	1	117	475.39	0.0001
1-5 d band width	<i>P</i> =0.2645		Area	3	93	8.05	0.0001
6-10 d band width	<i>P</i> =0.2267		Area	3	5.76	3.89	0.0768
Gut content weight							
	<i>P</i> =0.0001	<i>P</i> =0.7208	Area	3	16.2	0.36	0.7850
			SL	1	285	201.99	0.0001

able. Copepods dominated the catches in Chiniak Bay and over the shelf, whereas larval crabs were most prevalent in the Ugak and Kiliuda samples (Table 5B). In terms of overall abundance, mean prey densities were lowest among samples collected from the shelf and highest for the Chiniak Bay samples.

Discussion

The presence of age-0 pollock in bays and over the inner shelf, but not over the outer shelf, indicates that the principal pollock nursery off east Kodiak Island during autumn is relatively close to shore. Earlier studies of age-0 pollock in the western GOA focused on near-shore areas (Smith et al., 1984; Wilson, 2000) and did not document the absence of age-0 pollock over the outer shelf. Our results point to prey resource as a likely explanation for the observed distribution of and differences among age-0 walleye pollock.

Seasonal declines in zooplankton density underscore the importance of nearshore areas as pollock nurseries. Rogers et al.¹ and Kendall et al.² observed an order-of-magnitude autumnal decline in prey³ density off Kodiak Island during 1977-79 (Fig. 8). This decline was accompanied by a shoreward shift in the region of highest eu-

Table 3

Least-squares linear relationships used to describe the condition, growth, and feeding intensity of age-0 walleye pollock collected September 1993, Kodiak Island, Alaska. GCW = gut content weight.

Relationship	Location	Equation
Condition		
whole weight	Chiniak Bay	$\ln(g) = 3.228(\ln SLmm) - 12.646$
	Ugak Bay	$\ln(g) = 3.228(\ln SLmm) - 12.609$
	Kiliuda Bay	$\ln(g) = 3.228(\ln SLmm) - 12.659$
	Shelf	$\ln(g) = 3.228(\ln SLmm) - 12.698$
somatic weight	Chiniak Bay	$\ln(g) = 3.127(\ln SLmm) - 12.708$
	Ugak Bay	$\ln(g) = 3.127(\ln SLmm) - 12.702$
	Kiliuda Bay	$\ln(g) = 3.127(\ln SLmm) - 12.774$
	Shelf	$\ln(g) = 3.127(\ln SLmm) - 12.816$
Growth		
length-at-age	Chiniak Bay	$\text{age}(d) = 0.782(SLmm) - 22.294$
	Ugak Bay	$\text{age}(d) = 0.782(SLmm) - 26.928$
	Kiliuda Bay	$\text{age}(d) = 0.782(SLmm) - 21.346$
	Shelf	$\text{age}(d) = 0.782(SLmm) - 31.011$
Gut content weight	All combined	$\text{GCW}(g^{0.25}) = 0.007(SLmm) - 0.192$

² Kendall, A. W., Jr., J. R. Dunn, R. J. Wolotira Jr., J. H. Bowerman Jr., D. B. Dey, A. C. Matarese, and J. E. Munk. 1980. Zooplankton, including ichthyoplankton and decapod larvae, of the Kodiak shelf. NOAA NWAFWC proc. rep. 80-8, 393 p. Alaska Fishery Science Center, Seattle, WA.

³ All invertebrate zooplankters are considered potential age-0 pollock prey except cnidarians, ctenophores, siphonophores, and larval shrimps and crabs. Shrimp and crab were omitted from Figure 8 because density estimates were not available separately for the shelf and slope regions.

phausiid density. Similar to our findings, the estimates of larval crab densities from Rogers et al.'s and Kendall et al.'s studies were always highest in bays. In autumn,

the larger zooplankters are of principal importance to age-0 pollock because of size-related changes in diet (Table 5A, Merati and Brodeur, 1996).

By all accounts, age-0 pollock collected from Chiniak Bay fared as well or better than individuals in each of the other areas sampled. Wilson (2000) found that the density of age-0 pollock in the Chiniak Bay vicinity predicted Gulf-wide recruitment. However, these fish represent a minuscule part of the Gulf-wide population of age-0 pollock. Even if two cohorts, from spring- and summer-spawnings, were produced, it seems unreasonable to expect that local production would dramatically affect gulf-wide recruitment. Alternatively, the abundance and condition of age-0 pollock in this vicinity might reflect larger-scale processes that relate to gulf-wide recruitment. Identifying large-scale processes based on small-scale sampling, however, is complicated by variation at high spatial and temporal frequencies. For example, the relatively high density of pea crab (*Fabia subquadrata*) megalopae in combination with influxes of freshwater (Epifanio, 1988) indicate that local dynamics are important in sustaining prey populations in Ugak and Kiliuda bays. In contrast, Chiniak Bay might be more affected by influxes of oceanic prey. Such influxes could be facilitated by cross-shelf sea valleys, which extend into all the fjords that we sampled. Indeed, Kendall et al.,² Lagerloef (1983), and Stabeno et al. (2004) have all shown that the local sea valleys induce cross-shelf flow in the ACC. Furthermore, Inzce et al. (1997) found that zooplankton density was elevated in the Shelikof Sea Valley above the density found at adjacent shelf areas; a similar phenomenon, however, was not observed off northeastern Kodiak Island (Kendall et al.²). Compared to the other bays, Chiniak Bay might be best positioned to receive enriched ACC water that flows south from where it bifurcates at the entrance to Shelikof Strait. Such enriched water may also be an important transport mechanism for immigrating larval and juvenile pollock (Wilson, 2000).

Because of the inconsistency among our various indices (i.e., weight-at-length, length-at-age, otolith increment width), it is difficult to conclude that fish over the shelf and in Ugak and Kiliuda bays were prey limited. Over the shelf, recent growth rates were not low despite relatively small individual size and low prey density. For example, the low prey densities and small fish sizes over the shelf contrasted with recent fish growth that was not low. Age-0 pollock are capable of social foraging behavior to compensate for food scarcity (Ryer and Olla, 1992), but it is unclear that the associated energetic cost (Ryer and Olla, 1997) would depress body weight before slowing otolith growth. In contrast, fish in Kiliuda Bay had relatively slow recent growth and low body weight, but age-specific length was large. The observed differences in age-specific length are somewhat discounted by the fact that such differences may have arisen any time after hatching and are not necessarily indicative of recent differences in growth. Another complication was our inability to reconstruct the spatial history of the sampled fish;

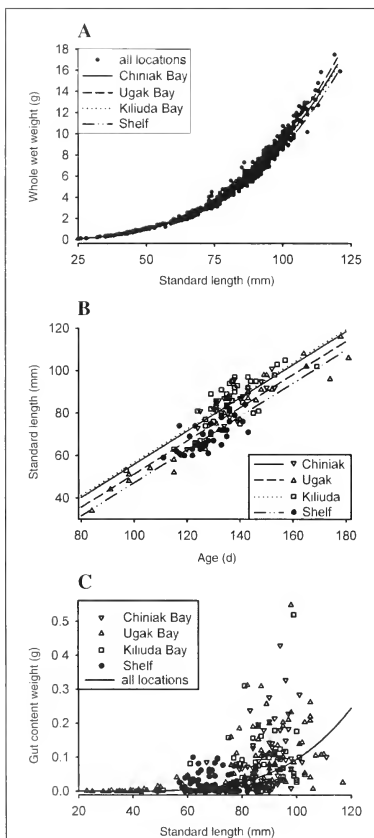


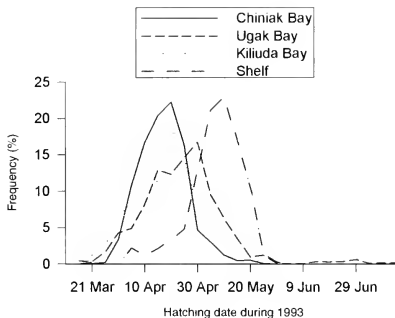
Figure 5

Least-squares regressions of age-0 walleye pollock (*Theragra chalcogramma*) length on weight (A), length on age (B), and gut content weight on length (C) for individuals collected from four areas off east Kodiak Island, 5–18 September 1993.

Table 4

Least-squares adjusted means of indices of body condition, growth, and gut content weight (GCW) of age-0 walleye pollock collected September 1993, Kodiak Island, Alaska. Means sharing the same superscript letter are not different (*post hoc* multiple comparison tests, $P > 0.05$).

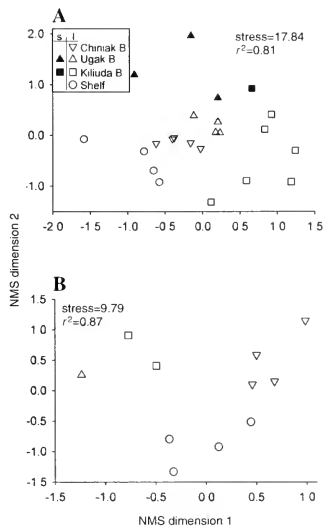
Location	Condition		Growth			GCW ($g^{0.25}$)
	whole wt. (ln g)	somatic wt. (ln g)	age-specific SL (mm)	1-5 d band width (mm)	6-10 d band width (mm)	
Chiniak Bay	1.47 ^{ob}	0.82 ^c	82.3 ^a	0.036 ^a	0.0333 ^{ob}	0.40
Ugak Bay	1.50 ^b	0.83 ^c	77.6 ^{ob}	0.027 ^{bc}	0.032 ^{ob}	0.43
Kiliuda Bay	1.45 ^{oc}	0.76 ^b	83.2 ^a	0.026 ^b	0.029 ^c	0.39
Shelf	1.42 ^c	0.72 ^b	73.6 ^b	0.030 ^c	0.036 ^b	0.36

**Figure 6**

Hatching-date composition of age-0 walleye pollock (*Theragra chalcogramma*) by area from samples collected near Kodiak Island, 5-18 September 1993.

in other words, we did not know where they had been prior to capture.

As evidenced by geographic variation in hatching-date distributions, cohort-specific differences persisted well into the juvenile stage and had important implications for inter-cohort differences in survival. The median hatching dates of fish in bays were similar to those estimated for north Kodiak Island by Brown and Bailey (1992). In contrast, fish over the shelf had substantially later hatching dates. There is little evidence of pollock spawning within our study area; therefore it seems likely that the differences in hatching dates reflect successive immigration of sequential cohorts. However, the presence of the youngest cohort, fish hatched during

**Figure 7**

Nonmetric multidimensional scaling (NMS) of samples based on age-0 walleye pollock (*Theragra chalcogramma*) diet composition (A), or zooplankton composition (B). Symbols indicate four different sampling areas. For diet, the small (<66 mm SL) fish in bays are represented by filled symbols.

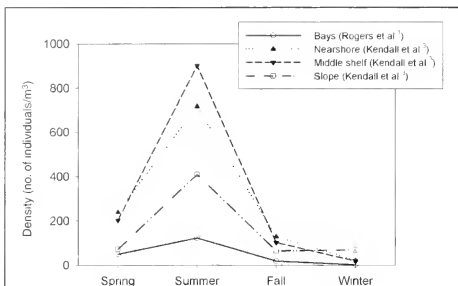


Figure 8

Seasonal variability in densities (no. of individuals/m³) of invertebrate zooplankton near Kodiak Island based on samples collected with 60-cm bongo nets with 0.333-mm mesh (modified from Rogers et al.¹, Kendall et al.²).

June and July, only in the innermost parts of Kiliuda Bay and Ugak Bay, may indicate an alternative mechanism such as local spawning and geographic differences in retention. Regardless, the relationship between fish size and hatching date indicates that large individuals were spawned early; thus, early spawned individuals might experience higher overwinter survival, which often increases with fish size (Sogard, 1997).

We chose to track echo sign in our study to reduce the sampling effort expended in areas devoid of age-0 pollock. This method maximized our chance of collecting the samples needed to study differences among age-0 pollock given the limited vessel time. Unfortunately, this method also introduced a bias, thereby reducing the utility of density estimates to indicate habitat suitability (Brown et al., 2000; Stoner et al., 2001) and to extrapolate from samples to at-sea populations. Our focus, however, was on other measures that might eventually provide a

Table 5

Numerical composition of age-0 pollock diet by location and predator SL (A), and composition of the plankton in 1-m² Tucker samples (B) concurrently collected during 5–18 September 1993, Kodiak Island, Alaska. "t" signifies trace (<0.05).

A		Prey (number of individuals/fish) [†]									No. of prey/fish
		Sample (n)	no. of fish	amphipod	chaetognath	copepod	crab larvae	cumacean	euphausiid	mysis	
Chiniak Bay	5	75	2.8	t	4.1	0.1	0.0	3.7	0.4	t	11.0
Ugak Bay											
≤66 mm	3	31	0.1	0.6	11.2	0.6	0.0	0.1	t	0.0	12.6
>66 mm	4	60	0.1	t	5.9	15.9	t	3.3	0.2	t	25.6
Kiliuda Bay											
≤66 mm	1	5	0.0	0.2	2.2	1.0	0.0	0.2	0.0	0.0	3.6
>66 mm	6	61	t	t	t	6.4	t	2.7	t	t	9.2
Shelf	6	65	0.3	0.0	0.1	0.1	t	2.8	0.4	0.1	3.8

[†] 0 < t < 0.05.

B		Zooplankton (number of individuals/m ³) [†]									total no./m ³
		Sample (n)	amphipod	chaetognath	copepod	crab larvae	euphausiid	fish larva	larvacean	mysis	
Chiniak Bay	4	t	9	332	1	23	t	4	2	4	375
Ugak Bay	1	t	13	12	48	2	t	3	1	t	80
Kiliuda Bay	2	t	13	40	82	28	t	17	4	3	188
Shelf	4	t	1	51	1	4	t	15	t	2	74

[†] 0 < t < 0.05. In zooplankton samples, cumaceans were not enumerated.

useful supplement to abundance distribution data (Beutel et al., 1999).

This study enabled us to conclude that Chiniak Bay is particularly well suited for rearing pollock probably because of influxes of zooplankton. It remains to be seen if Chiniak Bay contributes relatively high numbers of recruits, or if other counteracting factors such as predation exist. Nevertheless, we have demonstrated that differences among juvenile pollock exist at mesogeographic scales and that these differences are useful for inferring how specific areas might relate to the population dynamics of walleye pollock.

Acknowledgments

R. Brodeur provided the initial impetus for this study. P. Munro and D. Somerton accommodated our request to share ship time. The captain and crew of the NOAA ship *Miller Freeman* helped make our at-sea operations efficient and pleasurable. M. Busby assisted with field operations. We gratefully appreciate the comments of many people: K. Bailey, J. Napp, A. Stoner, S. Syrjala, N. Bartoo, the AFSC Publications Unit, and several anonymous reviewers.

Literature cited

- Bailey, K. M.
1989. Interaction between the vertical distribution of juvenile walleye pollock *Theragra chalcogramma* in the eastern Bering Sea, and cannibalism. *Mar. Ecol. Prog. Ser.* 53:205-213.
- Bailey, K. M., A. L. Brown, M. M. Yoklavich, and K. L. Mier.
1996. Interannual variability in growth of larval and juvenile walleye pollock, *Theragra chalcogramma*, in the western Gulf of Alaska, 1983-91. *Fish. Oceanogr.* 5(suppl. 1):137-147.
- Bailey, K. M., P. J. Stabeno, and D. A. Powers.
1997. The role of larval retention and transport features in mortality and potential gene flow of walleye pollock. *J. Fish. Biol.* 51(suppl. A):135-154.
- Beutel, T. S., R. J. S. Beeton, and G. S. Baxter.
1999. Building better wildlife-habitat models. *Ecography* 22(2):219-223.
- Brodeur, R. D., and M. T. Wilson.
1996a. A review of the distribution, ecology and population dynamics of age-0 walleye pollock in the Gulf of Alaska. *Fish. Oceanogr.* 5 (suppl. 1):148-166.
- Brodeur, R. D., and M. T. Wilson.
1996b. Mesoscale acoustic patterns of juvenile walleye pollock (*Theragra chalcogramma*) in the western Gulf of Alaska. *Can. J. Fish. Aquat. Sci.* 53(9):1951-1963.
- Brodeur, R. D., M. T. Wilson, G. E. Walters, and I. V. Melnikov.
1999. Forage fishes in the Bering Sea: distribution, species associations, and biomass trends. In *Dynamics of the Bering Sea* (T. R. Loughlin, K. Ohtani, eds.), p. 509-536. Univ. Alaska Sea Grant, Fairbanks, AK.
- Brown, A. L., and K. M. Bailey.
1992. Otolith analysis of juvenile walleye pollock *Theragra chalcogramma* from the western Gulf of Alaska. *Mar. Biol.* 112:23-30.
- Brown, A. L., M. S. Busby, and K. L. Mier.
2001. Walleye pollock *Theragra chalcogramma* during transformation from the larval to juvenile stage: otolith and osteological development. *Mar. Biol.* 139: 845-851.
- Brown, S. K., K. R. Buja, S. H. Jury, M. E. Monaco, and A. Banner.
2000. Habitat suitability index models for eight fish and invertebrate species in Casco and Sheepscot Bays, Maine. *N. Am. J. Fish. Manag.* 20:408-435.
- Carlson, H. R.
1995. Consistent yearly appearance of age-0 walleye pollock, *Theragra chalcogramma*, at a coastal site in southeastern Alaska, 1973-1994. *Fish. Bull.* 93(2): 386-390.
- Clarke, K. R., and R. M. Warwick.
2001. Change in marine communities: an approach to statistical analysis and interpretation, 2nd ed., 87 p. PRIMER-E, Plymouth, Cornwall, U.K.
- Coyle, K. O., A. J. Paul, and D. A. Ziemann.
1990. Copepod populations during the spring bloom in an Alaskan subarctic embayment. *J. Plank. Res.* 12(4):759-797.
- Epifanio, C. E.
1988. Transport of invertebrate larvae between estuaries and the continental shelf. In *Larval fish and shellfish transport through inlets* (M. P. Weinstein, ed.), p. 104-114. *Am. Fish. Soc. Symp.* 3, Bethesda, MD.
- Ince, L. S., D. W. Siefert, and J. M. Napp.
1997. Mesozooplankton of Shelikof Strait, Alaska: abundance and community composition. *Cont. Shelf Res.* 17(3):287-305.
- Kendall, A. W., Jr., and G. J. Duker.
1998. The development of recruitment fisheries oceanography in the United States. *Fish. Oceanogr.* 7(2): 69-88.
- Kendall, A. W. Jr., and S. J. Piquelle.
1989. Egg and larval distributions of walleye pollock *Theragra chalcogramma* in Shelikof Strait, Gulf of Alaska. *Fish. Bull.* 88:133-154.
- Kendall, A. W. Jr., J. D. Schumacher, and S. Kim.
1996. Walleye pollock recruitment in Shelikof Strait: applied fisheries oceanography. *Fish. Oceanogr.* 5(suppl. 1):4-18.
- Lagerloef, G.
1983. Topographically controlled flow around a deep trough transecting the shelf off Kodiak Island, Alaska. *J. Phys. Oceanogr.* 13:139-146.
- Littell, R. C., G. A. Milliken, W. W. Stroup, and R. D. Wolfinger.
1996. SAS System for mixed models, 633 p. SAS Institute Inc., Cary, NC.
- McCune B., and M. J. Mefford.
1999. PC-ORD. multivariate analysis of ecological data, vers. 4. 237 p. MjM Software Design, Gleneden Beach, OR.
- Merati, N., and R. D. Brodeur.
1996. Feeding habits and daily ration of juvenile walleye pollock, *Theragra chalcogramma*, in the western Gulf of Alaska. In *Ecology of juvenile walleye pollock, Theragra chalcogramma* (R. D. Brodeur, P. A. Livingston, T. R. Loughlin, A. B. Hollowed, eds.), p. 65-79. NOAA Tech. Rep. NMFS 126.
- Milliken, G. A., and D. E. Johnson.
2002. Analysis of messy data, vol. III, analysis of covariance, 605 p. Chapman and Hall/CRC, New York, NY.

- Nakatani, T., and T. Maeda.
1987. Distribution and movement of larval and juvenile walleye pollock (*Theragra chalcogramma*) in Funka Bay and adjacent waters. Bull. Jap. Soc. Sci. Fish. 53(9):1585-1591.
- Natsume, M., and M. Sasaki.
1995. Distribution of walleye pollock, *Theragra chalcogramma*, larvae and juveniles off the northern coast of Hokkaido. Sci. Rep. Hokkaido Fish. Exp. Stn. 47: 33-40.
- Patterson, K. R.
1992. An improved method for studying the condition of fish, with an example using Pacific sardine *Sardinops sagax* (Jenyns). J. Fish. Biol. 40:821-831.
- Reed, R. K., and J. D. Schumacher.
1986. Physical oceanography. In The Gulf of Alaska physical environment and biological resources (D. W. Hood and S. T. Zimmerman, eds.), p. 57-75. OCS Study MMS86-0095. Minerals Management Service, Springfield, VA.
- Ryer, C. H., and B. L. Olla.
1992. Social mechanisms facilitating exploitation of spatially variable ephemeral food patches in a pelagic marine fish. Anim. Behav. 44:69-74.
1997. Altered search speed and growth: social versus independent foraging in two pelagic juvenile fishes. Mar. Ecol. Prog. Ser. 153:273-281.
- Shida, O., O. Yamamura, and H. Miyake.
1999. Distribution and migration to offshore of age-0 walleye pollock, *Theragra chalcogramma*, along the Pacific coast of southeastern Hokkaido. Sci. Rep. Hokkaido Fish. Exp. Stn. 54:1-7.
- Sobolevskiy, E. I., L. V. Cheblykova, and V. I. Radchenko.
1992. Distribution of first-year pollock, *Theragra chalcogramma*, in the western Bering Sea. J. Ichthyol. 1: 119-130.
- Sogard, S. M.
1997. Size-selective mortality in the juvenile stage of teleost fishes: a review. Bull. Mar. Sci. 60(3):1129-1157.
- Smith, G. B., G. E. Walters, P. A. Raymore Jr., and W. A. Hirschberger.
1984. Studies of the distribution and abundance of juvenile groundfish in the northwestern Gulf of Alaska, 1980-1982. NOAA Tech. Memo. F/NWC-59, 100 p.
- Stabeno, P. N., A. Bond, A. J. Hermann, N. B. Kachel, C. W. Mordy, and J. E. Overland.
2004. Meteorology and oceanography of the northern Gulf of Alaska. Cont. Shelf Res. 24:859-897.
- Stabeno, P. J., R. K. Reed, and J. D. Schumacher.
1995. The Alaska Coastal Current: continuity of transport and forcing. J. Geophys. Res. 100(C2):2477-2485.
- Stoner, A. W., J. P. Manderson, and J. P. Pessutti.
2001. Spatially explicit analysis of estuarine habitat for juvenile winter flounder: combining generalized additive models and geographic information systems. Mar. Ecol. Prog. Ser. 213:253-271.
- Suthers, I. M.
1998. Bigger? Fatter? Or is faster growth better? Considerations on condition in larval and juvenile coral-reef fish. Aust. J. Ecol. 23:265-273.
- Tang, Q., W. Wang, Y. Chen, F. Li, X. Jin, X. Zhao, J. Chen, and F. Dai.
1995. Stock assessment of walleye pollock in the north Pacific Ocean by acoustic survey. J. Fish. China 19(1):8-20.
- Wilson, M. T.
2000. Effects of year and region on the abundance and size of age-0 walleye pollock, *Theragra chalcogramma*, in the western Gulf of Alaska, 1985-1988. Fish. Bull. 98:823-834.
- Wilson, M. T., R. D. Brodeur, and S. Hinckley.
1996. Distribution of age-0 walleye pollock (*Theragra chalcogramma*) in the western Gulf of Alaska. In Ecology of juvenile walleye pollock (R. D. Brodeur, P. A. Livingston, T. R. Loughlin, A. B. Hollowed, eds.), p. 11-24. NOAA Tech. Rep. NMFS 126.

Tagging studies on the jumbo squid (*Dosidicus gigas*) in the Gulf of California, Mexico

Unai Markaida

Departamento de Ecología, Centro de Investigación Científica y de Educación Superior de Ensenada (CICESE)

Ctra. Tijuana-Ensenada km 107

Ensenada, Baja California, Mexico

Present address: Departamento de Aprovechamiento y Manejo de Recursos Acuáticos

El Colegio de la Frontera Sur

Calle 10 x 61 No 264

Colonia Centro, 24000 Campeche, Mexico

Joshua J. C. Rosenthal

Institute of Neurobiology

University of Puerto Rico

201 Blvd del Valle

San Juan, Puerto Rico 00901

William F. Gilly

Hopkins Marine Station

Stanford University

Pacific Grove, California 93950

Email address (for W. F. Gilly, contact author): lgnye@stanford.edu

Dosidicus gigas, the only species in the genus *Dosidicus*, is commonly known as the jumbo squid, jumbo flying squid (FAO, see Roper et al., 1984), or Humboldt squid. It is the largest ommastrephid squid and is endemic to the Eastern Pacific, ranging from northern California to southern Chile and to 140°W at the equator (Nesis, 1983; Nigmatullin, et al., 2001). During the last two decades it has become an extremely important fisheries resource in the Gulf of California (Ehrhardt et al., 1983; Morales-Bojórquez et al., 2001), around the Costa Rica Dome (Ichii et al., 2002) and off Peru (Taïpe et al., 2001). It is also an active predator that undoubtedly has an important impact on local ecology in areas where it is abundant (Ehrhardt et al., 1983; Nesis, 1983; Nigmatullin et al., 2001; Markaida and Sosa-Nishizaki, 2003).

Ommastrephid squid, including the jumbo squid, are largely pelagic and may migrate long distances as part of their life cycle (Mangold, 1976). A

general pattern of long-distance migration for the jumbo squid over its entire range was proposed by Nesis (1983) and smaller-scale migrations within the Gulf of California have also been proposed according to the distribution of the fishery during 1979–80 (Klett, 1982; Ehrhardt et al., 1983). During this period squid were reported to enter the Gulf from the Pacific in January, to reach their northernmost limit (29°N) by April, and to remain in the central Gulf from May through August; the highest concentrations were found along the western (Baja California) coast. From September onward these squid appear to migrate eastward to the Mexican mainland coast and then southwards, to the mouth of the Gulf and back into the Pacific (Klett, 1982; Ehrhardt et al., 1983).

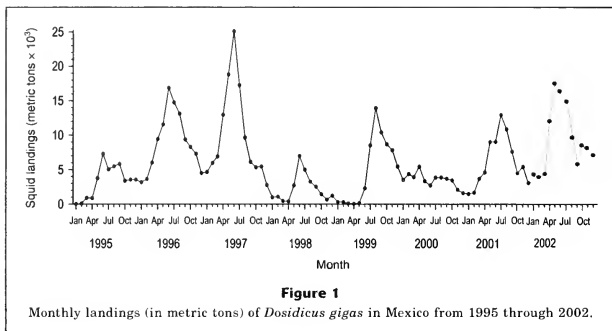
Since 1994 a seasonal pattern in the jumbo squid fishery has emerged in which large squid are abundant in the central Gulf essentially all year. During November to May, the fishery is centered in the area of Guaymas.

In Sta. Rosalia the fishery operates from May to November, which is also the period of peak landings (see Fig. 1; SEMARNAP, 1996, 1997, 1998, 1999, 2000; SAGARPA, 2001; SAGARPA¹) (see also Markaida and Sosa-Nishizaki, 2001). These generally reciprocal landing patterns are consistent with the abundance patterns described by Klett (1982), although the exact migrations proposed by Ehrhardt et al. (1983) have never been directly observed (Morales-Bojórquez et al., 2001).

All these studies concerning jumbo squid migrations have relied on analyses of landing statistics and catch data acquired by fishing stations on commercial squid-jigging vessels. Although migratory patterns of several other ommastrephid species of commercial importance have been directly demonstrated with conventional tag-and-recapture methods (Nagasawa et al., 1993), to our knowledge jumbo squid has not been studied in this manner. Given the commercial and ecological importance of this species, such studies would be valuable.

This paper describes conventional tag-and-recapture experiments on jumbo squid in the central Gulf of California. Tag-return rates were higher than in most previous studies of other ommastrephid species, and seasonal migrations between the Sta. Rosalia and Guaymas areas were directly demonstrated. Growth rates were also directly determined for the first time.

¹ SAGARPA (Secretaría de agricultura, ganadería, desarrollo rural, pesca y alimentación). Anuario Estadístico de Pesca. <http://www.sagarpa.gob.mx/conapesca/planeacion/anuario/anuario2001.zip> and <http://www.sagarpa.gob.mx/conapesca/planeacion/anuario2002>. [Accessed 26 July 2004.]



Materials and methods

Fieldwork was carried out in two separate experiments along both coasts of the Guaymas basin (see Fig. 2). This area of the central part of the Gulf of California accounts for more than 95% of Mexican jumbo squid landings. A total of 996 squid were tagged between 9 and 16 October 2001, in the general vicinity of Sta. Rosalia, Baja California Sur (B.C.S.), as indicated in Figure 2. Another 997 squid were tagged off Guaymas, Sonora, between 3 and 7 April 2002. Both experiments were conducted close to the anticipated end of the respective fishing seasons for each zone, because we hoped to obtain recaptures both locally and from more distant sites after the squid had migrated away from the fishing areas.

Squid were caught by commercial fishermen using hand-lines with 30-cm jigs and were tagged on deck with spaghetti-type, plastic cinch-up tags (Floy Tag Co., Seattle, WA) through the anterior edge of the dorsal mantle. This process took about 30 seconds, and the squid was then immediately released. All squid quickly jetted away with no obvious sign of trauma or physical impairment. Animals with any visible damage, primarily from cannibalistic attacks by other squid, were not tagged. In addition, dorsal mantle length (ML) was measured to the nearest mm for all squid in the Guaymas experiment.

Tag-return information was imprinted on the tag, and posters announcing the experiment were distributed at squid-landing ports and at local processing facilities in Sta. Rosalia, San Lucas, San Bruno, Mulege, Loreto and La Paz (B.C.S.), as well as in San Carlos, Guay-

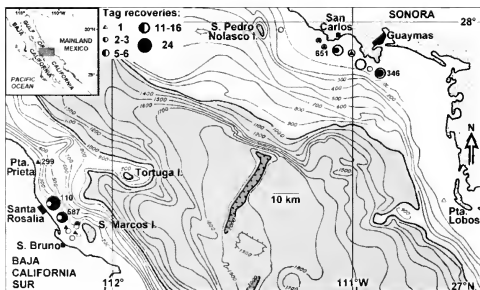
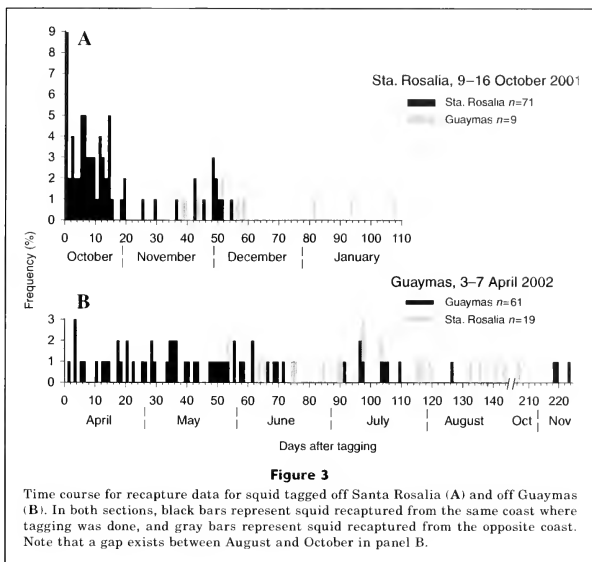


Figure 2

Map of the Guaymas basin in the central Gulf of California showing both coasts where the tagging experiments were performed. Area of detailed main map is indicated by a gray rectangle in upper leftmost inset. Numbers of tags deployed are in bold type in main map. Symbols for the numbers of tags recovered are indicated in the inset "Tag recoveries." Black symbols represent squid tagged off Sta. Rosalia; white symbols represent squid tagged off Guaymas. Depth contours are in meters. Adapted from Bischoff and Niemitz (1980).

mas, Yavaros (Sonora) and Mazatlan (Sinaloa) (Fig. 2). A monetary reward (\$50 US) was offered for each tag returned with information on recapture date and location. During the second experiment an additional reward was offered for information on squid ML and stage of sexual maturity as defined by Lipinski and Underhill (1995): immature (stages I–II), maturing (III) and mature (IV–V). Average daily growth rate (DGR) was calculated from the increase in ML between tagging and recapture divided by the number of days elapsed during this period.



Results

Timing of tag returns

A total of 80 tags (8.03%) were recovered for the squid tagged off Sta. Rosalia. Of these, 71 were recovered in the general vicinity of this port. More than a third of these tags (25) were discovered at commercial squid processing plants, where the mantles are manually cleaned before final processing. Squid were captured generally shortly after tagging; most of the tags (52) were recovered during the first 15 days (Fig. 3A). The shortest recapture period was only several hours. In this case, a squid tagged by the crew of one of our boats was caught about one km away by our second boat.

In addition to the Sta. Rosalia returns, another nine squid (0.9%) were recaptured off Guaymas, from 39 to 108 days after tagging (Fig. 3A). The temporal overlap in returns from the two localities (days 39–55) and the total lack of any subsequent Sta. Rosalia returns would indicate that a significant number, if not most, of the squid migrated from Sta. Rosalia to Guaymas and potentially elsewhere during this period (17 Nov–4 Dec).

In the second experiment, conducted off Guaymas, 80 tags (8%) were also recovered. Sixty-one were recovered

in the Guaymas area over an extended period from 2 to 224 days after tagging (Fig. 3B). In this case, the squid were recaptured more or less constantly at a low rate over the first 60 days. Surprisingly, only one tag was recovered at a processing plant during this period. Sporadic returns then continued in Guaymas over the next three months. It should be noted that there was little squid fishing activity in the area during September because of the beginning of the commercial shrimp season. The final three tags were recovered after 219–224 days (8–13 Nov). These squid were tagged on the same night and location seven months earlier.

Of the tags deployed in Guaymas, 19 (1.9%) were recovered in the Sta. Rosalia area in summer 2002 (28 May–29 August) from 54 to 207 days after tagging (Fig. 3B). Seven of these tags were recovered at squid factories. A period of overlapping returns occurred over days 54–72, and we interpreted this overlap in returns as being consistent with a seasonal mass migration from Guaymas to Sta. Rosalia. A second period of overlapping returns of similar duration occurred in July. However, in this case, returns from Guaymas continued throughout the entire summer and into the fall. It thus appears that some squid remained in the Guaymas area during this period.

Dependence of recapture rate on squid size

Squid tagged off Guaymas ranged from 32.7 to 83 cm ML (mean \pm SD) of 56.6 (\pm 7.5) cm ML [Fig. 4]. Recapture rate is clearly size dependent. No squid smaller than 46 cm ML were recaptured, and recapture rates were low (1.3–3.4%) for squid of 46–50 cm ML. However, recapture increased in roughly direct proportion to ML, reaching 15–20% for squid >70 cm ML.

Determination of daily growth rate (DGR)

Dorsal ML was measured from forty-four squid tagged off Guaymas after recapture at 4 to 224 days. ML values ranged between 46 and 80.7 cm. Variability in DGR determination, as indicated by the standard deviation (SD) of binned data from 20-day intervals, clearly decreased as the time to recapture increased. Thus, a significant negative correlation exists between the SD of DGR and recovery time ($r^2=0.88$, $P<0.01$, $n=6$) (Fig. 5). Six measurements of squid caught before 40 days yielded negative growth rates. This finding indicates that large discrepancies in DGR calculations exist in measurements on squid with short recapture times, because any errors in ML measurement are generally much larger. Growth rate estimates from squid captured after 40 days yielded values of 1.0–1.5 mm/day (SD of 0.05–0.6). We regard these as the only reliable data.

Further analysis of DGR was limited to squid captured after 40 days. Figure 6 illustrates DGR versus "mean" ML (average of ML at times of tagging and recapture) for selected squid of different sexes and stages of maturity. Probably the most reliable DGR estimates

come from the four squid that grew from 47–53 to 71–74 cm ML in 207–224 days, and these measurements yield a mean DGR of 1.05 (\pm 0.05) mm/day (Fig. 5 and ∇ in Fig. 6). Solid and dashed curves in Figure 6 represent DGR independently determined for both sexes through analysis of statolith increments (Markaida et al., 2004) for squid of a comparable size range. These growth rates are about twice those determined in the present study by direct ML measurements.

Discussion

Tag return rates

High recovery rates obtained in our study clearly demonstrate that *D. gigas* in the Gulf of California is suitable for tagging studies. This large species is relatively easily tagged with conventional plastic tags, and the tagging operation produced no obviously deleterious effects on the squid. These features make jumbo squid an attractive species for application of archival electronic tags or telemetry devices.

Despite extensive tagging efforts and intense commercial fisheries, recapture rates for other species of omastrephid squid have generally been much lower. In the extreme case, no recaptures whatsoever were obtained for the northern shortfin squid (*Illex illecebrosus*) tagged in offshore waters of Newfoundland (Hurley and Dawe, 1981). In other studies recaptures ranged from 0.03–0.1% for the Argentine shortfin squid (*I. argentinus*) in the Southwest Atlantic (Brunetti et al., 2000), to 1.0–6.2% for the European flying squid (*Todarodes sagittatus*) off Norway (Wiborg et al.²). The neon flying squid (*Ommastrephes bartramii*) from the North Pacific also yielded low rates (0.1–0.5%; Murata and Nakamura, 1998; see also Nagasawa et al., 1993). In 62 years of tagging studies of Japanese flying squid (*Todarodes pacificus*), only a few experiments carried out in the Sea of Japan and Tsugaru Strait yielded return rates that match those of the present study (up to 16.4%; see Nagasawa et al., 1993). The highest tag recovery rate (19–32%) was found for the northern shortfin squid in Newfoundland inshore areas (Hurley and Dawe, 1981). Recapture rates of up to 12.7% have also been reported for large, neritic loliginid squid (Nagasawa et al., 1993; Sauer et al., 2000).

In the present study, recapture rate was found to be directly proportional to mantle length, ranging from <3.5% for squid <50 cm

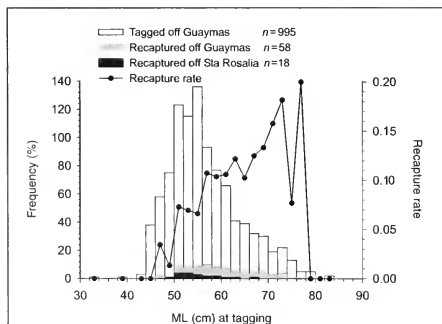


Figure 4

Mantle length (ML) distribution for all squid tagged off Guaymas (white bars) and for those recaptured off Guaymas (gray bars) and Santa Rosalia (black bars). Black circles represent recapture rate.

² Wiborg, K. F., J. Gjøsaeter, I. M. Beck, and P. Fossum. 1982. The squid *Todarodes sagittatus* (Lamarck). Distribution and biology in Northern waters, August 1981–April 1982. Council Meet. Int. Coun. Explor. Sea (K-30):1–17. ICES, Palægade 2-4, DK-1261, Copenhagen K, Denmark. info@ices.dk.

ML to 20% for squid close to 80 cm ML (Fig. 4). Reasons for this strong size-dependence are not clear. Smaller squid may either suffer a higher natural mortality rate or migrate southward out of the Guaymas basin more readily than the larger squid. We do not believe that the tagging process itself leads to such a difference in mortality rate, but this possibility cannot be ruled out.

Several factors are relevant to evaluating differences in recapture rates for jumbo squid and other ommastrephids. First, squid of the other species are not as large as jumbo squid. We are not aware of any other published data on size-dependence of recapture rates, but this phenomenon may be relevant. Second, the localized nature of the fisheries surrounding the Guaymas basin equates with high concentrations of squid in relatively small areas that are intensively fished. Most recent tagging studies of other ommastrephids have taken place in oceanic waters in the Sea of Japan and North Pacific, where the fishing zone is extremely large and far from any localized coastal fishing areas (Nagasawa et al., 1993). The extreme disparity in return rates for nearshore versus offshore studies in Newfoundland supports this idea. Third, an ambitious advertising campaign (posters) and the substantial reward offered for tag returns undoubtedly stimulated a high degree of cooperation in the largely artisanal Mexican fishery that is highly concentrated in Sta. Rosalia and Guaymas. A strong dependence of tag-return rate on rewards and advertising has been previously noted (see Nagasawa et al., 1993).

Seasonal migration

Results from this study directly demonstrate that jumbo squid in the Guaymas basin migrate across the Gulf on a seasonal basis. Squid appear to migrate from Sta. Rosalia to Guaymas during the second half of November and early December and to make the reverse trip in late May and early June. Thus, large squid (40–80 cm ML) remain available to fisheries surrounding the Guaymas basin throughout the year. These data support the idea that these fishing areas are feeding grounds (Markaida and Sosa-Nishizaki, 2001). What fraction of squid, if any, migrate southward out of the Guaymas basin and potentially into the Pacific cannot be ascertained from our data.

Transit time across the Gulf for the migrating squid appears to be fairly brief—probably less than 16 days based on the overlap of recaptures in both fishing areas. Assuming a straight-line distance of 130 km between

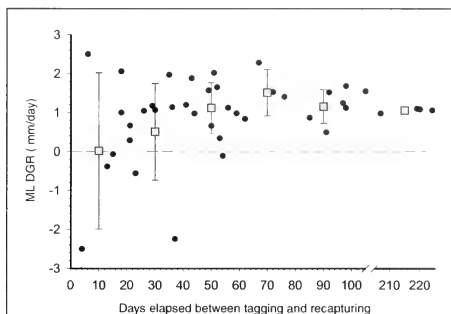


Figure 5

Daily growth rate (DGR) in mantle length (ML) determined for squid recaptured at different times after tagging. Black circles represent measurements from individual animals. Gray squares represent means ± 1 SD for squid grouped in 20-day bins. Note that a gap exists between 100 and 200 days.

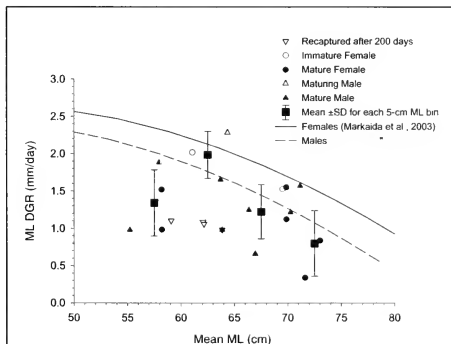


Figure 6

Relationship of daily growth rate (DGR) and mean mantle length (ML) (average of measured ML at time of tagging and time of recapture). Small symbols represent measurements from selected individual animals as follows: squid recaptured after >200 days (∇), immature female (\circ), mature female (\bullet), maturing male (Δ), mature male (\blacktriangle). Larger squares (\blacksquare) indicate means ± 1 SD for all data pooled into 5-cm bins. Analysis was limited to squid recaptured after 40 days and of identified sex. Curves represent DGR vs. ML relationship as determined by counting statolith increments for females (solid) and males (dashed) and are adapted from Markaida et al. (2004).

these areas, the average maintained speed during the migration would be about 8 km/day. A comparable figure can be derived from one of our first squid to be recaptured. This animal was tagged at Pt. Prieta (see Fig. 2) and recaptured 20 km away off Sta. Rosalia (Fig. 2) after three days.

This estimated velocity for a trans-Gulf migration is well within the range of rates observed in other studies of omastrephids (O'Dor, 1988). Jumbo squid tracked with acoustic telemetry off Peru covered 3–5 miles in 8–14 hours, or about 14 km/day (Yatsu et al., 1999). Neon flying squid tracked in the same way covered up to 22 km per day (Nakamura, 1993). Migration rates obtained from tagging studies yielded even higher estimates. Maximum speed for migrating short-finned squid has been estimated at 20–30 km/day (Dawe et al., 1981; Hurley and Dawe, 1981), and high rates have also been reported for the Japanese squid (see Nagasawa et al., 1993). Large loliginid squid have been reported to migrate at rates of 3 to 17 km/day (see Sauer et al., 2000).

Daily growth rates

Variance in DGR estimates from ML measurements decreased dramatically after 30 days after tagging, and became fairly consistent by 50 days. Clearly, estimates of DGR in our study are only reliable for these later times, and a DGR of 1–1.5 mm/day in ML is evident for squid in the 50–70 cm range of ML (Fig. 6). These absolute rates would correspond to relative rates of 0.15–0.22% increase in ML per day.

There are few comparable estimates of growth rates for other omastrephid squids based on tag-recapture studies. However, the neon flying squid grows 0.5–2.7 mm/day in the 18–48 cm ML range (Araya, 1983), and good agreement exists between growth rates obtained from tag-recapture studies and those from statolith aging studies (Yatsu et al., 1997). When converted to relative growth rate, this species would thus appear to grow substantially faster than the jumbo squid. The common Japanese squid grows 0.45 mm/day (Nagasawa et al., 1993), but for this species, mantle lengths were not given; therefore relative rates cannot be estimated.

More importantly, absolute growth rates determined by direct ML measurements in the present study disagreed with those derived from statolith aging methods (Markaida et al., 2004), and this discrepancy merits re-evaluation of previous longevity estimates. Squid of 50 cm ML are thought to be about 260 days old based on statolith ring counts, and our tag-recapture study revealed that it can take another 200 days to grow to 70 cm ML. The estimated age at this size would therefore be 460 days, about 100 days more than that estimated by statolith aging for squid of 70 cm ML (Markaida et al., 2004). Thus, the largest squid found in the Gulf of California (about 90 cm ML) might be up to 2 years old.

Reasons for the apparent underestimates in longevity with statolith aging are unclear. Difficulty in resolving

discrete rings late in life of a specimen is one possibility. Another is that the assumed daily ring deposition may not occur throughout the lifetime of a jumbo squid. No successful validation studies have been reported for this species, either in the laboratory or in the wild.

Squid distributions in the Gulf in relation to commercial landings

Although large-scale migrations of jumbo squid within the Guaymas basin are apparently responsible for the seasonal pattern in the commercial landings (Fig. 1; see also Markaida and Sosa-Nishizaki, 2001), the biological and oceanographic reasons for these migrations are not well established. The reciprocal pattern in squid distribution between the eastern and western central Gulf is correlated with the wind-driven upwelling seasonality in this area (Roden and Groves, 1959) and is probably highly influenced by this oceanographic feature. A similar situation exists in the life cycle of another important pelagic resource, the Pacific sardine (*Sardinops caeruleus*) (Hammann et al., 1988).

However, other biological factors are also probably important. Summer upwelling in the western Gulf is actually less intense than off the eastern coast in winter (Hammann et al., 1988; Santamaría-del-Angel et al., 1999), yet 80% of squid landings were made at Sta. Rosalia between 1995 and 1997 (Markaida and Sosa-Nishizaki, 2001). We propose that concentrations of spawning myctophids (lanternfishes) off Baja California in the summer (Moser et al., 1974) may be largely responsible for this disparity because these fish are a major prey item for squid in the Guaymas basin (Markaida and Sosa-Nishizaki, 2003).

Data in the present study also indicate that jumbo squid may be available to commercial fishing efforts off each coast for a longer period than previously thought. Our data indicate that squid were recovered in the waters off Guaymas throughout the year; therefore it is likely that some squid do not undergo the westward spring migration (Fig. 3B). However, it is not certain that the final returns from Guaymas after 7 months were of this resident stock, because they would have had time to migrate to Sta. Rosalia and back again. It is also unclear whether a resident stock of squid exists in the Sta. Rosalia area year-round. Strong northern winds in this area lead to a cessation of commercial fishing efforts during the winter months, and the lack of tag returns during winter may simply reflect this fact.

Long-distance migrations into and out of the Gulf of California

Although data in this paper have demonstrated seasonal migrations of jumbo squid within the Guaymas basin, migration patterns into this region from the southern Gulf and open Pacific (and back out) remain unknown. The much lower level of commercial fishing effort in these latter areas will greatly constrain efforts to elu-

cidate migrations over these longer distances using conventional tag-and-recapture approaches.

Presumably, as the largest eunektonic squid, jumbo squid should be able to perform large-scale migrations covering its whole geographic range as do other omastrephids (O'Dor, 1988). The high tag return rates achieved in the present study, in conjunction with the large size of the squid, make application of a variety of archival electronic tagging devices an attractive possibility. Such devices could reveal long-distance migrations across the large range of jumbo squid in a fishery-independent manner.

Acknowledgments

We acknowledge funding for this project by the Tagging of Pacific Pelagics (TOPP) program and the Census of Marine Life (COML). We thank Oscar Sosa-Nishizaki (CICSE, Ensenada) for administering this project in Mexico and providing laboratory space and facilities. Volunteer field workers in Sta. Rosalia included A. Novakovic, J. Schulz, S. Sethi (Stanford Univ.), and L. Roberson (California State University, Northridge). We are also indebted to personnel of Centro Regional de Investigación Pesquera, especially Manuel O. Nevárez, Paco Méndez, and Araceli Ramos, for their support during tagging and tag recovering at Guaymas, and to Sandra Patricia Garazar and Vicente Monreal for recovering tags in Sta. Rosalia. We extend our sincere gratitude to all fishermen and squid factory personnel for their cooperation.

Literature cited

Araya, H.
1983. Fishery, biology and stock assessment of *Ommastrephes bartramii* in the North Pacific Ocean. Mem. Nat. Mus. Victoria 44:269-283.

Bischoff, J. L., and J. W. Niemitz.
1980. Bathymetric maps of the Gulf of California: bathymetry of the Central Gulf Province, Map I-244. Miscellaneous Investigation Series, U. S. Geological Survey, Denver, CO. Sheet 3 of 4 sheets.

Brunetti, N. E., M. L. Ivanovic, G. R. Rossi, B. Elena, H. Benavides, R. Guerrero, G. Blanco, C. Marchetti, and R. Piñero.
2000. JAMARC-INIDEP joint research cruise on Argentine short-finned squid (*Illex argentinus*). January-March 1997. Argentine Final Report. INIDEP Inf. Tec. 34:1-36.

Dawe, E. G., P. C. Beck, H. S. Drew, and G. H. Winter.
1981. Long distance migration of a short-finned squid *Illex illecebrosus*. J. Northwest Atlantic Fish. Sci. 2:75-76.

Ehrhardt, N. M., P. S. Jacquemin, F. Garcia B., G. González D., J. M. López B., J. Ortiz C. and A. Solís N.
1983. On the fishery and biology of the giant squid *Dosidicus gigas* in the Gulf of California, Mexico. In Advances in assessment of world cephalopod resources (J. F. Caddy, ed.), p. 306-339. FAO Fish. Tech. Pap. 231.

Hamann, M.G., T. R. Baumgartner, and A. Badan-Dangon.
1988. Coupling of the Pacific sardine (*Sardinops sagax caeruleus*) life cycle with the Gulf of California pelagic environment. CalCOFI Rep. 29:102-109.

Hurley, G. V., and E. G. Dawe.
1981. Tagging studies on squid (*Illex illecebrosus*) in the Newfoundland area. North Atlantic Fisheries Organization (NAFO) SCR Doc., No. 80/II/33, serial no. 072. 11 p. NAFO, Dartmouth, Nova Scotia, Canada.

Ichii, T., K. Mahapatra, T. Watanabe, A. Yatsu, D. Inagake, and Y. Okada.
2002. Occurrence of jumbo flying squid *Dosidicus gigas* aggregations associated with the countercurrent ridge off the Costa Rica Dome during 1997 El Niño and 1999 La Niña. Mar. Ecol. Prog. Ser. 231:151-166.

Klett, A.
1982. Jumbo squid fishery in the Gulf of California, Mexico. In Proceedings of the International Squid Symposium, August 9-12, 1981, Boston, Massachusetts (prepared by the New-England Fisheries Development Found., Inc.), p. 81-100. UNIPUB, New York, NY.

Lipinski, M. R., and L. G. Underhill.
1995. Sexual maturation in squid: Quantum or continuum? S. Afr. J. Mar. Sci. 15:207-223.

Mangold, K.
1976. La migration chez les Céphalopodes. Oceanis 2(8):381-389. [In French.]

Markaida, U., and O. Sosa-Nishizaki.
2001. Reproductive biology of jumbo squid *Dosidicus gigas* in the Gulf of California, 1995-1997. Fish. Res. 54(1):63-82.
2003. Food and feeding habits of jumbo squid *Dosidicus gigas* (Cephalopoda: Ommastrephidae) from the Gulf of California, Mexico. J. Mar. Biol. Assoc. U.K. 83:507-522.

Markaida, U., C. Quiñónez-Velázquez, and O. Sosa-Nishizaki.
2004. Age, growth and maturation of jumbo squid *Dosidicus gigas* (Cephalopoda: Ommastrephidae) from the Gulf of California, Mexico. Fish. Res. 66(1):31-47.

Morales-Bojórquez, E., M. A. Cisneros-Mata, M. O. Nevárez-Martínez and A. Hernández-Herrera.
2001. Review of the stock assessment and fishery biology of *Dosidicus gigas* in the Gulf of California, México. Fish. Res. 54:83-94.

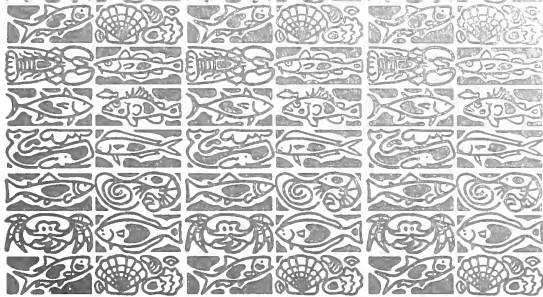
Moser, H. G., E. H. Ahlstrom, D. Kramer, and E. G. Stevens.
1974. Distribution and abundance of fish eggs and larvae in the Gulf of California. CalCOFI Rep. 17:112-128.

Murata, M., and Y. Nakamura.
1998. Seasonal migration and diel vertical migration of the neon flying squid, *Ommastrephes bartramii*, in the North Pacific. In Contributed papers to the international symposium on large pelagic squids, Tokyo, July 18-19, 1996 (T. Okutani, ed.), p. 13-30. Japan Marine Fishery Resources Research Center (JAMARC).

Nakamura, Y.
1993. Vertical and horizontal movements of mature females of *Ommastrephes bartramii* observed by ultrasonic telemetry. In Recent advances in cephalopod fisheries biology: contributed papers to 1991 CIAC international symposium and proceedings of the workshop on age, growth and population structure (T. Okutani, R. K. O'Dor, and T. Kubodera, eds.), p. 331-336. Tokai Univ. Press, Tokyo, Japan.

Nagasawa, K., S. Takayanagi, and T. Takami.
1993. Cephalopod tagging and marking in Japan: a review. In Recent advances in cephalopod fisheries

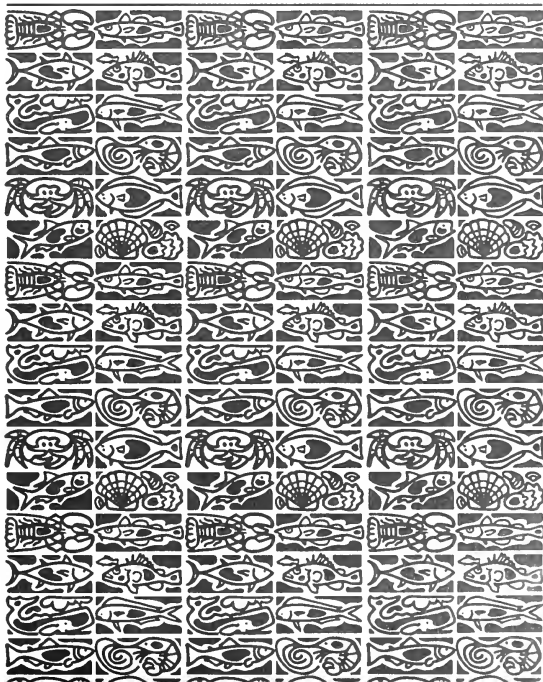
- biology: contributed papers to the 1991 Cephalopod International Advisory Council (CIAC) international symposium and proceedings of the workshop on age, growth, and population structure (T. Okutani, R. K. O'Dor, and T. Kubodera, eds.), p. 313-329. Tokay Univ. Press, Tokyo, Japan.
- Nesis, K. N.
1983. *Dosidicus gigas*. In Cephalopod life cycles, vol. 1, species accounts (P. R. Boyle, ed), p. 215-231. Academic Press, London, UK.
- Nigmatullin, Ch. M., K. N. Nesis, and A. I. Arkhipkin.
2001. A review of the biology of the jumbo squid *Dosidicus gigas* (Cephalopoda: Ommastrephidae). *Fish. Res.* 54:9-19.
- O'Dor, R. K.
1988. The energetic limits on squid distributions. *Malacologia* 29(1):113-119.
- Roden, G. I., and G. W. Groves.
1959. Recent oceanographic investigations in the Gulf of California. *J. Mar. Res.* 18:10-35.
- Roper, F. E., M. J. Sweeney, and C. E. Nauen.
1984. FAO species catalogue: vol. 3, Cephalopods of the world, 272 p. FAO, Rome.
- SAGARPA (Secretaría de agricultura, ganadería, desarrollo rural, pesca y alimentación).
2001. Anuario estadístico de pesca 2000. SAGARPA-CONAPESCA (Comisión Nacional de Acuacultura y Pesca), Mexico, 268 p. [In Spanish.]
- Santamaria-del-Angel, E., S. Alvarez-Borrego, R. Millán-Núñez, and F. E. Muller-Karger.
1999. On the weak effect of summer upwelling on the phytoplankton biomass of the Gulf of California. *Rev. Soc. Mex. Hist. Nat.* 49:207-212. [In Spanish, English abstract.]
- Sauer, W. H. H., M. R. Lipinski, and C. J. Augustyn.
2000. Tag recapture studies of the chokka squid *Loligo vulgaris reynaudii* d'Orbigny, 1845 on inshore spawning grounds on the south-east coast of South Africa. *Fish. Res.* 45:283-289.
- SEMARNAP (Secretaría del medio ambiente, recursos naturales y pesca). Distributed by the Mexican Secretary on Natural Resources.
1996. Anuario estadístico de pesca 1995, 235 p. SEMARNAP, Mexico. [In Spanish.]
1997. Anuario estadístico de pesca 1996, 232 p. SEMARNAP, Mexico. [In Spanish.]
1998. Anuario estadístico de pesca 1997, 241 p. SEMARNAP, Mexico. [In Spanish.]
1999. Anuario estadístico de pesca 1998, 244 p. SEMARNAP, Mexico. [In Spanish.]
2000. Anuario estadístico de pesca 1999, 271 p. SEMARNAP, Mexico. [In Spanish.]
- Taipe, A., C. Yamashiro, L. Mariategui, P. Rojas, and C. Roque.
2001. Distribution and concentrations of jumbo flying squid (*Dosidicus gigas*) off the Peruvian coast between 1991 and 1999. *Fish. Res.* 54:21-32.
- Yatsu, A., S. Midorikawa, T. Shimada, and Y. Uozumi.
1997. Age and growth of the neon flying squid, *Ommastrephes bartami*, in the North Pacific Ocean. *Fish. Res.* 29:257-270.
- Yatsu, A., K. Yamanaka, and C. Yamashiro.
1999. Tracking experiments of the jumbo squid, *Dosidicus gigas*, with an ultrasonic telemetry system in the Eastern Pacific Ocean. *Bull. Nat. Res. Inst. Far Seas Fish.* 36:55-60.



U.S. Department
of Commerce

Volume 103
Number 2
April 2005

Fishery Bulletin



**U.S. Department
of Commerce**

Carlos M. Gutierrez
Secretary

**National Oceanic
and Atmospheric
Administration**

Vice Admiral
Conrad C. Lautenbacher Jr.,
USN (ret.)

Under Secretary for
Oceans and Atmosphere

**National Marine
Fisheries Service**

William T. Hogarth
Assistant Administrator
for Fisheries



The *Fishery Bulletin* (ISSN 0090-0656) is published quarterly by the Scientific Publications Office, National Marine Fisheries Service, NOAA, 7600 Sand Point Way NE, BIN C15700, Seattle, WA 98115-0070. Periodicals postage is paid at Seattle, WA, and at additional mailing offices. POSTMASTER: Send address changes for subscriptions to *Fishery Bulletin*, Superintendent of Documents, Attn: Chief, Mail Last Branch, Mail Stop SSOM, Washington, DC 20402-9373.

Although the contents of this publication have not been copyrighted and may be reprinted entirely, reference to source is appreciated.

The Secretary of Commerce has determined that the publication of this periodical is necessary according to law for the transaction of public business of this Department. Use of funds for printing of this periodical has been approved by the Director of the Office of Management and Budget.

For sale by the Superintendent of Documents, U.S. Government Printing Office, Washington, DC 20402. Subscription price per year: \$55.00 domestic and \$68.75 foreign. Cost per single issue, \$28.00 domestic and \$35.00 foreign. See back for order form.

Fishery Bulletin

Scientific Editor
Norman Bartoo, Ph.D.

Associate Editor
Sarah Shoffler

National Marine Fisheries Service, NOAA
8604 La Jolla Shores Drive
La Jolla, California 92037

Managing Editor
Sharyn Matriotti

National Marine Fisheries Service
Scientific Publications Office
7600 Sand Point Way NE, BIN C15700
Seattle, Washington 98115-0070

Editorial Committee

Harlyn O. Halvorson, Ph.D.	University of Massachusetts, Boston
Ronald W. Hardy, Ph.D.	University of Idaho, Hagerman
Richard D. Methot, Ph.D.	National Marine Fisheries Service
Theodore W. Pietsch, Ph.D.	University of Washington, Seattle
Joseph E. Powers, Ph.D.	National Marine Fisheries Service
Harald Rosenthal, Ph.D.	Universität Kiel, Germany
Fredric M. Serchuk, Ph.D.	National Marine Fisheries Service
George Watters, Ph.D.	National Marine Fisheries Service

***Fishery Bulletin* web site: www.fishbull.noaa.gov**

The *Fishery Bulletin* carries original research reports and technical notes on investigations in fishery science, engineering, and economics. It began as the *Bulletin of the United States Fish Commission* in 1881; it became the *Bulletin of the Bureau of Fisheries* in 1904 and the *Fishery Bulletin of the Fish and Wildlife Service* in 1941. Separates were issued as documents through volume 46; the last document was No. 1103. Beginning with volume 47 in 1931 and continuing through volume 62 in 1963, each separate appeared as a numbered bulletin. A new system began in 1963 with volume 63 in which papers are bound together in a single issue of the bulletin. Beginning with volume 70, number 1, January 1972, the *Fishery Bulletin* became a periodical, issued quarterly. In this form, it is available by subscription from the Superintendent of Documents, U.S. Government Printing Office, Washington, DC 20402. It is also available free in limited numbers to libraries, research institutions, State and Federal agencies, and in exchange for other scientific publications.

Fishery Bulletin

Contents

Articles

- 229–245 Alonzo, Suzanne H., and Marc Mangel
Sex-change rules, stock dynamics, and the performance of spawning-per-recruit measures in protogynous stocks
- 246–257 Brandon, Elisif A. A., Donald G. Calkins,
Thomas R. Loughlin, and Randall W. Davis
Neonatal growth of Steller sea lion (*Eumetopias jubatus*) pups in Alaska
- 258–269 Brouwer, Stephen L., and Marc H. Griffiths
Reproductive biology of carpenter seabream (*Argyrozona argyrozona*) (Pisces: Sparidae) in a marine protected area
- 270–279 Burn, Douglas M., and Angela M. Doroff
Decline in sea otter (*Enhydra lutris*) populations along the Alaska Peninsula, 1986–2001
- 280–291 Carlson, John K., and Ivy E. Baremore
Growth dynamics of the spinner shark (*Carcharhinus brevipinna*) off the United States southeast and Gulf of Mexico coasts: a comparison of methods
- 292–306 Domeier, Michael L., Dale Kiefer, Nicole Nasby-Lucas,
Adam Wagschal, and Frank O'Brien
Tracking Pacific bluefin tuna (*Thunnus thynnus orientalis*) in the northeastern Pacific with an automated algorithm that estimates latitude by matching sea-surface-temperature data from satellites with temperature data from tags on fish
- 307–319 Fischer, Andrew J., M. Scott Baker Jr., Charles A Wilson,
and David L. Nieland
Age, growth, mortality, and radiometric age validation of gray snapper (*Lutjanus griseus*) from Louisiana
- 320–330 Grabowski, Robert C., Thomas Windholz, and Yong Chen
Estimating exploitable stock biomass for the Maine green sea urchin (*Strongylocentrotus droebachiensis*) fishery using a spatial statistics approach

The conclusions and opinions expressed in *Fishery Bulletin* are solely those of the authors and do not represent the official position of the National Marine Fisheries Service (NOAA) or any other agency or institution.

The National Marine Fisheries Service (NMFS) does not approve, recommend, or endorse any proprietary product or proprietary material mentioned in this publication. No reference shall be made to NMFS, or to this publication furnished by NMFS, in any advertising or sales promotion which would indicate or imply that NMFS approves, recommends, or endorses any proprietary product or proprietary material mentioned herein, or which has as its purpose an intent to cause directly or indirectly the advertised product to be used or purchased because of this NMFS publication.

- 331–343 Lowry, Mark S., and Karin A. Forney
Abundance and distribution of California sea lions (*Zalophus californianus*) in central and northern California during 1998 and summer 1999
- 344–354 Mackie, Michael C., Paul D. Lewis, Daniel J. Gaughan, and Stephen J. Newman
Variability in spawning frequency and reproductive development of the narrow-barred Spanish mackerel (*Scomberomus commerson*) along the west coast of Australia
- 355–370 Ruggerone, Gregory T., Ed Farley, Jennifer Nielson, and Peter Hagen
Seasonal marine growth of Bristol Bay sockeye salmon (*Oncorhynchus nerka*) in relation to competition with Asian pink salmon (*O. gorbuscha*) and the 1977 ocean regime shift
- 371–379 Shoji, Jun, and Masaru Tanaka
Distribution, feeding condition, and growth of Japanese Spanish mackerel (*Scomberomus niphonius*) larvae in the Seto Inland Sea
- 380–391 Wang, You-Gan, and Nick Ellis
Maximum likelihood estimation of mortality and growth with individual variability from multiple length-frequency data
- 392–403 Williams, Erik H., and Kyle W. Shertzer
Effects of fishing on growth traits: a simulation analysis

Notes

- 404–406 Burton, Michael L., Kenneth J. Brennan, Roldan C. Muñoz, and Richard O. Parker Jr.
Preliminary evidence of increased spawning aggregations of mutton snapper (*Lutjanus analis*) at Riley's Hump two years after establishment of the Tortugas South Ecological Reserve
- 411–416 Carpentieri, Paolo, Francesco Colloca, Massimiliano Cardinale, Andrea Belluscio, and Giandomenico D. Ardizzone
Feeding habits of European hake (*Merluccius merluccius*) in the central Mediterranean Sea
- 417–425 Gobert, Bertrand, Alain Guillou, Peter Murray, Patrick Berthou, Maria D. Oqueli Turcios, Ester Lopez, Pascal Lorange, Jérôme Huet, Nicolas Diaz, and Paul Gervain
Biology of the queen snapper (*Etelis oculatus*: Lutjanidae) in the Caribbean
- 426–432 Graham, Rachel T., and Daniel W. Castellanos
Courtship and spawning behaviors of carangid species in Belize
- 433–437 Hewitt, David A., and John M. Hoenig
Comparison of two approaches for estimating natural mortality based on longevity
- 438–444 Lindquist, David C., and Richard F. Shaw
Effects of current speed and turbidity on stationary light-trap catches of larval and juvenile fishes
- 445–452 Macchi, Gustavo J., Marcelo Pájaro, and Adrián Madirolas
Can a change in spawning pattern of Argentine hake (*Merluccius hubbsi*) affect its recruitment?
- 453–460 Raymundo-Huizar, Alma R., Horacio Pérez-España, Maite Mascaró, and Xavier Chiappa-Carrara
Feeding habits of the dwarf weakfish (*Cynoscion nannus*) off the coasts of Jalisco and Colima, Mexico
- 461–466 Wood, Anthony D.
Using bone measurements to estimate the original sizes of bluefish (*Pomatomus saltatrix*) from digested remains
- 467 Subscription form

Abstract—Predicting and understanding the dynamics of a population requires knowledge of vital rates such as survival, growth, and reproduction. However, these variables are influenced by individual behavior, and when managing exploited populations, it is now generally realized that knowledge of a species' behavior and life history strategies is required. However, predicting and understanding a response to novel conditions—such as increased fishing-induced mortality, changes in environmental conditions, or specific management strategies—also require knowing the endogenous or exogenous cues that induce phenotypic changes and knowing whether these behaviors and life history patterns are plastic. Although a wide variety of patterns of sex change have been observed in the wild, it is not known how the specific sex-change rule and cues that induce sex change affect stock dynamics. Using an individual based model, we examined the effect of the sex-change rule on the predicted stock dynamics, the effect of mating group size, and the performance of traditional spawning-per-recruit (SPR) measures in a protogynous stock. We considered four different patterns of sex change in which the probability of sex change is determined by 1) the absolute size of the individual, 2) the relative length of individuals at the mating site, 3) the frequency of smaller individuals at the mating site, and 4) expected reproductive success. All four patterns of sex change have distinct stock dynamics. Although each sex-change rule leads to the prediction that the stock will be sensitive to the size-selective fishing pattern and may crash if too many reproductive size classes are fished, the performance of traditional spawning-per-recruit measures, the fishing pattern that leads to the greatest yield, and the effect of mating group size all differ distinctly for the four sex-change rules. These results indicate that the management of individual species requires knowledge of whether sex change occurs, as well as an understanding of the endogenous or exogenous cues that induce sex change.

Sex-change rules, stock dynamics, and the performance of spawning-per-recruit measures in protogynous stocks

Suzanne H. Alonzo

Institute of Marine Sciences and the Center for Stock Assessment Research (CSTAR)
University of California Santa Cruz
1156 High Street
Santa Cruz, California 95064
Present address: Department of Ecology and Evolutionary Biology
Yale University
165 Prospect St., OML 427
New Haven, Connecticut 06511

E-mail address: Suzanne.Alonzo@yale.edu

Marc Mangel

Department of Applied Mathematics and Statistics
Jack Baskin School of Engineering and the Center for Stock Assessment Research (CSTAR)
University of California Santa Cruz
1156 High Street
Santa Cruz California 95064

Growth, survival, and reproduction all affect the dynamics of a population and its response to fishing and management (Quinn and Deriso, 1999; Haddon, 2001). However, these three key variables are influenced by many aspects of a species' biology, environment, and evolutionary history. There is an increasing realization that the management of populations requires an understanding of their behavior, life history strategies, and reproductive patterns (Sutherland, 1990; Huntsman and Schaaf, 1994; Collins et al., 1996; Greene et al., 1998; Sutherland, 1998; Beets and Friedlander, 1999; Coleman et al., 1999; Fulton et al., 1999; Kruuk et al., 1999; Constable et al., 2000; Cowen et al., 2000; Koeller et al., 2000; Fu et al., 2001; Apostolaki et al., 2002; Levin and Grimes, 2002). Although it is important to document the normal patterns of behavior and reproduction within a population, predicting and understanding a stock's response to novel conditions also requires knowledge of the degree of plasticity in behaviors that affect growth, survival, and reproduction, and the cues that induce phenotypic changes. Numerous examples exist of context- and condition-dependent behavior in fish

(e.g., Metcalfe et al., 1989; Snyder and Dingle, 1990; Schultz and Warner, 1991; Wainwright et al., 1991; Mittelbach et al., 1992; Nishibori and Kawata, 1993; Ridgeway and Shuter, 1994; Breden et al., 1995), and this kind of plasticity has the potential to affect the dynamics of a stock. For example, many commercially important species of fish change sex from female to male. Researchers have argued that this life history pattern will lead to different population dynamics and responses to fishing and management strategies than will the life history pattern of dioecious (separate-sex) species (e.g., Snyder and Dingle, 1990; Schultz and Warner, 1991; Wainwright et al., 1991; Nishibori and Kawata, 1993; Ridgeway and Shuter, 1994; Alonzo and Mangel, 2004). However, it is important to consider not only whether sex change occurs, but also how it occurs; whether plasticity in sex change exists and what cues determine sex change in an individual species.

A variety of patterns of sex change have been observed in the wild (Warner and Lejeune, 1985; Charnov, 1986; Shapiro, 1987; Charnov and Bull, 1989; Iwasa, 1990; Warner and Swearer, 1991; Lutnesky, 1994, 1996;

Kuwamura and Nakashima, 1998; Koeller et al., 2000; Nakashima et al., 2000). At one extreme, sex change may occur at a fixed size or age threshold. However, sex change is known in many species to be mediated by local factors such as population density, reproductive skew, sex ratio, and size distribution (Warner and Lejeune, 1985; Warner and Swearer, 1991; Lutnesky, 1994, 1996; Kuwamura and Nakashima, 1998; Koeller et al., 2000; Nakashima et al., 2000). In many sex-changing species, overlap exists between the sexes in size and age and this overlap indicates that sex change may also depend on individual experience and local conditions (Munoz and Warner, 2003). The pattern of sex change may have important implications for a species' response to fishing. For example, if the size at sex change is fixed, then the population sex ratio may be affected by size-selective fishing of males, resulting in sperm limitation and decreased larval production (Alonzo and Mangel, 2004). In contrast, if sex change is mediated at the level of the spawning group in single-male harems and mating group size remains the same, sex ratios are maintained if the largest female always changes sex. In such a case, larval production will be reduced only because of the decreased size distribution of the population due to fishing. However, if sex change is controlled by the reproductive skew in the group (e.g., the expected potential for reproduction as a male versus present fecundity as a female), then the largest individual might not change sex and the spawning group could be without a male (Munoz and Warner, 2003). This result would clearly lead to a much greater effect on the productivity of the stock. A detailed understanding of the factors determining sex change and the cascading effects on sperm production, fecundity, and sex ratio can be critical to predicting stock dynamics. Furthermore, most animals have "rules-of-thumb" which determine their behavior and reproduction. Although these rules will have evolved under normal conditions, in the presence of fishing or other human-induced disturbances, animals are likely to continue to use these behavioral rules on ecological time scales even if they no longer function to maximize reproduction.

Although previous fisheries models have examined sex change, a consensus does not exist regarding how sex change is predicted to affect stock dynamics. Some research has suggested that sex-changing stocks will be more sensitive to fishing and cannot be managed as if they were identical to separate-sex stocks (Bannerot et al., 1987; Punt et al., 1993; Huntsman and Schaaf, 1994; Coleman et al., 1996; Beets and Friedlander, 1999; Brule et al., 1999; Coleman et al., 1999; Armsworth, 2001; Fu et al., 2001). However, it has also been argued that, in the absence of sperm limitation, protogynous stocks should be less sensitive to size-selective fishing because female biomass and thus population fecundity should not decrease as much as in a dioecious population, making traditional management and theory conservative when applied to these species. In general, protogynous stocks have been predicted to be at risk of population crashes because of their potential for nonlin-

ear population dynamics in the presence of exploitation, yet there is no consensus regarding the importance of the exact pattern of sex change. For example, Armsworth (2001) examined protogynous stock dynamics when the probability of sex change was a fixed function of individual age and when the probability of sex change depended on the mean age of individuals in the population. He found that these two patterns of sex change had similar general dynamics and argued that management of a protogynous stock might not require knowledge of the precise pattern of sex change. In contrast, Huntsman and Schaaf (1994) and Coleman et al. (1999) have argued that a consideration of the pattern of sex change can be important to managing stocks. But, past theory has generally focused on comparing fixed patterns of sex change with fully compensating reproductive patterns that maintain a fixed sex ratio or ratio of female to male biomass. However, a variety of patterns of sex change exist and there is no reason to believe that all species have evolved to exhibit full compensation under natural conditions, let alone under new situations. Thus, it is important to consider how specific sex change rules will affect the dynamics and management of protogynous stocks and whether knowledge of the cues that determine sex change will be important.

We (Alonzo and Mangel, 2004) developed a general modeling approach for examining the impact of reproductive behavior and life history pattern on stock dynamics. Using this approach, we then compared the dynamics of a protogynous population with fixed size at sex change and an otherwise identical dioecious species (Alonzo and Mangel, 2004). These analyses showed that although dioecious and protogynous stocks clearly have distinct dynamics, simple statements arguing that one life history pattern is more or less sensitive to fishing cannot be made. Protogynous stocks with fixed patterns of sex change were predicted to experience sperm limitation and lowered larval recruitment at high fishing pressure, whereas the dioecious stock was predicted to show a large drop in mean population size even at low fishing mortality, but was not predicted to experience lowered fertilization rates due to size-selective fishing. Both stocks were predicted to be sensitive to fishing pattern, but a fixed pattern of sex change was predicted to put a population at risk of crashing if all male size classes were fished even at relatively low fishing mortality. Finally, classic spawning-per-recruit (SPR) measures were not predicted to be good indicators of changes in the mean population size of protogynous stocks because they cannot indicate whether a population is experiencing sperm limitation and whether this limitation may lead to decreased population size or cause the stock to crash with small changes in fishing mortality. Although we found that whether or not a stock changes sex was important, that knowledge alone was not sufficient to understand and predict the response of the stock to fishing or management. We also found that sperm production and mating system were important variables affecting the probability that a population

would experience sperm limitation and would affect the performance of traditional spawning-per-recruit measures. However, we did not consider the possibility that size at sex change may be plastic and depend on local social conditions or relative rather than absolute size. Plastic sex change may allow a protogynous species to compensate for any effect of size-selective fishing on the sex ratio of the population, rendering its dynamics identical to the dynamics of a dioecious species. However, as described above, a wide variety of patterns of sex change have been observed in the wild and have been proposed to occur. Therefore, the exact pattern of sex change and cue driving phenotypic changes may lead to unique stock dynamics. In this study we apply the same general method we used previously (Alonzo and Mangel, 2004) to examine the effect of four different patterns of sex change (one fixed and three plastic) on the stock dynamics of a protogynous species.

Methods

We applied the same general method and individual-based population dynamic model as our previous study (Alonzo and Mangel, 2004). However, we now included the effect of four different patterns of sex change on the stock dynamics and performance of spawning-per-recruit measures in a protogynous species. Individuals vary in age, size, sex, and location (i.e. mating site). We assumed annual time periods and determined individual survival, size, and reproduction as described below. We simulated 100 years prior to examining the impact of fishing on stock dynamics and then simulated 100 more years in the presence of fishing with a constant mean fishing-induced mortality. This allowed the population to reach a stable age, sex, and size distribution prior to fishing which is independent of initial conditions. Because a number of elements of the model are stochastic, we examined 20 simulations for each scenario and set of parameter values, which was more than sufficient in all cases to lead to low variability in the key measures of interest.

Fishing and adult survival

We assume age and size do not affect natural adult mortality, μ_A , and that adult mortality is density-independent. The fishery is size selective; if L represents fish size, F annual fishing mortality, L_f the size at which there is 50% chance an individual of that size will be taken, and r the steepness of the selectivity pattern, the fishing selectivity per size class $s(L)$ is given by

$$s(L) = \frac{1}{1 + \exp(-r(L - L_f))} \quad (1)$$

and adult annual survival is

$$\sigma(L) = \exp(-\mu_A - Fs(L)). \quad (2)$$

Population dynamics

The number of larvae that enter the population is determined by larval survival and the total production of fertilized eggs $P(t)$, which is determined by total fecundity and fertility within each mating site as described below. Larval survival is assumed to have both density-independent and density-dependent components (e.g., Cowen et al., 2000; Sale, 2002), and we use a Beverton-Holt recruitment function (Quinn and Deriso, 1999; Jennings et al., 2001) to calculate larval survival. The number of larvae surviving to recruit in any year t , $N_0(t)$, is given by

$$N_0(t) = (\alpha P(t)) / (1 + \beta P(t))$$

$$\text{if } (\alpha P(t)) / (1 + \beta P(t)) + \sum_{n=1} N_n(t) \leq N_{\max} \quad (3)$$

$$N_0(t) = \max\left(0, N_{\max} - \sum_{n=1} N_n(t)\right)$$

$$\text{if } (\alpha P(t)) / (1 + \beta P(t)) + \sum_{n=1} N_n(t) > N_{\max},$$

where α gives density-independent survival, β determines the strength of the density-dependence in the larval phase, and N_{\max} represents the maximum population size. We assume that the population is open between mating sites, a single larval pool exists, larval recruitment is random among mating sites, and there is no emigration to or immigration from outside populations.

Growth dynamics

Larvae that survive to recruit begin at size L_0 and growth is assumed to be deterministic and independent of sex or reproductive status. We calculate growth between age classes using a discrete time version of the von Bertalanffy growth equation (Beverton, 1987, 1992) where L_{inf} represents the asymptotic size and k is the growth rate. Then an individual of length $L(t)$ at time t will grow in the next time period to size $L(t+1)$:

$$L(t+1) = L_{\text{inf}}(1 - \exp(-k)) + L(t)\exp(-k). \quad (4)$$

Mating system

As in our previous model, we assume that reproduction occurs at the level of the mating group, and we examine the effect of varying mating group size and the number of mating sites. Juveniles and adults are assumed to exhibit site fidelity and larvae settle randomly among mating sites. The carrying capacity of the population is split equally among the mating sites and the total capacity of all mating sites exceeds the maximum population size in the absence of fishing as determined by

adult mortality and the recruitment function. As before (Alonzo and Mangel, 2004), we examine the following three cases: 1) the entire population mates at one site (1 mating site with up to 1000 individuals); 2) a few large mating groups exist (10 sites with a maximum of 100 individuals per site); and 3) many small mating aggregations exist (20 mating sites with a maximum of 50 individuals per site). We assume that within a mating site, individuals mate in proportion to their fertility and fecundity and that males that are large enough to change sex have a chance of reproducing that is proportional to their fertility and thus a large male reproductive advantage exists. This is equivalent to assuming that females exhibit a mate choice threshold (Janetos, 1980) that has evolved with the size at pattern of sex change and that male fertilization success is proportional to fertility.

Reproduction

We assume female fecundity $E(L)$ and male sperm production $S(L)$ can be represented by the allometric relationships $E(L)=aL^b$ and $S(L)=cL^b$ respectively where a , b and c are constants. We assume that at any body length males produce 1000 times more sperm than females produce eggs. This leads to the realistic pattern that (in the absence of fishing) fertilization rates are high and that multiple males are needed to fertilize all the eggs produced by females. We calculate the average expected fertilization rate per mating site based on the total production of sperm and eggs at the site, where S represents the number of sperm released (in millions) and E the number of eggs released at each mating site. The proportion of eggs fertilized per mating site p_F is given by

$$p_F = \frac{S}{1+(\kappa E + \chi)S}, \quad (5)$$

where κ and χ are constants fitted to data. The proportion of eggs fertilized (p_F) depends on both total sperm production (S) and egg production (E). If sperm production is very high in relation to egg production, fertilization rates will be at or near 100%. However, if total sperm production (S) decreases and egg production remains the same, fertilization rates will decrease. Similarly, as egg production (E) increases in relation to total sperm production (S) fertilization rates will decrease (see Fig. 2, Alonzo and Mangel, 2004). The number of eggs fertilized per group is $p_F E$ and the total production of fertilized eggs $P(t)$ is the sum of the number of eggs fertilized in all mating groups. For more details on the fertilization function and individual sperm production see Alonzo and Mangel (2004).

Patterns of sex change

We examine four possible patterns of sex change, determined by absolute or relative size of the individual. Although a variety of other possibilities exist, these

examples represent four plausible patterns that differ in the cues or mechanisms that induce sex change, the degree of compensation or plasticity assumed, and encompass the diversity that has been observed and hypothesized for a variety of sex-changing fish populations (Helfman, 1997).

Rule 1: Fixed For the first sex-change rule, we assume that the probability of sex change $p_C(L)$ is determined by the absolute length of the individual and is

$$p_C(L) = \frac{1}{1 + \exp(-\rho^a(L - L_C))}, \quad (6)$$

where L_C represents the size at which 50% of mature females change sex and ρ is a constant that determines the steepness of the probability function. With this sex change rule, we also assume that the probability an individual matures $p_M(L)$ is determined by absolute size. Once an individual matures, she remains female until sex change. L_M represents the length at which 50% of juveniles are expected to mature.

$$p_M(L) = \frac{1}{1 + \exp(-q(L - L_M))}, \quad (7)$$

where q determines the steepness of the probability function and where $L_C > L_M$.

Rule 2: Relative size For the second sex change rule, the mean size of all individuals in the mating group determines the probability of sex change for an individual. First, we find the mean size of all individuals at each mating site. We let L_i represent the mean size in the mating site i . Then the probability of sex change for an individual of length L is

$$p_i(L) = \frac{1}{1 + \exp(-\rho(L - (L_i + \Delta L_C)))}, \quad (8)$$

where ΔL_C represents the difference from the mean at which the probability of sex change is 0.5. For these analyses, we also assumed that the probability an individual matures also depends on the mean size of individuals at the mating site. Then the probability of maturity is

$$p_M(L) = \frac{1}{1 + \exp(-q(L - (L_i + \Delta L_M)))}, \quad (9)$$

where ΔL_M represents the difference from the population mean at which the probability an individual will mature is 0.5.

Rule 3: Relative frequency Sex change may also be induced by the social conditions at the mating site. For example, sex change may depend on the frequency of

other mature individuals or the frequency of smaller individuals. We examine the case where sex change depends on the frequency of smaller mature individuals. For each mature female, we find the frequency of mature individuals at the same mating site that are smaller. We let F_i represent the frequency of mature individuals that are smaller than the mature female and F_c represents the frequency at which 50% of the individuals are expected to change sex. Then the probability of sex change is

$$p_c(L) = \frac{1}{1 + \exp(-\rho(F_i - F_c))} \quad (10)$$

The probability of maturing depends on the frequency of smaller individuals. We let f_i represent the frequency of all smaller individuals at mating site i and f_M represent the frequency at which there is a 50% probability of an individual maturing. Then the probability of maturing is

$$p_M(L) = \frac{1}{1 + \exp(-q(f_i - f_M))} \quad (11)$$

Rule 4: Reproductive success Finally, we consider the case where sex change occurs when an individual's size-dependent expected reproductive success is greater as a male than as a female (Charnov, 1982). This pattern of sex change has been proposed to explain the observation that individual variation exists in size at sex change and that it is not always the largest individual in a group that changes sex (Munoz and Warner, 2003). We assume that a fish will change sex when its expected egg production at its current length ($E(L) = aL^b$ as given above) is exceeded by its expected paternity at the mating site which is given by the total egg production of all other females at the site multiplied by the focal individual's relative sperm production. This value is given by expected fertility $S(L)$ divided by the total sperm production (by all males at the site plus their own expected fertility) at the same mating site. We further assume that sex change occurs once a year in rank order from the largest to smallest female at the site. (For this scenario we assumed that the probability of maturing depends on absolute size as in Equation 7.) However, we still assume that individuals can only change sex once during their lifetime and only mature females can change sex. Thus, mature females change sex when their current expected fertilization success as a male is greater than their current expected fecundity as a female.

Measures of spawning stock biomass per recruit

We examine the same spawning-per-recruit measures as in our previous paper (Alonzo and Mangel, 2004) and compare the results of the patterns of sex change considered here with one another and with a hypothetical dioecious species, where sex is determined stochastically

at birth and the primary sex ratio is fixed. We compute the total spawning stock biomass per recruit starting from the beginning of fishing for the next 50 years. We use the generally recognized pattern that fish wet weight tends to be approximately proportional to the cube of fish length (Gunderson, 1997) to convert fish length, L , into relative biomass, $B(L) \sim L^3$. Then we calculate total, female, and male spawning stock biomass per recruit (SSBR). We also keep track of the total fecundity (egg production per recruit), fertility (sperm production per recruit), and eggs fertilized per recruit.

Parameter values

We use parameters based on previous research (Warner, 1975; Cowen, 1985; Cowen, 1990) on California sheephead (*Labridae*, *Semicossyphus pulcher*), a commercially important sex-changing fish, to provide evolutionarily and ecologically reasonable parameters for the model. Although the growth, survival, and reproduction of this species have been studied, less is known about the factors that induce sex change and mating behavior. In this species, sex change occurs at approximately 30 cm, although the exact pattern varies among populations (Warner, 1975; Cowen, 1990). It is not known whether sex change is fixed or socially mediated. For the first sex-change rule, we assume that individuals have a 50% chance of maturing (L_m) at 20 cm (the mean size of maturity observed in natural populations) and of changing sex at (L_c) 30 cm. This leads to a sex ratio of 2/3 mature females to 1/3 males on average and a mean length of 20 cm in the absence of fishing as is observed in the wild. For consistency, we also assume for the second sex-change rule, that individuals have a 50% chance of changing sex at 10cm ($\Delta L_c = 10$) above the mean size and have a 50% chance of maturing at the mean size in the mating site ($\Delta L_m = 0$). Similarly, for the third rule, the frequency of smaller mature individuals at which there is a 50% of sex change is assumed to be 0.67 and when 50% of all individuals are smaller, an individual will have a 0.5 probability of maturing. Therefore in the absence of fishing all four sex change rules lead to the same maturity and sex-change patterns as a function of age and size. For more information on the parameter values considered here, see Table 1.

Individual-based simulations are computationally very intensive. As a result, it was not feasible to explore a wide range of values for all parameters. Furthermore, because growth, mortality, reproduction, maturity, and sex change are coevolved characters within any species, it does not make sense in this context to vary them independently. Instead, we used estimates from California sheephead for as many parameters as possible (mortality, growth, fecundity, size at maturity, and sex change) and when necessary from a closely related species (fertilization rate). We then focused on exploring the effect, for this species, of varying the sex-change rule and fishing pattern while all other parameters remained the same. Our focus was on determining the impact of the sex change rule on the predicted stock

Table 1

The parameter values used in the model were based on available data for California sheephead (*Semicossyphus pulcher*). See text for details.

Parameter	Parameter values	Definition and source
Growth		
k	0.05	Growth rate (based on Cowen, 1990)
L_{inf}	90 cm	Asymptotic size (based on Cowen, 1990)
L_0	8 cm	Larval size at recruitment
Population		
N_{max}	1000	Maximum population size
μ_A	0.35	Adult mortality (based on Cowen, 1990)
α	0.0001	Density-independent larval mortality
β	$\alpha / (1 - \exp(-\mu_A)) N_{\text{max}}$ (3.33×10^{-7})	Larval recruitment function parameter (see text)
Fishing		
r	1 (0.1)	Steepness of selectivity curve
L_f	30 (25, 35)	Length at which 50% chance a fish will be removed
F	0-3	Fishing mortality
Reproduction		
a	7.04	Constant in the fecundity relationship (Warner, 1975)
b	2.95	Exponent in the allometric relationship (Warner, 1975)
c	$10^{-3}a$	Constant in the sperm production function (measured in millions of sperm)
x	0.000003	Slope of fertilization function parameter
z	0.09	Intercept of fertilization function parameter (based on Peterson et al., 2001) see text for details
Rule 1		
L_c	30 cm	Length at which 50% of fish change sex
ρ	1	Shape parameter in the sex-change function
L_m	20 cm	Length at which 50% of fish mature
q	1	Shape parameter in the maturity function
Rule 2		
ΔL_c	10 cm	Difference from the mean size at which $p_c(L) = 0.5$
ρ	1	Shape parameter in the sex-change function
ΔL_m	0 cm	Difference from the mean size at which $p_M(L) = 0.5$
q	1	Shape parameter in the maturity function
Rule 3		
F_c	0.67	Frequency of smaller mature individuals where $p_c(L) = 0.5$
ρ	50	Shape parameter in the sex-change function
F_m	0.50	Frequency of smaller individuals at which $p_M(L) = 0.5$
q	50	Shape parameter in the maturity function
Rule 4		
		No additional parameters required

dynamics rather than on exploring all possible parameter combinations. However, it would certainly be useful in the future to examine the same question using parameter estimates based on other commercially exploited species that change sex.

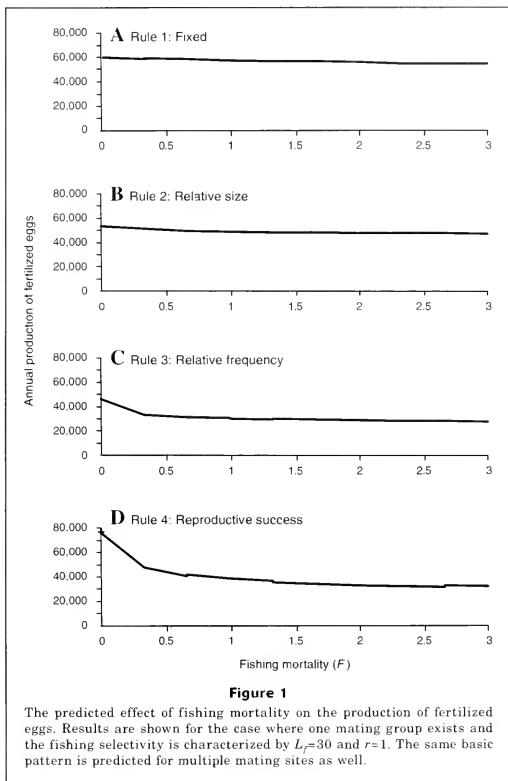
Results

We present the average across simulations of the mean population measures of the last 50 years for each simulation. The variation around the mean in all measures considered is hundredths of a percent of the mean or less. For the spawning-per-recruit (SPR) measures we give the mean value across the first 50 years of fishing

to ensure that the entire cohort under consideration had died before the end of the simulation. Parameter values used are given in Table 1

General dynamics

In all cases, size-selective fishing is predicted to decrease population size and decrease the mean length of fish in the population. Although all scenarios are predicted to lead to the same change in average fish length, the effect of fishing on predicted population size and the mechanisms leading to changes in population size differ between the four sex-change rules (Figs. 1 and 2, Table 2). The largest differences occur between the fixed rule and the three plastic patterns of sex change. How-

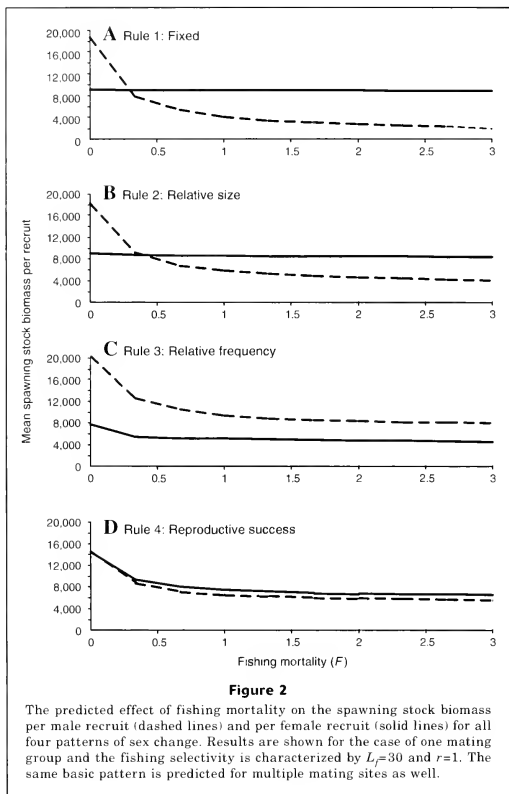


ever, the exact pattern of sex change has an important and qualitative effect on the predicted stock dynamics (Table 2). All three plastic patterns of sex change are predicted to show lower sperm limitation and higher fertilization rates in the presence of fishing than the fixed pattern of sex change (Table 2). However, associated with plastic sex change is also a greater predicted drop in egg production (total and fertilized) and mean population size than when the effect of size on the probability of sex change is fixed (Fig. 1, Table 2). This drop in egg production and mean population size occurs because female biomass is predicted to decrease as a result of the combination of fishing on larger individuals and smaller

sizes at sex change (Fig. 2). The basic patterns are the same for the case with multiple mating sites. Most of the significant reductions in stock size are predicted at high fishing mortality. However, it is important to remember that we have assumed that the stock is very resilient (Table 1), and our focus is on the differences among sex-change rules and fishing patterns rather than on absolute fishing mortality.

The effect of mating group size

Although mating group size is predicted to have an effect in most cases on the stock dynamics of the population,



the strongest effect is predicted when size at sex change is fixed or determined by the frequency of small fish in the population (Fig. 3, A and C). When the size at sex change is fixed, populations are predicted to crash when mating sites are very small (Fig. 3A). In the case where size at sex change is determined by expected reproductive success, group size is predicted to have no effect on the relative production of eggs and mean population size (Fig. 3D). However, for all the other rules of sex change considered, smaller mating sites are predicted to experience sperm limitation in the presence of fishing, leading to a decrease in the relative production of fertilized

eggs and a decrease in mean population size (Fig. 3). However, unlike in the case of fixed size at sex change, the smaller mating groups (20 mating sites with up to 50 individuals per site) are stable both in the presence and absence of fishing and are not predicted to collapse for most fishing patterns.

Sensitivity to fishing pattern

Rule 1 The size-selective pattern of the fishery has a large effect on the predicted stock dynamics when the size at sex change is fixed. When the selectivity of the

Table 2

A comparison of stock dynamics for four sex-change rules. Results are reported for the situation where the fishing selectivity pattern and the probability of sex change are both centered at the same size ($L_f=30$). These results assume a near knife-edge selectivity ($r=1$) and that one mating site exists. Numbers given are for the predicted relative change as a result of fishing (when $F=3$ compared to $F=0$). SSBR = spawning stock biomass per recruit.

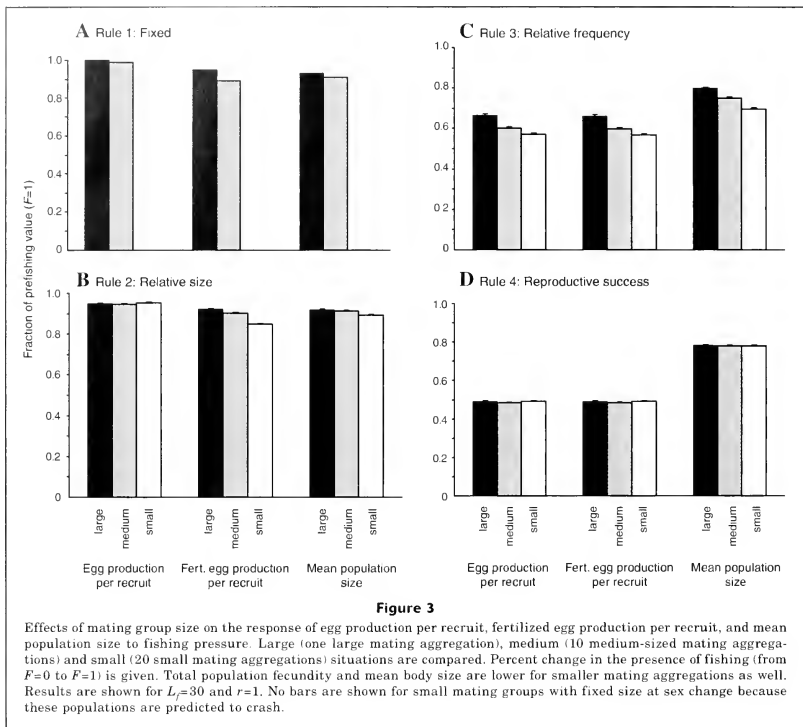
	Rule 1: Fixed	Rule 2: Relative size	Rule 3: Relative frequency	Rule 4: Reproductive success
Mean population size	90%	90%	73%	72%
Total SSBR	40%	45%	44%	39%
Male SSBR	11%	22%	39%	39%
Female SSBR	98%	92%	58%	39%
Sex ratio	0.67 → 0.92	0.67 → 0.84	No change	0.8 → 0.66
Mean size	88%	88%	88%	88%
Sperm production	11%	23%	40%	40%
Egg production	98%	93%	59%	41%
Fertilized egg production	88%	86%	59%	41%

fishery is centered below the mean size at sex change ($L_f=25$, $r=1$), the stock was predicted to crash at high fishing mortality ($F \geq 1$, Fig. 4A). Furthermore, when the selectivity pattern was not steep ($L_f=30$, $r=0.1$), the population was always predicted to crash even at low fishing mortality (and thus this case is not shown in Figs. 4A–6A). When the steepness of the fishery's selectivity changes, the size range over which fish are targeted also changes. Thus, smaller and younger fish are removed by the fishery when $r=0.1$ and hence a greater number of age classes are affected by fishing. At an extreme, fishing mortality could be high enough that all of the individuals in any size classes targeted by the fishery are removed. As a result, although the steepness of the selectivity function only affects the spread of the function mathematically, it has the biological effect of decreasing the size at which fish experience fishing mortality and can have a large effect on the size and age distribution of the population. In contrast, when the fishery's selectivity is steep ($r=1$) and only fish at or above the mean size at sex change ($L_f \geq 30$) are targeted, the effect of fishing on the population is predicted to be much less (Fig. 4A). Independent of the selectivity pattern, the population sex ratio is predicted to be more female-biased in the presence of fishing than in the absence of fishing. The lower the mean size removed by the fishery, the greater the predicted change in population sex ratio as a result of fishing (Fig. 5A). For situations in which the stock is not predicted to crash (i.e., $L_f \geq 30$ and $r=1$), yield is predicted to increase with diminishing returns with fishing mortality (Fig. 6A), catch is not predicted to decline with increased fishing mortality (at least up to $F=3$), and steep size-selective fishing patterns with lower size thresholds are predicted to lead to more yield (Fig. 6A).

Rule 2 When sex change is determined by the mean size of individuals in the mating site and the size-selectivity

is weak ($r=0.1$), the population is predicted to crash when $F \geq 1.67$ (Fig. 4B). This crash occurs because individuals do not escape fishing mortality even at small sizes. However, unlike when sex change is fixed (Fig. 4A), the population is predicted not to crash when the size selected by the fishery is less than the mean size at sex change in the absence of fishing ($L_f=25$, Fig. 4B). The larger the mean size selected by the fishery, the smaller the predicted effect of fishing on the mean population size and the population sex ratio (Figs. 4B and 5B). Although catch is predicted to increase with diminishing returns as fishing mortality increases from zero to three, the difference between the size-selectivity patterns is predicted to decrease and yield will be greater annually if larger fish are targeted (Fig. 6B).

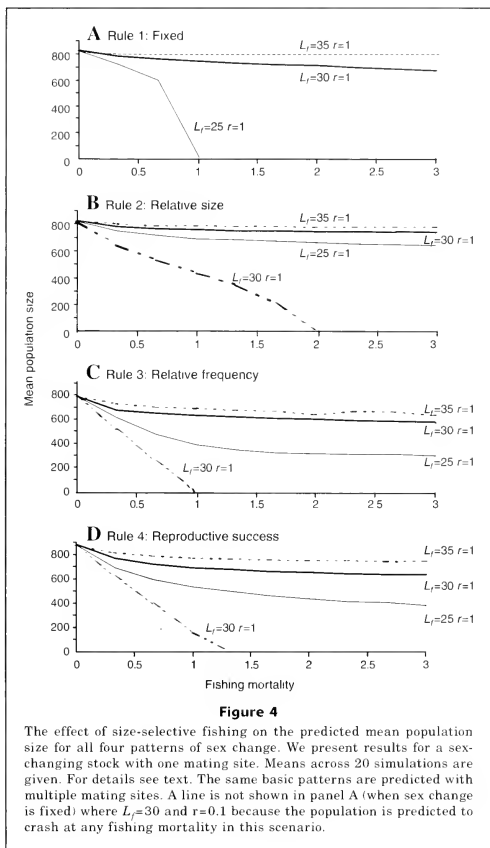
Rule 3 As above, when the probability of sex change depends on the relative frequency of smaller mature individuals, the population is predicted to crash whenever size-selectivity is weak because fish do not escape fishing even when small ($r=0.1$, Fig. 4C). Although the population is predicted not to crash when the size targeted by the fishery is less than the mean size at sex change in the absence of fishing ($L_f=25$, Fig. 4C), this fishing pattern is predicted to lead to a large decrease in mean population size and a marked decrease in population sex ratio (Figs. 4C and 5C). In contrast fishing selectivity that is centered at or above the mean size of sex change in the absence of fishing ($L_f=30$ and $L_f=35$) is predicted to lead to a weaker effect on mean population size and to almost no effect on the population sex ratio (Figs. 4C and 5C). However, in contrast to the two scenarios described above this pattern of sex change leads to the prediction that targeting fish at or larger than the normal mean size of sex change ($L_f=30$ and $r=1$) will lead to the greatest annual yield over time for most fishing mortalities (Fig. 6C).



Rule 4 As with all of the other patterns of sex change, populations with sex change based on expected reproductive success are predicted to crash whenever small fish experience fishing mortality ($r=0.1$, Fig. 4D). Furthermore, as with the other two plastic sex change rules, populations are predicted not to crash when fish below the normal mean size at sex change are included in the fishery because the population can compensate with smaller sizes at sex change in the presence of fishing (Fig. 4D). Although only small differences among fishing patterns are predicted in the mean population sex ratio, the effect on the population size is predicted to be greatest when many size classes are fished, and large differences are predicted between the fishing patterns in mean population size (Fig. 5D). Finally, in the scenario of sex change based on expected reproductive success,

the fishing pattern predicted to lead to the greatest catch is to target only fish above the normal mean size at sex change ($L_f=35$, Fig. 6D).

In summary, fishing is always predicted to decrease total production of fertilized eggs and mean population size. However, the strength of the effect depends both on fishing selectivity and the pattern of sex change (see above and Figs. 4–6). Although populations with fixed patterns of sex change are predicted to crash in the presence of fishing below the mean size at sex change, plastic patterns of sex change are predicted to lead to more resilience since these populations can compensate for the removal of large males more effectively. However, all scenarios are predicted to crash in the presence of fishing across a broad range of size classes (when $r=0.1$) even in completely compensatory patterns of sex change.



Yet, the exact response depends greatly on the specific pattern of sex change. For example, the population sex ratio is not predicted to change much in the presence of fishing when sex change is based on expected reproductive success and fishing pattern has little effect on the sex ratio (Fig. 5). However, when sex change is based on expected reproductive success, the annual yield is greater for fishing patterns with larger size thresholds (Fig. 6). In contrast, when sex change is determined by the mean size

of individuals at the mating site, sex ratio is predicted to increase with fishing and increase more when smaller size classes are fished. However, for this pattern of sex change, the smallest size threshold is also predicted to lead to the largest yield of the fishery, although as fishing mortality increases the difference between fishing patterns with differing size thresholds decreases. Therefore, the fishing pattern that will produce optimal yield will depend on the exact pattern of sex change (Fig. 6).

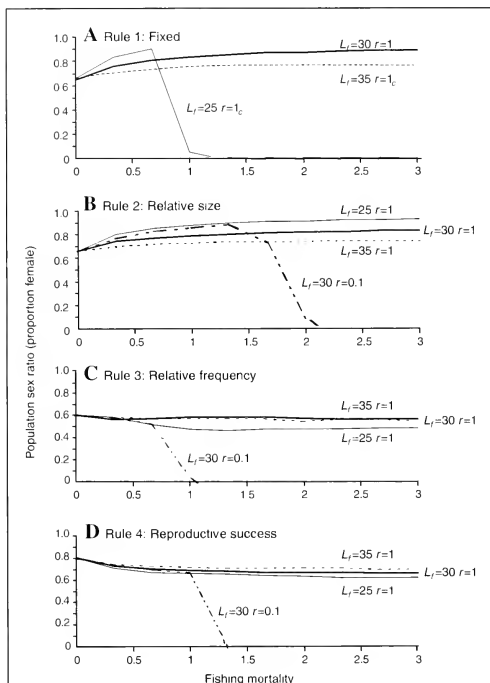


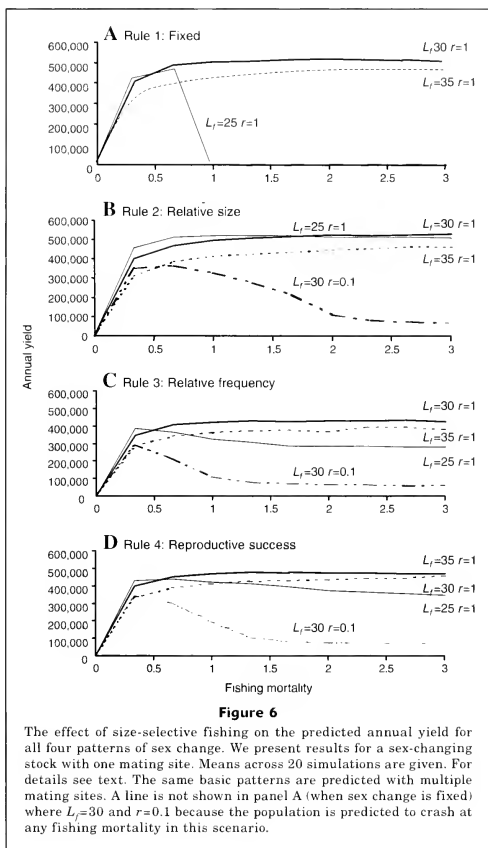
Figure 5

The effect of size-selective fishing on the predicted population sex ratio for all four patterns of sex change. We present results for a sex-changing stock with one mating site. Means across 20 simulations are given. For details see text. The same basic patterns are predicted with multiple mating sites. A line is not shown in panel A (when sex change is fixed) where $L_f=30$ and $r=0.1$ because the population is predicted to crash at any fishing mortality in this scenario.

Spawning-per-recruit (SPR) measures and a comparison of protogynous and dioecious stocks

Our previous results (Alonzo and Mangel, 2004) have shown that whether species change sex or are dioecious is predicted to have dramatic effects on both the stock dynamics and performance of classic SPR measures. However, our results show that the exact pattern of sex change, and not just whether the pattern is plastic

or fixed, can have a strong effect on these measures as well (Fig. 7). Because of the population dynamics of the model, all the scenarios represented in the present study show a great resiliency to fishing. Hence, the predicted changes in stock size are all above the common threshold of allowing a reduction of spawning per recruit measures to 40% of their values in the unfished condition. However, our aim is not determine if this population is overfished. Instead, it is to determine whether classic



spawning per recruit measures based on egg production or fecundity could accurately assess the status of sex-changing stocks. Although the fixed pattern of sex change is predicted to show the greatest difference between egg production per recruit and fertilized eggs produced per recruit, each population shows deviations between egg production and the production of fertilized eggs. Thus egg production alone cannot tell us how the population is being affected by fishing and classic

SPR measures based on population fecundity may be misleading for sex-changing stocks in cases where the sex-change rule is not completely compensatory (rules 1–3). It is also interesting to ask whether consistent differences exist (as has been suggested) in the resiliency of sex-changing stocks, compared to stocks with separate sexes. Our results indicate that sex change based on expected reproductive success is predicted to have very similar dynamics to the dioecious population.

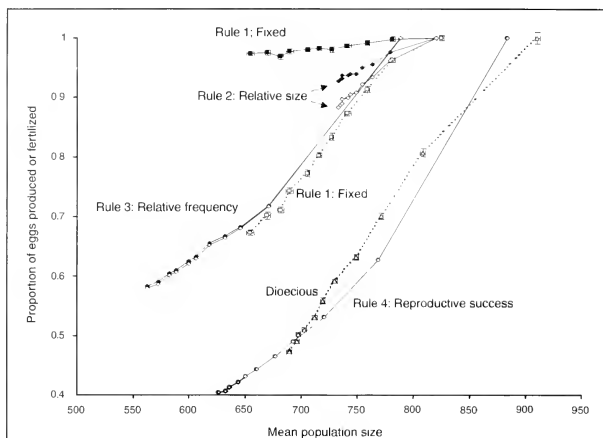


Figure 7

Spawning-per-recruit (SPR) measures for all four patterns of sex change and an otherwise identical dioecious stock: mean egg production per recruit (filled) and mean fertilized eggs per recruit (open) are shown for a population with one large mating group when $L_{\infty}=30$ and $r=1$. The same basic patterns are predicted for multiple mating sites. Each line represents the same range of fishing mortalities, and each point represents fishing mortality increasing from 0 to 3 in increments of $1/3$ moving from the right to the left. For the fourth rule (expected reproductive success), the two lines (eggs produced per recruit and eggs fertilized per recruit) overlap.

whereas sex change based on relative size or the relative frequency of individuals in a mating site is predicted to have similar dynamics to those for the fixed pattern of sex change. Thus, it is not possible to say that sex-changing stocks tend to be more or less resilient to fishing than are dioecious populations. However, the sex change rule clearly affects the predicted relationship between fishing mortality and the response of the stock to fishing.

Discussion

We apply a general approach using individual-based simulation models to determine the predicted effect of the pattern of sex change on the stock dynamics of a protogynous species. Although the model structure and parameter values considered will not apply to all commercially important protogynous species, it is important to realize that all the scenarios considered are identical except for the pattern of sex change. As a result, any predicted differences that arise between these situations are a result of the sex-change rule and indicate

that knowing simply that a species exhibits sex change but not what the behavioral rule of sex change is will lead to an incomplete ability to understand and predict the dynamics of the stock and its response to fishing or management strategies.

Independent of the sex-change rule, the protogynous stocks are always predicted to be sensitive to the size-selective fishing pattern. Mean population size is always predicted to decrease as fishing mortality increases, despite the fact that we have assumed that recruitment is strongly density dependent and that the species is very productive. Stocks are predicted to crash even at low fishing mortality when the size-selective fishing pattern targets all reproductive size classes and for the fixed sex change rule whenever all male sizes are targeted by the fishery. It will be necessary but not sufficient to avoid overfishing at spawning aggregations. Our results indicate that it will also be important to allow smaller and nonreproductive individuals to escape fishing as well. These results indicate that independent of the exact pattern of sex change, management strategies for all protogynous stocks need to be sensitive to the size-selectivity of

the fishing pattern in relation to size at maturity and size at sex change observed in the population, and a failure to do so can lead to a sudden and unexpected collapse of the fishery—a collapse from which it may be difficult to recover.

We assume in all cases that the same cues determine both the probability of maturity and the probability of sex change within a species. For example, when sex change was affected by the relative size of individuals at the mating site, we assume that this same cue affected the probability of maturing. This assumption has a large effect on the predicted dynamics of the stock. Alternatives exist. For example, the size at which fish mature could be determined by endogenous rather than exogenous factors even in a population where the probability of sex change is affected by external cues. If this were the case, the population can easily be fished into a situation where it cannot compensate for size-selective fishing and is predicted to crash for any fishing pattern that targets reproductive individuals. For example, when $L_c=30$ and $r=1$, populations with plastic size at maturity and sex change were not predicted to crash independent of fishing mortality. In contrast, simulations where populations were assumed to have fixed size at maturity rules ($L_m=20$) but plastic patterns of sex change crashed at most fishing mortalities with $L_c=30$ and $r=1$. Hence, knowledge of the cues determining both maturity and sex change will be important in predicting and understanding larval production and the effect of fishing on a population.

It is possible to argue that a protogynous species with fixed patterns of sex change may have very different dynamics than dioecious stocks, but the compensatory patterns of sex change will be less sensitive to fishing and exhibit dynamics very similar to their dioecious counterparts. However, our results indicate that even stocks with plastic patterns of sex change are predicted to have dynamics distinctly different from otherwise identical dioecious populations. For example, sperm limitation is predicted to occur for all sex change rules, except for the pattern where sex change is determined by expected reproductive success (rule 4). However, even a stock exhibiting the reproductive success rule has dynamics that are distinctly different from those of a dioecious species because a change in the size distribution of the population due to size-selective fishing is predicted to have a large effect on the productivity and sex ratio of the protogynous population. Similarly, mating group size is predicted to affect the stock dynamics in all cases except for the reproductive success rule. Therefore, although knowing the pattern of sex change is predicted to be important in understanding stock dynamics, it is also clear that the pattern of sex change must be considered in the context of the mating system of the stock, as well as in the context of the basic biology of the stock.

Protogynous stocks are thus predicted to be sensitive to the fishing pattern, and nonlinear stock dynamics are possible when fishing operations target a wide range of fish sizes. However, each stock is also predicted to

have a unique response to the same fishing pattern (Figs. 4–6) and to have different relationships between traditional spawning-per-recruit measures and changes in mean population size with fishing mortality (Figs. 1, 2, and 7). As a result, monitoring changes in spawning stock biomass per recruit or egg production per recruit alone will not make it possible to determine the relationship between these measures and mean population size or to know whether the population is at risk for large and sudden declines in population size. Our results indicate that although it is important to know whether sex change occurs when managing a stock, it will also be important to know what endogenous or exogenous cues induce sex change and how behavioral patterns and life history strategies affect the demographic rates of the stock.

Plasticity is not predicted to yield populations that have stock dynamics that are identical to those of dioecious species, and the performance of spawning-per-recruit measures and the relationship between egg production and population size differed greatly between all four patterns of sex change, despite the fact that the basic patterns of growth, survival, and fecundity were identical between all the scenarios considered. Because sperm limitation is more common with the fixed and relative size rules of sex change, these situations are predicted to have the greatest difference between classic SPR measures and the production of fertilized eggs. Clearly it is not just whether a population changes sex or not, but also how sex change is induced, that determines the population's predicted response to fishing and the performance of spawning-per-recruit measures in predicting and indicating the effect of fishing on the population.

Although it is important to know what life history strategy and behavioral patterns are observed in a species, these alone will not always be sufficient to predict expected changes in population size and productivity under new conditions. Instead, knowledge of the plasticity of behavioral and life history patterns, as well as information about the internal and external cues that induce phenotypic changes, may also be necessary. Phenotypic plasticity is often expressed as a threshold response (such as sex change) to a continuous endogenous or exogenous cue. Therefore, as predicted by our model, plasticity can generate nonlinear changes in important demographic characters. An understanding of the natural variation in behavior and life history combined with knowledge of fish vital rates and environmental conditions will lead to a better understanding of and ability to predict the response of a stock to fishing mortality, environmental changes, and specific management strategies.

Acknowledgments

This research was supported by National Science Foundation grant IBN-0110506 to Suzanne Alonzo and the Center for Stock Assessment Research (CSTAR).

Literature cited

- Alonzo, S. H., and M. Mangel.
2004. Size-selective fisheries, sperm limitation and spawning per recruit in sex changing fish. *Fish. Bull.* 102:1-13.
- Apostolaki, P., E. J. Milner-Gulland, M. K. McAllister, and G. P. Kirkwood.
2002. Modelling the effects of establishing a marine reserve for mobile fish species. *Can. J. Fish. Aquat. Sci.* 59:405-415.
- Armsworth, P. R.
2001. Effects of fishing on a protogynous hermaphrodite. *Can. J. Fish. Aquat. Sci.* 58:568-578.
- Bannerot, S., W. F. Fox, and J. E. Powers.
1987. Reproductive strategies and the management of snappers and groupers in the gulf of Mexico and Caribbean. In *Tropical snappers and groupers: biology and fisheries management*. (J. J. Polovina and S. Ralston, eds.), p. 561-603. Westview Press, Boulder, CO.
- Beets, J., and A. Friedlander.
1999. Evaluation of a conservation strategy: a spawning aggregation closure for red hind, *Epinephelus guttatus*, in the U.S. Virgin Islands. *Environ. Biol. Fish.* 55:91-98.
- Beverton, R. J. H.
1987. Longevity in fish: some ecological and evolutionary considerations. In *Evolution of longevity in animals*. (A. D. Woodhead and K.H. Thompson, eds.) p. 161-185. Plenum Press, New York, NY.
- Beverton, R. J. H.
1992. Patterns of reproductive strategy parameters in some marine teleost fishes. *J. Fish Biol.* 41 (Suppl. B) 41:137-160.
- Breden, F., D. Novinger, and A. Schubert.
1995. The effect of experience on mate choice in the Trinidad guppy, *Poecilia reticulata*. *Environ. Biol. Fish.* 42:323-328.
- Brule, T., C. Deniel, T. Colas-Marrufo, and M. Sanchez-Crespo.
1999. Red grouper reproduction in the southern Gulf of Mexico. *Trans. Am. Fish. Soc.* 128:385-402.
- Charnov, E. L.
1982. The theory of sex allocation, 355 p. Princeton Univ. Press, Princeton, NJ.
1986. Size advantage may not always favor sex change. *J. Theor. Biol.* 119:283-285.
- Charnov, E. L., and J. J. Bull.
1989. Non-Fisherian sex ratios with sex change and environmental sex determination. *Nature* 338:148-150.
- Coleman, F. C., A. Eklund, and C. B. Grimes.
1999. Management and conservation of temperate reef fishes in the grouper-snapper complex of the southeastern United States. *Am. Fish. Soc. Sym.* 23:233-242.
- Coleman, F. C., C. C. Koenig, and L. A. Collins.
1996. Reproductive styles of shallow-water groupers (Pisces: Serranidae) in the eastern Gulf of Mexico and the consequences of fishing spawning aggregations. *Environ. Biol. Fish.* 47:129-141.
- Collins, L. A., A. G. Johnson, and C. P. Keim.
1996. Spawning and annual fecundity of the red snapper (*Lutjanus campechanus*) from the northeastern Gulf of Mexico. In *Biology, fisheries, and culture of tropical groupers and snappers* (F. Arreguin-Sanchez, J. L. Munro, M. C. Balgos, and D. Pauly, eds.) p. 174-188. ICLARM (International Center for Living Aquatic Resources Management) conference proceedings 48, ICLARM, Makati City, Philippines.
- Constable, A. J., W. K. de la Mare, D. J. Agnew, I. Everson, and D. Miller.
2000. Managing fisheries to conserve the Antarctic marine ecosystem: practical implementation of the convention on the conservation of Antarctic marine living resources (CCAMLR). *ICES J. Mar. Sci.* 57:778-791.
- Cowen, R. K.
1985. Large-scale pattern of recruitment by the labrid, *Semicossyphus pulcher*: causes and implications. *J. Mar. Res.* 43:719-742.
1990. Sex change and life history patterns of the labrid, *Semicossyphus pulcher*, across an environmental gradient. *Copeia* 1990:787-795.
- Cowen, R. K., K. M. M. Lwiza, S. Sponaugle, C. B. Paris, and D. B. Olson.
2000. Connectivity of marine populations: open or closed? *Science* 287:857-859.
- Fu, C., T. J. Quinn, II, and T. C. Shirley.
2001. The role of sex change, growth and mortality in *Pandalus* population dynamics and management. *ICES J. Mar. Sci.* 58:607-621.
- Fulton, E., D. Kault, B. Mapstone, and M. Sheaves.
1999. Spawning season influences on commercial catch rates: computer simulations and *Plectropomus leopardus*, a case in point. *Can. J. Fish. Aquat. Sci.* 56:1096-1108.
- Greene, C., J. Umbanhowar, M. Mangel, and T. Caro.
1998. Animal breeding systems, hunter selectivity, and consumptive use in wildlife conservation. In *Behavioral ecology and conservation biology* (T. Caro, ed.) p. 271-305. Oxford Univ. Press, New York, NY.
- Gunderson, D. R.
1997. Trade-off between reproductive effort and adult survival in oviparous and viviparous fishes. *Can. J. Fish. Aquat. Sci.* 54:990-998.
- Haddon, M.
2001. Modelling and quantitative methods in fisheries, 406 p. Chapman and Hall, Boca Raton, FL.
- Helfman, G. S.
1997. The diversity of fishes, 528 p. Blackwell Science, Malden, MA.
- Huntsman, G. R., and W. E. Schaaf.
1994. Simulation of the impact of fishing on reproduction of a protogynous grouper, the grayshy. *No. Am. J. Fish. Manag.* 14:41-52.
- Iwasa, Y.
1990. Sex change evolution and cost of reproduction. *Behav. Ecol.* 2:56-68.
- Janetos, A. C.
1980. Strategies of female mate choice: a theoretical analysis. *Behav. Ecol. Sociobiol.* 7:107-112.
- Jennings, S., M. J. Kaiser, and J. D. Reynolds.
2001. *Marine fisheries ecology*, 417 p. Blackwell Science, Oxford, UK.
- Koeller, P., R. Mohn, and M. Etter.
2000. Density dependant sex change in northern shrimp, *Pandalus borealis*, on the Scotian Shelf. *J. No. Atl. Fish. Sci.* 27:107-118.
- Kruuk, L. E. B., T. H. Clutton-Brock, S. D. Albon, J. M. Pemberton, and F. E. Guinness.
1999. Population density affects sex ratio variation in red deer. *Nature* 399:459-461.

- Kuwamura, T., and Y. Nakashima.
1998. New aspects of sex change among reef fishes: Recent studies in Japan. *Environ. Biol. Fish.* 52:125-135.
- Levin, P. F., and C. B. Grimes.
2002. Reef fish ecology and grouper conservation and management. In *Coral reef fishes: dynamics and diversity in a complex ecosystem* (P. F. Sale, ed.), p. 377-390. Academic Press, Amsterdam, The Netherlands.
- Lutnesky, M. M. F.
1994. Density-dependent protogynous sex change in territorial-harem fishes: models and evidence. *Behav. Ecol.* 5:375-383.
1996. Size-dependent rate of protogynous sex change in the pomacanthid angelfish, *Centropyge potteri*. *Copeia* 1996:209-212.
- Metcalfe, N. B., F. A. Huntingford, W. D. Graham, and J. E. Thorpe.
1989. Early social status and the development of life-history strategies in Atlantic salmon. *Proc. Roy. Soc. Lond. B* 236:7-19.
- Mittelbach, G. G., C. W. Osenberg, and P. C. Wainwright.
1992. Variation in resource abundance affects diet and feeding morphology in the pumpkinseed sunfish (*Lepomis gibbosus*). *Oecologia* 90:8-13.
- Munoz, R. C., and R. R. Warner.
2003. A new version of the size-advantage hypothesis for sex change: Incorporating sperm competition and size-fecundity skew. *Am. Naturalist* 161:749-761.
- Nakashima, Y., Y. Sakai, K. Karino, and T. Kuwamura.
2000. Female-female spawning and sex change in a harem coral-reef fish, *Labroides dimidiatus*. *Zool. Sci.* 17:967-970.
- Nishibori, M., and M. Kawata.
1993. The effect of visual density on the fecundity of the guppy, *Poecilia reticulata*. *Environ. Biol. Fish.* 37:213-217.
- Petersen, C. W., R. R. Warner, D. Y. Shapiro, and A. Marconato.
2001. Components of fertilization success in the bluehead wrasse, *Thalassoma bifasciatum*. *Behav. Ecol.* 12:237-245.
- Punt, A. E., P. A. Garratt, and A. Govender.
1993. On an approach for applying per-recruit measures to a protogynous hermaphrodite, with an illustration for the slinger *Chrysoblephus puniceus* (Pisces: Sparidae). *S. Afr. J. Mar. Sci.* 13:109-119.
- Quinn, T. J., and R. B. Deriso.
1999. Quantitative fish dynamics, 542 p. Oxford Univ. Press, New York, NY.
- Ridgeway, M. S., and B. J. Shuter.
1994. The effects of supplemental food on reproduction in parental male smallmouth bass. *Environ. Biol. Fish.* 39:201-207.
- Sale, P. F.
2002. The science we need to develop more effective management. In *Coral reef fishes: dynamics and diversity in a complex ecosystem* (P. F. Sale, ed.), p. 361-376. Academic Press, Amsterdam, The Netherlands.
- Schultz, E. T., and R. R. Warner.
1991. Phenotypic plasticity in life-history traits of female *Thalassoma bifasciatum* (Pisces: Labridae): 2. Correlation of fecundity and growth rate in comparative studies. *Environ. Biol. Fish.* 30:333-344.
- Shapiro, D. Y.
1987. Reproduction in groupers. In *Tropical snappers and groupers: biology and fisheries management* (J. J. Polovina and S. Ralston, eds.), p. 295-328. Westview Press, Boulder, CO.
- Snyder, R. J., and H. Dingle.
1990. Effects of freshwater and marine overwintering environments on life histories of threespine sticklebacks: evidence for adaptive variation between anadromous and resident freshwater populations. *Oecologia* 84:386-390.
- Sutherland, W. J.
1990. Evolution and fisheries. *Nature* 344:814-815.
1998. The importance of behavioural studies in conservation biology. *Anim. Behav.* 56:801-809.
- Wainwright, P. C., C. W. Osenberg, and G. G. Mittelbach.
1991. Trophic polymorphism in the pumpkinseed sunfish (*Lepomis gibbosus* Linnaeus): effects of environment on ontogeny. *Funct. Ecol.* 5:40-55.
- Warner, R. R.
1975. The reproductive biology of the protogynous hermaphrodite *Pimelometopon pulchrum* (Pisces: Labridae). *Fish. Bull.* 73:262-283.
Warner, R. R., and P. Lejeune.
1985. Sex change limited by paternal care: A test using four Mediterranean labrid fishes, genus *Symphodus*. *Mar. Biol.* 87:89-100.
- Warner, R. R., and S. E. Swearer.
1991. Social control of sex change in the bluehead wrasse, *Thalassoma bifasciatum* (Pisces: Labridae). *Biol. Bull.* 181:199-204.

Abstract—The growth rate of Steller sea lion (*Eumetopias jubatus*) pups was studied in southeast Alaska, the Gulf of Alaska, and the Aleutian Islands during the first six weeks after birth. The Steller sea lion population is currently stable in southeast Alaska but is declining in the Aleutian Islands and parts of the Gulf of Alaska. Male pups (22.6 kg [± 2.21 SD]) were significantly heavier than female pups (19.6 kg [± 1.80 SD]) at 1–5 days of age, but there were no significant differences among rookeries. Male and female pups grew (in mass, standard length, and axillary girth) at the same rate. Body mass and standard length increased at a faster rate for pups in the Aleutian Islands and the western Gulf of Alaska (0.45–0.48 kg/day and 0.47–0.53 cm/day, respectively) than in southeast Alaska (0.23 kg/day and 0.20 cm/day). Additionally, axillary girth increased at a faster rate for pups in the Aleutian Islands (0.59 cm/day) than for pups in southeast Alaska (0.25 cm/day). Our results indicate a greater maternal investment in male pups during gestation, but not during early lactation. Although differences in pup growth rate occurred among rookeries, there was no evidence that female sea lions and their pups were nutritionally stressed in the area of population decline.

Neonatal growth of Steller sea lion (*Eumetopias jubatus*) pups in Alaska

Elisif A. A. Brandon

Department of Marine Biology
Texas A&M University at Galveston
5007 Avenue U
Galveston, Texas 77551
Present address: 97A Lowell Ave.
Newton, Massachusetts 02460

Donald G. Calkins

Alaska SeaLife Center
P.O. Box 1329
Seward, Alaska 99664

Thomas R. Loughlin

National Marine Mammal Laboratory
Alaska Fisheries Science Center, NMFS
7600 Sand Point Way, NE
Seattle, Washington 98115

Randall W. Davis

Department of Marine Biology
Texas A&M University at Galveston
5007 Avenue U
Galveston, Texas 77551
E-mail address (for R. W. Davis, contact author) davisr@tamug.edu

Sea lion (order Carnivora, family Otariidae) pups depend entirely on milk for neonatal growth (Bonner, 1984). Studies of sea lions and fur seals have shown that if a pup does not obtain enough milk from its mother, it will exhibit poor body condition (i.e., reduced lean mass and total lipid mass for a given age or standard length) and a reduced growth rate (Trillmich and Limberger, 1985; Ono et al., 1987). Poor body condition and reduced growth rate, in turn, may have lifelong consequences because neonatal growth is an important factor in determining adult size and survival (Bryden, 1968; Innes et al., 1981; Calambokidis and Gentry, 1985; Albon et al., 1992; Baker and Fowler, 1992; Gaillard et al., 1997; Boltnev et al., 1998; Tveraa et al., 1998; Burns, 1999). Because of their large size, aggressive behavior, sensitivity to disturbance, and the remote location

of their rookeries, less is known about the early growth of Steller sea lions (SSL) than of most other pinniped (seals, sea lions, and walrus) species. Higgins et al. (1988) measured body mass of SSL pups on Año Nuevo Island in California but only reweighed five pups to measure growth rates. Merrick et al. (1995) weighed SSL pups at a number of locations throughout the Gulf of Alaska and the Aleutian Islands but did not reweigh them to assess individual growth rates.

Genetic studies show that there are distinct eastern and western populations of SSL (Bickham et al., 1996, 1998) (Fig. 1). The eastern population comprises animals in California, Oregon, British Columbia, and southeast Alaska. The western population comprises animals in the Gulf of Alaska, the Aleutian Islands, the Bering Sea, the Commander Islands, Kamchatka, and the Kuril Islands. A severe popu-

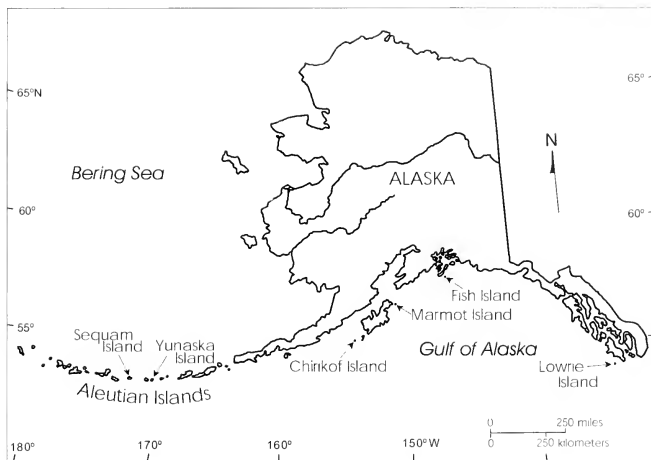


Figure 1

Study sites for Steller sea lions (*Eumetopias jubatus*) in Alaska. The Lowrie Island rookery in southeast Alaska has a stable population but rookeries at Fish, Marmot and Chirikof Islands in the Gulf of Alaska and Yunaska and Sequam Islands in the Aleutian Islands are areas where the population of Steller sea lions has declined.

lation decline (>80%) occurred in the western population between the 1970s and the 1990s. In 1997, these population changes led to the reclassification of the western population from "threatened" to "endangered" and a classification of the eastern population as "threatened" under the Endangered Species Act (U.S. Federal Register 62:24345–24355).

One hypothesis for the decline in population of SSLs is a decrease in food availability or quality in the Gulf of Alaska and the Aleutian Islands (Pascual and Adkison, 1994; York, 1994; Calkins et al., 1999; NMFS^{1,2}). If females are unsuccessful in obtaining sufficient food, pups will develop more slowly or die because of a decrease in milk supply. To examine the potential effects

of food availability on pup development, we measured growth rates of male and female pups from stable and declining populations of SSL in Alaska from 1990 to 1997. Our null hypothesis was that there was no difference in pup growth rates among rookeries in southeast Alaska, the Gulf of Alaska, and the Aleutian Islands. The alternative hypothesis was that pups grew at a faster rate in southeast Alaska, the area of stable population. However, our results showed that pups grew faster in the area of declining population during the first six weeks after birth. In addition, females invested more energy in male pups at all locations during gestation, but not during early lactation.

Materials and methods

Animals and study sites

From 1990 to 1997, SSL pups were studied at locations in southeast Alaska, the Gulf of Alaska, and the Aleutian Islands (Fig. 1 and Table 1). At Lowrie Island (54°51'N, 133°32'W) in southeast Alaska, measurements were made in 1993, 1994, and 1997. The rookery at Lowrie Island is in the area of the stable population (Calkins et al., 1999). In the Gulf of Alaska, measure-

¹ NMFS (National Marine Fisheries Service). 1992. Recovery plan for the Steller sea lion (*Eumetopias jubatus*), 92 p. Prepared by the Steller Sea Lion Recovery Team for the National Marine Fisheries Service, Silver Spring, MD. [Available from the National Marine Mammal Laboratory, 7600 Sandpoint Way, NE, Seattle, Washington 98115.]

² NMFS (National Marine Fisheries Service). 1995. Status review of the United States Steller sea lion (*Eumetopias jubatus*) population, 61 p. Prepared by the National Marine Mammal Laboratory, Alaska Fisheries Science Center. [Available from the National Marine Mammal Laboratory, 7600 Sandpoint Way, NE, Seattle, Washington 98115.]

Table 1

Locations, dates, and the number of Steller sea lion (*Eumetopias jubatus*) pups captured (n).

	Location	Dates	n
Stable population	Lowrie Island (1993)	26 May-5 June	25
		15-19 June	5
		3 July	1
	Lowrie Island (1994)	15-22 June	28
		24-30 June	9
		13-14 July	3
	Lowrie Island (1997)	5-12 June	25
		16-29 June	11
		9-10 June	20
Declining population	Fish Island (1995)	24-26 June	13
		13-14 July	12
		27 June	8
	Marmot Island (1990)	30 June	11
		27 June	21 ¹
	Marmot Island (1991)	15 July	11 ²
		11-17 June	20
	Chirikof Island (1993)	27-28 June	14
		7 July	11
	Yunaska and Seguam Islands (1997)	18 July	4
		8-16 June	16
		22-24 June	12
4 July		5	

¹ Nine known-age pups.² Six known-age pups.

ments were made in 1990, 1991, and 1994 on Marmot Island (58°12'N, 151°50'W), in 1993 on Chirikof Island (55°10'N, 155°8'W) and in 1995 on Fish Island (59°53'N, 147°20'W). On the Aleutian Islands of Seguam (52°30'N, 172°30'W) and Yunaska (52°45'N, 170°45'W), pups were studied in 1997. Data from Seguam and Yunaska Islands were combined because the islands are geographically close and can be considered part of one rookery complex. Rookeries in the Gulf of Alaska and the Aleutian Islands are in the area of declining population, although the rookery on Fish Island has not shown as precipitous a decline. Samples could not be obtained from all rookeries in all years because of logistical constraints and the need to minimize disturbance to rookeries. However, concurrent data were obtained from the declining and stable populations in 1993, 1994, and 1997.

Only pups that had an attached umbilical cord or an unhealed umbilicus were selected for study. The freshness of the umbilical cord was used as a rough estimate of age between 1 and 5 days (Davis and Brandon³).

Choosing only pups with fresh umbilical cords minimized the age bias (Trites, 1993) that occurs when pups are captured at different times and rookeries (Table 1).

Although pups were not selected by sex, sex was noted and used as a factor in analyses. Body mass (BM), standard length (SL), axillary girth (AG) (Am. Soc. Mammalogists, 1967) and body composition were measured for each pup. BM was measured to the nearest kilogram with a mechanical spring scale (Chatillon 160, Ametek, FL) on Marmot Island in 1990 and 1991 and on Lowrie Island in 1993. Body mass of pups at all other sites and years was measured to the nearest tenth of a kilogram by using an electronic scale (Rice Lake Weighing Systems, Rice Lake, WI; Ohaus I-20W, Ohaus, Pine Brook, NJ). Standard length was measured as a straight line from tip-of-nose to tip-of-tail, ventral surface down. Pups were restrained by hand and marked for later identification with hair bleach (Lady Clairol Maxi Blond, Clairol, Inc.) and with flipper tags attached in the axillary area of the fore-flippers.

Body composition was measured by using the labeled water method (Nagy 1975; Nagy and Costa, 1980; Costa, 1987; Bowen and Iverson, 1998). In this study, water labeled with a stable isotope of hydrogen (deuterium)

³ Davis, R. W. and A. A. Brandon. Unpubl. data. [Data are on file at Texas A&M University, 5007 Avenue U, Galveston, Texas 77551.]

was used to estimate total body water (TBW in kg and %TBW as a percentage of BM). Background concentration of deuterium was determined from blood samples taken from pups that were subsequently injected intramuscularly with 10 mL deuterium oxide (D_2O) (99% enriched, Cambridge Isotope Laboratories, Andover, MA). After a two-hour equilibration period (Costa, 1987), blood samples were taken to determine the dilution of injected deuterium in total body water.

Pups were recaptured at approximately two-week intervals over periods ranging in length from 18 to 38 days (average measurement period was 29.6 days) (Table 1) and were weighed, measured, and a blood sample was taken from each pup. Similar protocols were used at all rookeries, except Marmot Island in 1990 and 1991, when only BM and SL were measured, and the age of pups was not estimated. Therefore, no growth rates were obtained from these data.

Labeled water sample analysis

Blood samples were centrifuged in the field in serum separator tubes, and the serum was transferred to cryovials that were frozen at $-20^\circ C$ until analysis. Isotope-ratio mass spectrometry was used to determine the ratio of deuterium (2H) to hydrogen (H) (Laboratory of Biochemical and Environmental Studies at University of California, Los Angeles, CA). The hydrogen-isotope dilution space was calculated from this ratio by using Equation 3 in Schoeller et al. (1980). However, the hydrogen-isotope dilution space has been shown to underestimate TBW in a number of pinniped species (Reilly and Fedak, 1990; Arnould et al., 1996b), leading Bowen and Iverson (1998) to develop a single predictive equation to estimate %TBW from hydrogen-isotope dilution space in pinnipeds for which data on the accuracy of the hydrogen-isotope method are lacking. The equation

$$\%TBW = 0.003 + 0.968 H\text{-dilution space} \quad (1)$$

was used in the present study to correct the overestimated %TBW by 3.3% (Bowen and Iverson, 1998, Eq. 5). Percent total body lipid (%TBL, as a percentage of BM) was calculated by using predictive equations derived from the relationship between %TBW and %TBL for Antarctic fur seals (Arnould et al., 1996b):

$$\%TBL = 66.562 - 0.845 \%TBW. \quad (2)$$

%TBL was then compared between male and female pups and among rookeries.

Statistical analyses

Statistics were performed by using Systat (version 11, SPSS, Inc, Chicago, IL), and by first treating each study site and year as a separate "location," then combining data for multiple years at a location (e.g., Marmot Island and Lowrie Island) when no significant interannual differences were found. Significance was determined

at $P \leq 0.05$. Data were examined for heteroscedasticity (unequal variances) before analysis (Zar, 1984). All *post hoc* pairwise comparisons were made with the Tukey multiple comparison test. Data from the first capture (1–5 days of age) were analyzed for comparison by location and sex by using two-way ANOVA. Pup growth rate was estimated by performing a linear regression for each pup and extrapolating to $t = 0$ to estimate birth mass. Differences among means of pup growth rate and birth mass were then analyzed by using two-way ANOVA to determine differences by location and sex.

Results

Neonatal size

There were no significant differences by rookery in pup mass at 1–5 days of age (Table 2) and no significant interaction between rookery and sex. The only significant difference in SL of 1–5 day old pups was that both genders were significantly longer on Seguum and Yunaska Islands than on Fish Island ($P=0.0395$). Pups on Chirikof Island had significantly smaller AG than pups on Lowrie, Fish, and Seguum and Yunaska Islands ($P < 0.02$). Male and female pups were significantly different for all three morphometric measurements. Overall, male pups averaged 22.6 kg (± 2.21 SD, $n=71$) and female pups averaged 19.6 kg (± 1.80 SD, $n=74$) at first capture (1–5 days of age).

There was no significant difference by rookery or sex and no significant interaction between rookery and sex in %TBW or %TBL of pups at first capture. When all pups at all rookeries were combined ($n=116$), %TBW was 72.1% of BM (± 3.17 SD) and %TBL was 5.6% of BM (± 2.68 SD). Male pups had a significantly greater absolute TBW than female pups ($P < 0.0001$), as would be expected because of the difference in BM at birth. There was a significant correlation between TBW and BM (Pearson $r=0.945$, $P < 0.001$, $n=116$; $TBW (kg) = 0.6895 \times BM + 0.6618$).

Neonatal growth

Growth rates were treated as linear over the period monitored; there were not enough data to determine if growth was nonlinear. Male and female pups on the same rookery grew at the same rate (in BM, SL, and AG) during the first six weeks after birth (Fig. 2). When compared by rookery, BM increased at a faster rate for pups on Chirikof Island ($P=0.0005$) and on Seguum and Yunaska Islands ($P=0.0002$) than on Lowrie Island (Fig. 3 and Table 3). The increase in BM for pups on Fish Island did not differ significantly from that at other rookeries. Marmot Island pups grew significantly more slowly than pups on Seguum and Yunaska Islands ($P=0.0382$) but did not differ significantly from growth of pups at other rookeries.

Standard length increased at a faster rate for pups on Chirikof Island ($P=0.0068$) and Seguum and Yu-

Yunaska Islands ($P=0.0050$) than it did for pups on Lowrie Island (Table 3). Growth in SL was also faster on Chirikof ($P=0.0383$) and Seguam and Yunaska Islands ($P=0.0230$) than on Fish Island, whereas the increase in SL on Marmot Island did not differ significantly from the other rookeries. The increase in AG was significantly greater on Seguam and Yunaska Islands ($P=0.0021$) and Marmot Island ($P=0.0364$) than on Lowrie Island. There was no significant interaction between rookery and sex in the growth rate of BM, SL, and AG.

Body mass at birth extrapolated to $t = 0$ from growth rates did not differ by rookery. There was no significant interaction between rookery and sex, but extrapolated birth mass did differ by sex ($P<0.0001$). Male pups at all rookeries averaged 22.4 kg (± 2.36 SD, $n=39$), whereas female pups averaged 18.7 kg (± 2.08 SD, $n=35$). These extrapolated birth masses were similar to the average BM measured on the rookery for male (22.6 kg) and female (19.6) pups 1–5 days old. There was no correlation between extrapolated birth mass and growth rate (Pearson $r=-0.09$, $P=0.45$).

Table 2

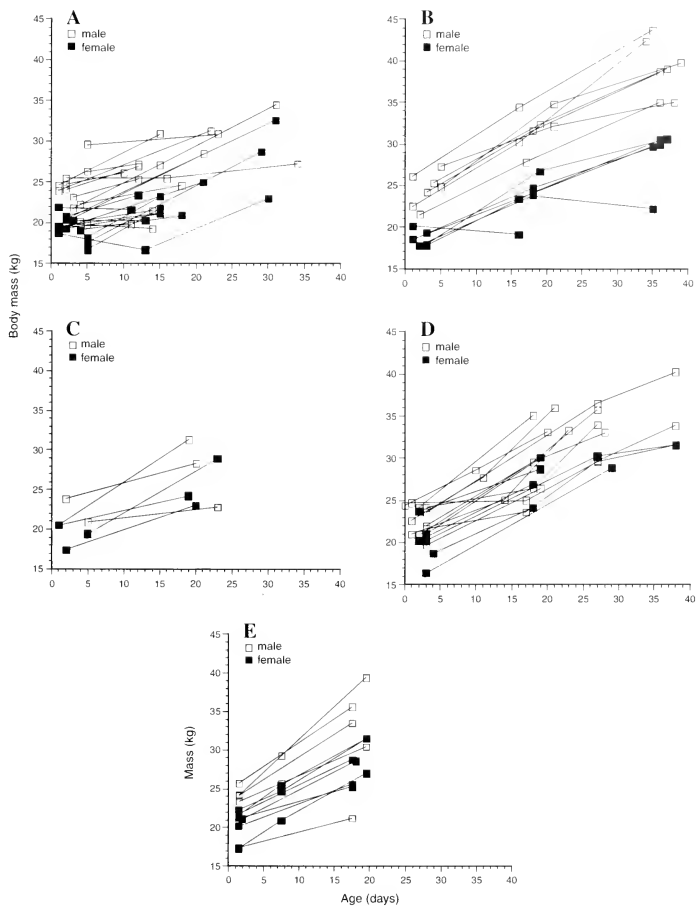
Body mass (BM), standard length (SL), and axillary girth (AG) of neonatal (1–5 day old) Steller sea lion (*Eumetopias jubatus*) pups in the stable (Lowrie Island) and declining (Fish Is., Marmot Is., Chirikof Is., Seguam Is., Yunaska Is.) populations (mean \pm SD). An asterisk (*) indicates significant differences from all other sites, and † indicates a significant difference between two sites. Standard length from Fish Is. was significantly different from SL on Seguam and Yunaska Is. Axillary girth on Chirikof Is. was significantly different from AG at all other sites. In all cases, males were significantly larger than females. There were no significant interannual differences; therefore data from all years at Lowrie Is. were combined.

Location	n	BM (kg)		SL (cm)		AG (cm)	
		male	female	male	female	male	female
Lowrie Is. (1993–97)	39M	22.1	19.5	98.3	94.1	64.9	64.3
	41F	± 2.20	± 1.67	± 4.56	± 3.96	± 3.33	± 5.01
Fish Is. (1995)	11M	22.6	19.2	96.2†	93.3†	68.5	64.0
	9F	± 1.69	± 2.39	± 26.76	± 6.39	± 2.96	± 4.00
Marmot Is. (1994)	3M	21.7	20.2	101.7	97.4	65.5	61.8
	6F	± 1.80	± 2.42	± 1.53	± 2.67	± 2.78	± 5.38
Chirikof Is. (1993)	11M	23.21	19.02	99.1	94.9	62.7*	60.1*
	9F	± 2.59	± 1.05	± 5.24	± 2.40	± 3.52	± 2.15
Aleutian Is. (Seguam and Yunaska Is.) (1997)	7M	24.2	20.5	101.4†	96.3†	67.7	63.9
	9F	± 1.97	± 1.88	± 4.29	± 2.55	± 3.50	± 3.66

Table 3

Steller sea lion (*Eumetopias jubatus*) pup growth from 0 to 40 days of age (mean \pm SD). There were no significant differences between male and female pups. BM=body mass; SL = standard length; AG=axillary girth. Underlining indicates that there were no significant differences within an underlined grouping (e.g., for body mass growth rate, C was significantly different from L, and A was significantly different from M and L).

Location	n	BM growth rate (kg/day)	SL growth rate (cm/day)	AG growth rate (cm/day)
Lowrie Is. (L)	26	0.23 \pm 0.176	0.20 \pm 0.322	0.25 \pm 0.244
Fish Is. (F)	13	0.35 \pm 0.171	0.22 \pm 0.183	0.41 \pm 0.235
Marmot Is. (M)	6	0.28 \pm 0.141	0.22 \pm 0.287	0.59 \pm 0.510
Chirikof Is. (C)	17	0.45 \pm 0.126	0.47 \pm 0.171	0.47 \pm 0.187
Aleutian Is. (A) (Seguam and Yunaska Is.)	12	0.48 \pm 0.168	0.53 \pm 0.163	0.59 \pm 0.257
ANOVA results		<u>L M F C A</u>	<u>L F M C A</u>	<u>L F C M A</u>

**Figure 2**

Change in body mass of individual Steller sea lion (*Eumetopias jubatus*) pups captured on (A) Lowrie Island in 1993, 1994, and 1997, (B) Fish Island in 1995, (C) Marmot Island in 1994, (D) Chirikof Island in 1993, and (E) Yunaska and Seguam Islands in 1997.

Discussion

Compared to other species of sea lions and fur seals, SSL pups are large, although this species produces smaller pups in relation to adult size than do smaller otariids (Kovacs and Lavigne, 1992; McLaren, 1993). In the present study, male pups averaged 22.6 kg and female pups averaged 19.6 kg at 1–5 days of age, which is in the range of birth masses reported in the literature. Two studies conducted before the recent population decline reported 17 kg for male pups at birth (Scheffer, 1945) and a range of 9.1–21.8 kg for male and female pups (Mathisen et al., 1962). Late in the population decline, studies reported a range of 16–23 kg for pups at birth in Alaska (Calkins and Pitcher, 1982) and an extrapolated birth mass of 17.9 kg for five pups for which growth rates were measured in California (Higgins et al., 1988).

This is the first, large-scale (in terms of sample size and geographic area) longitudinal study of growth in Steller sea lion pups. Growth rates reported in our study are the highest absolute growth rates reported for any sea lion or fur seal. This is to be expected because adult SSLs are the largest otariids (Kovacs and Lavigne, 1992). The growth rate of 0.38 kg/day measured for five SSL pups at Año Nuevo Island in California (Higgins et al., 1988) falls within the range of average growth rates measured in the present study (0.23–0.48 kg/day). The only other measurement of pup growth in SSLs was conducted on captive pups that were already

several months old. In terms of growth rate in relation to size at birth, SSL pups gained 1–2.3% of their birth weight per day (Lowrie Island and Seguam and Yunaska Islands, respectively, based on an average birth mass of 21.1 kg), which was faster than the relative growth rates reported for other otariid species (Kovacs and Lavigne, 1992, calculated from Table 1), except for northern fur seals. In contrast, seals (order Carnivora, family Phocidae) exhibit faster growth rates (1.3–5.6 kg/day or 8–26% birth weight per day) (Stewart and Lavigne, 1980; Bowen et al., 1985; Kovacs and Lavigne, 1985; Bowen et al., 1987; Bowen et al., 1992; Campagna et al., 1992). Although adult SSLs are larger than many species of phocid seals, phocids have much shorter lactation periods and their pups grow at a more accelerated rate than do otariids.

Male-female differences

Male pups weighed 15% more than females at birth, indicating a difference in maternal investment during gestation, which has been found in other otariids including Antarctic fur seals (Doigie et al., 1984; Lunn and Boyd, 1993; Goldsworthy, 1995; Boyd, 1996), South American fur seals (*Arctocephalus australis*) (Lima and Páez, 1995), California sea lions (Ono and Boness, 1996), and northern sea lions (*Otaria byronia*) (Cappozzo et al., 1991). These results are consistent with the predictions of Maynard-Smith's (1980) theory on sexual investment. Steller sea lion adults are extremely sexually dimorphic: females weigh 263 kg on average (maximum of approximately 350 kg); males weigh more than twice as much (average of 566 kg, maximum of approximately 1120 kg) (Calkins and Pitcher, 1982). In view of this dimorphism and the fact that size is more important to male fitness than to female fitness in a polygynous species (McCann, 1981) such as the SSL, theory predicts that males would be heavier than females at birth. Northern fur seal females with male fetuses are in poorer condition than mothers with female fetuses (Trites, 1992), and male fetuses grow at a faster rate than female fetuses (Trites, 1991), indicating that mothers invest more in male offspring during gestation.

However, there were no male-female differences in neonatal growth (BM, SL, and AG) rate in SSL during the first six weeks after birth. In a species as sexually dimorphic as SSL, one would expect males to grow at a faster rate than females during development. However, this difference may not occur until the animals are older. There is some evidence that male otariids undergo a sharp increase in growth rate near sexual maturity (McLaren, 1993; Bester and Van Jaarsveld, 1994), after females have already reached sexual maturity and their growth has slowed.

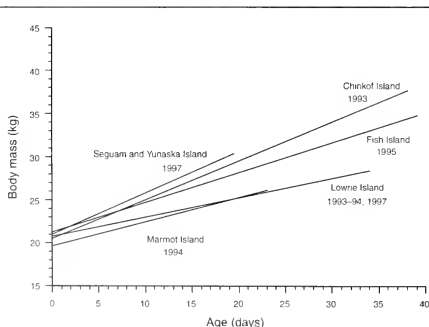


Figure 3

Summary of Steller sea lion (*Eumetopias jubatus*) pup growth (body mass) during the first six weeks after birth for all five rookeries. The length of each line indicates the length of the study period at that location. Pups from Seguam, Yunaska, and Chirikof Islands, in the declining population, grew significantly faster than pups from Lowrie Island, in the stable population. Pups from Seguam and Yunaska Islands also grew significantly faster than pups from Marmot Island.

Conflicting results have been reported in other growth studies of otariids. Several studies reported that male pups grew faster than female pups (Antarctic fur seals: Payne, 1979; Doidge et al., 1984; Antarctic and Subantarctic fur seals: Kerley, 1985; New Zealand fur seals: Matlin 1981). However, cross-sectional data on growth rate were used in these studies. Conversely, longitudinal data, considered to be more accurate, demonstrate no differences in neonatal growth rate between male and female Antarctic fur seal pups (Doidge and Croxall, 1989; Lunn et al., 1993; Lunn and Arnould, 1997); Goldsworthy (1995), however, is the exception. Ono and Boness (1996) collected longitudinal growth data on California sea lion pups and found that males grew faster than females, but they found no other evidence of differential maternal investment. In phocids, most studies have found no difference in neonatal male and female growth rates, regardless of whether the data were longitudinal or cross sectional (Stewart and Lavigne, 1980; Innes et al., 1981; Bowen et al., 1992). This is true for species with extreme sexual dimorphism such as elephant seals (McCann et al., 1989; Campagna et al., 1992). The only other study where growth rates for SSL pups were measured did not have a large enough sample size for a comparison between males and females (Higgins et al., 1988). No differences between male and female pups were found for suckling behavior or maternal attendance behavior (Higgins et al., 1988).

Total body lipid

Average %TBL of neonatal pups was low (5.6% BM). Steller sea pups are born with small energy stores and normally fast for short periods (about one day) while their mothers make foraging trips to sea. There have been few measurements of lipid content in otariid neonates. Jonker and Trites (2000) found a blubber content of 9.7% BM in five SSL pups in the first month after birth. However, this measurement does not correspond directly to body fat content because they measured blubber content by weighing the sculp (skin plus blubber) and then calculating the fraction of sculp that was blubber by measuring skin and blubber thicknesses. Using the same labeled water method as in the present study, Arnould et al. (1996b) found a %TBL of 9.4% BM in four Antarctic fur seal pups in the first month after birth. In a similar study of one-day-old Antarctic fur seal pups, Arnould et al. (1996a) found a %TBL of 7.0% BM for female pups and 4.9% BM for male pups. Also using labeled water, Oftedal et al. (1987a) found an average %TBL of 5% BM for neonatal California sea lion pups.

Arnould et al. (1996b) suggested two explanations for the higher lipid content that they found in Antarctic fur seal pups in comparison to California sea lion pups (Oftedal et al. 1987b). First, in colder habitats, a larger subcutaneous lipid store may be necessary for thermoregulation. The data here do not support that explanation. SSL live in a colder habitat than California sea lions, but have a similar %TBL. The more

likely explanation is that larger lipid stores are found in species in which pups normally fast longer while their mothers are foraging. Steller sea lion pups have the smallest lipid stores and shortest fasting periods (Brandon, 2000) of the three species.

Differences in pup size among rookeries

Although male and female pups differed significantly in size, there were no significant differences in pup size at birth among the rookeries studied. Rookery location should have less influence on pup size at birth than on neonatal growth because maternal foraging range is much greater during gestation than during lactation (Merrick and Loughlin, 1997). This greater maternal foraging range during gestation reduces, among rookeries, variation in maternal size and feeding conditions (quantity and quality of prey available) during gestation, both of which have been shown to influence pup birth mass in pinnipeds (Calambokidis and Gentry, 1985; Kovacs and Lavigne, 1986; Trites, 1991; Trites 1992). The lack of a difference in pup BM at birth among rookeries could also be explained by the fact that females that are "successful" (i.e., carry their fetuses to term) have a significantly better body condition than females that do not carry their fetuses to term (Pitcher et al., 1998). As a consequence of our study design, only those females that were successful were used, and therefore our sample was biased toward females in the population with better body condition. In addition, gestation is less energetically expensive than early lactation; therefore differences in food availability would have less of an effect during gestation (Robbins and Robbins, 1979; Albon et al., 1983; Oftedal, 1984).

Although most pup morphometrics at first capture did not differ among rookeries, growth parameters differed significantly (Table 3). Growth rates of pups on Seguum and Yunaska Islands (0.48 kg/day) and on Lowrie Island (0.23 kg/day) represented the extremes, whereas growth rates of pups on Chirikof, Marmot, and Fish Islands fell between these two extremes. In general, faster growth rates occurred in the west and slower growth rates in the east. In terms of mass, Seguum and Yunaska Islands and Chirikof Island pups grew twice as fast as Lowrie Island pups. A concurrent study of the attendance patterns of lactating females (Brandon, 2000) showed that foraging trip duration decreased from east (25.6 hours on Lowrie Island) to west (an average of 9.4 hours on Chirikof and Seguum Islands). Therefore, it is possible that the higher growth rates in SSL pups in the western Gulf of Alaska and Aleutian Islands resulted from shorter periods of fasting while females were foraging at sea (Arnould et al., 1996a; Goldsworthy, 1995).

Is food limiting growth in Steller sea lion pups in the area of population decline?

If the cause of the population decline were decreased food availability, which is one of the leading hypotheses

Pascual and Adkison, 1994; York, 1994; NMFS²), one might expect the animals in the declining population to show signs of nutritional stress compared to those in the stable population. The results for pup size and growth give no indication of food stress during early lactation. In fact, pups from the declining population on Seguam, Yunaska, and Chirikof Islands grew faster than pups from the stable population on Lowrie Island during the first six weeks. Similar results were also found in a study of pup BM (Merrick et al., 1995), in which pups were weighed on rookeries from Oregon to the Aleutian Islands in late June and early July from 1987 to 1994. Although the pups' ages were unknown, weighing date was used as a covariate in the analysis. Merrick et al. (1995) found a continuous increase in pup BM from Oregon to southeast Alaska and to the Aleutian Islands. These investigators also concluded that pup BM was on average greater in the declining population.

In most other studies of declining populations or differences among rookeries, such contradictory results have not been seen. A study of California sea lion pups during an ENSO (El Niño Southern Oscillation) event revealed lower pup growth during the period of food stress (Boness et al., 1991). Trillmich and Limberger (1985) have also seen clear effects of low food availability during an ENSO in Galapagos fur seals and sea lions. Antarctic fur seals are affected in predictable ways (increased pup mortality and increased female foraging time) during times of decreased food availability (Costa et al., 1989). Hood and Ono (1997) found that in the declining California population of SSLs, pups spent less time suckling when adult females made longer foraging trips in 1992 than in 1973 when the population was larger. The longer foraging trips suggested less abundant food resources.

Considering the results for SSL pup growth in light of the population decline, we suggest three alternative hypotheses: 1) food availability was never a factor in the population decline; 2) food availability caused the overall decline, but lactating females and their pups were not affected during early lactation; or 3) our study was conducted when pups and lactating females were no longer experiencing decreased food availability.

Faster rates of pup growth may be normal for the Aleutian Islands and western Gulf of Alaska despite the population decline. The declining and stable populations are genetically distinct (Bickham et al., 1996), and perhaps the differences seen in our study are normal differences between the two populations. It is impossible to determine if growth and foraging behavior have changed over time because historical data on maternal investment are sparse. Juveniles rather than neonates may be the affected age class in the declining population (Merrick et al., 1988), whereas lactating females are feeding on either different prey or age classes and not experiencing decreased food availability. York (1994) constructed a population model for SSLs in Alaska and concluded that the current population decline could be accounted for by increased juvenile mortality.

Alternatively, because our study was performed late in the decline, the higher growth rates could be the result of lower population density and less competition for food in the declining population. Trites and Bigg (1992) reported larger body sizes in northern fur seal populations during a period of decline. The northern fur seal population in the Pribilof Islands in the Bering Sea increased from the early 1900s to the 1950s. During this period, adult body size decreased. From 1950 to the 1970s the population declined and there was a concurrent increase in individual body size (Trites and Bigg, 1992). Scheffer (1955) hypothesized that increased body size was due to decreased competition for food, which in turn would be due to the lower population density. It is possible that the same density-dependent effects are occurring in the declining SSL population because our study was performed late in the decline, after the original cause may have abated. More information will be needed to determine the cause of the SSL decline and whether it is related to availability of food, especially for different age classes, and to different times of the year.

Acknowledgments

We thank T. Adams, R. Andrews, D. Bradley, J. Burns, M. Castellini, J. K. Chumbley, W. and S. Cunningham, J. Davis, F. Gulland, D. Gummeson, B. Heath, D. Johnson, S. Kanatous, D. Lidgard, R. Lindeman, R. Merrick, D. McAllister, L. Milette, K. Ono, L. Polasek, T. Porter, D. Rosen, J. Sease, T. Spraker, U. Swain, W. Taylor, A. Trites, D. van den Bosch, T. Williams, and the captain and crew of the RV *Medeia* for assistance in the field. We thank K. Andrews for the map and D. Brandon for assistance in data collection and analysis. G. Worthy, A. Trites, T. Lacher, D. Owens, and M. Reynolds reviewed an early version of this manuscript. Funding and logistical support in the field were provided by the Alaska Department of Fish and Game, the National Marine Fisheries Service/National Marine Mammal Laboratory, Texas A&M University, and the Texas Institute of Oceanography. This research was conducted under Marine Mammal permit no. 846 and 963.

Literature cited

- Albon, S. D., T. H. Clutton-Brock, and R. Langvatn.
1992. Cohort variation in reproduction and survival: implications for population demography. *In* The biology of deer (R. D. Brown, ed.), p. 15-21. Springer-Verlag, New York, NY.
- Albon, S. D., F. E. Guinness, and T. H. Clutton-Brock.
1983. The influence of climatic variation on the birth weights of red deer (*Cervus elaphus*). *J. Zool. (Lond.)* 203:295-298.
- American Society of Mammalogists.
1967. Standard measurements of seals. *J. Mammal.* 48:459-462.
- Arnould, J. P. Y., I. L. Boyd, and D. G. Socha.
1996a. Milk consumption and growth efficiency in Ant-

- arctic fur seal (*Arctocephalus gazella*) pups. *Can. J. Zool.* 74:254-266.
- Arnould, J. P. Y., L. L. Boyd, and J. R. Speakman.
1996b. Measuring the body composition of Antarctic fur seals (*Arctocephalus gazella*): validation of hydrogen isotope dilution. *Physiol. Zool.* 69:93-116.
- Baker, J. D., and C. W. Fowler.
1992. Pup weight and survival of northern fur seals *Callorhinus ursinus*. *J. Zool. (Lond.)* 227:231-238.
- Bestler, M. N., and A. S. Van Jaarsveld.
1994. Sex-specific and latitudinal variance in postnatal growth of the Subantarctic fur seal (*Arctocephalus tropicalis*). *Can. J. Zool.* 72:1126-1133.
- Bickham, J. W., T. R. Loughlin, J. R. Wickliffe, and V. N. Burkanov.
1998. Geographic variation in the mitochondrial DNA of Steller sea lions: haplotype diversity and endemism in the Kuril Islands. *Biosphere Conservation*, 1: 107-117.
- Bickham, J. W., J. C. Patton, and T. R. Loughlin.
1996. High variability for control-region sequences in a marine mammal: implications for conservation and biogeography of Steller sea lions (*Eumetopias jubatus*). *J. Mammal.* 77:95-108.
- Boltnev, A. I., A. E. York, and G. A. Antonelis.
1998. Northern fur seal young: interrelationships among birth size, growth, and survival. *Can. J. Zool.* 76: 843-854.
- Boness, D. J., O. T. Oftedal, and K. A. Ono.
1991. The effect of El Niño on pup development in the California sea lion (*Zalophus californianus*) I. Early postnatal growth. In Pinnipeds and El Niño: responses to environmental stress (F. Trillmich and K. Ono, eds.), p. 173-184. Springer-Verlag, Berlin.
- Bonner, W. N.
1984. Lactation strategies in Pinnipeds: problems for a marine mammalian group. *Symp. Zool. Soc. Lond.* 51:253-272.
- Bowen, W. D., and S. J. Iverson.
1998. Estimation of total body water in pinnipeds using hydrogen-isotope dilution. *Physiol. Zool.* 71:329-332.
- Bowen, D., D. J. Boness, and O. T. Oftedal.
1985. Birth to weaning in 4 days: remarkable growth in the hooded seal, *Cystophora cristata*. *Can. J. Zool.* 63:2841-2846.
1987. Mass transfer from mother to pup and subsequent mass loss by the weaned pup in the hooded seal, *Cystophora cristata*. *Can. J. Zool.* 65:1-8.
- Bowen, W. D., W. T. Stobo, and S. J. Smith.
1992. Mass changes of grey seal *Halichoerus grypus* pups on Sable Island: differential maternal investment reconsidered. *J. Zool. (Lond.)* 227:607-622.
- Boyd, I. L.
1996. Individual variation in the duration of pregnancy and birth date in Antarctic fur seals: the role of environment, age, and sex of fetus. *J. Mammal.* 77:124-133.
- Brandon, E. A. A.
2000. Maternal investment in Steller sea lions in Alaska. Ph.D. diss., 137 p. Texas A&M University, Galveston, TX.
- Bryden, M. M.
1968. Control of growth in two populations of elephant seals. *Nature* 217:1106-1108.
- Burns, J. M.
1999. The development of diving behavior in juvenile Weddell seals: pushing physiological limits in order to survive. *Can. J. Zool.* 77:737-747.
- Calambokidis, J., and R. Gentry.
1985. Mortality of northern fur seal pups in relation to growth and birth weights. *J. Wildl. Dis.* 21:327-330.
- Calkins, D. G., D. C. McAllister, K. W. Pitcher, and G. W. Pendleton.
1999. Steller sea lion status and trend in Southeast Alaska: 1979-1997. *Mar. Mammal Sci.* 15:462-477.
- Calkins, D. G., and K. W. Pitcher.
1982. Population assessment, ecology and trophic relationships of Steller sea lions in the Gulf of Alaska, 140 p. Final report to Outer Continental Shelf Environment Assessment Program, contract 03-5-022-69. Alaska Department of Fish and Game, Anchorage, AK.
- Campagna, C., B. J. Le Boeuf, M. Lewis, and C. Bisioli.
1992. Equal investment in male and female offspring in southern elephant seals. *J. Zool. (Lond.)* 226:551-561.
- Cappozzo, H. L., C. Campagna, and J. Monserrat.
1991. Sexual dimorphism in newborn Southern sea lions. *Mar. Mamm. Sci.* 7:385-394.
- Costa, D. P.
1987. Isotopic methods for quantifying material and energy intake of free-ranging marine mammals. In *Marine mammal energetics* (A. C. Huntley, D. P. Costa, G. A. J. Worthy, and M. A. Castellini, eds.), p. 43-66. Soc. Mar. Mammal. Special Publ. 1. Allen Press, Lawrence, KS.
- Costa, D. P., J. P. Croxall, and C. D. Duck.
1989. Foraging energetics of Antarctic fur seals in relation to changes in prey availability. *Ecology* 70:596-606.
- Dodge, D. W., and J. P. Croxall.
1989. Factors affecting weaning weight in Antarctic fur seals *Arctocephalus gazella* at South Georgia. *Polar Biol.* 9:155-160.
- Dodge, D. W., J. P. Croxall, and C. Ricketts.
1984. Growth rates of Antarctic fur seal *Arctocephalus gazella* pups at South Georgia. *J. Zool. (Lond.)* 203:87-93.
- Gaillard, J.-M., J.-M. Boutin, D. Delorme, G. Van Laere, P. Duncan, and J.-D. Lebreton.
1997. Early survival in roe deer: causes and consequences of cohort variation in two contrasted populations. *Oecologia* 112:502-513.
- Goldworthy, S. D.
1995. Differential expenditure of maternal resources in Antarctic fur seals, *Arctocephalus gazella*, and Heard Island, southern Indian Ocean. *Behav. Ecol.* 6:218-228.
- Higgins, L. V., C. P. Costa, A. C. Huntley, and B. J. Le Boeuf.
1988. Behavioral and physiological measurements of maternal investment in the Steller sea lion, *Eumetopias jubatus*. *Mar. Mammal Sci.* 4:44-58.
- Hood, W. R., and K. A. Ono.
1997. Variation in maternal attendance patterns and pup behaviour in a declining population of Steller sea lions (*Eumetopias jubatus*). *Can. J. Zool.* 75:1241-1246.
- Innes, S. R., E. A. Stewart, and D. M. Lavigne.
1981. Growth in Northwest Atlantic harp seals *Phoca groenlandica*. *J. Zool. (Lond.)* 194:11-24.
- Jonker, R. A. H., and A. W. Trites.
2000. The reliability of skinfold-calipers for measuring blubber thickness of Steller sea lion pups (*Eumetopias jubatus*). *Mar. Mamm. Sci.* 16:757-766.
- Kerley, G. I. H.
1985. Pup growth in the fur seals *Arctocephalus tropicalis* and *A. gazella* on Marion Island. *J. Zool. (Lond.)* 205:315-324.

- Kovacs, K. M., and D. M. Lavigne.
1985. Neonatal growth and organ allometry of North-west Atlantic harp seals (*Phoca groenlandica*). *Can. J. Zool.* 63:2793-2799.
1986. Maternal investment and neonatal growth in phocid seals. *J. Anim. Ecol.* 55:1035-1051.
1992. Maternal investment in otariid seals and walrus. *Can. J. Zool.* 70:1953-1964.
- Lima, M., and E. Paez.
1995. Growth and reproductive patterns in the South American fur seal. *J. Mammal.* 76:1249-1255.
- Lunn, N. J., and J. P. Y. Arnould.
1997. Maternal investment in Antarctic fur seals: evidence for equality in the sexes? *Behav. Ecol. Sociobiol.* 40:351-362.
- Lunn, N. J., and I. L. Boyd.
1993. Effects of maternal age and condition on parturition and the perinatal period of Antarctic fur seals. *J. Zool. (Lond.)* 229:55-67.
- Lunn, N. J., I. L. Boyd, T. Barton, and J. P. Croxall.
1993. Factors affecting the growth rate and mass at weaning of Antarctic fur seals at Bird Island, South Georgia. *J. Mammal.* 74:908-919.
- Mathisen, O. A., R. T. Baade, and R. J. Lopp.
1962. Breeding habits, growth and stomach contents of the Steller sea lion in Alaska. *J. Mammal.* 43:469-477.
- Mattlin, R. H.
1981. Pup growth of the New Zealand fur seal *Arctocephalus forsteri* on the Open Bay Islands, New Zealand. *J. Zool. (Lond.)* 193:305-314.
- Maynard-Smith, J.
1980. A new theory of sexual investment. *Behav. Ecol. Sociobiol.* 7:247-251.
- McCann, T. S.
1981. Aggression and sexual activity of male Southern elephant seals, *Mirounga leonina*. *J. Zool. (Lond.)* 195:295-310.
- McCann, T. S., M. A. Fedak, and J. Harwood.
1989. Parental investment in southern elephant seals, *Mirounga leonina*. *Behav. Ecol. Sociobiol.* 25:81-87.
- McLaren, I. A.
1993. Growth in pinnipeds. *Biol. Rev.* 68:1-79.
- Merrick, R. L., R. Brown, D. G. Calkins, and T. R. Loughlin.
1995. A comparison of Steller sea lion, *Eumetopias jubatus*, pup masses between rookeries with increasing and decreasing populations. *Fish. Bull.* 93:753-758.
- Merrick, R., P. Gearin, S. Osmet, and D. Withrow.
1988. Field studies of northern sea lions at Ugamak Island, Alaska, during the 1985 and 1986 breeding seasons. NOAA Tech. Memo. NMFS F/NWC-43, 60 p.
- Merrick, R. L., and T. R. Loughlin.
1997. Foraging behavior of adult female and young-of-the-year Steller sea lions in Alaskan waters. *Can. J. Zool.* 75:776-786.
- Nagy, K. A.
1975. Water and energy budgets of free-living animals: measurement using isotopically labeled water. In *Environmental physiology of desert organisms* (N. Hadley, ed.), p. 227-245. Dowden, Hutchinson, and Ross, Stroudsburg, PA.
- Nagy, K. A., and D. P. Costa.
1980. Water flux in animals: analysis of potential errors in the tritiated water method. *Am. J. Physiol.* 238: R454-R465.
- Oftedal, O. T.
1984. Body size and reproductive strategy as correlates of milk energy output in lactating mammals. *Acta Zoologica Fennica* 171:183-186.
- Oftedal, O. T., S. J. Iverson, and D. J. Boness.
1987a. Milk and energy intakes of suckling California sea lion *Zalophus californianus* pups in relation to sex, growth, and predicted maintenance requirements. *Physiol. Zool.* 60:560-575.
- Oftedal, O. T., D. J. Boness, and R. A. Tedman.
1987b. The behavior, physiology, and anatomy of lactation in the Pinnipedia. *Curr. Mammal.* 1:175-245.
- Ono, K. A., and D. J. Boness.
1996. Sexual dimorphism in sea lion pups: differential maternal investment, or sex-specific differences in energy allocation? *Behav. Ecol. Sociobiol.* 38:31-41.
- Ono, K. A., D. J. Boness, and O. T. Oftedal.
1987a. The effect of a natural environmental disturbance on maternal investment and pup behavior in the California sea lion. *Behav. Ecol. Sociobiol.* 21:109-118.
- Pascual, M. A., and M. D. Adkison.
1994. The decline of the Steller sea lion in the Northeast Pacific: demography, harvest, or environment? *Ecol. Appl.* 4:393-403.
- Payne, M. R.
1979. Growth in the Antarctic fur seal *Arctocephalus gazella*. *J. Zool. (Lond.)* 187:1-20.
- Pitcher, K. W., D. G. Calkins, and G. W. Pendleton.
1998. Reproductive performance of female Steller sea lions: an energetics-based reproductive strategy. *Can. J. Zool.* 76:2075.
- Reilly, J., and M. A. Fedak.
1990. Measurement of body composition in living gray seals by hydrogen isotope dilution. *J. Appl. Physiol.* 69:885-891.
- Robbins, C. H., and B. L. Robbins.
1979. Fetal and neonatal growth patterns and maternal reproductive efforts in ungulates and subungulates. *Am. Nat.* 114:101-116.
- Scheffer, V. B.
1945. Growth and behavior of young sea lions. *J. Mammal.* 26:390-392.
1955. Body size with relation to population density in mammals. *J. Mammal.* 39:493-515.
- Schoeller, D. A., E. van Santen, D. W. Peterson, W. Dietz, J. Jaspán, and P. D. Klein.
1980. Total body water measurement in humans with ¹⁸O and D₂ labeled water. *Am. J. Clin. Nutr.* 33:2686-2693.
- Stewart, R. E. A., and D. M. Lavigne.
1980. Neonatal growth of Northwest Atlantic harp seals, *Pagophilus groenlandicus*. *J. Mammal.* 61:670-680.
- Trillmich, F., and D. Limberger.
1985. Drastic effects of El Niño on Galapagos pinnipeds. *Oecologia*, 67:19-22.
- Trites, A. W.
1991. Fetal growth of northern fur seals: life-history strategy and sources of variation. *Can. J. Zool.* 69:2608-2617.
1992. Fetal growth and the condition of pregnant northern fur seals off western North America from 1958 to 1972. *Can. J. Zool.* 70:2125-2131.
1993. Biased estimates of fur seal pup mass: origins and implications. *J. Zool. (Lond.)* 229:515-525.
- Trites, A. W., and M. A. Bigg.
1992. Changes in body growth of northern fur seals

- from 1958 to 1974: density effects or changes in the ecosystem? *Fish. Oceanog.* 1:127-136.
- Tveraa, T., B.-E. Sæther, R. Aanes, and K. E. Erikstad.
1998. Body mass and parental decisions in the Antarctic petrel *Thalassiodroma antarctica*: how long should the parents guard the chick? *Behav. Ecol. Sociobiol.* 43:73-79.
- York, A. E.
1994. The population dynamics of Northern sea lions, 1975-1985. *Mar. Mammal Sci.* 10:38-51.
- Zar, J. H.
1984. *Biostatistical analysis*, 718 p. Prentice-Hall, Englewood Cliffs, NJ.

Abstract—The carpenter seabream (*Argyrozona argyrozona*) is an endemic South African spard that comprises an important part of the handline fishery. A three-year study (1998–2000) into its reproductive biology within the Tsitsikamma National Park revealed that these fishes are serial spawning late gonochorists. The size at 50% maturity (L_{50}) was estimated at 292 and 297 mm FL for both females and males, respectively. A likelihood ratio test revealed that there was no significant difference between male and female L_{50} ($P > 0.5$). Both monthly gonadosomatic indices and macroscopically determined ovarian stages strongly indicate that *A. argyrozona* within the Tsitsikamma National Park spawn in the astral summer between November and April. The presence of postovulatory follicles (POFs) confirmed a six-month spawning season, and monthly proportions of early (0–6 hour old) POFs showed that spawning frequency was highest (once every 1–2 days) from December to March. Although spawning season was more highly correlated to photoperiod ($r = 0.859$) than temperature ($r = -0.161$), the daily proportion of spawning fish was strongly correlated ($r = 0.93$) to ambient temperature over the range 9–22°C. These results indicate that short-term upwelling events, a strong feature in the Tsitsikamma National Park during summer, may negatively affect carpenter fecundity. Both spawning frequency and duration (i.e., length of spawning season) increased with fish length. As a result of the allometric relationship between annual fecundity and fish mass a 3-kg fish was calculated to produce fivefold more eggs per kilogram of body weight than a fish of 1 kg. In addition to producing more eggs per unit of weight each year, larger fish also produce significantly larger eggs.

Manuscript submitted 22 September 2003 to the Scientific Editor's Office.

Manuscript approved for publication 30 August 2004 by the Scientific Editor.
Fish. Bull. 103:258–269 (2005).

Reproductive biology of carpenter seabream (*Argyrozona argyrozona*) (Pisces: Sparidae) in a marine protected area

Stephen L. Brouwer

Marc. H. Griffiths

Department of Marine and Coastal Management

Private Bag X2

Rogge Bay 8012, South Africa

E-mail (for S. L. Brouwer): sbrouwer@deat.gov.za

The carpenter seabream (*Argyrozona argyrozona*), known as “carpenter” regionally, is an endemic South African spard found between St Helena Bay and KwaZulu-Natal (Fig. 1) (Smith and Heemstra, 1986). Although the third most important species in the line-fishery in terms of landed mass, catch per unit of effort (CPUE) on traditional fishing grounds, declined by 95% during the twentieth century (Griffiths, 2000). Despite the importance of this resource, little research attention has been given to this species. The only previous study on the reproductive biology of carpenter was based on specimens collected towards the western extreme of the distribution range (west of Cape Agulhas), where most of the fish examined were reproductively inactive (Nepgen, 1977). As a result spawning seasonality was not accurately delineated and sizes at 50% maturity were not calculated. Assuming carpenter to be determinate spawners, Nepgen (1977) overestimated batch fecundity by counting immature oocytes.

The objective of the present study was to provide information on spawning seasonality, size at maturity, and annual fecundity of carpenter in the Tsitsikamma National Park (TNP), a 75-km no-take marine protected area (MPA) that has existed for 38 years (Fig. 1). It was envisaged that in conjunction with other studies on carpenter (Brouwer and Griffiths¹) in exploited areas this information would assist in determining the affects of fishing on the life history of carpenter.

Materials and methods

Fish were caught from a research vessel at depths between 20 and 90 m by using handlines with baited hooks of 2/0–6/0 in size. An attempt was made to sample 60 fish per month between March 1996 and June 1999, although weather conditions did not always allow this number. Sampling involved measuring total and fork length (FL) (mm), whole mass (g), gutted mass (g), determining the sex of fish, and removing the gonads. Gonads were staged macroscopically according to a seven-stage maturity index (Table 1) and weighed to the nearest 0.1 g. The whole gonads were preserved in 10% neutrally buffered formalin or alternatively fixed in Bouin's solution for 48 hours and then stored in 60% ethanol. Preserved samples were processed for histological analysis according to the techniques described by Osborne et al. (1999).

Length at maturity was modelled by using a 2-parameter logistic ogive of the form

$$p_i = \frac{1}{1 + \exp^{-(L_i - L_{50})/\alpha}}$$

where p_i = the proportion of mature fish in size class i , sampled during the spawning season (November to April);

¹ Brouwer, S. L., and M. H. Griffiths. In prep. Stock separation and life history of *Argyrozona argyrozona* (Pisces: Sparidae) on the South African east coast.

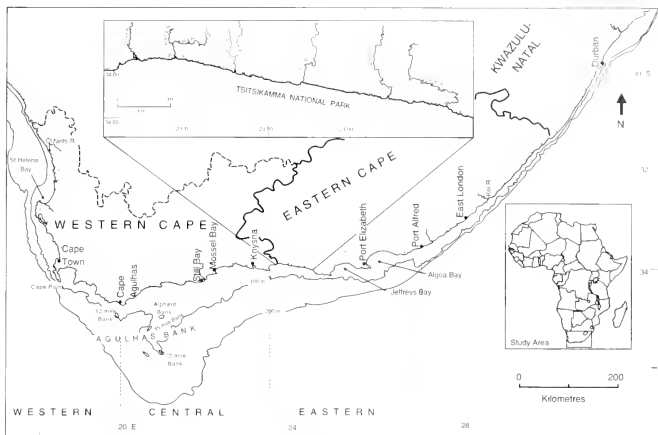


Figure 1

Map of the study area showing the position of the Agulhas Bank, Tsitsikamma National Park, 100- and 200-m isobaths and the places mentioned in the text.

Table 1

Classification and descriptions of macroscopic and microscopic ovary and testis stages of carpenter (*Argyrozoona argyrozoona*) sampled in the Tsitsikamma National Park.

Stage	Macroscopic	Microscopic
1 Juvenile female	Ovotestis appears as a thin transparent vessel.	Both ovarian and testicular tissues are present in equal proportions; however in the later stages ovarian tissue becomes dominant.
1 Juvenile male	Ovotestis appears as a thin transparent vessel.	Both ovarian and testicular tissue present in equal proportions; however in the later stages ovarian tissue becomes dominant.
2 Immature, resting female	Translucent orange tubes, no eggs visible to naked eye.	Cells in the perinucleolus stage have a large nucleus containing 8–15 nucleoli located along the periphery of the nucleus. There may be remnants of the testes on the periphery of the ovary.
2 Immature, resting male	Testes thin white and flaccid but larger than those in stage 1, no sperm in tissue.	No sperm cells are noticeable and the seminiferous tubules appear to be empty. Remnants of ovarian tissue may be present in the centre of the testes.
3 Active female	Oocytes visible to naked eye as tiny granules in gelatinous orange matrix; little increase in diameter of ovary.	Vitellogenesis begins in the oocytes, which become more rounded and begin to accumulate yolk (yolk vesicles). Yolk appears as a narrow ring of small yolk vesicles in the periphery of the cytoplasm.

continued

L_i = length of size class i ;
 L_{50} = the length at which 50% of the fish are sexually mature (stage 4+); and
 A = the width of the ogive.

The ogive was fitted by minimizing the negative log-likelihood. Differences in male and female L_{50} and a were tested by using a ratio test that minimizes the binomial log-likelihood of the form

$$-L = -\sum_{i=1}^n \left[m_i \times \ln \left(\frac{p_i}{1-p_i} \right) + n_i \times \ln(1-p_i) + \ln \left(\frac{n_i}{m_i} \right) \right],$$

where n = the number of samples in size class i ; and
 m_i = the number of mature fish in size class i .

Spawning frequency was estimated by using daily proportions of ovaries containing early postovulatory follicles (POFs), hereafter referred to as the spawn-

Table 1 (continued)

Stage	Macroscopic	Microscopic
3 Active male	Testes wider and triangular in cross section.	The seminal vesicles expand and become filled with spermatozoa.
4 Developing female	Ovary larger and orange-yellow in color. Eggs clearly discernible. Veins and arteries large and plentiful.	Yolk vesicles are common and primary yolk oocytes begin to appear, which are characterized by the formation of small spherical yolk granules.
4 Developing male	Testes wider and deeper, creamy white in colour, obvious presence of sperm in main sperm duct.	The seminiferous tubules of the testes are filled with spermatozoa, which are also present in the primary sperm duct.
5 Ripe female	Ovaries are large in diameter, may have a few hydrated eggs. Yellow oocytes take up all the space. Veins and arteries large and plentiful.	Tertiary yolk oocytes, characterized by large yolk plates, appear along with primary yolk and yolk vesicles. The nucleus becomes irregular in shape and smaller in size. The nucleus migrates to the animal pole of the cell after which hydration begins, resulting in increased transparency of the cells and an increase in cell size.
5 Ripe male	Sperm present in main sperm duct and in tissue. Gonad soft and breaks when lightly pinched.	The seminiferous tubules expand with copious amounts of spermatozoa that fill the lumen of the primary sperm duct.
6 Ripe, running female	Ovary amber in colour. Large with substantial proportion of gonad with hydrated eggs, which fill the lumen. Veins and arteries large and plentiful.	Filled with hydrated oocytes. Due to dehydration during the histological preparation, these oocytes appear as collapsed bags. Hydrated oocytes may squash and reshape the immature oocytes that surround them.
6 Ripe, running male	Free-flowing sperm extruded from fish when the abdomen is lightly squeezed. Testes very delicate and break easily when handled. Copious amounts of sperm present in main sperm duct and in tissue.	The seminiferous tubules of the testes appear distended and are filled with mature spermatozoa as is the lumen of the primary sperm duct.
7 Spent female	Ovary reduced in size similar to stage-2 flaccid ovary. Few yolked oocytes remaining. Ovary bloodshot.	Cells in various stages of atresia, and some hydrated and mature oocytes may be present in the tissue.
7 Spent male	Testes white in color, small shrivelled, and bloodshot.	The seminiferous tubules are no longer distended and have thicker walls than stage-6 tubules. They contain few spermatozoa, which are present in the lumen of the primary sperm duct. Large blood vessels are apparent in the tissue.

ing fraction (Hunter and Macewicz, 1985). POFs were aged by comparing them with known age POFs from spawning females under captive conditions. Female carpenter were held in a flow-through system at ambient sea temperature (mean 16°C, range 9.5–20°C) in 5000-liter circular tanks, were stimulated to ovulate with a commercially available GnRH-analogue (Davis, 1996). Three fish were sacrificed immediately after ovulation and then three fish every six hours over the following 48-hour period. Histological analysis of ovaries revealed three clearly defined POF stages (Fig. 2). The proportions of wild-caught fish with stage-1 POFs (the spawning fraction) were inverted to produce an estimate of spawning frequency (Wilson and Nieland, 1994).

Batch fecundity was estimated from counts of hydrated oocytes from ovaries without POFs or atretic oocytes (Hunter and Macewicz, 1985). A ± 1.00 -g section was removed from the middle of the right ovary. This was weighed to the nearest 0.01 g and the hydrated oocytes were separated according to the method described by Lowerre-Barbieri and Barbieri (1993). Hydrated oocytes were suspended in water and counted at 8–10 times magnification in a Bokkeroff tray and measured to 0.1 mm with an ocular micrometer along the longest diameter.

Annual fecundity was calculated as follows:

$$Af_t = \left(\frac{ls_j}{sf_j} \right) \times fb_t,$$

where Af_t = the annual fecundity for fish t ;

ls = the length of the spawning season (days) for fish of size class j ;

sf = the spawning frequency (days) for fish of size class j (all months combined); and

fb_t = the batch fecundity of fish t .

Spawning season was established by calculating the monthly proportions of macroscopic gonad stages and mean monthly gonadosomatic index (GSI) for fish larger than L_{50} :

$$GSI = \left(\frac{m_g}{m_s} \right) \times 100,$$

where m_g = the gonad mass (g); and

m_s = the somatic mass (g) (minus gonad and stomach mass).

In order to investigate the relationship between spawning and temperature, temperature data were collected at the sampling site with a Seamon Mini (Hugrun, Iceland) recorder stationed at a depth of 35 m on the reef from which the biological samples were collected. A thermistor array consisting of four underwater temperature recorders (UTRs) at depths of 12 m, 19 m, 27 m, and 35 m recorded the temperature every minute

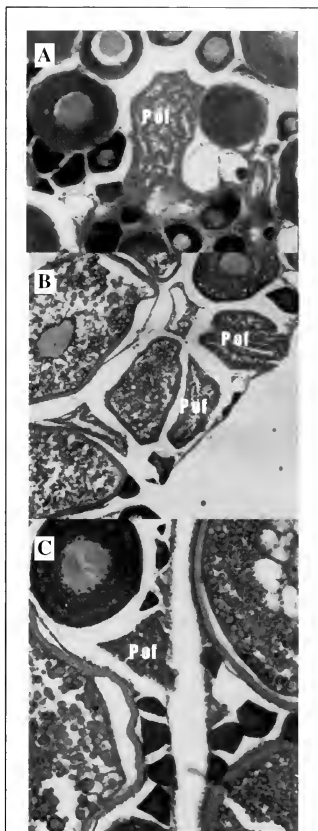


Figure 2

Postovulatory follicle (POF) stages determined from carpenter (*Argyrozona argyrozona*) chemically induced to spawn in an open circulating system housed at the Tsitsikamma National Park. (A) = stage 1 (0–6 hours), (B) = stage 2 (7–24) hours and (C) = stage 3 (25–48) hours.

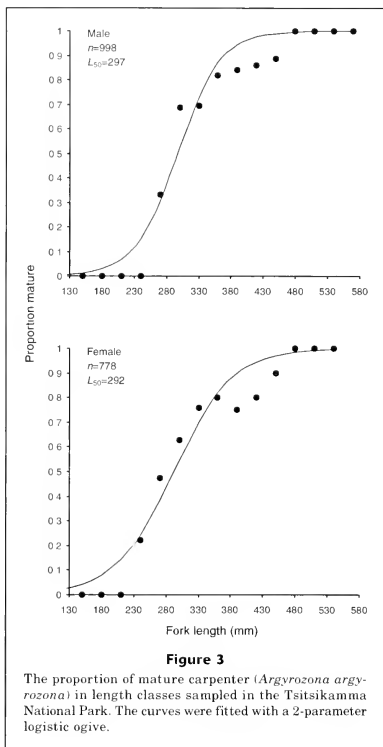
and stored an hourly average (Roberts²). Photoperiod data were downloaded from the South African Astronomical Observatory database.³ Pearson Rank correlation was used to measure the correlation between GSI and temperature, and GSI and photoperiod trends.

Results

Histological examination of the gonads revealed that although juveniles possess both testicular and ovarian tissue simultaneously (i.e., as hermaphrodites) they mature as either a male or female (Table 1) and are therefore late gonochorists (rudimentary hermaphrodites). Gametogenesis was similar to that described for other late gonochoristic sparids e.g., *Pterogymnus laniarius* (Booth and Hecht, 1997). The size at 50% maturity was estimated at 292 and 297 mm FL for females and males, respectively (Fig. 3), and in both cases is equivalent to an age of about five years (Brouwer and Griffiths 2004). A likelihood ratio test revealed that there was no significant difference between male and female L_{50} ($P>0.5$) or α ($P>0.1$). Complete (100%) maturity for both sexes occurred at 480 mm FL, an age of about 15 years (Brouwer and Griffiths 2004). The sex ratio was 1F:1.3M ($n=1776$); a chi-square test with Yates' correction factor revealed that this sex ratio was a significant difference from unity ($P<0.01$).

Three age-related POF stages were identified within the ovaries of captive spawned carpenter (Fig. 2). Stage-1 POFs (0–6 hours) were very loosely arranged and appeared as a long convoluted string with a large clearly defined lumen. The granulosa cells were clearly visible and widely spaced and had clearly visible nuclei (Melo, 1994). Stage-2 POFs (7–24 hours) are smaller and more densely packed but still have a visible lumen. The granulosa cells are closely packed and dense. Stage-3 POFs (25–48 hours) are small and densely packed. There is no lumen and the granulosa cells are closely arranged and no longer distinguishable from one another. After 48 hours at 16°C, POFs were no longer detectable.

Mean GSI and the proportions of ripe (stage-5) and ripe, running (stage-6) fish increased in November and remained high until April (Figs. 4 and 5), indicating that carpenter are summer spawners. The presence of early POFs from November to March (sample numbers being too low for April) supported the macroscopically determined spawning season. The monthly spawning fraction did, however, reveal that spawning frequency was highest in January and February when the fish spawned at two-day intervals and lowest in November and April when they were found to spawn every 2–3 days (Table 2).



Batch fecundity was positively correlated with both fish mass ($r=0.71$) and fork length ($r=0.71$). No correlation was found between fish length and relative batch fecundity (eggs/fish somatic mass) (Fig. 6). The proportion of fish with stage-1 POFs revealed that spawning frequency and length of the spawning season increased with fish length (Table 3). Accounting for size-related patterns in spawning season (Fig. 7) and frequency, we found that annual fecundity increased allometrically with mass (Fig. 8) and age (Table 4). Hydrated egg size was significantly smaller and more variable (average $1.0 \text{ mm} \pm 0.16$) in fish below the length at 100% maturity (480 mm FL) than those above this length ($1.1 \text{ mm} \pm 0.09$) (t -test, $P<0.005$).

² Roberts, M. J. 1999. CD-ROM, Tsitsikamma National Park oceanographic data, version 1.0. Marine and coastal management, Private Bag X2, Rogge Bay 8012, South Africa.

³ <http://www.sao.ac.za> [Accessed August 2000].

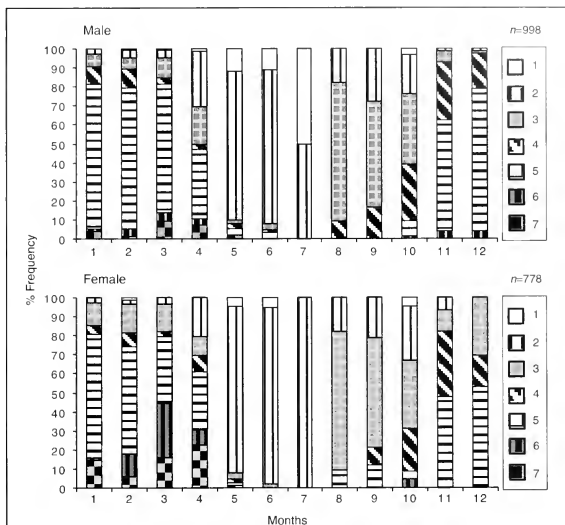


Figure 4

Monthly variation in the proportion of macroscopic gonad stages of carpenter (*Argyrosoma argyrosoma*) $>L_{50}$ caught in the Tsitsikamma National Park (March 1996–July 1999). Numbers in the legend refer to the gonad stages in Table 1. 1 = juvenile, 2 = immature, 3 = active, 4 = developing, 5 = ripe, 6 = ripe, running, and 7 = spent.

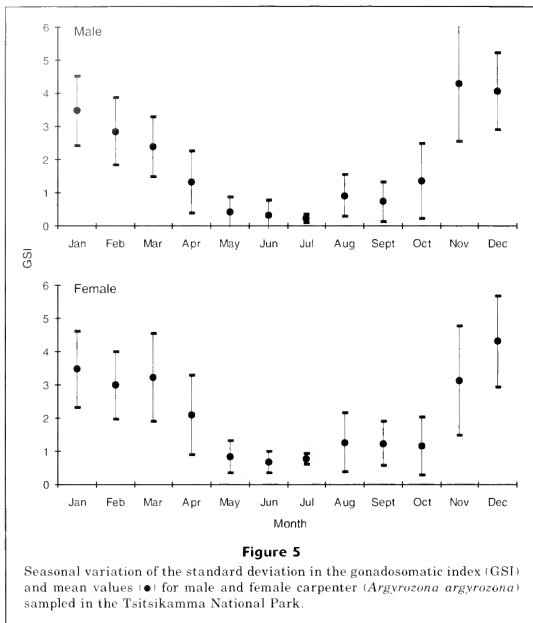
Table 2

Spawning frequency determined for carpenter (*A. argyrosoma*) from the proportion of ovaries with stage-1 POFs or macroscopically determined from hydrated oocytes.

Month	Spawning frequency (days)		% ovaries with hydrated oocytes	% ovaries with stage-1 POFs
	Macroscopic	POFs		
November	2.1 (44)	4.6 (23)	48	22
December	1.9 (53)	3.5 (21)	53	28
January	1.5 (119)	1.6 (5)	66	60
February	1.5 (160)	1.5 (35)	68	66
March	1.6 (99)	—	64	Not enough data
April	2.6 (49)	—	39	Not enough data

A positive relationship between temperature at the time of spawning (back-calculated from stage-1 POFs, assuming a delay of 6 hours) and the proportion of ova-

ries with stage-1 POFs indicated that spawning events were positively correlated with temperature ($r=0.93$) over the range 9°C and 22°C (Fig. 9). GSI was how-



ever strongly correlated ($r=0.86$) with photoperiod but exhibited a weak negatively relationship with seasonal temperature (Fig. 10).

Discussion

Late gonochorism, protandry, protogyny, and hermaphroditism are the recognized reproductive styles of sparids (Smale, 1988; Buxton and Garratt, 1990). Although carpenter were previously described as gonochoristic (Nepgen, 1977), microscopic examination of the gonads revealed that they are late gonochorists. The sex ratio calculated during this study (1 female:1.3 male) was typical for those observed for other late gonochorists (Griffiths et al., 2002).

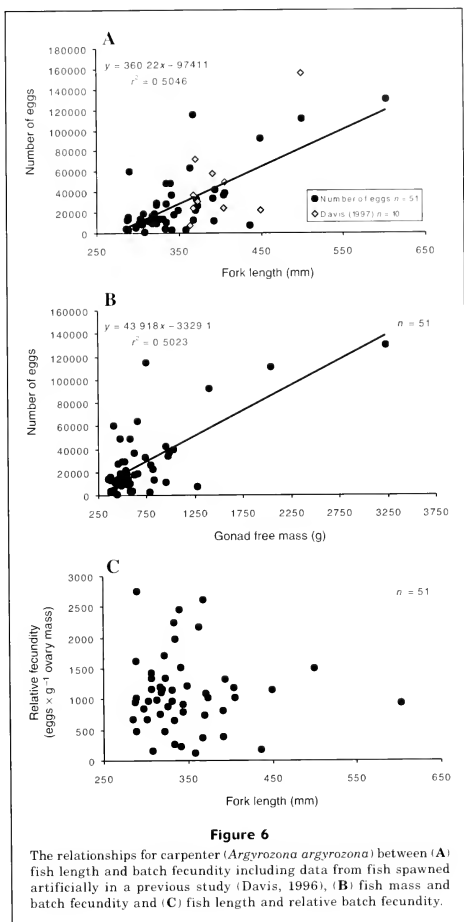
Upon reviewing 90 species of reef fish, Sadovy (1996) concluded that although GSIs reflect the gonad maturity patterns for a species, they are poor indicators of peak spawning times. By way of example, in red hind grouper (*Epinephelus guttatus*) yolked oocytes are present in the ovaries for four months of the year but actual spawning

Table 3

Spawning frequency (averaged over all months) and length of the spawning season calculated from the presence of stage-1 POFs in carpenter (*Argyrozona argyrozona*) ovaries in three size classes.

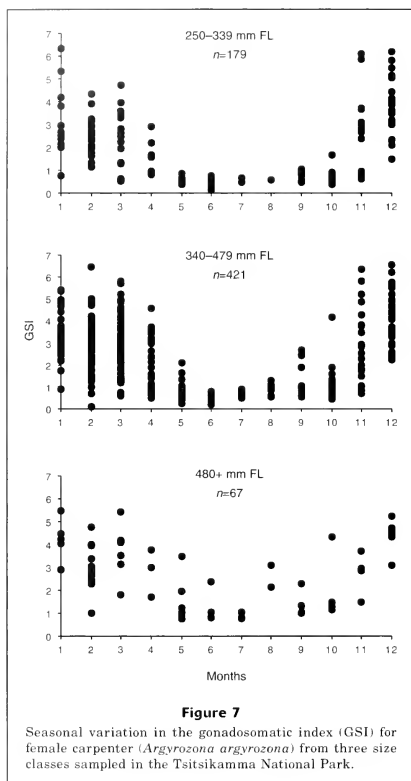
Size class (mm)	Average spawning frequency (days)	Spawning season (months)
250–339	9	6
340–479	4	7
480+	3.9	9

is limited to a period of 10 days (Sadovy, 1996). In the case of carpenter, however, the presence of POFs from November to April supports the six-month spawning season indicated by macroscopic methods (although in some larger individuals [>480 mm FL] hydrated



oocytes and POFs were found from October to May). Monthly spawning fraction and percentage of ovaries with hydrated oocytes nevertheless reached a peak during January and February (Table 2); these trends were not detected in the monthly GSIs. But given that the

macroscopic determinations of stage followed trends in the proportions of POFs that were present, we conclude that expensive and time-consuming histological analysis is not necessary for determining spawning peaks for this species.



Apart from being indicators of spawning seasonality, GSI trends can provide insight into the mating patterns of a species (Sadovy, 1996). Pair-spawning sparids such as *Chrysoblephus laticeps* have low male GSI ($\pm 10\%$ of female) during the spawning season (Buxton, 1990). Although the spawning behavior of carpenter has not been documented, the GSI of males (average 3.0 ± 1.4) was similar to that of females (average 3.3 ± 1.4) during the spawning season (Fig. 4). The large testes size suggests that carpenter are group spawners and that sperm competition is high (Sadovy, 1996). Further evidence for group spawning is the lack of sexual dimor-

phism in this species (Smale, 1988; Mann and Buxton, 1998; Griffiths et al., 2002).

Like many other South African sparids, carpenter are summer spawners (Buxton and Clarke, 1986; Buxton and Clarke, 1991; Buxton, 1993). Although various environmental cues have been suggested for this seasonal spawning, it is probably a combination of events that leads to gonad maturation and spawning. Smale (1988) and Garratt (1985) speculated that increases in gonad activity of *Petrus rupestris* and *Chrysoblephus puniceus* were attributed to an increase in photoperiod and water temperature respectively; Scott and Pankhurst (1992),

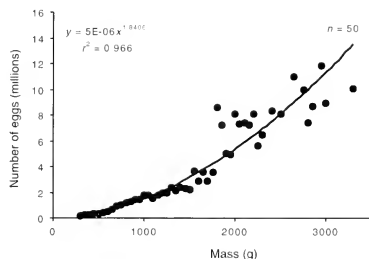


Figure 8

The relationship between annual fecundity and fish weight for carpenter (*Argyrozona argyrozona*) in the Tsitsikamma National Park.

however, showed that seasonal temperature regulated gonad development for *Pagrus aratus*. Based on the data collected during our study, photoperiod appears to be responsible for the onset of gonad maturation in carpenter; when day length increases (but water temperature is variable) in September and October, and their gonads begin to develop (Fig. 10). Photoperiod was also highly correlated with GSI ($r=0.86$), whereas temperature showed a weakly negative relationship ($r=-0.16$).

Nepgen (1977) calculated spawning frequency for this species with an oocyte-size-frequency analysis of inactive females. Finding only one peak in the oocyte-size-frequency distribution, he assumed that carpenter spawned only once a year. In our study POFs and various yolk stage oocytes were found to occur simultaneously, proving that carpenter are serial spawners. Accounting for monthly trends in spawning frequency and the length of the spawning season, carpenter in the Tsitsikamma National Park are estimated to spawn at least 30 times per year. This spawning frequency is similar to other predatory reef fishes, e.g., *Mycteroperca microlepis* (30–40 times per year) (Collins et al., 1998). Nevertheless, as with other species (Danilowicz, 1995), spawning fraction in carpenter during the spawning season was highly correlated with water temperature ($r=0.931$) (Fig. 9), indicating that short-term cold water upwellings, a common feature of the TNP during summer (Schumann et al., 1982), may negatively impact annual carpenter fecundity in this area.

Although fecundity in fishes is highly variable between individuals (Sadovy 1996), absolute fecundity increases with size (Hunter et al., 1985; Davis and West, 1993; Wilson and Nieland, 1994; Collins et al., 1998). In our study absolute annual fecundity increased markedly with fish size (Table 4) and spawning season was longer for large fish (Fig. 7) (Table 3). The positive

Table 4

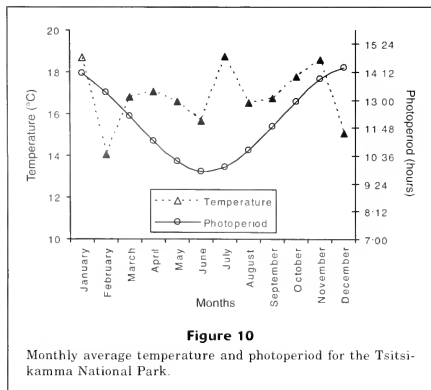
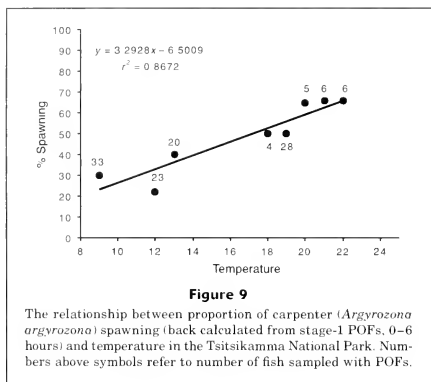
Age-based annual fecundity of carpenter (*Argyrozona argyrozona*) in the Tsitsikamma National Park.

Age (yr)	Number of eggs (millions)
1	0
2	0
3	0
4	0.143
5	0.288
6	0.367
7	0.441
8	0.870
9	1.014
10	1.228
11	1.498
12	1.706
13	1.763
14	2.260
15	2.233
16	2.427
17	3.132
18	3.175
19	5.363
20	6.308
21	6.308
22	7.815
23	7.430
24	6.480
25	7.421
26	8.363
27	8.363
28	8.064
29	10.397
30	11.808

correlation of batch fecundity and fish size ($r=0.71$), coupled with the increased length of the spawning season for the older fish, greatly increases the absolute annual fecundity of larger fishes (Fig. 8). Sadovy (1996) noted that for red snapper (*Lutjanus compechanus*) one large female (601 mm FL) will produce as many eggs as 212 small (420 mm FL) females. Similarly, one large female carpenter of 3.3 kg will produce as many eggs as 72 small ones of 0.3 kg. In addition to higher fecundity, the larger fish produce significantly larger eggs and presumably more viable larvae (Ojanguren et al., 1996; Pepin and Anderson, 1997).

Exploited populations were traditionally managed to maximize growth (Griffiths, 1997). However it is imperative to maintain sufficient numbers of reproduc-

tive adults to ensure egg production and avoid recruit-ment failure. To address proper management of line-caught fish in South Africa, spawner biomass per recruit models have been used (Griffiths, 1997). One assumption of this approach is that fecundity is linearly related to spawning biomass, regardless of individual size (Buxton, 1992). Because our study has shown that fecundity in carpenter is allometrically related to individual mass, egg-per-recruit models would be more appropriate for future stock assessment of this species.



Acknowledgments

We thank the staff at South African National Parks, for accommodation at the Tsitsikamma National Park and for use of their vessel. John Allen and Karoels Piterse are thanked for many hours at sea. Yolande Melo is thanked for her assistance with histological preparation and interpretation and Jeanine Van der Pol for assistance in laboratory and Tony Booth and two anonymous referees for constructive comments on this manuscript. This research was funded by the Marine Living Resources Fund.

Literature cited

- Booth, A. J., and T. Hecht.
1997. A description of gametogenesis in the panga *Pterogymnus laniarius* (Pisces: Sparidae) with comments on changes in maturity patterns over the past two decades. *S. Afr. J. Zool.* 32(2):49–53.
- Brouwer, S. L., and M. H. Griffiths.
2004. Age and growth of *Argyrozona argyrozona* (Pisces: Sparidae) in a Marine Protected Area: an evaluation of methods based on whole otoliths, sectioned otoliths and mark recapture. *Fish. Res.* 61:1–12.
- Buxton, C. D.
1990. The reproductive biology of *Chrysolephus laticeps* and *C. cristiceps* (Teleostei: Sparidae). *J. Zool. Lond.* 220:497–511.
1992. The application of yield-per-recruit models to two South African sparid reef species, with special consideration to sex change. *Fish. Res.* 15:1–16.
1993. Life-history changes in exploited reef fishes on the east coast of South Africa. *Environ. Biol. Fish.* 36: 47–63.
- Buxton, C. D., and J. R. Clarke.
1986. Age growth and feeding of the blue hottentot *Pachymetopon aeneum* (Teleostei: Sparidae) with notes on reproductive biology. *S. Afr. J. Zool.* 21:33–38.
1991. The biology of the white musselcracker *Sparodon durbanensis* (Pisces: Sparidae) on the Eastern Cape coast, South Africa. *S. Afr. J. Mar. Sci.* 10:285–296.
- Buxton, C. D., and P. A. Garratt.
1990. Alternative reproductive styles in seabreams (Pisces: Sparidae). *Environ. Biol. Fish.* 28:113–124.
- Collins, L. A., A. G. Johnson, C. C. Koenig, and M. S. Baker.
1998. Reproductive patterns, sex ratio, and fecundity in gage, *Mycteroperca microlepis* (Serranidae), a protogynous grouper from the northeastern Gulf of Mexico. *Fish. Bull.* 96:415–427.
- Danilowicz, B. S.
1995. The role of temperature in spawning of damselfish *Dascyllus albisella*. *Bull. Mar. Sci.* 57(3): 624–636.
- Davis, J. A.
1996. Investigations into the larval rearing of

- two South African sparid species. M.S. thesis, 138 p. Rhodes Univ., Grahamstown, Eastern Cape, South Africa.
- Davis, T. L. O., and G. J. West.
1993. Maturation, reproductive seasonality, fecundity, and spawning frequency in *Lutjanus vittus* (Quoy and Gaimard) from the North West shelf of Australia. Fish. Bull. 91:224-236.
- Garratt, P. A.
1985. The offshore linefishery of Natal. II. Reproductive biology of the sparids *Chrysoblephus puniceus* and *Cheimerius nufar*. Invest. Rep. Oceanogr. Res. Inst. 63:1-21.
- Griffiths, M. H.
1997. The application of per-recruit models to *Argyrosomus inodorus*, an important South African sciaenid fish. Fish. Res. 30:103-115.
2000. Long-term trends in the catch and effort of commercial linefish off South Africa's Cape Province: snapshots of the 20th century. S. Afr. J. Mar. Sci. 22:81-110.
- Griffiths, M. H., C. Wilke, A. J. Penny, and Y. Melo.
2002. Life history of white stumpnose *Rhabdosargus globiceps* (Pisces: Sparidae) off South Africa. S. Afr. J. Mar. Sci. 28:1-300.
- Hunter, J. R., N. C. H. Lo, and R. J. H. Leong.
1985. Batch fecundity and multiple spawning in fishes. In An egg production method for estimating spawner biomass of pelagic fish: application to the northern anchovy, *Engraulis mordax* (R. Lasker, ed.), 67-77. NOAA Tech. Rep. NMFS 36.
- Hunter, J. R., and B. J. Macewicz.
1985. Rates of atresia in the ovary of captive and wild northern anchovy *Engraulis mordax*. Fish. Bull. 83(2): 119-136.
- Lowerre-Barbieri, S. K., and L. R. Barbieri.
1993. A new method of oocyte separation and preservation for fish reproduction studies. Fish. Bull. 91: 165-170.
- Mann, B. Q., and C. D. Buxton.
1998. The reproductive biology of *Diplodus sargus capensis* and *D. cervinus hottentotus* (Sparidae) off the South-East Cape coast, South Africa. Cybium 22(1):31-47.
- Melo, Y. C.
1994. Spawning frequency of the anchovy *Engraulis capensis*. S. Afr. J. Mar. Sci. 14:321-331.
- Nepgen, C. S. V.
1977. The biology of the hottentot *Pachymetopon blochii* (Val.) and the silverfish *Argyrozona argyrozona* (Val.) along the cape south-west coast. Invest. Rep. Div. Sea Fish. Rep. S. Afr. 105:1-35.
- Ojanguren, A. F., and F. G. Reyes-Gavilan F. Brana.
1996. Effects of egg size on offspring development and fitness in brown trout, *Salmo trutta* L. Aquaculture 147(1-2):9-20.
- Osborne, R. F., Y. C. Melo, M. D. Hofmeyer, and D. W. Japp.
1999. Serial spawning and batch fecundity of *Merluccius capensis* and *M. paradoxus*. S. Afr. J. Mar. Sci. 21:2111-216.
- Peplin, D., C. Orr, and J. T. Anderson.
1997. Time to hatch and larval size in relation to temperature and egg size in Atlantic cod (*Gadus morhua*). Can. J. Fish. Aquat. Sci. 54 (suppl. 1):2-10.
- Sadovy, Y. J.
1996. Reproduction of reef fish species. In Reef fisheries (N. V. C. Polunin and C. M. Roberts, eds.), p. 15-59. Chapman and Hall, London.
- Schumann, E. H., L.-A. Perrins, and I. T. Hunter.
1982. Upwelling along the South Coast of the Cape province, South Africa. S. Afr. J. Sci. 78:238-242.
- Scott, S. G., and N. W. Pankhurst.
1992. Interannual variation in the reproductive cycle of the New Zealand snapper *Pagrus aratus* (Bloch & Schneider) (Sparidae). J. Fish Biol. 41:685-696.
- Smale, M. J.
1988. Distribution and reproduction of the reef fish *Petrus rupestris* (Pisces: Sparidae) off the coast of South Africa. A. Afr. J. Zool. 1988. 23(4):272-287.
- Smith, M. M., and P. C. Heemstra.
1986. Smiths Sea fishes, 1047 p. Southern Book Publishers, Johannesburg, South Africa.
- Wilson, C. A., and D. L. Nieland.
1994. Reproductive biology of red drum, *Sciaenops ocellatus*, from the neritic waters of the northern Gulf of Mexico. Fish. Bull. 92:841-850.

Abstract—During the 1990s, sea otter (*Enhydra lutris*) counts in the Aleutian archipelago decreased by 70% throughout the archipelago between 1992 and 2000. Recent aerial surveys in the Aleutians did not identify the eastward extent of the decline; therefore we conducted an aerial survey along the Alaska Peninsula for comparison with baseline information. Since 1986, abundance estimates in offshore habitat have declined by 27–49% and 93–94% in northern and southern Alaska Peninsula study areas, respectively. During this same time period, sea otter density has declined by 63% along the island coastlines within the south Alaska Peninsula study area. Between 1989 and 2001, sea otter density along the southern coastline of the Alaska Peninsula declined by 35% to the west of Castle Cape but density increased by 4% to the east, which may indicate an eastward extent of the decline. In all study areas, sea otters were primarily concentrated in bays and lagoon, whereas historically, large rafts of otters had been distributed offshore. The population declines observed along the Alaska Peninsula occurred at roughly the same time as declines in the Aleutian islands to the east and the Kodiak archipelago to the west. Since the mid-1980s, the sea otter population throughout southwest Alaska has declined overall by an estimated 56–68%, and the decline may be one of the most significant sea otter conservation issues in our time.

Decline in sea otter (*Enhydra lutris*) populations along the Alaska Peninsula, 1986–2001

Douglas M. Burn

Angela M. Doroff

Marine Mammals Management Office

U.S. Fish and Wildlife Service

1011 East Tudor Road

Anchorage, Alaska 99503

E-mail address (for D. M. Burn), douglas_burn@fws.gov

During the 1990s, the sea otter (*Enhydra lutris*) population in the Aleutian archipelago declined at a rate of 17.5%/yr and, overall, counts decreased by 70% throughout the archipelago between 1992 and 2000 (Doroff et al., 2003). By modeling population trends back to the mid-1980s, Burn et al. (2003) estimated the population in the Aleutian Island chain decreased by 65,000 sea otters and was at about 10% of its carrying capacity in 2000. The 2000 aerial survey of Doroff et al. (2003) did not identify an eastward extent of the population decline however; therefore additional sea otter surveys along the Alaska Peninsula were needed.

Historic information on population status and trends is sparse for sea otters along the Alaska Peninsula. Sea otters were exploited to near extinction in the commercial fur trades (1742–1911) and were removed from large portions of their historic range worldwide (Kenyon, 1969; Lensink, 1962). At the time of their protection in 1911 by an international fur seal treaty, there were 13 remnant populations remaining worldwide, 11 of which persisted and grew to recolonize much of the former range of this species (Kenyon, 1969). Studies of both remnant native and translocated sea otter populations have indicated a pattern of colonization with high population growth rates up to 20% per year, and an expansion into adjacent, unoccupied habitat (Estes, 1990).

One remnant population survived on the north side of the Alaska Pen-

insula near Unimak Island (Kenyon, 1969; Schneider, 1976). Sea otter habitat in this area is unique in that shallow water (less than 100 m) extends up to 50 km offshore, covering more than 10,000 km of open water. The remnant population in this area likely numbered fewer than 100 sea otters in 1911 (Kenyon, 1969). This population grew steadily and expanded its range to the northeast along the Peninsula until 1970, when extreme sea ice conditions temporarily reduced the range and likely the size of the population (Schneider and Faro, 1975). By 1976, most of the sea otters in this area were concentrated between Cape Mordvinof and Cape Leontovich (Schneider, 1976).

In addition to the remnant population on the north side of Unimak Island, there were also two remnant populations of sea otters located to the south of the Alaska Peninsula in the Sandman Reefs and the outer Shumagin Islands (Kenyon, 1969). Sea otter habitat along the southern Alaska Peninsula differs from the northern side and comprises primarily rocky, mixed substrate, and extensive offshore reefs (Brueggeman et al.¹). In the Sandman Reefs a small number of sea otters were sighted in

¹ Brueggeman, J. J., G. A. Green, R. A. Grotefendt, and D. G. Chapman. 1988. Aerial surveys of sea otters in the northwestern Gulf of Alaska and the southeastern Bering Sea. Minerals Management Service and NOAA final report, 87 p. Minerals Management Service, Anchorage, AK. [Contract no. 85-ABCV-00983.]

1922, and by 1962 the population had grown to an estimated 1625 sea otters (Lensing, 1962; Kenyon, 1969). Around the same time, the population in the Shumagin Islands was estimated to be 2724 sea otters (Kenyon, 1969).

The first systematic surveys of sea otter abundance along the north side of the Alaska Peninsula were conducted in the mid-1970s (Schneider, 1976), followed by surveys in 1982 and 1983 by Cimberg et al.² Brueggeman et al.¹ conducted quarterly surveys of both the northern and southern Peninsula in 1986 to assess sea otter abundance and seasonal distribution. The surveys conducted in 1986 provided seasonal estimates of abundance during a single, ice-free year, and a clear picture of habitat use in the mid-1980s along the Alaska Peninsula (Brueggeman et al.¹).

The sea otter surveys described above were concentrated along the western end of the Alaska Peninsula where remnant populations existed and appeared to have recovered. By the late 1980s, sea otters had also returned to the nearshore waters of the entire peninsula as far east as Cape Douglas (DeGange et al.³). Prior to this survey in 1989, little was known about sea otter distribution and abundance on the Alaska Peninsula east of Kupreanof Point.

The objectives of our study were 1) to assess current sea otter distribution and abundance along the northern and southern Alaska Peninsula, 2) to contrast our results with prior surveys conducted in 1986 and 1989, and 3) to relate these data to the observed sea otter population declines observed elsewhere in southwest Alaska. We repeated the aerial survey methods developed by Brueggeman et al.¹ for sea otter habitat along the Alaska Peninsula which consisted of a combination of strip transects in offshore habitat (to the 70-m isobath) and coastline surveys (≤ 1 km of shore) of island groups within the study area. We also repeated the coastline surveys of DeGange et al.² to determine the eastward extent of the decline.

Materials and methods

Offshore survey areas

The north Alaska Peninsula (NAP) study area ranged from Cape Mordvinof on Unimak Island in the west to Cape Seniavin in the east. This area was further subdivided

into two subunits (NAPa and NAPb), and a line at 162°W longitude divided the two subunits (Brueggeman et al.¹). The south Alaska Peninsula (SAP) study area ranged from the Ikatan Peninsula in the west to the Shumagin Islands in the east. The seaward extent of both the NAP and SAP study areas was the approximate 70-m depth contour (Fig. 1A).

The strip transect method developed by Brueggeman et al.¹ consisted of a series of transects oriented north-south which were spaced every three minutes of longitude throughout the study area. In 1986, surveys were flown in a DeHavilland Twin Otter aircraft equipped with bubble windows at an altitude of 92 m and an airspeed of 185 km/h. Two observers, one on each side of the aircraft, relayed sea otter sighting information to a data recorder seated in the aft section of the aircraft. Sea otter sightings were grouped into three distance intervals spaced at right angles to the transect line: 0.0–0.23 km, 0.23–0.46 km, and 0.46–0.93 km. These distance zones were determined by using a clinometer to place marks on the inside of the bubble windows. Environmental information on sea state, visibility, and glare was recorded throughout the survey.

In May 2000 and April 2001, we repeated the survey conducted by Brueggeman et al.¹ using similar methods, with the exception that our survey aircraft was an Aero Commander equipped with bubble windows and we grouped sea otter sightings into five distance intervals: 0.0–0.115 km, 0.115–0.23 km, 0.23–0.345 km, 0.345–0.46 km, and 0.46–0.575 km.

Coastline survey areas

In 1986, Brueggeman et al.¹ also surveyed the coastlines of 22 islands on the south side of the Alaska Peninsula quarterly at a distance of 0.46 km from shore, using the same aircraft, altitude, and airspeed as in the offshore area surveys (Fig. 1B). In 1989, DeGange et al.² surveyed the coastlines of these same islands and the Alaska Peninsula from False Pass to Cape Douglas (Fig. 1C). The 1989 survey was conducted from Bell 206 and Hughes 500 helicopters at a distance of 0.2 km from shore at an altitude of 92 m and an airspeed of 130 km/h. We used similar methods (0.23 km from shore, altitude 92 m, airspeed 185 km/h) to survey the coastlines of these 22 islands and the Alaska Peninsula in April and May 2001. The area of the offshore surveys was adjacent to, but did not overlap, the area of the coastline surveys. Coastline surveys were not conducted in the NAP study area.

Offshore survey analyses

Prior to the analysis of the 2000–01 offshore survey data, we tested several assumptions made in the 1986 analysis regarding the detectability of sea otters as a function of 1) survey strip width, 2) survey conditions, and 3) time of day. We examined the distribution of sea otter sightings by distance zone using a chi-square analysis to determine the appropriate survey strip width to use

² Cimberg, R. L., D. P. Costa, and P. A. Fishman. 1984. Ecological characterization of shallow subtidal habitats in the north Aleutian Shelf. OCSEAP Final Rep. no. 4197, 99 p. U.S. Dept. of Commerce, National Oceanographic and Atmospheric Administration, Anchorage, Alaska 99501.

³ DeGange, A. R., D. C. Douglas, D. H. Monson and C. M. Robbins. 1994. Surveys of sea otters in the Gulf of Alaska in response to the Exxon Valdez oil spill. Final report to the Exxon Valdez Oil Spill Trustee Council, Marine Mammal Study 6-7, 11 p. U.S. Fish and Wildlife Service, Anchorage, Alaska 99503.

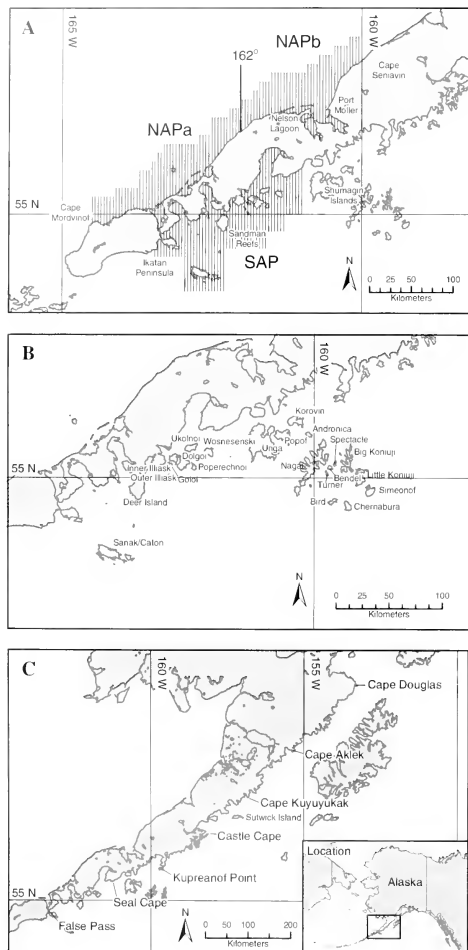


Figure 1

Sea otter (*Enhydra lutris*) survey areas along the Alaska Peninsula. (A) Offshore areas. (B) South Alaska Peninsula Islands. (C) Alaska Peninsula coastline. Surveyed areas in (B) and (C) include a 0.46-km zone adjacent to shore.

for estimating abundance. We calculated an encounter rate as the number of sea otter groups per km of survey effort and used this rate to examine the effects of time of day and environmental conditions (wave height, and visibility) on detectability of sea otters.

At the time of the surveys in 1986, researchers had documented a core resting period for sea otters which occurs about mid-day (Garshelis and Garshelis, 1984; Estes, 1977). As a result, Brueggeman et al.¹ subset the 1986 data using only effort and observations recorded between 0830 and 1430 hours local sun time for their abundance estimates. Recent studies indicate activity patterns for sea otters are strongly linked to sex, age, weather condition, season, and time of day (Gelatt et al., 2002). We tested the assumption that sea otters were more visible during the core resting period using a *t*-test of the encounter rate for each transect during presumed rest and nonrest periods for the 1986 and the 2000–01 data.

We measured the area of the NAP and SAP study areas using a geographic information system (Arc/Info). Our measurements differed from those of Brueggeman et al.¹ presumably because the original researchers had not used an equal-area map projection in their calculations. Like Brueggeman et al.¹ we estimated abundance of sea otters in the Alaska Peninsula offshore areas using the modified ratio of means estimator (method 1) of Estes and Gilbert (1978). Noting computational errors in the original analysis, we recalculated abundance estimates from the original 1986 data of Brueggeman et al.¹ The proportion of sea otters within the survey swath that went undetected by observers was not estimated in either our survey or the surveys of Brueggeman et al.¹; therefore all abundance estimates were biased low to an unknown degree. We computed the proportional change in abundance between survey periods ($(N_{t2} - N_{t1}) / N_{t1}$) as a range, using the minimum and maximum estimates from 1986 as a baseline and assuming no significant difference in the proportion of sea otters detected between surveys.

Coastline survey analyses

We calculated the area surveyed as the product of the coastline length and the survey strip width and calculated the density of sea otters per km² surveyed. Once

again assuming no significant difference in the proportion of sea otters detected between surveys, we computed the proportional change in density between survey periods ($(D_{t2}-D_{t1})/D_{t1}$) of sea otter density at each island within the study area between 2001 and 1986 (Brueggeman et al.¹) and each Alaska Peninsula coastline segment between 2001 and 1989 (DeGange et al.²).

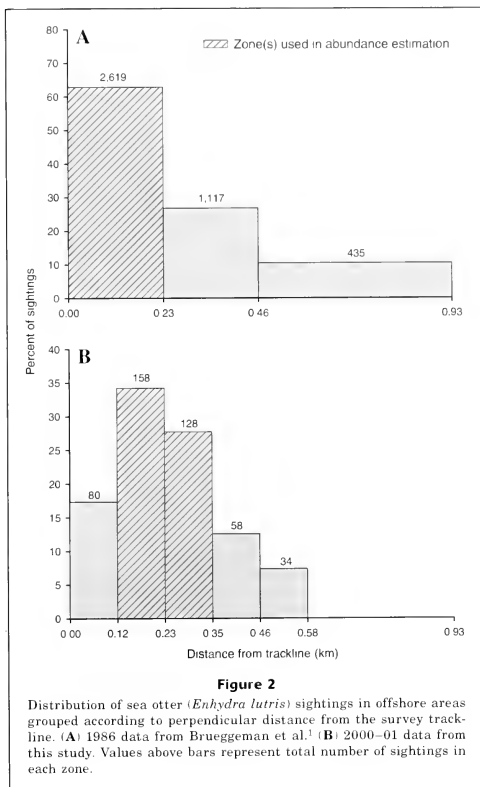
Results

Offshore surveys

In 1986, Brueggeman et al.¹ flew four surveys and an average of 3676 km of transect effort per survey. The majority (59%) of the 1986 survey effort was conducted in Beaufort sea state 2 (wind less than 7.4–11.1 km/h, no whitecaps) or less; and 95% of the survey effort was conducted with visibility categorized as good or better. In May 2000 and April 2001, we flew 6334 km of transects and 56% of our effort was conducted in Beaufort sea state 2 or less; 97% of our effort was conducted in visibility categorized as good or better.

In 1986, sea otter detection probability was not uniform between sighting zones ($\chi^2=1796$, $df=2$, $P<0.0001$) and substantially more sea otters were observed than expected in the 0.0–0.23 km distance zone (Fig. 2A). As a result, Brueggeman et al. (1988) used only this zone in their calculation of sea otter abundance. In our 2000–01 surveys, sea otter detection probability was also not uniform ($\chi^2=217$, $df=5$, $P<0.0001$). The observed frequency of sea otter sightings exceeded the expected value in our second (0.115–0.230 km) and third zones (0.230–0.345 km) but in the first zone (0.0–0.115 km) we recorded only half as many sea otter sightings as in the second zone (Fig. 2B). Therefore, only sightings from the second and third zones were used in our calculation of sea otter abundance. As a result, the overall width of the survey strip was the same for the 1986 and the 2000–01 surveys (0.46 km), but our strip was offset by 0.115 km from the trackline. The proportion of all sea otter sightings was similar between the usable zones in 1986 (62.8%) and 2000–01 (62.4%).

Sea otter encounter rate (otter groups/km) decreased as wave height increased and visibility conditions became worse in both the 1986 and 2000–01 surveys. As noted by Kenyon (1969), wave height has a profound influence on the ability of observers to detect sea otters. Prior to calculating abundance estimates for both



1986 and 2001, we subset both data sets to include only those transects where Beaufort sea state was ≤ 2 and visibility was categorized as good or excellent for counting sea otters. This procedure reduced the 1986 usable survey effort by 42%, and the 2000–01 survey efforts by 44%.

Sea otter encounter rates did not differ significantly between rest and nonrest periods in the 1986 data ($t=1.63$, $df=79$, $P<0.1064$). Likewise, there was no difference in encounter rates for rest and nonrest periods in 2000–01 ($t=-0.79$, $df=71.6$, $P<0.4327$). As a result, we did not exclude any survey effort and sea otter sightings based on time of day.

Table 1

Sea otter (*Enhydra lutris*) population estimates for Alaska Peninsula offshore study areas. Study areas: north Alaska Peninsula a [NAPa] = 6257 km²; and b [NAPb] = 5531 km²; south Alaska Peninsula (SAP) = 9469 km².

Survey area	Survey date	Total number of transects	Area sampled (km ²)	Number of otter groups	Density (groups/km ²)	Group abundance	Mean group size	Estimated abundance	95% confidence interval
NAPa	March 1986	35	446.2	243	0.545	3408	2.082	7096	±2558
	Late June–early July 1986	39	398.8	124	0.311	1945	2.177	4236	±1818
	August 1986	31	421.7	225	0.534	3338	2.169	7240	±2978
	October 1986	36	511.6	274	0.536	3351	1.982	6642	±2050
	May 2000	40	552.3	18	0.033	204	1.833	374	±318
NAPb	Late June–early July 1986	29	469.5	98	0.209	1155	1.939	2238	±840
	August 1986	6	120.4	23	0.191	1056	1.870	1975	±2212
	October 1986	14	314.3	42	0.134	739	1.214	897	±467
	May 2000	40	443.3	184	0.415	2296	1.897	4354	±3007
SAP	March 1986	26	358.3	254	0.709	6712	2.071	13,900	±6456
	Late June–early July 1986	33	424.8	227	0.534	5060	2.775	14,042	±5178
	October 1986	33	442.6	418	0.944	8943	1.957	17,500	±5768
	April 2001	38	631.2	22	0.035	330	3.045	1005	±1597

The estimated abundance of sea otters decreased by 91–94% in the NAPa study area, which ranged from 4236–7240 in 1986 to 374 in 2000 (Table 1). Estimated abundance increased by 95–385% in the NAPb study area, which ranged from 897 to 2238 in 1986 to 4354 in 2001. Overall, abundance estimates in the NAP study area declined by 27–49% between 1986 and 2000. Within the NAP area, sea otters were distributed primarily near the coast rather than further offshore as was observed in 1986 (Fig. 3). In May 2000, the majority of sightings occurred in the Port Moller and Nelson Lagoon areas, which had contained few otters during the 1986 surveys. Estimated abundance within the SAP study area declined by 93–94%, from 13,900–17,500 in 1986 to 1005 in 2001. Similar to the NAP results, areas that had previously supported dense aggregations of sea otters were largely vacant in 2001 and the areas of highest concentrations were in bays and lagoons.

Coastline survey analyses

Between 1986 and 1989 there was considerable variability in sea otter counts at islands in the south Alaska Peninsula study area (Table 2). Some areas had increased (Sanak, Caton, and the Pavlof Islands) while others decreased (Deer Island, Shumagin Islands). However by 2001, sea otter counts and density had decreased at nearly all islands and net losses of over 100 otters occurred at Deer, Dolgoi, Goloi, Unga, and Nagai islands. Overall, sea otter counts at these islands declined from 2174 in 1986 to 402 in 2001—a 63% decline in density.

In April and May 2001 we surveyed approximately 3800 km of coastline from Cape Douglas to False Pass (Table 3). Sea otter density in 2001 was 35% lower than

in 1989 for the three westernmost coastline segments from False Pass to Castle Cape (1782 km of coastline). To the east of Castle Cape, sea otter density was 4% greater in 2001 than in 1989 (2018 km of coastline). These results indicate that an eastward extent of the decline along the Alaska Peninsula may occur in the area of Castle Cape. Overall, sea otter density declined by 12.4% along the coastline of the Alaska Peninsula from False Pass to Cape Douglas between 1989 and 2001.

Discussion

When compared to surveys conducted in 1986, our results indicated that sea otter abundance has declined severely in the SAP and NAPa study areas along the Alaska Peninsula, whereas sea otter abundance increased in the NAPb study area (specifically Port Moller) and east of Castle Cape along the south side of the Peninsula. To determine the geographic extent and magnitude of the sea otter population decline, current data were needed to assess population abundance and trends along the Alaska Peninsula.

Variations in survey methods limited our ability to assess population trends for the Alaska Peninsula prior to 1986. In 1976, the sea otter population along the NAP was estimated to be 17,000 and continued range expansion was expected (Schneider, 1976). In 1982–83, seasonal estimates of sea otter abundance in the NAP study area varied between March (1454), August (10,325), and October (1880) which led Cimberg et al.² to speculate that there was a large-scale seasonal migration of sea otters between the Bering Sea and North Pacific Ocean. Sea otter distribution and abundance

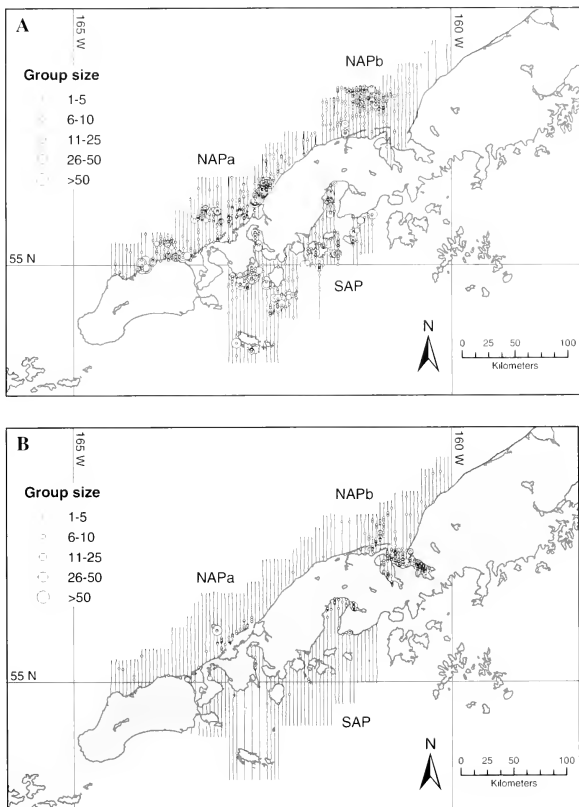


Figure 3

All survey transects and sea otter (*Enhydra lutris*) sightings in offshore areas. (A) Late June–early July 1986. (B) May 2000 (north Alaska Peninsula [NAP], a and b), April 2001 (south Alaska Peninsula [SAP]).

remained relatively constant over the spring, summer, and fall seasons for both the NAP and SAP study areas in 1986 which led Brueggeman et al.¹ to conclude that there was no indication that sea otters were redistributed from the northern to the southern Peninsula during the winter months. Instead, Brueggeman et al.¹

attributed the differences in the survey results between 1982–83 and 1986 to the viewing conditions and wind speed in which Cimberg et al.² conducted their March and October surveys. Although both the 1976 and 1983 estimates were adjusted for sea otters missed by observers, the 1986 estimates were not. Evans et al.⁴

Table 2

Alaska Peninsula island coastline lengths, sea otter (*Enhydra lutris*) counts, sea otter densities, and estimated population change. Survey strip width for the 1986 survey was 0.92 km, for 1989 it was 0.4 km, and for 2001 it was 0.46 km.

Island name	Coastline length (km)	Sea otters counted			Sea otter density (otters/km ²)			% change in density 1989–2001
		1986	1989	2001	1986	1989	2001	
Sanak and Caton	178	13	168	12	0.08	2.36	0.15	+84.6
Deer Island	61	245	71	19	4.35	2.90	0.67	-84.5
Dolgoi	94	185	93	15	2.14	2.47	0.35	-83.8
Goloi	14	113	62	1	8.77	11.07	0.16	-98.2
Inner Iliask	13	77	68	9	6.44	13.07	1.51	-76.6
Outer Iliask	17	82	305	4	5.24	44.85	0.51	-90.2
Wosnesenski	32	29	28	3	0.99	2.19	0.20	-79.3
Ukolnoi	38	54	133	21	1.54	8.75	1.20	-22.2
Poperechnoi	22	80	26	1	3.96	2.95	0.10	-97.5
Unga	231	568	275	182	2.67	2.98	1.71	-35.9
Popof	72	72	73	4	1.09	2.53	0.12	-88.9
Korovin	65	101	47	9	1.69	1.81	0.30	-82.2
Andronica	22	31	15	0	1.53	1.70	0.00	-100.0
Nagai	342	184	141	52	0.58	1.03	0.33	-43.5
Big Koniuji	160	52	18	33	0.35	0.28	0.45	+26.9
Turner and the Twins	16	6	9	0	0.41	1.41	0.00	-100.0
Bendel	17	35	7	2	2.24	1.03	0.26	-88.6
Spectacle	15	17	12	7	1.23	2.00	1.01	-17.6
Little Koniuji	95	65	20	0	0.74	0.53	0.00	-100.0
Simeonof	49	65	5	24	1.44	0.26	1.06	-26.2
Chernabura	30	20	2	0	0.72	0.17	0.00	-100.0
Bird	31	80	11	4	2.81	0.89	0.28	-90.0
Total	1614	2174	1589	402	1.46	2.46	0.54	-63.0

Table 3

Alaska Peninsula coastline segment lengths, sea otter (*Enhydra lutris*) counts, sea otter densities, and estimated population change. Survey strip width for the 1989 survey was 0.4 km; for 2001 it was 0.46 km.

Coastline segment 1989–2001	Coastline length (km)	Sea otters counted		Sea otter density (otters/km ²)		% change in density
		1989	2001	1989	2001	
False Pass to Seal Cape	715	622	461	2.17	1.40	-35.6
Seal Cape to Kupreanof Point	370	196	50	1.32	0.29	-77.8
Kupreanof Point to Castle Cape	697	48	25	0.17	0.08	-54.7
Castle Cape to Cape Kuyuyukak	639	1007	1193	3.94	4.06	+3.0
Cape Kuyuyukak to Cape Aklek	495	177	352	0.89	1.55	+72.9
Cape Aklek to Cape Douglas	814	570	497	1.75	1.33	-24.2
Sutwick Island	70	12	73	0.43	2.27	+429.0
Total	3800	2632	2651	1.73	1.52	-12.4

estimated that observers flying in a Twin Otter aircraft recorded 42% of the sea otters present within the area surveyed. Adjusting the 1986 results by this amount yields a range of 10,086–17,238; therefore the population may not have changed substantially between 1976 and 1986. By 2000 however, it is clear that sea otters had declined within the NAP study area, and although the data history for the SAP study area is even more sparse, there is little doubt that the population in this area has also declined severely since 1986.

The distribution of sea otters along the north side of the Alaska Peninsula is rather unique. Because of the broad shelf, large rafts of otters have been observed at distances of 50 km or more from shore. The area is also subject to seasonal sea ice that can have a profound impact on sea otter distribution, and in extreme ice years, result in significant mortality (Schneider and Faro, 1975). It is unclear if behavior and movement patterns in the NAP area are different from other areas in the north Pacific. In the 1960s and 1970s it was thought that sea otters along the northern Alaska Peninsula spent much, if not all, of their life in offshore waters (Kenyon, 1969; Lensink, 1962; Schneider, 1976). Cimberg et al.² suggested that sea otters may migrate through False Pass from the Bering Sea to the north Pacific Ocean during the winter months to avoid being trapped by shore-fast sea ice. Of the two study areas along the north side of the Alaska Peninsula, the NAPA study area located farther south and west is more likely to remain ice-free, and therefore may be important for the overall survival of sea otters in this area (Schneider and Faro, 1975). If sea otters remain concentrated throughout the year in Port Moller, which is in the NAPb study area, they may be vulnerable to mortality by extensive sea ice events in the future.

Information derived from sea ice data with spatial and temporal resolution suitable for evaluating the impacts of extensive sea ice on sea otters is not readily available. Detailed sea ice data for the NAP study area from the National Ice Center is only available for the period from 1997 to the present. In March 1999 shore-fast ice was present in both Port Moller and Izembek Lagoon, and nearshore areas were almost totally covered by sea ice. Similar conditions also occurred in January 2000. In both instances, sea otter mortality was reported by residents of Port Heiden, Alaska, located to the northeast of the NAP study area (Esslinger⁵; Snyder⁶). Human habitation in the NAP study area is extremely sparse in winter, which may explain why there were no reports of

sea otter mortality in this area. Given the degree of sea ice present, it is possible that the extreme ice conditions in 1999 and 2000 may have resulted in the death of some sea otters within our study area. The geographic pattern of the decline does not exactly fit what would be expected from sea ice however, because the decline occurred in the NAPA study area, which is presumed to be less vulnerable to these events. Although it is possible that extreme sea ice conditions may have been a contributing factor, it was likely not the sole cause of the decline in the NAP study area.

In our surveys of the NAP study area, sea otter abundance declined severely in NAPA but had increased in NAPb. It is unclear to what degree otters may move between these respective study areas. Quarterly surveys in 1986 did not indicate seasonal changes in distribution between the NAPA and NAPb portions of the study area. Monnett et al.⁷ used radio telemetry to study sea otter movements in the NAPA study area from 1986 through 1988 and found that study animals did not move between NAPA and NAPb or to the SAP study area as previously hypothesized by Cimberg et al.² The average distance between extreme locations was only 18.4 km; however, the sample size of sea otters in the Monnett et al.⁷ study was small ($n=14$). The large concentration of sea otters observed in Port Moller and Nelson Lagoon in May 2000 may be a seasonal event; large numbers of sea otters are typically observed in that area in May, but disperse by June (Murphy⁸). Compared to the ecology of other areas, the ecology of sea otters along the north side of the Alaska Peninsula is poorly understood and additional study is warranted.

In addition to changes in abundance there were also changes in sea otter distribution in the 2000–01 surveys. In 1986, sea otters were observed up to 50 km from shore during all surveys. In the 1970s and 1980s, large rafts of up to 1000 sea otters were distributed well offshore (Kenyon, 1969; Schneider, 1976; Bruggeman et al.¹). By 2001 sea otters were, with rare exception, located in bays and lagoons along the Peninsula rather than in the offshore habitat in both the NAP and SAP study areas. Estes et al. (1998) hypothesized that declines in sea otters in the Aleutian islands during the 1990s may have been caused by increased predation by killer whales (*Orcinus orca*). One line of evidence that led to this conclusion was a lower sea otter mortality in the sheltered area of Clam Lagoon than in the exposed area of Kuluk Bay on Adak Island. The observed distribution of sea otters within bays and lagoons along the Alaska Peninsula in 2000–01 is not inconsistent with the predation hypothesis of Estes et al. (1998). Alternatively, nearshore waters may constitute preferred

⁴ Evans, T. J., D. M. Burn, and A. R. DeGange. 1997. Distribution and relative abundance of sea otters in the Aleutian archipelago. Tech. Rep. MMM 97-5, 29 p. U. S. Fish and Wildl. Serv. Mar. Mamm. Manage. Office 1011 E Tudor Road, Anchorage, AK 99503.

⁵ George Esslinger. 1999. Personal commun. U.S. Geological Survey, Alaska Science Center. 1011 East Tudor Road, Anchorage, AK 99503-6103.

⁶ Jonathan Snyder. 2000. Personal commun. U.S. Fish and Wildl. Serv., Mar. Mamm. Manage. Office, 1011 East Tudor Road, Anchorage, AK 99503-6103.

⁷ Monnett, C., L. M. Rotterman, D. B. Sniff, and J. Sarvis. 1988. Movement patterns of western Alaska Peninsula sea otters. Minerals Management Service, OCSAP (Offshore Continental Shelf Engineering Assessment Program) Research Unit 688, 51 p.

⁸ Murphy, B. 2002. Personal commun. Alaska Department of Fish and Game, Division of Commercial Fisheries, 211 Mission Road, Kodiak, AK 99615-6399.

habitat for sea otters, and at low densities it is possible that these may be the only areas where they occur.

We are reasonably confident that the 2000–01 surveys yielded results that were comparable to baseline surveys because the methods were closely repeated. The difference in distribution of sea otter sighting zones may have been a result of different aircraft configurations. Although both aircraft were equipped with bubble windows, the size and shape of these windows were probably not identical. We accounted for any differences by selecting the zones best suited to estimate sea otter abundance for each survey period. In our data analysis, we also accounted for the effects of survey conditions (Beaufort sea state and viewing condition) in both data sets. Our results indicate that in addition to changes in sea otter abundance, distribution had changed markedly between study periods as well. Because sea otter distribution is currently concentrated closer to the coast, we recommend revising the survey design for future population surveys in this area. Rather than considering the offshore area as a single survey stratum, it would be more efficient to define nearshore and offshore survey strata and allocate survey effort accordingly.

To the west of the Alaska Peninsula study areas, the sea otter population in the Aleutian archipelago has declined to less than 10% of the estimated carrying capacity (Burn et al., 2003). Further westward in the Commander Islands, Russia, the sea otter population appears to have remained stable over the same time period (Burkanov and Burdin⁹). To the east of the Alaska Peninsula, sea otters have declined by an estimated 56% in the nearby Kodiak archipelago since 1989 (Doroff et al.¹⁰), but they appear to have remained relatively stable in the areas of Cook Inlet and Kenai Fjords (Bodkin et al.¹¹). According to the most recent population surveys, the geographic extent of the sea otter decline does not appear to have exceeded the range of the southwest Alaska population stock as described by Gorbics and Bodkin (2001), where the overall decline has been estimated at 56–68%. Because the cause of the decline remains unknown, areas at the periphery of the current decline should be regularly monitored in the future. Given the close proximity between the Aleutian Islands and the Commander Islands, Russia, future research there may improve our understanding of the cause of the decline in southwest Alaska.

The sea otter decline, which has occurred over a broad geographic area, encompasses different habitat types in southwest Alaska. The Aleutian Island chain is primarily volcanic in origin and the majority of habitat for foraging (waters <40 m) is concentrated relatively near shore and is primarily a rocky substrate. The Alaska Peninsula includes extensive soft-sediment offshore habitat available to sea otters. Despite these differences, the declines in sea otter populations are similar between the Alaska Peninsula and the Aleutian archipelago in both severity and time period, which may imply a common cause. In addition to sea otters, severe declines of harbor seals (*Phoca vitulina*), Steller sea lions (*Eumetopias jubatus*), and fur seals (*Callorhinus ursinus*) have also been documented within the same general region, which suggests broader ecosystem-level changes may be involved. Our survey results, along with evidence of a declining sea otter population in the Kodiak archipelago, prompted the U.S. Fish and Wildlife Service to propose listing sea otters in southwest Alaska as threatened under the U.S. Endangered Species Act. The population decline in southwest Alaska is one of the most significant conservation issues for the sea otters in our time.

Acknowledgments

We thank the following individuals and organizations for their contributions to 2000–01 surveys: Linda Comerici, Thomas Evans, Susanne Kalxdorff, and Rosa Meehan for their work as observers and data recorders during survey operations; Ralph Aiken, Tom Blaesing, and Dave Weintraub for their incomparable piloting skills; Izembek National Wildlife Refuge manager Rick Poetter and his staff for logistical support. Jay Brueggeman and Greg Green provided the original 1986 aerial survey information and assisted with data interpretation. We thank John Haddix for assistance with GIS analysis of the 1986 survey data. We also thank James Bodkin, Verena Gill, Mark Udevitz, and two anonymous reviewers for comments on an earlier draft of this manuscript.

Literature cited

- Burn, D. M., A. M. Doroff, and M. T. Tinker. 2003. Carrying capacity and pre-decline abundance of sea otters (*Enhydra lutris kenyoni*) in the Aleutian Islands. *Northwest. Nat.* 84:145–148.
- Doroff, A. M., J. A. Estes, M. T. Tinker, D. M. Burn, T. J. Evans. 2003. Sea otter population declines in the Aleutian archipelago. *J. Mammal.* 84:55–64.
- Estes, J. A. 1977. Population estimates and feeding behavior of sea otters. In *The environment of Amchitka Island, Alaska* (M. L. Merritt and R. G. Fuller, eds.), p. 511–526. U. S. Energy Resource and Development Administration, Springfield, VA.
1990. Growth and equilibrium in sea otter populations. *J. Anim. Ecol.* 59:385–401.

⁹ Burkanov, V. N., and A. M. Burdin. 2002. Distribution and abundance of sea otter, steller sea lion, and killer whale in the Commander Islands (Russia) during 2002. *North Pacific Wildlife Consulting, LLC Interim Report*, 37 p. North Pacific Wildlife Consulting, 12600 Elmwood Rd., Anchorage, AK 99516.

¹⁰ Doroff, A. M., D. M. Burn, R. A. Stovall, and V. A. Gill. In prep. Unexpected population declines of sea otters in the Kodiak archipelago, Alaska.

¹¹ Bodkin, J. L. D. H. Monson, and G. E. Esslinger. 2003. A report on the results of the 2002 Kenai Peninsula and Lower Cook Inlet aerial sea otter survey, 10 p. U.S. Geological Survey, Alaska Science Center Report. 1011 East Tudor Road, Anchorage, Alaska 99503.

- Estes, J. A., and J. R. Gilbert.
1978. Evaluation of an aerial survey of Pacific walrus (*Odobenus rosmarus divergens*). *J. Fish. Res. Board Can.* 53:1130-1140.
- Estes, J. A., M. T. Tinker, T. M. Williams, and D. F. Doak.
1998. Killer whale predation on sea otters linking oceanic and near shore ecosystems. *Science* 282:473-476.
- Garshelis, D. L., and J. A. Garshelis.
1984. Movements and management of sea otters in Alaska. *J. Wild. Manag.* 48(3):665-678.
- Gelatt, T. S., D. B. Siniff, and J. A. Estes.
2002. Activity patterns and time budgets of the declining sea otter population at Amchitka Island, Alaska. *J. Wild. Manag.* 66:29-39.
- Gorbics, C. S., and J. L. Bodkin.
2001. Stock structure of sea otters (*Enhydra lutris kenyoni*) in Alaska. *Mar. Mamm. Sci.* 17(3):632-647.
- Kenyon, K. W.
1969. The sea otter in the eastern Pacific Ocean. *N. Am. Fauna* 68:1-352.
- Lensink, C. J.
1962. The history and status of sea otters in Alaska. Ph.D. diss., 188 p. Purdue Univ., West La Fayette, IN.
- Schneider, K. B.
1976. Assessment of the distribution and abundance of sea otters along the Kenai Peninsula, Kamishak Bay, and the Kodiak archipelago. OCSEAP (Offshore Continental Shelf Engineering Assessment Program) final rep. no. 37, p. 527-626. Dept. of Commerce, National Oceanographic and Atmospheric Administration, Anchorage, AK.
- Schneider, K. B., and J. B. Faro.
1975. Effects of sea ice on sea otters (*Enhydra lutris*). *J. Mammal.* 56:91-101.

Abstract—The age and growth dynamics of the spinner shark (*Carcharhinus brevipinna*) in the northwest Atlantic Ocean off the southeast United States and in the Gulf of Mexico were examined and four growth models were used to examine variation in the ability to fit size-at-age data. The von Bertalanffy growth model, an alternative equation of the von Bertalanffy growth model with a size-at-birth intercept, the Gompertz growth model, and a logistic model were fitted to sex-specific observed size-at-age data. Considering the statistical criteria (e.g., lowest mean square error [MSE], high coefficient-of-determination, and greatest level of significance) we desired for this study, the logistic model provided the best overall fit to the size-at-age data, whereas the von Bertalanffy growth model gave the worst. For “biological validity,” the von Bertalanffy model for female sharks provided estimates similar to those reported in other studies. However, the von Bertalanffy model was deemed inappropriate for describing the growth of male spinner sharks because estimates of theoretical maximum size (L_{∞}) indicated a size much larger than that observed in the field. However, the growth coefficient ($k=0.14/\text{yr}$) from the Gompertz model provided an estimate most similar to that reported for other large coastal species. The analysis of growth for spinner shark in the present study demonstrates the importance of fitting alternative models when standard models fit the data poorly or when growth estimates do not appear to be realistic.

Growth dynamics of the spinner shark (*Carcharhinus brevipinna*) off the United States southeast and Gulf of Mexico coasts: a comparison of methods

John K. Carlson

Ivy E. Baremore

Southeast Fisheries Science Center
National Marine Fisheries Service, NOAA
3500 Delwood Beach Road
Panama City, Florida 32408
E-mail address (for J. K. Carlson): john.carlson@noaa.gov

Virtually every study concerned with describing the growth of elasmobranchs uses the von Bertalanffy growth equation (von Bertalanffy, 1938), despite criticism of the model (Knight, 1968; Roff, 1980). A review of the existing literature from 1962 to 2002 indicates that only about 12% of the published papers concerned with elasmobranch age and growth provide or have examined an alternative model (I.E.B., unpubl. data). Most studies on elasmobranch age and growth have simply fitted the von Bertalanffy model to observed or back-calculated size-at-age data without much concern about goodness-of-fit. In addition, appropriate age-structured assessments require accurate measures of the growth coefficient (k) of the population when calculating, for example, indirect estimates of natural mortality. A complete study on the age and growth of a species may require the application of multiple growth models, especially when data do not appear to fit a given model (e.g., when there is no statistical significance or when there is poor goodness-of-fit) or when results do not appear to be biologically realistic.

The spinner shark (*Carcharhinus brevipinna*) is a cosmopolitan species occurring in warm-temperate areas of the Atlantic Ocean, the Indian Ocean, and the western Pacific Ocean (Compagno, 1984). Off the United States east and Gulf of Mexico coasts, the spinner shark is managed under a large coastal shark complex (NMFS, 1993). Sharks within this complex are

considered to be relatively large, slow growing, long lived, and are currently overfished (Cortés et al.¹).

Although Allen and Wintner (2002) recently examined the age and growth of the spinner shark off South Africa, the only existing information on spinner sharks from U.S. waters is from Branstetter (1987), who examined just 15 animals from the Gulf of Mexico. The purpose of the present study is to re-examine the age and growth dynamics of the spinner shark off the U.S. southeast and Gulf of Mexico coasts. We compare and contrast four growth models to determine the model that best describes the growth data of the spinner shark.

Materials and methods

Sharks ($n=273$) were collected from 1995 to 2003 in the U.S. Exclusive Economic Zone from Galveston, Texas to Key West, Florida, in the Gulf of Mexico and in the U.S. south Atlantic Ocean from Charleston, South Carolina, to West Palm Beach, Florida (Fig. 1). Precaudal (PC), fork (FL) or total (TL) length (cm) were measured, and sex and maturity stage were determined for each shark. Total

¹ Cortés, E., L. Brooks, and G. Scott. 2002. Stock assessment of large coastal sharks in the U.S. Atlantic and Gulf of Mexico. Sustainable Fisheries Division contribution SFD-02/03-177, 64 p. Southeast Fisheries Science Center, 3500 Delwood Beach Rd., Panama City, FL, 32408.

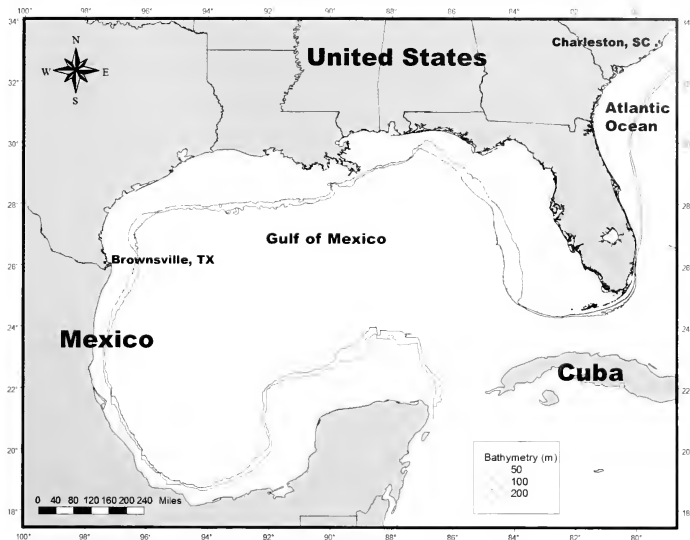


Figure 1

Map of the sampling area for spinner sharks (*Carcharhinus brevipinna*) showing areas and locations stated in the text.

length was measured as a straight line from the tip of the snout to the tip of the tail in a natural position. The weight (kg) of each shark was obtained when sampling conditions permitted. Vertebrae were removed from an area anterior to the first dorsal fin.

Vertebral sections were placed on ice after collection and frozen upon return to the laboratory. Thawed vertebrae were cleaned of excess tissue and soaked in a 5% sodium hypochlorite solution for 5–30 min to remove remaining tissue. After cleaning, vertebrae were soaked in distilled water for 30 minutes and stored in 95% isopropyl alcohol. Prior to examination, one vertebra from each shark was chosen at random, removed from alcohol, and dried. The vertebra was fixed to a clear glass slide with resin and sectioned with a Buehler 82 Isomet low-speed saw.

Sagittal sections of different thicknesses were cut from the vertebral centrum and stained with crystal violet, or alizarin red, or left unstained according to the methods of Carlson et al. (2003). Each vertebral section was mounted on a glass microscope slide with ProTex cytosal (Lerner Laboratories, Pittsburg, PA) and examined by using a dissecting microscope under transmitted light. The banding pattern was found to

be most apparent on unstained sagittal sections with a thickness of 0.3 mm.

Opaque bands representing summer growth and translucent bands representing winter growth were identified following the description and terms in Cailliet and Goldman (2004) (Fig. 2). Because no validation is available for this species, verification of the annual period of band formation was performed by using the relative marginal increment analysis (Branstetter and Musick, 1994; Natanson et al., 1995):

$$MIR = (VR - R_n) / (R_n - R_{n-1}),$$

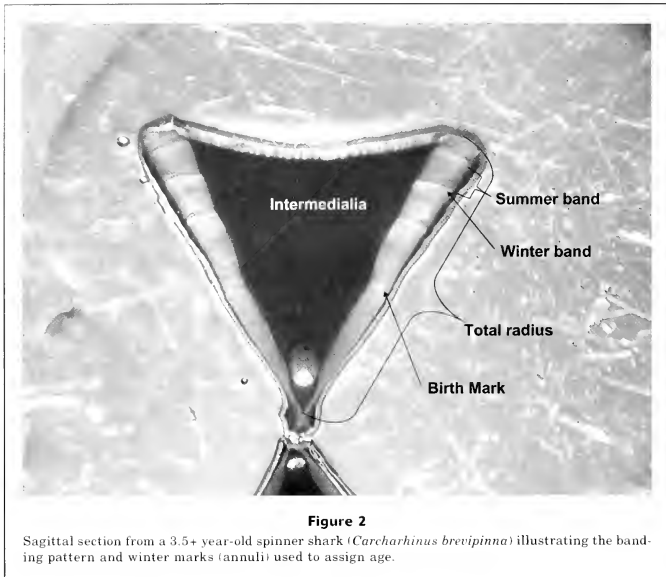
where MIR = the marginal increment ratio;

VR = the vertebral radius;

R_n = distance to the outer edge of the last complete band; and

R_{n-1} = distance to the outer edge of the next-to-last complete band.

Mean MIR was plotted against month to determine trends in band formation. A single factor analysis of variance was used to test for differences in arcsine-transformed (Zar, 1984) MIR data among months.



Both authors randomly read vertebrae independently without knowledge of sex or length of specimens. Vertebral age estimates for which the readers disagreed were reread simultaneously by using a digital camera and software (Pixera Studio version 2, Pixera Corporation, Los Gatos, CA). If no agreement between readings was reached, samples were discarded.

Several methods were used to evaluate precision and bias among age determinations following the recommendations in Cailliet and Goldman (2004). Percent agreement (PA=number agreed/number read) \times 100 and percent agreement plus or minus one year were calculated for 10 cm (e.g. 76–85 cm FL) length intervals to evaluate precision (Goldman, 2002). The index of average percent error (APE; Beamish and Fournier, 1981) was calculated to compare the average deviation of readings from the means of all readings for each vertebral section:

$$IAPE = \frac{1}{n} \sum_{j=1}^N \left[\frac{1}{r} \sum_{i=1}^r \frac{|x_{ij} - x_j|}{x_j} \right],$$

where n = number of sharks aged;
 r = number of readings;

x_{ij} = i^{th} age estimation of j^{th} shark at i^{th} reading;
and
 x_j = mean age calculated for the j^{th} shark.

Chi-square tests of symmetry following Hoenig et al. (1995) were used to determine if differences between readers were systematic or due to random error.

Several models were fitted to sex-specific observed size-at-age data to estimate the growth dynamics in spinner shark. Although back-calculated size-at-age length data would increase sample sizes for some ages (Cailliet, 1990), multiple back-calculated lengths-at-age are not independent samples and violate statistical assumptions in estimating parameters for a growth model (Vaughan and Burton, 1994). Vaughan and Burton (1994) pointed out that estimates of the model parameters may be biased because multiple back-calculated lengths cause an inaccurate number of degrees of freedom. Thus, we used data only from observed size-at-age.

In developing theoretical growth models, we assumed that 1) the birth mark is the band associated with a pronounced change in angle in the intermedialia, and we assigned an arbitrary birth date of 1 June, the approximate mid-point date when neonates were present in field collections, 2) translucent bands representing

winter growth form approximately six months later (i.e., 0.5 years) and 3) subsequent translucent bands representing winter growth form at yearly intervals, thereafter. Thus, ages (yr) were calculated by following the algorithm of Carlson et al. (1999): $age = birth\ mark + number\ of\ translucent\ winter\ bands - 1.5$. If only the birth mark was present, the age was 0+ years. All age estimates from growth band counts were based on the hypothesis of annual growth band deposition (Branstetter, 1987).

The von Bertalanffy growth model (von Bertalanffy, 1938) is described by using the equation

$$L_t = L_\infty(1 - e^{-k(t-t_0)}),$$

where L_t = mean fork length at time t ;

L_∞ = theoretical asymptotic length;

k = growth coefficient; and

t_0 = theoretical age at zero length.

An alternative equation of the von Bertalanffy growth model, with a size-at-birth intercept rather than the t_0 parameter (Van Dykhuizen and Mollet, 1992, Goosen and Smale, 1997; Carlson et al., 2003) is described as

$$L_t = L_0(1 - be^{-kt}),$$

where $b = (L_\infty - L_0)/L_\infty$; and

L_0 = length at birth.

Estimated median length at birth for spinner shark is 52 cm FL (Carlson, unpubl. data).

We also used the modified form of the Gompertz growth model (Ricker, 1975). The model is expressed following Mollet et al. (2002) as

$$L_t = L_0 \left(e^{G(1 - e^{-kt})} \right),$$

where $G = \ln(L_\infty/L_0)$.

For the Gompertz model, the estimated median asymptotic length for spinner shark is 220 and 200 cm FL for females and males, respectively (Carlson, unpubl. data).

A logistic model (Ricker, 1979) was also considered in the form

$$W_t = W_\infty / (1 + e^{-k(t-a)}),$$

where W_t = mean weight (kg) at time t ;

W_∞ = theoretical asymptotic weight;

k = (equivalent to g in Ricker, 1979) instantaneous rate of growth when $w \rightarrow 0$; and

a = (equivalent to t_0 in Ricker, 1979) time at which the absolute rate of increase in weight begins to decrease or the inflection point of the curve.

If weight was not available, length was converted to weight by using the regression: $weight = 0.0000209 \times FL^{2.9524}$ ($n=226$, $r^2=0.98$, range: 1.1–66.1 kg).

Table 1

A summary of the number of spinner sharks (*Carcharhinus brevipinna*), by month and sex, used for our estimates of age.

Month	Male	Female
January	8	3
February	0	0
March	0	13
April	0	3
May	25	6
June	15	47
July	35	22
August	30	35
September	4	13
October	0	0
November	0	0
December	0	0

All growth model parameters were estimated with Marquardt least-squares nonlinear regression. All models were implemented by using SAS statistical software (SAS version 6.03, SAS Institute Inc., Cary, NC). The goodness-of-fit of each model was assessed by examining residual mean square error (MSE), coefficient-of-determination (r^2), F from analysis of variance, level of significance ($P < 0.05$), and standard residual analysis (Neter et al., 1990).

Results

Morphometric relationships were developed to convert length measurements. Linear regression formulae were determined as $PC = 0.880(FL) + 1.503$, $n=163$, $r^2=0.88$, $P < 0.0001$; and $FL = 0.847(TL) - 3.497$, $n=260$, $r^2=0.99$, $P < 0.0001$.

Of the original 273 samples, 14 were deemed unreadable and were discarded (Table 1). The index of average percent error for the initial reading between authors was 10.6%. When grouped by 10-cm length intervals, agreement for combined sexes was reached for an average of 30.2% and 58.2% (± 1 band) of band counts for sharks less than 115 cm FL (Table 2). Above 115 cm FL, agreement was reached for 33.5% and 74.0% (± 1) of band counts for samples initially read. Hoenig's et al. (1995) test of symmetry indicated that there was bias between readers ($\chi^2=98.33$, $df=40$, $P < 0.001$).

Relative marginal increment analysis indicated that bands form annually during winter months (Fig. 3). The smallest relative increment was found in January and the greatest in July. The relative marginal increment ratio increased through spring months (March–May), peaked in summer (June–August), and then declined to fall. However, no statistical difference was found in MIR

values among months ($F=1.63$, $df=7$, $P=0.129$), likely because of the large variation in increment by months.

Under the statistical criteria established in our study, all growth models fitted the data well (Table 3). For males and females, models were highly significant ($P<0.001$) and exhibited high coefficients of determination ($r^2\geq 0.88$). Residual mean square error (MSE) was lowest for the logistic models. Notably, MSE was much

higher for the von Bertalanffy model males than for any other model. Plots of the residuals against predicted sizes indicated no pattern in the residuals for any model. The standard deviation of the residuals was lowest for the logistic models (Table 3).

Estimates of the asymptotic size varied depending on sex and model (Table 3; Figs. 4 and 5). For males, the highest asymptotic length was produced by the von Bertalanffy model ($L_\infty=421$ cm FL), intermediate lengths came from the von Bertalanffy model with a size-at-birth intercept ($L_\infty=279$ cm FL) and the Gompertz model ($L_\infty=200$, $G=1.38$), and lowest length was produced by the logistic model ($W_\infty=60.2$ kg, ~ 161 cm FL). For females, asymptotic sizes were highest and similar with the von Bertalanffy, von Bertalanffy model with a size-at-birth, and the Gompertz models (226, 202, and 220 cm FL, respectively) and lowest with the logistic model (62.6 kg or ~ 162 cm FL).

Among models with comparable growth coefficients, the von Bertalanffy model produced the lowest growth coefficient for both males and females ($k=0.03$ and $0.08/\text{yr}$, respectively). Growth coefficients were higher and fairly similar for the other two length models. The growth coefficient from the logistic weight model was 0.44 and 0.37 for males and females, respectively.

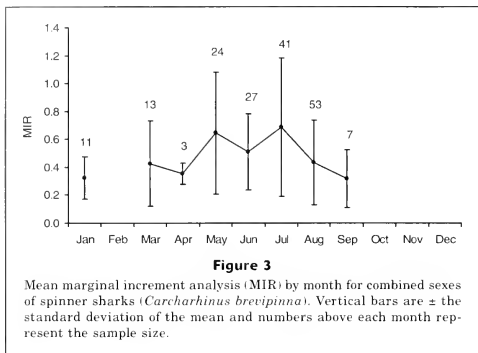


Figure 3

Mean marginal increment analysis (MIR) by month for combined sexes of spinner sharks (*Carcharhinus brevipinna*). Vertical bars are \pm the standard deviation of the mean and numbers above each month represent the sample size.

Table 2

Percent agreement and percent agreement (± 1 band) from the initial set of readings for spinner shark (*Carcharhinus brevipinna*).

FL interval	Sexes combined			Males			Females		
	Total read	Percent agreement	Percent agreement ± 1 band	Total read	Percent agreement	Percent agreement ± 1 band	Total read	Percent agreement	Percent agreement ± 1 band
46-55	8	75.0	100.0	2	100.0	100.0	6	66.7	100.0
56-65	62	32.3	83.9	25	20.0	64.0	37	40.5	81.1
66-75	10	20.0	60.0	4	0.0	50.0	6	33.3	66.7
76-85	36	30.6	66.7	17	29.4	47.1	19	31.6	84.2
86-95	28	14.3	28.6	13	23.1	30.8	15	6.7	26.7
96-105	15	20.0	40.0	5	0.0	40.0	10	30.0	40.0
106-115	21	19.0	28.6	10	10.0	20.0	11	27.3	36.4
116-125	16	37.5	68.8	10	40.0	90.0	6	33.3	33.3
126-135	12	41.7	75.0	2	50.0	50.0	10	40.0	80.0
136-145	5	60.0	100.0	5	60.0	100.0	0	—	—
146-155	10	40.0	60.0	6	50.0	83.3	4	25.0	25.0
156-165	12	41.7	58.3	8	62.5	87.5	4	0.0	25.0
166-175	11	36.4	63.6	4	50.0	75.0	7	28.6	57.1
176-185	12	16.7	66.7	6	33.3	83.3	6	0.0	50.0
186-195	1	0.0	100.0	0	—	—	1	0.0	100.0

The Gompertz model estimated size-at-birth (61 cm FL) within the range reported for spinner sharks. Size-at-birth off the United States southeast and Gulf of Mexico coasts has been reported to range from 50 to 65 cm FL depending on the study (Branstetter, 1987; Castro, 1993; Carlson, unpubl. data).

Observed size-at-age and longevity were different between males and females (Table 4). For most ages, females were larger. The oldest animals aged were 17.5+ years (female) and 13.5+ years (male).

Discussion

Considering our statistical criteria (e.g., lowest MSE, high r^2 , and level of significance), logistic models provided the best fits to the size-at-age data. The von Bertalanffy growth models, on the other hand, gave the worst fits. However, the criteria used to evaluate the models in this study may not be adequate. Because statistical fits have not been reported by other elasmobranch age and growth studies, we were not able to compare our criteria with other studies. Although not directly comparable, goodness-of-fit criteria used to select the best nonlinear gastric evacuation models have employed a combination of r^2 , residual sum of squares, standard deviation, or coefficient of variation of residuals (review in Cortés, 1997). Until a more rigorous criterion is developed for

growth models, efforts should continue to identify a best-fitting growth model.

We feel the von Bertalanffy model is inappropriate for describing the growth of male spinner shark. Asymptotic values indicated an unreasonable theoretical maximum size of 421 cm FL—much larger than sizes from recent fishery-dependent and fishery-independent sources (176–220 cm FL; Grace and Henwood, 1997; Morgan³; Carlson, unpubl. data). Asymptotic values from other models approach those actual values. Because of the relationship between k and L_{∞} , the von Bertalanffy growth coefficient was also much lower than expected. The growth coefficient from the Gompertz model was 0.14/yr, similar to those reported for other large coastal species in general (Cortés, 2000) and to those reported by Allen and Wintner (2002) for spinner sharks from South Africa.

The poor statistical fit and unrealistic biological estimates of the von Bertalanffy growth model for male spinner shark illustrates the importance of fitting alternative models to the data when estimates do not appear to be biologically real. Although sample size was well represented for most ages, the von Bertalanffy growth model did not reach an asymptote until well beyond the

³ Morgan, A. Personal commun. Program for Shark Research, Florida Museum of Natural History, Univ. Florida, P.O. Box 117800, Gainesville, FL, 32611.

Table 3

Estimates of growth and goodness-of-fit from four growth models fitted to observed size-at-age data for male and female spinner sharks (*Carcharhinus brevipinna*). Values in parentheses are standard errors. L_0 = size at birth. The standard deviation (SD) of the residuals is from standard residual analysis. MSE=mean square error. n/a=not available.

Model	Asymptotic size ¹ (cm FL)	Growth coefficient (/yr)	t_0 ² (yr)	L_0 (cm FL)	F	P	r^2	MSE	SD of residuals
Male									
von Bertalanffy	421.0 (±157.6)	0.03 (±0.02)	-4.58 (±0.65)	—	543.91	<0.001	0.91	543.91	11.91
von Bertalanffy with size-at-birth	279.1 (±39.4)	0.07 (±0.02)	n/a	52	946.24	<0.001	0.89	163.65	12.49
Gompertz	200 (G=1.38±0.09)	0.14 (±0.02)	n/a	60.5 (±1.9)	557.83	<0.001	0.91	141.23	11.78
Logistic	60.2 (±39.4)	0.44 (±0.05)	6.75 (±0.47)	—	483.00	<0.001	0.93	47.44	6.83
Female									
von Bertalanffy	226.2 (±18.6)	0.08 (±0.02)	-3.84 (±0.40)	—	612.20	<0.001	0.90	150.70	12.19
von Bertalanffy with size-at-birth	202.7 (±10.9)	0.11 (±0.01)	n/a	52	1047.19	<0.001	0.88	173.07	12.78
Gompertz	220 (G=1.17±0.4)	0.16 (±0.02)	n/a	60.7 (±1.6)	609.09	<0.001	0.90	151.39	12.21
Logistic	62.6 (±3.2)	0.37 (±0.03)	7.62 (±0.43)	—	572.84	<0.001	0.93	43.82	6.57

¹ Asymptotic size for the von Bertalanffy, von Bertalanffy with size-at-birth, and Gompertz models are in cm, whereas asymptotic size for the logistic model is in kg.

² t_0 is the theoretical age at zero length for the von Bertalanffy whereas t_0 for the logistic model represents time at which the absolute rate of increase in weight begins to decrease.

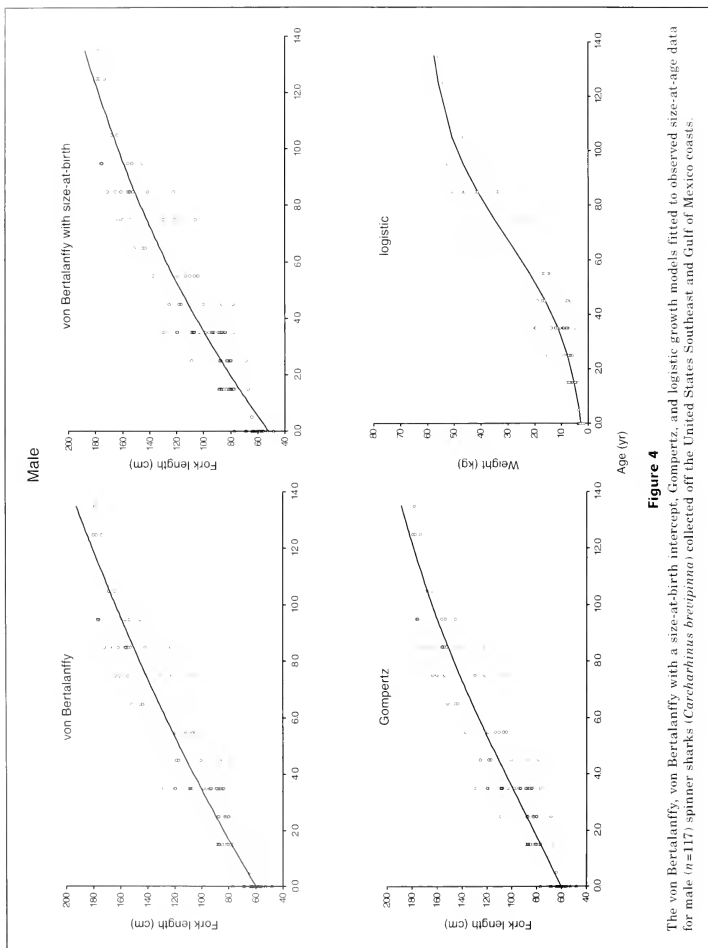
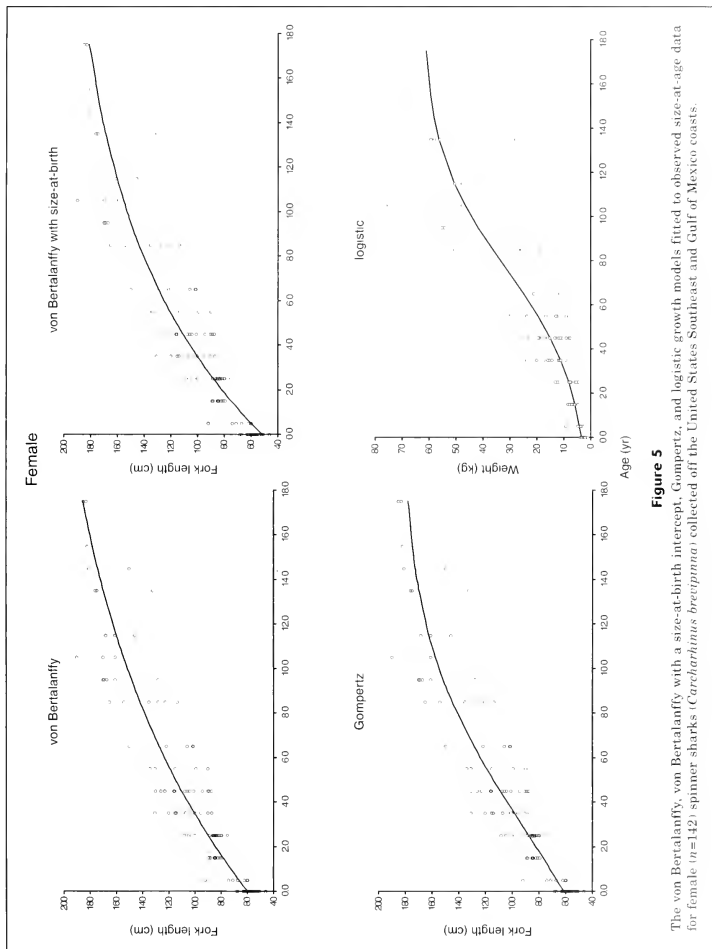


Figure 4 The von Bertalanffy, von Bertalanffy with a size-at-birth intercept, Gompertz, and logistic growth models fitted to observed size-at-age data for male ($n=117$) spinner sharks (*Carcharhinus brevipinna*) collected off the United States Southeast and Gulf of Mexico coasts.

**Figure 5**

The von Bertalanffy, von Bertalanffy with a size-at-birth intercept, Gompertz, and logistic growth models fitted to observed size-at-age data for female ($n=142$) spinner sharks (*Carcharhinus brevipinna*) collected off the United States Southeast and Gulf of Mexico coasts.

Table 4

Mean size-at-age (cm FL) for male and female spinner sharks (*Carcharhinus brevispinna*). SD=standard deviation.

	Age (yr)																		
	0.0	0.5	1.5	2.5	3.5	4.5	5.5	6.5	7.5	8.5	9.5	10.5	11.5	12.5	13.5	14.5	15.5	16.5	17.5
Male																			
Size	60.7	64.1	81.2	84.6	99.9	105.8	115.5	146.3	138.9	154.2	165.3	165.9	—	176.3	178.0	—	—	—	—
SD	5.3	—	5.9	11.4	13.8	17.9	11.0	4.2	23.4	13.9	13.4	3.0	—	3.1	—	—	—	—	—
n	29	1	12	8	21	7	7	3	6	10	7	2	—	3	1	—	—	—	—
Female																			
Size	59.0	69.3	84.4	86.9	106.9	106.9	117.1	116.2	—	136.3	160.8	173.7	158.3	—	164.7	165.5	182.0	—	184.0
SD	4.1	11.5	2.9	8.7	13.3	13.9	19.1	20.7	—	19.6	16.4	14.8	11.2	—	21.7	21.9	—	—	1.4
n	42	7	12	18	11	14	6	5	—	6	6	3	3	—	4	2	1	—	2

expected maximum size, resulting in an inflated asymptote and low growth coefficient. Branstetter and Stiles (1987) also encountered this problem with bull sharks (*Carcharhinus leucas*) but rather than fit an alternative growth model, those authors hand-fitted a curve through the upper data points. Results such as these may seriously bias estimates of k and any resulting population models because several indirect estimates of natural mortality (M) and longevity rely heavily on accurate estimates of k from a growth model (Fabens, 1965; Pauly, 1980; Chen and Watanabe, 1989; Jensen, 1996). For example, the method of Jensen (1996) for estimating M yields values ranging from 0.05/yr (with results from the von Bertalanffy model) to 0.23/yr (with results from the Gompertz model). Similarly, theoretical longevity estimates determined by the method of Fabens (1965) are 115.5 years and 21.6 years from the von Bertalanffy model and the Gompertz model, respectively.

In general, our estimates of age and growth for female spinner sharks from the von Bertalanffy model were similar to those reported by Allen and Wintner (2002) for spinner sharks collected off South Africa. Growth coefficients in their study were about 0.13/yr, L_{∞} was 250 cm FL, and observed longevity for females was up to 19+ years. Branstetter (1987), in his study on sharks collected in the Gulf of Mexico, reported an observed longevity up to 11+ years (combined sexes) and growth coefficients of about 0.21/yr. Because differences in life history traits (e.g., growth rates, size and age at maturity) between populations of blacktip and bull sharks from South Africa and United States waters have been proposed (Wintner and Cliff, 1995; Wintner et al., 2002, respectively), results from our study for spinner shark may be expected to be more similar to those of Branstetter (1987) rather than those of Allen and Wintner (2002). Although techniques (e.g., counting winter bands on sagittal vertebral sections) in Branstetter (1987) were similar to ours, the differences are likely a result of low sample size in the earlier study.

The index of average percent error (IAPE) in aging was at the higher end of the range of estimates pro-

vided in other studies that also used sagittal sections for aging. Values have been reported as low as 3.0% for the oceanic whitetip shark (*Carcharhinus longimanus*) (Lessa et al., 1999), and up to 13.0% for the blacktip shark (*Carcharhinus limbatus*) (Wintner and Cliff, 1995). Although IAPE indices are most commonly used to evaluate precision among age determinations, IAPE does not test for systematic differences and does not distinguish all sources of variation (Hoening et al., 1995). In addition, comparing IAPE values among studies may not be valid unless the study species is the same and from the same geographic area (Cailliet and Goldman 2004).

Although bands were readily discernible in most samples, the inexperience of one of the authors (reader 2) in reading and counting vertebral bands likely led to the higher IAPE and systematic bias. Generally, most systematic bias is a shift to increasing or decreasing counts with age (Morison et al. 1998), yet the bias in this study was the result of reader 2 consistently over aging sharks from the final agreed age regardless of the band count of the sample. Percent agreement was similar for samples above 115 cm FL as it was for samples below this size. Although a reference collection was aged by reader 2 prior to beginning this study, finely honed skills through experience are key elements in the technique of aging.

The trend in marginal increment analysis indicated that band formation occurs once a year during winter months—a result common to most studies where relative marginal increment analysis is used for carcharhinid sharks (e.g., Natanson et al., 1995; Carlson et al., 1999; Carlson et al., 2003). However, high variance in marginal increment analysis (MIR) within each month resulted in months not being statistically different, which is a widespread occurrence when using this method. Marginal increment analysis has been criticized as one of the most abused methods for validation of band formation (Campana, 2001). Problems with differentiating bands on the vertebral edge and application to older age classes may provide misleading results (Campana,

2001). Other methods have been used recently to report yearly band formation in sharks, including oxytetracycline marking (Simpfendorfer et al., 2002; Skomal and Natanson, 2003; Driggers et al., 2004) and bomb radiocarbon methods (Campana et al., 2002). However, validation exists for relatively few elasmobranch species (Cortés, 2000).

Two-phase growth models may be more appropriate for describing the growth of sharks, especially those that are longer lived. Soriano et al. (1992) developed a biphasic growth model which they applied to the long-lived Nile perch (*Lates niloticus*) to better describe their change in growth from zooplanktivores as juveniles to piscivores as adults. Growth by sharks could be regarded as being found in two phases: a rapid juvenile growth followed by a slower adult growth. From a bioenergetic perspective, this would follow a change from energy devoted to growth to energy devoted to reproduction. The logistic model could be regarded as a two-phase model and may help to describe this change. The shift from juvenile to adult would correspond to the inflection point (t_0) of the curve, which approximates biological age-at-maturity. In spinner sharks, age at maturity was reported to be about 6–7 years for males and 7–8 years for females (Branstetter, 1987). This estimate of age-at-maturity is similar to the inflection points from our logistic model of 6.75 and 7.62 years for males and females, respectively. Although each species should be evaluated separately, future studies should investigate the use of two-phase models to provide a more accurate description of the growth of elasmobranchs.

There have been few other examples of fitting alternative growth models to size-at-age data when results from the von Bertalanffy model were biologically incorrect or when models did not fit the data well. The present study represents the first attempt to do so for a species of shark. Comparison of age and growth models by Mollet et al. (2002) and Neer and Cailliet (2001) for two species of rays revealed that the Gompertz model best described their respective data although all models they tested fitted the data fairly well. For pelagic stingray (*Dasyatis violacea*) the Gompertz model predicted a more reasonable size-at-birth and growth rate than the von Bertalanffy growth model (Mollet et al., 2002). Neer and Cailliet (2001) reported a slightly better statistical fit for the Pacific electric ray (*Torpedo californica*) when using the Gompertz model. However, because the difference in model parameters was negligible, results were reported only for the von Bertalanffy model.

The von Bertalanffy growth model is still the most common model used to describe growth in fisheries literature, despite criticism by Roff (1980) who recommended its retirement. As pointed out by Roff (1980), the choice of using another equation should be determined by the variables that are being investigated and the results that are produced by the equation; for example, if the results appear to be biologically unrealistic. Our analysis of the growth of the spinner shark clearly demonstrates the value of this approach. Use of the von Bertalanffy growth model should continue because it

permits comparison of growth curves to information already published and in some cases adequately describes the growth of a given organism. However, the variety of statistical techniques and quality of each study make comparisons of von Bertalanffy growth curves between different populations difficult and results should be interpreted with caution regardless of what growth model is used (Roff, 1980).

Acknowledgments

We thank Enric Cortés, Pete Sheridan (NOAA Fisheries, Panama City Laboratory), and Miguel Arraya (Universidad Arturo Prat, Chile) for providing comments on earlier versions of this manuscript. Ken Goldman (Jackson State University) was especially helpful in discussion on precision and bias in age estimation, Miguel Arraya on the validity of the comparison of growth models, and Henry Mollet (Monterey Bay Aquarium) with the Gompertz model. Many different laboratories and institutions aided with the collection of vertebrae. George Burgess and Matt Callahan (University of Florida) provided samples from the directed shark longline fishery. Lisa Natanson (NOAA Fisheries, Narragansett Laboratory) obtained samples during their longline surveys from the U.S. south Atlantic Ocean. Observers Armando de Santiago, Carl Greene, Matt Rayl, Bill Habich, Mike Farni, Jacques Hill, and Jeff Pulver collected samples from the directed shark gillnet fishery. Mark Grace and Lisa Jones (NOAA Fisheries, Pascagoula Laboratory) provided samples from fishery-independent longline surveys. We also thank Linda Lombardi, Lori Hale, and numerous interns who assisted with the cleaning and processing of vertebrae samples.

Literature cited

- Allen, B. R. and S. P. Wintner.
2002. Age and growth of the spinner shark *Carcharhinus brevipinna* (Müller and Henle, 1839) off the KwaZulu-Natal coast, South Africa. *S. Afr. J. Mar. Sci.* 24: 1–8.
- Beamish, R. J., and D. A. Fournier.
1981. A method for comparing the precision of a set of age determinations. *Can. J. Fish. Aquat. Sci.* 38: 982–983.
- Branstetter, S.
1987. Age and growth estimates for blacktip, *Carcharhinus limbatus*, and spinner, *C. brevipinna*, sharks from the northwestern Gulf of Mexico. *Copeia* 1987:964–974.
- Branstetter, S., and J. A. Musick.
1994. Age and growth estimates for the sand tiger in the northwestern Atlantic Ocean. *Trans. Am. Fish. Soc.* 123:242–254.
- Branstetter, S., and R. Stiles.
1987. Age and growth estimates of the bull shark, *Carcharhinus leucas*, from the northern Gulf of Mexico. *Environ. Biol. Fish.* 20:169–181.
- Cailliet, G. M.
1990. Elasmobranch age determination and verifica-

- tion: an updated review. In Elasmobranchs as living resources: advances in biology, ecology, systematic and the status of the fisheries (H. L. Pratt Jr., S. H. Gruber and T. Taniuchi, eds.), p. 157-165. NOAA Tech. Rep. NMFS 90.
- Cailliet, G. M., and K. J. Goldman.
2004. Age determination and validation in chondrichthyan fishes. In The biology of sharks and their relatives (J. Carrier, J.A. Musick and M. Heithaus, eds.), p. 399-447. CRC Press, Boca Raton, FL.
- Campana, S. E.
2001. Accuracy, precision, and quality control in age determination, including a review of the use and abuse of age validation methods. *J. Fish. Biol.* 59:197-242.
- Campana, S. E., L. J. Natanson, and S. Myklevoll.
2002. Bomb dating and age determination of large pelagic sharks. *Can. J. Fish. Aquat. Sci.* 59(3):450-455.
- Carlson, J. K., E. Cortés, and D. M. Bethea.
2003. Life history and population dynamics of the finetooth shark, *Carcharhinus isodon*, in the north-eastern Gulf of Mexico. *Fish. Bull.* 101:281-292.
- Carlson, J. K., E. Cortés, and A. G. Johnson.
1999. Age and growth of the blacknose shark, *Carcharhinus acronotus*, in the eastern Gulf of Mexico. *Copeia* 1999:684-691.
- Castro, J. J.
1993. The shark nurseries of Bulls bay, South Carolina, with a review of the shark nurseries of the southeastern coast of the United States. *Environ. Biol. Fish.* 38:37-48.
- Chen, S. B., and S. Watanabe.
1989. Age dependence of natural mortality coefficient in fish population dynamics. *Nippon Suisan Gakkaishi* 55:205-208.
- Compagno, L. J. V.
1984. FAO species catalogue: sharks of the world. An annotated and illustrated catalogue of shark species known to date. FAO Fisheries Synopsis (125), vol. 4, part 1: Hexanchiformes to Lamniformes, 249 p. FAO, Rome.
- Cortés, E.
1997. A critical review of methods of studying fish feeding based on analysis of stomach contents: application to elasmobranch fishes. *Can. J. Fish. Aquat. Sci.* 54:726-738.
2000. Life history patterns and correlations in sharks. *Rev. Fish. Sci.* 8:299-344.
- Driggers, W. B., J. K. Carlson, D. Oakley, G. Ulrich, B. Cullum, and J. M. Dean.
2004. Age and growth of the blacknose shark, *Carcharhinus acronotus*, in the western North Atlantic Ocean with comments on regional variation in growth rates. *Environ. Biol. Fish.* 71:171-178.
- Fabens, A. J.
1965. Properties and fitting of the von Bertalanffy growth curve. *Growth* 29:265-289.
- Goldman, K. J.
2002. Aspects of age, growth, demographics, and thermal biology of two Lamniform shark species. Ph.D. diss., 219 p. Virginia Institute of Marine Science, Gloucester Point, VA.
- Goosen, A. J. J., and M. J. Smale.
1997. A preliminary study of the age and growth of the smoothhound shark *Mustelus mustelus* (Triakidae). *S. Afr. J. Mar. Sci.* 18:85-91.
- Grace, M., and T. Henwood.
1997. Assessment of the distribution and abundance of coastal sharks in the U.S. Gulf of Mexico and eastern seaboard, 1995 and 1996. *Mar. Fish. Res.* 59(4):23-32.
- Hoening, J. M., M. J. Morgan, and C. A. Brown.
1995. Analysing differences between two age determination methods by tests of symmetry. *Can. J. Fish. Aquat. Sci.* 52:364-368.
- Jensen, A. L.
1996. Beverton and Holt life history invariants result from optimal trade-off of reproduction and survival. *Can. J. Fish. Aquat. Sci.* 53:820-822.
- Knight, W.
1968. Asymptotic growth: an example of non-sense disguised as mathematics. *J. Fish. Res. Board Can.* 25:1303-1307.
- Lessa, R., F. M. Santana, and R. Paglerani.
1999. Age, growth, and stock structure of the oceanic whitetip, *Carcharhinus longimanus*, from the southwestern equatorial Atlantic. *Fish. Res.* 42:21-30.
- Mollet, H. F., J. M. Eczurra, and J. B. O'Sullivan.
2002. Captive biology of the pelagic stingray, *Dasyatis violacea* (Bonaparte, 1832). *Mar. Freshw. Res.* 53:531-541.
- Morison, A. L., S. G. Robertson, and D. G. Smith.
1998. An integrated system for production fish aging: image analysis and quality assurance. *N. Am. J. Fish. Manag.* 18:587-598.
- Natanson, L. J., J. G. Casey, and N. E. Kohler.
1995. Age and growth estimates for the dusky shark, *Carcharhinus obscurus*, in the western North Atlantic Ocean. *Fish. Bull.* 193:116-126.
- Neer, J. A., and G. M. Cailliet.
2001. Aspects of the life history of the Pacific electric ray, *Torpedo californica* (Ayres). *Copeia* 2001:842-847.
- Neter, J., W. Wasserman, and M. H. Kutner.
1990. Applied linear statistical models, 1408 p. Richard D. Irwin, Inc. Boston, MA.
- NMFS (National Marine Fisheries Service).
1993. Fishery management plan for sharks of the Atlantic Ocean, 167 p. Office of Fisheries Conservation and Management, National Marine Fisheries Service, NOAA, 1334 East-West Highway, Silver Springs, MD.
- Pauly, D.
1980. On the interrelationships between natural mortality, growth parameters, and mean environmental temperature in 175 fish stocks. *J. Cons. Int. Explor. Mer* 39:175-192.
- Ricker, W. E.
1975. Computation and interpretation of biological statistics of fish populations. *Bull. Fish. Res. Board Canada* 191:1-382.
1979. Growth rates and models. In *Fish physiology*, vol. VIII: Bioenergetics and growth (W. S. Hoar, D. J. Randall, and J. R. Brett, eds), p. 677-743. Academic Press, New York, NY.
- Roff, D. A.
1980. A motion for the retirement of the von Bertalanffy function. *Can. J. Fish. Aquat. Sci.* 37:127-129.
- Simpfendorfer, C. A., R. B. McAuley, J. Chidlow, and P. Unsworth.
2002. Validated age and growth of the dusky shark, *Carcharhinus obscurus*, from western Australian waters. *Mar. Freshw. Res.* 53:567-573.
- Skomal, G. B., and L. J. Natanson.
2003. Age and growth of the blue shark (*Prionace*

- glauca*) in the North Atlantic Ocean. Fish. Bull. 101:627-639.
- Soriano, M., J. Moreau, J. M. Hoenig, and D. Pauly.
1992. New functions for the analysis of two-phase growth of juvenile and adult fishes, with application to Nile perch. Trans. Am. Fish. Soc. 121:486-493.
- Van Dykhuizen, G., and H. F. Mollet.
1992. Growth, age estimation, and feeding of captive sevengill sharks, *Notorynchus cepedianus*, at the Monterey Bay Aquarium. Aust. J. Mar. Freshw. Res. 43:297-318.
- Vaughan, D. S., and M. L. Burton.
1994. Estimation of von Bertalanffy growth parameters in the presence of size-selective mortality: a simulated example with red grouper. Trans. Am. Fish. Soc. 123:1-8.
- von Bertalanffy, L.
1938. A quantitative theory of organic growth (inquiries on growth laws. II). Human Biology 10:181-213.
- Wintner, S. P., and G. Cliff.
1995. Age and growth determination of the blacktip shark, *Carcharhinus limbatus*, from the east coast of South Africa. Fish. Bull. 94:135-144.
- Wintner, S. P., S. F. J. Dudley, N. Kistnasamy, and B. Everett.
2002. Age and growth estimates for the Zambezi shark, *Carcharhinus leucas*, from the east coast of South Africa. Mar. Freshw. Res. 53:557-566.
- Zar, J. H.
1984. Biostatistical analysis, 718 p. Prentice Hall, Inc. Englewood Cliffs, NJ.

Abstract—Data recovered from 11 pop-up satellite archival tags and 3 surgically implanted archival tags were used to analyze the movement patterns of juvenile northern bluefin tuna (*Thunnus thynnus orientalis*) in the eastern Pacific. The light sensors on archival and pop-up satellite-transmitting archival tags (PSATs) provide data on the time of sunrise and sunset, allowing the calculation of an approximate geographic position of the animal. Light-based estimates of longitude are relatively robust but latitude estimates are prone to large degrees of error, particularly near the times of the equinoxes and when the tag is at low latitudes. Estimating latitude remains a problem for researchers using light-based geolocation algorithms and it has been suggested that sea surface temperature data from satellites may be a useful tool for refining latitude estimates. Tag data from bluefin tuna were subjected to a newly developed algorithm, called "PSAT Tracker," which automatically matches sea surface temperature data from the tags with sea surface temperatures recorded by satellites. The results of this algorithm compared favorably to the estimates of latitude calculated with the light-based algorithms and allowed for estimation of fish positions during times of the year when the light-based algorithms failed. Three near one-year tracks produced by PSAT tracker showed that the fish range from the California–Oregon border to southern Baja California, Mexico, and that the majority of time is spent off the coast of central Baja Mexico. A seasonal movement pattern was evident; the fish spend winter and spring off central Baja California, and summer through fall is spent moving northward to Oregon and returning to Baja California.

Tracking Pacific bluefin tuna (*Thunnus thynnus orientalis*) in the northeastern Pacific with an automated algorithm that estimates latitude by matching sea-surface-temperature data from satellites with temperature data from tags on fish

Michael L Domeier

Pfleger Institute of Environmental Research
901B Pier View Way
Oceanside, California 92054
E-mail address: Domeier@cs.com

Dale Kiefer

System Science Applications Inc.
PO Box 1589
Pacific Palisades, California 90272

Nicole Nasby-Lucas

Adam Wagschal

Pfleger Institute of Environmental Research
901B Pier View Way
Oceanside, California 92054

Frank O'Brien

System Science Applications Inc.
PO Box 1589
Pacific Palisades, California 90272

Current theories indicate the presence of a single stock of northern Pacific bluefin tuna (*Thunnus thynnus orientalis*) in the Pacific Ocean. Spawning adults have been recorded only from the western Pacific (Yamanaka et al., 1963; Yabe et al., 1966; Okiyama, 1974; Okiyama and Yamamoto, 1979; Nishikawa et al., 1985) but resulting offspring are known to either inhabit the western Pacific or to travel to the eastern Pacific (Sund et al., 1981; Bayliff, 1994; Itoh et al., 2003a) where they remain for an undetermined amount of time. Although it is believed that only a small fraction of the population migrates to the eastern Pacific, these fish are the basis for a fishery that occurs from May through October. A recent study has documented the migration of an archival-tagged juvenile northern Pacific bluefin tuna

from the western Pacific to the eastern Pacific in about two months, where it remained for eight months before being recaptured (Itoh, et al., 2003a). Conventional tagging studies have shown that Pacific bluefin tuna in the eastern Pacific eventually return to the western Pacific where they are believed to remain as adults (Sund et al., 1981; Bayliff, 1994). We provide this cursory summary merely as an introduction to our work, deferring the known details of Pacific bluefin biology to the excellent reviews that have been previously published (Bayliff, 1980, 1994; Sund et al., 1981). Work presented in the present study describes the use of electronic tags (pop-up satellite-transmitting archival tags and archival tags obtained from fish) and a newly developed sea surface temperature (SST) based geo-

Manuscript submitted 11 June 2004
to the Scientific Editor's Office.

Manuscript approved for publication
21 December 2004 by the Scientific Editor.
Fish. Bull. 103:292–306 (2005).

location algorithm to further our understanding of bluefin tuna movements in the eastern Pacific.

The light sensors on archival and pop-up satellite tags provide data on the time of sunrise and sunset, allowing one to calculate the approximate geographic position of an animal (Delong et al., 1992; Wilson et al., 1992; Hill, 1994; Bowditch, 1995; Sobel, 1995; Welch and Eveson, 1999; Hill and Braun, 2001; Metcalfe, 2001; Smith and Goodman; Gunn et al.²). The accuracy of the light-based geolocation estimates have been studied under controlled conditions (tags tethered to a moored buoy) and field conditions (tags attached to fish at a known location). Locations from tethered tags have been reported to be accurate to within ± 0.2 – 0.9° in longitude and ± 0.6 – 4.4° in latitude (Welch and Eveson, 1999, 2001; Musyl et al., 2001). Tagged tuna have provided light-based geolocation estimates within $\pm 0.5^\circ$ of longitude and ± 1.5 – 2.0° latitude (means of known locations (Schaefer and Fuller, 2002; Gunn et al.¹).

Light-based estimates are not precise and comparing studies that have examined the accuracy of this method is complicated by differences in tag hardware and geolocation algorithms used by different researchers. Other physical and biological factors complicate the issue further. Day length is not a good predictor of latitude during the spring and fall equinox, therefore estimates of latitude at times surrounding the equinox contain more error than at other times of the year (Hill and Braun, 2001). Latitude estimates are also more prone to error the closer the animal is to the equator (Hill and Braun, 2001). Additional errors can be introduced into estimates of both latitude and longitude by the behavior of the tagged animal (e.g., diving), bio-fouling of the tag, cloud cover, and wave action (Metcalfe, 2001).

Poor resolution of latitude estimates continues to be a problem for researchers using light-based geolocation algorithms. Under ideal theoretical conditions the variability in latitude error cannot be less than 0.7° and the expected variability in longitude will be a constant 0.32° (Hill and Braun, 2001). Sibert et al. (2003) developed an algorithm that applies a Kalman filter to light-based geolocation estimates in an attempt to reduce the error of these estimates. Although this approach smoothes data, it does not incorporate external data (data not collected by the tag) and therefore is still affected by errors inherent in the use of light-based geolocation es-

timates of latitude. It has been suggested that sea-surface-temperature (SST) and bathymetry data be used to refine light-based geolocation estimates (Block et al., 2001). These techniques are particularly useful when there is a north-to-south gradient of bathymetry or SST. The use of bathymetry to refine latitude requires an assumption that maximum diving depth is limited by the bottom depth; certainly this assumption introduces a new source of error. In addition, for animals that move off the continental shelf, bathymetry would be useless. The use of SST or bathymetry data to refine latitude necessitates the arduous task of matching tag data with another source of data.

It was our opinion that the accuracy of tracking marine animals could be improved through the development of an algorithm that automatically resolved latitude estimates by matching SST measurements from the tag to those taken from satellites. Here we present such an algorithm; one that was designed to operate in a geographic information system (GIS) environment, allowing for rapid analysis and display of archival and PSAT tag data. We demonstrate the algorithm and its product through the analyses of data we collected from Pacific bluefin tuna tagged in the eastern Pacific.

Materials and methods

Tagging in the field

Pacific bluefin tuna were captured on rod and reel from a recreational fishing vessel by using live bait and circle hooks. Fishing took place 123 nmi southwest, 86 nmi southwest, and 178 nmi south of San Diego in years 2000, 2001, and 2002, respectively. Fish were lifted into the boat with a vinyl sling and then placed on a soft mat, eyes were covered with a cloth, and the gills irrigated with seawater. The fish were then measured (fork length and girth), tagged, and immediately released. Sixteen fish were tagged with Wildlife Computers Inc. (Redmond, WA) pop-up satellite archival tags (PSATs), one fish was tagged with a Microwave Telemetry Inc. (Columbia, MD) PTT-100 PSAT, and seventeen fish were tagged with Lotek Wireless Inc. (Newmarket, Ontario) LTD2310 nontransmitting archival tags. The two types of PSATs either provided data once an hour (depth, water temperature, light level [Microwave Telemetry, Inc.]) or summarized data that had been collected every two minutes (Wildlife Computers, Inc.)—the difference being an artifact of the two tag manufacturers. The Lotek archival tags provided us with data every two minutes detailing the swimming depth, water temperature, internal fish temperature, and light level. Pressure sensor drift was adjusted by the tag manufacturers' software for PSAT tags and in the laboratory for the Lotek tags.

The PSAT tags were rigged with 300-lb monofilament leaders and a nylon dart. In 2000 and 2001 the dart was a "bluefin-type" provided by Eric Prince (NMFS-SEFSC); in 2002 a Pfleger Institute of Environmental Research (PIER) "umbrella" dart was used (Fig. 1).

¹ Smith, P., and D. Goodman. 1986. Determining fish movements from an "archival" tag: precision of geographical positions made from a time series of swimming, temperature and depth. NOAA Tech. Memo. NMFS-SWFC-60, 13 p. Southwest Fisheries Science Center, La Jolla, CA 92038.

² Gunn, J. S., T. W. Palacheck, T. L. O. Davis, M. Sherlock, and A. Bettleheim. 1994. The development and use of archival tags for studying the migration, behavior and physiology of southern bluefin tuna, with an assessment of the potential for transfer of the technology to groundfish research. In Proceedings of ICES mini-symposium on fish migration, 23 p. International Council for the Exploration of the Sea, Palaegade 2-4, DK-1261 Copenhagen K, Denmark.

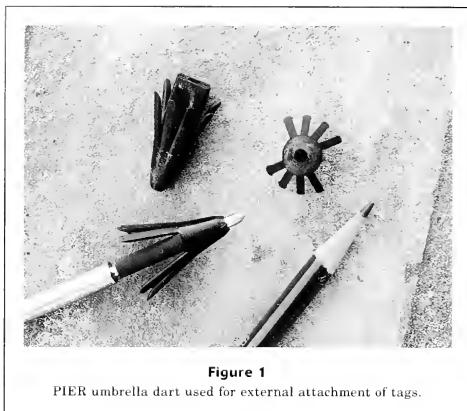


Figure 1
PIER umbrella dart used for external attachment of tags.

Each style of dart was inserted through the midline of the fish at the base of the second dorsal fin according to the method of Block et al. (1998).

Archival tags were surgically implanted either in the dorsal musculature below the first dorsal fin (when fork length was >110 cm) or into the peritoneal cavity (when fork length was <110 cm). The dorsal musculature implant was performed by making a 1-cm incision 3–5 cm below the first dorsal fin. A cold-sterilized trocar (14 mm diameter) was then inserted into the muscle, to a depth of 13–14 cm, within a plane parallel to the pterygiophores but angled 45 degrees to the anterior. The trocar was then removed and the tag was inserted so that the light stalk was angled toward the tail. The incision was then closed with a monocril suture material. This method was similar to that used by Musyl et al. (2003). Interperitoneal implants were done according to the method of Block et al. (1998).

PSAT Tracker algorithm and analysis system

We have developed an automated system, called the PSAT Tracker Information System (PTIS), to improve the accuracy and minimize the subjectivity and tedium of matching data from different sources (tag and satellite). It is an application of the Environmental Analysis System (EASy) (System Science Applications, Redondo Beach, CA) software that is specifically designed for handling four-dimensional information (latitude, longitude, depth, and time). We describe the system in terms of three processes; importing tag data and satellite imagery, calculation of the optimal path of the tag, and dynamic display of the path and associated tag information.

Importing tag data and setting parameters

The PSAT tracker information system was designed to support data formats of three tag manufacturers: Wildlife Computers, Microwave Telemetry, and Lotek. All three tag formats are imported into FIS and stored in a universal relational database format for processing. Key parameters used in the calculation of tracks include time and position of tag deployment, time and position of tag recovery, light-based estimates of longitude (provided by tag manufacturers), maximum swimming speed of the tagged fish (estimated and determined by the user), and a bracketed range of latitude within which the program will search for SST matches. Processing involves the temporal matching of SST as recorded by the tag with that measured from satellite imagery. It is important to note that the PTIS user-defined latitude bracket is unrelated to the light-based latitude estimates provided by the tag manufacturers; instead, it is simply a range set by the user to include all possible movement of the animal during the tag deployment. However, longitude estimates are tied to the tag manufacturers' light-based estimates; the user has the option of tying PTIS position estimates directly to the light-based estimates or allowing the algorithm to search a specified distance on either side of the light-based estimate.

For this study the maximum fish velocity was set at 4 knots. This was meant to be an inclusive rather than an exclusive value, broadening the range PSAT Tracker could search for SST matches. SST matches were also constrained to remain within ± 20 nautical miles ($\pm 0.33^\circ$) of the manufacturers' light-based estimates of longitude, based upon the observance by Hill and Braun

Table 1

Resolution of sea-surface-temperature data from satellites and tags (advanced very high resolution radiometer [AVHRR], moderate resolution spectroradiometer [MODIS], multichannel sea surface temperature algorithm [MCSST]).

Source	Accuracy (+C)	Spatial scale (km)	Temporal scale	Availability
AVHRR pathfinder	0.3–0.5	9	Daily	1985–present
AVHRR pathfinder	0.3–0.5	9	8-day composite	1985–present
MODIS	0.3	4.6	Daily	Oct 2000–present
MODIS	0.3	4.6	8-day composite	Oct 2000–present
MCSST (Miami)	0.5–0.7	18	Weekly composite	1981–Feb 2001
MCSST (NAVOCEANO)	0.5–0.7	18	Weekly composite	Sep 2001–present
Wildlife computer tag	0.05	—	1–12/day	—
Microwave telemetry tag	0.17	—	60 minutes	—
Lotek 2300 tag	0.1	—	2 minutes	—

(2001) that light-based longitude estimates have a year round constant error of ± 0.32 degrees.

Satellite imagery, temperature sensors, and land mask

The PSAT Tracker code provides an interface to automatically download, georeference, and display SST imagery. As many as three different types of imagery can be layered and prioritized to produce a collage of imagery for processing and display. Higher priority layers are searched first for SST matches before “drilling down” to lower layers. The sources and types of available SST data are numerous and have varied over the time frame of this study; different sensors and algorithms produced data of differing spatial and temporal resolution or accuracy (Table 1). To maximize the quality of the latitude estimates produced by the PSAT Tracker algorithm, we substituted better SST data as it became available. For this study SST imagery was prioritized as follows: 1) advanced very high resolution radiometer (AVHRR) or moderate resolution spectroradiometer (MODIS) daily data, 2) AVHRR or MODIS weekly data, and 3) multichannel sea surface temperature algorithm (MCSST) weekly data. The MCSST algorithm is a weekly (or 8-day) composite that is most helpful in analyzing regions of frequent cloud cover; this algorithm was applied by the University of Miami (Miami) from 1981 through February 2000 and has been applied by the Naval Oceanographic Office (NAVOCEANO) since September 2001. The MCSST algorithm provides a near complete picture of SST data for the study area; although AVHRR and MODIS data are higher resolution and more accurate.

The difference in the resolution and accuracy of temperature sensors on the tags verses those on the satellites (Table 1) are worth mentioning. The accuracy of the satellite SST data, particularly for MCSST/NAVOCEANO, is the limiting factor when attempting to match tag data to satellite data. The degree to which the satellite data and tag data must match can be set by the user in PSAT Tracker; for this study it was set

between the limit of MODIS and NAVOCEANO resolution (0.4°C).

There is a fourth layer that is superimposed upon the imagery. This is a land mask that is used to eliminate placing a tag on land and to insure that tags move around land barriers rather than across them.

Computation of the track

A detailed mathematical description of the computation for the best track would take more space than is available. Instead, we present a more general description of the algorithm and its logic, consisting of the following five steps that are summarized below and then subsequently described in detail.

- 1) Define the daily search area found within satellite SST imagery.
- 2) Define appropriate tag data (termed selection set) to match to satellite SST values found within the daily search area.
- 3) Select candidate points within each daily search area that provide the best match to the temperatures found in the selection set. The cost of each candidate point is largely determined by the difference between the tag and satellite SST values.
- 4) Calculate the cost for all possible steps, called arcs, between pairs of candidate points of adjacent daily search areas. The cost of each step is a function of the length of the arc that connects adjacent candidate points (the greater the distance, the greater the cost) and the cost of each individual candidate point (see step 3).
- 5) Sum the costs of all tracks and identifying the track with the lowest cost.

Step 1: Defining the daily search area A daily search area is defined by the tag manufacturers’ light-based solution for longitude, a user defined bracket for latitude and the value entered for maximum swimming

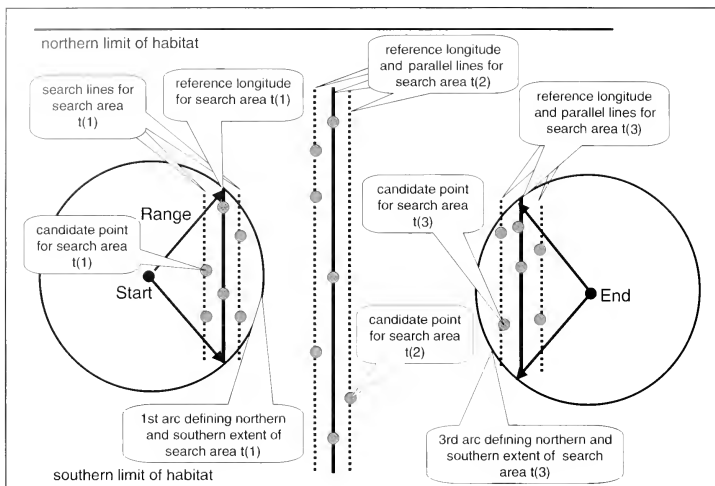


Figure 2

Definition of terms used to describe the PSAT Tracker algorithm. A search area is a region in a satellite thermal image where a search is conducted for pixels whose temperature values match those recorded by the tag at that time and when it is at the surface. The search area consists of a reference longitude line, defined by the daily calculation of latitude provided by the manufacturer's processed data record and parallel search lines that provide a hedge on this determination. The search area is uniquely defined by the time at which this calculation was determined. The northern and southern bounds of the search area are determined by either the habitat range or the maximum distance that the tagged fish can swim during each time step. Those pixels underlying the reference and search line, whose temperature best match the temperatures of the selection set of points from the tag, are chosen as candidate points. One candidate point from each search area will eventually define the best track.

speed of the fish. The latitudinal bounds of the daily search area are constrained in two ways, by the known (or unknown) bounds of the fish's habitat and by its maximum swimming speed. The northern and southern bounds of the habitat are entered by the user, and no areas are searched that are beyond these latitudes. These values are meant to be inclusive and can be determined from the literature or estimated by using latitude values provided by light-based geolocation algorithms. These bounds are set prior to processing and do not change throughout the processing; in this study the latitude search area was restricted to waters between 15 and 50 degrees north.

Each search area is centered on the light-based longitude estimate (termed the reference longitude). PSAT Tracker does not search every pixel of SST data for matches, but instead searches along parallel lines of longitude on either side of, and including, the reference

longitude. These lines, termed search lines, are spaced at equal distances from the reference longitude (Fig. 2). The user establishes the extent to which PSAT Tracker searches to the east and west of the reference longitude by choosing the number of search lines as well as their distance of separation. In this study four search lines were drawn on either side of the reference longitude; these parallels were drawn 5 nmi apart resulting in a 40 nmi wide daily search area. We refer to each search according to the time at which the reference longitude was determined, $t(i)$ (where t is the time for which the reference longitude was determined and i is the index for the sequence of daily search areas in the time series).

The maximum swimming speed of the fish can also constrain the latitudinal bounds of a daily search area. The farthest a fish can swim in a given time interval is simply the product of its maximum swimming speed and the length of the time interval. Thus, all possible posi-

tions that a fish can occupy when swimming in a fixed direction from the starting point of a track is the locus of points forming a circle whose center is at the starting point and whose radius is the product of its maximum swimming speed and the length of the time interval. Likewise, the farthest positions from which a fish can swim in given direction and reach the end point of the track is the locus of points forming a circle whose center is at the end point and whose radius is the product of its maximum swimming speed and the length of the time interval. The intersection of loci originating from either the start point or end point with a reference to longitude defines the most northern and southern extent of the search area for that reference longitude.

Because the distance of arcs whose center lies at the start point increases with time, whereas the distance of arcs whose center lies at the end point decreases with time, the latitudinal range of the search area is usually smallest at the start of the time series and at the end of the time series and is usually largest midway through the time series. The long time series obtained from the recovered archival tags creates a situation where the latitudinal extent of the search areas is largely determined by the northern and southern bounds of the habitat rather than by swimming speed. Swimming speed does, however, constrain east-west movement on a daily basis because the reference longitudes anchor the search areas.

Step 2: Selection sets for tag data The second step of processing involves selecting SST records (from the tag data set) that are coincident in time with the daily search area. The user can define the sea surface layer by entering a maximum depth of this layer; for this study the surface layer was defined as 0–1 m. The user can also determine how many values from the selection set should be used to search for SST matches. We chose a selection set consisting of three individual values for PSAT tags; however, because of the much higher frequency of measurements from the archival tags, we chose a selection set that consisted of a single average SST value for each day. The temperatures found in the selected set of points for a given daily search area would be used to calculate the location of pixels within the search area that the tag most likely visited.

Step 3: Choosing candidate points Selecting candidate points from which a best track will be chosen begins by assigning a temperature cost to pixels within the search area. The temperature cost for a given pixel, j , with a search area referenced by time, $t(i)$, $\Delta T[j, t(i)]$, is simply the absolute value of the difference in its temperature, $T_{sat}(j, t(i))$, and that of its closest match, k , from the selected set of tag points, $Ttag[k, t(i)]$:

$$\Delta T[j, t(i)] = |T_{sat}[j, t(i)] - Ttag[k, t(i)]|.$$

The temperature cost, $\Delta T[j, t(i)]$, is an inherited trait of a pixel and will be applied to all further calculations of the best track(s). If the temperature cost of any pixel

examined in a search area exceeds the cutoff value entered by the user, that pixel will be removed from further consideration. Pixels will also be removed if they lie over land.

Those pixels that remain are next subjected to an evaluation to determine if they qualify as candidate points. This evaluation is based upon the value of a cost function that weighs both the pixel's temperature cost described above, $\Delta T[j, t(i)]$, and the pixel's contribution to spreading coverage over the search area:

$$Cost[j, t(i)] = \Delta T[j, t(i)] + Spread\ Factor \times \Delta L[j, t(i)].$$

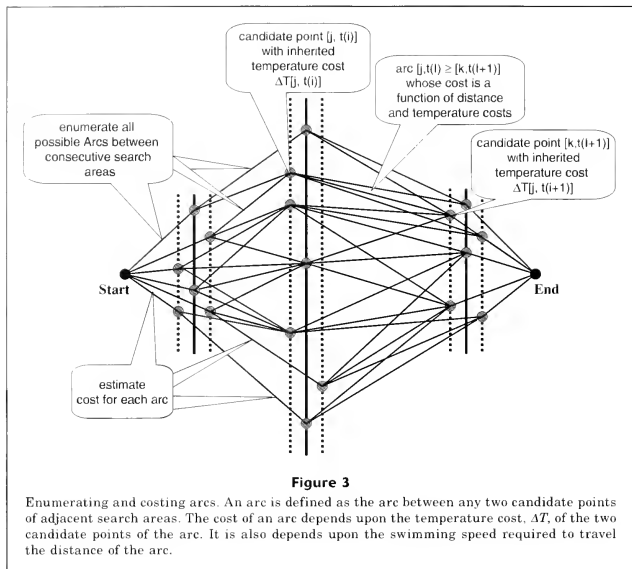
$\Delta L[j, t(i)]$ is the relative contribution a pixel makes to providing even latitudinal distribution along the reference longitude and search lines of the daily search area; the *Spread Factor* weights the relative importance of temperature costs with the benefit of obtaining an even distribution. Although the primary criterion for selecting candidate points is how well tag SST matches satellite imagery SST, we have found that this criterion alone can cause all the selected candidate points to be bunched together. Such aggregation will force the computed track into small regions of the search area without regard to the distribution of matching pixels in proceeding or succeeding search areas. To avoid this problem the *Spread Factor* function spreads candidate points in a north–south direction thereby providing smoother and more economical tracks. The degree to which the *Spread Factor* function spreads candidate points is controlled by the user by entering a weighted value. For this study we chose an intermediate value (5000 out of a possible 9999) and this value was constant for all evaluations.

The number of candidate points finally determined is determined by the user. For this study, five candidate points were identified for each search area. When the user defines the number of points to be evaluated in the search areas, pixels having the lowest cost are ranked and selected accordingly.

Step 4: Enumerate and calculate the cost of arcs After the candidate points have been chosen, the best track(s) is computed by choosing a single candidate point from each of the daily search areas in the time series. The best track is selected from all possible tracks by choosing the one of least cost. Thus, the solution is global rather than serial. The computation begins by calculating the cost of arcs between candidate points from adjacent search areas, and ends by summing the cost of all the arcs of a given track (Figs. 3 and 4).

The cost of an arc is a function of the temperature match for the pair of candidate points that define the arc, $\Delta T[j, t(i)]$ and $\Delta T[k, t(i+1)]$, as defined above. It also depends upon the minimum swimming speed required of the fish traveling between the two candidate points, *arc velocity min*, where

$$arc\ velocity\ min = \frac{distance\ between\ candidate\ pixels}{(t(i+1) - t(i))}.$$



The cost of the arc between candidate point j and candidate point k is

$$\text{arccost}(\{j, t(i)\} \rightarrow \{k, t(i+1)\}) = (\Delta T(j, t(i)) + \Delta T(k, t(i+1))) +$$

$$\text{DistFactor} \left(\frac{\text{arccmin}}{\text{velocity}} \right)$$

where velocity = the maximum sustained swimming speed of the fish; and

DistFactor = a factor that scales the cost of swimming at a given speed in relation to the sum of the temperature costs of the two candidate points.

Values for the DistFactor and Velocity are determined by the user. The rationale for such cost is that the best track should include an assessment of variations in swimming velocity as well as the costs of temperature. If swimming speed is judged to be an insignificant cost or too difficult to quantify, the DistFactor can be set to 0. If a land barrier lies between the pair of candidate points, the distance to swim around the barrier is calculated and included in the cost of the arc. In this study an interme-

diante value (5000 out of 9999) was assigned for the DistFactor , and this value was constant for all evaluations.

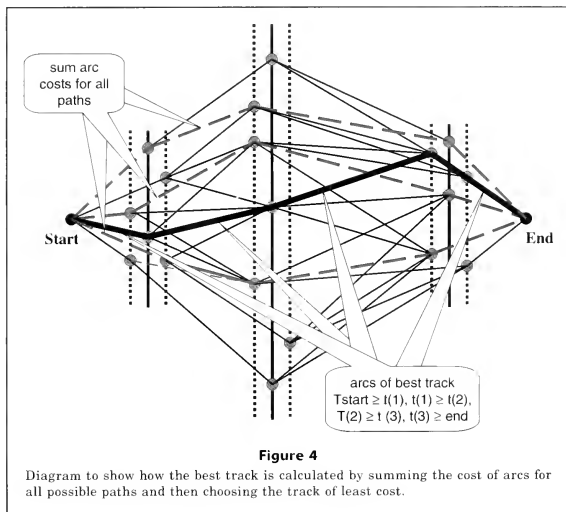
Step 5: Calculating the best track Finally, the algorithm calculates the sum of the arc costs for each track:

$$\text{Cost of tract} = \sum_{t_{\text{start}}}^{t_{\text{end}}} \text{arccost}(\{j, t(i)\} \rightarrow \{k, t(i+1)\}).$$

The costs for all possible tracks are then ranked, and the track(s) with the lowest cost(s) is then saved and available for display (Fig. 4). The track is saved in a table of the PSAT Tracker database; the table contains records of the latitude, longitude, time, and surface temperature of the candidate points that comprise the track, as well as records of surface temperature from the satellite imagery at regular intervals along the arcs between candidate points. Depending on the length of the time series, this process analyzes tens of thousands to hundreds of thousands of tracks and thus is the most time-consuming step of the algorithm.

Analyzing position data from PSAT Tracker

Location estimates provided by PSAT Tracker were subjected to spatial analysis to describe the move-



ment patterns and habitat use of Pacific bluefin tuna in the eastern Pacific. Monthly data were combined within each tag data set prior to performing utilization distribution analyses with the Home Range Extension for ArcView (version 1.1c, BlueSky Telemetry, Aberfeldy, Scotland) that employs the fixed kernel method (Rodgers and Carr, 1998). Results were displayed as volume contours displaying the main centers of activity for each fish during a given time period. Initial analyses allowed us to combine data so that figures could be minimized. For the archival tag data, consecutive months with similar spatial distribution were combined and individual fish with very similar tracks were combined. All data from fish that were PSAT tagged were combined by month because of the relatively sparse data compared with the data from the archival tags. PSAT tag data provided a glimpse at year-to-year variations in bluefin distribution (August 2000 through October 2002), whereas the archival tag data were for a single year and allowed for a monthly comparison within one year (August 2002 to September 2003).

The near daily position data provided through the PSAT Tracker analyses allowed us to calculate the swimming speed of each fish. This was done by simply dividing the horizontal distance between consecutive data records by the time between consecutive data records (1–4 days).

Results

Tag recoveries

Fifteen of the PSAT tags transmitted data after remaining on the fish from 2 to 191 days (Table 2). Unfortunately some of these tags did not transmit usable data. Fourteen of them provided a pop-up location and eleven of them transmitted enough data for some level of analyses of behavioral and movement patterns. The Microwave Telemetry PSAT tag provided an archival data set with a one-hour sampling schedule. The Wildlife Computer PSATs transmitted data summaries that included a daily water column profile of temperature (obtained from the deepest dive) and the percent time each fish spent within predetermined temperature and depth bins.

Four archival tags were recovered after a period at liberty of 16 hours to 385 days (Table 2). The 16-hour archival tag recovery was made from a recreational angler very near the point of release; this tag was not used for any analyses. The three tag recoveries made after 300 days came from a purse-seine vessel. Two of these three recaptured fish spent several weeks in a grow-out pen before the tags were discovered; the dates the fish were in the pen were not used for any analyses. The light stalks of tags 441 and 159 were damaged during recovery. For these tags, the internal temperature and pressure sensors were verified by Lotek data, but external

temperature and light level sensors could not be checked. For tag 233, none of the sensors could be verified because the tag had to be disassembled and destroyed by Lotek personnel in order to recover the data.

Table 2

Details of tagged Pacific bluefin tuna (*Thunnus thynnus orientalis*). WC=Wildlife Computer Tag, MT=Microwave Telemetry Tag, Lot=Lotek Tag.

Fish	Tag date	Weight (kg)	Time at liberty (days)
4 WC	13 August 2002	36	23
184 WC	13 August 2002	60	62
200 WC	13 August 2002	41	51
245 WC	2 August 2000	51	19
247 WC	2 August 2000	57	38
249 WC	2 August 2000	50	102
265 WC	2 August 2000	52	33
301 WC	2 August 2000	60	191
961 WC	3 August 2001	32	9
962 WC	3 August 2001	35	4
964 WC	3 August 2001	35	23
1041 WC	3 August 2001	26	2
1042 WC	2 August 2000	42	72
283 MT	13 August 2002	41	61
114 Lot	13 August 2002	52	16 (hours)
159 Lot	13 August 2002	52	375
233 Lot	14 August 2002	43	385
441 Lot	30 August 2002	12	323

PSAT Tracker algorithm

The archival tags provided large data sets that allowed for the comparison of the PSAT Tracker algorithm to the manufacturer's light-based geolocation solution. Because longitude estimates generated by PSAT Tracker are constrained by the light-based estimates, these values differed very little from the position estimates from the various tag manufacturers. Although similar, the PSAT Tracker latitude solutions were generally less erratic than those produced from the three light-based algorithms, particularly surrounding the times of the equinoxes (Figs. 5 and 6). The spring and fall equinoxes each produced approximately two months of unreliable latitude estimates for light-based algorithms.

Pacific bluefin tuna habitat use

Horizontal movement Tagged bluefin tuna ranged as far north as the California–Oregon border and nearly to the tip of Baja California, Mexico, to the south. Although this distance encompasses 2400 km of coastline, these fish spent the majority of their time in the southern part of the range, best illustrated by a home range analysis of the combined approximately year-long tracks of the three archival tagged bluefin (Fig. 7). Tagged off the northern coast of Baja California, Mexico, these three bluefin moved northward until November, followed by a southward migration to south-central Baja California where they spent the months of January through June (Fig. 8). The two larger archival-tagged fish reached the offshore waters of Oregon before turning south and the smaller fish did not venture north of San Francisco, California. The two larger fish spent much of the winter and spring (January–June) in the coastal bight between Punta Eugenia, Mexico, to the north and Cabo San Lazaro, Mexico, to the south, and the smaller fish had a more dispersed spring range north of Punta Eugenia. In July all three fish began to move to northern Baja, back into the general area where they were originally tagged and where they were subsequently recaptured (Fig. 8).

This general pattern of summer–fall movement northward followed by a winter migration southward and a winter–spring holding pattern off south-central Baja California was supported by data from fish with PSATs in years 2000 through 2002 (Fig. 9).

Although position data for the months of January through June generally placed the tagged bluefin off southern Baja, two of the three fish tagged with archival tags underwent rapid April excursions to the north before returning to the south (Fig. 10). Fish 159 traveled 2130 km, one way, before returning by 1 May; fish 441 made a similar move but did not go as far north (1285 km) and stopped its southward return 480 km north of its original starting point. The extreme

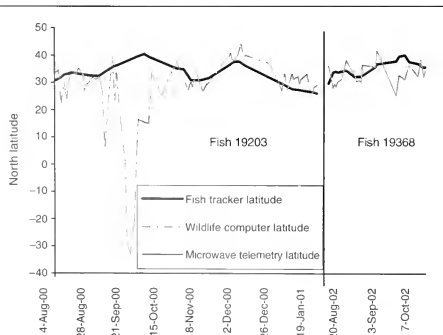


Figure 5

PSAT Tracker SST-based latitude solutions vs. Wildlife Computers and Microwave Telemetry light-based latitude estimates.

northern latitude estimates calculated by PSAT Tracker placed fish 441 slightly north of Point Conception, California, and fish 159 near the California–Oregon border before it returned to wintering grounds off Baja California (Fig. 10). This movement is corroborated by a westerly trend in longitudes and a dramatic drop in SSTs. For fish 159, SST dropped from 19.1°C on 4 April 2003 to 12.4°C on 18 April 2003. Similarly, fish 441 experienced an SST drop from 19.5°C to 13.5°C between 1 and 18 April.

Data from the archival tags provided near daily positions for each fish. The longest time between successive fixes was four days. The calculated swimming speeds between successive position fixes ranged from 0 to 14.7 knots for all three fish combined. The mean swimming speed for all three fish was 1.3 knots (± 1.3 kn).

Depth and temperature ranges Vertical movement was similar to that reported for other bluefin tuna (Block et al., 1997; Block, 2001; Kitagawa et al., 2004). Detailed analyses of vertical movement and temperature preferences and tolerances are beyond the scope of this article and will be presented in a future publication. In general, dives were most common during the day; maximum dive depths ranged from 341 to 382 m. Fish with archival tags spent nearly 70.1% of the time near the surface (<20 m deep). Ambient water temperatures ranged from 5.7°C to 25.0°C (mean=17.4°C). The internal temperature of fish tagged with archival tags ranged from 14.1°C to 29.5°C (mean=21.8°C); average internal temperatures of the fish were 4.4°C warmer than ambient waters and at times were up to 19.2°C warmer.

Discussion

Although we used SST matching as the sole means of estimating latitude for the fish tracks and spatial analyses presented in our study, the extent of the northward fall migration of juvenile Pacific bluefin tuna in the eastern Pacific has been corroborated by occasional commercial landings of Pacific bluefin tuna in Oregon (McCrae³). Because Pacific bluefin tuna are apparently capable of existing in the northern part of the eastern Pacific range, even during the colder months of the year, it is not clear what dictates the movement pattern of these fish. It is reasonable to speculate that the tuna are taking advantage of seasonal ocean warming to exploit distant prey when the physiological expense to maintain optimum body

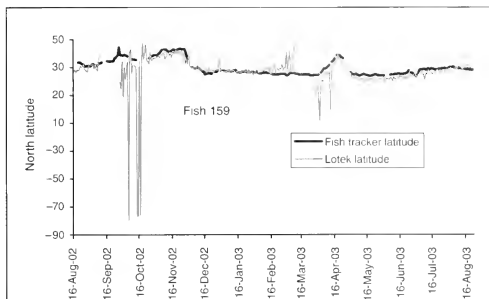


Figure 6

PSAT Tracker SST-based latitude solutions and Lotek light-based latitude estimates.

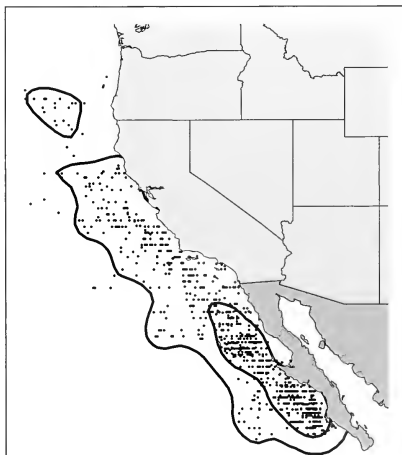
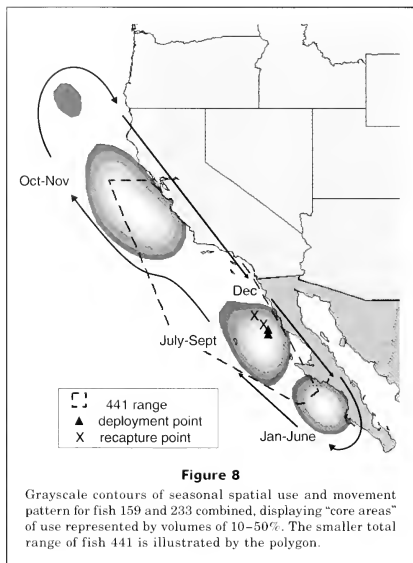


Figure 7

Fixed kernel home range analysis illustrating relative importance of the range of juvenile Pacific bluefin tuna (*Thunnus thynnus orientalis*) in the eastern Pacific; displayed are all points for fish 159, 233, and 441 and volume contours of 95% (outer line) and 50% (inner line) for all three fish combined. Isolated circle to the north is a 95% contour.

³ McCrae, J. 2004. Personal commun. Oregon Dept. Fish & Wildlife, Newport, OR 97365.

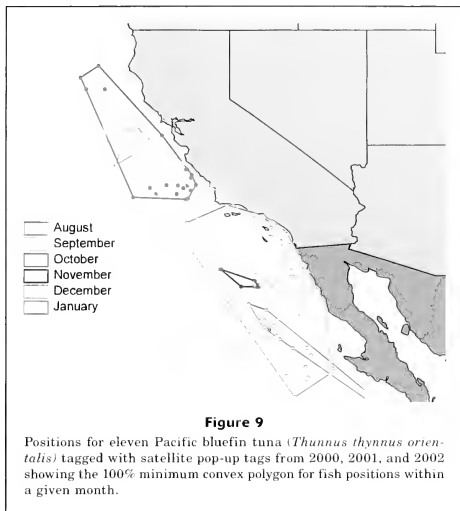


temperature is less. Temperature and depth tolerances and preferences indicated in our study are similar to those of bluefin tuna studied in other parts of the world (Carey and Teal, 1969; Carey and Lawson, 1973; Block et al., 1997; Kitagawa et al., 2000, 2004; Block et al., 2001; Brill et al., 2002; Itoh et al., 2003b).

The migration of a fish with an archival tag from the western Pacific to the eastern Pacific (Itoh et al., 2003a) provides an interesting comparison to our data. This individual, tagged off Japan, made the trans-Pacific migration in about two months and then resided in the eastern Pacific for about eight months before being recaptured by a recreational angler. The fish arrived off the coast of northern California in the month of January—a time when fish from our study were found to be at the southern extreme of their eastern Pacific range. By the month of March, the western Pacific migrant had traveled to the winter-spring grounds where it then seemed to behave in a pattern similar to that of fish tagged for our study. Whether or not the Itoh et al. (2003a) tagged fish illustrated a typical transition from trans-Pacific migrant to eastern Pacific resident will require more tag recoveries. It will be equally interesting to see future descriptions, from archival-tag data, of maturing Pacific bluefin tuna making the trip back to the western Pacific.

Two of the Pacific bluefin tuna with archival tags were captured and recaptured in very close proximity in both space and time of year. The computed tracks for these two fish, both relatively large for the eastern Pacific, also showed that they kept close to each other for most of the year. A smaller fish, tagged a month later, underwent a similar north to south movement, but did not range as far north, particularly, or south. Given our extremely low sample sizes, very little can be concluded, but the question is raised as to whether or not Pacific bluefin tuna of different year classes have distinct schools and migratory behaviors. It is also important to point out that the two larger fish were tagged in the dorsal musculature, whereas the smaller fish was tagged in the peritoneal cavity. The orientation of the light stalk is different for these two methods, one pointing towards the surface and the other in the shadow of the fish and pointing down. How this tag orientation may influence the detection of light and subsequent position estimates is unknown.

Two of our fish with archival made rapid northward migrations into much colder water in the early spring. This northward migration is similar to that made by Itoh's fish in the early spring of 1998. Because these movements occurred at a time when the light-based latitude estimates prove unreliable, it would not have



been possible to be certain that this rapid excursion was authentic without the aid of SST matching (as was also done by Itoh et al. [2003a]).

The PSAT Tracker algorithm provided relatively quick and automated geolocation estimates for data recovered from three separate types of tags deployed on Pacific bluefin tuna. Furthermore, the PSAT Tracker latitude solutions compared favorably to the light-based latitude estimates during non-equinox times of the year. The use of SSTs to resolve latitude allowed for spatial analyses of individual bluefin positions for every month of the year, whereas a strictly light-based approach would not provide reliable latitude position estimates for approximately 30% of a year-long track. PSAT Tracker also results in a global, rather than serial track solution. In essence this means that no single position estimate is selected without regard to the influence this position has on the overall track. A serial track is one that is produced by selecting each position without regard to the effect each selection has on the overall track. A serial track is also heavily biased by the start point and may weight the location estimates based upon the previous location estimate, allowing a single poor location estimate to ruin the remainder of the location estimates for the track.

It is instructive to compare our SST matching algorithm to the Kalman filter-based algorithm developed by Sibert et al. (2003). The Sibert et al. algorithm depends solely upon light data collected by the tag to

estimate latitude and longitude, whereas the PSAT Tracker algorithm depends upon the light field to provide an estimate of longitude and solely upon the sea surface temperature to provide an estimate of latitude. The initial estimates of both approaches are then refined according to a goodness-of-fit criterion that depends upon assumptions regarding the swimming behavior of the tagged fish. In the case of the Sibert et al.'s algorithm, the behavior of the fish is modeled in terms of a biased random walk model that describes the movement of the fish in terms of an advection-diffusion equation; the advective term describes the most probable displacement of the fish during a time step and the diffusive term describes the distribution of less likely displacements. The usefulness of the random walk model is largely determined by the adequacy of describing the distribution of swimming speed and direction of the fish. The algorithm also includes formulations of the dependence of the accuracy and precision of the estimates of latitude and longitude from the tag upon other factors. For example, around the equinox the weighting of the estimate of latitude from the tag measurements is greatly reduced (specifically an inverse cosine squared function of date.) The Sibert et al. algorithm simply searches for a track that minimizes discrepancies between the positions predicted from random walk model (the transition equation) and those predicted from the tag measurements (the measurement equation).

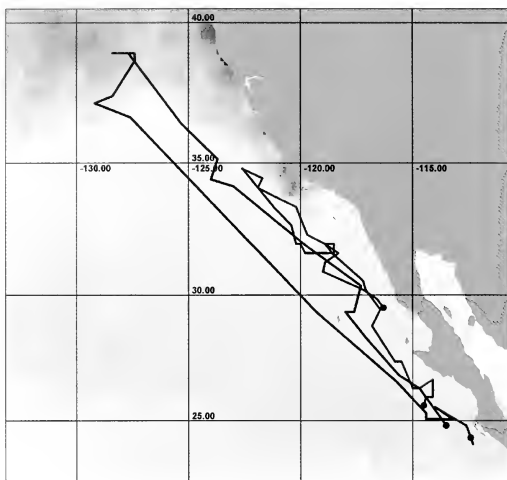


Figure 10

Track showing northward excursions of fish 159 (track extending to 38°) and 441 (track extending to 34.5°) between 1 April and 10 May 2003. Displayed SST imagery is a composite for the month of April showing a 7°C temperature gradient.

PSAT Tracker is similar to the Sibert et al. algorithm in that it invokes a model of fish behavior; there is a simple constraint on the maximum distance that a fish can swim during a time step, and shorter tracks that require lesser expenditures of energy by the fish are favored. Like the Sibert et al. algorithm, the PSAT Tracker also incorporates candidate points that are not limited to the initial light-based estimate of longitude but includes adjacent longitudes based upon the user's assessment of the accuracy of the initial estimate. Finally, both the Sibert et al. and the PSAT Tracker algorithms yield a solution that provides a best fit to the time series of satellite (in the case of PSAT Tracker) and tag measurements to the model of fish behavior.

Unfortunately, it is difficult to make a general assessment of the accuracy of either approach. In the case of the PSAT Tracker algorithm, the accuracy of the track will decrease in the absence of a north-south temperature gradient. We have not found a means of quantitatively determining the accuracy of PSAT Tracker calculations. However, the quality of the fit between pixel values of temperature from imagery and tag values for positions along the track is calculated as a χ^2 value. In the case of the Sibert et al. algorithm, the accuracy of the track will decrease during the period of the equinox when the latitudinal errors of the light-based estimates

are extremely large. Our data indicate that this period can be as long as two months surrounding each equinox (skewed towards winter). At such times the estimates of position derived by the Sibert et al. algorithm depend largely on the random walk model of fish movement, which provides only a generic description of movement. Although the algorithm provides values for the mean square errors of bias and randomness for the tag estimates of latitude and longitude, these values are not true values for error of predicting location; rather they represent of the discrepancy between the estimates of position by the random walk model, the formulation of the latitude estimation error, and the tag measurements. Additionally, the Sibert et al. algorithm does not exclude the possibility of placing a fish on land.

The PSAT Tracker worked well for this study because of the strong north-to-south temperature gradient that is presented in the northeastern Pacific. Studies conducted in regions with poor temperature gradients will continue to rely on light-based latitude estimates and approaches like the Sibert et al. algorithm. Further development of PSAT Tracker, or other SST-based geolocation algorithms, should explore a means of using light-based latitude positions in combination with SST matching when light data are reliable, but excluding light-derived latitude positions when they are unreliable.

Acknowledgments

This study was made possible through the support of the George T. Pflieger Foundation and the Offield Family Foundation. We thank those who helped us capture the fish in our study: Tom Pflieger, Tom Fullam, Tom Rotheric, Greg Stutzer and Chugey Sepulveda. Archival tags were recovered with the assistance of the Inter-American Tropical Tuna Commission.

Literature cited

- Bayliff, W. H.
1980. Synopsis of biological data on the northern bluefin tuna, *Thunnus thynnus* (Linnaeus, 1758), in the Pacific Ocean. Inter-Am. Trop. Tuna Comm. Spec. Rep. 2: 261-293.
1994. A review of the biology and fisheries for northern bluefin tuna, *Thunnus thynnus*, in the Pacific Ocean. FAO Fish. Tech. Paper 336, part 2:244-295.
- Block, B. A., H. Dewar, S. B. Blackwell, T. D. Williams, E. D. Prince, A. Boustany, C. F. Farwell, D. J. Dau, and A. Seitz.
2001. Archival and pop-up satellite tagging of Atlantic bluefin tuna. In Electronic tagging and tracking in marine fishes (J. R. Sibert and J. L. Nielsen, eds.), p. 65-68. Kluwer Academic Pubs, The Netherlands.
- Block, B.A., H. Dewar, T. Williams, E. Prince, C. Farwell, and D. Fudge.
1997. Archival and pop up satellite tagging of Atlantic bluefin tuna, *Thunnus thynnus*. In Proceedings of the 48th annual tuna conference, p. 10. Inter-Am. Trop. Tuna Comm., Lake Arrowhead, CA.
1998. Archival tagging of Atlantic bluefin tuna (*Thunnus thynnus thynnus*). MTS Journal 32:37-46.
- Bowditch, N.
1995. The American practical navigator: an epitome of navigation. Originally by Nathaniel Bowditch (1802), Publ. 9., 873 p. Defense Mapping Agency Hydrographic/Topographic Center, Bethesda, MD.
- Brill, R., M. Lutecavage, G. Metzger, P. Bushnell, M. Arendt, J. Lucy, C. Watson, and D. Foley.
2002. Horizontal and vertical movements of juvenile bluefin tuna (*Thunnus thynnus*), in relation to oceanographic conditions of the western North Atlantic, determined with ultrasonic telemetry. Fish. Bull. 100:155-167.
- Carey, F. G., and K. D. Lawson.
1973. Temperature regulation in free-swimming bluefin tuna. Comp. Biochem. Physiol. 44a:375-395.
- Carey, F. G., and J. M. Teal.
1969. Regulation of body temperature by the bluefin tuna. Comp. Biochem. Physiol. 28:205-213.
- Delong, R. I., B. S. Stewart, and R. D. Hill.
1992. Documenting migrations of northern elephant seals using day length. Mar. Mamm. Sci. 8:155-159.
- Hill, R.
1994. Theory of geolocation by light levels. In Elephant seals: population ecology, behavior, and physiology (B. J. LeBoeuf and R. M. Laws, eds.), p. 227-236. Univ. California Press, Berkeley, CA.
- Hill, R. D., and M. J. Braun.
2001. Geolocation by light-level. The next step: latitude. In Electronic tagging and tracking in marine fish-
erie (J. Sibert and J. Nielsen, eds.), p. 315-330. Kluwer Academic Press, Dordrecht, The Netherlands.
- Itoh, T., S. Tsuji and A. Nitta.
2003a. Migration patterns of young Pacific bluefin tuna (*Thunnus orientalis*) determined with archival tags. Fish. Bull. 101:514-534.
- 2003b. Swimming depth, ambient water temperature preference, and feeding frequency of young Pacific bluefin tuna (*Thunnus thynnus orientalis*) determined with archival tags. Fish. Bull. 101:535-544.
- Kitagawa, T., S. Kimura, H. Nakata, and H. Yamada.
2004. Diving behavior of immature, feeding Pacific bluefin tuna (*Thunnus thynnus orientalis*) in relation to season and area: the East China Sea and the Kuroshio-Oyashio transition region. Fish. Oceanogr. 13(3):161-180.
- Kitagawa, T., H. Nakata, S. Kimura, T. Itoh, S. Tsuji, and A. Nitta.
2000. Effect of ambient temperature on the vertical distribution and movement of Pacific bluefin tuna *Thunnus thynnus orientalis*. Mar. Ecol. Prog. Ser. 206:251-260.
- Metcalfe, J. D.
2001. Summary report of a workshop on daylight measurements for geolocation in animal telemetry. In Electronic tagging and tracking in marine fisheries (J. Sibert and J. Nielsen, eds.), p. 331-342. Kluwer Academic Press, Dordrecht, The Netherlands.
- Musyl, M. K., R. W. Brill, D. S. Curran, J. S. Gunn, J. R. Hartog, R. D. Hill, D. W. Welch, J. P. Eveson, C. H. Boggs, and R. E. Brainard.
2001. Ability of archival tags to provide estimates of geographical position based on light intensity. In Electronic tagging and tracking in marine fisheries (J. Sibert and J. Nielsen, eds.), p. 343-368. Kluwer Academic Press, Dordrecht, The Netherlands.
- Musyl, M. K., R. W. Brill, C. H. Boggs, D. S. Curran, T. K. Kazama, and M. P. Seki.
2003. Vertical movements of bigeye tuna (*Thunnus obesus*) associated with islands, buoys, and seamonts near the main Hawaiian islands from archival tagging data. Fish. Oceanogr. 12:152-169.
- Nishikawa, Y., M. Honma, S. Ueyanagi, and S. Kikawa.
1985. Average distribution of larvae of oceanic species of scombrid fishes, 1956-1981. Nat. Res. Institute of Far Seas Fisheries, Shimizu. 12:99.
- Okiyama, M.
1974. Occurrence of the postlarvae of bluefin tuna, *Thunnus thynnus*, in the Japan Sea. Japan Sea Reg. Fish. Res. Lab. Bull. 25:89-97.
- Okiyama, M., and G. Yamamoto.
1979. Successful spawning of some holepigelagic fishes in the Sea of Japan and zoogeographical implications. In Proceedings of the seventh Japan-Soviet joint symposium on aquaculture, p. 223-233. Tokai Univ. Press, Tokyo, Japan.
- Rodgers, A. R., and A. P. Carr.
1998. HRE: the home range extension for ArcView. User's manual, 27 p. Centre for Northern Forest Ecosystem Research, Ontario Ministry of Natural Resources, Thunder Bay, Ontario, Canada.
- Schaefer, K. M., and D. W. Fuller.
2002. Movements, behavior, and habitat selection of bigeye tuna (*Thunnus obesus*) in the eastern equatorial Pacific, ascertained through archival tags. Fish. Bull. 100:765-788.

- Sibert, J. R., M. K. Musyl, and R. W. Brill.
2003. Horizontal movements of bigeye tuna (*Thunnus obesus*) near Hawaii determined by Kalman filter analysis of archival tag data. *Fish. Oceanogr.* 12(3):141-151.
- Sobel, D.
1995. Longitude: the true story of a lone genius who solved the greatest scientific problem of his time, 184 p. Penguin Books, New York, NY.
- Sund, P. N., M. Blackburn, and F. Williams.
1981. Tunas and their environment in the Pacific Ocean: a review. *Oceanogr. Mar. Biol. Ann. Rev.* 19:443-512.
- Welch, D. W., and J. P. Eveson.
1999. An assessment of light-based geolocation estimates from archival tags. *Can. J. Aquat. Sci.* 56:13171-1327.
2001. Recent progress in estimating geolocation using daylight. *In* Electronic tagging and tracking in marine fisheries (Sibert and J. Nielsen, eds.), p. 3693-83. Kluwer Academic Press, Dordrecht, The Netherlands.
- Wilson, R. P., J. J. Ducamp, W. G. Rees, B. M. Culik, and K. Neikamp.
1992. Estimation of location: global coverage using light intensity. *In* Wildlife telemetry: remote monitoring and tracking of animals (J. G. Priede and S. M. Swift, eds.) p. 131-134. Ellis Horwood, New York, NY.
- Yabe, H., S. Ueyanagi, and H. Watanabe.
1966. Studies on the early life history of bluefin tuna *Thunnus thynnus* and on the larvae of the southern bluefin tuna *T. maccoyii*. *Rep. Nankai Reg. Fish. Res. Lab.* 23:95-129.
- Yamanaka, H., and staff (sic).
1963. Synopsis of biological data on kuromaguro *Thunnus orientalis* (Temminck and Schlegel) 1942 (Pacific Ocean). *FAO Fish Rep.* 6(2):180-217.

Abstract—The gray snapper (*Lutjanus griseus*) is a temperate and tropical reef fish that is found along the Gulf of Mexico and Atlantic coasts of the southeastern United States. The recreational fishery for gray snapper has developed rapidly in south Louisiana with the advent of harvest and seasonal restrictions on the established red snapper (*L. campechanus*) fishery. We examined the age and growth of gray snapper in Louisiana with the use of cross-sectioned sagittae. A total of 833 specimens, (441 males, 387 females, and 5 of unknown sex) were opportunistically sampled from the recreational fishery from August 1998 to August 2002. Males ranged in size from 222 to 732 mm total length (TL) and from 280 g to 5700 g total weight (TW) and females ranged from 254 to 756 mm TL and from 340 g to 5800 g TW. Both edge analysis and bomb radiocarbon analyses were used to validate otolith-based age estimates. Ages were estimated for 718 individuals; both males and females ranged from 1 to 28 years. The von Bertalanffy growth models derived from TL at age were $L_t = 655.4[1 - e^{-0.23(t/r)}]$ for males, $L_t = 657.3[1 - e^{-0.23(t/r)}]$ for females, and $L_t = 656.4[1 - e^{-0.22(t/r)}]$ for all specimens of known sex. Catch curves were used to produce a total mortality (Z) estimate of 0.17. Estimates of M calculated with various methods ranged from 0.15 to 0.50; however we felt that $M=0.15$ was the most appropriate estimate based on our estimate of Z . Full recruitment to the gray snapper recreational fishery began at age 4, was completed by age 8, and there was no discernible peak in the catch curve dome.

Age, growth, mortality, and radiometric age validation of gray snapper (*Lutjanus griseus*) from Louisiana

Andrew J. Fischer

Coastal Fisheries Institute
School of the Coast and Environment
Louisiana State University
Baton Rouge, Louisiana 70803-7503
E-mail address: afische@lsu.edu

M. Scott Baker Jr.

North Carolina Sea Grant
UNC-W Center for Marine Science
5001 Masonboro Loop Rd.
Wilmington, North Carolina 28409

Charles A. Wilson

Louisiana Sea Grant College Program
Louisiana State University
Baton Rouge, Louisiana 70803-7507

David L. Nieland

Coastal Fisheries Institute
School of the Coast and Environment
Louisiana State University
Baton Rouge, Louisiana 70803-7503

The gray snapper (*Lutjanus griseus*), commonly referred to as the mangrove snapper, is a temperate and tropical reef species that is found along the southeastern Atlantic coast of the United States from North Carolina to Bermuda, throughout the Gulf of Mexico (GOM), and south to Brazil (Johnson et al., 1994; Allman and Grimes, 2002). Gray snapper are fairly common along the Louisiana coast and are usually associated with complex structures such as oil and gas platforms, artificial reefs and other hard bottom substrates. In 1991 restrictions were put on the recreational red snapper (*Lutjanus campechanus*) fishery; these restrictions coincided with a rapid expansion of the gray snapper fishery in south Louisiana. Recreational anglers now typically target gray snapper once they have reached their bag limit of red snapper; thus peak gray snap-

per landings generally coincide with the red snapper recreational season (April–October). As a result, recreational landings of gray snapper in Louisiana have increased exponentially from 3.25 metric tons (t) in 1983 to 175 t in 2002 (NMFS¹). Currently there is a 305 mm (12 inches) minimum size and a recreational bag limit of 10 fish/person/day for gray snapper in the GOM.

Some background information is available for gray snapper in the southeastern United States, mainly from south Florida. Scientists have reported on early life history (Ruth-

Manuscript submitted 19 September 2003 to the Scientific Editor's Office.

Manuscript approved for publication 20 November 2004 by the Scientific Editor.
Fish. Bull. 103:307–319 (2005).

¹ NMFS (National Marine Fisheries Service). 2003. Fisheries Statistics and Economics Division. Unpubl. data. Website: http://www.st.nmfs.gov/pls/webpls/MF_ANNUAL_LANDINGS.RESULTS. [Accessed 25 August 2003.]

erford et al., 1989; Domier et al., 1997), population dynamics (Rutherford et al., 1989), juvenile food habits (Hettler, 1989), juvenile distribution (Chester and Thayer, 1990), and reproduction (Domeier et al., 1997; Allman and Grimes, 2002).

Few reports have been conducted on the age and growth of gray snapper. Manooch and Matheson (1981) used sectioned otoliths to age gray snappers from eastern Florida but did not validate their methods. Johnson et al. (1994) also used sectioned otoliths to age fish sampled from Fort Pierce, FL, to Grand Isle, LA, again without validation of methods. Burton (2001) validated the periodicity of opaque zone formation in gray snapper from east coast Florida waters with the use of marginal increment analysis of distal edge measurements. But gray snapper have never been fully examined in the northern GOM and comprehensive age, growth, and mortality data from the thriving Louisiana recreational fishery are virtually nonexistent.

The objectives of our study were to describe the age, growth, and mortality of gray snapper from the Louisiana recreational fishery. We obtained age information through examination of cross-sectioned sagittal otoliths, validated our aging techniques with the use of bomb-radiocarbon ^{14}C and edge analyses, produced mortality estimates with standard procedures, and modeled growth with the von Bertalanffy growth equation.

Methods and materials

Gray snapper were sampled from the Louisiana recreational harvest from August 1998 to August 2002 by personnel from the Louisiana State University Coastal Fisheries Institute and the Louisiana Department of Wildlife and Fisheries. Fish were opportunistically sampled at charter boat facilities in Port Fourchon, LA, and at spearfishing and hook and line fishing tournaments in Grand Isle and New Orleans, LA. Morphometric measurements (fork length [FL] and total length [TL] in mm, total weight [TW] in g) were taken, sex was determined by macroscopic examination of the gonads, and both sagittae were removed, rinsed, and air dried, weighed to the nearest 0.1 mg, and stored in coin envelopes until processed. For specimens in which TL was unavailable, TL was estimated from FL with the equation $TL = 1.048(FL) + 8.35$ (linear regression, $df=275$; $P<0.001$; $r^2=0.98$) calculated from specimens in which both TL and FL were available.

In order to estimate age of gray snapper, a transverse section (~1 mm thick) was taken containing the core of the left sagittal otolith of each specimen. Sections were made with a Hillquest model 800, thin-sectioning machine equipped with a diamond embedded wafering blade and precision grinder (Cowan et al., 1995). In instances where the left otolith was unavailable, the right was substituted. Examinations of otolith cross-sections were made under a dissecting microscope with transmitted light and polarized light filter from $20\times$ to $64\times$. Opaque zones were enumerated along the ventral side

of the sulcus acousticus from the core to the proximal edge (Wilson and Nieland, 2001). Two readers (AJF and MSB) performed opaque zone counts independently without knowledge of capture date or morphometric data. Otolith marginal edge condition was coded as opaque or translucent by using the criteria described by Beckman et al. (1989). Opaque zones were counted a second time when initial counts differed. In instances where a consensus between readers could not be reached, counts of the more experienced reader (AJF) were used. Between-reader variation in opaque zone counts was examined after the second readings of otolith sections were completed. Differences in counts were evaluated with the coefficient of variation (CV), index of precision (D) (Chang, 1982), and average percent error (APE) (Beamish and Fournier, 1981).

Ages of gray snapper were estimated from opaque annulus counts and capture date with the equation described by Wilson and Nieland (2001):

$$\text{Day age} = -182 + (\text{opaque increment count} \times 365) + \\ (m-1) \times 30 + d,$$

where m = the ordinal number (1–12) of month of capture; and

d = the ordinal number (1–31) of the day of the month of capture.

The 182 days subtracted from each age estimate are to account for the uniform hatching date of 1 July assigned for all gray snapper to coincide with peak spawning activity occurring in July (Domeier et al., 1997; Allman and Grimes, 2002). Age in years was assigned by dividing age (in days) by 365. Year of birth (YOB) was back calculated by subtracting our otolith-based age estimates from year of capture.

Validation of the periodicity of opaque zone formation in gray snapper otoliths was examined with two approaches. An advanced and accurate method of age validation uses a quantitative measurement of nuclear bomb-produced radiocarbon (^{14}C) that was accumulated in carbon-containing hard parts of marine organisms before, during, and after the atmospheric testing period of nuclear weapons (1958–65) (Baker and Wilson, 2001). Elevated levels of ^{14}C have been observed in hermatypic corals (Druffel, 1980, 1989) and this time-specific marker can be used to validate age estimates derived from hard parts in marine fishes (Kalish, 1993; Campana and Jones, 1998). Baker and Wilson (2001) recently validated red snapper otolith section age estimates using this technique with excellent results. This same method was applied in our study to the otolith cores of gray snapper hatched after the nuclear testing periods.

Gray snapper hatched prior to 1973 were not available for our study, and thus the steepest portion of the radiocarbon uptake curve could not be used to confirm age estimates. Consequently, no coral reference data for the general area were available after 1983. Because red snapper otoliths have been previously validated

with this same method (Baker and Wilson, 2001), we anticipated that gray snapper radiocarbon values would be roughly similar to red snapper values for a given YOB.

To obtain the oldest portion of the otolith for radiocarbon analysis, right otoliths of older gray snapper with an estimated YOB after the period of atmospheric testing (1973–95) were embedded in araldite epoxy resin and thin sectioned (~1 mm in thickness) through the core with an Isomet low-speed saw. The otolith core region was isolated from the otolith section by using the technique described in Baker and Wilson (2001). Cores were rinsed in double-distilled de-ionized water, allowed to air dry, weighed to the nearest 0.1 mg, and submitted to the accelerator mass spectrometry (AMS) facility in acid-washed 20-mL glass scintillation vials. The mean sample weight submitted for analyses was 12.8 mg.

At the AMS facility, otolith cores underwent acid hydrolysis with 85% phosphoric acid to yield CO_2 which was then made into graphite (pure C) by reduction at high temperature under vacuum. The graphite was pressed onto a target, loaded on the AMS unit and analyzed for radiocarbon. Samples were also analyzed for ^{13}C to correct for natural and machine fractionation effects. Radiocarbon values from individual otolith cores were reported as $\Delta^{14}\text{C}$ (mean \pm SD), the adjusted deviation from the radiocarbon activity of 19th century wood (Stuiver and Polach, 1977).

The periodicity of opaque zone formation was also examined with edge analysis. The marginal edge of each otolith was examined and coded as

- 1 opaque zone forming on otolith margin;
- 4 translucent zone forming on margin up to 1/3 complete;
- 5 translucent zone forming on margin 1/3 to 2/3 complete;
- 6 translucent zone forming on margin 2/3 to fully complete.

Percentages of otoliths with opaque margins were plotted by month of capture (Beckman et al., 1989; Campana, 2001; Wilson and Nieland, 2001) for all months in which specimens were available.

In order to examine the predictive capacity of otolith weight (W_0) to determine age in gray snapper, sex specific W_0 -age relationships were fitted by using a power function with least squares with the model: $\text{Age} = aW_0^b$. A likelihood ratio test (Cerrato, 1990) was used to test for differences between male and female models.

Male and female TW-TL relationships were independently fitted with linear regression to the model $W = aTL^b$ from \log^{10} -transformed data. Male and female regression coefficients were compared with an ANCOVA. Variability in age, TL, and TW-frequency distributions of males and females were compared with Komolgorov-Smirnov two-sample tests (Tate and Clelland, 1957; Sokal and Rohlf, 1995). Growth of gray snapper was modeled by using all specimens of known sex. Von Ber-

tanffy growth models of TL at age were fitted with nonlinear regression by least squares (SAS 6.11, SAS Institute, 1996, Cary, NC) in the form:

$$TL_t = L_\infty(1 - e^{-kt/t_0})$$

where t = age in years;

TL = TL at age t ;

L_∞ = the theoretical maximum TL; and

k = the growth coefficient.

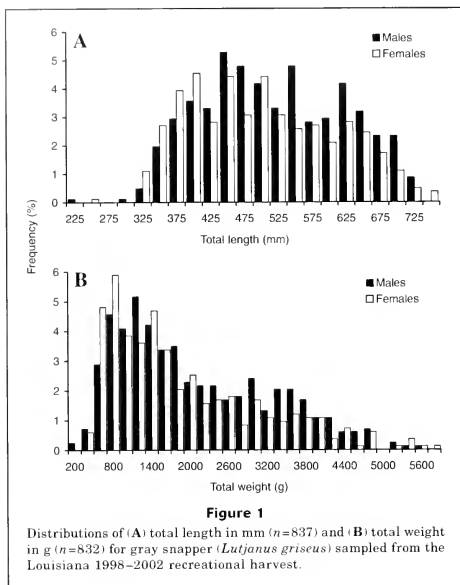
Because of a lack of smaller individuals in our sample population, no y -intercepts for t_0 were specified and models were forced through 0 (Szedlmayer and Shipp, 1994; Fischer et al., 2004) to better estimate juvenile growth. One growth model was generated for all specimens of known sex. Additional models were fitted independently for males and females. Likelihood ratio tests (Cerrato, 1990) were used to test for differences between male and female models.

The instantaneous total mortality rate (Z) was estimated from a catch curve (Nelson and Manooch, 1982; Burton, 2001) assuming our collections represented the actual age distribution of the population. These estimates were made with the regression method of plotting the \log_e age frequency on age. We used the absolute value of the slope of the linear descending right limb of the curve after full recruitment to estimate Z .

Estimates of instantaneous natural mortality (M) were computed with several methods. The first estimate of M was based on Hoenig's (1983) longevity-mortality relationship, where the mortality rate is based solely on the oldest specimen encountered in the data set. We also used Hoenig's (1983) relationship for natural mortality with modifications for sample size. Natural mortality was also computed with the method of Pauly (1980) assuming a mean annual water temperature of 25°C. Our mean annual water temperature estimate was derived from the data buoys operated by the National Oceanic and Atmospheric Administration's National Oceanographic Data Buoy Center from 1995 to 2001. Finally, M was calculated with the Ralston (1987) method, where the estimate of M is based solely on a simple regression involving the Brody growth coefficient (k). A significance level of 0.05 was used for all statistical analyses.

Results

We sampled 833 gray snapper (441 males, 387 females, and 5 individuals of unknown sex) from the recreational fishery of Louisiana for morphometric data and otoliths. The male:female ratio was 1:0.88; a χ^2 test indicated no significant difference between the proportions of males and females ($\chi^2=3.52$, $P=0.06$). Male and female specimens ranged from 222 to 732 mm TL and from 254 to 756 mm TL, respectively (Fig. 1A). Both sexes exhibited multimodal distributions; males were represented in the greatest numbers at 450 mm TL, compared to 400 mm



TL for females. A Kolmogorov-Smirnov two-sample test indicated no significant difference between male and female TL frequencies (maximum difference=9.45). Male and female TW ranged from 200 to 5700 g and 300 to 5800 g TW, respectively (Fig. 1B). Both sexes also displayed multimodal distributions in TW. A Kolmogorov-Smirnov two-sample test indicated a significant difference between sexes at 1600 g TW (maximum difference=9.67). A single predictive TL-TW regression was generated for both males and females:

$$TW = 3.31 \times 10^{-5} (TL^{2.85})$$

$$(F_{1, 822}=9,326.54; P<0.001; r^2=0.92).$$

Significant differences were found between sexes in TL-TW relationships (ANCOVA test of homogeneity of slopes, $F_{3,822}=7.25; P=0.007; r^2=0.92$). Therefore, separate models were fitted for each sex:

$$\text{Males} = TW = 2.04 \times 10^{-5} (TL^{2.93})$$

$$(F_{1, 436}=7588.29; P<0.001; r^2=0.95)$$

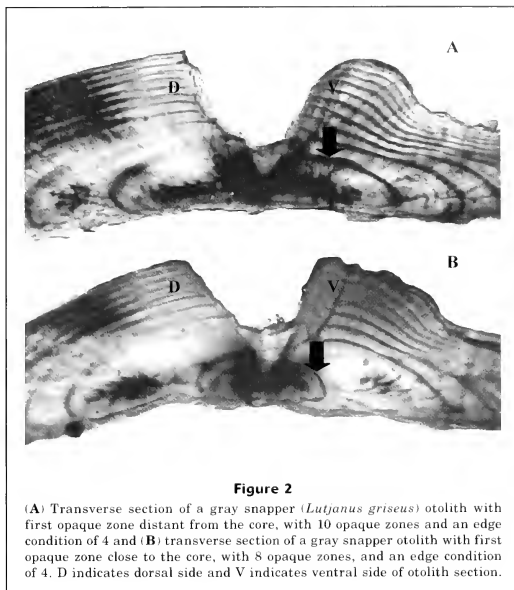
$$\text{Females} = TW = 5.5 \times 10^{-5} (TL^{2.77})$$

$$(F_{1, 385}=3,089.16; P<0.001; r^2=0.89)$$

Gray snapper otoliths are very similar in physical structure, although much smaller in actual size, to those of the red snapper. Opaque zones are easily distinguishable on the ventral side of the sulcus groove (Manooch and Matheson, 1981; Johnson et al., 1994; Shipp²) (Fig. 2, A and B).

Sagittae were collected from 721 gray snapper of which 718 were aged. Readers were unable to resolve opaque zones in three otolith sections because of poor sectioning. Readers agreed on the ages of 568 individuals (78.8%) after initial counts and differed by one opaque annulus for 154 specimens, two annuli for 18 specimens, and three annuli for 2 specimens. Readers agreed on 709 ages (98.7%) after the second reading. The average percent error (APE) was 0.5, coefficient of variation (CV) was 0.00078, and index of percent (D) was 0.0006.

² Shipp, R. L. 1991. Investigations of life history parameters of species of secondarily targeted reef fish and dolphin in the northern Gulf of Mexico. Proc. Fourth Annu. MARFIN Conf., San Antonio, TX, p 80–85. [Available from National Marine Fisheries Service, State/Federal Liaison Office, 9721 Executive Center DR. N., St. Petersburg, FL 33702.]

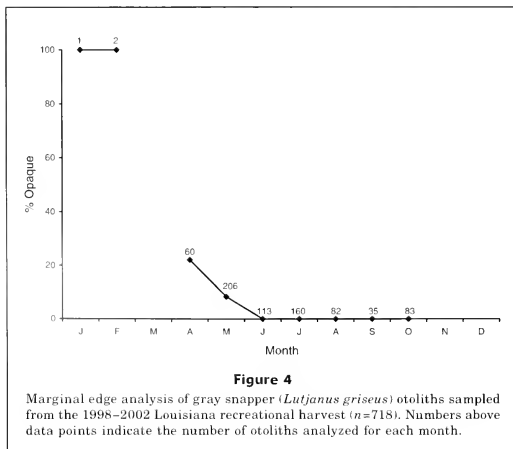
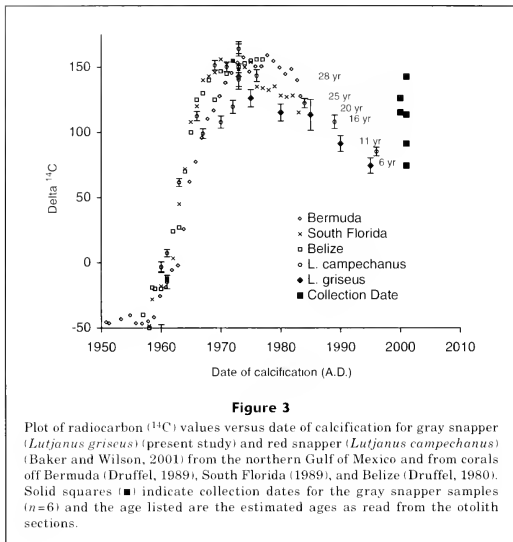
**Table 1**

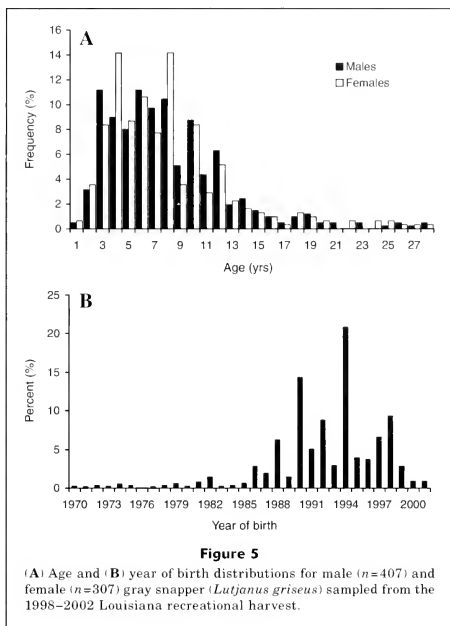
List of gray snapper (*Lutjanus griseus*) otoliths analyzed for stable carbon and bomb radiocarbon. "AMS wt." is the amount of otolith separated from the otolith section and submitted for accelerator mass spectrometry (AMS) radiocarbon analysis; FL=fork length. I.D.= our identification number.

NOS-AMS number	I.D.	Date caught	Otolith section age (yr)	Birth date	Otolith wt. (mg)	AMS wt. (mg)	$\delta^{13}\text{C}$ (‰)	$\delta^{14}\text{C}$ (‰)	
								Mean	±SD
OS-36337	320	2001	28	1973	639.1	9.9	-2.67	142.8	9.7
OS-36338	33	2000	25	1975	635.2	14.7	-2.55	126.2	6.7
OS-36339	5	2000	20	1980	536.7	15.0	-3.34	115.3	6.5
OS-36340	322	2001	16	1985	414.6	15.1	-5.27	113.5	11.9
OS-36341	316	2001	11	1990	306.5	9.8	-4.49	91.4	6.1
OS-36342	304	2001	6	1995	154.0	12.2	-5.73	74.5	5.9

The gray snapper ($n=6$) used for the radiocarbon age validation procedure ranged from 6 to 28 years of estimated age and were collected during 2000 and 2001 (Table 1). Furthermore, YOB ranged from 1973 to 1995. Gray snapper radiocarbon values were plotted

along with red snapper radiocarbon values from the northern Gulf of Mexico (Baker and Wilson, 2001) and coral radiocarbon values from Bermuda (Druffel, 1989), South Florida (Druffel, 1989), and Belize (Druffel, 1980) (Fig. 3). Radiocarbon values of gray snapper cores were





highest in 1973 and exhibited a steady decline to a low in 1995.

The periodicity of opaque annulus formation in gray snapper otoliths was further examined by plotting the monthly percentages of otoliths with opaque margins (Fig. 4). Although little data were available for the winter months, one specimen sampled in January and two specimens sampled in February 2001 each exhibited opaque marginal otolith edges indicating that opaque annulus formation occurs during the winter. Minimum percentages of otoliths with opaque margins during the months of April (22%) and May (8%) followed by an absence of opaque margins during the months of June through October indicate the cessation of opaque annulus formation by early spring and the onset of translucent annulus formation beginning in April and continuing through November.

Male and female gray snapper ranged in age from 1 to 28 years (Fig. 5A). There was no significant difference in age distributions between males and females (maximum difference=6.92 yr), but both sexes exhibited variable multimodal distributions in age frequency.

Year of birth (YOB) frequency was also multimodal, and the population was dominated by younger fish; 77% of males and 80% of females were aged at 10 years or younger (Fig. 5B).

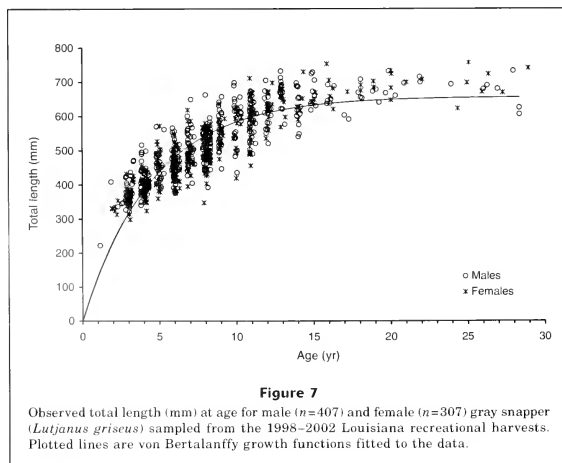
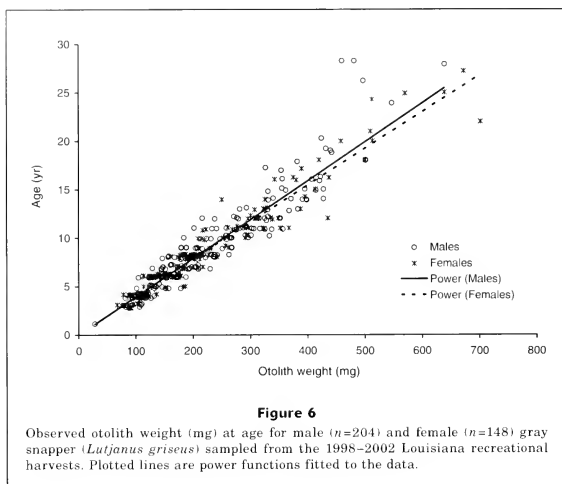
Significant differences in slopes were detected when plotting age- W_0 relationships between sexes (ANCOVA test of homogeneity of slopes, $F_{3,353} = 8.06$; $P = 0.0005$). Therefore, predictive models of age- W_0 were fitted separately for males and females using a power function with least squares as (Fig. 6)

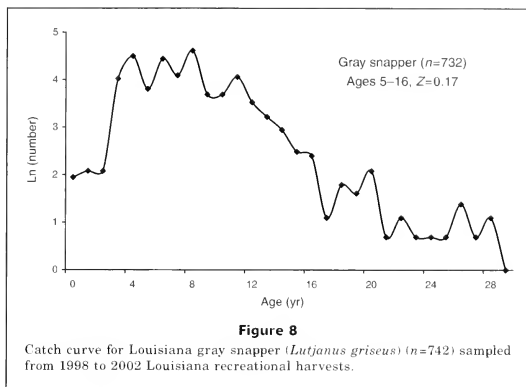
$$\text{Male age} = 0.0278 (W_0)^{1.06} \\ (F_{2,204} = 3,956.29, P < 0.001, r^2 = 0.89).$$

$$\text{Female age} = 0.0460 (W_0)^{0.97} \\ (F_{2,148} = 4,504.05, P < 0.001, r^2 = 0.90).$$

The single von Bertalanffy growth model to describe gray snapper TL at age (Fig. 7) was

$$L_t = 656.4[1 - e^{(-0.22/t)}] \\ (F_{2,714} = 32,217.6; P < 0.0001; r^2 = 0.72).$$



**Table 2**

Degrees of freedom (df), sum of squares (SS), mean square (MS), *F* value, and *P* values for the likelihood ratio test by which the full von Bertalanffy growth model (in which sexes were fitted independently) is compared with the reduced von Bertalanffy model (by fitting all specimens of known sex).

Model	df	SS	MS	<i>F</i>	<i>P</i>
Full	4714	1.9493 × 10 ⁸	48,732,614	16,341	<0.0001
Reduced	2714	1.9489 × 10 ⁸	97,447,139	32,217.6	<0.0001

However, a likelihood ratio test indicated growth models for males and females were significantly different from one another ($\chi^2=494.77$; df=2,714; $P<0.001$) (Table 2). The resultant sex-specific von Bertalanffy growth models were

$$\text{Male } L_t = 655.4\{1 - e^{[-0.23(t)]}\} \\ (F_{2,407}=19,732.9; P<0.001; r^2=0.73)$$

$$\text{Female } L_t = 657.3\{1 - e^{[-0.21(t)]}\} \\ (F_{2,307}=13,015.2; P<0.0001; r^2=0.72)$$

Instantaneous total mortality (*Z*) was calculated with catch curve analysis. Full recruitment to the gray snapper fishery began at age 4 and was completed by age 8 and there was no discernible peak in the catch curve dome (Fig. 8). For the purposes of *Z* estimation, age 4 was used as the age of full recruitment to the fishery. *Z* was estimated at 0.18 for all fish (age range: 5–28 years) and 0.17 for all fish when the age range was truncated at 16 years. The age range was truncated at 16 years because older age classes contained fewer than 10 individuals.

Estimates for natural mortality (*M*) for gray snapper varied substantially and were dependent upon the method used. Hoenig's (1983) longevity-mortality relationship produced the lowest estimate of 0.15. Hoenig's (1983) relationship modified for sample size yielded an estimate of 0.30. The regression method of Ralston (1987) produced an estimate of 0.40. Finally, Pauly's (1980) method using a mean annual water temperature of 25°C and parameter estimates L_∞ and *k* derived from the von Bertalanffy growth equations produced the highest estimate of 0.51.

Discussion

Validation of the periodicity of opaque zone formation is critical when using otoliths to determine the ages of fish (Beamish and McFarlane, 1983). The lack of data during the winter months prevented us from making a definitive statement on the timing of opaque zone formation based on edge analysis alone. However, we present evidence that suggests that opaque zone formation may

begin as early as December and proceed through May. Opaque zone formation beginning in December through spring has been shown to occur in the congeneric red snapper (Render, 1995; Patterson et al., 2001; Wilson and Nieland, 2001) as well as in a number of other teleosts in the northern GOM (Beckman et al., 1989, 1990, 1991; Thompson et al., 1999). Burton (2001) validated the periodicity of opaque zone formation for gray snapper along the Atlantic coast but reported the period of formation to occur during the summer months of June and July.

The natural decay of radiocarbon in the world ocean after the nuclear testing period is well documented (Broecker et al., 1985) and close agreement between gray snapper data and existing radiocarbon chronologies from the Gulf of Mexico, U.S. South Atlantic, and Caribbean provided additional evidence that our otolith-section-based age estimates of gray snapper were valid (Fig. 3). The ^{14}C values obtained from gray snapper otolith cores formed after the period of atmospheric testing of nuclear weapons were comparable to, if not slightly less than, those values found in red snapper from the northern Gulf of Mexico (GOM) (Baker and Wilson, 2001).

Although published coral radiocarbon chronologies are available for review and are made available in the present study, we are most confident in comparing gray snapper to the red snapper data for several reasons. First and foremost, these two species were collected from the same general area of the northern Gulf of Mexico and thus in theory should have similar radiocarbon chronologies (Broecker et al., 1985). Second, although the coral samples would seem to be the best possible items for comparison because of their known age, stationary location, and most importantly because multiple "birth dates" can be analyzed from one coral head, the gray snapper and red snapper samples were taken from different geographic areas and thus different water bodies. No known coral radiocarbon chronologies exist for the northern Gulf of Mexico. Radiocarbon chronologies have been shown to vary significantly in the world ocean by latitude (Broecker et al., 1985) and this trend in the reference corals can be seen in Figure 3, especially during the period of rapid radiocarbon uptake (1958–75). Finally, all otolith samples (gray snapper and red snapper) were analyzed for radiocarbon by the same AMS facility by using identical laboratory methods (Baker and Wilson, 2001). Delta ^{14}C data from the otoliths of gray snapper with presumed YOB back to 1973 (the oldest fish in our data set) clearly reflected the same pattern found in red snapper; high levels of oceanic radiocarbon attributable to previous nuclear testing followed by a slow but steady decline to a low in 1995 (Fig. 3). The gray snapper curve is slightly lower but parallel to the red snapper curve. Because of the inherent variability associated with individual fishes, it is inconceivable to think that the two species of snapper would have curves that completely lie on top of each other or on top of the coral chronologies for that matter. Although the two species are very similar in

many regards, we can only speculate that differences in juvenile life history patterns, habitat preferences, water column chemistry, and possibly otolith formation may account for the variation in radiocarbon chronologies. However, both the gray snapper and previously validated red snapper chronologies exhibit the same trend and indicate that our otolith-based age estimates are accurate.

The majority of radiocarbon fisheries age validation has produced otolith-based chronologies that resemble those from nearby reference corals or other fish species in the same general location (Campana, 2001). Campana and Jones (1998) observed extremely high and erratic radiocarbon values for black drum (*Pogonias cromis*) in the Chesapeake Bay. In that study, the radiocarbon values resembled the intermediate of surface oceanic (corals) and the much higher atmospheric values (Campana and Jones, 1998). The reasons for the erratic $\Delta^{14}\text{C}$ values remain unknown, but Campana and Jones speculated that the estuarine dependency of the species produced the variable activities of radiocarbon in individual fish for a given YOB. This was not the case with gray snapper, also a species that uses the shallow estuarine environment during the first years of its life. Because gray snapper is estuarine dependent, we fully expected the gray snapper radiocarbon values to be erratic and much higher than the reference corals. In contrast, gray snapper radiocarbon values were strikingly similar to, if not less than, red snapper and the reference coral radiocarbon values at all comparable YOBs (Fig. 3). Contrary to the opinions expressed by Campana and Jones (1998), our limited data suggested that estuarine dependency may have no effect on observed radiocarbon values, at least for gray snapper.

Although opaque zones are distinct in gray snapper otolith cross sections, the small size and apparent longevity of the species pose some challenges for age interpretation. In older fish, opaque zones are formed more closely together in the otolith, making accurate counts and accurate interpretation of the otolith margin more difficult. We observed considerable variability in the location of the first opaque zone in gray snapper; the first annulus was variously located somewhat distant from the core to close to and continuous with the otolith core (Fig. 2, A and B). Wilson and Nieland (2001) noted the same pattern in red snapper otoliths suggesting that this variability may be a function of the protracted red snapper spawning season, which is similar to that of gray snapper, and of the rapid growth rate during the juvenile stage. This variability in first opaque zone position accounted for the majority of disagreement between readers in initial age estimates; there was only 76.5% agreement. However, experience by both readers (AJF and MSB) with red snapper otoliths produced consensus of 98.8% after second readings.

Male and female gray snapper ranged in age from 1 to 28 years. Younger individuals composed the major portion of the fishery; 90% of the catch was aged less than 15 years. Maximum ages were greater than those reported in previous studies. Johnson et al. (1994) re-

ported maximum ages of 23 and 25 years for males and females, respectively; the oldest fish in the study was actually sampled from Grand Isle, LA. Burton (2001) reported a non-sex-specific maximum age of 24 years. Sampling for both of these studies was focused in Florida where there is higher fishing pressure on gray snapper (Burton, 2001) and this fishing pressure may explain the lesser maximum ages and paucity of older individuals in their sample populations.

Gray snapper exhibit multimodal distributions in age and YOY frequencies. Due to minimum size limits, very few individuals were represented below age 3. Age distributions exhibited an initial peak at 3 years, when gray snapper are beginning to recruit to the recreational fishery. Successive peaks in age-class abundance in our data set occurred every two years. In an examination of abundance by YOY a similar pattern was observed; strong year classes were followed by diminished year classes. Similar patterns of variability in year-class strength have been observed in black drum (*Pogonias chromis*) and red drum (*Scienops ocellatus*) in the northern GOM. Beckman et al. (1989) suggested that year-class variability in these species might be due to environmental factors during early life stages or biological controls on the population. If this observed consistent pattern is reflective of the gray snapper population off Louisiana, we suggest that the variation in year-class strength may be reflective of intra-species-specific year-class competition of juveniles competing for resources within the estuaries before recruiting to the offshore fishery.

Researchers continually search for effective, cost-efficient ways to acquire fish age data. Body size has been shown to be a poor value to use for estimating age in a number of fish species because of the considerable variability in size at age. Otolith growth has been shown to continue with age, independent of somatic growth. Otolith weight (W_o) has been used as a predictive tool to determine age in a number of fish species (Templeman and Squires, 1956; Beamish, 1979; Wilson and Dean, 1983; Secor et al., 1989; Beckman et al., 1991). Although a strong relationship has been demonstrated between W_o and age, especially for the younger age classes, considerable variability exists in W_o at age in older age classes. For example, the W_o of a 10-yr-old male gray snapper can range from 180 mg to 357 mg thus preventing a precise age estimate based on W_o alone. Although W_o data may provide general information on overall age distribution patterns of a population, we feel that annulus counts from otolith cross sections provide the most accurate age estimates for gray snapper.

Our overall (sexes combined) von Bertalanffy growth model estimated a maximum theoretical length (L_∞) of 656.4 mm TL. Although a likelihood ratio test indicated a significant difference between male and female models, this difference may be of limited biological significance because male and female models appear to be very similar. The presence of larger, older fish in our sample population resulted in our overall model

coming to an asymptote at a smaller L_∞ and having a larger respective k than previously reported (Manooch and Matheson, 1981; Johnson et al., 1994). Johnson et al. (1994) predicted an L_∞ of 792.25 mm using the regression method of Manooch and Matheson (1981) to back calculate lengths at age. Johnson et al. (1994) also obtained a much smaller estimate of k at 0.08 compared with a k value of 0.22 predicted in our model. A smaller estimate was not unexpected given the inverse correlation between L_∞ and k noted by Knight (1968). Because of the minimum size limitations on the recreational fishery, smaller (presumably younger) individuals below 304 mm TL were almost absent in our sample population. We chose to not specify a y-intercept for t_0 and to force our growth models through zero in order to obtain more accurate estimates of k . Forcing our models through zero also contributed to the differences in growth parameters between our study and those of Johnson et al. (1994). Like Johnson et al. (1994), Burton (2001) also estimated growth parameters by fitting back-calculated lengths at age. Burton's (2001) L_∞ estimates of 717 mm and 625 mm for north and south Florida, respectively, are similar to those found in our study. Burton's (2001) sample populations consisted of a number of fish below 200 mm TL. These smaller individuals had similar effects on his models as that of forcing our models through zero. Burton's estimates of k were 0.17 and 0.13 for north and south Florida, respectively, compared with a k of 0.22 for our overall model.

We estimated total instantaneous mortality (Z) to be 0.17 and full recruitment to the fishery at age 4. We chose to use the truncated age range of 5–16 years (versus 5–28 years) for Z estimation in order to have at least 10 samples in each age category. Our estimation of Z based on all age categories (5–28) was 0.18. Our estimate of Z is at the low end of the range of values reported by Johnson et al. (1994) ($Z=0.17-0.26$) for the Gulf of Mexico. It should be noted, however, that Johnson et al. (1994) pooled fish from five distinct geographical locations. Of the 432 fish analyzed in their study, 69% came from Grand Isle, LA ($n=104$) and Panama City, FL ($n=193$). The remaining 31% came from the central and southern coasts of Florida. Perhaps Johnson et al.'s (1994) estimates of Z would be lower if only the Louisiana samples were used. Our Z values, however, are much lower than those reported by Manooch and Matheson (1981) ($Z=0.39-0.60$) and Burton (2001) ($Z=0.34-0.95$) for the east coast of Florida.

Our low estimate of Z for gray snapper in Louisiana waters is clearly associated with the abundance of older, larger individuals in the population. Unlike the catch curves in previous studies that dealt with gray snapper populations on the east coast of Florida (Manooch and Matheson 1981; Burton 2001) and in the southeast in general (Johnson et al. 1994), the mode of our catch curve is not well defined. It is evident that gray snapper in the South Atlantic are heavily exploited (Burton, 2001), as evidenced from their age-frequency distribution and high estimates of Z .

Estimates of M ranged from 0.15 to 0.51 and were comparable to previous studies on gray snapper from the southeastern United States. Johnson et al. (1994) used the Pauly (1980) and Ralston (1987) methods to estimate M to range from 0.12 to 0.32 for the west coast of Florida, including Louisiana. Manooch and Matheson (1981) used the Pauly (1980) relationship to calculate $M = 0.22$. Burton (2001) used the same four methods as in our study and found M to range from 0.18 to 0.43. It is well known that estimates of mortality are highly variable and depend upon the parameters used to calculate them. The purpose of providing various estimates of M was to demonstrate to the reader the variability in this important life history parameter and to demonstrate how little we actually know about it. Adopting our estimate of Z , we feel that the Hoenig (1983) method ($M=0.15$) produced the most suitable estimate of M for gray snapper in Louisiana waters of the northern Gulf of Mexico. Based on the apparent age-size structure of the stock, historical landings data, and personal observation, all indications are that this species is lightly fished in this study area. Hoenig (1983) indicated that M should be roughly equivalent to Z if the population is lightly exploited. Our estimate of Z (0.17) was indeed roughly equivalent to M (0.15), supporting our belief that fisheries mortality (F) is not yet a significant threat to this fishery.

Gray snapper could become over-exploited if a large, intensive fishery developed in the northern Gulf of Mexico. Landings of gray snapper in Louisiana have increased dramatically over the last few years, partly because of the recent restrictions imposed on red snapper in the Gulf of Mexico. Compared to the gray snapper population structure in the South Atlantic, especially off the coast of south Florida (Manooch and Matheson, 1981; Burton, 2001), the Louisiana population appears to be healthy. Long-term heavy fishing pressure has probably affected the south Florida gray snapper population (Burton, 2001). As a result, the population structure of south Florida is dramatically different from that of Louisiana. Our estimates of Z are extremely low and indicate that fishing mortality (F) is currently not a significant factor for the gray snapper population in Louisiana waters. A low-intensity gray snapper fishery could take most of the resource without endangering future production.

Acknowledgments

Funding and assistance with sampling was provided by the Louisiana Department of Wildlife and Fisheries. We would also like to thank Josh Maier, Brett Blackmon, and Candace Aiken for sampling efforts and otolith processing as well as Brain Milan for providing juvenile gray snapper samples. We thank Steve Tomeny, the boat captains, and deck hands of Captain Steve Tomeny's charters in Port Fourchon, LA, as well as all the recreational fishermen that allowed us to sample their catch. We wish to thank Ann P. McNichol of National Ocean

Sciences (Accelerator Mass Spectrometry facility at the Woods Hole Oceanographic Institution) for otolith radiocarbon analyses.

Literature cited

- Allman, J. A., and C. B. Grimes.
2002. Temporal and spatial dynamics of spawning, settlement, and growth of gray snapper (*Lutjanus griseus*) from the West Florida shelf as determined from otolith microstructures. *Fish. Bull.* 100:391-403.
- Baker, M. S. Jr., and C. A. Wilson.
2001. Use of bomb radiocarbon to validate otolith section ages of red snapper *Lutjanus campechanus* from the northern Gulf of Mexico. *Limnol. Oceanogr.* 46:1819-1824.
- Beamish, R. J.
1979. New information on the longevity of the Pacific ocean perch (*Sebastes alutus*). *J. Fish. Res. Board Can.* 36: 1395-1400.
- Beamish, R. J., and D. A. Fournier.
1981. A method for comparing the precision of a set of age determinations. *Can. J. Fish. Aquat. Sci.* 38:982-983.
- Beamish, R. J., and G. A. McFarlane.
1983. The forgotten requirement for age for age validation in fisheries biology. *Trans. Am. Fish. Soc.* 112:735-743.
- Beckman, D. W., A. L. Stanley, J. H. Render, and C. A. Wilson.
1990. Age and growth of black drum in Louisiana waters of the Gulf of Mexico. *Trans. Am. Fish. Soc.* 119:537-544.
1991. Age and growth-rate estimation of sheephead, *Archosargus probatocephalus*, in Louisiana waters using otoliths. *Fish. Bull.* 89:1-8.
- Beckman, D. W., C. A. Wilson, and A. L. Stanley.
1989. Age and growth of red drum, *Sciaenops ocellatus*, from offshore waters of the northern Gulf of Mexico. *Fish. Bull.* 87:17-28.
- Broecker, W. S., T. Peng, G. Ostlund, and M. Stuiver.
1985. The distribution of bomb radiocarbon in the world ocean. *J. Geophys. Res.* 90:6953-6970.
- Burton, M. L.
2001. Age, growth, and mortality of gray snapper, *Lutjanus griseus*, from the east coast of Florida. *Fish. Bull.* 99:254-265.
- Campana, S. E., and C. M. Jones.
1998. Radiocarbon from nuclear testing applied to age validation of black drum, *Pogonias cromis*. *Fish. Bull.* 96: 185-192.
- Campana, S. E.
2001. Accuracy, precision and quality control in age determination, including a review of the use and abuse of age validation methods. *J. Fish Biol.* 59:197-242.
- Cerrato, R. M.
1990. Interpretable statistical tests for growth comparisons using parameters in the von Bertalanffy equation. *Can. J. Fish. Aquat. Sci.* 47:1416-1426.
- Chang, W. B.
1982. A statistical method for evaluating the reproducibility of age determination. *Can. J. Aquat. Sci.* 39:1208-1210.
- Chester, A. J., and G. W. Thayer.
1990. Distribution of spotted seatrout (*Cynoscion nebulosus*)

- sus*) and gray snapper (*Lutjanus campechanus*) juveniles in seagrass habitats of western Florida Bay. *Bull. Mar. Sci.* 46(2):345-357.
- Cowan, J. H. Jr., R. L. Shipp, H. K. Bailey IV, and D. W. Haywick. 1995. Procedure for rapid processing of large otoliths. *Trans. Am. Fish. Soc.* 124:280-282.
- Domier, M. L., C. C. Loenig, and F. C. Coleman. 1997. Reproductive biology of the gray snapper (*Lutjanus griseus*), with notes on spawning for other Western Atlantic snappers (*Lutjanidae*). In *Biology and culture of tropical groupers and snappers* (F. Arreguin-Sanchez, J. L. Munro, M. C. Balgos, and D. Pauly, eds.), p. 189-201. ICLARM Conf. Proc. 48.
- Druffel, E. M. 1980. Radiocarbon in annual coral rings of Belize and Florida. *Radiocarbon* 22:363-371.
1989. Decadal time scale variability of ventilation in the North Atlantic: high-precision measurements of bomb radio-carbon in banded corals. *J. Geophys. Res.* 94:3271-3285.
- Fischer, A. J., M. S. Baker Jr., and C. A. Wilson. 2004. Red snapper, *Lutjanus campechanus*, demographic structure in the northern Gulf of Mexico based on spatial patterns in growth rates and morphometrics. *Fish. Bull.* 102:593-603.
- Hettler, W. F., Jr. 1989. Food habits of juveniles of spotted seatrout and gray snapper in western Florida Bay. *Bull. Mar. Sci.* 44(1): 155-162.
- Hoenig, J. M. 1983. Empirical use of longevity data to estimate mortality rates. *Fish. Bull.* 82:898-903.
- Johnson, A. G., L. A. Collins, C. P. Keim. 1994. Age-size structure of gray snapper from the Southeastern United States: a comparison of two methods of back-calculating size at age from otolith data. *Proc. Annu. Conf. Southeast Assoc. Fish and Wildl. Agencies* 48:592-600.
- Kalish, J. M. 1993. Pre- and post-bomb radiocarbon in fish otoliths. *Earth Planet. Sci. Lett.* 114:549-554.
- Knight, W. 1968. Asymptotic growth: an example of nonsense disguised as mathematics. *J. Fish. Res. Board Can.* 25(6):1303-1307.
- Manooch, C. S., III, and R. H. Matheson III. 1981. Age, growth and mortality of gray snapper collected from Florida waters. *Proc. Annu. Conf. Southeast Assoc. Fish Wildl. Agencies* 35:331-344.
- Nelson, R. S., III, and C. S. Manooch III. 1982. Growth and mortality of red snappers in the west-central Atlantic Ocean and northern Gulf of Mexico. *Trans. Am. Fish. Soc.* 111:465-475.
- Patterson, W. F. III, James H. Cowan Jr., Charles A. Wilson, and Robert L. Shipp. 2001. Age and growth of red snapper, *Lutjanus campechanus*, from an artificial reef area off Alabama in the northern Gulf of Mexico. *Fish. Bull.* 99: 617-627.
- Pauly, D. 1980. On the interrelationships between natural mortality, growth parameters, and mean environmental temperature in 175 fish stocks. *J. Cons. Int. Explor. Mer* 39:175-192.
- Ralston, S. 1987. Mortality rates of snappers and groupers. In *tropical snappers and groupers: biology and fisheries management* (J. J. Polovina and S. Ralston, eds.), p. 375-404. Westview Press, Boulder, CO.
- Render, J. H. 1995. The life history (age, growth, and reproduction) of red snapper (*Lutjanus campechanus*) and its affinity for oil and gas platforms. PhD diss., 76 p. Louisiana State University, Baton Rouge, LA.
- Rutherford, E. S., T. W. Schmidt, and J. T. Tilmant 1989. Early life history of spotted sea trout (*Cynoscion nebulosus*) and gray snapper (*Lutjanus griseus*) in Florida Bay, Everglades National Park, Florida. *Bull. Mar. Sci.* 44(1):49-64.
- Rutherford, E. S., J. T. Tilmant, E. B. Thue, and T. W. Schmidt. 1989. Fishery harvest and population dynamics of gray snapper, *Lutjanus griseus*, in Florida Bay and adjacent waters. *Bull. Mar. Sci.* 44:139-154.
- Secor, D. H., J. M. Dean, and R. B. Baldevarona. 1989. Comparison of otolith growth and somatic growth in larval and juvenile fishes based on otolith length/fish length relationships. *Rapports et Proces-Verbaux des Reunions, Conseil International pour l'Exploration de la Mer* 191:431-438.
- Sokal, R. R., and F. J. Rohlf. 1995. *Biometry: the principles and practice of statistics in biological research*, 3rd ed., 887 p. W. H. Freeman and Co., New York, NY. [ISBN:0-7167-2411-1.]
- Stuiver, M., and H. Polach. 1977. Reporting of ¹⁴C data. *Radiocarbon* 19:355-363.
- Szedlmayer, S. T., and R. L. Shipp. 1994. Movement and growth of red snapper, *Lutjanus campechanus*, from an artificial reef area in the northeastern Gulf of Mexico. *Bull. Mar. Sci.* 55(2-3):887-896.
- Tate, M. W., and R. C. Clelland. 1957. Non-parametric and shortcut statistics in the social, biological, and medical sciences, p 93-94. Interstate Printers and Publishers, Inc., Danville, IL.
- Templeman, W., and H. J. Squires 1956. Relationship of otolith lengths and weights in the haddock *Melanogrammus aeglefinus* (L.) to the rate of growth of the fish. *J. Fish. Res. Board Can.* 13:467-487.
- Thompson, B. A., M. Beasley, and C. A. Wilson. 1999. Age distribution and growth of greater amberjack, *Seriola dumerilli*, from the north-central Gulf of Mexico. *Fish. Bull.* 97:362-372.
- Wilson, C. A., and J. M. Dean. 1983. The potential use of sagittae for estimating the age of Atlantic swordfish, *Xiphias gladius*. NOAA Tech. Rep. NMFS 8:151-156.
- Wilson, C. A., and D. L. Nieland. 2001. Age and growth of red snapper, *Lutjanus campechanus*, from the Northern Gulf of Mexico off Louisiana. *Fish. Bull.* 99:653-664.

Abstract—The objective of this study was to investigate the spatial patterns in green sea urchin (*Strongylocentrotus droebachiensis*) density off the coast of Maine, using data from a fishery-independent survey program, to estimate the exploitable biomass of this species. The dependence of sea urchin variables on the environment, the lack of stationarity, and the presence of discontinuities in the study area made intrinsic geostatistics inappropriate for the study; therefore, we used triangulated irregular networks (TINs) to characterize the large-scale patterns in sea urchin density. The resulting density surfaces were modified to include only areas of the appropriate substrate type and depth zone, and were used to calculate total biomass. Exploitable biomass was estimated by using two different sea urchin density threshold values, which made different assumptions about the fishing industry. We observed considerable spatial variability on both small and large scales, including large-scale patterns in sea urchin density related to depth and fishing pressure. We conclude that the TIN method provides a reasonable spatial approach for generating biomass estimates for a fishery unsuited to geostatistics, but we suggest further studies into uncertainty estimation and the selection of threshold density values.

Estimating exploitable stock biomass for the Maine green sea urchin (*Strongylocentrotus droebachiensis*) fishery using a spatial statistics approach

Robert C. Grabowski

School of Marine Sciences
5741 Libby Hall
University of Maine
Orono, Maine 04469
Present address: Flat 6, Falmer House
16-17 Marylebone High St
London, W1U 4NY, England
E-mail address: grabowskirc6@yahoo.com

Thomas Windholz

The GIS Training and Research Center
Idaho State University
Pocatello, Idaho 83209-8130

Yong Chen

School of Marine Sciences
5741 Libby Hall
University of Maine
Orono, Maine 04469

The green sea urchin (*Strongylocentrotus droebachiensis*) is an important resource of the fishing industry in the State of Maine, where it currently ranks fourth by value. The commercial fishing industry began in the late 1980s as a result of expanding foreign markets. Landings reached a peak of more than 22,000 metric tons (t) in 1993. However, declining stock abundances have caused landings to diminish over the last decade, and in 2001, less than 5,000 t were landed (Chen and Hunter, 2003). Considering the economic importance of the fishery and its persistent decline in yield, it is essential that we establish an accurate quantitative assessment of the stock in order to develop an effective management plan.

The Maine Department of Marine Resources (DMR) has collected fishery-dependent information since the beginning of the state's commercial fishery. This information, including catch and size-composition data, has formed the basis of most management decisions in the fishery. The fishery is

currently managed through limited entry, a restricted number of opportunity days, and sea urchin size limits, in which legal-size sea urchins have a test diameter between 52 mm and 76 mm. The fishing grounds are divided into two management areas based on spatial and temporal variations in spawning (Fig. 1), in which management differs only by fishing seasons (Vadas et al., 2002).

Chen and Hunter (2003) conducted the first formal stock assessment for the Maine green sea urchin in 2001. Fishery-dependent data and sea urchin life history parameters were used to assess the population dynamics of the Maine urchin stock. A length-based stock assessment model was used with a Bayesian approach to determine probabilistic estimates of current stock biomass and exploitation rate. The study estimated that the current stock biomass was extremely low, about 10% of the virgin biomass. Only fishery-dependent data were available at the time the stock assessment was conducted, but in

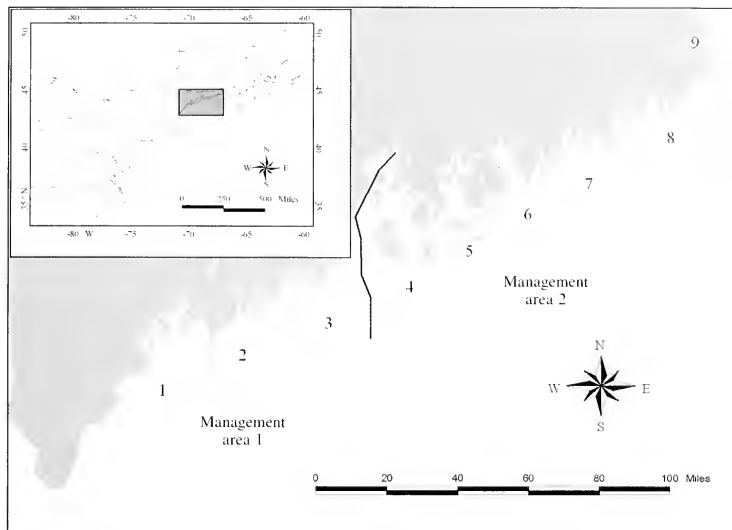


Figure 1

Map of the Maine coastline, showing the two management areas and the nine study strata from the fishery-independent survey program for green sea urchins (*Strongylocentrotus droebachiensis*).

2001 the DMR began an extensive fishery-independent survey program. This program generates large, spatially referenced, scientific data sets each year, which can be incorporated into stock assessments by using either fisheries population dynamics models or spatial analysis techniques.

Spatial statistics, also known as spatial statistics or geostatistics, encompasses a diverse group of techniques that can be used to model the spatial variability of a process, such as sea urchin density, to estimate the value at unobserved locations (Bailey and Gatrell, 1995; Petigas, 2001). Spatial variability is routinely divided into two categories: first- and second-order effects, or similarly, large- and small-scale variability. Large-scale variability is the variation in the mean value of the process over the study area, whereas small-scale variability is the spatial dependence of the process, in other words the similarity between neighboring sites (Bailey and Gatrell, 1995).

Intrinsic second-order methods, along with kriging, have become the most popular geostatistical tools and are now commonly used to estimate exploited fish stock biomass (e.g., Simard et al., 1992; Petigas, 1993; Pelle-

tier and Parma, 1994; Maravelias et al., 1996; Lembo et al., 1998; Maynou et al., 1998; Rivoirard et al., 2000; Petigas, 2001). Two assumptions must be met to use intrinsic geostatistical methods: 1) independence between the variable and the region's geometry and 2) stationarity (Petigas, 1993; Warren, 1998; Rivoirard et al., 2000). If these assumptions are violated, we can attempt to modify the data to make them more applicable or we must use other spatial analysis techniques to estimate the spatial patterns.

Tessellation is a spatial analysis technique that investigates first-order, or large-scale, spatial variability of a process (Ripley, 1981; Bailey and Gatrell, 1995). Triangulated irregular networks (TINs), or Delaunay triangulation, are the simplest and most common tessellation technique, in which a three-dimensional surface of contiguous, non-overlapping triangles is created by linear interpolation of the variable. TINs are most commonly used for visualization purposes but can be used to estimate the biomass of a process (Simard et al., 1992; Guan et al., 1999). They have received limited use in fisheries stock assessment, however, because if a stock exhibits stationarity, second-order methods tend

to provide more precise biomass estimates, as well as a quantification of their variances (Simard et al., 1992; Bailey and Gatrell, 1995; Guan et al., 1999).

The objective of our study is to investigate the spatial trends in green sea urchin density using spatial analysis techniques to estimate stock biomass. In doing so, we address the suitability of second-order methods to analyze a fishery with a target species that is highly spatially variable over a large, complex study area. We compare biomass estimates from several techniques to address the suitability of TINs for biomass estimation in the green sea urchin fishery.

Materials and methods

Data collection and processing

Sea urchin density and size-frequency information were obtained from the 2001 pilot study for the State's annual fishery-independent survey. The Department of Marine Resources conducted the survey in June and early July, after the fishing season had ended. The survey was restricted to rock and gravel habitats along the Maine coast and we used two modes of data collection, divers and video. In the first part of the study, divers sampled 144 sites according to a stratified random sampling design. The design consisted of 16 sites in each of 9 survey strata, where the width of a survey stratum was inversely proportional to the commercial landings in the region. At each site, SCUBA divers randomly sampled 30 quadrats (1 m² each) along three parallel linear transects set perpendicular to shore, for a total of 90 quadrats per site. The sampling intensity was divided equally among three depth zones: 0–5 m, 5–10 m, and 10–15 m. At each site, size-frequency data were obtained by randomly subsampling one quadrat in each depth zone, in which test diameters were measured for all individuals in the quadrat. An additional 148 sites were sampled, in a 15–40 m depth zone, with a video camera that recorded 10 quadrats (0.5 m² each) at each site. Because of the low sea urchin densities at these sites, test diameters were measured for all recorded specimens. Mean sea urchin density values were calculated for each site ($n=292$) and for each depth zone within a site ($n=580$). An analysis of variance (ANOVA) was used to test if there were significant differences in mean sea urchin density and test diameter among survey strata.

Five test diameter categories were created to more accurately represent the wide range of individual sea urchin weights. The categories were based on the state's minimum and maximum size restrictions, allowing us to separately estimate the biomass of sea urchins that have not yet recruited to the fishery, sea urchins within the fishery, and sea urchins that have escaped the fishery. The minimum (50 mm) and maximum (80 mm) size limits for our study were set slightly wider than the those of the state, because, according to the fishery regulations, up to 10% of the catch can be illegal-size sea urchins. Size-frequency data from sub-

sampled quadrats were applied to the mean sea urchin density for the specific depth zone and site, to generate density values for each size category. Weight per sea urchin was calculated from the mean length of the category by using a length-weight relationship (Scheibling et al., 1999).

Spatial interpolation

A sample semivariogram, often abridged to variogram, was generated from mean sea urchin densities by site, to examine the second-order spatial variation in the data set. The sample variogram was calculated with the following equation (Bailey and Gatrell, 1995):

$$\gamma(h) = \frac{1}{2n(h)} \sum_{S_i, S_j} (z_i - z_j)^2, \quad (1)$$

where S_i and S_j = sampling point pairs with (x,y) coordinates;

n = the number of sample point pairs;

h = the distance between pairs; and

z = mean urchin density for the sample.

Trends in the variogram provide insights into the viability of second-order methods for the sea urchin data.

Representations of the large-scale trends in sea urchin density were created by using Delaunay triangulated irregular networks (TINs) (ArcView 3.2a, 3D and Spatial Analyst Extensions, Redlands, CA). First, the sample points were plotted by using sea urchin density (/m²) as the z value. Second, each point was connected to the three nearest sites by linear interpolation, forming a continuous surface of nonoverlapping triangles (Fig. 2) (Bailey and Gatrell, 1995; Guan et al., 1999). Thus, the z value of any location within a triangular surface is based solely on the three nearest sites. TIN surfaces were generated for 40 different scenarios, according to the size category, depth zone, and management area, which minimizes variability and allows us to produce more realistic biomass estimates. Finally, using a customized C++ program,¹ we modified each surface to include only areas of appropriate sea urchin habitat. The green sea urchin is most commonly found on rocky substrate in the shallow subtidal (Scheibling and Hatcher, 2001), and, accordingly, the original survey program was limited to areas with predominately rock or gravel substrata in areas less than 40 meters deep. Therefore, we used a map of surficial geology to identify areas of the correct substrate type (1:100,000 scale) (Kelley et al., 1997) and digital gridded bathymetry data to create a plot of 5-m isoline contours. The bathymetry data source consisted of digital bathymetry data sets from sources such as NOAA and the Naval Oceanographic Office (15 arc second resolution) (Roworth and Signell, 2002).

¹ The C++ code used in this study is available upon request from the principal author (RCG).

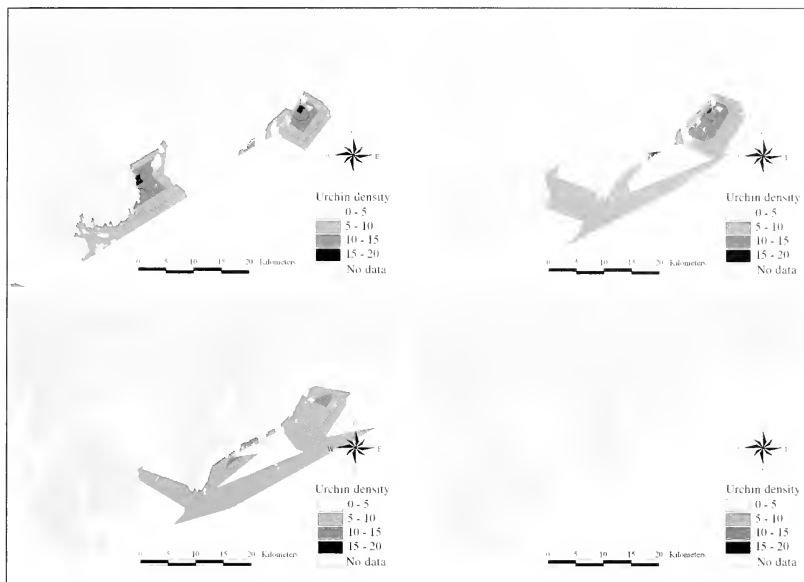


Figure 2

Representations of the triangulated irregular networks (TINs), used to characterize the large-scale patterns in green sea urchin (*Strongylocentrotus droebachiensis*) density (number of sea urchins/m²), for the 50–64 mm sea urchin size category in the central portion of management area 2. Top left, 0–5 m depth zone; top right, 5–10 m depth zone; bottom left, 10–15 m depth zone; bottom right, 15–40 m depth zone.

To determine total sea urchin biomass (b) for each scenario, the volume beneath the modified TIN surface was calculated, from Riemann sums, and multiplied by the mean weight (w) according to the following equation:

$$b = w \sum_{i=1}^n f(s_i)g, \quad (2)$$

where s_i = the spatial location (x, y) on an ASCII grid; n = the number of grids squares; $f(s_i)$ = the TIN surface and corresponds to a z value for each grid cell; and g = the grid cell size, which was 1.72 hectares for area 1 and 1.82 hectares for area 2.

Fishable biomass is defined as the biomass of all legal-size sea urchins and is simply the subset of the total biomass corresponding to legal-size sea urchins. Exploitable biomass corresponds to the legal-size sea

urchins that are available to the fishery. Some areas included in this study may not be subject to fishing pressure because of geographic isolation or low sea urchin densities. Because information on historical fishing grounds is insufficient, exploitable biomass was estimated by using a threshold density value. Only areas with densities greater than the threshold were included in the exploitable biomass estimates.

Two different types of threshold values were tested: 1) a threshold based on total sea urchin density and 2) a threshold based on the density of legal-size sea urchins. The threshold values make different assumptions about the fishery: method 1 assumes that fishermen target areas based on total sea urchin density, whereas method 2 assumes that fishermen target areas based on the density of legal-size sea urchins. Interviews were conducted with state sea urchin biologists and fishermen to determine an appropriate threshold value. The reported threshold values, the minimum total sea

urchin density that could attract fishermen, ranged from 20–50 sea urchin/m². For the first scenario, the mean density from the range of recommended values, 35 sea urchin/m², was selected. Therefore, the biomass of legal-size sea urchins was calculated only in areas where total sea urchin density was equal to or greater than 35/m². For the second scenario, we estimated that commercial divers target areas that have greater than 10 legal-size sea urchins/m².

Estimation of uncertainty and stock assessment

Because information on uncertainty cannot be directly obtained from the TIN method, cross validation was employed to approximate uncertainty in the estimation process. Cross validation involves randomly removing a site from a data set and predicting its value based on the other data points using the TIN process (Bailey and Gatrell, 1995). Residuals, or prediction errors, are calculated between the predicted and true values at the site. The process is repeated n times, resulting in an observed set of n prediction errors, or residuals. The frequency distribution and spatial distribution of residuals provide insights into the accuracy of the model; an ideal model would have a mean residual value of 0 and positive and negative residuals would be distributed randomly over the study area.

Sea urchin biomass values were also calculated with the arithmetic mean to provide comparisons with the spatially derived estimates. For total biomass, mean sea urchin densities by survey strata were multiplied by a spatially derived area estimate of suitable sea urchin habitat (<40 meters in depth) in the strata and the mean sea urchin mass per strata. Fishable biomass was calculated the same way but sea urchin density values were scaled by the proportion of legal-size sea urchins in the stratum. Finally, exploitation rates, or the ratio of commercial landings to the exploitable biomass estimates, were calculated to facilitate comparison with the results generated from the population dynamics stock assessment and a recent study on biological reference points (Chen and Hunter, 2003; Grabowski and Chen, 2004).

Results

Sea urchin density and size frequency, which were used to calculate biomass, varied considerably along the coast of Maine. Density (number of sea urchins/m²) differed significantly among survey strata ($P < 0.05$; ANOVA), showing a general large-scale trend of increasing density from stratum 1 to 9 (Table 1). Density also varied by depth; the sea urchin density in the 15–40 m depth zone was 0.32 sea urchins/m², significantly lower than those of the three shallow (<15 m) depth zones ($P < 0.05$, t -test), which each had approximately 9.50 sea urchins/m². Sea urchin test diameter varied from 3 mm to 114 mm (mean at 35.90 mm). Test diameter differed significantly among survey strata ($P < 0.05$; ANOVA), in which strata 4, 5, and 9 had the smallest size sea urchins, and strata

Table 1

Quadrat density counts (/m²) for the green sea urchin (*Strongylocentrotus droebachiensis*) by management area and survey strata. Sample size, n , is the number of quadrats observed.

Area	Stratum	Density				n
		Min.	Max.	Mean	SD	
1	1	0	36	0.17	1.62	1706
	2	0	130	2.57	10.63	1600
	3	0	141	3.20	11.29	1580
2	4	0	180	4.20	14.13	1490
	5	0	127	4.24	12.52	1580
	6	0	147	10.06	17.59	1530
	7	0	113	7.90	13.85	1498
	8	0	113	13.50	20.38	1570
	9	0	280	34.45	44.03	1540

Table 2

Sea urchin test diameter (mm) for green sea urchins (*Strongylocentrotus droebachiensis*) subsampled in the fishery-independent survey program.

Area	Stratum	Density				n
		Min.	Max.	Mean	SD	
1	1	7	80	38.69	21.07	29
	2	3	81	39.01	22.19	627
	3	4	89	45.25	18.90	855
2	4	3	89	32.99	19.82	1148
	5	3	77	29.25	17.56	1034
	6	4	110	39.87	16.23	1734
	7	5	92	47.23	16.07	1283
	8	3	114	42.11	16.86	2567
	9	3	114	28.84	12.90	5263

3 and 5 had the largest (Table 2). No meaningful trend was evident in the sample variogram, which showed a pure nugget effect (Fig. 3). This result indicates that the sea urchin density data were too spatially variable to be analyzed by intrinsic small-scale methods.

Total sea urchin biomass was estimated at approximately 250,000 metric tons (t), and legal-size sea urchins accounted for 165,000 t (Fig. 4). Most of the biomass was found in management area 2, which accounted for over 75% and 80% of the total and fishable biomass, respectively (Table 3). For both estimates, biomass varied by depth, being highest in the 0–5 m depth zone and lowest in the 15–40 m depth zone (Fig. 5).

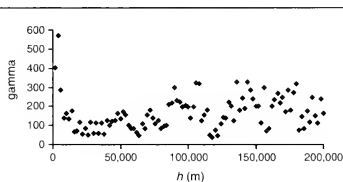
The two methods used to estimate exploitable biomass produced different biomass estimates with unique

Table 3

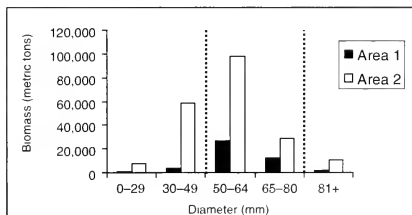
A summary of 2001 biomass estimates and 2000-2001 landings, in metric tons, for the Maine green sea urchin fishery. Biomass estimates for the TIN method and arithmetic mean were generated in this study, whereas the population dynamics estimates are from Chen and Hunter (2003). Area 1 consists of strata 1-3 and area 2 consists of strata 4-9. When possible, 95% confidence intervals are included, in italics.

	Area 1	Area 2	Total
TIN method			
Total biomass	45,868	204,304	250,172
Fishable biomass	39,060	126,725	165,786
Exploitable biomass			
Method 1	3645	5793	9438
Method 2	10,886	12,069	22,955
Arithmetic mean			
Total biomass	47,933	290,954	338,887
	<i>(42,399-54,331)</i>	<i>(274,632-307,977)</i>	<i>(317,031-362,308)</i>
Fishable biomass	24,241	90,185	114,426
	<i>(21,575-27,287)</i>	<i>(85,144-95,144)</i>	<i>(106,719-122,723)</i>
Population dynamics			
	6550	8452 ¹	15,002
	<i>(4041-9450)</i>	<i>(5866-11,701)</i>	<i>(10,307-21,151)</i>
2000-2001 landings			
	2148	3213	5361

¹ 2000 value.

**Figure 3**

Sample variogram of mean green sea urchin (*Strongylocentrotus droebachiensis*) density by site, showing small-scale variability, gamma (γ), with respect to the distance between sample point pairs, h .

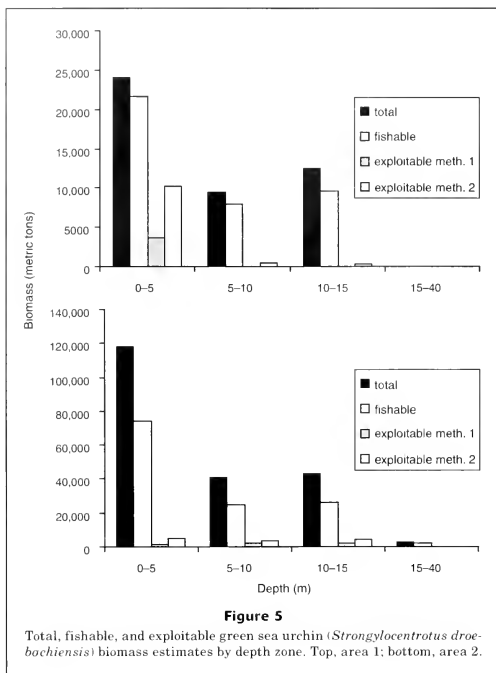
**Figure 4**

Total biomass by green sea urchin (*Strongylocentrotus droebachiensis*) test diameter according to management area. Sea urchins between 50 and 80 mm were considered legal size for this study, and the biomass within these limits, indicated by the dashed lines, constitutes the fishable biomass.

spatial distributions. Exploitable biomass estimates for method 2 were more than 2 times greater than those for method 1 (Table 3). With method 1, legal-size sea urchins were concentrated in the northeastern corner of management area 2, but with method 2, they were concentrated in the northeastern portion of area 1 and the central portion of area 2 (Fig. 6). Exploitable sea urchin biomass showed different patterns by management area and depth than did total biomass and fishable biomass (Fig. 5). For example, management area 1 had a larger share of the total exploitable biomass, 39% or 47%, for methods 1 and 2, respectively, and

this biomass was almost exclusively found in the 0-5 m depth zone, accounting for 98% or 93%, respectively, of the area's biomass.

TIN biomass estimates were similar to ones produced with the arithmetic mean but were higher for total biomass and lower for fishable biomass. Exploitation rates for method 1 were estimated at 0.59 and 0.55 for management areas 1 and 2, respectively, and 0.20 and 0.27 for method 2, respectively. Exploitation rates



from the population dynamics modeling approach were 0.38 and 0.57 (2000) for management areas 1 and 2, respectively.

Cross validation of sea urchin density surfaces yielded a mean residual of 0.50 (median=0, standard deviation=1.86, skewness=2.80, $n=60$) (Fig. 7). Residuals were greatest in regions with the highest spatial variability, such as sites within depth zones 1 and 2 and in the eastern survey strata.

Discussion

Spatial variability and distribution

The objective of this study was to investigate the spatial variability in green sea urchin density to estimate the biomass of the Maine stock. However, several factors limited the choice of spatial statistical approaches that

could be used to assess the fishery. In particular, the physical structure of the study area, the dependence of sea urchin variables upon the environment and a high degree of small-scale spatial uncertainty make small-scale approaches inappropriate.

First, the study area was neither uniform nor continuous. Because the aim of the fishery-independent survey program was to assess the whole population of sea urchins in Maine, the study area had to span the entire coastline. Consequently, the study area encompassed many features that create discontinuities in a spatial model at varying, yet relatively small, spatial scales. These features included the highly indented coastline, the presence of several hundred islands and the exclusion of regions because of environmental constraints. Second, green sea urchin variables were not independent of the study area; rather, they were dependent on several environmental, ecological, and anthropogenic factors. In particular, depth, substrate type,

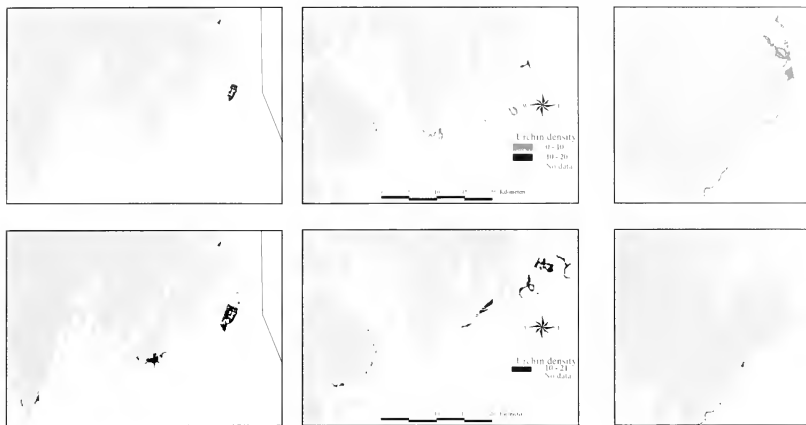


Figure 6

Final spatial representations of the density of exploitable green sea urchins (*Strongylocentrotus droebachiensis*). Top row, method 1: threshold was based on total sea urchin density. Bottom row, method 2: threshold was based on legal-size sea urchin density. Left column, eastern portion of management area 1; middle column, central portion of management area 2; right column, northeastern corner of management area 2.

benthic algal presence, and the presence and level of fishing or predatory activity all greatly affect urchin density, growth rates, and size frequency (Vadas et al., 1986; Scheibling and Hatcher, 2001). Mean sea urchin density and size frequency were not constant over the study area (Tables 1 and 2). Density exhibited large-scale spatial trends along the coast, which are related, at least, to depth and fishing activity. The eastward increase in total sea urchin density along the coast corresponded well with the historical patterns of commercial sea urchin fishing in the State of Maine (Table 1). The fishery began in the southwest, but as sea urchin densities dropped in those regions, the fishery steadily progressed northeastward along the coast. Spatial patterns in density by depth (0–15 m vs. 15–40 m) may have been caused, in part, by the difference in sampling techniques, yet the magnitude of the differences and support from ecological studies indicate that there is a pattern. Finally, sea urchin densities varied dramatically on small spatial scales—variations on the order of one magnitude within the same habitat, and sometimes only meters apart, are not uncommon (Scheibling and Hatcher, 2001). This variability was evident in the variogram analysis, which showed no meaningful small-scale spatial structure and thus no stationarity (Fig. 3).

We were interested in identifying a spatial statistical approach that would generate reasonable estimates

of stock biomass. The numerous discontinuities in the study area, the dependence of variables on ecological factors, and the high spatial variability indicated that an intrinsic spatial statistical approach was not appropriate for the investigation. Therefore, we needed an approach that was geared towards the detection and modeling of large-scale variability and that also exhibited some robustness to discontinuities caused by the indented coastline, islands, and habitat constraints. We believe the TIN approach used in this study satisfies these requirements, and, additionally, allows for varying levels of resolutions, with finer resolution in high density sampling areas.

Biomass estimates

We calculated exploitable biomass in two different ways because of the different assumptions they make about the fishery. Method 1 assumes that fishermen target areas based on total sea urchin density, whereas method 2 assumes that fishermen target areas based on the density of legal-size sea urchins. The spatial distributions of legal-size sea urchin density, which were used to calculate exploitable biomass, were distinctive and showed little overlap between methods (Fig. 6). The spatial distributions appear to reflect different aspects of the sea urchin fishery. When the threshold was based on total density (method 1), exploitable biomass was

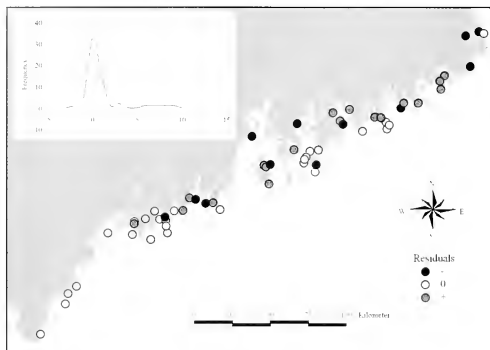


Figure 7

Spatial distribution of residuals and frequency distribution, insert (median=0, standard deviation=1.86, skewness=2.80, $n=60$), from the cross-validation study that addressed uncertainty in the TIN estimation process for estimating biomass for the green sea urchin (*Strongylocentrotus droebachiensis*) fishery.

concentrated in the eastern corner of management area 2, which is the most northeastern location on the coast of Maine. This area has high total sea urchin densities, but relatively low densities of legal-size adults, and is an important location for the trawling industry. When the threshold was based on the density of legal-size sea urchins (method 2), however, exploitable biomass was concentrated in the eastern portion of management area 1 and the central portion of area 2. These regions have lower average sea urchin densities, but higher percentages of legal-size adults, and are key fishing grounds for the state's dive-based fishery.

Because the two methods reflected different aspects of the fishery, it is not surprising that they produced different estimates of exploitable biomass (Table 3). Nevertheless, these estimates did not differ considerably from those of the population dynamics model. The spatial analysis estimates bordered the ones derived from the population dynamics model; method-1 estimates were smaller than those derived from the population dynamics model whereas method-2 estimates were larger. The biomass estimates were similar despite the fact that they were derived from different models (spatial analysis and population dynamics model) using entirely different data sources (fishery-independent and fishery-dependent).

The status of a fishery is often determined by comparing the current fishing mortality or stock biomass with biological reference points (BRPs) (Hilborn and Walters, 1992). The previous stock assessment study estimated that the sea urchin stock biomass in Maine is only about 10% of the virgin biomass, implying that the

fishery has been severely overfished. A preliminary investigation into BRPs recently estimated a BRP $F_{0.1}$ for the urchin fishery, based on a yield per recruit analysis, and concluded that estimates of the current exploitation rate are much higher than the BRP, which means that the fishery is being overfished (Grabowski and Chen, 2004). However, when we compare the TIN exploitation rates with the preliminary mean BRP $F_{0.1}$, which ranged from 0.37 to 0.43 depending upon uncertainty levels, we get an unclear assessment of the stock status. The fishery is being drastically overfished according to method 1, but is healthy according to method 2. We believe that the assessment generated by method 2 was unrealistically optimistic, considering the results from the stock assessment and the decade-long declining trend in landings.

Uncertainty and further studies

The TIN method was an appropriate spatial statistical approach for estimating biomass for the sea urchin fishery; however, a disadvantage of this technique is that there is no straightforward method to estimate the uncertainty in the biomass estimates. Because the technique does not incorporate a variance structure into the estimation process, we could not directly estimate uncertainty. Therefore, we used cross-validation to approximate the uncertainty associated with the TIN method (Fig. 7). We found that the mean residual did not equal zero, indicating that there is a global bias in the TIN surfaces and that biomass estimates were likely overestimated (Simard et al., 1992). This bias was most likely caused

by a combination of the underlying patterns in spatial variability, the linear interpolation method employed in TIN formation, and the effects of sample selection in the cross-validation study. There are several possible ways to reduce the bias in the estimation process, such as incorporating a smoothing function or weighting based on neighbors into the TIN model. This procedure would not completely address uncertainty, however, because it would only acknowledge uncertainty in the TIN estimation process. To obtain confidence intervals for biomass estimates, we needed to incorporate uncertainty in mean density and in TIN estimation. We are currently investigating methods to estimate confidence intervals, such as using a Monte Carlo simulation approach. A thorough examination and quantification of uncertainty is beyond the scope of this article.

In this study, we identified a basic approach for investigating spatial patterns, and estimating stock biomass in situations where second-order methods are inappropriate. The TIN technique generated realistic biomass estimates that are similar to those derived with other approaches, but before we can recommend this technique for the green sea urchin fishery, several points must be addressed. First, the two methods used to estimate exploitable biomass must be integrated because they reflect different aspects of the fishery and result in different stock assessments. Second, a process must be established to estimate threshold levels because they have a large control over exploitable biomass estimates. Finally, a technique must be developed to estimate uncertainty in biomass. We would also recommend further investigations into tracking fishing pressure and identifying its effects on the benthic ecosystem and the spatial distribution of sea urchins.

Acknowledgments

We would like to thank the staff at the Maine Department of Marine Resources for collecting and compiling the sea urchin fishery data. We would especially like to thank Margaret Hunter and Robert Russell from the DMR, Kathryn Wisz, our laboratory assistant, Ryan Weatherbee, for his help with the manuscript, and Olivier Mette, for his technical assistance. This project was partially supported by grants from the Northeast Consortium (UNH SUB 302-628), the Maine Department of Marine Resources (G1102012), and the Sea Urchin Zone Council to Y. Chen and a Maine Marine Science Fellowship from the Marine Department of Marine Resources and the University of Maine School of Marine Sciences to R. Grabowski.

Literature cited

- Bailey, T., and A. Gatrell.
1995. *Interactive spatial data analysis*, 413 p. Pearson Education, Essex, England.
- Chen, Y., and M. Hunter.
2003. Assessing the green sea urchin (*Strongylocentrotus droebachiensis*) stock in Maine, USA. *Fish. Res.* 60:527-537.
- Guan, W., R. H. Chamberlain, B. M. Sabol, and P. H. Doering.
1999. Mapping submerged aquatic vegetation with GIS in the Caloosahatchee Estuary: evaluation of different interpolation methods. *Mar. Geod.* 22:69-92.
- Grabowski, R., and Y. Chen.
2004. Incorporating uncertainty into the estimation of the biological reference points $F_{0.1}$ and F_{max} for the Maine green sea urchin (*Strongylocentrotus droebachiensis*) fishery. *Fish. Res.* 68:367-371.
- Hilborn, R., and C. J. Walters.
1992. *Quantitative fisheries stock assessment: choice, dynamics and uncertainty*, 570 p. Chapman and Hall, New York, NY.
- Kelley, J. T., W. A. Barnhardt, D. F. Belknap, S. M. Dickson, and A. R. Kelley.
1997. The seafloor revealed: the geology of the northwestern Gulf of Maine inner continental shelf, 55 p. Open file source 96-6. Maine Geological Survey, Natural Resources Information and Mapping Center, Augusta, ME.
- Lembo, G., T. Silecchia, P. Carbonara, A. Acrivulis, and M. T. Spedicato.
1998. A geostatistical approach to the assessment of the spatial distribution of *Parapenaeus longirostris* (Lucas, 1846) in the central-southern Tyrrhenian Sea. *Crustaceana* 72:1093-1095.
- Maravelias, C. D., D. G. Reid, E. J. Simmonds, and J. Haralabous.
1996. Spatial analysis and mapping of acoustic survey data in the presence of high local variability: geostatistical application to North Sea herring (*Clupea harengus*). *Can. J. Fish. Aquat. Sci.* 53:1497-1505.
- Maynou, F. X., F. Sarda, and G. Y. Conat.
1998. Assessment of the spatial structure and biomass evaluation of *Nephrops norvegicus* (L.) populations in the northwestern Mediterranean by geostatistics. *ICES J. Mar. Sci.* 55:102-120.
- Pelletier, D., and A. M. Parma.
1994. Spatial distribution of Pacific halibut (*Hippoglossus stenolepis*): an application of geostatistics to longline survey data. *Can. J. Fish. Aquat. Sci.* 51:1506-1518.
- Petigas, P.
1993. Geostatistics for fish stock assessments: a review and an acoustic application. *ICES J. Mar. Sci.* 50:285-298.
2001. Geostatistics in fisheries survey design and stock assessment: models, variances and applications. *Fish and Fisheries* 2:231-249.
- Ripley, B. R.
1981. *Spatial statistics*, 252 p. John Wiley & Sons, New York, NY.
- Rivoirard, J., J. Simmonds, K. G. Foote, P. Fernandes, and N. Bez.
2000. Geostatistics for estimating fish abundance, 206 p. Blackwell Science, Oxford, UK.
- Roworth, E., and R. Signell.
2002. Construction of a digital bathymetry for the Gulf of Maine. <http://woodshole.er.usgs.gov/project-pages/oracles/gomaine/bathy/data.htm>. [Accessed 22 October 2002.]
- Scheibling, R. E., A. W. Hennigar, and T. Balch.
1999. Destructive grazing, epiphytism, and disease: the dynamics of sea urchin-kelp interactions in Nova Scotia. *Can. J. Fish. Aquat. Sci.* 56:2300-2314.

- Scheibling, R. E., and B. G. Hatcher.
2001. The ecology of *Strongylocentrotus droebachiensis*.
In Edible sea urchin biology and ecology (J. M. Lawrence,
ed.), p. 271-304. Elsevier, New York, NY.
- Simard, Y., P. Legendre, G. Lavoie, and D. Marcotte.
1992. Mapping, estimating biomass, and optimizing sam-
pling programs for spatially autocorrelated data: case
study of the northern shrimp (*Pandalus borealis*). Can.
J. Fish. Aquat. Sci. 49:32-45.
- Vadas, R. L., R. W. Elner, P. E. Garwood, and I. G. Babb.
1986. Experimental aggregation behavior in the sea ur-
chin *Strongylocentrotus droebachiensis*. Mar. Biol. 90:
433-448.
- Vadas, R. L., Sr., B. D. Smith, B. Beal, and T. Dowling.
2002. Sympatric growth morphs and size bimodal-
ity in the green sea urchin (*Strongylocentrotus*
droebachiensis). Ecol. Monogr. 72:113-132.
- Warren, W. G.
1998. Spatial analysis for marine populations: factors
to be considered. In Proceedings of the North Pacific
symposium on invertebrate stock assessment and man-
agement (G. S. Jamieson and A. Campbell, eds.), p.
21-28. Can. Spec. Publ. Fish. Aquat. Sci. 125.

Abstract—The abundance and distribution of California sea lions (*Zalophus californianus*) in central and northern California was studied to allow future evaluation of their impact on salmonids, the ecosystem, and fisheries. Abundance at-sea was estimated by using the strip transect method from a fixed-wing aircraft with a belly viewing port. Abundance on land was estimated from 126-mm-format aerial photographs of animals at haulouts between Point Conception and the California–Oregon border. The sum of these two estimates represented total abundance for central and northern California. Both types of survey were conducted in May–June 1998, September 1998, December 1998, and July 1999. A haulout survey was conducted in July 1998. The greatest number of sea lions occurred near Monterey Bay and San Francisco Bay for all surveys. Abundance was high in central and northern California in 1998 when warm water from the 1997–98 El Niño affected the region and was low in July 1999 when cold water La Niña conditions were prevalent. At-sea abundance estimates in central and northern California ranged from 12,232 to 40,161 animals, and haulout abundance was 13,559 to 36,576 animals. Total abundance of California sea lions in central and northern California was estimated as 64,916 in May–June 1998, 75,673 in September 1998, 56,775 in December 1998, and 25,791 in July 1999. The proportion of total abundance to animals hauled-out for the four complete surveys ranged from 1.77 to 2.13, and the mean of 1.89 was used to estimate a total abundance of 49,697 for July 1998. This multiplier may be applicable in the future to estimate total abundance of California sea lions off central and northern California if only the abundance of animals at haulout sites is known.

Manuscript submitted 1 October 2002
to the Scientific Editor's Office.

Manuscript approved for publication
14 December 2004 by the Scientific Editor.

Fish. Bull. 103:331–343 (2005).

Abundance and distribution of California sea lions (*Zalophus californianus*) in central and northern California during 1998 and summer 1999

Mark S. Lowry

National Marine Fisheries Service
Southwest Fisheries Science Center
8604 La Jolla Shores Dr.
La Jolla, California 92037
E-mail address: mark_lowry@noaa.gov

Karin A. Forney

National Marine Fisheries Service
Southwest Fisheries Science Center
110 Shaffer Road
Santa Cruz, California 95060

The California sea lion (*Zalophus californianus*) is distributed from central Mexico to British Columbia, Canada. Four islands off southern California (Santa Barbara, San Clemente, San Nicolas, and San Miguel Islands) form the reproductive center for the U.S. population, although some pupping occurs at various other haulout sites in central California (Pierotti et al., 1977; Keith et al., 1984). The number of individuals off California varies throughout the year because sea lions from Mexico enter and leave California waters and individuals from California migrate southward into Mexico or northward as far as British Columbia, Canada (Bartholomew, 1967; Bigg, 1988; and Huber, 1991). In southern California, the abundance of California sea lions peaks during the summer breeding season (Bartholomew, 1967; Odell, 1975). In central and northern California, the number of sea lions typically increases in the autumn during the northward migration, declines in winter, increases in spring as sea lions move to rookeries in southern California and Mexico, and declines in summer (Orr and Poulter, 1965; Mate, 1975; Sullivan, 1980; and Griswold, 1985; Bonnell et al.¹).

Since the mid-1970s, the California sea lion population in the United States has expanded at an average of 5.0% per year and was most

recently estimated to be between 204,000 and 214,000 individuals in 1999 (Forney et al.²). This estimate is roughly 2.7 times greater than in 1981–83 (Bonnell et al.¹). As the U.S. sea lion population has grown, concerns have arisen about potential impacts on commercially harvested fish stocks. California sea lions feed on a variety of fish and cephalopods, some of which are commercially important species, such as salmonids (*Oncorhynchus* spp.), Pacific sardines (*Sardinops sagax*), northern anchovy (*Engraulis mordax*), Pacific mackerel (*Scomber japonicus*), Pacific whiting (*Merluccius productus*), rockfish (*Se-*

¹ Bonnell, M. L., M. O. Pierson, and G. D. Farrens. 1983. Pinnipeds and sea otters of central and northern California, 1980–1983: status, abundance, and distribution. Center for Marine Studies, Univ. California, Santa Cruz. OCS Study MMS 84-0044, 220 p. Prepared for Pacific OCS Region, Minerals Management Service, U.S. Department of Interior, Camarillo, Calif. 93010, contract no. 14-12-0001-29090.

² Forney, K. A., J. Barlow, M. M. Muto, M. Lowry, J. Baker, G. Cameron, J. Mobley, C. Stinchcomb, and J. V. Carretta. 2000. U.S. Pacific marine mammal stock assessments: 2000. NOAA Tech. Memo.: NOAA-TM-NMFS-SWFSC-300, 276 p. National Marine Fisheries Service, Southwest Fisheries Science Center, 8604 La Jolla Shores Drive, La Jolla, CA 92037.

bastes spp.), and market squid (*Loligo opalescens*) (Lowry et al. 1990, 1991; Lowry and Carretta, 1999; Weise, 2000). Effects on these resources have been estimated for Monterey Bay only, where during the 1997–98 El Niño sea lions consumed an estimated 269.1 to 804.7 metric tons (t) of salmon, 988.4 to 2206.8 t of sardine, and 533.4 to 1827.4 t of rockfishes annually (Weise, 2000). Recently, salmon in central and northern California have experienced population declines and some stocks have been listed as threatened or endangered under the U.S. Endangered Species Act. Although a variety of factors are responsible for the decline (e.g., logging, dams, agriculture, fishing), some salmonid populations are at such reduced levels that predation by sea lions may negatively affect their recovery (NMFS³). Sea lions also have been documented as interfering with recreational fisheries by consuming bait and chum and depredating hooked fish (Fluharty⁴).

Existing methods of population assessment have been based on pup counts obtained at California sea lion rookeries near the end of the breeding season and total population has been estimated by extrapolating data from a life history model (Barlow and Boveng, 1991; Boveng⁵; Barlow et al.^{6,7}; Forney et al.²). However, this approach cannot be used outside of the breeding season or in nonbreeding areas. Previous studies of California sea lion abundance and distribution in central and northern California during 1980–82 (Bonnell et al.¹)

³ NMFS (National Marine Fisheries Service). 1997. Investigation of scientific information on the impacts of California sea lions and Pacific harbor seals on salmonids and on the coastal ecosystems of Washington, Oregon, and California. NOAA Tech. Memo. NMFS-NWFSC-28, 172 p. Northwest Fisheries Science Center, 2527 Montlake Blvd. E., Seattle, WA 98112-2097 and National Marine Fisheries Service, Northwest Region, 7600 Sand Point Way N.E., Seattle, WA 98115-0070.

⁴ Fluharty, M. J. 1999. California sea lion interactions with commercial passenger fishing vessel fisheries: a review of log book data from 1994, 1995, and 1996. California Department of Fish and Game Admin. report 99-2, 21 p. [Available from California Department of Fish and Game, Marine Region, San Diego Field Office, 4949 Viewridge Avenue, San Diego, CA 92123.]

⁵ Boveng, P. 1988. Status of the California sea lion population on the U. S. west coast. National Oceanographic and Atmospheric Administration admin. report LJ-88-07, 26 p. Northwest Fisheries Science Center, 8604 La Jolla Shores Drive, La Jolla, CA 92037.

⁶ Barlow, J., R. L. Brownell Jr., D. P. DeMaster, K. A. Forney, M. S. Lowry, S. Osmek, T. J. Ragen, R. R. Reeves, and R. J. Small. 1995. U.S. Pacific marine mammal stock assessments. NOAA Tech. Memo. NMFS, NOAA-TM-NMFS-SWFS-219, 162 p. National Marine Fisheries Service, Southwest Fisheries Science Center, 8604 La Jolla Shores Drive, La Jolla, CA 92037.

⁷ Barlow, J., K. A. Forney, P. Scott Hill, R. L. Brownell Jr., J. V. Carretta, D. P. DeMaster, F. Julian, M. S. Lowry, T. Ragen, R. and R. Reeves. 1997. U.S. Pacific marine mammal stock assessments: 1996. NOAA Tech. Memo. NMFS, NOAA-TM-NMFS-SWFS-248, 223 p. National Marine Fisheries Service, Southwest Fisheries Science Center, 8604 La Jolla Shores Drive, La Jolla, CA 92037.

and 1995–96 (Beeson and Hanan⁸) included only animals on land; animals at sea were either not considered or were included as a rough estimate. An assessment approach was, therefore, needed to provide quantitative estimates of California sea lion abundance in central and northern California that included both animals at sea and on land.

This study uses a combination of the strip-transect method (to estimate at-sea abundance) and aerial photographic counts (to estimate abundance of sea lions on land) in order to estimate the total abundance of California sea lions in central and northern California. Abundances were estimated separately for seven latitudinal zones within central and northern California. This study also describes distribution of sea lions by age and sex class in central and northern California, describes offshore distribution of sea lions, and introduces a new multiplier that can be used to estimate the total abundance of California sea lions at sea and on land, when only an estimate of the number of animals on land is available.

Methods

Survey dates and areas

Surveys were conducted during May–June, July, September, and December 1998, and July 1999. The May–June survey occurred when salmonid smolts were migrating out of rivers (NMFS³), the July survey when the United States stock of California sea lions was expected to be distributed mostly in California coastal waters, and the September and December surveys when adult salmon were migrating into rivers (NMFS³). The study area encompassed the waters and shoreline of central and northern California from Point Conception (34°26.8'N, 120°28.0'W) to the California–Oregon border (42°00.0'N, 124°12'W) within approximately sixty nautical miles of the coast (Fig. 1).

Strip-transect surveys

A twin-engine, high-wing Partenavia PN68C- or PN68-observer model aircraft was flown at an airspeed of 185 km/h during strip-transect and coastal haulout surveys. Abundance of sea lions at sea was determined by using the strip-transect method because previous aerial surveys in central California indicated that densities of sea lions would be too great in some areas to obtain reliable measures of perpendicular distances for line-transect density estimation. Previous aerial surveys using line transect methods, conducted at 213 m altitude, indicated a relatively flat detection function for sea lions between

⁸ Beeson, M. J., and D. A. Hanan. 1996. An evaluation of pinniped-fishery interactions in California. Report to the Pacific States Marine Fisheries Commission, 47 p. [Available from Pacific States Marine Fisheries Commission, 205 SE Spokane St., Suite 100, Portland, OR, 97202-6413.]

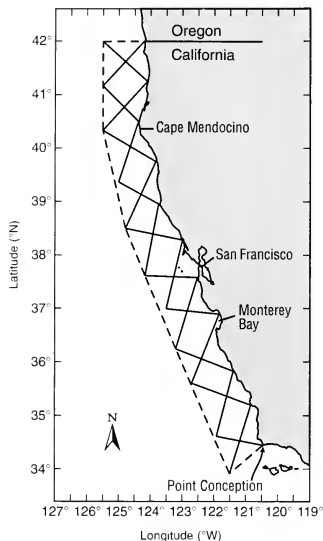


Figure 1

Strip-transect lines (solid lines) within the study area (dashed line) used for estimating at-sea abundance of California sea lions (*Zalophus californianus*) in central and northern California.

approximately 85 meters left and right of the transect line (Fig. 2; Carretta, personal commun.⁹). Therefore, strip transect assumptions, that all individuals within the observed strip are detected, were expected to be valid within 85 meters left and right of the transect line. In our study we lowered the altitude of the aircraft to 183 m to increase the detection probability for sea lions in the water, especially in Beaufort 3–4 sea states. At that altitude, the viewing area of a single observer viewing from the belly window extended from directly below (90°) to a declination angle of 65° on each side, resulting in a total strip width of 170 m, or 85 m on each side of the viewing window.

Transects followed predetermined lines that systematically zig-zagged the study area (Fig. 1). Surveys were conducted in Beaufort sea states of 0–4. The lines were flown from south to north to take advantage of

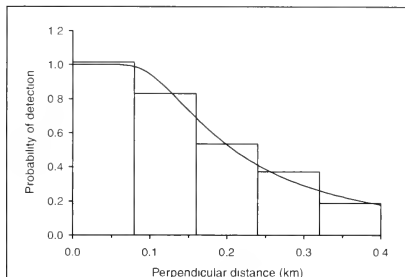


Figure 2

Probability density function for California sea lion (*Zalophus californianus*) sightings from an aircraft flying at an altitude of 213 meters in Beaufort sea states 0–4. Figure was provided by J. Carretta, National Marine Fisheries Service, Southwest Fisheries Science Center, La Jolla, CA, 92037.

sun angle and to minimize sun glare, except on a few overcast days when southbound flights provided ample visibility. Geographical positions were recorded at one-minute intervals directly to a laptop computer by a serial cable connected to the aircraft's global positioning system (GPS). The following data were collected: number of California sea lions, GPS position, percentage of cloud cover over the survey area, name of the observer and data recorder, Beaufort sea state, transect number, and percentage of glare. Percentage of glare was defined as the proportion of the viewing area in which the observer could not see into the water because of surface reflection caused by sun or cloud glare. During the May–June survey we used a recorder, observer, and a resting person—the resting person rotating with the observer approximately every 30 minutes. During the July, September, and December surveys, the resting person was eliminated and the observer and recorder rotated at approximately 30-minute intervals.

Abundance at sea

We used the nonparametric Kruskal-Wallis test for two-way comparisons of the effects of glare and sea state on California sea lion sighting rates. For these tests, each transect segment with constant viewing conditions was randomly assigned to one of five substrata, which served as replicate samples for the tests. Viewing conditions with significantly lower sighting rates were excluded from the abundance analyses to reduce bias caused by missed animals.

Two *a posteriori* geographic strata were created, inshore (50,546 km² total surface area) and offshore

⁹ Carretta, J. 1998. Personal commun. Southwest Fisheries Science Center, NMFS, La Jolla, California, 92037.

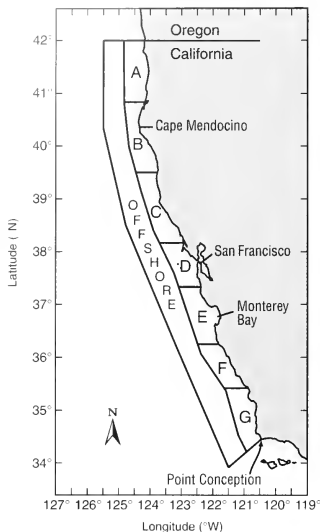


Figure 3

A posteriori stratification of study area into "offshore" stratum and into seven zones (A through G) within the "inshore" stratum for estimating abundance of California sea lions (*Zalophus californianus*) from strip-transect data and haulout count data.

(56,526 km² total surface area), using transect intersect points as the dividing line (Fig. 3). Differences between the definition of haulout sites for the surveys in this study and during previous surveys in 1980–82 and 1995 (Bonnell et al.¹, and Beeson and Hanan⁸) made it necessary to create additional zones within the inshore stratum to allow comparisons of the three data sets. The inshore stratum was thus divided into seven zones ("A" through "G"), separated at the following latitudes: 1) 35°25'N; 2) 36°15'N; 3) 37°20'N; 4) 38°10'N; 5) 39°30'N; and 6) 40°50'N (Fig. 3). The zones were separated where gaps occurred in the distribution of haulout areas along the coastline. Total area sizes for the seven zones were the following: A: 7647 km²; B: 7206 km²; C: 8025 km²; D: 6153 km²; E: 7790 km²; F: 6030 km², and G: 7695 km². At-sea abundance was obtained separately for offshore and inshore strata, and for each zone within the inshore stratum, by using a modified strip-transect formula that included a correction, $g(0)$, for diving animals that were not available to be seen:

$$N_i = \frac{nA}{WLg(0)} \quad (1)$$

where N_i = corrected total abundance (corrected for animals below the surface);
 n = number of individuals sighted within the strip-transect;
 A = total size of study area (in km²);
 W = the strip width (in km);
 L = distance surveyed (in km) calculated as the sum of the great circle distances between position fixes; and
 $g(0)$ = probability that a sea lion will be visible at the surface within the strip viewed by the observer as the aircraft passes over the water.

Coefficients of variation (CV) and lognormal 95% confidence limits of these abundance estimates were calculated by using standard formulae (Buckland et al., 1993).

Probability of missing submerged sea lions

We estimated the probability of seeing sea lions at the surface, $g(0)$, from dive data in Feldkamp et al. (1989) derived from 14 foraging trips made by seven lactating adult female California sea lions during late breeding-season:

$$g(0) = \frac{t+s+r}{t+s+r+d} \quad (2)$$

where t = average time (hours) spent at the surface between dives within diving bouts by an adult female sea lion;
 s = average time (h) spent swimming near the surface between diving bouts by an adult female sea lion;
 r = average time (h) spent resting at the surface between diving bouts by an adult female sea lion; and
 d = average time (h) spent diving during diving bouts by an adult female sea lion.

From seven female sea lions, Feldkamp et al. (1989) calculated averages of 12.0 hours (no SD given) spent at the surface between dives within diving bouts (t), 21.9 hours (SD=9.5 hours) spent swimming near the surface between diving bouts (s), 1.6 hours (SD=1.6) spent resting at the surface between diving bouts (r), and 17.3 hours (SD=6.7) spent diving during diving bouts (d). We calculated the CV for $g(0)$ from the standard deviations of diving data. In using these data we assumed that between dives, sea lions swam near the surface and at a depth where they would be seen by an observer in the aircraft and that sea lions were not visible to an observer in the aircraft during dives. Dive data were not available for other age and sex classes; therefore,

it was assumed that the proportion of time spent at or near the surface was similar for adult females and other age and sex classes and did not vary significantly within region, season, and year.

Photographic surveys

The aircraft was flown from north to south directly over the coastline or slightly offshore at an altitude of 183 to 213 m (typically 213 m) to locate sea lions onshore. The low altitude ensured that California sea lions could be detected on rocky substrates, aided in identification of different pinniped species, and enabled accurate counts from aerial photographs. All hauled-out California sea lions onshore were photographed. At the Farallon Islands, the aircraft was flown at an altitude of 366 to 457 m (typically 396 m) to prevent disturbance of nesting seabirds. Multiple passes were made over large rocks or islands to ensure that the entire rock or island was photographed. Surveys were made without regard to tidal conditions at any time of day between approximately two hours after sunrise and two hours before sunset.

Sea lions were photographed with a 126-mm-format KA-76 camera (Chicago Aerial Industries, Inc., Chicago, IL) equipped with image motion compensation (IMC) and operated at a cycle rate that achieved 67% overlap between adjacent frames. The geographical position of each photograph was recorded by linking the camera (mounted vertically inside the belly of the aircraft) to a computer and GPS unit. A 152-mm focal-length lens was used for low altitude photography (i.e., 183–213 m) and a 305-mm focal-length lens was used for higher altitude photography (i.e., 366–457 m). Kodak Aerochrome MS Film 2448, a very fine-grained, medium-speed, color transparency film, or Aerochrome HS Film SO-359, a very fine-grained, high-speed, color transparency film, was used. The camera was set at an aperture of $f/5.6$ and a shutter speed between 1/400 and 1/2000 second.

Photographic counts

Sea lions were counted from photographs illuminated with a light table by using a 7-30X zoom binocular microscope. Counts were obtained for five age and sex class categories: pups, juveniles, adult females or young males of similar size, subadult males, and adult males. Age and sex class distinctions were determined from size and other external characteristics (e.g., hair color on head, presence of sagittal crest, chest size, fore flipper width, snout shape, and body coloration). Animals of each age and sex class were marked on a clear acetate plastic overlay with different colored pens as each was counted. Marks on the acetate were then compared and verified with overlapping photographs. The acetate was placed on another photograph at the exact position of the coastline where the count ended previously and the count was continued on the uncounted portion. One count was made for each rock, island, or mainland haulout site.

All counts were conducted by the first author, who is an experienced counter with high intercount reliability (Lowry, 1999). Geographical positions (latitude and longitude) were assigned to each haulout site.

Analysis of haulout data

Counts of sea lions made in this study were compared to those obtained by earlier investigators in 1980–82 (Bonnell et al.¹) and 1995–96 (Beeson and Hanan²) by using nested ANOVAs and paired *t*-tests. The null hypothesis of no difference in zonal counts was used to examine differences in counts by zone, season, year, and survey. The counts were 0.45 power transformed (with Systat 6.0 for Windows, SPSS Inc., Chicago, IL) because their distribution was skewed toward zero.

Results

Sighting rates and $g(0)$

No difference was found ($P > 0.05$) for number of sightings, total animals seen, and mean group size during Beaufort sea state conditions 1 through 4. A sharp decline in sighting rates was observed when sightings were grouped into glare categories of 0–24% ($n=27.3$ sightings/1000 km), 25–49% ($n=17.5$ sightings/1000 km), 50–74% ($n=10.7$ sightings/1000 km), and 75–100% ($n=0$ sightings/1000 km). Sighting rates were significantly greater at 0–49% glare than at 50–100% glare ($P < 0.001$ for all surveys combined); therefore, only data collected in 0–49% glare were used for at-sea abundance estimation. With only data collected in 0–49% glare, we used 48–76% of kilometers surveyed and 79–89% of sightings.

The probability of sighting a sea lion at the surface, $g(0)$, was estimated as 0.67 (with a CV of $g(0)=0.12$).

At-sea abundance

Strip-transect survey effort totaled 1272 km during 26–30 May 1998, 2856 km during 12–28 September 1998, 2993 km during 1–11 December 1998, and 1175 km during 13–21 July 1999 (Fig. 4). No transect survey was conducted in July 1998 because of persistent low clouds and high winds. Transect distances in 0–49% glare conditions are given in Table 1. Nearly all sightings were within the inshore stratum, and most were within 20 nautical miles from the mainland coast (Fig. 5). Corrected at-sea abundance estimates for sea lions in the study area (Table 1) were 28,340 (May 1998), 40,161 (September 1998), and 24,720 animals (December 1998). For July 1999, a corrected abundance estimate for the inshore stratum in July 1999 was 11,492 animals (Table 1). From the total abundance estimated in the three 1998 surveys, the average proportion represented by the offshore stratum was 0.073 (range: 0.000–0.204). From this proportion, we estimated that there were about 829 sea lions in the unsurveyed offshore stratum

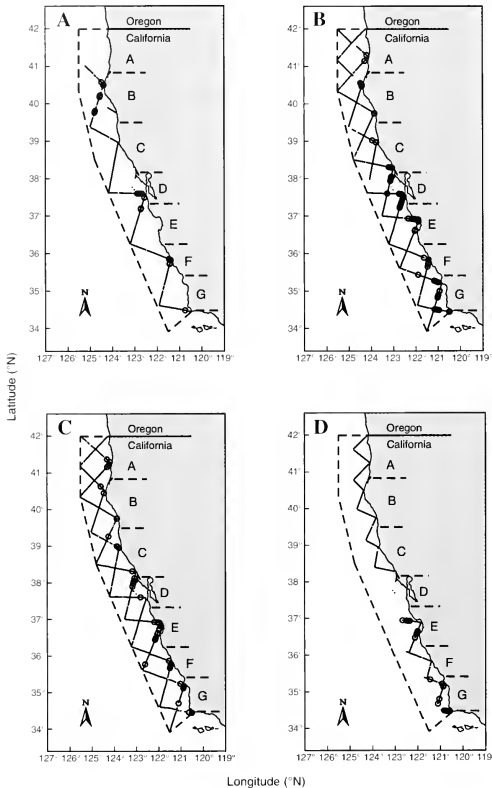


Figure 4

California sea lions (*Zalophus californianus*) sightings (o) during strip-transect surveys flown in Beaufort sea states 0-4 and 0-49% glare conditions (solid zig-zag line). (A) 26-30 May 1998, (B) 12-28 September 1998, (C) 1-11 December 1998, and (D) 13-21 July 1999.

in July 1999, and this number was used to extrapolate a total at-sea abundance estimate within the study area of 12,232 sea lions. CVs of corrected estimates were 0.32 (May 1998), 0.26 (September 1998), 0.50 (December 1998), and 0.43 (July 1999; Table 1).

During the May-June 1998 survey, sea lions were most abundant in the northern part of the study area

(Table 1). In September 1998, sea lions were most abundant in the central part of the study area (zones D and E). In December 1998 they were most abundant in the southern portion of the study area (zones E and F). During July 1999, sea lions were most abundant in the south-central portion of the study area (zone E).

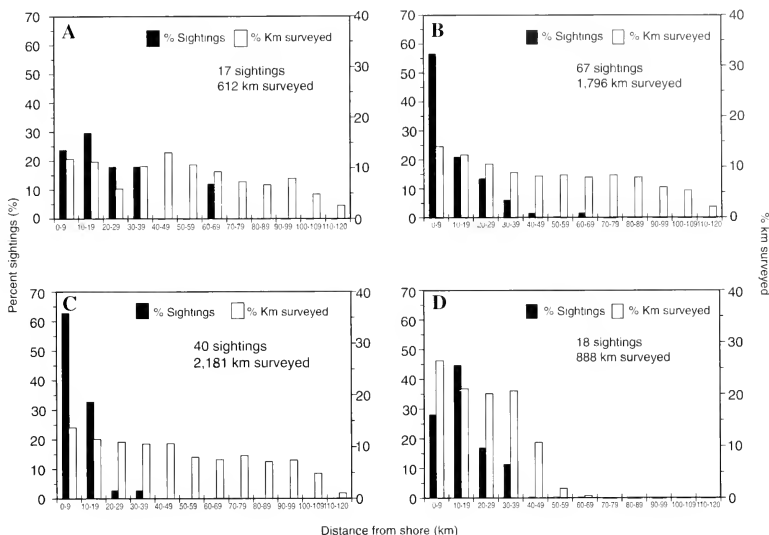


Figure 5

Distances from shore for California sea lions (*Zalophus californianus*) sighted and kilometers from shore for California sea lions that were surveyed during strip transect surveys in Beaufort sea state 0-4 and 0-49% glare conditions. (A) 26-30 May 1998, (B) 12-28 September 1998, (C) 1-11 December 1998, and (D) 13-21 July 1999.

Haulout abundance

In 1998 and 1999, aerial photographic surveys of sea lion haulouts in central and northern California were conducted during 31 May-8 June 1998, 7-18 July 1998, 11-20 September 1998, 14-16 December 1998, and 6-11 July 1999. For the July 1998 survey, low clouds prevented aerial surveys of the coastline from Point Sal (34°54.1'N, 120°40.0'W) to Point Conception (counts from 1999 were used for these areas) and from the Klamath River (41°32.5'N, 124°04.7'W) to Humboldt Bay (40°45.4'N, 124°14.4'W). To estimate abundance in the latter missed area, we obtained ground counts from the mainland at all haulouts except Turtle Rocks (41°08.0'N, 124°10.9'W) and Redding Rock (41°20.6'N, 124°10.5'W). In July 1999 a low cloud layer prevented surveys of the coastline between Golden Gate Bridge (37°51.1'N, 122°34.0'W) and just north of Año Nuevo Island (37°06'N, 122°20'W). This gap should have had virtually no effect on the total counts, however, because there is only one minor haulout in this region.

The number of sea lions hauled-out in the study area (Table 2) were 36,576 (May 1998), 26,260 (includes estimate, July 1998), 35,512 (September 1998), 32,055 (December 1998), and 13,559 (July 1999). There was no significant difference in total number of sea lions between the seven zones ($P=0.229$) and between seasons ($P=0.179$; Table 3). More sea lions were counted in 1998-99 than during previous surveys in 1980-82 and 1995-96 ($P<0.003$ for both tests), but no difference in counts was found between 1980-82 and 1995-96 surveys ($P=0.232$; Table 3).

In 1998, the greatest numbers of sea lions were found in zone D and E (Table 2), corresponding to the San Francisco and Monterey Bay regions; most animals hauled out at Año Nuevo Island and South Farallon Islands. Juveniles and adult-females or young-males were the most prevalent age and sex classes found in the study area in 1998 (Table 2). More adult males were counted during the May-June 1998 survey than during other surveys. In 1998 the number of pups in the study area ranged from 22 (December 1998) to 149 (May-June 1998).

Table 1

Abundance estimates for California sea lions (*Zalophus californianus*) at sea from sightings during strip-transect surveys in the central and northern California study area during three surveys in 1998 and one survey in 1999, under 0–49% glare and Beaufort 0–4 sea state conditions. No survey was conducted within the offshore stratum in July 1999. Insufficient kilometers were surveyed for estimating at-sea abundance, $CV(N_i)$, and 95% confidence limits for strata noted with a dash (—). Corrected estimates are based on $g(0)$ calculated from dive studies on lactating adult females during late breeding season (Feldkamp et al., 1989).

Stratum	No. of sightings	No. of animals	Kilometers surveyed (km)	Corrected			
				CV (N_i)	Abundance (N_i)	Lower 95% CL	Upper 95% CL
26–30 May 1998							
Inshore: zone A	—	—	0	—	—	—	—
Inshore: zone B	5	6	96	—	3977	—	—
Inshore: zone C	—	—	19	—	—	—	—
Inshore: zone D	6	6	63	—	5156	—	—
Inshore: zone E	—	—	0	—	—	—	—
Inshore: zone F	4	4	118	—	1793	—	—
Inshore: zone G	—	—	6	—	—	—	—
Inshore: total	15	16	302	0.29	23,541	11,224	49,376
Offshore	2	3	310	1.01	4799	561	41,040
Inshore + offshore	17	19	612	0.32	28,340	15,237	52,713
12–28 September 1998							
Inshore: zone A	1	1	121	—	556	—	—
Inshore: zone B	5	5	140	—	2256	—	—
Inshore: zone C	6	7	117	—	4235	—	—
Inshore: zone D	18	23	108	—	11,552	—	—
Inshore: zone E	16	25	146	—	11,752	—	—
Inshore: zone F	5	5	69	—	3852	—	—
Inshore: zone G	15	16	220	—	4919	—	—
Inshore: total	66	82	919	0.27	39,595	24,210	64,757
Offshore	1	1	877	1.1	566	82	3923
Inshore + offshore	67	83	1796	0.26	40,161	24,205	66,635
1–11 December 1998							
Inshore: zone A	4	4	213	—	1262	—	—
Inshore: zone B	6	7	219	—	2026	—	—
Inshore: zone C	4	4	238	—	1185	—	—
Inshore: zone D	2	3	124	—	1303	—	—
Inshore: zone E	15	25	175	—	9773	—	—
Inshore: zone F	3	18	59	—	16,129	—	—
Inshore: zone G	6	6	175	—	2316	—	—
Inshore: total	40	67	1203	0.5	24,720	9333	65,479
Offshore	0	0	977	0	0	0	0
Inshore + offshore	40	67	2181	0.5	24,720	9726	62,831
13–21 July 1999							
Inshore: zone A	0	0	124	—	0	—	—
Inshore: zone B	0	0	174	—	0	—	—
Inshore: zone C	0	0	185	—	0	—	—
Inshore: zone D	—	—	0	—	—	—	—
Inshore: zone E	11	14	146	—	6573	—	—
Inshore: zone F	0	0	135	—	0	—	—
Inshore: zone G	7	9	128	—	4762	—	—
Inshore: total	18	23	888	0.5	11,492	4,358	30,304
Offshore (estimated)	0	0	23	0.9	829	183	3752
Inshore + offshore	18	23	911	0.43	12,232	5427	27,572

Table 2

Counts of California sea lions (*Zalophus californianus*) made from 126-mm-format aerial color photographs for five age- and sex-class categories found in seven zones along the central and northern California coast during four surveys in 1998 and one survey in 1999.

Zone	Pups	Juveniles	Adult females or young males	Subadult males	Adult males	Total
31 May–8 June 1998						
A	0	299	1948	1554	528	4329
B	0	3195	1534	2371	911	8011
C	0	698	751	513	530	2492
D	11	3639	5821	1636	555	11,662
E	99	3481	2993	678	464	7715
F	5	186	380	93	52	716
G	34	684	886	32	15	1651
All	149	12,182	14,313	6877	3055	36,576
7–18 July 1998						
A	0	358	206	148	22	734
B	0	2382	116	162	62	2722
C	0	320	287	190	101	898
D	55	1918	7318	1283	290	10,864
E	54	2920	3226	564	178	6942
F	12	63	510	125	50	760
G	0	779	1362	92	30	3340 ¹
All	121	8740	13,025	2564	733	26,260 ¹
11–20 September 1998						
A	0	73	1325	1548	559	4165
B	0	1136	351	938	173	2598
C	0	524	594	584	56	2028
D	18	1506	8453	1136	100	11,213
E	22	2122	8056	671	188	11,059
F	6	470	1440	78	24	2018
G	0	1224	1175	29	3	2431
All	46	7985	21,394	4984	1103	35,512
14–16 December 1998						
A	0	27	105	162	123	663
B	0	193	1790	2950	429	5362
C	0	54	201	995	516	1766
D	1	765	10,310	632	97	11,805
E	12	1566	8035	311	103	10,027
F	9	307	903	84	15	1318
G	0	201	831	63	19	1114
All	22	3359	22,175	5197	1302	32,055
6–11 July 1999						
A	0	111	167	5	4	287
B	0	6	6	1	1	14
C	0	0	0	1	0	1
D	3	193	970	109	91	1366
E	4	1226	5652	398	65	7345
F	0	270	578	90	14	952
G	0	919	2426	186	63	3594
All	7	2725	9799	790	238	13,559

¹ Includes 1077 unknown age- and sex-class sea lions that were estimated to have been missed in zone G.

Table 3

Results of four nested ANOVAs on haulout counts of California sea lions (*Zalophus californianus*) found in 7 zones within central and northern California (refer to text and Fig. 3 for zone descriptions). The tests of ANOVA revealed differences between zones, season, years, and surveys. 1980–82 surveys were conducted by Bureau of Land Management (Bonnell et al.¹) and 1995–96 surveys were conducted by the California Department of Fish and Game (Beeson and Hanan⁸). Year was nested within survey, season was nested within year, and zone was nested within season.

Source	Sum-of-squares	df	Mean-square	F-ratio	P
1998–99 surveys					
Season	1427.2	3	475.7	2.177	0.179
Zone (season)	9157.0	24	381.5	1.746	0.229
1998–99 surveys vs. summer and autumn 1995 and winter 1996 surveys					
Survey	1610.7	1	1610.7	11.449	0.003
Season (survey)	2019.4	5	403.9	2.871	0.037
Zone (season)	11,008.8	24	458.7	3.260	0.003
1998–99 surveys vs. 1980–82 surveys					
Survey	1731.6	1	1731.6	21.224	<0.001
Year (survey)	2235.9	3	745.3	9.135	<0.001
Season (year)	3576.5	12	298.0	3.653	<0.001
Zone (season)	14,761.2	24	615.0	7.538	<0.001
1980–82 surveys vs. summer and autumn 1995 and winter 1996 surveys					
Survey	81.9	1	81.9	1.457	0.232
Year (survey)	649.0	3	216.3	3.849	0.013
Season (year)	3491.5	10	349.1	6.211	<0.001
Zone (season)	11,027.6	24	459.5	8.174	<0.001

In 1999, the majority of sea lions were found between the San Francisco Bay area and Point Conception (zones D through G). Zone E had the greatest number of sea lions (Table 2); the majority of these animals hauled out at Año Nuevo Island. As in 1998, juveniles and adult-females or young-males were the most prevalent age and sex classes (Table 2). Only seven pups were counted in the study area during July 1999. The number of sea lions counted in 1999 was 52% of that counted in July 1998.

Total abundance

There was a significant correlation ($r=0.468$, $P=0.024$) between at-sea abundance and haulout abundance within zones. Total abundance of California sea lions in central and northern California during 1998 was estimated to be 64,916 in May–June, 75,673 in September, and 56,775 in December. Total abundance in July 1999 was estimated at 25,791 individuals. The proportion of total abundance to animals hauled-out was 1.77, 2.13, 1.77, and 1.90, respectively, with a mean of 1.89 and a CV for small samples (Sokal and Rohlf, 1995) of 0.09. Using the mean multiplier of 1.89 on haulout counts obtained in July 1998 (Table 2), when at-sea abundance could not be estimated, we estimated total abundance as 49,697 ($CV=0.09$) animals for that period.

Discussion

This abundance study of California sea lions in central and northern California successfully integrated two methods: 1) strip transect surveys to estimate abundance at sea; and 2) aerial photographic surveys to estimate haulout abundance. The $g(0)$ detection probability derived from previously published dive data allowed estimation of total abundance, including animals expected to be underwater during at-sea strip transect surveys. Previous surveys where transect methods similar to ours were used in the Southern California Bight in 1975–78 and in central and northern California in 1980–83 (Bonnell and Ford, 1987; Bonnell et al.^{1,10}) did not have information for deriving $g(0)$, and, therefore, densities of sea lions at sea were underestimated in these studies.

California sea lions were abundant in central and northern California during May through September

¹⁰ Bonnell, M. L., B. J. Le Boeuf, M. O. Pierson, D. H. Dettman, G. D. Farrrens, C. B. Heath, R. F. Gantt, and D. J. Larsen. 1980. Summary of marine mammal and seabird surveys of the Southern California Bight area 1975–1978. Vol. 3: Investigators reports, part 1—pinnipeds of the Southern California Bight, 535 p. Univ. Calif., Santa Cruz, Calif. 95064. Final Report to the Bureau of Land Management, under Contract AA550-CT7-367. [NTIS PB81-248-71.]

1998 when waters were warm because of the strong 1997–98 El Niño. Increased abundance of juveniles and adult females were observed in this region during previous El Niños (Huber, 1991; Sydeman and Allen, 1999) and during our May–June, July, and September 1998 surveys. The increase in adult females in central California in 1998 resulted in an increase in the number of pups counted at Año Nuevo and South Farallon Islands (106 pups in 1998 vs. 23 in 1997), and below normal births at rookeries in southern California (Lowry, unpubl. data, Forney et al.²). In contrast to 1998, during the summer of 1999 fewer sea lions were found in central and northern California, especially north of San Francisco (zones A, B, and C), and greater numbers were found at rookeries in southern California (M. Lowry, unpubl. data) when waters were cold as a result of the La Niña oceanographic condition that began in October 1998 (Hayward et al., 1999).

The abundance and distribution of California sea lions were distinctly different between El Niño and La Niña periods. During El Niño, sea lions were very abundant in central and northern California, and were distributed throughout the region. In contrast, during summer 1999 (our only survey that year [La Niña]), sea lions were less abundant than during summer 1998, and they were distributed only south of the San Francisco Bay area. The abundance and distribution pattern of summer 1999 is similar to the observed abundance and distribution pattern described by earlier studies (Chambers, 1979; Griswold, 1985; Weise, 2000; Bonnell et al.). During periods of elevated sea lion abundance in central and northern California, such as those observed during the 1998 El Niño, we would expect 1) increased consumption of prey species because of more sea lions feeding in the area, 2) increased pressure on coastal fisheries resources because sea lions feed on commercially valuable species (see Lowry et al., 1990, 1991; Lowry and Carretta, 1999; Weise, 2000), and 3) increased interactions with commercial and sport fisheries. The opposite would occur during periods of low sea lion abundance during non-El Niño years. Greater abundance of California sea lions in central and northern California during the 1997–98 El Niño event, therefore, would be expected to have a greater effect on salmonids and other sea lion prey species, and on fisheries than would occur during non-El Niño years.

Abundance of sea lions in central and northern California during 1998 was greater in May–June (spring) and September (fall) and less in July (summer) and December (winter). This bimodal phenomenon, also observed in the past (Sullivan, 1980; Bonnell et al.), is due to migrating subadult and adult male sea lions on their way to (in fall) and from (in spring) Oregon (Mate, 1975), Washington, and British Columbia (Bigg, 1988). However, these seasonal differences were not significantly different, likely because of low power (only one year of data), or because the animals behaved differently from other years. In fact, fewer subadult and adult males were present at southern California rookeries during the 1998 July census (near the end of breeding

season) than were present during 1997 and 1999 (M. Lowry, unpubl. data). The large number of sea lions in central and northern California during 1998 was the result of a more numerous population (U.S. population estimated at 204,000 to 214,000 in 1999) than existed when previous surveys were conducted in 1980–82 and 1995–96 (U.S. population estimated at 76,000 in 1982 and at 167,000 to 188,000 in 1995) (Barlow et al.; Forney²; Bonnell et al.¹, and Beeson and Hanan³).

In central and northern California, California sea lions have been sighted during aerial surveys (Carretta and Forney¹¹; present study) and tracked with satellite tags (Melin and DeLong, 2000; Melin, 2002) up to 100 nautical miles from shore. However, our surveys indicated that they forage predominantly within 20 nautical miles from shore.

The strip transect method assumes that all animals within a strip are sighted by the observer. Although we found no difference in sighting rate between Beaufort sea state scales 0–1, 2, 3, and 4, Carretta et al.¹² found during their 1998–99 line transect survey in waters off San Clemente Island, California, that the effective strip width of pinniped sightings at 213 m altitude was slightly less in Beaufort sea states 3–4 (184 m on each side) than in Beaufort sea states 0–2 (256 m on each side). Their results suggest that if our analysis suffered from reduced detection probability at high sea states, then we may have underestimated at-sea abundance of sea lions or increased the variance of at-sea sea lion abundance. This potential negative effect was minimized in our surveys by surveying at a lower altitude (183 m) than the 213 m altitude surveyed by Carretta et al.¹²

The $g(0)$ correction derived from dive and foraging studies of lactating adult-female California sea lions during late breeding season (July–August) may be an additional source of error in our at-sea abundance estimates. It may not be representative of nonlactating adult females and other age- and sex-class sea lions, and it may not be representative for all seasons or different oceanographic cycles (e.g., El Niño and non-El Niño). Dive data from various ages and sexes are needed to test these assumptions, but existing dive data from a single age+sex group provided a rough correction to account for animals underwater during at-sea

¹¹ Carretta, J. V. and K. A. Forney. 1993. Report of two aerial surveys for marine mammals in California coastal waters utilizing a NOAA DeHavilland twin otter aircraft March 9–April 7, 1991 and February 8–April 6, 1992. NOAA Tech. Memo. NMFS, NOAA-TM-NMFS-SWFSC-185, 77 p. National Marine Fisheries Service, Southwest Fisheries Science Center, 8604 La Jolla Shores Drive, La Jolla, CA 92037.

¹² Carretta, J. V., M. S. Lowry, C. E. Stinchcomb, M. S. Lynn, and R. E. Cosgrove. 2000. Distribution and abundance of marine mammals at San Clemente Island and surrounding offshore waters: results from aerial and ground surveys in 1998 and 1999. National Oceanographic and Atmospheric Administration admin. report LJ-00-02, 51 p. Southwest Fisheries Science Center, 8604 La Jolla Shores Drive, La Jolla, CA 92037.

surveys. Seasonal differences may exist, but data in Feldkamp et al., (1989, 1991) and Melin (2002) indicate that these differences are negligible. Feldkamp et al. (1991) showed differences in diving behavior during El Niño and non-El Niño, but Melin (2002) did not find as much difference in diving behavior during El Niño and non-El Niño (with the exception of longer transit time to foraging grounds during El Niño).

Error in age- and sex-class abundance estimates at haulouts is also affected by subjectivity and inter-observer differences in age and sex classification of sea lions. Therefore, age- and sex-class counts provided in these surveys, although conducted by a single experienced observer (M. Lowry), serve as approximate indices of sea lion age- and sex-class distributions in central and northern California. These indices will be useful for future attempts to estimate consumption of prey by sea lions along central and northern California, given that nutritional requirements differ among age and sex classes.

By estimating abundance of sea lions on land as well as at-sea, we were able to derive a multiplier for estimating total abundance from counts of animals hauled out on land. This multiplier can be applied to future land counts of California sea lions in central and northern California to estimate total abundance, as has been done for harbor seals in California, Oregon, and Washington (Huber et al., 2001; Barlow et al.⁶; Forney et al.²). It may also be useful for estimating total abundance from counts of sea lions hauled out in Oregon, Washington, and British Columbia because the age- and sex-class structure of sea lions is similar to that found in central and northern California. However, the multiplier should not be used for smaller areas (such as the zones in the inshore stratum) or for other species, because regional and interspecies differences may exist. In particular, it would not be appropriate for regions where sea lions reproduce, such as in the Southern California Bight (SCB) and in Mexico, because adult females that are rearing pups may spend a different proportion of their time at sea. For that reason, it would be judicious to conduct concurrent offshore and haulout surveys in the SCB and Mexico to derive a correction factor for each geographical region of the sea lion's range. Multipliers could also be derived for smaller areas (such as our zones) by conducting suitably designed smaller-scale at-sea surveys in conjunction with counts of animals hauled out, or by using satellite or radio telemetry tags to directly measure the relative times at sea and on land.

The multiplier for deriving total abundance from haulout counts provides researchers and resource managers with an alternative method for estimating total population abundance or abundance of a stock. Abundance estimates derived with this new approach can be compared to abundance estimates obtained with more conventional methods (such as the life history model), and may provide a means for estimating total abundance when life history data are unavailable.

The approach used in the present study may be particularly useful for estimating abundance at times and places unrelated to breeding activities, or for periods when breeding is disrupted, as with El Niño conditions. Abundance estimates and distributional data provided by these methods can be used to determine where and when the greatest effects on salmon and other prey species may occur. Diet studies at major hauling areas in conjunction with abundance surveys to derive consumption estimates are required to determine the effect of California sea lions on salmon and other sea lion prey species of the region.

Acknowledgments

This research was supported financially by the Office of Protected Resources, National Marine Fisheries Service. We greatly appreciate the assistance given by Jim Gilpatrick, Charlie Stinchcomb, and, especially, Scott Benson of Moss Landing Marine Laboratories during the surveys. Jay Barlow provided guidance. Special thanks to Morgan Lynn of the Southwest Fisheries Science Center who kept the photographic equipment functioning properly. Henry Orr of the Southwest Fisheries Science Center helped with illustrations. Research within Gulf of the Farallones National Marine Sanctuary and Monterey Bay National Sanctuary was conducted under National Marine Sanctuary Permit GFNMS/MBNMS-20-98. This research was conducted under MMPA Research Permit No. 774-1437. We greatly appreciated the reviews and comments by Jay Barlow, Jeff Laake, Jim Harvey, and three anonymous reviewers.

Literature cited

- Barlow, J., and P. Boveng.
1991. Modeling age-specific mortality for marine mammal populations. *Mar. Mamm. Sci.* 7:50-65.
- Bartholomew, G. A.
1967. Seal and sea lion populations of the Channel Islands. *In Proc. of the symp. on the biology of the Calif. Islands* (R. N. Philbrick, ed.), p. 229-243. Santa Barbara Botanic Garden, p. 229-243. Santa Barbara, CA.
- Bigg, M. A.
1988. Status of the California sea lion, *Zalophus californianus*, in Canada. *Can. Field Nat.* 102:307-314.
- Bonnell, M. L., and R. G. Ford.
1987. California sea lion distribution: a statistical analysis of aerial transect data. *J. Wildl. Manage.* 51: 13-20.
- Buckland, S. T., D. R. Anderson, K. P. Burnham, and J. L. Laake.
1993. Distance sampling: estimating abundance of biological populations, 446 p. Chapman and Hall, London.
- Chambers, J. R.
1979. Population studies of California sea lions near Diablo Canyon, California. M.A. thesis, 154 p. California Polytechnic State Univ., San Luis Obispo, CA.

- Feldkamp, S. D., R. L. DeLong, and G. A. Antonelis.
1989. Diving patterns of California sea lions, *Zalophus californianus*. *Can. J. Zool.* 67:872-883.
- Feldkamp, S. D., R. L. DeLong, and G. A. Antonelis.
1991. Effects of El Niño 1983 on the foraging patterns of California sea lions (*Zalophus californianus*) near San Miguel Island, California. In *Pinnipeds and El Niño: responses to environmental stress* (F. Trillmich and K. A. Ono, eds.) p. 146-155. Springer-Verlag, Berlin and Heidelberg, Germany.
- Griswold, M. D., Jr.
1985. Distribution and movements of pinnipeds in Humboldt and Del Norte counties, California. M.A. thesis, 101 p. Humboldt State University, Arcata, CA.
- Hayward, T. L., T. R. Baumgartner, D. M. Checkley, R. Durazo, G. Gaxiola-Castro, K. D. Hyrenbach, A. W. Mantyla, M. M. Mullin, T. Murphree, F. B., Schwing, P. E., Smith, and M. J. Tegner.
1999. The state of the California Current in 1998-1999: transition to cool-water conditions. *CalCOFI Rep.* 40:29-62.
- Huber, H. R.
1991. Changes in the distribution of California sea lions north of the breeding rookeries during the 1982-83 El Niño. In *Pinnipeds and El Niño: responses to environmental stress* (F. Trillmich and K. A. Ono, eds.) p. 129-137. Springer-Verlag, Berlin and Heidelberg, Germany.
- Huber, H. R., S. J. Jeffries, R. F. Brown, R. L. DeLong, and G. VanBlaricom.
2001. Correcting aerial survey counts of harbor seals (*Phoca vitulina richardsi*) in Washington and Oregon. *Mar. Mamm. Sci.* 17:276-293.
- Keith, E. O., R. S. Condit, and B. J. Le Boeuf.
1984. California sea lions breeding at Año Nuevo Island, California. *J. Mamm.* 65:695.
- Lowry, M. S.
1999. Counts of California sea lion (*Zalophus californianus*) pups from aerial color photographs and from the ground: a comparison of two methods. *Mar. Mamm. Sci.* 15:143-158.
- Lowry, M. S., and J. V. Carretta.
1999. Market squid (*Loligo opalescens*) in the diet of California sea lions (*Zalophus californianus*) in southern California (1981-1995). *CalCOFI Rep.* 40:196-207.
- Lowry, M. S., C. W. Oliver, C. Macky, and J. B. Wexler.
1990. Food habits of California sea lions, *Zalophus californianus*, at San Clemente Island, California, 1981-1986. *Fish. Bull.* 88:509-521.
- Lowry, M. S., B. S. Stewart, C. B. Heath, P. K. Yochem, and J. M. Francis.
1991. Seasonal and annual variability in the diet of California sea lions, *Zalophus californianus*, at San Nicolas Island, California, 1981-86. *Fish. Bull.* 89:331-336.
- Mate, B. R.
1975. Annual migrations of the sea lions *Eumetopias jubatus* and *Zalophus californianus* along the Oregon USA coast. *Rapp. P.-V. Reun. Cons. Int. Explor. Mer* 169:455-461.
- Melin, S. R.
2002. The foraging ecology and reproduction of California sea lion (*Zalophus californianus californianus*). Ph.D. diss., 150 p. Univ. Minnesota, Minneapolis, MI.
- Melin, S. R., and R. L. DeLong.
2000. At-sea distribution and diving behavior of California sea lion females from San Miguel Island, California. In *Proceedings of the fifth California Islands symposium* (D. R. Browne, K. L. Mitchell, and H. W. Chaney), p. 407-412. Prepared by MBC Applied Environmental Sciences, 3000 Redhill Ave., Costa Mesa, CA 92626 under MMS (Minerals Management Service) contract no. 14-35-01-96-RC-30801 from the U.S. Dep. Interior, MMS, Pacific OCS Region.
- Odell, D. K.
1975. Breeding biology of the California sea lion, *Zalophus californianus*. *Rapports et Proces-verbaux de Reunions* 169:374-378.
- Orr, R. T., and T. C. Poulter.
1965. The pinniped population of Año Nuevo Island, California. *Proc. Calif. Acad. Sci.* 32:377-404.
- Pierotti, R. J., D. G. Ainley, and T. J. Lewis.
1977. Birth of a California sea lion on Southeast Farallon Island. *Calif. Fish Game* 63:64-66.
- Sokal, R. R., and F. J. Rohlf.
1995. *Biometry: the principles and practice of statistics in biological research*, 887 p. W.H. Freeman and Co., New York, NY.
- Sullivan, R. M.
1980. Seasonal occurrence and haul-out use in pinnipeds along Humboldt County, California. *J. Mamm.* 61:754-760.
- Sydeman, W. J., and S. G. Allen.
1999. Pinniped population dynamics in central California: correlations with sea surface temperature and upwelling indices. *Mar. Mamm. Sci.* 15:446-461.
- Weise, M. J.
2000. Abundance, food habits and annual fish consumption of California sea lions (*Zalophus californianus*) and its impact on salmonid fisheries in Monterey Bay, California. M.S. thesis, 103 p. Moss Landing Marine Laboratories, Moss Landing, CA, and San Jose State Univ., San Jose, CA.

Abstract—The narrow-barred Spanish mackerel (*Scomberomorus commersoni*) is widespread throughout the Indo-West Pacific region. This study describes the reproductive biology of *S. commersoni* along the west coast of Australia, where it is targeted for food consumption and sports fishing. Development of testes occurred at a smaller body size than for ovaries, and more than 90% of males were sexually mature by the minimum legal length of 900 mm TL compared to 50% of females. Females dominated overall catches although sex ratios within daily catches vary considerably and females were rarely caught when spawning. *Scomberomorus commersoni* are seasonally abundant in coastal waters and most of the commercial catch is taken prior to the reproductive season. Spawning occurs between about August and November in the Kimberley region and between October and January in the Pilbara region. No spawning activity was recorded in the more southerly West Coast region, and only in the north Kimberley region were large numbers of fish with spawning gonads collected. Catches dropped to a minimum when spawning began in the Pilbara region, when fish became less abundant in inshore waters and inclement weather conditions limited fishing on still productive offshore reefs. Final maturation and ovulation of oocytes took place within a 24-hour period, and females spawned in the afternoon-evening every three days. A third of these spawning females released batches of eggs on consecutive days. Relationships between length, weight, and batch fecundity are presented.

Variability in spawning frequency and reproductive development of the narrow-barred Spanish mackerel (*Scomberomorus commersoni*) along the west coast of Australia

Michael C. Mackie

Paul D. Lewis

Daniel J. Gaughan

Stephen J. Newman

Western Australian Marine Research Laboratories
Department of Fisheries

Government of Western Australia

West Coast Drive

Waterman, Western Australia 6020, Australia

E-mail address (for M.C. Mackie) mmackie@fish.wa.gov.au

The narrow-barred Spanish mackerel (*Scomberomorus commersoni*) is a prized food fish targeted by fishermen throughout its range in the Indo-West Pacific region (Collette and Nauen, 1983). Reaching over 2.4 m in length and 45 kg in weight, this pelagic species is seasonally abundant in coastal waters where it often schools in large numbers. In Australian waters, the commercial mackerel fishery targets these schools using trolling methods, and 2362 metric tons were caught in 2001–02 for domestic and overseas markets (ABARE, 2003).

Scomberomorus commersoni is also a premier sport fishing species, targeted by an increasing number of recreational anglers throughout its broad Australian distribution. The combined commercial and recreation take of *S. commersoni* has put significant pressure on stocks in Queensland (QLD) waters, leading to a possible decline in the spawning stock abundance (McPherson and Williams, 2002). The biology of *S. commersoni* in these waters has been well studied (e.g., Munro, 1942; McPherson, 1981, 1992, 1993). Biological information is also available for *S. commersoni* in waters of the Northern Territory (NT; Buckworth¹), where stocks are still recovering from a prolonged period of exploitation by foreign gill-net operators that ended in 1986. In contrast, little is known about the stock status

and biology of *S. commersoni* in Western Australian (WA) waters, despite the fact that catches are similar to those taken in QLD and the NT, and commercial fishermen have expressed concern about increasing fishing pressure on this species in WA. Recent moves to overhaul management of the mackerel fishery in WA (in which *S. commersoni* is the dominant species) have further highlighted the need for more information on the biology and stock status of *S. commersoni* along the WA coast.

Research to enable a stock assessment of *S. commersoni* in WA waters was therefore commenced in 1999. Description of reproductive biology was a key focus of this study, since this information is required for stock assessment models and for management controls such as minimum legal lengths, which were previously set with little knowledge of the biology of *S. commersoni* in WA. Information on other reproductive parameters, such as batch fecundity and spawning behavior, which are also required for

¹ Buckworth, R. C. 1999. Age structure of the commercial catch of Northern Territory narrow-barred Spanish mackerel. Final Report to the Fisheries Research and Development Corporation (FRDC) on project no. 1998/159. Fishery report 42, 27 p. Department of Business Industry and Resource Development, Darwin, Northern Territory, 0800, Australia.

stock assessments, is unavailable or insufficiently described in the literature for this species. The objective of our study was, therefore, to provide a comprehensive description of the reproductive biology of *S. commerson* in Western Australian waters.

Material and methods

Collection and processing of samples

Scomberomorus commerson were collected onboard vessels operating from a number of locations along the WA coast between 1998 and 2002 (Fig. 1). These locations were pooled into three regions to reflect differences in fishing methods within the mackerel fishery (Kimberley—east of 120° E, Pilbara—north of 23° S to the Kimberley border, and West Coast—south of 23° S; Fig. 1). *Scomberomorus commerson* are seasonally abundant in coastal waters although low numbers are caught in the Pilbara region during the “off-season.” Samples were therefore collected throughout the year from this region only.

Fresh *S. commerson* collected from commercial and recreational fishermen were measured (total length [TL] and fork length [FL] in mm) and, where possible, weighed to 0.1 kg (whole weight [WW] and clean weight [viscera and gonads removed]). Heads were removed and measured from tip of the mouth to firm edge of the operculum (mm), and weighed with gills intact (± 0.1 gm). Gonads were removed from the fish within hours of capture, macroscopically staged (see below), weighed where possible (± 0.01 g), and preserved in 10% formalin and seawater solution. Frozen head and viscera obtained from commercial and recreational fishermen were also measured and weighed as above. The thawed gonads were macroscopically staged by using a simplified staging system (see below) that is used in less detailed reproductive analyses.

Preserved gonads were blotted dry with a paper towel and weighed. A 4-mm slice from the mid-region was processed by using standard histological techniques and stained with Harris's haematoxylin and eosin for microscopic examination. Full details of methods used in the collection and analysis of *S. commerson* gonads are provided in Mackie and Lewis.²

Biological analyses

Gonads were staged macroscopically and microscopically. Macroscopic staging employed five developmental steps that were compatible with the microscopic staging system (Mackie and Lewis²):

² Mackie, M. C., and P. D. Lewis. 2001. Assessment of gonad staging systems and other methods used in the study of the reproductive biology of narrow-barred Spanish mackerel, *Scomberomorus commerson*, in Western Australia. Fisheries Research Report 136, 25 p. Department of Fisheries, Perth, Western Australia 6020, Australia. <http://www.fish.wa.gov.au/res/broc/frf/fr136/index.html>. [Accessed January 15 2002.]

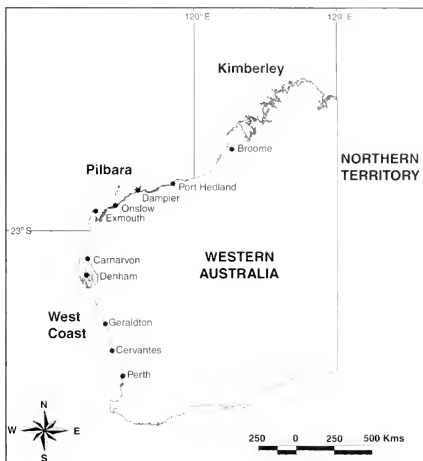


Figure 1

Sampling locations used in the study of the narrow-barred Spanish mackerel (*Scomberomorus commerson*) reproductive biology.

Juvenile (J)	undifferentiated.
Females	
stage 1	immature (“virgin” in other studies);
stages 2–3	mature, resting;
stage 4	reproductively developed;
stage 5	spawning (“running, ripe” in other studies).
Males	
stage 1	immature (“virgin” in other studies);
stage 2	mature resting;
stage 3	reproductively developed, ripe;
stage 4	spawning (“running, ripe” in other studies).

The microscopic staging system had more stages and allowed a more detailed description of spawning:

Juvenile (J)	undifferentiated.
Females	
stage 1	immature (“virgin” in other studies);
stage 1a	immature, developing;
stage 2	mature, resting;
stage 3	mature, developing;
stage 4	reproductively developed;
stage 5a	prespawning;
stage 5b	spawning (“running, ripe” in other studies);
stage 5c	postspawning;
stage 6	spent.

Males

stage 1	immature ("virgin" in other studies);
stage 1a	immature, developing;
stage 2	mature, resting;
stage 3	reproductively developed, ripe;
stage 4	spawning.

The immature, developing stage identified females that were immature and unlikely to spawn but had ovaries containing cortical alveoli stage oocytes (which otherwise identified mature, developing females).

Division of the microscopic staging system for ovaries into three spawning stages was based on the presence of migratory nucleus stage or hydrated oocytes within the ovarian lamellae (stage 5a), the presence of hydrated oocytes within the ovarian lumen (stage 5b), and the presence of postovulatory follicles (POFs) in the lamellae (stage 5c). In tropical fish species POFs may remain up to 24 hours in the ovaries before being resorbed (West, 1990), and there is evidence suggesting this is the case for *S. commerson* in Queensland waters (McPherson, 1993). In the present study POFs observed in the ovaries of females were categorized as either "new" or "old" based on their degree of degeneration (Mackie and Lewis²).

Gonadosomatic indices (GSIs) were calculated by using ratios of gonad weight to whole body weight, head weight, and head length. The latter two ratios were used to assess the usefulness of head and viscera samples in future monitoring of *S. commerson*.

Scorpaenopsis commerson is a serial-spawning species (Munro, 1942). Estimates of batch fecundity were made for preserved prespawning (stage 5a) ovaries from counts of hydrated oocytes within three samples taken from the anterior, middle, and posterior region of one lobe (each 130–200 mg). A section of each ovary was also processed by using histological methods to confirm suitability for estimation of fecundity. Some ovaries were subsequently rejected for fecundity estimates because the most mature batch of oocytes had not fully hydrated and were less easy to distinguish from earlier stage oocytes. These ovaries tended to provide an overestimate of batch fecundity (Mackie et al.³).

The daily timing and frequency of spawning were determined for females captured in the Kimberley region during September 1999 when 94% of ovaries were retained for histological analysis ($n=344$). Spawning frequency was determined as the inverse of the spawning fraction (the number of ovaries with hydrated or migratory nucleus stage (MNS) oocytes divided by the total number of mature ovaries in the catch). These data were compared with estimates made by using the number of ovaries macroscopically identified as having

hydrated oocytes. Analyses of sex ratios were based on data where the whole catch or a known random sample of the catch was processed.

Results

The gonads of 5128 male, female, and juvenile *S. commerson* were macroscopically staged during this study. Of these, 1624 were also processed with histological techniques for more detailed analyses.

Biological analyses

Body lengths ranged from 58 to 1720 mm FL (62 to 1840 mm TL), and whole weights ranged from 0.0015 to 40.6 kg. Regression analyses incorporating step-wise reduction (using analysis of variance) of a fully parameterized model indicated that differences in length and weight relationships between regions and sex were minor compared to measurement error. Thus, the simplest models which adequately explain the pooled data were

$$\text{Whole weight (kg)} = 3.40e - 9 \times \text{FL (mm)}^{3.12} \quad (n=2842) \\ (\text{SE of constants: } a=2.78e-10, b=0.01)$$

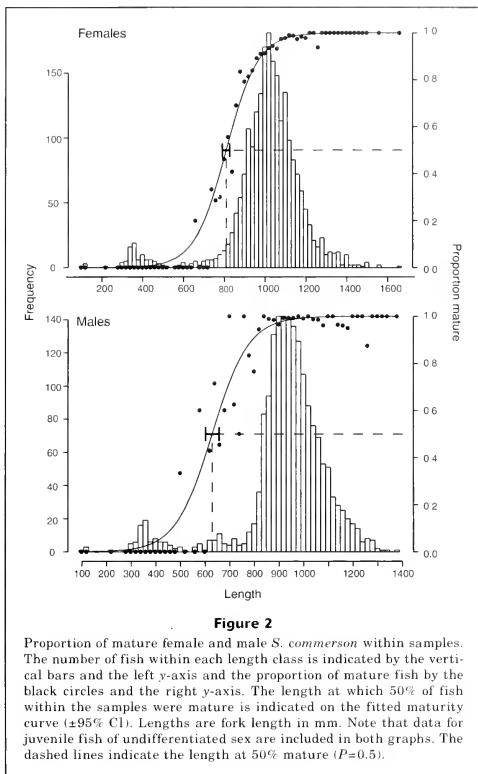
$$\text{TL (mm)} = 42.74 + (1.06 \times \text{FL (mm)}) \\ (n=1679, r^2=0.996)$$

Overall sex ratios were biased towards females, with the M:F ratio varying between 1:1.2 and 1:1.6 in the three regions. However, there was considerable variation between samples, from a peak M:F ratio of 1:2.6 for samples obtained in the nonreproductive period, to a male bias of 1.1:1 in pooled samples obtained during the peak spawning period. This slight male bias during the spawning period occurred in successive years; the sex bias, however, was variable between daily samples. Sex ratios also changed over from a male to female bias with increasing size class, with a 1:1 ratio occurring at about 1000–1050 mm FL.

Ovarian weight ranged from 2.00 to 1908.30 g and testes from 0.84 to 840.10 g. Gonads of juvenile *S. commerson* were small and contained no recognizable germ tissue. The smallest fish with differentiated gonads was a 301-mm-FL male. The smallest female was 396 mm FL. Two abnormally large juveniles (1170 and 1251 mm FL) were captured whose gonads had remained unusually small and undifferentiated. Body lengths of immature females (largest=1195 mm FL [13.8 kg WW]) overlapped substantially with those of mature females (smallest=641 mm FL [2.3 kg WW]).

Estimates of the size at which 50% of females were mature were calculated by using all available data as well as data taken only during the reproductive season (October to April). Data for each area were pooled to provide sufficient samples (virtually all samples of immature fish were obtained from the Pilbara region). Both data sets provided similar estimates; 809 mm FL, ± 9.8 SE (898 mm TL) for all data, and 788 mm

³ Mackie, M. C., D. J., Gaughan, and R. C. Buckworth. 2003. Stock assessment of narrow-barred Spanish mackerel (*Scorpaenopsis commerson*) in Western Australia. Final report to the Fisheries Research and Development Corporation (FRDC) on project no. 1999/151, 242 p. Department of Fisheries, Perth, Western Australia, 6020.

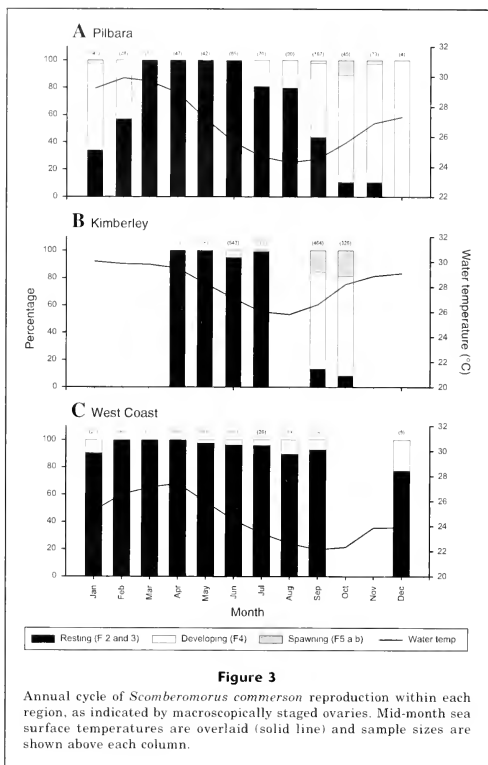


FL (± 14.5 SE) for data taken during the reproductive period. The size at which 10% of females were mature was 638 mm FL (± 19.6 SE), with 90% mature by 981 mm FL (± 7.2 SE) (Fig. 2A).

There was also considerable overlap between the lengths of immature and mature males. The largest immature male was 1140 mm FL (11.3 kg WW), whereas the smallest mature male (stage 3) was 491 mm FL (1.0 kg WW). The size at which 10% of males were mature was 465 mm FL (± 24.9 SE), the size at which 50% of males were mature was 628 mm FL (± 13.8 SE) or 706 mm TL, and the size at which 90% were mature was 791 mm FL (± 10.5 SE) (Fig. 2B).

Development of oocytes is asynchronous and all stages of oocytes are present at the same time within reproductively active ovaries. This reproductive feature, along with the maturation of multiple batches of oocytes (as evidenced by presence of both POFs and hydrated or MNS oocytes in spawning ovaries), confirms that female *S. commerson* are serial or partial spawners (Hunter et al., 1985).

Relationships between batch fecundity and body parameters were obtained from counts of hydrated oocytes within prespawning (stage 5a) ovaries. Size of females for which batch fecundity was determined ranged from 857 to 1143 mm FL and from 5.3 to



12.7 kg WW. Both relationships were explained with power curves:

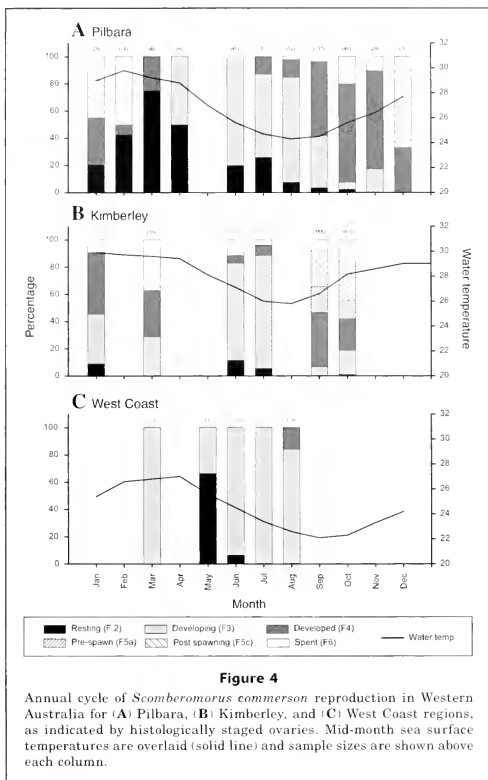
$$\text{Batch fecundity} = 0.0011 \times FL^{2.896} \quad (r^2=0.441, n=21)$$

$$\text{Batch fecundity} = 31087 \times WW^{1.384} \quad (r^2=0.714, n=19).$$

Annual reproductive cycle

Female *S. commerson* within the Pilbara region were non-reproductive between March and June, during the downward cycle of water temperatures (Figs. 3 and 4). As water temperatures reached a minimum in July and August (around 24°C), a small proportion of mature ovaries had

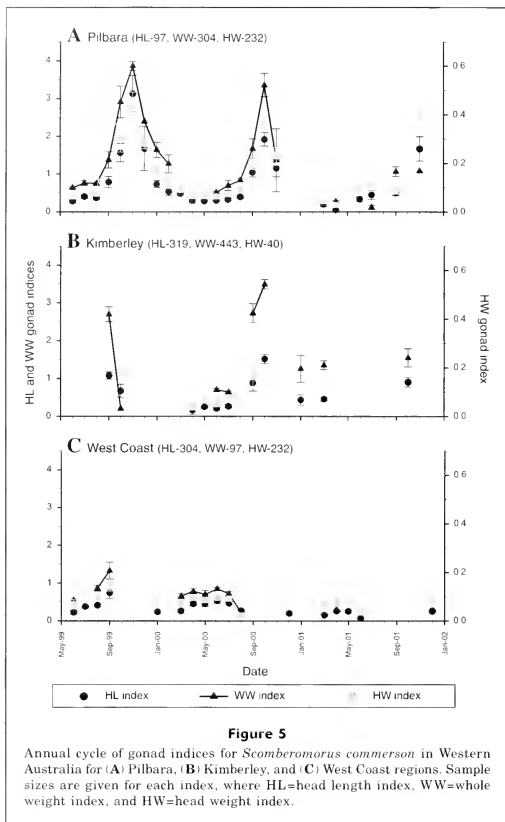
become reproductively developed (stage 4). The proportion of developed ovaries during September (the start of the upward cycle of water temperatures) varied noticeably between years in the Pilbara region, from 18.5% to 79% in 2001 and 2000, respectively. A small number of females were also actively spawning when sampled during September 2000. Peak reproductive activity extended from October to January, and spawning females were captured during this period in 1999 and 2000 when the sea surface temperature (SST) was rising from about 25.5° to 28.5°C. By February, when SST peaked at approximately 30°C, reproductive development was declining and the ovaries of most females were spent or resting.



The annual reproductive cycle of ovaries in the Kimberley region follows a similar pattern to that in the Pilbara region (Figs. 3 and 4). However, because 30–50% of females captured in Kimberley waters during September 1999 and 2000 were actively spawning, it appears that *S. commerson* commence spawning at least one month earlier in this region. About 60% of females were also spawning when sampled during October 1999 and 2000, although only 35% were spawning during this month in 2001. If spawning in the Kimberley region commenced in August and concluded in November (same duration as in the Pilbara region), the associated SST ranged from approximately 26.5–27°C

to 29–30°C (annual maximum approx 30–31°C; Figs. 3 and 4). Sampling of developed ovaries in March also indicated that the reproductive period for *S. commerson* in the Kimberley region may be more protracted than in the Pilbara region.

In the West Coast region few reproductively developed ovaries and no spawning ovaries were obtained; *S. commerson* are rarely captured in this region during the peak spawning period observed in the northern regions. The maximum sea surface temperature (SST) in this region of around 28°C is above the lower temperature range of spawning in the two northern regions. Reproductively developed ovaries obtained from the



West Coast region were collected over a range of SSTs, including when it was at a minimum (Figs. 3 and 4).

Gonadosomatic indices calculated from whole weight, head weight, and head length exhibited similar patterns and confirmed the spawning cycle determined from examination of ovaries (Fig. 5). The most complete data set was for females from the Pilbara region. In this region indices were minimal between March and August and increased considerably during September as ovaries became reproductively developed. Peak indices occurred

in November 1999 and October 2000, coinciding with peaks in the proportion of spawning (stage 5) ovaries in the samples. The drop in gonad indices during December 1999 showed that the supplies of vitellogenic oocytes within the ovaries were reduced by this time, even though many females were still spawning (Fig. 4). This drop continued until March when all the ovaries in the samples were in the resting stage. Data for 2001 indicate that decreased GSIs during the reproductive season were comparable to data from the previous two

Table 1

Ovarian development of *Scomberomorus commerson* sampled in the Kimberley region during the spawning season. POFs = postovulatory follicles. Ovaries in prespawning, spawning, postspawning, and spent stages of development are indicated by 5a, 5b, 5c, and 6, respectively. Note that data for stage 5c includes only females that had spawned on the day of capture (i.e., excluding ovaries containing old POFs only). Data for "Old POFs" includes all ovaries containing old POFs as well as other evidence of recent or imminent spawning.

Year	Total caught	Histological analysis		Morning				Afternoon					
		Total	Number mature	Total	5a	5b	5c	Old POFs	Total	5a	5b	5c	Old POFs
1999	344	325	306	171	59	0	0	70	135	1	1	23	51
2000	406	115	103	59	22	0	0	21	44	0	0	15	13

years. Data for the Kimberley and West Coast regions were limited but concurred with gonad staging data and also confirmed the low reproductive status of *S. commerson* within the West Coast region.

Spawning

Evidence of spawning was found in 237 of the histologically processed ovaries. Thirty-eight percent ($n=90$) of these were about to spawn when captured (stage 5a), 62% ($n=147$) had recently spawned (stage 5c), and one was running, ripe (stage 5b). The ovaries of only two macroscopically staged females were also running, ripe. Most of these spawning fish ($n=219$) were captured in the north Kimberley region (eighteen from the Pilbara region). The most southern location from which a spawning female was obtained was Exmouth (one recently spawned fish), and no females captured in the West Coast or more southern regions showed histological (or macroscopic) evidence of spawning.

Spawning females collected during 1999 and 2000 were either prespawning (stage 5a) and caught in the morning, or had recently spawned (stage 5c) and were caught in the afternoon (Table 1). The absence of hydrated oocytes in the afternoon and new POFs in the morning showed that the entire cycle of oocyte maturation, ovulation, and spawning is completed within a 24-hour period. Because no new POFs were present in ovaries sampled during the morning the transition from new to old POFs occurs during the night, within about 12 hours of spawning. The lack of evidence to show that females spawned on more than two consecutive days indicates that old POFs are unrecognizable after 24 hours.

Spawning fraction was estimated by using data obtained in the Kimberley region during September 1999 when 95% ($n=344$) of ovaries were examined by using histological methods. Analyses were based on the number of prespawning (stage 5a) ovaries sampled during the morning (usually between 0600–0900 h). Afternoon samples (usually 1500–1800 h) were not used because

the number of spawning fish was likely to be underestimated because of the low catchability of running, ripe (stage 5b) females. Thirty-five percent ($n=59$) of mature females in the morning samples were about to spawn (stage 5a). Spawning frequency was therefore 2.9 days. Comparison of spawning fractions in samples of at least ten females showed higher spawning fractions (33–56%) for the Kimberley region compared with the Pilbara region (4–28%).

Spawning fraction was also estimated for the morning samples as the proportion of macroscopically staged mature ovaries that contained hydrated oocytes. Thirty-one of the 180 mature females were identified as such, providing an estimated spawning fraction of 17.2%, and a spawning frequency of 5.8 days.

Thirty-six percent ($n=54$) of spawning females (stages 5, a–c) had spawned on two consecutive days. For example, 39 ovaries contained oocytes in the MNS or hydrated stage of development (i.e., spawning was imminent when fish were captured) and also contained old POFs. Another 15 ovaries had both old and new POFs.

Discussion

Scomberomorus commerson has a gonochoristic life history in which the gonad differentiates into an ovary or testis at around 300–400 mm FL. Males differentiate and reach sexual maturity at a smaller body size than females, as is the case with the congeneric species *S. maculatus* and *S. cavalla* (Beamariage, 1973; Schmidt et al., 1993). Consequently, more than 90% are sexually mature by the time the minimum legal length of 900 mm TL is reached in the fishery. In contrast only 50% of females are mature at 898 mm TL. Although mortality of released undersize fish may be high because of difficulties in removing fishing hooks, this size limit deters fishermen from targeting small fish and relatively few are captured (Mackie et al. 3).

Biases in sex ratios have been observed in several species of *Scomberomorus* (e.g. Trent et al., 1981; Sturm

and Salter, 1990; Begg, 1998). In the case of *S. commerson*, females usually dominate size classes above the MLL because they grow faster and reach a larger maximum size (McPherson, 1992; Mackie et al.³). However, they are rarely caught when actively spawning, despite observations by fishermen of leaping fish that might indicate that they are still present on the fishing grounds. Regional differences in fishing gear can also affect catchability. The lighter monofilament and reel outfits used in the Pilbara and West Coast regions likely catch larger fish than the heavier rope and thick monofilament hand-hauled rigs used by Kimberley fishermen that do not allow the fish to be "played" (i.e. do not allow the fish to swim) and may result in more gear failure.

The spring-summer spawning pattern observed in our study is similar to that of *S. commerson* along the east coast of Australia (McPherson, 1981). Water temperature may influence spawning in fish by affecting gametogenesis, gonad atresia, and spawning behavior (Lam, 1983). In WA waters *S. commerson* spawn as water temperatures are rising and, as found in Queensland, may compensate for latitudinal differences in temperatures by spawning earlier in northern waters (McPherson, 1981). No evidence of spawning activity was found within the West Coast region although the annual range of water temperatures overlap with those in which spawning occurs farther north. Restricted spawning by *S. commerson* on the east coast occurs at similar latitudes to northern parts of the West Coast region, and anecdotal evidence suggests that spawning may be restricted in some years in this region.

During the spawning period the average female *S. commerson* may spawn every three days and about one third of fish spawn on consecutive days. Female fish similarly spawn every 2–6 days and possibly on consecutive days in Queensland waters (McPherson, 1993). Our study showed that estimates based on the fraction of histologically staged prespawning (stage 5a) ovaries provided the best estimate of spawning frequency. However, only samples taken during the morning can be used for this analysis because of decreased catchability of running, ripe females in the afternoon. In comparison, macroscopic staging of ovaries with hydrated oocytes underestimated spawning frequency because migratory nucleus oocytes (which comprised 54% of histologically staged, prespawning [stage 5a] ovaries) cannot be identified. It is also impossible to identify fish that have spawned on more than one occasion with macroscopic criteria, resulting in a further underestimate of spawning activity (by 25% for *S. commerson*).

Maturation, ovulation, and spawning of oocytes by female *S. commerson* was completed within a 24-h cycle in the Kimberley region compared to 24–36 hours in Queensland waters (McPherson, 1993). Maturation of the oocytes is underway by sunrise and probably completed in all spawning ovaries by mid to late morning to allow for ovulation prior to spawning in the afternoon. Few samples were obtained at or after dusk because fish are generally not catchable, indicating that a high

incidence of spawning at this time because only one spawning fish was obtained during the study. Dusk spawning is prominent among pelagic spawning species that inhabit tropical reefs (Thresher, 1984). However, spawning in the afternoon is less common and may be linked to large tidal cycles and strong currents in the north of WA, as indicated for the brown stripe snapper (*Lutjanus vitta*) that also spawns in the afternoon in the Pilbara region (Davis and West, 1993).

Batch fecundity of *S. commerson* has not previously been recorded and such data are rare for other *Scomberomorus* species. Fecundity estimates for *S. commerson* from the Indian Peninsula (Devaraj, 1983) were not comparable because those data appeared to be obtained from counts of both vitellogenic and previtellogenic oocytes. Although the current study provided fecundity estimates only for females up to 13 kg whole weight, it shows that *S. commerson* is highly fecund (the highest estimated batch fecundity of 1.2 million eggs was obtained from an ovary that was less than half the weight of the heaviest ovary sampled). This study highlighted the need to histologically check that oocytes in the spawning batch are fully hydrated because fecundity may otherwise be over-estimated. Similarly, fecundity will be under-estimated if ovulation has commenced. The best time to collect gonad samples so that these biases are minimized is during the mid to late afternoon for this species.

Fishing activity is also regulated by the reproductive cycle. About 3–6 months prior to the spawning season catches of *S. commerson* by commercial fishermen increase as large numbers of smaller *S. commerson* appear on offshore reefs sometime between March and May, and soon after throughout the coastal waters of WA (Mackie⁴). By the time reproductive development in ovaries begins (approximately August and September in the Kimberley and Pilbara regions, respectively) catches have peaked or are declining. In the Pilbara region commercial catches have dropped to a minimum when spawning begins, as fish become less abundant in inshore waters and inclement weather conditions limit fishing on still productive offshore reefs. Because *S. commerson* generally do not make substantial longshore movements (Buckworth et al.⁵), it is likely that most spawning activity occurs at offshore locations in this region (e.g., in mid to outer areas of the continental shelf), although anecdotal evidence indicates that

⁴ Mackie, M. C. 2001. Spanish mackerel stock status report. In State of the fisheries report 1999/2000 (J. W. Penn, W. J. Fletcher, and F. Head, eds.), p. 71–75. Department of Fisheries, Perth, Western Australia, 6020. <http://www.fish.wa.gov.au/sof/1999/comm/nc/commnc26.html>. Accessed 10/2/2001.

⁵ Buckworth, R. C., S. J. Newman, J. R. Oviden, R. J. G. Lester, and G. R. McPherson. 2004. In prep. The stock structure of northern and western Australian spanish mackerel. Final report to the Fisheries Research and Development Corporation (FRDC) on project no. 1998/159. Department of Business Industry and Resource Development, Darwin, Northern Territory, 0800, Australia.

large, more solitary individuals may spawn in inshore waters.

Catches of *S. commerson* peak and decline rapidly along the Kimberley coast during the main spawning period because of declining fish abundance and weather conditions. As in the Pilbara region, few *S. commerson* are caught at this time in southern or midsections of the Kimberley coast. Fishermen must therefore undertake extensive trips north to the remaining productive grounds located between 12.5° and 15°S latitude where the majority of *S. commerson* spawning activity was encountered in the present study. Although it is possible that *S. commerson* in other areas of the Kimberley region may move offshore to spawn, it is also possible that some move northward, mixing and spawning with otherwise temporally and spatially discrete northern populations, in a similar manner to *S. cavalla* in U.S. waters (Broughton et al., 2002).

Monitoring of the WA fishery for *S. commerson* is likely to be based on the collection of head and gonad samples because limited funding and large distances will restrict future research trips. Onboard storage of filleted frames for research purposes is also prohibited by the large body size of *S. commerson*. In contrast, the head of this species is relatively small and easy to store, and as shown in the present study, provides a general measure of reproductive activity through calculation of head-to-gonad ratios. These ratios can also be supplemented by staging the gonads by using the macroscopic staging system developed for this species (Mackie and Lewis²). Head length can also be used to estimate body length of *S. commerson* (Mackie et al.³) and the otoliths contained in the head can be used to determine age. Although data gathered by such means is less accurate than that obtained from whole, fresh samples, it presents the best option for gathering ongoing data in sufficient quantities for meaningful analyses.

Acknowledgments

The authors thank the numerous commercial and recreational fishermen who assisted in the collection of samples and provided invaluable advice. The assistance of Department of Fisheries staff and volunteers on field trips is also appreciated. We also thank Rod Lenanton, Rick Fletcher, and Peter Stephenson for reviewing the manuscript, and to the Fisheries Research and Development Corporation for funding Project 1999/151, of which this study formed a part.

Literature cited

- ABARE (Australian Bureau of Agricultural and Resource Economics).
2003. Australian fisheries statistics 2002, 69 p. ABARE, Canberra, New South Wales, Australia.
Beaumariage, D. S.
1973. Age, growth and reproduction of king mackerel

- Scomberomorus cavalla*, in Florida. Florida Mar. Res. Pub. 1:1-45.
Begg, G. A.
1998. Reproductive biology of school mackerel (*Scomberomorus queenslandicus*) and spotted mackerel (*S. munroi*) in Queensland east-coast waters. Mar. Freshw. Res. 49:261-270.
Broughton, R. E., L. B. Stewart, and J. R. Gold.
2002. Microsatellite variation suggests substantial gene flow between king mackerel (*Scomberomorus cavalla*) in the western Atlantic Ocean and Gulf of Mexico. Fish. Res. 54:305-316.
Collette, B. B., and C. E. Nauen.
1983. FAO Species catalogue, Vol 2: scombrids of the world. FAO Fish. Synop. 125:1-137.
Davis, T. L. O., and G. J. West.
1993. Maturation, reproductive seasonality, fecundity, and spawning frequency in *Lutjanus vittatus* (Quoy and Gaimard) from the North West Shelf of Australia. Fish. Bull. 91:224-236.
Devaraj, M.
1983. Maturity, spawning and fecundity of the king seer, *Scomberomorus commerson* (Lacepede), in the seas around the Indian Peninsula. Ind. J. Fish. 30(2):203-230.
Hunter, J. R., N. C. H. Lo, and R. J. H. Leong.
1985. Batch fecundity in multiple spawning fishes. In An egg production method for estimating spawning biomass of pelagic fish: application to the northern anchovy (*Engraulis mordax*) (R. Lasker, ed.), p. 67-77. NOAA Tech. Rep. NMFS 36.
Lam, T. J.
1983. Environmental influences on gonadal activity in fish. In Reproduction, part B. Behaviour and fertility control (W. S. Hoar, D. J. Randall, and E. M. Donaldson, eds.), p. 65-115. Academic Press, New York and London.
McPherson, G. R.
1981. Preliminary report: Investigations of Spanish mackerel (*Scomberomorus commerson*) in Queensland waters. In Northern pelagic fish seminar (D. J. Grant and D. G. Walter, eds.), p. 51-58. Australian Government Publishing Service, Canberra, New South Wales, Australia.
1992. Age and growth of the narrow-barred Spanish mackerel (*Scomberomorus commerson* Lacepede, 1800) in north-eastern Queensland waters. Aust. J. Mar. Freshw. Res. 43:1269-1282.
1993. Reproductive biology of the narrow-barred Spanish mackerel (*Scomberomorus commerson* Lacepede, 1800) in Queensland waters. Asian Fish. Sci. 6:169-182.
McPherson, G. R., and L. E. Williams.
2002. Narrow-barred Spanish mackerel. In Queensland's fisheries resources: current condition and recent trends 1988-2000 (L. E. Williams, ed.), p. 88-93. Information Series Q102012, Department of Primary Industries Queensland, Brisbane, Australia.
Munro, I. S. R.
1942. The eggs and early larvae of the Australian barred Spanish mackerel, *Scomberomorus commersoni* (Lacepede) with preliminary notes on the spawning of that species. Proc. Royal Soc. Qld. 54:33-48.
Schmidt, D. J., M. R. Collins, and D. M. Wyanski.
1993. Age, growth, maturity and spawning of Spanish mackerel, *Scomberomorus maculatus* (Mitchell), from the Atlantic coast of the southeastern United States. Fish. Bull. 91:526-533.

- Sturm, M. G. deL., and P. Salter
1990. Age, growth and reproduction of the king mackerel, *Scomberomorus cavalla* (Cuvier), in Trinidad waters. Fish Bull. 88:361-370.
- Thresher, R. G.
1984. Reproduction in reef fishes, 391 p. T.F.H. Publications Pty Ltd., Neptune City, NJ.
- Trent, L., R. O. Williams, R. G. Taylor, C. H. Saloman, and C. S. Manooch.
1981. Size and sex ratio of king mackerel, *Scomberomorus cavalla*, in the southeastern United States. NOAA Tech. Memo. NMFS-SEFC 62:1-59.
- West, G.
1990. Methods of assessing ovarian development in fishes: a review. Aust. J. Mar. Freshw. Res. 41:192-222.

Abstract—Recent research demonstrated significantly lower growth and survival of Bristol Bay sockeye salmon (*Oncorhynchus nerka*) during odd-numbered years of their second or third years at sea (1975, 1977, etc.), a trend that was opposite that of Asian pink salmon (*O. gorbuscha*) abundance. Here we evaluated seasonal growth trends of Kvichak and Egegik river sockeye salmon (Bristol Bay stocks) during even- and odd-numbered years at sea by measuring scale circuli increments within each growth zone of each major salmon age group between 1955 and 2000. First year scale growth was not significantly different between odd- and even-numbered years, but peak growth of age-2. smolts was significantly higher than age-1. smolts. Total second and third year scale growth of salmon was significantly lower during odd- than during even-numbered years. However, reduced scale growth in odd-numbered years began after peak growth in spring and continued through summer and fall even though most pink salmon had left the high seas by late July (10–18% growth reduction in odd vs. even years). The alternating odd and even year growth pattern was consistent before and after the 1977 ocean regime shift. During 1977–2000, when salmon abundance was relatively great, sockeye salmon growth was high during specific seasons compared to that during 1955–1976, that is to say, immediately after entry to Bristol Bay, after peak growth in the first year, during the middle of the second growing season, and during spring of the third season. Growth after the spring peak in the third year at sea was relatively low during 1977–2000. We hypothesize that high consumption rates of prey by pink salmon during spring through mid-July of odd-numbered years, coupled with declining zooplankton biomass during summer and potentially cyclic abundances of squid and other prey, contributed to reduced prey availability and therefore reduced growth of Bristol Bay sockeye salmon during late spring through fall of odd-numbered years.

Seasonal marine growth of Bristol Bay sockeye salmon (*Oncorhynchus nerka*) in relation to competition with Asian pink salmon (*O. gorbuscha*) and the 1977 ocean regime shift

Gregory T. Ruggerone

Natural Resources Consultants, Inc.
1900 West Nickerson Street, Suite 207
Seattle, Washington 98119
E-mail address: GRuggerone@nrccorp.com

Ed Farley

National Marine Fisheries Service
11305 Glacier Highway
Juneau, Alaska 99801

Jennifer Nielsen

Biological Resources Division
U.S. Geological Survey
Anchorage, Alaska 99503

Peter Hagen

Alaska Dept. of Fish and Game
P.O. Box 25526
Juneau, Alaska 99802-5526

Competition among Pacific salmon (*Oncorhynchus* spp.) for food resources in the North Pacific Ocean and Bering Sea is a potentially important mechanism affecting salmon growth and population dynamics. Reduced growth at sea may lead to delayed maturation (Rogers, 1987), lower reproductive potential (Groot and Margolis, 1991), or greater risk of predation (Juanes, 1994).

Density-dependent growth in the ocean has been observed among sockeye (*O. nerka*), pink (*O. gorbuscha*), and chum salmon (*O. keta*), which are the most abundant species among Pacific salmon (Rogers¹; Eggers et al.²). Density-dependent growth may occur during early marine life (Peterman, 1984) or during the homeward migration period when the potential for high growth rate (Ishida et al., 1998) may be influenced by high concentrations of salmon (Rogers and Ruggerone, 1993).

Since the early 1970s, salmon abundance in the North Pacific Ocean has increased, whereas body size for many populations of all salmon species has declined (Bigler et al., 1996). However, greater abundance of adult sockeye salmon returning to Bristol Bay, Alaska, was associated with increased growth during the first and second years at sea, followed by relatively low growth during the third year at sea, and greater adult size at a given abundance (Ruggerone et al.,

¹ Rogers, D. E. 2001. Estimates of annual salmon runs from the North Pacific, 1951–2001. Report SAFS-UW-0115. 11 p. School of Aquatic Sciences, Univ. Washington, Seattle, WA.

² Eggers, D. M., J. Irvine, M. Fukawaki, and V. Karpenko. 2003. Catch trends and status of North Pacific salmon. Doc. no. 723. 34 p. North Pacific Anadromous Fisheries Commission (NPAFC), 889 Pender Street, Vancouver, Canada.

2002). Increased growth of Bristol Bay sockeye salmon during the first two years at sea was associated with greater adult returns, but high abundance apparently led to increased competition and reduced growth during the third year.

The potential for competition for food between Asian pink salmon and Bristol Bay sockeye salmon stocks is great in the North Pacific Ocean and Bering Sea. Trophic level, diet, and feeding behavior of pink salmon overlap significantly with sockeye salmon (Welch and Parsons, 1993; Davis et al., 2000; Kaeriyama et al., 2004). Asian pink salmon are highly abundant, averaging approximately 162 million adults in odd-numbered years and 104 million adults in even-numbered years, 1955 to 2000 (Rogers¹). Bristol Bay sockeye salmon and Asian pink salmon overlap in the central North Pacific Ocean and the Bering Sea. Greatest overlap is with pink salmon from the eastern Kamchatka Peninsula and Sakhalin Island (French et al., 1976; Takagi et al., 1981; Myers et al.³), which are especially abundant, as shown by average harvests of 79,000 metric tons (t) in odd-numbered years and 33,000 t in even-numbered years, 1955–99 (Sinyakov, 1998; Anonymous⁴).

Evidence for competition between Asian pink and Bristol Bay sockeye salmon was provided in a recent investigation by Ruggerone et al. (2003). During 1955–97, annual sockeye salmon scale growth during the second and third years at sea was significantly reduced during odd- compared to even-numbered years. Adult sockeye salmon length was relatively low when sockeye salmon overlapped with abundant odd-year pink salmon during the year prior to homeward migration. Furthermore, smolt-to-adult survival of Bristol Bay sockeye salmon was significantly lower when they encountered odd-year pink salmon during the second year at sea. However, Bristol Bay sockeye salmon encountered relatively few pink salmon during their first year at sea and no competition effect was observed during this early marine period.

In our study we examined the seasonal growth of Bristol Bay sockeye salmon scales in an effort to determine the approximate timing and duration of reduced growth during odd-numbered years at sea that was observed by Ruggerone et al. (2003). Scale circuli increments and annuli are correlated with salmon body size (Clutter and Whitesel, 1956; Fukuwaka and Kaeriyama, 1997; Fukuwaka, 1998). We compared seasonal scale growth before and after 1977 to examine seasonal growth trends associated with the twofold increase in Bristol Bay sockeye salmon abundance and the 1977

ocean regime shift (Rogers, 1984; Beamish and Bouillon, 1993; Rogers¹). We also examined the hypothesis that seasonal growth during the second growing season was dependent on previous marine growth (Aydin, 2000). These hypotheses were tested by using scales from Kvichak River and Egegik River sockeye salmon, which averaged approximately 16 million fish per year or approximately 57% of the annual sockeye salmon run to Bristol Bay, 1955–2000.

Methods

For our study, we used scales from four age groups of Kvichak River sockeye salmon and three age groups of Egegik River sockeye salmon collected from the late 1950s through 2000 (Fig. 1). Adult salmon scales were obtained from the Alaska Department of Fish and Game (ADFG) archive in Anchorage, Alaska, and from the School of Aquatic and Fishery Sciences, University of Washington. Scales have been collected annually for measuring and quantifying age composition for management of the fisheries in Alaska. We selected scales from salmon sampled in the Kvichak and Egegik rivers rather than in the ocean fisheries to reduce the possibility of mixed stocks in the scale collection. Scale collections from the Kvichak River began in 1955, whereas collections from Egegik River began in 1960. Major freshwater and ocean age groups from Kvichak (ages 1.2, 1.3, 2.2, 2.3) and Egegik (ages 1.3, 2.2, 2.3) sockeye salmon were measured. Age was designated by European notation, i.e. the number of winters spent in freshwater before going to sea (1 winter=age-1, or two winters=age-2.) followed by the number of winters spent at sea (two winters=age-2 or 3 winters=age-3.). Nearly all Bristol Bay sockeye salmon mature after spending two or three winters at sea.

Scales were selected for measurement in this study only when 1) we agreed with the age determination previously made by ADFG, 2) the scale shape indicated that the scale was removed from the "preferred area" (Koo, 1962), and 3) circuli and annuli were clearly defined and not affected by scale regeneration or significant resorption along the measurement axis. We measured up to 50 scales per year, representing equal numbers of male and female salmon from each age group within each stock.

Scale measurements followed procedures described by Davis et al. (1990) and Hagen et al.⁵ After selecting a scale for measurement, the scale was scanned from a microfiche reader and its image was stored as a high resolution digital file. High resolution (3352×4425 pixels) allowed the entire scale to be viewed and provided enough pixels to be seen between narrow circuli

¹ Myers, K. W., K. Y. Aydin, R. V. Walker, S. Fowler, and M. L. Dahlberg. 1996. Known ocean ranges of stocks of Pacific salmon and steelhead as shown by tagging experiments, 1956–1995. Report FRI-UW-9614, 159 p. School of Aquatic and Fishery Sciences, Univ. Washington, Seattle, WA.

⁴ Anonymous. 2002. Biostatistical information on salmon catches, escapement, outmigrants number, and enhancement production in Russia in 2001. Doc. no. 646, 14 p. NPAFC, 889 Pender Street, Vancouver, Canada.

⁵ Hagen, P. T., D. S. Oxman, and B. A. Agler. 2001. Developing and deploying a high resolution imaging approach for scale analysis. Doc. 567, 11 p. North Pacific Anadromous Fish Commission, 889 Pender Street, Vancouver, Canada.

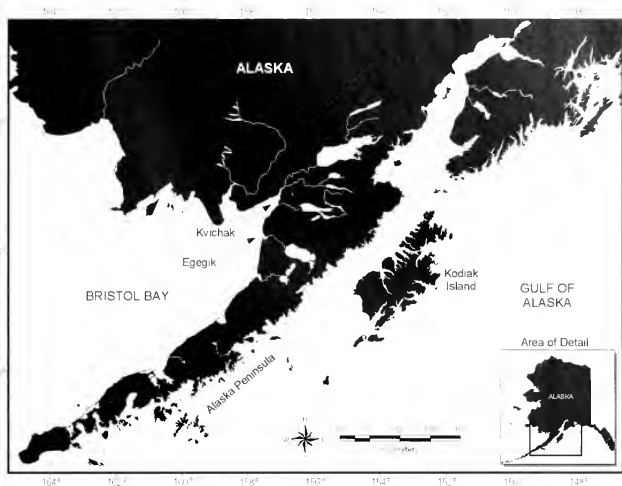


Figure 1

Map of Bristol Bay, Alaska, and the location of the Kvichak and Egegik river systems.

to ensure accurate measurements of circuli spacing. The digital image was loaded in Optimas 6.5 (Media Cybernetics, Inc., Silver Spring, MD) image processing software to collect measurement data with a customized program. The scale image was displayed on a digital LCD flat panel tablet. The scale measurement axis was determined by a perpendicular line drawn from a line intersecting each end of the first saltwater annulus. Distance (mm) between circuli was measured within each growth zone (i.e., from the scale focus to the outer edge of the first freshwater (FW1) annulus, between the first and second freshwater (FW2) annuli, within the spring plus (FWPL) growth zone, within each annual saltwater (SW1, SW2, SW3) growth zone, and from the last ocean annulus to the edge of the scale (i.e., the saltwater plus [SWPL] growth zone).

Data analysis

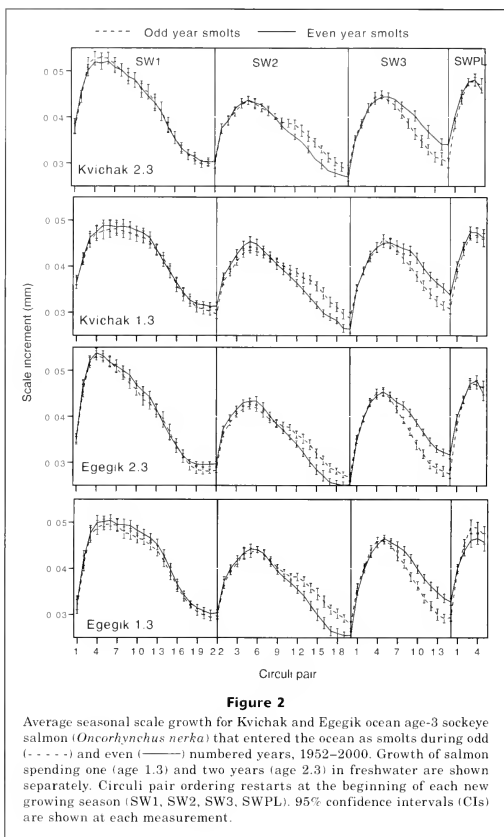
Mean scale circuli increments (distance between adjacent circuli pairs) of each age group and stock were calculated for each year when 10 or more scales were available. Typically, 40 to 50 scales of each age group and stock were measured in a given year. To facilitate evaluation of trends between odd- and even-numbered years at sea, scale circuli measurements were described in terms of the odd- or even-numbered year when the salmon entered

the ocean. Thus, a salmon smolt entering the Bering Sea during an even-numbered year interacted with abundant odd-year Asian pink salmon during its second growing season (SW2) and less abundant even-year pink salmon during its third year, if it remained at sea. The number of circuli pairs considered in our analysis differed by growth zone, ranging from 22 circuli (SW1) to 20 circuli (SW2) to 15 circuli (SW3) in order to represent the majority of salmon. Analyses of seasonal scale growth trends were based on the mean of annual mean scale circuli increments, percentage change in scale circuli increments during odd- versus even-numbered years, and percentage change in odd- and even-year growth during periods before and after the 1977 ocean regime shift. A two-sample *t*-test was used to test for differences between odd- and even-numbered year scale growth at each circuli pair. Correlation was used to determine whether an individual's growth during the second growing season was related to previous growth at sea.

Results

First year (SW1) growth of ocean age-3 sockeye salmon

Kvichak and Egegik river sockeye salmon scale growth (distance between adjacent circuli) increased rapidly



after the fish entered Bristol Bay during May and early June, reaching peak growth near the fifth circuli (Fig. 2). Thereafter, growth declined steadily to a minimum at the first ocean annulus (circuli 18–22).

Peak scale growth of age-2. smolts was significantly greater compared with that of age-1. smolts for both Kvichak ($df=79$, $t=5.757$, $P<0.001$) and Egegik salmon ($df=73$, $t=4.667$, $P<0.001$). During the first eight circuli, age-2. smolts averaged 6.5% greater growth

than age-1. smolts. Thereafter (circuli 11–20), growth of age-2. smolts declined more rapidly and averaged 2.3% (Kvichak) to 6.1% (Egegik) less than growth of age-1. smolts.

Within the SW1 growth period, no statistically significant difference in circuli growth was detected between smolts entering the ocean during odd- and even-numbered years ($P>0.05$). However, there was a trend for greater growth among even-year smolts in some

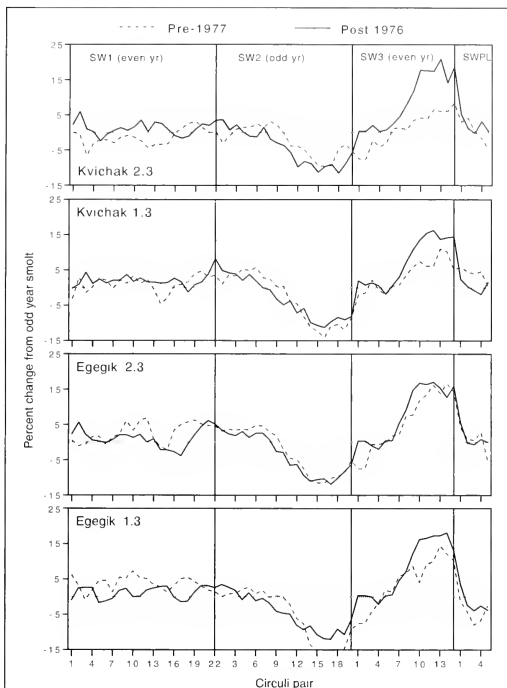


Figure 3

Percent change in scale growth of ocean age-3 sockeye salmon (*O. nerka*) entering the ocean during even-numbered years compared to odd-numbered years. Growth patterns represent ocean developmental periods prior to 1977 (---) and after 1976 (—). Even-year smolts encountered odd-year pink salmon (*O. gorbuscha*) during their second year at sea (SW2), but they encountered even-year pink salmon during their third year at sea (SW3). Age 1.3=1 year in freshwater and 3 years in saltwater; age 2.3=2 years in freshwater and 3 years in saltwater.

portions of SW1, including the annulus (circuli 18–22) and immediately after peak growth (circuli 7 to 13) (Figs. 2 and 3).

SW1 growth of both even- and odd-year smolts tended to be greater after the 1977 climate shift than prior to this period, except for the last few circuli (Fig. 4). The greatest difference in growth between these two periods occurred immediately after entry into Bristol

Bay (circuli 1–3) and during the last part of the SW1 growth period (circuli 13–19). This bimodal pattern of growth between the two periods was somewhat consistent among both stocks and freshwater age groups. However, Kvichak age 2.3 salmon experienced especially high early marine growth that was 17% greater, on average, after 1976. Following peak scale growth in spring, Egegik age 1.3 sockeye salmon experienced a

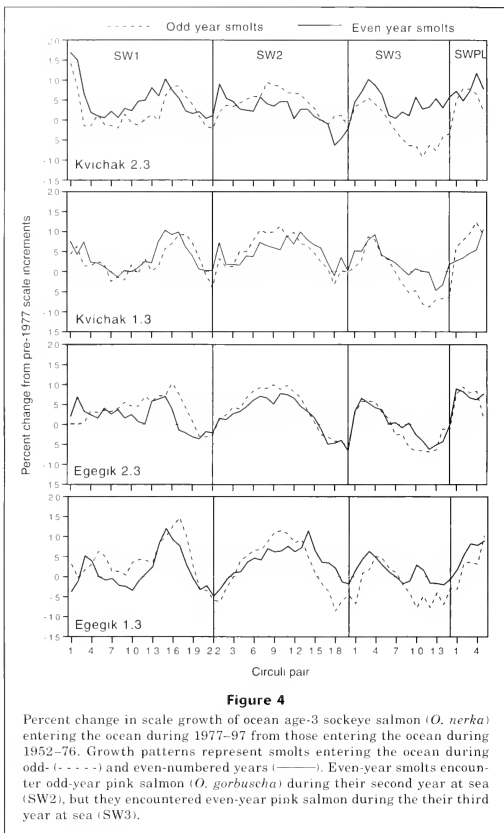


Figure 4

Percent change in scale growth of ocean age-3 sockeye salmon (*O. nerka*) entering the ocean during 1977-97 from those entering the ocean during 1952-76. Growth patterns represent smolts entering the ocean during odd- (---) and even-numbered years (—). Even-year smolts encounter odd-year pink salmon (*O. gorbuscha*) during their second year at sea (SW2), but they encountered even-year pink salmon during their third year at sea (SW3).

15% increase in growth after 1976. In contrast, growth near the winter annulus (circli 20-22) was up to 5% lower after the 1977 climate shift.

Second year (SW2) growth of ocean age-3 sockeye salmon

At the beginning of the second growing season (SW2), when Bristol Bay sockeye salmon are farthest south

in the North Pacific Ocean (French et al., 1976), scale growth of both stocks and age groups increased rapidly, but the rate of increase was 59% less than that of SW1 and 37% less than SW3 growth (Fig. 2). Peak growth occurred near circli 5 or 6 and it averaged 15% lower than that of SW1 growth.

During their second year at sea, even-year sockeye smolts inhabited the North Pacific and Bering Sea when Asian pink salmon were abundant in offshore waters

Table 1

Summary of two sample *t*-tests for evaluating the circuli number at which sockeye scale growth began to differ between odd- versus even-numbered years of the second and third seasons at sea. Between-year differences in circuli growth were greater after the circuli number shown in this table. No consistent pattern of differences between odd- and even-numbered years was observed during the first season at sea. Age "1.2" is a fish that has spent one year in fresh water and two years in salt water. SW2=2 years in saltwater.

Age	Ocean period	Stock	Circuli no.	df	<i>t</i> -value	<i>P</i> (two tailed)
1.2	SW2	Kvichak	C11	43	2.412	0.020
2.2	SW2	Kvichak	C11	44	3.283	0.002
2.2	SW2	Egegik	C11	39	3.434	0.001
1.3	SW2	Kvichak	C12	42	3.068	0.004
	SW3	Kvichak	C8	42	3.126	0.003
1.3	SW2	Egegik	C11	38	2.140	0.038
	SW3	Egegik	C7	38	2.527	0.016
2.3	SW2	Kvichak	C11	43	2.711	0.010
	SW3	Kvichak	C8	43	2.384	0.022
2.3	SW2	Egegik	C11	39	3.061	0.004
	SW3	Egegik	C7	39	2.728	0.010

(i.e., during odd-numbered years). Initial scale growth prior to the SW2 peak in spring was the same between odd- and even-numbered years, although there was a tendency for greater growth following the SW1 annulus of even-year smolts (Fig. 3). Immediately after peak growth near circuli 11, scale growth of even-year smolts became significantly less than that of odd-year smolts (Table 1). The growth differential continued through the end of the SW2 growing season and it reached a maximum reduction of -10% to -18% near circuli 14 to 18 (Fig. 3). This pattern was consistent before and after the 1977 climate shift and among each stock and age group. The reduced growth of even-year smolts during SW2 corresponded with high abundance of pink salmon in the central North Pacific Ocean during odd-numbered years.

Scale growth during SW2 of both odd- and even-year smolts tended to be greater after the 1977 climate shift (Fig. 4), a period when abundance of Bristol Bay sockeye salmon and Asian pink salmon was great. This pattern was consistent among both age groups of Kvichak and Egegik River sockeye salmon. Greatest growth differential between the two periods (up to 10%) occurred just after peak growth (circuli 5 to 15), a pattern that differed markedly from both SW1 and SW3. In contrast to the relatively large increase in growth shown in the central portion of SW2 after 1977, growth at the beginning of SW2 was similar during both periods and growth at the end of SW2 was relatively low after the climate shift.

Third year (SW3) growth of ocean age-3 sockeye salmon

Scale growth at the beginning of the third year at sea increased rapidly, peaked near circuli 5-6, then declined

steadily through the year (Fig. 2). Peak growth during SW3 was intermediate to the relatively high peak growth during SW1 and relatively low peak growth during SW2.

During their third year at sea, even-year sockeye smolts inhabited the North Pacific and Bering Sea when relatively few Asian pink salmon were in offshore waters (i.e., even-numbered years). Prior to peak growth, SW3 growth of even-year smolts was similar or below that of odd-year smolts (Fig. 3), a pattern that continued from the previous season. Immediately following the peak, growth of even-year smolts significantly increased in relation to odd-year smolts (Table 1), and growth remained relatively high throughout the remaining season (Fig. 2). Growth of even-year smolts was approximately 5% to 15% greater than that of odd-year smolts from circuli 8 to the annulus (Fig. 3). Differences in growth during even- versus odd-numbered years tended to be greater after 1976 when both pink and sockeye salmon were relatively abundant.

Peak SW3 scale growth was up to 10% greater after the mid-1970 regime shift during both odd- and even-numbered years (Fig. 4). However, after the peak growing season, scale growth was typically lower after 1976. The relatively low growth after 1976 was especially pronounced among odd-year smolts that inhabited the ocean during odd-numbered years when Asian pink salmon were abundant in offshore waters. Scale growth of odd-year smolts during SW3 was as much as 10% lower than that prior to 1977.

Scale growth during both SW3 and SW2 were significantly reduced during odd-numbered years at sea (Table 1). However, SW3 scale growth during odd- versus even-years diverged immediately after the peak, whereas

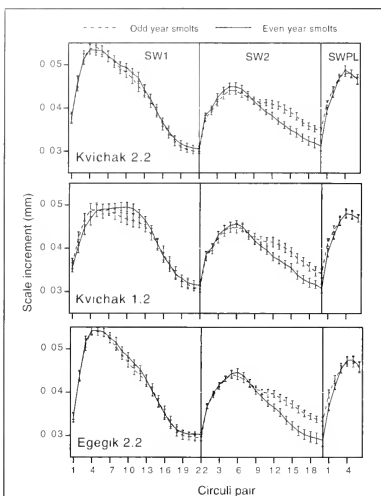


Figure 5

Seasonal scale growth of Kvichak and Egegik ocean age-2 sockeye salmon (*O. nerka*) that entered the ocean as smolts during odd- (---) and even- (—) numbered years, 1952–2000. Growth of salmon spending one (age 1.2) and two years (age 2.2) in freshwater are shown separately. Circuli pair ordering restarts at the beginning of each new growing season (SW1, SW2, SWPL). 95% CIs are shown at each measurement. Age 1.2=1 year in freshwater and 2 years in saltwater.

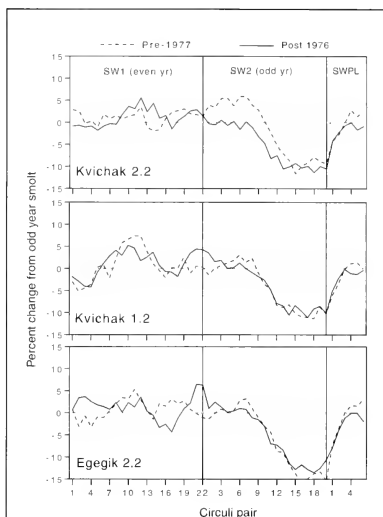


Figure 6

Percent change in scale growth between ocean age-2 sockeye salmon (*O. nerka*) entering the ocean during even years and those entering during odd-numbered years. Growth patterns represent ocean rearing periods prior to 1977 (---) and after 1976 (—). Even-year smolts encountered odd-year pink salmon (*O. gorbuscha*) during the second year at sea (SW2).

growth during SW2 diverged two or three circuli after the peak (Fig. 2). Late season growth of even-year smolts during SW3 was greater than late season growth during SW1 and SW2, whereas growth of odd-year smolts during SW3 was intermediate to SW1 and SW2 growth. These relatively large, older fish experienced a longer growing season, especially during even-numbered years, when few pink salmon were present.

Growth during homeward migration (SWPL) of ocean age-3 sockeye salmon

The peak return of sockeye salmon to Bristol Bay occurs near 3 July. Scale growth during the homeward migration peaked at circuli 3 and 4, then declined (Fig. 2). Peak growth was less than that of SW1, but greater than SW2 and SW3 growth. No growth difference was detected between odd- and even-year migrants during

the period of homeward migration. Spring growth after 1976 was 5–10% greater than that during the earlier time period (Fig. 4).

First year ocean (SW1) growth of ocean age-2 sockeye salmon

Scale growth patterns of ocean age-2 Kvichak and Egegik sockeye salmon were remarkably similar to that of ocean age-3 sockeye, especially among those having the same freshwater age (Fig. 5). Sockeye salmon that had spent two winters in freshwater had significantly greater SW1 peak growth compared with those spending one winter in freshwater (Kvichak stock: $df=85$, $t=6.772$, $P<0.001$). Growth of age-2. smolts during the first eight circuli averaged 9% higher compared to age-1. smolts. However, as with ocean age-3 salmon, postpeak growth of age-2 smolts averaged 3.5% less than that of age-1.

smolts. Growth of even- and odd-year smolts during the first growing season was not significantly different but even-year smolts tended to have somewhat greater growth immediately following peak growth (circuli 7–13) and at the end of the growing season (circuli 19–22) (Fig. 6).

SW1 growth was markedly greater after 1976 when salmon abundance was relatively high compared with the growth during 1952–1976 (Fig. 7). Greater growth during the recent time period was most pronounced immediately after entry to Bristol Bay and after peak growth (circuli 13–18), but it was relatively low at the end of the growing season (circuli 20–22). These patterns were generally consistent between odd- and even-year smolt years.

Second year (SW2) growth of ocean age-2 sockeye salmon

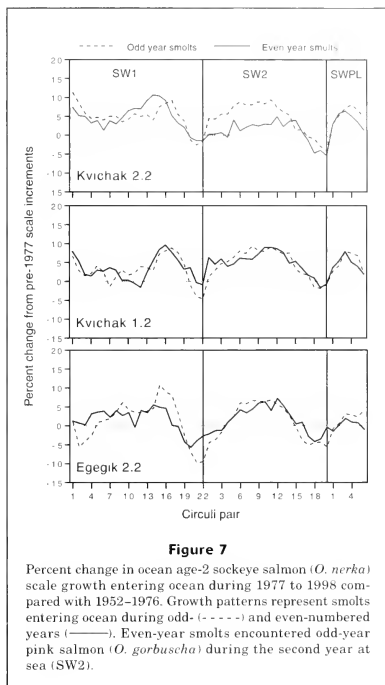
SW2 scale growth patterns of ocean age-2 sockeye salmon were similar to SW2 patterns of ocean age-3 sockeye salmon. Scale growth of odd- and even-year smolts was similar until scale growth of even-year smolts significantly declined approximately three circuli after peak growth (Fig. 5, Table 1). Lower growth of even-year smolts continued to the end of the growing season. Scale growth of even-year migrants during their second year at sea was approximately 10% to 15% less than that of odd-year migrants (Fig. 6). Low growth of even-year migrants was associated with odd-numbered years at sea—a trend that was observed among SW2 and SW3 growth periods of ocean age-3 sockeye salmon.

Scale growth during SW2 was greater after 1976 when salmon abundance was relatively high compared with the growth before 1977, especially during the middle of the growing season (Fig. 7). However, after 1976, growth near the end of the growing season (circuli 17–20) tended to be below average. These patterns were consistent among the two stocks and three age groups.

Late season growth of ocean age-2 sockeye salmon during the second year at sea differed from that of ocean age-3 sockeye salmon (Figs. 2 and 5). Growth after circuli 8 of SW2 was significantly greater among ocean age-2 compared with ocean age-3 sockeye salmon ($df=283$, $t=12.81$, $P<0.001$), averaging 11% greater growth.

Growth during homeward migration (SWPL) of ocean age-2 sockeye salmon

Scale growth of ocean age-2 sockeye salmon during the homeward migration peaked at circuli 4, then declined. Prior to peak growth, even-year migrants experienced approximately 5% less growth than odd-year migrants, a pattern that was similar prior to and after the climate shift (Fig. 6). Low initial growth during SWPL appeared to be a continuation of relatively low growth during SW2. No difference in peak growth between odd- and even-years was apparent. Growth tended to be higher after the mid-1970s (Fig. 7).



Relationship between early marine and late SW2 scale growth

We examined correlations between early marine scale (SW1 growth through the first eight circuli of SW2) and late SW2 growth (circuli 11 to annulus), corresponding with periods before and after the divergent scale growth pattern observed between odd- and even-numbered years. Negative correlations between early marine and late SW2 scale growth were observed among each stock and age group, before and after the 1977 regime shift, and among fish inhabiting the ocean during odd- or even-numbered years. Negative correlations between early marine and late SW2 scale growth were observed among each stock and age group, before and after the 1977 regime shift, and among fish inhabiting the ocean during odd- or even-numbered years (Table 2). Only one of the 28 correlations (Egegik age-2.2, early period, odd SW2 year) was statistically insignificant. Thus, individual sockeye salmon that experienced somewhat low growth during early marine life tended to have somewhat high growth during later portions of their second year at sea, regardless of whether they competed with pink salmon. The strength of the

Table 2

Correlation between early marine scale growth (SW1 through SW2, circuli 1-8) and SW2 scale growth after growth difference in odd and even numbered years (SW2, circuli 11 to annulus). Measurements based on individual fish (*n*). Correlation coefficient and statistical significance are shown for each age group and stock during early (pre-1977) and recent (post-1976) periods for odd- and even-numbered years at sea. SW2=2 years in saltwater.

Age	Stock	Period	SW2 year	<i>r</i>	<i>n</i>	<i>F</i> -value	<i>P</i> -value
1.2	Kvichak	Early	Even	-0.11	408	5.18	<0.025
		Early	Odd	-0.20	429	18.20	<0.001
		Recent	Even	-0.22	550	27.84	<0.001
		Recent	Odd	-0.24	596	36.07	<0.001
2.2	Kvichak	Early	Even	-0.14	592	12.17	<0.001
		Early	Odd	-0.14	523	10.16	<0.002
		Recent	Even	-0.31	549	56.23	<0.001
		Recent	Odd	-0.17	568	16.78	<0.001
2.2	Egegik	Early	Even	-0.14	428	8.61	<0.004
		Early	Odd	-0.06	441	1.33	0.249
		Recent	Even	-0.14	551	10.21	<0.002
		Recent	Odd	-0.09	599	4.81	<0.030
1.3	Kvichak	Early	Even	-0.15	270	6.53	<0.020
		Early	Odd	-0.15	333	7.50	<0.010
		Recent	Even	-0.35	517	71.18	<0.001
		Recent	Odd	-0.20	504	21.89	<0.001
1.3	Egegik	Early	Even	-0.15	191	4.32	<0.040
		Early	Odd	-0.22	210	10.51	<0.002
		Recent	Even	-0.23	453	24.67	<0.001
		Recent	Odd	-0.27	479	38.60	<0.001
2.3	Kvichak	Early	Even	-0.15	347	7.78	<0.010
		Early	Odd	-0.16	376	10.12	<0.002
		Recent	Even	-0.24	438	25.86	<0.001
		Recent	Odd	-0.18	407	13.38	<0.001
2.3	Egegik	Early	Even	-0.16	460	12.35	<0.001
		Early	Odd	-0.23	416	23.94	<0.001
		Recent	Even	-0.18	546	17.94	<0.001
		Recent	Odd	-0.17	543	16.11	<0.001

correlations was low, but the consistent pattern among stocks, age groups, and time periods indicates that the negative correlations were not spurious.

Discussion

Previous research documented reduced annual scale growth of Nushagak Bay (Bristol Bay) sockeye salmon during odd-numbered years of their second and third years at sea (Ruggerone et al., 2003). The primary finding of our investigation was that salmon scale growth reduction during odd-numbered years did not occur throughout the second and third years at sea. During the second year at sea, scale growth reduction began three to five circuli after peak scale growth. During the third year at sea, scale growth reduction began immediately after peak growth. This finding was consistent among all

age groups of both Kvichak and Egegik sockeye salmon prior to and after the mid-1970s regime shift that led to greater sockeye salmon abundance. Comparison of seasonal scale growth patterns before and after the regime shift indicated that the recent period of high sockeye salmon abundance was associated with relatively high growth 1) immediately after entry to Bristol Bay, 2) after peak scale growth during the first growing season, 3) during the middle of the second growing season, and 4) during the third spring but followed by below average growth during the remaining summer and fall.

Timing of peak scale growth and differences in scale growth between odd- and even-numbered years

The approximate time period of peak scale growth can be estimated from previous studies of salmon circuli formation at sea and timing of peak prey production. Bilton

and Ludwig (1966) reported that sockeye salmon in the Gulf of Alaska tended to form annuli during December and January, whereas salmon sampled farther west in the relatively cold waters below the Aleutian Islands appeared to form annuli during March (Birman, 1960). For example, sockeye salmon collected from the eastern range of Bristol Bay sockeye salmon in the Gulf of Alaska (e.g., 152–160°W) averaged 1.2 circuli beyond the winter annulus during January and 3.6 circuli in April. We observed peak circuli growth of Kvichak and Egegik sockeye salmon to occur near circuli 5 to 6 (all ages), indicating that peak scale growth occurred from approximately early May to mid-June. This finding is consistent with scale growth in the year of homeward migration when Bristol Bay sockeye salmon averaged approximately 1 to 2 circuli after peak circuli growth before reaching Bristol Bay, on average, during the first week in July. The estimated date of peak scale growth is also consistent with observations of peak biomass of zooplankton in the Gulf of Alaska and Bering Sea, which typically occurs during May or June (Brodeur et al., 1996; Coyle et al., 1996; Mackas et al., 1998; Mackas and Tsuda, 1999). However, Ishida et al. (1998) reported that salmon growth was greatest between June and July, a period apparently later than peak scale growth and peak zooplankton biomass. Furthermore, scale growth may lag behind body growth (Bilton, 1975). Based on these observations, the observed divergence in scale growth between odd- and even-numbered years likely began after zooplankton biomass declined and during a period of high potential body growth of salmon.

Differences in SW2 scale growth between odd- and even-numbered years at sea began three to five circuli after peak growth, rather than immediately after the peak as shown among fish during their third year at sea (SW3). Because younger salmon begin circuli formation earlier in winter than do older salmon (Bilton and Ludwig, 1966; Martinson and Helle, 2000), it is likely that the differences in time of SW2 scale growth was only slightly later than that scale growth during SW3. The reason for the somewhat later differences between odd and even years of younger sockeye salmon might relate to the degree of diet overlap with pink salmon. In the central North Pacific Ocean and Bering Sea, pink salmon in their second growing season have greater diet overlap with larger sockeye salmon (Davis, 2003), such as sockeye salmon in their third season at sea. Thus, competition for prey may be greatest between pink salmon and the larger, older sockeye salmon, leading to earlier growth differences between the SW3 than the SW2 growth period. Alternatively, this pattern may reflect differences in the distribution of age-2 and age-3 sockeye salmon: age-3 salmon maybe distributed farther west where overlap with Asian pink salmon is greater.

Interactions with pink salmon and prey

Spatial and temporal overlap between Asian pink salmon and Bristol Bay sockeye salmon are important factors

that affect the degree of competition. Little or no overlap occurs between these stocks during the first growing season (SW1) and there are typically small numbers of pink salmon originating from Bristol Bay (Rogers¹). Little sampling has occurred during winter (Myers⁶), but data collected during fall and spring indicate that some overlap between Asian pink salmon and Bristol Bay sockeye begins in the central North Pacific Ocean during winter (French et al., 1976; Takagi et al., 1981; Myers et al.³). The degree of overlap likely increases into spring when both species reach their southernmost distribution, which is somewhat farther south for pink salmon. As the temperature begins to increase, both species migrate northwest—pink salmon leading the migration. Both species enter the Bering Sea but many Bristol Bay salmon and some Asian pink salmon remain in the North Pacific Ocean. In June, some Asian pink salmon leave the high seas for coastal areas, whereas others remain offshore through July (Myers et al.³; Azumaya and Ishida, 2000). During odd-numbered years, pink salmon are more broadly distributed on the high seas and catch per effort in the Bering Sea remains high through at least mid-July (up to 400 fish per 30 tans (1.5 km) of gill net) compared with that during even-numbered years (Azumaya and Ishida, 2000). Catch per effort of pink salmon during July is somewhat lower in the central North Pacific Ocean. Most pink salmon in the Bering Sea likely originate from the eastern Kamchatka Peninsula, which supports a major Asian population that is dominated by odd-year pink salmon. Thus, the period of overlap between Asian pink salmon and Bristol Bay sockeye salmon is from approximately winter through July and greatest overlap likely occurs during late spring through at least mid-July.

The relatively slow growth of sockeye salmon scales during odd-numbered years at sea began in the period of overlap with pink salmon and continued for months after pink salmon left the high seas. This finding indicates that prey availability was reduced for months after most pink salmon left the high seas. Sugimoto and Tadokoro (1997) examined zooplankton biomass during June and July, 1950–81 and concluded that Asian pink salmon caused the observed alternating pattern of zooplankton biomass in the central North Pacific Ocean and the eastern Bering Sea. Shiomoto et al. (1997) examined macrozooplankton biomass in the central North Pacific Ocean during 1985–94 and also concluded that Asian pink salmon, especially those from the eastern Kamchatka Peninsula, reduced the biomass of macrozooplankton. Shiomoto et al. (1997) noted that lower zooplankton biomass was still apparent in the central North Pacific Ocean after many pink salmon had migrated into the Bering Sea. These findings support the hypothesis that predation by pink salmon altered zooplankton biomass from spring through at least July.

⁶ Myers, K. 1996. Survey on overwintering salmonids in the North Pacific Ocean: Kaiyo Maru, 5 January–29 January 1996. Report FRI-UW-9607, 54 p. Univ. Washington, Seattle, WA.

Timing of peak zooplankton biomass occurs later in the year in northern regions, but zooplankton biomass typically declines during summer and fall (Batten et al., 2003). Declining zooplankton biomass in epipelagic waters is related, in part, to the ontogenetic migration to deep waters of some major zooplankton species, such as *Neocalanus* spp. (Mackas and Tsuda, 1999). Declining zooplankton biomass during summer likely enhanced the effect of competition exerted by pink salmon during odd-numbered years. July through at least September is a period of high potential salmon growth (Ishida et al., 1998); therefore sockeye salmon may be especially influenced by prey reduction during this period. During early spring, when scale growth of sockeye salmon was great and did not differ between odd- and even-numbered years, prey availability was apparently sufficient to minimize the effects of competition. Walker et al. (1998) reported that density-dependent growth of Asian pink salmon occurred after late June—a finding that is consistent with our study.

The transition from foraging on zooplankton to foraging on squid for both pink and sockeye salmon may also contribute to the alternating-year pattern of sockeye salmon growth. Aydin (2000) suggested that pink and sockeye salmon may begin to feed intensively on micronekton squid after reaching sufficient size during their second growing season. Pink salmon reportedly begin feeding on squid during spring, whereas sockeye salmon may not begin to feed on squid until summer because sockeye salmon are smaller. During odd-numbered years, pink salmon may have reduced the availability of squid to sockeye salmon and influenced the observed differences in scale growth after spring. In support of this hypothesis, sampling of sockeye and pink salmon during a recent 10-year period in the Bering Sea (June and July) indicated a 58% reduction among sockeye salmon and 32% reduction among pink salmon in the weight of squid consumed during odd- compared to even-numbered years (Davis, 2003). Few annual estimates of squid abundance are available, but Sobolevsky (1996) estimated that epipelagic squid biomass in the western Bering Sea was approximately five times greater in an even-year (1990) than in an odd-year (1989). Population dynamics and life history of squid are not well known (Nesis, 1997; Brodeur et al., 1999), but their apparent one- or two-year life history, in conjunction with predation by pink salmon, may lead to an alternating-year pattern of squid abundance that re-enforces the alternating-year pattern of sockeye salmon growth.

Ruggerone et al. (2003) reported that Bristol Bay sockeye salmon that inhabited the ocean in odd-numbered years of their second year at sea experienced lower smolt-to-adult survival compared with sockeye salmon that were present during even-numbered years. Lower survival was believed to be related to competition with Asian pink salmon. Our findings suggest that this mortality was likely related to reduced growth during late spring through fall, rather than during the first winter. We hypothesize that reduced sockeye

salmon growth during the second year at sea led to lower energy reserves and to greater mortality during the second winter, but predation on smaller salmon may also be an important factor (Nagasawa, 1998). Bioenergetic modeling of salmon by Aydin (2000) indicated the greatest difference between the need for prey and prey availability is during winter. Nagasawa (2000) reported exceptionally low prey availability and corresponding low lipid content for salmon in the North Pacific Ocean during winter. Ishida et al. (1998) examined salmon on the high seas and determined that condition factor of all salmon species was lowest during late winter. Beamish and Mahnken (2001) provided evidence that relatively low growth of salmon during summer and fall can lead to significant growth-related mortality during the first winter at sea. Growth-related mortality appears to occur among Bristol Bay sockeye salmon in response to competition with pink salmon, but this competition-related mortality primarily occurs during the second winter at sea.

Bristol Bay sockeye salmon are broadly distributed across the North Pacific Ocean and Bering Sea. They occur in several oceanographic regions in which dominant prey may vary (e.g., the Bering Sea [euphausiids, squid, fish], subarctic current [squid], ridge domain [small zooplankton], the Alaska stream [small zooplankton, squid, fish], and the coastal domain [fish, euphausiids]) (Pearcy et al., 1988; Aydin, 2000). The alternating-year pattern of scale growth was persistent among adult Kvichak and Egegik sockeye salmon of all age groups returning to Bristol Bay even though many of these fish likely inhabited different ocean habitats. Thus, the observed scale growth pattern is either highly persistent in most of these ocean habitats or it is especially important in certain key regions inhabited by Bristol Bay sockeye salmon.

Salmon growth in relation to the regime shift of the mid-1970s

Several studies indicate that a significant change in the species assemblage of the North Pacific Ocean began near 1977 and concurrent with a dramatic shift in physical oceanic regimes (Francis et al., 1998; Anderson and Piatt, 1999). Pacific salmon abundance, including Bristol Bay sockeye salmon, more than doubled after this period (Rogers¹). Zooplankton and squid biomass have appeared to increase substantially, especially in coastal regions, since the mid-1970s (Brodeur and Ware, 1992; Brodeur et al., 1996). Furthermore, Mackas et al. (1998) reported that the period of maximum zooplankton biomass shifted one or two months earlier after the mid-1970s. In comparison, seasonal scale growth of Kvichak and Egegik sockeye salmon during the first and second years at sea tended to be high after the regime shift. This pattern was also observed in annual scale measurements of sockeye salmon (Ruggerone et al., 2002). Spring scale growth of sockeye salmon after the regime shift was relatively high immediately after entry of sockeye salmon into Bristol Bay and during

their third year at sea, but spring growth was relatively low during the second year. Growth during the second year was relatively high during summer, a pattern that was different from SW1 and SW3 growth. Seasonal scale growth patterns of sockeye salmon indicate that the response of salmon to the 1977 ocean regime shift varied with age and season but that the greater growth during early marine life was associated with greater adult returns. The shift in seasonal growth patterns of sockeye salmon likely reflected their opportunistic foraging behavior and the changes in prey species abundances caused by climate change (Kaeriyama et al. 2004).

Greater growth of sockeye salmon when they initially entered the Bering Sea after the 1977 ocean regime shift may reflect differences in seaward migration patterns. Prior to the 1977 regime shift, juvenile sockeye salmon were observed in a narrow band that extended from the shore along the Alaska Peninsula to as far as 50 km offshore (Straty, 1981; Hartt and Dell, 1986). However, recent survey results indicate that juvenile sockeye salmon are broadly distributed in the eastern Bering Sea from the Alaska Peninsula to north of 58°N and that the highest catch rates occur beyond 50 km offshore (Farley et al.⁷). Zooplankton are more abundant in offshore, deeper waters of Bristol Bay than within near shore waters (Straty, 1981; Napp et al., 2002), indicating that the recent northerly seaward migration patterns of juvenile sockeye salmon may place them in areas of higher prey densities and lead to higher early marine growth rates.

Sockeye salmon scale growth during the third year of growth (SW3) was relatively low after 1977, indicating that density-dependent growth was most apparent during this late life stage when mortality is likely relatively low (Ruggerone et al., 2002). Our study indicated the reduced SW3 growth after the 1977 regime shift occurred after peak spring growth, indicating that interspecific competition was most apparent during summer and fall. During the spring homeward migration (SWPL) period, scale growth was above average after 1977. Age-specific size of adult sockeye salmon returning to Bristol Bay was density dependent, but size at a given density was greater after 1977 (Rogers and Ruggerone, 1993; Ruggerone et al., 2003).

Salmon survival and scale growth

Biologists have suggested that rapid growth early in life can lead to greater growth in subsequent periods because larger animals have a greater variety of prey and prey size available to them (Pearcy et al., 1999). Aydin (2000) hypothesized that rapidly growing salmon in their first year at sea would more quickly reach a threshold size for feeding on abundant, energy-rich micronekton squid, leading to even greater growth in their second year. However, comparison of early marine scale growth (SW1 through SW2, circuli 8) with late season SW2 growth of individual Kvichak and Egegik sockeye salmon indicated a negative rather than positive relationship. Individual salmon having relatively great early marine scale growth tended to experience reduced scale growth during the later portion of their second year when sockeye salmon reach the size needed to readily consume larger prey such as squid. This finding reflects the growth of sockeye salmon survivors and not those that died at sea. Thus, we interpret this counterintuitive finding as an indication that slow growing sockeye salmon during late SW2 survived primarily when their early marine growth was relatively high. Salmon that experienced both low early marine growth and low SW2 growth apparently did not survive and were not represented in the scale collection. These observations do not necessarily reject the hypothesis that high early marine growth leads to high subsequent growth. In fact, other analyses of sockeye scales indicate spring growth is positively correlated with fall growth within a given year (G. Ruggerone, unpubl. data).

Effect of freshwater age on seasonal scale growth

Scale growth during the first year at sea was different among salmon spending one versus two winters in freshwater. Early SW1 scale growth of sockeye salmon spending two winters in freshwater (age-2) was significantly greater than that of salmon spending only one winter in freshwater. This trend might reflect differences in migration timing or size (or both) of age-2 versus age-1 smolts. Age-2 smolts are approximately 17 mm longer than age-1 smolts and most age-2 smolts enter marine waters before age-1 smolts (Crawford and West⁸). After peak growth in spring, scale growth of age-1 smolts exceeded that of age-2 smolts. The different early marine growth patterns of age-1 and age-2 smolts did not appear to significantly affect the size of the fish at the end of the growing season. For example, during 1958–72, age-2.1 sockeye salmon sampled immediately south of the Aleutian Islands were 25 mm longer than age-1.1 sockeye salmon (French et al., 1976). The size difference between age-2 and age-1 smolts declined to 8 mm during the second growing season.

⁷ Farley, E. V., Jr., R. E. Haight, C. M. Guthrie, and J. E. Pohl. 2000. Eastern Bering Sea (Bristol Bay) coastal research on juvenile salmon, August 2000. Doc. 499, 18 p. North Pacific Anadromous Fish Commission, 889 Pender Street, Vancouver, Canada.

Farley, E.V., Jr., C.M. Guthrie, S. Katakura, and M. Koval. 2001. Eastern Bering Sea (BASIS) Coastal research on juvenile salmon, August 2001. Doc. 560, 19 p. NPAFC, 889 Pender Street, Vancouver, Canada.

Farley, E.V., Jr., B.W. Wing, A. Middleton, J. Pohl, L. Hulbert, M. Trudel, J. Moss, T. Hamilton, E. Parks, C. Lagoudakis, and D. McCallum. 2002. Eastern Bering Sea (BASIS) Coastal Research (August–2002) on Juvenile Salmon. Doc. 678, 27 p. NPAFC, 889 Pender Street, Vancouver, Canada.

⁸ Crawford, D. L., and F. W. West. 2001. Bristol Bay sockeye salmon smolt studies for 2000. Reg. Info. Rept. 2A01-12, 164 p. Alaska Dept. Fish Game, 333 Raspberry Road, Anchorage, AK.

Difference in growth by ocean age

Barber and Walker (1988) reported that peak SW2 scale growth for Bristol Bay sockeye salmon (Ugashik stock) was less than peak growth during SW1 and SW3. They suggested that this trend reflected lower prey availability for sockeye salmon in the North Pacific Ocean than in the Bering Sea (Mackas and Tsuda, 1999). But Bristol Bay sockeye salmon also develop in the Bering Sea during their second growing season (French et al., 1976; Myers et al.³). Kvichak and Egegik sockeye salmon scales, 1955–2000, exhibited relatively low growth throughout SW2 year compared to SW1 and SW3 years. We suggest that low SW2 growth may also be related to the inability of sockeye salmon to efficiently capture large prey (Aydin, 2000) and to a lower bioenergetic efficiency when consuming smaller prey. Salmon in their third year at sea may experience greater prey availability and capture efficiency because they are larger.

Late season growth of ocean age-2 sockeye salmon during SW2 was significantly greater than that of ocean age-3 sockeye salmon. This finding indicates that the greater size-at-age of ocean age-2 sockeye salmon compared to ocean age-3 sockeye salmon at the end of the second growing season (French et al., 1976) may be largely related to increased growth during the later portion of the second growing season at sea.

Conclusions

Seasonal scale growth patterns of Kvichak and Egegik sockeye salmon exhibited significant differences in SW2 and SW3 scale growth during odd- versus even-numbered years. Differences in scale growth did not begin until after peak scale growth and difference began somewhat later for younger SW2 sockeye salmon. The persistence of this pattern over the past 45 years may be caused by pink salmon, especially those from eastern Kamchatka that are highly abundant during odd-numbered years. During odd-numbered years, pink salmon reduced prey abundance prior to migrating to coastal areas in June and July (Shimamoto et al., 1997; Sugimoto and Tadokoro, 1997). This prey reduction, coupled with declining abundance and ontogenetic vertical migrations of some zooplankton (Mackas and Tsuda, 1999), appears to have influenced (reduced) growth of sockeye salmon from early summer through fall of odd-numbered years. We hypothesize that the alternating odd- and even-year growth pattern of sockeye salmon may be reinforced by the one- or two-year life cycle of prey, such as squid, whose abundance may be out-of-phase with the two-year cycle of pink salmon. These data, coupled with previous findings of reduced smolt-to-adult survival of sockeye salmon that interacted with odd-year pink salmon during the second year at sea (Ruggerone et al., 2003), indicate that reduced growth of salmon during the second year at sea can lead to measurable salmon mortality. Sockeye mortality associated with pink salmon likely occurs during winter when demand

for prey by salmon exceeds the low availability of prey (Aydin, 2000), but it may also occur in response to size-selective predation. Our study indicates that salmon growth and survival are influenced by complex food web interactions, which are likely to significantly shift under various scenarios of climate change that affect temperature, CO₂, and phytoplankton community structure of the Bering Sea (Hare et al.⁹).

Acknowledgments

We appreciate the efforts of biologists and technicians of the Alaska Department of Fish and Game who collected salmon scales and associated data, and B. Agler and D. Oxman who helped compile the data. S. Goodman assisted with graphics. The manuscript benefited from comments provided by N. Davis, G. Duker, and two anonymous reviewers. This study was funded by the Global Change Program, Biological Resources Division, U.S. Geological Survey.

Literature cited

- Anderson, P. J., and J. F. Piatt.
1999. Community reorganization in the Gulf of Alaska following ocean climate regime shift. *Mar. Ecol. Progr. Ser.* 189:117–123.
- Aydin, K. Y.
2000. Trophic feedback and carrying capacity of Pacific salmon (*Oncorhynchus* spp.) on the high seas of the Gulf of Alaska. Ph.D. diss., 396 p. Univ. Washington, Seattle, WA.
- Azumaya, T., and Y. Ishida.
2000. Density interactions between pink salmon (*Oncorhynchus gorbuscha*) and chum salmon (*O. keta*) and their possible effects on distribution and growth in the North Pacific Ocean and Bering Sea. *North Pacific Anadr. Fish Comm. Bull.* 2:165–174.
- Barber, W. E., and R. J. Walker.
1988. Circuli spacing and annulus formation: is there more than meets the eye? The case for sockeye salmon, *Oncorhynchus nerka*. *J. Fish Biol.* 32:237–245.
- Batten, S. D., D. W. Welch, and T. Jonas.
2003. Latitudinal differences in duration of development of *Neocalanus plumchrus* copepodites. *Fish. Oceanogr.* 12:201–208.
- Beamish, R. J., and D. R. Bouillon.
1993. Pacific salmon production trends in relation to climate. *Can. J. Fish Aquat. Sci.* 50:1002–1016.
- Beamish, R. J., and C. Mahnken.
2001. A critical size and period hypothesis to explain natural regulation of salmon abundance and linkage to climate and climate change. *Progr. Oceanogr.* 49: 423–437.
- ⁹ Hare, C. E., G. R. DiTullio, P. D. Torell, R. M. Kudela, Y. Zhang, K. Leblanc, S. F. Riseman, and D. A. Hutchins. 2004. Experimental determination of climate change effects on Bering Sea biogeochemistry and phytoplankton community structure. *Am. Soc. of Limnology and Oceanography and The Oceanography Society Ocean Research 2004 Conference*; 15–20 February 2004, Honolulu, HI, 1 p.

- Bigler, B. S., D. W. Welch, and J. H. Helle.
1996. A review of size trends among North Pacific salmon (*Oncorhynchus* spp.). *Can. J. Fish. Aquat. Sci.* 53: 445-465.
- Bilton, H. T.
1975. Factors affecting the formation of scales. *Int. North Pacific Fish. Comm. Bull.* 32:102-108.
- Bilton, H. T., and S. A. M. Ludwig.
1966. Times of annulus formation on scales of sockeye, pink, and chum salmon in the Gulf of Alaska. *J. Fish. Res. Board Can.* 23:1403-1410.
- Birman, I. B.
1960. Times of formation of annuli on the scales of Pacific salmon, and the rate of growth of pink salmon. (Doklady Akad. Nauk SSSR 132:1187-1190). *Transl. Fish Res. Board Can.* No. 327.
- Brodeur, R. D., B. W. Frost, S. R. Hare, R. C. Francis, and W. J. Ingraham Jr.
1996. Interannual variations in zooplankton biomass in the Gulf of Alaska, and covariation with California current zooplankton biomass. *Calif. Coop. Oceanic Invest. Rep.* 37:80-99.
- Brodeur, R. S., McKinnell, K. Nagasawa, W. Pearcy, V. Radchenko, and N. Takagi.
1999. Epipelagic nekton of the North Pacific subarctic and transition zones. *Progr. Oceanogr.* 43:365-397.
- Brodeur, R. D., and D. M. Ware.
1992. Long-term variability in zooplankton biomass in the subarctic Pacific Ocean. *Fish. Oceanogr.* 1:32-38.
- Clutter, R. L., and L. E. Whitesel.
1956. Collection and interpretation of sockeye salmon scales. *Bull. Int. Pac. Salmon Fish. Comm.* 9, 159 p.
- Coyle, K. O., V. G. Chavtur, and A. I. Pinchuk.
1996. Zooplankton of the Bering Sea: a review of Russian-language literature. *In Ecology of the Bering Sea: a review of Russian literature* (O. A. Mathisen, K. O. Coyle, eds.), p. 97-133. Alaska Sea Grant, Fairbanks, AK.
- Davis, N. D.
2003. Feeding ecology of Pacific salmon (*Oncorhynchus* spp.) in the central North Pacific Ocean and central Bering Sea, 1991-2000. Ph.D. diss., 190 p. Hokkaido Univ., Hakodate, Japan.
- Davis, N. D., K. Y. Aydin, and Y. Ishida.
2000. Diel catches and food habits of sockeye, pink, and chum salmon in the central Bering Sea in summer. *North Pacific Anadr. Fish Comm. Bull.* 2:99-109.
- Davis, N., K. W. Myers, R. V. Walker, and C. K. Harris.
1990. The Fisheries Research Institute's high seas salmonid tagging program and methodology for scale pattern analysis. *Am. Fish. Soc. Symp.* 7:863-879.
- Francis, R. C., S. R. Hare, A. B. Hollowed, and W. S. Wooster.
1998. Effects of interdecadal climate variability on the oceanic ecosystems of the NE Pacific. *Fish. Oceanogr.* 7:1-21.
- French, R., H. Bilton, M. Osako, and A. Hartt.
1976. Distributions and origin of sockeye salmon (*Oncorhynchus nerka*) in offshore waters of the North Pacific Ocean. *Int. North Pacific Fish. Comm. Bull.* 34:1-113.
- Fukuwaka, M.
1998. Scale and otolith patterns prove history of Pacific salmon. *North Pacific Anadr. Fish Comm. Bull.* 1: 190-198.
- Fukuwaka, M., and M. Kaeriyama.
1997. Scale analyses to estimate somatic growth in sockeye salmon, *Oncorhynchus nerka*. *Can. J. Fish. Aquat. Sci.* 54:631-636.
- Groot, C., and L. Margolis.
1991. Pacific salmon life histories, 564 p. UBC Press, Vancouver, British Columbia, Canada.
- Hartt, A. C., and M. B. Dell.
1986. Early oceanic migrations and growth of juvenile Pacific salmon and steelhead trout. *Int. North Pacific Fish. Comm. Bull.* 46:1-105.
- Ishida, Y., S. Ito, Y. Ueno, and J. Sakai.
1998. Seasonal growth patterns of Pacific salmon (*Oncorhynchus* spp.) in offshore waters of the North Pacific Ocean. *North Pacific Anadr. Fish Comm. Bull.* 1:66-80.
- Juanes, F.
1994. What determines prey size selectivity in piscivorous fishes? *In Theory and application in fish feeding ecology* (D. J. Stouder, K. L. Fresh, and R. J. Feller, eds.), p. 79-100. Univ. South Carolina Press, Columbia, SC.
- Kaeriyama, M., M. Nakamura, R. Edpalina, J. R. Bower, M. Yamaguchi, R. V. Walker, and K. W. Myers.
2004. Change in the feeding ecology and trophic dynamics of Pacific salmon (*Oncorhynchus* spp.) in the central Gulf of Alaska in relation to climate events. *Fish. Oceanogr.* 13:197-207.
- Koo, T. S. Y.
1962. Age and growth studies of red salmon scales by graphical means. *In Studies of Alaska red salmon* (T.S.Y. Koo, ed.), p. 49-121. *Publ. Fish., New Series 1*, University of Washington, Seattle.
- Mackas, D. L., R. Goldblatt, and A. G. Lewis.
1998. Interdecadal variation in developmental timing of *Neocalanus plumchrus* populations at Ocean Station P in the subarctic North Pacific. *Can. J. Fish. Aquat. Sci.* 55:1878-1893.
- Mackas, D. L., and A. Tsuda.
1999. Mesozooplankton in the eastern and western subarctic Pacific: community structure, seasonal life histories, and interannual variability. *Progr. Oceanogr.* 43:335-363.
- Martinson, E. C., and J. H. Helle.
2000. Time of annulus formation of chum salmon in the North Pacific Ocean in 1998 and 1999. *North Pacific Anadr. Fish Comm. Bull.* 2:13-144.
- Nagasawa, K.
1998. Predation by salmon sharks (*Lamna ditropis*) on Pacific salmon (*Oncorhynchus* spp.) in the North Pacific Ocean. *North Pacific Anadr. Fish Comm. Bull.* 1:419-433.
2000. Winter zooplankton biomass in the Subarctic North Pacific, with a discussion on overwintering survival strategy of Pacific salmon (*Oncorhynchus* spp.). *North Pacific Anadr. Fish Comm. Bull.* 2:21-32.
- Napp, J. M., C. T. Baier, R. D. Brodeur, K. O. Coyle, N. Shiga, and K. Mier.
2002. Interannual and decadal variability in zooplankton communities of the southeastern Bering Sea shelf. *Deep-Sea Res. Series II* 49: 5991-6008.
- Nesis, K. N.
1997. Gonatid squids in the subarctic North Pacific: ecology, biogeography, niche diversity and role in the ecosystem. *Adv. Mar. Ecol.* 32: 245-324.
- Pearcy, W. G., K.Y. Aydin, and R. D. Brodeur.
1999. What is the carrying capacity of the North Pacific Ocean for salmonids. *PICES Press* 7:17-23.

- Pearcy, W. G., R. D. Brodeur, J. Shenker, W. Smoker, and Y. Endo.
1988. Food habits of Pacific salmon and steelhead trout, midwater trawl catches, and oceanographic conditions in the Gulf of Alaska, 1980-1985. *Bull. Ocean. Res. Inst.* 26:29-78.
- Peterman, R. M.
1984. Density-dependent growth in early ocean life of sockeye salmon (*Oncorhynchus nerka*). *Can. J. Fish. Aquat. Sci.* 41:1825-1829.
- Rogers, D. E.
1984. Trends in abundance of Northeastern Pacific stocks of salmon. *In* The influence of ocean conditions on the production of salmonids in the North Pacific (W. G. Pearcy, ed.), p. 100-127. Oregon State Univ., Corvallis, OR.
1987. The regulation of age at maturity in Wood River sockeye salmon (*Oncorhynchus nerka*). *Can. Spec. Publ. Fish. Aquat. Sci.* 96:78-89.
- Rogers, D. E., and G. T. Ruggerson.
1993. Factors affecting the marine growth of Bristol Bay sockeye salmon. *Fish. Res.* 18:89-103.
- Ruggerson, G. T., J. Nielsen, E. Farley, S. Ignell, P. Hagen, B. Agler, D. Rogers, J. Bumgarner.
2002. Long-term trends in annual Bristol Bay sockeye salmon scale growth at sea in relation to sockeye abundance and environmental trends, 1955-2000. *In* Technical report 4: Joint meeting on causes of marine mortality of salmon in the North Pacific and North Atlantic oceans and in the Baltic Sea (IBSFC, NASCO, NPAFC, PICES, eds.), p. 56-58. NPAFC, Vancouver, B.C.
- Ruggerson, G. T., M. Zimmermann, K. W. Myers, J. L. Nielsen, and D. E. Rogers.
2003. Competition between Asian pink salmon (*Oncorhynchus gorbuscha*) and Alaskan sockeye salmon (*O. nerka*) in the North Pacific Ocean. *Fish. Oceanogr.* 12:209-219.
- Shiomoto, A., K. Tadokoro, K. Nagasawa, and Y. Ishida.
1997. Trophic relations in the subarctic North Pacific ecosystem: possible feeding effect from pink salmon. *Mar. Ecol. Progr. Ser.* 150:75-85.
- Sinyakov, S. A.
1998. Stock conditions of Pacific salmon in Kamchatka and its fisheries management. *Nat. Res. Inst. Far Seas Fish., Salmon Report Series* 45:281-293.
- Sobolevsky, Y. I.
1996. Species composition and distribution of squids in the western Bering Sea. *In* Ecology of the Bering Sea: a review of Russian literature (O. A. Mathisen and K. O. Coyle, eds.), p. 135-141. Alaska Sea Grant, Fairbanks, AK.
- Straty, R. R.
1981. Trans-shelf movements of Pacific salmon. *In* The Eastern Bering Sea shelf: oceanography and resources (D. W. Hood and J. A. Calder, eds.), p. 575-610. NOAA, Dept. Commerce, Washington D.C.
- Sugimoto, T., and K. Tadokoro.
1997. Interannual-interdecadal variations in zooplankton biomass, chlorophyll concentration and physical environment in the subarctic Pacific and Bering Sea. *Fish. Oceanogr.* 6:74-93.
- Takagi, K., K. V. Aro, A. C. Hartt, and M. B. Dell.
1981. Distributions and origin of pink salmon (*Oncorhynchus gorbuscha*) in offshore waters of the North Pacific Ocean. *Int. North Pacific Fish. Comm. Bull.* 40:1-195.
- Walker, R. V., K. W. Myers, and S. Ito.
1998. Growth studies from 1956-95 collections of pink and chum salmon scales in the central North Pacific Ocean. *North Pacific Anadr. Fish Comm. Bull.* 1:54-65.
- Welch, D. W., and T. R. Parsons.
1993. ^{13}C , ^{15}N values as indicators of trophic position and competitive overlap for Pacific salmon (*Oncorhynchus* spp.). *Fish. Oceanogr.* 2:11-23.

Abstract—Distribution of eggs and larvae and feeding and growth of larvae of Japanese Spanish mackerel (*Scomberomorus niphonius*) were investigated in relation to their prey in the Sea of Hiuchi, the Seto Inland Sea, Japan, in 1995 and 1996. The abundance of *S. niphonius* eggs and larvae peaked in late May, corresponding with that of clupeid larvae, the major prey organisms of *S. niphonius* larvae. The eggs were abundant in the northwestern waters and the larvae were abundant in the southern waters in late May in both years, indicating a southward drift during egg and yolk sac stages by residual flow in the central part of the Sea of Hiuchi. Abundance of clupeid larvae in southern waters, where *S. niphonius* larvae were abundant, may indicate a spawning strategy on the part of first-feeding *S. niphonius* larvae to encounter the spatial and temporal peak in ichthyoplankton prey abundance in the Seto Inland Sea. Abundance of the clupeid larvae was higher in 1995 than in 1996. Feeding incidence (percentage of stomachs with food; 85.3% in 1995 and 67.7% in 1996) and mean growth rate estimated from otolith daily increments (1.05 mm/d in 1995 and 0.85 mm/d in 1996) of *S. niphonius* larvae in late May were significantly higher in 1995. Young-of-the-year *S. niphonius* abundance and catch per unit of fishing effort of 1-year-old *S. niphonius* in the Sea of Hiuchi was higher in 1995, indicating a more successful recruitment in this year. Spatial and temporal correspondence with high ichthyoplankton prey concentration was considered one of the important determinants for the feeding success, growth, and survival of *S. niphonius* larvae.

Distribution, feeding condition, and growth of Japanese Spanish mackerel (*Scomberomorus niphonius*) larvae in the Seto Inland Sea

Jun Shoji

Masaru Tanaka

Laboratory of Estuarine Ecology
Field Science Education and Research Center
Kyoto University
Kita-shirakawa, Sakyo, Kyoto 606-8502, Japan
E-mail address (for J. Shoji) shoji@kais.kyoto-u.ac.jp

Scomid fishes are considered to have adopted a survival strategy characterized by fast growth and the ability to consume large prey at an early age (Hunter, 1981). Their larvae have morphological features such as large eyes and mouths, with which piscivory and fast growth can be achieved in early life stages. Among scombrids, extremely early piscivory and fast growth have been observed in the early life stages of Spanish mackerels (*Scomberomorus* fishes). Fish larvae were dominant in stomachs of *Scomberomorus* larvae in three regions: 1) *S. semifasciatus*, *S. queenslandicus*, and *S. commerson*, in Australian waters (Jenkins et al., 1984), 2) Spanish mackerel (*S. maculatus*) and king mackerel (*S. cavalla*) in the southeastern United States (Finucane et al., 1990), and 3) Japanese Spanish mackerel (*S. niphonius*) in the Seto Inland Sea, Japan (Shoji et al., 1997). Larval growth rate was reported to be approximately 1.0 mm/d in king and Spanish mackerels (DeVries et al., 1990; Peters and Schmidt, 1997) and *S. niphonius* (Shoji et al., 2001). Tanaka et al. (1996) demonstrated precocious development of an adult-type digestive system (with a functional stomach and pyloric caecum) occurred in first feeding *S. niphonius* larvae. They suggested that *Scomberomorus* fish have adopted a specialized feeding strategy, namely piscivory and fast growth from the time of first

feeding, which reduces the duration of the larval stage, the period of greatest vulnerability to predation (Houde, 1987).

Ichthyoplankton prey seem to be indispensable for growth and survival during larval period of *Scomberomorus* fish. Under laboratory conditions, Fukunaga et al. (1982) reported that *S. niphonius* larvae preferred fish larvae to invertebrate plankton prey (rotifer and *Artemia* nauplii). Shoji and Tanaka (2001) demonstrated that *S. niphonius* larvae began to cannibalize siblings when they were supplied with only invertebrate plankton prey. *Scomberomorus* larvae would need to exert greater searching effort and to swim fast to capture ichthyoplankton prey because they are larger and much less abundant in water than invertebrate plankton prey (Sheldon et al., 1972). *Scomberomorus* larvae with a high swimming performance have been shown to have high levels of larval mortality due to starvation. Margulies (1993) demonstrated by histological analysis that Pacific sierra (*S. sierra*) larvae could not survive beyond 48 hours without feeding in the Panama Bight. Shoji et al. (2002) observed that the point-of-no-return for *S. niphonius* larvae was one day after first feeding in laboratory experiments. *Scomberomorus niphonius* larvae fed after 1- or 2-days starvation showed significantly retarded growth during the following period

of adequate feeding compared to fish that had been fed from the time of first feeding. These observations suggest that ichthyoplankton prey availability can strongly influence growth and survival of *S. niphonius* larvae.

Scomberomorus niphonius is distributed in the coastal waters of Japan and supports important commercial fisheries in the Seto Inland Sea. The total catch exceeded 6000 metric tons (t) in the middle 1980s but decreased to less than 1000 t in the late 1990s in the Seto Inland Sea. Spawning migration of *S. niphonius* into the Seto Inland Sea occurs in May (Kishida and Aida, 1989) and the larvae are distributed in May and June in the Sea of Hiuchi, the central Seto Inland Sea (Kishida, 1988). In order to ensure that catches remain at stable levels and to establish more efficient fisheries management, it is necessary to accumulate biological information to elucidate the recruitment process of the species.

The objective of the present study is 1) to investigate spatial and temporal distribution of *S. niphonius* larvae and their prey and 2) to compare feeding conditions and growth of *S. niphonius* larvae for two consecutive years with contrasting levels of recruitment, 1995 and 1996, in the Seto Inland Sea, Japan. The catch-per-unit-of-fishing-effort (CPUE: no. of fish/boat/day) of 1-year-old *S. niphonius* (Fig. 1) fished by drift gill net in May, the major fishing season for the species, at the Kawarazu Fisherman's Association (Fig. 2) has been used as a recruitment index in the Sea of Hiuchi (Kishida, 1991). The CPUE fluctuated tenfold in the 1990s (Ehime Prefecture Chuyo Fisheries Experimental Station Toyo Branch¹) and indicated recruitment in 1995 was more successful. Egg, larval, and larval prey distributions, larval feeding incidence and growth, and young-of-the-year (YOY) fish abundance were investigated in 1995 and 1996 in the Sea of Hiuchi.

Materials and methods

Ichthyoplankton sampling

Three research cruises were carried out in 1995 (11–16 April, 24–28 May, and 20–23 June) and in 1996 (10–13 May, 27–30 May, and 18–21 June) in the Sea of Hiuchi (Fig. 2). Ichthyoplankton sampling and hydrographic survey were conducted from the RV *Shirafuji* (138 t) of the National Research Institute of Fisheries and Environment of Inland Sea (NRIFEIS). Double oblique tows from the surface to 5 m above the bottom were made by using a bongo net (0.7-m diameter, 0.315-mm mesh) at 80 stations during the cruises in 1995 and at 50 stations in 1996. Average depth of the Sea of Hiuchi is approximately 17.8 m (Montani, 1996). *Scomberomorus*

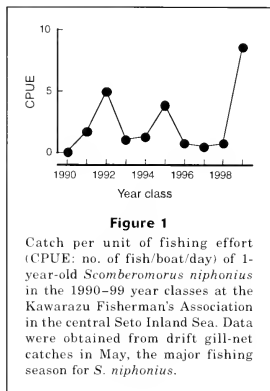


Figure 1

Catch per unit of fishing effort (CPUE: no. of fish/boat/day) of 1-year-old *Scomberomorus niphonius* in the 1990–99 year classes at the Kawarazu Fisherman's Association in the central Seto Inland Sea. Data were obtained from drift gill-net catches in May, the major fishing season for *S. niphonius*.

niphonius larvae were quickly sorted from the samples and were preserved in 95% ethanol. Other ichthyoplankton were fixed in 10% formalin seawater for sorting in the laboratory. Flow meters were mounted in the mouth of the net to determine the filtered volume. Each tow followed a salinity-temperature-depth sensor cast to measure the water temperature and salinity profiles at each station.

YOY fish abundance

YOY *S. niphonius* have been reported to occur in the southern part of the Sea of Hiuchi from late June to early July (Watanabe, 1994). To detect a potential difference in *S. niphonius* recruitment abundance between 1995 and 1996, YOY fish abundance was assessed in the southern part of the Sea of Hiuchi. YOY *S. niphonius* were collected from catches by a seine fishery in the southern part of the Sea of Hiuchi (Fig. 2). The seine fishery primarily targets young and adult Japanese anchovy (*Engraulis japonicus*). The codend of the net has a 2-mm mesh aperture and was towed by two boats for about 1 hour at a ship velocity of 3 to 4 knots. Two to 10 kg of the catch by the seine fishery was sampled weekly (five times each year) from mid June to late July in 1995 and 1996. YOY abundance was expressed as the number of *S. niphonius* per 10 kg of the catch.

Laboratory procedures

Larval SL was measured to the nearest 0.1 mm, and stomach contents were identified under a dissecting microscope. After removal of *S. niphonius* larvae, the bongo-net samples were processed to estimate concentrations (no./100 m²) of *S. niphonius* eggs. Larvae of two

¹ Ehime Prefecture Chuyo Fisheries Experimental Station Toyo Branch, 2000. Unpubl. data. Kawarazu, Toyo, Ehime 799-1303, Japan.

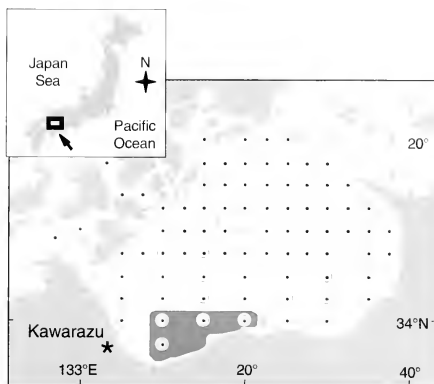


Figure 2

Map of the Sea of Hiuchi, central Seto Inland Sea, showing the sampling stations where ichthyoplankton were collected with a bongo net during the three cruises in 1995 (closed small circles) and in 1996 (large open circles). Catch data for 1-year-old *S. niphonius* were obtained at Kawarazu Fisherman's Association (asterisk). Young-of-the-year Japanese Spanish mackerel were collected by the seine fishery in the southern waters indicated by the shaded area.

clupeid species, gizzard shad (*Konosirus punctatus*) and Japanese sardine (*Sardinops melanostictus*), that were the major prey organisms of the post-first-feeding *S. niphonius* larvae (see "Results" section) were counted to estimate prey concentrations.

Scomberomorus niphonius larvae were aged by counting daily increments on otoliths. Right-side sagittal otoliths were removed under a dissecting microscope and the number of increments on the otolith were counted using an image-analysis system (ARP, version 4.21, Ratoc System Engineering Co., Ltd., Tokyo, Japan) connected to a compound light microscope at 400 to 1000 \times magnification. Daily increments begin to be deposited on the sagittal otoliths of *S. niphonius* larvae at first feeding (Shoji and Tanaka, 2004). *Scomberomorus niphonius* larvae initiate feeding on day 5 under 19.0 $^{\circ}$ C (Shoji et al., 2001). Larval age was therefore estimated by adding five to the increment count because the water temperature in the southern part of the Sea of Hiuchi where *S. niphonius* larvae were abundant ranged between 18 $^{\circ}$ and 20 $^{\circ}$ C (see "Results" section) in late May. Data from cruises in late May only (the second cruise in both years) were included in the feeding and growth analyses because no *S. niphonius* larvae were collected during the first cruise and too few were collected during the third cruise in both years.

Results

Physical environment

The surface water temperature was higher in the southeastern area and lower in the northwestern area in all cruises. Mean surface temperatures (\pm SD) were 12.3 $^{\circ}$ (\pm 0.4), 18.6 $^{\circ}$ (\pm 1.2), and 20.5 $^{\circ}$ (\pm 0.6) $^{\circ}$ C in 11–16 April, 24–28 May, and 20–23 June, 1995, and were 14.3 $^{\circ}$ (\pm 0.6), 19.0 $^{\circ}$ (\pm 1.3), and 19.4 $^{\circ}$ (\pm 1.0) $^{\circ}$ C in 10–13 May, 27–30 May, and 18–21 June 1996, respectively (Fig. 3). Salinity ranged between 32.5 and 34.3 ppt and was lower in the southeastern area in all cruises. In late May, during the seasonal peak in abundance of *S. niphonius* larvae, the mean surface temperature was slightly higher in 1996 although there was no significant difference between the two years (ANOVA: $F=3.14$, $P=0.08$).

Scomberomorus niphonius eggs and larvae

A total of 1018 eggs and 272 larvae of *S. niphonius* were collected during the cruises. No eggs and larvae of *S. niphonius* were collected during the first cruise in both years. The egg and larval abundance peaked in late May and decreased thereafter in both years (Fig. 4, A and B). The eggs were abundant in the northwestern waters in

late May where the surface temperature was between 17° and 19°C (Fig. 5). The larvae were abundant in the middle to southern waters, where the surface temperature was between 18° and 20°C in late May (Fig. 6). There was no significant difference in egg and larval abundance in late May between the two years (ANOVA: $F=0.03$, $P=0.87$ for eggs; $F=0.02$, $P=0.89$ for larvae).

Clupeid larvae

Of the 107,252 larvae collected throughout the cruises, clupeid larvae were most dominant, accounting for 57.2% in number. Gizzard shad and Japanese sardine larvae accounted for 76.4% and 23.6% of clupeid larvae, respectively. A seasonal change in abundance of clupeid larvae and a peak in abundance in late May in both years were evident (Fig. 4C). Maximum abundance (no./m²) was more than 400 in late May in 1995 in the southern

waters and there was no station where the abundance exceeded 300/m² in 1996 (Fig. 7). The difference in abundance of clupeid larvae in late May between the two years was significant (ANOVA: $F=8.12$, $P=0.005$).

Feeding

Clupeid larvae (gizzard shad, Japanese sardine, and unidentified clupeid larvae) were the most dominant items in the stomachs of *S. niphonius* larvae (Table 1). Feeding incidence (percentage of stomachs with food) was significantly higher in 1995 than in 1996 (chi square test; $df=1$, $\chi^2=8.538$, $P=0.0035$).

Growth

Age of *S. niphonius* larvae collected in late May in 1995 and 1996 was estimated to be between 5 and 14 days

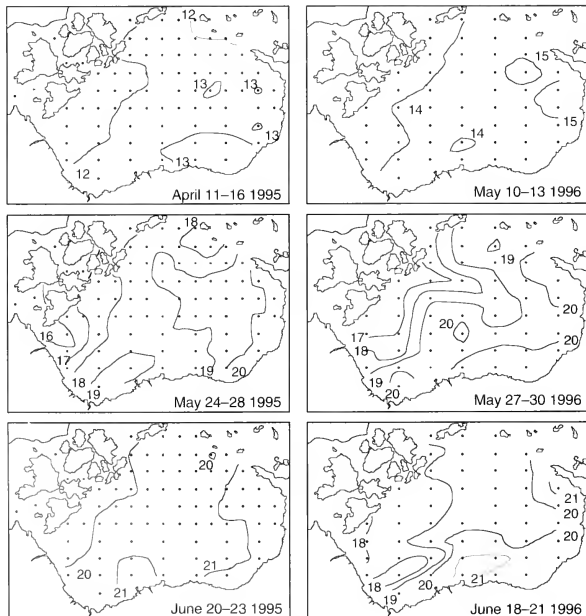


Figure 3

Contour plots of the surface water temperature (°C) of the Sea of Hiuchi during the three cruises in 1995 and 1996.

after hatching. Relationships between larval age (A) and SL (L , mm) were best described by a linear regression for each year (Fig. 8):

$$1995: L = 1.05A - 1.39 \quad (n=102, r^2=0.87, P<0.0001)$$

$$1996: L = 0.85A - 0.15 \quad (n=93, r^2=0.80, P<0.0001).$$

The slope of the equation for 1995 was significantly higher than that for 1996 (ANCOVA: $df=1$, $F=11.01$, $P=0.001$).

YOY *S. niphonius* abundance

YOY *S. niphonius* (14.6–122.8 mm in TL) were collected by the seine fishery in the Sea of Hiuchi from late June through late July in 1995 and 1996. Mean (\pm SE) abundance of YOY *S. niphonius* in 1995 (7.7 [\pm 2.1] individuals/m²) was significantly higher than that in 1996 (0.6 [\pm 0.4] individuals/m²; Mann-Whitney U -test; $P=0.006$, Fig. 9).

Discussion

Spawning strategy

Abundance of *S. niphonius* eggs and larvae peaked in late May in 1995 and 1996. A similar pattern was observed in the abundance of clupeid larvae, indicating that spawning of *S. niphonius* was synchronized with

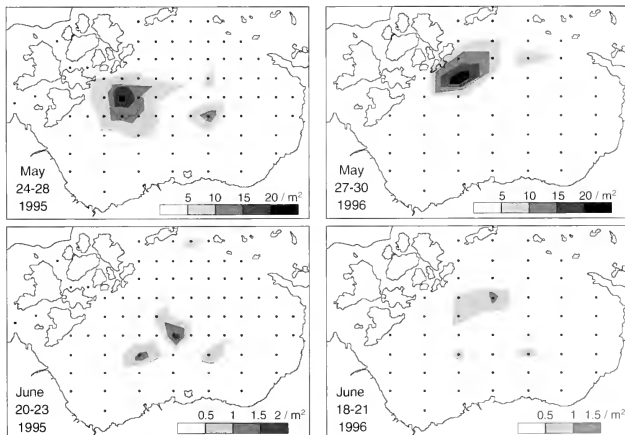
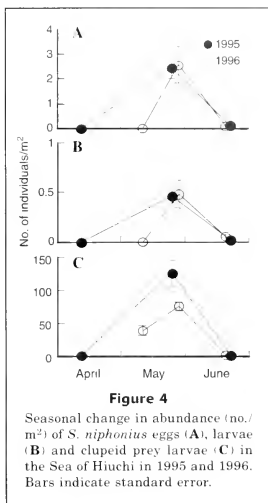


Figure 5
Horizontal distribution of *S. niphonius* eggs in the Sea of Hiuchi in 1995 and 1996.

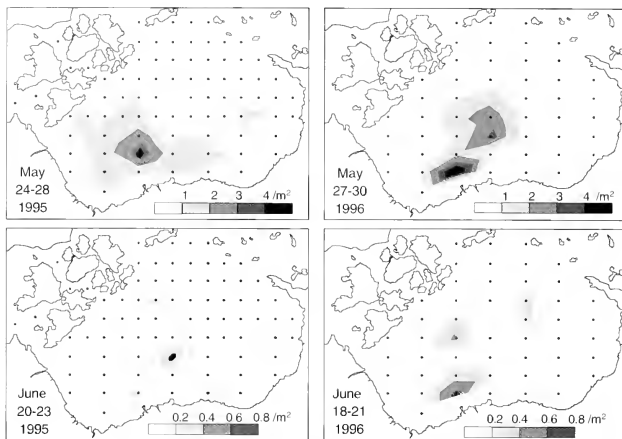


Figure 6

Horizontal distribution of *S. niphonius* larvae in the Sea of Hiuchi in 1995 and 1996.

that of clupeid fishes in the central Seto Inland Sea. Piscivorous fishes tend to spawn earlier than other fishes in freshwater ecosystems so that they attain sufficient size to enable consumption of other young fishes by the onset of piscivory (Keast, 1985). Because *S. niphonius* larvae are piscivorous from the first feeding stage, spawning that is synchronized with the seasonal peak in abundance of clupeid larvae would be advantageous for survival of *S. niphonius* larvae.

Larvae of *S. niphonius* were abundant in the southern part of the Sea of Hiuchi in late May 1995 and 1996 while eggs were abundant in the northwestern waters during the same season. This difference in horizontal distribution patterns of eggs and larvae seems to be associated with the drift by a residual flow (current) from northern to southern waters. In the central part of the Sea of Hiuchi, a residual flow in the middle (5–15 m) layers proceeds southward at a speed of about 5 cm/s (=4.32 km/d; Yanagi et al., 1995). Yolksac larvae of *S. niphonius* are abundant in the 5- to 10-m layers in the Sea of Hiuchi (Kishida, 1988) and do not exhibit diel vertical migration (Shoji et al., 1999). The horizontal distance between the stations with the highest egg and larval abundance in late May was approximately 15 km in 1995 and 20 km in 1996. Given that the yolksac stage is five days for mackerel larvae under 19°C (Shoji et al., 2001), drift distance while larvae are entrained in the southward residual flow during the yolksac stage would be estimated to be approximately 20 km. The estimate for the drift distance during the yolksac stage

Table 1

Feeding incidence (percentage of stomachs with prey) and stomach contents of *S. niphonius* larvae collected in late May of 1995 and 1996 in the Sea of Hiuchi.

	1995	1996
No. of larvae examined	102	93
No. of larvae feeding	87	63
Feeding incidence (%)	85.3	67.7
Size range (SL, mm)	4.2–13.8	4.5–14.2
Stomach contents		
	<i>n</i>	<i>n</i>
<i>Sardinops melanostictus</i>	4	2
<i>Konosirus punctatus</i>	21	14
Unidentified clupeids	19	11
<i>Engraulis japonicus</i>	2	4
Unidentified Clupeiformes	34	22
Mugilidae	3	2
Gobiidae	13	9
Total	96	64

approximates the horizontal distance between the stations of egg and larval highest abundance. It is therefore plausible that the larvae were transported by the southward residual flow to the southern part of the Sea

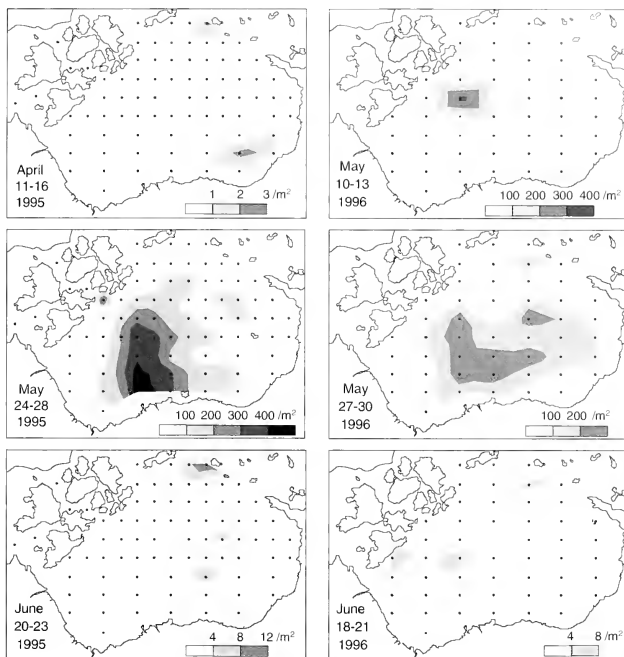


Figure 7

Horizontal distribution of clupeid larvae in the Sea of Hiuchi during the three cruises in 1995 and in 1996.

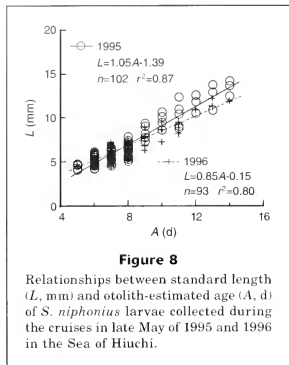
of Hiuchi where clupeid larva concentration was high in late May. We suggest that spawning of *S. niphonius* in the northern part of the Sea of Hiuchi would enable their first-feeding larvae to meet high prey abundance in the southern part.

Significance of high ichthyoplankton prey

Water temperature and prey concentration would be possible factors that can influence growth rates of *S. niphonius* larvae. In aquaria, the mean absolute growth rate of *S. niphonius* larvae fluctuated between 0.87 and 1.28 mm/d depending on temperature between 18.2° and 22.6°C (Fukunaga et al., 1982; Shoji et al., 2001). In the present study, the mean surface temperature of the Sea of Hiuchi in late May was slightly higher in 1996, although the difference was not significant.

The higher abundance of clupeid larvae in 1995 would better explain the higher larval growth rate in 1995. The mean larval growth rate in late May 1995, 1.05 mm/d, approximates those reported in aquaria at the same temperature (1.03 mm/d at 20.8°C; Fukunaga et al., 1982) where *S. niphonius* larvae were provided with an excess of prey, indicating that the prey concentration in late May 1995 met larval requirements. It is likely that the lower growth rate in late May 1996 resulted from lower prey concentration. This conclusion is supported by results of the stomach content analysis: the larval feeding incidence was significantly lower in May 1996. We conclude that clupeid larvae concentration had a significant effect on growth of the *S. niphonius* larvae.

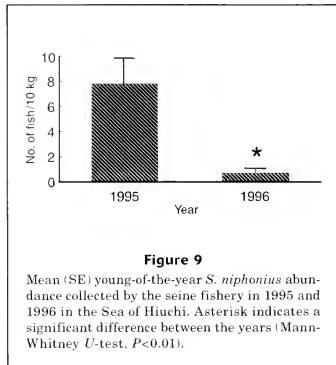
In the Sea of Hiuchi, clupeid larvae abundance greatly increased from April to May. We suggest that the prey



availability for *S. niphonius* larvae fluctuated depending for the most part on seasonal change in abundance of gizzard shad larvae that were dominant in the Sea of Hiuchi. The difference in clupeid larval abundance in late May between 1995 and 1996 may be explained by between-year difference in gizzard shad spawning stock biomass. The total catch of gizzard shad in the southern Sea of Hiuchi (coastal waters of Ehime Prefecture) in 1995 (372 t) was higher than that in 1996 (217 t: Ehime Prefecture Agriculture, Forestry and Fisheries Statistics Association, 1998).

Implications for recruitment

Variability in larval growth rate can influence survival during the larval period by affecting the length of the early life stages because total mortality is positively correlated with the length of these early life stages (Houde, 1987). Campana (1996) demonstrated a significant correlation between growth to the end of the pelagic juvenile stage (90 d) and the year-class strength of Atlantic cod on the Georges Bank and suggested that the adult cohort strength could be predicted from growth during early life stages. In the present study, egg and larval *S. niphonius* abundance during their peak-occurrence period did not differ between 1995 and 1996, whereas YOY and 1-year-old *S. niphonius* were more abundant in 1995. These results indicate more successful recruitment and higher larval growth rate in 1995 although there are no data available for years other than 1995 and 1996. Larvae of *S. niphonius* initiate feeding at 5.59 mm SL at 18.5°C (Shoji et al., 2002). Given the mean larval growth rate in 1995 (1.05 mm/d) and 1996 (0.88 mm/d), the critical period (from first feeding to the onset of schooling at the early juvenile stage, 19.6 mm SL; Masuda et al., 2003) is estimated as 13.3 days in 1995 and 16.5 days in 1996. For *S. niphonius*, even a slight increase in larval stage



duration due to retarded growth can greatly reduce larval survival because the larval daily mortality coefficient is expected to be extremely high (>0.6 ; Grimes and Kingsford, 1996). The lower recruitment of *S. niphonius* in 1996 may be partly explained by the prolonged larval period (3.2 d) which could have led to lower survival (1/6.82, assuming the daily mortality coefficient is 0.6) during the larval period of that year.

Acknowledgments

We thank M. Fukuda, N. Suzuki, N. Kohno, and the crew of RV *Shirafuji* of NRIFEIS and staff of Asagi-Suisan Co. Ltd. for their assistance with field sampling. We also thank T. Maehara and N. Murata, Ehime Prefecture Chuyo Fisheries Experimental Station Toyo Branch, and Y. Maki, Kawarazu Fisherman's Association, for their help in collecting young-of-the-year Japanese Spanish mackerel and data on the catch of 1-year-old fish. Two anonymous reviewers and M. Takahashi, National Research Institute of Fisheries Science, provided valuable comments on the manuscript.

Literature cited

- Campana, S. E.
1996. Year-class strength and growth rate in young Atlantic cod *Gadus morhua*. Mar. Ecol. Prog. Ser. 135: 21-26.
- DeVries, D., C. Grimes, K. Lang, and B. White.
1990. Age and growth of king and Spanish mackerel larvae and juveniles from the Gulf of Mexico and U.S. South Atlantic Bight. Environ. Biol. Fish. 29:135-143.
- Ehime Prefecture Agriculture and Forestry Statistics Association.
1998. Agriculture, forestry and fisheries statistics of Ehime Prefecture, fiscal 1996, 278 p. Ehime Prefec-

- ture Agriculture and Forestry Statistics Association, Matsuyama, Japan.
- Finucane, J. H., C. B. Grimes., S. P. Naughton.
1990. Diets of young king and Spanish mackerel off the southeast United States. *Northeast Gulf Sci.* 11: 145-153.
- Fukunaga, T., N. Ishibashi, and N. Mitsuhashi.
1982. Artificial fertilization and seedling propagation of Spanish mackerel. *Saibai-giken* 11:29-48.
- Grimes, C. B., and M. J. Kingsford.
1996. How do riverine plumes of different sizes influence fish larvae: do they enhance recruitment? *Mar. Freshw. Res.* 47:191-208.
- Houde, E. D.
1987. Fish early life dynamics and recruitment variability. *Am. Fish. Soc. Symp.* 2:17-29.
- Hunter, J. R.
1981. Feeding ecology and predation of marine fish larvae. *In* Marine fish larvae (R. Lasker, ed.), p. 33-77. Univ. Washington Press, Seattle, WA.
- Jenkins, G. P., N. E. Milward, and R. F. Harwick.
1984. Food of larvae of Spanish mackerels, genus *Scomberomorus* (Teleostei: Scombridae), in shelf waters of the Great Barrier Reef. *Aust. J. Mar. Freshw. Res.* 35: 477-482.
- Keast, A.
1985. The piscivore guild of fishes in small freshwater ecosystems. *Environ. Biol. Fish.* 12:119-129.
- Kishida, T.
1988. Vertical and horizontal distribution of eggs and larvae of Japanese Spanish mackerel in the central waters of the Seto Inland Sea. *Bull. Jap. Soc. Sci. Fish.* 54:1-8.
1991. Fluctuations in year-class strength of Japanese Spanish mackerel in the central Seto Inland Sea. *Bull. Jap. Soc. Sci. Fish.* 57:1103-1109.
- Kishida, T., and K. Aida.
1989. Maturation and spawning of Japanese Spanish mackerel in the central and western waters of the Seto Inland Sea. *Bull. Jap. Soc. Sci. Fish.* 55:2065-2074.
- Margulies, D.
1993. Assessment of the nutritional condition of larval and early juvenile tuna and Spanish mackerel (Pisces: Scombridae) in the Panama Bight. *Mar. Biol.* 115:317-330.
- Masuda, R., J. Shoji, S. Nakayama, and M. Tanaka.
2003. Developing of schooling behavior in Spanish mackerel *Scomberomorus niphonius* during early ontogeny. *Fisheries Sci.* 69:772-776.
- Montani, S.
1996. Relationships between environment and fisheries in the Seto Inland Sea. *In* Resource and environment of the Seto Inland Sea (T. Okaichi, S. Komori, and H. Konishi, eds.), p. 1-37. Koseisha Koseikaku, Tokyo, Japan.
- Peters, J. S., and D. J. Schmidt.
1997. Daily age and growth of larval and early juvenile Spanish mackerel, *Scomberomorus maculatus*, from the South Atlantic Bight. *Fish. Bull.* 95:530-539.
- Sheldon, R. W., A. Prakash, and W. H. Sutcliffe Jr.
1972. The size distribution of particles in the ocean. *Limnol. Oceanogr.* 17:327-340.
- Shoji, J., M. Aoyama, H. Fujimoto, A. Iwamoto, and M. Tanaka.
2002. Susceptibility to starvation by piscivorous Japanese Spanish mackerel *Scomberomorus niphonius* (Scombridae) larvae at first feeding. *Fisheries Sci.* 68:59-64.
- Shoji, J., T. Maehara, M. Aoyama, H. Fujimoto, A. Iwamoto, and M. Tanaka.
2001. Daily ration of Japanese Spanish mackerel *Scomberomorus niphonius* larvae. *Fish. Sci.* 67: 238-245.
- Shoji, J., T. Maehara, and M. Tanaka.
1999. Diel vertical movement and feeding rhythm of Japanese Spanish mackerel larvae in the central Seto Inland Sea. *Fish. Sci.* 65:726-730.
- Shoji, J., and M. Tanaka.
2001. Strong piscivory of Japanese Spanish mackerel larvae from their first feeding. *J. Fish Biol.* 59: 1682-1685.
2004. Effect of prey concentration on growth of piscivorous Japanese Spanish mackerel *Scomberomorus niphonius* larvae in the Seto Inland Sea, Japan. *J. Appl. Ichthyol.* 20:271-275.
- Tanaka, M., T. Kaji, Y. Nakamura, and Y. Takahashi.
1996. Developmental strategy of scombrid larvae: High growth potential related to food habits and precocious digestive system development. *In* Survival strategies in early life stages of marine resources (Y. Watanabe, Y. Yamashita, and Y. Oozeki, eds.), p. 125-139. A. A. Balkema, Rotterdam.
- Watanabe, A.
1994. Fish caught by seine fisheries in the Sea of Hiuchi. *Proceed. the Sea of Hiuchi Res. Meet.* 2:4-9. Ehime Prefecture Chuyo Fisheries Experimental Station, Matsuyama, Ehime, Japan.
- Yanagi, T., H. Tsukamoto, S. Igawa, and K. Shiota.
1995. Recruitment strategy of swimming crab, *Portunus trituberculatus*, in Hiuchi-nada, Japan. *Fish. Oceanogr.* 4:217-229.

Abstract—We consider estimation of mortality rates and growth parameters from length-frequency data of a fish stock and derive the underlying length distribution of the population and the catch when there is individual variability in the von Bertalanffy growth parameter L_{∞} . The model is flexible enough to accommodate 1) any recruitment pattern as a function of both time and length, 2) length-specific selectivity, and 3) varying fishing effort over time. The maximum likelihood method gives consistent estimates, provided the underlying distribution for individual variation in growth is correctly specified. Simulation results indicate that our method is reasonably robust to violations in the assumptions. The method is applied to tiger prawn data (*Penaeus semisulcatus*) to obtain estimates of natural and fishing mortality.

Maximum likelihood estimation of mortality and growth with individual variability from multiple length-frequency data

You-Gan Wang

CSIRO Mathematical and Information Sciences
65 Brockway Road
Floreat Park
Western Australia 6014, Australia
E-mail address: You-Gan.Wang@csiro.au

Nick Ellis

CSIRO Marine Research
P.O. Box 120
Cleveland, Queensland 4163, Australia

Estimation of growth and mortality is fundamental in fisheries because stock assessment and management rely on these population parameters. Length-frequency-based methods become important when aging techniques are either not possible or very expensive. Existing methods such as that of Beverton and Holt (1956) assume that recruitment is continuous and constant throughout the year, which leads to a population with an exponentially distributed age structure. Existing modifications to Beverton and Holt's method comprise some simple recruitment patterns or distributions (Ssentongo and Larkin 1973; Ebert 1980; Hoenig 1987; Wetherall et al. 1987). As pointed out by Vetter (1988), the existing methods for estimating mortality in the literature have strong limitations and disadvantages. In particular, they require the following assumptions:

- 1) each individual follows the same von Bertalanffy growth curve;
- 2) the recruitment is either continuous and constant throughout the year (as in Beverton and Holt [1956] and Wetherall et al. [1987]) or is a pulse function (as in Hoenig [1987]);
- 3) the total instantaneous mortality rate, z , is constant.

As pointed out by Sainsbury (1980), it is more realistic to allow individual variability in growth. For example, using tag-recapture data, Wang et al. (1995) found substantial individual variability for the tiger prawn species *P. semisulcatus*.

Estimation of mortality relies on the distribution of the lengths, which is determined by the age distribution, mortality rates, and the individual variability in growth rates. If individual variability in growth is ignored, an inappropriate length distribution will be generated, leading to biases in parameter estimates. It is also biologically interesting to quantify the individual variability in growth, which has important implications in fisheries management. Although it is well understood that variability leads to increased uncertainty in estimates, it is less well recognized (among the fisheries community) that variability can also lead to bias. Wang and Ellis (1998) analyzed the effect of ignoring individual variability in a simplified context of constant recruitment and a single length-frequency record. They found that, in the presence of individual variability, existing methods gave positively biased parameter estimates. More details about the background can be found in Ebert (1973), Askland (1994), and Wang and Ellis

(1998). See DeLong et al. (2001) for alternative approaches to length-frequency data where individual variability is taken into account.

In our study, we develop a new framework for analyzing length-frequency data. In particular, we incorporate 1) individual variability in growth parameters; and 2) an arbitrary recruitment function. The model is flexible enough to incorporate various sizes at recruitment and a fishing selectivity function. However, we did not use these aspects in the analysis of tiger prawn data. Some analytical expressions are derived for these generalizations. A maximum likelihood approach is developed for estimation of mortality and growth parameters. Separation of fishing mortality from natural mortality is possible only when there is substantial contrast in the effort pattern. We also require a known recruitment pattern, and sampling times are spread out so that the length-frequency data will contain information on growth and mortality. Simulation studies are carried out to determine the performance of the method. The simulated data are generated from the recruitment pattern of the brown tiger prawn (*Penaeus esculentus*) in the northern prawn fishery of Australia. Finally we apply the maximum likelihood method to length-frequency data from grooved tiger prawn data (*P. semisulcatus*) in the northern prawn fishery of Australia.

Materials and methods

The model

We assume that the growth of individuals follow a von Bertalanffy curve so that the length at age a (relative to some origin t_0) is given by

$$L(a) = L_{\infty}(1 - e^{-ka}). \quad (1)$$

In this study, age is always defined to be relative to t_0 , i.e. t_0 is absorbed into a for the purpose of identifiability. We will consider estimation of (k, L_{∞}) only because t_0 is not estimable from length-frequency data with aging data. Note that this does not mean t_0 is assumed to be 0. To provide a general treatment we relax each of the assumptions mentioned in the introduction. First we relax assumption 1 by letting the maximum length, L_{∞} , vary within the population. We denote the density function of L_{∞} as $p(x)$, which has a mean of L_{∞} and a variance of σ^2 . It is possible that recruits to the fishery have a range of sizes. To allow for this range we let the size at recruitment, L_0 , be a random variable with density function $u(s)$. In practice, one may be able to use information from other studies (such as subadult abundance) to arrive at an approximate parametric form for $u(s)$.

If $f_t(l)$ is the probability density function of L at time t , then

$$f_t(l) = \int_0^{\infty} \int_l^{\infty} p(x|L_0 = s) f_t(l|L_{\infty} = x, L_0 = s) u(s) dx ds, \quad (2)$$

where $f_t(l|L_{\infty} = x, L_0 = s)$ is the conditional probability density function of L at time t when L_{∞} is known to be x and the size at recruitment is s . Note the lower limit of the inner integral is l because L_t cannot be less than an individual's length.

Let the age (again, relative to t_0) at recruitment of an individual be A_0 . From Equation 1, we have age a at length l is $a = -k^{-1} \log(1 - l/L_{\infty})$ and hence the conditional distribution, $f_t(l|L_{\infty} = x, L_0 = s)$, which may be written as $f_t(l|x, s)$ for brevity, can be expressed by using the conditional distribution of age $h_t(a|L_{\infty} = x, A_0 = a_0)$ (see Wang et al., 1995), as

$$f_t(l|x, s) = \frac{1}{k(x-1)} h_t(-k^{-1} \log(1 - l/x) | x, a_0). \quad (3)$$

We now generalize assumptions 2 and 3 by introducing the intensity function of recruitment, $r(t)$, and the total instantaneous mortality, $z(t)$, which are arbitrary functions of time t . The total mortality would depend on time through the fishing mortality component F , where $z(t) = M + F(t)$ and M is the constant natural mortality.

The age distribution satisfies

$$h_t(a|L_{\infty} = x, A_0 = a_0) \propto \exp\left[-\int_{a_0}^a z(t - a + y) dy\right] r(t - a + a_0). \quad (4)$$

This equation states that the density of individuals of age a is proportional to the intensity of recruitment at the time when these individuals were recruited, namely $t - a + a_0$, multiplied by a reduction factor due to mortality over the intervening period. We therefore have

$$h_t(a|x, s) = h_t(a|L_{\infty} = x, A_0 = -k^{-1} \log(1 - s/x)) \times \exp\left[-\int_{-k^{-1} \log(1 - s/x)}^a z(t - a + y) dy\right] r(t - a - k^{-1} \log(1 - s/x)) \quad (5)$$

and Equation 3 becomes (after substituting for a and shifting the dummy variable y)

$$f_t(l|x, s) \propto \frac{1}{x-1} \exp\left[-\int_{-k^{-1} \log\left(\frac{x-l}{x-1}\right)}^t z(y) dy\right] r\left(t - k^{-1} \log\left(\frac{x-s}{x-1}\right)\right). \quad (6)$$

Let us consider the case of fixed recruitment length, i.e., $L_0 = l_0$, and define a parameter vector, β , consisting of (k, L_{∞}, s) , and other parameters quantifying mortality and catchability. Equation 2 then reduces to a single integral over x ,

$$f_t(l|\beta) \propto \int_l^{\infty} p(x) \exp\left[-\int_{-k^{-1} \log\left(\frac{x-l_0}{x-1}\right)}^t z(y) dy\right] r\left(t - k^{-1} \log\left(\frac{x-l_0}{x-1}\right)\right) \frac{dx}{x-1}. \quad (7)$$

A more convenient form for computation arises after changing the integration variable from the asymptotic length x to time since recruitment, $t-a+a_0$,

$$\tau = k^{-k} \log \left(\frac{x-l_0}{x-1} \right). \quad (8)$$

The expression (Eq. 7) then becomes

$$f_j(l|\beta) \approx \int_1^{\infty} p(x(\tau)) \exp \left(- \int_{t-\tau}^t z(y) dy \right) r(t-\tau) \frac{d\tau}{1-e^{-k\tau}}. \quad (9)$$

In the special case of constant recruitment, i.e., $r(t)=1$, and constant mortality, $z(t)=z$, $f_j(l|\beta)$ becomes independent of time as first obtained by Powell (1979).

Maximum likelihood estimation

Let $p_{ij}(\beta)$ be the expected proportion of individuals in the i th length class (l_{i-1} , l_i) on the j th occasion, where $i=1, 2, \dots, N$; and let n_{ij} be the corresponding observed numbers. The value of $p_{ij}(\beta)$ can be obtained from the density function $f_j(l|\beta)$ given by Equation 2. Thus

$$p_{ij}(\beta) = \frac{\int_{l_{i-1}}^{l_i} f_j(l|\beta) dl}{\int_{l_0}^{l_N} f_j(l|\beta) dl}, \quad (10)$$

in which $f_j(l|\beta)$ is the (unnormalized) density function on the j th occasion. Under a multinomial model, estimation of the parameter vector β relies on the procedure

$$\text{maximize } \sum_{i,j} n_{ij} \log p_{ij}(\beta) \text{ with respect to } \beta. \quad (11)$$

The sum is the log-likelihood function up to a constant independent of the parameters. The probability, p_{ij} , can be approximated as $f_j(l_{i+1/2})/\sum_j f_j(l_{i+1/2})$, which is the normalized value of the density function for the j th occasion at the midpoint of the i th length class.

If sampling effort is known and expected catch is assumed to be a known function of effort and population abundance, the log-likelihood function in Equation 11 can be easily modified to incorporate effort information. For example, if the total number of individuals on each occasion, $n_j = \sum_i n_{ij}$, is assumed to follow a Poisson model with overdispersion parameter v , the log-likelihood function becomes

$$\sum_{i,j} n_{ij} \log p_{ij}(\beta) + v \sum_j \left\{ n_j \log \lambda_j(\beta) - \lambda_j(\beta) \right\}, \quad (12)$$

where $\lambda_j(\beta)$ is the expected total number in the sample on the j -th occasion and depends on effort. One way to model this dependence is $\lambda_j(\beta) = \phi p_j(\beta) e_j$, where e_j is the

sampling effort, ϕ is the total abundance index over all occasions; and p_j is the expected proportion of individuals on the j th occasion (i.e., the relative abundance), so that ϕp_j is the expected catch per unit of effort. In this case we can obtain the maximum likelihood estimate of ϕ as $\sum_j n_j / \sum_j e_j p_j$. The probability, p_j , can be approximated as $\sum_i f_j(l_{i+1/2}) / \sum_i f_j(l_{i+1/2})$. Here v is introduced to allow for overdispersion in the Poisson model. It plays a weighting role for the two terms in Equation 12, and the second summation can be regarded as auxiliary information. If n_j is assumed to follow a Poisson distribution exactly, we have $v=1$.

In our simulation and tiger prawn studies we specify a case of fixed, known recruitment length, l_0 , and $f_j(l|\beta)$ is obtained from Equation 7 or 9. For definiteness we set the constant of proportionality implicit in these equations to one.

The integrals in Equations 7 and 9 present some subtleties for their evaluation, so that some details of the numerical implementation might be of interest. For the simulation study we used Equation 7. The integral was performed on an l -dependent grid of 41 and 81 quantiles of the L_x distribution $p(x)$ and then improved upon by using the Richardson extrapolation. Note that there is an apparent singularity at $x=1$. However, by decomposing the mortality into a mean and deviation term, $z(y) = \bar{z} + z(y) - \bar{z}$, we find that the factor involving mortality is proportional to $(x-l)^{\bar{z}/k}$. Hence the integrand is proportional to $(x-l)^{\bar{z}/k}$, and, because $\bar{z}/k - 1 > -1$, the singularity is integrable (i.e., the integral is finite). We used a quadrature scheme designed for integrands of the form $(x-l)^{\bar{z}/k} p(x)$, $\bar{z}/k > -1$, to perform the integral in the neighborhood of $x=1$.

For the tiger-prawn study we used Equation 9. The integral was performed on uniform grids of 41 and 81 points over the interval $\tau \in (0, 1.5)$ years and, as before, was improved by using the Richardson extrapolation. We used our knowledge that tiger prawns live for about 18 months to determine the upper limit of integration. Note that despite appearances, this integral contains no singularity because $x(\tau) \rightarrow \infty$ as $\tau \rightarrow 0$, and therefore the factor $p(x(\tau))/(1-e^{-k\tau}) \rightarrow 0$. The effort integral within the integrand was computed by linear interpolation between cumulative totals of the weekly effort.

The prototype implementation of our maximum likelihood method was written in S-plus software (Lucent Technologies) by using the optimizer "nlminb." However, to improve the performance for a large number of simulations, the program was recoded in C by using Powell's optimization routine with numerical derivatives (Press et al., 1992). The C code and some relevant reports are available on request.

Results

Simulation studies

We simulated length-frequency data based on the recruitment pattern of tiger prawns *P. esculentus* in

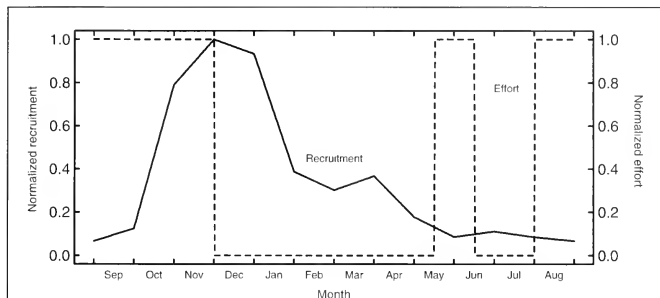


Figure 1

The empirical recruitment pattern (solid line) of the tiger prawn *Penaeus esculentus* in the northern prawn fishery of Australia and the fishing effort pattern (dashed line).

the northern prawn fishery of Australia. This pattern has been derived from experimental trawls in which the number of individuals in the lowest length class are counted (Wang and Die, 1996). We assume the recruitment and effort patterns are the same in each year (Fig. 1). The effort pattern (dashed line) consists of two constant-fishing periods: 15 May to 15 June, and 1 August to 1 December. The unit of effort, E , depends on the unit of catchability, q , because the fishing mortality $F=qE$ must have unit yr^{-1} ; therefore we let $E=1$ during the fishing season. Note that the proportion of the year that is fished is $\int E(t)dt=5/12$.

The growth component of our models has $l_{\infty}=40$ mm and $k=3yr^{-1}$; the instantaneous natural mortality is $M=2yr^{-1}$; and the instantaneous fishing mortality, F , during the fishing season is $4yr^{-1}$ (i.e., $q=4$, because in our units, $F=q$). The resulting annual mortality, $Z=\int z(t)dt=M+qE(t)dt=2+4\times 5/12=11/3$. The values for mortality come from Somers and Wang (1996). We assume that all recruits have length 19.5 mm. The L_{∞} distribution is normal (standard deviation 4 mm) but is truncated at 19.5 mm. The truncated normal distribution at l_0 is simply a conditional normal distribution conditional on being greater than l_0 .

We generate twelve length-frequency data sets, one for the beginning of each month. We choose a monthly time interval because the data from our case study in the next section were sampled at roughly monthly intervals. In addition, because the recruitment pattern is periodic it is sufficient to analyze one year of data.

We obtain each monthly length-frequency data set by taking a sample of size 1000 from the theoretical length distribution $f_l(l)$ given by Equation 6, which depends on the recruitment pattern, the effort pattern, and the distribution of L_{∞} . That is, for each of the 12 time points t , we evaluate numerically the right-hand

side of Equation 6 over a set of finely spaced l values (i.e., every 0.25 mm), aggregate the $f_l(l)$ to 1-mm intervals and finally normalize the function by dividing by the sum of $f_l(l)$. This results in an array of probabilities for an individual's length in each 1-mm interval. It is then straightforward to sample from the corresponding multinomial distribution.

We then obtain parameter estimates from the twelve months of simulated data. The process is repeated 100 times to provide a reasonable estimate of the sampling variance of the parameters. In practice, (k, l_{∞}) can often be estimated from a different study. We therefore consider two models. In model 1, we assume all five parameters are unknown, and, in model 2, we assume that l_{∞} and k are known and we estimate M, F , and α . It is also common practice (e.g., Sullivan, 1992) to assume that M is known and to estimate the remaining parameters; this is the case in our model 3.

The results are summarized in Table 1. All the parameters are quite well estimated, even for model 1. Estimates of both natural mortality and fishing mortality are quite reliable when growth parameters are assumed known. There is also a modest reduction in the standard deviation when (k, l_{∞}) are assumed known.

We have also tested for robustness by performing the estimation process on data generated from a log-normal distribution. The results are shown in Table 1. For model 1 the estimates of M and F have a larger and opposite bias, whereas the absolute bias for Z is somewhat smaller. Model 2 improves the estimates dramatically, despite the fact that an incorrect distribution (the truncated normal) is being used in the model. Note that the variation in the estimates of total annual mortality, Z , is somewhat less than that for F and M ; this is because F and M are highly negatively correlated (typically 94%). In model 3 the estimate of

Table 1

Mean parameter estimates and standard deviations (in parentheses) for simulated tiger prawn (*Penaeus esculentus*) data. The model assumes an underlying truncated normal L_{∞} distribution. The data are generated from two underlying L_{∞} distributions: the truncated normal and the lognormal. With model 1 all parameters are unassumed to be unknown; with model 2 (k, l_{∞}) are assumed to be known; with model 3 M is assumed to be known.

Model	k	l_{∞}	α	Z	M	F
Underlying truncated normal distribution						
True	3	40	4	3.67	2	4
1	2.99 (0.05)	40.00 (0.19)	4.02 (0.08)	3.65 (0.05)	1.98 (0.15)	3.99 (0.34)
2	3	40	4.01 (0.07)	3.65 (0.04)	2.00 (.11)	3.95 (0.28)
3	2.99 (0.05)	40.02 (0.15)	4.01 (0.07)	3.65 (0.05)	2	3.95 (0.12)
Underlying lognormal distribution						
True	3	40	4	3.67	2	4
1	3.02 (0.07)	39.53 (0.22)	4.28 (0.08)	3.53 (0.05)	1.51 (0.16)	4.84 (0.35)
2	3	40	4.14 (0.07)	3.62 (0.04)	1.93 (0.11)	4.05 (0.28)
3	2.96 (0.06)	39.92 (0.17)	4.16 (0.07)	3.57 (0.05)	2	3.76 (0.11)

F is negatively biased, but once again the standard deviation is reduced.

Application to tiger prawns (*P. semisulcatus*)

The data for this application consist of a six-year sequence of experimental length-frequency data from the trawling region around Albatross Bay in the eastern Gulf of Carpentaria, Australia. The data consist of catches of tiger prawns from 11 mm to 59 mm (carapace length) for each of 69 times ranging from March 1986 to March 1992. The catches from several stations covering the trawling region at each time (over a few consecutive days) are aggregated. Sampling was done roughly every lunar month.

We use the catch data for the smaller size classes to obtain two types of recruitment patterns: the *aperiodic* pattern and the *quasiperiodic* pattern. The aperiodic pattern is constructed by summing over all individuals with length 21 mm or less for each occasion. The resulting sequence of plotted time points is then joined up by straight lines. The quasiperiodic pattern is generated from the aperiodic pattern by averaging corresponding points across years to give a single annual pattern. The pattern for all six years is generated from the annual pattern by applying, for each biological year, a scale factor that is found by averaging the catch over all size classes within the year. The start of the biological year is defined as the time when the annual pattern reaches its minimum (see Fig. 2).

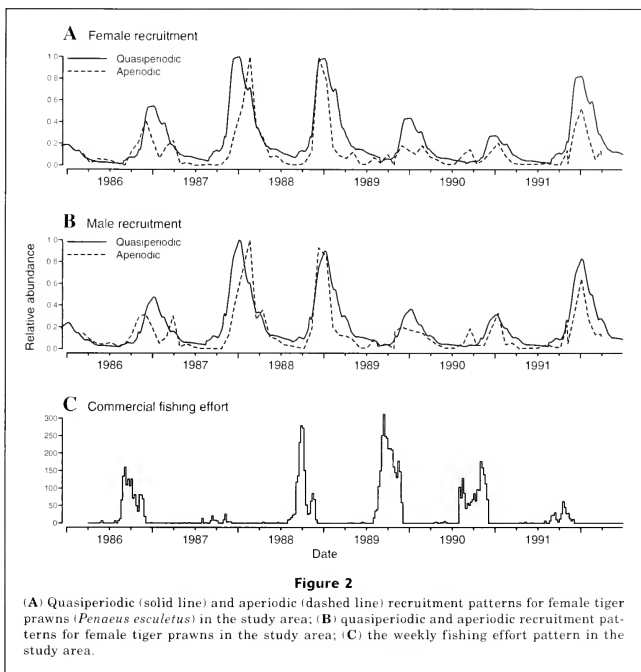
The effort pattern comes from commercial log books collected from fishermen for the period from 1986 to 1992 in the area. Effort is measured in boat-days (see Fig. 2). There is substantial contrast in the effort both within years (due to seasonal closures) and across years. This contrast may allow us to separate fishing mortality from natural mortality.

The instantaneous fishing mortality $F(t)$ is assumed to be $qE(t)$. The mean total mortality $Z = M + q\bar{E}$, where \bar{E} is the mean effort over the study period. Given the results of the simulation study, we expect the parameter Z may be more reliably estimated than either M or q , whose estimates are negatively correlated.

We further assume that the L_{∞} distribution is a truncated normal distribution. This choice is based on the shape of the observed length distribution from July to September, the period when this distribution should approximate the asymptotic length distribution. The truncated normal distributions are then reparameterized in terms of the mean l_{∞} and variance σ^2 of this underlying normal distribution. It is more convenient to use these parameters than the mean l_{∞} and variance σ^2 of the truncated normal distribution. Note that l_{∞} is always larger than l_{∞} and σ is always less than σ . However, in this application the two sets of parameters are nearly interchangeable because over the range of estimated values l_{∞} exceeds l_{∞} by at most 0.5 mm and σ exceeds σ by at most 0.6 mm (see Table 2).

We define a recruit to be an individual with length l_0 , which can be chosen at discretion. We examine a range of candidate values of l_0 between 19.5 mm and 27.5 mm, to find out which values provide the most suitable definition of recruitment for this data set, i.e., that which leads to the least violation of model assumptions.

In our application the recruitment pattern was derived from size classes 21 mm or less. If we use this pattern at say 23.5 mm then we need to shift the pattern slightly to later times. It is not apparent to what degree we should shift the pattern; therefore we shall estimate the degree of shift. We call this parameter the *lag*. We expect the lag to increase with l_0 . Also note that the derived recruitment pattern is an average over different size classes and hence it is an average over different times. The absolute timing of the pattern is



therefore uncertain and so the lag parameter adopts the role of estimating this uncertainty.

We do have sampling effort information, so that it would be reasonable to consider incorporating into the likelihood the Poisson term for the total catch as mentioned in section 3. Information on total catch per occasion would improve estimates of mortality. However, preliminary analysis found that there was a mismatch of the expected total catch with the observed total catch. Therefore, it appears to be unrealistic to assume that the catch is proportional to the sampling effort. In the subsequent data analysis we use the form of the log-likelihood in Equation 11, which uses the shape of the observed distribution and takes the total catch as given.

We have estimated all the parameters k , l_x , α , M , q , and the lag simultaneously (model 1). To achieve a better understanding of the data, we also estimate parameters for a range of fixed values of M (model 3).

This is common practice in the fisheries literature (e.g. Sullivan, 1992). Estimates of q for corresponding values of M can be useful in some contexts where the outcome of an analysis is insensitive to the joint pairs (M, q) (Somers and Wang, 1996). Taking the rough values of Somers and Wang (1996) and Wang and Die (1996) as a guide, we choose the values $M=1, 2$, and $3yr^{-1}$. The utility of considering a range of values of M applies equally to considering a range of values for (k, l_x) . Somers and Kirkwood (1991), Wang et al. (1995) and Wang (1998) have all reported estimates of (k, l_x) for this species, and we would like to incorporate this information. However, it is well known that estimates of the growth parameters are strongly correlated. We therefore considered a range of feasible pairs (k, l_x) and estimated the remaining parameters under model 2. The fixed values we used were, for males, (2, 39.3), (3, 37.7), and (4, 36.1), and for females, (2, 53.1), (3, 47.4), and (4, 41.7). These values were obtained by a

Table 2

Parameter estimates for tiger prawn (*Penaeus semisulcatus*) data. F_{89} is the estimated fishing mortality in 1989. $\text{cor}(M, F_{89})$ is the jackknifed correlation between M and F_{89} . The last column is the objective value per unit of effort. With model 1 all parameters are assumed to be unknown; with model 2 (k, l_0) are assumed to be known; with model 3 M is assumed to be known.

Model	M	F_{89}	Z	k	l_0	σ^0	$\text{cor}(M, F_{89})$	-2log
Males: quasiperiodic recruitment								
1	4.1	2.3	5.2	9.3	33.4	4.5	-0.82	72.96
2	2.9	0.3	3.1	2	39.3	5.1	-0.78	74.43
2	3.7	0.6	3.9	3	37.7	4.3	-0.35	73.99
2	3.4	2.1	4.4	4	36.1	4.3	-0.25	73.60
3	1	2.2	2.0	5.3	32.3	4.8	—	73.05
3	2	1.9	2.9	6.7	32.5	4.8	—	73.03
3	3	0.0	3.0	7.6	32.3	4.8	—	73.15
Males: aperiodic recruitment								
1	1.3	1.6	2.0	5.0	32.6	4.8	-0.67	72.91
2	2.8	0.4	3.0	2	39.3	5.8	-0.79	74.65
2	3.7	0.1	3.7	3	37.7	4.7	-0.81	74.31
2	3.5	0.5	3.7	4	36.1	4.5	-0.64	73.84
3	1	1.8	1.8	4.9	32.4	4.8	—	72.93
3	2	1.0	2.5	5.9	32.5	4.8	—	72.93
3	3	0.0	3.0	7.0	32.5	4.8	—	73.01
Females: quasiperiodic recruitment								
1	4.2	1.7	5.0	5.6	42.2	7.1	-0.65	86.83
2	3.9	0.3	4.1	2	53.1	8.3	-0.83	87.94
2	4.0	0.7	4.3	3	47.4	6.9	-0.66	87.31
2	2.7	1.3	3.3	4	41.7	7.7	-0.71	86.91
3	1	2.6	2.2	4.1	38.8	8.3	—	87.10
3	2	1.8	2.8	4.4	39.9	7.9	—	86.92
3	3	1.6	3.7	5.1	40.7	7.5	—	86.87
Females: aperiodic recruitment								
1	2.6	0.9	3.0	4.9	39.2	8.2	-0.67	86.90
2	3.9	0.1	4.0	2	53.1	13.5	-0.80	88.43
2	4.3	0.1	4.4	3	47.4	9.7	-0.70	87.88
2	3.0	0.8	3.4	4	41.7	8.1	-0.71	87.04
3	1	2.1	2.0	3.6	39.3	8.4	—	87.07
3	2	0.8	2.4	2.8	41.5	8.5	—	86.94
3	3	0.6	3.3	5.0	39.4	8.1	—	86.91

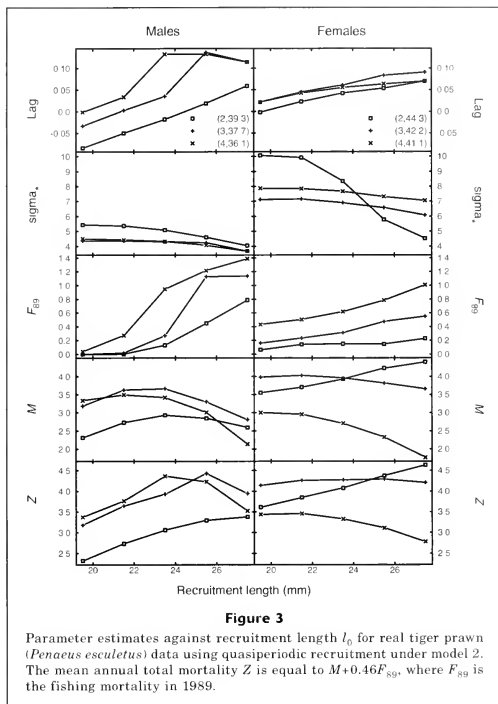
simple linear fit to the estimates in the three papers mentioned above.

The estimates of M from model 1 appear more reasonable for the aperiodic recruitment pattern. The correlations between M and F_{89} (the fishing mortality in 1989) are not as strong as in the simulation example. This is encouraging and indicates that there may be enough contrast in the effort pattern to separate fishing mortality from natural mortality.

The estimates of l_0 and σ for model 3 are not sensitive to M . However k and M are quite strongly related. In the case of constant recruitment $r(t)$ and mortality $z(t)=Z$, it is well known that k and Z are perfectly correlated, and only their ratio Z/k is able to be estimated. The separation of M and k therefore relies on there being adequate contrast in recruitment and effort.

For model 2 there is little difference between the two recruitment models. The estimates of M show moderate dependence on (k, l_0) , but without trend. These estimates are generally somewhat higher than we expect from prior studies. But for the natural mortality rate, this is the first time we have obtained estimates of M , which is larger than what we have assumed in previous stock assessments, around 2.3 per year (Wang and Die, 1996). Estimates of F_{89} are too variable to be relied upon. All models agree reasonably on the σ parameter.

Our model assumes recruitment at a fixed length, l_0 , which has to be chosen. In Figure 3 the parameter estimates for fixed (k, l_0) are plotted against l_0 for the quasiperiodic recruitment model. Parameter estimates are consistent for given l_0 provided that all model assumptions are satisfied. However, when l_0 is too small



or too large, there is bound to be a violation of those assumptions, leading to high sensitivity of the estimates to changes in l_0 . Therefore, we say the most reasonable value for l_0 is that for which the estimates are most slowly varying in the immediate neighborhood of l_0 . On the basis of σ , M and Z for males, $l_0=23.5$ would be a reasonable choice. We exclude q from consideration because its standard deviation is comparable to its magnitude (see Table 2). In addition we exclude the lag because we expect it to increase approximately monotonically with l_0 , as indeed it does. There is no clear choice for females; therefore we choose $l_0=23.5$, the same as for males. This choice is consistent with the consideration that l_0 should be somewhere between 20 mm and 30 mm, but in the lower half of the range so that more data can be included in the estimation (because lengths must exceed l_0).

Also shown in Table 2 are jackknife estimates of the standard deviations. The jackknifing is done by dropping the length-frequency record from each occasion in turn and re-estimating the parameters. From the over-all estimate $\hat{\theta}$ and the jackknife estimate $\hat{\theta}_i$ from dropping the i^{th} occasion we obtain a pseudo-value $\hat{\theta} - (n-1)\theta_i/n$, where in our case $n=69$. The jackknifed standard deviation is simply the standard deviation of these pseudo-values. We also show the jackknifed correlation between M and q , which is simply the correlation between the corresponding pseudo-values. In most cases there is a large negative correlation.

The fishing mortality in 1989 (the year of peak effort), F_{89} , is simply proportional to q with constant of proportionality 2865, the number of boat-days of effort in that year. The mean total annual mortality Z is $M+0.46F_{89}$ because the mean annual effort was

1320 boat-days. The mostly high negative correlations between M and F_{99} (equivalently, q) may explain why Z tends to have a smaller standard deviation than either M or F_{99} . The results of Figure 3 can be regarded as a sensitivity study on the effect of changing l_0 . The purpose of this sensitivity study is not to estimate l_0 but rather to check that the model assumptions have not been violated for the given l_0 .

The results are fairly similar for the two recruitment models although there are differences: the quasiperiodic recruitment model gives larger F_{99} estimates and smaller σ estimates. Our method assumes that the recruitment pattern is known without error; therefore the preferred recruitment pattern should be the one with less error. Let us suppose that the true recruitment pattern consists of a periodic pattern with random variation both within years and between years. If the within-year variation is sufficiently large in comparison with the between-year variation, then the quasiperiodic pattern should be used. On the other hand, if the between-year variation is large, then the aperiodic pattern is preferred. Based on the objective values ($-2\log$) in Table 2, model 2 with quasiperiodic recruitment pattern and fixed k at 4yr^{-1} appears to be the best model for both males and females.

Figure 4 shows the 40 length-frequency records for females with the largest total catch. Overlaid is the expected catch (given the total catch) from the model with (k, l_∞) fixed at (3, 47.4) for quasiperiodic recruitment (solid line) and for aperiodic recruitment (dashed line). Because the integral for the expected length distribution is singular in the neighbourhood of l_0 , the first few size classes are omitted from the estimation; only data with length above l_0+2 are used in the estimation. The fit is quite reasonable for most records. It is interesting to compare the performance of the two recruitment models. In early 1988, when recruitment occurred later than usual (see Fig. 2), the aperiodic model tracks the data more closely than the quasiperiodic model, especially in March. On the other hand, the quasiperiodic model fits better in October 1990, whereas the aperiodic model predicts higher abundance of small females because of a recruitment "blip" in September, which was perhaps due to sampling variation.

Discussion

Methods such as McDonald and Pitcher's (1979), ELEFAN (Pauly et al., 1981), and Sparre's (1987) operate on multiple length-frequency data and attempt to identify cohorts in the frequency pattern. Essentially they estimate the growth parameters by tracing cohorts in time; then they estimate mortality by measuring the evolution in abundance of a cohort. For mortality estimation these methods need catch-per-unit-of-effort data. Sparre's method bears some similarity to ours because it attempts to fit the length distribution of a cohort to a normal distribution whose variance is a parameter to be estimated. Our method does not require separation

of cohorts because samples are assumed to come from a length distribution which may be multimodal. Another advantage of our method is that it is not necessary to have information about sampling effort and thus may greatly reduce the complexity of sampling. However, our approach needs a known recruitment pattern.

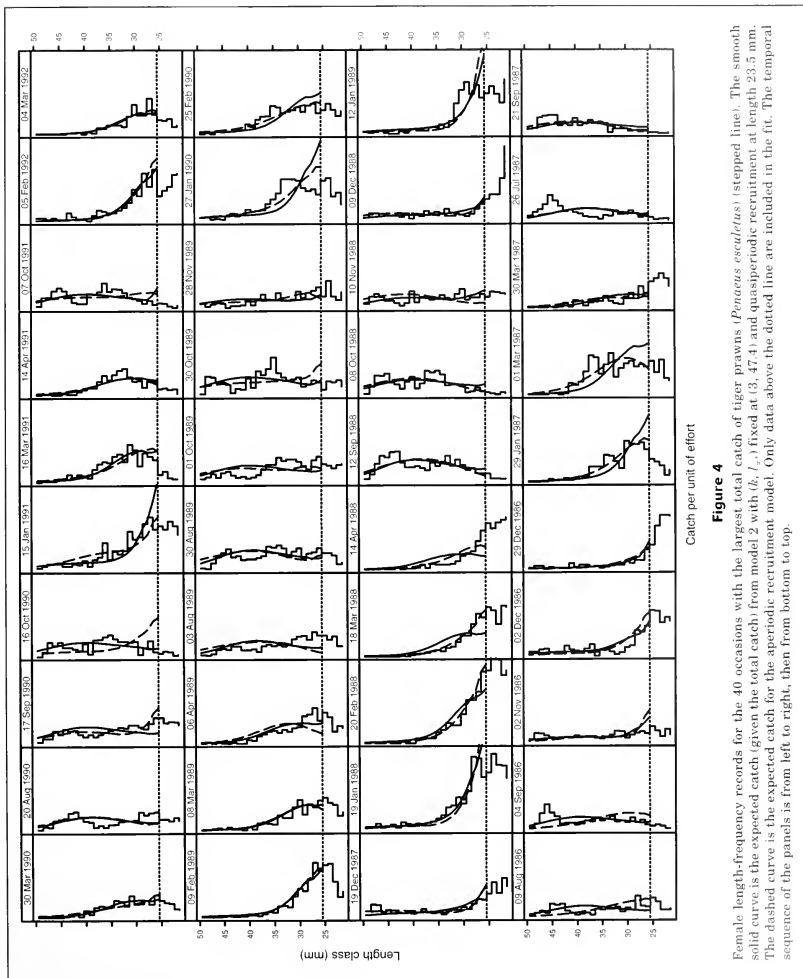
In our application, recruitment was assumed to occur at a fixed length, l_0 , which had to be chosen. We used prior information to constrain l_0 to lie somewhere between 20 mm and 30 mm. We then found the sensitivity of the estimates to changes in l_0 and chose a value that reduced this sensitivity. This choice could be further refined if more accurate constraints were available from other sources. Alternatively, Wang and Somers (1996), who also used l_0 to account for continuous recruitment in estimating growth parameters, have provided guidelines for choosing l_0 .

Deriso and Parma (1988) and Sullivan et al. (1990) reported methods based on stochastic growth. Sullivan (1992) also applied the Kalman filter approach for estimating population parameters. Their models differ from ours in the way random variation is incorporated in the growth model. In their models the length increment from one time step to the next follows a distribution whose mean is given by a fixed growth model. As Wang and Thomas (1995) have demonstrated, this is equivalent to assuming that the growth rate changes randomly from time to time. In our model each individual follows a deterministic growth curve whose L_∞ parameter is chosen from a random distribution. An individual with larger than average growth at one time step will have above-average growth at subsequent time steps. Perhaps further modeling effort could be directed into combining these approaches.

DeLong et al. (2001) have reported a method for estimating density-dependent natural mortality and the growth rate from length-frequency data for juvenile winter flounder not subject to fishing mortality. Other growth parameters (l_∞ and the variability of k) were fixed by using information from other sources. Because their data were recorded in the latter half of the year, when recruitment was nearly complete, recruitment was not a complicated issue. In contrast, we had the challenge of a species that recruits all year round. The degree of fit in DeLong et al.'s Figure 5 is comparable to that in our Figure 4.

Our methods are based on distributional assumptions that must be tested for robustness, because, in practice, the L_∞ distribution of real prawn populations will not equal any of our mathematical distributions. We have found that, even for our ideal model, akin to any other existing model, biases occur for moderate to large coefficients of variation when violation of distributional assumptions occurs.

Our model is motivated by the trawl data from the tiger prawn fishery and relies on 1) known recruitment pattern, 2) contrast in commercial fishing effort for estimation of M and F simultaneously, and 3) contrast in sampling times. Requirement 3 is to spread sampling effort so that growth and mortality information



are in the data. We fitted a variety of different models. The objective function $-2\log(\text{likelihood})$ values in Table 2 should be used only as guidelines and should not drive the analysis or be used for model selection. Tiger prawns are subject to very high total mortality and hence are short-lived species. Our method is also applicable to longer-lived species. However, for application to other fisheries, some modification of the model may be necessary to incorporate relevant information in the model. Simulation studies may have to be carried out to see how reliable the modified version is for parameter estimation because many factors, such as growth rate and commercial effort patterns, will determine if parameter estimates can be found or how reliable they are if they can be found.

We aim to obtain growth and mortality parameter estimates simultaneously. However, this may be too ambitious, especially for short-lived species unless other information can be incorporated to assist estimation. For instance, Ebert (1973) found estimation of even two parameters (natural and fishing mortality) unreliable and had to assume one of them. This is perhaps why natural mortality is assumed to be known in traditional cohort analysis. Also Askland's method (1994), one of the most recent cohort-analysis methods, requires a known M . Nevertheless, in practice, (k, L_{∞}) may be estimated from different types of data. The results based on model 2 (assuming (k, L_{∞}) are known) indicate that both M and F can then be estimated more reliably when there is substantial contrast in the effort pattern. Another assumption is that catchability does not change over time. This may not be necessarily true when new technology is introduced into the fishery (Bishop et al., 2000). The assumption that growth parameters are known greatly reduces the complexity of estimating the remaining unknown parameters and improves the performance of the proposed methods.

We have chosen to allow only L_{∞} to be random because, unlike tag-recapture data, the length-frequency data do not have multiple measures from each individual. Each individual is measured only once. Therefore, it might be problematic to allow random K and correlation between K and L_{∞} . Such an attempt using length-frequency data may lead to misleading conclusions because the conclusion will be model-driven instead of data-driven. Parameter estimates obtained by fixing M as a constant are deemed more reliable.

We provided a framework for length-frequency data analysis that incorporates continuous recruitment, selectivity, and time-dependent fishing mortality. We have also provided guidelines for how to compute the likelihood function, which depends on rather delicate integrals. Such a model would be very useful for many fisheries because such unified models are not available in the literature. Our work provides a sensible case study. Application of our method may require incorporation of specific information in a fishery. We believe our model, which generalizes the traditional model and is somewhat complicated, has provided us with some use-

ful results for future stock assessment and evaluation of management strategies.

Acknowledgments

This research project was partly supported by the Fisheries Research and Development Corporation of Australia. We gratefully acknowledge the helpful suggestions and comments of David Die, André Punt, Neil Loneragan, and two anonymous referees.

Literature cited

- Askland, M.
1994. A general cohort analysis method. *Biometrics* 50:917-932.
- Beverton, R. J. H., and S. J. Holt.
1956. A review of methods for estimating mortality rates of fish in exploited fish populations, with special reference to sources of bias in catch sampling. *Rapp. P.-V. Réun., Cons. Int. Explor. Mer* 140: 67-83.
- Bishop, J., D. Die, and Y.-G. Wang.
2000. A generalized estimating equations approach for analysis of fishing power in the Australian Northern Prawn Fishery. *Aust. N. Z. J. Stat.* 42:159-177.
- DeLong, A. K., J. S. Collie, C. J. Meise, and J. C. Powell.
2001. Estimating growth and mortality of juvenile winter flounder, *Pseudopleuronectes americanus*, with a length-based model. *Can. J. Fish. Aquat. Sci.* 58:2233-2246.
- Deriso, R. B., and A. M. Parma.
1988. Dynamics of age and size for a stochastic population model. *Can. J. Fish. Aquat. Sci.* 45:1054-1068.
- Ebert, T. A.
1973. Estimating growth and mortality rates from size data. *Oecologia* 11:281-298.
1980. Estimating mortality from growth parameters and a size distribution when recruitment is periodic. *Limnol. Oceanogr.* 26:764-769.
- Hoening, J. M.
1987. Estimation of growth and mortality parameters for use in length-structure stock production models. *In* Length-based methods in fisheries research (D. Pauly and G. R. Morgan, eds.), p. 121-128. ICLARM Conf. Proc. 13.
- McDonald, P. D., and T. J. Pitcher.
1979. Age groups from size-frequency data: a versatile and efficient method of analyzing distribution mixtures. *J. Fish. Res. Board Can.* 36:987-1001.
- Pauly, D., J. Ingles, and T. Neal.
1981. Application to shrimp stocks of objective methods for the estimation of growth, mortality and recruitment-related parameters from length-frequency data (ELEFAN I and II). *In* Penaeid shrimps: their biology and management (J. A. Gulland and B. J. Rothschild, eds.), p.220-234. Fishing News Books Ltd., Farnham, England.
- Powell, D. G.
1979. Estimation of mortality and growth parameters from the length frequency of a catch. *Rapp. P.-V. Réun., Cons. Int. Explor. Mer* 175:167-169.

- Press, W. H., S. A. Teukolsky, W. T. Vetterling, and B. P. Flannery. 1992. Numerical recipes in C: the art of scientific computing (2nd ed.). Cambridge Univ. Press, Cambridge, England.
- Sainsbury, K. J. 1980. Effect of individual variability on the von Bertalanffy growth equation. *Can. J. Fish. Aquat. Sci.* 37:241-247.
- Somers, I. F., and G. P. Kirkwood. 1991. Population ecology of the grooved tiger prawn, *Penaeus semisulcatus*, in the North-western Gulf of Carpentaria, Australia: growth, movement, age structure and infestation by the bobryd parasite *Epipenaeon ingens*. *Aust. J. Mar. Freshw. Res.* 42:349-367.
- Somers, I. F., and Y.-G. Wang. 1996. A bioeconomic analysis of seasonal closures in Australia's multispecies Northern Prawn Fishery. *N. Am. J. Fish. Manag.* 17:114-130.
- Sparre, P. 1987. A method for estimating growth, mortality and gear selection/recruitment parameters from length-frequency samples weighted by catch per effort. *In* Length-based methods in fisheries research. ICLARM Conf. Proc. 13 (D. Pauly and G. R. Morgan, eds.), p. 75-102.
- Ssentongo, G. W., and P. A. Larkin. 1973. Some simple methods of estimating mortality rates of exploited fish populations. *J. Fish. Res. Board Can.* 30:695-698.
- Sullivan, P. J. 1992. A Kalman filter approach to catch-length analysis. *Biometrics* 48:237-257.
- Sullivan, P. J., H. L. Lai, and V. F. Gallucci. 1990. A catch-at-length analysis that incorporates a stochastic model of growth. *Can. J. Fish. Aquat. Sci.* 47:184-198.
- Vetter, E. F. 1988. Estimation of natural mortality in fish stocks: a review. *Fish. Bull.* 86:25-43.
- Wang, Y.-G. 1998. An improved Fabens method for estimation of growth parameters in the von Bertalanffy model with individual asymptotes. *Can. J. Fish. Aquat. Sci.* 55:397-400.
- Wang, Y.-G., and D. Die. 1996. Stock-recruitment relationship of the tiger prawns (*Penaeus esculentus* and *Penaeus semisulcatus*) in the Australian Northern Prawn Fishery. *Aust. J. Mar. Freshw. Res.* 47:87-95.
- Wang, Y.-G., and N. Ellis. 1998. Effect of individual variability on estimation of population parameters from length-frequency data. *Can. J. Fish. Aquat. Sci.* 55:2393-2401.
- Wang, Y.-G., and I. F. Somers. 1996. A simple method for estimating growth parameters from multiple length-frequency data in presence of continuous recruitment. *Fish. Res.* 28:45-56.
- Wang, Y.-G., and M. R. Thomas. 1995. Accounting for the individual variability in the von Bertalanffy growth model. *Can. J. Fish. Aquat. Sci.* 52:1368-1375.
- Wang, Y.-G., M. R. Thomas, and I. F. Somers. 1995. A maximum likelihood approach for estimating growth parameters from tag-recapture data. *Can. J. Fish. Aquat. Sci.* 52:252-259.
- Wetherall, J. A., J. J. Polovina, and S. Ralston. 1987. Estimating growth and mortality in steady-state fish stocks from length-frequency data. *In* Length-based methods in fisheries research (D. Pauly, and G. R. Morgan, eds.), p. 53-75. ICLARM Conf. Proc. 13.

Abstract—Fisheries often target individuals based on size. Size-selective fishing can create selection differentials on life-history traits and, when those traits have a genetic basis, may cause evolution. The evolution of life-history traits affects potential yield and sustainability of fishing, and it is therefore an issue for fishery management. Yet fishery managers usually disregard the possibility of evolution, because little guidance is available to predict evolutionary consequences of management strategies. We attempt to provide some generic guidance. We develop an individual-based model of a population with overlapping generations and continuous reproduction. We simulate model populations under size-selective fishing to generate and quantify selection differentials on growth. The analysis comprises a variety of common life-history and fishery characteristics: variability in growth, correlation between von Bertalanffy growth parameters (K and L_{∞}), maturity rate, natural mortality rate (M), M/K ratio, duration of spawning season, fishing mortality rate (F), maximum size limit, slope of selectivity curve, age at 50% selectivity, and duration of fishing season. We found that each characteristic affected the magnitude of selection differentials. The most vulnerable stocks were those with a short spawning or fishing season. Under almost all life-history and fishery characteristics examined, selection differentials created by realistic fishing mortality rates are considerable.

Effects of fishing on growth traits: a simulation analysis

Erik H. Williams

Kyle W. Shertzer

Center for Coastal Fisheries and Habitat Research
101 Pivers Island Road
Beaufort, North Carolina 28516
E-mail address: Erik.Williams@noaa.gov

Fishing is typically size selective. It almost always targets the larger individuals of a population and can thus shift the spawning stock towards smaller, slower-growing individuals. If somatic growth has some genetic basis, size-selective fishing may cause evolution toward a smaller size-at-age.

Changes in somatic growth are well documented in field data, and several studies implicate fishing (Ricker, 1981; Harris and McGovern, 1997; Haugen and Vollestad, 2001; Sinclair et al., 2002). However, with typical field data, it is difficult to rule out other explanations. Changes in growth could result from fluctuations in population density or the environment. Furthermore, they may not be evolutionary, but instead expressions of phenotypic variability. Because of such possibilities, the idea that fishing can cause evolution has often been accepted because of compelling theoretical arguments, rather than on empirical support. However, the laboratory experiments of Conover and Munch (2002) demonstrated that size selection can cause evolution of growth traits. More and more, fishing-induced evolution is considered not just possible, but prevalent (Law, 2000; Stockwell et al., 2003).

The evolution of growth traits, despite wide acknowledgement of the potential for evolution of these traits, is usually a low priority in fishery management. However, it raises at least four management concerns. First, any reduction in growth rate or maximum size can decrease recreational and economic value (Miller and Kapuscinski, 1994). Second, size selection could reduce genetic variability (Falconer and Mackay, 1996),

unpredictably altering correlated traits and population fitness. Third, evolution may not easily be reversed, even with after-the-fact management. Fourth, the evolution of growth and other life-history traits can modify population dynamics (Bronikowski et al., 2002; Shertzer and Ellner, 2002) and therefore potential yield (Edley and Law, 1988; Heino 1998). Evolution in fishes can be rapid (Reznick et al., 1997; Hendry et al., 2000; Quinn et al., 2001), so that evolutionary, population, and fishery dynamics occur on similar time-scales (Sinervo et al., 2000; Shertzer et al., 2002; Yoshida et al., 2003). These dynamics imply that evolution matters for fishery management on the time-scale of years or decades.

For fishing to cause evolution, two conditions must be met. There must be a selection differential on a phenotypic trait and a genetic basis must exist for the trait's expression (i.e., the trait must be heritable). Selection differential is defined as the difference in the mean phenotypic trait value of parents before and after selection (e.g., size-selective fishing). Stokes and Law (2000) argued that, under exploitation levels in many of today's fisheries, "selection differentials on body size should be substantial and measurable." Even so, attempts to estimate selection differentials of actual fish stocks have been rare (but see Law and Rowell, 1993; Miller and Kapuscinski, 1994). This lack of estimates is surprising, given that the data needed are often available, as noted by Law (2001).

The second necessary condition, heritability, is defined as the proportion of phenotypic variability in offspring

that is due to the genotypes of the parents. It can range from zero to one, with a higher value potentially speeding the evolutionary response to selection. Field estimates of heritability in fish size are uncommon because in nature it is difficult (although not impossible; McAllister et al., 1992) to separate genetic and environmental effects on phenotypes. Almost all estimates come from laboratory experiments (e.g., Hadley et al., 1991; Conover and Munch, 2002; Vandeputte et al., 2002), mostly on populations from aquaculture breeding programs (e.g., Gjedrem, 1983; Jarayabhand and Thavorniyutikarn, 1995; Henryon et al., 2002). One might expect laboratory experiments to over-estimate natural heritabilities, because experiments tend to reduce environmental effects on total phenotypic variance, but estimates from the laboratory have been similar to those from the field (Weigensberg and Roff, 1996). The laboratory experiments indicate that heritabilities in fish growth traits may vary widely among populations but are high enough to allow rapid evolution, given a large enough selection differential.

Models of evolutionary response to selective harvest have usually taken one of two approaches: quantitative genetics (e.g., Law, 1991; Ratner and Lande, 2001) or life-history optimization (e.g., Blythe and Stokes, 1999). In the present study, we take a different approach. Rather than attempt to predict evolution explicitly, we focus on selection differentials, a necessary (but not sufficient) condition for an evolutionary response.

We use simulation analyses to compute selection differentials caused by fishing. The simulation model is one common in fisheries. It consists of an age-structured population following von Bertalanffy growth, with fishing and reproduction modeled as continuous processes.

Our goal is to compare selection differentials across a variety of life-history and fishery characteristics. We quantify selection differentials on growth parameters and body size. If growth traits are heritable, those life-history and fishery characteristics with the largest selection differentials are most likely to generate an evolutionary response. Armed with such knowledge, fishery managers can weigh potential evolutionary effects when choosing a fishing strategy.

Materials and methods

To compute selection differentials caused by size-selective fishing we used an individual-based model (Fig. 1). To initialize the model, 250,000 individual phenotypes were generated. Each was assigned a set of life-history parameters and then duplicated. One copy entered an unfished population that experienced only natural mortality; the

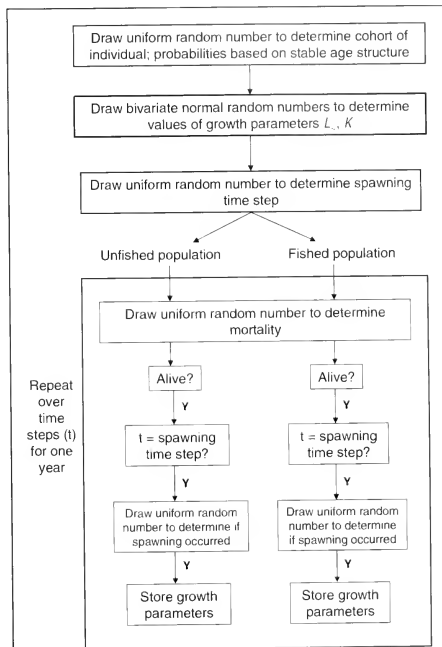


Figure 1

Flow diagram of the individual-based model. 250,000 individuals were initialized and then duplicated; one copy entered an unfished population, the other entered a fished population. Both populations were simulated for a single year with monthly time steps. Selection differentials on the growth parameters were computed as the difference between mean trait values of the unfished and fished parents.

other copy entered a fished population that experienced both natural and fishing mortality. Growth, survival, and reproductive success of individuals were simulated with monthly time steps for a single year. At the end of the simulation, selection differentials on growth parameters were computed as the percent change between the mean values of spawners in the two populations.

Model structure

The model comprised three basic life-history functions: growth, survival, and reproduction. For each individual,

size was assumed a function of age (a) and followed the von Bertalanffy model,

$$l(a) = L_{\infty}[1 - e^{-K(a-t_0)}], \quad (1)$$

where $l(a)$ = the length-at-age of an individual;

L_{∞} = the theoretical maximum length;

K = the growth rate, and

t_0 = the theoretical age when size would have been zero.

In our study, each individual's age and size were updated at each monthly time step.

Survival was computed differently for the two populations. In the unfished population, individuals survived with a probability depending only on the natural mortality rate (M /yr). In the fished population, individuals survived with a probability depending on both the natural mortality rate and the size-specific fishing mortality rate. Size selectivity [$s(l)$] by the fishery increased with length according to the logistic equation

$$s(l) = \frac{1}{1 + e^{-\beta_s(l-L_s)}}, \quad (2)$$

where β_s = the slope of the selectivity curve; and

L_s = the length at 50% selectivity.

The function $s(l)$ describes the proportion of the fully-selected fishing mortality rate (F) experienced by individuals of length l . The size-specific fishing mortality rate, therefore, is $s(l)F$ per year. Fishing was applied over a fishing season of duration D_f .

The probability of reproduction was assumed equal to the probability of maturity [$m(a)$]. In the model, maturity increases with age and is independent of length. Although maturity likely relates to length through bioenergetics, the relationship was not modeled here because it is, in general, poorly understood. Like selectivity (Eq. 2), $m(a)$ was modeled by a logistic equation, but with a slope parameter, β_m , and age at 50% maturity, A_m .

In nature, values of life-history parameters K and A_m are related to a stock's natural mortality rate. A higher natural mortality rate reduces the expected lifespan and consequently tends to be associated with a higher growth rate (K) and a younger age at maturity (A_m). In the simulation, K and A_m were related to natural mortality by life-history invariants (detailed later). Life-history invariants have a strong theoretical and empirical basis (Roff, 1984; Beverton, 1992; Charnov, 1993) and have been valuable in other fishery applications (Mangel, 1996; Charnov and Skuladottir, 2000; Frisk et al., 2001; Williams and Shertzer, 2003).

Simulation

To initialize the simulation, individuals were assigned at random to a cohort. The number of cohorts was determined as the age at which approximately 1% of the population would be expected to remain under natural

mortality [$-\ln(0.01)/M$, rounded to the nearest integer]. Probabilities of cohort membership decayed exponentially with age according to M ; the probability of the oldest cohort was adjusted to include the remaining fraction of fish (i.e., a plus group). The probabilities were scaled to sum to one, and a uniform random number was drawn to determine an individual's cohort.

Next, individuals were assigned parameter values for von Bertalanffy growth. The value of t_0 was fixed at 0.5 yr. Values of L_{∞} and K were chosen uniquely for each individual. Following Xiao (1994), L_{∞} and K were assumed to follow a bivariate normal distribution with standard deviations σ_L and σ_K , respectively, and correlation ρ .

Finally, individuals were assigned a time step (month) within the year to attempt spawning. The time step was chosen from months distributed uniformly over a spawning season of duration, D_s .

Once assigned parameter values, each individual was duplicated. One copy entered the unfished population, the other the fished population. The populations were simulated in parallel over a single model year.

The simulation iterated each individual through monthly time steps. At each step, the simulation computed growth and checked for survival and reproduction. In the unfished population, the monthly probability of survival was $\exp(-M/12)$. In the fished population, the monthly probability of survival during the fishing season depended on natural mortality and on the size-specific fishing mortality. For simplicity, we assumed size within a month was fixed so that the probability of survival was $\exp[-(M/12 - s(l_0)F)/D_f]$, where l_0 was an individual's size at the beginning of the month. Outside the fishing season, only natural mortality applied. To check for survival, a uniform random number was drawn and compared to the survival probability appropriate for the population.

Each individual surviving to its assigned spawning time had the opportunity to reproduce. In that case, a uniform random number was drawn and compared to the probability of reproduction. If reproduction was successful, the individual's growth parameters went into a pool of parents used to compute selection differentials.

Growth parameters L_{∞} and K jointly determine size-at-age, and it is on these parameters that we describe selection differentials. At the end of the simulation year, we computed a selection differential on each growth parameter as the percent difference between mean trait values (L_{∞} or K) of the unfished and fished parents. Based on the differences in L_{∞} and K , we also computed upper and lower bounds of selection differentials on size-at-age. The bounds occur where age approaches t_0 or ∞ . Because each population consisted of the same set of individuals at the beginning of the year, any difference in growth traits between parents at the end of the year could be attributed solely to fishing.

Base model and variations

We began with a base model built on parameter values chosen or computed to represent common life-history and

Table 1

Parameter values used in the base model. Formulas for the growth rate (K) and the age at 50% maturity (A_m) are life-history invariant relationships from Charnov (1993) and Beverton (1992), respectively. The formula for L_s is the length at age A_m , according to von Bertalanffy growth. A value of ∞ for slope parameters corresponds to a knife-edge curve.

Parameter	Description	Formula	Value
M	Natural mortality rate (per year)	Fixed	0.2
F	Fishing mortality rate (per year)	Fixed	0 to 10
\bar{L}_∞	Mean asymptotic size in growth function	Fixed	1000
\bar{K}	Mean growth rate in growth function	$M/1.65$	0.12
t_0	Location parameter in growth function	Fixed	-0.5
CV_L	Coefficient of variation in L_s	Fixed	20%
CV_K	Coefficient of variation in K	Fixed	20%
ρ	Correlation between L_s and K	Fixed	0
β_s	Slope of the size selectivity curve	Fixed	∞
β_m	Slope of the maturity curve	Fixed	∞
A_m	Age at 50% maturity	$\log\{[3\bar{K} + M]/M\} / \bar{K}$	8.55
L_s	Length at 50% selectivity	$\bar{L}_s[1 - \exp(-\bar{K}(A_m - t_0))]$	666
D_S	Duration of spawning season (yr)	Fixed	1
D_F	Duration of fishing season (yr)	Fixed	1

fishery characteristics (Table 1). We then conducted a variety of sensitivity analyses.

In the base model, the natural mortality rate (M) was set at 0.2/yr, a value common for many fish species. Sensitivity analyses used $M = 0.1, 0.4,$ or 0.8 . The value of M affects the values of $K, A_m,$ and L_s , according to the life-history invariant relationships (Table 1). The relationship between M and K is often referred to as the M/K ratio. Charnov (1993) suggested a central value for fishes of $M/K=1.65$, which we used in the base model. Beverton (1992) examined the M/K ratio for fishes and found a range of 0.5 to 2.5. We used this range in our sensitivity analyses to examine the effect of the M/K ratio on selection differentials (Table 2).

The base model treated L_s and K as independent variables ($\rho=0$, Table 1). Often these parameters are correlated. A meta-analysis by He and Stewart (2001) of 235 fish populations indicated a correlation value of -0.28. The negative correlation could be expected from a trade-off between growth rate (represented by K) and maximum size (represented by L_s), as has been suggested in studies of bioenergetics (Stearns, 1992; Hutchings, 1993; Mangel, 1996). Our sensitivity analyses considered negative values of correlation that range from -0.25 to -1.

With the base model, selectivity and maturity were assumed to be "knife-edge," a functional form often used in fisheries for convenience. Also, in the base model the size at 50% selectivity (L_s) was assumed to occur at an age equal to the age at 50% maturity (A_m). Although

these fishery characteristics are common, selectivity and maturity may not be knife-edge or coincide. In sensitivity analyses, we examined different shapes of selectivity and maturity curves (Fig. 2). We also examined the affect of shifting the age at 50% selectivity from -2 to 2, in relation to the base case. This shift corresponds to a range in L_s values from 574 to 738. For simplicity, we held F constant for these sensitivity analyses, implying constant effort but resulting in different amounts of removals.

Under logistic selectivity, the oldest, largest fish receive the highest rate of exploitation. Yet often the largest fish are unavailable to a fishery because of migration patterns or regulations (e.g., a maximum size limit). Thus our sensitivity analyses included a cap on susceptible sizes. The cap was set at 70, 80, or 90% of L_s .

Using the base model, we examined the effects of annual fishing mortality rate over values that range from $F=0$ to $F=10$ /yr, which is 0 to 50 times the natural mortality rate. Fishing mortality was applied continuously throughout the year (i.e., $D_F=1$). In sensitivity analyses, we examined shorter fishing seasons ranging from one to six months. The F was still an annual rate but was applied over fewer months and adjusted so that the number of fish removed was the same as when $D_F=1$. For seasons shorter than a full year, fishing was assumed to occur at the beginning of the year.

Like the fishing season, the duration of the spawning season was a full year in the base model ($D_S=1$).

Table 2

Percent selection differential on the von Bertalanffy growth coefficient (K) at fishing mortality = 0.8/yr. Columns correspond to the levels of the coefficient of variation ($CV=0\%$, 10% , 20%) in K and in the asymptotic length (L_∞). Any combination with 0% CV in K is not presented because it results in zero selection differential. The first row corresponds to the base model and subsequent rows correspond to changes in the base model: correlation between L_∞ and K (ρ), slope of maturity curve (β_m), natural mortality (M), M/K ratio, duration of annual spawning season (D_S), maximum size limit (L_{95}), slope of selectivity curve (β_s), change in age at 50% selectivity (A_s) in relation to the base case, and duration of annual fishing season (D_F).

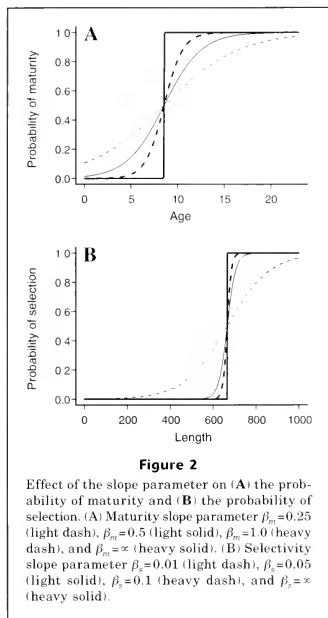
	Parameter values					
	L_∞ : 0% CV	L_∞ : 10% CV	L_∞ : 20% CV	L_∞ : 0% CV	L_∞ : 10% CV	L_∞ : 20% CV
	K : 10% CV	K : 10% CV	K : 10% CV	K : 20% CV	K : 20% CV	K : 20% CV
Base	0.7	0.5	0.3	2.1	1.7	1.2
$\rho = -1$	0.7	-0.7	-1.3	2.1	0.2	-2.3
$\rho = -0.75$	0.7	-0.3	-0.8	2.1	0.8	-0.9
$\rho = -0.5$	0.7	0.0	-0.4	2.1	1.1	0.1
$\rho = -0.25$	0.7	0.3	0.0	2.1	1.4	0.6
$\beta_m = 0.25$	0.2	0.2	0.1	0.7	0.7	0.6
$\beta_m = 0.5$	0.3	0.3	0.2	1.1	1.1	0.9
$\beta_m = 1$	0.5	0.4	0.3	1.7	1.4	1.1
$M = 0.1$	0.4	0.4	0.3	1.6	1.5	1.2
$M = 0.4$	0.7	0.4	0.3	2.0	1.5	1.0
$M = 0.8$	0.6	0.3	0.2	1.6	1.1	0.7
$M/K = 0.5$	0.6	0.3	0.1	1.9	1.0	0.6
$M/K = 1$	0.4	0.3	0.2	1.5	1.3	0.8
$M/K = 2$	0.5	0.4	0.3	1.9	1.6	1.2
$M/K = 2.5$	0.8	0.6	0.4	2.4	2.1	1.5
$D_S = 1/12$	1.6	1.0	0.6	4.5	3.6	2.3
$D_S = 3/12$	1.4	0.9	0.5	4.1	3.3	2.2
$D_S = 6/12$	1.1	0.8	0.5	3.3	2.7	1.8
$L_{95} = 700$	0.0	0.0	0.0	-0.1	-0.1	0.0
$L_{95} = 800$	0.2	0.0	0.0	0.3	0.2	0.0
$L_{95} = 900$	0.4	0.2	0.1	1.1	0.8	0.3
$\beta_s = 0.01$	0.3	0.2	0.2	1.1	1.0	0.8
$\beta_s = 0.05$	0.6	0.4	0.3	1.9	1.6	1.2
$\beta_s = 0.1$	0.6	0.5	0.3	2.0	1.7	1.2
$A_s = -2$	0.1	0.2	0.2	1.1	1.2	1.0
$A_s = -1$	0.4	0.4	0.3	1.7	1.6	1.1
$A_s = 1$	0.6	0.5	0.3	2.1	1.7	1.2
$A_s = 2$	0.5	0.4	0.3	1.9	1.6	1.1
$D_F = 1/12$	1.5	1.0	0.6	4.3	3.5	2.3
$D_F = 3/12$	1.3	0.9	0.6	3.9	3.1	2.1
$D_F = 6/12$	1.2	0.7	0.5	3.3	2.6	1.8

In sensitivity analyses, the spawning season ranged from one to six months and was assumed to occur at the end of the year.

A selection differential cannot exist without phenotypic variation. The base model assumed a coefficient of variation (CV) of 20% in both L_∞ and K . For sensitivity analyses, combinations of 0%, 10%, and 20% CV in L_∞ and K were examined for the influence of growth variability on selection differentials of L_∞ and K .

Results

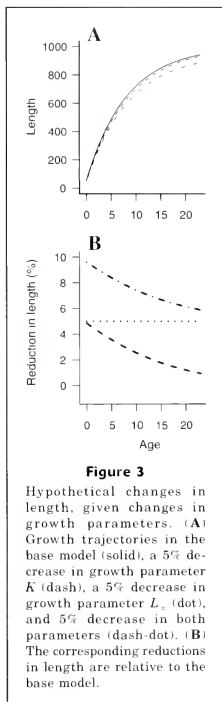
Changes in growth parameters L_∞ and K affect size-at-age jointly, resulting in non-uniform selection differentials across ages (Fig. 3). The selection differentials on size are bounded by the differentials at the extreme ages, t_0 and ∞ . At the youngest age, the selection differential on size is limited by the sum of the selection differentials on L_∞ and K plus their product. (At age t_0 , the selection differential on size is undefined.) As age



increases, the selection differential on size increases or decreases monotonically toward an asymptote, the selection differential on L_∞ . Thus selection differentials on size across all ages are bounded by those at $L_\infty + K$ and $L_\infty - K$. The selection differential on the smallest fish (age approaching t_0) is an upper bound when the selection differential on K is positive, and a lower bound when negative. These properties are important for interpreting how selection differentials on size-at-age correspond to differentials on L_∞ and K .

Using the base model, we computed selection differentials on L_∞ and K as functions of fishing mortality, over the range $F=0$ to $F=10/\text{yr}$. The selection differentials increased with F nonlinearly, resulting in a concave relationship (Fig. 4). However for $F < 2.0$, the relationship is nearly linear.

The alternative models also revealed linear relationships between selection differentials and F , for $F < 2.0$ (figures not shown). In addition, those relationships have a zero intercept (by definition, no fishing, no selection differential). Because the relationships are (nearly) linear and have a common intercept, the rank of selec-



tion differentials among models does not change across values of F . A model that bears the highest selection differential at $F=0.2$ does so at $F=2.0$. We therefore present results of sensitivity analyses for a single value of F ($F=0.8/\text{yr}$), with the understanding that for other values of F (up to 2.0), magnitudes of selection differentials can be inferred and ranks among models are maintained.

Increased variation in L_∞ and K tended to increase the selection differentials, and interaction between the two growth parameters (Tables 2 and 3). Selection differentials on L_∞ were generally larger than those on K . In the base model, the largest selection differential on each growth parameter occurred when variation in the focal parameter was highest and variation in the other parameter was zero. The selection differentials on size-at-age were largest when variation in both parameters was highest (20% CV for both L_∞ and K).

Life-history parameters

The correlation (ρ) between L_∞ and K was assumed to be zero in the base model and negative in sensitivity analyses. The effect of correlation depended on variation in the growth parameters. When the CV was zero for either parameter, correlation had no effect on selection differentials (Tables 2 and 3). When the CV was positive for both, a negative correlation decreased selection differentials in relation to those from the base model (Tables 2 and 3). For decreased values of the correlation coefficient (i.e., stronger negative correlation), the percent selection differentials on K decreased, whereas the percent selection differentials on L_∞ either decreased or remained constant. The percent selection differentials on the size near age t_0 ranged from 3.7% to -0.1% for values of ρ from 0 to -1. The percent selection differentials on L_∞ remained relatively constant, ranging from 2.1% to 2.5%, with the highest at $\rho=0$ (Fig. 5).

Knife-edge maturity ($\beta_m = \infty$) resulted in larger selection differentials than did other maturity curves (Tables 2 and 3). As the slope of the maturity curve became more gradual, the selection differentials decreased. For β_m values greater than 1, the selection differentials on size were similar to those of the knife-edge case (Fig. 5).

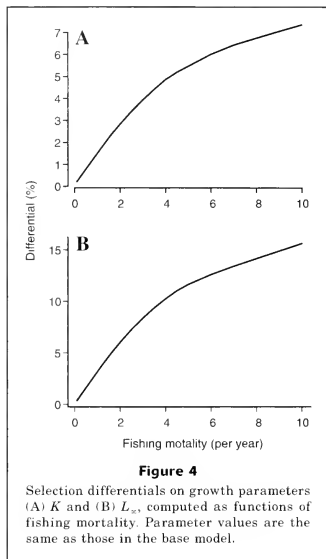
The effect of M on selection differentials was relatively small (Tables 2 and 3). Changes in M from 0.1 to 0.8 led to small changes in selection differentials (Fig. 5). The largest selection differentials tended to occur near intermediate values of M (Tables 2 and 3, Fig. 5). This nonlinear response in the selection differentials is not surprising because changes in M affected the values of K , A_m , and maximum age nonlinearly (Table 1).

Changes in the M/K ratio did not reveal a clear trend (Tables 2 and 3, Fig. 5). As with M , the M/K ratio affects other parameters; therefore changes in M/K could be expected to produce a nonlinear response in the selection differentials. The percent selection differential on L_∞ was lowest at an intermediate value of $M/K=2$ (Table 3). The percent selection differentials on K showed no consistent trend (Table 2). For M/K values from 0.5 to 2.5, the selection differentials on size across ages ranged from 2.3% to 4.0% (Fig. 5).

Decreases in the spawning season duration (D_s) caused a near linear increase in the selection differentials (Tables 2 and 3, Fig. 5). A compressed spawning duration of one month resulted in a range of 5.0% to 7.4% selection differential on size across ages (Fig. 5). Of all the life-history parameters examined in this analysis, spawning duration had the greatest effect.

Fishery parameters

A limit (L_u) on sizes susceptible to the fishery decreased the selection differentials (Tables 2 and 3, Fig. 5). The percent selection differential at all ages was zero for $L_u = 800$ and -0.1% for $L_u = 700$ (Fig. 5). In these analyses, F was held constant. Consequently, smaller values of L_u correspond to fewer fish removed. An alternative approach would have been to maintain constant catch



by increasing F , which would have led to selection differentials larger than those in Tables 2 and 3.

Knife-edge selectivity ($\beta_s = \infty$) caused larger selection differentials than did selectivity curves with more gradual slopes (Tables 2 and 3). For β_s greater than 0.1, the selection differential rapidly converged to that of the knife-edge case (Fig. 5). As with L_u , F was held constant across β_s sensitivity analyses.

A change in the ages of fishery selectivity had little effect on selection differentials (Tables 2 and 3, Fig. 5). When selectivity was set to a larger age or size, the selection differential decreased slightly. In this case, selectivity was occurring after maturity, allowing more fish to reproduce before reaching sizes selected by the fishery. However if harvest had been held constant instead of F , the selection differentials would have been larger. When selectivity was set to a smaller age or size, the selection differential decreased slightly or remained constant. This result is due to a reduction in the time exposed to differential fishing mortality. Differential fishing mortality occurs only on the sizes where selectivity is less than one; otherwise fishing mortality is constant for all individuals. Under von Bertalanffy growth, younger fish grow more quickly. A decrease in the age or size of selectivity shifts the fishing pressure to ages with quicker growth, reducing the time

Table 3

Percent selection differential on the von Bertalanffy asymptotic length (L_∞) at fishing mortality = 0.8/yr. Columns correspond to the levels of the coefficient of variation (CV=0%, 10%, 20%) in L_∞ and in the growth coefficient (K). Any combination with 0% CV in L_∞ is not presented because it results in zero selection differential. The first row corresponds to the base model and subsequent rows correspond to changes in the base model: correlation between L_∞ and K (ρ), slope of maturity curve (β_m), natural mortality (M), M/K ratio, duration of annual spawning season (D_S), maximum size limit (L_u), slope of selectivity curve (β_s), change in age at 50% selectivity (A_s) in relation to the base case, and duration of annual fishing season (D_F).

	Parameter values					
	L_∞ : 0% CV K: 10% CV	L_∞ : 10% CV K: 10% CV	L_∞ : 20% CV K: 10% CV	L_∞ : 0% CV K: 20% CV	L_∞ : 10% CV K: 20% CV	L_∞ : 20% CV K: 20% CV
Base	1.0	2.7	0.9	2.7	0.8	2.5
$\rho = -1$	1.0	2.8	0.7	2.7	-0.1	2.3
$\rho = -0.75$	1.0	2.7	0.7	2.6	0.2	2.2
$\rho = -0.5$	1.0	2.8	0.8	2.7	0.4	2.3
$\rho = -0.25$	1.0	2.8	0.9	2.7	0.6	2.4
$\beta_m = 0.25$	0.3	1.2	0.3	1.1	0.3	1.1
$\beta_m = 0.5$	0.5	1.8	0.5	1.8	0.5	1.7
$\beta_m = 1$	0.8	2.4	0.7	2.4	0.7	2.2
$M = 0.1$	0.8	2.6	0.7	2.5	0.7	2.4
$M = 0.4$	1.0	2.8	1.0	2.7	0.8	2.6
$M = 0.8$	1.0	2.6	1.0	2.6	0.8	2.4
$M/K = 0.5$	1.4	3.2	1.4	3.2	1.3	3.1
$M/K = 1$	0.9	2.7	0.9	2.7	0.8	2.5
$M/K = 2$	0.9	2.5	0.8	2.5	0.7	2.3
$M/K = 2.5$	1.1	2.8	1.0	2.7	0.8	2.5
$D_S = 1/12$	2.2	5.6	2.0	5.5	1.7	5.0
$D_S = 3/12$	2.0	5.1	1.8	5.0	1.5	4.6
$D_S = 6/12$	1.6	4.4	1.5	4.3	1.3	3.9
$L_u = 700$	-0.1	-0.1	-0.1	-0.1	-0.1	-0.1
$L_u = 800$	0.0	-0.1	0.0	-0.1	-0.1	-0.1
$L_u = 900$	0.3	0.5	0.2	0.5	0.1	0.4
$\beta_s = 0.01$	0.5	1.9	0.5	1.9	0.5	1.8
$\beta_s = 0.05$	0.9	2.7	0.9	2.6	0.8	2.5
$\beta_s = 0.1$	1.0	2.7	0.9	2.7	0.8	2.5
$A_s = -2$	0.4	2.1	0.4	2.1	0.4	2.1
$A_s = -1$	0.7	2.5	0.7	2.5	0.7	2.4
$A_s = 1$	1.0	2.8	1.0	2.7	0.9	2.5
$A_s = 2$	1.0	2.7	0.9	2.6	0.8	2.4
$D_F = 1/12$	2.2	5.5	2.0	5.3	1.6	4.8
$D_F = 3/12$	1.9	4.9	1.7	4.8	1.5	4.4
$D_F = 6/12$	1.6	4.2	1.5	4.1	1.2	3.7

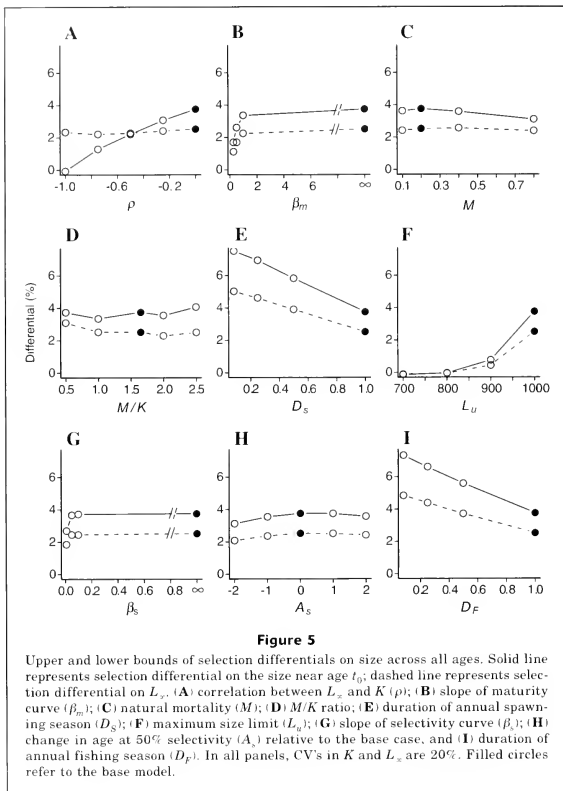
individuals experience differential fishing pressure and therefore the potential for selection differentials. If harvest had been held constant instead of F , the selection differentials would have been larger.

The fishing season duration (D_F) affected selection differentials in ways similar to the spawning season duration (Tables 2 and 3, Fig. 5). A fishing season of one month resulted in an upper bound of selection differentials that ranged from 4.8% to 7.3% over all ages

(Fig. 5). Of all the fishery parameters examined in this analysis, a concentrated fishing season resulted in the largest selection differentials.

Discussion

The individual-based simulation approach used here simplifies computation of selection differentials and



isolates the cause—fishing. Yet with any simulation analysis, one must interpret results in light of model assumptions. With our model maturity was assumed to be a function of age, and the computation of selection differentials were consequently focused to those on growth traits and size. If maturity were considered a function of size, it too would have been subject to a selection differential. Changes in size or age at maturity have been considered in other studies (Stokes and Blythe, 1993; Haugen and Vollestad, 2001; Olsen et al., 2004) and are likely connected to growth parameters through bioenergetic constraints.

A central assumption is that somatic growth follows the von Bertalanffy model. That model was chosen because of its successful track record (Chen et al., 1992; Quinn and Deriso, 1999). Life-history characteristics other than growth are assumed to follow life-history invariant relationships. The invariants constrain biological parameters to values that represent an “average stock.” Of course, no stock is truly average, and therefore our sensitivity analyses incorporate considerable deviation from life-history invariants.

In our simulation, the largest selection differentials occurred when the spawning or fishing seasons were

compressed. We modeled fishing seasons at the beginning of the year and spawning seasons at the end of the year, and in a single-year simulation, the annual timing of the fishing and spawning seasons will affect selection differentials. For example, if the one-month fishing season had been modeled at the end of the year, the selection differential would be smaller because of the 11 months of spawning prior to fishing mortality. Over multiple years, however, the annual timing of the fishing and spawning seasons is less important than their duration and overlap.

Our model simulated selection differentials at the onset of a fishery. As a fishery progresses, selection differentials should decrease as life-history parameters shift in the direction of selection. A multiyear simulation of evolution would require knowledge or assumptions about heritability and trait distributions, both of which are likely to be dynamic. Even so, a short-term simulation, where selection differentials and heritability are assumed to be static, may be an informative approximation.

We simulated evolution of the base-model population, assuming a static heritability of 0.2 and selection differentials of 2.5% for L_{∞} and 1.2% for K (values from Tables 2 and 3 with 20% CV's in both parameters). Two simulations were conducted with different values for fishing mortality. With $F = 4M$, five years of evolution led to a 9.0% decrease in the capacity of spawning biomass. With $F = M$, five years led to a 2.3% decrease.

With real fishery data it is often impossible to document conclusively that fishing causes a genetic change in growth. Any such change may be hard to measure, fall within the range of statistical variability due to sampling, or be masked by strong year classes. Selection for reduced growth may be compensated by density-dependent effects (for example, lower abundance leaving more resources for survivors to allocate towards growth). Even when a change can be demonstrated, fishing is just one potential explanation. Alternative explanations include environmentally driven evolution and reaction norms (i.e., phenotypic expressions of a genotype-environment interaction).

Nonetheless, size-selective fishing is widespread and often accompanies changes in somatic growth rates (Ricker, 1981; Harris and McGovern, 1997; Haugen and Vøllestad, 2001; Sinclair et al., 2002). Until recently, the question was whether fishing can cause changes in growth that are evolutionary, and the answer was "yes ... probably." The laboratory experiments of Conover and Munch (2002) removed any doubt. However, those experiments represented an extreme fishery in terms of its potential to inflict a selection differential: high F compressed in time (90% of population removed in one day), knife-edge selectivity, non-overlapping generations, and a population where all individuals are susceptible.

The goal of our study was to shed light on selection differentials created by fishing under realistic ranges of life-history and fishery characteristics. Understanding how life-history characteristics affect selection differ-

entials is important for identifying which stocks are most susceptible to evolution of growth traits. For example, susceptibility increases with compression of the spawning season. Fish species with compressed spawning seasons, such as many anadromous species, may be at higher risk of evolution from size-selective fisheries.

Understanding how fishery patterns affect selection differentials has direct management implications because it is the fishery parameters that can be controlled. For example, our results indicate that size-selective fisheries compressed in time are apt to cause high selection differentials. Managers should avoid "derby" style harvests, such as the annual Pacific herring sacroe fisheries, which are completed in only a few days. Other management strategies could reduce selection differentials, such as slot limits, reduction in the slope of selectivity curves, and partial selectivity after the age at maturity. However, because no size-selective fishing pattern can preclude some directional selection on growth, management by area closures may be the best option for avoiding fishery-induced evolution of growth traits.

As fishing technology improves, so does the ability to fully and rapidly exploit fish populations, and thus increase the potential for evolutionary responses. Still, when overfishing depletes a stock, low abundance is usually the paramount concern. With appropriate management, stock abundance may recover, but pre-fishing growth capacity may recover more slowly or not at all if genetic variation is lost. Given plausible heritabilities of growth traits, this analysis shows that under a wide variety of life-history and fishery characteristics, selection differentials are large enough to allow for rapid evolution.

Acknowledgments

We thank R. Muñoz, M. Prager, and D. Vaughan for comments on the manuscript. This work was supported by the National Marine Fisheries Service through its Southeast Fisheries Science Center.

Literature cited

- Beverton, R. J. H.
1992. Patterns of reproductive strategy parameters in some marine teleost fishes. *J. Fish. Biol.* 41(suppl. B):137-160.
- Blythe, S. P., and T. K. Stokes.
1993. Size-selective harvesting and at-at-maturity. I: Some theoretical implications for management of evolving resources. *In* The exploitation of evolving resources (T. M. Stokes, J. M. McGlade, and R. Law, eds.), p. 232-247. Lecture Notes in Biomathematics 99. Springer-Verlag, Berlin.
- Bronikowski, A. M., M. E. Clark, F. H. Rodd, and D. N. Reznick.
2002. Population-dynamic consequences of predator-induced life history variation in the guppy (*Poecilia reticulata*). *Ecology* 83:2194-2204.

- Charnov, E. L.
1993. Life history invariants: some explorations of symmetry in evolutionary ecology, 159 p. Oxford Univ. Press, Oxford, England.
- Charnov, E. L., and U. Skuladottir.
2000. Dimensionless invariants for the optimal size (age) of sex change. *Evol. Ecol. Res.* 2:1067-1071.
- Chen, Y., D. A. Jackson, and H. H. Harvey.
1992. A comparison of von Bertalanffy and polynomial functions in modeling fish growth data. *Can. J. Fish. Aquat. Sci.* 49:1228-1235.
- Conover, D. O., and S. B. Munch.
2002. Sustaining fisheries yields over evolutionary time scales. *Science* 297:94-6.
- Edley, M. T., and R. Law.
1988. Evolution of life histories and yields in experimental populations of *Daphnia magna*. *Biol. J. Linn. Soc.* 34:309-326.
- Falconer, D. S., and T. F. C. Mackay.
1996. An introduction to quantitative genetics, 4th ed., 245 p. Longman Group Ltd., Harlow, Essex, England.
- Frisk, M. G., T. J. Miller, and M. J. Fogarty.
2001. Estimation and analysis of biological parameters in elasmobranch fishes: a comparative life history study. *Can. J. Fish. Aquat. Sci.* 58:969-981.
- Gjedrem, T.
1983. Genetic variation in quantitative traits and selective breeding in fish and shellfish. *Aquaculture* 33:51-72.
- Hadley, N. H., R. T. Dillon, and J. J. Manzi.
1991. Realized heritability of growth rate in the hard clam *Mercenaria mercenaria*. *Aquaculture* 93:109-119.
- Harris, P. J., and J. C. McGovern.
1997. Changes in the life history of red porgy, *Pagrus pagrus*, from the southeastern United States, 1972-1994. *Fish. Bull.* 95:732-747.
- Haugen, T. O., and L. A. Vøllestad.
2001. A century of life-history evolution in grayling. *Genetica* 112-113 and 475-491.
- He, J. X., and D. J. Stewart.
2001. Age and size at first reproduction of fishes: predictive models based only on growth trajectories. *Ecology* 82:784-791.
- Heino, M.
1998. Management of evolving fish stocks. *Can. J. Fish. Aquat. Sci.* 55:1971-1982.
- Henryon, M., A. Jokumsen, P. Berg, I. Lund, P. B. Pederson, N. J. Olesen, W. J. Sierendrecht.
2002. Genetic variation for growth rate, feed conversion efficiency, and disease resistance exists within a farmed population of rainbow trout. *Aquaculture* 209:59-76.
- Hendry, A. P., J. K. Wenburg, P. Bentzen, E. C. Volk, T. P. Quinn.
2000. Rapid evolution of reproductive isolation in the wild: evidence from introduced salmon. *Science* 290:516-518.
- Hutchings, J. A.
1993. Adaptive life histories effected by age-specific survival and growth rate. *Ecology* 74:673-684.
- Jarayabhand, P., and M. Thavornyutikarn.
1995. Realized heritability estimation on growth rate of oyster, *Saccostrea cucullata* Born, 1778. *Aquaculture* 138:111-118.
- Law, R.
1991. On the quantitative genetics of correlated characters under directional selection in age-structured populations. *Phil. Trans. R. Soc. Lond. B* 331:213-223.
2000. Fishing, selection, and phenotypic evolution. *ICES J. Mar. Sci.* 57:659-668.
2001. Phenotypic and genetic changes due to selective exploitation. *In* Conservation of exploited species (J. D. Reynolds, G. M. Mace, K. H. Redford, and J. G. Robinson, eds.), p. 323-342. Cambridge Univ. Press, Cambridge, England.
- Law, R., and C. A. Rowell.
1993. Cohort-structured populations, selection responses, and exploitation of the North Sea cod. *In* The exploitation of evolving resources (T. K. Stokes, J. M. McGlade, and R. Law, eds.), p. 155-173. Lecture Notes in Biomathematics 99. Springer-Verlag, Berlin, Germany.
- Mangel, M.
1996. Life history invariants, age at maturity and the ferocet trout. *Evol. Ecol.* 10:249-263.
- McAllister, M. K., R. M. Peterman, and D. M. Gillis.
1992. Statistical evaluation of a large-scale fishing experiment designed to test for a genetic effect of size-selective fishing on the British Columbia pink salmon (*Oncorhynchus gorbuscha*). *Can. J. Fish. Sci.* 49:1294-1304.
- Miller, L. M., and A. R. Kapuscinski.
1994. Estimation of selection differentials from fish scales: a step towards evaluating genetic alteration of fish size in exploited populations. *Can. J. Fish. Sci.* 51:774-783.
- Olsen, E. M., M. Heino, G. R. Lilly, M. J. Morgan, J. Brattey, B. Ernande, and U. Dieckmann.
2004. Maturation trends indicative of rapid evolution preceded the collapse of northern cod. *Nature* 428:932-935.
- Quinn, T. J., II, and R. B. Deriso.
1999. Quantitative fish dynamics, 542 p. Oxford Univ. Press, New York, NY.
- Quinn, T. P., M. T. Kinnison, and M. J. Unwin.
2001. Evolution of Chinook salmon (*Oncorhynchus tshawytscha*) populations in New Zealand: pattern, rate, and process. *Genetica* 112-113:493-513.
- Ratner, S., and R. Lande.
2001. Demographic and evolutionary responses to selective harvesting in populations with discrete generations. *Ecology* 82:3093-3104.
- Reznick, D. N., F. H. Shaw, F. H. Rodd, and R. G. Shaw.
1997. Evaluation of the rate of evolution in natural populations of guppies (*Poecilia reticulata*). *Science* 275:1934-1937.
- Ricker, W. E.
1981. Changes in the average size and average age of Pacific salmon. *Can. J. Fish. Aquat. Sci.* 38:1636-1656.
- Roff, D. A.
1984. The evolution of life-history parameters in teleosts. *Can. J. Fish. Aquat. Sci.* 41:984-1000.
- Shertzer, K. W., and S. P. Ellner.
2002. Ecology storage and the evolution of population dynamics. *J. Theor. Biol.* 215:183-200.
- Shertzer, K. W., S. P. Ellner, G. F. Fussmann, and N. G. Hairston Jr.
2002. Predator-prey cycles in an aquatic microcosm: testing hypotheses of mechanism. *J. Anim. Ecol.* 71:802-815.
- Sinclair, A. F., D. P. Swain, and J. M. Hanson.
2002. Disentangling the effects of size-selective mortal-

- ity, density, and temperature on length-at-age. *Can. J. Fish. Aquat. Sci.* 59:372-382.
- Sinervo, B., E. Svensson, and T. Comendant.
2000. Density cycles and an offspring quantity and quality game driven by natural selection. *Nature* 406:985-988.
- Stearns, S. C.
1992. *The evolution of life histories*, 379 p. Oxford Univ. Press, Oxford, England.
- Stockwell, C. A., A. P. Hendry, and M. T. Kinnison.
2003. Contemporary evolution meets conservation biology. *Trends Ecol. Evol.* 18:94-101.
- Stokes, T. K., and S. P. Blythe.
1993. Size-selective harvesting and at-at-maturity. II: Real populations and management options. *In* The exploitation of evolving resources (T. K. Stokes, J. M. McGlade, and R. Law (eds.), p. 232-237. *Lecture Notes in Biomathematics* 99, Springer-Verlag, Berlin.
- Stokes, K., and R. Law.
2000. Fishing as an evolutionary force. *Mar. Ecol. Prog. Ser.* 208:307-309.
- Vandeputte, M., E. Quillet, and B. Chevassus.
2002. Early development and survival in brown trout (*Salmo trutta fario* L.): indirect effects of selection for growth rate and estimation of genetic parameters. *Aquaculture* 204:435-445.
- Weigensberg, I., and D. A. Roff.
1996. Natural heritabilities: can they be reliably estimated in the laboratory. *Evolution* 50:2149-2157.
- Williams, E. H., and K. W. Shertzer.
2003. Implications of life-history invariants for biological reference points used in fishery management. *Can. J. Fish. Aquat. Sci.* 60:710-720.
- Yoshida, T., L. E. Jones, S. P. Ellner, G. F. Fussmann, and N. G. Hairston Jr.
2003. Rapid evolution drives ecological dynamics in a predator-prey system. *Nature* 424:303-306.
- Xiao, Y.
1994. Von Bertalanffy growth models with variability in, and correlation between, K and L_{∞} . *Can. J. Fish. Aquat. Sci.* 51:1585-1590.

Preliminary evidence of increased spawning aggregations of mutton snapper (*Lutjanus analis*) at Riley's Hump two years after establishment of the Tortugas South Ecological Reserve

Michael L. Burton

Kenneth J. Brennan

Roldan C. Muñoz

Richard O. Parker Jr.

Center for Coastal Fisheries and Habitat Research
National Marine Fisheries Service
National Oceanic and Atmospheric Administration
101 Pivers Island Rd.
Beaufort, North Carolina 28516-9722
E-mail address: Michael.Burton@noaa.gov

In this note we describe the re-formation of a spawning aggregation of mutton snapper (*Lutjanus analis*). A review of four consecutive years of survey data indicates that the aggregation may be increasing in size. Mutton snapper are distributed in the temperate and tropical waters of the western Atlantic Ocean from Florida to southeastern Brazil (Burton, 2002). Juveniles and subadults are found in a variety of habitats such as vegetated sand bottoms, bays, and mangrove estuaries (Allen, 1985). Adults are found offshore on coral reefs and other complex hardbottom habitat. They are solitary and wary fish, rarely found in groups or schools except during spawning aggregations (Domeier et al., 1996). Spawning occurs from May through July at Riley's Hump (Domeier et al., 1996) and peaks in June, as indicated by gonadosomatic indices (M. Burton, unpubl. data). Mutton snapper are highly prized by Florida fishermen for their size and fighting ability, and the majority of landings occur from Cape Canaveral, through the Florida Keys, including the Dry Tortugas (Burton, 2002).

Reports of spawning aggregations of tropical reef fishes are abundant in the fisheries literature. Most documented aggregations of commercially important fishes are attributed to

members of the grouper family, Serranidae, including observations of spawning Nassau grouper (*Epinephelus striatus*), red hind (*E. guttatus*), and tiger grouper (*Mycteroperca tigris*) in the Caribbean (see review in Domeier and Colin, 1997, and references therein). Eklund et al. (2000) observed black grouper (*M. bonaci*) aggregating during their spawning season just outside no-take zones along the Florida Keys reef tract. Samoily and Squire (1994) and Samoily (1997) documented spawning aggregations of coral trout (*Plectropomus leopardus*) from the Great Barrier Reef, and Johannes (1988) described the aggregating behavior of squaretail coral grouper (*P. arcuatus*) from the Solomon Islands. Most recently, Sala et al. (2003) observed aggregating behavior in two species of serranids—the sawtail grouper (*M. prionura*) and the leopard grouper (*M. rosacea*) from the Gulf of California.

There are fewer descriptions of spawning aggregations of the commercially important snappers (Lutjanidae) in the literature. Wicklund (1969) described spawning behavior of lane snapper (*Lutjanus synagris*) from southeast Florida, Carter and Perrine (1994) described a spawning aggregation of dog snapper (*L. jocu*) from Belize, and Sala et al. (2003)

described spawning behavior in two lutjanids from the Gulf of California (yellow snapper, *L. argentiventris*; Pacific dog snapper, *L. novemfasciatus*). Mutton snapper (*L. analis*) are perhaps the best known snapper to form spawning aggregations. Craig (1966) observed concentrated commercial fishing on an apparent "spawning run" of mutton snapper in August at Long Cay, Belize. Domeier and Colin (1997) described an aggregation of *L. analis* in the Turks and Caicos Islands in April 1992, and Domeier et al. (1996) identified a spawning aggregation at Riley's Hump.

Because of their predictable nature with respect to location and time, spawning aggregations become extremely vulnerable to heavy exploitation once discovered by fishermen. The majority of annual catches of Nassau grouper in some areas come from annual spawning aggregations (Colin, 1992; Aguilar-Perera and Aguilar-Dávila, 1996), whereas other aggregations have been completely extirpated (Olsen and LaPlace, 1978; Sadovy and Eklund, 1999; Heyman, 2003). Russ (1991) observed that uncontrolled fishing on spawning aggregations could lead to recruitment overfishing. During a May 1991 survey of Riley's Hump, a site of a known mutton snapper spawning aggregation in the Dry Tortugas, Florida, Domeier and Colin (1997) noted that fish were more scattered and far less abundant than they were at the Turks and Caicos site. The authors suggested that this difference was attributable to heavy commercial fishing pressure at Riley's Hump during the several years prior to 1991.

Although recent literature indicates that fishing pressure on Riley's Hump has been intensive for several years prior to 1991 (Domeier and Colin, 1997), anecdotal information indicates otherwise. According to a commercial hook-and-line fisherman who fished on Riley's Hump from 1978 through 2001, the first known

Manuscript submitted 20 December 2003
to the Scientific Editor's Office.

Manuscript approved for publication
29 December 2004 by the Scientific Editor.
Fish. Bull. 103:404–410 (2005).

instance of commercial fishing on this area occurred in 1968 by a fisherman named Riley.¹ However, the navigation device in common use in 1968 was LORAN (long range navigation) A; thus, the likelihood of a fisherman finding the exact spot where he fished previously was much less likely than with today's global positioning system (GPS) receivers. Large-scale commercial fishing of Riley's Hump began in 1976, with the introduction of the improved LORAN C navigation system.

Commercial fishermen began fishing the area with longline gear in 1979, and fish traps were introduced there in 1984. This was the period of the most intensive fishing; longliners harvested between 10 and 21 metric tons per trip and fish trappers typically landed an average of 11.5 metric tons (Gladding¹). It is necessary to rely on knowledgeable fishermen for anecdotal data such as this because the National Marine Fisheries Service (NMFS) did not separate out individual species in their data sets prior to 1986, instead consolidating all snappers into an unclassified snapper category. After 1986, landings from the Dry Tortugas were included with the rest of the Florida Keys in a Monroe County total; therefore it is virtually impossible to obtain an exact magnitude of the landings from the Dry Tortugas for this time frame without information from knowledgeable fishermen who were involved in the fishery at the time. In addition to the commercial effort, a small fleet of headboats ran multiday fishing trips to Riley's Hump and other areas in the Dry Tortugas (Dixon²).

Fishermen began to realize declining catches in the mid-1980s and brought this to the attention of the fishery management councils. The Gulf of Mexico Fishery Management Council (GMFMC) enacted a spawning-season closure in 1992, prohibiting fishing on Riley's Hump in May and June (Gulf of Mexico Fishery Management Council, 1992). An analysis of pre- and postclosure commercial landing data revealed that, as a result of the closure, there was a shift in effort to the months on either side of the period of closure, and landings during the two-month closure decreased in only one of the months while annual landings increased (Burton, 1997). After further urging by fishermen and an effort by the Tortugas Working Group (a group of stakeholders appointed by the Florida Keys National Marine Sanctuary [FKNMS] Advisory Council), the Tortugas South Ecological Reserve (TSER) was created in July 2001 specifically to protect the spawning aggregation and habitat of mutton snapper. Current regulations prohibit all uses of the reserve, except continuous transit through the reserve, for any vessels without a FKNMS research permit. The authors initiated data collection on Riley's Hump in July 2001 to document the effect of the newly designated ecological reserve on abundance of snappers and groupers.

Materials and Methods

Study area

Riley's Hump is a carbonate bank of Holocene origin located 20 km southwest of the Dry Tortugas National Park (DTNP) island of Garden Key (Ft. Jefferson). Riley's Hump sits in the northeast corner of the TSER within the FKNMS (Fig. 1). The area has a predominantly low-relief hardbottom and patchy hard coral and scattered gorgonian sponge-soft coral communities. Rising to within 30 m of the surface, Riley's Hump covers an area of approximately 10 km². Habitat mapping efforts by Franklin et al. (2000), who used a nine-tier habitat classification scheme, and visual observations from SCUBA dives revealed that Riley's Hump consisted mostly of areas of rocky outcropping and some patchy hard bottom in sand. More detailed multibeam mapping showed that the top of the bank is relatively flat and has an escarpment on the south side of the bank dropping from 30 m to well over 50 m deep (Fig. 2) (Mallinson et al., 2003).

Sampling

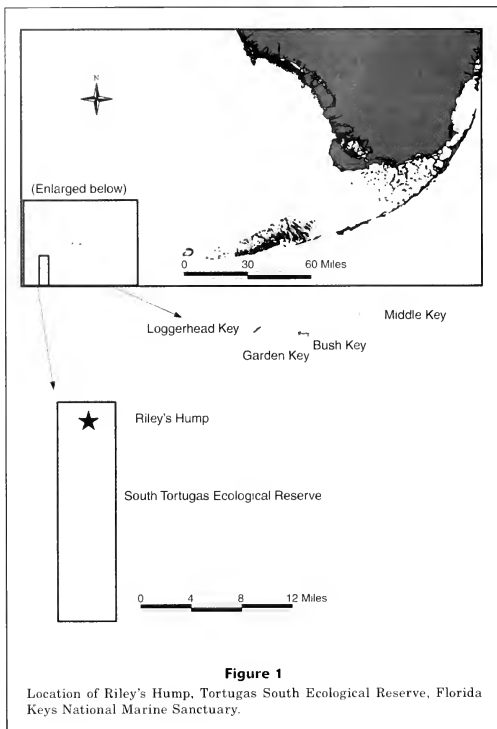
Initial sampling stations were selected in 2001 by dividing the top of Riley's Hump into a grid consisting of 0.40-km² sections and by conducting a census with the ship's depth sounder in order to identify (within as many grids as possible) reef habitat that could be reached by dives. Ten initial stations were selected according to this procedure. Five more stations were added in 2002 at the recommendation of our vessel captain, Peter Gladding (Fig. 2). Two-man dive teams conducted several 30-m visual census strip transects (Brock, 1954) at each station during the summer months of each year, enumerating all species of snappers and groupers observed.

Results

We summarize our observations of mutton snapper abundance and behavior on Riley's Hump in Table 1, along with the observation's relation in time to the lunar calendar. The initial sighting of an unusually large group of mutton snapper occurred on 17 July 2001. A group of 10 fish was observed by the senior author at station 2 (Fig. 2). The fish were swimming 0.5–1 m apart in a group approximately 1.5 m above the seafloor. The next year, on 27 May 2002, we observed a larger group of approximately 75–100 mutton snapper on the same site, station 2 (Fig. 2). These fish were exhibiting similar behavior to that observed the preceding year. The group remained schooled while the dive team completed one 30-m visual transect and then slowly dispersed as the divers returned to the aggregation location. On 15 June 2003, a team of divers discovered an aggregation of over 200 individual mutton snapper at station 12 (Fig. 2). The fish repeatedly swam up to the diver doing the census transects and then slowly turned and swam

¹ Gladding, P. 2003. Personal commun. 27A 12th Avenue, Stock Island, FL 33040.

² Dixon, R. 2003. Personal commun. CCFHR, NMFS, NOAA, 101 Pivers Island Rd., Beaufort, NC 28516-9722.



away. The aggregation was spread out over a wide area, was not as dense as in the previous two sightings, and exhibited the milling behavior similar to that described by Thresher (1984) for several other species of lutjanids. This aggregation remained at the site throughout the entire 20-minute census dive. Later that day, divers recording their observations at nearby station 2 reported a group of approximately 100 mutton snapper. These fish were more widely dispersed and maintained a distance of 3–5 m from divers. Finally, on 4 July 2004, the senior author and another diver encountered a large school of approximately 300 mutton snapper at station 12, exhibiting behavior similar to that observed during the preceding year.

Discussion

We believe that the large groups of fish encountered at station 12 in June 2003 and again in July 2004 were spawning aggregations based on their behavior and on the timing and location of the aggregation. First, behavior of the snappers themselves was not typical of nonspawning individuals. Although Humann (1997) described them as being very curious, mutton snapper are typically described as solitary animals (Domeier and Colin, 1997), cautious of divers, and not allowing close approach. Many large reef fishes exhibit similar solitary behavior, such as Nassau grouper (Smith, 1972) and black grouper (Eklund et al., 2000). The

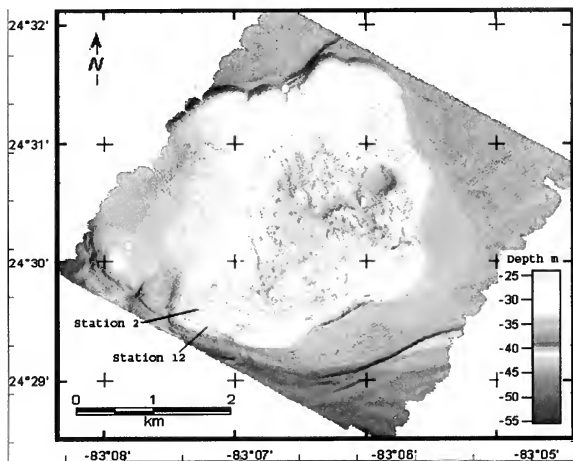


Figure 2

Multibeam bathymetric image of the top of Riley's Hump showing locations of visual census stations (white circles) and mutton snapper aggregation sightings (stations 2 and 12). Bathymetric image was provided courtesy of D. Naar and B. Donahue, Univ. S. Florida, from Mallinson et al., 2003.

Table 1
Observations on mutton snapper (*Lutjanus analis*) on Riley's Hump and their behavior as noted by the authors.

Date and station	Numbers observed	Behavior	Moon phase
28 May–1 June 1999	Solitary <i>L. analis</i> observed on 3 of 11 dives	Slowly swimming, diver avoidance	Full moon May 30
31 July–3 Aug 2000	Solitary <i>L. analis</i> observed on 5 of 6 dives	Slowly swimming, diver avoidance	New moon July 30
17 Jul 2001 Station 2	10	Swimming in a tightly packed group, 1.5 m off bottom	3 days before new moon
27 May 2002 Station 2	75–100	Swimming in tightly packed group, 1.5 m off bottom	1 day after full moon
15 June 2003 Station 2	75–100	Widely dispersed, diver avoidance	1 day after full moon
Station 12	200+	Widespread aggregation, actively swimming, did not avoid divers	
4 July 2004 Station 12	300	Widespread aggregation, actively swimming, did not avoid divers	2 days after full moon

senior author completed over 115 dives on Riley's Hump from 1995 through 2004, and the typical mutton snapper sighting during dives made outside the spawning season (February, 5 dives; August, 5 dives; October, 7 dives) was a single fish. In these instances, the closest approach allowed by the fish was 3 m, and when an attempt was made to approach, the fish would swim away, maintaining separation. The only exceptions to this behavior were the four sightings in which groups of fish were apparently unconcerned with the presence of divers (Table 1). Johannes (1981) described a condition he termed "spawning stupor" in *P. arcuatus* from Palau. He took this term from the Palauan fishermen's description of the fish as "stupid." We do not believe that "stupid" in this context means unaware, but more closely approximates Johannes et al.'s (1999) modified description of spawning stupor as more of a lack of concern about divers. Mutton snapper in the spawning aggregation we observed seemed aware of our presence because they approached and retreated from the divers many times. Domeier and Colin (1997) asserted that spawning or courtship behavior is easily broken off by a diver's close approach or SCUBA exhalation, although Johannes et al. (1999) offered evidence showing that this is not always the case. We conducted our dive operations primarily in the day and thus did not witness spawning, which is thought to occur at dusk or later (Domeier and Colin, 1997). Courtship behavior has not been described for mutton snapper except by Domeier and Colin (1997) who observed that fish in the Turks and Caicos aggregation "milled in a dense school from the bottom to within a few meters of the surface." The mutton snapper we observed exhibited this milling behavior and did not change it because of our presence.

Consistent timing of spawning with respect to a specific lunar phase has long been thought to be a characteristic of many spawning aggregations. Johannes (1978) noted that the majority of fishes with known lunar-associated spawning rhythms spawned near the full or new moon. However, the published literature does not provide strong support for a correlation between spawning of most lutjanid species and any single lunar phase. The lane snapper aggregation observed by Wicklund (1969) occurred just after the new moon but has not been corroborated since this single observation. Spawning of dog snapper in Belize was variable, however, occurring three days after the new moon on Cay Glory (Carter and Perrine, 1994) and just after the full moon on English Cay (Domeier and Colin, 1997). Spawning peaks for gray snapper off Key West, Florida, were also variable, occurring on the new and full moons of June–August, although the strongest spawning peak was associated with the last quarter moon of August, half way between the new and full moons (Domeier et al., 1996). Back-calculated spawning dates of gray snapper collected in ichthyoplankton samples near Beaufort Inlet, North Carolina, have indicated that spawning takes place primarily at the time of the new moon and secondarily at the time of the full moon (Tzeng et al., 2003).

Evidence of mutton snapper spawning tends to support the argument that the species spawns during a full moon, in contrast to the examples of other lutjanids above. Mutton snapper aggregations off Gladden Spit, Belize, peaked during the April and May full moons and were heavily exploited by fishermen (Heyman et al., 2001). Domeier and Colin's (1997) observation of a mutton snapper aggregation off West Caicos occurred on the April 1992 full moon, and Domeier collected specimens with hydrated oocytes from the Riley's Hump location within one day of the full moon in May 1991 (Domeier and Colin, 1997). Our observation of a small group of about 10 mutton snapper at Riley's Hump in July 2001 occurred three days before the new moon. Our observations of groups of approximately 100, 200, and 300 fish, however, occurred one day after the full moons of May 2002 and June 2003, and two days after the full moon of July 2004, respectively. In contrast, the back-calculated spawning dates of mutton snapper collected in ichthyoplankton samples near Beaufort Inlet, NC, indicated that spawning occurred from two days after the full moon to three days before the new moon and that peak spawning occurred between the full moon and last quarter moon phase (Hare³). These data are not inconsistent, however, with our observations of fish beginning to aggregate on or around the full moon for spawning. Our sightings of such large groups of mutton snapper around the full moon indicate activity associated with a spawning aggregation.

Finally, many species of reef fishes consistently aggregate to spawn at specific locations at regular intervals (e.g., daily, annually). The two main hypotheses as to why reef fishes do this are to offer increased chances of 1) immediate survival of eggs and larvae, and 2) entrainment of larvae in favorable currents for transport to suitable nursery habitat (Johannes, 1978; Lobel, 1978; Gladstone, 1994), although the former hypothesis currently has more support (Hensley et al., 1994; Peterson and Warner, 2002). Without invoking the hypothesis of local adaptation to the aggregation sites on Riley's Hump, several studies have indicated that the physical oceanography of the region is favorable for transporting larvae spawned at Riley's Hump up the Florida Keys reef tract (Lee et al., 1994; Lee and Williams, 1999) and even as far north as Vero Beach, Florida (Domeier, 2004), presumably to suitable habitat. We believe that the specific location on Riley's Hump where we observed aggregations supports our conclusion that these were spawning aggregations.

In describing lutjanid behavior Thresher (1984) said, "A key feature of reproduction . . . is an extensive spawning migration to select areas along the outer reef." Observations in the literature of reef fish spawning aggregations occurring on the outer reef edge, on seaward extensions or promontories, near the shelf-edge

³ Hare, J. 2002. Personal commun. Center for Coastal Fisheries and Habitat Research, National Ocean Service, NOAA, 101 Pivers Island Rd., Beaufort, NC 28516-9722.

break, on the reef slope or near drop-offs are numerous (Randall and Randall, 1963; Smith, 1972; Munro, 1974; Colin, 1992; Shapiro et al., 1993; Sadovy et al., 1994a, 1994b; Samoilys and Squire, 1994; Sala et al., 2003, and others). Heyman (2003) described a single promontory on a Belize reef that harbored spawning aggregations of 26 different species throughout the year. The mutton snapper aggregation from West Caicos (Domeier and Colin, 1997) occurred on a reef near a drop-off into deep water. The south end of Riley's Hump drops quickly from 35 m to well over 50 m. The two sites where we have observed unusually large numbers of mutton snapper are in the vicinity of this drop-off. Station 2, where we observed aggregations of various sizes in all four years, is approximately 300 m inshore of the edge, whereas station 12, where we observed the largest aggregation in June 2003 and July 2004, is within 150 m of the edge (Fig. 2).

We conclude from behavior, timing, and location that we are observing spawning aggregations of mutton snapper beginning to re-form on Riley's Hump following more than two decades of intensive exploitation. Although the numbers we observed are not close to anecdotal descriptions of the numbers of fish caught during the height of the commercial fishery at this location, it is encouraging to note that we have seen an increasing number of fish for each successive year that we have surveyed these stations. It is too early to say definitively whether the fish are actually becoming more abundant, but preliminary indications are that one effect of the TSER has been to increase numbers of mutton snapper. Current research plans include continued annual monitoring of transects and increased exploration for additional spawning sites, as well as an expansion of our surveys to the last quarter and new-moon phases in order to continue to try to document the exact timing of spawning.

Acknowledgments

We gratefully acknowledge and dedicate this paper to Peter Gladding, master of the FV *Alexis M*, for his superb boat handling skills and knowledge of Riley's Hump; Peter recently lost his battle with cancer and we will greatly miss his guidance and company on our trips. We acknowledge the contributions of Richard Stoker, first mate of the *Alexis M* for his repeated suggestions and help that improved our research efforts; Don Field, Don Demaria, Bill Gordon, and Ian Workman for their assistance at various times with diving efforts; Lisa Wood for her help with the figures; Jon Hare, Erik Williams, Michael Prager, and three anonymous reviewers for constructive reviews of the manuscript that greatly improved it.

Literature cited

- Aguilar-Perera, A., and W. Aguilar-Dávila.
1996. A spawning aggregation of Nassau grouper *Epinephelus striatus* (Pisces: Serranidae) in the Mexican Caribbean. *Environ. Biol. Fish.* 45:351-361.
- Allen, G. R.
1985. Snappers of the world. An annotated and illustrated catalogue of lutjanid species known to date. FAO Fish. Synop. 125:1-208.
- Brock, V. E.
1954. A preliminary report on a method of estimating reef fish populations. *J. Wildl. Manage.* 18:297-308.
- Burton, M. L.
1997. The effect of spawning season closures on landings of two reef associated species. *Proc. Gulf. Caribb. Fish. Inst.* 50:896-918.
2002. Age, growth and mortality of mutton snapper, *Lutjanus analis*, from the east coast of Florida, with a brief discussion of management implications. *Fish. Res.* 59:31-41.
- Carter, J., and D. Perrine.
1994. A spawning aggregation of dog snapper, *Lutjanus jocu* (Pisces: Lutjanidae) in Belize, Central America. *Bull. Mar. Sci.* 55:228-234.
- Colin, P.
1992. Reproduction of the Nassau, grouper, *Epinephelus striatus* (Pisces: Serranidae) and its relationship to environmental conditions. *Environ. Biol. Fish.* 34:357-377.
- Craig, A. K.
1966. Geography of fishing in British Honduras and adjacent coastal waters. Tech. Rep. Coastal Studies Lab. No. 28, Louisiana State Univ., Baton Rouge, LA.
- Domeier, M. L.
2004. A potential larval recruitment pathway originating from a Florida marine protected area. *Fish. Oceanogr.* 13:287-294.
- Domeier, M. L., and P. L. Colin.
1997. Tropical reef fish spawning aggregations: defined and reviewed. *Bull. Mar. Sci.* 60:698-726.
- Domeier, M. L., C. Koenig, and F. Coleman.
1996. Reproductive biology of gray snapper (*Lutjanus griseus*) with notes on spawning for other western Atlantic snappers (Lutjanidae). In *Biology and culture of tropical groupers and snappers* (F. Arreguin-Sanchez, J. L. Munro, M. C. Balgos, and D. Pauly, eds.), p. 189-201. International Center for Living Aquatic Resources Management Conference Proceedings 48, ICLARM, Makati City, Philippines.
- Eklund, A. M., D. B. McClellan, and D. E. Harper.
2000. Black grouper aggregations in relation to protected areas within the Florida Keys National Marine Sanctuary. *Bull. Mar. Sci.* 66:721-728.
- Franklin, E. C., J. S. Ault, S. G. Smith, J. Luo, G. A. Meester, G. A. Diaz, M. Chiappone, D. W. Swanson, S. L. Miller, and J. A. Bohnsack.
2000. Benthic habitat mapping in the Tortugas region, Florida. *Mar. Geodesy* 26:19-34.
- Gladstone, W.
1994. Lek-like spawning, parental care and mating periodicity of the triggerfish *Pseudobalistes flavimarginatus* (Balistidae). *Environ. Biol. Fish.* 39:249-257.
- Gulf of Mexico Fishery Management Council.
1992. Help proposed for mutton snapper. *Gulf Fishery News* 12(4):2.
- Hensley, D. A., R. S. Appeldoorn, D. Y. Shapiro, M. Ray, and R. G. Turingan.
1994. Egg dispersal in a Caribbean coral reef fish,

- Thalassoma bifasciatum*. 1. Dispersal off the reef platform. *Bull. Mar. Sci.* 54:256-270.
- Heyman, W.
2003. Session introduction: conservation of multi-species reef fish spawning aggregations. *Proc. Gulf Caribb. Fish. Inst.* 54:650-651.
- Heyman, W. D. R. T. Graham, B. Kjerfve, and R. E. Johannes.
2001. Whale sharks *Rhinocodon typus* aggregate to feed on fish spawn in Belize. *Mar. Ecol. Prog. Ser.* 215:275-282.
- Humann, P.
1997. Reef fish identification: Florida, Caribbean, Bahamas, 2nd ed., 396 p. New World Publications, Inc. Jacksonville, FL.
- Johannes, R. E.
1978. Reproductive strategies of coastal marine fishes in the tropics. *Environ. Biol. Fish.* 3: 65-84.
1981. Words of the lagoon: fishing and marine lore in the Palau district of Micronesia. 245 p. Univ. California Press, Berkeley, CA.
1988. Spawning aggregation of the grouper *Plectropomus aeorolatus* (Ruppel) in the Solomon Islands. In *Proceedings of the 6th international coral reef symposium*, Townsville, Australia, 1988 (J. H. Choat, D. Barnes, M. A. Borowitzka, J. C. Coll, P. J. Davies, P. Flood, B. G. Hatcher, D. Hopley, P. A. Hutchings, D. Kinsey, G. R. Orme, M. Pichon, P. F. Sale, P. Sammarco, C. C. Wallace, C. Wilkinson, E. Wolanski, and O. Bellwood, eds.), p. 751-755. Sixth International Coral Reef Symposium Executive Committee, Townsville, Australia.
- Johannes, R. E., L. Squire, T. Graham, Y. Sadovy, and H. Renguul.
1999. Spawning aggregations of groupers (Serranidae) in Palau. *Mar. Conserv. Res. Ser. Publ.* 1, 144 p. The Nature Conservancy, Arlington, VA.
- Lee, T. N., M. E. Clarke, E. Williams, A. F. Szmant, and T. Berger.
1994. Evolution of the Tortugas Gyre and its influence on recruitment in the Florida Keys. *Bull. Mar. Sci.* 54:621-646.
- Lee, T. N., and E. Williams.
1999. Mean distribution and seasonal variability of coastal currents and temperature in the Florida Keys with implications for larval recruitment. *Bull. Mar. Sci.* 64:35-56.
- Lobel, P.
1978. Diel, lunar and seasonal periodicity in the reproductive behavior of the pomacanthid fish, *Centropyge potteri*, and some other reef fishes in Hawaii. *Pac. Sci.* 32:193-207.
- Mallinson, D., A. Hine, P. Hallock, S. Locker, E. Shinn, D. Naar, B. Donahue, and D. Weaver.
2003. Development of small carbonate banks on the south Florida platform margin: response to sea level and climate change. *Mar. Geol.* 199:45-63.
- Munro, J. L.
1974. The biology, ecology and bionomics of Caribbean reef fishes. Mullidae (goatfishes). *Res. Rept.* 3, 44 p. Zool. Dept., Univ. West Indies, Kingston, Jamaica.
- Olsen, D. A., and J. A. LaPlace.
1978. A study of a Virgin Islands grouper fishery based on a breeding aggregation. *Proc. Gulf Caribb. Fish. Inst.* 31:130-144.
- Peterson, C. W., and R. R. Warner
2002. The ecological context of reproductive behavior. In *Coral reef fishes: dynamics and diversity in a complex ecosystem* (P. F. Sale, ed.), p. 103-118. Academic Press, New York, NY.
- Randall, J. E., and H. A. Randall.
1963. The spawning and early development of the Atlantic parrotfish, *Sparisoma rubripinne*, with notes on other scarid and labrid fishes. *Zoologica* 48:49-60.
- Russ, G. R.
1991. Coral reef fisheries: effects and yields. In *The ecology of fishes on coral reefs* (P. F. Sale, ed.), p. 601-635. Academic Press, New York, NY.
- Sadovy, Y., P. L. Colin, and M. L. Domeier.
1994a. Aggregation and spawning in the tiger grouper, *Mycteroperca tigris* (Pisces: Serranidae). *Copeia* 1994:511-516.
Sadovy, Y., and A. M. Eklund.
1999. Synopsis of biological data on the Nassau grouper, *Epinephelus striatus* (Bloch, 1972) and the jewfish, *E. itojara* (Lichtenstein, 1822). NOAA Tech. Rep. NMFS 146, 68 p.
Sadovy, Y., A. Rosario, and A. Román.
1994b. Reproduction in an aggregating grouper, the red hind, *Epinephelus guttatus*. *Environ. Biol. Fish.* 41:269-286.
- Sala, E., O. Aburto-Orapeza, G. Paredes, and G. Thompson.
2003. Spawning aggregations and reproductive behavior of reef fishes in the Gulf of California. *Bull. Mar. Sci.* 72:103-121.
- Samoilys, M.
1997. Periodicity of spawning aggregations of coral trout *Plectropomus leopardus* (Pisces:Serranidae) on the northern Great Barrier Reef. *Mar. Ecol. Prog. Ser.* 160:149-159.
- Samoilys, M., and L. Squire.
1994. Preliminary observations on the spawning behavior of coral trout, *Plectropomus leopardus* (Pisces: Serranidae) on the Great Barrier Reef. *Bull. Mar. Sci.* 54:332-342.
- Shapiro, D. Y., Y. Sadovy, and M. A. McGehee.
1993. Size, composition and spatial structure of the annual spawning aggregation of the red hind, *Epinephelus guttatus* (Pisces: Serranidae). *Copeia* 1993:399-406.
- Smith, C. L.
1972. A spawning aggregation of Nassau grouper, *Epinephelus striatus* (Bloch). *Trans. Am. Fish. Soc.* 101:257-261.
- Thresher, R. E.
1984. Reproduction in reef fishes, 399 p. T.F.H. Publications, Neptune City, NJ.
- Tzeng, M. W., J. A. Hare, and D. G. Lindquist.
2003. Ingress of transformation stage gray snapper, *Lutjanus griseus* (Pisces: Lutjanidae) through Beaufort Inlet, North Carolina. *Bull. Mar. Sci.* 72:891-908.
- Wicklund, R.
1969. Observations on spawning of lane snapper. *Underw. Nat.* 6:40.

Feeding habits of European hake (*Merluccius merluccius*) in the central Mediterranean Sea

Paolo Carpentieri

Francesco Colloca

Department of Animal and Human Biology

University "La Sapienza"

Viale dell'Università 32

00185 Rome, Italy

E-mail address (for P. Carpentieri) paolo.carpentieri@uniroma1.it

Massimiliano Cardinale

Institute of Marine Research

National Board of Fisheries

P.O. Box 4

45 332, Lysekil, Sweden

Andrea Belluscio

Giandomenico D. Ardzzone

Department of Animal and Human Biology

University "La Sapienza"

Viale dell'Università 32

00185 Rome, Italy

European hake (*Merluccius merluccius*) is an important predator of deeper shelf-upper slope Mediterranean communities. It is a neobenthic species distributed over a wide depth range (20–1000 m) throughout the Mediterranean Sea and the north east Atlantic region (Fisher et al., 1987). Notwithstanding the ecological and economic importance (Oliver and Massuti, 1995) of hake in the Mediterranean, many aspects of its biology (e.g., recruitment and reproduction), due to multiple spawning (Sarano, 1986) and the current state of exploitation, are poorly understood (Arneri and Morales-Nin, 2000).

Recent studies on hake feeding habits in the Mediterranean (Papaconstantinou and Caragitsou, 1987; Bouaziz et al., 1990; Oliver and Massuti, 1995) have focused on 0–3 age groups using data from trawl catches (Recasens et al., 1998; Colloca et al., 2000). For this reason, trophic habits of older individuals (Bozzano et al., 1997) and possible ontogenetic-related diet changes are almost

unknown. Therefore, in this study we combined samples from trawl and gillnet fisheries collected in the same fishing ground (Colloca et al., 2000) to address these issues.

Materials and methods

The study area is located off the central western coasts of Italy, covering 13,404 km² between 20 and 700 meters depth (outer boundaries: latitude 40°52'64", longitude 13°23'13"; latitude 42°20'30", longitude 11°16'32").

Monthly size-stratified samples were obtained from spring 1997 to winter 1998 both from bottom-trawls, gillnet commercial-vessels, and from commercial landings. Trawlers catch mainly 0–2 year-old juveniles; they rarely capture adults (Aldebert et al., 1993; Abella et al., 1997; Ardzzone and Corsi, 1997). The gillnet fishery exploits mainly adults of the species (>25 cm TL).

Caught fish were kept on ice, subsequently frozen to prevent di-

gestion of their stomach contents, taken to the laboratory, measured (total length: TL) to the nearest 1 mm, and weighed to the nearest 0.01 g. Sex and maturity stage were also recorded. Maturity state was determined by macroscopic analysis of the gonads by using the maturity scale for partial spawners (Holden and Raitt, 1974).

Stomachs were removed and their contents weighed to the nearest 0.001 g. Prey items were identified and sorted into taxonomic groups to the species level whenever possible. When the state of digestion was more advanced, prey were checked and grouped into unidentified fish, cephalopods, or crustaceans. The degree of digestion of the prey was not considered in the analysis. Empty stomachs and those with partially everted or unidentified contents were excluded from the total sample.

With the exception of the largest individuals (grouped into two heterogeneous length classes), all remaining hakes in the sample were grouped into 5-cm length classes. The study of size-related diet variations was based on these groups. The contribution of each food item to the diet of these fish length groups was evaluated by using the index of relative importance (IRI, Pinkas et al., 1971) as modified by Hacunda (1981): $IRI = F(N + W)$.

This index, expressed as

$$IRI\% = IRI - \frac{IRI}{\sum IRI} \times 100,$$

incorporates the percentage by number ($N\%$), wet weight ($W\%$), and frequency of occurrence ($F\%$) (Hyslop, 1980). Hierarchical cluster analysis and nonmetric multidimensional scaling (NMDS), based on Bray-Curtis similarity and on the IRI%, were used for classification and ordination of hake size classes (Clarke and Warwick, 1994).

Manuscript submitted 27 April 2003 to the Scientific Editor's Office.

Manuscript approved for publication 13 December 2004.

Fish. Bull. 103:411–416 (2005).

Results

A total of 2761 hakes between 5 and 90 cm TL were collected (Table 1). The total number of prey was about 1700, divided into 46 different species. Cluster and NMDS analysis (stress=0.02) based on the IRI allowed the identification of four groups below 50% similarity that were separated along a size gradient (Fig. 1).

Euphausiids (*Nectiphanes couchi*, IRI=76%) and mysids (*Lophogaster typicus*, IRI=22%) dominated the diet of group A (hake between 5 and 10.9 cm TL), and decapods were the secondary prey.

Group B (hake from 11 to 15.9 cm TL) showed a more heterogeneous diet characterized by a high occurrence of euphausiids but also with a considerable number of decapods (IRI=18%). Decapods were represented by a wide variety of species, such as *Chlorotocus crassicornis*, *Alpheus glaber*, *Plesionika heterocarpus*, *Pasiphaca sivado*, and *Solenocera membranacea*. Pisces and mysids showed lower percentages (IRI=15% and 4%, respectively). Sepioliidae (IRI=0.9%), *Sepietta oweniana* and *Alloteuthis media*, dominated among cephalopods.

The data suggest a gradual change towards a fully piscivorous diet (Fig. 2) which begins around 16 cm TL and is completed when sexual maturity is attained (TL=32 cm for males and TL=38.5 cm for females; Colloca et al., 2002).

The importance of teleosts strongly increased in group C (hake from 16 to 35.9 cm TL), where they accounted for 91% of hake diet. The main prey were Clupeiformes (IRI=61%), *Sardina pilchardus* and *Engraulis encrasicolus*. Fish (IRI=96%) represented almost the entire diet of group D (>36 cm TL). In this group a shift towards Centranchthidae (*Spicara flexuosa*, *Centranchthus cirrus*) and a simultaneous decline in consumption of Clupeiformes was observed. Among decapods (IRI=4%), two species occurred most frequently: *Processa* spp. and *S. membranacea*. Euphausiids, mysids, and cephalopods were absent in the diet of hakes larger than 36 cm TL.

Cannibalism of hake juveniles also accounted for some of the diet and increased with predator size. In hake between 36 and 40 cm TL cannibalism represented 12% of IRI, reaching the highest values (IRI=17%) among larger individuals (TL >51 cm).

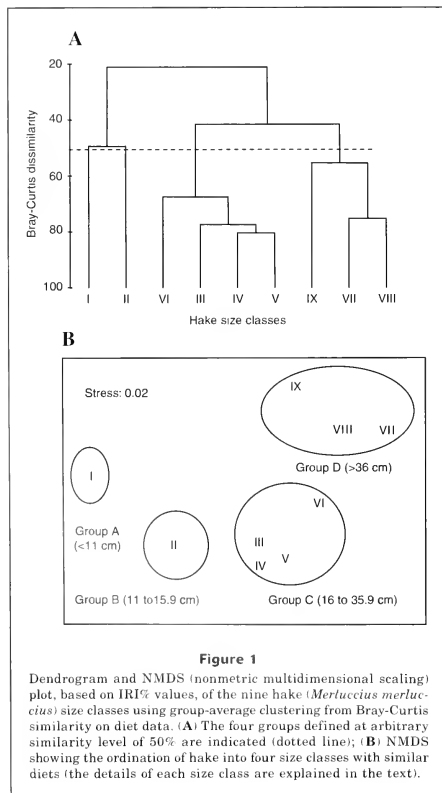


Figure 1

Dendrogram and NMDS (nonmetric multidimensional scaling) plot, based on IRI% values, of the nine hake (*Mertuacius merluccius*) size classes using group-average clustering from Bray-Curtis similarity on diet data. (A) The four groups defined at arbitrary similarity level of 50% are indicated (dotted line); (B) NMDS showing the ordination of hake into four size classes with similar diets (the details of each size class are explained in the text).

Discussion

Hake is a top predator that occupies different trophic levels during its ontogenetic development. Hake size classes are differentiated along food niche dimensions according to different prey sizes or different prey taxa. Hake diet shifted from euphausiids, consumed by the smaller hakes (<16 cm TL), to fishes consumed by larger hakes. Before the transition to the complete ichthyophagous phase, hake showed more generalized feeding habits where decapods, benthic (Gobiidae, *Callionymus* spp., *Arnoglossus* spp.) and nectonic fish (*S. pilchardus*, *E. encrasicolus*) dominated the diet, and cephalopods had a lower incidence. Specific size-related differences in prey spectrum seem to be associated with different spatial distributions or genetic needs (or with both) (Flamigni, 1984; Jukic and Arneri, 1984; Velasco and Olaso, 1998).

The patterns observed in the present study indicated a strong partitioning among hake

Table 1

Number of hakes and values of IRI (index of relative importance) (%) for the nine size classes. The four groups identified from the cluster analysis are indicated.

Size group	A		B		C			D		
	I	II	III	IV	V	VI	VII	VIII	IX	
Length (cm)	5.0–10.9	11.0–15.9	16.0–20.9	21.0–25.9	26.0–30.9	31.0–35.9	36.0–40.9	41.0–50.9	51.0–90.0	
Number of hakes	202	430	564	454	555	224	139	107	75	
Stomach contents	93	215	239	173	170	78	45	35	26	
Prey										
Cephalopoda										
<i>Alloteuthis media</i>		0.22	0.02	0.01						
<i>Sepietta oweniana</i>		0.02	0.02	0.01						
Unid. Sepiolidae		0.35	0.30	0.03						
Unid. Cephalopoda		0.42	0.10	0.01	0.02					
Crustacea										
<i>Alpheus glaber</i>		0.02	0.33	0.05	0.22	0.05	0.81	1.54		
Aristeidae			0.01	0.02						
<i>Aristeus antennatus</i>		0.02								
<i>Chlorotocus crassicornis</i>		1.61	1.83	1.09	1.10	0.48				
Crangonidae			0.01	0.01						
Pandalidae		0.03		0.01						
<i>Parapenaeus longirostris</i>				0.01						
<i>Pasiphaea multidentata</i>		0.02		0.01						
<i>Pasiphaea sivado</i>		0.20	0.04	0.05	0.02	0.05			0.33	
<i>Plesionika heterocarpus</i>		0.11	0.01							
<i>Plesionika</i> sp.		0.62	0.07	0.01	0.04	0.05				
<i>Pontocaris lacazei</i>		0.01	0.02	0.01			0.20			
<i>Pontophilus spinosus</i>		0.01	0.01	0.03	0.05	0.20				
<i>Processa</i> sp.		0.25	0.06	0.06	0.15	1.77	0.83	1.54		
<i>Solenocera membranacea</i>		0.04	0.02	0.05	0.34	0.58	3.27	3.53		
<i>Squilla</i> sp.					0.05					
Unid. Decapoda	3.05	19.91	6.19	2.84	2.73	1.45		1.58	1.32	
<i>Lophogaster typicus</i>	28.77	4.34	0.16			0.01				
<i>Nectiphanes couchi</i>	54.10	31.83	0.37							
Unid. Euphasiacea	13.99	3.43	0.11							
Unid. Isopoda	0.07	0.02	0.01							
Pisces										
<i>Argentina sphyraena</i>				0.08	0.41	1.06	4.04	3.29	2.34	
<i>Arnoglossus laterna</i>			0.01	0.01						
<i>Arnoglossus</i> sp.			0.01	0.01	0.01					
<i>Callionymus</i> sp.			0.01	0.01	0.01	0.06				
Centranchidae				0.03	0.11	2.60	2.43	11.23	53.97	
<i>Centranchus cirrus</i>						1.93	26.54	4.62	3.80	
<i>Clorophthalmus agassizi</i>			0.01							
<i>Conger conger</i>							0.34	0.85		
<i>Echiodon dentatus</i>					0.05					
<i>Engraulis encrasicolus</i>		1.95	11.61	1.28	4.45	9.91	0.87	1.27	1.86	
<i>Gadiculus argenteus</i>					0.08	0.65	0.31	0.58		
Gobiidae		0.04	0.02	0.01	0.01	0.05				
<i>Gobius quadrimaculatus</i>			0.02	0.02	0.01					
<i>Lepidotrigla dieuzedei</i>				0.01	0.01				0.78	
<i>Lesuerigobius friesii</i>			0.01	0.02	0.03					
<i>Merluccius merluccius</i>					0.07	0.18	12.00	4.10	17.95	

continued

Table 1 (continued)

Size group	A		B			C			D		
	I	II	III	IV	V	VI	VII	VIII	IX		
Pisces (continued)											
<i>Mullus barbatus</i>						0.12	0.44		0.49		
Myctophidae		0.30	0.28	0.03	0.15						
<i>Nettastoma melanurum</i>		0.02		0.01	0.01						
<i>Sardina pilchardus</i>		0.05	45.23	72.55	46.19	62.0	5.20	12.77	10.31		
<i>Sphyræna sphyraena</i>							0.60	4.98			
<i>Spicara flexuosa</i>				0.02	0.10	1.33	12.63	21.83	0.01		
<i>Spicara</i> sp.						0.37	4.57	0.54	1.69		
<i>Trachurus trachurus</i>					0.09	0.13	1.60	1.93			
<i>Trisopterus m. capelanus</i>			0.02	0.01	0.01	0.05					
Unid. Osteichthyes	0.04	34.19	33.14	21.61	43.44	15.01	23.09	22.90	4.25		
<i>Raja</i> sp.								0.50			

size classes. Two main thresholds associated with ontogenesis-related diet changes have been identified. The first one was observed around 16 cm TL and corresponded to a significant change in depth distribution. The second, around 36 cm TL, corresponded to the attainment of sexual maturity (Colloca et al., 2002).

Although hakes are demersal fishes, they feed typically upon fast-moving pelagic prey that are ambushed in the water column (Alheit and Pitcher, 1995). There is evidence that hakes feed in mid-water or near the surface at night, undertaking daily vertical migrations (Hickling, 1927; Papaconstantinou and Caragitsou, 1987; Orsi-Relini et al., 1989) which are more frequent for juveniles. Small hakes feed daily on small Euphausiacea (*Nectiphanes couchi*). This school-forming planktonic crustacean carries out vertical migrations at night (Casanova, 1970; Franqueville, 1971; Vallet and Dauvin, 2001). They rise to near the surface at night to feed on phytoplankton and sink during daylight between 50 and 800 m depth (Buchholz et al., 1995). Juveniles of *M. merluccius* may follow such migrations, moving from near the bottom, 100–200 m depth, to midwater at night (Frogliola 1973; Papaconstantinou and Caragitsou, 1987; Orsi-Relini et al., 1989). Nocturnal vertical migration behavior has been described for gadoids such as hake and cod and is considered responsible for the reduction of trawl catches of these fish at night (Beamish, 1966; Bowman and Bowman, 1980).

Considerable diet changes have been observed after the first year of life (>16 cm TL) when juveniles move from nursery areas on the shelf-break and upper slope to the middle shelf (Andaloro et al., 1985; Ardizzone and Corsi, 1997). The data indicate that such migration is induced by a change in trophic requirements. In this size class, diet changed to fish prey (Clupeiformes), and the importance of the small epipelagic crustaceans

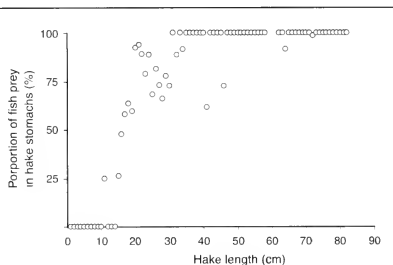


Figure 2

Proportion (%) of fish prey occurring in the diet of hake (*Merluccius merluccius*) during its growth.

(Euphausiacea) strongly decreased. Clupeiforms *S. pilchardus* and *E. encrasicolus* are distributed largely on the continental coastal shelf forming schools usually deeper than 25 m (Fisher et al., 1987).

The size-depth distribution pattern of hake was confirmed by experimental trawl surveys carried out in the Mediterranean (Relini and Piccinetti, 1996; Relini et al., 1999). Juveniles (modal length of 10 cm TL) are found mostly between 100 and 200 m depth. Intermediate hakes reach the highest abundance mainly on the shelf (<100 m). Large hakes (>36 cm) are found in a wide depth range but concentrate on the shelf break during the spawning period (Recasens et al., 1998; Colloca et al., 2000; Alvarez et al., 2001).

Growth induces a continuous qualitative and quantitative change in diet that is reflected in the increasing

mean weight of prey and decreasing mean number of prey items per stomach. The shift towards large fish prey (i.e., Centracanthidae) usually occurs slightly before maturity—the life history stage with much higher energetic demands due to gonad development (Ross, 1978). A similar pattern was observed for Atlantic cod (*Gadus morhua*) where sexual maturation and spawning are also associated with an ontogenetic change in diet (Paz et al., 1993). Thus, increased energy demands related to sexual requirements, gonad development, and breeding activity appear to be the critical factors driving the changes in feeding strategy of *M. merluccius*.

In large hakes (>36 cm), cannibalism played an important role and should be carefully considered in stock-recruitment analyses. Studies carried out in the Mediterranean (Macpherson, 1977; Bozzano et al., 1997) and in the Atlantic (Guichet, 1995; Link and Garrison, 2002) showed that cannibalism has some importance for hake. In silver hake (*M. bilinearis*), cannibalism notably increased with ontogeny (Link and Garrison, 2002). In the large cape hakes, *M. capensis*, hake is the dominant food item (50% of the diet) for individuals larger than 60 cm (Roel and Macpherson, 1988). Conversely, a low cannibalism rate was observed for *M. paradoxus* in the same area (Payne et al., 1987). This could be a response to the greater accessibility of conspecifics compared to other species. As Payne et al. (1987) pointed out, small hake are not found in the vicinity of adults of the species. This is supported by the observed size segregation by depth, which is more pronounced in *M. paradoxus* than in *M. capensis* (Gordoa and Duarte, 1991). Density-dependent cannibalism may be an important source of natural mortality that can stabilize fish populations (Smith and Reay, 1991), and for *M. capensis*, cannibalism has even been considered the main cause of natural mortality (Leonart et al., 1985; Payne and Punt, 1985).

Our results on the trophic ecology of hake are of primary importance for future management of fish assemblages where this species plays an important predatory role. Multispecies management requires quantitative data on fish diet to elucidate the relationships between species and, consequently, to forecast temporal biomass fluctuations, under specific fishing regimes, in an integrated manner.

Literature cited

- Abella, A., J. F. Caddy, and F. Serena.
1997. Do natural mortality and availability decline with age? An alternative yield paradigm for juvenile fisheries, illustrated by the hake *Merluccius merluccius* fishery in the Mediterranean. *Aquat. Living. Resour.* 10:1-14.
- Aldebert, Y., L. Recasens, and J. Leonart.
1993. Analysis of gear interaction in a hake fishery: the case of the Gulf of Lions (NW Mediterranean). *Sci. Mar.* 57:207-217.
- Alheit, J., and T. J. Pitcher (eds.).
1995. Hake: fisheries, ecology and markets, 478 p. Chapman and Hall, London.
- Alvarez, P., L. Motos, A. Uriarte, and J. Egana.
2001. Spatial and temporal distribution of European hake, *Merluccius merluccius* (L.), eggs and larvae in relation to hydro-biological conditions in the Bay of Biscay. *Fish. Res.* 50:111-128.
- Andaloro, F., P. Arena, and S. Prestipino Giarratta.
1985. Contribution to the knowledge of the age, growth and feeding of hake *Merluccius merluccius* (L. 1758) in the Sicilian channel. *FAO Fish Rep.* 336:93-97.
- Ardizzone, G. D., and F. Corsi.
1997. Atlas of Italian demersal fishery resources. *Biol. Mar. Medit.* 4(2), 568 p.
- Arneri, E., and B. Morales-Nin.
2000. Aspects of the early life history of European hake from the central Adriatic. *J. Fish. Biol.* 53:1155-1168.
- Beamish, F. W. H.
1966. Vertical migration of demersal fish in the northwest Atlantic. *J. Fish. Res. Board Can.* 23: 109-139.
- Bouaziz, A., F. Djabali, and C. Maurin.
1990. Régime alimentaire du merlu (*Merluccius merluccius*, L., 1758) en baie de Bou Ismail. *Rapp. Comm. int. Mer Médit.* 32(1):273.
- Bowman, R. E., and E. W. Bowman.
1980. Diurnal variation in the feeding intensity and catchability of the silver hake (*Merluccius bilinearis*). *Can. J. Fish. Aquat. Sci.* 37:1562-1572.
- Bozzano, A., L. Recasens, and P. Sartor.
1997. Diet of the European hake *Merluccius merluccius* (Pisces: Merlucciidae) in the Western Mediterranean (Gulf of Lions). *Mar. Sci.* 61(1):1-8.
- Buchholz, F., C. Buchholz, J. Reppin, and J. Fischer.
1995. Diel vertical migration of *Meganectiphanes norvegica* in the Kattegat: comparison of net catches and measurements with acoustic Doppler current profilers. *Helgol. Wiss. Meeresunters* 49:849-866.
- Casanova, B.
1970. Répartition bathymétrique des euphausiacés dans le bassin occidental de la Méditerranée. *Rev. Trav. Inst. Pêches Marit.* 34(2):205-219.
- Clarke, K. R., and R. M. Warwick.
1994. Change in marine communities: an approach to statistical analysis and interpretation, 144 p. Natural Environment Research Council, UK.
- Colloca, F., A. Belluscio, and G. D. Ardizzone.
2000. Sforzo di pesca, cattura e gestione dello stock di nasello (*Merluccius merluccius*, L.) in un'area del tirreno centrale. *Biol. Mar. Medit.* 7(1):117-129.
- Colloca, F., P. Gentilioni, A. Belluscio, P. Carpentieri, and G. D. Ardizzone.
2002. Estimating growth parameters of the European hake (*Merluccius merluccius*) through the analysis and validation of annual increments in otoliths. *Arch. Fish. Mar. Res.* 50 (2):174-179.
- Fisher, W., W. M. Bauchot, and M. Schneider.
1987. Fiches FAO d'identification pour les besoins de la pêche révision 1. Méditerranée et mer Noire. Zone de pêche 37, vol. 2: Vertébrés, p. 761-1530. FAO, Rome.
- Flamigni, C.
1984. Preliminary utilization of trawl survey data for hake (*Merluccius merluccius*, L.) population dynamics in the Adriatic Sea. *FAO Fish. Rep.* 290:109-115.
- Franqueville, C.
1971. Macroplankton profond (invertébrés) de la Méditerranée nord-occidentale. *Tethys* 3(1):11-56.

- Froglio, C.
1973. Osservazioni sull'alimentazione del merluzzo (*Merluccius merluccius* L.) del Medio Adriatico. In Atti V Congresso Naz. Soc. It. Biol. Mar. (N. Salentina, ed.), p. 327-341.
- Gordoa, A., and C. M. Duarte.
1991. Internal school density of Cape hake (*Merluccius capensis*). Can. J. Fish. Aquat. Sci. 48:2095-2099.
- Guichet, R.
1995. The diet of European hake (*Merluccius merluccius*) in the northern part of the Bay of Biscay. ICES J. Mar. Sci. 52:21-31.
- Hacunda, J. S.
1981. Trophic relationships among demersal fishes in a coastal area of the Gulf of Maine. Fish. Bull. 79: 775-788.
- Hickling, C. F.
1927. The natural history of the hake. Parts 1 and II. Fish. Invest. Serv. II, 10 (2), 112 p.
- Holden, M. J., and D. F. S. Raitt.
1974. Manual of fisheries science. Part 2: Methods of resources investigation and their application. FAO Fish. Tech. Paper 115, 214 p. FAO, Rome.
- Hyslop, E. J.
1980. Stomach content analysis: a review of methods and their application. J. Fish Biol. 17:411-429.
- Jukic, S., and E. Arneri.
1984. Distribution of hake (*Merluccius merluccius*, L.) striped mullet (*Mullus barbatus*, L.) and pandora (*Pagellus erythrinus*, L.) in the Adriatic Sea. FAO Fish. Rep. 290:85-91.
- Leonart, J. J. Salat, and E. Macpherson.
1985. CSPA, an expanded VPA with cannibalism. Application to a hake population. Fish. Res. 12:119-146.
- Link, J. S., and L. P. Garrison.
2002. Changes in piscivory associated with fishing induced changes to the finfish community on Georges Bank. Fish. Res. 55:71-86.
- Macpherson, E.
1977. Estudio sobre relaciones tróficas en peces bentónicos de la costa catalana. Ph.D. diss., 369 p. Universitat de Barcelona, Barcelona.
- Oliver, P., and E. Massuti.
1995. Biology and fisheries of western Mediterranean hake (*M. merluccius*). In Fish and fisheries series 15, hake, fisheries, ecology and markets (J. Alheit and T. J. Pitcher), p. 181-202. Chapman and Hall, London.
- Orsi Relini, L., F. Fiorentino, and A. Zamboni.
1989. Spatial-temporal distribution and growth of *Merluccius merluccius* recruits in the Ligurian Sea. Observations on the O group. Cybium (13):263-270.
- Papaconstantinou, C., and E. Caragitsou.
1987. The food of hake (*Merluccius merluccius*) in Greek Seas. Vie Milieu 37:77-83.
- Payne, A. I. L., B. Rose, and R. W. Leslie.
1987. Feeding of hake and a first attempt at determining their trophic role in the South African west coast marine environment, in The Benguela and comparable ecosystem (A. I. L. Payne, J. A. Gulland and K. H. Brink, eds.). S. Afr. J. Mar. Sci. 5:471-501.
- Payne, A. I. L., and A. E. Punt.
1985. Biology and fisheries of South African cape hakes (*M. capensis* and *M. paradoxus*). Hake—fisheries, ecology and markets. Chapman and Hall, London.
- Paz, J., J. M. Casas, and G. Perez-Gandaras.
1993. The feeding of cod (*Gadus morhua*) on Flemish Cap, 1989-90. NAFO Scientific Council Studies 19, p. 41-50.
- Pinkas, L., M. S. Oliphant, and I. L. K. Iverson.
1971. Food habits of albacore, bluefin tuna and bonito in California waters. Calif. Dep. Fish Game Fish. Bull. 152:1-150.
- Recasens, L., A. Lombarte, B. Morales-Nin, and G. J. Torres.
1998. Spatiotemporal variation in the population structure of the European hake in the NW Mediterranean. J. Fish. Biol. 53:387-401.
- Relini, G., and C. Piccinetti.
1996. Ten years of trawl surveys in Italian seas (1985-1995). FAO Fish. Rep. 533:21-41.
- Relini, G., J. Bertrand, and A. Zamboni.
1999. Synthesis of the knowledge on bottom fishery resources in central Mediterranean (Italy and Corsica). Biol. Mar. Medit. 6, 868 p.
- Roel, B., and E. Macpherson.
1988. Feeding of *Merluccius capensis* and *M. paradoxus* off Namibia. S. Afr. J. Mar. Sci. 6:227-643.
- Ross, S. T.
1978. Trophic ontogeny of the leopard searobins, *Priodontes scitulus* (Pisces: Triglidae). Fish. Bull. 76:225-234.
- Sarano, F.
1986. Cycle ovarien du Merlu, *Merluccius merluccius*, poisson a ponte fractionnee. 2ev. Trav. Inst. Peches Marit. 48:65-67.
- Smith, C., and P. Reay.
1991. Cannibalism in teleost fish. Rev. Fish Biol. Fish 1:41-64.
- Vallet, C., and J. C. Dauvin.
2001. Biomass changes and benthic-pelagic transfers throughout the Benthic Boundary Layer in the English Channel. J. Plankton Research, vol. 23(9):903-922.
- Velasco, F., and I. Olaso.
1998. European hake *Merluccius merluccius* (L., 1758) feeding in the Cantabrian Sea: seasonal, bathymetric and length variations. Fish. Res. 38:33-44.

Biology of queen snapper (*Etelis oculatus*: Lutjanidae) in the Caribbean

Bertrand Gobert

Institut de Recherche pour
le Développement (IRD)
Technopôle Brest-Iroise
BP 70
29280 Plouzané, France
E-mail address: gobert@ird.fr

Alain Guillou

Institut Français de Recherche
pour l'Exploitation de la Mer (Ifremer)
Boulevard Jean Monnet
BP 171
34203 Sète Cedex, France

Peter Murray

Organization of Eastern Caribbean States
(OECS)
Environment and Sustainable
Development Unit
The Morne
PO Box 1383
Castries, Saint Lucia

Patrick Berthou

Institut Français de Recherche
pour l'Exploitation de la Mer (Ifremer)
BP 70
29280 Plouzané, France

Maria D. Oqueli Turcios

38, rue Desaix
75015 Paris, France

Ester Lopez

Département Halieutique
Ecole Nationale Supérieure Agronomique de
Rennes
65, rue de Saint-Brieuc
CS 84215
35042 Rennes Cedex, France

Pascal Lorange

Jérôme Huet

Institut Français de Recherche pour
l'Exploitation de la Mer (Ifremer)
BP 70
29280 Plouzané, France

Nicolas Diaz

Boyer
97129 Lamentin
Guadeloupe, French West Indies

Paul Gervain

Rue Authé 2
Petit Paris
97100 Basse Terre
Guadeloupe, French West Indies

tation of the queen snapper is poorly documented, and very few detailed catch statistics are available; in all cases, the amounts landed in each country are small (probably not exceeding a few tens of tons per year), but the potential production of these resources has never been estimated.

Owing to the depth of its habitat and to the relatively small economic importance of the fisheries for queen snapper on the local scale, very little is known about the biology of *E. oculatus*. It is generally cited in species checklists or in general descriptions of deepwater fisheries. Very few studies actually have focused on the species itself (Murray, 1989; Murray and Charles, 1991; Murray et al., 1992; Murray and Moore, 1992; Murray and Neilson, 2002).

The objective of this study is to present new information about the biology of *E. oculatus*, obtained from fishing experiments undertaken since the 1980s in the French West Indies (Martinique, Guadeloupe, Saint-Barthelemy, and the French part of Saint-Martin), Dominica and Saint-Lucia, and from a study conducted in the late 1990s on the artisanal and semi-industrial fisheries off the Caribbean coast of Honduras.

Material and methods

Areas studied

The data were collected from various research projects (Fig. 1 and Table 1):

The queen snapper (*Etelis oculatus*) is among the deepest dwelling species of the family Lutjanidae, and the only Atlantic species of *Etelis*. Its distribution covers the tropical western Atlantic Ocean, from North Carolina to the eastern tip of Brazil, at depths of 130 to 450 m (Allen, 1985).

Although it reaches a large size and presents no risk of ciguatera (Lorange¹), the species is exploited by only a few fisheries in the Caribbean. Most often it is only a minor part of the catch of line fisheries that focus on the whole community of deep snappers, or on more abundant species such as vermilion snapper (*Rhom-*

boplites aurorubens) or silk snapper (*Lutjanus vivanus*) (e.g., in Venezuela: Mendoza and Larez, 1996). In a few cases, however, *E. oculatus* is specifically sought by fishermen; for example, in Saint-Lucia within a traditional fishery operating during the months when migratory pelagics are not fished (Murray et al., 1992), or in Bermuda where it has been caught irregularly (pulse fishery) since the ban on potfishing (Luckhurst, 1996). Commercial exploitation is only beginning in the French West Indies, but is much more developed in Barbados (Prescod et al., 1996) and Puerto Rico (Matos-Caraballo, 2000). Exploi-

¹ Lorange, P. 1988. La ciguatera des poissons sur les bancs de Saint-Barthélemy, Saint-Martin et Anguilla. Doc. Sci. Pôle Caraïbe 15, 31 p. [Available from Ifremer, Pointe Fort, 97231 Le Robert, France.]



Figure 1

Study area and locations sampled for queen snapper (*Etelis oculatus*) by Caribbean fisheries 1982–2001.

- 1) On the French parts of the wide shelf shared by St-Martin, St Barthélemy, and Anguilla (abbreviated as SMSBA shelf in the text), exploratory fishing experiments were conducted to assess the fishing potential and the risk of ciguatoxicity (Lorance²). The deep slopes of the bank (200–300 m) were fished in 1986–87, using bottom longlines, trammel nets, and secondarily bottom gill nets.
- 2) In Martinique, exploratory fishing experiments were conducted in 1986–87 on various parts of the shelf slope (100–300 m), and some observations were made in 1982 and 1988–91, mainly with gill nets and trammel nets (Guillou³).
- 3) In Saint-Lucia, observations were made in 1987 on the commercial fishery, and fishing experiments were conducted in 1992 with longlines and gill nets.
- 4) In Dominica, fishing experiments were conducted in 1992 with longlines and gill nets.
- 5) In Guadeloupe, experiments were conducted in 2001 with gill nets in the range 200–400 m (Diaz et al., in press); some small *Etelis* were also caught with 10-mm-mesh traps used for a survey of deep crustacean resources.
- 6) In the Bay Islands, off the Caribbean coast of Honduras, a fisheries survey was conducted in 1999–2000 as part of a coastal zone management project (Berthou et al.⁵). This artisanal fishery uses mainly handlines to catch snappers and groupers on the shelf, but a fraction of the fishing effort is directed towards the deepwater snappers on the shelf slopes.
- 7) In Honduras, the landings of the semi-industrial fishing fleet based in Roatán (Bay Islands) were studied, through catch statistics of the export firms and by sampling in the collecting centers (de Rodellec⁶). These fleets target snappers and groupers over the entire Caribbean shelf of Honduras, and fish with handlines.

² Lorance, P. 1989. Ressources demersales et descriptions des pêcheries des bancs de St-Martin et St Barthelemy. Rapp. Int. Dir. Ressources Vivantes Ifremer, DRV-89.039-RH/Martinique, 75 p. [Available from Ifremer, Pointe Fort, 97231 Le Robert, France.]

³ Guillou, A. 1989. Ressources demersales du talus insulaire de la Martinique. Rapp. int. Dir. Ressources Vivantes Ifremer DRV-89.037-RH/Martinique, 121 p. [Available from Ifremer, Pointe Fort, 97231 Le Robert, France.]

⁴ Guillou A., A. Lagin, and P. Murray. 1996. Observations réalisées sur la biologie et la pêche du «gros yeux» *Etelis oculatus* Val. aux Petites Antilles de 1982 à 1992. Doc. Sci. Pôle Caraïbe 33, 137 p. [Available from Ifremer, Pointe Fort, 97231 Le Robert, France.]

⁵ Berthou P., M. D. Oqueli, E. Lopez, B. Gobert, C. Macabiau, and P. Lespagnol. 2001. Diagnostico de la pesca artesanal de la Islas de la Bahía, Honduras. Proyecto Manejo Ambiental de las Islas de la Bahía (PMAIB), Informe Tecnico PES-06, vol 1, 194 p. [Available from PMAIB, Roatán, Islas de la Bahía, Honduras.]

⁶ de Rodellec, A. 2001. Les débarquements de poissons destinés à l'exportation dans l'île d'Utilá (Iles de la Bahía, Honduras). Unpubl. report, IRD-Brest, 51 p. [Available from IRD, BP 70, 29280 Plouzané, France.]

Table 1

Summary of sample sizes and depth ranges of queen snapper (*Etelis oculatus*) by area and fishing gear, in exploratory or commercial fishing operations (SMSBA=Saint Martin-Saint Barthélemy-Anguilla).

Area	Trammel nets (exploratory)	Gill nets (exploratory)	Lines (exploratory)	Lines (commercial)	Depth range (m)
Martinique	300	209	6		140-300
SMSBA shelf	249		406		230-430
Saint-Lucia			34	394	210-290
Dominica		191	20		180-300
Guadeloupe		1133			195-410
Bay Islands				794	unknown
Honduran shelf				3948	unknown

Fishing gears used

In all islands but Guadeloupe, gill nets had mesh sizes of 65 mm (knot to knot) and a stretched height of 6.4 m. In Guadeloupe, mesh was 60 mm and height was 4 m; in addition, the nets were given more slack than in Martinique to increase their efficiency, and thus caught a wider size range of fish.

Trammel nets had mesh sizes of 40 mm (knot to knot) on the central panel and 200 mm on the outer panels, and were 2 m high. All nets (trammel nets and gill nets) were set overnight (15 to 20 hours of fishing time) in units of 200 or 300 m.

Three types of longlines were used in the fishing experiments. Vertical longlines were derived from those used by fishermen in the Lesser Antilles and had about 20 hooks on 40 cm-long secondary lines. Pole longlines were adapted from a technique used in Florida and Puerto-Rico: poles about 2 m long are fastened to the main line lying on the bottom, each having 12 to 25 hooks on very short secondary lines (20 to 30 cm). Reinforced longlines are horizontal longlines whose main line is heavier, in order to fish on very rough grounds. All longlines were hauled after 30 to 45 minutes fishing. For the analysis, no distinction was made between samples of these three types of longlines. Various kinds of longlines are used in the small-scale queen snapper fishery in Saint-Lucia. Handlines used in the artisanal and semi-industrial Hondurian fisheries are either mono- or multifilament, and bear one or several hooks. No detailed observations were made on the size of hooks or on the bait used in the commercial queen snapper fisheries.

Data collected

None of these studies was specifically designed for the study of *E. oculatus*, and therefore the nature and amount of available information (sampling coverage though time, space, and depth) for this species were variable. Species identification (Allen, 1985; Anderson,

1987) could be done reliably in the field for adults and juveniles, but had to be confirmed under the microscope for the smallest individuals (less than 10 cm). Fish length was the only information recordable from professional landings (St-Lucia, Honduras); fishing experiments yielded more detailed data, by order of decreasing frequency: length (fork length FL, total length TL, or both; unless specified, all lengths mentioned in the text are fork lengths), weight, and sexual stage, and occasionally a few additional observations (such as unusual number or length of fin rays). Sexual stages were identified by using the macroscopic scale defined by Barnabé (1973) and were coded as follows: 1 (immature, without identifiable sex), 2 (immature, of identifiable sex), 3 (mature), 4 (prespawning), 5 (spawning), 6 (postspawning), and 7 (resting). Depth was recorded only in the fishing experiments; for gillnet and trammel-net stations, it was measured at each end of the net, and the depth used in the analysis was the average of these two values.

Length-frequency analysis

In most cases, length-frequency analysis was strongly hindered by gear selectivity and sample sizes. We attempted to estimate L_{∞} and Z/K with the method of Wetherall et al. (1987) applied to the sample of the semi-industrial Hondurian fishery. All other samples were unsuitable for length-frequency analysis because of severe violations of one or several assumptions, principally regarding constant catchability above the full selection length, which was obviously not the case for the three gears used in the fishing experiments.

Results

Depth distribution

During the fishing experiments, *E. oculatus* of marketable size (i.e., larger than about 20 cm) were caught

between 140 and 430 m. In Martinique, the trammel nets were set between 100 and 300 m but did not catch any *E. ocellatus* in the shallowest part of this range. In Guadeloupe, gill nets were set down to 410 m, but the deepest catch of queen snapper was 340 m. No *E. ocellatus* were caught in shallower (<80 m) fishing experiments with any of the gears used (traps, gill nets, trammel nets, and longlines) on the SMSBA shelf. According to some local fishermen, however, queen snappers can be caught from about 100 m down to 550 m (Lorance²).

Depth-size relationship

No clear relationship between depth and average size of fish was found in the fishing experiments (Fig. 2). This is not unexpected given the selectivity of some gears (gill nets) and the small sample sizes in most depth strata outside the main fishing range (250–300 m); 70% of the 456 fish caught by longlines were in the 290 m depth stratum, and five or fewer fish were caught in most of the other strata.

A different picture emerges from the analysis of the professional fisheries of Honduras. Multivariate analysis (principal component analysis followed by hierarchical classification) applied to the landings by species revealed the two different categories of fish caught by the two types of semi-industrial vessels operating from Roatán (de Rodellec⁶), the shelf-operating fleet and the slope-operating fleet. The first category of fish were dominated by shallow species such as *Ocyurus chrysurus* (59.8%), *Lutjanus analis* (7.8%), and several grunts (Haemulidae), whereas *E. ocellatus* accounted for only 2.2%. On the other hand, the second category comprised mainly deep snappers: *L. vivanus* (39.6%), *E. ocellatus* (22.4%), *R. aurorubens* (6.9%) or *L. buccanella* (1.9%). The two divisions of the fleet independently exploit the continental shelf and the deep slope. Although actual depth of fishing operations is unknown, the shelf-operating fleet probably catches *E. ocellatus* in the deepest part of its working area (i.e., at the shallowest part of the species' bathymetric range), whereas the slope-operating fleet exploits the main habitat of the deepwater snappers. The size structures of *Etelis* catches (Fig. 3, A and B) strongly indicate that only the fish up to 45–50 cm live on the shelf or its edge, whereas individuals of all sizes, and particularly the largest ones, inhabit the shelf slope.

A similar observation was made for the island of Roatán, where the artisanal fleet is the least developed of the archipelago: fishermen using small (<6 m) and often (57%) nonpowered canoes fish quite close to the shore and catch a large diversity of coastal reef fishes, a large proportion of which are juveniles. *Etelis ocellatus* is rarely caught by these small-scale fishermen but is so only as individuals smaller than 50 cm, sometimes as small as 16 cm (Fig. 3C).

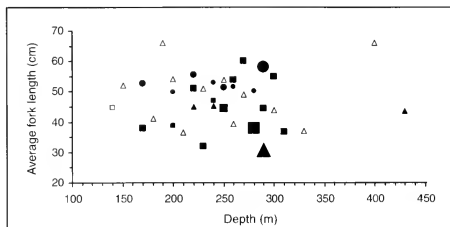


Figure 2

Average fork length of queen snapper (*Etelis ocellatus*) by depth (m) strata in the fishing experiments with gill nets (circles), trammel nets (squares), and lines (triangles). Sample sizes are indicated by size of the symbols: empty symbol ($n < 10$), filled symbol by increasing size ($n = 11-20, 21-50, 51-100, > 100$).

Habitat of early juveniles

Some observations were made from very small (smaller than 10 cm) individuals of *E. ocellatus*. Off Guadeloupe, a few of them were entangled in gill nets at 300 m depth (Fig. 3D); on the same island, previous exploratory fishing operations with small-mesh traps caught six juveniles ranging from 5.5 to 7 cm FL at 490 m depth; off Dominica, one small individual (8.5 cm TL) was found in the stomach of a predator caught at a depth greater than 200 m (see below). In spite of the general tendency of increasing size with depth found for the larger individuals, these observations show that the habitat of early postsettlement juveniles is not restricted to the shallowest part of the species depth range.

Morphometric relationships

The main morphometric relations were computed from the fish sampled in commercial or scientific fishing operations in the Lesser Antilles (Martinique, Saint-Lucia, SMSBA shelf). Because the differences between relations for males and females were insignificant, only global equations are given (Table 2).

Maximum size and weight

The largest individual caught was 90 cm FL in the Lesser Antilles (Guadeloupe) and 86 cm in Honduras, and the maximum weight recorded was 6280 g, in the Lesser Antilles; fish were not weighed individually in Honduras.

Sex-related length differences

When sex was recorded, the largest fish were always female, and no male was found above 70 cm. The difference between size-structure of male and female catches

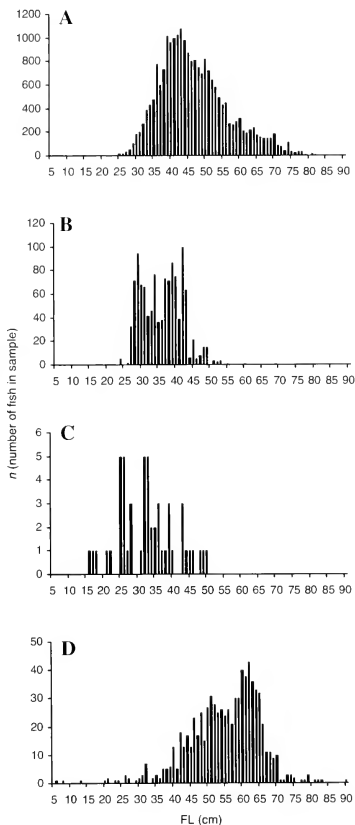


Figure 3

Length-frequency distributions for queen snapper (*Etelis oculatus*) catches. (A) Semi-industrial deepwater Hondurian line fishery ($n=3415$). (B) Semi-industrial shallow-water Hondurian line fishery ($n=387$). (C) Artisanal line fishery of Roatán (Honduras) ($n=52$). (D) Gillnet exploratory fishing in Guadeloupe ($n=779$). (E) Trammel-net exploratory fishing in all areas: males ($n=231$). (F) Trammel-net exploratory fishing in all areas: females ($n=227$).

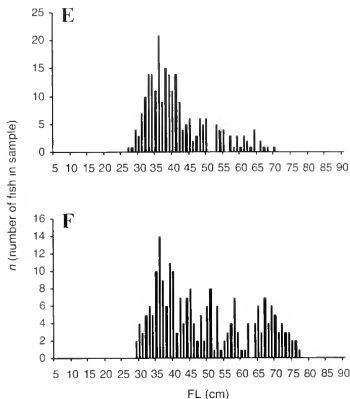


Figure 3 (continued)

was particularly clear for trammel nets (Fig. 3, E and F): the mode corresponding to fish gilled in the small-mesh central panel had similar characteristics for both sexes (range 25–45 cm and peak at 36 cm), as opposed to the diffuse mode for fish >45 or 50 cm (predominantly females) entangled in the large-mesh outer panels. With many fewer fish ($n=23$ for both sexes), the longline samples showed a similar difference between sizes of males (maximum 55 cm, mean 43.8 cm) and females (maximum 71 cm, mean 51.8 cm). In Guadeloupe, the sex of fish was not determined, but the existence of two modes in the overall size structure of gillnet catches (Fig. 3D) could possibly be related to this sex-related length difference.

Growth and mortality

The data collected in the various surveys did not allow any reliable analysis of the growth of *E. oculatus*. Because growth may be different for males and females, the length-frequency distributions of the large samples (where sex was not determined) from Honduras could not be processed rigorously to estimate life-history population parameters. However, in order to provide preliminary information on such a little known species, the regression method of Wetherall et al. (1987) was used in the modified version of FiSAT (Gayanilo et al., 1996) to estimate L_{∞} and Z/K . With a satisfactory fit of the regression line ($r=0.986$), the estimates were $L_{\infty}=90.57$ cm and $Z/K=3.73$. For the reason mentioned above (together with other weaknesses related to possible violations of the hypotheses underlying the regression

Table 2
Morphometric relationships established for queen snapper (*Etelis oculatus*).

Parameters	Equation	Sample size	r
FL (cm) – TL (cm)	$TL = 2.7458 + 1.1644 \times FL$	842	0.987
TL (cm) – FL (cm)	$FL = -1.0028 + 0.8368 \times TL$	842	0.987
FL (cm) – W (g)	$W = 0.02748 \times FL^{2.8348}$	499	0.990
TL (cm) – W (g)	$W = 0.03006 \times FL^{2.8147}$	487	0.990

method), these estimates have to be seen only as indications that the asymptotic length of *E. oculatus* is quite large and that the Hondurian population is moderately exploited (if $M = 2K$, as suggested by Ralston (1987) for snappers, then $Z/K = 3.73$ and $E = F/Z = 0.46$).

Reproduction

Macroscopic observations of gonads were recorded for 309 fish whose sex could be identified (118 males and 191 females); all stages of the reproductive cycle were observed, but only 20 individuals were in the prespawning to postspawning stages, and a single one was found to be in the process of spawning.

The smallest fish with developing gonads was 36 cm for females and 29 cm for males (Fig. 4). Although only part of the length range of males was adequately sampled (100 out of the 118 fish were smaller than 44 cm), it appears that the progressive build-up of the reproductive male population occurs between about 30 cm and 45 cm. The picture is clearer for females, whose sample size was larger and more evenly spread over the length range: above 54 cm, all females were found to be in a reproductive cycle. The maturing process therefore occurs at clearly lower sizes for males (30–45 cm) than for females (35–55 cm). Females in advanced reproductive stages (postspawning and resting stages) were observed across the length range, including the smallest adult sizes, those below 45 cm (Fig. 4).

A full analysis of the seasonality of reproduction is not possible because data were collected in only seven months, out of which only four (May, June, November, and December) yielded samples large enough for the analysis (21 to 72 females per month). No females were found to be spawning, but most of the pre- and post-spawning stages (14 out of 17) were observed in November and December, and half of maturing females were fished during the last quarter of the year (Fig. 5). However, 74% of females at sexual rest (resting stage) were caught in May and June. Additional pieces of information confirm this pattern: the only spawning individual, a male, was observed in November (Dominica); females gonads in advanced stage of vitellogenesis were observed in September (Guadeloupe); no mature individual was found in Honduras in April–June. These observations show that an active spawning period occurs at the end of the year (even if all fish caught at this period were

not close to the spawning phase), as opposed to late spring which is a period of sexual inactivity.

Such limited results leave open the overall interpretation of the annual reproductive cycle of *E. oculatus*. In particular, according to the fishermen working on the SMSBA shelf, the species could have an extended spawning season, lasting from November to April or May.

Predators and prey

No systematic observations were made on the trophic relationships of *E. oculatus*, but a few occasional recordings were made of its predators and prey. The only record of a predator was that of a beardfish (*Polymixia lowei*: Polymixiidae) measuring 40 cm TL containing a very small queen snapper (8.5 cm TL) and which was caught deeper than 200 m. This is the first record of such a food item for this beryciform fish whose diet had so far been reported to comprise cephalopods (Cervigon, 1991). The stomachs of *E. oculatus* that could be observed were most often empty; on a few occasions, unidentified squids were the only items present. This was the case for three fish (58 to 62 cm) caught at 430 m depth.

Discussion

Etelis oculatus was found on the upper part of the continental and insular slopes, from about 150 to 450 m; this observed range confirms previous indications (Allen, 1985), but the bathymetric distribution of the species could possibly extend beyond the maximum depth fished in these surveys. The presence of *E. oculatus* in shallower waters of the shelf seems possible, according to a statement that juveniles can be found in less than 30 m (Appeldoorn et al., 1987) and to the reported catch of one fish (size not recorded) at 59 m depth by a trawl survey off southeastern United States (Cuellar et al., 1996). However the present data, other fishery-independent surveys focusing on snappers (i.e., Marciano et al., 1996, down to 128 m), and most studies on Caribbean coastal fisheries strongly indicate that the species is very rare on the shelf itself.

Within the observed depth range, there is a tendency for the largest fish to be found in the deeper areas, as observed in the closely related Pacific species

E. carbunculus and *E. coruscans* (Brouard and Grandperrin⁷), other deepwater lutjanids (Boardman and Weiler, 1980; Cuellar et al., 1996), and many reef fish species. The maximum size recorded for large samples (90 cm FL) is much greater than the 60 cm TL indicated by Allen (1985) but is consistent with other field observations, such as 94 cm TL in Saint-Lucia (Murray, 1989) or 100 cm TL in Venezuela (Cervigon, 1991).

No reliable growth estimate could be obtained because males and females showed very different size structures, and the only data suitable for length-frequency analysis were data for which the sexes had not been determined.

Important differences were found between sexes in terms of size structure and maturation size. Male *E. oculatus* attain a smaller length than females, and are much rarer above 45 cm. Sex-ratios skewed in favor of females in large size classes were observed in the most complete studies of snapper populations (Grimes, 1987), including Pacific deepwater snappers (Brouard and Grandperrin⁷), and probably result from a difference in growth and mortality between the sexes; in Cuba, for instance, females of most snapper species have been found to grow faster than males (Claro and Garcia-Arteaga, 2001). In the present study, sex-specific growth and mortality estimates were not available, but our interpretation seems likely because other possible causes could be ruled out, such as selectivity of nets (morphometric relationships are identical for both sexes) and fish behavior in relation to fishing gear (differences between sexes, however, were observed in trammel nets and lines whose catch mechanism is completely different). Different habitat preferences, which can lead to sex-related size structures in reef species (Garcia-Cagide et al., 2001), seem unlikely in our study because the deep slopes have fewer habitat gradients than the shallower reef environments and because no relation was found between depth and sex-ratio. A similar difference between males and females was found for reproductive size. Male snappers generally mature at a slightly smaller size than females, but sex does not appear as a significant factor of variation for relative length at first reproduction, as opposed to depth or continental or insular habitat (Grimes, 1987).

In the Lesser Antilles, *E. oculatus* spawns at the end of the year and has a period of sexual rest during from late spring through early summer. These results are not sufficient to establish the entire annual reproductive pattern, and even these partial findings cannot be applied to other parts of the Caribbean because snapper populations of continental and insular shelves generally show different seasonal patterns of reproduction (Grimes, 1987). This indication of a spawning period for *E. oculatus* in the cold season contrasts with the two eteline species (*Aprion virescens* and *E. coruscans*) studied in Hawaii, which have a protracted spawning period extending through the summer (May or June through October or November) (Everson et al., 1989).

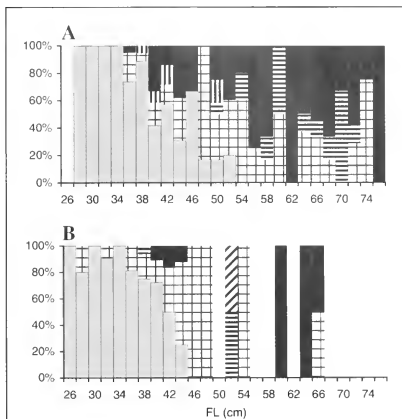


Figure 4

Proportion of sexual stages by 2-cm length classes for (A) female ($n=191$) and (B) male ($n=118$) queen snapper (*Etelis oculatus*): immature fish (gray), maturing fish (large squares), postspawning (horizontal bars), spawning (oblique bars), postspawning (vertical bars), sexual rest (black). Empty areas indicate the absence of data for the length class.

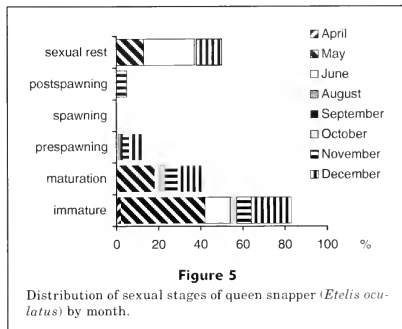


Figure 5

Distribution of sexual stages of queen snapper (*Etelis oculatus*) by month.

⁷ Brouard, F., and R. Grandperrin. 1985. Les poissons profonds de la pente récifale externe à Vanuatu. South Pacific Commission, 17^{me} conférence technique régionale des pêches, Nouméa (Nouvelle Calédonie) 5-9 August 1985. SPC/Fisheries 17/WP.12, 131 p. [Available from SPC, BP D5, 98848 Noumea Cedex, New-Caledonia, France.]

The data collected in these studies did not allow the analysis of the aggregation pattern of *E. ocellatus*. In the Pacific, *E. coruscans* was found to form feeding aggregations near underwater promontories and these aggregations had important consequences for catchability (Ralston et al., 1986). For the deeper living alfonsoins (*Beryx* spp.) and orange roughy (*Hoplostethus atlanticus*), fisheries have shown their ability to quickly fish down aggregations once they are discovered (Lorance and Dupouy, 2001). Added to "K-selected" life-history strategies (high longevity, slow growth, late reproduction) and irregular recruitment, this aggregating behavior reinforces the vulnerability of deepwater species to overfishing (Koslow et al., 2000).

Recently gained knowledge about the exploitation of seamount and deep bank fish resources (Clark, 2001) cannot be applied directly to *E. ocellatus* and the other slope-dwelling snappers which, although they are the deepest dwelling species of the family, are much closer in terms of demographic strategy to their shallow relatives (longevity 10–20 years; Manooch, 1987) than to these truly deep species (longevity 50 to more than 100 years; Koslow et al., 2000). However, less extreme life history traits do not protect deep snappers against overfishing, as shown by the example of *E. coruscans* and *E. caruncululus* in Hawaii (Simonds, 1995). The limited fishery data available on *E. ocellatus* in the Caribbean do not seem to show evidence of a similar situation so far, but the stocks are being increasingly fished without much scientific basis (i.e., catch statistics) for management (Mahon, 1990; FAO, 1993). Regulation measures continue to be defined (Diaz et al., in press), but so far they are based only on conservative rules of thumb because of a lack of reliable biological information. To address this lack of information, future research on *E. ocellatus* therefore should address, in particular, sex-specific growth, reproductive biology, and fine-scale distribution patterns.

Acknowledgments

The data presented here were collected and processed with the help of many people; the authors particularly wish to thank E. Burgos, T. and J. Chapelle, P. Galera, J. Grelot, A. Lagin, P. Lespagnol, L. Reynal, J. Robin, B. Séret, and the Chief Fisheries Officers of Dominica and Saint-Lucia.

Literature cited

Allen, G. R.

1985. FAO species catalogue. Vol. 6. Snappers of the world. An annotated and illustrated catalogue of lutjanid species known to date. FAO Fish. Synop. 125, vol. 6:1–208.

Anderson, W. D.

1987. Systematics of fishes of the family Lutjanidae (Perciformes: Percoidae), the snappers. In *Tropical snappers*

and groupers, biology and fisheries management (J. J. Polovina and S. R. Ralston, eds), p. 1–31. Westview Press, Boulder, CO.

Appeldoorn, R., G. D. Dennis, and O. Monterrosa Lopez.

1987. Review of shared demersal resources of Puerto Rico and the Lesser Antilles region. FAO Fish. Rep. 383:36–106.

Barnabé, G.

1973. Contribution à la connaissance de la croissance et de la sexualité du Loup (*Dicentrarchus labrax* L.) de la région de Sète. Ann. Inst. Oceanogr. Paris (nouv. ser.) 49:49–75.

Boardman, C., and D. Weiler.

1980. Aspects of the life history of three deepwater snappers around Puerto Rico. Proc. Gulf Carib. Fish. Inst. 32:158–172.

Cervignon, F.

1991. Los peces marinos de Venezuela, 951 p. Fundación Científica Los Roques, Caracas, Venezuela.

Claro, R., and J. P. García-Arteaga

2001. Growth patterns of fishes of the Cuban shelf. In *Ecology of the marine fishes of Cuba* (R. Claro, K. C. Lindeman, and L. R. Parenti, eds.), p. 149–178. Smithsonian Institution Press, Washington and London.

Clark, M.

2001. Are deepwater fisheries sustainable? The example of orange roughy (*Hoplostethus atlanticus*) in New Zealand. Fish. Res. 51:123–135.

Cuellar, N., G. R. Sedberry, D. J. Machowski, and M. R. Collins.

1996. Species composition, distribution and trends in abundance of snappers of the southeastern USA, based on fishery-independent sampling. ICLARM Conf. Proc. 48:59–73.

Diaz, N., P. Gervain, and V. Druault-Aubin.

- In press. Queen snapper (*Etelis ocellatus*) experimental deep-sea gillnet fishery in Guadeloupe (F.W.I.). Proc. Gulf Carib. Fish. Inst. 55.

Everson A. R., H. A. Williams, and B. M. Ito.

1989. Maturation and reproduction in two Hawaiian eteline snappers, uku, *Aprion virescens*, and onaga, *Etelis coruscans*. Fish. Bull. 87:877–888.

FAO (Food and Agricultural Organization of the United Nations).

1993. Marine fishery resources of the Antilles. FAO Fish. Tech. Paper 326:1–235.

García-Cagide A., R. Claro, and B. V. Koshelev.

2001. Reproductive patterns of fishes of the Cuban shelf. In *Ecology of the marine fishes of Cuba* (R. Claro, K. C. Lindeman, and L. R. Parenti, eds.), p. 73–114. Smithsonian Institution Press, Washington and London.

Gayanilo F., P. Sparre, and D. Pauly.

1996. FAO-ICLARM stock assessment tools. User's manual. FAO Comput. Inform. Ser. Fisheries 8:1–126.

Grimes C. B.

1987. Reproductive biology of the Lutjanidae: a review. In *Tropical snappers and groupers: biology and fisheries management* (J. J. Polovina and S. R. Ralston, eds.), p. 239–294. Westview Press, Boulder, CO.

Koslow J. A., G. Boehlert, J. D. M. Gordon, R. L. Haedrich, P. Lorance, and N. Parin.

2000. Continental slope and deep-sea fisheries: implications for a fragile ecosystem. ICES J. Mar. Sci. 57:548–557.

- Lorance P., and H. Dupouy.
2001. CPUE abundance indices of the main target species of the French deep-water fishery in ICES sub-areas V-VII. *Fish. Res.* 51:137-149.
- Luckhurst B. E.
1996. Trends in commercial fishery landings of groupers and snappers in Bermuda from 1975 to 1992 and associated fishery management issues. ICLARM Conf. Proc. 48:277-288.
- Mahon, R.
1990. Fishery management options for Lesser Antilles countries. FAO Fish. Tech. Paper 313:1-126.
- Manooch, C. S.
1987. Age and growth of snappers and groupers. In *Tropical snappers and groupers: biology and fisheries management* (J. J. Polovina and S. R. Ralston, eds.), p. 329-373. Westview Press, Boulder, CO.
- Marcano, L. A., R. Guzman, and G. J. Gomez.
1996. Exploratory fishing with traps in oceanic islands off eastern Venezuela during 1992. ICLARM Conf. Proc. 48:331-336.
- Matos-Caraballo, D.
2000. Overview of Puerto Rico's small-scale fisheries statistics: 1994-1997. *Proc. Gulf Carib. Fish. Inst.* 51:215-231.
- Mendoza, J. J., and A. Larez.
1996. Abundance and distribution of snappers and groupers targeted by the artisanal medium range fishery off northeastern Venezuela (1981-1992). ICLARM Conf. Proc. 48:266-276.
- Murray, P. A.
1989. A comparative study of methods for determining mean length-at-age and von Bertalanffy growth parameters for two fish species. M. Phil. thesis, 222 p. Univ. West Indies, Cave Hill, Barbados.
- Murray, P. A., and A. V. Charles.
1991. Some considerations for increasing landings of the queen snapper, *Etelis oculatus* Val., in the Saint Lucian fishery. FAO Fish. Rep. 431 (suppl):75-77.
- Murray P. A., L. E. Chinnery, and E. A. Moore.
1992. The recruitment of the queen snapper, *Etelis oculatus* Val., into the St. Lucian fishery: recruitment of fish and recruitment of fisherman. *Proc. Gulf Carib. Fish. Inst.* 41:297-303.
- Murray, P. A., and E. A. Moore.
1992. Some morphometric relationships in *Etelis oculatus* Valenciennes (Queen snapper), landed in St. Lucia, W.I. *Proc. Gulf Carib. Fish. Inst.* 41:416-421.
- Murray, P. A., and J. D. Neilson.
2002. A method for the estimation of the von Bertalanffy growth rate parameter by direct examination of otolith microstructure. *Proc. Gulf Carib. Fish. Inst.* 53:516-525.
- Prescod, S. D., H. A. Oxenford, and C. Taylor.
1996. The snapper fishery of Barbados: present status and a preliminary assessment of the potential for expansion. *Proc. Gulf Carib. Fish. Inst.* 44:159-179.
- Ralston, S.
1987. Mortality rates of snappers and groupers. In *Tropical snappers and groupers: biology and fisheries management* (J. J. Polovina and S. R. Ralston, eds.), p. 375-404. Westview Press, Boulder, CO.
- Ralston, S., R. M. Gooding, and G. M. Ludwig.
1986. An ecological survey and comparison of bottom fish resource assessments (submersible versus handline fishing) at Johnston atoll. *Fish. Bull.* 84:141-155.
- Simonds, K.
1995. Federal state cooperation in managing deepwater bottom fish in Hawaii. South Pacific Commission workshop on the management of South Pacific inshore fisheries, Noumea (New Caledonia), 26 Jun-7 Jul 1995. South Pac. Comm. Tech. Doc. Intergr. Coast. Fish. Manag. Proj. 12:299-309.
- Wetherall, J. A., J. J. Polovina, and S. Ralston.
1987. Estimating growth and mortality in steady state fish stocks from length-frequency data. ICLARM Conf. Proc. 13:53-74.

Courtship and spawning behaviors of carangid species in Belize

Rachel T. Graham

Wildlife Conservation Society
PO Box 37
Punta Gorda, Belize
E-mail address: rgraham@wcs.org

Daniel W. Castellanos

Monkey River Village
Toledo District, Belize

Many species of reef fish aggregate seasonally in large numbers to spawn at predictable times and sites (Johannes, 1978; Sadovy, 1996; Domeier and Colin, 1997). Although spawning behavior has been observed for many reef fish in the wild (Wicklund, 1969; Smith, 1972; Johannes, 1978; Sadovy et al., 1994; Aguilar Perera and Aguilar Davila, 1996), few records exist of observations on the courtship or natural spawning for the commercially important family Carangidae (jacks) (von Westernhagen, 1974; Johannes, 1981; Sala et al., 2003). In this study, we present the first observations on the natural spawning behavior of the economically-valuable permit (*Trachinotus falcatus*) (Linnaeus, 1758) from the full to new moon period at reef promontories in Belize, with notes on the spawning of the yellow jack (*Caranxoides bartholomaei*) (Cuvier, 1833), and the courtship of five other carangid species.

Permit belong to the family Carangidae and are broadly distributed in the western Atlantic Ocean from Massachusetts to southeastern Brazil, including the Caribbean Sea and Gulf of Mexico (Smith, 1997). Considered an inshore pelagic species (Valdez Muñoz and Mochek, 2001) that spawns offshore, permit utilize a range of habitats that include coastal mangroves and seagrass beds, reef flats, and fore-reef areas during their life-cycle (Crabtree et al., 2002). Permit are reported to feed during the day and may show similar feeding

characteristics to the closely related *T. carolinus* that displays a clear circadian rhythm entrained to the light phase during its feeding period (Heilman and Spieler, 1999). According to otolith analysis of fish caught in Florida, permit live to at least 23 years and reach a maximum published fork length of 110 cm and a weight of 23 kg (Crabtree et al., 2002).^{1,2} Permit are gonochoristic and Crabtree et al. (2002) recorded 50% sexual maturity for females at 547 mm FL or 3.1 years and males at 486 mm FL and 2.3 years. Permit exhibit a protracted spawning season from March to September in Cuba (García-Cagide et al., 2001) and from March to July in Florida (Crabtree et al., 2002). High gonadosomatic indices recorded for March and maturation of oocytes noted in late June–July (Crabtree et al., 2002) support the observations by García-Cagide et al. (2001) that permit are batch spawners and have an asynchronous cycle of vitellogenesis. Spawning cue by the full moon has been recorded in many species of reef and inshore fish (Johannes, 1978, 1981; Moyer et al., 1983; Crabtree, 1995; Hoque et al., 1999). Macroscopic gonadal analysis and observations on the timing of courtship and spawning in several carangid species in the wild (Johannes, 1981; Sala et al., 2003), coupled with gonadal sampling observations on the captive spawning behavior of the related bluefin trevally (*Caranx melampygus*) (Moriwake et al., 2001), further indicate that permit and other carangids

display circa lunar periodicity when spawning naturally.

Permit represent a valuable resource for recreational fishermen throughout their range. In Florida, recreational fisheries land more than 100,000 fish per year, but declines in landings from 1991 to date prompted regulation (Crabtree et al., 2002) and a move towards catch-and-release of fish. As such, Belize is rapidly becoming known as a world-class fly-fishing location due to its abundance of permit. The fishery is highly lucrative: flyfishers pay up to US\$500 per day in Belize to catch and release a permit. This niche tourism industry has also become an economic alternative for local fishermen (Heyman and Graham³). Consequently, information on the timing and behavior of reproduction of permit can underpin conservation efforts that focus on a vulnerable stage in their life cycle.

¹ The IGFA (International Game Fishing Association) notes a record length for permit of 122 cm FL, 2001. Database of IGFA angling records until 2001. IGFA, Dania Beach, Florida, 33004.

² The United Nations notes a maximum weight of 36 kg for a permit. (Cervigon, F., R. Cipriani, L. Fischer, L. Garibaldi, M. Hendrickx, A. J. Lemus, R. Márquez, J. M. Poutiers, G. Robaina and B. Rodríguez. 1992. Fichas FAO de identificación de especies para los fines de la pesca. Guía de campo de las especies comerciales marinas y de aguas salobres de la costa septentrional de Sur América, 513 p. FAO, Rome.

³ Heyman W. D., and R. T. Graham. 2000. The voice of the fishermen of Southern Belize, 44 p. TIDE (Toledo Institute for Environment and Development), P.O. Box 150, Punta Gorda, Belize.

Materials and methods

Turneffe Elbow (17°09'N, 87°54'W) and Gladden Spit (16°35'N, 88°00'W) are two sites located on the Belize Barrier Reef that were monitored for abundance and behavior of many species of spawning reef fish between 1999 and 2002. Both sites are promontories with a sloping reef shelf that drops off steeply at a depth of 35–45 m to over 1000 m into the southern tip of the Cayman Trench. According to the spawning aggregation criteria developed by Domeier and Colin (1997), Turneffe Elbow and Gladden Spit attract, respectively, an estimated 13 and 27 species of reef fish that aggregate seasonally to spawn (Graham, 2003).

We logged over 270 hours of underwater monitoring of reef fish spawning aggregations at Turneffe Elbow and Gladden Spit, primarily from the full-moon to the new-moon from March to July from 2000 through 2002. Additional dives took place variously over the course of 3–5 days during the same lunar period from 1999 to 2002. Most dives for monitoring spawning aggregations took place between 0830 and 1100 hours, at midday, and between 1600 to 1730 hours of each diving day. Dives began 150–250 m north of both spawning aggregation sites and proceeded to the south along the reef platform edge. Dive depth usually began at about 30 m and decreased to 15 m as the dive progressed because of SCUBA decompression constraints. Dives normally lasted between 35 and 50 minutes. Horizontal and vertical visibility rarely dropped below 20–25 m.

Results and discussion

During 10 dive surveys (15 diving hours) at Turneffe Elbow, we observed a large school of 250 to 500 permit aggregating on the reef promontory (Table 1). The aggregated fish slowly swam into the south current along the south-facing sloping fore-reef shelf at 5–15 m depth and the steep drop-off located at ~30–35 m. The school streamed down to the spur and groove formations at about 20 m depth on the reef shelf and rose up into the upper water column again. Permit were loosely grouped and displayed little fear of divers, a behavior commonly observed among a range of other fish species that aggregate to spawn (Graham, 2003). Several individuals displayed a dark patch located above and behind the pectoral fin on both flanks. Permit displayed this same behavior coloration change during each encounter.

On 22 August 2000, 7 days after the full moon, at ~1730 (41 minutes before sunset at 1811 hours local time) we conducted our standard north to south fish census dive at a depth of ~20–30 m along the fore-reef drop off. During all dives horizontal and vertical visibility was at least 20 m and often over 40 m. We observed a school of ~300 permit descend from 5–15 m depth above the fore-reef drop-off to 25 m directly on the shelf edge. At ~1745 hours (26 min before sunset) within-group activity increased as permit schooled densely on

the edge of the reef drop-off. At ~1750 hours, a subgroup of eight permit left the dense school and ascended in the water column to ~18 m depth. The lead individual initiating the ascent was ~100 cm FL and was pursued by seven fish ranging from ~55 to 75 cm FL. The pursuing fish nuzzled the larger fish's vent as it rose in the water column. All fish displayed a dark flank patch behind their pectoral fins. The lead permit then ceased its ascent at ~15 m, tilted its head down slightly and convulsed rapidly, releasing a puff of gametes. Pursuing permit tried to position their vents as closely as possible to the lead individual's while releasing their gametes. The resulting gamete cloud was less than 50 cm in diameter and dispersed within seconds (Fig. 1). Following gamete release, all fish descended quickly to the main school still located ~25 m below. Within moments this behavior was repeated and observed in two smaller groups of permit before all observations ceased because of a lack of light.

At Gladden Spit, we observed slightly different permit spawning behavior. On 7 April 2002 (10 days after the full moon), the aggregation remained in a restricted area ~100 m north of where we previously witnessed the spawning of several species of fish and ~30 m east of where we have also observed groups of *Epinephelus striatus*, *Mycteroperca tigris*, *M. venenosus*, and *M. bonaci* aggregate to spawn (Graham, 2003). Ambient water temperature was 27.7°C as measured by a temperature logger (Onset Corp. Tidbit data logger) moored at the spawning site at 30 m depth.

At least 300 permit—many of them large individuals (~70–90 cm FL)—schooled densely into a ball at ~1700 hours (66 minutes before sunset local time) near the reef shelf drop-off at a depth of ~40–48 m. Subgroups comprised five to nine fish, and the lead fish was much larger than the pursuers. Subgroups rapidly rose up on the periphery of the school, spawned at the apex of the aggregation, and descended towards the bottom of the school again. Spawning was more frenetic than that observed at Turneffe Elbow. Permit subgroups behaved in the same manner as that observed at Turneffe during spawning, and all spawning individuals displayed a large dark flank patch behind the pectoral fins.

Based on our observations of courtship and spawning behavior, our estimate of spawning season for permit in Belize may stretch from February to the end of October, beyond the period of March to September as suggested by Garcia-Cagide et al. (2001) and Crabtree et al. (2002). Permit may also reach larger sizes than published by Crabtree et al. (2002); we estimated the largest individual permit observed at Turneffe Elbow in Belize to be ~120 cm FL, which may indicate that permit exceed a lifespan of 23 years.

We could not determine if the lead permit was female and the pursuing permit were males because no individuals were caught for gonadal analysis. However, carangids are gonochoristic and it is highly likely that the lead fish in the spawning rush was female. Garcia-Cagide et al. (2001) noted that spawning females are often larger than mature males in several species of

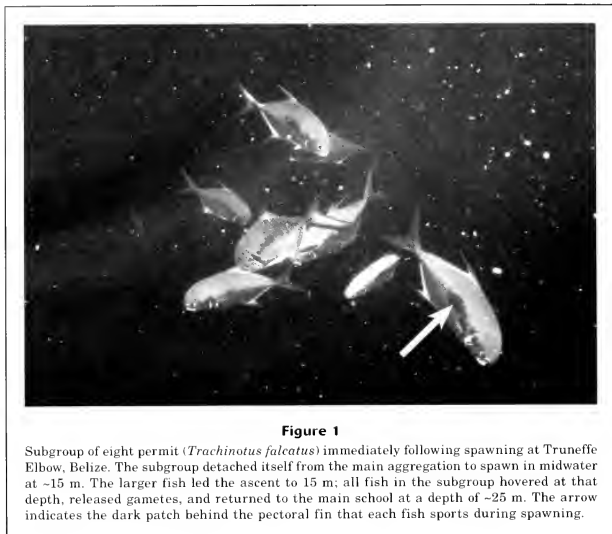


Figure 1

Subgroup of eight permit (*Trachinotus falcatus*) immediately following spawning at Truneffe Elbow, Belize. The subgroup detached itself from the main aggregation to spawn in midwater at ~15 m. The larger fish led the ascent to 15 m; all fish in the subgroup hovered at that depth, released gametes, and returned to the main school at a depth of ~25 m. The arrow indicates the dark patch behind the pectoral fin that each fish sports during spawning.

reef fish. This is also supported by our observations of gonochoristic spawners such as the cubera snapper (*Lutjanus cyanopterus*) and the dog snapper (*L. jocu*) that display a pattern of group, broadcast spawning where larger females are swollen with roe and lead the subgroup spawning ascents (Graham, 2003).

Group spawning behavior in the yellow jack (*C. bartholomaei*) closely resembled that of permit. We recorded yellow jacks schooling at Gladden Spit on only two occasions (Table 1). On 7 April 2002, we observed that the yellow jacks spawned at ~1705 hours (61 minutes before sunset local time) at Gladden Spit, less than 50 m south of the school of spawning permit. The jacks schooled densely at ~40–45 m and subgroups of 5 to 8 fish detached themselves from within the school, ascending rapidly to ~35 m, releasing gametes at the apex, and descending into the school again. Observations ceased shortly thereafter because of depth constraints and decreasing light.

Not all species of carangids are group spawners. Pair spawning has been observed in species such as *C. ignobilis* and *Alectis indicus* in the Pacific (von Westernhagen, 1974) and *C. sexfasciatus* in the Gulf of California (Sala et al., 2003). We have also observed on numerous occasions pair courtship in crevalle jack (*C. hippos*), horse-eye jack (*C. latus*), and bar jack (*Carangoides*

ruber) in schools exceeding 1000 fish, in rainbow runner (*Elagatis bipinnulata*) in schools of up to ~300 fish, and occasionally greater amberjack (*Seriola dumerili*) in schools numbering ~120 individuals, primarily following during the full-moon and waning moon periods between February and October (Table 1). These five species displayed extended pair courtship within and outside a large aggregation of conspecific fish as they swam along the edge of the reef drop-off. All courting pairs observed showed similar behavior. The chasing fish nuzzled the gonopore of the lead fish (whose head and upper body half had turned black but whose fins were lighter, Fig. 2, A and B) during prolonged chases, often swimming close to and at a perpendicular angle to the lead fish. *Seriola dumerili* also displayed dichromatism; the pursuing fish turned a vivid electric blue and exhibited a scrawled pattern on its upper flanks, similar to that displayed by the scrawled filefish (*Aluterus scriptus*). Occasionally, 1–10 individuals that did not display coloration changes followed the courting pairs. These five species may also pair spawn because their courtship behavior parallels that of *C. sexfasciatus*, observed by Sala et al. (2003) to spawn in pairs from the full moon to waning crescent periods from July to September. However, we did not observe any release of gametes during all pair courtship behavior.

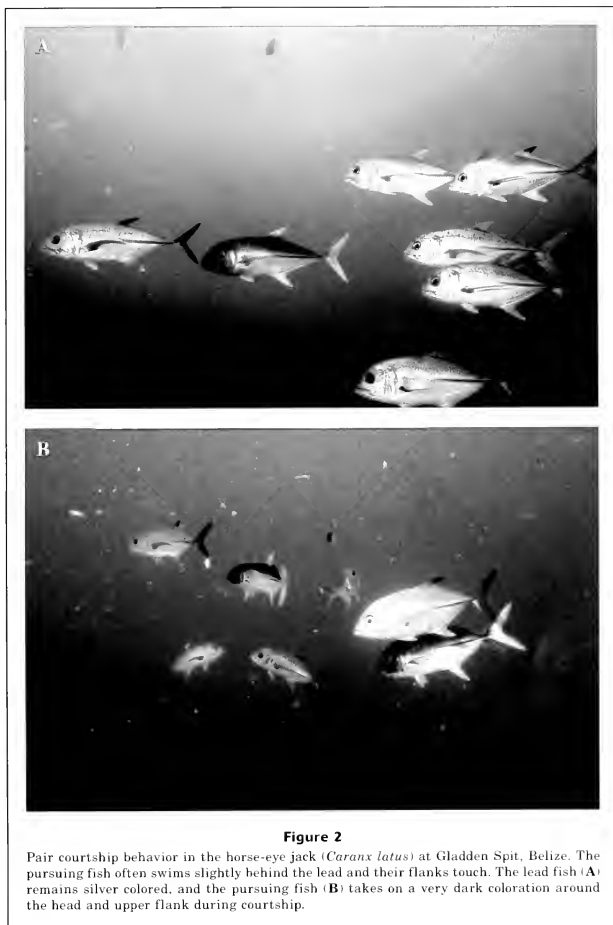


Figure 2

Pair courtship behavior in the horse-eye jack (*Caranx latus*) at Gladden Spit, Belize. The pursuing fish often swims slightly behind the lead and their flanks touch. The lead fish (A) remains silver colored, and the pursuing fish (B) takes on a very dark coloration around the head and upper flank during courtship.

Conclusions

Our observations confirm that permit spawn offshore at reef promontories that support other reef fish spawning aggregations. Permit demonstrate group broadcast

spawning behavior and spawning events take place close to sunset. Further observations indicate that other species of carangids, such as yellow jack are also group broadcast spawners, occupying the same spatiotemporal spawning niche as permit. If observed courtship behav-

Table 1

Timing and lunar phase of observations on the schooling, courtship, and spawning of seven carangids at two reef promontories in Belize from April 1999 to July 2002. fm = full moon; dafm = days after full moon; dbfm = days before full moon. Sch = schooling; C = courting and color change; Spawn = spawning observed.

Date	Dive start time	Moon phase	Location	Species	Behavior
2 Apr 1999	12:04	2 dafm	Gladden	Yellow jack	Sch
3 Apr 1999	10:25	3 dafm	Gladden	Crevalle	Sch
5 Apr 1999	16:40	5 dafm	Gladden	Crevalle, horse-eye, rainbow runner	Sch
2 May 1999	16:50	2 dafm	Gladden	Bar jack, crevalle	Sch
5 May 1999	5:40	5 dafm	Gladden	Horse-eye, crevalle	Sch, C
30 May 1999	12:45	fm	Gladden	Amberjack, bar jack	Sch, C
3 Jun 1999	9:10	4 dafm	Gladden	Horse-eye, bar jack	Sch
4 Jun 1999	15:30	5 dafm	Gladden	Crevalle	Sch
30 Jun 1999	12:00	2 dafm	Gladden	Bar jack, horse-eye	Sch
27 Sep 1999	16:30	2 dafm	Gladden	Crevalle, amberjack	Sch, C
28 Sep 1999	10:50	3 dafm	Gladden	Crevalle, bar jack, horse-eye	Sch
	16:30	3 dafm	Gladden	Horse-eye, amberjack	Sch, C
24 Mar 2000	17:15	4 dafm	Gladden	Horse-eye	Sch, C
17 Apr 2000	16:25	1 dbfm	Gladden	Horse-eye, crevalle	Sch, C
18 Apr 2000	16:25	fm	Gladden	Bar jack, rainbow runner	Sch
19 Apr 2000	17:10	1 dafm	Gladden	Horse-eye	Sch, C
20 May 2000	17:00	2 dafm	Gladden	Crevalle	Sch, C
23 May 2000	16:45	5 dafm	Gladden	Amberjack	Sch, C
24 May 2000	16:21	6 dafm	Gladden	Bar jack	Sch
25 May 2000	-16:30	7 dafm	Gladden	Crevalle	Sch
26 May 2000	16:00	8 dafm	Gladden	Horse-eye, crevalle	Sch, C
23 Jun 2000	17:30	7 dafm	Gladden	Bar jack	Sch, C
18 Aug 2000	15:36	3 dafm	Gladden	Bar jack	Sch
	15:36	3 dafm	Gladden	Horse-eye, rainbow runner	Sch, C
19 Aug 2000	-12:00	4 dafm	Gladden	Bar jack, crevalle	Sch
20 Aug 2000	15:00	5 dafm	Turneffe	Horse-eye	C
	15:00	5 dafm	Turneffe	Permit	Sch
20 Aug 2000	17:00	5 dafm	Turneffe	Permit	Sch, C
	17:00	5 dafm	Turneffe	Amberjack, bar jack	Sch, C
21 Aug 2000	15:00	6 dafm	Turneffe	Crevalle, horse-eye	Sch, C
	15:00	6 dafm	Turneffe	Permit	Sch
22 Aug 2000	17:30	7 dafm	Turneffe	Horse-eye	C
	17:30	7 dafm	Turneffe	Permit	Spawn
14 Oct 2000	17:30	1 dafm	Gladden	Horse-eye, crevalle	C
15 Oct 2000	17:30	2 dafm	Gladden	Rainbow runner	C
17 Oct 2000	16:30	4 dafm	Turneffe	Horse-eye, crevalle	C
	16:30	4 dafm	Turneffe	Permit, amberjack	Sch
18 Oct 2000	16:30	5 dafm	Turneffe	Horse-eye, crevalle, amberjack, permit	C
13 Dec 2000	16:30	2 dafm	Gladden	Horse-eye	Sch
9 Apr 2001	16:00	1 dafm	Gladden	Horse-eye	C
8 May 2001	11:15	1 dafm	Gladden	Crevalle	C
9 May 2001	-10:30	2 dafm	Gladden	Crevalle	Sch
7 Jun 2001	17:00	1 dafm	Gladden	Crevalle, bar jack, horse-eye	Sch

continued

Table 1 (continued)

Date	Dive start time	Moon phase	Location	Species	Behavior
8 Jun 2001	17:00	2 dafm	Gladden	Amberjack, crevalle, horse-eye	Sch, C
9 Jun 2001	11:00	3 dafm	Gladden	Crevalle, horse-eye	Sch
10 Jun 2001	17:50	4 dafm	Gladden	Crevalle, horse-eye	Sch, C
3 Oct 2001	~17:00	1 dafm	Turneffe	Horse-eye	C
6 Feb 2002	16:00	9 dafm	Turneffe	Horse-eye, permit	Sch
7 Feb 2002	8:30	10 dafm	Turneffe	Horse-eye, permit	C
	16:30	10 dafm	Gladden	Horse-eye, crevalle, bar jack	Sch
28 Mar 2002	16:48	fm	Gladden	Crevalle, permit	Sch
	16:48	fm	Gladden	Horse-eye	C
29 Mar 2002	16:30	1 dafm	Gladden	Crevalle, bar jack, horse-eye	Sch
30 Mar 2002	16:45	2 dafm	Gladden	Crevalle, horse-eye	Sch
31 Mar 2002	16:40	3 dafm	Gladden	Horse-eye	Sch
1 Apr 2002	16:35	4 dafm	Gladden	Bar jack, horse-eye	Sch
3 Apr 2002	9:40	5 dafm	Gladden	Bar jack, horse-eye	Sch
7 Apr 2002	10:30	9 dafm	Gladden	Bar jack	Sch
	16:30	9 dafm	Gladden	Permit, yellow jack	Spawn
	16:30	9 dafm	Gladden	Bar jack	Sch
6 May 2002	9:40	9 dafm	Gladden	Horse	Sch
27 May 2002	12:18	1 dafm	Gladden	Horse-eye	C
30 May 2002	11:07	4 dafm	Gladden	Horse-eye	Sch
31 May 2002	16:20	5 dafm	Gladden	Crevalle	Sch
1 Jun 2002	16:15	6 dafm	Gladden	Bar jack, rainbow runner	Sch
2 Jun 2002	16:15	7 dafm	Gladden	Bar jack, horse-eye	Sch
29 Jun 2002	12:00	5 dafm	Turneffe	Permit, horse-eye	Sch
1 Jul 2002	15:00	7 dafm	Gladden	Bar jack, crevalle, horse-eye	Sch

ior is included, the spawning season for permit and horse-eye jacks is protracted from February through October, and the five other carangid species described in the present study spawned within this period. Protection of permit stocks throughout their life cycle, and particularly during their spawning season, underpins the associated rapidly growing and economically lucrative flyfishing tourism. Future directions of study should include a study of permit movement patterns between feeding and spawning grounds and mortality rates of catch-and-release fishing.

Acknowledgments

We would like to thank two anonymous reviewers who provided helpful suggestions for the improvement of this paper. The fieldwork and observations were supported by grants from the UK Darwin Initiative and the UK's Natural Environment Research Council. We worked under permits provided by the Belize Department of Fisheries.

Literature cited

- Aguilar Perera, A., and W. Aguilar Davila.
1996. A spawning aggregation of Nassau grouper *Epinephelus striatus* (Pisces: Serranidae) in the Mexican Caribbean. *Environ. Biol. Fishes* 45:351-361.
- Crabtree, R. E.
1995. Relationship between lunar phase and spawning activity of tarpon, *Megalops atlanticus*, with notes on the distribution of larvae. *Bull. Mar. Sci.* 56:895-899.
- Crabtree, R. E., P. B. Hood, and D. Snodgrass.
2002. Age, growth and reproduction of permit (*Trachinotus falcatus*) in Florida waters. *Fish. Bull.* 100:26-34.
- Domeier, M. L., and P. L. Colin.
1997. Tropical reef fish spawning aggregations: defined and reviewed. *Bull. Mar. Sci.* 60:698-726.
- García-Cagide, A., R. Claro, and B. V. Koshelev.
2001. Reproductive patterns of fishes of the Cuban shelf. In *Ecology of the marine fishes of Cuba* (R. Claro, K. C. Lindeman and L. R. Parenti, eds.), p. 73-114. Smithsonian Institution Press, Washington DC.
- Graham, R. T.
2003. Behavior and conservation of whale sharks on the

- Belize Barrier Reef. Ph.D. diss., 408 p. Environment Department, Univ. York, York, UK.
- Houlman, M. J., and R. W. Spieler.
1999. The daily feeding rhythm to demand feeders and the effects of timed meal-feeding on the growth of juvenile Florida pompano, *Trachinotus carolinus*. *Aquaculture* 180:53-64.
- Hoque, M. M., A. Takemura, M. Matsuyama, S. Matsuura, and K. Takano.
1999. Lunar spawning in *Stigonus canaliculatus*. *J. Fish Biol.* 55:1213-1222.
- Johannes, R. E.
1978. Reproductive strategies of coastal marine fishes in the tropics. *Environ. Biol. Fishes* 3: 65-84.
- Johannes, R. E.
1981. Words of the lagoon: fishing and marine lore in the Palau, District of Micronesia, p. 245. Univ. California Press, Berkeley, CA.
- Moriwake, A. M., V. N. Moriwake, A. C. Ostrowski, and C. S. Lee.
2001. Natural spawning of the bluefin trevally *Caranx melampygus* in captivity. *Aquaculture* 203(1-2): 159-164.
- Moyer, J. T., R. E. Thresher, and P. L. Colin.
1983. Courtship, spawning and inferred social organization of American angelfishes (Genera *Pomacanthus*, *Holacanthus* and *Centropyge*: *Pomacanthidae*). *Environ. Biol. Fishes* 9:25-39.
- Sadovy, Y.
1996. Reproduction of reef fishery species. *In* Reef fisheries (N. V. C. Polunin and C. M. Roberts, eds.), p. 15-59. Chapman and Hall, London.
- Sadovy, Y., P. L. Colin, and M. L. Domeier.
1994. Aggregation and spawning in the tiger grouper, *Mycteroperca tigris* (Pisces: Serranidae). *Copeia* 1994:511-516.
- Sala, E., O. Aburto-Oroperca, G. Paredes, and G. Thompson.
2003. Spawning aggregations and reproductive behavior of reef fishes in the Gulf of California. *Bull. Mar. Sci.* 72(1):103-121.
- Smith, C. L.
1972. A spawning aggregation of Nassau grouper, *Epinephelus striatus* (Bloch). *Trans. Am. Fish. Soc.* 101:257-261.
1997. National Audubon Society field guide to tropical marine fishes of the Caribbean, the Gulf of Mexico, Florida, the Bahamas, and Bermuda, 718 p. Alfred A. Knopf, Inc., New York, NY.
- Valdez Muñoz, E., and A. D. Moche.
2001. Behavior of marine fishes of the Cuban shelf. *In* Ecology of the marine fishes of Cuba (R. Claro, K. C. Lindeman and L. R. Parenti, eds.), p. 53-72. Smithsonian Institution Press, Washington DC.
- von Westernhagen, H.
1974. Observation on the natural spawning of *Alectis indicus* (Ruppell) and *Caranx ignobilis* (Forsk.) (Carangidae). *J. Fish Biol.* 6:513-516.
- Wicklund, R.
1969. Observations on spawning of the lane snapper. *Underwater Naturalist* 6:40.

Comparison of two approaches for estimating natural mortality based on longevity*

David A. Hewitt

John M. Hoenig

Virginia Institute of Marine Science

The College of William and Mary

P.O. Box 1346

Gloucester Point, Virginia 23062

E-mail address (for D. A. Hewitt): dhewitt@vims.edu

Vetter (1988) noted that her review of the estimation of the instantaneous natural mortality rate (M) was initiated by a discussion among colleagues that identified M as the single most important but least well-estimated parameter in fishery models. Although much has been accomplished in the intervening years, M remains one of the most difficult parameters to estimate in fishery stock assessments. A number of novel approaches using tagging and telemetry data provide promise for making reliable direct estimates of M for a given stock (Hearn et al., 1998; Frusher and Hoenig, 2001; Hightower et al., 2001; Latour et al., 2003; Pollock et al., 2004). However, such methods are often impracticable and fishery scientists must approximate M by using estimates made for other stocks of the same or similar species or by predicting M from features of the species' life history (Beverton and Holt, 1959; Beverton, 1963; Alverson and Carney, 1975; Pauly, 1980; Hoenig, 1983; Peterson and Wroblewski, 1984; Roff, 1984; Gunderson and Dygert, 1988; Chen and Watanabe, 1989; Charnov, 1993; Jensen, 1996; Lorenzen, 1996).

We are concerned with two approaches for predicting M based solely on the longevity of the members of a stock—an approach that can be used when data are not available to make direct estimates of the parameter. One is a linear regression model (Hoenig, 1983) and the other is a simple rule-of-thumb approach. Hoenig (1983) found that

M was inversely correlated with longevity across a wide variety of taxa and recommended use of the following predictive equation relating the maximum age observed in the stock (t_{max}) to M :

$$\ln(\hat{M}) = 1.44 - 0.982 \times \ln(t_{max}). \quad (1)$$

The rule-of-thumb approach consists of determining the value of M such that 100(P)% of the animals in the stock survive to the age t_{max} ; thus,

$$\hat{M} = \frac{-\ln(P)}{t_{max}}. \quad (2)$$

The challenge in this approach is determining an appropriate value for the proportion P .

The rule-of-thumb approach has the potential to be used widely because it is presented in Quinn and Deriso (1999) and stock assessment manuals of the Food and Agriculture Organization of the United Nations (FAO; Sparre and Venema, 1998; Cadima, 2003). The approach has recently been used extensively, in the specific form $M=3/t_{max}$, in work related to stock assessments for blue crab (*Callinectes sapidus*). In this note, we 1) show that the regression model and the rule-of-thumb approach can be compared directly; 2) illustrate the difference in the estimates of M generated by the two approaches; 3) discuss the origins and current use of the rule-of-thumb approach; and 4) recommend that the regression model be used instead of the rule-of-thumb approach.

Methods

With the rule-of-thumb approach, the fraction of a population that survives to a given age is used to estimate M . This approach is equivalent to a quantile estimator (Bury, 1975). Suppose the fraction surviving to age t is described by the negative exponential function

$$\frac{N_t}{N_0} = e^{-Zt}, \quad (3)$$

where Z is the total instantaneous mortality rate. The quantile estimator is of the form

$$P = e^{-Zt_p}, \quad (4)$$

where t_p is the age at which 100(P)% of the population remains. In the case where $P = 0.05$, the estimator, based on data from a sample of the population, is

$$0.05 = e^{-Zt_{0.05}}, \quad (5)$$

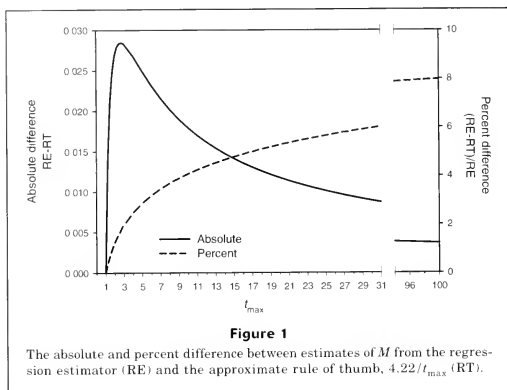
where 5% of the animals in the sample are older than age $t_{0.05}$.

To estimate M , an empirical approach is usually taken where $t_{0.05}$ is replaced with t_{max} :

$$0.05 = e^{-Mt_{max}}, \quad (6)$$

where t_{max} is either the oldest age observed in the stock or the oldest age found in the literature for the species of interest. When age composition data are used from an exploited stock, Equation 6 will provide an estimate of M only if fishing mortality is reasonably close to zero ($M=Z$) or if there is a refuge where older animals can accumulate. If exploitation affects all

* Contribution 2637 of the Virginia Institute of Marine Science, The College of William and Mary, Gloucester Point, VA 23062.



animals in the stock, Equation 6 is unlikely to provide a reliable estimate of M .

The rule of thumb for approximating M follows directly from Equation 6:

$$-\ln(0.05) = \hat{M} \times t_{\max} \quad (7)$$

$$\hat{M} = \frac{2.996}{t_{\max}} = \frac{3}{t_{\max}}$$

Most importantly, note that the use of 0.05 or any other proportion in the equations is arbitrary because we have no reason to believe that t_{\max} pertains to any particular quantile.

We show in the present study that this arbitrary rule of thumb for approximating M is unnecessary, as an empirical method (Hoenig, 1983) provides an analogous estimate based on a substantial data set. Equation 1 is based on the same model as that in Equation 3 and was developed from a regression of $\ln(M)$ on $\ln(t_{\max})$ from data on 134 stocks of 79 species of fish, mollusks, and cetaceans. It can be shown to be of the same form as the rule-of-thumb approach as follows:

$$e^{\ln(M)} = e^{1.44 - 0.982 \cdot \ln(t_{\max})}$$

$$\hat{M} = \frac{e^{1.44}}{e^{0.982 \cdot \ln(t_{\max})}} \quad (8)$$

$$= \frac{4.22}{(t_{\max})^{0.982}}$$

$$\approx \frac{4.22}{t_{\max}}$$

Results

We substituted 1.0 for 0.982 in Equation 8 to allow the development of a simple, approximate rule of thumb for direct comparison with $3/t_{\max}$. As a result, this rule of thumb strictly applies only to the case where $t_{\max} = 1$. Estimates from the regression estimator in Equation 1 are always greater than estimates from Equation 8 for $t_{\max} > 1$, although the difference is usually small (Fig. 1).

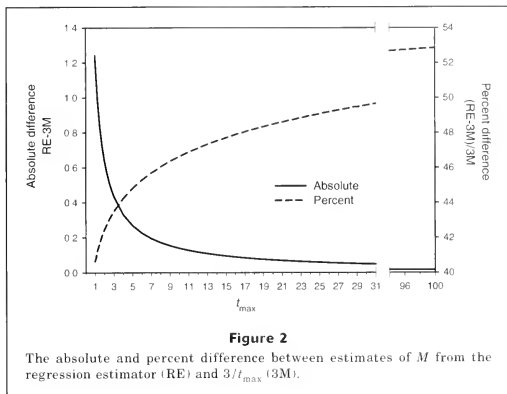
Estimates from the regression estimator are typically 40–50% greater than estimates from $3/t_{\max}$ (Fig. 2). For example, if a maximum age of eight years is used for blue crab in Chesapeake Bay (Rugolo et al., 1998), $3/t_{\max}$ gives an estimate for M of 0.375/yr and the regression estimator gives 0.548/yr.

Perhaps the most significant result is the finding that rearrangement of the regression model yields an estimate of an appropriate value for P in Equation 2. The value of 4.22 in Equation 8 approximately corresponds to $-\ln(0.015)$, indicating that the average longevity for stocks in the data set used by Hoenig (1983) is the age at which about 1.5% of the stock remains alive (versus 5% in $3/t_{\max}$).

Discussion

Development of the rule-of-thumb approach

The rule-of-thumb approach appears to have arisen independently in four different places. Cadima (2003) supported the approach by citing the early work of Tanaka (1960). Sparre and Venema (1998) based their presen-



tation on the work of Alagaraja (1984), who provided the mathematics of a method that Sekharan (1975) used without description. Interestingly, Shepherd and Breen (1992) rearranged Equation 3 to obtain the rule of thumb based on the results of Hoenig (1983). This latter presentation is provided in Quinn and Deriso (1999). In all of these cases, the proportion of animals surviving to t_{\max} is assumed to be some arbitrarily small value, typically 1% or 5%.

The development and use of the specific form $3/t_{\max}$ in blue crab work occurred altogether separately. Its use began with an assessment for the Chesapeake Bay stock, in which Rugolo et al. (1998) used an estimate of M based on "the ICES [International Council for the Exploration of the Sea] convention; that is, 5% survivorship at maximum age following negative exponential depletion." The approach is more explicitly defined in their original document (Rugolo et al.¹) as $M = (3/\text{maximum age})$. The report also states that "this convention ... is widely used for many east coast finfish stocks (NMFS [National Marine Fisheries Service]/NEFSC [Northeast Fisheries Science Center], ASMFC [Atlantic States Marine Fisheries Commission])." Following its introduction by Rugolo et al. (Rugolo et al.¹; Rugolo et al., 1998), the $3/t_{\max}$ approach has been used in nearly all blue crab

stock assessment work conducted on the east coast of the United States (Miller and Houde²; Miller, 2001; Murphy et al.³; Helsen et al., 2002; Kahn⁴).

The references used by Rugolo et al. (1998) in support of what they termed the "ICES convention" (Anthony⁵; Vetter, 1988) do not mention the $3/t_{\max}$ approach. Rather than advocating a method for determining M , Anthony⁵ called for standardization of the range of ages to include in the calculation of yield-per-recruit for a stock; this range of ages was termed the stock's "fishable life span." He proposed that the fishable life span should be defined such that the oldest age would be that

¹ Rugolo, L., K. Knotts, A. Lange, V. Crecco, M. Terceiro, C. Bonzek, C. Stagg, R. O'Reilly, and D. Vaughan. 1997. Stock assessment of Chesapeake Bay blue crab (*Callinectes sapidus*), 267 p. Report of the Technical Subcommittee of the Chesapeake Bay Stock Assessment Committee of the National Marine Fisheries Service, NOAA (National Oceanic and Atmospheric Administration). NOAA Chesapeake Bay Office, 410 Severn Avenue, Suite 107, Annapolis, MD 21403.

² Miller, T. J., and E. D. Houde. 1999. Blue crab target setting, 167 p. Final report to the Living Resources Subcommittee of the Chesapeake Bay Program. University of Maryland Center for Environmental Science (UMCES) Technical Series No. TS-177-99. Chesapeake Bay Program, U.S. EPA (Environmental Protection Agency), 410 Severn Avenue, Annapolis, MD 21403.

³ Murphy, M. D., C. A. Meyer, and A. L. McMillen-Jackson. 2001. A stock assessment for blue crab, *Callinectes sapidus*, in Florida waters, 56 p. FMRI (Florida Marine Research Institute) Inhouse Report Series IHR 2001-008. Florida Fish and Wildlife Conservation Commission, FMRI, 100 Eighth Avenue SE, St. Petersburg, FL 33701.

⁴ Kahn, D. M. 2003. Stock assessment of Delaware Bay blue crab (*Callinectes sapidus*) for 2003, 52 p. Delaware Department of Natural Resources and Environmental Control, Division of Fish and Wildlife, P.O. Box 330, Little Creek, DE 19961.

⁵ Anthony, V. C. 1982. The calculation of $F_{0.1}$: a plea for standardization, 16 p. Northwest Atlantic Fisheries Organization (NAFO) Serial Document N557, SCR 82/VI/64. NAFO Secretariat, P.O. Box 638, Dartmouth, Nova Scotia B2Y 3Y9, Canada.

at which 5% or less of the initial recruits survived. The use of Anthony's standard to approximate M makes the assumption that the fishable life span of an exploited stock is the same as the longevity of the members of the stock in an unexploited condition. It is unlikely that this assumption will be met unless the fishery is at an early stage in its development because fishing may alter the age structure of the stock (Hilborn and Walters, 1992). We note that although a limited number of scientists involved with ICES have used $3/t_{\max}$ in a general way, the method has not been adopted as a convention within ICES (O'Brien⁶). Furthermore, we did not find evidence that the approach is currently in common use in stock assessments on the east coast of the United States, with the exception of those for blue crab. Nonetheless, the rule-of-thumb approach certainly has the potential to be used widely, given its repeated presentation in fishery literature and its accumulated momentum in blue crab work.

Recommendations

The power of empirical relationships for predicting natural mortality can be rather limited (Vetter, 1988; Pascual and Iribarne, 1993), and the uncertainty associated with parameter estimates should be taken into account whenever possible (Patterson et al., 2001). Furthermore, methods for directly estimating M are likely to be preferable to making predictions based on life history features. Nonetheless, such estimates may be needed when available data are inadequate for making a direct estimate. Given the results of our comparison, we recommend that the regression estimator be used instead of the rule-of-thumb approach when longevity is used to predict M . The regression estimator is based on a least squares fit to an extensive data set and thus matches experience better than a rule-of-thumb approach based on an arbitrary constant.

We recommend that use of the $3/t_{\max}$ rule of thumb be abandoned, despite it being entrenched in blue crab literature. For a species like blue crab, for which t_{\max} is less than 10 years, the differences in the estimates of M from the regression estimator and $3/t_{\max}$ are not trivial (~45%). Although the regression estimator was based on data for fish, mollusks, and cetaceans (Hoenig, 1983) and may not be applicable to other exploited taxa, such as crustaceans, the model had a good fit to the data across widely disparate taxa. Finally, estimates of M for blue crab based on longevity are controversial because of continued difficulty in determining an appropriate t_{\max} . In the absence of data to directly estimate M for this species, we suggest that the most prudent course

of action is a review and comparison of other methods for predicting M .

Acknowledgments

We thank Doug Vaughan for helping investigate the use of the rule-of-thumb approach, and Russell Burke, Romuald Lipcius, Jacques van Montfrans, and three anonymous reviewers for helpful comments on the manuscript. D.A.H. gratefully acknowledges the support of the Willard A. Van Engel (WAVE) Fellowship for Crustacean Research. This work was supported by funding from the NOAA Chesapeake Bay Office, award no. NA03NMF4570376.

Literature cited

- Alagaraja, K.
1984. Simple methods for estimation of parameters for assessing exploited fish stocks. *Indian J. Fish.* 31:177-208.
- Alverson, D. L., and M. J. Carney.
1975. A graphic review of the growth and decay of population cohorts. *J. Cons. Int. Explor. Mer* 36:133-143.
- Beverton, R. J. H.
1963. Maturation, growth and mortality of clupeid and engraulid stocks in relation to fishing. *Rapp. P.-V. Réun. Cons. Int. Explor. Mer* 154:44-67.
- Beverton, R. J. H., and S. J. Holt.
1959. A review of the lifespans and mortality rates of fish in nature, and their relation to growth and other physiological characteristics. In *The lifespan of animals*, CIBA Foundation colloquia on ageing, vol. 5 (G. E. W. Westenholme and M. O'Connor, eds.), p. 142-177. Little, Brown and Company, Boston, MA.
- Bury, K. V.
1975. Statistical models in applied science, 625 p. John Wiley and Sons, New York, NY.
- Cadima, E. L.
2003. Fish stock assessment manual. FAO Fish. Tech. Pap. 393, 161 p. FAO, Rome.
- Charnov, E. L.
1993. Life history invariants: some explorations of symmetry in evolutionary ecology. Oxford Univ. Press, New York, NY.
- Chen, S., and S. Watanabe.
1989. Age dependence of natural mortality coefficient in fish population dynamics. *Nippon Suisan Gakkaishi* 55:205-208.
- Frusser, S. D., and J. M. Hoenig.
2001. Estimating natural and fishing mortality and tag reporting rate of southern rock lobster (*Jasus edwardsii*) from a multiyear tagging model. *Can. J. Fish. Aquat. Sci.* 58:2490-2501.
- Gunderson, D. R., and P. H. Dygert.
1988. Reproductive effort as a predictor of natural mortality rate. *J. Cons. Int. Explor. Mer* 44:200-209.
- Hearn, W. S., K. H. Pollock, and E. N. Brooks.
1998. Pre- and post-season tagging models: estimation of reporting rate and fishing and natural mortality rates. *Can. J. Fish. Aquat. Sci.* 55:199-205.

⁶ O'Brien, C. M. 2004. Personal commun. Chair of ICES Working Group on Methods of Fish Stock Assessments and ICES Resource Management Committee. CEFAS (Centre for Environment, Fisheries and Aquaculture Science) Lowestoft Laboratory, Pakefield Road, Lowestoft, Suffolk NR33 0HT, England.

- Helser, T. E., A. Sharov, and D. M. Kahn.
2002. A stochastic decision-based approach to assessing the status of the Delaware Bay blue crab stock. In Incorporating uncertainty into fishery models (J. M. Berkson, L. L. Kline, and D. J. Orth, eds.), p. 63-82. Am. Fish. Soc., Symposium 27, Bethesda, MD.
- Hightower, J. E., J. R. Jackson, and K. H. Pollock.
2001. Use of telemetry methods to estimate natural and fishing mortality of striped bass in Lake Gaston, North Carolina. Trans. Am. Fish. Soc. 130:557-567.
- Hilborn, R., and C. J. Walters.
1992. Quantitative fisheries stock assessment: choice, dynamics and uncertainty, 570 p. Chapman and Hall, New York, NY.
- Hoening, J. M.
1983. Empirical use of longevity data to estimate mortality rates. Fish. Bull. 82:898-903.
- Jensen, A. L.
1996. Beverton and Holt life history invariants result from optimal trade-off of reproduction and survival. Can. J. Fish. Aquat. Sci. 53:820-822.
- Latour, R. J., J. M. Hoening, D. A. Hepworth, and S. D. Frusher.
2003. A novel tag-recovery model with two size classes for estimating fishing and natural mortality, with implications for the southern rock lobster (*Jasus edwardsii*) in Tasmania, Australia. ICES J. Mar. Sci. 60:1075-1085.
- Lorenzen, K.
1996. The relationship between body weight and natural mortality in juvenile and adult fish: a comparison of natural ecosystems and aquaculture. J. Fish Biol. 49:627-647.
- Miller, T. J.
2001. Matrix-based modeling of blue crab population dynamics with applications to the Chesapeake Bay. Estuaries 24:535-544.
- Pascual, M. A., and O. O. Iribarne.
1993. How good are empirical predictions of natural mortality? Fish. Res. 16:17-24.
- Patterson, K., R. Cook, C. Darby, S. Gavaris, L. Kell, P. Lewy, B. Mesnil, A. Punt, V. Restrepo, D. W. Skagen, and G. Stefansson.
2001. Estimating uncertainty in fish stock assessment and forecasting. Fish and Fisheries 2:125-157.
- Pauly, D.
1980. On the interrelationships between natural mortality, growth parameters, and mean environmental temperature in 175 fish stocks. J. Cons. Int. Explor. Mer 39:175-192.
- Peterson, I., and J. S. Wroblewski.
1984. Mortality rate of fishes in the pelagic ecosystem. Can. J. Fish. Aquat. Sci. 41:1117-1120.
- Pollock, K. H., H. Jiang, and J. E. Hightower.
2004. Combining telemetry and fisheries tagging models to estimate fishing and natural mortality rates. Trans. Am. Fish. Soc. 133:639-648.
- Quinn, T. J. H., and R. B. Deriso.
1999. Quantitative fish dynamics, 542 p. Oxford Univ. Press, New York, NY.
- Roff, D. A.
1984. The evolution of life history parameters in teleosts. Can. J. Fish. Aquat. Sci. 41:989-1000.
- Rugolo, L. J., K. S. Knotts, A. M. Lange, and V. A. Crecco.
1998. Stock assessment of Chesapeake Bay blue crab (*Callinectes sapidus* Rathbun). J. Shellfish Res. 17:493-517.
- Sekharan, K. V.
1975. Estimates of the stocks of oil sardine and mackerel in the present fishing grounds off the west coast of India. Indian J. Fish. 21:177-182.
- Shepherd, S. A., and P. A. Breen.
1992. Mortality in abalone: its estimation, variability and causes. In Abalone of the world: biology, fisheries and culture (S. A. Shepherd, M. J. Tegner, and S. A. Guzman del Proo, eds.), p. 276-304. Fishing News Books, Cambridge, UK.
- Sparre, P., and S. C. Venema.
1998. Introduction to tropical fish stock assessment, Part 1: manual. FAO Fish. Tech. Pap. 306/1, rev. 2, 407 p. FAO, Rome.
- Tanaka, S.
1960. Studies on the dynamics and the management of fish populations. Bull. Tokai Reg. Fish. Res. Lab. 28:1-200.
- Vetter, E. F.
1988. Estimation of natural mortality in fish stocks: a review. Fish. Bull. 86:25-43.

Effects of current speed and turbidity on stationary light-trap catches of larval and juvenile fishes

David C. Lindquist

Richard F. Shaw

Coastal Fisheries Institute
School of the Coast and Environment
Louisiana State University
Baton Rouge, Louisiana 70803

E-mail address (for D. C. Lindquist): dlindq1@lsu.edu

Light traps are one of a number of different gears used to sample pelagic larval and juvenile fishes. In contrast to conventional towed nets, light traps primarily collect larger size classes, including settlement-size larvae (Choat et al., 1993; Hickford and Schiel, 1999; Hernandez and Shaw, 2003), and, therefore, have become important tools for discerning recruitment dynamics (Sponaugle and Cowen, 1996; Wilson, 2001). The relative ease with which multiple synoptic light trap samples can be taken means that larval distribution patterns can be mapped with greater spatial resolution (Doherty, 1987). Light traps are also useful for sampling shallow or structurally complex habitats where towed nets are ineffective or prohibited (Gregory and Powles, 1985; Brogan, 1994; Hernandez and Shaw, 2003).

As with any sampling gear, there are concerns about light trap sampling biases and efficiency. Light traps are taxon-selective because they target fishes that are photopositive and able to swim to and enter the trap (Thorold, 1992; Choat et al. 1993; Hernandez and Shaw, 2003), and size-selective because both phototactic behavior and swimming abilities change during ontogeny (Stearns et al., 1994; Fisher et al., 2000). Unlike conventional towed nets, it is difficult, if not impossible, to quantify the volume of water sampled by light traps. This is largely due to external, environmental factors such as lunar phases, current speed or water

clarity, which may have a large impact on catch rates (Doherty, 1987; Meekan et al., 2000).

Few studies have attempted to address the effects of environmental factors on light trap performance. Catches have been found to be lower during full moons as compared to new moons, either because of the greater ambient illumination interfering with light trap efficiency (Gregory and Powles, 1985; Hickford and Schiel, 1999) or because of higher abundances of presettlement fish during the darker lunar phases (Johannes, 1978; Robertson et al., 1988). Thorold (1992) showed that catches were greater for light traps drifting with the current as compared to traps anchored in the current flow. Anderson et al. (2002) found that anchored light traps were less efficient at a high-current sampling site as compared with a low-current sampling site. The latter two studies, however, did not provide any information on catch rates with variation in current speed. The purpose of this study was to assess the relationships between catch rates from stationary (anchored or tethered) light traps at offshore petroleum platforms and concurrent measurements of current speed and turbidity.

Materials and methods

Study sites

Larval and juvenile fishes were collected at five oil and gas platforms

(platforms) in the north-central Gulf of Mexico. These platforms included: Mobil's Green Canyon 18 (27°56'37"N, 91°0'45"W; sampled from July 1995–June 1996); Mobil's Grand Isle 94B (28°30'57"N, 90°07'23"W; April–August 1996); Exxon's South Timbalier 54G (28°50'01"N, 90°25'00"W; April–September 1997); Santa Fe-Snyder's Main Pass 259A (29°19'32"N, 88°01'12"W; May–September 1999); and Murphy Oil's Viosca Knoll 203 (29°46'53"N, 88°19'59"W; May–October 2000). All platforms had similar underwater structural complexity, and had well-developed biofouling communities when sampled.

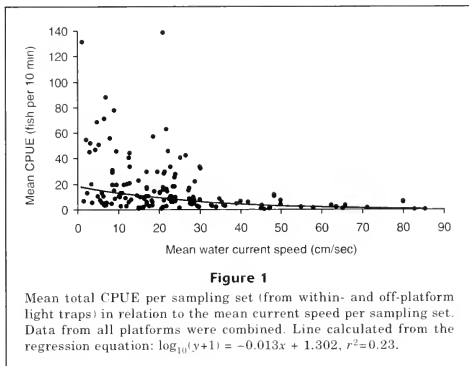
Sampling procedures

Sampling procedures have been described in detail elsewhere (Hernandez and Shaw, 2003) and will be briefly described here. Fish collections were made by using a modified quatrefoil light trap with a Brinkman Starfire II halogen light (250,000 candlepower) powered through an umbilical by a 12-volt marine battery. Light traps were deployed in surface waters within the platform structure along a stainless-steel guidewire (within-platform light trap), and tethered and floated in surface waters to a distance of 20 m from the down-current side of the platform (off-platform light trap). Light traps were deployed with their lights off, fished with lights on for 10–15 min, and retrieved with lights off.

Sampling was undertaken generally twice monthly coincident with new and full moon phases. During each trip, light traps were fished during four to six sets per night, starting at least one hour after sunset and ending at least one hour before sunrise, over two to three consecutive nights. Each sample set consisted of a within-platform light trap collec-

Manuscript submitted 4 February 2004
to the Scientific Editor's Office.

Manuscript approved for publication
1 December 2004 by the Scientific Editor.
Fish. Bull. 103:438–444 (2005).



tion and an off-platform light trap collection in random order. During sampling, turbidity (Nephelometric turbidity unit: NTU) was measured every 5 sec by using a Hydrolab DataSonde3 suspended in surface waters within the platform structure. Current speed and direction were measured every 10 min with an InterOcean S4 Current Meter suspended 1–2 m below the surface on the up-current side of the platform. Because the platform structure undoubtedly reduced current speeds (Forristall, 1996), current data taken from this location should be considered as relative estimates for the light trap collections.

Samples were preserved in 10% buffered formalin and transferred to ethanol within 12 hours. Fish were enumerated and identified to the lowest possible taxonomic level. Preflexion larvae were measured to notochord length, and postflexion and juvenile fish were measured to standard length. Data from light trap catches were standardized to a catch per unit of effort (CPUE) of number of fish per 10 minutes.

Data analyses

We assumed that there were no inter-location differences in the relationship between light trap CPUE and current speed or turbidity; therefore, data from all platforms for the months May to September were combined. The relationship between total light trap CPUE and current speed or turbidity was analyzed by using regression analysis. Current speed and turbidity were analyzed separately, rather than in a multiple regression analysis, because there was a limited number of sampling sets where we had data for light trap CPUE, current speed and turbidity together ($n=60$, or 31% and 37% of the available turbidity and current data, respectively). There were no significant differences in the regression coef-

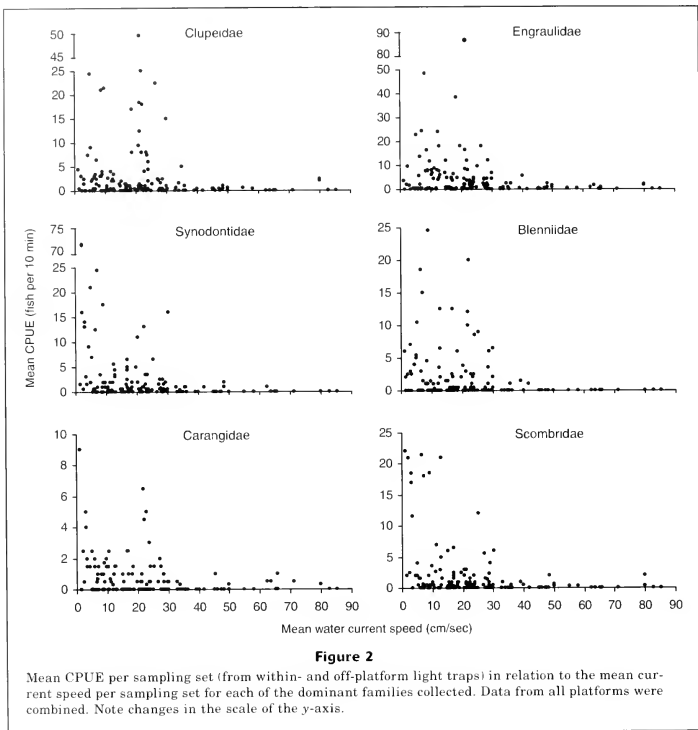
ficients of CPUE vs. current speed or turbidity between within- and off-platform light traps ($P>0.15$); therefore, the CPUEs from both light traps were averaged for each sampling set. Mean total CPUEs were log-transformed ($\log_{10}(y+1)$) and analyzed with the mean current speed or turbidity from each respective sampling set. Mean CPUEs were also calculated for the dominant families collected; however, regression analyses could not be performed because variances remained heterogeneous after transformation.

To investigate how fish size (i.e., locomotive ability) influenced light trap catches with increasing current speed, length-frequency distributions of all fishes collected at different current speed intervals (0–9, 10–19, 20–29, 30–39, 40–49 and >49 cm/sec) were compared by using Kolmogorov-Smirnov tests ($\alpha=0.05$). The length-frequency figures were subdivided by three ecological groupings: clupeiforms (Clupeidae and Engraulidae); demersal taxa (predominantly Synodontidae and Blenniidae); and scombrids and carangids, to further assess whether any changes in the size of fish collected over the current intervals were due to a particular group. All statistics were performed with SAS version 6.12 (SAS Institute, Cary, NC).

Results

Current speed

Mean total CPUEs generally decreased with increasing current speed (Fig. 1). At current speeds ≤ 30 cm/sec, light trap catches were highly variable (CPUEs ranged from 0 to 138 fish per 10 min); however, CPUEs >20 fish per 10 min occurred only at these lower speeds. Although there were fewer samples at speeds >30 cm/sec,



CPUEs were mostly <5 fish per 10 min at these speeds. There was a significant linear relationship between log-transformed mean total CPUE data and mean current speed ($\log_{10}(y+1) = -0.013x + 1.302$, $r^2=0.23$; $F=49.61$, $P<0.0001$).

Each of the dominant families collected by light traps showed a similar pattern of highest mean CPUEs at current speeds <30 cm/sec and relatively low mean CPUEs at higher current speeds (Fig. 2). Clupeidae, Engraulidae, and Blenniidae showed a slight trend of highest CPUEs at intermediate current speeds (10–30 cm/sec), whereas the other families generally had highest CPUEs at the lowest speeds (<10 cm/sec). Synodontidae and Blenniidae were rarely collected at current speeds >40 cm/sec, and small numbers of Clupeidae,

Engraulidae, Carangidae, and Scombridae were collected at speeds up to 80 cm/sec.

As current speeds increased, light trap collections became limited to smaller size classes of fish (Fig. 3). For the first three current intervals, i.e., 0–9, 10–19, and 20–29 cm/sec, a broad range of sizes were collected and the distributions had median lengths of 15–19 mm. However, beginning at the fourth current interval, 30–39 cm/sec, the size distributions shifted toward an increasingly greater proportion of the catch <10 mm in length. This trend was most pronounced at the two highest current intervals, 40–49 and >49 cm/sec, both of which had distributions with median lengths of 5 mm. The size distributions from the two highest current intervals were the only distributions that were not

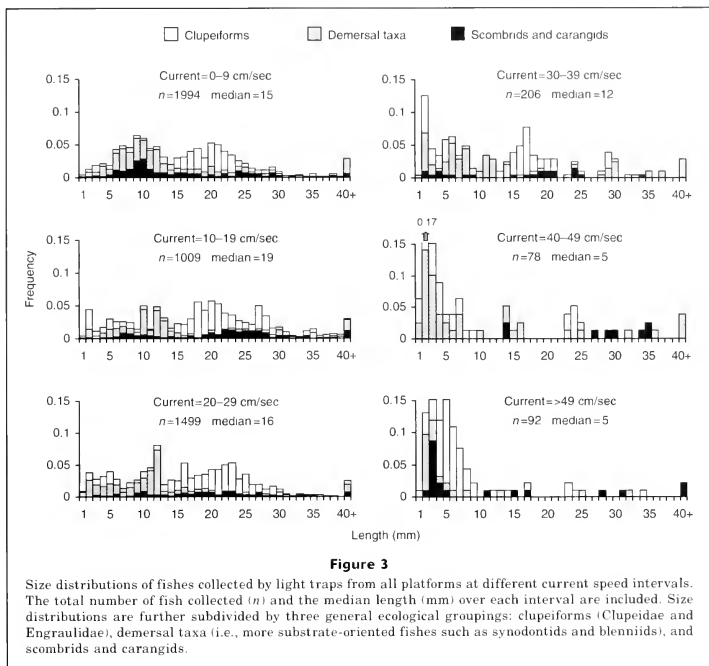


Figure 3

Size distributions of fishes collected by light traps from all platforms at different current speed intervals. The total number of fish collected (n) and the median length (mm) over each interval are included. Size distributions are further subdivided by three general ecological groupings: clupeiforms (Clupeidae and Engraulidae), demersal taxa (i.e., more substrate-oriented fishes such as synodontids and blenniids), and scombrids and carangids.

significantly different from each other ($P=0.11$). The decrease in the frequency of fishes larger than 10 mm at the higher current intervals was not limited to any particular ecological grouping, i.e., pelagic fishes such as clupeiforms, scombrids, and carangids were as rare as demersal taxa.

Turbidity

Mean total CPUEs generally decreased with increasing turbidity (Fig. 4). Highest catches (CPUEs >50 fish per 10 min) predominantly occurred at turbidities below 1.0 NTU, whereas at higher turbidities catches were generally lower. There was a significant linear relationship between log-transformed mean total CPUE data and mean turbidity ($\log_{10}(y+1) = -0.25x + 1.48$, $r^2 = 0.08$; $F = 11.86$, $P = 0.0007$).

The majority of the dominant families showed a similar pattern of highest mean CPUEs at turbidities <1.0

NTU, and relatively low mean CPUEs at higher turbidities (Fig. 5). Clupeidae, however, showed a pattern of high CPUEs at turbidities <0.5 NTU and between 1.0 and 2.0 NTU.

Discussion

Light trap catches of larval and juvenile fishes appeared to be negatively affected by increasing current speeds at platforms. This was expected because stronger currents may interfere with a fish's ability to swim to and enter a light trap (Doherty, 1987; Thorrold, 1992; Anderson et al., 2002). Doherty (1987) predicted that, for stationary (anchored or tethered) light traps, catches should increase initially with current speed as more water is sampled, but then decrease as current speed interferes with catchability. Although mean total CPUEs clearly decreased with increasing current speed, they

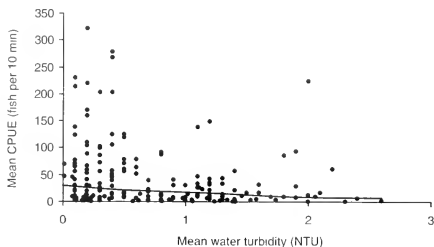


Figure 4

Mean total CPUE per sampling set (from within- and off-platform light traps) in relation to the mean turbidity per sampling set. Data from all platforms were combined. The line was calculated from the regression equation: $\log_{10}(y+1) = -0.25x + 1.48$, $r^2=0.08$. Included in the analysis, but not shown in the plot, were three points from 583 to 878 CPUE between 0.2 to 0.5 NTU.

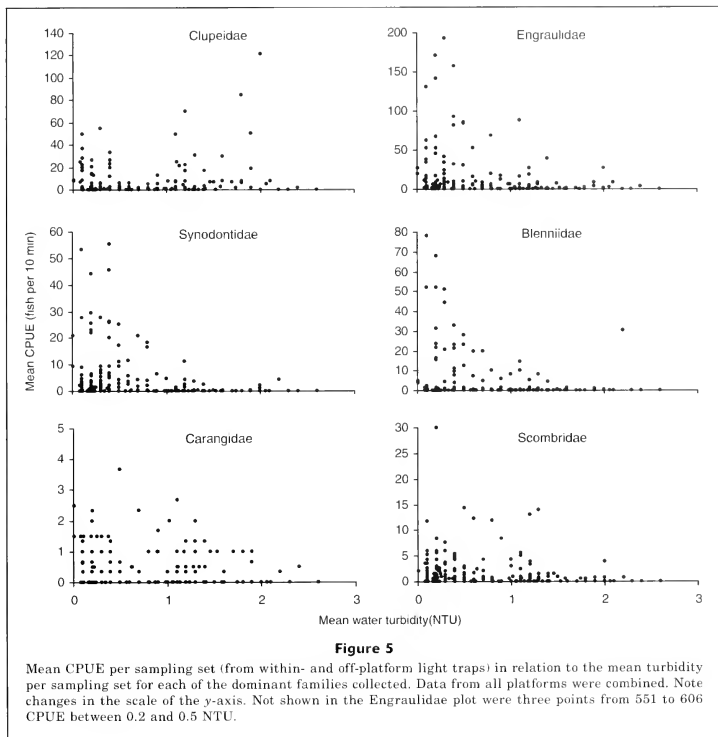
did not appear to peak at some intermediate current level. These results, however, represented the total catch of all fishes, and the relationship between current speed and light trap catches may be more taxon specific (Doherty, 1987). When analyzed at the family level, a bell-shaped relationship may have occurred for Clupeidae, Engraulidae, and Blenniidae; however, the pattern was indistinct and there was generally little difference among families.

The lack of any strong differences in the relationship between light trap CPUEs and current speed among the dominant families was unexpected, considering the potential differences in swimming abilities. Because larvae and juveniles of demersal fishes are generally believed to have lower swimming speeds (Blaxter, 1986), it was anticipated that catches of synodontids and blenniids would have been more negatively affected by increasing current speed than relatively stronger-swimming pelagic taxa (e.g., scombrids and carangids). Perhaps larvae of demersal taxa have greater swimming capabilities than previously considered, as has been recently found for certain settlement-stage larval reef fishes (sustained swimming speeds of 20–60 cm/sec; Stobutzki and Bellwood, 1994; Leis and Carson-Ewart, 1997). However, despite possible strong swimming abilities, few larval and juvenile demersal or pelagic fishes were collected at current speeds >40 cm/sec, and of these the majority were preflexion larvae that were undoubtedly passively entrained in the light trap. It is possible that the larvae and juveniles of taxa collected at platforms were unable to maintain the metabolic power required to swim against the stronger currents over extended distances from the light trap (Fisher and Bellwood, 2002).

Currents may have interfered with the functioning of the light traps. Assuming that larval and juvenile fishes were able to swim against the stronger currents, their ingress into the light trap may have been impeded by turbulence created by the current flow around the trap. If turbulence occurred after some critical current speed, then this may explain the lower CPUEs beginning at around 30 cm/sec observed for each of the dominant families.

Higher turbidity also appeared to have a negative effect on light trap catches at platforms. Light trap catch efficiency should be greatly impaired by highly turbid waters because greater light attenuation would reduce the effective sampling radius of the trap. In addition, the phototactic response of larval and juvenile fishes may be lower at lower light intensities (Gehrke, 1994; Stearns et al., 1994). However, it is uncertain whether the relatively small range of turbidities (0.1–2.6 NTU) sampled during this study would result in a significant decrease in light trap catch efficiency, particularly given the intensity of the light source used (250,000 candlepower). The observed patterns may have been a reflection of intrusions of turbid coastal and Mississippi River plume water at the platforms, during which light trap catches comprised large numbers of coastal clupeids and relatively few other taxa (Fig. 5).

Although they were treated separately for the purposes of this study, the effects of current speed and turbidity also may have been interrelated. A positive relationship between turbidity and current speed was found for a limited data set where both variables were available ($r^2=0.28$, $P<0.0001$). It is unlikely that this relationship was caused by the resuspension of benthic sediments, given the water depth at the platforms (20–230 m), but



particles may have been flushed from the platforms and their associated biofouling communities by currents. In a comparison of light trap catches between adjacent beach and rocky shore habitats, Hickford and Schiel (1999) attributed lower catches at the beach to lower water clarity caused by sediment resuspension by wave action. Therefore, high current speeds at platforms may have indirectly affected light trap catch efficiency by reducing water clarity.

Results from this study have clear implications for future studies with light traps. At platforms, light trap CPUEs began to decline noticeably at current speeds of 30 cm/sec, and by 40 cm/sec catches of active swimming larval stages (i.e., all but preflexion stages) were rare. This finding suggests that, for comparison studies,

estimates of relative abundance from light traps may be biased where there is considerable variation in current flow (Doherty, 1987; Anderson et al., 2002). Drifting traps may be used to avoid the confounding effect of differential water flow (Thorold, 1992); however such a deployment method may not be applicable when habitats of interest are fixed (e.g., platforms, coral reefs). In such cases, the best course may be to not consider light trap samples at high current speeds (≥ 40 cm/sec). For turbidity, study results were not as clear; however, temporal or spatial variation in turbidity also would undoubtedly bias light trap results. Short of using light traps at times or locations of similar water clarity, an adjustable light source may be incorporated into light trap design so that equivalent light intensities, and

therefore sampling fields, can be maintained across a variety of water conditions. The alternative would be to standardize the volumes of water sampled by light traps; however, considering the suite of external factors that affect light trap efficiency, such attempts may be fruitless (Meekan et al., 2000).

Acknowledgments

We would like to thank A. Scarborough-Bull, C. Wilson, D. Stanley, J. Ditty, F. Hernandez Jr., J. Cope, J. Plunket, T. Farooqi, and all of those who assisted in the field and laboratory for their assistance and efforts during this research. We also thank Exxon USA, Inc., Mobil USA Exploration and Production, Inc., Santa Fe-Snyder Oil Corp., and Murphy Oil Corp. for access to their oil and gas platforms and logistical support, the crews of GC 18, GI 94B, ST 54G, MP 259A and VK 203 for their assistance and hospitality, and two anonymous reviewers for their helpful comments on this manuscript. This research was funded by the Minerals Management Service-Louisiana State University-Coastal Marine Institute (contract no. 14-35-0001-30660-19961).

Literature cited

- Anderson, T. W., C. T. Bartels, M. A. Hixon, E. Bartels, M. H. Carr, and J. M. Shenker.
2002. Current velocity and catch efficiency in sampling settlement-stage larvae of coral reef fishes. *Fish. Bull.* 100:404-413.
- Blaxter, J. H. S.
1986. Development of sense organs and behaviour of teleost larvae with special reference to feeding and predator avoidance. *Trans. Am. Fish. Soc.* 115:98-114.
- Brogan, M. W.
1994. Distribution and retention of larval fishes near reefs in the Gulf of California. *Mar. Ecol. Prog. Ser.* 115:1-13.
- Choat, J. H., P. J. Doherty, B. A. Kerrigan, and J. M. Leis.
1993. A comparison of towed nets, purse seine, and light-aggregation devices for sampling larvae and pelagic juveniles of coral reef fishes. *Fish. Bull.* 91:195-209.
- Doherty, P. J.
1987. Light-traps: selective but useful devices for quantifying the distributions and abundances of larval fishes. *Bull. Mar. Sci.* 41:423-431.
- Fisher, R., and D. R. Bellwood.
2002. The influence of swimming speed on sustained swimming performance of late-stage reef fish larvae. *Mar. Biol.* 140:801-807.
- Fisher, R., D. R. Bellwood, and S. D. Job.
2000. Development of swimming abilities in reef fish larvae. *Mar. Ecol. Prog. Ser.* 202:163-173.
- Forristall, G. Z.
1996. Measurements of current blockage by the Bullwinkle platform. *J. Atmos. Ocean. Technol.* 13:1247-1266.
- Gehrke, P. C.
1994. Influence of light intensity and wavelength on phototactic behaviour of larval silver perch *Budyonius budyonius* and golden perch *Macquaria ambigua* and the effectiveness of light traps. *J. Fish Biol.* 44:741-751.
- Gregory, R. S., and P. M. Powles.
1985. Chronology, distribution, and sizes of larval fish sampled by light traps in macrophytic Chemung Lake. *Can. J. Zool.* 63:2569-2577.
- Hernandez, F. J., Jr., and R. F. Shaw.
2003. Comparison of plankton net and light trap methodologies for sampling larval and juvenile fishes at offshore petroleum platforms and a coastal jetty off Louisiana. *In Fisheries, reefs and offshore development* (D. R. Stanley and A. Scarborough-Bull, eds.), p. 15-38. *Am. Fish. Soc. Symp.* 36.
- Hickford, M. J. H., and D. R. Schiel.
1999. Evaluation of the performance of light traps for sampling fish larvae in inshore temperate waters. *Mar. Ecol. Prog. Ser.* 186:293-302.
- Johannes, R. E.
1978. Reproductive strategies of coastal marine fishes in the tropics. *Environ. Biol. Fish.* 3:65-84.
- Leis, J. M., and B. M. Carson-Ewart.
1997. *In situ* swimming speeds of the late pelagic larvae of some Indo-Pacific coral reef fishes. *Mar. Ecol. Prog. Ser.* 159:165-174.
- Meekan, M. G., P. J. Doherty, and L. White Jr.
2000. Recapture experiments show the low sampling efficiency of light traps. *Bull. Mar. Sci.* 67:875-885.
- Robertson, D. R., D. G. Green, and B. C. Victor.
1988. Temporal coupling of production and recruitment of larvae of a Caribbean reef fish. *Ecology* 69:370-381.
- Sponaugle, S., and R. K. Cowen.
1996. Nearshore patterns of coral reef fish larval supply to Barbados, West Indies. *Mar. Ecol. Prog. Ser.* 133:13-28.
- Stearns, D. E., C. J. Holt, R. B. Forward, and P. L. Pickering.
1994. Ontogeny of phototactic behavior in red drum larvae (*Sciaenidae*, *Sciaenops ocellatus*). *Mar. Ecol. Prog. Ser.* 104:1-11.
- Stobutzki, I. C., and D. R. Bellwood.
1994. An analysis of the sustained swimming abilities of presettlement and postsettlement coral-reef fishes. *J. Exp. Mar. Biol. Ecol.* 175:275-286.
- Thorrold, S. R.
1992. Evaluating the performance of light traps for sampling small fish and squid in open waters of the central Great Barrier Reef lagoon. *Mar. Ecol. Prog. Ser.* 89:277-285.
- Wilson, D. T.
2001. Patterns of replenishment of coral-reef fishes in the nearshore waters of the San Blas Archipelago, Caribbean Panama. *Mar. Biol.* 139:735-753.

Can a change in the spawning pattern of Argentine hake (*Merluccius hubbsi*) affect its recruitment?*

Gustavo J. Macchi

Consejo Nacional de Investigaciones Científicas y Técnicas (CONICET)
Rivadavia 1917
1033 Buenos Aires, Argentina
Present address: Instituto Nacional de Investigación y Desarrollo Pesquero (INIDEP)
Paseo Victoria Ocampo N° 1. CC. 175
Mar del Plata, 7600, Argentina
E-mail address gmacchi@inidep.edu.ar

Marcelo Pájaro

Adrián Madirolas

Instituto Nacional de Investigación y Desarrollo Pesquero (INIDEP)
Paseo Victoria Ocampo N° 1 CC. 175
Mar del Plata, 7600, Argentina

Argentine hake (*Merluccius hubbsi*) inhabit waters of the Southwest Atlantic Ocean between 22° and 55°S, at depths ranging from 50 to 500 m (Cousseau and Perrota, 1998). This species has historically been among the more abundant fish resources in the Argentine Sea, where its biomass has ranged between one and two million metric tons annually since 1986 (Aubone et al., 2000). In this area, there are two identified fishing stocks, limited by the 41°S parallel. The southern group (Patagonian stock) is the more important with an abundance of about 85% of the total biomass estimated for this species in 1999 (Aubone et al., 2000). During the late 1990s, the spawning biomass of both stocks and their recruitment indices declined drastically, both of which were attributed to an increase in exploitation (Aubone et al., 2000).

The Patagonian stock of Argentine hake spawns from November through March and peak spawning occurs in January (Macchi et al., 2004). This species is a batch spawner and has indeterminate annual fecundity, which is to say that unyolked oocytes continuously mature and are spawned throughout the reproductive season (Macchi and Pájaro, 2003). Thus, to estimate total fecundity, it is necessary to determine the number of

eggs released at one spawning (batch fecundity) and to estimate the number of batches spawned in a reproductive season (spawning frequency). Macchi et al. (2004) estimated these parameters for the southern stock of *M. hubbsi*. They analyzed total egg production during the reproductive season and determined that the size composition of the spawning fraction influences the reproductive potential of the stock.

Reproductive activity of the Patagonian hake historically has taken place mainly in coastal waters off the Chubut province at depths near 50 m, in the area known as Isla Escondida (43°30'–44°S) (Ciechowski et al., 1983). Since 1997–98, a movement of reproductive hake to deeper waters and a decrease in fish density have been observed (Ehrlich et al.¹). These changes, mainly in the location of the spawning area, may have affected the reproductive potential of this species, reducing the survival of eggs and larvae. If so, we would expect a negative effect on the number of juveniles recruited after this period.

In this note, we hypothesize that a change in spawning site for Patagonian hake can affect species recruitment. We studied temporal changes in the location and density of spawning aggregations, egg production, and

recruitment of this stock in different years between 1988 and 2001.

Materials and methods

Samples of *M. hubbsi* were collected from the area where the Patagonian stock is known to reproduce during four acoustic surveys in December 1988, 1993, 1996, and 2000 and during six trawl cruises carried out in January between the years 1996 and 2001.

Acoustic surveys covered the Isla Escondida area between 43° and 45°S (Fig. 1). A SIMRAD EK400/QD echointegrator was used for the 1988 survey and a SIMRAD EK500 echosounder and BI500 postprocessing program were employed for subsequent surveys. To avoid possible biases due to the presence of fish in the near-bottom, acoustic transects were carried out at night when hake assume a more pelagic behavior. Trawl catches were carried out during the day, when fish are concentrated close to the bottom, and immediately after each acoustic transect. Because trawls were intentionally biased to those areas of higher fish density, their positions were different between 1988 and 2000. Nevertheless, the study area, transect design, and sampling effort were similar for all cruises covering the main spawning shoals.

In January, information was collected from trawl surveys to assess the Patagonian stock of juvenile hake between 1996 and 2001. These cruises covered a wide area between 43° and 47°S that included a section

* Contribution 1357 from the Instituto Nacional de Investigación y Desarrollo Pesquero, Mar del Plata, Argentina.

¹ Ehrlich, M. D., P. Martos, A. Madirolas, and R. P. Sánchez. 2000. Causes of spawning pattern variability of anchovy and hake on the Patagonian shelf. ICES CM 2000/N:06.

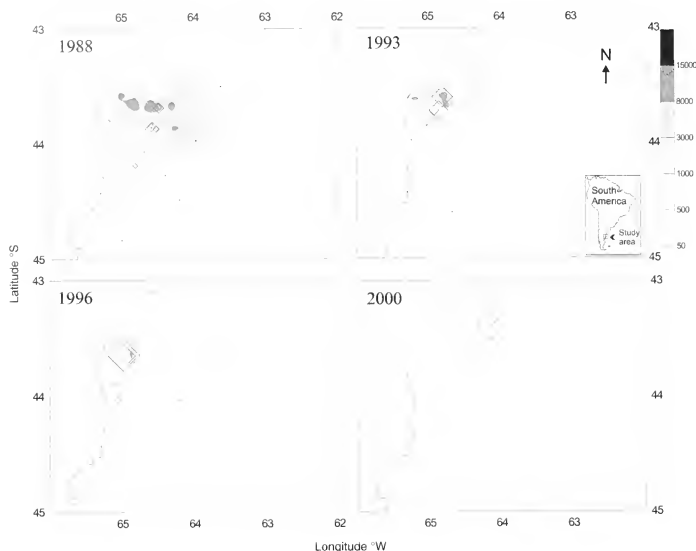


Figure 1

Distribution and density (s_A) of Argentine hake (*Merluccius hubbsi*) estimated from acoustic surveys carried out during December (1988, 1993, 1996, and 2000) in the Isla Escondida area. The size of the symbols is proportional to the percentage of spawning females (with hydrated oocytes). Vertical shaded scale represents scattering coefficient values (s_A), where $7.14 s_A$ units = $1 t/\text{nautical mile}^2$.

of the main spawning ground of hake. Thus, to analyze spawning individuals we used only data from 33 fish stations located offshore within the spawning area between $43^{\circ}30'$ and 46°S (Fig. 2). Trawl station sites were the same during all cruises. In January of 1996 and 2001 additional information from catches obtained inshore near Isla Escondida was analyzed (Fig. 2).

Argentine hake were collected with a bottom net with a mouth width of about 20 m, a height of about 4 m, and with 20-mm mesh at the inner cover of the codend. Total length (TL) in cm, total weight (TW) in g, and sex were recorded for each fish sampled; for females a subsample was randomly selected from different trawl stations (Table 1) and the maturity stage was determined for each individual. A macroscopic maturity key of five stages designed for biological studies was employed: 1) immature; 2) developing and partially spent; 3) spawning (gravid and running); 4) spent; and 5) resting (Macchi and Pájaro, 2003). This scale was validated by the histological analysis of ovaries collected

during December 2000 and January 2001 (Macchi et al., 2004). Females were classified as reproductively active or inactive, according to the presence of yolked oocytes and atresia stages following the criteria of Hunter et al. (1992). When we consider the codes used in the visual assessment of maturity, stages 2 and 3 corresponded to active females, which were capable of spawning at the time of capture or in the near future (Hunter et al., 1992).

Abundance of active females was estimated from data collected during each survey. Information obtained from sampling the trawl catch was expanded to obtain estimates of the number of individuals per length class, following the method described by Macchi et al. (2004).

During December, information from acoustic surveys was used to assign a different weight to each trawl station, based on the relative density and size of the school targeted by the trawl. The transect segment that contained a given trawl was determined and the average value of the water column scattering coefficient

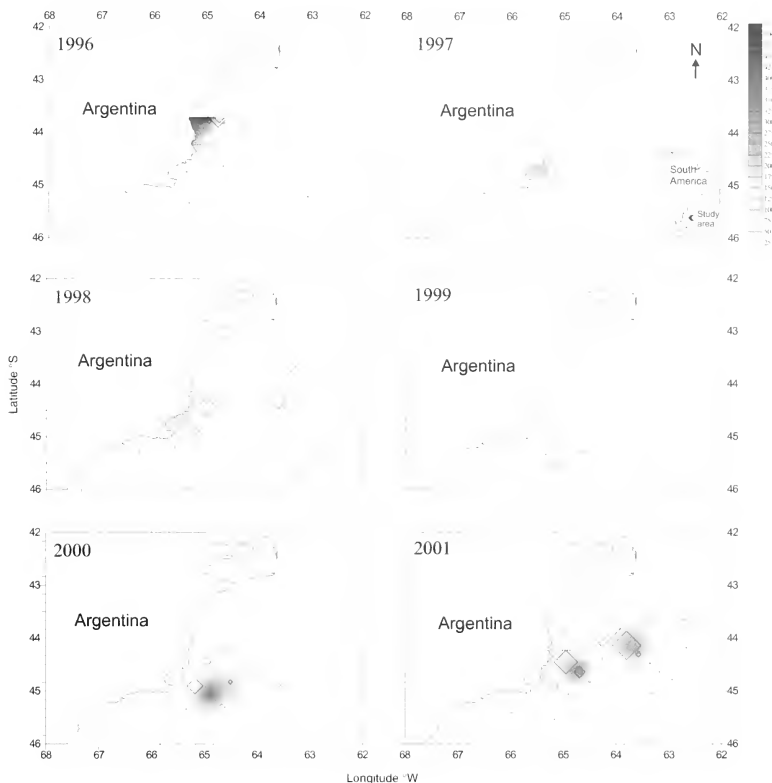


Figure 2

Distribution and density of Argentine hake (*Merluccius hubbsi*) estimated from trawl surveys carried out during January (1996–2001) in the offshore area. The size of the symbols is proportional to the percentage of spawning females (with hydrated oocytes). The square shows the Isla Escondida area. Vertical shaded scale represent biomass in t/nautical mile².

(sA) was calculated and weighed by the corresponding number of acoustic observations.

The number of active females for each survey was estimated by multiplying the number of hake within each length class by the proportion of females and the proportion of active females for that length class obtained for that survey (Marshall et al., 1998). The sum

of values estimated across the size range was an index of the number of reproductive females in the sampled area during that survey.

Egg production of the Patagonian hake in December during the period 1988–2000 and in January from 1996 to 2001 was based on estimates of three variables: the abundance of active females per length class, the

Table 1

Number of Argentine hake (*Merluccius hubbsi*) sampled during research surveys carried out in the north Patagonian area in December and January, between 1988 and 2001.

Period	Number of trawls	Number of individuals sampled	Number of females subsampled
December			
1988	18	9527	2054
1993	6	2156	1060
1996	9	1563	690
2000	12	4390	708
January			
1996	38	17,715	1509
1997	33	12,687	842
1998	33	15,804	1092
1999	33	14,987	817
2000	33	14,389	958
2001	37	17,944	856

batch-fecundity-size relationship, and spawning frequency. The batch fecundity-total-length relationship and the spawning frequency values used for December (1988-2000) and for January (1996-2001) were those estimated in December 2000 and January 2001, respectively (Macchi et al., 2004). We assumed that these values were applicable to all previous years, because in general, annual differences of these variables were not significant for hake females of the same length range (Macchi et al., 2004).

Egg production by length for each month was estimated by multiplying the number of active females in each length class by the batch fecundity corresponding to that length class and by the number of spawnings estimated for each month. The sum of the egg production values estimated across the size range was the total number of eggs produced in the sampled area during each month (December or January) in different years.

To analyze the relationship between egg production and recruitment, estimates of the relative abundance at age 1 (number of individuals per trawl hour) of Argentine hake were used as a recruitment index. These data were obtained from samples to assess hake juveniles collected from the whole area covered during the cruises carried out in January 1997-2001. In 2002, this index was estimated with samples collected in the same area, but in a different month (March) (GEM, unpubl. data²). The number of age-1 individuals in year $t+1$ was the recruitment index corresponding to the year t .

Results

Abundance of hake and location of spawning females

Figure 1 shows the acoustic densities estimated for Argentine hake and the distribution of spawning females

(with hydrated oocytes) in the Isla Escondida area during December 1988, 1993, 1996, and 2000. A decline in hake abundance from 1988 to 2000 was observed—in particular, a drastic decrease in 2000, when the mean density value (14.6 t/nautical mile²) was thirty times less than that estimated in 1988 (469.2 t/nautical mile²). During December 1988-96, spawning females were mainly located in the northern area (between 43° and 44°S) inshore at depths lower than 50 m. In 2000 reproductive activity was concentrated at the same latitude as in previous years, but offshore (Fig. 1).

In January 1996 the highest densities of *M. hubbsi* and the spawning females of this species were located in the Isla Escondida area (Fig. 2). Between 1997 and 2000 we did not obtain data from this zone, but the increase in the proportion of spawning hake in deep waters observed since 1998 indicates a spatial change in the reproductive area. During January 2000 and 2001, in addition to the increase of reproductive females offshore, the abundance of hake was higher than that estimated previously for the same area (Fig. 2). In January 2001, trawl stations located near Isla Escondida showed very low values of hake density, in contrast to that observed offshore. This contrast could be attributed to the movement of individuals from the traditional spawning area near the coast to deeper water.

Egg production

Egg production estimated for December in the Isla Escondida area showed a considerable decrease from 1988 to 2000 (Fig. 3). The number of eggs produced

² GEM (Grupo de Evaluación Merluza). 2002. Evaluación del estado del recurso merluza (*Merluccius hubbsi*) al sur de 41° S, año 2002. Unpubl report. INIDEP, CC. 175, Mar del Plata (7600), Argentina.

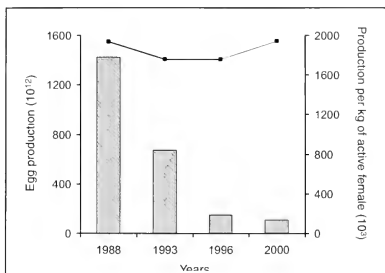


Figure 3

Egg production of Argentine hake (*Merluccius hubbsi*) estimated for December (1988, 1993, 1996, and 2000) in the Isla Escondida area (bars), and production by unit-weight of reproductively active female (line) for the same month.

per unit of weight (kg of active females) declined from 1988 to 1996, and to a value of around 1700 eggs/kg in the last year (Fig. 3). During December 2000, however, relative egg production increased to 2000 eggs/kg, which can be attributed to the effect of a higher proportion of larger females in reproductive activity. In fact, when the percentage of eggs produced by length class was analyzed, the distribution obtained for December 2000 was different from that for 1988, 1993, and 1996 (Fig. 4). During the earlier years, production mainly depended on young females (<50 cm TL), whereas in December 2000 most of the eggs produced (about 70%) were spawned by females larger than 50 cm TL.

Egg production estimated for the offshore area in January increased from 1996 to 2001 (Fig. 5), in contrast to that observed during December in shallow water near Isla Escondida. The number of eggs produced per unit of weight of active females was similar in 1996 and 1997 (about 1600 eggs/kg), but increased in 1998–2001 to about 1800 eggs/kg. This increase was similar to that observed for December 2000, which was attributed to the higher proportion of larger females within the spawning fraction of hake. In fact, percentage-distribution of eggs produced by length class showed a change beginning in 1998 (Fig. 6). In 1996 and 1997, 70% of the eggs were produced by young females (<50 cm TL), but subsequent production of old females increased to 60% in 1998–99 and to 70% in 2000–01.

Recruitment

Relative abundance data for hake at age 1 (year $t+1$) in the north Patagonian area were contrasted with the egg production obtained in January from the previous year (t). To estimate egg production, only information

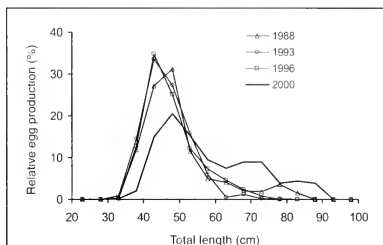


Figure 4

Relative egg production (%) by length class estimated for Argentine hake (*Merluccius hubbsi*) from December 1988, 1993, 1996, and 2000.

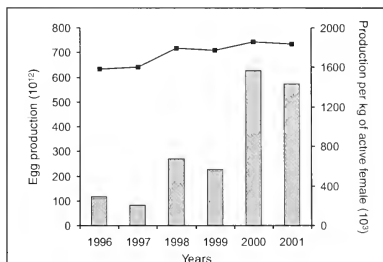


Figure 5

Egg production of Argentine hake (*Merluccius hubbsi*) estimated for January (1996–2001) in the offshore area (bars), and production by unit-weight of reproductively active female (line) for the same month.

from the offshore area was used; thus, the number of eggs estimated was a fraction of that produced by all spawning females in January. However, the increase in egg production observed offshore for the parental stock in 2000 and 2001 was coincident with higher values of age-1 recruitment estimated one year later during 2001 and 2002, respectively (Table 2).

Discussion

The spatial pattern of *M. hubbsi* spawning aggregations inshore and offshore of the north Patagonian area between 1988 and 2001 has changed since 1998. This

Table 2

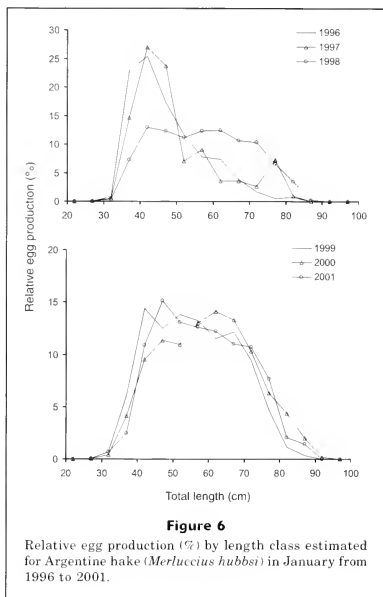
Egg production estimates for Argentine hake (*Merluccius hubbsi*) for January cruises (1996–2001) taken offshore of the north Patagonian area, and indices of abundance at age 1 corresponding to these annual classes.

Year	Egg production (10 ¹²)	Index of age-1 hakes (individuals per trawl hour)
1996	116.625	
1997	81.774	347
1998	270.512	438
1999	228.020	133
2000	627.484	250
2001	572.485	1367
2002		2444

change was characterized by a decrease in density on shoals and a movement of spawning females to deeper water, with a more scattered distribution than in the early 1990s. Our results confirm previous observations reported by Ehrlich et al.¹, who analyzed ichthyoplankton samples collected from 1973 to 1999, in the traditional spawning area of Isla Escondida. These authors did not observe significant environmental anomalies that might have affected the spawning of hake and associated the change with the high levels in fishing exploitation in the 1990s. These shifts in the pattern of reproduction led to the following question: "How does the movement of the center of spawning affect the recruitment of Patagonian hake?"—given that different environmental conditions could be present in the new spawning area.

Our analyses show that the abundance of active females offshore of the north Patagonian area increased from 1998 to 2001, coinciding with a significant decrease in hake biomass in the shallow waters of Isla Escondida. During these years, demographic changes in the offshore area were characterized by an increase of larger females (>50 cm TL) compared to previous years. The increase in proportion of older individuals in spawning condition may result in a greater contribution to egg production because of the higher fecundity produced by larger females (Mairteinsdottir and Thorarinnsson, 1998). In fact, egg production estimated for the offshore Patagonian hake during January showed an increase since 1998, with the highest values in 2000 and 2001 (400% more than those estimated in 1996–97). A high proportion (70%) of these eggs were spawned by females larger than 50 cm TL (≥ 5 -year old, Otero et al., 1986), whereas in January 1996 and 1997 eggs were mainly produced by young females.

Because of the displacement of active females to deep water, the offshore north Patagonian area from 43°30' to 45° S and between 50 m and 100 m depths was considered an important section of the spawning ground for Patagonian hake after 1998. The comparison between the January 1996 and 2001 surveys, in which inshore

**Figure 6**

Relative egg production (%) by length class estimated for Argentine hake (*Merluccius hubbsi*) in January from 1996 to 2001.

and offshore samples of the north Patagonian area were collected, demonstrated this change. In January 1996, spawning of Patagonian hake was concentrated inshore (Isla Escondida), whereas in January 2001 reproduction of this stock took place mainly offshore (Fig. 2). For this reason, the offshore egg production value obtained after 1998 was considered a representative index of the spawning area.

Relative abundance of hake at age 1 (number of individuals/hour) in the north-Patagonian area, showed a decline from 1996 to 2000 and an increase in 2001 and 2002, reaching the highest values of the study period. The recruitment index obtained for 2001 (1367 individuals/h) was about twice that estimated for 2001 (1367 individuals/h). According to Santos et al.,³ it is possible that this value has been overestimated, because it was determined

³Santos, B. A., E. B. Louge, and R. Castrucci. 2003. Estudio de las variaciones conjuntas de la temperatura y de la salinidad del área de cría de la merluza con los índices de abundancia de los grupos de edad 0, 1 y 2. (enero 1995–enero 2002). Tech. Rep. 10/03, 6 p. INIDEP, CC. 175, Mar del Plata (7600), Argentina.

from samples collected two months later (March) than those during 1996–2001. These authors suggested that the spatial distribution or catchability of juvenile hake could have changed from January to March, resulting in a greater abundance index during 2002.

The higher recruitment levels observed for Patagonian hake during 2001 and 2002 were coincident with higher indices of egg production estimated offshore in January during the two previous years (2000 and 2001). Therefore, in principle we concluded that the change in spatial location of spawners in the Patagonian stock did not appear to negatively affect the recruitment of this species. The next question to be answered is: "Why were recruitment indices in the early 2000s higher than in previous years?"

Several authors have analyzed the spawner-recruit relationship in different species and have concluded that recruitment is often positively correlated with spawner biomass estimated from virtual population analysis (VPA) (Myers and Barrowman, 1996). In the case of Patagonian hake, the increase in abundance at age 1 observed in 2001 and 2002 was not associated with higher values of the VPA-based spawner biomass in previous years (GEM, unpubl. data²). Thus, environmental and ecological factors affecting prerecruit mortality should be considered, mainly in association with a no-fishing area implemented in 1997. Moreover, the demographic composition and the nutritional state of spawning females (maternal effect) are other factors that have been related to recruitment levels (Trippel et al., 1997; Kjesbu et al., 1998; Cardinale and Arrhenius, 2000).

Analysis of hydrographic characteristics from the north-Patagonian waters in the 1980s and 1990s indicated that the Patagonian shelf, including the Isla Escondida area, is a relatively stable environment (Erhlich et al.²). On the other hand, analysis of temperature and salinity data collected from 1995 to 2002 in the nursery area of the Patagonian stock (San Jorge Gulf), showed that higher values of salinity and temperature during the time of hatching were associated with higher indices of abundance at age 1, one year later (Santos et al.³).

The high proportion of larger females in the offshore area mainly in 2000 and 2001 may have affected the quality as well as the quantity of hake progeny. In general, older females produce larger eggs and larger larvae with higher rates of survival, in combination with more egg batches over a longer spawning season (Kjesbu et al., 1996; Trippel, 1998). Previous reports showed that *M. hubbsi* older than 5-years have a longer spawning season (Macchi et al., 2004) and produce heavier eggs than young females do (Pájaro et al.⁴). Thus, an increase in the proportion of older spawning females in

the stock may result in improved recruitment, as has been reported for other species (Mairteinsdóttir and Thorarinnsson, 1998).

The fishing regulation for Patagonian hake implemented in the late 1990s mainly affected bottom trawlers and the factory freezer fleet, which applied greater fishing effort in the north Patagonian area during the 1990s. It is possible that this decline in harvesting pressure by trawlers on Patagonian hake after 1997 influenced the reproductive success of this species. Stress can have a negative impact on fish reproduction (Campbell et al., 1994; Clearwater and Pankhurst, 1997). The potential effects of trawl avoidance can affect the reproductive physiology and behavior during spawning, which could lead to the production of fewer viable juveniles (Morgan et al., 1999).

Finally, other factors, such as predation and feeding conditions within the new spawning ground of Patagonian hake, can affect survival of the early life stages. In addition, future studies should include a comparison between the inshore and offshore waters of the north-Patagonian area with respect to the abundance of jellyfish (i.e., *Medusa* and *Ctenophora*), which are known to be major predators of fish eggs and larvae (Bailey, 1984; Fancett, 1988).

Acknowledgments

We thank Jorge Hansen for assistance with the method used to estimate fish abundance. We would also like to thank Hector Cordo for reading and making suggestions to improve the manuscript.

Literature cited

- Aubone, A., S. Bezzi, R. Castrucci, C. Dato, P. Ibañez, G. Iruata, M. Pérez, M. Renzi, B. Santos, N. Scarlato, M. Simonazzi, L. Tringali, and F. Villarino.
2000. *Merluza (Merluccius hubbsi)*. In *Síntesis del estado de las pesquerías marítimas argentinas y de la Cuenca del Plata. Años 1997–1998, con una actualización de 1999* (S. Bezzi, R. Akselman and E. Boschi, eds.), p. 29–40. INIDEP, Mar del Plata, Argentina.
- Bailey, K. M.
1984. Comparison of laboratory rates of predation on five species of marine fish larvae by three planktonic invertebrates. Effects of larval size on vulnerability. *Mar. Biol.* 79:303–309.
- Campbell, P. M., T. G. Pottinger, and J. P. Sumpter.
1994. Preliminary evidence that chronic confinement stress reduces the quality of gametes produced by brown and rainbow trout. *Aquaculture* 120:151–169.
- Cardinale, M., and F. Arrhenius.
2000. The influence of stock structure and environmental conditions on the recruitment process of Baltic cod estimated using a generalized additive model. *Can. J. Fish. Aquat. Sci.* 57: 2402–2409.
- Ciechomski, J. D., R. P. Sánchez, C. A. Lasta, and M. D. Erhlich.
1983. Distribución de huevos y larvas de anchoíta (*En-*

⁴ Pájaro, M. E., Louge, G. J., Macchi, N., Radovani, and L. Rivas. 2002. Calidad de los ovocitos de la población patagónica de merluza (*Merluccius hubbsi*) durante la época de puesta estival. *Tech. Rep.* 55/02, 13 p. INIDEP, CC. 175, Mar del Plata (7600), Argentina.

- graulis anchoita*) y de merluza (*Merluccius hubbsi*), evaluación de sus efectivos desovantes y análisis de los métodos empleados. Contrib. Inst. Nac. Invest. Desarr. Pesq. (Mar del Plata) 432:3-37.
- Clearwater, S. J., and N. W. Pankhurst.
1997. The response to capture and confinement stress of plasma cortisol, plasma sex steroids and vitellogenic oocytes in the marine teleost, red gurnard. *J. Fish Biol.* 50:429-441.
- Cousseau, M. B., and R. G. Perrota.
1998. Peces marinos de Argentina. Biología distribución y pesca, 163 p. INIDEP, Mar del Plata, Argentina.
- Fancett, M. S.
1988. Diet and prey selectivity of scyphomedusae from Port Phillip Bay, Australia. *Mar. Biol.* 98:503-509.
- Hunter, J. R., B. J. Macewicz, N. C. H. Lo, and C. A. Kimbrell.
1992. Fecundity, spawning, and maturity of female Dover sole *Microstomus 13 pacificus*, with an evaluation of assumptions and precision. *Fish. Bull.* 90:101-128.
- Kjesbu, O. S., P. Solemdal, P. Bratlan, and M. Fonn.
1996. Variation in annual egg production in individual captive Atlantic cod (*Gadus morhua*). *Can. J. Fish. Aquat. Sci.* 53:610-620.
- Kjesbu, O. S., P. R. Witthames, P. Solemdal, and M. Greer Walker.
1998. Temporal variations in the fecundity of Arcto-Norwegian cod (*Gadus morhua*) in response to natural changes in food and temperature. *J. Sea Res.* 40:303-321.
- Macchi G. J., and M. Pájaro.
2003. Comparative reproductive biology of some commercial marine fishes from Argentina. *Fisken Og Havet* 12:69-77.
- Macchi, G. J., M. Pájaro, and M. Ehrlich.
2004. Seasonal egg production pattern of the Patagonian stock of Argentine hake (*Merluccius hubbsi*). *Fish. Res.* 67:25-38.
- Mairteinsdottir, G., and K. Thorarinnsson.
1998. Improving the stock-recruitment relationship in Icelandic cod (*Gadus morhua* L.) by including age diversity of spawners. *Can. J. Fish. Aquat. Sci.* 55:1372-1377.
- Marshall, T., O. S. Kjesbu, N. A. Yragina, P. Solemdal, and O. Ulltang.
1998. Is spawner biomass a sensitive measure of the reproductive and recruitment potential of Northeast Arctic cod? *Can. J. Fish. Aquat. Sci.* 55:1766-1783.
- Morgan, M. J., C. E. Wilson, and L. W. Crim.
1999. The effect of stress on reproduction in Atlantic cod. *J. Fish Biol.* 54(3):477-488.
- Myers, R. A., and N. J. Barrowman.
1996. Is fish recruitment related to spawner abundance? *Fish. Bull.* 94:707-724.
- Otero, H. O., M. S. Giangioje, and M. A. Renzi.
1986. Aspectos de la estructura de población de la merluza (*Merluccius hubbsi*). II Distribución de tallas y edades. Estudios sexuales. Variaciones estacionales. *Publ. Com. Tec. Mix. Fr. Mar.* 1(1):147-179.
- Trippel, E. A.
1998. Egg size and viability and seasonal offspring production of young Atlantic cod. *Trans. Am. Fish. Soc.* 127:339-359.
- Trippel, E. A., O. S. Kjesbu, and P. Solemdal.
1997. Effects of adult age and size structure on reproductive output in marine fishes. In *Early life history and recruitment in fish populations* (R. C. Chambers and E. A. Trippel, eds.), p. 31-62. Chapman & Hall, New York, NY.

Feeding habits of the dwarf weakfish (*Cynoscion nannus*) off the coasts of Jalisco and Colima, Mexico

Alma R. Raymundo-Huizar

Centro Universitario de la Costa, Departamento de Ciencias
Universidad de Guadalajara
Av. Universidad 203
Puerto Vallarta, Jalisco, CP 48280 México

Horacio Pérez-España

Centro de Ecología y Pesquerías
Universidad Veracruzana
Dr. Castelazo s/n. Xalapa
Veracruz, CP 91190 México

Maite Mascaró

Laboratorio de Ecología y Conducta
Unidad Académica Sisal
Universidad Nacional Autónoma de México
Sisal, Yucatán, CP 97355 México

Xavier Chiappa-Carrara

Unidad de Investigación en Ecología Marina, FES-3
México, DF, CP 09230 México
Present address: Unidad Académica Sisal
Universidad Nacional Autónoma de México
Sisal, Yucatán, CP 97355 México
E-mail address (for X. Chiappa-Carrara, contact author): chiappa@servidor.unam.mx

Sciaenids from the Pacific coast of Mexico are used as a second-class fish species for human consumption (Aguilar-Palomino et al., 1996). The dwarf weakfish (*Cynoscion nannus*) (Castro-Aguirre and Arvizu-Martínez, 1976) is often caught as bycatch in the shrimp fishery but, because of its small size (<27 cm TL, total length), it is not considered a valuable resource. This species can be found in great numbers in waters between 100 and 812 m (Allen and Robertson, 1994; Fischer et al., 1995) associated with the soft-bottom regions off the coast of Jalisco and Colima (González-Sansón et al., 1997).

Previous studies of the trophic biology of the Sciaenidae (Chao and Musík, 1977; Campos and Corrales, 1986; Chao, 1995; Peláez-Rodríguez, 1996; Cruz-Escalona, 1998; Lucena et al., 2000) have shown that they

feed on a variety of small fish and benthic invertebrates (Allen and Robertson, 1994). However, there are few studies concerning the feeding habits of *C. nannus*, and its dietary preferences are not known. Considering its abundance, *C. nannus* must play an important role in the trophic relationships of soft-bottom ecosystems in this region.

Most studies describing the feeding habits of fish have used the normalized version of the breadth niche index proposed by Levins (1968). This index is based both on the number of food resources and on the proportion of prey used by a species. The appropriate distribution function for this index ensures sample independence among prey found in any particular stomach. Distribution functions based either on the number or the relative biomass or volume of dietary items do

not ensure such independence, given that all items found in any particular stomach are statistically associated (Hurlbert, 1984). Therefore, neither the number nor the relative biomass or volume of dietary items should be used to calculate the Levins index. The only distribution function that ensures statistical independence is that which is based on the proportion of stomachs in which a certain food resource is found (Krebs, 1999).

Considering the ecological importance of studying the feeding habits of this abundant fish species, we examined trophic breadth variations (temporally and ontogenetically) of *C. nannus*. When attempting to correctly apply the Levins index, we used the distribution function of prey that ensures statistical independence among sampling units.

Materials and methods

The sampling area was located in the central region of the continental shelf off the Pacific coast of Mexico, where the mouth of the river Cuitzamal, in Punta Farallón, Jalisco (19°22'N, 105°01'W), is the northern limit, and Cuyutlán, Colima (18°55'N, 104°08'W), is the southern limit. Samples of *C. nannus* were collected on a monthly basis from January to December 1996 (except February, August, and September) on the research vessel *BIP V*, equipped with a trawl net with a pair of codends. Sampling was carried out over seven transects perpendicular to the coast, each comprising four bathymetric strata: 20, 40, 60, and 80 m mean depth.

Fish were individually identified, measured (TL, ± 1 mm), and the total weight of each fish was recorded to the nearest 0.1 g. The stomachs of individual fish were dissected and preserved in 10% neutralized formalin. Stomach contents were analyzed

Manuscript submitted 16 May 2003
to the Scientific Editor's Office.

Manuscript approved for publication
20 December 2004 by the Scientific Editor.
Fish. Bull. 103:453-460 (2005).

with a stereoscopic microscope and dietary items were identified to the lowest taxonomic level possible by using specialized keys. Garth (1958), Rodriguez de la Cruz (1987), Hendrickx and Salgado-Barragan (1991), and Hendrickx (1996), were consulted for crustacean identification, whereas Jordan and Evermann (1896–1900), Castro-Aguirre (1978), Allen and Robertson (1994), Thomson et al. (2000), and FAO guides were used for fish identification (Fischer et al., 1995).

Both the number of individuals and weight of each dietary category were quantified, and mean proportions in terms of number ($\%N_i$) and biomass ($\%W_i$) were calculated according to Tirasin and Jørgensen (1999):

$$\% \bar{X}_i = \frac{\sum_{j=1}^{n_j} X_{ij}}{\sum_{r=1}^k \sum_{j=1}^{n_j} X_{ij}} \times 100,$$

where X_{ij} = the number or weight of each taxa i in the j^{th} stomach; and

k = the number of dietary components found in all stomachs analyzed, n_j .

The percent frequency of occurrence of each component was also obtained ($\%F$). Finally, the index of relative importance for each dietary category was calculated (IRI, Pinkas et al., 1971; Rosecchi and Nouaze, 1987):

$$IRI_i = (\%N_i + \%P_i) \times \%F_i.$$

Relative importance index values were expressed as a percentage of the total items analyzed (Cortés, 1997) and results were graphically represented as a rectangle of base $\%F$ and height $\%N + \%W$.

Variance analysis was applied on transformed $W = \sin^{-1}(\sqrt{W})$ gravimetric proportions of the dietary components (Zar, 1999) to evaluate both monthly and ontogenetic variations in the feeding habits of *C. nanus*. The number [$q=1+3.322(\text{Log}_{10}n)$] and width of size classes ($w=R_{TL}/q$) were considered for analysis, where n is the sample size and $R_{TL}=TL_{\text{max}}-TL_{\text{min}}$.

For the analysis of trophic niche breadth, the normalized version of the index proposed by Levins (1968) was used. This index combines both the number of prey resources used (k) (i.e., the trophic spectrum) and the relative frequency with which each prey resource is consumed (j). This represents the distribution function of prey proportions in diet (Hespenheide 1975; Hurlbert, 1978):

$$Ba = \frac{\left(\sum_{j=1}^{n_j} p_j^2 \right)^{-1}}{k-1}.$$

Because the ensemble of prey found in any given stomach does not constitute independent samples (Hurlbert, 1984), p_j was calculated as the proportion of indi-

vidual fish (N_j) that consumed a certain food resource in relation to the number of resources used by the total number of fish:

$$p_j = \frac{N_j}{\sum_{j=1}^k N_j} \text{ so that } \sum p_j = 1.$$

Ba values range between 0 and 1. Zero values indicate that fish feed on only one prey type, representing the minimum diet breadth and high feeding specialization. Unity values, on the other hand, indicate that the species consumed all k food resources in the same proportion ($p_j=1/k$), representing no selection among prey types and the widest possible trophic niche (Gibson and Ezzi, 1987; Labropoulou and Eleftheriou, 1997). Ba values were calculated on the basis of matrix resources (Colwell and Futuyama, 1971) both for each month and for each size class. The percentage similarity measure (R) between size classes q' and q'' (Renkonen, 1938; Schoener, 1970; Hurlbert, 1978) was calculated as

$$R_{q'q''} = 1 - \frac{1}{2} \left[\sum_{j=1}^k |p_{j,q'} - p_{j,q''}| \right],$$

where $p_{j,q}$ is the proportion of individual fish in each size class that consumed a certain food resource, calculated over the total number of stomachs per size class.

Confidence intervals (CI_{95%}) of Ba were obtained by means of the bootstrap method (Mueller and Altenberg, 1985; Efron and Tibshirani, 1986) by considering two thousand resamplings of the data (Hamilton, 1991).

Results

The 311 *Cynoscion nanus* examined ranged from 7.5 to 20.6 cm TL. Food was found in 287 (92%, ranging from 85% to 98% among size classes) stomachs. The trophic spectrum of *C. nanus* is composed of 29 dietary items (Table 1), which were classified into four general categories: penaeid shrimp, fish, stomatopods, and cephalopods.

Penaeid shrimp constituted the principal dietary category of *C. nanus* ($N_{\bar{x}}=82.5\%$, $W_{\bar{x}}=35.4\%$; $F_{\bar{x}}=43.9\%$, $IRI_{\bar{x}}=74.6\%$; Fig. 1), of which juvenile stages were the most frequent ($F_{\bar{x}}=23.4\%$). Fish were the second most important category ($N_{\bar{x}}=6.5\%$, $W_{\bar{x}}=36.5\%$, $F_{\bar{x}}=37.7\%$, $IRI_{\bar{x}}=14.5\%$), followed by stomatopods of the *Squilla* genus ($N_{\bar{x}}=5.8\%$, $W_{\bar{x}}=8.6\%$, $F_{\bar{x}}=25.5\%$, $IRI_{\bar{x}}=6.6\%$). The cephalopod *Loliopsis diomedae* was the last category in order of importance ($N_{\bar{x}}=1.0\%$, $W_{\bar{x}}=12.4\%$, $F_{\bar{x}}=4.2\%$, $IRI_{\bar{x}}=1.8\%$).

Overall, significant differences in diet were found between individuals of different size classes ($F=1.03$; $P<0.05$). Values of the percentage similarity of diet (R) between size classes were, in general, $<50\%$ (Table 2). R -values were relatively high only among size classes 2

Table 1

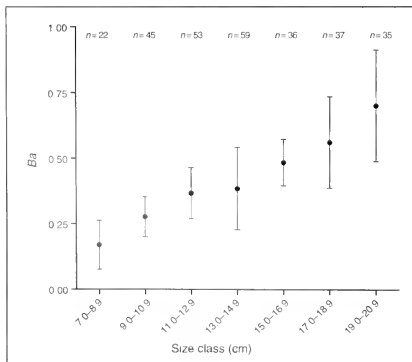
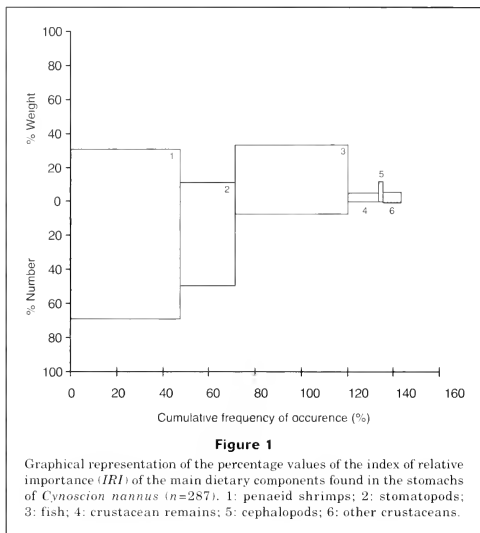
Composition of the trophic spectrum of *Cynoscion nannus* (7.5 cm \pm TL \pm 20.6 cm; $n=287$) from the coast of Jalisco and Colima (mean percentage by weight [g: %W], frequency of occurrence [%F], number [%N], and index of relative importance [%IRI] of prey).

Dietary categories		%W	%F	%N	%IRI
Cephalopods	<i>Loliopsis diomedae</i>	12.4	4.2	1.0	1.8
	Remains	0.1	0.4	0.1	0.0
Stomatopods	<i>Squilla</i> sp.	5.9	19.7	4.0	6.4
	<i>S. panamensis</i>	1.5	1.7	0.8	0.1
	<i>S. hancocki</i>	0.5	1.7	0.4	0.0
	<i>S. mantoidea</i>	0.7	2.5	0.7	0.1
Penaeid shrimps	<i>Solenocera</i> sp.	7.6	10.9	4.3	4.2
	<i>S. florea</i>	2.2	1.3	0.6	0.1
	<i>S. mutator</i>	3.8	2.9	4.6	0.8
	<i>Trachypnaeus brevisuturae</i>	3.5	5.4	2.3	1.0
	Juvenile shrimps	18.2	23.4	70.8	68.4
Other crustaceans	Carideans	1.3	4.2	0.9	0.3
	<i>Panulirus</i> sp. larvae	0.1	0.4	0.1	0.0
	Other crustacean larvae	0.1	0.4	0.3	0.0
	Euphausiids	0.5	1.3	2.3	0.1
	Microcrustaceans	0.2	0.4	0.1	0.0
	Unidentified remains	4.2	13.8	—	1.9
Fish	<i>Cynoscion nannus</i>	2.1	0.8	0.4	0.1
	<i>Cherublemma emmelas</i>	1.3	1.7	1.0	0.1
	<i>Polydactylus opercularis</i>	1.6	1.3	0.4	0.1
	<i>Ophidium</i> sp.	0.7	0.4	0.8	0.0
	<i>Monolele</i> sp.	0.9	0.4	0.1	0.0
	<i>Symphurus</i> sp.	0.1	0.4	0.1	0.0
	<i>Bregmaceros bathymaster</i>	1.6	2.5	0.7	0.2
	Anguilliformes	1.2	2.1	0.5	0.1
	Leptocephalus larvae	8.9	4.2	1.1	1.4
	Other fish larvae	1.4	1.7	1.0	0.1
	Unidentified remains	16.6	22.2	0.3	12.3
Anelids	<i>Polychaeta</i>	0.62	1.26	0.38	0.0

Table 2

Percentage similarity values (R) of the diet between size classes (cm, TL) of *Cynoscion nannus* ($n=287$) from the coast of Jalisco and Colima.

Size class (cm)	Size class (cm)					
	7.0–8.9	9.0–10.9	11.0–12.9	13.0–14.9	15.0–16.9	17.0–18.9
9.0–10.9	37.0					
11.0–12.9	44.2	54.2				
13.0–14.9	33.5	65.1	51.1			
15.0–16.9	31.0	47.6	51.4	64.1		
17.0–18.9	12.5	31.6	39.6	38.0	40.4	
19.0–20.9	29.3	45.8	44.3	47.9	40.1	21.6



through 5 (51.1%–65.1%). The trophic spectrum of the smallest *C. nannus* (7 cm \leq TL \leq 10.9 cm, n=67) was composed by crustaceans ($W_x=68\%$), mostly carideans and stomatopods ($W_x=20\%$). The diet of intermediate individuals (11 cm \leq TL \leq 16.9 cm, n=148) was composed by penaeid shrimp, fish, and stomatopods. Only fish of the size classes grouped in this range showed percentages of diet similarity $>50\%$. Among *C. nannus* between 17 and 18.9 cm TL (n=37), the value of consumed fish biomass attained 69%, whereas that of penaeid shrimp reached 20%. Only among the larger individuals (19 cm \leq TL \leq 20.9 cm; n=35) did cephalopods attain high gravimetric values ($W_x=45\%$) followed by penaeid shrimp ($W_x=38\%$).

Values of trophic niche breadth for each size class indicated ontogenetic variation in the diet (Fig. 2). The smallest individuals fed on a smaller number of prey species and showed a trend towards higher trophic specialization. Larger individuals, however, had a wider trophic spectrum and fed on a greater number of different prey species.

Temporal variations in the dietary composition of *C. nannus* were significant ($F=3.58$; $P<0.05$). During the first months of the year, *C. nannus* consumed a higher percentage of fish ($W_x=37.2\%$,

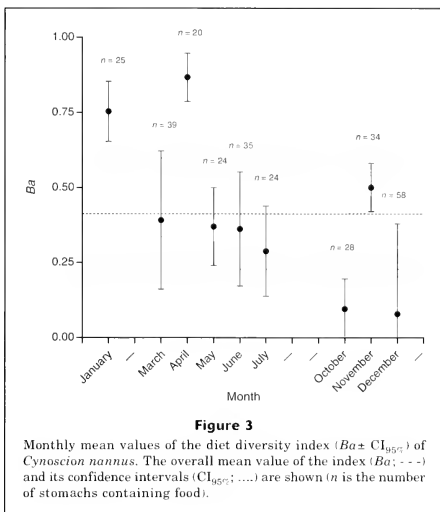


Figure 3
Monthly mean values of the diet diversity index ($Ba \pm CI_{95\%}$) of *Cynoscion nannus*. The overall mean value of the index (Ba ; - - -) and its confidence intervals ($CI_{95\%}$;) are shown (n is the number of stomachs containing food).

whereas towards the end of the year, penaeid shrimp were eaten in higher proportions ($W_x = 50.6\%$). During May, stomatopods and carideans were found with higher biomass values than during the rest of the year ($W_x = 68.2\%$ and 20% , respectively). Cephalopods were found in most months with biomass values ranging from 4% to 34% of consumed biomass.

The mean value of diet diversity was $0.41 (\pm 0.18 CI_{95\%})$. Although the number of dietary categories for *C. nannus* that were identified was high (29 prey types), there were a few items with significant importance. Monthly variations in Ba ranged from 0.1 to 0.8 (Fig. 3). During most of the period analyzed, Ba values were not significantly different from each other as shown by the lack of overlap between $CI_{95\%}$. The only exceptions were January and April, when $CI_{95\%}$ was above the mean $Ba \pm CI_{95\%}$ value, and October when $CI_{95\%}$ was below the mean Ba .

Discussion

Cynoscion nannus is a carnivorous fish that feeds on at least 29 different prey types. Although cannibalistic behavior has been reported for several fish species in a variety of habitats and life-history strategies (Smith and Reay, 1991), *C. nannus* as a prey type was

found in only 0.8% (two individuals >15.0 cm TL) of all stomachs analyzed. According to the IRI values, crustaceans—specifically juvenile shrimp and stomatopods of the genus *Squilla*—appear to be the most important items in the diet. The type of substrate can influence the feeding habits of these fish. For example, Minello and Zimmerman (1984) observed that under experimental conditions, the feeding preferences of *C. nebulosus* (16 cm \leq TL \leq 21 cm) for *Farfantepenaeus aztecus* varied depending on the substrate. These authors suggested that substrate characteristics determine the burrowing capacity of *F. aztecus* and thus predator avoidance. In the study area, juvenile shrimp and stomatopods of the genus *Squilla* can be abundantly found in soft-bottom habitats (González-Sansón et al., 1997). Both the cephalopod (*Loliopsis diomedea*) and the fish species found in the stomach contents of *C. nannus* are pelagic or demersal species, indicating that the feeding activities of *C. nannus* are not exclusively limited to the benthos, and that this species can forage throughout the water column. Results in the present study provide evidence that fish feeding at different water depths have access to a broader variety of prey types. This has been shown both for other Sciaenidae (Chao and Musík, 1977; Campos and Corrales, 1986; Chao, 1995; Peláez-Rodríguez, 1996; Cruz-Escalona, 1998), and other species of demersal fish (Lucena et al., 2000).

It should be noted that graphic representations of the IRI values are more accurate in describing the diet of fish species (Cortés, 1997). Our results (Fig. 1) demonstrate that the three indices representing the relative importance of each food item highlight the influence that the percentages of occurrence, by number and by weight, have on the overall IRI values.

The temporal analysis of the trophic spectrum of *C. nannus* showed that during October, November, and December this species fed mainly on penaeid shrimps. Fish prey were abundant in stomachs collected only during March, April, June, and November. Stomatopods were present all year round, but only abundant during May. Low *Ba* values in October were due to the prevailing consumption of *Solenocera* spp. Monthly differences in the diet of *C. nannus* were most probably in accordance with the seasonal variations in prey species abundance, which in turn determined their availability. Lucena et al. (2000) found that temporal variations in the diet of *C. guatucupa* from southern Brazil are related to seasonal production cycles of prey, mainly fish and crustaceans, thus supporting the view that sciaenids can generally be considered opportunistic species.

Results of this study showed ontogenetic variations in the trophic spectrum of *C. nannus*. The smallest individuals (7 cm \leq TL \leq 10.9 cm) feed mainly on stomatopods, whereas larger individuals (\geq 11 cm TL), consume less stomatopods and more penaeid shrimp and fish. Merriner (1975) also found ontogenetic variations in the diet of *C. regalis*, where the smallest individuals (age group "0") fed on crustaceans and small fish. The relative importance of shrimp, however, decreased as *C. regalis* increased in size, and individuals of age group "2" generally consumed different species of clupeids, depending on the local abundance of each prey species. The measure of percentage similarity among size classes (Table 2) shows that *C. nannus* share a limited number of resources. Only fish belonging to intermediate lengths feed on the same prey types in percentages greater than 50% for the total number of food resources used.

Ontogenetic changes in the diet of *C. nannus* observed in the present study are due to differences in diet composition and proportions of consumed prey. These results suggest that food types are ingested unequally as fish grow and that morphological and physiological changes take place. As fish grow, the size of their mouth increases proportionally, their swimming capacity is modified, and their energetic requirements vary. Thus, larger fish have different feeding requirements than smaller ones and will attempt to satisfy them by consuming a larger variety of prey types. As *C. nannus* grow, *Ba* values increase and the trophic spectrum of the species grows wider (Fig. 2). Our results indicate that there is a pattern of differential use of food resources throughout the different size classes of *C. nannus*, and suggest a possible ecological strategy to reduce intraspecific competition for food in the population (Schoener, 1974; Werner, 1979).

The increasing variety of food resources used as predators increase in size is a common pattern among marine organisms, including invertebrates (Rangeley and Thomas, 1987; Mascaró and Seed, 2001). These ontogenetic variations in food preferences can be explained by changes in foraging behavior where predators of certain size classes actively select their prey (Jubb et al., 1983; Allan et al., 1987). Alternatively, they can be the result of passive mechanisms that do not involve individual decisions associated with age or life stages, such as differences in the predator's mouth structures, changes in movement velocity of both prey and predator, and spatial or temporal variations in habitat as predators increase in size (Hughes, 1979; Rodrigues et al., 1987).

To show that *Ba* values are affected by the type of prey distribution function used, we calculated the mean diet diversity index using 1) the proportion of the number of prey (N ; $Ba=0.03$), 2) the percent frequency of occurrence of prey (F ; $Ba=0.16$), and 3) the proportion of prey biomass (W ; $Ba=0.32$). The values obtained were then compared to those calculated by considering the proportion of individuals (N^* ; $Ba=0.41$) that use a certain food resource for the total number of stomachs analyzed. *Ba* values calculated by using N , F , and W are markedly lower than the *Ba* value obtained by using N^* . These differences serve to underline the importance of complying strictly with the property of statistic independence of sampling units when the feeding habits of a species are being studied.

Given the numerical importance of *C. nannus* as part of demersal assemblages, observations on the trophic spectrum of this and other species can help to generate a conceptual model of the trophic webs and dynamics of the feeding relations among communities found on the continental shelf of Jalisco and Colima, an area that has received little attention in the past.

Acknowledgments

J. Arciniega, R. García de Quevedo, and V. Landa-Jaime kindly verified the taxonomic status of prey. We also thank L. E. Hidalgo-Arcos for his technical support and S. Bowers who edited the text.

Literature cited

- Aguiar-Palomino, B., J. Mariscal-Romero, G. González-Sansón, and L. E. Rodríguez-Ibarra.
1996. Ictiofauna demersal de fondos blandos de la plataforma continental de Jalisco y Colima, México, en la Primavera de 1995. *Cienc. Mar.* 22:469-481.
- Allan, J. D., A. S. Flecker, and N. L. McClintock.
1987. Prey preference of stoneflies: sedentary vs. mobile. *Oikos* 49:323-331.
- Allen, G. R., and R. Robertson.
1994. Fishes of the tropical Eastern Pacific, 380 p. Univ. Hawaii Press, Honolulu, HI.

- Campos, J., and A. Corrales.
1986. Preliminary results on the trophic dynamics of the Gulf of Nicoya, Costa Rica. *An. Inst. Cienc. Mar y Limnol. Univ. Nal. Autón. México* 13:329-334.
- Castro-Aguirre, J. L.
1978. Catálogo sistemático de los peces marinos que penetran a las aguas continentales de México, con aspectos zoogeográficos y ecológicos. Dep. Pesca, Inst. Nal. Pesca (México), Ser. Cient. 19, 298 p.
- Castro-Aguirre, J. L., and J. Arvizu-Martínez.
1976. Una nueva especie de *Cynoscion*, del Pacífico de México (Pisces: Sciaenidae: Otholithinae). *Rev. Soc. Mex. Hist. Nat.* 37:323-329.
- Chao, L. N.
1995. Familia Sciaenidae. In *Guía FAO para la identificación de especies para los fines de la pesca. Pacífico Centro-oriental. Vertebrados, parte 1* (W. Fischer, F. Krupp, W. Schneider, C. Sommer, K. E. Carpenter, and V. H. Niem, eds.), p. 647-1200. FAO, Rome.
- Chao, L. N., and J. A. Musick.
1977. Life history, feeding habits and functional morphology of juvenile sciaenid fishes from the York River estuary, Virginia. *Fish. Bull.* 75:675-702.
- Colwell, R. K., and D. J. Futuyma.
1971. On the measurement of niche breadth and overlap. *Ecology* 52:567-576.
- Cortés, E.
1997. A critical review of methods of studying fish feeding based on analysis of stomach contents: application to elasmobranch fishes. *Can. J. Fish. Aquat. Sci.* 54:726-738.
- Cruz-Escalona, V. H.
1998. Análisis trófico de la ictiofauna de la laguna de San Ignacio, B.C.S. M.Sc. thesis, 128 p. Instituto Politécnico Nacional, México.
- Efron, B., and R. Tibshirani.
1991. Statistical analysis in computer age. *Science* 253:390-395.
- Fischer, W., F. Krupp, C. Sommer, C. E. Carpenter, and V. H. Niem.
1995. Guía FAO para la identificación de especies para los fines de pesca. Pacífico centro-oriental. FAO II-III:647-1200.
- Garth, J. S.
1958. Brachyura of the Pacific coast of America; Oxyryncha: Majidae. *Allan Hancock Pacific Expeditions* 21(1-2):1-854.
- Gibson, K. N., and I. A. Ezzi.
1987. Feeding relationships of a demersal fish assemblage on the west coast of Scotland. *J. Fish Biol.* 31: 55-69.
- Gonzalez-Sansón, G., B. Aguilar-Palomino, J. Arciniega-Flores, R. García de Quevedo-Machain, E. Godínez-Domínguez, V. Landa-Jaime, J. Mariscal-Romero, J. E. Michel-Morfin, and M. Saucedo-Lozano.
1997. Variación espacial de la abundancia de la fauna de fondos blandos en la plataforma continental de Jalisco y Colima, México (Primavera 1995). *Cienc. Mar.* 23:93-110.
- Hamilton, L. C.
1991. Bootstrap programming. *Stata Tech. Bull.* 4:18-27.
- Hendrickx, M. E.
1996. Los camarones Penaeoidea bentónicos (Crustacea: Decapoda: Dendrobranchiata) del Pacífico mexicano, 147 p. CONABIO-Instituto de Ciencias del Mar y Limnología, Universidad Nacional Autónoma de México.
- Hendrickx, M. E., and J. Salgado-Barragan.
1991. Los estomatópodos (Crustacea: Hoplocarida) del Pacífico mexicano. *An. Inst. Cienc. Mar y Limnol. Univ. Nal. Autón. México, Publ. Esp.* 10, 200 p.
- Hespenheide, H. A.
1975. Prey characteristics and predator niche width. In *Ecology and evolution of communities* (M. L. Cody and J. M. Diamond, eds.), p. 158-180. Harvard Univ. Press., Boston, MA.
- Hughes, R. N.
1979. Optimal diets under the energy maximization premise: the effects of recognition time and learning. *Am. Nat.* 113:209-221.
- Hurlbert, S. H.
1978. The measurement of niche overlap and some relatives. *Ecology* 59:67-77.
1984. Pseudoreplication and the design of ecological field experiments. *Ecol. Monogr.* 54:187-211.
- Jordan, D. S., and B. W. Evermann.
1896-1900. The fishes of North and Middle America: a descriptive catalogue of the species of fish-like vertebrates found in the waters of North America, North of the Isthmus of Panama. *Bull. U.S. Nat. Mus.* 47(1-4):1-3313.
- Jubb, R. N., R. N. Hughes, and T. ap Rheinallt.
1983. Behavioral mechanisms of size-selection by crabs *Carcinus maenas* feeding on the mussels *Mytilus edulis*. *J. Exp. Mar. Biol. Ecol.* 66:81-87.
- Krebs, C. J.
1999. Ecological methodology, 620 p. Benjamin/Cummings, Menlo Park, CA.
- Labropoulou, M., and A. Eleftheriou.
1997. The foraging ecology of two pairs of congeneric demersal fish species: importance of morphological characteristics in prey selection. *J. Fish Biol.* 50:324-340.
- Levins, R.
1968. Evolution in changing environments: some theoretical explorations, 120 p. Princeton Univ. Press, Princeton, NJ.
- Lucena, F. M., T. Vaske Jr., J. R. Ellis, and C. M. O'Brien.
2000. Seasonal variation in the diets of bluefish, *Pomatomus saltatrix* (Pomatomidae) and striped weakfish, *Cynoscion gtuatucupo* (Sciaenidae) in southern Brazil: implications of food partitioning. *Environ. Biol. Fish.* 57:423-434.
- Mascaró, M., and R. Seed.
2001. Foraging behaviour of juvenile *Cynoscion maenas* (L.) and *Cancer pagurus* L. *Mar. Biol.* 139:1135-1145.
- Merriner, J. V.
1975. Food habits of the weakfish, *Cynoscion regalis*, in North Carolina waters. *Chesapeake Sci.* 16:74-76.
- Minello, T. J., and R. J. Zimmerman.
1984. Selection for brown shrimp, *Penaeus aztecus*, as prey by the spotted seatrout, *Cynoscion nebulosus*. *Contrib. Mar. Sci.* 27:159-167.
- Mueller, L. D., and L. Altenberg.
1985. Statistical inference on measures of niche overlap. *Ecology* 66:1204-1210.
- Peñáz-Rodríguez, E.
1996. Relaciones ecológicas de los peces ictiófagos demersales de la zona de pesca comercial de Alvarado, Veracruz. B.Sc. thesis, 84 p. Universidad Nacional Autónoma de México, México.
- Pinkas, L., M. S. Oliphant, and I. L. K. Iverson.
1971. Food habits of albacore, bluefin tuna and bonito in

- California waters. Calif. Dep. Fish Game, Fish Bull. 152:1-105.
- Rangeley, R. W., and M. L. H. Thomas.
1987. Predatory behavior of juvenile shore crab *Carcinus maenas*. J. Exp. Mar. Biol. Ecol. 108:191-197.
- Renkonen, O.
1938. Statistisch-okologische Untersuchungen über die terrestrische Käferwelt der finnischen Bruchmoore. Ann. Zool. Soc. Zool-Bot. Fenn. Vanamo 6:1-231.
- Rodriguez, C. L., S. Nojima, and T. Kikuchi.
1987. Mechanics of prey size preference in the gastropod *Neverita didyma* preying on the bivalve *Ruditapes philippinarium*. Mar. Ecol. Prog. Ser. 40:87-93.
- Rodriguez de la Cruz, M. C.
1987. Crustaceos Decapodos del Golfo de California. Secretaria de Pesca, Mexico 2:145-306
- Rosecchi, E., and Y. Nouaze.
1987. Comparaison de cinq indices alimentaires utilisés dans l'analyse des contenus stomacaux. Rev. Trav. Inst. Pêches Mar. Nantes 49:111-123.
- Schoener, T. W.
1970. Nonsynchronous spatial overlap of lizards in patchy habitats. Ecology 51:408-418.
1974. Resource partitioning in ecological communities. Science 185:27-39.
- Smith, C., and P. Reay.
1991. Cannibalism in teleost fish. Rev. Fish Biol. Fish. 1:41-64.
- Thomson, D. A., L. T. Findley, and A. N. Kerstitch.
2000. Reef fishes of the Sea of Cortez, 407 p. Univ. Texas Press, Austin, TX
- Tirasin, E. M., and T. Jørgensen.
1999. An evaluation of the precision of diet description. Mar. Ecol. Prog. Ser. 182:243-252.
- Werner, E. E.
1979. Niche partitioning by food size in fish communities. In Predator-prey systems in fisheries management (R. H. Stroud and H. Clepper, eds.), p 311-322. Sport Fishing Institute, Washington, DC.
- Zar, J. H.
1999. Biostatistical analysis, 663 p. Prentice Hall, Englewood Cliffs, NJ.

Using bone measurements to estimate the original sizes of bluefish (*Pomatomus saltatrix*) from digested remains

Anthony D. Wood

Box 200
Graduate School of Oceanography
University of Rhode Island Bay Campus
South Ferry Rd.
Narragansett, Rhode Island 02882
E-mail address: awood@gso.uri.edu

The ability to estimate the original size of an ingested prey item is an important step in understanding the community and population structure of piscivorous predators (Scharf et al., 1998). More specifically, knowledge of original prey size is essential for deriving important biological information, such as predator consumption rates, biomass of the prey consumed, and selectivity of a predator towards a specific size class of prey (Hansel et al., 1988; Scharf et al., 1997; Radke et al., 2000). To accurately assess the overall "top-down" pressure a predator may exert on prey community structure, prey size is crucial. However, such information is often difficult to collect in the field (Trippel and Beamish, 1987). Stomach-content analyses are the most common methods for examining the diets of piscivorous fish, but the prey items found are often thoroughly digested and sometimes unidentifiable. As a result, obtaining a direct measurement of prey items is frequently impossible.

Because of the problems of reconstructing original prey size directly from prey remains, numerous methods involving correlations between measurements of specific morphological features of the prey and prey size (length) have been devised. External body measures such as eye diameter, and caudal peduncle depth (Crane et al., 1987; Serafy et al., 1996; Scharf et al., 1997), as well as numerous internal measures such as pharyngeal arch length (Fickling and Lee, 1981; McIntyre and Ward, 1986; Radke et al., 2000), vertebral diameter (Pikhu and Pikhu, 1970; Feltham and Marquiss, 1989), and a variety of skeletal bones (Newsome, 1977; Hansel et al., 1988; Scharf et al., 1998) have been used to generate models for predicting original prey size.

The bluefish (*Pomatomus saltatrix*) is a voracious piscivore and is among the top predatory fish species in the western North Atlantic Ocean (Buckel et al., 1999). Bluefish are an important fish both commercially and recreationally, and over the past two decades stocks off the eastern coast of the United States have experienced a dramatic decline. From 1978 through 1996, the commercial landings and spawning stock biomass of bluefish declined by over 60% (Fahay et al.¹). A variety of mechanisms have been proposed to explain this dramatic decline, including intense predation by large apex predators. It is known that bluefish act as an important prey species for a number of apex predators in the North Atlantic, most notably the shortfin mako (*Isurus oxyrinchus*). Stillwell and Kohler (1982) sampled 399 makos from 1972–79 and found that bluefish made up 85% of the diet by volume. The mako diet has recently been reviewed and it appears that the incidence of bluefish in the diet has increased (assume 1 mL=1 g for flesh) to 94% of their diet by weight (Wood et al.²). Bluefish have also been found to be important in the diet of bluefin tuna (*Thunnus thynnus*) (Chase, 2002), swordfish (*Xiphias gladius*) (Stillwell and Kohler, 1985),

blue shark (*Prionace glauca*) (Kohler, 1989), and the thresher shark (*Alopias vulpinus*) (Kohler³).

The motivation for this study came from field sampling shortfin mako (*Isurus oxyrinchus*) stomach contents where it was observed that bluefish jaw bones and various other skull bones were often intact, even if the rest of the prey fish was digested. To generate accurate estimates of the original prey size a series of predictive equations was generated by regressing bluefish skull bone measurements with the fork length (FL) and total length (TL) of the fish. Five skull bones were chosen to obtain measurements for the relationships: the dentary, maxilla, premaxilla, opercle, and cleithrum (Fig. 1). These five bones were chosen because they are strong bones (with the exception of the opercle), covered by extensive musculature, and assumed to be resilient to digestion.

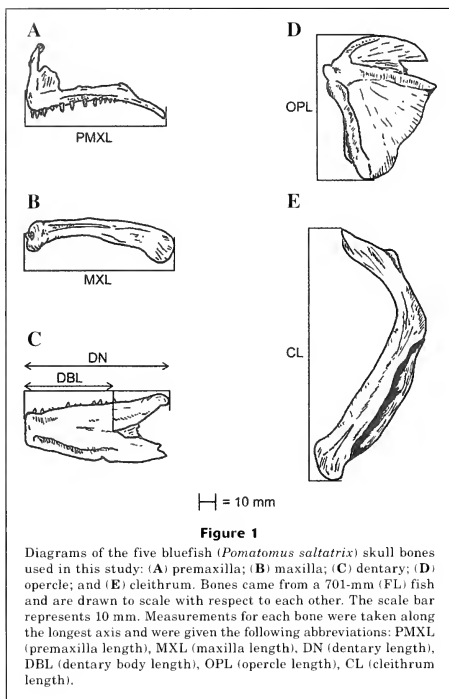
Materials and methods

During June–September of 2000 and 2001, bluefish were collected by rod and reel and by otter trawl in Narragansett Bay, RI, and at bluefish fishing tournaments along the northeast coast of the United States from Ocean

¹ Fahay, M. P., P. L. Berrien, D. L. Johnson, and W. W. Morse. 1999. Essential fish habitat source document: Bluefish, *Pomatomus saltatrix*, life history and habitat characteristics. NOAA Tech. Memo. NMFS-NE-144, 68 p. U.S. Department of Commerce, NOAA, NMFS-NEFSC, Woods Hole, MA.

² Wood, A. D., B. Wetherbee, N. E. Kohler, F. Juanes and C. Wilga. 2004. In prep. Predator prey interaction between the shortfin mako (*Isurus oxyrinchus*) and bluefish (*Pomatomus saltatrix*).

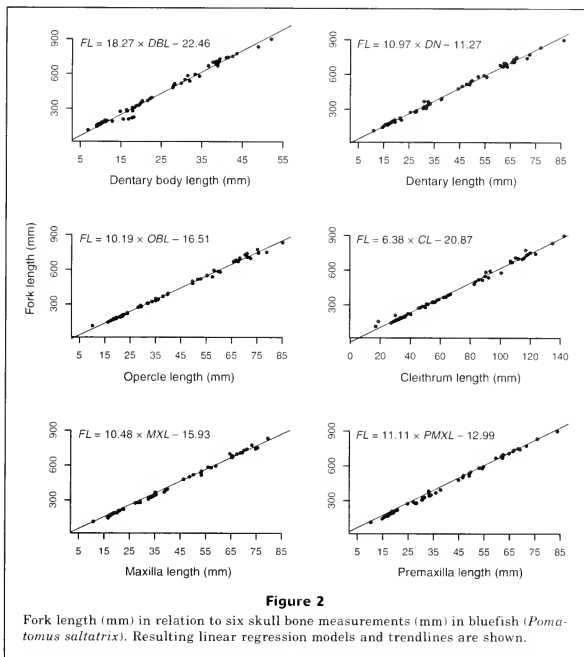
³ Kohler, N. E. 2001. Personal commun. NMFS Narragansett lab, 28 Tarzwell Drive, Narragansett, RI 02882.



City, MD, north to Bayshore, NY. Upon retrieval, the fork length (FL) and total length (TL) of each fish were measured to the closest mm. The heads of the bluefish were then removed by cutting approximately 5 cm behind the pectoral girdle, and all heads were immediately placed on ice. Samples were returned to the laboratory and kept in a cool room on ice until the selected bones could be extracted and measured (within 24 hours). Bones were extracted by immersing the bluefish heads in boiling water for a short period of time (between 30 and 180 seconds, depending on the size of the fish and on the amount of musculature around the bones). The dentary, maxilla, premaxilla, opercle, and cleithrum were dissected from the left side of each fish and measured to the nearest 0.1 mm by using 0–150 mm dial calipers. Measurements were taken linearly along the

longest axis of each bone and the following abbreviations were used to indicate lengths: DBL (dentary body length), DN (dentary length), OPL (opercle length), CL (cleithrum length), MXL (maxilla length), and PMXL (premaxilla length) (Fig. 1). In cases where left bones were damaged, or it was determined that an accurate measurement could not be retrieved, right-side bones were measured in place of the damaged bones.

Least squares regression analyses, which reveal the relationship of each of the bone measurements to FL and TL, were then conducted to generate predictive equations. The strength of each of the correlations was judged by both the r^2 values and by calculating the mean percent prediction error for each model, where the percent prediction error for a model (Sharf et al., 1997) is calculated by the following equation:



$$\frac{(\text{Observed} - \text{Predicted})}{(\text{Predicted})} \times 100.$$

To determine if any one bone or set of bones provided the best predictor equation, comprehensive models involving sets of bones were fitted in a stepwise linear algorithm by using the Akaike information criterion (AIC) as the criterion for model selection. Models were generated in both a forwards and backwards manner in order to confirm that the same model was returned in all cases.

Results

Fork length (FL) and total length (TL) measurements were taken from 58 bluefish ranging from 110 mm to 900 mm FL. The resulting regression equations correlating skull bone measurements to FL (Fig. 2) were highly significant ($P=0.005$ for the dentary correlation and

$P<0.001$ for the rest of the models). The r^2 values for the FL predictive equations ranged from 0.988 to 0.997, and the mean percent predictive errors ranged from -0.03 to 1.19 (Table 1). Similarly, all of the resulting models correlating the bone measurements to total length (Fig. 3) were highly significant ($P<0.001$, r^2 values ranging from 0.987 to 0.996, and mean percent predictive errors ranging from -0.11 to 1.07 [Table 1]).

Bones were ranked from best predictor to worst predictor for both the FL and TL models by using the Akaike information criterion (AIC). In both cases the premaxilla was ranked the best predictor bone, followed by the maxilla, the opercle, the dentary, the cleithrum, and finally dentary body length. The bone measurements included in the stepwise multiple regression model for predicting fork length were PMXL, OPL, and DN (Table 2). In the best predictor model for total length, PMXL, OPL, DN and CL were included (Table 2).

Table 1

Resulting predictive equations of fork and total length in relation to several skull bone measures with corresponding coefficient of determination (r^2) and P -values, and mean percent predictive errors (%PE) for each model.

Bone	Fork length	r^2	P -value	%PE
Dentary body length (DBL)	$FL = 18.27(DBL) - 22.46$	0.988	<0.001	0.54
Dentary (DN)	$FL = 10.97(DN) - 11.27$	0.996	0.005	-0.03
Opercle (OPL)	$FL = 10.19(OPL) - 16.51$	0.997	<0.001	0.28
Cleithrum (CL)	$FL = 6.38(CL) - 20.87$	0.993	<0.001	1.19
Maxilla (MXL)	$FL = 10.48(MXL) - 15.93$	0.997	<0.001	0.31
Premaxilla (PMXL)	$FL = 11.11(PMXL) - 12.99$	0.997	<0.001	0.26
Bone	Total length	r^2	P -value	%PE
Dentary body length (DBL)	$TL = 20.20(DBL) - 27.69$	0.987	<0.001	0.46
Dentary (DN)	$TL = 12.13(DN) - 15.42$	0.996	<0.001	-0.11
Opercle (OPL)	$TL = 11.27(OPL) - 21.13$	0.996	<0.001	0.15
Cleithrum (CL)	$TL = 7.05(CL) - 26.13$	0.994	<0.001	1.07
Maxilla (MXL)	$TL = 11.59(MXL) - 20.43$	0.996	<0.001	0.19
Premaxilla (PMXL)	$TL = 12.28(PMXL) - 17.20$	0.996	<0.001	0.14

Table 2

Independent variables included in the stepwise linear regression models used to estimate original bluefish fork length and total length.

	Variables included in forward stepwise regression model	Variables included in backward stepwise regression model
Fork length	PMXL, OPL, DN	PMXL, OPL, DN
Total length	PMXL, OPL, DN, CL	PMXL, OPL, DN, CL

Discussion

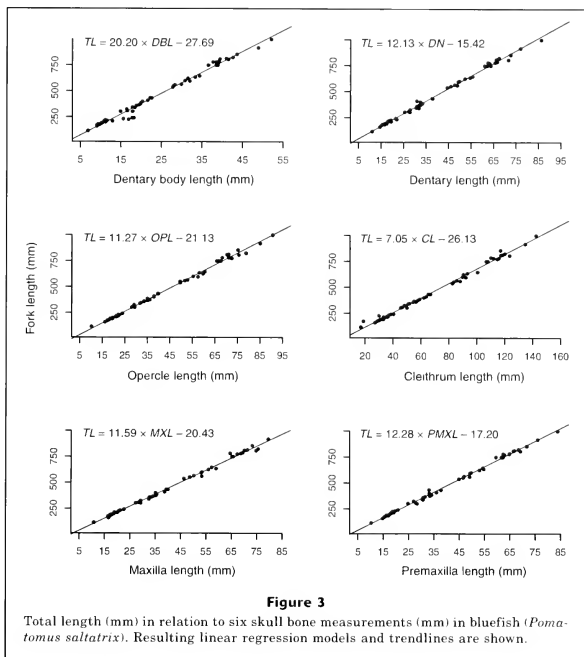
This study revealed that measurements of five skull bones can be used as accurate predictors of original fork length and total length of bluefish. Although the methods of other studies were incorporated in this study, the information is the first of its kind for bluefish and may serve as a tool for the future study of this species in the North Atlantic.

In recent years there has been growing concern over the stability of the bluefish stock and an increased effort to gather information on the possible mechanisms affecting bluefish abundance and distribution in the western North Atlantic.⁴ One of the proposed mecha-

nisms that could be adversely influencing the recovery of bluefish is top-down pressure by a number of apex predators in the North Atlantic. Although indiscriminant predation on bluefish may not be a significant pressure on the stock, size selective predation can dramatically alter the structure of the prey community (McIntyre and Ward, 1986; Trippel and Beamish, 1987; Sharf et al., 1997).

In order to study the consumption rates of key predators in an ecosystem it is necessary to gather information on the sizes of the prey being consumed (Elliot and Persson, 1978; Sharf et al., 1998). However, it is often difficult to estimate the original size of a prey item from stomach content data because of the complications caused by digestion. Erosion of the prey bones from digestive juices can lead to measurement error or bias when prey sizes are back-calculated from digested parts (Sharf et al., 1998). Although bias from digestion is a concern that should be addressed in studies, internal bones and hard parts of fishes have been shown to be excellent predictors of original prey size (Trippel and

⁴ In 1997 Rutgers University and the NMFS organized a workshop to study the factors that could be contributing to the depressed state of the bluefish stock. A similar concern was expressed by Congress at this time, and the Rutgers and NMFS workshop led to a request for proposals for bluefish-related research in 1998, 1999, and 2000.



Beamish, 1987; Hansel, 1988, Sharf et al., 1998). In addition, the bones used in the present study are strong bones (with the exception of the opercle, that are liable to resist digestive erosion.

All the relationships generated in the present study yielded very accurate predictions of original prey size, but the jaw bones are of special interest. Bluefish can be classified as predators that exhibit a biting behavior during predation. Fish that show this type of predation behavior have very heavy, robust jaw bones (Norton, 1995). The jaw bones (maxilla, premaxilla, and dentary) of bluefish are both easily identifiable and likely resistant to digestion, and when combined with the adequacy with which original size can be determined from these bones (based on AIC rankings and %PE), they are the best option for researchers interested in back-calculating original bluefish sizes.

The results of this study provide a means to further analyze the stomach contents of bluefish predators beyond identifying, and quantifying prey items.

The usefulness of this type of data has been shown repeatedly for a number of species (McIntyre and Ward, 1986; Feltham and Marquiss, 1989; Serafy et al., 1996; Sharf et al., 1997; Sharf et al., 1998). The ability to back-calculate the original size of a prey leads to the enhancement of diet studies and allows for more accurate estimates of predator consumption rates. The lack of this kind of data and correlations for many key prey species in the Atlantic and elsewhere is surprising.

Acknowledgments

Funding for this study was provided by the Bluefish-Striped Bass Dynamics Research Program at Rutgers University in cooperation with the National Marine Fisheries Service (grant NA97FE0363). I am indebted to the numerous fishing tournament directors, as well as the fishermen at the tournaments for allowing me to collect many of the bluefish needed for this study. I am

also especially grateful to Abby McLean for her help with the exhausting task of measuring bones. Finally, I wish to thank Francis Juanes for encouraging me to pursue and publish this study and Jeremy Collie and two anonymous reviewers for comments that helped to improve this manuscript.

Literature cited

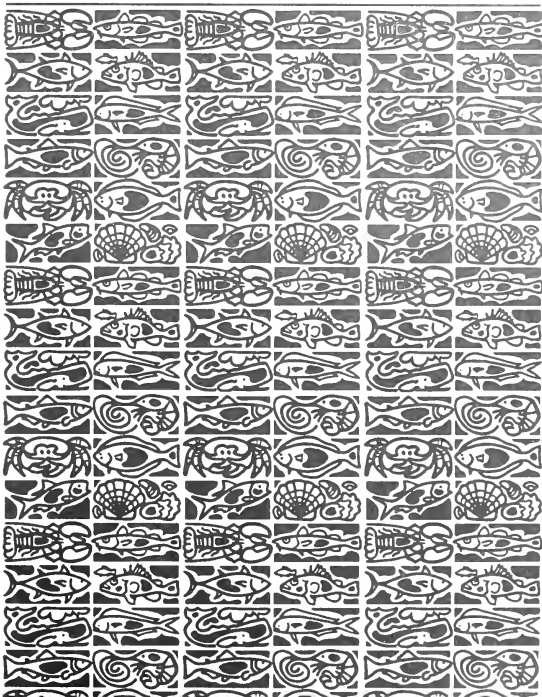
- Buckel, J. A., M. J. Fogarty, and D. O. Conover.
1999. Foraging habits of bluefish, *Pomatomus saltatrix*, on the U.S. east coast continental shelf. *Fish. Bull.* 97:758-775.
- Chase, B. C.
2002. Differences in diet of Atlantic bluefin tuna (*Thunnus thynnus*) at five seasonal feeding grounds on the New England continental shelf. *Fish. Bull.* 100:168-180.
- Crane, S. A., J. M. Fenaughty, and R. W. Gauldie.
1987. The relationship between eye diameter and fork length in the spiny oreo dory, *Allocyttus sp.* *N.Z.J. Mar. Freshw. Res.* 21:641-642.
- Elliott, J. M., and L. Persson.
1978. The estimation of daily rates of food consumption for fish. *J. Anim. Ecol.* 47:977-991.
- Feltham, M. J., and M. Marquiss.
1989. The use of first vertebrae in separating, and estimating the size of, trout (*Salmo trutta*) and salmon (*Salmo salar*) in bone remains. *J. Zool.* 219:113-122.
- Fickling, N. J., and R. L. G. Lee.
1981. Further aids to the reconstruction of digested prey lengths. *Fish Manage.* 12:107-110.
- Hansel, H. C., S. D. Duke, P. T. Lofy, and G. A. Gray.
1988. Use of diagnostic bones to identify and estimate original lengths of ingested prey fishes. *Trans. Am. Fish. Soc.* 117:55-62.
- Kohler, N. E.
1989. Aspects of the feeding ecology of the blue shark, *Prionace glauca*, in the western North Atlantic. *Diss. Abst. Int. Pt. B-Sci. & Eng.* 49:1-179.
- McIntyre, D. B., and F. J. Ward.
1986. Estimating fork lengths of fathead minnows, *Pimephales promelas*, from measurement of pharyngeal arches. *Can. J. Fish. Aquat. Sci.* 43:1294-1297.
- Newsome, G. E.
1977. Use of opercular bones to identify and estimate lengths of prey consumed by piscivores. *Can. J. Zool.* 55:733-736.
- Norton, S. F.
1995. A functional approach to ecomorphological patterns of feeding in cottid fishes. *Environ. Biol. Fishes* 44:61-78.
- Pikhu, E. Kh., and E. R. Pikhu.
1970. Reconstruction of the size of fishes swallowed by predators from fragments of their vertebral column. *J. Ichthyol. (USSR)*, vol. 10:706-709.
- Radke, R. J., T. Petzoldt, and K. Wolter.
2000. Suitability of pharyngeal bone measures commonly used for reconstruction of prey fish length. *J. Fish Biol.* 57:961-967.
- Scharf, F. S., J. A. Buckel, F. Juanes, and D. O. O'Connor.
1997. Estimating piscine prey size from partial remains: Testing for shifts in foraging mode by juvenile bluefish. *Environ. Biol. Fishes* 49:377-388.
- Scharf, F. S., R. M. Yetter, A. P. Summers, and F. Juanes.
1998. Enhancing diet analyses of piscivorous fishes in the northwest Atlantic through identification and reconstruction of original prey sizes from ingested remains. *Fish. Bull.* 96:575-588.
- Serafy, J. E., C. M. Schmitz, T. R. Capo, M. E. Clarke, and J. S. Ault.
1996. Total length estimation of red drum from head dimensions. *Prog. Fish-Cult.* 58:289-290.
- Stillwell, C. E., and N. E. Kohler.
1982. Food, Feeding Habits, and Estimates of Daily Ration of the Shortfin Mako (*Isurus oxyrinchus*) in the Northwest Atlantic. *Can. J. Fish. Aquat. Sci.* 39:407-414.
1985. Food and feeding ecology of the swordfish *Xiphus gladius* in the western North Atlantic Ocean with estimates of daily ration. *Mar. Ecol. Prog. Ser.* 22:239-247.
- Trippel, E. A., and F. W. H. Beamish.
1987. Characterizing piscivory from ingested remains. *Trans. Am. Fish. Soc.* 116:773-776.



U.S. Department
of Commerce

Volume 103
Number 3
July 2005

Fishery Bulletin



**U.S. Department
of Commerce**

Carlos M. Gutierrez
Secretary

**National Oceanic
and Atmospheric
Administration**

Vice Admiral
Conrad C. Lautenbacher Jr.,
USN (ret.)

Under Secretary for
Oceans and Atmosphere

**National Marine
Fisheries Service**

William T. Hogarth
Assistant Administrator
for Fisheries



The *Fishery Bulletin* (ISSN 0090-0656) is published quarterly by the Scientific Publications Office, National Marine Fisheries Service, NOAA, 7600 Sand Point Way NE, BIN C15700, Seattle, WA 98115-0070. Periodicals postage is paid at Seattle, WA, and at additional mailing offices. POSTMASTER: Send address changes for subscriptions to *Fishery Bulletin*, Superintendent of Documents, Attn: Chief, Mail List Branch, Mail Stop SSOM, Washington, DC 20402-9373.

Although the contents of this publication have not been copyrighted and may be reprinted entirely, reference to source is appreciated.

The Secretary of Commerce has determined that the publication of this periodical is necessary according to law for the transaction of public business of this Department. Use of funds for printing of this periodical has been approved by the Director of the Office of Management and Budget.

For sale by the Superintendent of Documents, U.S. Government Printing Office, Washington, DC 20402. Subscription price per year: \$55.00 domestic and \$68.75 foreign. Cost per single issue: \$28.00 domestic and \$35.00 foreign. See back for order form.

Fishery Bulletin

Scientific Editor
Norman Bartoo, Ph.D.

Associate Editor
Sarah Shoffler

National Marine Fisheries Service, NOAA
8604 La Jolla Shores Drive
La Jolla, California 92037

Managing Editor
Sharyn Matriotti

National Marine Fisheries Service
Scientific Publications Office
7600 Sand Point Way NE, BIN C15700
Seattle, Washington 98115-0070

Editorial Committee

Harlyn O. Halvorson, Ph.D.	University of Massachusetts, Boston
Ronald W. Hardy, Ph.D.	University of Idaho, Hagerman
Richard D. Methot, Ph.D.	National Marine Fisheries Service
Theodore W. Pietsch, Ph.D.	University of Washington, Seattle
Joseph E. Powers, Ph.D.	National Marine Fisheries Service
Harald Rosenthal, Ph.D.	Universität Kiel, Germany
Fredric M. Serchuk, Ph.D.	National Marine Fisheries Service
George Watters, Ph.D.	National Marine Fisheries Service

***Fishery Bulletin* web site: www.fishbull.noaa.gov**

The *Fishery Bulletin* carries original research reports and technical notes on investigations in fishery science, engineering, and economics. It began as the Bulletin of the United States Fish Commission in 1881; it became the Bulletin of the Bureau of Fisheries in 1904 and the *Fishery Bulletin* of the Fish and Wildlife Service in 1941. Separates were issued as documents through volume 46; the last document was No. 1103. Beginning with volume 47 in 1931 and continuing through volume 62 in 1963, each separate appeared as a numbered bulletin. A new system began in 1963 with volume 63 in which papers are bound together in a single issue of the bulletin. Beginning with volume 70, number 1, January 1972, the *Fishery Bulletin* became a periodical, issued quarterly. In this form, it is available by subscription from the Superintendent of Documents, U.S. Government Printing Office, Washington, DC 20402. It is also available free in limited numbers to libraries, research institutions, State and Federal agencies, and in exchange for other scientific publications.

Fishery Bulletin

Contents

Articles

- 469–488 Dressel, Sherri C., and Brenda L. Norcross
Using poststratification to improve abundance estimates from multispecies surveys: a study of juvenile flatfishes
- 489–500 Francis, Malcolm P., and Clinton Duffy
Length at maturity in three pelagic sharks (*Lamna nasus*, *Isurus oxyrinchus*, and *Prionace glauca*) from New Zealand
- 501–515 Fritz, Lowell W., and Eric S. Brown
Survey- and fishery-derived estimates of Pacific cod (*Gadus macrocephalus*) biomass: implications for strategies to reduce interactions between groundfish fisheries and Steller sea lions (*Eumetopias jubatus*)
- 516–523 Greig, Thomas W., M. Katherine Moore, Cheryl M. Woodley, and Joseph M. Quattro
Mitochondrial gene sequences useful for species identification of western North Atlantic Ocean sharks
- 524–535 Hawkins, Sharon L., Jonathan Heifetz, Christine M. Kondzela, John E. Pohl, Richard L. Wilmot, Oleg N. Katugin, and Vladimir N. Tuponogov
Genetic variation of rougheye rockfish (*Sebastes aleutianus*) and shortraker rockfish (*S. borealis*) inferred from allozymes
- 536–543 Sulikowski, James A., Jeff Kneebone, Scott Elzey, Joe Jurek, Patrick D. Danley, W. Huntingt Howell, and Paul C. W. Tsang
The reproductive cycle of the thorny skate (*Amblyraja radiata*) in the western Gulf of Maine

The conclusions and opinions expressed in *Fishery Bulletin* are solely those of the authors and do not represent the official position of the National Marine Fisheries Service (NMFS) or any other agency or institution.

The National Marine Fisheries Service (NMFS) does not approve, recommend, or endorse any proprietary product or proprietary material mentioned in this publication. No reference shall be made to NMFS, or to this publication furnished by NMFS, in any advertising or sales promotion which would indicate or imply that NMFS approves, recommends, or endorses any proprietary product or proprietary material mentioned herein, or which has as its purpose an intent to cause directly or indirectly the advertised product to be used or purchased because of this NMFS publication.

Notes

- 544–552 Fey, Dariusz P., Gretchen E. Bath Martin, James A. Morris, and Jonathan Hare
Effect of type of otolith and preparation technique on age estimation of larval and juvenile spot (*Leiostomus xanthurus*)
- 553–558 Piner, Kevin R., Melissa A. Haltuch, and John R. Wallace
Preliminary use of oxygen stable isotopes and the 1983 El Niño to assess the accuracy of aging black rockfish (*Sebastes melanops*)
- 559 Subscription form

Abstract—Population assessments seldom incorporate habitat information or use previously observed distributions of fish density. Because habitat affects the spatial distribution of fish density and overall abundance, the use of habitat information and previous estimates of fish density can produce more precise and less biased population estimates. In this study, we describe how poststratification can be applied as an unbiased estimator to data sets that were collected under a probability sampling design, typical of many multispecies trawl surveys. With data from a multispecies survey of juvenile flatfish, we show how poststratification can be applied to a data set that was not collected under a probability sampling design, where both the precision and the bias are unknown. For each of four species, three estimates of total abundance were compared: 1) unstratified; 2) poststratified by habitat; and 3) poststratified by habitat and fish density (high fish density and low fish density) in nearby years. Poststratification by habitat gave more precise and (or) less design-biased estimates than an unstratified estimator for all species in all years. Poststratification by habitat and fish density produced the most precise and representative estimates when the sample size in the high fish-density and low fish-density strata were sufficient (in this study, $n \geq 20$ in the high fish-density stratum, $n \geq 9$ in the low fish-density stratum). Because of the complexities of statistically testing the annual stratified data, we compared three indices of abundance for determining statistically significant changes in annual abundance. Each of the indices closely approximated the annual differences of the poststratified estimates. Selection of the most appropriate index was dependent upon the species' density distribution within habitat and the sample size in the different habitat areas. The methods used in this study are particularly useful for estimating individual species abundance from multispecies surveys and for retrospective studies.

Manuscript submitted 28 December 2001 to the Scientific Editor's Office.

Manuscript approved for publication 31 March 2005 by the Scientific Editor.
Fish. Bull. 103:469–488 (2005).

Using poststratification to improve abundance estimates from multispecies surveys: a study of juvenile flatfishes

Sherri C. Dressel

Brenda L. Norcross

Institute of Marine Science
School of Fisheries and Ocean Sciences
University of Alaska Fairbanks
245 O'Neill Building
Fairbanks, Alaska 99775-7220

Present Address (for S. C. Dressel): Alaska Department of Fish and Game
Commercial Fisheries Division
802 3rd Street
P.O. Box 240020
Douglas, Alaska 99824-0020

E-mail address (for S. C. Dressel): sherr_dressel@fishgame.state.ak.us

Scientists must be able to assess population abundance with a high degree of confidence to achieve the goals of fishery management (Quinn, 1985). To do this, survey designs and estimation methods that minimize the variance in estimates of abundance are needed. Recently, the National Research Council (NRC, 2000) recommended incorporating habitat information and commercial fisheries data in population assessments. Both of these data may result in lower variances in estimates of abundance.

Habitat type and habitat quality are becoming more widely recognized as primary determinants for the distribution and survival of marine fish species (Murawski and Finn, 1988; Gadomski and Caddell, 1991; Reichert and van der Veer, 1991; Norcross et al., 1999). Until recently, however, few studies have been directed toward defining fish habitat or using habitat associations to help decrease the variability in abundance estimation (Scott, 1995). In response to the growing recognition of the importance of habitat, the Magnuson-Stevens Fishery Conservation and Management Act was amended in 1996 (Public Law 104–297) so that the National Marine Fisheries Service (NMFS) and regional fishery management councils must describe and identify essential

fish habitat (EFH) for managed species. Similarly, a recent report from the NRC calls for methods that link environmental data to stock assessments (NRC, 2000).

Poststratification can be used in a number of different ways to address the NRC recommendations. Although poststratification is not a new statistical method, it is one that is not commonly used for estimating groundfish population abundance and can be used to meet these newly defined challenges. In contrast to a stratified sampling design, poststratification is a method that allocates samples to strata after they have been collected. As a result, habitat data collected during a survey can be used for stratification. When poststratification is applied to data that have been collected under a simple random sampling design, the poststratification estimator is unbiased and may produce more precise estimates than those from a simple random sampling estimator. Poststratified estimates will be nearly as precise as stratified sampling with proportional allocation, in which the sample sizes in each stratum are proportional to stratum sizes, if stratum sample sizes are large ($n > 20$) and errors in estimates of strata areas are negligible (Cochran, 1977; Pollock et al., 1994;

Scheaffer et al., 1996). If poststratification is applied to data from a multispecies survey, 1) abundance data for each species can be poststratified with different habitat variables or 2) abundance data for every species can be poststratified with the same variables, but different stratum boundaries can be used for each species.

Many large-scale multispecies groundfish surveys are conducted by using a stratified random sampling design (Azarovitz, 1981; Halliday and Koeller, 1981; Pitt et al., 1981; Martin¹; Weinberg et al.²). Depth, distance from or along shore, latitude, distance along depth contours, or broad geographic features (such as bays, capes, banks, gullies, and slopes) are used as stratum boundaries in trawl surveys because they have been shown to be related to species distributions. These factors are fixed spatially, allowing samples to be allocated to strata prior to sampling. The same boundaries are used for all species, and boundaries generally remain the same over years.

When conducting a multispecies survey with a stratified random sampling design, optimal stratification for one species may not be optimal for others (Koeller, 1981; NRC, 2000). Because the placement of strata boundaries is critical for precise stratified estimates (Cochran, 1977), use of a stratified sampling design for a multispecies survey may result in only small gains in precision for some or all species. Poststratification is possible for data that have been collected under a stratified design. It can be used to stratify data more finely for individual species. Under stratified random sampling, a simple random sample is taken in each stratum. Thus, data within each stratum can be poststratified separately with additional variables and the abundance estimates from each of the strata can be summed. The resultant estimator is unbiased and likely will be more precise than that of the original stratified design if sample sizes in poststratified strata are large enough.

Often, researchers need to estimate abundance from data sets that were not recorded under a probability sampling design (a design in which randomness is built into the survey design, such as simple random sampling or stratified random sampling). Finances and logistics, for example, may make it impossible to collect data under a probability sampling design, researchers may want to estimate species abundance from commercial fisheries or other nonsurvey data, or previously collected data sets that were not recorded under a probability

sampling design may be used for retrospective studies. In this article, we refer to data collection without a probability sampling design as "haphazard sampling." The use of haphazardly collected data for estimating abundance is undesirable because they cannot be evaluated by the theorems of probability theory (Krebs, 1989). Although undesirable, it is often necessary to analyze haphazardly collected data and effective methods are needed to do so.

Poststratification can be applied to data that were not collected with a probability sampling design. When poststratification is applied to data not collected under a probability sampling design, the poststratification estimator, a design-based estimator, may be biased. When analyzing such data, it is important both to maximize the precision and to minimize the bias. Poststratification has been applied to nonprobability samples in other studies to increase the precision (Hall and Boyer, 1988) and decrease the bias of estimators (Buckland and Anganuzzi, 1988; Hall and Boyer, 1988; Anganuzzi and Buckland, 1989).

Poststratification can be useful, but has some drawbacks. With poststratification, sample sizes within strata are random variables—which are an additional source of variability over that of a stratified sampling variance estimator (Thompson, 1992; Scheaffer et al., 1996). The variance of a poststratified estimator can be estimated by using standard stratified sampling variance equations and by incorporating an additional approximate term to account for the random sample sizes present with poststratification (Scheaffer et al., 1996). Alternatively, the variance of a poststratified estimator can be estimated by conditioning on sample sizes and by applying the standard stratified sampling variance equation (Thompson, 1992). For accurate poststratification estimates, the proportion of total possible samples in each stratum (for this study the proportion of the total survey area included in each stratum) must be known or approximated closely enough that the error in the approximation is negligible (Cochran, 1977). Error in estimates of stratum sizes causes bias in poststratified estimates of abundance. Because error in the estimation of stratum size is unaccounted for in the estimated variance of poststratified estimates, the estimated variances may be underestimates of the true error (Cochran, 1977).

This study had two goals. The first goal was to evaluate the benefits and drawbacks of using poststratification to incorporate habitat and fish-density information into estimates of abundance from multispecies survey data that were not collected under a probability sampling design. To achieve this goal, this study compared three estimates of total abundance and variance (unstratified, poststratified by habitat, poststratified by habitat and estimates of fish density in neighboring years) for each of four species. The comparison was made to determine whether poststratification of haphazardly sampled data with habitat and fish-density information increases the precision and helps account for possible bias in abundance estimates.

¹ Martin, M. H. 1997. Data report: 1996 Gulf of Alaska bottom trawl survey. NOAA Tech. Memo. NMFS-AFSC-82, 235 p. National Technical Information Service, U.S. Department of Commerce, 5285 Port Royal Road, Springfield, Virginia 22161.

² Weinberg, K. L., M. E. Wilkins, R. R. Lauth, and P. A. Raymore Jr. 1994. The 1989 Pacific west coast bottom trawl survey of groundfish resources: Estimates of distribution, abundance, and length and age composition. NOAA Tech. Memo. NMFS-AFSC-33, 168 p., plus appendices. National Technical Information Service, U.S. Department of Commerce, 5285 Port Royal Road, Springfield, Virginia 22161.

Because this study is an observational study with haphazard sampling, the precision and bias cannot be directly assessed. Instead, we estimated and compared the precision by using unstratified and poststratified estimators. We qualitatively estimated the relative amount of design bias (i.e., how representative the estimates are) with the use of habitat. In previous studies (Norcross et al., 1995; 1997; 1999), depth and sediment were identified as habitat characteristics closely associated with the distribution of the four species in this study. From depth, sediment, and fish abundance data collected in this study we were able to identify ranges of habitat characteristics associated with areas of high, low, and no fish density. By estimating the proportion of area (km^2) in the study area characterized by the ranges of depth and sediment, it was possible to estimate the proportion of the survey area with high, low, and no fish density. Because samples in our study were not randomly allocated, the probability of selection was not equal among all samples in the survey area. The resulting numbers of samples taken in areas of high, low, and no fish density were not in proportion to the size (km^2) of those areas as it would have been with repeated simple random sampling. Therefore, by comparing the relative size of high, low and no fish-density areas in the survey area with the relative number of samples in those areas, we made qualitative estimates of the design bias associated with the estimators. Although an assessment of the relative amount of design bias made in this way is only an approximation, it is helpful when using haphazardly collected data in order to provide some indication of the amount of design bias based on the disproportion of samples in an area to the size of that area.

Because of the complexities of statistically testing the annual stratified data, the second goal of our study was to develop indices of abundance that closely approximated the annual differences of poststratified estimates and that could easily be tested for statistically significant changes between years. To achieve the second objective, three indices of annual relative abundance were constructed and compared with respect to their estimated relative precision and design bias: one from all sites in the survey area, one from all sites within the species' habitat, and one from all sites within an area of high fish density within the species' habitat.

The data for this study were obtained from six years of juvenile groundfish surveys conducted in Kalsin Bay and Middle Bay, Kodiak Island, Alaska. The four species studied were age-0 rock sole (*Lepidopsetta* spp.), age-1 yellowfin sole (*Pleuronectes asper*), age-0 Pacific halibut (*Hippoglossus stenolepis*), and age-0 flathead sole (*Hippoglossoides elassodon*). The survey data were collected during the six-year survey under three different survey designs, none of which were strictly randomized, but each involved some degree of haphazard

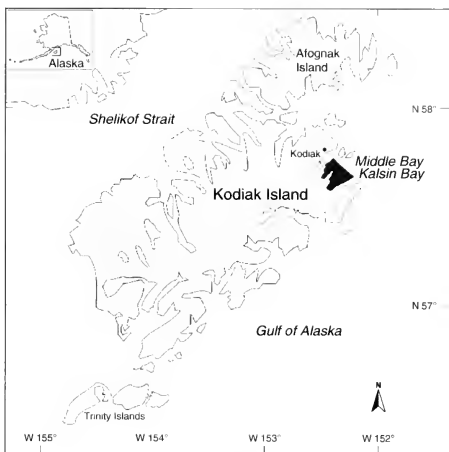


Figure 1

Study area (in black) in Middle and Kalsin Bays, Kodiak Island, Alaska.

sampling due to weather, sediment structure, and other logistical restrictions for beam trawling in small bays off the Gulf of Alaska (Norcross et al.³). Although many trawl survey data sets to which these methods could be applied are collected under a probability sampling design where the estimator is unbiased, the haphazardly collected data set used in our study was chosen to show how poststratification can be applied when both the precision and the bias of the estimator are unknown.

Methods

Sampling

Middle and Kalsin Bays are part of Chiniak Bay, 10 nmi south of the town of Kodiak, Alaska. The total size of the study area, 87 km^2 , included the combined areas of both bays and the areas directly outside the mouths of the bays (Fig. 1). Middle Bay is 8 km long and has depths of 50 m at the mouth of the bay and an area of 21 km^2 . Kalsin Bay is 8 km long, has depths greater than 100 m

³ Norcross, B. L., B. A. Holladay, A. A. Abookire, and S. C. Dressel. 1998. Defining habitats for juvenile groundfishes in Southcentral Alaska with emphasis on flatfishes. Vol. 1, Final Study Report, OCS Study MMS 97-0046, 131 p. Coastal Marine Institute, Univ. Alaska Fairbanks, Fairbanks, AK 99775.

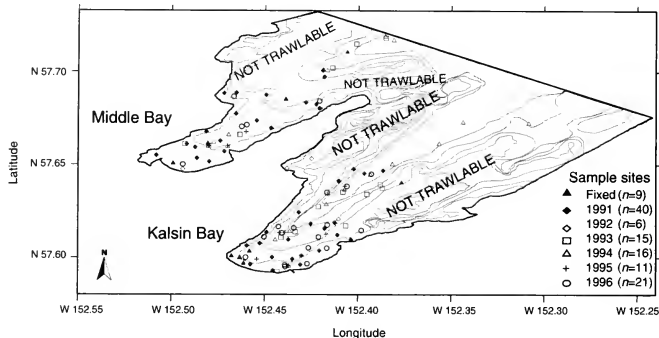


Figure 2

Kalsin and Middle Bay sample sites (1991–96) and bathymetry. Fixed (sampled every year) sites are noted.

at the mouth of the bay, and encompasses an area of 34 km². Rocky cliffs and islands surround the mouths of the bays, and rocks in the sediment made several areas untrawlable (Fig. 2). Although trawling was not conducted in these areas, depth and sediment data were collected. In this analysis, untrawlable areas were still considered possible flatfish habitat and were included in the measurements of the size of the total study area.

Annual cruises were conducted in Middle and Kalsin Bays for two weeks in August from 1991 to 1996. Juvenile flatfish were collected by using 3.05 and 3.66 m plumb-staff beam trawls (Gunderson and Ellis, 1986). Trawl nets were made of 7-mm square net mesh and had a 4-mm codend liner that retained flatfish as small as 11 mm. Sampling methods were consistent for all six years (Norcross et al., 1995; Norcross et al.³). Collections at each sample site included a tow of 10 minutes or less, a vertical CTD (conductivity, temperature and depth) cast, and a sediment grab (0.06-m³ Ponar grab). The sampling area of each tow was determined by the width of the beam trawl, which was 0.74 of the beam length (Gunderson and Ellis, 1986), and distance towed was based on global positioning system (GPS) coordinates. Fish were identified to the lowest possible taxon and measured to the nearest millimeter total length. At the time of collections, all rock sole were identified as *Pleuronectes bilineatus*. Following Orr and Matarese's (2000) revision of the genus, we refer to these fishes as *Lepidopsetta* spp. in this article because both species, *L. bilineata* and *L. polyxystra*, were identified in the study area during 1996 sampling. Fish ages were determined by length-frequency analysis. Fish catch-per-unit-of-effort (CPUE) values were standardized to a 1000-m² tow area.

Sampling designs varied from year to year (Norcross et al.³). Extensive exploratory sampling was conducted

from 1991 through 1994 to describe juvenile flatfish distributions in relation to habitat characteristics (Norcross et al., 1995; 1997). The goal in these years was to sample over the widest range of areas and habitat characteristics possible within the depth, sediment, weather, and logistical constraints. In 1995 and 1996, sampling was stratified by depth and percent sand in sediment. The sample allocation and the number of strata differed in 1995 and 1996 (Norcross et al.³). Because of logistical constraints, samples were not randomly allocated within each stratum. Within these sampling designs, nine fixed sites were chosen, each with different depth and sediment combinations and with high abundances of one of the four species. Each of the nine fixed sites was sampled at least once in each of the six years. For this study, survey data in each year were treated as unstratified samples that were not collected under a probability sampling design.

Analysis

Poststratification Habitat preferences of juvenile flatfishes, as defined by depth and sediment variables, have been identified as affecting the distribution and abundance of juvenile flatfish around Kodiak Island (Norcross et al., 1995; 1997; 1999; Mueter and Norcross, 1999) and elsewhere (Pearcy, 1978; Tanda, 1990; Burke et al., 1991; Rogers, 1992; Walsh, 1992). Four areas were defined for use in estimating total and relative abundance: habitat, nonhabitat, high fish-density (HFD) and low fish-density (LFD) areas. Percent sand was used as a continuous variable of sediment type. Suitable habitat (habitat area) was defined for each species as ranges of depth and percent sand in which the species was caught during one or more

of the six sampling years. Unsuitable habitat (nonhabitat area) was defined for each species as ranges of depth and percent sand in which the species was never caught. Within the habitat area, the area of high fish density for each year was defined as ranges of depth and percent sand associated with CPUEs in the 75th-100th percentile of nonzero catches in the five other years. The area of low fish density was defined as the remaining habitat area not incorporated in the HFD area.

In order for the poststratification method to estimate abundance accurately (high precision and low bias), the size of each stratum must be known or closely approximated (Cochran, 1977; Scheaffer et al., 1996). When using habitat variables to determine stratum sizes, the accuracy of stratum sizes defined by the boundaries is heavily dependent upon the number and distribution of habitat variable measurements. For our study, 243 depth and percent sand measurements collected over the six years at trawl locations were used to determine stratum boundaries. The ranges of depth and percent sand that defined the four areas for each species were contoured over the study area by using a minimum curvature algorithm (Surfer, 1995). The size of each stratum in relation to the size of the entire study area was then visually estimated to the nearest square kilometer. Although not used in our study, a digital representation of the size of each stratum and the size of the study area is recommended to produce more precise estimates.

To assess the advantages and disadvantages of using poststratification to estimate abundance, three estimates of total abundance were calculated and compared for each species in each year. An unstratified estimate of total abundance was calculated from samples across the entire survey area, with no differentiation with regard to habitat. The unstratified estimate of total abundance was calculated with the standard simple random sampling equation

$$\hat{\tau} = N\bar{y},$$

where $\hat{\tau}$ = the estimated population total;

N = the total number of possible samples in the survey area; and

\bar{y} = the mean CPUE of all sites sampled in a year.

The estimated variance for the unstratified estimator was calculated as

$$\hat{V}(\hat{\tau}) = N^2 \left(\frac{s^2}{n} \right) \left(\frac{N-n}{N} \right),$$

where $\hat{V}(\hat{\tau})$ = the estimated variance of the population total estimate;

N = the total number of possible samples in the survey area;

n = the total number of samples taken; and

s^2 = the sample variance.

The estimate poststratified by habitat was calculated as

$$\hat{\tau}_{st} = \sum_{i=1}^L N_i \bar{y}_i,$$

where $\hat{\tau}_{st}$ = the estimated population total;

L = the number of strata (here $L=2$, habitat and nonhabitat);

N_i = the total number of possible samples in stratum i (samples were standardized to 1000 m², therefore $N_i \times 1000$ m² = stratum size); and

\bar{y}_i = the mean CPUE in stratum i .

A third estimate, poststratified by habitat and fish density, was calculated with the same poststratification estimator with $L=3$. This poststratification estimator used the HFD area of that year as one stratum, the LFD area of that year as the second stratum, and the nonhabitat area as the third. An approximate variance estimator (Scheaffer et al., 1996),

$$\hat{V}_p(\hat{\tau}_{st}) = \frac{N(N-n)}{n} \sum_{i=1}^n \frac{N_i}{N} s_i^2 + \frac{N^2}{n^2} \sum_{i=1}^n \left(1 - \frac{N_i}{N} \right) s_i^2,$$

was used to estimate the variance of each poststratification estimator,

where \hat{V}_p = the estimated poststratified variance of $\hat{\tau}_{st}$,
the estimated population total;

N = the total number of possible samples in the survey area;

n = the total number of samples taken;

N_i = the total number of possible samples in stratum i ; and

s_i^2 = the sample variance in stratum i .

The first term of the variance equation is the variance of a stratified sample mean under proportional allocation. The second term shows the amount of increase in variance expected from post- rather than prestratification (Scheaffer et al., 1996).

Relative efficiency statistics were calculated for pairwise comparisons of the precision of the unstratified and the two poststratified estimates. Pairwise comparisons of the estimates were made for each species in each year. Relative efficiency was calculated as

$$R.E. = \frac{V_A}{V_B},$$

where V_A represents the variance of an unstratified estimate or a stratified sample with fewer strata than the estimate of variance represented by V_B .

The variance of an estimate is directly affected by the sample size (Zar, 1996). In our study, three total abundance estimates and their respective variances were

calculated and compared for each of the 24 species-year combinations. One of the three total abundance estimates was most precise for each of the species-year combinations. For each species-year combination, the habitat stratum sample size (used in the estimate poststratified by habitat), the HFD stratum sample size, and the LFD stratum sample size (both used in the estimate poststratified by habitat and fish density) were plotted in relation to the total abundance estimator that was most precise in order to investigate the influence of sample size on the relative precision of the three total abundance estimators.

Indices of abundance Three indices were constructed for each species in each year to determine interannual variations in relative abundance (mean CPUE): an all-site index, a habitat index, and a HFD index. For each species and year, the all-site index was the mean CPUE from all sites sampled. The habitat index was the mean CPUE from all sites sampled within the species' habitat area. The HFD index was the mean CPUE from all sites sampled within the species' HFD area.

CPUE values were not normally distributed and therefore the Kruskal-Wallis nonparametric analysis of variance test was used to test the three indices for each species' differences in mean CPUE among years. For species that showed significant differences ($\alpha=0.05$), a Tukey HSD (honestly significant difference) multiple comparison test for unequal sample sizes was conducted to determine which years differed ($\alpha=0.05$). The Tukey multiple comparison test was used because it is robust with respect to departures from population normality and homogeneity of variance (Keselman, 1976). The results for the three indices for each species were compared to see how the differences in estimating abundance with the three indices affected conclusions of significant differences in abundance between years.

Numerous sources of bias can affect estimators of abundance from survey data. The poststratification estimator and other design-based estimators may be biased when applied to data that were not collected under a probability sampling design, as done in the present study. For a qualitative estimate of possible design bias in the estimates, the annual proportion of sample sites in each stratum (habitat, nonhabitat, HFD, and LFD strata) were compared with the proportion of area (km^2) in that stratum. First, we compared the size of the habitat area, in relation to the size of the total survey area, with the number of samples taken in the habitat area, in relation to the number taken in the total survey area.

$$\frac{\text{Size of the habitat area}}{\text{Size of the total survey area}} ; \frac{\text{Number of samples taken in the habitat area}}{\text{Number of samples taken in the total survey area}}$$

number of samples taken in the HFD area, in relation to the number taken in the total habitat area.

$$\frac{\text{Size of the HFD area}}{\text{Size of the habitat area}} ; \frac{\text{Number of samples taken in the HFD area}}{\text{Number of samples taken in the habitat area}}$$

Recognizing that the distribution of individuals varied within and across strata, two measures were used to better understand the distribution of each species in each year. The proportion of zero catches (e.g., a "zero catch" for rock sole indicates a tow in which no rock sole were caught) and the mean CPUE of nonzero catches were calculated for each species in each year over four areas: the total survey area, the habitat area, the HFD area, and the LFD area.

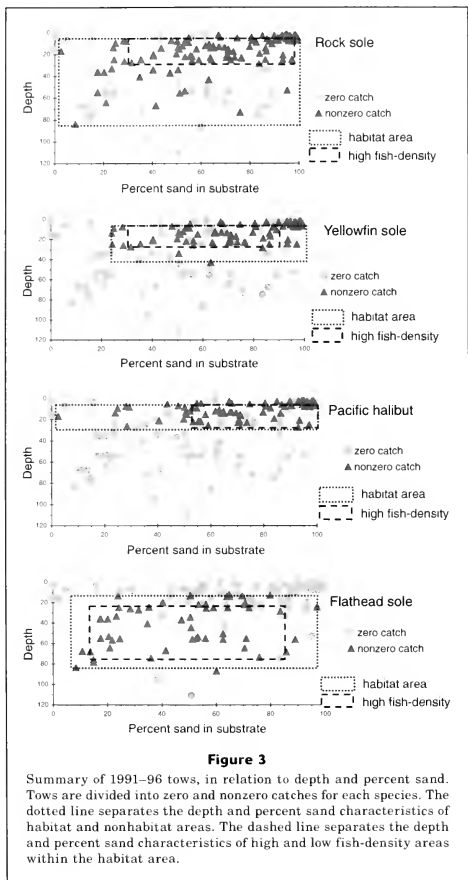
Results

Fish CPUE statistics were calculated for a total of 244 quantitative tows over the six sampling years (Fig. 2) in habitats ranging from 1 to 111 m depth and from 0% to 99% sand. Based on compiled data from all six years, the habitat area for rock sole was defined by 1–84 m depth and 2–99% sand; for yellowfin sole, by 2–43 m depth and 24–99% sand; for Pacific halibut, by 2–27 m depth and 2–99% sand; and for flathead sole, by 12–87 m depth and 8–97% sand (Fig. 3). The HFD area, defined by depth and percent sand, was determined for each of the four species in each of the six years (Table 1, Fig. 3). Although the range of depth and the range of percent sand were determined independently in each year, they remained quite constant for each species over the six sampling years.

The size of habitat area in relation to total area ranged across species from 0.62 to 0.92 and, for each species, the proportion of habitat sites to total sites varied among years (Table 2). The proportion of sample sites in habitat to sample sites in the total survey area ranged from 0.88 to 1.00 for rock sole, 0.60 to 0.87 for yellowfin sole, 0.52 to 0.93 for Pacific halibut, and 0.29 to 0.67 for flathead sole. The relative number of samples taken in each species' habitat area exceeded the relative size of their habitat area (i.e., a positive disproportion of samples in habitat), except for rock sole in 1991 and 1994, yellowfin sole in 1993 and 1994, Pacific halibut in 1993 and 1994, and all years for flathead sole. On average, rock sole had a 5% positive disproportion of samples in its habitat area, yellowfin sole and Pacific halibut had an 11% positive disproportion of samples in their habitat area, and flathead sole had a 15% negative disproportion of samples in its habitat area.

The size of the HFD area in relation to habitat area, and the number of sites sampled in the HFD area in relation to the number sampled in the entire habitat area, varied over the six sampling years for each of the four species (Table 2). On average over the six years,

Second, we compared the size of the HFD area, in relation to the size of the total habitat areas, with the



rock sole had a 10% negative disproportion of samples in the HFD area, Pacific halibut had a 3% negative disproportion of samples in the HFD area, and flathead sole had a 28% negative disproportion of samples in the HFD area. For yellowfin sole, the average distribution of samples between the high and low fish-density areas was in direct proportion to the size of the areas, i.e., there was no disproportion of samples.

Two measures were used to characterize the distribution of a species within their habitat: the proportion of zero catches and the mean of nonzero catches in high and low fish-density areas. As expected, for all species the average proportion of zero catches over all sites was greater than the proportion of zero catches in the habitat or HFD areas (Table 3). For rock sole, yellowfin sole, and flathead sole, the average proportion of zero

Table 1

Characteristics defining 1991–96 high fish-density areas for each species of flatfish. Ranges of depth and percent sand, defining the high fish-density (HFD) area, and the associated spatial coverage within the bay (km^2). Each year's HFD area was determined as the range of depth and percent sand associated with the 75th–100th percentile of nonzero catch from the other five years.

Species	Year	Depth (m)		Percent sand in sediment		Size (km^2)
		minimum	maximum	minimum	maximum	
Rock sole (<i>Lepidopsetta</i> spp.)	1991	3.0	27.3	31.5	99.2	52
	1992	3.0	36.0	20.2	99.2	56
	1993	3.0	27.3	31.5	99.2	52
	1994	3.0	27.3	31.5	98.8	52
	1995	3.0	27.3	31.5	99.2	52
	1996	3.0	25.0	47.8	99.2	46
	average	3.0	28.3	32.4	99.2	52
Yellowfin sole (<i>Pleuronectes asper</i>)	1991	1.7	23.0	40.5	98.6	33
	1992	2.3	25.0	24.2	86.7	29
	1993	2.3	25.0	24.2	86.7	29
	1994	2.3	25.0	24.2	86.7	29
	1995	2.3	25.0	24.2	86.7	29
	1996	2.3	25.0	24.2	86.7	29
	average	2.2	24.7	26.9	88.7	30
Pacific halibut (<i>Hippoglossus stenolepis</i>)	1991	2.5	25.0	52.3	99.3	39
	1992	2.3	27.0	52.3	99.3	41
	1993	2.3	27.0	52.3	99.3	41
	1994	2.3	27.0	52.3	99.3	41
	1995	2.0	27.0	64.6	99.3	33
	1996	2.3	25.5	52.3	98.4	37
	average	2.3	26.4	54.4	99.1	39
Flathead sole (<i>Hippoglossoides elassodon</i>)	1991	19.8	87.0	17.4	89.1	42
	1992	25.5	87.0	10.7	89.1	38
	1993	19.8	87.0	8.4	70.7	34
	1994	19.8	67.5	10.7	89.1	40
	1995	19.8	87.0	17.4	89.1	42
	1996	19.8	64.0	17.4	89.1	39
	average	20.8	79.9	13.7	86.0	39

catches in the LFD area was higher than in the HFD area. For Pacific halibut, the average proportion of zero catches remained approximately constant across the entire habitat area. The relative mean nonzero catch between the LFD and HFD areas varied across species, ranging from 37% to 82% (Table 4).

In each of the 24 species-year combinations, three estimates of population abundance were compared, except for flathead sole in 1992 when no samples were taken in the flathead sole HFD area (Fig. 4). In every case in which the proportion of habitat stratum-size sites to total study area sites exceeded the proportion of habitat stratum size to total study area size (Table 2), the unstratified estimate was greater than the estimate poststratified by habitat (Fig. 4). In every case that the proportion of habitat stratum sites to total study area sites was less than the proportion of habitat stratum size to total study area,

the unstratified estimate was less than the estimate poststratified by habitat. Similarly, in every case that the proportion of HFD stratum sites to habitat stratum sites exceeded the proportion of HFD stratum size to habitat stratum size (Table 2), the estimate poststratified by habitat was greater than the estimate poststratified by habitat and fish density (Fig. 4). In all but two cases in which the proportion of HFD stratum sites to habitat stratum sites was less than the proportion of HFD stratum size to habitat stratum size, the estimate poststratified by habitat was less than the estimate poststratified by habitat and fish density. The two exceptions were for Pacific halibut in 1991 and 1996, where the difference between poststratified estimates was small. In 1991, the estimate poststratified by habitat was 2.9% (8116 fish) greater than the estimate poststratified by habitat and fish density; in 1996, it was 0.56% (4905 fish) greater.

Table 2

A comparison of the relative number of sample sites and relative size (km²) of the habitat area, high fish-density (HFD) area, and total study area. Comparisons include the size of the habitat area versus the size of the study area, the number of sites sampled in the habitat area versus the number sampled in the total study area, the size of the HFD area versus the size of the habitat area, and the number of sites sampled in the HFD area versus the number sampled in the habitat area.

Species	Habitat size/Total study size (km ²)		Habitat sites/Total sites												
			Year												
	All years							average	1991	1992	1993	1994	1995	1996	average
Rock sole (<i>Lepidopsetta</i> spp.)	0.92							0.92	1.00	1.00	0.88	1.00	1.00	0.97	
Yellowfin sole (<i>Pleuronectes asper</i>)	0.66							0.78	0.87	0.63	0.60	0.80	0.80	0.75	
Pacific halibut (<i>Hippoglossus stenolepis</i>)	0.62							0.73	0.93	0.58	0.52	0.80	0.80	0.73	
Flathead sole (<i>Hippoglossoides elassodon</i>)	0.67							0.43	0.29	0.67	0.56	0.60	0.60	0.52	

Species	High fish-density size/Habitat size (km ²)								High fish-density sites/Habitat sites							
	Year								Year							
	1991	1992	1993	1994	1995	1996	average	1991	1992	1993	1994	1995	1996	average		
Rock sole (<i>Lepidopsetta</i> spp.)	0.65	0.70	0.65	0.65	0.65	0.58	0.65	0.64	0.73	0.42	0.45	0.55	0.50	0.55		
Yellowfin sole (<i>Pleuronectes asper</i>)	0.58	0.51	0.51	0.51	0.51	0.51	0.52	0.76	0.46	0.47	0.40	0.50	0.50	0.52		
Pacific halibut (<i>Hippoglossus stenolepis</i>)	0.72	0.76	0.76	0.76	0.61	0.69	0.72	0.69	0.86	0.79	0.62	0.63	0.54	0.69		
Flathead sole (<i>Hippoglossoides elassodon</i>)	0.72	0.66	0.59	0.69	0.72	0.67	0.68	0.52	0.00	0.50	0.43	0.50	0.44	0.40		

Calculations of relative efficiency among the three total abundance estimators showed increases in estimated precision with stratification (Table 5). In most cases (18 out of 24), the estimate poststratified by habitat was more precise (corresponding to a lower standard error in Fig. 5) than the unstratified estimate. Of the 16 (of 23) cases in which the precision of both poststratified estimates were greater than that of the unstratified estimate, in half the estimate poststratified by both habitat and density was more precise than the estimator poststratified by habitat alone.

Sample sizes across the survey area and in each sub-area (habitat, high fish-density, and low fish-density areas) (Table 6) strongly influenced the precision of estimates. Habitat sample sizes for all species-year combinations ranged from 4 to 45 (proportion of samples taken in habitat ranged from 0.286 to 1.000); HFD sample sizes ranged from 0 to 29 (proportion of samples taken in the HFD area ranged from 0.0 to 0.8); and LFD sample sizes ranged from 4 to 16 (proportion of samples taken in the LFD area ranged from 0.125 to 0.583). Although the number of samples in both the high and low fish-density areas (Fig. 6, A and B) likely affected estimates poststratified by habitat and fish density, the number of samples in the HFD area appears to have had the primary influence on the precision of estimates. The species-year combinations for which the unstratified estimate was the most precise occurred when habi-

tat sample sizes ranged from 4 to 22 (Fig. 7) and HFD stratum sample sizes ranged from 6 to 11 (Fig. 6A). The species-year combinations for which the estimate poststratified by habitat was the most precise occurred when habitat sample sizes ranged from 12 to 30 (Fig. 7) and when sample sizes in the HFD stratum ranged from 6 to 15 (Fig. 6A). The species-year combinations for which the estimate poststratified by habitat and fish density was most precise occurred when habitat sample sizes ranged from 15 to 45 (Fig. 7) and HFD stratum sample sizes ranged from 10 to 29 (Fig. 6A). Estimates poststratified by habitat and fish density were the most precise for all three cases in which the HFD stratum sample size was greater than 20 (corresponding to LFD stratum sample sizes ranging from 9 to 16) (Fig. 6, A and B). Both of the poststratified estimates were more precise than the unstratified estimate when habitat stratum sample sizes were greater or equal to 24 (Fig. 7) and when HFD stratum sizes were greater or equal to 12 (Fig. 6A).

Statistically significant changes in annual abundance varied among indices and species. There were significant changes in annual mean CPUE in all indices for rock sole and Pacific halibut, in two indices for yellowfin sole and in no indices for flathead sole (Table 7). Rock sole abundance was significantly greater in 1992 than all other years except 1996. Individual indices indicated that rock sole 1996 abundance was greater than that

Table 3

Annual and average proportion of zero catches in the total survey area, habitat area, high fish-density (HFD) areas and low fish-density (LFD) areas for rock sole (*Lepidopsetta* spp.), yellowfin sole (*Platromectes asper*), Pacific halibut (*Hippoglossus stenolepis*), and flathead sole (*Hippoglossoides elassodon*).

Year	Proportion of zero catches															
	Rock sole				Yellowfin sole				Pacific halibut				Flathead sole			
	Total survey	Habitat	HFD	LFD	Total survey	Habitat	HFD	LFD	Total survey	Habitat	HFD	LFD	Total survey	Habitat	HFD	LFD
1991	0.224	0.156	0.069	0.308	0.408	0.237	0.241	0.222	0.571	0.417	0.440	0.364	0.776	0.476	0.273	0.700
1992	0.133	0.133	0.000	0.500	0.533	0.462	0.167	0.714	0.267	0.214	0.250	0.000	0.714	0.250	—	0.250
1993	0.375	0.375	0.100	0.571	0.500	0.200	0.143	0.250	0.583	0.286	0.273	0.333	0.542	0.313	0.000	0.625
1994	0.360	0.273	0.100	0.417	0.800	0.667	0.833	0.556	0.520	0.077	0.125	0.000	0.520	0.143	0.167	0.125
1995	0.050	0.050	0.000	0.111	0.400	0.250	0.125	0.375	0.250	0.063	0.000	0.167	0.600	0.333	0.333	0.333
1995	0.133	0.133	0.067	0.214	0.433	0.292	0.250	0.333	0.333	0.167	0.154	0.182	0.733	0.556	0.250	0.800
Average	0.213	0.187	0.056	0.354	0.512	0.351	0.293	0.408	0.421	0.204	0.207	0.174	0.647	0.345	0.205	0.472

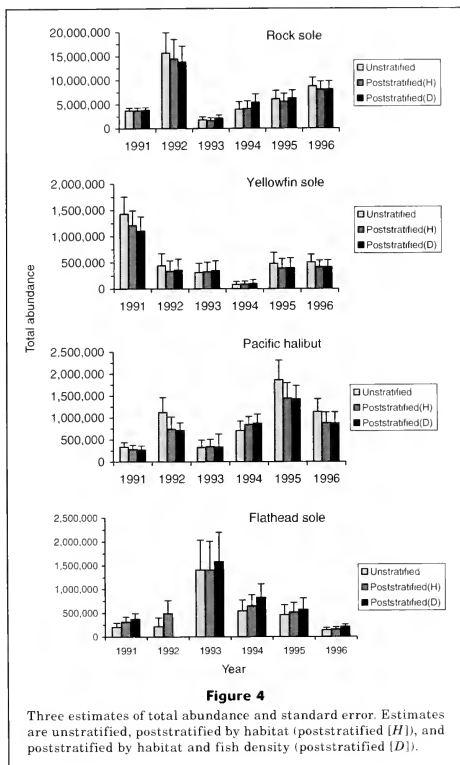
of 1992 and 1993. Tukey *post hoc* tests on the yellowfin sole all-site and habitat indices showed that 1991 yellowfin abundance was greater than that of 1994. All three indices showed that Pacific halibut abundance was greater in 1995 than in 1991 and 1993. Individual indices also indicated that Pacific halibut abundance was greater in 1995 than in 1992, 1994, and 1996.

Discussion

The Chiniak Bay multispecies survey was designed to estimate the abundance of four species with equal emphasis. Because the distribution of species varied greatly throughout the bay, what might have been an optimal stratification for individual species was compromised to develop a stratification scheme that was as effective as possible for all target species. Because we do not believe sampling was optimal for any one of the species, a poststratification method of analysis was investigated to increase the precision of abundance estimates for each species individually and to account for possible bias due to the uneven and nonrandom distribution of sampling sites over space and time.

The need for stratification and the concern about the distribution of sampling sites arise because of the varying distributions of species in the study region. Knowledge of the spatial distributions of species is important when estimating abundance from trawl surveys. A random distribution of individuals is often taken as a starting point for defining spatial distributions in ecology (Taylor et al., 1978). It is also a primary assumption for many survey sampling designs and analysis measures. The assumption of randomly distributed individuals often is not appropriate, however, because the concentration of fish varies over time and space in relation to environmental factors (Murawski and Finn, 1988; Gadomski and Caddell, 1991; Reichert and van der Veer, 1991; Norcross et al., 1999). If habitat (Fiedler and Reilly, 1994; Reilly and Fiedler, 1994) and related spatial population density distributions (Buckland and Anganuzzi, 1988) are not accounted for when calculating abundance estimates, precision can decrease and results can be seriously biased. Inaccurate results can have strong management repercussions.

In situations such as that of the present study, where the sample does not properly represent the population, poststratification is appropriate (Scheaffer et al., 1996). By comparing poststratified and unstratified estimates of abundance, we found that in every species-year combination for which the three estimates of abundance differed (Fig. 3), the poststratified estimates reduced the effect of the disproportion of samples allocated between habitat and nonhabitat areas and between high and low fish-density areas. For instance, in 1992, a disproportionately large number of samples were taken in Pacific halibut habitat (Table 2). We suspect, therefore, that the unstratified estimate of abundance was an overestimate of true population abundance. The disproportionately large number of samples taken in Pacific halibut



habitat was adjusted by poststratifying by habitat. The estimate poststratified by habitat was less than the unstratified estimate of abundance, as we suspect the true abundance was. Poststratification by habitat and neighboring years' halibut density adjusted not only for the disproportionately large number of samples in the habitat area but also for the disproportionately large number of samples in the HFD area (Table 2). The estimate poststratified by habitat and halibut density was less than both the estimate poststratified by habitat and the unstratified estimate, as we suspect was the case for the true Pacific halibut abundance.

In 1992, the number of samples in yellowfin sole habitat was disproportionately large, but the number

of samples in the HFD area was disproportionately small (Table 2). In this case, we suspect the unstratified estimate of abundance was an overestimate of true abundance because of the overabundance of samples in the habitat area. We also believe, however, that it was not a very large overestimate because of the disproportionately small number of samples in the HFD area. Poststratifying by habitat adjusted for the disproportionately large number of samples in the habitat area and produced an estimate that was less than the unstratified estimate. Poststratifying by habitat and fish density adjusted for both the disproportionately large number of samples in the habitat area and the disproportionately small number of samples in the HFD

Table 4

The mean catch per unit of effort (CPUE) of nonzero catches in the habitat, high fish-density (HFD), and low fish-density (LFD) areas and the proportion of the mean CPUE of nonzero catches in LFD and habitat areas in relation to those in the HFD area.

	Species			
	Rock sole (<i>Lepidopsetta</i> spp.)	Yellowfin sole (<i>Pleuronectes asper</i>)	Pacific halibut (<i>Hippoglossus stenolepis</i>)	Flathead sole (<i>Hippoglossoides classodon</i>)
Habitat nonzero mean	85.3	15.6	16.8	16.0
HFD nonzero mean	105.4	20.7	17.9	20.6
LFD nonzero mean	52.2	7.6	14.7	9.5
Habitat mean/concentration mean	0.81	0.75	0.94	0.78
LFD mean/HFD mean	0.50	0.37	0.82	0.46

Table 5

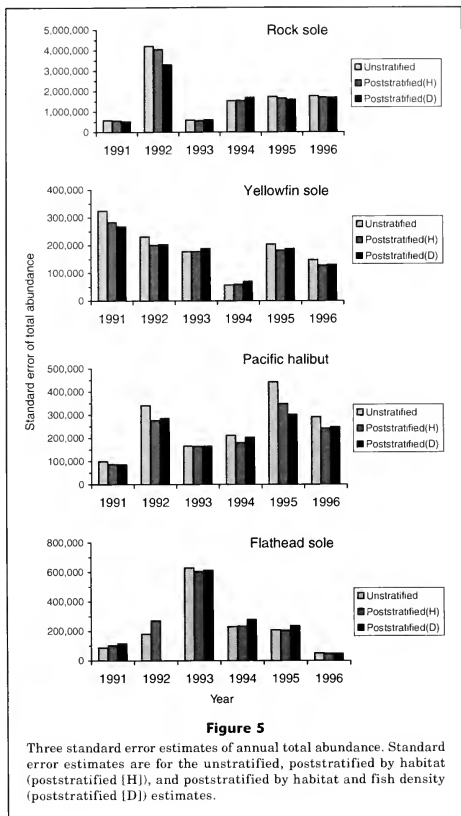
Unstratified total abundance estimates (*U*), total abundance estimates poststratified by habitat (*H*), and total abundance estimates poststratified by habitat and fish density (*D*) are compared by using annual relative efficiency statistics.

Species	Relative efficiency comparison	Year					
		1991	1992	1993	1994	1995	1996
Rock sole (<i>Lepidopsetta</i> spp.)	<i>H</i> to <i>U</i>	1.076	1.081	1.084	0.985	1.083	1.084
	<i>D</i> to <i>H</i>	1.129	1.496	0.865	0.834	1.089	0.999
	<i>D</i> to <i>U</i>	1.214	1.618	0.937	0.821	1.179	1.084
	conclusion	<i>D</i> > <i>H</i> > <i>U</i>	<i>D</i> > <i>H</i> > <i>U</i>	<i>H</i> > <i>U</i> > <i>D</i>	<i>U</i> > <i>H</i> > <i>D</i>	<i>D</i> > <i>H</i> > <i>U</i>	<i>H</i> > <i>D</i> > <i>U</i>
Yellowfin sole (<i>Pleuronectes asper</i>)	<i>H</i> to <i>U</i>	1.318	1.317	0.988	0.922	1.266	1.324
	<i>D</i> to <i>H</i>	1.111	0.969	0.890	0.715	0.936	0.967
	<i>D</i> to <i>U</i>	1.465	1.277	0.880	0.659	1.186	1.280
	conclusion	<i>D</i> > <i>H</i> > <i>U</i>	<i>H</i> > <i>D</i> > <i>U</i>	<i>U</i> > <i>H</i> > <i>D</i>	<i>U</i> > <i>H</i> > <i>D</i>	<i>H</i> > <i>D</i> > <i>U</i>	<i>H</i> > <i>D</i> > <i>U</i>
Pacific halibut (<i>Hippoglossus stenolepis</i>)	<i>H</i> to <i>U</i>	1.272	1.521	1.007	1.369	1.607	1.440
	<i>D</i> to <i>H</i>	1.029	0.936	0.996	0.792	1.340	0.949
	<i>D</i> to <i>U</i>	1.309	1.424	1.003	1.084	2.155	1.366
	conclusion	<i>D</i> > <i>H</i> > <i>U</i>	<i>H</i> > <i>D</i> > <i>U</i>	<i>H</i> > <i>D</i> > <i>U</i>	<i>H</i> > <i>D</i> > <i>U</i>	<i>D</i> > <i>H</i> > <i>U</i>	<i>H</i> > <i>D</i> > <i>U</i>
Flathead sole (<i>Hippoglossoides classodon</i>)	<i>H</i> to <i>U</i>	0.726	0.449	1.075	0.973	1.025	1.056
	<i>D</i> to <i>H</i>	0.786	—	0.976	0.705	0.746	0.992
	<i>D</i> to <i>U</i>	0.571	—	1.049	0.686	0.765	1.047
	conclusion	<i>U</i> > <i>H</i> > <i>D</i>	<i>U</i> > <i>H</i>	<i>H</i> > <i>D</i> > <i>U</i>	<i>U</i> > <i>H</i> > <i>D</i>	<i>H</i> > <i>U</i> > <i>D</i>	<i>H</i> > <i>D</i> > <i>U</i>

area. As a result, the estimate poststratified by habitat and fish density was greater than the estimate poststratified by habitat, but lower than the unstratified estimate. According to our results, it is unlikely that the estimates poststratified by habitat and fish density were the most representative estimates of abundance because poststratification adjusted for the disproportionate distribution of samples between areas.

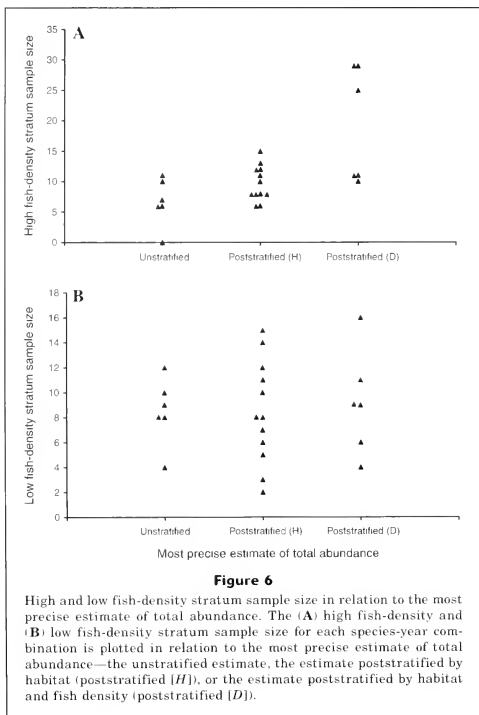
Another reason to poststratify the data is to increase the precision of abundance estimates. Poststratified

estimates in our study were generally more precise than unstratified estimates, given sufficient sample sizes (Table 5). Poststratification by habitat characteristics increased the precision of abundance estimates in three-quarters of all species-year combinations. This finding indicates a close link between habitat type and fish abundance and agrees with poststratification results in other studies (Pollock et al., 1994; Reilly and Fiedler, 1994). Estimates poststratified by both habitat and fish density were also generally more precise than



unstratified estimates but were not consistently more precise than the estimates poststratified by habitat alone. The six cases in which estimates poststratified by habitat and fish density were the most precise show that some species have strong density gradients within habitat areas and that the incorporation of fish density information from neighboring years can be beneficial for increasing precision. Being able to predict the distribution of fish density in one year from that of neighboring years indicates annual consistency in species distribution in relation to habitat characteristics.

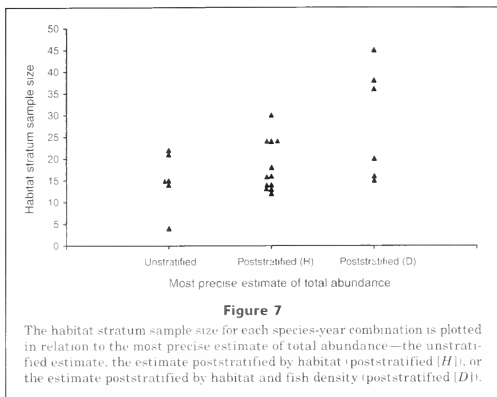
The present study indicates that when estimating abundance from haphazardly sampled data, the estimator poststratified by habitat is superior to the unstratified estimator regardless of sample size. The estimate poststratified by habitat was more precise than the unstratified estimate in 18 of the total 24 species-year combinations. These 18 species-year combinations occurred across nearly the full range of habitat stratum sample sizes, from 12 to 45. The six cases in which the estimate poststratified by habitat was less precise than the unstratified estimate were affected by the propor-



tion of samples in unsuitable habitat. As a measure of variability, the magnitude of the variance is dependent on the magnitude of the data (Zar, 1996). Thus, the variances of trawl catches decrease as the observed means decrease (Taylor, 1953). A lower variance, therefore, does not necessarily indicate a better estimator, but instead may reflect lower population abundance. In the six cases in this study where the variance of the unstratified estimate was less than the variance of the estimate poststratified by habitat, the unstratified abundance estimate was less than the abundance estimate poststratified by habitat. The low unstratified abundance estimates in these six cases were the result of a disproportionately large number of samples in nonhabitat areas in relation to the size of the nonhabitat areas. Therefore, although the unstratified estimate was more precise, it was also likely to be an underestimate of the

true abundance. Thus, we suggest that the estimate poststratified by habitat is the most desirable estimator in these situations, despite the decrease in precision in relation to the unstratified estimator.

In many cases, small sample size was likely the reason that the estimates poststratified by habitat and fish density were not the most precise of the three estimates. Poststratification produces precise estimates when the overall sample size and the sample size in each stratum are large (Scheaffer et al., 1996). In our study, the estimator poststratified by habitat and fish density was the most precise estimator of the three when sample size in the HFD stratum was 20 or greater and the sample size in the LFD stratum was 9 or greater. The number of samples in the HFD stratum appears to have had a larger influence on the precision of estimates stratified by habitat and fish density than the number of samples

**Table 6**

Annual number of tows made across all strata in habitat and nonhabitat strata, and in the high and low fish-density strata within the habitat stratum.

Species	Stratum	Year					
		1991	1992	1993	1994	1995	1996
Rock sole (<i>Lepidopsetta</i> spp.)	all	49	15	24	25	20	30
	habitat and nonhabitat	45 and 4	15 and 0	24 and 0	22 and 3	20 and 0	30 and 0
	high fish density and low fish density	29 and 16	11 and 4	10 and 14	10 and 12	11 and 9	15 and 15
Yellowfin sole (<i>Pleuronectes asper</i>)	all	49	15	24	25	20	30
	habitat and nonhabitat	38 and 11	13 and 2	15 and 9	15 and 10	16 and 4	24 and 6
	high fish density and low fish density	29 and 9	6 and 7	7 and 8	6 and 9	8 and 8	12 and 12
Pacific halibut (<i>Hippoglossus stenolepis</i>)	all	49	15	24	25	20	30
	habitat and non-habitat	36 and 13	14 and 1	14 and 10	13 and 12	16 and 4	24 and 6
	high fish density and low fish density	25 and 11	12 and 2	11 and 3	8 and 5	10 and 6	13 and 11
Flathead sole (<i>Hippoglossoides elassodon</i>)	all	49	14	24	25	20	30
	habitat and non-habitat	21 and 28	4 and 10	16 and 8	14 and 11	12 and 8	18 and 12
	high fish density and low fish density	11 and 10	0 and 4	8 and 8	6 and 8	6 and 6	8 and 10

in the LFD stratum (Fig. 6, A and B). This study supports the conclusion of Scheaffer et al. (1996) but also indicates that the sample size in the HFD stratum may have a larger influence on the precision of the resultant estimate.

As concluded in other studies (Fiedler and Reilly, 1994; Pollock et al., 1994; Reilly and Fiedler, 1994;

Bernard et al., 1998), we found that poststratification can provide increased precision and decreased bias for estimates. Small stratum sample sizes, however, can make it impossible to detect heterogeneity among strata and fail to give increased precision (Powell et al., 1995; Friedland et al., 1999). The wide range of sample sizes among strata across species-year combinations exempli-

Table 7

Kruskal-Wallis test statistics for differences in annual relative abundance and, for significant Kruskal-Wallis statistics, the corresponding significant Tukey *post hoc* pairwise differences. Statistics were calculated for the all-site, habitat, and high fish-density indices.

Species	Index	Kruskal-Wallis (*indicates statistically significant difference)	Tukey <i>post hoc</i> significant differences	
Rock sole (<i>Lepidopsetta</i> spp.)	All-site	$P=0.0003^*$	1992>1991 ($P<0.0006$)	
			1992>1993 ($P<0.0001$)	
			1992>1994 ($P<0.0009$)	
			1992>1995 ($P<0.0124$)	
			1996>1993 ($P<0.0301$)	
	Habitat	$P=0.0008^*$	1992>1991 ($P<0.0012$)	
			1992>1993 ($P<0.0001$)	
			1992>1994 ($P<0.0022$)	
	High fish density	$P=0.0035^*$	1992>1995 ($P<0.0149$)	
1996>1993 ($P<0.0351$)				
1992>1991 ($P<0.0005$)				
1992>1993 ($P<0.0003$)				
Yellowfin sole (<i>Pleuronectes asper</i>)	All-site	$P=0.0033^*$	1991>1994 ($P<0.0096$)	
	Habitat	$P=0.0022^*$	1991>1994 ($P<0.0374$)	
	High fish density	$P=0.1240$		
	Pacific halibut (<i>Hippoglossus stenolepis</i>)	All-site	$P=0.001^*$	1995>1991 ($P<0.0013$)
				1995>1993 ($P<0.0012$)
				1995>1994 ($P<0.0359$)
		Habitat	$P=0.0004^*$	1995>1991 ($P<0.0018$)
				1995>1993 ($P<0.0077$)
				1995>1991 ($P<0.0002$)
High fish density	$P=0.0002^*$	1995>1992 ($P<0.0127$)		
		1995>1993 ($P<0.0004$)		
		1995>1996 ($P<0.0249$)		
Flathead sole (<i>Hippoglossoides elassodon</i>)	All-site	$P=0.1955$		
	Habitat	$P=0.2950$		
	High fish density	$P=0.5151$		

fies an important drawback to using the poststratification method. Because strata criteria are unknown when sampling, it is not possible to insure that there will be sufficient samples in each poststratified stratum. When resulting sample sizes in some strata are small, poststratification may be ineffective at increasing precision. If the resulting sample size in one or more strata is one, the poststratification variance will be inestimable. If the resulting sample size in one or more strata is zero, poststratification may not be possible.

Because sample size is a limiting factor for increased precision with poststratification, there are strong implications for survey design. Many multispecies surveys are conducted by using a stratified random sampling design. There are two ways to apply poststratification to a

stratified survey. First, for an unbiased estimator, each stratum of the stratified survey can be poststratified individually (Cochran, 1977). For the poststratification estimator to have increased precision beyond that of stratified random sampling, each of the original strata must have a large number of samples to allow sufficient samples in each poststratified stratum. Therefore, investigators who intend to poststratify data within a stratified random survey for unbiased estimates need to construct large strata with many samples in the original sampling design. Second, if poststratification is applied to data that were not collected under a probability sampling design, the estimator may be more precise, but may be biased. For the analysis of data that were not collected under a probability sampling

design, developing an index of relative abundance from all samples, or samples in the habitat or HFD areas, is an easy and effective way to estimate statistically significant changes in abundance among years. To determine which tows should be included in an index to effectively approximate the variations in the annual total abundance estimates, it is helpful to compare the size of the habitat area over years and to study the distribution of species density within the habitat area. The goal of creating an index should be to include the most information possible, while avoiding undue influence from the haphazard distribution of sample sites.

If the total study area is the same in each year, the choice of whether to use the all-site index should depend on whether the size of the habitat area is constant over the compared years. In this study, the defined habitat area for each species was the same over the six years compared. Therefore, for an index of relative abundance, the habitat index retained all necessary information and reduced possible bias due to the disproportionate distribution of haphazard samples between habitat and nonhabitat areas. When a temporally dependent stratification variable, such as temperature, is used to define the placement of stratum boundaries, however, the size of the habitat area may vary between years. If the annual size of the habitat area varies, some common size would need to be chosen for the relative index to approximate the annual changes in the total abundance estimates. The all-site index could be used for this purpose, but the index will be affected by any disproportionate distribution of samples between habitat and nonhabitat areas. Another possible way to do this would be to include all tows from the habitat area each year, plus as many zero catches from the nonhabitat area necessary to be proportional to the annual size of the nonhabitat area. Such an approach would not depend on actual tows in nonhabitat area but would depend on the estimated size of the habitat and nonhabitat areas and the sample size in the habitat area.

If the size of habitat area is the same in each year, the choice of whether to use the habitat index should depend on whether the distribution of species density is constant throughout the habitat area. If a species' density distribution is approximately constant across the habitat area, a haphazard distribution of sample sites should have little influence. Constructing an index from all habitat tows may then be desired to retain the largest sample size and the most information possible. Alternatively, if a species has a strong density gradient within its habitat area, a disproportionate distribution of sites in relation to the size of high and low fish-density areas may provide an unrepresentative estimate of abundance from the habitat index. In this case, if a sufficient number of samples are taken in the HFD area, constructing an index from samples within the species' HFD area alone may provide an effective index while minimizing the effect of a disproportional distribution of haphazard samples within the habitat area.

A comparison of the number of zero catches and the mean nonzero catch between the high and low fish-

density areas provides information about the density distribution of species within a habitat area. The proportion of zero catches of rock sole, yellowfin sole, and flathead sole and the mean nonzero catch between high and low fish-density areas indicated density gradients within the habitat areas. Unlike these three species, the proportion of Pacific halibut zero catches was approximately the same in the HFD area as across the entire habitat area and the difference in mean nonzero catch between low and high fish-density areas was only approximately half that of the other species. Therefore, it appears that the Pacific halibut density distribution across the defined habitat area varied little compared with the other three species.

In this study, we suggest that the habitat index was the most appropriate for all four species. For each species in our study, the size of the habitat area remained the same across all six years. Thus, the habitat index eliminated the influence of disproportionately allocated samples in habitat and nonhabitat areas. For Pacific halibut, the relatively homogenous distribution of abundance across the habitat area indicates that the effect of disproportionate samples between high and low fish-density areas is small and that samples across the entire habitat area are helpful in describing annual differences in abundance. For rock sole, yellowfin sole, and flathead sole, the difference in the proportion of zero catches and nonzero mean abundance between the high and low fish-density areas was considerable. As a result, differences in annual abundance suggested by the habitat index may be affected by the inconsistent disproportion of samples between high and low fish-density areas over years. Although it would be preferable to use the HFD index in these cases, annual sample sizes in the HFD area were so small that we recommend the habitat index instead. Recognizing that the habitat index will not account for the annual disproportion of samples between the high and low fish-density areas, we used the comparison of the size and the number of samples taken in high and low fish-density areas to flag differences in annual index abundance estimates that might be over- or underestimates. If this method is applied in a management context, the levels of the factors describing the density distribution of the species (i.e., difference in the percent of zero catches and the percent difference in mean nonzero catch between years) can be set as criteria and kept constant over years to eliminate subjectivity between years or between species. For example, if the percent of zero catches in high and low fish-density regions differ by 40% and the mean nonzero catch in the HFD area is 30% greater than that in the LFD area, the HFD index should be used. Otherwise, the habitat index should be used.

For many surveys, identifying habitat and fish-density areas for poststratification and index construction is possible with currently available information. The estimation methods used in the present study can be applied to any survey for which abundance and environmental measurements are available for each sampled site and the environmental measurements are related to species

abundance in a consistent way. For example, the NMFS Bering Sea trawl survey includes measurements of depth and surface and bottom temperatures at all trawl sites (Goddard and Walters⁴) that could be used for post-stratification. Similarly, the Pacific West Coast trawl survey includes measurements of surface and bottom temperature and salinity at all stations (Lauth et al.⁵) that could be used. Poststratification allows for use of a wide range of stratification variables, including temporally dependent variables that are not available before sampling is complete, e.g., temperature and salinity.

For surveys where habitat information is not collected at trawl sites, habitat information from other sources can be paired with fish distribution information after collections have been made. For instance, when habitat information is available, but has not been collected at each site, spatial statistics can be used to krig the habitat information over the study area and to predict the specific habitat data value at the sampling sites. If there is a consistent relationship between species abundance and the habitat variable, the catch and habitat data paired at sample sites can then be used to identify areas of suitable habitat and areas of high fish density within suitable habitat. How well habitat and HFD areas are estimated will depend on the number and distribution of habitat measurements, the contouring algorithms used, and the estimates of areas within contours. Even if species are not distributed in direct response to particular environmental characteristics, the characteristics may serve as proxies for effects that are more difficult to measure (Perry and Smith, 1994). Once habitat and HFD areas are identified, poststratification can be conducted for total abundance estimates, and statistically significant changes between years can be assessed with an index of relative abundance. These methods could yield more accurate estimates of abundance for use by managers. The goal of most sampling plans is to provide statistical estimates with the smallest possible confidence limits at the lowest cost (Krebs, 1989). Thus, being able to use data collected independently of a survey should be appealing.

The NRC (2000) recommends using data from commercial or sportfishing vessels in scientific assessments of abundance. A primary difficulty in using commercial fisheries data for scientific estimates of abundance is that the data do not represent random samples of the fish population. As a result, commercial fisheries data

present a biased perspective of the population that may change over time and may not correlate well with actual fish abundance (NRC, 2000). Although commercial fishery-dependent data may provide biased estimates of abundance, fishery-dependent data also provide large sample sizes and a wide range of information not available from other sources. For example, commercial and sportfishing data often provide broader geographic and temporal coverage. Poststratification of haphazard data from commercial and sportfishing sources may be one way to reduce inherent bias and provide useable scientific information. For instance, Buckland and Anganuzzi (1988) described how data collected on commercial tuna fishing vessels can be used to estimate dolphin abundance when survey data are not sufficient. The data collection sites were not randomly selected. Instead, the sampling sites were directly related to dolphin sightings, because dolphins and tuna schools are often closely associated. As a result, areas of high dolphin density corresponded with areas of high fishing effort. Poststratification was used to decrease the bias resulting from nonrandom distribution of both search effort and dolphin schools. A second example is a retrospective study that combined survey and commercial fishing data. In this study (Halliday⁶), 1958–60 poststratified survey data were used to develop a relationship between the survey abundance of the 1954–1959 year classes and their abundance estimates from commercial fishery data. This relationship was then used, along with 1969 survey data, to predict the size of the 1966–68 year classes. The same process was used to predict the size of later year classes with later years of survey data.

Poststratification also facilitates the use of a single data set for multiple objectives. Collecting data is costly and many data sets are collected and analyzed for a single objective and then not used again. Although it is preferable to use data for multiple objectives, it can be difficult to meet statistical assumptions when the data are re-used for a different purpose. For example, a multispecies survey may be stratified according to the distribution of one or more of the most commercially valuable species collected. An example is the stratification of Pacific west coast bottom trawl surveys in 1980, 1983, and 1986, which were focused to improve the precision of canary and yellowtail rockfish abundance estimates (Weinberg et al.²). If the stratification used was not effective for decreasing the variance of abundance estimates for other species, treating the data as if they were haphazardly collected, recognizing that the estimator may be biased, and poststratifying the data by habitat variables that are closely related to the

⁴ Goddard, P., and G. Walters. 1998. 1995 bottom trawl survey of the eastern Bering Sea continental shelf. AFSC Processed Report 98-08, 170 p. Resource Assessment and Conservation Engineering Division, Alaska Fisheries Science Center, NMFS, NOAA, 7600 Sand Point Way N.E., Seattle, Washington, 98115.

⁵ Lauth, R. R., M. E. Wilkins, and P.A. Raymore Jr. 1997. Results of trawl surveys of groundfish resources of the West Coast upper continental slope from 1989 to 1993. NOAA Tech. Memo. NMFS-AFSC-79, 342 p. National Technical Information Service, U.S. Department of Commerce, 5285 Port Royal Road, Springfield, Virginia 22161.

⁶ Halliday, R. G. 1970. 4T-V-W haddock: recruitment and stock abundance in 1970–72. ICNAF Res. Doc 70/75, 12 p. Approved for citation by Tissa Amaratunga, Deputy Executive Secretary, Northwest Atlantic Fisheries Organization. [Available from the Secretariat Library, Northwest Atlantic Fisheries Organization, 2 Morris Drive, Burnside Industrial Park, Dartmouth, Nova Scotia, Canada, B3B 1K8.]

distribution of the other species may be a beneficial way to make multiple uses of the data. Although the post-stratified estimator may be biased, poststratification may provide large gains in precision and a decrease in bias in relation to an unstratified estimator. Large increases in precision may be worth the acceptance of some bias.

Multispecies surveys are often not optimal for estimating the abundance of individual species but are often necessary because of limited time and financial resources. As a result, researchers need to explore alternative sampling and analysis designs to increase the precision of individual species abundance estimates (NRC, 2000). Poststratification is a method that can be applied to any number of species by using a wide range of habitat and other variables that can be stratified. Because of the dramatic increase in habitat information that is likely to be collected in response to the expanded emphasis in the Magnuson-Stevens Act (NRC, 2000) and because of the adaptability of poststratification for handling a multitude of types of data sets, the method of poststratification may provide increased usefulness for scientific researchers.

Acknowledgments

We thank Eric Munk and National Marine Fisheries Service Kodiak Laboratory for the vessel and field assistance from 1993 to 1996 and Bruce Short for field assistance in 1991 and 1992. Additionally, we thank Brenda Holladay, Franz Mueter, Brad Allen, Ed Roberts, and Cindy VanDamm, who helped with the fieldwork for this project, and Franz Mueter, Michael Simpkins, Robert Foy, and Arny Blanchard for constructive advice. For critical review of this article, we thank Milo Adkison, Alison Banks, Allison Barns, Cathy Coon, Judy Hamilton, Sue Hills, Heather Patterson, Andy Seitz, Dana Thomas, Albert Tyler, and other anonymous reviewers. This project was funded by Saltonstall-Kennedy NOAA (contracts number NA16FD021601, NA26FD0156, NA47FD0351), Minerals Management Service through the University of Alaska Coastal Marine Institute (task order numbers 11983, 12041, 18445), and the Rasmuson Fisheries Research Council.

Literature cited

- Anganuzzi, A. A. and S. T. Buckland.
1989. Reducing bias in trends in dolphin abundance, estimated from tuna vessel data. *Rep. Int. Whal. Comm.* 39:323-334.
- Azarovitz, T. R.
1981. A brief historical review of the Woods Hole Laboratory trawl survey time series. *In* Bottom trawl surveys (W. G. Doubleday and D. Rivard, eds.), p. 62-67. *Can. Spec. Publ. Aquat. Sci.* 58.
- Bernard, D. R., A. E. Bingham and M. Alexandersdottir.
1998. Robust harvest estimates from on-site roving-access creel surveys. *Trans. Am. Fish. Soc.* 127:481-495.
- Buckland, S. T. and A. A. Anganuzzi.
1988. Estimated trends in abundance of dolphins associated with tuna in the eastern tropical Pacific. *Rep. Int. Whal. Comm.* 38:411-437.
- Burke, J. S., J. M. Miller and D. E. Hoss.
1991. Immigration and settlement pattern of *Paralichthys dentatus* and *P. lethostigma* in an estuarine nursery ground, North Carolina, U.S.A. *Neth. J. Sea Res.* 27(3/4):393-405.
- Cochran, W. G.
1977. Sampling techniques, 3rd ed., 413 p. John Wiley & Sons, Inc., New York, NY.
- Fiedler, P. C., and S. B. Reilly.
1994. Interannual variability of dolphin habitats in the eastern tropical Pacific. II: Effects on abundances estimated from tuna vessel sightings, 1975-1990. *Fish. Bull.* 92:451-463.
- Friedland, K. D., J.-D. Dutil, and T. Sadusky.
1999. Growth patterns in postsmolts and the nature of the marine juvenile nursery for Atlantic salmon, *Salmo salar*. *Fish. Bull.* 97:472-481.
- Gadomski, D. M., and S. M. Caddell.
1991. Effects of temperature on early-life-history stages of California Halibut *Paralichthys californicus*. *Fish. Bull.* 89:567-576.
- Gunderson, D. R. and I. E. Ellis.
1986. Development of a plumb staff beam trawl for sampling demersal fauna. *Fish. Res.* 4:35-41.
- Hall, M. A. and S. D. Boyer.
1988. Incidental mortality of dolphins in the eastern tropical Pacific tuna fishery in 1986. *Rep. Int. Whal. Comm.* 38:439-441.
- Halliday, R. G., and P. A. Koeller.
1981. A history of Canadian groundfish trawling surveys and data usage in ICNAF Divisions 4TVWX. *In* Bottom trawl surveys (W. G. Doubleday and D. Rivard, eds.), p. 27-41. *Can. Spec. Publ. Fish. Aquat. Sci.* 58.
- Keselman, H. J.
1976. A power investigation of the Tukey multiple comparison statistic. *Educ. Psychol. Meas.* 35:97-104.
- Koeller, P. A.
1981. Distribution and sampling variability in the southern Gulf of St. Lawrence groundfish surveys. *In* Bottom trawl surveys (W. G. Doubleday and D. Rivard, eds.), p. 194-217. *Can. Spec. Publ. Fish. Aquat. Sci.* 58.
- Krebs, C. J.
1989. Ecological methodology, 654 p. HarperCollins Publishers, New York, NY.
- Mueter, F. J., and B. L. Norcross.
1999. Linking community structure of small demersal fishes around Kodiak Island, Alaska, to environmental variables. *Mar. Ecol. Prog. Ser.* 190:37-51.
- Murawski, S. A., and J. T. Finn.
1988. Biological bases for mixed-species fisheries: species co-distribution in relation to environmental and biotic variables. *Can. J. Fish. Aquat. Sci.* 45:1720-1735.
- NRC (National Research Council).
2000. Improving the collection, management, and use of marine fisheries data, 222 p. Ocean Studies Board, Commission on Geosciences, Environment, and Resources. National Academy Press, Washington, D.C., MD.
- Norcross, B. L., A. Blanchard, and B. A. Holladay.
1999. Comparison of models for defining nearshore flatfish nursery areas in Alaskan waters. *Fish. Oceanogr.* 8(1):50-67.

- Norcross, B. L., B. A. Holladay, and F. J. Muter.
1995. Nursery area characteristics of pleuronectids in coastal Alaska, USA. *Neth. J. Sea Res.* 34(1-3):161-175.
- Norcross, B. L., F. J. Muter, and B. A. Holladay.
1997. Habitat models for juvenile pleuronectids around Kodiak Island, Alaska, USA. *Fish. Bull.* 95:504-520.
- Orr, J. W., and A. C. Matarese.
2000. Revision of the genus *Lepidopsetta* Gill, 1862 (Teleostei: Pleuronectidae) based on larval and adult morphology, with a description of a new species from the North Pacific Ocean and Bering Sea. *Fish. Bull.* 98:539-582.
- Pearcy, W. G.
1978. Distribution and abundance of small flatfishes and other demersal fishes in a region of diverse sediments and bathymetry off Oregon. *Fish. Bull.* 76:629-640.
- Perry, R. L., and S. J. Smith.
1994. Identifying habitat associations of marine fishes using survey data: an application to the Northwest Atlantic. *Can. J. Fish. Aquat. Sci.* 51:589-602.
- Pitt, T. K., R. Wells, and W. D. McKone.
1981. A critique of research vessel otter trawl surveys by the St. John's Research and Resource Services. In *Bottom trawl surveys* (W. G. Doubleday and D. Rivard, eds.), p. 42-61. *Can. Spec. Publ. Fish. Aquat. Sci.* 58.
- Pollock, K. H., C. M. Jones, and T. L. Brown.
1994. Angler survey methods and their applications in fisheries management, 371 p. *Am. Fish. Soc. Spec. Publ.* 25, Bethesda, MD.
- Powell, L. A., W. R. Clark, and E. E. Klaas.
1995. Using post-release stratification to detect heterogeneity in mallard survival. *J. Wildl. Manage.* 59(4):683-690.
- Quinn, T. J., II.
1985. Sampling considerations. In *Fisheries dynamics: harvest management and sampling* (P. R. Mundy, T. J. Quinn II, and R. B. Deriso, eds.), 60 p. Washington Sea Grant Tech. Rep. 85-01. Seattle, WA.
- Reichert, M. J. M., and H. W. van der Veer.
1991. Settlement, abundance, growth and mortality of juvenile flatfish in a subtropical tidal estuary (Georgia, U.S.A.). *Neth. J. Sea Res.* 27(3/4):375-391.
- Reilly, S. B., and P. C. Fiedler.
1994. Interannual variability of dolphin habitats in the eastern tropical Pacific. I: Research vessel surveys, 1986-1990. *Fish. Bull.* 92:434-450.
- Rogers, S. I.
1992. Environmental factors affecting the distribution of sole (*Solea solea* (L.)) within a nursery area. *Neth. J. Sea Res.* 29(1-3):153-161.
- Scheaffer, R. L., W. Mendenhall III, and L. Ott.
1996. Elementary survey sampling, 5th ed., 501 p. Duxbury Press, Belmont, CA.
- Scott, B.
1995. Oceanographic features that define the habitat of Pacific Ocean perch, *Sebastes alutus*. *Fish. Oceanogr.* 4(2):147-157.
- Surfer.
1995. *Surfer user's guide*, vers. 6, 530 p. Golden Software, Inc., Golden, CO.
- Tanda, M.
1990. Studies on burying ability in sand and selection to the grain size for hatchery-reared marbled sole and Japanese flounder. *Nippon Suisan Gakkaishi* 56:1543-1548.
- Taylor, C. C.
1953. Nature of variability in trawl catches. *Fish. Bull.* 54:145-166.
- Taylor, L. R., I. P. Woivod, and J. N. Perry.
1978. The density-dependence of spatial behaviour and the rarity of randomness. *J. Anim. Ecol.* 47:383-406.
- Thompson, S. K.
1992. *Sampling*, 343 p. John Wiley & Sons, Inc., New York, NY.
- Walsh, S. J.
1992. Factors influencing distribution of juvenile yellowtail flounder (*Limanda ferruginea*) on the Grand Bank of Newfoundland. *Neth. J. Sea Res.* 29(1-3):193-202.
- Zar, J. H.
1996. *Biostatistical analysis*, 662 p. Prentice Hall, Upper Saddle River, NJ.

Abstract—Reproductive data collected from porbeagle, shortfin mako, and blue sharks caught around New Zealand were used to estimate the median length at maturity. Data on clasper development, presence or absence of spermatophores or spermatozuogmata, uterus width, and pregnancy were collected by observers aboard tuna longline vessels. Direct maturity estimates were made for smaller numbers of sharks sampled at recreational fishing competitions. Some data sets were sparse, particularly over the vital maturation length range, but the availability of multiple indicators of maturity made it possible to develop estimates for both sexes of all three species.

Porbeagle shark males matured at 140–150 cm fork length and females at about 170–180 cm. New Zealand porbeagles therefore mature at shorter lengths than they do in the North Atlantic Ocean. Shortfin mako males matured at 180–185 cm and females at 275–285 cm. Blue shark males matured at about 190–195 cm and females at 170–190 cm; however these estimates were hampered by small sample sizes, difficulty obtaining representative samples from a population segregated by sex and maturity stage, and maturation that occurred over a wide length range. It is not yet clear whether regional differences in median maturity exist for shortfin mako and blue sharks.

Length at maturity in three pelagic sharks (*Lamna nasus*, *Isurus oxyrinchus*, and *Prionace glauca*) from New Zealand

Malcolm P. Francis

National Institute of Water and Atmospheric Research
301 Evans Bay Parade
Greta Point
Wellington, New Zealand
E-mail address: m.francis@niwa.co.nz

Clinton Duffy

Department of Conservation
Private Bay 68908
Auckland, New Zealand

The attainment of sexual maturity in sharks is a major developmental milestone which has a large impact on their distribution, behavior, and biology. Immature sharks often associate with each other regardless of sex, but after maturity sexual segregation is the norm. Mature males and females may come together only to mate, resulting in movements that may range from small-scale aggregation of dispersed individuals to long-range migrations over thousands of kilometers.

The process of maturation, and the subsequent need to channel energy into reproduction, affect the growth rate of at least some shark species. Immature male and female porbeagles grow at the same rate, and the growth rate of both sexes slows at maturity; however females mature at a greater age than males and therefore their period of fast immature growth lasts longer and they grow larger than males (Natanson et al., 2002).

The maximum reproductive lifespan of a shark species is the time elapsed between the age at maturity and the maximum age. In conjunction with the duration of the reproductive cycle, the reproductive lifespan determines the maximum number of litters a female shark can produce in her lifetime. Population modeling indicates that shark species that mature at a young age have a greater capacity to recover from exploitation than

sharks that mature later (Smith et al., 1998). Thus age at maturity is a crucial factor influencing the productivity of a species.

Age at maturity can be estimated directly from paired age-and-maturity estimates taken from the same shark, but often such data are not available, or are too few to provide precise estimates. Consequently it is often necessary to estimate age at maturity indirectly from length at maturity and a growth curve.

In the present study we estimate the length at maturity for three species of large pelagic sharks in New Zealand waters: porbeagle (*Lamna nasus* (Bonnaterre, 1788)), shortfin mako (*Isurus oxyrinchus* Rafinesque, 1810), and blue (*Prionace glauca* (Linnaeus, 1758)) sharks. These species are commonly caught by tuna longliners fishing around New Zealand (Francis et al., 2001). Longline fishing effort declined from a high of over 25 million hooks per year in the early 1980s, to a low of 2–4 million hooks in 1995–98, largely because of a reduction in the number of foreign licensed vessels (Francis et al., 2001). Since then, the domestic longline fleet has expanded, and fishing effort exceeded 10 million hooks in 2001–02 (Ayers et al., 2004). Because of concern over the sustainability of the catches of both target and nontarget species in this fishery, the New Zealand Ministry

of Fisheries introduced individual transferable quotas for a number of pelagic species, including the three sharks, in October 2004.

Despite the panglobal distributions of porbeagle, shortfin mako, and blue sharks, and their importance in the catches of pelagic longline fisheries worldwide, comparatively little effort has been devoted to estimating their length (or age) at maturity. In the northwest Atlantic Ocean, the length at maturity of male and female porbeagles has been well determined (Jensen et al., 2002), but preliminary data from the southwest Pacific Ocean indicate that females mature at a much smaller length there (Francis and Stevens, 2000). Mollet et al. (2000) found significant differences in the length at maturity of female shortfin makos between the Northern and Southern hemispheres; however there is little information on the length at maturity of male makos (Stevens, 1983). Blue sharks have been studied in a number of regions worldwide (Pratt, 1979; Stevens, 1984; Hazin et al., 1994; Nakano, 1994; Castro and Mejuto, 1995), but size and sex segregation have made it difficult to obtain representative samples of both sexes from which to determine length at maturity.

In the southwest Pacific Ocean, estimates of length at maturity are lacking or uncertain for at least one sex of all three species. Although all species make long distance movements, and presumably have wide-ranging stocks, the interhemispheric differences in length at maturity reported for female porbeagles and shortfin makos indicate that it is not safe to transfer estimates from one region to another. The aim of the present study is to develop region-specific estimates of length at maturity for male and female porbeagle, blue and shortfin mako sharks, and to determine whether this parameter varies globally. These results will contribute to efforts to determine the productivity and stock status of pelagic sharks in New Zealand waters.

Materials and methods

Data sources

Reproductive data were collected from two main sources. The first consisted of sharks sampled by the authors at recreational fishing competitions, or occasionally sharks retained by commercial fisheries or research vessels. The second source consisted of data and occasionally embryos and female reproductive tracts collected by Ministry of

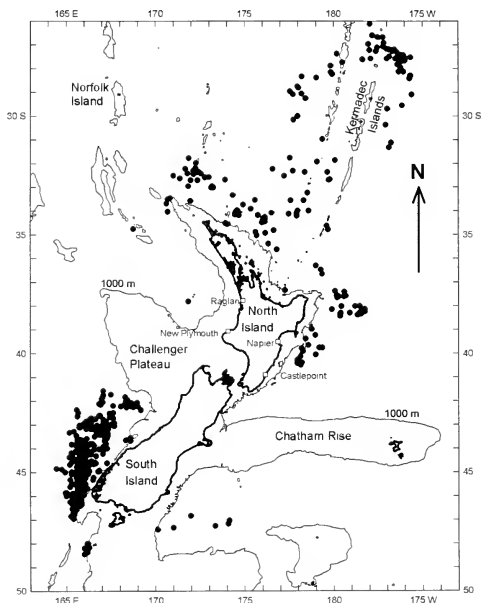


Figure 1

Start-of-set positions of tuna longline sets during which observers sampled porbeagle (*Lamna nasus*), shortfin mako (*Isurus oxyrinchus*), and blue (*Prionace glauca*) sharks. Also shown are the North Island ports where sharks landed during fishing competitions were sampled.

Fisheries observers aboard commercial tuna longline vessels (Fig. 1). Sharks obtained from fishing competitions provided the opportunity to measure a wide range of reproductive parameters on relatively small samples, whereas sharks observed on tuna longline vessels provided large samples but limited reproductive data.

Sharks obtained from fishing competitions

Competition sharks consisted mainly of makos and blue sharks sampled at fishing competitions around the North Island (Fig. 1). Most sharks were sampled from the Hawke Bay competition held annually in February or March from the port of Napier. Other significant competitions were sampled at Castlepoint, Raglan, and New Plymouth. All except two of the competition sharks were collected in summer (January–March) and samples

spanned the period from 1986 to 2004. In the early years, only data on length, sex, weight, and maturity were collected. In later years, detailed reproductive data were also collected. The following length measurements were made as point-to-point straight line distances to the whole centimeter below actual length:

- Total length (TL_{nat}): tip of snout to a perpendicular dropped from the tip of tail to the midline (with the tail in the natural position);
- Total length (TL_{dex}): tip of snout to tip of tail (with the tail flexed towards the midline to provide maximum extension);
- Fork length (FL): tip of snout to fork in the tail;
- Precaudal length (PCL): tip of snout to the upper precaudal pit (mako and porbeagle sharks) or the origin of the upper caudal lobe (blue sharks).

Total weight was measured on accurate scales provided at the fishing competitions, on research vessels, or in commercial fish processing sheds.

In males, inner clasper length was measured between the anterior margin of the cloaca and the posterior clasper tip, and expressed as a percentage of fork length:

$$\text{Clasper length index (CLI)} = 100 (\text{clasper length}/FL).$$

The degree of clasper calcification and development was determined and included an assessment of whether the terminal cartilages could be splayed open, whether a spur was present and erupted, and whether the entire clasper could be rotated. In some males sampled in later years, the degree of development of the testes, epididymis, and ampulla at the posterior end of the epididymis was also recorded, and occasionally testes were weighed and measured (following dissection from the epigonal organ if necessary). The presence or absence of spermatophores or spermatozeugmata in the ampulla epididymis was noted. (Spermatophores are masses of encapsulated sperm, and they are found in porbeagle and mako sharks; spermatozeugmata are unencapsulated masses of naked sperm that are found in blue sharks [Pratt and Tanaka, 1994]).

In females, the reproductive system was examined, and in later years a number of measurements were taken. Uterus width was measured near the middle of the body cavity and expressed as a percentage of fork length:

$$\text{Uterine width index (UWI)} = 100 (\text{uterus width}/FL).$$

The maximum diameter of ova, where they were sufficiently developed to be visible in the ovary, was recorded, and the diameter of the oviducal gland was measured. Ovarian dimensions and weight were mea-

sured after dissection (if necessary) from the epigonal organ. Any contents of the uteri were noted; embryos were measured and sex was determined. The presence or absence of a hymen (cloacal membrane occluding the vaginal opening) was recorded.

For both males and females, a direct assessment of maturity (hereafter called direct maturity) was made by using all the available reproductive data. A three-stage classification scheme was used: immature, maturing, and mature. Mature sharks were defined as those in which the reproductive system was judged to be fully functional and capable of delivering reproductive products. For analysis purposes, maturing sharks were grouped with immature sharks.

Sharks sampled by observers

Observers sampled tuna longline sets from around the New Zealand region (Fig. 1). Data from blue and mako sharks were obtained throughout the sampled area, but porbeagles came mainly from the southwestern South Island. Most sharks were sampled in autumn–winter (April–July) over the period 2001–2003. The “standard” length measurement for sharks was FL, but frequently observers also recorded TL_{nat} or PCL.

Observers were provided with instructions and photographs indicating the reproductive data they needed to collect, but they were not provided with any practical training. The main data they collected were the following: inner clasper lengths, presence or absence of spermatophores or spermatozeugmata in the ampulla epididymis (for males); uterus width, maximum ovum diameter, and whether the shark was pregnant or not (for females).

Examination of observer pregnancy records for blue sharks indicated numerous probable errors: uterus widths from sharks scored as pregnant were frequently less than 18 mm, which seems implausible considering that ova are ovulated at about 18 mm, and pregnant sharks are unlikely to have such small uteri (Pratt, 1979; Natanson¹). This problem was apparent for several observers, some of whom were very experienced (although they had no previous experience examining shark reproductive systems). We suspect that they may have scored some female blue sharks as pregnant if the ovary contained large yolky ova (this problem did not occur for mako and porbeagle sharks, which have much smaller ovarian ova). We therefore used observer blue shark pregnancy records only if they were supported by appropriate comments on the data sheet (e.g., mention of embryos or ovulated eggs in uteri), or if the observers retained embryos or intact uteri for us to examine.

Observers did not assess direct maturity; therefore we were unable to derive direct maturity ogives for observer sharks.

¹ Natanson, L. 2004. Unpubl. data. National Marine Fisheries Service, 28 Tarzwell Drive, Narragansett, Rhode Island 02882-1152.

Table 1

Regression equations used to convert shark lengths reported in the literature. r^2 = the coefficient of determination; n = sample size. Measurement method acronyms are defined in the "Materials and methods" section, except that CFL = curved fork length and CTL = curved total length (both measured over the curve of the body).

Species	Regression equation	r^2	n	Data range (cm)	Source
Porbeagle	$FL = -6.943 + 0.893 TL_{nat}$	0.997	103	61–181 FL	This study
	$FL = 0.90 + 0.95 CFL$	0.997	172	83–253 FL	S. Campana ²
Mako	$CFL = -1.7101 + 0.9286 CTL$	0.997	199	65–338 CFL	Kohler et al., 1995
	$FL = 0.973 + 0.968 CFL$	0.999	30	113–287 FL	This study
	$FL = 0.766 + 1.100 PCL$	0.997	999	61–346 FL	This study
	$FL = 0.821 + 0.911 TL_{nat}$	0.993	399	70–346 FL	This study
Blue	$FL = -0.90 + 0.98 CFL$	0.99	789	123–286 FL	S. Campana ²
	$FL = -1.615 + 0.838 TL_{nat}$	0.990	273	50–270 FL	This study
	$FL = 0.745 + 1.092 PCL$	0.998	12,657	34–326 FL	This study

¹ Refers to footnote 2 in the general text.

Data analysis

For each shark species and sex, we were interested in determining the length at which 50% of the individuals in a population reached full sexual maturity. That length is the median length at maturity, hereafter referred to as "median maturity."

Many shark species show abrupt transitions in the sizes of reproductive organs near length at maturity. To locate such transitions in clasper length, we fitted "split" linear regressions to CLI data plotted against FL. Split regressions consist of two simple linear regressions fitted to different nonoverlapping data ranges that meet at a point called the breakpoint (Kováč et al., 1999). A split regression has the form

$$CLI = f(FL - p) + h \text{ for } FL < p$$

$$CLI = g(FL - p) + h \text{ for } FL \geq p,$$

where f and g are slope parameters for the two limbs of the regression, and h and p are the y-axis and x-axis coordinates of the breakpoint, respectively. The parameters f , g , h , and p were estimated by least squares by using the curve fitting routine in the Sigmaplot statistical and graphing package (Sigmaplot, vers. 9.01, Systat Software Inc., Richmond, CA). The length at the breakpoint was corrected for downward rounding of FL by adding 0.5 cm.

Maturity ogives were fitted to the direct maturity data separately by sex by using probit analysis (Pearson and Hartley, 1962). The analyses were performed on individual FL measurements, but we also calculated the proportions of mature individuals in 10-cm length classes to illustrate the trends. Probit analysis assumes that the length at which a randomly selected fish reaches maturity is normally distributed. Two pa-

rameters, the mean and standard deviation of the normal distribution, were fitted. Each maturity ogive is the cumulative distribution function for the associated normal distribution. The probit function was fitted by maximum likelihood, and 95% confidence limits were estimated by the bootstrap method. The mean of the normal distribution is an estimate of the median maturity, and it was corrected for downward rounding of FL by adding 0.5 cm.

All shark length measurements provided in the present study are FL, unless otherwise stated. For comparison with our results, we converted measurements from the literature to FL where necessary using the regression equations in Table 1. Literature reports of total length were assumed to be TL_{nat} unless otherwise stated. Scientists working on sharks in the northeastern United States, and eastern Canada have typically measured lengths over the curve of the body rather than as straight line distances (Natanson³; Campana²; Pratt³), notwithstanding some published statements to the contrary (Pratt, 1979; Kohler et al., 1995).

Results

Porbeagle shark

In male porbeagles, CLI showed two strong inflection points: the first at about 110 cm, and the second, esti-

² Campana, S. E. 2004. Personal commun. Bedford Institute of Oceanography, P.O. Box 1006, Dartmouth, Nova Scotia, Canada B2Y 4A2.

³ Pratt, H. L. 2004. Personal commun. Mote Marine Laboratory, 24244 Overseas Highway, Summerland Key, FL 33042.

mated by split linear regression fitted to sharks longer than 110 cm, at 142.7 cm (95% confidence interval (CI) 140.7–144.7 cm) (Fig. 2). Thus rapid elongation of the claspers began at about 110 cm and was completed by 143 cm. Spermatophores first appeared in the posterior reproductive tract at 135 cm and by about 152 cm 50% of males contained spermatophores. The percentage of sharks with spermatophores peaked at 165 cm (82% of males) and then declined to about 50%, although sample sizes were small in the longer length groups (Table 2).

In females, UWI began increasing at a length of about 145 cm, but many larger, nonpregnant sharks showed no expansion of the uteri (Fig. 3). Three females with UWI of about 4–5% were postpartum, and two with UWI about 11% and one with UWI of about 4% were pregnant. Pregnant females measured 167–202 cm (mean 184 cm, $n=55$). Of 19 females longer than 175 cm that were scored by observers for pregnancy, 10 (53%) were pregnant, two (11%) were postpartum, and seven (37%) were resting (or possibly immature).

Apart from a 185-cm pregnant female, all whole porbeagles examined by us were immature; therefore no attempt was made to estimate maturity directly.

Shortfin mako shark

CLI showed two strong inflection points in male makos; the first at about 140 cm and the second (estimated by split linear regression) at 185.1 cm (CI 182.5–187.7 cm) (Fig. 4). The smallest male with spermatophores was 136 cm, but this measurement was an outlier and may have been an error; the next smallest was 156 cm. Fifty percent of males contained spermatophores by 178 cm, and 100% by about 235 cm. Sample sizes were reasonable over the transition range but small above 230 cm (Table 2).

Male makos examined by us showed little overlap in length between immature and mature sharks (Fig. 4), but sample sizes were small in all length classes (Table 2). The smallest mature male was 182 cm and the largest immature male was 183 cm long. The median maturity estimated by probit analysis was 182.9 cm (CI 180.7–185.1 cm) (Fig. 4).

In females, UWI began increasing at a length of about 275 cm, and all larger sharks had expanded uteri (Fig. 5). Only one pregnant female mako has been recorded from New Zealand waters, and it was 290 cm FL (Duffy and

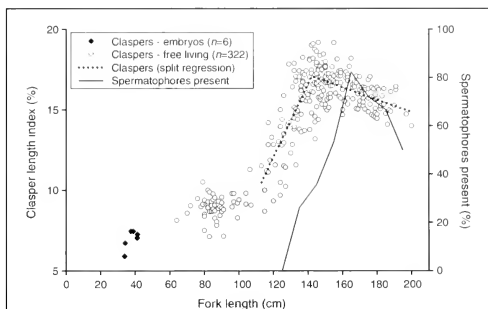


Figure 2

Maturation of male porbeagle sharks (*Lamna nasus*): variation in clasper development and presence of spermatophores in the reproductive tract.

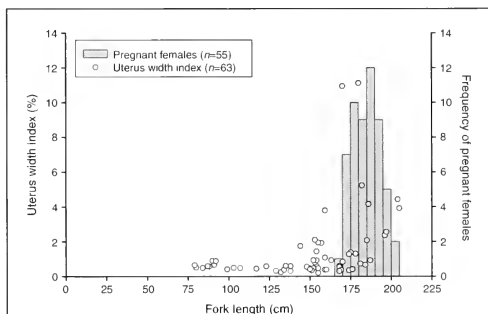


Figure 3

Maturation of female porbeagle sharks (*Lamna nasus*): variation in uterus width index, and length-frequency distribution of pregnant females.

Francis, 2001); no uterus width measurement was available for that shark. The remaining makos over 275 cm were either postpartum or resting. The maximum ovum diameter began increasing in sharks longer than 250 cm (in shorter sharks, ova were barely visible or were invisible) (Fig. 6). The diameter of the oviducal gland increased abruptly between 250 and 270 cm, but ovary dimensions showed no abrupt change in size (Fig. 6).

Median maturity was estimated directly from a sample of 88 females (Table 3). The smallest mature female

Table 2

Sample sizes by 10-cm length class for the assessment of maturity in male porbeagle, mako, and blue sharks.

Length class midpoint (cm)	Shortfin mako shark				
	Porbeagle shark		Blue shark		Direct maturity
	Spermatophores	Spermatophores	Spermatophores	Spermatozeugmata	
45	0	0	0	0	1
55	0	0	0	0	3
65	0	0	0	0	2
75	2	0	0	0	0
85	15	0	1	1	0
95	4	0	0	2	1
105	0	3	1	2	0
115	2	3	3	0	0
125	8	3	0	1	0
135	23	4	8	1	0
145	28	4	11	3	1
155	30	9	4	6	5
165	17	10	6	13	3
175	18	19	3	4	6
185	6	16	7	20	4
195	4	15	1	21	6
205	1	27	1	18	6
215	0	19	4	15	4
225	0	14	1	12	1
235	0	8	0	20	8
245	0	5	1	26	2
255	0	3	0	19	1
265	0	0	0	11	1
275	0	1	0	6	2
285	0	0	0	2	0
295	0	0	0	1	1
Total	158	163	52	204	58

Table 3

Sample sizes by 10-cm length class for the assessment of maturity in female mako and blue sharks.

Shortfin mako shark		Blue shark	
Length class midpoint (cm)	Direct maturity	Length class midpoint (cm)	Direct maturity
55	0	215	10
65	0	225	10
75	0	235	6
85	0	245	9
95	0	255	4
105	0	265	3
115	2	275	1
125	2	285	2
135	2	295	3
145	10	305	1
155	6	315	0
165	3	325	3
175	1	335	2
185	3	345	1
195	0	Total	88
205	4		26

was 274 cm and the longest immature female was 300 cm. Median maturity was estimated by probit analysis to be 280.1 cm (CI 267.5–292.9 cm), but sample sizes were very small over the transitional range (Fig 5). The nonoverlap of the CIs between males and females showed that median maturity differs significantly between the sexes.

Blue shark

The relationship between CLI and FL was essentially linear in blue sharks, and no apparent inflections were evident (Fig. 7). The smallest male with spermatozeugmata was 164 cm; 50% of males contained spermatozeugmata by 194 cm, and 100% by about 260 cm.

Samples of male blue sharks examined by us were small (Table 2). Maturation occurred over a wide length range: the smallest mature male was 157 cm and the largest immature male was 237 cm long. The direct estimate of median maturity was correspondingly variable (192.1 cm, CI 178.1–206.3 cm) (Fig. 7).

The UWI increased abruptly above about 170 cm in some sharks, all of which were pregnant (Fig. 8). Other non-pregnant sharks up to about 220 cm FL, which were presumably subadults, had UWIs less than 2%. Pregnant females ranged from 166 to 252 cm (mean 203 cm) (Fig. 8).

Only 26 females were available for direct maturity estimation (Table 3). The smallest recorded mature female was 142 cm, but this seems exceptional; the next smallest was 172 cm. The longest immature female was 185 cm. The number of sharks in the maturation length range was inadequate for determining median maturity (Table 3), although we have shown the probit analysis ogive in Figure 8.

Discussion

Maturity estimates

To be sexually mature, a male shark must be able to produce viable sperm and have the means to deliver them to a female. Similarly, females must be able to produce viable eggs and nourish the developing embryos through to parturition. An assessment of the degree of development of all parts of the reproductive system and the presence or absence of reproductive products is the best way to determine sexual maturity. We used

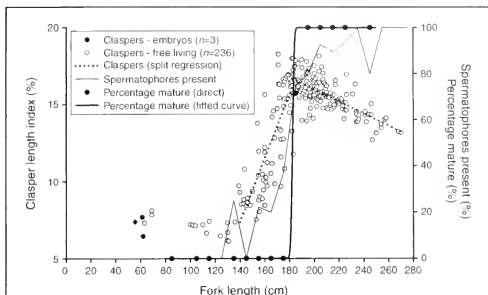


Figure 4

Maturation of male shortfin mako sharks (*Isurus oxyrinchus*): variation in clasper development, presence of spermatozeugmata in the reproductive tract, and direct maturity estimation determined from a suite of maturity indicators.

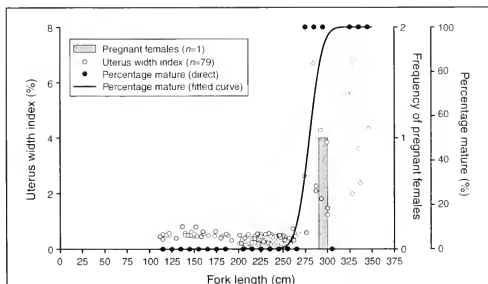


Figure 5

Maturation of female shortfin mako sharks (*Isurus oxyrinchus*): variation in uterus width index, and direct maturity estimation from a suite of maturity indicators. The only pregnant female recorded from New Zealand waters is also indicated.

this approach to score the maturity status of individual sharks and thereby derive direct median maturity estimates. However, the sample sizes available for this approach were sometimes small, and confidence limits ranged from unrealistically low (because of lack of overlap of immature and mature sharks) to high; therefore it was not possible to rely entirely on these estimates.

We supplemented our direct maturity estimates with measurements or assessments (made by observers) of some key components and products of the reproductive

system. The presence or absence of spermatophores or spermatozeugmata is a good indicator of the ability of a male to produce viable sperm, but it is not infallible: such structures sometimes lack viable sperm (Pratt and Tanaka, 1994). Furthermore, male reproductive products may not be present year-round: blue sharks appear to have a seasonal cycle of spermatozeugmata production in the western central Atlantic (Hazin et al., 1994), although Pratt (1979) found no evidence of a cycle in the western North Atlantic. Thus the presence of spermatophores and spermatozeugmata does not

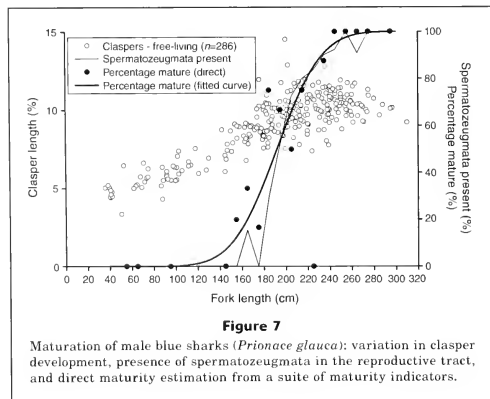
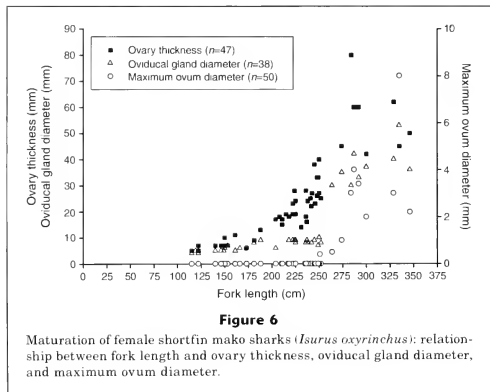
necessarily confirm reproductive viability, and their absence does not confirm immaturity. Similarly, fully calcified claspers that can be rotated, splayed open, and possess an anchoring mechanism may confer an ability to mate, but they do not necessarily confirm an ability to deliver viable products; however the lack of fully developed claspers presumably does prevent successful copulation.

In the present study, either the length at which clasper development was completed in half the male population, or the length at which 50% of males possessed spermatophores or spermatozeugmata, whichever was higher, provided an estimate of the lower bound of the median maturity. The actual median maturity may be higher than this estimate if some males had reproductive products that lacked viable sperm, or if some other feature of the reproductive system (e.g., the siphon system) was insufficiently developed to enable delivery of sperm to the female.

An analogous argument applies to female sharks. Full development of the uterus and oviducal gland, and production of vitellogenic ovarian ova, are all required for successful reproduction. Expansion of the uterus, as measured here by UWI, may not be a sufficient condition by itself. Thus the length at which half the female population had expanded uteri places a lower bound on the median maturity.

The smallest length at which females were pregnant, and the length-frequency distributions of pregnant females, are not by themselves good indicators of median maturity. A better indicator would be the length at which half the females in a population first become pregnant, but this is impossible to determine. Furthermore, pregnancy estimates could be confounded by unrepresentative sampling of a population that may be segregated by reproductive status and by nonparticipation of some females during breeding because they are "resting" between pregnancies. Nevertheless, pregnancy absolutely confirms maturity; therefore it is a useful adjunct to other measures of maturity.

The presence or absence of a hymen has been used in some studies to indicate maturity. However it should not be used for that purpose because adolescent (premature) mating occurs in at least some species of sharks, including blue sharks (Pratt, 1979). Furthermore, the absence of a hymen may not even be a good indicator of mating: we observed



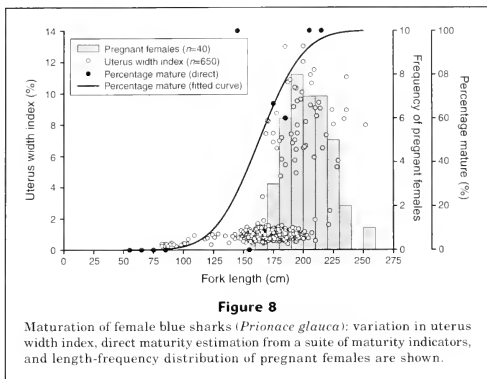


Figure 8

Maturation of female blue sharks (*Prionace glauca*): variation in uterus width index, direct maturity estimation from a suite of maturity indicators, and length-frequency distribution of pregnant females are shown.

Table 4

Summary of length at maturity indicators in porbeagle, shortfin mako, and blue sharks, and estimates of median length at maturity. Table entries are fork lengths in centimeters. Direct maturity estimates were derived by examination of a suite of maturity indicators. Italics indicate estimates based on small sample sizes over the maturation length range. "—" indicates that an estimate was not possible.

Sex	Maturity indicator	Porbeagle shark	Shortfin mako shark	Blue shark
Males	50% with spermatophores	152	178	194
	Rapid clasper elongation complete	143	185	—
	Direct maturity estimate	—	183	192
	Median length at maturity	140–150	180–185	190–195
Females	Rapid expansion of uterus begins	145	275	170
	First females pregnant	167	— ¹	166
	Direct maturity estimate	—	280	—
	Median length at maturity	170–180	275–285	170–190

¹ Only one pregnant female (290 cm FL) has been recorded from New Zealand.

some female shortfin makos in which the membrane was very thin and partially perforated, but had clearly not been damaged by copulation. We believe that the hymen disintegrates naturally with growth in makos; the same possibility was proposed for blue sharks by Pratt (1979).

Using a combination of our direct maturity estimates, and other indicators of maturity based on larger samples of sharks, we generated overall estimates of median maturity for both sexes of the three pelagic sharks (Table 4).

Porbeagle shark

In male porbeagles, the length at which 50% of sharks had spermatophores (152 cm) was longer than the length

at which clasper elongation was complete (143 cm) (Table 4). However the percentage of males having spermatophores did not reach 100% in the longer length groups (Fig. 2), indicating that some mature males were reproductively inactive. This finding is consistent with reports from the western North Atlantic that male porbeagles have a seasonal cycle of spermatophore production, with a minimum in winter–spring (Jensen et al., 2002). If some mature males lacked spermatophores, the length at which 50% of males had spermatophores in our study was probably greater than the median maturity. The lack of a direct maturity estimate limits our ability to estimate the median maturity, but it is likely in the range 140–150 cm.

Similarly, we have no direct estimate of female porbeagle maturity. There was a considerable gap between

the length at which rapid expansion of the uterus began (145 cm) and the length of the smallest pregnant female (167 cm). UWI values less than 2% occurred for females up to about 185 cm (Fig. 3), but this does not mean that a high proportion of females in this length group had narrow uteri; uterus width measurements were not available for most of our pregnant females and therefore large UWI values are underrepresented in Figure 3. Most pregnant females were 170–200 cm long. We estimate that median maturity in females is about 170–180 cm, but this estimate requires confirmation. It is essentially the same as that provided by Francis and Stevens (2000) for New Zealand and Australian porbeagles (their New Zealand data were a smaller subset of the data used in the present study).

Although our estimates of median maturity for both males and females are uncertain, it is clear that porbeagles from New Zealand mature at considerably smaller lengths than they do in the North Atlantic. In the western North Atlantic, males mature at about 166 cm and females at 208 cm (Jensen et al., 2002). Data from the eastern North Atlantic (Gauld, 1989; Ellis and Shackley, 1995) are insufficient to estimate length at maturity, but the pregnant females reported by Gauld (1989) were considerably longer (199–248 cm) than those from New Zealand.

Porbeagles from the North Atlantic also grow larger than those from New Zealand: in the North Atlantic, sharks longer than 200 cm are common (Gauld, 1989; Campana et al., 2001), whereas around New Zealand and Australia they are very rare (Francis et al., 2001; Stevens and Wayte⁴). Differences in length at maturity between the North Atlantic and New Zealand and the proportion of sharks in the longer length classes indicate the existence of separate populations in the two regions—a conclusion that is supported by the disjunct distribution of porbeagles in the Northern and Southern Hemispheres (Compagno, 2001).

Shortfin mako shark

Our direct maturity estimate for male makos (183 cm) was based on a small sample size, and the small overlap between the lengths of immature and mature sharks is implausible. However, the lengths at which clasper development was completed, and at which 50% of males had spermatophores, were similar to the direct estimate (Table 4). Median maturity for males is therefore about 180–185 cm.

Our direct maturity estimate for female makos (280 cm) was based on few sharks over the maturation length range but was consistent with the length at which rapid uterus expansion began (275 cm). Our best estimate of median maturity in females is 275–285 cm.

Stevens (1983) used the degree of clasper calcification and an inflection in clasper length to estimate the length at maturity of males from New South Wales as 176 cm. In South Africa, males were estimated to mature at 177–188 cm (Cliff et al., 1990), but very few immature sharks were available. Our estimate of median maturity in New Zealand males (180–185 cm) is therefore similar to those from elsewhere.

Mollet et al. (2000) reported lengths at maturity for female makos of 298 cm total length in the Northern Hemisphere and 273 cm total length in the Southern Hemisphere. However, some of the 25 cm difference was due to Northern Hemisphere measurements having been taken over the curve of the body and Southern Hemisphere measurements having been taken in a straight line. Using appropriate conversion regressions, their Northern Hemisphere median maturity is equivalent to 267 cm FL, and their Southern Hemisphere median maturity is equivalent to 248 cm FL. When Mollet et al.'s Southern Hemisphere data are analysed separately for two subregions, South Africa and Australia, the estimated lengths at maturity are 244 cm ($n=50$) and 254 cm ($n=32$) respectively (Mollet⁵). The former is consistent with Cliff et al.'s (1990) estimate of 243 cm for South Africa, and the latter is consistent with Stevens's (1983) estimate of 255 cm for eastern Australia (both those estimates were made from subsets of the data used by Mollet et al. [2000]).

Our estimate of median maturity in New Zealand females (275–285 cm) is substantially higher than Mollet's⁵ estimate for Australia (254 cm). Because tagged makos have moved between New Zealand and eastern Australia in both directions (Chan, 2001; Hartill and Davies, 2001; Holdsworth and Saul, 2003), we think it is unlikely that the difference is due to the presence of distinct populations in the two regions. We suspect that the difference is a result of possible length estimation errors (some of the Australian shark lengths were calculated from recorded weights, with a length-weight regression [Stevens, 1983; Mollet et al., 2000]), and the result of small sample sizes over the length range at maturation. For our direct maturity estimate, we had only 19 New Zealand sharks over the length range 240–290 cm, and Mollet⁵ had 15 sharks.

Interestingly, our estimate of median maturity in New Zealand females is also greater than Mollet et al.'s (2000) estimate for the western North Atlantic, thus removing the reported between-hemisphere difference. We believe that larger, accurately measured samples of female makos are required before definitive statements can be made about length at maturity in the various regions.

Blue shark

In male blue sharks from New Zealand, CLI lacked an inflection near the length of maturity—a feature that

⁴ Stevens, J. D., and S. E. Wayte. 1999. A review of Australia's pelagic shark resources. FRDC Proj. Rep. 98/107, 64 p. [Available from CSIRO Marine Research, PO Box 1538, Hobart, Tasmania 7001, Australia.]

⁵ Mollet, H. 2004. Personal commun. Moss Landing Marine Laboratories, 8272 Moss Landing Road, Moss Landing, CA 95039.

has also been reported elsewhere (Pratt, 1979; Hazin et al., 1994). Thus clasper length was not useful in estimating length at maturity. Our direct maturity estimate was similar to the length at which 50% of sharks had spermatozeugmata and indicated that median maturity occurs at about 190–195 cm (Table 4).

In females, maturation occurred over a wide length range, as reported elsewhere (Hazin et al., 1994). Taking into account the length distributions of pregnant females and females with low UWI values (Fig. 8), we believe median maturity is likely in the range 170–190 cm.

In other blue shark studies, estimation of the length at maturity has also been hindered by small sample sizes, or even a complete absence of immature or mature sharks. In the western North Atlantic, males mature at about 178 cm, and females at around the same length, although few mature females have been available (Pratt, 1979). In the Gulf of Guinea, Atlantic Ocean, 50% of females were pregnant at 180 cm (Castro and Mejuto, 1995). In Australian studies, a lack of immature sharks made it impossible to estimate maturity adequately (Stevens, 1984; Stevens and McLoughlin, 1991). In the North Pacific Ocean, 50% of males had spermatozeugmata at 166 cm and 50% of females were pregnant at 174 cm (Nakano, 1994). Thus worldwide estimates of maturity in blue sharks are similar to ours from New Zealand, except perhaps for a smaller length at maturity of males in the North Pacific. Unlike females in most species of sharks, female blue sharks do not appear to mature at a length greater than that for mature males.

Acknowledgments

We thank the Ministry of Fisheries for funding this study under research project TUN2002/01, and providing access to data collected by observers. Lynda Griggs (NIWA) assisted with data extracts and interpretation, and Chris Francis (NIWA) carried out the probit analyses. Lisa Natanson, Wes Pratt, Steve Campana, and Henry Mollet kindly provided unpublished data and advice on their interpretation.

Literature cited

- Ayers, D., M. P. Francis, L. H. Griggs, and S. J. Baird.
2004. Fish bycatch in New Zealand tuna longline fisheries, 2000–01 and 2001–02. N.Z. Fish. Assess. Rep. Rep. 2004/46. 47 p.
- Campana, S. E., L. Marks, W. Joyce, and S. Harley.
2001. Analytical assessment of the porbeagle shark (*Lamna nasus*) population in the Northwest Atlantic, with estimates of long-term sustainable yield. Can. Sci. Advisory Secretariat Res. Doc. 2001/067, 59 p.
- Castro, J. A., and J. Mejuto.
1995. Reproductive parameters of blue shark, *Prionace glauca*, and other sharks in the Gulf of Guinea. Mar. Freshw. Res. 46:967–973.
- Chan, R. W. K.
2001. Biological studies on sharks caught off the coast of New South Wales. Ph.D. diss., 323 p. Univ. New South Wales, Sydney, New South Wales, Australia.
- Cliff, G., S. F. J. Dudley, and B. Davis.
1990. Sharks caught in the protective gill nets off Natal, South Africa. 3. The shortfin mako shark *Isurus oxyrinchus* (Rafinesque). Sth Afr. J. Mar. Sci. 9:115–126.
- Compagno, L. J. V.
2001. Sharks of the world. An annotated and illustrated catalogue of shark species known to date. FAO Species Cat. Fishery Purposes 1, vol. 2, 269 p. FAO, Rome.
- Duffy, C., and M. P. Francis.
2001. Evidence of summer parturition in shortfin mako (*Isurus oxyrinchus*) sharks from New Zealand waters. N. Z. J. Mar. Freshw. Res. 35:319–324.
- Ellis, J. R., and S. E. Shackley.
1995. Notes on porbeagle sharks, *Lamna nasus*, from the Bristol Channel. J. Fish Biol. 46:368–370.
- Francis, M. P., L. H. Griggs, and S. J. Baird.
2001. Pelagic shark bycatch in the New Zealand tuna longline fishery. Mar. Freshw. Res. 52:165–178.
- Francis, M. P., and J. D. Stevens.
2000. Reproduction, embryonic development and growth of the porbeagle shark, *Lamna nasus*, in the south-west Pacific Ocean. Fish. Bull. 98:41–63.
- Gauld, J. A.
1989. Records of porbeagles landed in Scotland, with observations on the biology, distribution and exploitation of the species. Scot. Fish. Res. Rep. 45, 16 p.
- Hartill, B., and N. M. Davies.
2001. New Zealand billfish and gamefish tagging, 1999–2000. NIWA Tech. Rep. 106, 29 p.
- Hazin, F. H. V., K. Kihara, K. Otsuka, C. E. Boeckman, and E. C. Leal.
1994. Reproduction of the blue shark, *Prionace glauca*, in the southwestern equatorial Atlantic Ocean. Fish. Sci. 60:487–491.
- Holdsworth, J., and P. Saul.
2003. New Zealand billfish and gamefish tagging 2001–02. N.Z. Fish. Assess. Rep. 2003/15, 39 p.
- Jensen, C. F., L. J. Natanson, H. L. Pratt, N. E. Kohler, and S. E. Campana.
2002. The reproductive biology of the porbeagle shark, *Lamna nasus*, in the western North Atlantic Ocean. Fish. Bull. 100:727–738.
- Kohler, N. E., J. G. Casey, and P. A. Turner.
1995. Length-weight relationships for 13 species of sharks from the western North Atlantic. Fish. Bull. 93:412–418.
- Kováč, V., G. H. Copp, and M. P. Francis.
1999. Morphometry of the stone loach, *Barbatula barbatula*: do mensural characters reflect the species' life history thresholds? Environ. Biol. Fish. 56:105–115.
- Mollet, H. F., G. Cliff, H. L. Pratt, and J. D. Stevens.
2000. Reproductive biology of the female shortfin mako, *Isurus oxyrinchus* Rafinesque, 1810, with comments on the embryonic development of lamnoids. Fish. Bull. 98:299–318.
- Nakano, H.
1994. Age, reproduction and migration of blue shark in the North Pacific Ocean. Bull. Nat. Res. Inst. Far Seas Fish. 31:141–256.
- Natanson, L. J., J. J. Mello, and S. E. Campana.
2002. Validated age and growth of the porbeagle shark (*Lamna nasus*) in the western North Atlantic Ocean. Fish. Bull. 100:266–278.

- Pearson, E. S., and H. O. Hartley.
1962. Biometrika tables for statisticians. Vol. 1, 2nd ed., 240 p. Cambridge Univ. Press, Cambridge, UK.
- Pratt, H. L.
1979. Reproduction in the blue shark, *Prionace glauca*. Fish. Bull. 77:445-470.
- Pratt, H. L., and S. Tanaka.
1994. Sperm storage in male elasmobranchs: a description and survey. J. Morph. 219:297-308.
- Smith, S. E., D. W. Au, and C. Show.
1998. Intrinsic rebound potentials of 26 species of Pacific sharks. Mar. Freshw. Res. 49:663-678.
- Stevens, J. D.
1983. Observations on reproduction in the shortfin mako *Isurus paucus*. Copeia 1983:126-130.
1984. Biological observations on sharks caught by sport fishermen off New South Wales. Aust. J. Mar. Freshw. Res. 35:573-590.
- Stevens, J. D., and K. J. McLoughlin.
1991. Distribution, size and sex composition, reproductive biology and diet of sharks from Northern Australia. Aust. J. Mar. Freshw. Res. 42:151-199.

Abstract—Survey- and fishery-derived biomass estimates have indicated that the harvest indices for Pacific cod (*Gadus macrocephalus*) within a portion of Steller sea lion (*Eumetopias jubatus*) critical habitat in February and March 2001 were five to 16 times greater than the annual rate for the entire Bering Sea-Aleutian Islands stock. A bottom trawl survey yielded a cod biomass estimate of 49,032 metric tons (t) for the entire area surveyed, of which less than half (23,329 t) was located within the area used primarily by the commercial fishery, which caught 11,631 t of Pacific cod. Leslie depletion analyses of fishery data yielded biomass estimates of approximately 14,500 t (95% confidence intervals of approximately 9,000–25,000 t), which are within the 95% confidence interval on the fished area survey estimate (12,846–33,812 t). These data indicate that Leslie analyses may be useful in estimating local fish biomass and harvest indices for certain marine fisheries that are well constrained spatially and relatively short in duration (weeks). In addition, fishery effects on prey availability within the time and space scales relevant to foraging sea lions may be much greater than the effects indicated by annual harvest rates estimated from stock assessments averaged across the range of the target species.

Survey- and fishery-derived estimates of Pacific cod (*Gadus macrocephalus*) biomass: implications for strategies to reduce interactions between groundfish fisheries and Steller sea lions (*Eumetopias jubatus*)

Lowell W. Fritz

National Marine Mammal Laboratory
Alaska Fisheries Science Center
National Marine Fisheries Service
7600 Sand Point Way NE
Seattle, Washington 98115
E-mail address: lowell.fritz@noaa.gov

Eric S. Brown

Resource Assessment and Conservation Engineering
Alaska Fisheries Science Center
National Marine Fisheries Service
7600 Sand Point Way NE
Seattle, Washington 98115

For the past 30 years, the Steller sea lion (*Eumetopias jubatus*) population in western Alaska has declined (Braham et al., 1980; Sease and Gudmundson¹). The species was listed as threatened under the U.S. Endangered Species Act (ESA) in 1990 after evidence of a major decline in abundance in the core of its range from the Kenai Peninsula in south-central Alaska to Kiska Island in the western Aleutian Islands (Braham et al., 1980; Merrick et al., 1987). After the decline was first observed in the eastern Aleutian Islands in the early 1970s (Braham et al., 1980), it spread eastward to Prince William Sound and westward through Russia during the next decade (Merrick et al., 1987; Loughlin et al., 1992). From the early 1970s to 1990, counts of adult and juvenile Steller sea lions declined by over 70%, but annual rates of decline were most severe between 1985 and 1989 (–15%/yr; Loughlin et al., 1992). During the 1990s, the decline slowed to approximately –5%/yr and may have temporarily abated in many areas by 2002 (Sease and Gudmundson¹).

Understanding the causes for the decline and lack of recovery in the Steller sea lion population has largely eluded scientists and managers,

despite the millions of dollars spent on scientific research (Ferrero and Fritz²) and numerous reviews by academic (Alaska Sea Grant³; DeMaster and Atkinson⁴; NRC, 1996; 2003) and governmental panels (Kruse et al.⁵; NMFS^{6,7,8,9}). Although recent reviews

¹ Sease, J. L., and C. J. Gudmundson. 2002. Aerial and land-based surveys of Steller sea lions (*Eumetopias jubatus*) from the western stock in Alaska, June and July 2001 and 2002. NOAA Tech. Memo. NMFS-AFSC-131, 45 p. Alaska Fisheries Science Center, 7600 Sand Point Way NE, Seattle WA 98115.

² Ferrero, R. C., and L. W. Fritz. 2002. Steller sea lion research coordination: a brief history and summary of recent progress. NOAA Tech. Memo. NMFS-AFSC-129, 34 p. Alaska Fisheries Science Center, 7600 Sand Point Way NE, Seattle WA 98115.

³ Alaska Sea Grant. 1993. Is it food? Addressing marine mammal and seabird declines. Workshop summary rep. AK-SG-93-01, 59 p. Univ. Alaska Fairbanks, Alaska Sea Grant College Program, Fairbanks AK 99775.

⁴ DeMaster, D., and S. Atkinson. (eds.). 2002. Steller sea lion decline: Is it food? II. Workshop summary. rep. AK-SG-02-02, 80 p. Univ. Alaska Fairbanks, Alaska Sea Grant College Program, Fairbanks AK 99775.

^{5, 6, 7, 8, 9} See next page.

(Kruse et al.⁵; DeMaster and Atkinson⁴; NRC, 2003) concluded that "top-down" forces, such as predation or illegal shooting, are greater threats to recovery of the Steller sea lion population, they could not eliminate "bottom-up" factors from consideration. NRC (2003) suggested that NMFS conduct an adaptive management experiment to determine the magnitude of one such "bottom-up" force, nutritional stress resulting from competition with fisheries for prey (NMFS^{6,7,8,9}; NRC, 2003). The North Pacific is home to some of the largest fisheries in the world, particularly those for groundfish such as Pacific cod (*Gadus macrocephalus*) and walleye pollock (*Theragra chalcogramma*). Steller sea lions eat a wide variety of fish and cephalopods, including Pacific cod, walleye pollock, Atka mackerel (*Pleurogrammus monopterygius*), arrowtooth flounder (*Atherestes stomias*), salmon (*Oncorhynchus* spp.), herring (*Clupea pallasii*), capelin (*Mallotus villosus*), eulachon (*Thaleichthys pacificus*), sand lance (*Ammodytes hexapterus*), squid, and octopus (Sinclair and Zeppelin, 2002). A large proportion of their diet, however, is composed of semidemersal or pelagic schooling fish, particularly fish in spawning migrations or aggregations nearshore. These same species are often targeted at the same time and in the same areas by groundfish fisheries, particularly those fisheries that use trawl gear. Concerns about the potential of fisheries to create localized depletions of prey in important sea lion foraging habitats have led to controversial groundfish fishery restrictions throughout most of Alaska (NMFS^{8,9}).

⁵ Kruse, G. H., M. Crow, E. E. Krygier, D. S. Lloyd, K. W. Pitzer, L. D. Rea, M. Ridgway, R. J. Small, J. Stinson and K. M. Wynne. 2001. A review of proposed fishery management actions and the decline of Steller sea lions (*Eumetopias jubatus*) in Alaska: a report by the Alaska Steller sea lion restoration team. Regional information report 5/01-04, 106 p. Alaska Dep. Fish and Game, P.O. Box 25526, Juneau AK 99802.

⁶ NMFS (National Marine Fisheries Service). 1998. Endangered Species Act Section 7 Consultation on an Atka mackerel fishery under the BSAI groundfish FMP between 1999 and 2002; authorization of a walleye pollock fishery under the BSAI FMP between 1999 and 2002; and under the GOA FMP between 1999 and 2002. 189 p. NMFS Protected Resources Division, Alaska Region, P.O. Box 21668, Juneau, AK 99802.

⁷ NMFS. 2000. Endangered Species Act. Section 7: Consultation, biological opinion and incidental take statement on the authorization of the Bering Sea-Aleutian Islands and Gulf of Alaska groundfish fisheries based on the Fishery Management Plans. 352 p. NMFS Protected Resources Division, Alaska Region, P.O. Box 21668, Juneau, AK 99802.

⁸ NMFS. 2001. Endangered Species Act. Section 7: Consultation, biological opinion and incidental take statement on the authorization of the Bering Sea-Aleutian Islands and Gulf of Alaska groundfish fisheries based on the Fishery Management Plans as modified by Amendments 61 and 70, 206 p. NMFS Protected Resources Division, Alaska Region, P.O. Box 21668, Juneau, AK 99802.

⁹ NMFS. 2003. Supplement to the Endangered Species Act. Section 7: Consultation, biological opinion and incidental take statement of October 2001, 179 p. NMFS Protected Resources Division, Alaska Region, P.O. Box 21668, Juneau, AK 99802.

Assessment models and fisheries harvest strategies have determined the overall fishing mortality rate that can be allowed for the stock and the amount of biomass that can be removed. In practice, however, catches are not uniformly distributed across the range of the assessed stock nor are they distributed equally throughout the year. Although there is evidence that the Atka mackerel trawl fishery has created localized depletions of its target species (NMFS⁶ Lowe and Fritz, 1997; NRC, 2003), this finding has not been generally applied to fisheries for other sea lion prey. Trawl fisheries in the Aleutian Islands may have, in certain instances, reduced local abundances of Atka mackerel by as much as 90% (Lowe and Fritz, 1997). Atka mackerel and its fishery have characteristics that permitted analysis of fishery data in this way. The species does not possess a swim bladder and thus makes a poor acoustic target. As a consequence, the Atka mackerel fishery does not target on an acoustic signal, but instead trawls in areas where the species is known to congregate. Through the analysis of time series of catch and effort statistics from local fisheries with Leslie's equation (Ricker, 1975; Hilborn and Walters, 1992; Gunderson, 1993), estimates of the initial abundance of Atka mackerel (prefishery) and its catchability (proportion of the stock caught with one unit of effort) were made within the context of certain assumptions, which included the following: 1) the population being fished is closed, or alternatively that immigration and growth are equal to emigration plus natural mortality, 2) catchability over the course of the fishery remains constant, and 3) changes in catch per unit of effort (CPUE) are directly related to changes in fish density. These assumptions may be met for marine species if the area fished is well defined (e.g., is surrounded by habitat that is unsuitable for the species), the duration of the fishing season is relatively short, or the species is relatively sedentary (Polovina, 1986; Ralston, 1986; Joll and Penn, 1990; Miller and Mohn, 1993). Although they indicate that fisheries have created local depletions of Atka mackerel, these models are difficult to apply to other North Pacific fisheries because of a lack of fishery-independent estimates of biomass and by circumstances unique to the Atka mackerel fishery (e.g., the fishery trawls in areas where the species is known to congregate rather than uses acoustic signal, Atka mackerel are patchily distributed, and patches are separated by areas with low fish density).

To obtain information on the winter distribution of groundfish in areas used by foraging Steller sea lions and groundfish fisheries, the Alaska Fisheries Science Center of the National Marine Fisheries Service conducted a bottom trawl survey for groundfish in the southeastern Bering Sea north of Unimak Island in February–March 2001 (Fig. 1). This area is important to the Pacific cod fishery in winter because cod aggregate in this area to spawn (Shimada and Kimura, 1994). It is also recognized as an important foraging area for Steller sea lions because it is designated as critical habitat under the ESA (NMFS^{7,8}).

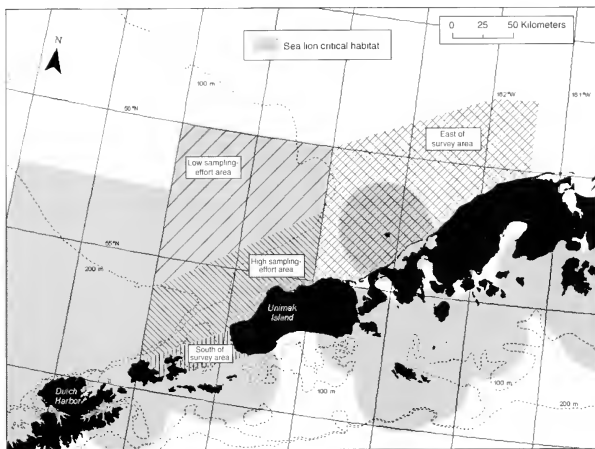


Figure 1

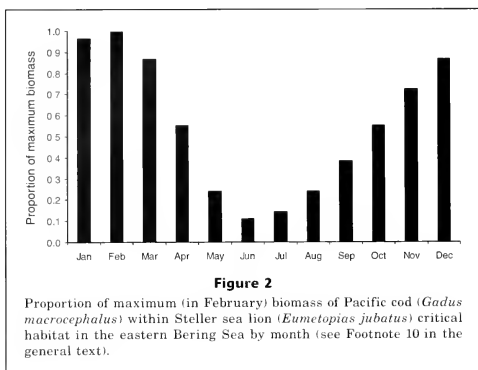
The four areas (high and low sampling-effort survey areas, the area east of the survey area, and the area south of the survey area) in the southeastern Bering Sea that were surveyed in February–March 2001 for groundfish with a bottom trawl survey used for analysis of Pacific cod (*Gadus macrocephalus*) fishery data. Steller sea lion (*Eumetopias jubatus*) critical habitat is also shown.

In this article, estimates of Pacific cod biomass from Leslie depletion analyses of fishery data are compared with those derived from a bottom trawl survey conducted in the same area at the same time. These two methods are independent because they use completely different data to estimate the same parameter, Pacific cod biomass. If they yield similar results, they would support each other in the estimate of local area cod biomass and support the use of Leslie depletion analyses of data from relatively short and spatially well-defined fisheries operations for making such estimates. Furthermore, these comparisons increase our understanding of the potential local effects of a fishery in areas important for sea lion foraging and permit comparison with the results of assessments of the Pacific cod stock in the entire eastern Bering Sea (Thompson and Dorn, 2002). In this instance, if the change in Pacific cod abundance attributable to the fisheries north of Unimak Island is not greater than what would have occurred if catch were evenly distributed throughout the year and across the range of the stock, then it could be argued that no localized depletion occurred. However, if the local change in abundance is greater than expected, does this constitute a localized depletion of the species? The answer ultimately depends on the extent to which the fishery negatively affects the target species (e.g., by reducing recruitment) or, as

in our case, by reducing the foraging success of sea lions, which, in turn, could lead to reduced survival or reproductive rates. Although we do not know what the threshold levels of change in local prey densities are for foraging Steller sea lions, it is first necessary to determine the level of change in local abundance that may be attributable to fisheries.

There are several aspects of Pacific cod life history in the eastern Bering Sea that make it difficult to use fishery data and the Leslie depletion method to estimate local area biomass. The most important may be that the population in the area fished may not be closed over the time period analyzed. Pacific cod spawn north of Unimak Island in late winter but apparently arrive in groups and, after spawning, leave the area and spread out on the eastern Bering Sea shelf to feed during the remainder of the year (Shimada and Kimura, 1994; Thompson and Dorn, 2002). Seasonal emigration from and immigration into spawning areas in critical habitat, modeled with a combination of fishery and survey data by NMFS scientists¹⁰ (Fig. 2), provide a baseline

¹⁰ NMFS. 2000. Estimation of monthly Pacific cod biomass inside Steller sea lion critical habitat. In Biological opinion questions, NMFS-AKC analytical team. Unpubl. manuscript, 112 p. Alaska Fisheries Science Center, 7600 Sand Point Way NE, Seattle WA 98115.



against which possible changes related to local fisheries can be compared. The model results indicate that the highest biomass in critical habitat (largely on the shelf north of Unimak Island) occurs in February, declines to about 10% of the peak in June, and then slowly rebuilds through the summer and fall. Changes in the behavior of Pacific cod immediately prior to or after spawning, such as the formation of dense aggregations or the temporary cessation of feeding, would affect catchability by both trawl and fixed gears. However, abrupt changes in catchability due to the formation of aggregations should be evident within the time series of catch and effort data, and changes in feeding habits would not affect the catchability by trawl gear.

Methods

Bottom trawl survey

Stations sampled during the bottom trawl survey were selected by using a stratified random scheme. Two strata were defined: one with a high and another with a low degree of sampling effort, based on the expected distribution and abundance of Pacific cod from fishery information. In the nearshore or high sampling-effort stratum (7765 km²), 38 stations were sampled, whereas 19 stations were sampled in the larger (12,112 km²), offshore low sampling-effort stratum (Fig. 1). All survey tows were conducted during daylight hours from 16 February to 1 March 2001 aboard the FV *Northwest Explorer* and the FV *Ocean Harvester*. The 49-m FV *Northwest Explorer* was equipped with two 1800-hp engines, and the 33-m FV *Ocean Harvester* had a single 1250-hp engine. Both vessels were house-forward trawlers that had stern ramps, multiple net storage reels, and paired

hydraulic trawl winches with 1280–2190 m of 2.54-cm diameter steel cable. Each vessel carried a full complement of navigation and fishing electronics, including global positioning systems (GPS), video position plotters, radars, and depth sounders.

A Poly-Nor'eastern high-opening bottom trawl rigged with roller gear was used to sample the groundfish community at each selected location. The trawl net was constructed of 12.7-cm stretched-mesh polyethylene web and had a 3.2-cm stretched-mesh nylon liner in the codend. Accessory gear for the Nor'eastern trawl included three 54.9 m, 1.6 cm diameter galvanized wire rope bridles, and 1.8 × 2.7 m steel V-doors weighing approximately 850 kg each.

Biomass (B) estimates for each stratum surveyed were computed by multiplying the average CPUE (in units of kg/km²) for all hauls (n) in a stratum by its area (A). Haul CPUE was calculated as the weight of cod caught (kg) divided by the area swept (a), which was the length of the tow multiplied by the average net width determined by sonic mensuration equipment:

$$B = \frac{\sum_{n} \text{kg}}{n} \times A.$$

Confidence bounds on stratum biomass estimates were computed from the standard deviation of the haul CPUEs. For haul CPUEs we assumed a catchability¹¹ of 1 for Pacific cod (all cod within the area swept by

¹¹ Note that catchability within the survey biomass estimation procedure has a different literal definition than in the Leslie equation.

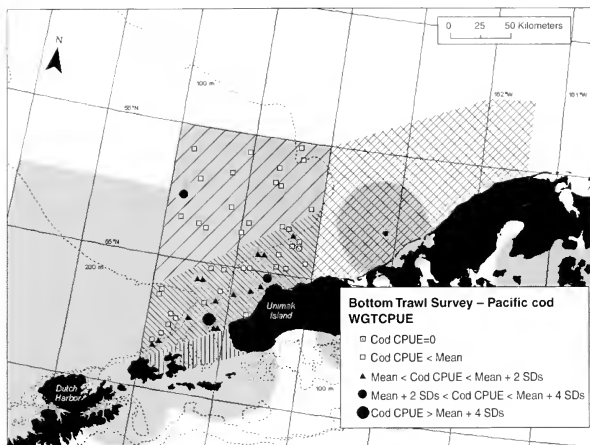


Figure 3

Catch per unit of effort (CPUE=kg/km²) of Pacific cod (*Gadus macrocephalus*) during the February–March 2001 bottom trawl survey of the southeastern Bering Sea. “Wgtcpue” refers to the CPUE of Pacific cod from individual hauls (Table 2). Area shading is the same as that in Figure 1.

the net are captured) and that it is constant over the course of the survey. This assumption is also made in the Leslie analyses of fishery data. In addition, each haul is assumed to be a random, normally distributed estimate of the density of cod within the stratum. Therefore, the average of the haul CPUEs of cod was assumed to be an unbiased estimate of the true density of cod, allowing linear extrapolation from the CPUE within the area swept to a biomass estimate for each stratum.

Analysis of fishery data

Fishery observers record a wide variety of information about each haul taken by a fishing vessel, including retrieval location, depth, date and time of catch, and total catch weight (all referred to hereafter as “haul data”). In addition, the catch of a randomly chosen subset of hauls was sampled to determine the species composition of the haul and the length distribution of the target species (see Nelson et al. 1981 and NMFS¹² for observer sampling methods). Observer data were queried for any

hauls with any gear in which Pacific cod were caught in the eastern Bering Sea and Aleutian Islands region in 2001. The geographic distribution of the observed Pacific cod catch was used to estimate the distribution of the actual catch of Pacific cod from January–April 2001 in four areas of the southeastern Bering Sea (Fig. 1): the high and low sampling-effort areas surveyed in February–March 2001, and two areas outside of the area surveyed—one to the east, and one to the south. To account for Pacific cod catches in both unsampled hauls and on unobserved vessels, the observed catch of cod was multiplied by the ratio of total-to-observed catch by processing sector and gear type (Table 1). For this procedure, the catch of the unobserved portion of the fleet is assumed to be similar to the observed portion. Ratios of total-to-observed catch by sector and gear ranged from 1.02 to 33.94, but for the majority of the catch, the ratios were less than 2 (Table 1).

A simple Leslie analysis of fishery catch and effort data was conducted on data collected by observers on-board vessels targeting groundfish. For the basic Leslie model (Ricker, 1975; Hilborn and Walters, 1992; Gunderson, 1993) a deterministic linear relationship between CPUE and cumulative catch is assumed:

$$\frac{C_t}{I_t} = qB_0 - qK_t,$$

¹² NMFS. 1996. Manual for biologists aboard domestic groundfish vessels, 431 p. U.S. Dep. Commer., NOAA, NMFS, Alaska Fisheries Science Center, 7600 Sand Point Way, NE, Seattle, WA 98115.

Table 1

Observed and total estimates of total catches of Pacific cod by processor and gear type in the Bering Sea-Aleutians Island region in 2001, and the ratio of Total ÷ Observed catches. CP=catcher processor; CV=catcher vessel.

Gear	Catches and ratio	Processor type		
		CP	CV	Other
Trawl	Total (t)	29,398	21,354	734
	Observed (t)	19,316	8590	720
	Ratio	1.52	2.49	1.02
Hook and line	Total (t)	96,238	637	11,331
	Observed (t)	52,920	19	11,109
	Ratio	1.82	33.94	1.12
Pot	Total (t)		16,506	478
	Observed (t)		4741	469
	Ratio		3.48	1.02

where C_t = catch in time period t ;

f_t = effort in t ;

q = catchability;¹¹

B_0 = underlying (or initial) biomass; and

K_t = cumulative catch through t .

Current catch, effort, and cumulative catch are required by the model, whereas catchability and initial biomass are estimated from it. The catch and effort time series used in these analyses were 1) daily aggregates of observed cod catch in metric tons (t) and effort by vessels targeting cod by area (i.e., the high sampling-effort [HSE] area, the low sampling-effort area [LSE], the area east [AE] and the area south [AS] of the survey area), and 2) daily cumulative catch of cod by gear for all vessels. CPUE metrics were defined for each gear: 1) trawl as the catch of cod (t) per hour of observed trawling per day; 2) pot as the catch of cod (t) per 20 pots observed per day; and 3) hook and line as the catch of cod (t) per 1000 hooks observed per day. These metrics were chosen so that the CPUE for each gear would be in approximately the same range to permit being plotted together on the same axis. Changing the unit-of-effort definition (number of pots or hooks fished, for instance) has no effect on the significance of the results. Hauls for which cod was the target species were defined as those in which the catch of cod was at least 20% of the total groundfish catch; target levels of 40% and 60% were also explored for trawl fisheries. Catch and effort from these hauls alone, in which cod was the target species, were used for CPUE calculations, whereas cumulative catch was derived from the total catch of cod from all vessels regardless of their target species.

The relationship between trawl vessel length and CPUE was investigated but was not included in the Leslie analyses. It was expected that CPUE would be

directly related to vessel length. With increasing vessel length, horsepower would increase as would the vessel's ability to use larger nets. Vessel length (a surrogate variable for horsepower) could be a significant covariate in the relationship between CPUE and cumulative catch.

Results

Bottom trawl survey

Mean CPUE (kg/km²) of Pacific cod in the smaller HSE survey stratum was almost three times higher than in the larger LSE stratum, resulting in mean biomass estimates of 31,312 t and 17,720 t of Pacific cod, respectively (Table 2 and Fig. 3). The highest recorded CPUE of cod was recorded for a haul on the northeast side of Unimak Pass (Fig. 3). Hauls with CPUEs above the mean were distributed throughout the HSE stratum in depths less than 200 m. Only one of the 18 hauls in the LSE stratum had a CPUE larger than the mean. For the HSE stratum, the 95% confidence interval on the mean biomass estimate was 19,284–43,339 t.

Fishery data

Total catch of Pacific cod Approximately 30,500 t of Pacific cod were caught in the four areas of the southeastern Bering Sea from 1 January to 30 April 2001 (Table 3 and Fig. 4). Almost 60% of this total catch was collected in the HSE survey stratum, whereas 25% and 12% of the total catch were collected in the AE and AS of the survey area, respectively; only 4% was collected in the LSE survey stratum. Based on the distribution of the observed catch of cod by gear, approximately half of the total catch was collected by trawls, a third by hook and line (=longline), and 14% by pots.

The distribution of cod catch by area primarily reflects the distribution of the fishery targeting Pacific cod (Fig. 4). Of the 5813 t of cod that was observed caught by the cod trawl fleet (with at least 20% of each haul composed of cod), 86% was caught in the HSE stratum in over 4600 hours of observed trawling. Most of the remainder (13% or 781 t) was caught east (AE) of the survey area, primarily between the HSE stratum and the 20 nautical mile (nmi) radius trawl exclusion zone encompassing sea lion critical habitat around Sea Lion Rocks and Amak Island (Figs. 1 and 4). There was little trawl effort targeting Pacific cod in the LSE stratum (only 10 observed hours of trawling) or south (17 hours observed) of the survey area. The cod pot fleet worked primarily south of the survey area (57% of their catch) and in the HSE stratum (31%) in areas where conflicts with trawl gear would be minimized. The cod longline fleet worked in both the HSE stratum and to the east of the survey area, and had only trace amounts of catch in the other areas (Table 3).

Percentage of Pacific cod in the haul The distribution of the percentage of cod in the total catch of each haul

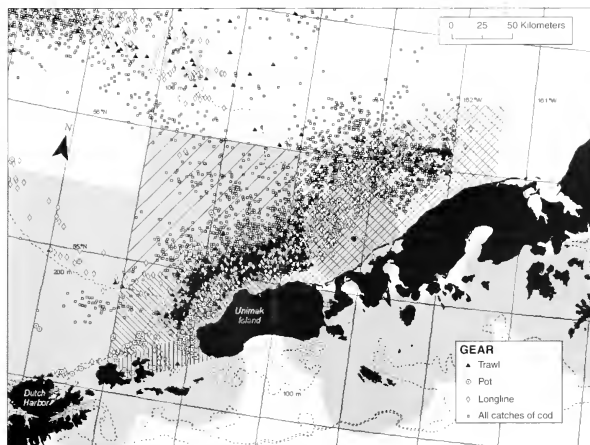


Figure 4

Locations of groundfish fishery catches of Pacific cod (*Gadus macrocephalus*) in the south-eastern Bering Sea, January–April 2001. The cod target fishery is separated by gear type (trawl—at least 20% of the haul by weight was cod). “All catches of cod” refers to bycatch in trawl fisheries targeting other species. Area shading is the same as that seen in Figure 1.

Table 2

Results (catch and biomass of Pacific cod) and haul data from the bottom trawl survey of the southeastern Bering Sea conducted in February–March 2001. Low and high sampling-effort strata are shown in Figure 1. (CPUE=catch per unit of effort; CI=confidence interval).

	Survey stratum		Total
	Low sampling effort	High sampling effort	
Number of hauls	19	38	57
Number of hauls with cod	19	37	56
Mean CPUE (kg cod/km ²)	1463	4032	3176
Range in CPUE	65–12,681	0–21,299	0–21,299
Standard deviation of CPUE	2776	4676	4292
Area of stratum (km ²)	12,112	7765	19,877
Area of stratum sampled (km ²)	0.472	0.927	1.399
% of stratum area sampled	0.004%	0.012%	0.007%
Biomass (t)	17,720	31,312	49,032
95% CI on biomass (t)	1513–33,928	19,284–43,339	20,796–77,267

indicates that the vast majority of the fleet using pots or longline gear were targeting Pacific cod. The total catch of 350 of 351 observed hauls of pots and 777 of 797 observed hauls of longlines was composed of at least

60% cod (Table 4). Therefore, use of a 20% threshold to identify the cod fleet for the longline and pot vessels was unnecessary. For the trawl fleet, however, more than half the observed hauls had less than 10% cod, and

63% had less than 20% cod. These trawl vessels were targeting fish species other than Pacific cod, such as rock sole, and caught some cod (as bycatch) in the process. The distribution of hauls that had greater than 20%

cod (by 10% bins) was relatively flat, varying only from 4% to 7% between bins and having no clear threshold or breakpoint. Use of a low threshold proportion of cod (such as 20%) would likely include some hauls in which

Table 3

Catch and effort statistics for Pacific cod fisheries in the southeastern Bering sea by strata (Fig. 1) in January–April 2001. Statistics include total catch estimates (in metric tons (t); all gear and fisheries), observed catch by all fisheries (by gear type), and observed catch and effort by fisheries targeting Pacific cod (by gear type). Three levels of Pacific cod catches from trawl gear are listed and are based on the minimum proportion of cod in each haul.

	Strata				Total
	East of sampling area	High sampling effort	Low sampling effort	South of sampling area	
Catch					
Total catch	7691	17,875	1,200	3724	30,491
Observed catch—all fisheries					
Trawl	1628	5737	324	32	7720
Pot	85	655	152	1198	2091
Longline	2493	2001	45	116	4654
Total	4205	8393	521	1345	14,465
Observed catch—Pacific cod fisheries					
Trawl (20% cod in each haul)	781	4993	7	32	5813
Trawl (40% cod in each haul)		4119			
Trawl (60% cod in each haul)		3364			
Pot	85	655	152	1198	2090
Longline	2493	2001	45	116	4654
Effort					
Trawl (hours; 20% cod in each haul)	677	4644	10	17	5348
Trawl (hours; 40% cod in each haul)		3768			
Trawl (hours; 60% cod in each haul)		2903			
Pot (number of pots)	1857	10,130	1119	14,816	27,922
Longline (no. of hooks)	4,220,051	3,265,606	88,880	165,585	7,740,122

Table 4

Frequency distribution of the percentage of cod in each haul by gear for the groundfish fishery in the four areas of the eastern Bering Sea (Fig. 1) in January–April 2001

% cod	Trawl		Longline		Pot	
	No. of hauls	% of total	No. of hauls	% of total	No. of hauls	% of total
<10%	1810	52	0	0	0	0
10–20%	371	11	1	0	0	0
20–30%	237	7	2	0	1	0
30–40%	169	5	1	0	0	0
40–50%	126	4	5	1	0	0
50–60%	126	4	11	1	0	0
60–70%	151	4	40	5	2	1
70–80%	166	5	120	15	4	1
80–90%	181	5	334	42	37	11
90–100%	161	5	283	36	307	87
Total	3498		797		351	

other species were targeted. On the other hand, the use of a high threshold (such as 60%) might exclude hauls where Pacific cod was the target species. Therefore, a range of trawl target definitions from 20% to 60% was used. The cod trawl fleet distribution shown in Figure 4 was defined by the 20% threshold. If the 40% or 60% thresholds are used, most of the cod trawl effort shown in the HSE area remains, whereas some of the effort in the eastern portions of the AE of the survey area is not coded as the effort of a cod-target fishery.

Distribution of Pacific cod catch Cod catches accumulated differently in the three primary areas fished (Fig. 5). In the HSE area, cod catches rose steadily from 1 January through early April, and totaled approximately 13,000 t. There was a brief increase in the rate of cod catch in mid-April, but by approximately 20 April, the cod fishery in the HSE area had essentially finished with a catch total of 17,875 t. In the AE of the survey area, cod catches accumulated steadily from 1 January through 2 March, and totaled 6340 t. There was a brief increase in catch rates for 6 days from 25 through 30 March, after which the cod fishery in the AE of the survey area was finished with a catch total of 7691 t. In the AS of the survey area, there was little cod fishing effort prior to 22 February, and it lasted only through 27 March, by which time almost 3500 t had been caught; catches through 30 April from the AS of the survey area totaled 3724 t. There was very little cod fishery effort in the LSE area (Table 3), and only 1200 t of cod were caught (principally as bycatch in other fisheries) through 30 April 2001.

The longline fleet began fishing for Pacific cod in both the HSE area and AE of the survey area on 1 January (Fig. 5). In the HSE area, daily average longline CPUE (t cod per 1000 hooks per day) remained relatively low and steady, ranging from 0.3–0.7 through January. The longline fleet left the HSE area for approximately two weeks, resuming effort again on 13 February and continuing through 6 March. Longline CPUEs were generally higher in late February than they were in January, ranging from approximately 0.7 to 1.2. The longline fleet again returned to the HSE area on 19–24 March, but daily average CPUEs were <0.5. There was sporadic longline fishing for cod in the HSE area through April, and CPUEs ranged from 0.3 to 1.0. In the AE of the survey area, the longline fleet fished continuously from 1 January through 2 March, and daily average CPUE declined from a range of 0.7–1.0 on 1–7 January to a range of 0.3–0.5 on 24 February–2 March.

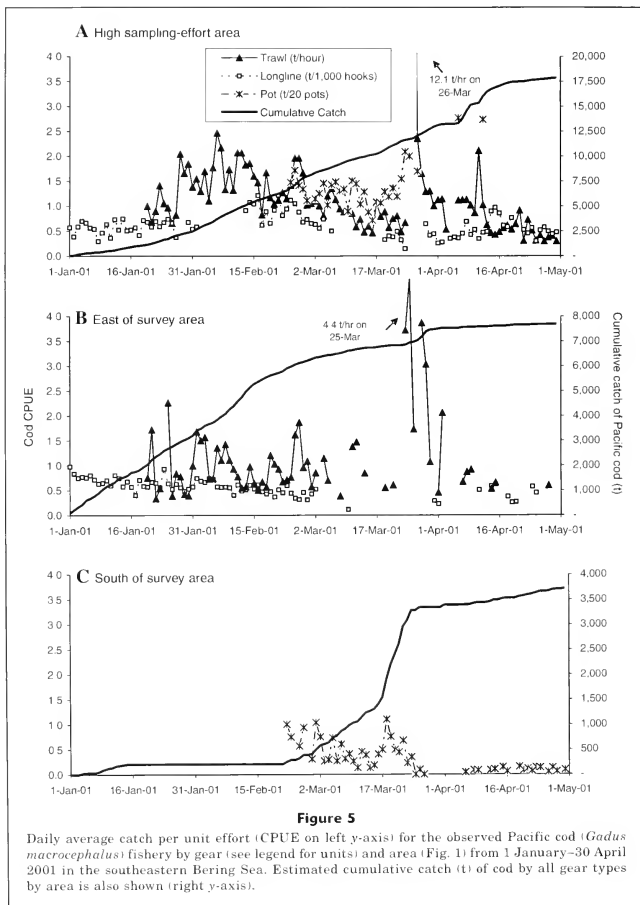
The trawl fishery for cod began on 20 January in both the HSE area and AE of the survey area (Fig. 5). In the HSE area, trawl CPUE (t cod per hour trawled per day) increased from a range of 0.7–1.4 on 20–27 January to a range of 1.3–2.5 on 6–15 February. From 16 February–1 March, trawl CPUEs were slightly lower, ranging from 0.8 to 2.0, after which they declined further, ranging only from 0.5 to 1.3 from 2–24 March. On 26 March, the average CPUE increased substantially to over 12 but quickly declined to less than 1.0 by 1 April. This

was followed by another short-lived increase in CPUE on 11 April, after which daily average CPUEs remained below 1.0 through April. In the AE of the survey area, CPUEs were highly variable (between 0.4 and 2.3) and there was little observable trend between 20 January and early March. On 25 March, however, average CPUE increased to over 4 and ranged between 0.4 and 3.9 through 2 April, after which there was only sporadic effort and daily average CPUEs were less than 1.

The pot fishery for cod began on 22 February south of the survey area and on 24 February in the HSE area (Fig. 5). In the AS of the survey, pot CPUE (t cod per 20 pots per day) decreased from a range of 0.3–1.0 from 22 February–1 March, to a range of 0.2–0.5 on 8–17 March. However, on 18 March, pot CPUE increased to 1.1, and remained between 0.5 and 0.8 through 22 March, after which it quickly declined to very low levels. In the HSE area, pot CPUE ranged between 0.7 and 1.7 from 24 February to 23 March. However, on 24–25 March, CPUE was greater than 2. Pot cod fishing occurred on only three more days through the end of April in the HSE area: on 27 March, 6 April, and 12 April. Although daily average CPUEs on the last two days were the highest recorded in the pot fishery in 2001, observed catches on these days totaled only 4 and 5 t of cod, respectively.

Leslie depletion analyses Leslie depletion analyses were conducted on four sets of Pacific cod fishery data collected in the HSE area and on two sets of data collected in the AE of the survey area (Table 5). In the HSE area, longline fishery data collected prior to 13 February and trawl fishery data collected prior to 6 February were excluded from the analyses because CPUE data indicated that fish were immigrating into the area in January in preparation for spawning (Fig. 5). It is unlikely that the increase in CPUE was due to a change in catchability because the increase was evident whether bait was used (pots and longlines) or not (trawls). Data indicating an increase in the abundance of cod north of Unimak Island in January and a peak in February were in agreement with a generalized model of cod abundance in Steller sea lion critical habitat in the eastern Bering Sea (Fig. 2) and seasonal cod movements from tagging data (Shimada and Kimura, 1994). The time series was truncated at 24 March because of the evidence within the fisheries data (increase in CPUE) that another group of cod had immigrated to the HSE area and AE of the survey area in late March or that catchability had increased substantially (Fig. 5). In addition, daily average CPUEs from hauls that had at least 20%, 40%, and 60% Pacific cod by weight were regressed against cumulative catch to see what effect the target definition might have on the regression results.

All Leslie regressions with longline or trawl fishery data from the HSE area were highly significant ($P < 0.000001$; Table 5 and Fig. 6). Coefficients of determination (r^2) for the longline and the trawl-20% data were both greater than 0.6. Regression coefficients



(slopes) in all cases were negative and significantly different from zero. Collectively, these results strongly indicate that cod fishery CPUE was negatively correlated with cumulative catch. Initial biomass estimates (B_0) from the four regressions were similar and ranged between 14,119 and 14,806 t, with 95% confidence in-

tervals ranging from approximately 9000 to 25,000 t. Use of different fishery catch levels (20%, 40%, 60% cod in each haul) had little effect on the initial biomass estimate but changed the estimate of q , which increased directly with the threshold proportion of cod in each haul (Table 5 and Fig. 7).

Table 5

Results of Leslie depletion analyses on cod trawl and longline fishery data collected in the (A) high sampling-effort (HSE) survey area and (B) east of the survey area (Fig. 2). Dates when data were collected are listed, along with the regression parameters (q =slope and y -intercept= qB_0) and statistics (P =probability that slope is not significantly different from 0, r =Pearson correlation coefficient, and 95% confidence interval (CI) on B_0). For the trawl fishery in the HSE area, three different levels catch for the target fishery were used (20%, 40%, or 60% of the total catch per haul was cod). Cumulative catches in each area are defined as the catch from 1 January through the end of the period analyzed.

A High sampling-effort survey area

	Gear			
	Longline 13 Feb–24 Mar	Trawl 20% 6 Feb–24 Mar	Trawl 40% 6 Feb–24 Mar	Trawl 60% 6 Feb–24 Mar
Cumulative catch (t)	11,631	11,631	11,631	11,631
B_0 (t)	14,251	14,806	14,119	14,410
95% CI on B_0 (t)	9608–22,195	10,549–21,570	9526–21,942	8989–24,860
q	0.000115	0.000172	0.000207	0.000212
y -intercept	1.6395	2.5442	2.9246	3.0573
P	<0.000001	<0.000001	<0.000001	<0.000001
No. of days (n)	27	47	46	46
r^2	0.712	0.635	0.577	0.479

B East of survey area

	Gear	
	Longline 1 Jan–2 Mar	Trawl 20% 20 Jan–21 Mar
Cumulative catch (t)	6340	6837
B_0 (t)	14,671	
95% CI on B_0 (t)	10,934–20,936	
q	0.000053	
y -intercept	0.7707	
P	<0.000001	0.65
No. of days (n)	61	49
r^2	0.515	0.004

Although a portion of the AE of the sampling area is also critical habitat, the majority of it is not. Cod are thought to move from the areas east and south of the survey area to aggregate within critical habitat, particularly north of Unimak Island, for spawning (Shimada and Kimura, 1994; Thompson and Dorn, 2002). Leslie analyses were conducted on longline data collected from 1 January to 2 March in the AE of the survey area, and on trawl data collected from 20 January to 21 March. The longline data yielded a highly significant negative relationship between CPUE and cumulative catch ($P<0.000001$), whereas the trawl data did not ($P=0.65$; Table 5 and Fig. 6).

Trawl fishery CPUE in the HSE area was not correlated with daily average vessel length for the period 20 January–30 April 2001 ($P=0.16$; $r^2=0.02$; Fig. 8). The data from the analysis period 6 February–24 March are highlighted in Figure 8. Although there was a significant linear relationship between vessel

length and CPUE for this shorter period ($P=0.004$), the correlation coefficient was low ($r^2=0.16$), indicating that daily average CPUE and vessel length were poorly correlated.

Discussion

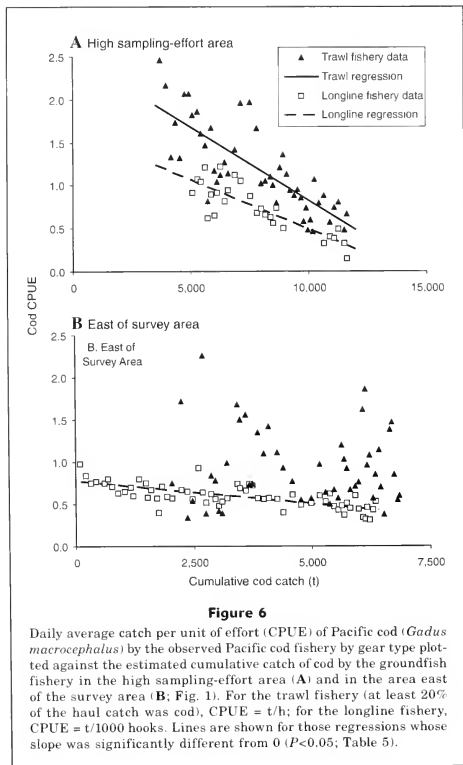
The bottom trawl survey point estimate of cod biomass in the HSE area (31,312 t) is approximately twice the values derived from analyses of fishery data (approximately 14,500 t). This is in part because the fishery worked almost exclusively within the eastern two-thirds of the HSE area. Restratifying the HSE survey yields biomass estimates of 23,329 t for the eastern two-thirds used by the fishery and 7983 t for the western portion. The fishery-derived biomass estimates for the eastern portion of the HSE survey area are within the 95% confidence bounds on the survey estimate (12,846–33,812 t).

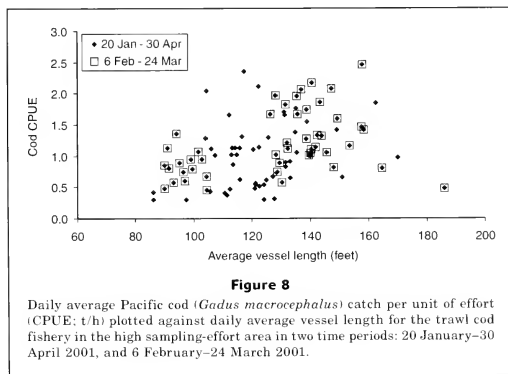
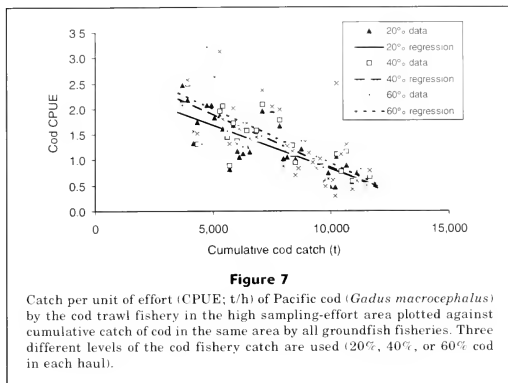
In addition, the survey biomass estimate for the eastern two-thirds of the HSE area is within or close to the upper 95% confidence bounds of the Leslie analyses of trawl and longline Pacific cod fishery data (Table 5).

One possible explanation for the lower fishery-derived estimates in the eastern portion of the HSE area is that emigration of fish after spawning contributed to the low CPUEs observed near the end of the fishery time series. If this emigration occurred, however, it went largely undetected in the neighboring areas. Emigration over the course of the fishery would decrease CPUEs faster than what would be attributable to fisheries alone, which would, in turn, decrease the estimate of initial biomass.

Plots of fishery CPUEs of Pacific cod were very similar for all gears used in each area. This finding indicates that these time series are useful as indices of relative cod abundance. Similarly, inferences can be made through analyses of fishery CPUE data regarding fish movement from area to area (or lack thereof) to a possible cause in the observed declines in CPUE (or local abundance). For instance, the lack of fishery CPUE increases in areas to the north, east, and south of the HSE survey area in March indicates that emigration was not a significant factor in the CPUE decline observed in both the longline and trawl fishery CPUE data from early February through 24 March. In fact, in the AE of the survey area through 2 March, longline CPUE declined, indicating that either fish left this area (to the north) or were reduced in abundance by fishing and were not replenished. Although the time series from the AS of the survey area is short, there is no indication that cod moved there in early March. There is also no evidence that cod moved north to the LSE survey area because the longline or pot fleets targeting cod did not move there, nor did the proportion of cod in trawl hauls increase (otherwise they would have been labeled as a cod-target fishery). It is possible that cod emigrating from the HSE area were so dispersed or their catchabilities were much lower than those for residents in other areas that their presence went undetected, but there is no evidence to suggest that either of these were any more likely than the more simple assumption that changes in CPUE within the fished area represented real changes in local abundance even after accounting for some level of emigration. If cod immigration exceeded emigration for the HSE area during early March as CPUEs were declining, then fishery-derived estimates of initial biomass calculated in our study are biased high.

Pot fishery CPUE data in the AS of the sampling area and in the HSE area indicated that there was an influx of Pacific cod from the south in mid-March. This was evident from the increase in pot fishery CPUE on 18 March in the AS of the survey area and beginning on 24 March in the HSE area. Cod may have moved into nearshore sections of the HSE area where they would be more vulnerable to pot gear than to trawlers. However, on 25–26 March, trawl CPUE on the border of the HSE area and the AE of the survey area increased substantially, indicating that these fish had moved offshore to areas worked by trawlers, or that they became highly aggregated (perhaps just prior to spawning). The late-March "pulse" of Pacific cod biomass was probably smaller than the



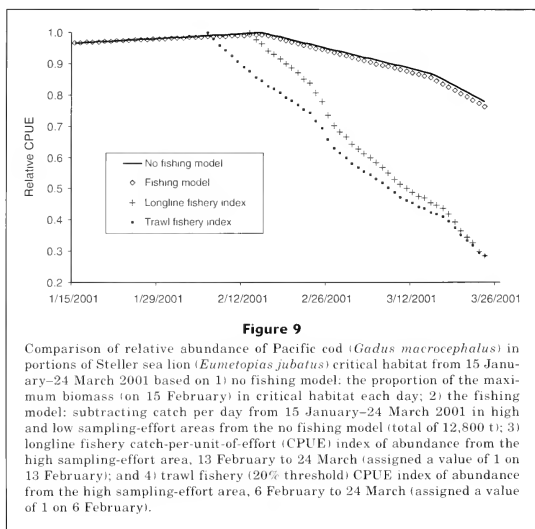


initial influx that peaked in early February because it sustained the fishery for only 1–2 weeks, and resulted in cod catches of only approximately 7500 t from all four areas.

In the stock assessment for Pacific cod in the eastern Bering Sea and Aleutian Islands (BSAI; Thompson and Dorn, 2002), the estimate of age 3+ biomass in 2001 was approximately 1.284 million t, whereas the female spawning biomass was approximately 359,000 t. Doubling the latter to account for male spawner biomass, the survey and fishery data discussed in the present study indicate that only 4% of the adult spawning and 3% of the age 3+ biomass was in the HSE area, and

only about 7% and 4%, respectively, in the entire area surveyed. The area north of Unimak Island is thought to be one of the principal spawning grounds for Pacific cod in the eastern Bering Sea (Shimada and Kimura, 1994; Thompson and Dorn, 2002). The results reported in the present study may indicate that either 1) this is not one of the principal spawning grounds for Pacific cod in the eastern Bering Sea and most spawning occurs elsewhere, 2) the stock assessment estimates are too high, or 3) Pacific cod aggregated in the area after the survey occurred.

Biomass estimates from the assessment are approximately twice those derived directly from bottom trawl



surveys of the entire Bering Sea shelf conducted in summer (Thompson and Dorn, 2002). This difference stems from highly domed-shaped selectivity-at-length schedules for the summer surveys and most fishery catches of cod (Thompson and Dorn, 2002). As a consequence, the model “assumes” that fewer cod are caught in proportion to their actual abundance at lengths greater than 45 cm for the survey catch and 80 cm for the fishery catch. However, it is unclear how large cod avoid capture during surveys or by longline, pot, and trawl fishery gear as implied by the dome-shaped selectivity-at-length schedules.

A seasonal model of Pacific cod movement patterns into and out of Steller sea lion critical habitat (Fig. 2) indicates that relative Pacific cod biomass inside critical habitat is highest in February, then drops 13% in March and 44% by April. If these values are assigned to the middle of each month and daily values are extrapolated linearly, the relative change from 15 February through 24 March is 23% (Fig. 9). Fishery indices of abundance in the HSE area in January and February are consistent with this seasonal pattern, with both trawl and longline CPUEs increasing from January to February. According to Figure 2 and the 2001 age 3+ biomass estimate (Thompson and Dorn, 2002), catches through 24 March within the entire survey area (12,806 t) represented only 1% of the BSAI stock and

should have reduced the relative biomass of cod within critical habitat by only an additional 2%. Thus, the total reduction in relative cod biomass within critical habitat from mid-February through late March after accounting for fishing and emigration should have been 25% (Fig. 9). Longline and trawl fishery CPUE data in the HSE area provide an independent estimate of relative cod biomass. Both indices indicate that the reduction in relative cod biomass within the HSE survey area through 24 March was 71–46% greater than that predicted by the model.

Catches and biomass estimates of Pacific cod for different time periods and areas can be used to compute harvest indices (catch divided by observed biomass). For instance, the harvest index within the entire survey area (based on the catch from 1 January through 24 March and the survey biomass estimate) was 26% (12,806 or÷49,032). If the focus is narrowed to only the HSE survey area through 24 March, the harvest index was 37% (11,631 or÷31,312). However, both the fish and the fishery were concentrated within the HSE area. The eastern two-thirds of the HSE survey area had survey and fishery-derived biomass estimates of 23,418 t and ~14,500 t, respectively. With the area of fishery effort more precisely defined, local harvest indices increase even further, ranging from 50% (11,631 or÷23,329) to 80% (11,631 or÷14,500).

The annual harvest rate of BSAI cod in 2001 was estimated to be approximately 11% (Thompson and Dorn, 2002). The total catch of cod in the BSAI through 24 March represented only 44% of the total catch of Pacific cod in 2001. Therefore, the harvest rate through 24 March should only have been 44% of 11%, or about 5%. The local harvest indices estimated in the present study, which ranged from 26% to 80%, were five to 16 times greater than that on the BSAI Pacific cod stock as a whole in 2001. Much of the area used by the fishery is designated as critical habitat for the endangered Steller sea lion, primarily because of the prey resources available within it. In addition, the fisheries occurred in the winter and early spring, when sea lions are most likely to consume Pacific cod (Sinclair and Zeppelin, 2002). It is not known how or if cod fishery catches in this area affect Steller sea lion foraging success. One objective of the Pacific cod fishery management regulations is to minimize the competitive interactions between locally intense fisheries and Steller sea lions. The suite of groundfish fishery regulations enacted in 2001 and 2002 work together to avoid adverse modification of critical habitat under the ESA. However, based on the observations during 2001 discussed in the present study, regulations for the eastern Bering Sea Pacific cod fishery should be reviewed to ensure that they meet these management objectives.

Acknowledgments

We thank D. DeMaster, G. Duker, B. Fadely, J. Lee, T. Loughlin, S. Lowe, S. Moore, and especially M. Sigler for their reviews of early versions of the manuscript. We also give heartfelt thanks to the captains and crews of the FV *Northwest Explorer* and FV *Ocean Harvester*, AFSC personnel (E. Acuna, T. Buckley, W. Floering, L. Haaga, R. Harrison, E. Jorgensen, G. Lang, D. Nebanzahl, D. Nichol, and K. Smith) who conducted the bottom trawl survey in February–March 2001, and the numerous fishery observers working onboard commercial vessels at that time.

Literature cited

- Braham, H. W., R. D. Everitt, and D. L. Rugh.
1980. Northern sea lion population decline in the eastern Aleutian Islands. *Fish. Bull.* 44:25–33.
- Gunderson, D. R.
1993. *Surveys of fisheries resources*, 248 p. John Wiley & Sons, Inc. New York, NY.
- Hilborn, R., and C. J. Walters.
1992. *Quantitative fisheries stock assessment: choice, dynamics and uncertainty*, 570 p. Chapman and Hall, New York, NY.
- Joll, L. M., and J. W. Penn.
1990. The application of high-resolution navigation systems to Leslie-DeLury depletion experiments for the measurement of trawl efficiency under open-sea conditions. *Fish. Res.* 9:41–55.
- Loughlin, T. R., A. S. Perlov, and V. A. Vladimirov.
1992. Range-wide survey and estimation of total number of Steller sea lions in 1989. *Mar. Mam. Sci.* 8: 220–239.
- Lowe, S. A., and L. W. Fritz.
1997. Atka mackerel. In *Stock assessment and fishery evaluation report for the groundfish resources of the Bering Sea-Aleutian Islands regions as projected for 1998*, 653 p. North Pacific Fishery Management Council, P.O. Box 103136, Anchorage, AK 99501.
- Merrick, R. L., T. R. Loughlin, and D. G. Calkins.
1987. Decline in abundance of the northern sea lion, *Eumetopias jubatus*, in 1956–86. *Fish. Bull.* 85: 351–365.
- Miller, R. J., and R. K. Mohn.
1993. Critique of the Leslie method for estimating sizes of crab and lobster populations. *N. Am. J. Fish. Manage.* 13:676–685.
- NRC (National Research Council).
1996. *The Bering Sea ecosystem*, 307 p. The National Academies Press, Washington, DC.
2003. Decline of the Steller sea lion in Alaskan waters: untangling food webs and fishing nets, 204 p. The National Academies Press, Washington, DC.
- Nelson, R., Jr., R. French, and J. Wall.
1981. Sampling by U.S. observers on foreign fishing vessels in the eastern Bering Sea and Aleutian Islands region, 1977–78. *Mar. Fish. Rev.* 43(5):1–19.
- Polovina, J. J.
1986. A variable catchability version of the Leslie model with application to an intensive fishing experiment on a multispecies stock. *Fish. Bull.* 84:423–428.
- Ralston, S.
1986. An intensive fishing experiment for the caridean shrimp, *Heterocarpus laevigatus*, at Alamagan Island in the Mariana archipelago. *Fish. Bull.* 84:927–934.
- Ricker, W. E.
1975. Computation and interpretation of biological statistics of fish populations. *Bull. Fish. Res. Board Canada* 191, 382 p.
- Shimada, A. M., and D. K. Kimura.
1994. Seasonal movements of Pacific cod (*Gadus macrocephalus*) in the eastern Bering Sea and adjacent waters based on tag-recapture data. *Fish. Bull.* 92: 800–816.
- Sinclair, E. H., and T. K. Zeppelin.
2002. Seasonal and spatial differences in diet in the western stock of Steller sea lions (*Eumetopias jubatus*). *J. Mammal.* 83: 973–990.
- Thompson, G. G., and M. W. Dorn.
2002. Assessment of the Pacific cod in the eastern Bering Sea and Aleutian Islands area. In *Stock assessment and fishery evaluation report for the groundfish resources of the Bering Sea-Aleutian Islands regions*, p. 121–206. North Pacific Fishery Management Council, 605 W 4th Avenue, Suite 306, Anchorage, AK 99501.

Abstract—Molecular-based approaches for shark species identification have been driven largely by issues specific to the fishery. In an effort to establish a more comprehensive identification data set, we investigated DNA sequence variation of a 1.4-kb region from the mitochondrial genome covering partial sequences from the 12S rDNA, 16S rDNA, and the complete valine tRNA from 35 shark species from the Atlantic fishery. Generally, within-species variability was low in relation to interspecific divergence because species halotypes formed monophyletic groups. Phylogenetic analyses resolved ordinal relationships among Carcharhiniformes and Lamniformes, and revealed support for the families Sphyrnidae and Triakidae (within Carcharhiniformes) and Lamnidae and Alopiidae (within Lamniformes). The combination of limited intraspecific variability and sufficient between-species divergence indicates that this locus is suitable for species identification.

Mitochondrial gene sequences useful for species identification of western North Atlantic Ocean sharks

Thomas W. Greig

M. Katherine Moore

Cheryl M. Woodley

National Ocean Service
National Center for Coastal Ocean Science
Center for Coastal Environmental Health and Biomolecular Research at Charleston
219 Fort Johnson Road
Charleston, South Carolina 29412-9110
E-mail address (for T. W. Greig): Thomas.Greig@noaa.gov

Joseph M. Quattro

Department of Biological Sciences
School of the Environment
University of South Carolina
Columbia, South Carolina 29208

Seventy-three species of sharks inhabit the United States territorial waters of the Atlantic Ocean, Gulf of Mexico, and Caribbean Sea (Compagno, 1984a, 1984b). All but one (spiny dogfish, *Squalus acanthias*, managed separately) are managed under the current Fisheries Management Plan (FMP) for highly migratory species (NMFS¹). Thirty-three species are of lesser commercial importance and are relegated to the "deepwater and other" species management group, and 19 species cannot be landed commercially or recreationally ("prohibited species" group). The remaining 20 species are of interest to the commercial shark fishery and are categorized as large coastal species (LCS), small coastal species (SCS), and pelagic species management units in the current FMP. Although these management units are practical, it is clear that species respond uniquely to exploitation and therefore should be managed on a species-by-species basis (Castro et al., 1999; NMFS²). Species-level management is widely recommended (e.g., FAO Marine Resource Service, 2000) but is complicated by the paucity of species-specific fisheries data, stemming, in part, from an inability to accurately identify species.

Many commercially important species (e.g., within Carcharhiniformes) are difficult to identify whole, and this task is more daunting if individuals are processed (head, entrails, and fins are removed); unfortunately, at-sea processing is widespread in the industry (Castro³). Although current U.S. legislation prohibits the practice of "finning" (where fins are retained and carcasses are discarded at sea,

¹ NMFS (National Marine Fisheries Service). 2003. Final amendment 1 to the fishery management plan for Atlantic tunas, swordfish and sharks, 599 p. Office of Sustainable Fisheries, Highly Migratory Species Management Division, NMFS, NOAA, 1315 East West Highway, SSMC3, Silver Spring, MD 20910.

² NMFS (National Marine Fisheries Service). 2001. Final United States national plan of action for the conservation and management for sharks, 90 p. Office of Sustainable Fisheries, Highly Migratory Species Management Division, NMFS, NOAA, 1315 East West Highway, SSMC3, Silver Spring, MD 20910.

³ Castro, J. I. 1993. A field guide to the sharks commonly caught in commercial fisheries of the southeastern United States. NOAA Tech. Memo. NMFS-SEFSC-338, 47 p. Southeast Fisheries Science Center, NMFS, NOAA, 75 Virginia Beach Dr., Miami, FL 33149.

the landing of fins is allowed where carcasses and fins are off-loaded at the same time in a no more than 1:20 (fin-to-carcass) weight ratio. However, serious problems can arise in matching off-loaded fins to processed carcasses. In and of itself, the landing of shark fins can be lucrative; fins accounted for more than 50% of the total Atlantic shark fishery value in 2002 (NMFS⁴). Because preferences exist for fins from certain species, exvessel prices for specific types of fin vary considerably (e.g., Weber and Fordham, 1997). It is perhaps not surprising that augmenting the fin-to-carcass ratio with spoiled meat or “finning” target species out of season (and subsequently attributing the fins to fish that are allowed to be caught during the season) might not be uncommon (Vannuccini, 1999). Clearly, these possibilities lead to the challenge of matching collected fins to processed carcasses. Therefore, accurate and reliable species identification methods are paramount for law enforcement and sound species management.

Molecular species identification research on sharks has been driven largely by resolution of specific problems associated with the fishery. For example, Heist and Gold (1999) used mtDNA sequence data to develop restriction fragment assays that differentiate 11 species of carcharhiniform sharks commonly encountered in the LCS fishery. Similarly, Pank et al. (2001) used multiplex PCR to differentiate two morphologically similar shark species (*Carcharhinus obscurus* and *C. plumbeus*)—an approach that was expanded by Shivji et al. (2001) to include five additional species (with some overlap of species included by Heist and Gold 1999). Both approaches are relatively rapid, inexpensive, and easily implemented; however, they appear most applicable when the number of species investigated is limited. In sum, of the thirty-nine species of sharks that are not in the “deepwater and other” management group, molecular species identification assays have been developed for fifteen species (9 LCS, 3 pelagic, and 3 in the prohibited species management groups) (Heist and Gold, 1999; Pank et al., 2001; Shivji et al., 2001), leaving 24 species without molecular methods for identification.

Some investigators have instead turned to DNA sequence analysis to resolve issues of species identification (Takeyama et al., 2001; Akimoto et al., 2002; Jerome et al., 2003). This approach is exemplified best by the recent development of computer interfaces that allow access to and analysis of large DNA databases (DNA Surveillance, Ross et al., 2003; ARB, Ludwig et al., 2004). Simply put, these databases circumvent the tedious process of scanning large taxonomically diverse DNA repositories (e.g., GenBank) by allowing the user to access (DNA Surveillance) or maintain (ARB) taxonomically restricted sets of reference sequences. Users

can submit “unknown” sequences to compare against specified sequence subsets; subsequent analyses are returned as genetic distances (between unknown and reference sequences) and include a phylogenetic hypothesis.

The power of this approach lies in the ease with which reference sequences can be added to the database, in the “quality-control” that can be exerted over subsequent additions to the reference sequences, and in the ease with which geographic variation within species can be included. The success of this approach, however, hinges on the information contained in the gene in the reference database. The inception of this approach, as applied to commercially important sharks, requires a sufficiently informative set of reference sequences against which searches can be made. The aforementioned molecular approaches (RFLP, multiplex PCR) include a diversity of gene regions (mitochondrial DNA, nuclear ITS); thus no comprehensive data set exists for commercially landed Atlantic shark species. Fortunately, recent work with a 2.4-kb fragment of the mitochondrial genome (spanning 12S rDNA to 16S rDNA) to examine the phylogenetic relationships among shark orders has shown that this region may be useful in resolving relationships at this taxonomic level (Douady et al., 2003). Unfortunately, sampling within orders was limited, and it is thus unknown whether this region contains sufficient phylogenetic signal at lower taxonomic levels.

We present here mtDNA sequence data of a smaller fragment of the same region containing partial sequence information for the mitochondrial 12S rDNA, 16S rDNA, and the complete valine tRNA from 35 shark species (including all 20 commercially exploited species, 12 of 19 prohibited species, the spiny dogfish, and two species of *Mustelus*). We suggest that a suitable locus for species-identification purposes will permit identification of unequivocally distinct species (i.e., large genetic differentiation between species compared to within species) and offer the potential for meaningful phylogenetic comparisons (important when “query” animals are absent or not adequately represented in a molecular database). Keeping in mind issues of species identification and fisheries management, we examine this mtDNA region for patterns of genetic variability and assess its utility in phylogenetic reconstruction. We then discuss the use of this region for the underpinnings of a validated reference DNA database suitable for forensic and fisheries management applications.

Methods

Sample collection

Voucher Atlantic Ocean shark samples (muscle, fin, or blood) were obtained from the CCEHBR Marine Forensics archive in Charleston, SC (Table 1). Samples were accompanied by species certification and chain-of-custody forms. Muscle and fin samples were either frozen at

⁴ NMFS (National Marine Fisheries Service). 2003. Stock assessment and fishery evaluation report for Atlantic highly migratory species (SAFE), 274 p. Office of Sustainable Fisheries, Highly Migratory Species Management Division, NMFS, NOAA, 1315 East West Highway, SSMC3, Silver Spring, MD 20910.

Table 1

Scientific and common names of samples, number of individuals sampled (*n*), species codes, and Genbank accession numbers. Taxonomy follows Campagno (1984, 2001). Species codes correspond to a representative individual in the National Ocean Service Marine Forensics Program (CCEHBR, Charleston, SC) tissue archive with that particular haplotype (except for *Heterodontus francisci* Hfra1).

Order	Family and species	Common name	Code (<i>n</i>)	Accession
Carcharhiniformes	Carcharhinidae			
	<i>Carcharhinus acronotus</i>	Blacknose	Cacr003(3)	AY830721
	<i>C. altimus</i>	Bignose	Cal001(2)	AY830722
	<i>C. brevipinna</i>	Spinner	Cbre001(3)	AY830723
	<i>C. falciformis</i>	Silky	Cfal003(1)	AY830725
			Cfal006(1)	AY830726
	<i>C. isodon</i>	Finetooth	Ciso004(1)	AY830727
			Ciso101(1)	AY830728
			Ciso115(1)	AY830729
	<i>C. leucas</i>	Bull	Cleu003(3)	AY830730
	<i>C. limbatus</i>	Blacktip	Clim004(1)	AY830731
			Clim006(2)	AY830732
	<i>C. longimanus</i>	Oceanic whitetip	Clon000(1)	AY830736
			Clon002(1)	AY830733
			Clon005(1)	AY830734
			Clon006(1)	AY830735
	<i>C. obscurus</i>	Dusky	Cobs000(1)	AY830737
			Cobs001(3)	AY830738
	<i>C. perezii</i>	Caribbean reef	Cper001(2)	AY830739
			Cper002(2)	AY830740
	<i>C. porosus</i>	Smalltail	Cpor001(1)	AY830743
	<i>C. plumbeus</i>	Sandbar	Cpla004(2)	AY830741
			Cpla023(1)	AY830742
	<i>C. signatus</i>	Night	Csig002(1)	AY830744
	<i>Galeocerdo cuvier</i>	Tiger	Geuv003(3)	AY830746
	<i>Negaprion brevirostris</i>	Lemon	Nbre005(1)	AY830756
	<i>Prionace glauco</i>	Blue	Pgla004(1)	AY830760
			Pgla0020(1)	AY830761
			Pgla0022(1)	AY830762
	<i>Rhizoprionodon terraenovae</i>	Sharpnose	Rter001(2)	AY830763
		Rter026(1)	AY830764	
Sphyrnidae				
<i>Sphyrna lewini</i>	Scalloped hammerhead	Slew003(2)	AY830768	
<i>S. mokorran</i>	Great hammerhead	Smok003(3)	AY830769	
<i>S. tiburo</i>	Bonnethead	Stib016(2)	AY830770	
		Stib018(1)	AY830771	
<i>S. zygaena</i>	Smooth hammerhead	Szyg681(6)	AY830772	
Triakidae				
<i>Mustelus canis</i>	Smooth dogfish	Mcan003(3)	AY830754	
<i>M. norrisi</i>	Florida smoothhound	Mnor001(2)	AY830755	
Lamniformes	Alopiidae			
	<i>Alopias superciliosus</i>	Bigeye thresher	Asup001(1)	AY830718
			Asup006(1)	AY830719
	<i>A. vulpinus</i>	Thresher	Avul002(1)	AY830720
	Lamnidae			
	<i>Carcharodon carcharias</i>	White	Ccar002(3)	AY830724
	<i>Isurus oxyrinchus</i>	Shortfin mako	Ioxy005(1)	AY830747
			Ioxy032(1)	AY830748
			Ioxy051(1)	AY830749
	<i>I. paucus</i>	Longfin mako	Ipau002(2)	AY830750
		Ipau005(1)	AY830751	
<i>Lamna nasus</i>	Porbeagle	Lnas001(2)	AY830752	
		Lnas003(1)	AY830753	

continued

Table 1 (continued)

Order	Family and species	Common name	Code (n)	Accession
	Odontaspidae			
	<i>Carcharias taurus</i>	Sand tiger	Otau004(1) Otau005(1) Otau007(1)	AY830757 AY830758 AY830759
Orectolobiformes	Ginglymostomatidae			
	<i>Ginglymostoma cirratum</i>	Nurse	Geir001(2)	AY830745
Hexanchiformes	Hexanchidae			
	<i>Hexanchus vitulus</i>	Bigeye sixgill	Hvit1(1)	AY830716
	<i>Heptranchias perlo</i>	Sevengill	Hper1(1)	AY830715
Squaliformes	Squalidae			
	<i>Squalus acanthias</i>	Spiny dogfish	Saca002(1) Saca003(2)	AY830765 AY830766
Squatiformes	Squatinae			
	<i>Squatina dumeril</i>	Atlantic angel	Sdum001(3)	AY830767
Heterodontiformes	Heterodontidae			
	<i>Heterodontus francisci</i>	Horn shark	Hfra(1)	NC003137

-80°C, dried, or stored in 70% EtOH. Blood was stored at room temperature in sodium dodecyl sulfate-urea (SDS-urea: 1% SDS, 8M urea, 240 mM Na₂HPO₄, 1mM EDTA pH 6.8). Total nucleic acids were extracted from frozen, dried, and EtOH-preserved samples by using DNeasy Tissue Kits and following manufacturer's recommendations (Qiagen, Valencia, CA). DNA was isolated from blood in SDS-urea according to White and Densmore (1992; protocol 11). Extracted DNA was visualized by electrophoresis in a 1% agarose gel stained with 0.4 ng/mL of ethidium bromide in 1× Tris-borate-EDTA (TBE: 89 mM Tris-borate, 2 mM Na₂EDTA, pH 8). A 1-kb DNA ladder (Promega, Madison, WI) was used as a size standard.

Amplification and sequencing

Primers 12SA-5' and 16SA-3' (Palumbi, 1996) were used to amplify an approximately 1400-bp region spanning the 3' end of the 12s rDNA, the valine tRNA, and the 5' end of the 16s rDNA region of mitochondrial DNA (mtDNA). Samples were amplified in 50 µL reactions containing ~50 ng of template DNA, 20 mM Tris-HCl pH 8.4, 50 mM KCl, 0.2 mM each dNTP, 2 mM MgCl₂, 20 mM each primer, and 2.5 units *Taq* DNA polymerase (Gibco BRL, Rockville, MD). Thermal cycling consisted of an initial denaturation at 94°C for 1.5 minutes, followed by 30 cycles of 40 seconds at 94°C, 40 seconds at 52°C, and 50 seconds at 72°C, and a final extension step of 15 minutes at 72°C. Negative controls (no template) were included in each set of reactions. PCR products were gel-purified as described in Rosel and Block (1996) and 20–50 ng were used as template for ABI Big Dye Terminator (v. 1.0, Applied Biosystems, Foster City, CA) cycle sequencing reactions. Sequence was obtained with amplification primers 12SA-5', 16SA-3' and two additional internal sequencing primers. Sequencing reaction

products were precipitated with ethanol, washed according to sequencing kit instructions, dried in a Savant Speedvac Plus, and resuspended in 4 µL of loading dye (5:1 Hi-Di formamide:dextran blue). Fragments were analyzed on an Applied Biosystems 377 automated DNA sequencer.

Sequence analysis and alignment

Sequences were edited with SEQUENCHER (vers. 3.0; Gene Codes Corp., Detroit, MI). We included three additional sequences from GenBank: horn shark (*Heterodontus francisci*, NC003137) to represent the family Heterodontidae, thorny skate (*Raja radiata*, AF106038), rabbit fish (*Chimaera monstrosa*, AJ310140), and the Atlantic guitarfish (*Rhinobatis lentiginosus*, AY830717—this study) to serve as outgroups for phylogenetic analyses. Sequences were aligned by using a linear hidden Markov model (HMM) as implemented in SAM (Sequence Alignment and Modeling System; Hughey and Krogh, 1996; Karplus et al., 1998) with default settings. The alignment file is available from the senior author.

Phylogenetic hypotheses were constructed by using the maximum parsimony (MP) and neighbor-joining (NJ) algorithms implemented in PAUP 4.0b10 (Sinauer Associates, Sunderland, MA). NJ analyses employed a variety of pairwise distance measures, but the distance measure used had little or no effect on the recovered topologies. Phylogenies recovered with MP with equally weighted characters were generally concordant with those recovered by NJ, particularly when bootstrap consensus trees were compared. For ease of interpretation, we report NJ analyses using p-distances as a metric. Bootstrapping (Felsenstein, 1985) was used to estimate the reliability of NJ reconstructions (1000 pseudoreplicates).

Results

Sequence variation and divergence

An approximately 1.4-kb gene region was amplified and sequenced from 93 samples representing 35 shark species. Fifty-seven of the 93 individuals had unique haplotypes (Table 1, Fig. 1). An alignment of these haplotypes with several outgroups with the SAM algorithm resulted in a 1510 position consensus alignment after the introduction of gaps. Of these 1510 aligned positions, 717 positions were variable and 543 were parsimony informative. Transition outweighed transversion substitutions by a factor of 4.27. Considering only phylogenetically informative sites within the ingroup, we found that nucleotide composition did not differ significantly among haplotypes (A: 35.9%, C: 21.9%, G: 16.9%, T: 25.3%; $\chi^2=175.6$, $P=0.39$).

Phylogenetic analysis

Unweighted parsimony analysis produced 24 equally parsimonious trees of length 2733 (CI=0.39, RI=0.74) that differed primarily in the relationships among haplotypes within species (not shown). Neighbor-joining analyses produced nearly identical topologies regardless of the distance metric used. When differences were noted, they often involved trivial placements of individual variants within species or the placement of branches that were poorly supported by bootstrap analyses regardless of the reconstruction method employed. For this reason, we present phylogenetic hypotheses generated by neighbor-joining, using p-distances as a surrogate for all analyses.

Most clades containing multiple haplotypes within species were highly supported by bootstrap analyses. Of 16 species represented by more than a single sequence, 15 were recovered as monophyletic groups in 100% of 1000 bootstrap replicates (Fig. 1). Sequence divergence within species was generally trivial compared to among-species divergences. For example, sequence divergence among haplotypes within species of *Carcharhinus* differed by approximately two orders of magnitude from that among species within the genus (average p-distance of 0.05% and 4.16%, respectively). The exception involved haplotypes observed within *C. plumbeus* that were supported as monophyletic by fewer than 70% of 1000 bootstrap replicates in MP and NJ analyses. Interestingly, a sister group relationship between *C. plumbeus* and *C. altimus* was highly supported by bootstrapping, and average sequence divergence within species (0.14%) was only about one-third of that observed between these two (0.43%).

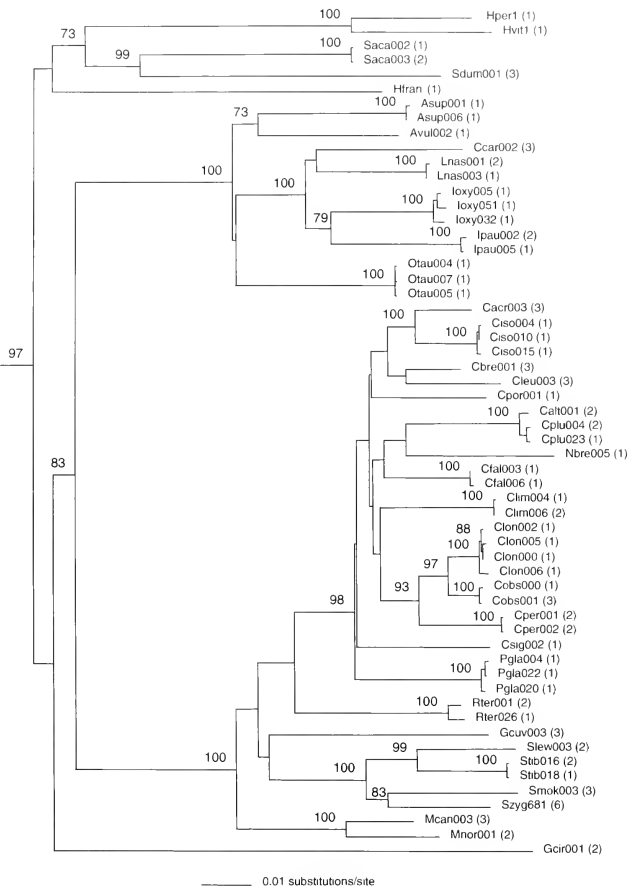
Some higher order relationships were recovered with high bootstrap support. Notably the Carcharhiniformes were strongly supported as monophyletic, as were the families Sphyrnidae and Triakidae. The family Carcharhinidae was poorly supported as monophyletic, although a group that included *Negaprion*, *Prionace*, and all *Carcharhinus* was observed in a large number of

bootstrap replicates. *Carcharhinus* was paraphyletic in the NJ topology, and *Negaprion* was nested within the genus, but this relationship received little support from bootstrapping. The Lamniformes were monophyletic and strongly supported by bootstrapping. Within this order, only the family Lamnidae received strong support, whereas support for a monophyletic Alopiidae was moderate. The order Hexanchiformes was recovered as a monophyletic group; however bootstrap support for this grouping was low.

Discussion

Our goal was to assess whether the 12s–16s region of the shark mitochondrial genome contained sufficient genetic variation and phylogenetic signal to be useful in species identification. Of the 35 species examined, 6 species were each represented by a single individual, and 16 of the remaining 29 species contained variants at the mtDNA locus examined. Importantly, all within-species variants formed strongly supported monophyletic groups concordant with morphologically based species descriptions. Intraspecific variability was low in relation to interspecific divergence at this locus and in no instance was a paraphyletic relationship between species observed. The combination of limited intraspecific variability combined with sufficient between-species divergence indicates that this locus is suitable for species identification.

Two exceptions to this generalization of low within versus large between-species differentiation exist in our phylogenetic hypothesis—one involving the sister species pair *C. plumbeus* and *C. altimus*. In an alignment of mitochondrial sequences from these species, only 5 or 7 transition substitutions were observed across approximately 1.4 kb of sequence data. Interestingly, Heist and Gold (1999) included these two taxa in their cytochrome-*b* RFLP analysis, and again, Atlantic samples of *C. plumbeus* and *C. altimus* differed by only a single transition in 395 basepairs (0.25%), and there were more substitutions observed between Atlantic and Pacific *C. plumbeus* than between Atlantic samples of *C. plumbeus* and *C. altimus* (Table 2 in Heist and Gold 1999). The next most closely related pair of taxa in our phylogenetic hypothesis comprised two other Carcharhiniforms, *C. longimanus* and *C. obscurus*, a taxon pair differing by approximately 1.44% sequence divergence, compared with an average of 0.06% within taxon diversity. These two taxa were considered by Shivji et al. (2001) while developing a multiplex PCR assay for six commercially important pelagic species. Specifically, assays developed to diagnose *C. obscurus* could not discriminate between *C. obscurus* and *C. longimanus*, two closely related species in our phylogenies. The *C. plumbeus* and *C. altimus* species pair was not considered by Shivji et al. (2001); thus no comparison to the Heist and Gold (1999) cytochrome-*b* sequence/RFLP or the 12s–16s data set presented in our study was possible. We are currently analyzing additional samples,

**Figure 1**

Neighbor-joining tree showing relationship of observed 12s-16s haplotypes among 36 species of shark. Codes are defined in Table 1 and numbers in parentheses indicate the number of individuals found with the indicated haplotype. Bootstrap support is indicated as numbers immediately above the relevant node (only values greater than 70% are shown). The phylogeny was rooted with several outgroup taxa (*Heterodontus francisci* (NC003137), *Raja radiata* (AF106038), *Chimaera monstrosa* (AJ310140), and *Rhinobatis lentiginosus* (AY830717)).

including a more comprehensive geographical survey of these four species to confirm that the genetic differences observed are diagnostic. However, it is clear that DNA sequence-based approaches appear more powerful in discriminating closely related species pairs and less likely to produce false positives than other DNA-based assays.

Although it was not our intent to conduct an exhaustive analysis of higher-order relationships among western North Atlantic shark species, some interesting results nonetheless deserve mention. First, the orders Carcharhiniformes and Lamniformes were strongly supported as monophyletic, as were the families Sphyrnidae, Triakidae, and Lamnidae that were included in the study. The order Hexanchiformes was likewise monophyletic, but bootstrap support for this grouping was low. The family Carcharhinidae was poorly supported as monophyletic, which is consistent with previous studies (Naylor, 1992; Nelson, 1994; Musick et al., 2004). Interestingly, our phylogenetic hypotheses place the family Triakidae basal to all other families within the Carcharhiniformes, following Compagno (1988), but this position was not strongly supported and is predicated on limited sampling of Carcharhiniform families (only four of eight were included in our analysis). Clearly this gene region contains some phylogenetically useful information regarding shark relationships, confined principally to higher-level groupings.

We are careful in judging the utility of a locus for species identification on the basis of phylogenetic signal alone. Clearly, rapidly evolving molecular markers are valuable tools for species identification but might not be appropriate for reconstructing phylogenetic relationships at certain scales. Conversely, those regions containing sufficient signal to generate reasonable phylogenetic reconstructions (i.e., general concordance with accepted phylogenetic relationships based on other independent characters) must be useful (and appropriate) markers for species identification. Further, these regions are amenable to the addition of uncharacterized species and the inclusion of intraspecific diversity (e.g., diverged mtDNA lineages within species). Importantly, however, DNA sequence-based approaches offer the potential to assign at least some level of taxonomic characterization to unknown or unrepresented samples. Although the use of DNA sequencing has historically been viewed as cost prohibitive, the genomic revolution over recent years has spawned cost-effective sequencing services, making routine sequencing of samples for species identification not only practical but optimal.

The size of the amplification product in the present study might place limitations on the application of this method to the poor-quality tissue and DNA often encountered in forensic studies. It has been our experience that the primers used in our study consistently have generated strong amplification products with DNA isolated from a variety of tissue types, including dried tissue and fins; however, we have yet to explore the range of amplifications possible using tissues more commonly

encountered in forensic cases. To circumvent potential problems with large amplifications on degraded DNA samples, we have constructed a preliminary, searchable DNA-sequence database using the FASTA program (Univ. Virginia, Charlottesville, VA; Pearson, 1999) and the 12s-16s sequences presented in the present study. Our preliminary analyses indicate that all species examined in the study can be uniquely identified from approximately 400 bp of sequence generated by the 12SA-5' primer. We are examining the limitations of sequence length in combination with the search accuracy of this informative fragment.

We are mindful of the restriction placed on these analyses due to limited within-taxon sampling (particularly within-family) and of the incomplete representation (notably the *Pristophoriformes*) of all orders of sharks and are aware that the phylogenetic affinities presented in this study could change with the addition of characters and taxa. These caveats notwithstanding, we believe that a taxonomically restricted DNA sequence database offers certain advantages over perhaps more rapid RFLP or multiplex PCR assays. DNA databases 1) can be "curated" (additions and access to the database can be selective) and distributed as an alignment suitable for further subsequent statistical or phylogenetic manipulation; 2) can be easily amended to include additional taxa, genetic variation within species, and additional gene loci more appropriate at various taxonomic scales; 3) allow for unequivocal assignment (subject to limits of discrimination of those loci included) of species identification while making available the raw data necessary for the development of more rapid assays (RFLP/Multiplex PCR) for select taxa (note that the opposite is not necessarily true); and, 4) facilitate the identification of those taxa not currently represented in the database through phylogenetic analysis.

In summary, we have found that the sequence of the 12S-16S region of the mtDNA that we examined contains ample information for discriminating between the shark species studied and shows promise for the placement of species not yet examined within the correct phylogenetic group (family). We are continuing to examine geographic variation within and among species and to assay genetic variability at nuclear loci in an effort to resolve potential introgression and (or) hybridization events. As information is added to our database, either in the form of additional species or loci, our species identification method will become more robust.

Acknowledgments

Much of this work derived directly from forensic case work conducted by Ann Colbert for the National Marine Fisheries Service. Robert Chapman provided primer sets and guidance. Laura Webster conducted initial surveys of shark mtDNA variability and assisted in sample acquisition. Shannon Leonard and David Carter assisted

in DNA sequencing. The authors thank Trey Knott, Ron Lundstrum, Laura Webster and two anonymous reviewers for their critical review of this manuscript. This project was funded partially by grants from the Cooperative Institute for Fisheries Molecular Biology (FISHTEC; NOAA/NMFS (RT/F-1)) and SC SeaGrant (R/MT-5) to JMQ.

Literature cited

- Akimoto S, S. Kinoshita, K. Sezaki, I. Mitani, and S. Watabe.
2002. Identification of alfonsoino and related fish species belonging to the genus *Beryx* with mitochondrial 16S rRNA gene and its application on their pelagic eggs. *Fish. Sci.* 68 (6):1242-249.
- Castro, J. I., C. M. Woodley, and R. L. Brudeck.
1999. A preliminary evaluation of the status of shark species. *Fish. Tech. Paper* 380, 72 p. FAO Rome.
- Compagno, L. J. V.
1984a. FAO species catalogue. Vol 4. Sharks of the world. An annotated and illustrated catalogue of shark species known to date. Part 1 Hexanchiformes to Lamniformes. FAO, Fish. Synop. 125, vol.4, pt.1, 249 p. FAO, Rome.
1984b. FAO species catalogue. Vol 4. Sharks of the world. An annotated and illustrated catalogue of shark species known to date. Part 2: Carchariformes. FAO Fish. Synop. 125, vol.4, pt. 2, p. 251-655. FAO, Rome.
1988. Sharks of the order Carcharhiniformes. 486 p. Princeton Univ. Press, Princeton, NJ.
2001. Sharks of the world. An annotated and illustrated catalogue of shark species known to date. Volume 2: Bullhead, mackerel and carpet sharks (Heterodontiformes, Lamniformes and Orectolobiformes). FAO species catalogue for fishery purposes, no. 1, vol. 2, 269 p. FAO, Rome.
- Douady C. J. D. Dosay, M. S. Shivji, and M. J. Stanhope.
2003. Molecular phylogenetic evidence refuting the hypothesis of Batoidea (rays and skates) as derived sharks. *Mol. Phylo. Evol.* 26:215-221.
- Felsenstein, J.
1985. Confidence limits on phylogenies: an approach using the bootstrap. *Evolution* 39:783-791.
- FAO (Food and Agriculture Organization) Marine Resource Service.
2000. Fisheries management. 1. Conservation and management of sharks. FAO Technical guidelines for responsible fisheries, no. 4, suppl. 1, 37 p. FAO, Rome.
- Heist, E. J., and J. R. Gold.
1999. Genetic identification of sharks in the U.S. Atlantic large coastal shark fishery. *Fish. Bull.* 97:53-61.
- Hughes R, and A. Krogh.
1996. Hidden Markov models for sequence analysis: extension and analysis of the basic method. *CABIOS* 12(2):95-107.
- Jerome M., C. Lemaire, J. M. Bautista, J. Fleurencem and M. Etienne.
2003. Molecular phylogeny and species identification of sardines. *J. Agr. Food Chem.* 51(1):43-50.
- Karpus, K., C. Barrett, and R. Hughley.
1998. Hidden Markov models for detecting remote protein homologies. *Bioinformatics* 14:846-856.
- Ludwig, W. O., Strunk, R., Westram, L., Richter, H., Meier, Yadhukumar, A. Buchner, T. Lai, S. Steppi, G. Jobb, W. Forster, I. Brettske, S. Gerber, A.W. Ginhart, O. Gross, S. Grumann, S. Hermann, R. Jost, A. König, T. Liss, R. Lussmann, M. May, B. Nonhoff, B. Reichel, R. Strehlow, A. Stamatakis, N. Stuckmann, A. Vilbig, M. Lenke, T. Ludwig, A. Bode, and K. H. Schleifer.
2004. ARB: a software environment for sequence data. *Nuc. Acids Res.* 32 (4):1363-1371.
- Musick, J. A., M. M. Harbin, and L. J. V. Compagno.
2004. Historical zoogeography of the Selachii. *In* Biology of sharks and their relatives (J. C. Carrier, J. A. Musick, and M. R. Heithaus, eds.), p. 33-78. CRC Press, Boca Raton, FL.
- Naylor, G. J. P.
1992. The phylogenetic relationships among requiem and hammerhead sharks: inferring phylogeny when thousands of equally most parsimonious trees result. *Cladistics* 8:295-318.
- Nelson, J. S.
1994. *Fishes of the world* 3rd ed., 600 p. John Wiley and Sons, Inc. New York, NY.
- Palumbi, S. R.
1996. Nucleic acids II: the polymerase chain reaction. *In* Molecular systematics, 2nd ed. (D. M. Hillis, C. Moritz and B. , eds.), p 205-247. Sinauer Associates, Sunderland, MA.
- Pank, M., M. Stanhope, L. Natanson, N. Kohler, and M. Shivji.
2001. Rapid and simultaneous identification of body parts from morphologically similar sharks *Carcharhinus obscurus* and *Carcharhinus plumbeus* (Carcharhinidae) using Multiplex PCR. *Mar. Biotech.* 3:231-240.
- Pearson, W. R.
1999. Flexible sequence similarity searching with the FASTA3 program package. *Methods Mol. Biol.* 132: 185-219.
- Rosel P. E., and B. A. Block.
1996. Mitochondrial control region variability and global population structure in the swordfish, *Xiphias gladius*. *Mar. Biol.* 125:11-22.
- Ross H. A., G. M. Lento, M. L. Dalebout, M. Goode, G. Ewing, P. McLaren, A. G. Rodrigo, S. Lavery, and C. S. Baker.
2003. DNA surveillance: web-based molecular identification of whales, dolphins, and porpoises. *J. Hered.* 94:111-114.
- Shivji, M., S. Clarke, M. Pank, L. Natanson, N. Kohler, and M. Stanhope.
2001. Genetic identification of pelagic shark body parts for conservation and trade monitoring. *Cons. Gen.* 16(4):1036-1047.
- Takeyama, H., S. Chow, Tsuzuki, and T. Matsunaga.
2001. Mitochondrial DNA sequence variation within and between tuna *Thunnus* species and its application to species identification. *J. Fish Biol.* 58(6):1646-1657.
- Vannuccini, S.
1999. Shark utilization, marketing and trade. FAO Fisheries Technical Paper 389, 470 p. FAO, Rome.
- Weber, M. L., and S. V. Fordham.
1997. Managing shark fisheries: opportunities for international conservation. TRAFFIC international and Center for Marine Conservation report, 61 p. TRAFFIC, Washington, DC.
- White P.S., and L. D. Densmore III.
1992. Mitochondrial DNA isolation. *In* Molecular genetic analysis of populations: a practical approach (A. R. Hoelzel ed.), p. 29-58. Oxford Univ. Press, Oxford, U.K.

Abstract—Rougheye rockfish (*Sebastes aleutianus*) and shortraker rockfish (*Sebastes borealis*) were collected from the Washington coast, the Gulf of Alaska, the southern Bering Sea, and the eastern Kamchatka coast of Russia (areas encompassing most of their geographic distribution) for population genetic analyses. Using starch gel electrophoresis, we analyzed 1027 rougheye rockfish and 615 shortraker rockfish for variation at 29 protein-coding loci. No genetic heterogeneity was found among shortraker rockfish throughout the sampled regions, although shortraker in the Aleutian Islands region, captured at deeper depths, were found to be significantly smaller in size than the shortraker caught in shallower waters from Southeast Alaska. Genetic analysis of the rougheye rockfish revealed two evolutionary lineages that exist in sympatry with little or no gene flow between them. When analyzed as two distinct species, neither lineage exhibited heterogeneity among regions. *Sebastes aleutianus* seems to inhabit waters throughout the Gulf of Alaska and more southern waters, whereas *S. sp. cf. aleutianus* inhabits waters throughout the Gulf of Alaska, Aleutian Islands, and Asia. The distribution of the two rougheye rockfish lineages may be related to depth where they are sympatric. The paler color morph, *S. aleutianus*, is found more abundantly in shallower waters and the darker color morph, *Sebastes sp. cf. aleutianus*, inhabits deeper waters. *Sebastes sp. cf. aleutianus*, also exhibited a significantly higher prevalence of two parasites, *N. robusta* and *T. trituba*, than did *Sebastes aleutianus*, in the 2001 samples, indicating a possible difference in habitat and (or) resource use between the two lineages.

Manuscript submitted 24 November 2003 to the Scientific Editor's Office.

Manuscript approved for publication 28 March 2005 by the Scientific Editor.
Fish. Bull. 103:524–535 (2005).

Genetic variation of rougheye rockfish (*Sebastes aleutianus*) and shortraker rockfish (*S. borealis*) inferred from allozymes

Sharon L. Hawkins

Jonathan Heifetz

Christine M. Kondzela

John E. Pohl

Richard L. Wilmot

Auke Bay Laboratory
Alaska Fisheries Science Center
National Marine Fisheries Service
11305 Glacier Highway
Juneau, Alaska, 99801-8626
E-mail address: Sharon.Hawkins@noaa.gov

Oleg N. Katugin

Vladimir N. Tuponogov

Pacific Research Fisheries Centre (TINRO-Centre)
4 Shevchenko Alley
Vladivostok 690950, Russia

Information about the biology and population dynamics of rougheye rockfish (*S. aleutianus*) and shortraker rockfish (*S. borealis*) is limited, and uncertainty exists about current stock abundance and long-term productivity. As adults, these two species are similar in appearance, have the same zoogeography, and share the same habitat. They were classified as a single species, *S. aleutianus* (Jordan and Evermann, 1898), until Barsukov (1970) described *S. borealis*. Tsuyuki and Westheim (1970) also described *S. borealis* that same year (initially as *S. caenaemeticus*), using biochemical methods. The distribution of rougheye rockfish is reported from Japan to southeastern Kamchatka (excluding the Sea of Okhotsk), to Navarin Canyon in the Bering Sea, throughout the Aleutian Islands, and south to San Diego, California (Tokranov and Davydov, 1997). Shortraker rockfish has a similar distribution; however, this species is much more abundant than rougheye rockfish in Russia—eastern Russian *Sebastes* biomass was composed of more than 90% shortraker and less than 1% rougheye rockfish for most regions, excepting the Com-

mander Islands (Tokranov and Davydov, 1997). Both species have been reported at depths to 875 m (Allen and Smith, 1988), although longline (Sigler and Zenger¹) and trawl surveys (NMFS triennial groundfish survey) indicate they are most abundant on the upper continental slope at 300–400 m depths. Krieger and Ito (1999) found the two species difficult to distinguish visually when viewed from a submersible but believed that the highly sedentary adults of both species share the same habitat, preferring substrates of sand or mud and frequent boulders and steep slopes.

Rougheye and shortraker rockfish are highly prized commercially but are particularly sensitive to overexploitation because of slow growth, late maturation, and long life spans. Half of rougheye rockfish are mature at 20

¹ Sigler, M. F., and H. H. Zenger Jr. 1994. Relative abundance of Gulf of Alaska sablefish and other groundfish based on the domestic longline survey, 1989. U. S. Dep. Commer., NOAA Tech. Memo. NMFS-AFSC-40, 79 p. Auke Bay Laboratory, 11305 Glacier Hwy., Juneau, AK 99801.

years of age (McDermott, 1994). Rougheye rockfish have been estimated to attain ages in excess of 200 years and shortraker rockfish in excess of 150 years (Munk, 2001). These two species are currently managed together as the "shortraker-rougheye" assemblage within waters managed under a North Pacific Fishery Management Council (NPFMC) fishery management plan. Commercial catch levels in NPFMC areas of the Bering Sea, the Aleutian Islands, and the Gulf of Alaska averaged 2400 t each year from 1999 to 2001 (Heifetz et al., 2002; Spencer and Reuter, 2002).

The annual catch quota for rockfish and most groundfish managed by the NPFMC is apportioned among five relatively large geographic areas: the eastern, central, and western Gulf of Alaska, the Aleutian Islands, and the eastern Bering Sea. Previous work in the Gulf of Alaska has indicated geographical segregation of the two rougheye species (Moles et al., 1998; Hawkins et al.²). Based on earlier designations of the International North Pacific Fisheries Commission, area boundaries have little biological basis. If the population structure of a particular species has different geographic boundaries than the boundaries of the designated management areas for the species, there is risk of over-harvest. The objective of this study is to examine the population structure of rougheye and shortraker rockfish by using allozyme variation. This is the first population structure study of these two species that encompasses all the North Pacific management areas and most of their biological ranges.

Methods

Collection

Adult rougheye rockfish were collected with bottom trawls from the Gulf of Alaska in 1993, the eastern Bering Sea in 1994, and from the Washington coast in 1998. They were also collected by longline from waters north of Unalaska Island in the Aleutian Islands in 1996, the central Gulf of Alaska and the northwestern Bering Sea near Russia in 1997, and north of Unalaska Island (Aleutian Islands) and in the eastern and central Gulf of Alaska in 2001. Shortraker rockfish were collected with bottom trawls from the Gulf of Alaska in 1993, the eastern Bering Sea in 1994, and by longline in the northwestern Bering Sea near Russia in 1997. Dates, locations, and sample sizes are reported in Table 1 and Figure 1.

Approximately 2–3 mL of liver, heart, and muscle were taken from each fish, temporarily stored in either a freezer (–20°C) or in liquid nitrogen, shipped to the

Auke Bay Laboratory, Alaska, and stored at –80°C. Eye tissue was taken from the 1993 Southeast Alaska samples but was not collected during subsequent sampling efforts because initial experimentation yielded limited results from this tissue. Samples of heart tissue were sent to the University of Alaska for DNA analysis. Only liver tissue was taken from the Shumagin and Aleutian Islands rougheye rockfish samples in 2001 (regions 9b, 14a, and 16a). The right gill arch and a 4-inch section of the gut were sampled for parasite analysis from the rougheye rockfish 2001 Gulf of Alaska samples. These fish were also photographed, preserved in 10% formalin, and shipped to the Alaska Fisheries Science Center for future morphological studies.

Laboratory analysis

Protein enzymes from each sample were separated by horizontal starch-gel electrophoresis as described by Aebersold et al. (1987). Enzymes were screened by staining eye, heart, liver, and muscle tissue on each of six buffer systems (Table 2) by using general staining procedures (Harris and Hopkinson, 1976; Aebersold et al., 1987), and *Sebastes*-specific procedures (Seeb, 1986). Enzyme screening was designed to detect interspecific allelic mobility differences and to identify intraspecific multilocus enzymes by tissue. Therefore, each tissue type from both rougheye and shortraker rockfish were run together on each gel buffer. Of 47 enzymes screened, 23 enzymes representing 29 loci were resolved for all rougheye rockfish except the Russian collection, for which 25 loci were resolved, and the collections from regions 9b, 14a, and 16a, for which only liver samples were taken and 7 loci were resolved (data available from senior author). Twenty-nine loci were resolved for all shortraker rockfish collections except the Russian collection, for which 24 loci were resolved (data available from senior author). The loci used in subsequent analyses and the level of variation are listed in Table 2. Nomenclature for identified loci were assigned according to the American Fisheries Society guidelines for standardization (Shaklee et al., 1990).

Data analysis

Fish sampled from stations in close proximity were combined to form regional collections (Table 1 and Fig. 1). The software package GENEPOP (vers. 3.4, Montpellier University, Montpellier, France) was used to calculate genotypic frequencies for each region and to test for departure from expected Hardy-Weinberg equilibrium frequencies. Homogeneity of allele frequencies among regional collections was tested with log-likelihood ratio analysis (G-test; Sokal and Rohlf, 1981). F_{is} and F_{st} were calculated with FSTAT (Goudet, 1995).

Heterogeneity among the collections and within some of the collections of rougheye rockfish was such that the fish were easily divided into two distinct "types" according to their genotypes at five loci: ACP^* , $IDDH^*$, MPI^* , $PGM-2^*$, and XO^* (Table 3 and data available from

² Hawkins, S. L., J. Heifetz, J. Pohl, and R. Wilmot. 1997. Unpubl. data. Genetic population structure of rougheye rockfish (*Sebastes aleutianus*) inferred from allozyme variation. Alaska Fisheries Science Center, Quarterly Report Feature, July–Aug–Sept. Auke Bay Laboratory, 11305 Glacier Hwy., Juneau, AK 99801.

Table 1

Regional group, location, sample size (*n*) of *S. aleutianus*, *S. sp. cf. aleutianus*, U = unknown type of *S. aleutianus*, *S. borealis*, and latitude, longitude, depth, and date of collections.

Region	Location	<i>Sebastes</i>			Lat. N	Long. W	Depth (m)	Date	
		<i>aleutianus</i> (<i>n</i>)	<i>sp.cf.</i> (<i>n</i>)	<i>borealis</i> (<i>n</i>)					
1	North Washington State	79	3		47.6	125.2	118–421	1998	
2	S.E. Alaska, Dixon entrance	20	21	36	54.5	133.5	152–228	1993	
3	S.E. Alaska, S. Baranoff Is.	32	16	10	56.0	135.2	176–260	1993	
4	S.E. Alaska, Cross Sound	27	4	15	58.1	136.9	77–249	1993	
5	S.E. Alaska, Cape Fairweather	19	1	1	38	58.4	139.3	123–241	1993
5a	S.E. Alaska, Cape Fairweather	2	6	2	58.4	140.4	300–400	2001	
6	S.E. Alaska, Yakutat	50	3	4	53	59.3	141.2	102–198	1993
6a	S.E. Alaska, Yakutat	6	10	6	59.2	141.1	300–400	2001	
7	S.E. Alaska, Cape Suckling	22	0	1	32	59.8	143.4	81–217	1993
7a	S.E. Alaska, Cape Suckling	5	42	2	59.3	143.1	300–600	2001	
8	S. of Prince William Sound	4	43		58.2	148.4	300–600	1997	
8a	S. E. of Prince William Sound	2	17		59.1	147.2	300–400	2001	
9	Kodiak Island, S.W.	12	86	99	56.3	152.1	270–400	1996	
9a	Kodiak Island, S.W.	11	0	8	58.0	152.2	140–150	2001	
9b	Shumagin Island, S.W.	5	0	2	55.4	159.4	145	2001	
10	South of Amlia Island								
	S. between Atka & Amlia Is	0	76	105	51.8	173.9	303–320	1994	
	South of Amlia Island	0	12		51.5	173.3	163–650	1996	
11	South Atka Pass								
	South Atka Pass	0	22	34	51.7	175.5	309–407	1994	
	South of Atka Island	0	25	1	20	51.5	175.1	185–820	1996
12	South Tanaga Island								
	South of Tanaga Island	0	70	57	51.6	177.6	372–381	1994	
	West of Tanaga Island	0	24	12	51.4	178.1	90–705	1996	
13	North of Semisopochnoi Island	0	28		52.5	180.0	213	1994	
14	North Atka Pass	0	30	37	52.1	175.0	108–940	1996	
14a	North of Amlia Island	0	11	2	52.5	173.5	230–350	2001	
15	N. of Islands of Four Mountains	0	34	12	53.0	170.1	172–630	1996	
16	North Unalaska Island								
	North of Unalaska Island	5	0		53.7	167.0	195	1994	
	North of Unalaska Island	6	44		53.7	167.0	121–350	1997	
16a	North of Unalaska Island	8	3	1	53.6	167.5	85–303	2001	
17	northwest Bering Sea, Russia	0	55		60.5	179.3E	390–384	1997	
	northwest Bering Sea, Russia			55	60.3	171.4E	457–533	1997	

senior author). We identified these types as *Sebastes aleutianus* and *Sebastes sp. cf. aleutianus* (a species that has putatively not been described but is similar to *S. aleutianus*). The *S. aleutianus* type is characterized by individuals with genomes of predominately ACP*100; IDDH*100, and *500; MPI*129; PGM-2*100, *83, *91, and *117; and XO*100. The *Sebastes sp. cf. aleutianus* type is characterized by individuals with genomes of predominately ACP*46; IDDH*500 and *750; MPI*100; PGM-2 *83, *74, and *63; and XO*109. We used 25 loci to perform multidimensional scaling analysis of individual rougheye genotypes to illustrate separation of the two types.

We chose STRUCTURE, a Bayesian clustering model (Pritchard et al., 2000) to gain greater statistical rigor in identifying individual types and possible hybrids of rougheye rockfish. This model seeks to identify populations in a mixture without the availability of baseline samples from the separate populations. The proportions of each individual's genome belonging to the population identified by the model and the separate population allele frequencies are simultaneously estimated. A 90% probability interval is computed for each individual's inferred genome source proportions. For this analysis, we used 25 loci, 100,000 iterations, and a 10,000 burn-in period. This model assumes that loci are in Hardy-

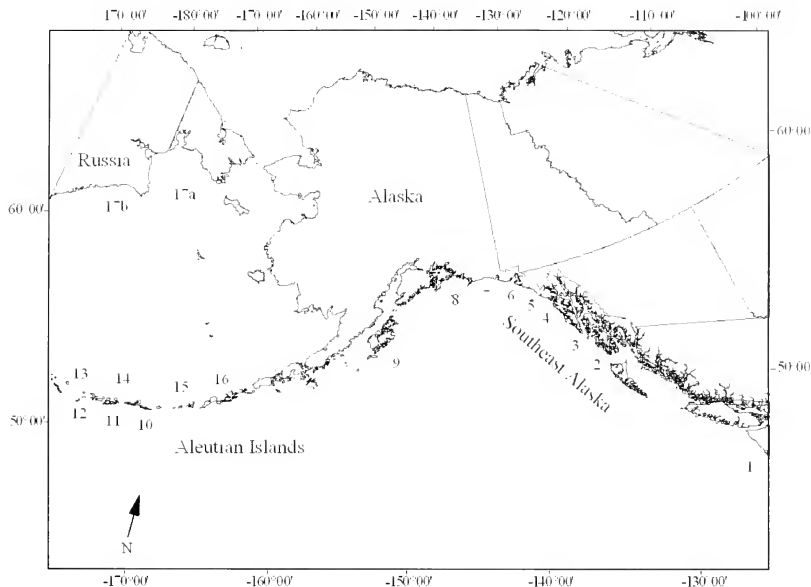


Figure 1

Location of rougheye (*Sebastes aleutianus*) and shortraker rockfish (*Sebastes borealis*) collection sites, which correspond to locations in Table 1.

Weinberg equilibrium within populations and in linkage equilibrium with one another within populations. These assumptions were tested with the PC program GENEPOP (vers. 3.4, Univ. Montpellier, Montpellier, France).

Regional groups were separated into two groups of rougheye rockfish types according to the multidimensional scaling analysis and Bayesian clustering model and were retested for Hardy-Weinberg equilibrium and homogeneity of allelic frequencies (*G*-test) among regions for each type. Chord distance (Cavalli-Sforza and Edwards, 1967) for 25 loci was used to assess the overall similarities of allelic frequencies for the two rougheye rockfish types with multidimensional scaling analysis (Rohlf, 2000). Only 25 loci were used because the Russian collection was missing data at 4 loci. Regions 9b, 14a, and 16a were therefore not included in these analyses because of the limited number of loci available.

Because the two rougheye rockfish types exhibited a distinct yet puzzling pattern of distribution—nearly all *S. sp. cf. aleutianus* in the Aleutian Is-

lands, nearly all *S. aleutianus* in the central Gulf of Alaska, and both types in sympatry in Southeast Alaska—we collected rougheye rockfish at different depths in 2001 (regions 5a–9a, 9b, 16a). We ran a Mann-Whitney rank sum test (SigmaStat, vers. 2.0, SPSS, Chicago, IL) to test for significant differences of the mean, standard deviation, and range of depths between the two rougheye rockfish types. A single depth of 350 m was used to approximate depth of catch for the 2001 Southeast Alaska rougheye rockfish collections (regions 5a, 6a, and 7a) because depths were reported only as a range from 300 to 600 m. Had we chosen a deeper average depth in the range, the difference in depth between the two rougheye rockfish types would have been (and in actuality may be) even greater. Because the two rougheye types were found in sympatry, we analyzed the length data to determine if size differences existed between the two types. Linear regressions were used to examine the relationships between length (tip of snout to fork of tail) and depth of capture of both shortraker rockfish and the two rougheye rockfish types.

Table 2

Enzymes with associated International Union of Biochemistry Numbers (IUBNC), locus name (Shaklee et al., 1990), tissue(s), buffers), and level of variability for *Sebastes aleutianus*. RE=both *Sebastes* sp. cf. *aleutianus* and *Sebastes aleutianus*, and SR=*Sebastes borealis*. Tissue: M=muscle; H=heart; and L=liver. Buffers: 1= R (Ridgway et al., 1970); 2 = MF (Markert and Faulhaber, 1965); 3=CA6.1 and 4- CA6.9 (Clayton and Tretiak, 1972, modified pH); 5 = TC (Shaw and Prasad, 1970); and 6 = CAME7.4 (modified from Clayton and Tretiak, 1972). Var. RE and Var. SR: 0 = monomorphic; 1 = frequency common allele >0.95; 2 = frequency common allele <0.95 for at least one region. — = Loci were not reliably scored in that species. + = loci were not reliably scored in all populations and were not used in most analyses.

Enzyme	IUBNC no.	Locus	Tissue	Buffer	Var. RE	Var. SR
Acid phosphatase	3.1.3.2	ACP ⁸	L	3	2	—
Aconitate hydratase	4.2.1.3	mAH ⁶	H	5,6	1	1
		sAH ⁶	L	3,4	2	1
Adenosine deaminase	3.5.4.4	ADA-1 ²	M,H	3,6	0	2
Adenylate kinase	2.7.4.3	AK ⁹	M,H,L	6	0	0
Alcohol dehydrogenase	1.1.1.1	ADH ⁷	L	3	2 ¹	2
Aspartate aminotransferase	2.6.1.1	sAAT ⁶	L	1	2 ¹	0
		mAAT ⁶	M,H,L	3,4,6	1	1
beta-N-Acetylgalactosaminidase	3.2.1.53	bGALA ¹	L	4	0 ¹	0
Creatine kinase	2.7.3.2	CK-1 ³ +	H	3,6	1	0
Fumarate hydratase	4.2.1.2	FH ⁶	H,L	5	0 ¹	1
Glucose-6-phosphate isomerase	5.3.1.9	GPI-A ⁶	M,H,L	1,3	1	2
		GPI-B ⁶	M,H	1,3	1	1
Glycerol-3-phosphate dehydrogenase	1.1.1.8	G3PDH ¹	M	2	0	1
Iditol dehydrogenase	1.1.1.15	IDDH ⁶	L	1	2	—
Isocitrate dehydrogenase	1.1.1.42	IDHP-1 ⁺	H	3	1	1
		IDHP-2 ¹	L	3	1	1
Lactate dehydrogenase	1.1.1.27	LDH ⁶	M,H	3	0	0
Malate dehydrogenase	1.1.1.37	MDH-1 ⁶	M,H	3,6	1	—
		MDH-2 ⁶	M,H,L	3,4,6	1	1
Malic enzyme	1.1.1.40	mMEP ⁶	M,H	3,6	2 ¹	2
Mannose-6-phosphate isomerase	5.3.1.8	MPI ⁶	H	6	2	2
Dipeptidase (glycyl-leucine)	3.4.-.	PEPA ⁶	M,H,L	2	2	1
Tripeptide aminopeptidase (leu-gly-gly)	3.4.-.	PEPB ⁶	M,H,L	1	0	0
		PEPD ⁺	M,H	2	—	2
		PEP-LT ⁶ +	M,H	2	—	1
Phosphoglucomutase	5.4.2.2	PGM-1 ⁶	M,H,L	1,5	2 ¹	2
		PGM-2 ⁶	H	5	2	2
6-Phosphogluconate dehydrogenase	1.1.1.44	PGDH ⁶	M,H,L	3	2 ¹	0
Triose-phosphate isomerase	5.3.1.1	TPI-1 ⁶	M,H	1,3	0	0
		TPI-2 ⁶	M,H	1,3	—	2
Xanthine Oxidase		XO ⁶	L	2	2 ¹	0

¹ *Sebastes* sp. cf. *aleutianus* level of variability was 1.

Parasite analysis

Although not an objective of the study, parasites were opportunistically sampled from the 2001 Gulf of Alaska collections of rougheye rockfish to determine if depth or species subtype might have been a factor in the geographical segregation noted by Moles et al. in 1998. This would also allow us to determine if the parasite data supported results of the current allozyme work. The rougheye rock-

fish were examined for the proportion of fish with the gill parasites *Neobrachiella robusta*, *Trochopus trituba*, or the visceral parasite *Corynosoma* sp. by using the procedures of Moles et al. (1998). A categorical analysis of variance (SAS procedure, CATMOD; vers. 8.02, Cary, NC 1989) was used to test whether parasite prevalence differed among the two types of rougheye rockfish.

Table 3

Allelic frequencies of five loci for all samples by type that best distinguish *Sebastes aleutianus* and *Sebastes* sp. cf. *aleutianus*.

Locus	n	Allele					
ACP*		100	46	83			
<i>aleutianus</i>	242	0.896	0.087	0.017			
sp. cf. <i>aleutianus</i>	486	0.094	0.905	0.001			
IDDH*		100	500	750	999		
<i>aleutianus</i>	287	0.73	0.268	0.002	0		
sp. cf. <i>aleutianus</i>	658	0.03	0.507	0.462	0.001		
MPI*		100	129	110			
<i>aleutianus</i>	283	0.343	0.656	0.001			
sp. cf. <i>aleutianus</i>	540	0.74	0.26	0			
PGM-2*		100	83	74	63/69/59**	80	91/117**
<i>aleutianus</i>	270	0.775	0.185	0.005	0	0.002	0.028
sp. cf. <i>aleutianus</i>	586	0.003	0.333	0.508	0.147	0.009	0
XO*		100	109				
<i>aleutianus</i>	295	0.844	0.156				
sp. cf. <i>aleutianus</i>	660	0.011	0.989				

** indicates pooled alleles.

Results

Shortraker rockfish and rougheye rockfish had different common alleles (fixed) for 10 of 29 loci examined (*sAH**, *CK-A1**, *GPI-A**, *G3PDH**, *IDHP-2**, *PEPA**, *PEPB**, *PEP-LT**, *PGM-2**, and *SOD**). These are inexpensive markers that can be used to differentiate shortraker rockfish from rougheye rockfish when precise field identification, particularly in younger fish, is necessary but difficult.

Shortraker rockfish

Nine loci (31%) were monomorphic for all regions, 11 loci (38%) were variable (with the frequency of the common allele greater than 0.95 for all regional groups), and 9 loci (31%) had a common allele frequency of less than 0.95 for at least one regional group. For the Russian collection, data were unavailable from five loci (*FH**, *midHP**, *MPI**, *PGM-2**, and *TPI-2**). Average heterozygosity of each regional group fell within a narrow range of 0.09–0.11, and produced an overall average for 29 loci of 0.10. All regional genotypic proportions closely agreed with those expected under Hardy-Weinberg equilibrium; of 128 chi-square tests, only four (3%) differed significantly ($P < 0.05$) from expected values. No significant ($P < 0.05$) heterogeneity was detected with G-tests among

regional groups, and thus no subpopulations or stock structure was evident with this suite of allozymes.

Although no genetic differentiation was detected among shortraker rockfish throughout their geographic distribution, size of fish and depth of capture differed between shortraker rockfish from the Aleutian Islands and those from Southeast Alaska. Aleutian Island shortraker rockfish were significantly smaller (mean 43.6 cm [\pm SD 7.0], range: 24–70 cm) and were caught in deeper water (309–407 m) than Southeast Alaska shortraker rockfish (mean 66.5 cm [\pm SD 10.5], range: 45–101 cm at 138–260 m depths). A regression of fish length on depth of capture yielded a significant r^2 value of 0.452 ($P < 0.001$).

Rougheye rockfish

Significant departure from Hardy-Weinberg equilibrium occurred in 37 out of 226 possible tests (16%); a value greater than the 11 that would be expected by chance alone at the $P = 0.05$ level of probability (Table 4). Thirty-six of the departures were due to an absence of heterozygotes, a situation known as the Wahlund effect, which typically indicates the presence of a mixture of populations for presumably neutral genetic loci. Most of the departure from Hardy-Weinberg expectations occurred at *ACP**, *IDDH**, *MPI**, *PGM-2**, and *XO**. Only

Table 4

Loci not in Hardy Weinberg equilibrium ($P < 0.05$). N/A = insufficient sample size for analysis.

Location	Mixture	<i>S. aleutianus</i> ¹	<i>S. sp. cf. aleutianus</i> ¹
Dixon Entrance	ACP, sAH, IDDH PGM-2, XO	ACP, IDDH	ACP, IDDH
S. Baranof Island	ACP, IDDH, XO PGM-1, PGM-2	ACP, PGM-1	None
Cross Sound	ACP, IDDH, XO	None	N/A
Cape Fairweather	ACP, PGM-2	ACP	N/A
Yakutat	ACP, MPI PGM-2, XO	MPI	N/A
Cape Suckling	None	None	N/A
Prince William Sound	IDDH, PGM-2, XO	N/A	None
Kodiak	ACP, IDDH PGM-2, XO	None	ACP
Amlia Island	None	N/A	None
South Atka Pass	MPI	N/A	MPI
South Tanaga Island	PEPA, PGM-2	N/A	PEPA
North Semisopchnoi Island	IDDH	N/A	IDDH
North Atka Pass	None	N/A	None
N. Is. Of Four Mountains	None	N/A	None
North Unalaska Island	ACP, PGM-2, XO	ACP, XO	None
Washington	sAH, IDDH, MPI PGM-2	sAH, MPI	N/A
Russia	None	N/A	None

¹ As determined from the program STRUCTURE (Pritchard et al., 2000).

PGM-2* in the South Tanaga Island sample was due to an excess of heterozygotes.

Inbreeding coefficients (F_{is}) indicated deviation from panmixia. The values ranged from -0.050 for IDHP-1* to 0.772 for ACP*. The mean value over all loci in all collections was 0.140. Statistically significant F_{is} values were found at ACP* (0.521), MPI* (0.135), PGM-2* (0.109), and XO* (0.524). All were the result of heterozygote deficiencies. The mean F_{is} value for the *S. aleutianus* type collections dropped to 0.062 and for the *S. sp. cf. aleutianus* types, to 0.048.

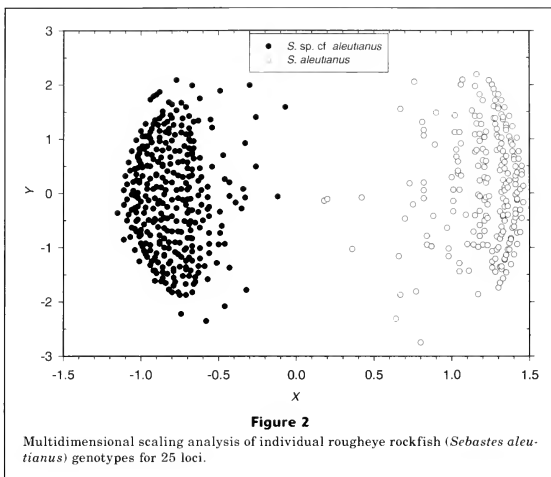
Eight of the loci showed statistically significant F_{st} values: sAAT* (0.007), ACP* (0.572), sAH* (0.037), IDDH* (0.189), MDH-2* (0.007), MPI* (0.123), PGM-2* (0.206), and XO* (0.551). The mean F_{st} value for all loci in all collections was 0.215. When analyzed by pure *S. aleutianus*-type and *S. sp. cf. aleutianus*-type, the mean F_{st} values dropped to 0.013 and 0.012, respectively.

Two rougheye types

The results of the rougheye rockfish analyses allowed us to segregate rougheye rockfish individuals into two types: *S. aleutianus* and *Sebastes sp. cf. aleutianus*. Multidimensional scaling analysis with individual genotypes (Fig. 2) yielded two distinct clusters with little

overlap. This outcome was confirmed by the Bayesian clustering model in STRUCTURE (Pritchard et al., 2000), which identified two types. We calculated the inferred source proportions of genomes for 1027 individuals using 25 loci that were scored in most individuals. One hundred sixty-six individuals were missing data for more than 30% of the 25 loci used and were omitted from the analysis. Most of the individuals had a very high proportion of their genome from one type; for 851 individuals, the program assigned at least 0.80 of the individual's genes to one of the two ancestral lines, and all had an upper 90% probability limit that included 1.0. These fish were likely all purebreds. Ten individuals had an inferred proportion of ancestry from one lineage of less than 0.80 and two did not include an upper probability interval of 1.0. These individuals were possibly hybrids. If any of these 10 individuals were actual hybrids of the two rougheye rockfish types, none were of the first generation (i.e., heterozygotes at all differentiating loci).

Significant differences of allele frequencies (G-test) were detected between the two types at 14 loci: $P < 0.001$ for sAAT*, ACP*, ADH*, sAH*, IDDH*, MDH-2*, mMEP*, MPI*, PGDH*, PGM-1*, PGM-2*, and XO*; and $P < 0.05$ for mAAT* and GPI-B*. When the two types were analyzed independently by area (Table 4), all but two collections were in Hardy-Weinberg equilibrium



(South Tanaga Island *Sebastes* sp. cf. *aleutianus* type, $P=0.042$, and North Unalaska Island *S. aleutianus* type, $P=0.023$). The G-test analysis indicated no heterogeneity among regions except for the Russian sample, which was significantly different from all other samples ($P<0.05$). Average heterozygosity was 0.09 for *S. aleutianus* and 0.08 for *Sebastes* sp. cf. *aleutianus*.

A significant difference in overall depth of capture ($P<0.001$) was detected between *Sebastes* sp. cf. *aleutianus* (mean 330+ m) and *S. aleutianus* (mean 208 m). We obtained both shallow and deep collections from the central Gulf of Alaska. The fish captured at shallow depths, 77–249 m (regions 4–7, 9a, 9b, $n=134$), were nearly all (94%) *S. aleutianus*, whereas the deeper dwelling fish, 270–600 m (regions 5a–7a, 8, 8a, 9, $n=204$), were mostly (87%) *Sebastes* sp. cf. *aleutianus*. Both types were captured, some within a single haul, in southern Southeast Alaska (regions 2 and 3, $n=89$) at depths of 150–260 m (Fig. 3).

A highly significant correlation of fish length (15–65 cm) and depth of capture (77–260 m) was detected for *S. aleutianus* in Southeast Alaska, with smaller fish in shallower water and larger fish in deeper water ($r^2=0.415$, $P<0.001$). No length-depth trend was noted for *Sebastes* sp. cf. *aleutianus*.

Results of the parasite analysis for the 2001 rougheye rockfish showed that *Sebastes* sp. cf. *aleutianus* had a significantly higher prevalence of both *Neobrachiella robusta* ($P=0.003$) and *Trochopus trituba* ($P=0.022$) than did *S. aleutianus* (Table 5).

Discussion

The most notable conclusion of our study was that two genetically distinct types of rougheye rockfish exist. This conclusion corroborates prior biochemical studies in which Tsuyuki et al. (1968) and Tsuyuki and Westrheim (1970) conducted hemoglobin electropherogram analyses on *S. aleutianus* and *S. caenaemeticus* (= *S. borealis*) and detected four blood types. Three blood types characterized *S. aleutianus*—two distinct types and a rare hybrid type. The fourth type characterized *S. borealis*. Seeb (1986) examined allozymes from several species of North Pacific rockfish and found two color morphs of rougheye rockfish fixed for alternate alleles at three loci. At one of the loci, *ACP*^a, we detected a small percentage of a shared allele, likely because of our larger sample size. We were unable to resolve the other two loci, *GAP*^a (IUBNC no. 1.2.1.12 Glyceraldehyde-3-phosphate dehydrogenase,) and *GAM*^a (B-Galactosaminidase). Although we are unable to report fixed loci differences between the two rougheye rockfish types, we did detect significant allele frequency differences at nearly half of the loci examined. Allelic mobilities of *Sebastes aleutianus* were similar to those of Seeb's "*Sebastes aleutianus*," and allelic mobilities of *Sebastes* sp. cf. *aleutianus* were similar to Seeb's "*Sebastes aleutianus* unknown." Because simultaneous hemoglobin and allozyme studies have never been done, we are currently unable to correlate allozyme types with the blood types reported by Tsuyuki et al. (1968) and Tsuyuki and Westrheim (1970).

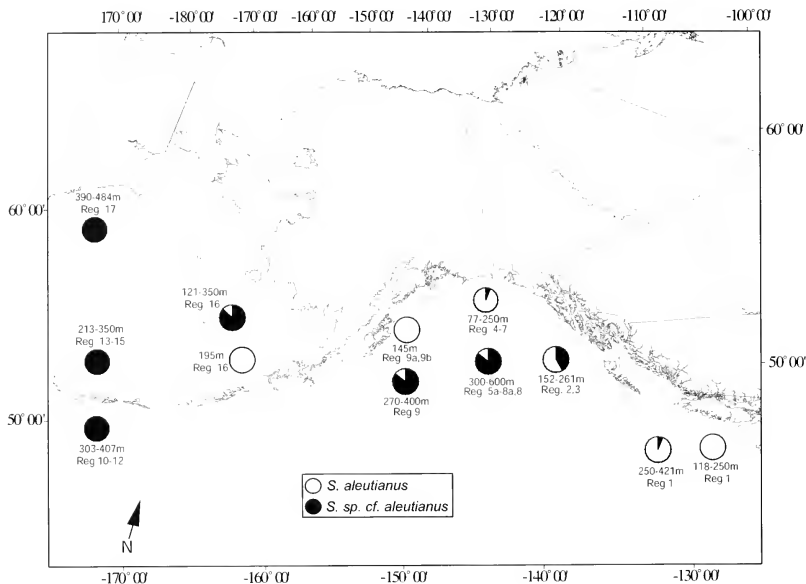


Figure 3

Proportions of *Sebastes aleutianus* and *S. sp. cf. aleutianus* in relation to depth of capture.

Table 5

Prevalence of parasites (percentage) in both rougheye rockfish types and results of categorical analysis of variance.

	Parasite prevalence		Significance probability	
	<i>sp. cf. aleutianus</i> (n=61)	<i>S. aleutianus</i> (n=18)	Type	Size of fish
<i>Neobrachiella robusta</i>	0.57	0.11	0.003*	0.442
<i>Trochopus trituba</i>	0.49	0.17	0.022*	0.339
<i>Corynosoma sp.</i>	0.90	0.83	0.448	0.326

The Cavalli-Sforza-Edwards (CSE) chord distance (for 29 loci) between the two *S. aleutianus* types, 0.35 (SD=0.05), was a value comparable to that for other closely related rockfish species. Seeb (1986) reported CSE distances between rockfish species ranging from 0.07 to 0.75 for 28 loci. Identical mobilities at the majority of loci indicated a close relationship between the two types, which probably existed as a single type at an earlier geologic time. Given that Tsuyuki and

Westrheim (1970) detected (2%) hybrids of the two blood types and we did not detect fixed differences between the two rougheye rockfish types, some gene flow may be occurring. However, the low effective number of migrants and the sympatric distribution of the population indicate that the gene flow is limited. Because rockfish have internal fertilization, sibling species may co-occur and there is little chance of cross-fertilization of gametes.

The initial objective of our study did not include collection of morphological data, but in light of the genetic differences detected, and the color morphs detected by Seeb (1986), morphology of the two lineages should be more closely examined. Upon processing the 2001 fish, we noted that many were easily identified as either light or dark in color, although some appeared intermediate. The obvious light-colored individuals were all found genetically to be *S. aleutianus*, whereas the darker specimens were typically *Sebastes* sp. cf. *aleutianus*. Although Tsuyuki and Westrheim (1970) reported no distinguishing meristic or morphometric characters between *S. aleutianus* blood types, Seeb (1986) separated rougheye rockfish morphologically and by color into two groups: one that was light pink and had spines under the orbit of the eye (*S. aleutianus*); the other was darker and had a considerable area of black on the mouth and jaw and often lacked orbital spines (*S. aleutianus* unknown). The lack of orbital spines in *Sebastes* sp. cf. *aleutianus* is an important observation because this feature is a key characteristic in distinguishing *S. aleutianus* from *S. borealis*.

Initial observations of the distribution of the 1993 rougheye samples displayed a pattern of predominately *S. aleutianus* in the Gulf of Alaska and almost entirely *S. sp. cf. aleutianus* in the Aleutian Islands. A parasite study (Moles et al., 1998) performed on the same rough-eye rockfish reported a significantly greater ($P < 0.05$) prevalence of three parasites in the Aleutian Island samples. Upon close examination of the depth of the sample collection, we noted that the Aleutian Islands samples were collected in deeper waters than those collected in the Gulf of Alaska. Thus subsequent sampling strategies focused on a possible depth niche. Parasite data from both the shallow and deep water 2001 rough-eye collections showed a significant prevalence of two parasites in the deeper host, *Sebastes* sp. cf. *aleutianus* (Table 5). The prevalence of the parasite *T. tributa* may be dependent on host habitat. Because the hosts (two *aleutianus* types) exhibited significantly different prevalences of the parasite *T. tributa*, they may be using different resources (different diets) and (or) exhibiting ecological segregation (Moles et al., 1998).

Both *Sebastes aleutianus* types are found in the Gulf of Alaska and occur in sympatry, although the majority of *S. sp. cf. aleutianus* are distributed at deeper depths (Fig. 3). Bathymetric segregation has been noted in other closely related rockfish. *Sebastes fasciatus* and *Sebastes mentella* in the Atlantic Ocean elude abundance estimates because of a lack of easily identifiable morphological characteristics. In the laboratory, these two species are nearly fixed at alternate alleles at the allozyme locus MDH*. A bathymetric segregation is detected, where *S. fasciatus* is found at depths of 132–315 m, *S. mentella* at depths greater than 355 m, and both species and possible hybrids at intermediate depths (Rubec et al., 1991). Another species pair, *Sebastes carnatus* and *Sebastes chrysomelas*, are both shallow-dwelling species (depth less than 20 m) that coexist only in a narrow zone of overlap that separates exclusive depth

ranges. Factors organizing their segregation are largely behavioral because both species expand their depths in the absence of the other species (Larson, 1980). Rough-eye rockfish may exhibit a similar strategy. Deep sampling efforts near Washington state have indicated that the distribution of *S. sp. cf. aleutianus* may diminish in southern ranges and it appears that the distribution of *S. aleutianus* does not extend to the western Aleutian Islands and Asia. This pattern of distribution has been noted in other closely related species, such as the northern and southern species of *Lepidopsetta* (Orr and Matarese, 2000). The poorly understood ontogenetic and seasonal movements of rougheye and other rockfish further confound the picture. For example, *S. altivelis* and *S. alascanus* were long thought to be deep-dwelling and shallow-dwelling congeneric species, respectively. It is now known that *S. altivelis* is a permanent deepwater resident, whereas *S. alascanus* settles in shallow water, then migrates to deep water with the onset of sexual maturity. Competition between these two species may be reduced by size differences; for example, where they are sympatric, *S. alascanus* is much larger than *S. altivelis* (Vetter and Lynn, 1997). Although length data for rougheye rockfish in sympatry are limited, a single haul ($n=29$) near Dixon Entrance (depth of capture = 213 m) yielded both types, and nearly all the *S. aleutianus* individuals were much larger (mean 56.3 cm) than *Sebastes* sp. cf. *aleutianus* (mean 37.2 cm). No age data are currently available to add insight into these results. The trend of smaller fish in shallower waters and larger fish in deeper waters was significant for *S. aleutianus* in the Gulf of Alaska. This was not detected for *Sebastes* sp. cf. *aleutianus*, although their full depth range may not have been sampled. Perhaps only younger *Sebastes* sp. cf. *aleutianus* were collected, and the older, larger fish are deeper and remain unsampled. It would be beneficial to analyze juvenile rougheye rockfish to ascertain genetic type composition at different depths.

A significant size difference existed between fish in the Gulf of Alaska and those of the Aleutian Islands, especially among shortraker rockfish. Aleutian fish were smaller, despite collection at greater depth. Growth and age of maturation differences among differing latitudes and longitudes have been noted in other rockfish species (Westrheim, 1973; Archibald et al., 1981; Field, 1984; Lunsford, 1999). The size difference among shortraker rockfish has been previously noted (Orlov, 2001; Matala, 2004) and raises more questions than it answers. It is still unknown whether these differences are caused by different age classes or regional ecological differences.

Allozyme data did not reveal heterogeneity within either rougheye rockfish type or within shortraker rockfish throughout the sampled geographic range. Although no heterogeneity was detected with our suite of allozyme loci, other genetic markers, such as microsatellite loci, may provide finer resolution of population structure. A recent study of shortraker microsatellite variation revealed geographically restricted homogeneity among allele frequencies—a model consistent with the assump-

tion of limited movement (Matala, 2004). Conversely, Orlov (2001) proposed a synopsis of horizontal adult migration (with increased size of shortraker rockfish at spawning grounds) and oceanic dispersal of larvae and juveniles.

In conclusion, it appears there are species-level differences between the two rougheye rockfish types. We have considered the darker morph *Sebastes* sp. cf. *aleutianus* as the new type. The paler *S. aleutianus* morph conforms more to the original *S. aleutianus* type description, an individual of which was captured at a 55-m depth in the Gulf of Alaska. It is likely that the distribution of the new species *S. sp cf aleutianus* stretches from the Gulf of Alaska and west to Asia. The distribution of *S. aleutianus* encompasses the Gulf of Alaska and extends south to California, and the species is found in more shallow waters where it is sympatric with *S. sp cf aleutianus*. An understanding of the basic life history, distribution, and biomass of a species is critical for successful resource management. Ito (1999) suggested that the major fisheries management survey effort is the NMFS Gulf of Alaska triennial trawl survey, which may be inadequate to assess the shortraker-rougheye rockfish assemblage because its multispecies sampling design covers mostly depths less than 200 m. This survey may, therefore, be completely missing *Sebastes* sp. cf. *aleutianus* altogether. An important consideration for management is knowledge of exploitation rates. Given the sensitivity of long-lived rockfish species to over-exploitation, basic biological studies should be undertaken of these species to understand characteristics such as growth, maturity, and natural mortality.

Acknowledgments

We dedicate this article in fond memory of H. R. Carlson. His research provided a highly significant contribution to our understanding of juvenile rockfish life history and homing in adult rockfish, and he was anxiously awaiting completion of our study. We thank Hanhvan Nguyen for her support in the laboratory, and we thank all participants in the haul and longline surveys for providing the collections. We also thank James Orr, Jerry Pella, and Phillip Rigby for earlier reviews of the manuscript, and Adam Moles for the parasite determinations.

Literature cited

- Aebersold, P. B., G. A. Winans, D. J. Teel, G. B. Milner, and F. M. Utter.
1987. Manual for starch gel electrophoresis: a method for the detection of genetic variation. NOAA Tech. Rep. NMFS 61, 20 p.
- Allen, J. M., and B. G. Smith.
1988. Atlas and zoogeography of common fishes in the Bering Sea and northeastern Pacific. NOAA Tech. Rep. NMFS 66, 151 p.

- Archibald, C. P., W. Shaw, and B. M. Leaman.
1981. Growth and mortality estimates of rockfishes (Scorpaenidae) from B.C. coastal waters of 1977-1979. Can. Tech. Rep. Fish. Aquat. Sci. 1048, 61 p.
- Barsukov, V. V.
1970. Species composition of the genus *Sebastes* in the North Pacific. Description of a new species. Dokl. Acad. Nauk SSSR Ser. Biol. 195(4):994-997.
- Cavalli-Sforza, L. L., and A. W. F. Edwards.
1967. Phylogenetic analysis: models and estimation procedures. *Evol.* 21:550-570.
- Clayton, J. W., and D. N. Treliak.
1972. Amine-citrate buffer for pH control in starch gel electrophoresis. *J. Fish. Res. Board Can.* 29:1167-1172.
- Field, L. J.
1984. Bathymetric patterns of distribution and growth in three species of nearshore rockfish from the southeastern Gulf of Alaska. M.S. thesis, 88 p. Univ. Washington, Seattle, WA.
- Goudet, J.
1995. FSTAT: Computer program to calculate F-statistics. *J. Hered.* 86:485-486.
- Harris, H., and D. A. Hopkinson.
1976. Handbook of enzyme electrophoresis in human genetics, 120 p. American Elsevier, New York, NY.
- Heifetz, J., D. L. Courtney, D. M. Clausen, D. Hanselman, J. T. Fujioka, and J. N. Ianelli.
2002. Slope rockfish. In Stock assessment and fishery evaluation report for the groundfish resources of the Gulf of Alaska, p. 296-382. North Pacific Fishery Management Council, 605 W. 4th Ave. Anchorage, AK 99501.
- Ito, D.H.
1999. Assessing shortraker and rougheye rockfishes in the Gulf of Alaska: addressing a problem of habitat specificity and sampling capability. Ph.D. diss., 205 p. Univ. Washington, Seattle, WA.
- Jordan, D. S., and B. W. Evermann.
1898. The fishes of North and Middle America: a descriptive catalogue of the species of fish-like vertebrates found in the waters of North America, north of the Isthmus of Panama, Part III. *Bull. U.S. Natl. Mus.* 47:2183-3136.
- Krieger, K., and D. Ito.
1999. Distribution and abundance of shortraker rockfish, *Sebastes borealis*, and rougheye rockfish, *S. aleutianus*, determined from a manned submersible. *Fish. Bull.* 97:264-272.
- Larson, R. J.
1980. Competition, habitat selection, and the bathymetric segregation of two rockfish (*Sebastes*) species. *Ecol. Monogr.* 50(2):221-239.
- Lunsford, C.
1999. Distribution patterns and reproductive aspects of Pacific ocean perch (*Sebastes alutus*) in the Gulf of Alaska. M.S. thesis, 154 p. Univ. Alaska Fairbanks, Fairbanks, AK.
- Markert, C. L., and I. Faulhaber.
1965. Lactate dehydrogenase isozyme patterns of fish. *J. Exp. Zool.* 159:319-332.
- Matala, A. P., A. K. Gray, J. Heifetz, and A. J. Gharrett.
2004. Population structure of Alaskan shortraker rockfish, *Sebastes borealis*, inferred from microsatellite variation. *Environ. Biol. Fish.* 69:201-210.

- McDermott, S. F.
1994. Reproductive biology of rougheye and shortraker rockfish, *Sebastes aleutianus* and *Sebastes borealis*. M. S. thesis, 76 p. Univ. Washington, Seattle, WA.
- Moles, A., J. Heifetz, and D. Love.
1998. Metazoan parasites as potential markers for selected Gulf of Alaska rockfishes. *Fish. Bull.* 96:912-916.
- Munk, K. M.
2001. Maximum ages of groundfishes in waters off Alaska and British Columbia and considerations of age determination. *Alaska Fish. Res. Bull.* 8(1):12-21.
- Orlov, A. M.
2001. Ocean current patterns and aspects of life history of some northwestern Pacific scorpaenids. In *Spatial Processes and Management of Marine Populations* (G. H. Kruse, N. Bez, A. Booth, M. W. Dorn, S. Hills, R. N. Lipcius, D. Pelletier, C. Roy, S. J. Smith, and D. Witherell, eds.), p. 161-184. Univ. Alaska Sea Grant College Program, Fairbanks, AK-SG-01-02.
- Orr, J. W., and A. C. Matarese.
2000. Revision of the genus *Lepidopsetta* Gill, 1862 (Teleostei: Pleuronectidae) based on larval and adult morphology, with a description of a new species from the North Pacific Ocean and Bering Sea. *Fish. Bull.* 98:539-582.
- Pritchard, J. K., M. Stephens, and P. Donnelly.
2000. Inference of population structure using multilocus genotype data. *Genetics* 155:945-959.
- Ridgway, G. J., S. W. Sherburne, and R. D. Lewis.
1970. Polymorphisms in the serum esterases of Atlantic herring. *Trans. Am. Fish. Soc.* 99:147-151.
- Rohlf, F. J.
2000. NTSYS-pc, numerical taxonomy and multivariate analysis system, vers. 2.1, 38 p. Exeter software, Setauket, NY.
- Rubec, P. J., J. M. McGlade, B. L. Trottier, and A. Ferron.
1991. Evaluation of methods for separation of Gulf of St. Lawrence beaked redbishes, *Sebastes fasciatus* and *S. mentella*: malate dehydrogenase mobility patterns compared with extrinsic gasbladder muscle passages and anal fin ray counts. *Can. J. Fish. Aquat. Sci.* 48:640-660.
- Seeb, L. W.
1986. Biochemical systematics and evolution of the Scorpaenid genus *Sebastes*. Ph.D. diss., 176 p. Univ. Washington, Seattle, WA.
- Shaklee, J. B., F. W. Allendorf, D. C. Morizot, and G. S. Whitt.
1990. Gene nomenclature of protein-coding loci in fish. *Trans. Am. Fish. Soc.* 119:2-15.
- Shaw, C. R., and R. Prasad.
1970. Starch gel electrophoresis of enzymes: a compilation of recipes. *Biochemical Genetics* 4:297-320.
- Sokal, R. R., and F. J. Rohlf.
1981. *Biometry*, 2nd ed., 859 p. W. H. Freeman and Company, New York, NY.
- Spencer, P. D., and R. F. Reuter.
2002. Other red rockfish. In *Stock assessment and fishery evaluation report for the groundfish resources of the Bering Sea/Aleutian Islands Regions*, p. 559-578. North Pacific Fishery Management Council, 605 W. 4th Ave., Anchorage, AK 99501.
- Tokranov, A. M., and I. I. Davydov.
1997. Some aspects of biology of the shortraker rockfish *Sebastes borealis* (Scorpaenidae) in the Pacific waters of Kamchatka and western part of the Bering Sea: 1. Spatial and bathymetric distribution. *J. Ichthyol.* 37(9):761-768.
- Tsuyuki, H., E. Roberts, R. H. Lowes, and W. Hadaway.
1968. Contribution of protein electrophoresis to rockfish (Scorpaenidae) systematics. *J. Fish. Res. Board Can.* 25(11):2477-2501.
- Tsuyuki, H., and S. J. Westheim.
1970. Analyses of the *Sebastes aleutianus*-*S. melanostomus* complex, and description of a new scorpaenid species, *Sebastes caenemaeticus*, in the northeast Pacific Ocean. *J. Fish. Res. Board Can.* 27:2233-2254.
- Vetter, R. D., and E. A. Lynn.
1997. Bathymetric demography, enzyme activity patterns, and bioenergetics of deep-living scorpaenid fishes (genera *Sebastes* and *Sebastolobus*): paradigms revisited. *Mar. Ecol. Progr. Ser.* 155:173-188.
- Westheim, S. J.
1973. Age determination and growth of Pacific ocean perch (*Sebastes alutus*) in the northeast Pacific Ocean. *J. Fish. Res. Board Can.* 30:235-247.

Abstract—The thorny skate (*Amblyraja radiata*) is a large species of skate that is endemic to the waters of the western north Atlantic in the Gulf of Maine. Because the biomass of thorny skates has recently declined below threshold levels mandated by the Sustainable Fisheries Act, commercial harvests from this region are prohibited. We have undertaken a comprehensive study to gain insight into the life history of this skate. The present study describes and characterizes the reproductive cycle of female and male thorny skates, based on monthly samples taken off the coast of New Hampshire, from May 2001 to May 2003. Gonadosomatic index (GSI), shell gland weight, follicle size, and egg case formation, were assessed for 48 female skates. In general, these reproductive parameters remained relatively constant throughout most of the year. However, transient but significant increases in shell gland weight and GSI were observed during certain months. Within the cohort of specimens sampled monthly throughout the year, a subset of females always had large prevulatory follicles present in their ovaries. With the exception of June and September specimens, egg cases undergoing various stages of development were observed in the uteri of specimens captured during all other months of the year. For males ($n=48$), histological stages III through VI (SIII–SVI) of spermatogenesis, GSI, and hepatosomatic index (HSI) were examined. Although there appeared to be monthly fluctuations in spermatogenesis, GSI, and HSI, no significant differences were found. The production and maintenance of mature spermatozoa (SVI) within the testes was observed throughout the year. These findings collectively indicate that the thorny skate is reproductively active year round.

The reproductive cycle of the thorny skate (*Amblyraja radiata*) in the western Gulf of Maine

James A. Sulikowski

Jeff Kneebone

Scott Elzey

Zoology Department
University of New Hampshire
Durham, New Hampshire 03824

Present address: Florida Program for Shark Research,
Florida Museum of Natural History
University of Florida
P.O. Box 117800
Gainesville, Florida 32611

E-mail address (for J. A. Sulikowski): jsulikow@hotmail.com

Joe Jurek

Yankee Fishing Coop
Route 1A
Seabrook, New Hampshire 03874

Patrick D. Danley

Department of Biology
University of Maryland
College Park, Maryland 20742

W. Hunting Howell

Zoology Department
University of New Hampshire
Durham, New Hampshire 03824

Paul C. W. Tsang

Department of Animal and
Nutritional Sciences,
University of New Hampshire
Kendall Hall, 129 Main St.
Durham, New Hampshire 03824

The thorny skate (*Amblyraja radiata*) is a member of the family Rajidae (Robins and Ray, 1986; Collette and Klein-MacPhee, 2002). It is a cosmopolitan species, endemic to both sides of the Atlantic Ocean, from Greenland and Iceland to the English Channel in the eastern Atlantic (Compagno et al., 1989), and from Greenland and Hudson Bay, Canada, to South Carolina, in the western Atlantic (Robins and Ray, 1986; Collette and Klein-MacPhee, 2002). Despite such a wide distribution, knowledge pertaining to the reproductive biology of this species is limited. Templeman (1982) reported the occurrence of egg capsules in *A. radiata*, and Templeman (1987), Del Rio (2002), and Sosebee¹ examined size at sexual maturity.

In the Gulf of Maine, these skates were generally discarded as bycatch because of their low commercial value NEFMC.^{2,3} Recently, the rapidly expanding markets for skate wing has made this species commercially more viable, especially because *A. radiata* meets the minimum 1¼ pound-cut pectoral fin size sought by processors (Sosebee¹; NEFMC²). Although no comprehensive published data for reproductive cycles currently exist for thorny skates in the Gulf of Maine,

information from the few skate species studied so far indicates that sexual maturity at a late age, low fecundity, and a relatively long life span may also be characteristics of *A. radiata*'s life history (Winemiller and Rose, 1992; Zeiner and Wolf, 1993; Francis et al., 2001; Frisk et al., 2001; Sulikowski et al., 2003). When these characteristics are coupled with the practice of selective removal of large individuals, the thorny skate population in the Gulf of Maine may be highly susceptible to over-exploitation by commercial fisheries (Brander 1981; Hoenig and Gruber, 1990; Casey and Myers 1998; Dulvy et al., 2000; Frisk et al., 2001). Because of an in-

¹ Sosebee, K. 2002. Maturity of skates in northeast United States waters. Scientific Council Research Document NAFO. no. 02/134, 17 p. [Available from the Northwest Atlantic Fisheries Organ., Dartmouth, NS.]

² New England Fishery Management Council (NEFMC). January 2001. 2000 stock assessment and fishery evaluation (SAFE) report for the northeast skate complex. 179 p. NEFMC, 50 Water Street, Mill 2 Newburyport, MA 01950.

³ New England Fishery Management Council (NEFMC). 2003. Skate fisheries management plan, 142 p. 50 Water St., Mill 2 Newburyport, MA 01950.

creasing commercial importance, declines in biomass levels, and a paucity of specific biological information, commercial harvests of thorny skates in the U.S. portion of the western North Atlantic are now prohibited. Thus, obtaining life history information for this skate species is not only timely (Simpfendorfer, 1993; Frisk et al., 2001), but it has become imperative. The objective of the present study was to describe the patterns of several morphological reproductive parameters manifested during the reproductive cycle of female and male *A. radiata* collected in the western Gulf of Maine.

Materials and methods

Sampling

Thorny skates were captured by otter trawl in an area approximately 900 square miles centered at 42° 50' N and 70° 15' W in the Gulf of Maine. These locations varied from 30 to 40 km off the coast of New Hampshire. Collection of skates occurred between the 10th and 20th of each month beginning May 2001 and ending May 2003. A comparison of samples taken from the same month between different years revealed no variability. Furthermore, the skates sampled in the present study were obtained from the same population and geographic location. Thus, the data from the same months for different sampling years were grouped together.

Skates were maintained alive on board the FV *Mystique Lady* until transport to the University of New Hampshire's Coastal Marine Laboratory (CML). There, individual fish were euthanized (0.3 g/L bath of MS222). Total length (TL in mm) was measured as a straight line distance from the tip of the rostrum to the end of the tail, and disc width (DW in mm) as a straight line distance between the tips of the widest portion of pectoral fins. Total wet weight (kg) was also recorded. For males, clasper length was measured as the straight line distance from the posterior point of the cloaca to the end of the clasper. The gonadosomatic index (GSI) and hepatosomatic index (HSI) were calculated as gonad weight divided by total body weight multiplied by 100, and liver weight divided by total body weight multiplied by 100, respectively. The epigonal organ was included in both male and female GSI measurements because of its close association with the gonads (Maruska et al., 1996).

Criteria used to determine reproductively active skates

Females whose reproductive tracts contained ovarian follicles with a minimum diameter of 25 mm and had a shell gland weighing at least 30 g were considered mature (capable of egg encapsulation and oviposition). These numbers were determined from our observations of reproductive tracts containing egg cases that were either fully formed or undergoing various stages of formation. Males with calcified claspers 200 mm long or greater, and with a proportion of mature spermato-

cysts in the testes of 25% or greater were considered reproductively capable of fertilizing an ovulated follicle. These criteria are consistent with previous studies that reported similar characteristics for other mature elasmobranch species (Koob et al., 1986; Heupel et al., 1999; Conrath et al., 2002; Sulikowski et al., 2004). Male and female thorny skates that did not meet all the criteria were considered to be immature. We also looked for some other indicators of reproductive activity, such as mating bites on female pectoral fins, and evidence of mating activity on male claspers, but they were either absent or not apparent in specimens examined during the study. Sperm storage was not assessed in the present investigation.

Gross morphology of the female reproductive tract

After removal of reproductive tracts, the ovaries, shell glands, and uteri were dissected out, blotted dry, and weighed to the nearest gram. Ovarian follicle dynamics were evaluated by measuring the diameter (with a caliper) and counting all follicles ≥ 1 mm in diameter (Tsang and Callard, 1987; Snelson et al., 1988; Sulikowski et al., 2004). For this data set, we averaged the size of the largest single follicle found on the right and left ovaries of each skate. Average follicle diameters, average ovary weights, and average shell gland weights were analyzed to assess temporal patterns during the reproductive cycle.

Histology of the testis

From male specimens, testes were removed, blotted dry, and weighed to the nearest gram. A single 2–3 mm thick segment was removed from the central portion of a single lobe in the medial area of an individual testis (Maruska et al., 1996; Sulikowski et al., 2004), placed in a tissue cassette, and fixed in 10% buffered formalin until processed by the University of New Hampshire Veterinary Diagnostic Laboratory. There, the sample was dehydrated, embedded in paraffin, sectioned, and stained with hematoxylin and eosin. Prepared slides of testicular tissue were examined and classified into stages of spermatogenic development following the criteria described by Maruska et al. (1996), Hamlett and Koob (1999), and Tricas et al. (2000). For the developmental stages of spermatogenesis described in other elasmobranchs, hormone analyses have confirmed that stages III through VI are associated with reproductive readiness (Heupel et al., 1999; Tricas et al. 2000; Sulikowski et al. 2004). For this reason, we focused our efforts on these specific stages in the thorny skate. Briefly, these stages have the following characteristics: stage III, spermatocysts; stage IV, spermatids; stage V, immature spermatozoa; and stage VI, mature spermatozoa (Maruska et al., 1996). In the present study, the mean proportion of testis occupied by each of these stages was measured along a straight line distance across one representative full lobe cross section of the testis (Maruska et al., 1996; Conrath et al., 2002).

Statistical analyses

The results are presented as means \pm SEM and evaluated by Kruskal Wallis analysis of variance followed by a Tukey's *post hoc* test. Statistical significance was accepted at $P < 0.05$. To determine whether a relationship exists in measured morphological and histological reproductive parameters, a Pearson correlation analysis (denoted as r) was performed.

Results

The lack of a robust sample size presents a potential limitation for our study. However, over the last decade, there

has been an increasingly precipitous decline in thorny skate populations in the Gulf of Maine, especially larger size specimens (NEFMC^{2,3}). These declines were evident in our sampling trips, because large, mature individuals were rarely caught in most trawls. The data presented in this article are the result of 84 sampling trips that took place over the course of two years (approximately three to four trips per month). Moreover, the recent prohibition on thorny skate landings has put an end to any prospects regarding collection of additional specimens in the foreseeable future. Thus, the data set we have presented represents the best available information on the reproductive cycle for this species.

Size ranges

Mature female skates ($n=48$) ranged from 820 to 1050 mm TL (mean=917 \pm 7 SEM) and from 4.4 to 10.2 kg (mean=7.7 \pm 0.2 SEM) in total body mass. Mature male skates ($n=48$) ranged from 800 to 1040 mm TL (mean=952 \pm 11 SEM), and from 5.4 to 10.8 kg (mean=8.4 \pm 0.3 SEM) in total body mass.

Assessment of morphological parameters in the female reproductive tract

In females, the average GSI of skates captured in July was lower ($P < 0.05$) than those captured in October and December, and those from September were lower than the specimens captured in October, November, and December (Fig. 1A). Because the number of samples from April consisted of only two skates, we were unable to test for statistical differences between other months. Despite this limitation, the two specimens from April displayed similar values to those in July. Average HSI (Fig. 1B) did not change ($P > 0.05$) over the sampling period. However, the average shell gland weight (Fig. 1C) from skates captured in October was greater ($P < 0.05$) than those captured in September. Because all shell glands from skates captured in February were in the process of encapsulating ovulated eggs, we were unable to obtain accurate individual shell gland weights.

There were no differences ($P > 0.05$) observed in the average diameter of the two largest follicles (Fig. 1D), and no pattern of follicle dynamics was discerned. Also, fully formed egg cases, or those in the process of formation, were found in the uteri of skates captured during all months of the year, except June and September.

Additional analysis revealed that GSI was correlated to shell gland weight ($r=0.53$) and average follicle diameter ($r=0.4$). Furthermore, HSI was also correlated to shell gland weight ($r=0.53$) and average follicle diameter ($r=0.7$).

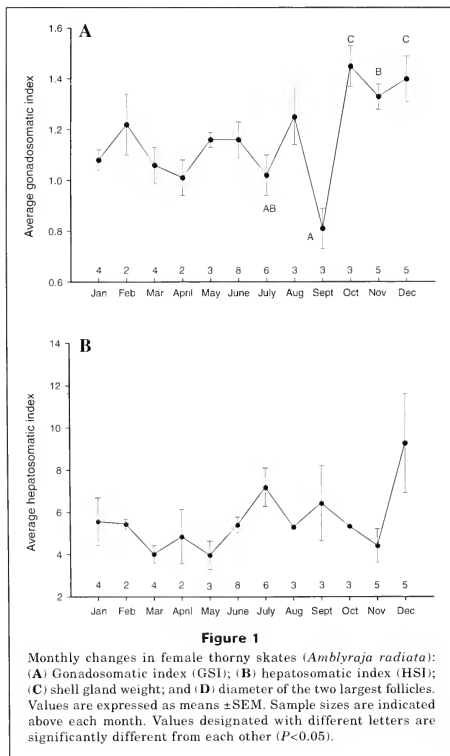


Figure 1

Monthly changes in female thorny skates (*Amblyraja radiata*): (A) Gonadosomatic index (GSI); (B) hepatosomatic index (HSI); (C) shell gland weight; and (D) diameter of the two largest follicles. Values are expressed as means \pm SEM. Sample sizes are indicated above each month. Values designated with different letters are significantly different from each other ($P < 0.05$).

Assessment of morphological parameters in the male reproductive tract

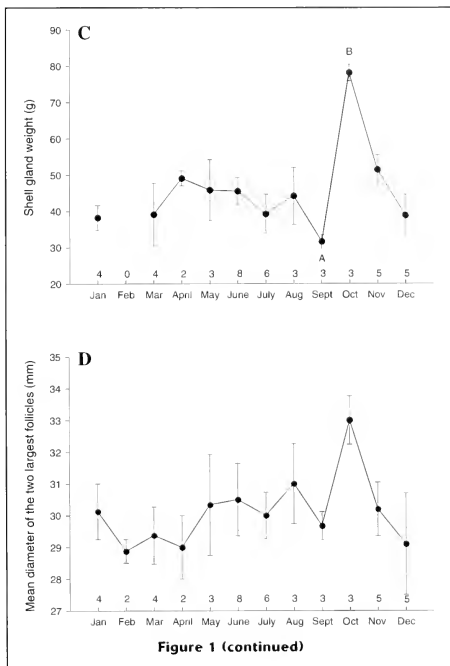
Histological stages III through VI (SIII–SVI) of spermatogenesis were examined, and GSI and HSI were determined for the 48 males collected during 24 months of sampling. Although the relative proportion of these four stages did not differ among months, it is notable that the production and maintenance of mature spermatocysts (SVI) within the testes persisted throughout the year (Fig. 2A). Similarly, no significant seasonal differences were found in HSI or GSI (Fig. 2, B and C, respectively). In addition, there were weak to no correlations between spermatogenesis and either HSI or GSI ($r = -0.07$ and 0.13 , respectively).

Synchronicity between male and female reproductive cycles

Results from the male and female morphological reproductive parameters indicated that thorny skates are capable of reproducing throughout the year in the western Gulf of Maine. When GSI, follicle diameter in relation to percent composition of SVI, or shell gland weight in relation to percent composition of SVI were compared between male and female thorny skates, no apparent correlation was detected (Fig. 3, A–C). In contrast, when percent composition of SVI (spermatogenesis) was plotted against percentage of captured female skates with egg cases, a strong synchronicity ($r = 0.51$) was observed (Fig. 4).

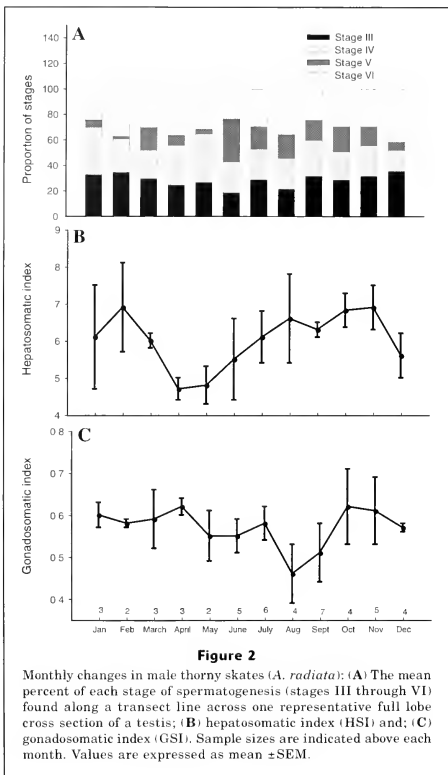
Discussion

Elasmobranchs display a wide range of reproductive strategies with morphological and physiological specializations for oviparous or viviparous reproduction (Wourms and Demski, 1993; Hamlett and Koob, 1999). These strategies are associated with one of three basic types of reproductive cycles: 1) reproduction throughout the year, 2) a partially defined annual cycle with one or two peaks, and 3) a well-defined annual or biennial cycle (Wourms, 1977; Hamlett and Koob, 1999). Among oviparous elasmobranchs, some species exhibit cycles with clearly delineated period(s) of reproductive activity interspersed between periods of little or no activity. For example, in the clearnose skate (*Raja eglanteria*), the patterns of estradiol concentrations and follicle dynamics indicate the presence of a well-defined annual reproductive cycle, in which mating and egg deposition take place from December to mid May (Rasmussen et al., 1999). Likewise, hormone and morphological data also indicate a defined annual cycle in the epaulette shark (*Hemiscyllium ocellatum*) (Heupel et al., 1999) and that reproductive activities take place from July to December.



In contrast, other oviparous elasmobranchs exhibit reproductive activity year round. For example, the present study revealed that female thorny skates are capable of reproducing throughout the year. This conclusion was based on GSI, shell gland weight, diameter of the largest prevulatory follicles, and the presence of egg cases in specimens collected over the course of the study. We also observed that GSI and shell gland weight were highest in October. Thus, the period (or periods) of enhanced reproductive activity appears to be an integral part of continuous cycles, although the specific measured parameters or when these periods occur may vary between species.

In a study of thorny skates sampled from August to December in NAFO Division 3N, females were found to be reproductively active over the entire sampling interval, and peak egg case production occurred in September (Del Río, 2002). In contrast, although large prevulatory follicles were present and oviposition occurred throughout the reproductive cycle of the lesser spotted dogfish

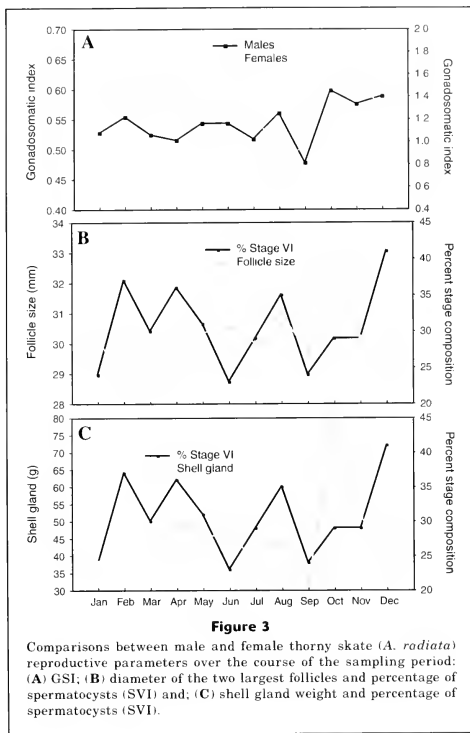


(*Scyliorhinus canicula*) (Henderson and Casey, 2001), ovary weight and egg deposition peaked during spring. Similarly, several morphological parameters and steroid hormones have been shown to peak in female winter skates (*Leucoraja ocellata*) during the summer, and egg-case production is highest in the fall (Sulikowski et al., 2004). Lastly, in *L. erinacea*, examination of follicle dynamics and egg-case production indicated that a higher proportion of females are reproductively active during two periods of time in the reproductive cycle: in the winter and in the summer (Richards et al., 1963).

The fairly consistent pattern of HSI in female thorny skates over the reproductive cycle indicated that liver

reserves (such as lipids and proteins used for oocyte growth) were stored and metabolized continuously throughout the year without a significant change in whole organ biomass. This is in contrast to other oviparous species, such as *S. canicula*, which displayed seasonal variations in liver mass as a result of lipid deposition occurring during different times of the reproductive cycle (Craik, 1978).

The continual presence of mature spermatocysts within the testes over the entire sampling period indicated that male thorny skates are also capable of reproducing throughout the year. Information describing the annual reproductive cycles of oviparous male elasmobranchs is



very limited because studies have focused on changes in morphological parameters (i.e., Richards et al., 1963; Craik, 1978) or steroid hormone analyses (i.e., Sumpter and Dodd, 1979; Rasmussen et al., 1999) in females. To our knowledge, the only two species in which quantitative methods were used to describe annual reproductive patterns in males were *H. ocellatum* (Heupel et al., 1999) and *L. ocellata* (Sulikowski et al., 2004). These two species exhibit contrasting strategies in their respective reproductive cycles. For example, similar to male thorny skates from the present study, male winter skates appear capable of continuous production of mature spermatocysts throughout the year (Sulikowski et al., 2004). In contrast, examination of the testes and circulating hormone concentrations in *H. ocellatum* indicated that sperm production and androgen concen-

tration display a concurrent seasonal cycle that peaks from June to October (Heupel et al., 1999).

The lack of correlation between GSI and stage of spermatogenesis in the thorny skate was not surprising because studies do not support the assumption that relative gonad size (or storage products in the liver) and reproductive readiness are positively correlated (Teshima, 1981; Parsons and Grier, 1992; Maruska et al., 1996). For instance, neither peak sperm production (Maruska et al., 1996) nor the pattern of testosterone concentration was correlated with GSI in *Dasyatis sabina* (Snelson et al. 1997) or *L. ocellata* (Sulikowski et al., 2004).

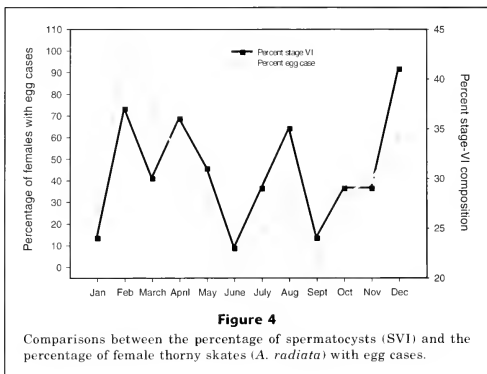
Relatively few studies have assessed whether cyclical patterns of reproductive morphological parameters or hormone concentrations are coordinated between

males and females over the course of their reproductive cycles. Among them, coordinated peaks in gonad weight and steroid hormone concentrations in winter skates (Sulikowski et al., 2004) and epaulette sharks (Heupel et al., 1999) were observed in males and females over an annual cycle. In the present study, mature spermatocysts (SVI) and percentage of female thorny skates with egg cases were also synchronized over the course of the study. In contrast, Henderson and Casey (2001) found that the gonadal cycles of male and female lesser spotted dogfish were asynchronous, which they hypothesized to be due to the storage of sperm by females. Sperm storage has been documented in other female elasmobranch species as well (e.g., Pratt, 1993; Maruska et al., 1996) and is thought to be a feature primarily of species that are nomadic or segregated by sex (Pratt, 1993). In the current study, *A. radiata* was neither segregated by sex (both genders were captured in the same area and in the same trawls) nor found to be nomadic in their movement patterns (Templeman, 1987; Sulikowski, unpubl. observ.). Moreover, because males are capable of producing viable sperm and females appear to be reproductively active throughout the year, there is probably no need for the population of thorny skates that we sampled to store sperm. On the basis of the above information, we believe that the reproductive cycle in the sampled population of thorny skates is coordinated over an annual cycle.

In summary, according to the reproductive strategies outlined by Wourms (1977) and later by Hamlett and Koob (1999), the results of the present study indicate that thorny skates have a reproductive cycle that is continuous throughout the year. For females, this conclusion was based on ovary weight, shell gland weight, and diameter of the largest follicles (the previtellogenic follicles). For males, this conclusion was based on the presence of mature spermatocysts within the testes over the course of the sampling period. Moreover, comparisons between the proportion of mature spermatocysts within the testes and the percentage of egg-case-bearing females indicate that the reproductive cycles of male and female thorny skates are synchronized. Currently, analyses of circulating steroid hormone concentrations are in progress for the thorny skates used in the present study, which may provide additional insight into the regulation and timing of reproductive events in this species.

Acknowledgments

Collection of skates was conducted on the FV *Mystique Lady*. We thank Noel Carlson for maintenance of the fish



at the U.N.H. Coastal Marine Laboratory. This project was supported by a Northeast Consortium grant (no. NA16FL1324) to PCWT, JAS, and PDD.

Literature cited

- Brander, K.
1981. Disappearance of common skate *Raja batis* from Irish Sea. *Nature* 290 (5801):48–49.
- Casey, J. M., and R. A. Myers.
1998. Near extinction of a large widely distributed fish. *Science* 28:690–692.
- Collette, B., and G. Klein-MacPhee
2002. *Fishes of the Gulf of Maine*, 3rd ed., p. 62–66. Smithsonian Institution Press, Washington, D.C.
- Compagno, L. J. V., D. A. Ebert, and M. J. Smale.
1989. Guide to the sharks and rays of southern Africa, 158 p. New Holland (Publ.) Ltd., London.
- Conrath, C. L., J. Gelsleichter, and J. A. Musick.
2002. Age and growth of the smooth dogfish, *Mustelus canis*, in the northwest Atlantic. *Fish. Bull.* 100:674–682.
- Craik, J. C. A.
1978. An annual cycle of vitellogenesis in the elasmobranch *Scyliorhinus canicula*. *J. Mar. Biol. Assoc. UK* 58:719–726.
- Del Río, J. L.
2002. Some aspects of the thorny skate, *Amblyraja radiata*, reproductive biology in NAFO Division 3N. NAFO SCR Doc. 02/118, serial no. N4739, 14 p.
- Dulvy, N. K., J. D. Metcalfe, J. Glanville, M. G. Pawson, and J. D. Reynolds.
2000. Fishery stability, local extinctions, and shifts in community structure in skates. *Cons. Biol.* 14: 283–293.
- Francis, M., C. O., Maolagáin, and D. Stevens.
2001. Age, growth, and sexual maturity of two New Zealand endemic skates, *Dipturus nasutus* and *D.*

- innominatus*. N.Z.J. Mar. Freshw. Res. 35:831-842.
- Frisk, M. G., T. J. Miller, and M. J. Fogarty.
2001. Estimation and analysis of biological parameters in elasmobranch fishes: a comparative life history study. Can. J. Fish. Aquat. Sci. 58:969-981.
- Hamlett W. C., and T. J. Koob.
1999. Female reproductive system. In Sharks, skates and rays: the biology of elasmobranch fish (W. C. Hamlett, ed.), 515 p. Johns Hopkins Univ. Press, Baltimore, MD.
- Henderson, A. C., and A. Casey.
2001. Reproduction and growth in the lesser-spotted dogfish *Scyliorhinus canicula* (Elasmobranchii: Scyliorhinidae), from the west coast of Ireland. Can. Biol. Mar. 42:397-405.
- Heupel M. R., J. M. Whittier, and M. B. Bennett.
1999. Plasma steroid hormone profiles and reproductive biology of the epaulette shark, *Hemiscyllium ocellatum*. J. Exp. Zool. 284:586-594.
- Hoenig, J., and S. H. Gruber.
1990. Life history patterns in the elasmobranchs: Implications for fisheries management. In Elasmobranchs as living resources: advances in the biology, ecology, systematics and the status of the fisheries (H. L. Pratt Jr. S. H. Gruber, and T. Tanuchi, eds.), p. 1-16. NOAA Technical Report, NMFS 90.
- Koob T. J., P. Tsang, and I. P. Callard.
1986. Plasma estradiol, testosterone and progesterone levels during the ovulatory cycle of the little skate, *Raja erinacea*. Biol. Reprod. 35:267-275.
- Maruska K. P., E. G. Cowie, and T. C. Tricas.
1996. Periodic gonadal activity and protracted mating in elasmobranch fishes. J. Exp. Zool. 276: 219-232.
- Parsons G. R., and H. J. Grier.
1992. Seasonal changes in the shark testicular structure and spermatogenesis. J. Exp. Zool. 261:173-184.
- Pratt, H. L.
1993. The storage of spermatozoa in the oviductal glands of western North Atlantic sharks. Environ. Biol. Fish. 35:139-149.
- Rasmussen L. E. L., D. L. Hess, and C. A. Luer.
1999. Alterations in serum steroid concentrations in the clearnose skate, *Raja eglanteria*: correlations with season and reproductive status. J. Exp. Zool. 284:575-585.
- Richards S. W., D. Merriman, and L. H. Calhoun.
1963. Studies in the marine resources of southern New England. IX. The biology of the little skate *Raja erinacea*, Mitchell. Bull. Bingham. Oceanogr. Coll. 18:311-407.
- Robins, C. R., and G. C. Ray.
1986. A field guide to Atlantic coast fishes of North America, 354 p. Houghton Mifflin Co., Boston, MA.
- Simpfendorfer, C. A.
1993. Age and growth of the Australian sharpnose shark, *Rhizoprionodon taylori*, from north Queensland, Australia. Environ. Biol. Fish. 36:233-241.
- Snelson F. F. Jr, S. E. Williams-Hopper, and T. H. Schmid.
1988. Reproduction and ecology of the Atlantic stingray, *Dasyatis sabina*, in Florida coastal lagoons. Copeia 1988:729-739.
- Snelson F. F. Jr, L. E. L. Rasmussen, M. R. Johnson, and D. L. Hess.
1997. Serum concentrations of steroid hormones during reproduction in the Atlantic stingray, *Dasyatis sabina*. Gen. Comp. Endocrinol. 108:67-79.
- Sulikowski, J. A., M. D. Morin, S. H. Suk and W. H. Howell.
2003. Age and growth of the winter skate, *Leucoraja ocellata*, in the Gulf of Maine. Fish. Bull. 101:405-413.
- Sulikowski J. A., P. C. W. Tsang, and W. Hannting Howell.
2004. An annual cycle of steroid hormone concentrations and gonad development in the winter skate, *Leucoraja ocellata*, from the western Gulf of Maine. Mar. Biol. 144:845-853.
- Sampter J. P., and J. M. Dodd.
1979. The annual reproductive cycle of the female lesser spotted dogfish, *Scyliorhinus canicula*, and its endocrine control. J. Fish. Biol. 15:687-695.
- Templeman, W.
1982. Development, occurrence and characteristics of egg capsules of the thorny skate, *Raja radiata*, in the Northwest Atlantic. J. Northw. Atl. Fish. Sci. 3:47-56.
- Templeman, W.
1987. Differences in sexual maturity and related characteristics between populations of thorny skate *Raja radiata* in the northwest atlantic. J. Northw. Atl. Fish. Sci. 44 (1):155-168.
- Teshima, K.
1981. Studies on the reproduction of the Japanese smooth dogfishes, *Mustelus manazo* and *Mustelus griseus*. J. Shimonoseki. Univ. Fish. 29:113-199.
- Tricas T. C., K. P. Maruska, and L. E. L. Rasmussen.
2000. Annual cycles of steroid hormone production, gonad development, and reproductive behavior in the Atlantic stingray. Gen. Comp. Endocrinol. 118:209-225.
- Tsang P., and I. P. Callard.
1987. Morphological and endocrine correlates of the reproductive cycle of the aplacental viviparous dogfish, *Squalus acanthias*. Gen. Comp. Endocrinol. 66:182-189.
- Winemiller, K. O., and K. A. Rose.
1992. Patterns of life history diversification in North American fishes: implication for population regulation. Can. J. Fish. Aquat. Sci. 49:2196-2218.
- Wourms, J. P.
1977. Reproduction and development in chondrichthyan fishes. Am. Zool. 17:379-410.
- Wourms, J. P., and L. S. Demski.
1993. The reproduction and development of sharks, skates, rays and ratfishes: introduction, history, overview and future prospects. Environ. Biol. Fish. 38:7-21.
- Zeiner, S. J., and P. G. Wolf.
1993. Growth characteristics and estimates of age at maturity of two species of skates (*Raja binoculata* and *Raja rhina*) from Monterey Bay, California. In Conservation biology of elasmobranchs, p. 87-90. NOAA Technical Report NMFS 115.

Effect of type of otolith and preparation technique on age estimation of larval and juvenile spot (*Leiostomus xanthurus*)

Dariusz P. Fey

Sea Fisheries Institute
Dept. of Fisheries Oceanography and Marine Ecology
ul. Kollataja 1
81-332 Gdynia, Poland
E-mail address: dfeym@mirgdynia.pl

Gretchen E. Bath Martin

James A. Morris

Jonathan A. Hare

NOAA National Ocean Service
Center for Coastal Fisheries and Habitat Research
101 Pivers Island Road
Beaufort, North Carolina 28516-9722

Otoliths of larval and juvenile fish provide a record of age, size, growth, and development (Campana and Neilson, 1985; Thorrold and Hare, 2002). However, determining the time of first increment formation in otoliths (Campana, 2001) and assessing the accuracy (deviation from real age) and precision (repeatability of increment counts from the same otolith) of increment counts are prerequisites for using otoliths to study the life history of fish (Campana and Moksness, 1991). For most fish species, first increment deposition occurs either at hatching, a day after hatching, or after first feeding and yolk sac absorption (Jones, 1986; Thorrold and Hare, 2002). Increment deposition before hatching also occurs (Barkmann and Beck, 1976; Radtke and Dean, 1982). If first increment deposition does not occur at hatching, the standard procedure is to add a predetermined number to increment counts to estimate fish age (Campana and Neilson, 1985).

Accuracy and precision of increment counts is in part determined by the increment formation rate, which has been reviewed elsewhere (Campana and Neilson, 1985; Jones, 1986; Geffen, 1987), and by the type of otolith (asteriscus, sagitta, or lapillus) and the preparation technique

used for aging. In most age and growth studies of larval and juvenile fish, the sagitta, the largest of the three otoliths, has been used (Campana and Neilson, 1985), but there are many examples of fish species that can be aged accurately by using the lapillus (e.g., Hoff et al., 1997; Bestgen and Bundy, 1998; Escot and Granado-Lorencio, 1998; Morioka and Machinandiarena, 2001). Although infrequently used, the asteriscus has provided age information with similar or even better precision and accuracy than the sagitta and lapillus (David et al., 1994). However, the microstructure of asterisci is usually not as clear as that of sagittae or lapilli, and the extraction of asterisci is relatively time consuming and laborious (Campana and Neilson, 1985; Neilson and Geen, 1985). As for otolith preparation, two general techniques are common: 1) polishing of one or both sides of a sectioned otolith in transverse view, and 2) polishing of one side of the whole sagitta (Secor et al., 1992). Sagittae and lapilli provide the same accuracy and precision for age estimation; however, lapilli may be easier to process for age determination and may not require processing at all (e.g., Ichimaru and Katsunori, 1995).

Spot (*Leiostomus xanthurus*) is an important fishery species along the southeast coast of the United States (Mercer, 1987) and is a dominant species in coastal ecosystems owing to its abundance (Walter and Austin, 2003). Studies of spot have illuminated processes that affect the abundance of estuarine-dependent species (Warlen and Chester, 1985; Flores-Coto and Warlen, 1993; Ross, 2003). Further, spot has been used as an experimental organism for examining larval ecology (Govoni et al., 1985; Govoni and Hoss, 2001) and otolith chemistry (Bath Martin et al., 2000, 2004; Bath-Martin and Thorrold, 2005). Although spot has been widely studied and is an important ecological and fishery species, basic information necessary for otolith analyses is not available.

Our goal was to provide a foundation for the use of otolith increment counts in examining the ecology of larval and juvenile spot. Our specific objectives were 1) to determine the timing of first-increment formation of spot (*Leiostomus xanthurus*) and 2) to assess the accuracy and precision of age estimates from increment counts made with different combinations of otoliths and preparation techniques. Specifically, four combinations of otoliths (sagittae and lapilli) and preparation techniques were compared: 1) a transverse section of the sagitta (polished on one side TSS-1); 2) a transverse section of the sagitta (polished on two sides TSS-2); 3) a whole sagitta (polished on one side WS-1); and 4) a whole lapillus (polished on one side WL-1).

Materials and methods

First increment formation

Six male and six female spot were induced to spawn by injection of human chorionic gonadotropin (HCG) hormone at the NOAA Beaufort Laboratory. Eggs were incubated in a 100-L

Manuscript submitted 14 May 2004 to the Scientific Editor's Office.

Manuscript approved for publication 29 March 2005 by the Scientific Editor.
Fish. Bull. 103:544–552 (2005).

tank at constant temperature (20°C) and salinity (30‰), under 12 h light:12 h dark photoperiod. These conditions were maintained throughout the rearing period. Hatching occurred three days after spawning. Larvae were fed rotifers throughout the experiment and supplemented with enriched *Artemia* from day 20 through day 30. Larvae were collected 4 days ($n=5$), 12 days ($n=7$), and 27 days ($n=5$) after hatching, and live total length (L_T) measurements were made. Larvae were then preserved in 95% ethanol.

Sagittae and lapilli were dissected with fine-tipped forceps and embedded on microscope slides. The increments were clearly visible and otoliths did not require any additional preparation. All increment counts were conducted three times by one person on different occasions with a 100× oil objective and a Nikon E600 microscope with transmitted light. The light was polarized to obtain better visibility. The reader did not know the ages of the fish.

Known fish age and the number of observed increments were used to determine the time of first increment formation on both the sagittae and lapilli. The number of increments deposited between sampling dates divided by elapsed days indicated periodicity of increment formation.

Accuracy and precision

The experimental protocol and conditions were the same as in the previous examination of first increment formation, except that fish were reared for 53 days and artificial diet was added after day 30. Larvae ($n=24$, 8.8–16.1 mm L_T , mean=11.8 mm L_T) were collected 34 days after hatching, and juveniles ($n=34$, 19.4–28.1 mm L_T , mean=24.3 mm L_T) were collected 53 days after hatching.

Sagittae and lapilli were dissected from fish with fine-tipped forceps and embedded for sectioning on the transverse plane (right sagitta) or polishing on the sagittal plane (left whole sagitta and lapillus). Priority was given to transverse sections, and if the right sagitta was damaged during preparation, the left sagitta was used ($n=8$). Otoliths were sectioned with a slow-speed saw with dual diamond wafering blades. Sections were then ground on one side with 1000-grit sandpaper and polished with 0.3- μ m alumina paste. After increments were counted on the proximal side of sections that were polished on one side (see below for details), sections were flipped over, ground, and polished to the core to provide a section that was polished on two sides. The left whole sagitta and lapillus were ground and polished in the sagittal plane with 0.3- μ m alumina paste. One person made all the increment counts three times for each preparation technique on different occasions with a 100× oil objective on a Nikon E600 microscope with transmitted light. The reader knew the study design, but not the ages of the fish.

The mean number of increments counted from sagittae and lapilli prepared with different techniques were compared with known ages to determine the accuracy of

the different aging methods. The statistical significance of differences in increment counts (accuracy) was evaluated with a one-way ANOVA. Increment formation rate was determined by comparing the number of increments counted to known age, and by comparing the difference in the number of increments between 34- and 54-day-old fish and the number of actual days between these increments (20 days).

Precision of increment counts from different otoliths and preparation techniques was determined with the coefficient of variation (CV), calculated by using the three increment counts made for each individual type of otolith and preparation technique (Chang, 1982). The differences in CV values among the four age estimation methods were analyzed by using a Kruskal-Wallis ANOVA. The statistical significance of observed differences were estimated with a *post hoc* Tukey HSD for unequal n test. All the statistical data analyses were performed with Statistica 6.0 software (StatSoft Inc., Tulsa, OK).

Results

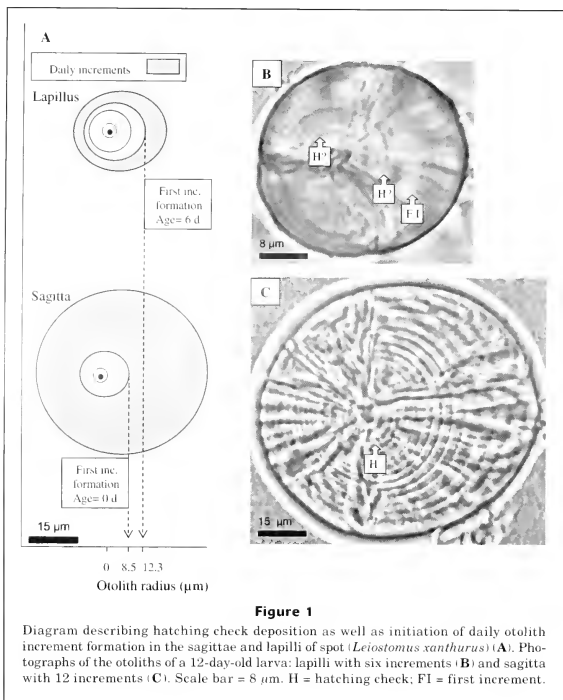
First-increment formation

First-increment formation on the sagitta occurred at hatching, but there may be problems in resolving increments near the core. Increment counts on sagittae were variable for 4-day-old larvae. Four increments were visible on the sagittae of one individual. The first increment was more pronounced than the others and was interpreted as a hatching check. This increment was approximately 8 μ m from the core. On the sagittae of the remaining four 4-day-old larvae, only one increment was visible corresponding to the location of the perceived hatching check. Despite the apparent nondaily increment formation in 4-day-old larvae, an average of 12.3 (range 12–13) increments were visible on the sagittae of 12-day-old larvae, and an average of 26.5 (range 26–27) were visible on the sagittae of 27-day-old larvae. The first increment observed on the sagittae of 12- and 27-day-old larvae corresponded to the location of the first increment observed in the sagittae of 4-day-old larvae (Fig. 1).

First increment formation on the lapillus occurred 6–7 days after hatching. No increments were visible on the lapilli of 4-day-old larvae. In older larvae, an average of 6.4 (range 6–7) increments were observed on 12-day-old larvae and an average of 20.3 (range 20–21) increments were observed on the lapilli of 27-day-old larvae. Additionally, lapilli of 12 and 27-day old larvae exhibited two checks in the area between the otolith core and the first increment, but it was difficult to distinguish which check, if either, was formed at hatching (Fig. 1).

Accuracy and precision

Increments were clearly visible regardless of otolith preparation technique (Fig. 2). Increment width increased from



the core towards the otolith edge. In both sagittal preparations, increment counts could not easily be made along one radius owing to changes in the growth trajectories (Fig. 2A) and to discontinuities in increment formation (Fig. 2B). However, increment counts could be made along one radius in the lapilli (Fig. 2C)—an advantage that may facilitate measurements of otolith increment widths in future studies.

A hatching check was identified in the sagittae of 34-day-old larvae and 54-day-old juveniles at a location approximately 8.4 μm radius from the core (Table 1). In addition to the hatching check, another well-defined increment was observed in the core area of the sagittal otoliths (Fig. 3A), and this second check was likely related to a dietary switch to exogenous feeding. In most fish the second check was separated from the hatching check by an average of 5.2 increments ($n=49$, $SD=0.59$). However, in some fish ($n=9$), no increments were visible

between the hatching check and the other well-defined increment. This observation indicates that there may be problems resolving increments near the core, similar to the results presented above regarding the timing of first increment formation. Owing to the apparent problems discerning increments near the core, the second check was used as a starting point for increment counts. Using the second check as a starting point influenced accuracy but provided a clear starting point for increment counts in all sagittal otolith preparations.

In the lapilli, increment deposition began from a pronounced check visible at ca. 12.3 μm radius from the otolith core (Fig. 3B). This check was found at the same distance from the core in lapilli of 12- and 27-day-old larvae in the experiment on first-increment formation (Table 1). Beginning increment counts from this check would underestimate age by 6–7 days owing to the timing of first-increment formation on the lapilli.

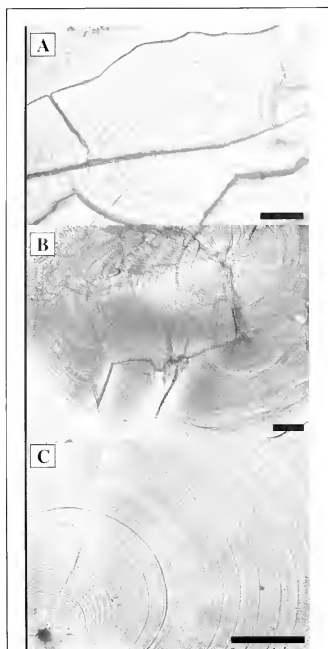


Figure 2

Otolith microstructure of an early-juvenile laboratory-reared spot (*Leiostomus xanthurus*): (A) transverse section of the sagitta (polished on two sides); (B) whole sagitta (polished on one side); and (C) whole lapillus (polished on one side). Scale bar = 30 μ m.

Increment formation occurred daily in both sagittae and lapilli after the early larval period. The difference in number of increments counted from sagittae and lapilli from fish sampled 34 and 53 days after hatching reflected the time elapsed between these two samplings (Table 2) and indicated daily increment formation between the larval and early juvenile stage. The same daily increment formation was also observed for larvae sampled 12 and 27 days after hatching during the experiment on first-increment formation (Table 2).

The accuracy of larval age estimates were similar for all the sagittae and lapilli preparation methods (ANO-

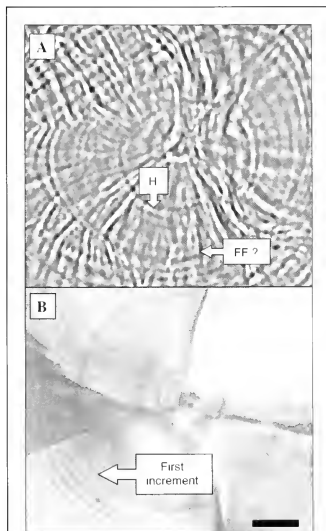


Figure 3

Central otolith area of early-juvenile laboratory-reared spot (*Leiostomus xanthurus*): (A) transverse section of sagitta (polished on two sides); five increments are visible between hatching check (H) and, presumably, first feeding check (FF?); (B) whole lapillus (polished on one side) with daily increments deposited after the check was formed six days after hatching. Scale bar = 10 μ m.

VA, $P > 0.05$; Fig. 4A). For juveniles, however, there was a significant difference in the number of counted increments among sagitta preparation methods (ANOVA, $P < 0.001$) (Fig. 4B). A lower number of increments were enumerated from transverse sections of sagittae (with one side polished) (*post hoc*: Tukey HSD for unequal n , $P < 0.001$). Moreover, ~25% of otoliths within this group were not readable.

All the otolith preparation techniques, except the P1S transverse sections of sagitta from juveniles, underestimated the age from hatching by 9–10 days. A 6–7 day difference was expected between known age and lapilli increment counts, owing to the time of first-increment formation. Thus, actual fish age was underestimated by approximately 2–4 days with lapilli increment counts. A 5-day difference was expected between known age and

Table 1

The distance from otolith core to first increment in the sagittae (first increment formed on the first day after hatching) and in the lapilli (first increment formed six days after hatching) of laboratory-reared spot (*Leiostomus xanthurus*).

Otolith	n	Distance to the first increment (μm)		
		Mean	SD	Range
Sagittae—experiment on first-increment formation	17	8.3	0.76	6.7–9.9
Sagittae ¹ —experiment on accuracy and precision of aging technique	36	7.8	0.91	6.7–8.8
Lapilli—experiment on first-increment formation	17	12.3	0.54	11.5–13.2
Lapilli—experiment on accuracy and precision of aging technique	25	12.2	0.61	11.0–14.2

¹ Data for both whole sagittae (polished on one side) along sagittal view, and transverse sections of sagittae polished on two sides.

Table 2

Number of increments deposited on the otoliths of laboratory-reared spot (*Leiostomus xanthurus*) between sampling days in comparison with number of days between sampling days.

Otolith	Sampling days (days after hatching)	Days between sampling	Number of increments between sampling ²
Sagittae—experiment on first-increment formation	12 and 27	15	14.3
Sagittae ¹ —experiment on accuracy and precision of age determination	34 and 53	19	18.3
Lapilli—experiment on first-increment formation	12 and 27	15	14.1
Lapilli—experiment on accuracy and precision of age determination	34 and 53	19	18.6

¹ Data for both whole sagittae (polished on one side) and for transverse sections of sagittae (polished on two sides).

² No variance is given because the value represents difference between two average increment numbers obtained for two different groups of fish.

whole-sagittae increments counts, owing to the initiation of increments from a second check, which formed approximately 5 days after hatching. With whole-sagittae increment counts, actual fish age was underestimated by approximately 5 days.

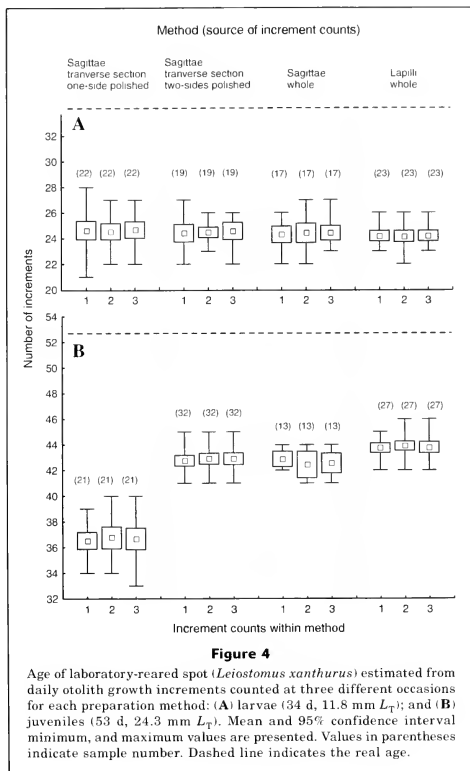
The coefficients of variation (CV), which indicates the precision of age estimates, varied from 1.4% to 8.3% (Fig. 5). CVs were statistically different among age estimation methods for both larvae and juveniles (Kruskal-Wallis ANOVA, $P < 0.001$). Lapilli from both larvae and juveniles had lowest CVs, indicating high precision. Whole sagittae and P2S transverse sections for juveniles were comparable, but lower precision for larvae was observed. However, if transverse sections are used for aging, the preparation of both sides is important in the case of larvae (with regard to precision; see Fig. 5) and mandatory in the case of juveniles (with regard to accuracy; see Fig. 4B). In addition, the confidence of the otolith reader in increment recognition (Fig. 5) indicated that the most clear and easy to count increments were found in the lapilli.

Discussion

First-increment formation

In prior studies, the age of larval and juvenile spot was estimated by adding five days to the number of increments counted from sagittae (e.g., Warlen and Chester, 1985; Flores-Coto and Warlen, 1993; Ross, 2003). Our research indicated that increment formation in sagittae occurred at hatching. The only study validating first-increment formation in spot used linear regression analysis for laboratory-reared fish (Peters et al.¹). The intercept of their regression line (age in relation to number of increments) indicated that the first increment

¹ Peters, D. S., Jr., J. C. DeVane, M. T. Boyd, L. C. Clements, and A. B. Powell. 1978. Preliminary observations on feeding, growth and energy budget of larval spot (*Leiostomus xanthurus*). In Ann. Rep. Southeast Fish. Cent., Beaufort Lab. to U.S. Dep. Energy, p. 377–397. Beaufort Laboratory, National Marine Fisheries Service, Beaufort, NC.



formed five days after hatching, which corresponds to a time of exogenous feeding initiation in spot (Powell and Gordy, 1980; Powell and Chester, 1985). The other validation experiments on spot (Hettler, 1984; Siegfried and Weinstein, 1989) provided no information on first increment deposition time. In lapilli, increment deposition occurred six days after hatching, but no other studies are available for spot to compare and evaluate these results.

The inconsistency in the time of first increment formation on the sagittae between the present study and Peters et al.'s study¹ may be the result of underestimation by the latter because they did not section or pol-

ish the otoliths. Spot otoliths are relatively large and thick and both sagittae and lapilli are difficult to read without otolith preparation for fish older than 25–30 days (~7–9 mm TL). Peters et al.¹ found no increments in sagittae of four- to five-day-old fish. Although in the present study increments were not clear in sagittae of four-day-old spot, fish collected from the same tanks, 8 and 23 days later, had visible increments since hatching. Even if it is difficult to explain why the increments in sagittae of four-day-old fish were not visible, results presented in the present study support the conclusion that first increment formation occurred at hatching.

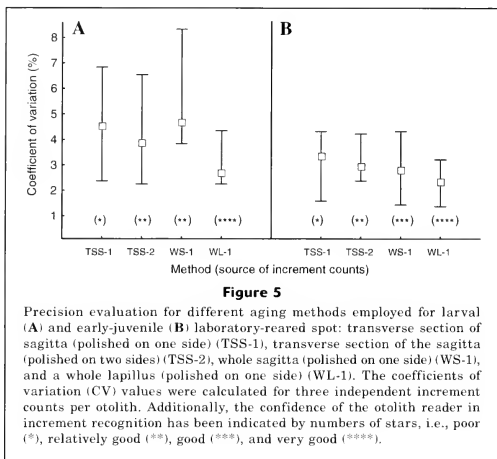


Figure 5

Precision evaluation for different aging methods employed for larval (A) and early-juvenile (B) laboratory-reared spot: transverse section of sagitta (polished on one side) (TSS-1), transverse section of the sagitta (polished on two sides) (TSS-2), whole sagitta (polished on one side) (WS-1), and a whole lapillus (polished on one side) (WL-1). The coefficients of variation (CV) values were calculated for three independent increment counts per otolith. Additionally, the confidence of the otolith reader in increment recognition has been indicated by numbers of stars, i.e., poor (*), relatively good (**), good (***), and very good (****).

Accuracy and precision of age estimates among different types of otoliths and preparation techniques

Lack of distinct patterns in daily growth increments in otoliths of laboratory-reared fish (e.g., David et al., 1994) could make it difficult to conduct laboratory-based ecological experiments with larval fish. Hettler (1984) attempted to validate increment formation rate in the sagittal otoliths of laboratory-reared spot (13–16 mm SL). Within eight days after tetracycline marking, otolith radii increased approximately 18%, but no increments were observed. Stegfried and Weinstein (1989) confirmed daily increment formation in the sagittae of field-reared spot larvae, but those reared in the laboratory produced 17 increments instead of the expected 30. Our results, on the other hand, provided direct validation of daily increment formation in the sagittae and lapilli of laboratory-reared spot (Table 2).

Even though increment formation was found to occur daily, there were inaccuracies in the estimate of age from otolith increment counts. Twenty-four increments were counted on the sagittae of 34-day-old larvae; if five increments were added for time between first-increment formation and formation of the second check (the starting point of counts used in the present study), age was still underestimated by 4–5 days. Similarly, 24 increments were counted on the sagittae of 34-day-old larvae; if 6–7 days were added to account for the timing of increment formation in the lapillus, age was underestimated by 3–4 days. Similar inaccuracies in age estimates were derived for 53-day-old juveniles. Peters et al.¹ also found age inaccuracies of five days from

sagittal increments and concluded that first-increment formation occurred five days after hatching. Given our results and those of Hettler (1984) and Stegfried and Weinstein (1989), we conclude that the likely explanation for age inaccuracies is that the increments near the core of the otolith become harder to read as more otolith material is laid down and this process results in the appearance of fewer increments. These inaccuracies would contribute to a 10–15% underestimation of age from sagittae and a 3–11% underestimation of age from lapilli. To account for these inaccuracies, five increments should be added to increment counts to estimate age.

Lapilli, compared with sagittae, exhibited very clear patterns with increments (Fig. 2) and provided more precise results for the ages of larval and juvenile spot. Although there is no study presenting age data obtained from lapilli for larval or juvenile spot, lapilli have been used successfully for aging many other fish species. Ichimaru and Katsunori (1995) preferred the lapillus as a source of age data for two species of flyingfishes larvae (*Cypselurus heterurus doederleini* and *Cypselurus hiraii*) because increments were as clear as those in the sagittae, yet the lapilli did not require any preparation. Bestgen and Bundy (1998) reported increments deposited on sagittae of Colorado squawfish (*Ptychocheilus lucius*) were difficult to distinguish after fish were 30 days old and thus lapilli were used to age older fish. Lapilli were the preferred otoliths for age determination of young Lost River sucker (*Delostes luxatus*) and shortnose sucker (*Chasmistes brevirostris*) because of their readability and conservative growth pattern (Hoff et al., 1997). Escot and Grando-Lorencio (1998) concluded

that increments in lapilli of *Barbus sclateri* (Pisces: Cyprinidae) were more clearly defined than in sagittae and asterisci. Similarly, our results demonstrate the utility of lapilli for larval and juvenile fish age estimates.

In addition to the choice of the most suitable type of otolith, the choice of the most appropriate preparation method is an important aspect of larval and juvenile fish age determination (Secor et al., 1992). Analysis of P1S whole sagittae provided in the current study similar precision and confidence in age determination as transverse sections. Although analysis of sagittal transverse sections have been applied to spot (Siegfried and Weinstein, 1989), the most frequently used method has been the analysis of whole sagittae in sagittal view (Hettler, 1984; Warlen and Chester, 1985; Powell et al., 1990; Flores-Coto and Warlen, 1993; Ross, 2003). Recently, Ross (2003) was able to age 40–160 day-old spot juveniles, analyzing whole sagittae along the sagittal view; however, polishing on both sides was frequently necessary. For whole lapilli, however, only one preparation method (i.e., polishing along the sagittal plane) was used in the present study and the results were more satisfactory than those obtained for sagittae and hence no other preparation method (i.e., sectioning) seemed to be required.

In conclusion, first-increment formation occurs at hatching in the sagittae and at 6–7 days after hatching in the lapilli. Increment formation rate occurs daily in both the sagittae and the lapilli. With sagittal and lapillar increment counts, age was underestimated and the cause appeared to be difficulty in discerning increments near the core. Whole lapilli (prepared by polishing one side along the sagittal section) provided age accuracy similar to that of the three sagittal preparations, but higher precision. Future studies would benefit from using the lapillus for ecological studies of the early life history of spot.

Acknowledgments

The authors thank Elisabeth Laban for consultation during otolith preparation and analysis, as well as Dean Ahrenholz and Jennifer Potts for reviewing the earlier version of the manuscript. This research was performed while the first author held a National Research Council Research Associateship Award at the NOAA Beaufort Laboratory.

Literature cited

- Barkmann, R. C., and A. Beck.
1976. Incubating eggs of the Atlantic silverside on nylon screen. *Prog. Fish-Cult.* 38:148–150.
- Bath Martin, G. E., and S. R. Thorrold.
2005. Temperature and salinity effects on magnesium, manganese, and barium incorporation in otoliths of larval spot (*Leiostomus xanthurus*). *Mar. Ecol. Prog. Ser.* 293:233–240.
- Bath Martin, G. E., S. R. Thorrold, and C. M. Jones.
2004. Temperature and salinity effects on strontium incorporation in otoliths of larval spot (*Leiostomus xanthurus*). *Can. J. Fish. Aquat. Sci.* 63:34–42.
- Bath Martin, G. E., S. R. Thorrold, C. M. Jones, S. E. Campana, J. W. McLaren, and J. W. H. Lam.
2000. Strontium and barium uptake in aragonitic otoliths of marine fish. *Geochim. Cosmochim. Acta* 64:1705–1714.
- Bestgen, K. R., and J. M. Bundy.
1998. Environmental factors affect daily increment deposition and otolith growth in young Colorado squawfish. *Trans. Am. Fish. Soc.* 127:105–117.
- Campana, S. E.
2001. Accuracy, precision and quality control in age determination, including a review of the use and abuse of age validation method. *J. Fish Biol.* 59:197–242.
- Campana, S. E., and E. Mokness.
1991. Accuracy and precision of age and hatch date estimation from otolith microstructure examination. *ICES J. Mar. Sci.* 48:303–316.
- Campana, S. E., and J. D. Neilson.
1985. Microstructure of fish otoliths. *Can. J. Fish. Aquat. Sci.* 42:1014–1032.
- Chang, W. Y. B.
1982. A statistical method for evaluating the reproducibility of age determination. *Can. J. Fish. Aquat. Sci.* 39:1208–1210.
- David, A. W., J. J. Isley, and C. B. Grimes.
1994. Differences between the sagitta, lapillus, and asteriscus in estimating age and growth in juvenile red drum, *Sciaenops ocellatus*. *Fish. Bull.* 92:509–515.
- Escot, C., and C. Granado-Lorenco.
1998. Morphology of the otoliths of *Barbus sclateri* (Pisces: Cyprinidae). *J. Zool.* 246:89–94.
- Flores-Coto, C., and S. M. Warlen.
1993. Spawning time, growth, and recruitment of larval spot *Leiostomus xanthurus* into a North Carolina estuary. *Fish. Bull.* 91:8–22.
- Geffen, A. J.
1987. Methods of validating daily increment deposition in otoliths of larval fish. In *Age and growth of fish* (R. C. Summerfelt and G. E. Hall, eds.), p. 223–240. Iowa State Univ. Press, Ames, IA.
- Govoni, J. J., A. J. Chester, D. E. Hoss, and P. B. Ortner.
1985. An observation of episodic feeding and growth of larval *Leiostomus xanthurus* in the northern Gulf of Mexico. *J. Plank. Res.* 7:137–146.
- Govoni, J. J., and D. E. Hoss.
2001. Comparison of the development and function of the swimbladder of *Brevoortia tyrannus* (Clupeidae) and *Leiostomus xanthurus* (Sciaenidae). *Copeia* 2001(2):430–442.
- Hettler, W. F.
1984. Marking otoliths by immersion of marine fish larvae in tetracycline. *Trans. Am. Fish. Soc.* 113:370–373.
- Hoff, C. R., D. J. Logan, and D. F. Markle.
1997. Otolith morphology and increment validation in young Lost River and shortnose suckers. *Trans. Am. Fish. Soc.* 126:488–494.
- Ichimaru, T., and T. Katsunori.
1995. Otolith increment formation of flyingfishes larvae, *Cypselurus heterurus doederleini* and *Cypselurus hiraii*

- under rearing conditions. Bull. Nagasaki Prefect. Inst. Fish. 21:1-6.
- Jones, C. M.
1986. Determining age of larval fish with the otolith increment technique. Fish. Bull. 83:289-298.
- Mercer, L. P.
1987. Fishery management plan for spot (*Leiostomus xanthurus*). ASMFC Fishery Management Report 11:1-81. Atlantic States Marine Fisheries Commission, Washington, D.C.
- Morioka, S., and L. Machinandiarena.
2001. Comparison of daily increment formation pattern between sagittae and lapilli of ling (*Genypterus blacodes*) larvae and juveniles collected off Argentina. N.Z.J. Mar. Freshw. Res. 35:111-119.
- Neilson, J. D., and G. H. Geen.
1985. Effects of feeding regimes and diel temperature cycles on otolith increment formation in juvenile salmon (*Oncorhynchus tshawytscha*). Fish. Bull. 83:91-101.
- Powell, A. B., and A. J. Chester.
1985. Morphometric indicis of nutritional conditions and sensitivity to starvation of spot larvae. Trans. Am. Fish. Soc. 114:338-347.
- Powell, A. B., A. J. Chester, J. J. Govoni, and S. M. Warlen.
1990. Nutritional condition of spot larvae associated with Mississippi River Plume. Trans. Am. Fish. Soc. 119:957-965.
- Powell, A. B., and H. R. Gordy.
1980. Egg and larval development of the spot, *Leiostomus xanthurus* (Sciaenidae). Fish. Bull. 78:701-714.
- Radtke, R. L., and J. M. Dean.
1982. Increment formation in the otoliths of embryos, larvae, and juveniles of the mummichog, *Fundulus heteroclitus*. Fish. Bull. 80:201-215.
- Ross, S. W.
2003. The relative value of different estuarine nursery areas in North Carolina for transient juvenile marine fishes. Fish. Bull. 101:384-404.
- Secor, D. H., J. M. Dean, and E. H. Laban.
1991. Otolith removal and preparation for microstructural examination: a user's manual. Technical Publ. 1991-01, 85 p. The Electronic Power Research Institute and the Bell W. Baruch Institute for Marine and Coastal Sciences, Columbia, SC.
- Siegfried, R. C. II, and M. P. Weinstein.
1989. Validation of daily increments deposition in the otolith of spot (*Leiostomus xanthurus*). Estuaries 12:180-185.
- Thorrold, S. R., and J. A. Hare.
2002. Otolith applications in reef fish ecology. In Coral reef fishes: dynamics and diversity in a complex ecosystem (P. F. Sale, ed.), p. 243-264. Academic Press, San Deigo, CA.
- Walter, J. F., and H. M. Austin.
2003. Diet composition of large striped bass (*Morone saxatilis*) in Chesapeake Bay. Fish. Bull. 101:414-423.
- Warlen, S. M., and A. J. Chester.
1985. Age, growth, and distribution of larval spot, *Leiostomus xanthurus*, off North Carolina. Fish. Bull. 83:587-599.

Preliminary use of oxygen stable isotopes and the 1983 El Niño to assess the accuracy of aging black rockfish (*Sebastes melanops*)

Kevin R. Piner

Southwest Fisheries Science Center
National Marine Fisheries Service, NOAA
8604 La Jolla Shores Drive
La Jolla, California 92037
E-mail address: Kevin.Piner@noaa.gov

Melissa A. Haltuch

School of Aquatic and Fishery Sciences
University of Washington,
1122 NE Boat Street
Seattle, Washington 98105

John R. Wallace

Northwest Fisheries Science Center
National Marine Fisheries Service,
2725 Montlake Blvd East
Seattle, Washington 98112

Black rockfish (*Sebastes melanops*) range from California to Alaska and are found in both nearshore and shallow continental shelf waters (Love et al., 2002). Juveniles and subadults inhabit shallow water, moving deeper as they grow. Generally, adults are found at depths shallower than 55 meters and reportedly live up to 50 years. The species is currently managed by using information from an age-structured stock assessment model (Ralston and Dick, 2003).

In many studies, ages are assumed to be accurate and there is no effort to validate the accuracy of the ages (Beamish and McFarlane, 1983). Recent methods of age validation rely upon environmental events that serve as time markers (Campana, 2001). Bomb radiocarbon released during nuclear bomb testing has been used to validate fish ages (Kalish et al., 1996; Campana, 1997; Kalish et al., 1997). Unfortunately, bomb radiocarbon can be used only for fish that lived during the informative period (~1960–70); thus the technique has been used primarily on older ages. For many stock assessments, the validation of younger ages is more

critical because of their importance in estimating vital rates, such as growth and maturity schedules.

In this note we apply the well-studied relationship between water temperature and the ratio of oxygen stable isotopes in otoliths to assess the accuracy of young black rockfish ages. Oxygen isotope ratios serve as a record of past water temperatures because the isotope ratio is incorporated into the otolith in near equilibrium with the ratio found in the environment (Patterson et al., 1993; Thorrold et al., 1997) and ambient water temperatures are inversely correlated with $^{18}\text{O}/^{16}\text{O}$ ratios (Gao et al., 2001). Calcified structures have a strong history of being used in environmental reconstructions based on incorporated trace elements and isotopes (Chivas et al., 1985; Holmden et al., 1997). Otolith microchemistry has been used to successfully reconstruct the environmental history of fish and to answer questions about natal homing (Thorrold et al., 2001) and population mixing (Campana et al., 1999). Variation in oxygen isotopes has been used to confirm visually observed growth increments

(Campana, 2001). Recently, stable oxygen isotopes from Pacific halibut (*Hippoglossus stenolepis*) otoliths were used to examine regime shifts in the Northeast Pacific for the identification of changes in bottom water temperatures (Gao and Beamish, 2003). In addition, otolith chemistry may be used to identify environmental events that serve as natural tags for such studies (Campana and Thorrold, 2001). We used a strong regional environmental event, the 1983 El Niño, as a time marker to judge the accuracy of age assignment for black rockfish <15 years of age. The 1983 El Niño produced anomalously warm oceanic conditions along the coastlines in the eastern Pacific; therefore the stable oxygen isotope ratio from 1983 should reflect this change in oceanic conditions.

Materials and methods

We obtained nine pre-aged black rockfish otoliths collected during 1987–91 from recreationally caught fish off Cape Lookout, Oregon (~45.25°N, 145°W), from approximately 15–30 m water depth. One otolith was aged by Oregon Department of Fish and Wildlife scientists by using the traditional break-and-burn method; the matching otolith was used in the stable isotope analysis. Fish from a range of years and ages (Table 1) were selected to include the 1983 El Niño year. A time series of annual summer bottom water temperatures from the same region and depth where the black rockfish otolith samples were obtained, were provided by the Pacific Hindcast from the Columbia University International Research Institute for Climate Prediction, Palisades, New York.

To estimate the year containing the warmest oceanic conditions, we examined otolith material from all opaque growth zones within each otolith for oxygen isotopes ($^{18}\text{O}/^{16}\text{O}$) and

Manuscript submitted 13 February 2004
to the Scientific Editor's Office.

Manuscript approved for publication
8 February 2005 by the Scientific Editor.
Fish. Bull. 103:553–558 (2005).

Table 1

Age-specific $\delta^{18}\text{O}$ values for each black rockfish (*Sebastes melanops*), along with annulus age and collection year. Values replaced by "N/A" indicates samples that were not reported by the stable isotope laboratory.

Age	Sample number								
	1987-33	1987-86	1987-98	1988-7	1988-100	1991-27	1991-86	1991-168	1991-178
0+	-0.96	N/A	-0.633	-0.357	1.209	N/A	-0.128	-2.06	0.756
1+	-1.17	0.914	-0.981	-0.513	0.725	-0.53	-0.114	-1.77	0.948
2+	-0.42	0.654	-0.644	-0.504	-0.544	-0.42	-0.358	-1.09	0.869
3+	-0.04	0.461	-0.518	-0.579	1.037	-0.39	-0.409	-0.64	0.741
4+	0.42	1.006	-0.202	-0.320	N/A	-0.09	-0.082	-0.85	0.338
5+	0.28	0.946	-0.037	-0.257	N/A	-0.22	-0.218	-0.73	N/A
6+		0.957	0.630	0.137	N/A	-0.05	0.1067	0.35	0.785
7+				0.962		1.0	0.512	1.08	1.054
8+						N/A	0.805	1.07	1.113
9+						N/A	1.053	N/A	1.404
10+						N/A	1.164	N/A	1.510
11+						N/A	1.881		
Annulus age (yr)	6	7	7	8	7	12	12	11	11
Collection year	1987	1987	1987	1988	1988	1991	1991	1991	1991

assigned to a year of formation based on estimated age and capture year. Chemical assay and otolith processing were completed at the Stable Isotope Laboratory of the University of Michigan. Each otolith was embedded in epoxy resin and cut transversally with a low-speed diamond-bladed saw. Three or four thin sections ~150 μm thick were removed from the center of each otolith. The thin sections were then glued with cyanoacrilate glue to petrographic glass slides. Samples from multiple thin sections were combined for a single assay. Each opaque growth zone was sampled by using a MerchanteK Micro-milling system and assays were completed with a Finnigan 251 MAT mass spectrometer. All measurements were reported in standard Vienna Pee Dee Belemnite (VPDB) and notation as $\delta\text{‰}$ (per mil), where

$$\delta^{18}\text{O} = \left(\left(\frac{^{18}\text{O}/^{16}\text{O}}{^{18}\text{O}/^{16}\text{O}} \right)_{\text{sample}} / \left(\frac{^{18}\text{O}/^{16}\text{O}}{^{18}\text{O}/^{16}\text{O}} \right)_{\text{standard}} \right) - 1 \times 1000.$$

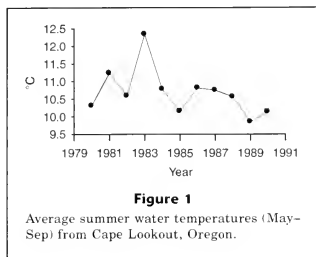
A time series of $\delta^{18}\text{O}$ was constructed for each fish by using the assay from each year-specific sample of the otolith material. Assay results from the collection year were not included because of differences in the season of capture. Years with missing results were due to micromilling or assay errors that resulted in no results reported by the stable isotope laboratory.

To gauge the accuracy of age assignments, we fitted a linear model to each time series and analyzed the residuals from the linear model fit. The $\delta^{18}\text{O}$ value corresponding to the negative residual of greatest magnitude from that linear model would be associated with the anomalously warmest oceanic conditions (El Niño).

If the age assignments were correct, that portion of the otolith corresponding to 1983 would have the negative residual of greatest magnitude because the observed $\delta^{18}\text{O}$ value was much lower than the linear model predicted. Temporal shifts of the most anomalous negative residual with respect to 1983 were interpreted as either an under- or over-estimation of age.

A randomization procedure (20,000 iterations) was used to determine if the magnitude of the average residual in any year was more negative than expected, thus identifying the signal associated with the 1983 El Niño. The residuals from the linear models within each of the fish were randomized with respect to year. Randomized residuals from all iterations were averaged across all fish to produce a distribution of averages. The original year-specific residual averages were compared to the randomization distribution to estimate statistical significance. We rejected the hypothesis of any year with an average residual ≥ 0 if less than 5% of the randomizations produced a negative average residual of equal or greater magnitude than the observed year-specific average residual, thus identifying anomalously warm years.

An iterative sensitivity analysis was performed by retrospectively removing sequential blocks of years of data and by estimating the statistical significance of the originally determined anomalous years with the reduced data sets. All data taken from years more recent than the cutoff year were removed, and the linear model fitting and randomization procedures were recalculated. The cutoff year was sequentially changed beginning with 1989 to 1986.



Results

The period 1980–90 was characterized by an isolated and historically strong 1983 El Niño event (Fig. 1), that resulted in a 1–2°C increase in water temperatures along the Oregon coast. Average summer water temperatures declined slightly over this period. The $\delta^{18}\text{O}$ values measured in each fish resulting from this period (Table 1) showed strong patterns that indicated temperature differences both within fish (between years) and between fish (same year). In addition, many fish contained trends in $\delta^{18}\text{O}$ across time (Fig. 2). Precision of the reported $\delta^{18}\text{O}$ measurements ranged from 0.01 to 0.07‰ (SD).

The residual patterns (Fig. 3A) showed that anomalously warm conditions existed in otolith material corresponding to those of 1983 ($n=9$, $P=0.0338$) and 1985 ($n=7$, $P=0.0409$). Both old (ages 11–12) and young (ages 6–8) fish appeared to have similar temporal patterns of residuals; however in older fish this pattern shifted by 1–2 years toward more recent years (Fig. 3B). The year-specific averaged residuals of the age 6–8 fish depicted a single anomalously warm year corresponding to 1983. The anomalously warm year in the age 11–12 fish was 1984–85, thus explaining the significance result in 1985. The results of the randomization test were not sensitive to the exclusion of data from the four most recent years (Table 2).

Discussion

The location of the anomalously warm signal in 1983, in the youngest and likely the more accurately aged fish, supports the hypothesis that the 1983 El Niño can be detected by using oxygen stable isotopes. From this analysis, we concluded that the break-and-burn aging method is accurate on average but has a potential tendency toward underaging fish >10 years.

Confirmation of the annual banding pattern in the otoliths of other *Sebastes* species has been accomplished by using a variety of methods. Woodbury (1999) confirmed the accuracy of age assignment in widow (*Se-*

Table 2

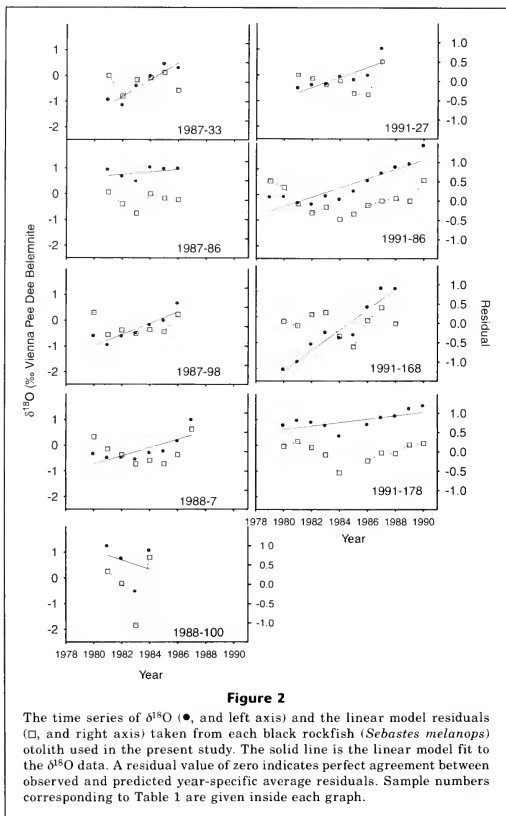
Results of the retrospective analysis that estimated the statistical significance of the magnitude of the average negative residual from the years 1983 and 1985. Assay results from otolith material formed after the cutoff year were removed from the randomization analysis.

Cutoff year	1983	1985
1989	$^{\circ}0.03$	$^{\circ}0.05$
1988	$^{\circ}0.03$	$^{\circ}0.05$
1987	$^{\circ}0.04$	$^{\circ}0.06$
1986	$^{\circ}0.05$	$^{\circ}0.26$

bastes entomelas) and yellowtail (*S. flavidus*) rockfish, using the change in growth increment width associated with El Niño. Piner et al. (in press) has used bomb radiocarbon to confirm the annual pattern of otolith banding in canary rockfish (*S. pinniger*) and has reported a possible underaging bias for older fish. Andrews et al. (1999) used radiometric age determination to confirm the longevity of long-lived species. However, a larger study on black rockfish with stable isotopes is necessary to conclusively determine age estimates accurately and potential underaging bias.

The 1983 El Niño was chosen for the present study because it was one of the strongest recorded in the century (Sharp and McClain, 1993). Warm water conditions associated with the 1983 El Niño were sufficient to slow growth (MacLellan and Saunders, 1995; Woodbury, 1999) and alter reproductive patterns (VenTresca et al., 1995) in species occupying similar geographic ranges. In contrast, this study attempted to indirectly measure the environment experienced by black rockfish without the need to infer changes to biological processes. Nevertheless, our results appear to support the conclusions of MacLellan and Saunders (1995) and Woodbury (1999) that the anomalous oceanic conditions in 1983 are identifiable.

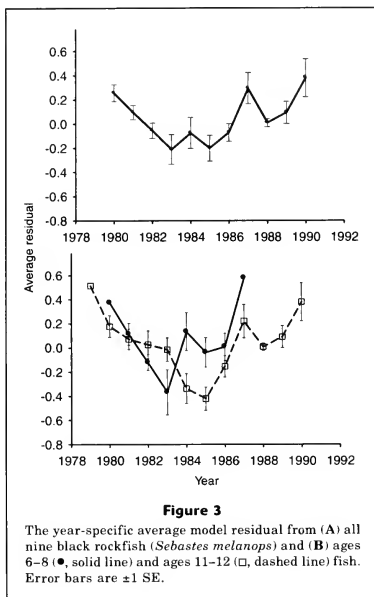
The analysis of model residuals rather than raw isotope ratios is more appropriate because of the obvious $\delta^{18}\text{O}$ temporal trend in some samples. Otolith processing difficulties also may have contributed to the trend. The opaque region of the otolith decreases in size with increasing age. The narrowing of the otolith region associated with older ages made precise sampling more difficult and may have resulted in accidental sampling from otolith material outside the opaque region. The sampling of otolith material from outside the opaque region may have contributed otolith material formed in cooler waters in contrast to the sampling of areas of the otolith associated with younger ages. The increasing trend in $\delta^{18}\text{O}$ was not explained solely by the decreasing temporal trend of summer water temperatures. However, an additional component of that trend may be the result of age-dependent fish movement to cooler waters that are deeper or more



northerly. Furthermore, the isotope variability between fish may be due to fish inhabiting different areas in the early periods of life or to temporal differences in growth. Finally, changes in calibration of the spectrometer between assays may be a source of uncertainty.

A critical assumption behind the present study was that the lowest $\delta^{18}\text{O}$ corresponds to the warmest water temperature, and consequently the 1983 El Niño that serves as the time marker. The $\delta^{18}\text{O}$ values may be impacted by salinity in addition to water temperature

(Dorval, 2004), and we assumed that salinity was constant and that the changes in $\delta^{18}\text{O}$ values were largely influenced by changes in temperature. A further confounding element to this kind of study is the ability of fish to move and potentially select microhabitats with different temperatures than that of the average local environment. Natural date-specific markers also must be monitored over a number of years to ensure that they remain identifiable within the otolith (Campana, 2001). We addressed this concern by selecting fish of



various ages and from various collection dates and by performing the same analysis on each fish. Lastly, this method of age validation can be difficult to implement for fish with small otoliths or for long-lived fish because of the difficulties in obtaining sufficient otolith material from small growth increments.

The detection of El Niño events using $\delta^{18}\text{O}$ may allow the use of this recurring climatic event as a natural tag for age validation. Because previous studies that used El Niño events as time markers were forced to measure biological reactions to environmental changes, the use of $\delta^{18}\text{O}$ may be an improvement because it avoids assuming the intermediate step, namely that environment affects a biological process. The results from this study, however, were based on a small sample size and are, therefore, only preliminary. Further work in this area is warranted.

Acknowledgments

We are grateful to Maria Marcano of the University of Michigan geochemical laboratory for her help in setting

up the assays. Bill Miller of the Oregon Department of Fish and Wildlife provided aging expertise. We thank the Sea Grant Fellowship in Population Dynamics and the National Marine Fisheries Service Northwest Fisheries Science Center for financial support. Finally, the anonymous reviewers and Christian Reiss greatly helped our efforts.

Literature cited

- Andrews, A. H., K.H. Coale, J. L. Nowicki, C., Lundstrom, Z. Palacz, J. E. Burton, and G. M. Cailliet.
1999. Application of an ion-exchange separation technique and thermal ionization mass spectrometry to ^{226}Ra determination in otoliths for radiometric age determination of long-lived fishes. *Can. J. Fish. Aquat. Sci.* 56:1329-1338.
- Beamish, R. J., and G. A. McFarlane.
1983. The forgotten requirement for age validation in fisheries biology. *Trans. Am. Fish. Soc.* 112(6):735-743.
- Campana, S. E.
1997. Use of radiocarbon from nuclear fallout as a dated

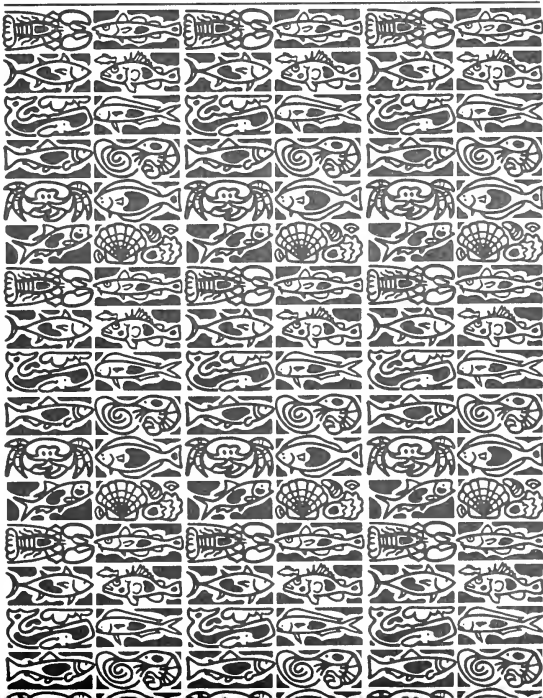
- marker in the otoliths of haddock (*Melanogrammus aeglefinus*). Mar. Ecol. Prog. Ser. 150(1-3):49-56.
2001. Accuracy, precision and quality control in age determination, including a review of the use and abuse of age validation methods. J. Fish. Biol. 59(2):197-242.
- Campana, S. E., G. A. Chouinard, J. M. Hanson, and A. Frechet. 1999. Mixing and migration of overwintering Atlantic cod (*Gadus morhua*) stocks near the mouth of the Gulf of St. Lawrence. Can. J. Fish. Aquat. Sci. 56(10):1873-1881.
- Campana, S. E., and S. R. Thorrold. 2001. Otoliths, increments, and elements: keys to a comprehensive understanding of fish populations? Can. J. Fish. Aquat. Sci. 58(1):30-38.
- Chivas, A. R., P. DeDecker, and J. M. G. Shelley. 1985. Strontium content of ostracods indicates lacustrine paleosalinity. Nature 316(6025):251-253.
- Dorval, E. 2004. Relating water and otolith chemistry in Chesapeake Bay, and their potential to identify essential seagrass habitats for juveniles of an estuarine-dependent fish, spotted seatrout (*Cynoscion nebulosus*). Ph.D. diss., 134 p. Old Dominion Univ., Norfolk, VA.
- Gao, Y. W., and R. J. Beamish. 2003. Stable isotope variations in otoliths of Pacific halibut (*Hippoglossus stenolepis*) and indications of the possible 1990 regime shift. Fish. Res. 60(2-):393-404.
- Gao, Y., H. P. Schwarz, U. Brand, and E. Moksness. 2001. Seasonal stable isotope records of otoliths from ocean-pen reared and wild cod, *Gadus morhua*. Environ. Biol. Fish. 61(4):445-453.
- Holmden, C., R. A. Creaser, and K. Muehlebachs. 1997. Paleosalinities in ancient brackish water systems determined by Sr-87/Sr-86 ratios in carbonate fossils: a case study from the Western Canada Sedimentary Basin. Geoch. Cosmochim. Acta. 61(10):2105-2118.
- Kalish, J. M., J. M. Johnston, J. S. Gunn, and N. P. Clear. 1996. Use of the bomb radiocarbon chronometer to determine age of southern bluefin tuna (*Thunnus maccoyii*). Mar. Ecol. Prog. Ser. 143(1-3):1-8.
- Kalish, J. M., J. M. Johnston, D. C. Smith, A. K. Morison, and S. G. Robertson. 1997. Use of the bomb radiocarbon chronometer for age validation in the blue grenadier (*Macruronus novaezelandiae*). Mar. Biol. 128(4):557-563.
- Love, M. S., M., Yoklavich, and L. Thorsteinson. 2002. The rockfishes of the Northeast Pacific, 404 p. Univ. California Press, Los Angeles, CA.
- MacLellan, S. E., and M. W. Saunders. 1995. A natural tag on the otoliths of Pacific hake (*Merluccius productus*) with implications for age validation and migration. In Recent developments in fish otolith research (D. H. Secor, J. M. Dean, and S. E. Campana, eds.), p. 567-580. Univ. South Carolina Press, Columbia, SC.
- Patterson, W. P., G. R. Smith, and K.C. Lohmann. 1993. Continental paleothermometry and seasonality using isotopic composition of aragonitic otoliths in freshwater fishes. Geophys. Monogr. 78:191-202.
- Piner, K. R., O. S. Hamel, J. L. Menkel, J. R. Wallace, and C. E. Hutchinson. In press. Age validation of canary rockfish (*Sebastes pinniger*) from off the Oregon coast (USA) using the bomb radiocarbon method. Can. J. Fish. Aquat. Sci.
- Ralston, S., and E. J. Dick. 2003. The status of black rockfish (*Sebastes melanops*) off Oregon and northern California in 2003. In Status of the Pacific coast groundfish fishery through 2003 and stock assessment and fishery evaluation, 75 p. Pacific Fishery Management Council, Portland, OR.
- Sharp, G. D., and D. R. McClain. 1993. Fisheries, El Niño-Southern oscillation and upper ocean temperature records: an eastern Pacific example. Oceanography 6:13-22.
- Thorrold, S. R., S. E. Campana, C. M. Jones, and P. K. Swart. 1997. Factors determining delta super(13)C and delta super(18)O fractionation in aragonitic otoliths of marine fish. Geochim. Cosmochim. Acta 61(14):2909-2919.
- Thorrold, S. R., C. Latkoczy, P. K. Swart, and C. M. Jones. 2001. Natal homing in a marine fish metapopulation. Science 291(5502):297-299.
- VenTresca, D. A., R. H. Parrish, J. L. Houk, M. L. Gingas, S. D. Short, and N. L. Crane. 1995. El Niño effects on the somatic and reproductive condition of blue rockfish, *Sebastes mystinus*. Calif. Coop. Oceanic Fish. Invest. Report 36:167-174.
- Woodbury, D. 1999. Reduction of growth in otoliths of widow and yellowtail rockfish (*Sebastes entomelas* and *S. flavidus*) during the 1983 El Niño. Fish. Bull. 97:680-89.



U.S. Department
of Commerce

Volume 103
Number 4
October 2005

Fishery Bulletin



**U.S. Department
of Commerce**

Carlos M. Gutierrez
Secretary

**National Oceanic
and Atmospheric
Administration**

Vice Admiral
Conrad C. Lautenbacher Jr.,
USN (ret.)

Under Secretary for
Oceans and Atmosphere

**National Marine
Fisheries Service**

William T. Hogarth
Assistant Administrator
for Fisheries



The *Fishery Bulletin* (ISSN 0090-0656) is published quarterly by the Scientific Publications Office, National Marine Fisheries Service, NOAA, 7600 Sand Point Way NE, BIN C15700, Seattle, WA 98115-0070. Periodicals postage is paid at Seattle, WA, and at additional mailing offices. POSTMASTER: Send address changes for subscriptions to *Fishery Bulletin*, Superintendent of Documents, Attn.: Chief, Mail List Branch, Mail Stop 8550M, Washington, DC 20402-9373.

Although the contents of this publication have not been copyrighted and may be reprinted entirely, reference to source is appreciated.

The Secretary of Commerce has determined that the publication of this periodical is necessary according to law for the transaction of public business of this Department. Use of funds for printing of this periodical has been approved by the Director of the Office of Management and Budget.

For sale by the Superintendent of Documents, U.S. Government Printing Office, Washington, DC 20402. Subscription price per year: \$55.00 domestic and \$68.75 foreign. Cost per single issue: \$28.00 domestic and \$35.00 foreign. See back for order form.

Fishery Bulletin

Scientific Editor
Adam Moles, Ph.D.

National Marine Fisheries Service, NOAA
8604 La Jolla Shores Drive
La Jolla, California 92037

Managing Editor
Sharyn Matriotti

National Marine Fisheries Service
Scientific Publications Office
7600 Sand Point Way NE, BIN C15700
Seattle, Washington 98115-0070

Editorial Committee

Harlyn O. Halvorson, Ph.D.	University of Massachusetts, Boston
Ronald W. Hardy, Ph.D.	University of Idaho, Hagerman
Richard D. Methot, Ph.D.	National Marine Fisheries Service
Theodore W. Pietsch, Ph.D.	University of Washington, Seattle
Joseph E. Powers, Ph.D.	National Marine Fisheries Service
Harald Rosenthal, Ph.D.	Universität Kiel, Germany
Fredric M. Serchuk, Ph.D.	National Marine Fisheries Service
George Watters, Ph.D.	National Marine Fisheries Service

***Fishery Bulletin* web site: www.fishbull.noaa.gov**

The *Fishery Bulletin* carries original research reports and technical notes on investigations in fishery science, engineering, and economics. It began as the *Bulletin of the United States Fish Commission* in 1881; it became the *Bulletin of the Bureau of Fisheries* in 1904 and the *Fishery Bulletin of the Fish and Wildlife Service* in 1941. Separates were issued as documents through volume 46; the last document was No. 1103. Beginning with volume 47 in 1931 and continuing through volume 62 in 1963, each separate appeared as a numbered bulletin. A new system began in 1963 with volume 63 in which papers are bound together in a single issue of the bulletin. Beginning with volume 70, number 1, January 1972, the *Fishery Bulletin* became a periodical, issued quarterly. In this form, it is available by subscription from the Superintendent of Documents, U.S. Government Printing Office, Washington, DC 20402. It is also available free in limited numbers to libraries, research institutions, State and Federal agencies, and in exchange for other scientific publications.

U.S. Department
of Commerce
Seattle, Washington

Volume 103
Number 4
October 2005

Fishery Bulletin

Contents

Articles

- 561–573 Kingsford, Michael J., and Julian M. Hughes
Patterns of growth, mortality, and size of the tropical damselfish *Acanthochromis polyacanthus* across the continental shelf of the Great Barrier Reef
- 574–587 Kotwicki, Stan, Troy W. Buckley, Taina Honkalehto, and Gary Walters
Variation in the distribution of walleye pollock (*Theragra chalcogramma*) with temperature and implications for seasonal migration
- 588–600 Luthy, Stacy A., Robert K. Cowen, Joseph E. Serafy, and Jan R. McDowell
Toward identification of larval sailfin (*Istiophorus platypterus*), white marlin (*Tetrapturus albidus*), and blue marlin (*Makaira nigricans*) in the western North Atlantic Ocean
- 601–619 McDonough, Christopher J., William A. Roumillat, and Charles A. Wenner
Sexual differentiation and gonad development in striped mullet (*Mugil cephalus* L.) from South Carolina estuaries
- 620–634 Megalofonou, Persefoni, Constantinos Yannopoulos, Dimitrios Damalas, Gregorio De Metrio, Michele Defflorio, Jose M. de la Serna, and David Macias
Incidental catch and estimated discards of pelagic sharks from the swordfish and tuna fisheries in the Mediterranean Sea
- 635–647 Narimatsu, Yoji, Daiji Kitagawa, Tsutomu Hattori, and Hirobumi Onodera
Reproductive biology of female Rikuzen sole (*Dexistes rikuzenius*)

The conclusions and opinions expressed in *Fishery Bulletin* are solely those of the authors and do not represent the official position of the National Marine Fisheries Service (NOAA) or any other agency or institution.

The National Marine Fisheries Service (NMFS) does not approve, recommend, or endorse any proprietary product or proprietary material mentioned in this publication. No reference shall be made to NMFS, or to this publication furnished by NMFS, in any advertising or sales promotion which would indicate or imply that NMFS approves, recommends, or endorses any proprietary product or proprietary material mentioned herein, or which has as its purpose an intent to cause directly or indirectly the advertised product to be used or purchased because of this NMFS publication.

- 648–658 Porter, Steven M.
Temporal and spatial distribution and abundance of flathead sole (*Hippoglossoides elassodon*) eggs and larvae in the western Gulf of Alaska
- 659–669 Prince, Eric D., Robert K. Cowen, Eric S. Orbesen, Stacy A. Luthy, Joel K. Llopiz, David E. Richardson, and Joseph E. Serafy
Movements and spawning of white marlin (*Tetrapturus albidus*) and blue marlin (*Makaira nigricans*) off Punta Cana, Dominican Republic
- 670–684 Stanley, Richard D., and Allen R. Kronlund
Life history characteristics for silvergray rockfish (*Sebastes brevispinis*) in British Columbia waters and the implications for stock assessment and management
- 685–696 Weise, Michael J., and James T. Harvey
Impact of the California sea lion (*Zalophus californianus*) on salmon fisheries in Monterey Bay, California
- 697–711 Welsford, Dirk C., and Jeremy M. Lyle
Estimates of growth and comparisons of growth rates determined from length- and age-based models for populations of purple wrasse (*Notolabrus fucicola*)

Notes

- 712–719 Bishop, Melanie J., Charles H. Peterson, Henry C. Summerson, and David Gaskill
Effects of harvesting methods on sustainability of a bay scallop fishery: dredging uproots seagrass and displaces recruits
- 720–724 Diaz, Guillermo A., and Joseph E. Serafy
Longline-caught blue shark (*Prionace glauca*): factors affecting the numbers available for live release
- 725–727 Fey, Dariusz P., and Jonathan A. Hare
Length correction for larval and early-juvenile Atlantic menhaden (*Brevoortia tyrannus*) after preservation in alcohol
- 728–736 Hare, Jonathan A., and John J. Govoni
Comparison of average larval fish vertical distributions among species exhibiting different transport pathways on the southeast United States continental shelf
- 737 Acknowledgment of reviewers
- 738 List of titles
- 741 List of authors
- 743 List of subjects
- 747 Subscription form

Abstract—Age-based analyses were used to demonstrate consistent differences in growth between populations of *Acanthochromis polyacanthus* (Pomacentridae) collected at three distance strata across the continental shelf (inner, mid-, and outer shelf) of the central Great Barrier Reef (three reefs per distance stratum). Fish had significantly greater maximum lengths with increasing distance from shore, but fish from all distances reached approximately the same maximum age, indicating that growth is more rapid for fish found on outer-shelf reefs. Only one fish collected from inner-shelf reefs reached >100 mm SL, whereas 38–67% of fish collected from the outer shelf were >100 mm SL. The largest age class of adult-size fish collected from inner- and mid-shelf locations comprised 3–4 year-olds, but shifted to 2-year-olds on outer-shelf reefs. Mortality schedules (*Z* and *S*) were similar irrespective of shelf position (inner shelf: 0.51 and 60.0%; mid-shelf: 0.48 and 61.8%; outer shelf: 0.43 and 65.1%, respectively). Age validation of captive fish indicated that growth increments are deposited annually, between the end of winter and early spring. The observed cross-shelf patterns in adult sizes and growth were unlikely to be a result of genetic differences between sample populations because all fish collected showed the same color pattern. It is likely that cross-shelf variation in quality and quantity of food, as well as in turbidity, are factors that contribute to the observed patterns of growth. Similar patterns of cross-shelf mortality indicate that predation rates varied little across the shelf. Our study cautions against pooling demographic parameters on broad spatial scales without consideration of the potential for cross-shelf variability.

Patterns of growth, mortality, and size of the tropical damselfish *Acanthochromis polyacanthus* across the continental shelf of the Great Barrier Reef

Michael J. Kingsford

Julian M. Hughes

Reef and Ocean Ecology Laboratory
School of Marine Biology and Aquaculture
James Cook University
James Cook Drive
Townsville, Queensland, Australia 4811
E-mail address (for M. J. Kingsford): Michael.Kingsford@jcu.edu.au

Coral reefs are spatially diverse and heterogeneous marine environments. The Great Barrier Reef (GBR) is the largest reef system and represents a near-continuous matrix of over 2400 individual reefs spanning a distance of some 2000 km along the coast of Queensland, eastern Australia (Fig. 1). Coral reef habitats are subject to the influences of environmental (e.g., exposure and proximity to coastlines), as well as biotic processes (e.g., availability of food). Strong cross-shelf abiotic and biotic gradients (Wilkinson and Cheshire, 1988) have the potential to influence patterns of abundance and demographic characteristics of fishes associated with coral reefs. Several studies have examined the broad-scale abundance and distribution of a wide variety of organisms across the continental shelf of the GBR, including hard corals (Done, 1982), soft corals (Dinesen, 1983), crustaceans (Preston and Doherty, 1990, 1994), algae (McCook et al., 1997), and reef fishes (Williams, 1982, 1983; Williams and Hatcher, 1983; Russ, 1984a, 1984b; Newman and Williams, 1996; Newman et al., 1997; Gust et al., 2001, 2002). Great cross-shelf differences in abundance are common within and among taxa. Although environmental gradients have often been implicated as causing these patterns and it is also known that environmental features

influence demographic characteristics (e.g., growth), there have been few comparisons of demographic characteristics by geography and spatial scale.

Demographic measures are crucial to understanding population dynamics. Population demographics of a number of many fish species have been shown to vary at spatial scales ranging from 100's of m to 100's of km (Gillanders, 1995; Meekan et al., 2001; Gust et al., 2002). With the exception of data on a few commercially important taxa (Munro and Williams, 1985; Williams et al., 2003) and some others (e.g., acanthurids and scarids; Choat and Axe, 1996), there are few data on demographic parameters of coral reef fishes and even less on spatial variation within these parameters. Variation in demographics may be common across the shelf. For example, significant differences in the size frequency, growth, mortality, and longevity in populations of three scarids (*Scarus frenatus*, *S. niger*, and *Chlorurus sordidus*) and an acanthurid (*Acanthurus lineatus*) have been shown between mid- and outer-shelf locations on the northern GBR (Gust et al., 2001, 2002). Dudgeon et al. (2000) found evidence that high levels of genetic exchange occurred between populations of these fishes on mid- and outer-shelf reefs and concluded that observed differ-

Table 1

Distance strata and reefs sampled during September and October 2001 over the continental shelf of the central Great Barrier Reef near Townsville, Australia, for analyses of growth patterns, mortality, and size of the tropical damselfish *Acanthochromis polyacanthus*.

Distance strata	Reef sampled	Date(s) sampled	Average distance (km) to coast of the three sites \pm SE
Inner shelf	Orpheus Island	4 and 5 Sep 2001	15.3 \pm 0.6
	Pandora Reef	3 Sept 2001	16.4 \pm 0.3
	Havannah Island	3 and 4 Sep 2001	25.1 \pm 0.3
Mid-shelf	Bramble Reef	15 Oct 2001	41.1 \pm 0.5
	Britomart Reef	16 Oct 2001	38.7 \pm 3.0
	The Slashers	20 Oct 2001	85.3 \pm 2.4
Outer shelf	Pith Reef	18 Oct 2001	74.4 \pm 0.9
	Barnett Patches	17 Oct 2001	62.6 \pm 1.8
	Myrmidon Reef	19 Oct 2001	110.4 \pm 0.8

ences in the demographic and life history features represented phenotypic plasticity.

Acanthochromis polyacanthus (Bleeker) is one of a few species of fish that are found in abundance at all distances across the Great Barrier Reef (Williams, 1982, 1983) and, therefore, was ideal for comparisons of cross-shelf patterns of demographic characteristics. *Acanthochromis polyacanthus* is a polymorphic gonochoristic pomacentrid and site-attached planktivore that inhabits reefs of the Indo-Australian Archipelago and adjacent regions (Allen, 1975). It is extremely wide spread and abundant along (north-south) the GBR (Williams, 1982, 1983). It is unusual among marine reef fishes and unique among damselfishes in that it lacks a dispersive planktonic larval stage (Robertson, 1973). Instead, adult *A. polyacanthus* lay demersal eggs and after hatching, both parents defend a brood of larvae and juveniles for several months (Robertson, 1973; Allen, 1975; Thresher, 1985a, 1995b; Kavanagh, 2000). In contrast to other taxa, therefore, dispersal is likely to be slow within and among reefs. *Acanthochromis polyacanthus* is one of the best studied coral reef fishes on the GBR with respect to predation (Connell, 1996, 1998, 2000), genetics and evolution (Doherty et al., 1994, 1995; Planes and Doherty, 1997a, 1997b), behavior (Robertson, 1973; Allen, 1975; Thresher, 1985a, 1995b; Nakazono, 1993; Kavanagh, 1998), reproductive success (Thresher, 1983), and early life history (Kavanagh, 2000), but no data exist on age, growth, and demographic parameters, such as mortality rates (but see estimates of juvenile mortality while larvae and juveniles are brooded by adults; Connell, 1996).

The objective of this study was to compare the demographic characteristics of *A. polyacanthus* across the continental shelf. Our approach was to sample replicate reefs in the central region of the GBR at multiple distance strata from shore (inner-, mid- and outer-shelf distances). In addition, we chose a section of the GBR where *A. polyacanthus* exhibited the same color pattern

(brown anterior and white posterior) and are known to be genetically isolated (Planes and Doherty, 1997b). Any variation in demographic parameters, therefore, could be largely attributed to phenotypic plasticity. The specific objectives of this study were the following: 1) to validate the deposition of annual growth increments for fish of a wide range of sizes and ages by using tetracycline, 2) to describe patterns of growth of populations of *A. polyacanthus* within and among distance strata; 3) to describe the age and size structures of populations of *A. polyacanthus* within and among distance strata, and; 4) to calculate the instantaneous mortality and survival rates (Z) of populations of *A. polyacanthus* within and among distance strata.

Materials and methods

Study sites and sampling design

Spatial variation in demographics and structures of cross-shelf populations of *A. polyacanthus* was determined by using a partially hierarchical sampling design. Individuals of a wide range of sizes were collected from three replicate reefs within each of three distance strata (inner-, mid- and outer-shelf) spanning the width of the continental shelf of the central Great Barrier Reef near Townsville, Australia (Fig. 1, Table 1). At least 16 fish were collected with hand spears from each of three sites on each reef during September and October 2001. All fish collected were the same brown and white morph (Allen, 1975).

Sample processing

All fish were measured (standard length [SL] to the nearest mm) and weighed (to the nearest 0.01 g). Sagittal otoliths were extracted, cleaned in freshwater to remove the sagittal membrane, and allowed to dry

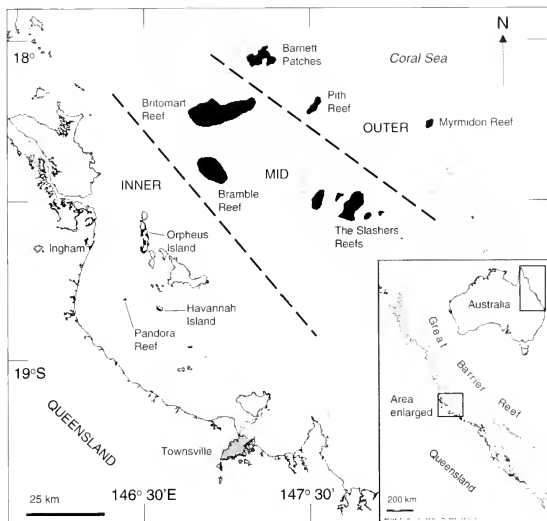


Figure 1

Map of the nine reefs on the central Great Barrier Reef where *Acanthochromis polyacanthus* were collected. Distance strata from the mainland (i.e. inner-, mid- and outer-shelf distances) are also indicated.

overnight. One otolith from each fish was then imbedded in Struers Epofix resin that was allowed to harden overnight in a drying oven at 60°C. A thin (250–300 µm) transverse section perpendicular to the long axis of the otolith was then taken through the core (primordium) of the otolith with a Buehler low-speed saw with two spaced diamond blades. This section was polished by hand with 9-µm lapping film to remove saw blade marks, thereby making the internal structure of the otolith more clearly visible. The polished section was then fixed to a labelled glass microscope slide with Crystal bond thermoplastic glue.

Analysis of growth increments

The opaque zones visible in the internal structure of the otolith were counted along a radius from the primordium to the outer edge of the largest sagittal lobe of the otolith with a compound microscope (Leica DMLB) and white incident light source. Alternating translucent and opaque increments were interpreted as annuli. Sections were coded and examined in random order and the opaque increments counted on two occasions by the

same observer (JMH) separated by four weeks. Counts of annuli were compared between these two occasions in order to assess the confidence that could be placed in the interpretation of otolith structure. If increment counts differed by more than two between counting occasions, then the otoliths were re-examined. If, following a third reading, agreement between the third and one of the two other counts was not reached (all matching counts were used in analyses), then the otolith was not included in the analysis; 4.6% of otoliths were rejected on this basis ($n=715$ fish).

Validation of growth increments

The periodicity of growth increment formation was validated by marking a group of fish (of various sizes) reared in captivity with the antibiotic tetracycline hydrochloride (Sigma-Aldrich, Ballerup, Denmark). Small (known to be 0+ fish) and large fish were chosen to determine if annuli are formed early and late in life. Fish were held at the MARFU Aquarium Facility, James Cook University. For the duration of the experiment, the fish were held in several 70–500 L aquaria at this facility.

Adult fish were injected in the coelomic cavity with 0.05 g/mL tetracycline in sterile saline solution at concentrations equivalent to 0.05 g/kg body weight (McFarlane and Beamish, 1987). The approximate weight of each individual was estimated from the relationship between weight and SL. Juveniles were mass marked by immersion in a tetracycline solution (concentration: 0.5g/L) in seawater for 12 hours (overnight). The tetracycline generally forms a very effective time-marker in otoliths; it fluoresces when viewed under ultraviolet light (Geffen, 1992).

The experiment commenced in May 2002 and fish were sacrificed after six months, one year (June 2003), and one-and-a-half years (November 2003). Ten fish had readable otoliths for which validation was attempted. Otolith sections were viewed with a compound microscope and incident ultraviolet light in a darkened room. When a fluorescing tetracycline band was identified, its position in relation to the edge was measured. The section was then examined under reflected white light and measurements of increment widths and marginal increments were recorded. Known time at liberty, expressed as a proportion of one year, was then compared with estimated time at liberty by using the growth of the otoliths. If estimated time at liberty equalled actual time at liberty, it supported the hypothesis that opaque increments were deposited annually. Juveniles and adults were collected on each occasion to determine whether increments were deposited annually, early and late in life.

The length of time for increment formation was also estimated by calculating the number of days after tetracycline treatment. The number of days after treatment was estimated by comparing the position of the tetracycline mark with that of the last (marginal) opaque increment and the width of a full annual increment with the following formula:

$$\text{Number of days after treatment} = \frac{TE - MI}{IW} \times 365,$$

where *TE* = otolith growth after treatment;
MI = the marginal increment; and
IW = the final full increment width.¹

Growth

It was hypothesized that patterns of growth would vary with distance from the coast. Growth rates were described by using von Bertalanffy growth functions that provided the best fit to size-at-age data when compared with estimates of the Schnute growth function (Schnute, 1981). The von Bertalanffy expression for length at age *t* (L_t), as a function of time is

$$L_t = L_\infty [1 - e^{-K(t-t_0)}],$$

where L_∞ = the asymptote of the growth curve (average maximum length);
 L_t = length at age *t*;
 K = the rate at which the growth curve approaches the asymptote (L_∞);
 t = age of fish in years;
 t_0 = the theoretical origin of the growth curve (i.e., the hypothetical age of the fish when it has no length); and
 e = the base of the natural logarithm.

Differences in growth curves for *A. polyacanthus* from each reef sampled were visualized by using the technique of Kimura (1980), where 95% confidence ellipses were generated around the parameter estimates of K and L_∞ . Confidence ellipses that did not overlap indicated differences in growth parameters and enabled the pooling of data from sites within reefs at each distance stratum. The parameter t_0 was constrained to minus 0.05 to take into account the approximate size of *A. polyacanthus* at hatching (5 mm; Kavanagh, 1998, 2000).

Mortality

The instantaneous rate of mortality (Z) was calculated by using log-linear regression analyses of age-frequency data sets for *A. polyacanthus* populations from each reef (Pauly, 1984). With this method, recruitment was assumed to be consistent over time at each reef. The natural logarithm of the number of fish sampled from each age class was compared with their corresponding age. Year classes to the left of the age-frequency mode were excluded from the analysis because our sampling technique was biased against small *A. polyacanthus*. Fish greater than 60 mm were collected. The slope of the regression line between year classes estimated the instantaneous mortality rate (Z):

$$Z = F + M,$$

where F = fishing mortality; and
 M = natural mortality (Gust et al., 2002).

Because there is no fishery for *A. polyacanthus* on the GBR, F equals zero and therefore Z estimates natural mortality only. Annual survival rate estimates were then calculated according to the equation $S = e^{-Z}$ (Ricker, 1975). Comparisons of the slopes of age-frequency relationships (for estimates of Z) were made by using analysis of covariance (ANCOVA) according to the procedures of Zar (1999). Data from each site were pooled for each reef because in many cases sample sizes were too small to provide reliable estimates of mortality at the site level. Similarities in mortality rates among replicate reefs within distance strata allowed us to pool data at the strata level so that comparisons of mortality between shelf positions could be made.

¹ We assumed similar IWs for fish older than 3 years. For fish 3 years or younger the IW was calculated as an average from all experimental fish.

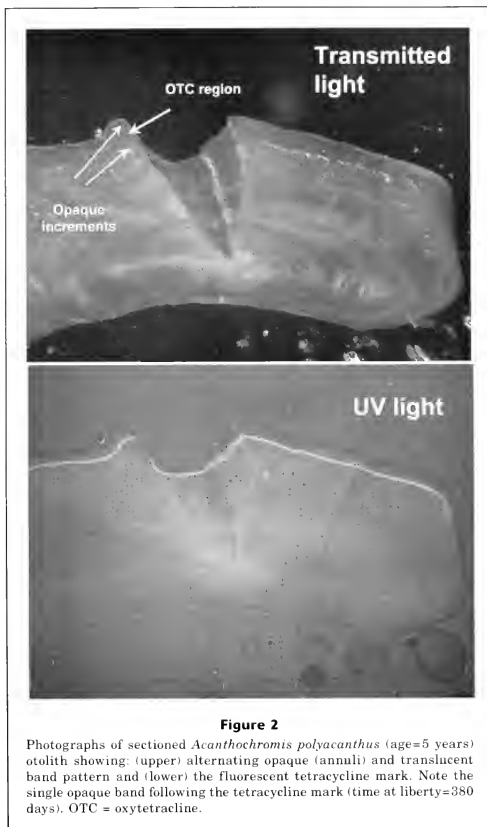


Figure 2

Photographs of sectioned *Acanthochromis polyacanthus* (age=5 years) otolith showing: (upper) alternating opaque (annuli) and translucent band pattern and (lower) the fluorescent tetracycline mark. Note the single opaque band following the tetracycline mark (time at liberty=380 days). OTC = oxytetracycline.

Results

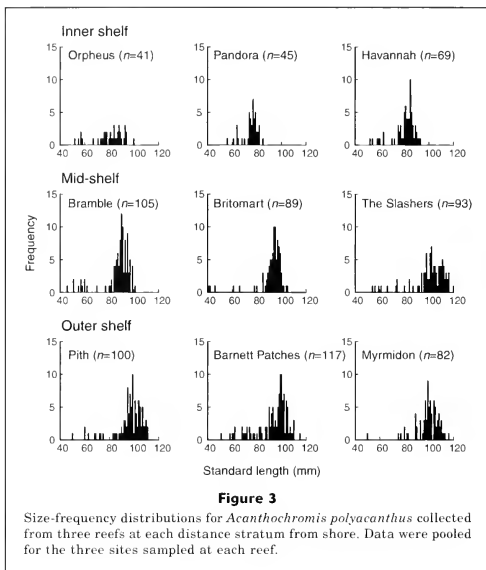
Age validation

All fish treated with tetracycline had clear fluorescent marks in their otoliths (Fig. 2). The positions of the fluorescent tetracycline bands in relation to the otolith margin were consistent with the deposition of opaque zones on an annual basis (Table 2). In general, percent agreement was over 75% (7/10 fish). Differences between actual and estimated time at liberty were probably

related to slight variation in the small measurements that were made (i.e., fractions of a mm). The timing of deposition of the opaque increment was estimated to occur in spring because new increments were found at the edge of otoliths of fish that had been marked in May and sacrificed about 200 days later.

Size and age structures

There were large differences in the size-frequency distributions of fish sampled across the shelf (Fig. 3). At



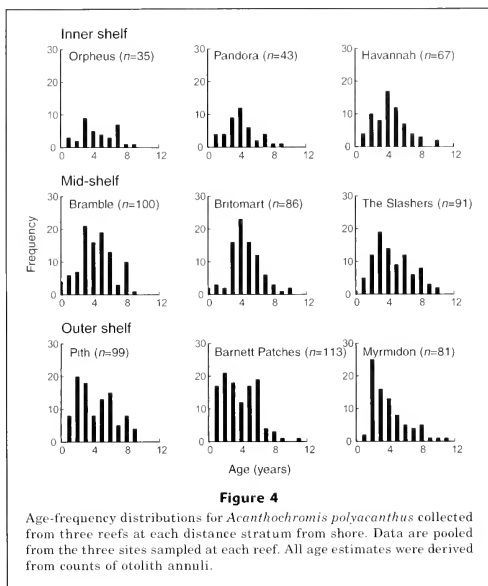
inner-shelf reefs ($n=155$), only one fish >100 mm was collected. In contrast, between 38% and 54% of fish collected from outer-shelf reefs were >100 mm. A mix of inner- and outer-shelf size-frequency distributions was evident for mid-shelf reefs. Bramble and Britomart reefs had 1% and 7% of fish >100 mm, respectively, whereas The Slashers had the highest proportion of fish >100 mm collected of any reef (67%) including the largest individual fish collected (120 mm); however, this result was more characteristic of outer-shelf reefs. Another conspicuous feature of the cross-shelf size frequencies was the very narrow size range of adult fish collected on inner-shelf reefs in comparison to the size range of fish collected from mid- and outer-shelf locations (Fig. 3). Size selectivity due to the collection technique (hand spear) restricted the numbers of fish <60 mm that could be collected.

Maximum age of *A. polyacanthus* was similar at all reefs sampled (Fig. 4; inner shelf: 9–10 yr, mid-shelf: 9–10 yr, outer shelf: 10–11 yr). The largest age class of fish on the inner- and mid-shelf reefs comprised 3–4 year olds, whereas on the outer-shelf reefs, 2-year-old fish made up the largest proportion of the populations. The two oldest fish were both collected from outer-shelf reefs (Myrmidon and Barnett Patches) and were both

11 years old. Strong age-structured cohorts of fish were found at some reefs within the same distance stratum and these cohorts were found only at these reefs and distance stratum. For example, there were strong year classes at Pith and Barnett Patches in years 5 and 6 that were not found at Myrmidon (Fig. 4).

Growth

Variation in patterns of growth was greater among distance strata across the shelf than among reefs within a distance strata (Fig. 5). There was variation in growth between individuals from reefs within each shelf position and this resulted in variable size-at-age relationships (Fig. 5). From inner-shelf reefs, fish from Pandora showed small asymptotic sizes and thus had lower average L_{∞} ($L_{\infty}=77.4$ mm) compared to fish from Orpheus and Havannah ($L_{\infty}=87.0$, 84.2 mm, respectively; Table 3). Distinct, non-overlapping ellipses formed in 95% confidence interval plots of L_{∞} in relation to K confirmed that growth curves for fish from Pandora differed from those at Orpheus and Havannah (Fig. 5). Fish collected from mid-shelf reefs (Bramble, Britomart, and The Slashers) showed differences in growth among all reefs (non-overlapping 95% confidence ellipses; Fig. 5). Growth of fish

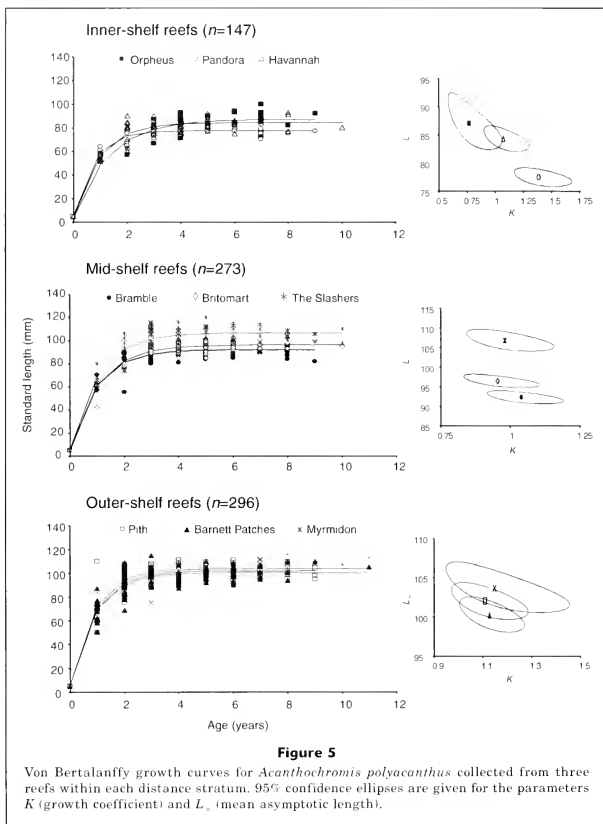
**Table 2**

Validation data with the use of tetracycline to determine the periodicity and timing of opaque ring deposition for *Acanthochromis polyacanthus* with the use of tetracycline as a time marker. TAL = time at liberty expressed as a proportion of one year and derived from growth measurements from reared fish treated with tetracycline. TC = tetracycline.

Fish age (yr)	TC to marginal increment (mm)	TAL (mm)	TAL as proportion of year	Estimated days from TC marking	Actual days from TC marking	Percent agreement = (estimated/actual) × 100
1	0.0423	0.30	0.43	110	158	69
1	0.0463	0.33	0.43	120	158	76
1	0.1784	0.94	0.97	344	355	97
5	0.0686	0.80	1.04	291	380	76
5	0.0739	0.83	1.04	304	380	80
5	0.1077	1.00	1.52	365	556	66
5	0.0805	0.81	1.52	295	556	53
6	0.1471	1.46	1.47	532	537	99
7	0.1034	0.90	1.12	327	409	80
7	0.0919	1.30	1.52	474	556	85

from the outer reefs (Pith, Barnett Patches, and Myrmidon), however, was similar for fish from each of these reefs (overlapping 95% confidence ellipses; Fig. 5).

Average maximum length (L_{∞}) varied across the shelf and differences among strata were generally greater than within-distance strata. The K values for all three



shelf positions were similar and indicated that K values for *A. polyacanthus* converge at asymptotic sizes at approximately the same rate of growth, irrespective of proximity to the coast (Fig. 5 and Table 3). However, an obvious trend for increased L_{∞} occurred with increasing distance from the coast (inner shelf: ~83 mm, mid-shelf: ~99 mm, outer shelf: ~102 mm). The growth parameters of fish from The Slashers were more similar to those of fish taken from the outer-shelf reefs than to those we defined *a priori* as mid-shelf (Fig. 6). The Slashers are in fact much farther from the coast (85 km), as are Pith

Reef (74 km) and Barnett Patches (63 km) on the outer shelf, than the other two mid-shelf reefs (Britomart: 39 km, Bramble: 41 km) (Fig. 1, Table 1).

Mortality

Mortality rates for *A. polyacanthus* did not differ significantly between replicate reefs within inner-shelf (test for slopes $df_{(2,19)}$, $F=0.982$, $P=0.39$), mid-shelf (test for slopes $df_{(2,19)}$, $F=1.334$, $P=0.29$) or outer-shelf (test for slopes $df_{(2,19)}$, $F=0.658$, $P=0.53$) locations (Table 4).

Age frequencies, therefore, were pooled at the shelf level (within distance strata; Fig 7).

Acanthochromis polyacanthus mortality rates did not differ significantly between the inner-, mid- and outer-shelf strata (test for slopes $df_{8, 63}$, $F=0.367$, $P=0.70$) (Fig. 6). Although mortality estimates were progressively lower with increased distance from the coast, this trend was not significant (inner shelf: -0.51 , mid-shelf: -0.48 , outer shelf: -0.43 ; Fig. 6, Table 4). Associated survival rate estimates (S) varied between reefs by $\sim 9\%$ per annum at inner- and mid-shelf strata and by $\sim 6\%$ per annum on the outer shelf (Table 3). The mean difference in survival rates for *A. polyacanthus* between the inner and mid-shelf was -2% and between the mid- and outer shelf was -3% (Table 4).

Discussion

The demographic parameters of L_{∞} and patterns of growth for populations of *A. polyacanthus* varied across the shelf on the central GBR. Although there was variation in body size and growth among reefs within a distance stratum, it was minor compared to overall cross-shelf patterns. In this study, mortality estimates and maximum age were similar for populations of fish across the shelf. Thus, in order to explain the cross-shelf trend in body size, fish must have grown faster with increasing distance from shore (Fig. 7, Table 1).

Despite the relative paucity of age-based studies on reef fishes (Choat and Robertson, 2002), variable rates of growth have been previously demonstrated for fish at local scales (hundreds of metres to kilometers; Fowler and Doherty, 1992), medium scales (kilometers to tens of kilometers; Choat and Axe, 1996; Hart and Russ, 1996; Newman et al., 1996; Meekan et al., 2001; Gust et al., 2002), and large scales (thousands of kilometers; Choat and Robertson, 2002). Gust et al. (2002) found that growth patterns of scarids varied between the reef crests of mid- and outer-shelf sampling locations on the northern GBR. In contrast to the results from the current study, however, outer-shelf populations of scarids had smaller asymptotic sizes and slower growth rates than mid-shelf populations. The factors influencing patterns of growth, therefore, vary by group.

Differences in the shape of growth curves between geographic regions or areas may be determined by both genetic and environmental influences (Sebens, 1987). Populations of reef fish are generally considered to be genetically open systems (Sale, 1991) and it is considered unlikely that adaptation of such populations to local conditions through genetic selection can occur (Warner, 1991). *Acanthochromis polyacanthus*, how-

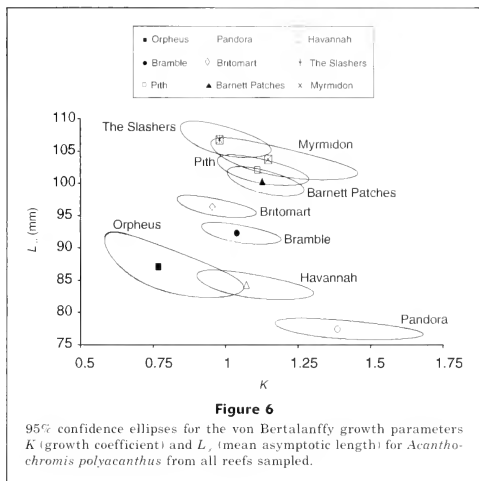


Table 3

Parameters from von Bertalanffy growth models on the fishes collected from different distance strata and reefs.

Shelf location and reef	n	L_{∞}	K	r^2
Inner shelf				
Orpheus Island	36	87.03	0.77	0.83
Pandora Reef	44	77.43	1.39	0.92
Havannah Island	67	84.23	1.07	0.81
Mid-shelf				
Bramble Reef	97	92.24	1.04	0.83
Britomart Reef	85	96.37	0.95	0.87
The Slashers	91	106.73	0.98	0.75
Outer shelf				
Pith Reef	100	101.98	1.11	0.76
Barnett Patches	114	100.27	1.13	0.78
Myrmidon Reef	82	103.66	1.15	0.70

ever, possesses a unique life history trait among reef fishes in that it lacks a dispersive larval phase. The major implication of this characteristic is the potential for genetic isolation of populations of these fish. Even reefs that are in relatively close proximity to one another (100's of m) may become "genetic islands" isolated by any barrier that proves impassable to adults (e.g., deep water). Without gene flow, reproductively isolated

Table 4

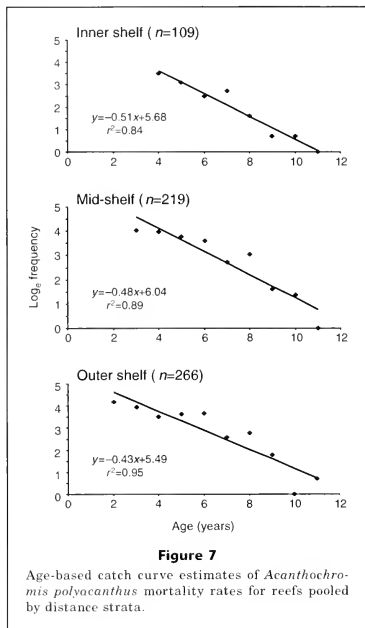
Estimates of mortality (M) for fishes collected from different distance strata and reefs. Pooled values are for all reefs within one distance stratum. n = number of fish in sample. S = animal survival rate.

Reef	n	M	Pooled M	S (%)	Pooled S (%)
Inner shelf			0.51		60.0
Orpheus Island	30	0.29		74.8	
Pandora Reef	34	0.40		67.0	
Havannah Island	45	0.42		65.7	
Mid-shelf			0.48		61.8
Bramble Reef	83	0.44		64.4	
Britomart Reef	63	0.48		61.9	
The Slashers	73	0.34		71.2	
Outer shelf			0.43		65.1
Pith Reef	91	0.32		72.6	
Barnett Patches	96	0.40		67.0	
Myrmidon Reef	79	0.38		68.4	

populations are expected to diverge over time with respect to their genetic composition (Doherty et al., 1994). Numerous studies have examined the genetic relationships between populations of *A. polyacanthus* on the GBR (Doherty et al., 1994, 1995; Planes and Doherty, 1997a, 1997b). Isozyme analyses of populations of different color morphs at various spatial scales have shown significant genetic variation at both the regional (1000's of km) and local (100's of m) level, which under normal circumstances would suggest separate species for each color morph (Doherty et al., 1994; Planes and Doherty, 1997a). However, differences in the growth rates of *A. polyacanthus* across the continental shelf in this study are unlikely to reflect genetic differences between the populations sampled because all individuals collected were of the same color morph and were from a relatively small area (about 400 km², cf. 450,000 km² for the entire GBR).

Environmental influences that can affect patterns of growth include predation pressure, temperature, and related effects on metabolism, variations in resources (e.g., abundance of planktonic food), and variation in water condition (e.g., turbidity).

High rates of predation may "drive" faster growth (Werner, 1984), or conversely, select for early maturation and smaller adult size (Reznick et al., 1990; Hutchings, 1997). It is unlikely that the cross-shelf patterns in growth that we found were determined by differences in mortality rates. Some data on serranid abundance (Williams, 1982) and anecdotal accounts have indicated that predator abundance is greatest on mid- and outer reefs of the GBR (Gust et al., 2001). Our measures of instantaneous mortality (Z) and age maximum, however, did not vary with distance from the mainland. Furthermore, in contrast to the patterns that Gust et

**Figure 7**

Age-based catch curve estimates of *Acanthochromis polyacanthus* mortality rates for reefs pooled by distance strata.

al. (2001) found for scarids, L_{∞} increased with distance from the coast. Mortality rates have been shown to vary among locations within reefs for several species of coral reef fish (Aldenhoven, 1986; Eckert, 1987; Sale and Ferrell, 1988; Beukers and Jones, 1997) including *A. polyacanthus* juveniles (Connell, 1996), as well as over larger spatial scales (Meekan et al., 2001; Gust et al., 2002). In contrast to these last two studies, particularly that of Gust et al. (2002), mortality rates for *A. polyacanthus* were similar at all three cross-shelf strata. We acknowledge, however, that no data were available on mortality rates of fish from zero to two years of age. It is possible that mortality rates do vary with distance from shore over this age range.

An increase in adult size may occur when individuals experience a decline in average temperature during development (Atkinson, 1994). It is also well established that metabolism and growth are increased at higher ambient temperatures in ectotherms (Schmidt-Nielsen, 1990). Differences in temperature between the water bodies spanning inner-, mid- and outer-shelf positions in the central GBR do occur; relatively shallow near-

shore waters are the warmest and outer-shelf waters are the coolest (Wolanski, 2001). The opposite pattern of growth to the one observed in this study would be predicted by this cross-shelf gradient in water temperature. It is also considered unlikely that local upwelling events on outer-shelf reefs could produce the observed differences, but they could influence primary productivity and abundance of food (zooplankton) through nutrient-rich waters. An increase in average annual temperature correlates with maximum age in some fishes (review Choat and Robertson, 2002), but we found no differences in age maximum across the shelf. We conclude that any differences in temperature across the shelf are not persistent enough to affect cross-shelf patterns of growth of *A. polyacanthus*.

Differences in growth profiles can be more realistically attributed to cross-shelf variation in some limiting resource(s). This variation in resources may influence the quality and quantity of food, suitable nest sites, refuges from predators and (or) wave exposure, and density of conspecifics and (or) other species that compete with *A. polyacanthus* for resources. Correlative studies have concluded that the distribution and abundance of coral reef fishes is strongly influenced (directly and indirectly) by physical factors such as wave exposure, sediment loads, water depth, and topographical complexity, as well as by biological factors (Williams, 1982). These factors also have the potential to affect growth rates.

A combination of reduced resource levels and high population densities on outer-shelf reefs strongly indicated that growth profiles represent density dependence in scarids (Gust et al., 2001, 2002). Density of con- and hetero-specifics was not recorded for our study, but densities of *A. polyacanthus* were clearly greatest on the mid- and outer-shelf reefs. This observation is contrary to the pattern noted by Williams (1982) who found greatest abundances of *A. polyacanthus* on inner- and mid-shelf reefs. Thresher (1983) suggested that food abundance is a limiting resource for *A. polyacanthus* and interspecific competition for food does occur. Thus, it is plausible that variation in abundance of and competition for food across the shelf may have influenced the growth rates observed in the present study. The large differences in cross-shelf densities and L_{∞} 's of *A. polyacanthus* indicate that competition may be less important than variation in quantity and quality of food across the shelf.

Biomass of planktivores is generally highest at mid-shelf reefs on the central GBR (Williams and Hatcher, 1983). Although data on cross-shelf abundance and distribution of plankton are limited, Williams and Hatcher attributed this pattern to the increased availability of food (zooplankton) in mid-shelf waters. Upwelling of cold, nutrient-rich water from the edge of the continental shelf results in high biomasses of phytoplankton. Aging of the water (time since upwelling) is accompanied by a shift in dominant planktonic biomass to herbivorous and then carnivorous zooplankton. This shift in biomass composition occurs simultaneously with the prevailing wind-driven passage of water across the shelf and

ultimately leads to the greatest biomass of zooplankton occurring in mid-shelf waters (Andrews and Gentien, 1982; Sammarco and Crenshaw, 1984; Williams et al., 1988). Food quality has also been previously shown to limit growth and reproduction in herbivorous coral reef fishes (Horn, 1989; Choat, 1991).

Despite a high abundance of zooplankton near shore, these waters also have higher turbidity than mid- and outer-shelf reefs. Visual impairment caused by very turbid waters may hinder the ability of fish to feed on planktonic organisms and this hypothesis has been suggested as a factor contributing to the low relative abundances of planktivorous fish on inner-shelf reefs (Williams et al., 1986). It is possible that this factor may retard the growth and influence the maximum size of planktivores like *A. polyacanthus* by effectively reducing food availability. Interestingly, lowest L_{∞} values were found at the most turbid inshore reef, Pandora. Lower visibility near shore, however, did not appear to affect the mortality rates of *A. polyacanthus* at inner-shelf reefs.

There were clear differences in growth, size maxima, and age structures for populations of *A. polyacanthus* across the continental shelf of the central GBR. Although *Acanthochromis polyacanthus* grew faster and to a larger size with increasing distance from the mainland, cross-shelf mortality rates and maximum ages were similar. Because these populations of fish are unlikely to be genetically distinct, we suggest that biotic and physical processes are the most plausible cause of these cross-shelf patterns. Increased abundance of zooplankton in mid- and outer-shelf waters, coupled with potential visual impairment associated with high turbidity levels on the inner shelf, are likely mechanisms that explain the observed patterns, but multifactorial manipulative experiments are required to determine the relative contribution of these factors to variation in demographic parameters. Our study therefore cautions against pooling demographic parameters over broad spatial scales without considering cross-shelf variation.

Acknowledgments

We would like to thank H. Patterson, C. Bunt, W. Robbins, and the crew of the RV *Orpheus* for field assistance during this study. We also thank J. Ackerman for analytical advice and expertise and J. H. Choat for constructive comments on the manuscript. We also thank John Morrison and the staff of MARFU for assistance with the maintenance of aquarium fish. The project was partly funded by an ARC Grant to MJK. This is a contribution from Orpheus Island Research Station.

Literature cited

- Aldenhoven, J. M.
1986. Local variation in mortality rates and life history estimates of the coral reef fish *Centropyge bicolor* (Pisces: Pomacanthidae). Mar. Biol. 92:237-244.

- Allen, G. R.
1975. Damselfishes of the South Seas, 240 p. Tropical Fish Hobbyist Publications, Neptune City, NJ.
- Andrews J. C., and P. Gentien.
1982. Upwelling as a source of nutrients for the Great Barrier Reef ecosystems: a solution to Darwin's question? *Mar. Ecol. Prog. Ser.* 8:257-269.
- Atkinson, D.
1994. Temperature and organism size—a biological law for ectotherms? *Adv. Ecol. Res.* 25:1-58.
- Beukers, J. J., and G. P. Jones.
1997. Habitat complexity modifies the impact of piscivores on a coral reef fish population. *Oecologia* 114: 50-69.
- Choat, J.
1991. The biology of herbivorous fishes on coral reefs. *In* The ecology of fishes on coral reefs (P. F. Sale, ed.), p. 120-155. Academic Press, San Diego, CA.
- Choat, J., and L. Axe.
1996. Growth and longevity in acanthurid fishes: an analysis of otolith increments. *Mar. Ecol. Prog. Ser.* 134:15-26.
- Choat, J., and D. R. Robertson.
2002. Age-based studies. *In* Coral reef fishes (P. F. Sale, ed.), p. 57-80. Academic Press, Amsterdam, The Netherlands.
- Connell, S. D.
1996. Variations in mortality of a coral reef fish: links with predator abundance. *Mar. Biol.* 126:347-352.
1998. Effects of predators on growth, mortality and abundance of a juvenile reef fish: evidence from manipulations of predator and prey abundance. *Mar. Ecol. Prog. Ser.* 169:251-261.
2000. Is there safety-in-numbers for prey? *Oikos* 88(3):527-532.
- Dinesen, Z. D.
1983. Patterns in the distribution of soft corals across the central Great Barrier Reef. *Coral Reefs* 1:229-236.
- Doherty, P. J., S. Planes, and P. Mather.
1994. *Acanthochromis polyacanthus*, a fish lacking larval dispersal, has genetically differentiated populations at local and regional scales on the Great Barrier Reef. *Mar. Biol.* 121(1):11-21.
1995. Gene flow and larval duration in seven species of fish from the Great Barrier Reef. *Ecology* 76(8):2373-2391.
- Done, T. J.
1982. Patterns in the distribution of coral communities across the central Great Barrier Reef. *Coral Reefs* 1:95-107.
- Dudgeon, C. L., N. Gust, and D. Blair.
2000. No apparent genetic basis to demographic differences in scarid fishes across the continental shelf of the Great Barrier Reef. *Mar. Biol.* 137:1059-1066.
- Eckert, G. J.
1987. Estimates of adult and juvenile mortality for labrid fishes at One Tree Reef, Great Barrier Reef. *Mar. Biol.* 95:167-171.
- Fowler, A. J., and P. J. Doherty.
1992. Validation of annual growth increments in the otoliths of two species of damselfish from the southern Great Barrier Reef. *Aust. J. Mar. Freshw. Res.* 43:1057-1068.
- Geffen, A. J.
1992. Validation of otolith increment deposition rate. *In* Otolith microstructure examination and analysis (D. K. Stevenson, and S. E. Campana, eds.), p. 101-113. Can. Spec. Publ. Fish. Aquat. Sci. 117.
- Gillanders, B. M.
1995. Feeding ecology of the temperate marine fish *Achoerodus viridis* (Labridae): size, seasonal and site-specific differences. *Mar. Freshw. Res.* 46(7):1009-1020.
- Gust, N., J. H. Choat, and J. L. Ackerman.
2001. Demographic plasticity in tropical reef fishes. *Mar. Biol.* 140:1039-1051.
- Gust, N., J. H. Choat, and M. McCormick.
2002. Spatial variability in reef fish distribution, abundance, size and biomass: a multi-scale analysis. *Mar. Ecol. Prog. Ser.* 214:237-251.
- Hart, A. M., and G. R. Russ.
1996. Response of herbivorous fishes to crown of thorns starfish *Acanthaster planci* outbreaks III. Age, growth, mortality and maturity indices of *Acanthurus nigrofasciatus*. *Mar. Ecol. Prog. Ser.* 136:25-35.
- Horn, M. H.
1989. Biology of marine herbivorous fishes. *Oceanogr. Mar. Biol. Annu. Rev.* 27:167-272.
- Hutchings, J. A.
1997. Life history responses to environmental variability in early life. *In* Early life history and recruitment in fish populations (R. C. Chambers, and E. A. Trippel, eds.), p. 139-168. Chapman & Hall, London, UK.
- Kavanagh, K.
1998. Notes on the frequency and function of glancing behavior in juvenile *Acanthochromis* (Pomacentridae). *Copeia* 1998(2):493-496.
2000. Larval brooding in the marine damselfish *Acanthochromis polyacanthus* (Pomacentridae) is correlated with highly divergent morphology, ontogeny and life-history traits. *Bull. Mar. Sci.* 66(2):321-37.
- Kimura, D. K.
1980. Likelihood methods for comparison of von Bertalanffy growth curves. *Fish. Bull.* 77:765-776.
- McCook, L. J., I. R. Price, and D. W. Klumpp.
1997. Macro algae on the Great Barrier Reef: causes or consequences, indicators or models of reef degradation? *Proc. 8th Int. Coral Reef Symp.* 2:1851-1856.
- McFarlane, G. A., and R. J. Beamish.
1987. Selection of dosages of oxytetracycline for age validation studies. *Can. J. Fish. Aquat. Sci.* 44:905-909.
- Meekan, M. G., J. L. Ackerman, and G. M. Wellington.
2001. Demography and age structures of coral reef damselfishes in the tropical eastern Pacific Ocean. *Mar. Ecol. Prog. Ser.* 212:223-232.
- Munro, J. L., and D. M. Williams.
1985. Assessment and management of coral reef fisheries: biological, environmental and sociological aspects. *Proc. 5th Int. Coral Reef Congr.* 4:545-581.
- Nakazono, A.
1993. One-parent removal experiment in the brood-caring damselfish, *Acanthochromis polyacanthus*, with preliminary data on reproductive biology. *Aust. J. Mar. Freshw. Res.* 44(5):699-707.
- Newman, S. J., and D. M. Williams.
1996. Variation in reef associated assemblages of the Lutjanidae and Lethrinidae at different distances offshore in the central Great Barrier Reef. *Environ. Biol. Fish.* 46:123-138.
- Newman, S. J., D. M. Williams, and G. R. Russ.
1996. Age validation, growth and mortality rates of the tropical snappers (Pisces: Lutjanidae) *Lutjanus adtii* (Castelnau, 1873) and *L. quinquefasciatus* (Bloch, 1790)

- from the central Great Barrier Reef, Australia. Mar. Freshw. Res. 47:575-584.
1997. Patterns of zonation of assemblages of the Lutjanidae, Lethrinidae and Serranidae (Epinephelinae) within and among mid shelf and outer shelf reefs in the central Great Barrier Reef. Mar. Freshw. Res. 48:119-128.
- Pauly, D.
1984. Fish population dynamics in tropical waters. ICARM Stud. Rev. 8:1-325.
- Planes, S., and P. J. Doherty.
1997a. Genetic and color interactions at a contact zone of *Acanthochromis polyacanthus*: a marine fish lacking pelagic larvae. Evolution 51(4):1232-1243.
1997b. Genetic relationships of the color morphs of *Acanthochromis polyacanthus* (Pomacentridae) on the northern Great Barrier Reef. Mar. Biol. 130(1):109-117.
- Preston, N. P., and P. J. Doherty.
1990. Cross-shelf patterns in the community structure of coral dwelling Crustacea in the central region of the Great Barrier Reef. 1. Agile shrimps. Mar. Ecol. Prog. Ser. 66:47-61.
1994. Cross-shelf patterns in the community structure of coral dwelling Crustacea in the central region of the Great Barrier Reef. 2. Cryptofauna. Mar. Ecol. Prog. Ser. 104:27-38.
- Reznick, D. N., H. Bryga, and J. A. Endler.
1990. Experimentally-induced life history evolution in a natural population. Nature 346:357-359.
- Ricker, W. E.
1975. Computation and interpretation of biological statistics of fish populations. 392. Bull. Fish. Res. Board Canada 191, Ottawa, Canada.
- Robertson, D. R.
1973. Field observations on the reproductive behavior of a pomacentrid fish, *Acanthochromis polyacanthus*. Zeitschrift für Tierpsychologie 32:319-324.
- Russ, G.
1984a. Distribution and abundance of herbivorous grazing fishes in the central Great Barrier Reef I. Levels of variability across the entire continental shelf. Mar. Ecol. Prog. Ser. 20:23-34.
1984b. Distribution and abundance of herbivorous grazing fishes in the central Great Barrier Reef II. Patterns of zonation of mid-shelf and outer-shelf reefs. Mar. Ecol. Prog. Ser. 20:35-44.
- Sale, P. F.
1991. Reef fish communities: open non equilibrium systems. In The ecology of fishes on coral reefs (P. F. Sale, ed.), p. 564-598. Academic Press, San Diego, CA.
1988. Early survivorship of juvenile coral reef fishes. Coral Reefs 7:117-124.
- Sammarco, P. W., and H. Crenshaw.
1984. Plankton community dynamics of the central Great Barrier Reef lagoon: analysis of data from Ikeda et al. Mar. Biol. 82:167-180.
- Schmidt-Nielsen, K.
1990. Animal physiology: adaptation to environment, 4th ed., 602 p. Cambridge Univ. Press, Cambridge, UK.
- Schnute, J.
1981. Versatile growth model with stable parameters. Can. J. Fish. Aquat. Sci. 38:1128-1140.
- Sebens, K. P.
1987. The ecology of indeterminate growth in animals. Annu. Rev. Ecol. Syst. 18:371-407.
- Thresher, R. E.
1983. Habitat effects on reproductive successes in the coral reef fish, *Acanthochromis polyacanthus*. Ecology 64:1184-1199.
1985a. Distribution, abundance and reproductive success in the coral reef fish *Acanthochromis polyacanthus*. Ecology 66:1139-1150.
1985b. Brood-directed parental aggression and early brood loss in the coral reef fish *Acanthochromis polyacanthus*. Anim. Behav. 33:897-907.
- Warner, R. R.
1991. The use of phenotypic plasticity in coral reef fishes as tests of theory in evolutionary ecology. In The ecology of fishes on coral reefs (P. F. Sale, ed.), p. 387-398. Academic Press, San Diego, CA.
- Werner, E. E.
1985. The mechanisms of species interactions and community organization in fish. In Ecological communities (D. R. Strong, ed.), p. 360-382. Princeton Univ. Press, Princeton, NJ.
- Wilkinson, C. R., and A. C. Cheshire.
1988. Cross shelf variations in coral reef structure and function - influences of land and ocean. Proc. 6th Int. Coral Reef Symp. 1:227-233.
- Williams, D. M.
1982. Patterns in the distribution of fish communities across the central Great Barrier Reef. Coral Reefs 1:35-43.
1983. Longitudinal and latitudinal variation in the structure of reef fish communities. In The inaugural Great Barrier Reef conference (J. T. Baker, R. M. Carter, P. W. Sammarco, and K. P. Stark, eds.), p. 265-270. James Cook Univ. Press, Townsville, Queensland, Australia.
- Williams, D. M., and A. I. Hatcher.
1983. Structure of fish communities on outer slopes of inshore, mid-shelf and outer shelf reefs of the Great Barrier Reef. Mar. Ecol. Prog. Ser. 10:239-250.
- Williams, D. M., P. Dixon, and S. English.
1988. Cross-shelf distribution of copepods and fish larvae across the central Great Barrier Reef. Mar. Biol. 99:577-589.
- Williams, D. M., G. Russ, and P. J. Doherty.
1986. Reef fish: large-scale distribution and recruitment. Oceanus 29(2):76-82.
- Williams, D. M., C. R. Davies, B. D. Mapstone, and G. R. Russ.
2003. Scales of spatial variation in demography of a large coral reef fish: an exception to the typical model? Fish. Bull. 101: 673-683.
- Wolanski, E.
2001. Oceanographic processes of coral reefs: physical and biological links in the Great Barrier Reef, 356 p. CRC Press, Boca Raton, FL
- Zar, J. H.
1999. Biostatistical analysis, 4th ed., 663 p. Prentice Hall, Upper Saddle River, NJ.

Abstract—Aspects of the feeding migration of walleye pollock (*Theragra chalcogramma*) in the eastern Bering Sea (EBS) were investigated by examining the relationship between temperatures and densities of fish encountered during acoustic and bottom trawl surveys conducted in spring and summer between 1982 and 2001. Bottom temperature was used as an indicator of spring and summer warming of the EBS. Clusters of survey stations were identified where the density of walleye pollock generally increased or decreased with increasing water temperature. Inferences about the direction and magnitude of the spring and summer feeding migration were made for five length categories of walleye pollock. Generally, feeding migrations appeared to be northward and shoreward, and the magnitude of this migration appeared to increase with walleye pollock size up to 50 cm. Pollock larger than 50 cm showed limited migratory behavior. Pollock may benefit from northward feeding migrations because of the changes in temperature, zooplankton production, and light conditions. Ongoing climate changes may affect pollock distribution and create new challenges for pollock management in the EBS.

Variation in the distribution of walleye pollock (*Theragra chalcogramma*) with temperature and implications for seasonal migration

Stan Kotwicki

Troy W. Buckley

Taina Honkalehto

Gary Walters

Resource Assessment and Conservation Engineering Division

Alaska Fisheries Science Center

National Marine Fisheries Service, NOAA

7600 Sand Point Way NE

Seattle, Washington 98115-6349

E-mail (for S. Kotwicki): Stan.kotwicki@noaa.gov

Walleye pollock (*Theragra chalcogramma*; referred to as "pollock" in this article) migrate seasonally. Such migrations have been described for the northern Sea of Japan (Maeda, 1986; Maeda et al., 1988, 1989; Kooka et al., 1998), Korean waters (Shuntov et al., 1993), the Okhotsk Sea (Shuntov et al., 1987), and the western and central Bering Sea (Fadeyev, 1989; Bulatov and Sobolevskiy, 1990; Efimkin, 1991; Radchenko and Sobolevskiy, 1993; Shuntov et al., 1993; Balykin, 1996). Generally, these authors have described a spring and summer migration from spawning grounds to forage areas (referred to as a "feeding migrations" by many authors) and a winter migration of pollock returning to spawning grounds (e.g., Maeda et al., 1988; Radchenko and Sobolevskiy, 1993). This pattern of migration is believed to occur in the eastern Bering Sea (EBS) where it has received considerable attention (Takahashi and Yamaguchi, 1972; Francis and Bailey, 1983; Pola, 1985; Shuntov, 1992; Shuntov et al., 1993; Stepanenko, 2001), but the evidence for this pattern of migration is sparse. In addition, there is a lack of information on the magnitude of, routes of, and size-dependent differences in seasonal migrations.

Temperature (and other factors closely related to temperature) affects the distribution and movements of pollock. Pola (1985) simulated

temperature-induced migrations of pollock in the EBS occurring during May and June. Pollock appear to avoid some temperatures (Swartzman et al., 1994) and prefer environmental conditions that are linked to food availability associated with temperature gradients and fronts along the EBS slope (Swartzman et al., 1995). Water temperature is an especially important indicator of the transition from winter conditions to those supporting a spring bloom of phytoplankton and then zooplankton. In the EBS, the simulated onset of the feeding migration of pollock was delayed in colder years (Pola, 1985).

Annual surveys documenting the spatial distribution of fishes in relation to water temperatures can be used to infer details about their migratory behavior. Using annual survey data, Mountain and Murawski (1992) found that the relationship between the distribution of seasonally migrating species and water temperature could indicate a change in the overwintering location of the fish, or a change in the timing of the spring migration, or both. In the eastern Bering Sea, bottom trawl (BT) surveys and echo-integration-trawl (EIT) surveys are conducted in late spring and summer (Honkalehto et al.^{1, 2}; Acuna et al.²), when water tem-

Manuscript submitted 20 November 2004 to the Scientific Editor's Office.

Manuscript approved for publication 30 March 2005 by the Scientific Editor. Fish. Bull. 103:574–587 (2005).

^{1, 2} See next page for footnote texts.

peratures are generally rising on the eastern Bering Sea shelf (Overland et al., 1999; Stabeno et al., 2001). Interannual variability in climatic conditions and survey timing create variability in mean water temperatures encountered during the surveys (Acuna et al.²).

We describe the variability in distribution of pollock with temperature and propose that this variability may be explained by the fact that pollock migrate to feeding grounds during spring and summer. Temperature is used in our study as an indicator of how far into an idealized seasonal warming cycle each survey has occurred. Thus, the distribution of pollock observed in a warm year would be considered to be representative of that seen later in a seasonal warming cycle in a cold year. Generally, feeding migrations appeared to be northward and shoreward, and the magnitude of this migration appeared to increase with walleye pollock size up to 50 cm. Pollock larger than 50 cm showed limited migratory behavior. Pollock may benefit from northward feeding migrations because of the changes in temperature, zooplankton production, and light conditions.

Materials and methods

Data used in this investigation were collected by BT and EIT surveys conducted by the Alaska Fisheries Science Center.

Since 1982, BT surveys have been conducted annually over a standard area of the EBS, at the centers of 20 × 20 nautical-mile grids (Fig. 1). The corners of the grid block were also sampled in areas surrounding St. Matthew Island and the Pribilof Islands. The same

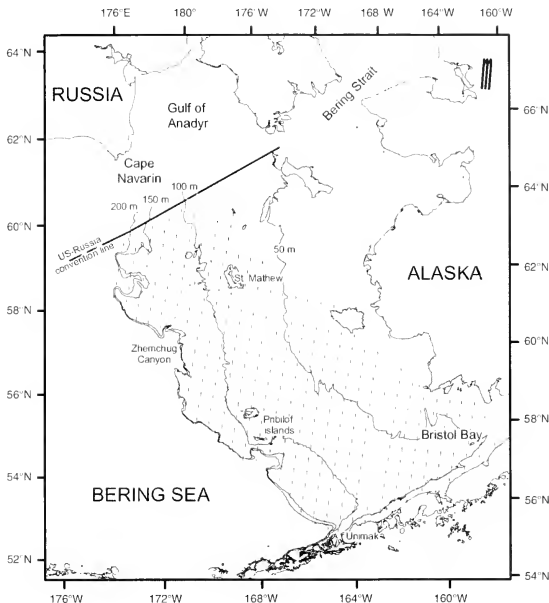


Figure 1

Locations of AFSC bottom trawl stations (dots) and echo-integration survey transects (lines) in the eastern Bering Sea where walleye pollock (*Theragra chalcogramma*) were collected during bottom trawl surveys and echo-integration trawl surveys in spring and summer between 1982 and 2001.

standard trawl (83-112 eastern otter trawl) was used every year (Acuna et al.²) and surveys usually began in late May or early June, and ended in August. Surveys always began in the northeastern corner of the Bristol Bay and proceeded westward. Samples were collected by tows for 30 minutes at 1.54 m/s (intended speed). Temperature data were collected during each tow using an expendable bathythermograph (XBT) until 1992 and after 1992 with a micro-bathythermograph (MBT) attached to the headrope of the trawl. Catches were sorted by species and weight; number of fish caught and length-frequency data were collected for each tow.

Echo integration trawl survey transects were designed to coincide with north-south lines of BT stations. Similar to the BT survey, the EIT survey began also in the eastern Bristol Bay and proceeded westward. The time lag between the survey varied from 0 to 30 days. Acoustic data were collected with a Simrad EK500 quantitative echo sounding system. Biological

¹ Honkalehto, T., N. Williamson, and S. de Blois. 2002a. Echo integration-trawl survey results for walleye pollock (*Theragra chalcogramma*) on the Bering Sea shelf and slope during summer 1999. U.S. Dep. Commerce, NOAA Tech. Memo. NMFS-AFSC-125.77 p.

² Acuna, E., P. Goddard, and S. Kotwicki (compilers). 2003. 2002 bottom trawl survey of the eastern Bering Sea continental shelf. AFSC Processed Report 2003-01, 169 p. Alaska Fish. Sci. Cent., NOAA Natl. Mar. Fish. Serv., 7600 Sand Point Way NE, Seattle, WA 98115.

data were collected by midwater trawl, bottom trawl, and Methot trawl (see Honkalehto et al.¹ for details). Pollock length data from trawls were aggregated into analytical strata based on echosign type, geographic proximity of hauls, and similarity in size composition of hauls. Estimates of numbers of pollock by size were derived by scaling acoustic measurements with the target strength-to-length relationship described in Traynor (1996). Temperature data were collected with an MBT mounted on the headrope of the trawl, although many of the profiles did not reach bottom because the trawls usually targeted midwater fish aggregations. For that reason, we elected not to use the temperature data collected during the EIT survey. Because both surveys were conducted at approximately the same time of year, we used the mean bottom temperature from the BT survey as an index temperature for the EIT survey. We used EIT data collected in years 1994, 1996, 1997, 1999, and 2000.

Because of the semidemersal nature of pollock (Bailey et al., 1999a) and assuming that pollock do not dive as a boat and trawl approaches, BT data are assumed to describe the demersal part of the pollock stock within 3 m of the bottom. EIT data represented the midwater part of the stock from 3 m above the bottom to 14 m below the surface. In our calculations, we used two density measures: CPUE in kg/ha for the BT data and biomass (tons) per 20-mile square for EIT data (the term "density" will be used in the present study to refer to both of these measures). Echo integration trawl survey 20-mile squares were centered on the BT survey stations, so that both sets of data could be easily compared (the term "station" will be used here to refer to BT survey stations as well as EIT survey squares). Because of known age-dependent behavioral differences between pollock (e.g., Shuntov et al., 1993; Bailey et al., 1999a), we investigated five different length classes of pollock; up to 20 cm (mostly 1-year-old pollock), 21–29 cm (mostly 2-year-old pollock), 30–39 cm, 40–49 cm, and pollock >50 cm. Because of differences in the year-class strengths between years, we scaled the data by dividing the density data for each station by the average fish density for each year within each length class. Thus, a station with a density value of 1 has an average density for a given year and a station with a value of 5 has a density 5 times larger for a given year.

If the pollock distribution in the EBS is assumed to be dynamic and related to temperature, the relationship between temperature and pollock density will be different at each spatial location. This means that if pollock moved from location A to location B over a period of rising temperatures, we expected a negative relationship between density and temperature in location A and an offsetting positive relationship in location B. To study these relationships in the EBS, we applied a two-step approach. In the first step, we identified possible locations where pollock density may be changing with temperature. In the second step, we identified locations of most significant biomass changes with temperature and quantified these changes.

First step—identifying areas of change in fish density with temperature

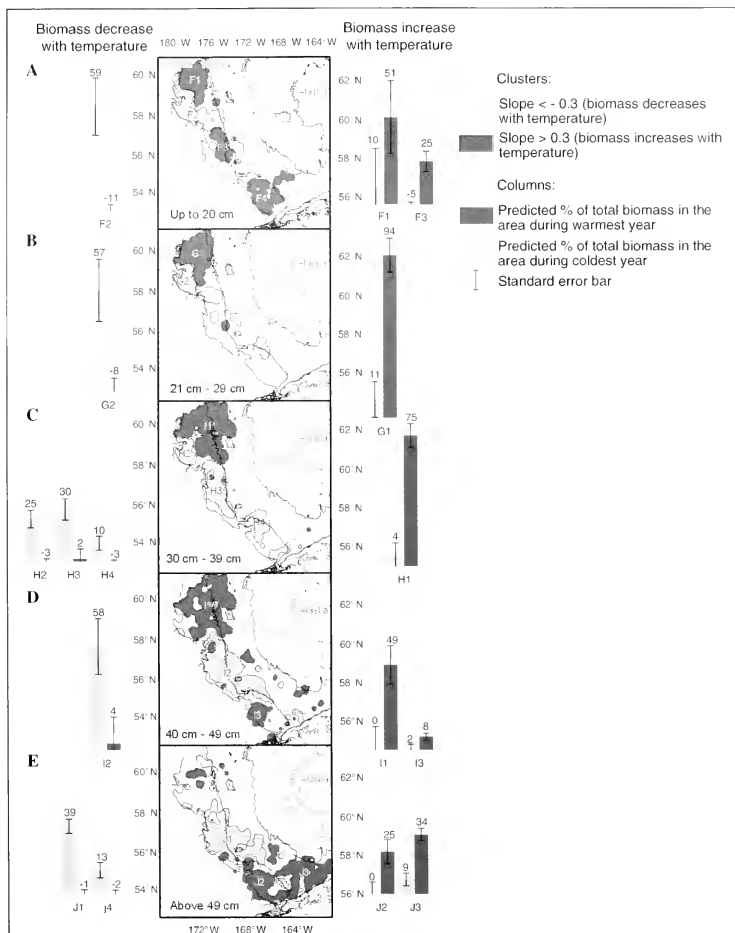
For both types of surveys, we calculated the slope of the linear regression of scaled density against bottom temperature for each station over the time series (e.g., a slope value of 1 indicates an increase of 1 unit of density per degree increase of temperature). Slopes in the range between -0.3 and 0.3 were ignored because they represented areas of low fish density or areas of no significant changes in fish density between years. Each station slope was then plotted on a map to visualize the spatial relationship between these two variables for the BT and EIT surveys.

To contour areas with similar slopes, we interpolated the data using inverse distance-weighted squared interpolation (IDW). This method was chosen because IDW is an exact interpolator, where the maximum and minimum values in the interpolated surface can occur only at sample points and values at all sampling points are true measured values (ArcGIS, Geostatistical Analyst Help, 2003, ESRI, Redlands, CA). Using these maps, we identified the main spatially correlated clusters of stations with positive or negative slopes of the linear regression of pollock density against temperature (Figs. 2 and 3). Stations were assigned to clusters visually by using slope maps that overlapped the stations map. For practical reasons we investigated only clusters with four stations or more. Twenty-eight clusters were identified for BT survey and 17 clusters were identified for EIT survey (Figs. 2 and 3).

Second step—identifying areas of most significant changes in biomass with temperature and quantifying these changes

For each cluster, we calculated mean temperature and percentage of total biomass of pollock present in this cluster in each year. Total biomass and biomass within clusters were calculated as outlined in Wakabayashi et al. (1985). The relationship between mean bottom temperature and percentage of pollock biomass within each cluster was then fitted to a linear regression model. Because the error variances for the BT survey were not constant (variance increased with fish density), we weighted the regression by the inverse of the variance (Neter et al., 1996). For the EIT survey, we made no assumptions about the variance that was due to a small number of observations (only five years of data).

The relative strength of the relationship between the percentage of pollock biomass and temperature within each cluster was characterized by the *P*-value of the slope (Table 1) (the *P*-values are not a true measure of statistical significance because the stations were not chosen randomly). Only clusters with the strongest relationships were used in the interpretation of results. Because the number of data points (years) in each analysis was equal within the survey (BT surveys—20 points, EIT surveys—5 points), *P*-values indicate relative strength of the temperature-biomass relationship. We plotted histograms of *P*-values for

**Figure 2**

Clusters of positive and negative slopes of the linear regression of pollock (*Theragra chalcogramma*) density (detected by echo-integration trawl survey) when plotted against temperature. Columns represent predicted percent biomass of fish in these clusters within the observed range of temperatures. Predicted percent of biomass is shown only for clusters with the strongest relationship between temperature and fish density with the exception of cluster F1 (see results for explanation). Labels are located at the geographic centers of the clusters.

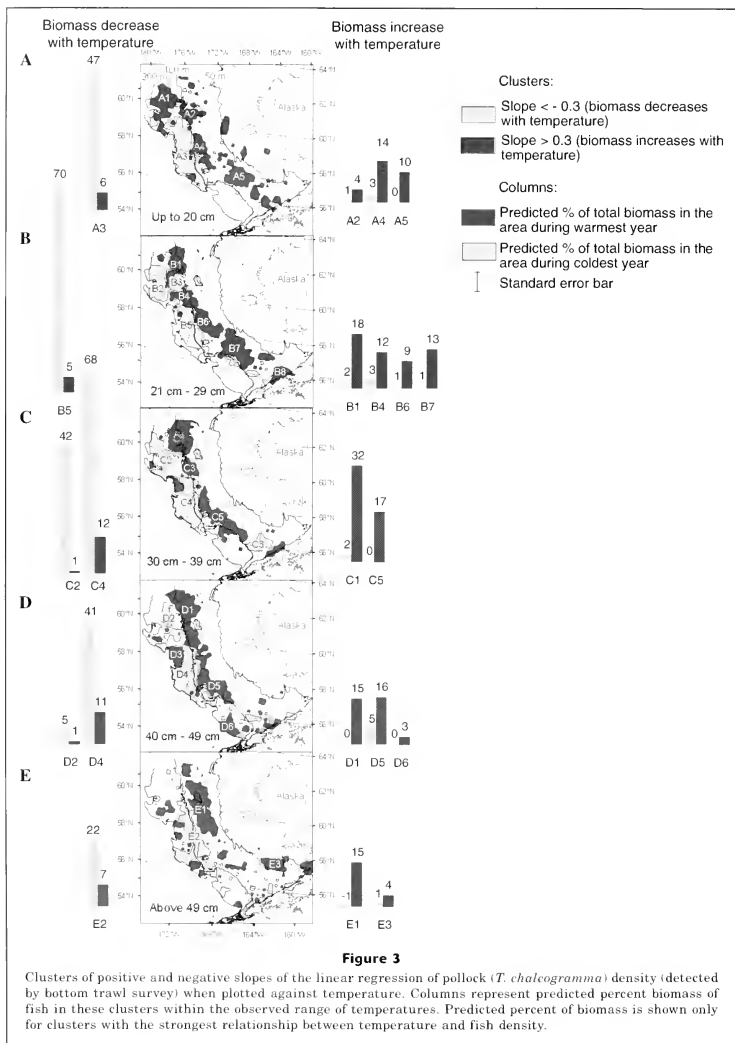
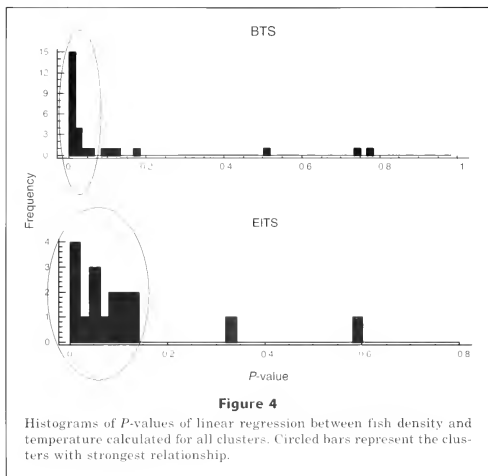


Table 1

Results of linear regression analyses and predicted percent of total biomass in each cluster within an observed range of temperatures.

Cluster	Slope	Standard error of slope	Intercept	r^2	P	Percentage at min. temperature	Standard error of min. percentage	Percentage at max. temperature	Standard error of max. percentage
Botton trawl survey									
A1	3.0706	4.579	7.2013	0.024	0.511	8.82	5.07	15.49	4.89
A2	1.1579	0.382	1.6145	0.338	0.007	0.55	0.36	4.31	1.01
A3	-24.0232	6.812	98.8454	0.409	0.002	47.04	5.33	5.79	6.38
A4	3.3081	1.254	2.9747	0.279	0.017	3.14	1.22	13.75	2.84
A5	2.7928	0.837	-0.5577	0.382	0.004	0.08	0.47	10.13	2.65
B1	6.2744	1.655	4.5969	0.444	0.001	1.98	1.21	18.30	3.13
B2	-5.7916	3.445	24.2379	0.136	0.110	21.73	6.37	5.44	3.34
B3	-0.2449	0.839	4.9690	0.005	0.774	4.86	2.07	4.07	0.70
B4	3.6720	1.880	1.4972	0.175	0.066	2.83	0.52	12.05	4.33
B5	-26.2623	7.642	106.0603	0.396	0.003	70.17	14.89	5.08	4.06
B6	1.9462	0.756	2.9913	0.269	0.019	0.62	1.12	9.27	2.31
B7	3.4809	1.408	-0.5292	0.253	0.024	0.77	0.23	13.03	4.94
B8	0.5026	0.350	0.0979	0.103	0.168	0.10	0.44	2.47	1.30
C1	10.9174	2.355	10.7957	0.544	0.000	2.28	0.31	32.32	6.32
C2	-17.9173	5.809	60.4987	0.346	0.006	42.49	7.89	0.51	5.72
C3	1.1807	0.731	1.5962	0.127	0.124	0.84	1.20	4.68	1.26
C4	-26.8246	7.771	116.1162	0.398	0.003	68.32	10.03	12.06	6.27
C5	5.3395	1.413	-3.3847	0.442	0.001	0.11	1.79	16.77	2.65
C6	-1.4934	0.843	6.3588	0.148	0.094	4.77	2.07	0.89	0.28
D1	5.4677	1.368	7.2510	0.470	0.001	-0.15	0.44	15.42	3.55
D2	-1.9038	0.850	5.7227	0.218	0.038	4.50	1.39	0.87	0.45
D3	0.9668	2.954	2.9573	0.006	0.747	4.89	1.28	6.65	4.19
D4	-14.3609	5.356	65.9267	0.285	0.015	41.08	8.45	10.70	2.89
D5	3.6882	1.411	2.7672	0.275	0.018	4.92	1.18	15.81	3.02
D6	2.3974	0.830	-8.0125	0.317	0.010	0.04	0.31	2.60	0.81
E1	4.5778	0.733	6.1399	0.684	0.000	-1.45	1.13	14.86	1.56
E2	-5.7776	1.910	26.8244	0.337	0.007	22.13	3.71	7.32	1.24
E3	0.6479	0.217	0.9447	0.332	0.008	0.91	0.28	3.80	1.01
Echo-integration trawl survey									
F1	16.0479	13.649	-1.2116	0.315	0.324	10.35	21.80	51.49	20.57
F2	-27.5255	9.304	79.2218	0.744	0.059	59.39	14.86	11.18	14.02
F3	11.7970	3.622	-13.4672	0.779	0.047	-4.97	5.76	25.28	5.46
F4	5.1896	8.463	-3.8753	0.111	0.583	-0.13	13.52	13.17	12.75
G1	32.3770	4.047	-12.0017	0.955	0.004	11.32	6.46	94.33	6.10
G2	-25.5850	10.151	75.6302	0.679	0.086	57.20	16.22	-8.40	15.30
H1	28.0501	4.012	-16.7011	0.942	0.006	3.51	6.41	75.42	6.05
H2	-10.6961	2.999	32.2026	0.809	0.037	24.50	4.79	-2.93	4.52
H3	-11.0388	3.249	38.1076	0.793	0.042	30.16	5.19	1.85	4.90
H4	-5.0998	2.465	13.8907	0.587	0.130	10.22	3.94	-2.86	3.71
I1	19.1934	7.184	-13.8822	0.704	0.075	-0.06	11.48	49.15	10.83
I2	-21.2245	8.449	73.6602	0.677	0.086	58.37	13.50	3.95	12.73
I3	2.3497	1.169	-0.0335	0.573	0.138	1.66	1.87	7.68	1.93
J1	-15.6292	2.465	50.1504	0.930	0.007	38.89	3.94	-1.18	3.72
J2	9.6097	4.374	-6.9678	0.616	0.115	-0.04	6.99	24.59	6.59
J3	9.7424	1.675	1.5600	0.918	0.010	8.58	2.68	33.56	2.53
J4	-5.8055	2.571	17.1422	0.629	0.109	12.96	4.11	-1.92	3.88



each survey (Fig. 4) and the groups of clusters with the strongest relationships between fish biomass and temperature were chosen for further investigations. These groups consisted of 21 clusters from BT surveys with *P*-values between 0.000 and 0.066 and 15 clusters from EIT surveys with *P*-values between 0.004 and 0.138. Using linear regression models (biomass against temperature), we calculated the predicted percentage of the total pollock biomass for each of these clusters (Table 1) within the temperature range observed during surveys (Fig. 5).

To evaluate a spatial scale on which biomass redistribution occurred for the EIT surveys, we calculated mean distance between clusters of negative and positive slope (Table 2). To obtain these values, we generated 100 random points within each of the clusters and calculated the mean distance between all possible pairs of points from both clusters. We did not attempt to calculate this distance for the BT surveys because of the much more complicated nature of the BT cluster maps.

Results

Northward and inshore shifts in pollock distribution in warmer years were found in the EBS for all length categories. The location and magnitude of these shifts and distance between clusters differed with the survey type and length categories. In the present study we address changes in pollock distribution by length category within each survey.

Table 2

Mean distance between largest echo-integration trawl (EIT) survey clusters. Clusters for pollock >50 cm were not calculated because of low selectivity of the EIT survey for these fish.

Clusters	Mean distance (km)	99% confidence interval (km)
F2-F1	241.3	2.3
G2-G1	217.5	2.5
H4, H3, H2-H1	368.3	4.7
I2-I1	453.7	3.9

Echo-integration trawl survey

The biomass of pollock <20 cm in cluster F2 near Zem-chung Canyon at latitude 59°N decreased (with increasing temperature) from about 59% of the total biomass of pollock in the coldest year to 0% in the warmest year (Fig. 2A). This decrease was partially offset by the increase in pollock biomass in area F3, northwest of the Pribilof Islands. The relatively weak relationship (*P*-value=0.324) between pollock biomass and temperature in cluster F1 (north of F2) was caused by the extremely high abundance of <20 cm pollock within cluster F4 during 1997. Therefore the percentage of total

biomass was particularly low in clusters F1, F2, and F3 for that year. In cluster F1 we observed an increase in biomass from 10% to 51%.

For pollock 21–29 cm, changes between cluster G2 and G1 resembled changes between clusters F2 and F1. The percentage of total biomass in these two clusters changed from 57% to 0% and from 11% to 94%, respectively (Fig. 2B).

A slightly different situation was observed for pollock 30–39 cm (Fig. 2C). We identified three clusters of decreasing biomass with temperature: H2, H3, and H4 located, respectively, northwest of Zhemchug Canyon, northwest and east of the Pribilof Islands. Overall predicted biomass change in H2, H3, and H4 decreased from 65% to 2%. The offset for this negative change was found in cluster H1, where we noted a positive change from 4% to 75%.

Areas with decreasing fish biomass for pollock 40–49 cm were located within cluster I2 (Fig. 2D). Biomass decreased from 58% in the coldest year to 4% in the warmest year. We observed temperature-related increases in biomass mostly north of I2 in cluster I1 (0%–49%).

A quite different situation was observed for pollock >50 cm (Fig. 2E). Although pollock of this size seemed to concentrate northwest and northeast of the Pribilof Islands (similar to pollock 30–49 cm) during cold years; in warm years they were found in EIT surveys mainly in the southeast, as opposed to the smaller fish that are found mainly in the north. Results for pollock >50 cm should be treated cautiously because only a very small part of the entire population of pollock this size can be detected with the EIT survey (Ianelli et al.³). Because of the benthic habits of pollock >50 cm (Shuntov et al., 1993), most were detected in BT surveys.

Overall, our analysis of EIT survey data indicated a northward temperature-related shift of 50–80% of pollock <50 cm in two major areas. With increasing temperature, the density of pollock <40 cm decreased northwest of Zhemchug Canyon in a large area at 100 m to 200 m depths. Similarly, the density of pollock 30–49 cm decreased northwest of the Pribilof Islands. Offsetting these decreases, pollock density increased in the northernmost area of the survey (close to the U.S.-Russia Convention Line).

Although the direction of the shift was the same for all length categories up to 50 cm, the mean distance between the clusters with negative slopes and clusters with positive slopes increased with fish size (Table 2).

Bottom trawl survey

For pollock <20 cm, we observed a decrease in pollock biomass with temperature in cluster A3 covering the

area west of the Pribilof Islands and north to Zhemchug Canyon (Fig. 3A). We observed an increase in pollock biomass in shallower areas north of Pribilof Island (A4), as well as in the areas of 50–100 m depth east from the Pribilof Islands (A5). The magnitude of change was somewhat smaller than that observed for the EITS survey (see Fig. 3A for details).

For pollock 20–29 cm, we observed a decrease in biomass from 70% to 5% in the area northwest of the Pribilof Islands (cluster B5). A cumulative increase in biomass from 7% to 52% of total biomass was observed in clusters B1 and B4 north of B5, and in clusters B6 and B7 in shallower waters (Fig. 3B). Relatively weak relationships were found between pollock biomass and temperature for clusters B2, B3, and B8.

For pollock 30–39 cm, we observed a temperature-related decrease in biomass in clusters C2 and C4 (42% to 1%, and 68% to 12% accordingly) (Fig. 2C). Increase in biomass was observed in cluster C1 (2–32%) north from C2. Positive change was also observed in cluster C5 (0–17%) within the shallow (<100 m) part of the southeastern Bering Sea shelf.

Clusters D2 and D4 represented areas where we observed a significant decrease in biomass for pollock 40–49 cm (from 5% to 1%, and from 41% to 11%) (Fig. 3D). Increased biomass was detected in cluster D1 located north from D4 and in D5 located to the east of D4 in shallower waters.

Very small changes were detected for pollock >50 cm. Although three clusters had a relatively strong pollock biomass and temperature relationship, the magnitude of biomass changes within the range of observed temperatures was quite small (Fig. 3E).

Overall, as with the EIT surveys, northward shifts in distribution in warmer years were found in the BT survey data for pollock <30 cm. The magnitude of these northward shifts was somewhat smaller (15–30%) than those detected by EIT surveys. In addition, these data suggested an inshore eastward redistribution of pollock in warmer years. Changes for pollock >50 cm were evident but small (in the range of 15%).

Discussion

Inferring seasonal pollock migration from interannual variations in distribution

Interannual differences in the timing of the migration from spawning grounds to forage areas are related to water temperatures. The relationship between temperature and the spatial distribution of a seasonally migrating species could represent either a change in the winter location of the stock or a change in the timing of the migration or both (Mountain and Murawski, 1992). Although the evidence is not conclusive, data suggest that most pollock populations spawn in late winter or early spring in the same locations year after year (Bailey et al., 1999a). For example, large, prespawning aggregations of pollock have been surveyed around

³ Ianelli, J. N., T. Buckley, T. Honkalehto, N. Williamson, and G. Walters. 2001. Bering Sea-Aleutian Islands walleye pollock assessment for 2002. In Stock assessment and fishery evaluation report for the groundfish resources of the Bering Sea/Aleutian Islands regions, p. 1–105. North Pac. Fish. Manag. Council, Anchorage, AK.

Bogoslof Island every year since 1988 in the winter (Honkalehto et al.⁴). Further support that temperature is related to the timing of the postspawning migration may come from temperature effects on physiological aspects of spawning. Cold water temperatures may delay the onset of spawning and extend the spawning period of walleye pollock as has been found for another gadid (Kjesbu, 1994) and for flatfish (Lange and Greve, 1997) in the Atlantic.

The surveyed distribution of pollock in warmer years should be more representative of that seen later in a typical spring-summer warming cycle than the distribution of pollock seen in colder years. Bottom temperatures generally increased over the EBS and northern Bering Sea (NBS) during spring and summer (Overland et al., 1999; Khen et al., 2001; Stabeno et al., 2001). Our results show that the warmer the bottom water during spring-summer groundfish surveys, the farther away pollock <50 cm are found from their major spawning grounds. Thus, we interpret areas having lower pollock density with increasing temperature (clusters with negative slope) to be areas from which pollock are emigrating, and areas having higher pollock density with increasing temperature (clusters with positive slope) to be areas to which pollock are immigrating (Figs. 2 and 3).

Routes and directions of the migrations

As the water warms during spring and summer, pollock generally migrate northward, northwestern, and inshore to shallower waters. Larger pollock (>30 cm) begin their feeding migration from spawning grounds. In many areas (white areas—Figs. 2 and 3) we did not detect a significant increase or decrease in pollock abundance in relation to temperature, e.g., in the major pollock spawning area north of Unimak Island (Hinckley, 1987; Bulatov, 1989), and this finding may indicate that migration progressed beyond this area before it was surveyed, even in the coldest years, or that migrations were not pronounced in this area. However, we observed a very large decrease in biomass with increasing temperature in the Pribilof Islands area (i.e., within clusters A3, B5, C4, D4, E2, H3, and I2), which is another important pollock spawning location (Maeda and Hirakawa, 1977; Hinckley, 1987; Bulatov, 1989; Bailey et al., 1999a). An offsetting increase in biomass was observed in the northernmost part of the survey area (clusters B1, C1, D1, F1, G1, H1, and I1) and in shallower waters (clusters A4, A5, B6, B7, C5, and D5), which may indicate that pollock migrate north and inshore during the warming season. Echo integration trawl data indi-

cate that smaller pollock (<29 cm) probably begin their migration from overwintering areas (clusters F2 and G2) located mainly northwest of the Zhemchug Canyon. These results agree with observations made by Bailey et al. (1999b) that small age-0, age-1, and age-2 pollock are distributed farther north than larger age-3 and older pollock. Migrations continued generally northward to the U.S.-Russia Convention Line. The near-bottom part of the pollock population (detected in the BT survey) also migrates northeastward into shallower waters. At this point we cannot describe the exact starting and ending points of migration but only the general direction, because surveys are performed after most of the spawning has been completed, and we lacked data for the NBS, where part of the pollock EBS population is probably migrating.

The direction of movements indicated by the EIT survey data and the BT survey data were somewhat different because of the effect of depth on the availability of pollock to each survey. As pollock migrate into shallower water they become more available to the BT survey and less available to the EIT survey. Therefore the BT survey indicates greater movement into shallower water, whereas the EIT survey indicates greater movement in a northerly direction.

Seasonal migrations by pollock in the EBS are broadly recognized as occurring but have not been well substantiated; however, most of the general observations and descriptions are in agreement with our results. It is generally recognized that the feeding migration of some EBS pollock takes them northwestern beyond our survey area and into Russian waters (Shuntov et al., 1992; 1993; Stepanenko, 2001). Pola (1985), in her numerical simulation of pollock migrations in the EBS identified two types of pollock feeding migration. One was temperature induced in the northward direction, and the other was seasonal in the northeastern direction toward shallower waters. Shuntov et al. (1993) considered migrational activity to start with the onset of sexual maturity, but our findings indicate that immature pollock do undergo feeding migrations in a northwestern direction, but over shorter distances than those traveled by mature pollock. Stepanenko (2001) also recognized migration by immature pollock. Only a few pollock tagged in the EBS have been recovered (Yoshida, 1985), but the relationships between the release and recovery locations are consistent with our findings of a northwestern feeding migration during the spring and summer over most of the EBS shelf and a northeastward migration into shallower water on the southeast EBS shelf.

Length-based differences in migration patterns

Our analysis of the EIT surveys indicates that the migrations of pollock <30 cm are shorter than those of pollock 30–50 cm. The distance pollock need to cover from clusters F2 and G2 to clusters F1 and G1 (241.3 km and 217.5 km) is much shorter than the distance to be covered by larger fish from clusters H4, H3, H2,

⁴ Honkalehto, T., N. Williamson, D. Hanson, D. McKelvey, and S. de Blois. 2002b. Results of the echo integration-trawl survey of walleye pollock (*Theragra chalcogramma*) conducted on the southeastern Bering Sea shelf and in the southeastern Aleutian Basin near Bogoslof Island in February and March 2002. AFSC Processed Report 2002-02, 49 p. Alaska Fish. Sci. Cent., NOAA, Natl. Mar. Fish. Serv., 7600 Sand Point Way NE, Seattle, WA 98115.

and I2 to clusters H1 and I1 (368.3 km and 453.7 km, respectively). Similar size-dependent differences in the distance of seasonal migrations were reported for Pacific hake (*Merluccius productus*), another gadoid from the north Pacific (Dorn, 1995). These observations may support the length-based hypothesis of Nøttestad et al. (1999) for feeding migrations in pelagic fish. Focusing on the energetic cost-benefit relationship of long distance migration, they concluded that migration distance is a function of length, weight, and age. Smaller fish may undergo shorter feeding migrations because the energetic cost of migration can exceed their total energy intake resulting from the of greater hydrodynamic drag associated with smaller fish size.

Migrations of the largest pollock (>50 cm), detected from the BT survey data, were of much lower magnitude than those of smaller fish. Our models indicate that only about 15% of fish in this length category move between clusters in the northeastern direction toward shallower waters. These small changes detected in BT data contradict those seen in EIT data. Whereas a small northward shift in biomass (mostly from cluster E2 to cluster E4) was detected with BT data, a southeastward shift was detected with EIT data. However, because the EIT survey is not well suited for estimating the distribution of pollock >50 cm, we are inclined to put more weight on the BT data to explain temperature-related changes in biomass distribution for this length category. Larger pollock (>50 cm) appear to change their migratory behavior. Shuntov (1992) noticed that the distribution of larger pollock (>54 cm) fundamentally differs from that of smaller pollock and that larger pollock are more benthic in behavior and feeding. Stepanenko (2001) did not observe any migrations to the Russian zone for pollock six years or older. We propose that the difference in the migratory behavior between pollock <50 cm and pollock >50 cm is linked to a well-known shift toward a diet of fish with increasing pollock size (Bailey and Dunn, 1979; Dwyer et al., 1987).

Why do pollock migrate?

Pollock feeding migrations in the EBS may be driven by a combination of four factors: temperature, zooplankton production, currents, and length of daylight.

Changes in the water temperature may affect pollock migrations. Bottom water temperature over the Bering Sea shelf rises between April and September (Pavlov and Pavlov, 1996; Overland et al., 1999; Khen et al., 2001; Stabeno et al., 2001). Our results indicate that with rising temperature pollock generally migrate northward and inshore. Pollock appear to avoid temperatures below 0°C (Swartzman et al., 1994); therefore a seasonal increase in temperature above 0°C can open new geographic areas for migration. Temperature was presented as one of several important stimuli affecting fish movements by Harden Jones (1968) and by Wielgolaski (1990), who noticed that capelin (*Mallotus villosus*), Atlantic cod (*Gadus morhua*), and haddock (*Melanogrammus aeglefinus*) in the Barents Sea migrate

north towards a preferred temperature, either directly to satisfy metabolic requirements, or indirectly, as when attracted by food organisms.

Seasonal patterns in zooplankton production and prey availability largely coincide with seasonal patterns in pollock migration and distribution. The role of food availability in driving fish-feeding migrations has been described for other zooplanktivores such as Pacific hake (Dorn, 1995), Atlantic herring (*Clupea harengus*), blue whiting (*Micromesistius poulassou*), mackerel (*Scomber scombrus*) and capelin (Nøttestad et al., 1999). In the Bering Sea, the abundance of zooplankton is high on the EBS and NBS shelf throughout spring and summer, but it remains high in autumn only in the NBS (Springer et al., 1989; Chuchukalo et al., 1996; Coyle et al., 1996). Copepods and euphausiids are major prey groups for pollock during spring and summer in the northwest area of the EBS shelf, but in autumn, 30–49 cm pollock increase their feeding on fish and decapods (Dwyer et al., 1987) which may be related to a decrease in the availability of these prey (Willette et al., 1999) in this area. Further north in the Navarin-Anadyr area, copepods and euphausiids remain major prey components in the diet of pollock <50 cm through summer and autumn (Shuntov et al., 2000). The migration pattern of pollock indicates they may follow their food supply as the production and abundance of zooplankton proceeds northward. Pollock larger than 50 cm do not undergo northward feeding migrations because small pollock, other fish, and benthos are the main components of the diet (Dwyer et al., 1987; Yoshida, 1994; Shuntov et al., 2000).

In the area of pollock migrations northwest of Pribilof Islands current speeds are in the range of 1–5 cm/s at the 100 m depth and they generally run in the northwest direction (Stabeno et al., 2001). Current direction coincides with the direction of pollock migrations, so that the cost of the migration may be offset by swimming in the same direction as the transporting current (Nøttestad et al., 1999). Water currents can also influence fish migration indirectly by providing visual stimuli arising from the moving background (Harden Jones, 1968) or by transporting food. Springer et al. (1989) suggested that the transport of zooplankton by the northwest current may cause greater levels of zooplankton concentration in the NBS. Because of the lack of data on current speed, he speculated that a current velocity in the range of 20 cm/s was needed to explain these high levels of zooplankton in the NBS if the high levels of zooplankton are based only on currents. The latest observations of current on the Bering Sea shelf do not support these hypotheses (Stabeno et al., 2001). However northwestern currents may contribute to higher zooplankton biomass in the NBS.

Nøttestad et al. (1999) suggested that light conditions may play a role in fish feeding migrations because during summer day-length increases the farther north fish travel, thus potentially increasing feeding duration for pelagic visual predators. Pollock are visual predators and light conditions affect feeding efficiency of pollock

(Ryer and Olla, 1999; Ryer et al., 2002); therefore it may be that longer days at northern latitudes make a northward feeding migration beneficial by possibly providing an extended window of search time if the pollock happen to be in a locally depauperate area. However, day-length remains long enough in the entire Bering Sea for pollock to feed to satiation, and their gastric evacuation rate is slow (Dwyer et al., 1987), making the need to entirely fill their stomachs every day very unlikely.

At this time it is impossible to assess which factor is most important in driving pollock migrations, but in summary we can conclude that pollock, as visual pelagic predators, benefit from northward feeding migrations during seasonal warming. Because three of the factors (excluding current) are similar throughout the Northern Hemisphere, we should see similar migration patterns for other pelagic fish of the north. Other examples include Pacific hake migrating along the North American west coast from California to British Columbia (Francis and Bailey, 1983; Dorn, 1995). Herring in the Norwegian Sea undergo seasonal feeding migrations in the northwestern direction from the south-central coast of Norway to the areas located northeast of Iceland (Ferno, 1998). Blue whiting, mackerel, and capelin from the north Atlantic undergo northward feeding migrations (Nøttestad et al., 1999). Pacific saury (*Cololabis saira*), chub mackerel (*Scomber japonicus*), Pacific sardine (*Sardinops sagax melanosticta*), and Japanese anchovy (*Engraulis japonicus*) from the western North Pacific are reported to migrate northwards during the summer (Novikov, 1986). Capelin, Atlantic cod, and haddock in the Barents Sea migrate north towards a "preference" temperature during summer (Wielgolaski, 1990). All these species have characteristics similar to those of Bering Sea pollock—that is, a pelagic or semipelagic life style, a diet of zooplankton, winter or spring spawning activity, and feeding migrations that take place during spring and summer.

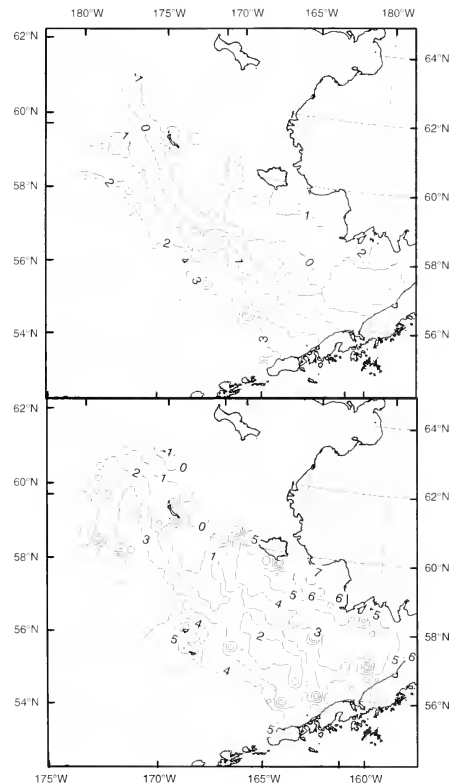


Figure 5

Bottom water temperature contours during the bottom trawl survey in the coldest year (1999—upper map) and warmest year (1996—lower map).

Why is temperature important?

Temperature may affect the proportion of the stock that is in the standard EBS survey area. Ianello et al.,⁵ using population modeling, estimated that fewer pollock were detected during the BT survey in the EBS with increasing temperature, and fewer pollock would indicate that pollock are probably leaving the survey area during seasonal migrations. We conclude that a significant part of the EBS pollock population migrates into the Navarin-Anadyr area, which can have an impact on the way the EBS stock is managed. We should account for landings of pollock in the Navarin-Anadyr area, estimate how much of these landings include pollock from the EBS stock, and use this estimate in determining the EBS total allowable catch. Further research is needed to quantify the proportion of the EBS stock migrating into the Russian fishing zone and to estimate the number of pollock caught there. Stokes⁵ suggested that the biomass estimates from the NBS are in the range of 0.5–1.0 million

⁵ See next page for footnote text.

metric tons per annum and the exploitation rate is in the range of 0.5 million metric tons (50–100% of the total estimate).

Ongoing climate changes may affect pollock distribution between the U.S. and Russian EEZs. Stabeno and Overland (2001) reported a shift toward an earlier spring transition in the Bering Sea. This can affect the starting time of pollock migrations and the length of time fish spend in the Russian EEZ, increasing the availability of fish to the Russian fleet. This situation should encourage us to closely monitor changes in migration patterns of pollock in the Bering Sea.

Significant bias or error variation may be caused by the interaction of fish movement with survey protocol. For even relatively low fish migration velocities (<0.5 m/s), bias in estimated fish biomass can be very large (McAllister, 1998). Therefore, fish migration vectors should be estimated to minimize the bias created by not taking into account these migrations in biomass estimates.

Acknowledgments

The authors thank Angie Greig and Jan Benson for an introduction to ArcGIS and help with geospatial problems that occurred during analyses of data. We also want to thank Kevin Bailey, Jerry Hoff, Jim Ianelli, Jay Orr, David Somerton, Phyllis Stabeno, Gary Stauffer, Neal Williamson, and three anonymous reviewers for discussions and review of earlier versions of this manuscript.

Literature cited

- Bailey, K., and J. Dunn.
1979. Spring and summer foods of walleye pollock, *Theragra chalcogramma*, in the eastern Bering Sea. *Fish. Bull.* 77:304–308.
- Bailey, K. M., T. J. Quinn II, P. Bentzen, and W. S. Grant.
1999a. Population structure and dynamics of walleye pollock, *Theragra chalcogramma*. *Adv. Mar. Biol.* 37:179–255.
- Bailey, K. M., D. M. Powers, J. M. Quattro, G. Villa, A. Nishimura, J. J. Traynor, and G. Walters.
1999b. Population ecology and structural dynamics of walleye pollock (*Theragra chalcogramma*). In *Dynamics of the Bering Sea* (T. R. Loughlin and K. Ohtani, eds.), p. 581–614. Univ. Alaska Sea Grant publ. AK-SG-99-03, Fairbanks, AK.
- Balykin, P. A.
1996. Dynamics and abundance of western Bering Sea pollock. In *Ecology of the Bering Sea*, p. 177–182. Alaska Sea Grant Report 96-01, Fairbanks, AK.
- Bulatov, O. A.
1989. Reproduction and abundance of spawning pollock in the Bering Sea. In *Proceedings of the international symposium on the biology and management of walleye pollock*; November 14–16, 1988, Lowell Wakefield Fisheries Symposium, p. 199–208. Alaska Sea Grant Report 89-1, Anchorage, AK.
- Bulatov, O. A., and E. I. Sobolevskiy.
1990. Distribution, stocks, and fishery prospects of walleye pollock in the open waters of the Bering Sea. *Biologiya Morya* 5:297–304.
- Chuchukalo, V. I., N. A. Kuznetsova, and V. V. Napazakov.
1996. Seasonal distribution of euphausiids in the Bering and Okhotsk Sea and adjacent waters of Pacific Ocean. *Izv. TINRO*, 119:256–281.
- Coyle, K. O., V. G. Chaytor, and A. I. Pinchuk.
1996. Zooplankton of the Bering Sea: a review of Russian-language literature. In *Ecology of the Bering Sea*, p. 97–134. Alaska Sea Grant Report 96-01, Fairbanks, AK.
- Dorn, M. W.
1995. The effects of age composition and oceanographic conditions on the annual migration of Pacific whiting, *Merluccius productus*. *CalCOFI Rep.* 36:97–105.
- Dwyer, D. A., K. M. Bailey, and P. A. Livingston.
1987. Feeding habits and daily ration of walleye pollock (*Theragra chalcogramma*) in the eastern Bering Sea, with special reference to cannibalism. *Can. J. Fish. Aquat. Sci.* 44:1972–1984.
- Efimkin, A. Y., and V. I. Radchenko.
1991. State of food resources and distribution of epipelagic fish in the western Bering Sea in the fall. *Sov. J. Mar. Biol.* (English translation from *Biologiya Morya*) 17(1):18–28.
- Fadeyev, N. S.
1989. Spatial and temporal variability of the eastern Bering Sea walleye pollock size composition in relation to its migrations. In *Proceedings of the international symposium on the biology and management of walleye pollock*; November 14–16, 1988, Lowell Wakefield Fisheries Symposium, p. 325–347. Alaska Sea Grant Report 89-1, Anchorage, AK.
- Ferno, A., T. J. Pitcher, W. Melle, L. Nottestad, S. Mackinson, C. Hollingworth, and O. A. Misund.
1998. The challenge of the herring in the Norwegian Sea: making optimal collective spatial decisions. *Sarsia* 83:149–167.
- Francis, R. C., and K. M. Bailey.
1983. Factors affecting recruitment of selected gadoids in the northeast Pacific and east Bering Sea. In *From year to year* (W. S. Wooster, ed.), p.35–60. Washington Sea Grant WSG-No.83-3, Univ. Washington, Seattle, WA.
- Harden Jones, F. R.
1968. Fish migration. St. Martin's Press, New York, NY.
- Hinckley, S.
1987. The reproductive biology of walleye pollock, *Theragra chalcogramma*, in the Bering Sea, with reference to spawning stock structure. *Fish. Bull.* 85:481–498.
- Khen, G. V., A. I. Kafanov, and E. O. Basyuk.
2001. Chapter 7: General characteristics. In *Hydro-meteorology and hydrochemistry of the seas, vol 10: Bering Sea* (Terzyev, F. S., B. M. Zatchnoy, and A. P. Alexeyev, eds.), p. 122–136. St. Petersburg Gidrometeoizdat, St. Petersburg, Russia. [In Russian.]

⁵ Stokes, T. K. 2000. Review of Alaska pollock assessment. Appendix 3 in *Eastern Bering Sea walleye pollock stock assessment for 2001* (J. N. Ianelli, L. Fritz, T. Honkalehto, N. Williamson, and G. Walters), p. 179–188. In *Stock assessment and fishery evaluation report for the groundfish resources of the Bering Sea/Aleutian Islands regions*. North Pac. Fish. Manag. Council, Anchorage, AK.

- Kjesbu, O. S.
1994. Time of start of spawning in Atlantic cod (*Gadus morhua*) females in relation to vitellogenic oocyte diameter, temperature, fish length and condition. *J. Fish Biol.* 45(5):719-735.
- Kooka, K., T. Takatsu, Y. Kamei, T. Nakatani, and T. Takahashi.
1998. Vertical distribution and prey of walleye pollock in the northern Japan Sea. *Fish. Sci.* 64(5):686-693.
- Lange, U., and W. Greve.
1997. Does temperature influence the spawning time, recruitment, and distribution of flatfish via its influence on the rate of gonadal maturation? *Dtsch. Hydrogr. Z.* 49(2/3):251-263.
- Maeda, T.
1986. Life cycle and behavior of adult pollock (*Theragra chalcogramma* (Pallas)) in waters adjacent to Funka Bay, Hokkaido Island, Symposium on biology, stock assessment, and management of pollock, Pacific cod and hake in the North Pacific region. INPFC Bull. 45:39-65.
- Maeda, T., and H. Hirakawa.
1977. Spawning grounds and distribution pattern of the Alaska pollock in the eastern Bering Sea. *Bull. Jap. Soc. Sci. Fish.* 43:39-45. [In Japanese, English summary.]
- Maeda, T., T. Nakatani, T. Takahashi, S. Takagi, and B. Melteff.
1989. Distribution and migration of adult walleye pollock off Hiyma, Southwestern Hokkaido. In *Proceedings of the international symposium on the biology and management of walleye pollock*; November 14-16, 1988, Lowell Wakefield Fisheries Symposium, p. 325-347. Alaska Sea Grant Report, 89-1, Anchorage, AK.
- Maeda, T., T. Takahashi, and T. Nakatani.
1988. Distribution, migration and spawning grounds of adult walleye pollock *Theragra chalcogramma* in the coastal waters of Hiyma Subprefecture, Hokkaido. *Bull. Fac. Fish. Hokkaido Univ.* 39(4):216-229.
- McAllister, M. K.
1998. Modeling the effects of fish migration on bias and variance in area swept estimates of biomass: a vector based approach. *Can. J. Fish. Aquat. Sci.* 55:2622-2641.
- Mountain, D. G., and S. A. Murawski.
1992. Variation in the distribution of fish stocks on the northeast continental shelf in relation to their environment, 1980-1989. *ICES Mar. Sci. Symp.* 195:424-432.
- Neter, J., M. H. Kutner, C. J. Nachtsheim, and W. Wasserman.
1996. *Applied linear regression models*, 3rd ed., 720 p. Irwin, Chicago, IL.
- Nottestad, L., J. Giske, J. C. Holst, and G. Huse.
1999. A length-based hypothesis for feeding migrations in pelagic fish. *Can. J. Fish. Aquat. Sci.* 56(suppl.):26-34.
- Novikov, Y. V.
1986. Some trends of distribution and migration of common pelagic fishes of the northwestern Pacific Ocean. *J. Ichthyol.* 26(2):161-172.
- Overland, J. E., S. A. Salo, H. K. Lakshmi, and C. A. Clayson.
1999. Thermal stratification and mixing on the Bering Sea shelf. In *Dynamics of the Bering Sea* (T. R. Loughlin and K. Ohtani, eds.), p. 129-146. Univ. Alaska Sea Grant, AK-SG-99-03, Fairbanks, AK.
- Pavlov, V. K., and P. V. Pavlov.
1996. Oceanographic description of the Bering Sea. In *Ecology of the Bering Sea: a review of Russian literature*. (O. A. Mathisen, and K. O. Coyle eds.), p. 135-141. Alaska Sea Grant College Program Report 96-01, Fairbanks, AK.
- Pola, N. B.
1985. Numerical simulations of fish migrations in the eastern Bering Sea. *Ecol. Model.* 29:327-351.
- Radchenko, V. I., and Y. I. Sobolevskiy.
1993. Seasonal spatial distribution dynamics of walleye pollock in the Bering Sea. *J. Ichthyol.* 33(2):63-76.
- Ryer, C. H., A. Lawton, R. J. Lopez, and B. L. Olla.
2002. A comparison of the functional ecology of visual vs. nonvisual foraging in two planktivorous marine fishes. *Can. J. Fish. Aquat. Sci.* 59(8):1305-1314.
- Ryer, C. H., and B. L. Olla.
1999. Light-induced changes in the prey consumption and behavior of two juvenile planktivorous fish. *Mar. Ecol. Prog. Ser.* 181:41-51.
- Shuntov, V. P., E. P. Dulepova, K. M. Gorbatenko, A. M. Slabin-skii, and A. Y. Efimkin.
2000. Feeding of the walleye pollock *Theragra chalcogramma* in the Anadyr-Navarin region of the Bering Sea. *J. Ichthyol.* 40(3):362-369.
- Shuntov, V. P., A. F. Volkov, O. S. Temnykh, and E. P. Dupoleva.
1993. Pollock in the ecosystems of the Far East seas. 425 p. TINRO, Vladivostok Russia. [In Russian.]
- Shuntov, V. P.
1992. Functional structure of the distribution area of walleye pollock in the Bering Sea. *Russ. J. Mar. Biol./Biol. Morya* 17(4):189-198. [A translation from *Biol. Morya*, 1991.]
- Shuntov, V. P., A. F. Volkov, V. I. Matveev, L. V. Cheblukova, and A. V. Gudz.
1987. Development of productive zones in the Sea of Okhotsk during the autumn. *Russ. J. Mar. Biol./Biol. Morya* 12(4):241-247. [A translation from *Biol. Morya* 1986.]
- Springer, A. M., C. P. McRoy, and K. R. Turco.
1989. The paradox of pelagic food webs in the northern Bering Sea—II. Zooplankton communities. *Cont. Shelf Res.* 9(4):359-386.
- Stabeno, P. J., and J. E. Overland.
2001. Bering Sea shifts toward an earlier spring transition. *Eos. Trans. Am. Geophys. Union* 82(29):317-321.
- Stabeno, P. J., N. A. Bond, N. B. Kachel, S. A. Salo, and J. D. Schumacher.
2001. On the temporal variability of physical environment over the south-eastern Bering Sea. *Fish. Oceanogr.* 10(1):81-98.
- Stepanenko, M. A.
2001. Relationship between age and spatial distribution of walleye pollock in the eastern and northwestern Bering Sea. *Izv. TINRO*, 128:125-135. [In Russian.]
- Swartzman, G., E. Silverman, and N. Williamson.
1995. Relating trends in walleye pollock (*Theragra chalcogramma*) abundance in the Bering Sea to environmental factors. *Can. J. Fish. Aquat. Sci.* 52(2):369-380.
- Swartzman, G., W. Stuetzle, K. Kulman, and M. Pwojowski.
1994. Relating the distribution of pollock schools in the Bering Sea to environmental factors. *ICES J. Mar. Sci.* 51(4):481-492.
- Takahashi, Y., and H. Yamaguchi.
1972. Stock of Alaska pollock in the eastern Bering

- Sea. Bull. Jap. Soc. Sci. Fish. 38:389-399. [In Japanese, English summary.]
- Traynor, J. J.
1996. Target strength measurements of walleye pollock (*Theragra chalcogramma*) and Pacific whiting (*Merluccius productus*). ICES J. Mar. Sci. 53:253-258.
- Wakabayashi, K., R. G. Bakkala, and M. S. Alton.
1985. Methods of the US-Japan demersal trawl surveys. INPFC Bull. 44:7-29.
- Wielgolaski, F. E.
1990. A Barents Sea fish resources and migration model. FiskDir. Skr. Ser. HavUnders. 18:381-409.
- Willette, T. M., T. Cooney, and K. Hyer.
1999. Predator foraging mode shifts affecting mortality of juvenile fishes during the subarctic spring bloom. Can. J. Fish. Aquat. Sci. 56:364-376.
- Yoshida, H.
1985. Research on clarification of Alaska pollock resources in the Bering Sea and waters around the Kamchatka Peninsula. Can. Transl. Fish. Aquat. Sci. 5140:1-39.
1994. Food and feeding habits of pelagic walleye pollock in the central Bering Sea in summer, 1976-1980. Sci. Rep. Hokkaido Fish. Exp. Stn. 45:1-35.

Abstract—The identification of larval istiophorid billfishes from the western North Atlantic Ocean has long been problematic. In the present study, a molecular technique was used to positively identify 27 larval white marlin (*Tetrapturus albidus*), 96 larval blue marlin (*Makaira nigricans*), and 591 larval sailfish (*Istiophorus platypterus*) from the Straits of Florida and the Bahamas. Nine morphometric measurements were taken for a subset of larvae (species known), and lower jaw pigment patterns were recorded on a grid. Canonical variates analysis (CVA) was used to reveal the extent to which the combination of morphometric, pigment pattern, and month of capture information was diagnostic to species level. Linear regression revealed species-specific relationships between the ratio of snout length to eye orbit diameter and standard length (SL). Confidence limits about these relationships served as defining characters for sailfish >10 mm SL and for blue and white marlin >17 mm SL. Pigment pattern analysis indicated that 40% of the reflexion blue marlin examined possessed a characteristic lower jaw pigment pattern and that 62% of sailfish larvae were identifiable by lower jaw pigments alone. An identification key was constructed based on pigment patterns, month of capture, and relationships between SL and the ratio of snout length to eye orbit diameter. The key yielded identifications for 69.4% of 304 (blind sample) larvae used to test it; only one of these identifications was incorrect. Of the 93 larvae that could not be identified by the key, 71 (76.3%) were correctly identified with CVA. Although identification of certain larval specimens may always require molecular techniques, it is encouraging that the majority (92.4%) of istiophorid larvae examined were ultimately identifiable from external characteristics alone.

Manuscript submitted 14 July 2004
to the Scientific Editor's Office.

Manuscript approved for publication
6 April 2005 by the Scientific Editor.

Fish. Bull. 103:588–600 (2005).

Toward identification of larval sailfish (*Istiophorus platypterus*), white marlin (*Tetrapturus albidus*), and blue marlin (*Makaira nigricans*) in the western North Atlantic Ocean*

Stacy A. Luthy

Robert K. Cowen

Rosenstiel School of Marine and Atmospheric Science
University of Miami
4600 Rickenbacker Causeway
Miami, Florida 33149

Present address (for S. A. Luthy): Baruch Marine Field Laboratory
P.O. Box 1630
Georgetown, South Carolina 29442

Email address (for S. A. Luthy): stacy@belle.baruch.sc.edu

Joseph E. Serafy

National Marine Fisheries Service
Southeast Fisheries Science Center
75 Virginia Beach Drive
Miami, Florida 33149

Jan R. McDowell

The Virginia Institute of Marine Science
School of Marine Science
College of William and Mary
P.O. Box 1346
Gloucester Point, Virginia 23062

Research on the early life history of exploited fishes benefits management efforts by elucidating the temporal and spatial distribution of spawning, cohort strength, and biological and physical factors affecting recruitment (Lasker, 1987). The ability to confidently identify specimens to species is necessary in any early life history study (Collette and Vecchione, 1995). This has not yet been achieved for larval billfishes of the family Istiophoridae from the Atlantic Ocean: sailfish (*Istiophorus platypterus*), blue marlin (*Makaira nigricans*), white marlin (*Tetrapturus albidus*), and longbill spearfish (*Tetrapturus pfluegeri*).

Larval istiophorids are easily distinguished from larval swordfish (*Xiphias gladius*, family Xiphiidae). However, larval istiophorids are dif-

ficult to identify below the family level. Full fin-ray complements are not present until a larva reaches 20 mm in length, and even then, meristic counts are of limited use for identification because of significant overlap in counts among species. At best, species possibilities can be eliminated only for specimens with counts in the extremes of their ranges (Richards, 1974). The only definitively diagnostic count is the vertebral formula for *Makaira* (11 precaudal and 13 caudal) versus that of the other istiophorids (12 precaudal and 12 caudal) (Richards, 1974). Larger blue marlin lar-

* Contribution SFD-2003-0010 from NOAA Fisheries Sustainable Fisheries Division, Southeast Fisheries Science Center, 75 Virginia Beach Drive, Miami, Florida 33149.

vae may also be identified by the presence of a complex lateral line. Ueyanagi (1964) found this character in Pacific blue marlin of 20 mm standard length (SL), but the smallest SL of an Atlantic blue marlin from a recent collection in which a complex lateral line was visible was 26.9 mm. At lengths <20 mm, specific identification of istiophorids is even more uncertain. Ueyanagi (1963; 1964) based the identification of Indo-Pacific istiophorids <5 mm SL on four characters: 1) anterior projection of the eye orbit; 2) the position of the tip of the snout in relation to the middle of the eye; 3) presence of pigments on the branchiostegal and gular membranes; and 4) whether the pectoral fins are rigid—a character that applies to larval black marlin (*Makaira indica*), a species not known to spawn in the Atlantic Ocean. For fish >5 mm SL, the characters of relative snout length and eye size are used. Ueyanagi (1964) described sailfish, striped marlin (*Tetrapturus audax*, the Pacific counterpart to white marlin), and shortbill spearfish (*Tetrapturus angustirostris*) between 10 and 20 mm SL as having long snouts. The short snout group comprised blue marlin and black marlin. The angles at which the pterotic and preopercular spines protrude from the body have also been useful in identifying Indo-Pacific specimens (Ueyanagi, 1974a).

A troubling aspect of current larval istiophorid identification methods is the difficulty in using some of the above characters. If a specimen is fixed with its mouth open, snout position with respect to eye is an unreadable character (Richards, 1974), and misidentifications can occur (Ueyanagi, 1974a). Evaluation of certain characters (e.g., whether the eye orbit projects anteriorly) can be highly subjective. The lack of confirming identification characters compounds the problem; if just one character cannot be assessed, identification may not be possible (Richards, 1974). An additional problem is the apparently high variability in characters such as pigment locations and head spine angles in Atlantic istiophorids (Richards, 1974).

Most of the larval specimens examined by Ueyanagi came from the Indo-Pacific; he assumed that the same identification characters would apply to their Atlantic counterparts (Ueyanagi, 1963, 1974a). Although recent genetic evidence supports Morrow and Harbo's (1969) opinion that Atlantic and Indo-Pacific sailfish are actually populations of a global species (Finnerty and Block, 1995; Graves and McDowell, 1995), morphological differences have been noted in sailfish, especially at 90 cm. Specifically, the pectoral fin is longer, in relation to the body, in Atlantic sailfish than in Indo-Pacific sailfish. Differences in the spread of the caudal fin and maximum total length have also been observed. These characters were the impetus behind the separation of sailfish, at least to subspecies, by ocean basin (Nakamura, 1974). Regardless of the taxonomic status of the Atlantic and Indo-Pacific billfishes, physical attributes of istiophorid species may vary by region. Therefore, the assumption that the larvae of Atlantic istiophorids can be identified by using the same characters attributed to Indo-Pacific istiophorids may not be valid.

Billfishes are not the only group whose larval identification has proven difficult. Species of the genus *Sebastes*, the rockfishes, have some morphological and pigmentation differences as larvae, but identification was difficult and uncertain until genetic methods were employed (Rocha-Olivares et al., 2000). Fulford and Rutherford (2000) solved a similar problem by combining allozyme analysis of larval tissues with landmark-based morphometrics to distinguish between species of the genus *Morone*. In each study, a molecular technique was used to confirm larval species identity, facilitating the development of morphometric identification techniques.

Several molecular methods for identifying adult billfishes have been developed (Chow, 1993; Innes et al., 1998; McDowell and Graves, 2002). In the present study, larval istiophorids from Atlantic waters were identified to species using restriction fragment length polymorphism (RFLP) analysis of a 1.2-kb segment of nuclear DNA, as described for adult billfishes by McDowell and Graves (2002). In this article we present data for genetically identified istiophorid larvae, analyses of morphometric and qualitative characters, and a key for the identification of larval istiophorids of the Straits of Florida and the Bahamas.

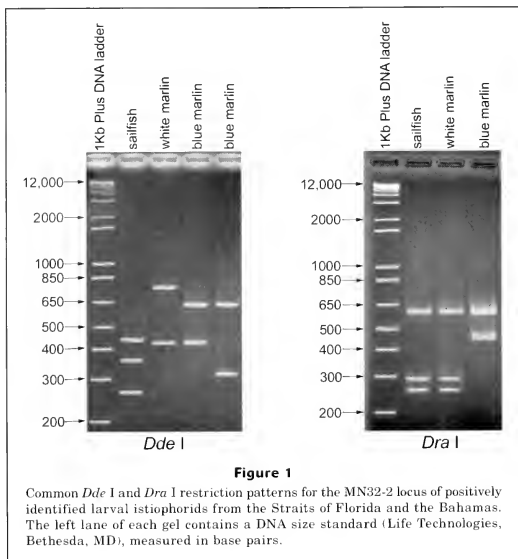
Materials and methods

Larval material

Larval istiophorids were collected between June 1998 and April 2002 from the Straits of Florida and Exuma Sound, Bahamas. Several preservation fluids were used, but the majority of the larvae (~1000) were preserved in 70–95% ethanol. Butylated hydroxytoluene (BHT) saturated ethanol was used to preserve 150 larvae. Approximately 300 larvae were fixed in 10% unbuffered formalin and then transferred to 70% ethanol. In the laboratory, each fish was assigned a unique identification number and stored separately.

Molecular identification

Total DNA was extracted from the right eyeball of each larva, using either a quick-digest method (Ruzzante et al., 1996) or a standard high-molecular weight DNA extraction protocol (Sambrook et al., 1989). Larval identification was achieved by PCR amplification of the nuclear locus MN32-2 (Buonaccorsi et al., 1999), and subsequent RFLP analysis (restriction endonucleases *Dra* I and *Dde* I, Life Technologies, Bethesda, MD). If the restriction fragment pattern (Fig. 1) of a larva matched one of those described for a known-identity adult, the larva was assigned to that species. See McDowell and Graves (2002) for detailed protocols and reaction parameters. Preliminary attempts to amplify DNA from formalin-fixed larvae failed; only ethanol-preserved specimens were used in subsequent molecular work.



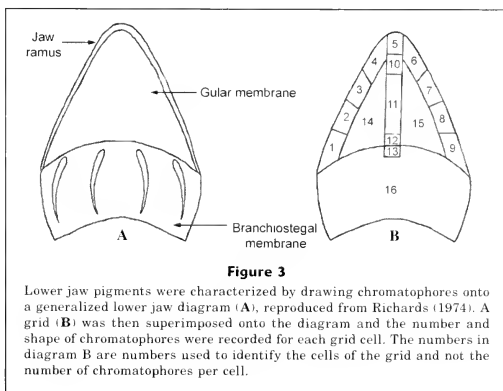
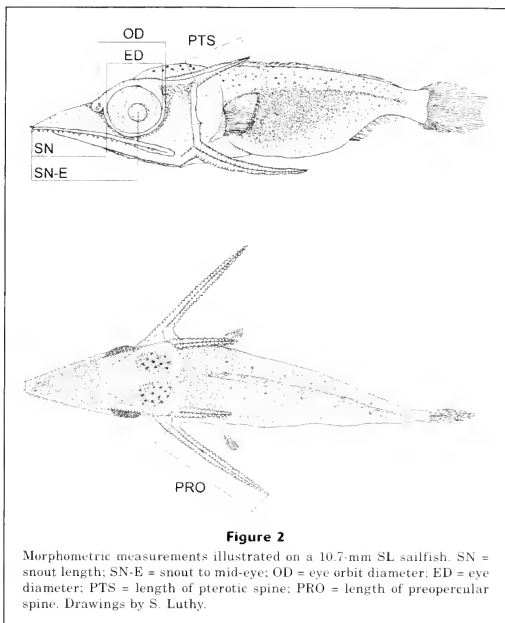
Characters

A subset of the molecularly identified istiophorid larvae were examined to ascertain which morphological characters might aid in specific identification and possibly obviate the need for future molecular work. The measurements made by Richards (1974) served as a starting point for quantitative larval descriptions: standard length (SL); snout length (SN); tip of the snout to the center of the eyeball (SN-E); diameter of the eye (ED); diameter of the eye orbit (OD); head length (HL); and difference in length between the upper and lower jaws (JD). To this suite were added measurements of the preopercular (PRO) and pterotic (PTS) head spines. All measurements were taken with Image-Pro Plus software (version 4.5, Media Cybernetics, Silver Spring, MD), and each specimen was viewed through a CoolSNAP-PROcf monochrome digital camera (Media Cybernetics, Silver Spring, MD) which was connected to a Leica MZ12 dissecting microscope (at magnifications 0.8–10.0 \times). Each larva was soaked in tap water for one minute before measurements were taken, to rehydrate the fish and facilitate handling. SL and PRO measurements were made from the dorsal view, JD measurements were made from the ventral view, and all other measurements were made from the left lateral view (Fig. 2). Because the preopercular spine often prevents

an istiophorid larva from lying on its side, a side view was obtained by using the surface tension of the still-wet larva to adhere it to the side wall of a Petri dish. Care was taken to maintain the two points of measurement on a plane parallel to the microscope lens.

Pigments observed on the ventral surface of the lower jaw rami, gular membrane, and branchiostegal membranes of each larva were drawn onto a generalized diagram of the larval istiophorid lower jaw (Fig. 3). A grid was then superimposed on the diagram, and the shape (pointate or stellate) and number of chromatophores in each grid cell were recorded. Pigment data were also recorded as binary presence or absence per grid cell. Two other categorical variables assessed were flexion stage (i.e., preflexion, flexing, postflexion) and the position of the tip of the snout with regard to a plane passing through the center of the eye and the mid-line of the body (i.e., below, even, above). Although the latter character is useful for identifying Indo-Pacific istiophorids (Ueyanagi, 1963, 1964), in our collection it was highly variable within species, and therefore it was not analyzed further.

Month of capture was considered a partially discriminating character based on differences in the length and timing of spawning seasons of local populations. Spawning seasons were determined by de Sylva and Breder (1997) by gonad histology studies.



Data analyses

Canonical variates analysis (CVA) was used to visualize the separation between species and the relative importance of all variables (morphometric characters, pigment patterns, and month of capture) in that separation. Results from the CVA were used to help drive character selection for subsequent analyses. The significance of the canonical axes was obtained with a Monte Carlo permutation test (499 iterations). The canonical analyses were performed with the software CANOCO (version 4.5, Microcomputer Power, Ithaca, NY), and plotted with the associated software CANODRAW.

In the CVA, all the molecularly identified white marlin (21) and blue marlin (68) with full measurement sets (i.e., no missing values) and a subset of sailfish (135) with full measurement sets were compared. Every attempt was made to include fish from different locations, different years and months of collection, and across the full available size range of each species, in order to capture as much intra- and inter-species variation as possible. Forward selection was used as a guide for the creation of a reduced set of variables by retaining those that were significant for discrimination at $\alpha=0.05$ in a Monte Carlo permutation test (499 iterations). Months that were excluded by selection were restored to the variable set to insure that the entire spawning season was represented. It was assumed that pigment on the right lower jaw ramus was of equal importance as pigment in the corresponding location on the left lower jaw ramus; thus if a pigment grid from only one side of the jaw was selected, the corresponding grid from the other side of the jaw was added back to the reduced set.

In addition to its function as an exploratory tool for character selection, CVA with the reduced set of variables was used to identify unknown larvae to species. Ordination coordinates of an unknown larva were obtained by summing the products of the canonical coefficients and the character values for the unknown (standardized to mean 0, standard deviation 1). The identity of an unknown larva was determined by its placement in the ordination with respect to the reference larva.

The CVA provided clues as to which individual pigment grid cells were important for species discrimination, but cluster analysis was employed to examine overall lower jaw pigment patterns. Simple average link cluster analysis of Jaccard similarity indices was executed on pigment grid cell presence (binary coding) in the suite of lower jaw grid cells with BioDiversity Pro¹ software for the 26 white marlin with undamaged lower jaws and for equal numbers of randomly chosen blue marlin and sailfish. Analyses were conducted on all larvae together, and separately by flexion stage. Pigment drawings of the individual larvae within single-

species clusters were examined visually for commonalities. If a pattern was detected, the entire database of pigment position, number, and shape of all molecularly identified larvae was searched for that pattern. Lower jaw pigment patterns that were confined to one species only were deemed diagnostic characters.

Lower jaw pigment patterns alone did not resolve the differences among the species sufficiently for identification of all larvae. Therefore, for each species, continuous variables related linearly to SL were regressed against SL by using SAS (version 8.02, SAS Institute, Cary, NC) software. Two ratios were also examined in this way—snout length divided by eye orbit diameter, and snout length divided by eye diameter. Both ratios were suggested by the results of the full-model CVA because the influence of snout length was large and opposite in sign to the large and similar vectors of orbit diameter and eye diameter. The former ratio was also considered by Ueyanagi (1963, 1964, 1974b) to be an important distinguishing character for istiophora larvae. The same larvae that were used in the CVA analyses were used for the regressions, plus three white marlin, two sailfish, and two blue marlin that were excluded from CVA because of a missing measurement. Suitability of the characters for linear regression was assessed visually. Confidence intervals of 95%, 99%, and 99.9% were constructed around the regressions. Intersections of the three levels of confidence intervals for the three species were examined for maximum discrimination at the smallest standard length. The relationships that provided the best separation were included in the identification key.

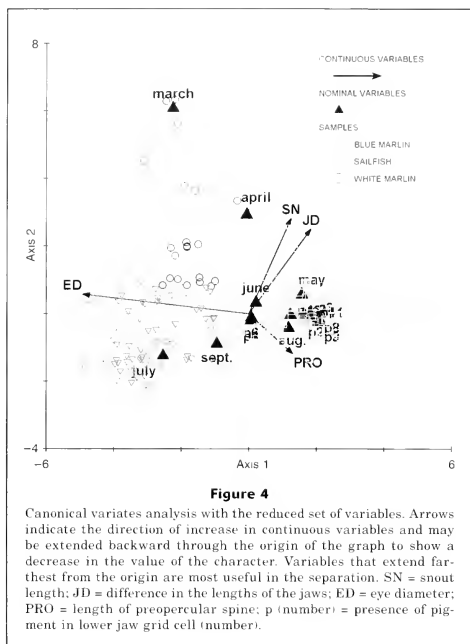
The identification key was constructed from the various characters that showed differences among the three species. All of the larvae used in developing the key were tested with it, as well as 12 blue marlin and 61 sailfish that were previously excluded from the analyses. A set of 50 larvae were independently identified by two observers unfamiliar with the key (naive observers). The only information about the fish provided to them was month of capture, so that each made his own measurements and pigment evaluations. The percent accuracy of their identifications was taken as a measure of the utility of the key.

Results

Molecular identification

The molecular identification technique was applied to 1044 larvae. Amplification success rates appear to have been negatively affected by the addition of BHT to ethanol and by the use of the Ruzzante et al. (1996) DNA extraction protocol. Overall, 714 (68.4%) istiophorids were successfully identified to the species level. Sailfish represented 82.8% of this group (591 larvae), whereas 96 blue marlin (13.4%) and 27 white marlin (3.8%) were identified. No longbill spearfish were identified. Sailfish larvae (2.9 mm–18.3 mm SL) were collected from April

¹ McAleece, N., P. J. D. Lambshead, G. L. J. Paterson, and J. D. Gage. 1997. The National History Museum and The Scottish Association for Marine Science. Website: <http://www.sams.ac.uk/>. [Accessed 5 February 2003.]



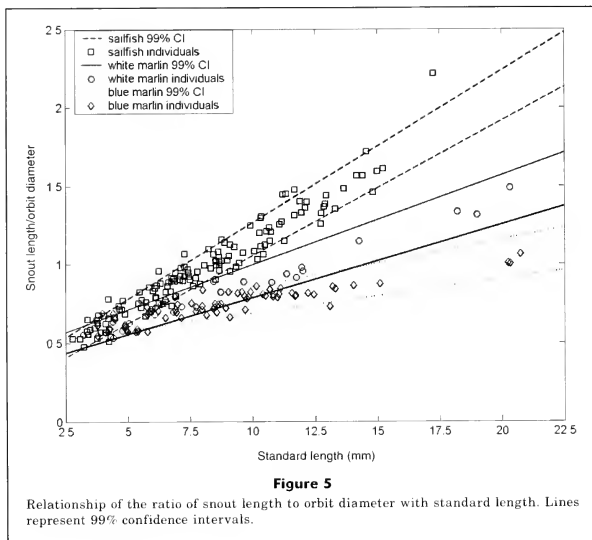
through September, white marlin (4.5 mm–20.3 mm SL) were collected from March through June, and larval blue marlin (3.8 mm–22.1 mm SL) were collected from June through September. Month of capture closely matched the reported spawning seasons for these species in the western North Atlantic: April through October for sailfish, March through June for white marlin, and July through October for blue marlin (de Sylva and Breder, 1997). Because blue marlin larvae were also caught in June, the blue marlin spawning season was expanded to include that month for the purposes of the identification key.

Canonical variates analysis

In the CVA with all variables included, separation of the three species was achieved with little overlap. Sailfish larvae were separated from the marlins along canonical axis 1 (eigenvalue=5.45). The separation was driven mainly by ED, OD, and lower jaw pigmentation. White marlin larvae separated from blue marlin primarily

along canonical axis 2 (eigenvalue=0.79), largely by month of capture, as well as SN, SN-E, and JD. The overall ordination was significant at $P=0.002$.

The forward selection process, along with the re-addition of counterpart pigment grids and the full spawning season, yielded the following 21 out of 32 variables: March, April, May, June, July, August, September, SN, JD, ED, PRO, and pigment grids 1–4, 6–9, 11, and 12. The following variables were ultimately excluded from the data set: SL, SN-E, OD, HL, PTS, and pigment grids 5, 10, and 13–16. The degree of species overlap was similar to that in the full model (Fig. 4). This overall ordination was also significant at $P=0.002$. The eigenvalue of the first canonical axis was 4.71, whereas the eigenvalue of the second canonical axis was 0.71. Coordinates obtained from the canonical coefficients and character values, standardized by reference set character means and standard deviations (Table 1), accurately placed test “unknowns” in the ordination of the reference larvae.



Lower jaw pigment patterns

Sailfish of all flexion stages with chromatophores on one or both sides of the lower jaw rami and sometimes in the middle of the gular membrane comprised single-species clusters. Examination of all molecularly identified larvae showed that many sailfish had pigment on the posterior $\frac{1}{3}$ of the lower jaw, but a few marlins also had stray pigments in that region. The minimum criterion to identify sailfish by lower jaw pigment without misidentifying other species was pigment in at least three of lower jaw pigment grids 1, 2, 3, 7, 8, 9, and 11. The shape and number of chromatophores within the grids was inconsequential. Not all sailfish larvae possessed the putative sailfish pattern, but 61.8% of molecularly identified sailfish (353 of 571 with intact lower jaws) could be identified by their lower jaw pigments alone.

Preflexion and flexing blue marlin also formed single-species clusters owing to the pattern of a single, pointed chromatophore in each of lower jaw grid cells 4 and 6, but without any other pigment (except occasionally in grid cell 12 or 13). However, not all small blue marlin exhibited this pattern. Eight of the 20 (40%) prefixion, molecularly identified blue marlin with intact lower jaws could be accurately identified by lower jaw pigments. Although some

postflexion white marlin had a similar pattern, no prefixion or flexing larvae of other species were misidentified as blue marlin by virtue of this pigment pattern.

Linear regressions

Residual plots showed no deviations from homogeneity of variance. Snout length, snout to mid-eye, ratio of snout length to eye diameter, and ratio of snout length to orbit diameter were all linearly related to SL. Jaw difference was linear and appeared to be helpful for discriminating istiophorids >12 mm SL, but too few larvae of this size were available for meaningful regressions. The ratio of snout length to orbit diameter provided the most separation between the species as indicated by the full model CVA. The 99% upper limit of the regression of this ratio against SL for white marlin was used to separate sailfish from both marlin species at 10 mm SL. If white marlin is ruled out as a possibility by month of capture, sailfish can be separated from blue marlin by the blue marlin upper 99% confidence limit for the regression of the ratio of snout length to orbit diameter at 8 mm SL. The lower 99% confidence limit for the regression of the ratio of white marlin snout length to orbit diameter separated them from blue marlin at 17 mm SL (Fig. 5, Table 2).

Table 1

Canonical coefficients, mean, and standard deviation of each character from the canonical variates analysis (reduced set of characters). The coordinate of a larva on canonical axis 1 (x) can be found by $x = \sum c_{1i} z_i$, where c = canonical coefficient and z = (character value - character mean)/character standard deviation. The coordinate of a larva on canonical axis 2 (y) can be found by $y = \sum c_{2i} z_i$. PRO = pre-opercular; SN = snout length; ED = eye diameter; and JD = difference in length between upper and lower jaws.

i (iterative count)	Character	Canonical coefficient, c_{1i} , for canonical axis 1	Canonical coefficient, c_{2i} , for canonical axis 2	Character mean (reference set)	Character standard deviation (reference set)
1	March	-0.0963	0.7538	0.0134	0.1149
2	April	0.0772	0.7354	0.0357	0.1856
3	May	0.1961	0.7347	0.1786	0.3830
4	June	0.1267	0.6460	0.3036	0.4598
5	July	-0.0369	-0.2988	0.2054	0.4040
6	August	0.3465	0.2116	0.2143	0.4103
7	September	0.0000	0.0000	0.0491	0.2161
8	PRO	0.6697	-0.6728	2.0781	0.7076
9	SN	3.1678	0.9640	1.4978	0.8711
10	ED	-2.8386	0.0739	1.2011	0.4426
11	JD	-0.9464	-0.4947	0.1806	0.2222
12	Pigment 1	0.1450	-0.1156	0.2366	0.4250
13	Pigment 2	0.3483	-0.0953	0.2366	0.4250
14	Pigment 3	0.3564	0.1262	0.3036	0.4598
15	Pigment 4	0.0887	-0.2251	0.7768	0.4164
16	Pigment 6	-0.0263	-0.1084	0.8214	0.3830
17	Pigment 7	-0.0375	-0.1584	0.3259	0.4687
18	Pigment 8	0.2684	-0.0507	0.2098	0.4072
19	Pigment 9	0.3262	-0.0603	0.2545	0.4356
20	Pigment 11	0.4757	-0.1622	0.4241	0.4942
21	Pigment 12	0.2250	-0.1191	0.3438	0.4750

Table 2

Regression of the ratio of snout length to orbit diameter against standard length. r^2 = coefficient of determination and n = number of fish in sample.

Species	Regression equation	r^2	n
Sailfish (<i>Istiophorus platypterus</i>)	SN:OD = 0.092SL + 0.242	0.94	137
White marlin (<i>Tetrapturus albidus</i>)	SN:OD = 0.052SL + 0.373	0.95	24
Blue marlin (<i>Makaira nigricans</i>)	SN:OD = 0.026SL + 0.510	0.74	70

Identification methods

Combination of species diagnostic lower jaw pigment patterns, regression equations, and month of capture resulted in the identification key found in Table 3. Of the 304 larvae that were examined with the key by the authors, only one was misidentified. This was an 8.02-mm blue marlin that was mistakenly identified as a sailfish by question 6a in part I of the key. Of the remaining fish, 31 larvae, all between 4 mm and 10 mm SL could not be identified with the key. An additional

62 larvae, again mostly less than 10 mm SL, could be narrowed down to only two species possibilities. Overall, 69.1% of the fish were correctly identified to species. Accuracy improved with size. Eighty-five of the 93 larvae that could not be identified by the key were plotted as unknowns on the ordination (reduced set of variables), at which time correct identification was obtained for 71 of them. Seven larvae could not be identified at all, and seven were incorrectly identified because they were plotted at the interface of two species groupings. The remaining eight were incompatible with CVA because

Table 3

Key for ethanol-preserved larvae and postlarval specimens of Istiophoridae caught in the Straits of Florida and the Bahamas.

Part I: for larvae <10 mm standard length (SL)

1a	Preflexion or flexing; a single, pointate chromatophore in each of lower jaw pigment grids 4 and 6; with or without a single pigment in either grid 12 or 13; no other lower jaw pigments	<i>Makaira nigricans</i>	2
1b	Not as above		2
2a	Any flexion stage; chromatophores of any number or shape in 3 or more of lower jaw pigment grids 1, 2, 3, 7, 8, 9, 11	<i>Istiophorus platypterus</i>	3
2b	Not as above		3
3a	Larva caught in March, April, or May	either <i>Istiophorus platypterus</i> or <i>Tetrapturus albidus</i>	4
3b	Larva caught in June or later		4
4a	Larva caught in June	either <i>Istiophorus platypterus</i> , <i>Tetrapturus albidus</i> , or <i>Makaira nigricans</i>	5
4b	Larva caught in July, August, September, or October		5
5a	Standard length ≥ 8 mm		6
5b	Standard length <8 mm	either <i>Istiophorus platypterus</i> or <i>Makaira nigricans</i>	6
6a	Snout length / orbit diameter $>0.030SL + 0.551$	<i>Istiophorus platypterus</i>	6
6b	Snout length / orbit diameter $\leq 0.030SL + 0.551$	<i>Makaira nigricans</i>	6

Part II: for larvae ≥ 10 mm SL

1a	Chromatophores of any number or shape in 3 or more of lower jaw pigment grids 1, 2, 3, 7, 8, 9, 11	<i>Istiophorus platypterus</i>	2
1b	Without the above lower jaw pigment pattern		2
2a	Snout length / orbit diameter $>0.057SL + 0.427$	<i>Istiophorus platypterus</i>	3
2b	Snout length / orbit diameter $\leq 0.057SL + 0.427$		3
3a	Larva caught in March, April, or May	<i>Tetrapturus albidus</i>	4
3b	Larva caught in June or later		4
4a	Larva caught in July, August, September, or October	<i>Makaira nigricans</i>	5
4b	Larva caught in June		5
5a	Standard length ≥ 17 mm		6
5b	Standard length <17 mm	either <i>Makaira nigricans</i> or <i>Tetrapturus albidus</i>	6
6a	Snout length / orbit diameter $\geq 0.047SL + 0.319$	<i>Tetrapturus albidus</i>	6
6b	Snout length / orbit diameter $<0.047SL + 0.319$	<i>Makaira nigricans</i>	6

a measurement was missing. Thus, when the key and CVA analyses were combined, 92.4% of the tested larvae were correctly identified.

One of the two naive observers found that one larva out of the test set of 50 was too damaged to be evaluated. He correctly identified 35 larvae and found 14 to be unidentifiable with the key. Overall, his success rate was 71.4%. The other observer correctly identified 30 larvae, misidentified one (the larva not evaluated by the other observer and the same larva misidentified by the authors), and found 19 to be unidentifiable by the key. His overall success rate was 60%. The difference in the number of larvae that could not be identified with the key was the result of differences in interpretation of the lower jaw pigment position for larvae less than 10 mm SL.

Discussion

Because adults of four istiophorid species are found in the Straits of Florida and Bahamian waters, a reliable larval identification technique for these species is necessary (Voss, 1953). Incorrect species identifications can have serious ramifications on other areas of istiophorid early life history research. For example, studies on early growth would suffer if a larval blue marlin, which is thought to reach 174 cm lower jaw fork length (LJFL) by age one (Prince et al., 1991), were to be confused with a larval sailfish, which reportedly grows to only 108.9 cm LJFL (Hedgepeth and Jolley, 1983; Prager et al., 1995) by age one.

Few characters are available to separate the species of larval istiophorids (Richards, 1974). Although

a single character may be used to separate fish into groups, early work has lacked a means to confirm the identity of the groups. Molecular techniques provided a solution to this problem. A limitation of the molecular identification technique that we used was that only those larvae preserved in ethanol could be identified. Formalin fixation does not always preclude the use of PCR-based methods, but work is usually limited to small fragments; 570 bp is considered large for successful amplification (Shedlock et al., 1997). In the present study, DNA quality was too low in the formalin-fixed istiophorid larvae for PCR to amplify the 1.2-kb MN32-2. Consequently, only ethanol-preserved larvae could be used for key development and testing. Because of likely differences in length shrinkage between larvae preserved only in ethanol and those fixed in formalin, it is possible that the regressions presented in the present study are not valid for the latter.

No longbill spearfish were among the molecularly identified larvae; thus this species could not be included in the key. Very little is known about the longbill spearfish, but it is reported that larvae are found offshore (Ueyanagi et al., 1970), and that even adults are quite rare in United States and Bahamian waters (Robins, 1975). The longbill spearfish spawning season appears to range from late November to early May and peaks in February (Robins, 1975; de Sylva and Breder, 1997). Although there is some overlap in the spawning season of longbill spearfish with the spawning seasons of other Atlantic istiophorids, because of the rarity and predominantly offshore occurrence of the longbill spearfish, its absence from the key may not pose major problems for the identification of istiophorid larvae from our study area.

The larval istiophorids used to create and test the identification key were all captured either in the Straits of Florida or in Bahamian waters and were all smaller than 22 mm SL. Caution must be used when applying the key to larvae from other parts of the world or to larger sizes. Ueyanagi (1963) assumed that species pairs from different oceans (white marlin and striped marlin [*Tetrapturus audax*], longbill spearfish and shortbill spearfish [*Tetrapturus angustirostris*], Atlantic and Pacific blue marlin, Atlantic and Pacific sailfish) would be identifiable by the same characters. Although these pairs exhibit the same RFLP patterns at the MN32-2 locus (McDowell and Graves, 2002), we have not tested the key with Pacific larvae and cannot be certain that their measurements would fall within the same regression limits or that they would have the same lower jaw pigment patterns. Even within the Atlantic Ocean, spawning seasons vary with location (e.g., Bartlett and Haedrich [1968] collected larval blue marlin off the coast of Brazil in February and March). Month of capture was crucial in our analyses for discriminating between small marlins when spawning season overlap is minimal; therefore our key may need adjustment to reflect local spawning seasons when applied to other locations.

As in Indo-Pacific istiophorid larvae (Ueyanagi, 1964, 1974b), snout length, eye orbit diameter, and lower jaw

pigmentation are important characters for identifying larval istiophorids of the western Atlantic. However, white marlin differ markedly from their Indo-Pacific counterpart, striped marlin. White marlin larvae, long-held as members of the "long-snout group" of istiophorids, actually more closely resemble the short-snouted blue marlin until 17 mm standard length (Fig. 6). After they reach this size, snout length is intermediate between that of blue marlin and sailfish. This result cautions against the assumption that even large larvae with short snouts are blue marlin. Snout length may be useful as a character in phylogeny studies.

The identification methods presented in the present study reduce subjectivity in the evaluation of characters. This study also brings to light the caveats of using lower jaw pigment patterns as a means of identification and limits which pigment patterns qualify as diagnostic. Although there is a family of lower jaw pigment patterns that appears to mark sailfish only, if this character were the only means of identifying sailfish, nearly 40% of our sailfish (as confirmed by RFLP analysis) would have been misidentified or escaped classification. Likewise, the preflexion blue marlin pigment pattern will not lead to misidentifications, but too many preflexion blue marlin lack the pattern to justify its use as a stand-alone identification character. Lower jaw pigment patterns have also been suggested as potentially useful characters for separation of subspecific populations of both sailfish (Ueyanagi, 1974a, 1974b) and striped marlin in the Indo-Pacific (Nishikawa, 1991). The hypothesis of pigment-delineated sailfish populations was not borne out (Leis et al., 1987), and the high variability of lower jaw pigments among larvae of each species from our study area casts further doubt on the notion of using pigments alone to distinguish populations.

Our identification key does not enable separation of species for certain classes of istiophorid larvae. For example, larvae that are caught in June, are less than 10 mm SL, and possess none of the diagnostic lower jaw pigment patterns are especially problematic. In these "dead end" cases, discriminant analysis (CVA) is useful. Although a few larvae were misidentified with the CVA, these larvae were plotted near the interface of two species groupings; this position alerts the user to the fact that misidentification is a possibility. One disadvantage of using CVA (or any discriminant analysis) for identification is that all of the variables must have a value, meaning that a larva with broken preopercular spines, for example, cannot be entered into the analysis. When the species possibilities are narrowed down to blue marlin and either sailfish or white marlin, it may be feasible to identify larvae by vertebral formula. Richards (1974) suggests that this is difficult with larvae less than 20 mm SL, but it is the method that Prince et al. (1991) used to identify blue marlin that were 5–10 mm SL. Molecular identification is always an option for resolving dead ends.

The identification of larval istiophorids has never been an easy task. Molecular identification is reliable, but can be relatively more labor intensive and expensive

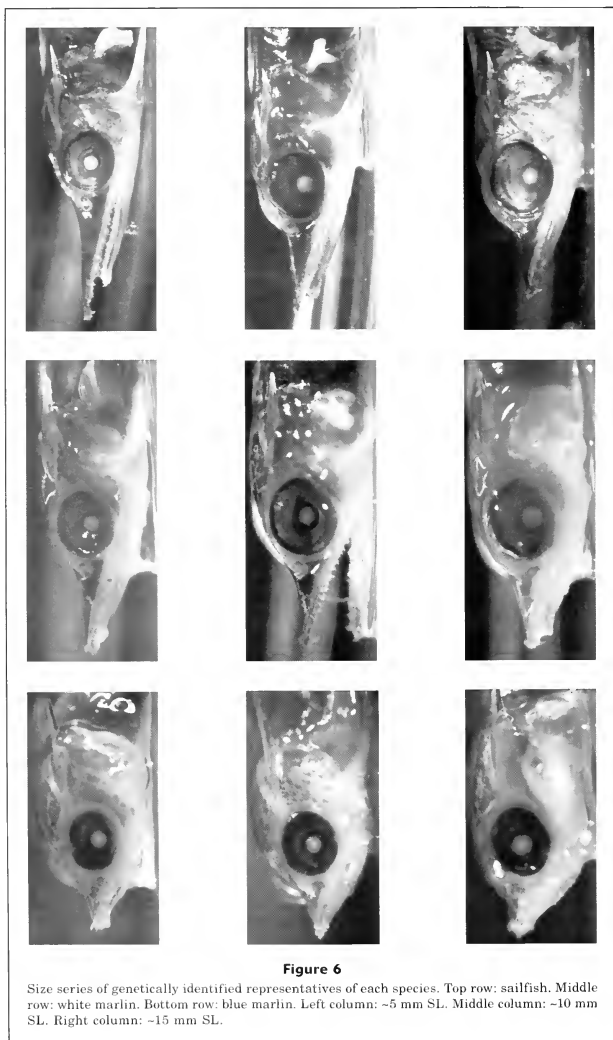


Figure 6

Size series of genetically identified representatives of each species. Top row: sailfish. Middle row: white marlin. Bottom row: blue marlin. Left column: ~5 mm SL. Middle column: ~10 mm SL. Right column: ~15 mm SL.

than traditional methods. The creation of a key based on characters developed from molecularly identified Atlantic larvae makes it possible to use more traditional methods to make reliable identifications. Despite the limitations of the key, it works well for larvae caught in our area. We recommend further testing with istiophorid larvae from other waters, and the inclusion of longbill spearfish larvae.

Acknowledgments

The authors appreciate financial support provided by Network Miami and Anheuser Busch, the American Institute of Marine Science, the Miami Billfish Tournament's Captain H. Vernon Jr. Scholarship, the International Light Tackle Tournament Association, and the University of Miami's Center for Sustainable Fisheries. We thank G. Diaz, K. Gracie, L. Leist, M. Williams, O. Bowen, C. Schmitz, C. Faunce, D. Schuller, G. Meyers, and M. Feeley for volunteering their time for specimen collection and J. Post, T. Capo, J. Ault, S. Smith, and J. Luo for early instruction. Laboratory advice and commiseration were provided by C. Campbell, P. Walsh, J. van Wye, and all the members of the VIMS genetics laboratory. We offer special thanks to J. Graves, in whose laboratory the molecular work was carried out. We are grateful to T. Grothues for sharing his CVA wisdom and to J. Llopiz, D. Richardson, and K. Denit for testing our key. W. Richards, D. deSylva, and C. Paris were instrumental in the interpretation of identification characters. This work could not have been carried out without the generosity and enthusiasm of D. Frazel and his family in donating their time and the use of their boat. Larvae were collected under NMFS permits HMS-EFP-00 through 03, and under University of Miami animal care protocols (02-063).

Literature cited

- Bartlett, M. R., and R. L. Haedrich.
1968. Neuston nets and South Atlantic larval blue marlin (*Makaira nigricans*). *Copeia* 1968:469-474.
- Buonaccorsi, V. P., K. S. Reece, L. W. Morgan, and J. E. Graves.
1999. Geographic distribution of molecular variance within the blue marlin (*Makaira nigricans*): a hierarchical analysis of allozyme, single-copy nuclear DNA, and mitochondrial DNA markers. *Evolution* 53:568-579.
- Chow, S.
1993. Identification of billfish species using mitochondrial cytochrome *b* gene fragment amplified by polymerase chain reaction. *Collect. Vol. Sci. Pap. ICCAT* 41:549-556.
- Collette, B. B., and M. Vecchione.
1995. Interactions between fisheries and systematics. *Fisheries* 20:20-25.
- de Sylva, D. P., and P. R. Breder.
1997. Reproduction, gonad histology, and spawning cycles of North Atlantic billfishes (Istiophoridae). *Bull. Mar. Sci.* 60:668-697.
- Finnerty, J. R., and B. A. Block.
1995. Evolution of cytochrome *b* in the Scombroidei (Teleostei)—molecular insights into the billfish (Istiophoridae and Xiphiidae) relationships. *Fish. Bull.* 93:78-96.
- Fulford, R. S., and D. A. Rutherford.
2000. Discrimination of larval *Morone* geometric shape differences with landmark-based morphometrics. *Copeia* 2000:965-972.
- Graves, J. E., and J. R. McDowell.
1995. Inter-ocean genetic divergence of istiophorid billfishes. *Mar. Biol.* 122:193-203.
- Hedgepeth, M. Y., and J. W. Jolley.
1983. Age and growth of sailfish, *Istiophorus platypterus*, using cross sections from the fourth dorsal fin spine. *In Proceedings of the international workshop on age determination of oceanic pelagic fishes: tunas, billfishes, and sharks* (E. D. Prince and L. M. Pulos, eds.), p. 131-135. NOAA Tech. Rep. 8.
- Innes, B. H., P. M. Grewe, and R. D. Ward.
1998. PCR-based genetic identification of marlin and other billfish. *Mar. Freshw. Res.* 49:383-388.
- Lasker, R.
1987. Use of fish eggs and larvae in probing some major problems in fisheries and aquaculture. *Am. Fish. Soc. Symp.* 2:1-16.
- Leis, J. M., B. Goldman, and S. Ueyanagi.
1987. Distribution and abundance of billfish larvae (Pisces, Istiophoridae) in the Great Barrier Reef Lagoon and Coral Sea near Lizard Island, Australia. *Fish. Bull.* 85:757-765.
- McDowell, J. R., and J. E. Graves.
2002. Nuclear and mitochondrial DNA markers for specific identification of istiophorid and xiphiid billfishes. *Fish. Bull.* 100:537-544.
- Morrow, J. E., and S. J. Harbo.
1969. A revision of the sailfish genus *Istiophorus*. *Copeia* 1969:34-44.
- Nakamura, I.
1974. Some aspects of the systematics and distribution of billfishes. *In Proceedings of the international billfish symposium; Kailua-Kona, Hawaii, 9-12 August 1972. Part 2: Review and contributed papers* (R. S. Shomura and F. Williams, eds.), p. 45-53. NOAA Tech. Rep. NMFS SSRF-675.
- Nishikawa, Y.
1991. On the melanophore patterns on lower jaw of the larvae of striped marlin. *Bull. Natl. Res. Inst. Far Seas Fish.* 28:15-19.
- Prager, M. H., E. D. Prince, and D. W. Lee.
1995. Empirical length and weight conversion equations for blue marlin, white marlin, and sailfish from the North-Atlantic Ocean. *Bull. Mar. Sci.* 56:201-210.
- Prince, E. D., D. W. Lee, J. R. Zweifel, and E. B. Brothers.
1991. Estimating age and growth of young Atlantic blue marlin *Makaira nigricans* from otolith microstructure. *Fish. Bull.* 89:441-459.
- Richards, W. J.
1974. Evaluation of identification methods for young billfishes. *In Proceedings of the international billfish symposium; Kailua-Kona, Hawaii, 9-12 August 1972. Part 2: Review and contributed papers* (R. S. Shomura and F. Williams, eds.), p. 62-72. NOAA Tech. Rep. NMFS SSRF-675.
- Robins, C. R.
1975. Synopsis of biological data on the longbill spearfish, *Tetrapturus pfluegeri*, Robins and de Sylva. *In*

- Proceedings of the international billfish symposium; Kailua-Kona, Hawaii, 9-12 August 1972. Part 3: Species synopsis (R. S. Shomura and F. Williams, eds.), p. 28-37. NOAA Tech. Rep. NMFS SSRF-675.
- Rocha-Olivares, A., H. G. Moser, and J. Stannard.
2000. Molecular identification and description of pelagic young of the rockfishes *Sebastes constellatus* and *Sebastes enstifer*. Fish. Bull. 98:353-363.
- Ruzzante, D. E., C. T. Taggart, and D. Cook.
1996. Spatial and temporal variation in the genetic composition of a larval cod (*Gadus morhua*) aggregation: Cohort contribution and genetic stability. Can. J. Fish. Aquat. Sci. 53:2695-2705.
- Sambrook, J., E. F. Fritsch, and T. Maniatis.
1989. Molecular cloning: a laboratory manual, p. 9.17-9.19. Cold Spring Harbor Laboratory Press, Cold Spring Harbor, NY.
- Shedlock, A. M., M. G. Haygood, T. W. Pietsch and P. Bentzen.
1997. Enhanced DNA extraction and PCR amplification of mitochondrial genes from formalin-fixed museum specimens. Biotechniques 22:394-400.
- Ueyanagi, S.
1963. Methods for identification and discrimination of the larvae of five istiophorid species distributing in the Indo-Pacific. Rep. Nankai Reg. Fish. Res. Lab. 17:137-150. [In Jap., Engl. sum.]
1964. Description and distribution of larvae of five istiophorid species in the Indo-Pacific. Mar. Biol. Assoc. India. Proc. Symp. Scombroid Fish. Mandapam Camp, Part 1:499-528.
- 1974a. On an additional diagnostic character for the identification of billfish larvae with some notes on the variations in pigmentation. In Proceedings of the international billfish symposium, Kailua-Kona, Hawaii, 9-12 August 1972. Part 2: Review and contributed papers (R. S. Shomura and F. Williams, eds.) p. 73-78. NOAA Tech. Rep. NMFS SSRF-675.
- 1974b. Present state of billfish larval taxonomy. In The early life history of fish (J. H. S. Blaxter, ed.), p. 649-658. Springer-Verlag, New York, NY.
- Ueyanagi, S., S. Kikawa, M. Uto, and Y. Nishikawa.
1970. Distribution, spawning, and relative abundance of billfishes in the Atlantic Ocean. Bull. Far Seas Fish. Res. Lab. 3:15-55.
- Voss, G. L.
1953. A contribution to the life history and biology of the sailfish, *Istiophorus americanus* Cuv. and Val., in Florida waters. Bull. Mar. Sci. Gulf Carib. 3:206-240.

Abstract—This study examined the sexual differentiation and reproductive dynamics of striped mullet (*Mugil cephalus* L.) in the estuaries of South Carolina. A total of 16,464 specimens were captured during the study and histological examination of sex and maturity was performed on a subsample of 3670 fish. Striped mullet were sexually undifferentiated for the first 12 months, began differentiation at 13 months, and were 90% fully differentiated by 15 to 19 months of age and 225 mm total length (TL). The defining morphological characteristics for differentiating males was the elongation of the protogonial germ tissue in a corradating pattern towards the center of the lobe, the development of primary and secondary ducts, and the lack of any recognizable ovarian wall structure. The defining female characteristics were the formation of protogonial germ tissue into spherical germ cell nests, separation of a tissue layer from the outer epithelial layer of the lobe-forming ovarian walls, a tissue bud growing from the suspensory tissue that helped form the ovary wall, and the proliferation of oocytes and oocytes. Sexual maturation in male striped mullet first occurred at 1 year and 248 mm TL and 100% maturity occurred at age 2 and 300 mm TL. Female striped mullet first matured at 2 years and 291 mm total length and 100% maturity occurred at 400 mm TL and age 4. Because of the open ocean spawning behavior of striped mullet, all stages of maturity were observed in males and females except for functionally mature females with hydrated oocytes. The spawning season for striped mullet recruiting to South Carolina estuaries lasts from October to April; the majority of spawning activity, however, occurs from November to January. Ovarian atresia was observed to have four distinct phases. This study presents morphological analysis of reproductive ontogeny in relation to size and age in South Carolina striped mullet. Because of the length of the undifferentiated gonad stage in juvenile striped mullet, previous studies have proposed the possibility of protandric hermaphroditism in this species. The results of our study indicate that striped mullet are gonochoristic but capable of exhibiting nonfunctional hermaphroditic characteristics in differentiated mature gonads.

Manuscript submitted 11 March 2003 to the Scientific Editor's Office.

Manuscript approved for publication 31 May 2005 by the Scientific Editor.

Fish. Bull. 103:601–619 (2005).

Sexual differentiation and gonad development in striped mullet (*Mugil cephalus* L.) from South Carolina estuaries*

Christopher J. McDonough

William A. Roumillat

Charles A. Wenner

Marine Resources Research Institute
South Carolina Department of Natural Resources
217 Fort Johnson Road
Charleston, South Carolina 29412

E-mail address (for C. J. McDonough): mcdonoughc@dnr.sc.gov

The striped mullet (*Mugil cephalus* L.) is distributed circumglobally in tropical and semitropical waters between latitudes 42°N and 42°S (Thomson, 1963; Rossi et al., 1998). Even though considered a marine species, striped mullet are euryhaline and can be found year round throughout the full range of estuarine salinities in the southeastern United States (Jacot, 1920; Anderson, 1958). Striped mullet are important throughout the world for commercial fisheries and aquaculture. In the southeastern United States there are large-scale commercial fisheries for striped mullet in North Carolina and Florida. South Carolina and Georgia have much more limited landings (NMFS¹).

The commercial effort in the southeastern United States targets "roe" fish (fish containing roe) during the fall spawning migration. Throughout the rest of the year mullet are fished commercially for human consumption (particularly the west coast of Florida) and bait (Anderson, 1958). Striped mullet have a significant economic impact in the southeast where they represented a landings value of 16.4 million dollars from 1994 to 2000 (NMFS¹). Striped mullet landings in the Gulf of Mexico were significantly higher with a landings value of 86.2 million dollars for the same time period. Striped mullet are also one of the most important forage fishes that occur in the estuaries of the southeast and represent a significant food source for upper level piscivores (Wenner et al.²).

General information on the biology of striped mullet has been well documented (Jacot, 1920; Anderson, 1958; Thomson, 1963, 1966; Chubb et al., 1981) but limited information is available on the reproductive biology of wild populations (Anderson, 1958; Stenger, 1959; Greeley et al., 1987; Render et al., 1995). There is a large body of work concerning striped mullet reproduction in aquaculture but many of these studies have concentrated on females by using artificial manipulation of the reproductive cycle. Although the maturation process of oocytes may be the same as that in wild striped mullet, the environment and conditions under which maturation occurred in these studies was artificial (Shehadeh et al., 1973; Kuo et al., 1974; Pien and Liao, 1975; Kelly, 1990; Tamaru et al., 1994; Kuo, 1995). This lack of in-

* Contribution 564 of the Marine Resources Research Institute, South Carolina Dept. of National Resources, Charleston, SC 29412.

¹ NMFS (National Marine Fisheries Service). 2001. Unpubl. data. Statistics and Economic Division, 1315 East-West Highway, Silver Spring, Md. 20910. <http://www.st.nmfs.gov/st1/index.html>.

² Wenner, C. A., W. A. Roumillat, J. E. Moran, M. B. Maddox, L. B. Daniel, and J. W. Smith. 1990. Investigations on the life history and population dynamics of marine recreational fishes in South Carolina, part 1, p. 2–22. Completion reports, Project F-37, Charleston, and Project F-31, Brunswick. South Carolina Marine Resources Research Institute, P.O. Box 12559 Charleston, S.C. 29422.

formation on reproductive biology is surprising given the worldwide importance of mullet. In particular, there have been very few studies where sexual differentiation of immature striped mullet has been examined in conjunction with histological confirmation of maturity stage in reproductively capable adults. One notable exception was the work of Stenger (1959), who although thorough in histological confirmation of the male and female developmental stages in relation to length, did not take age into consideration at differentiation or maturity. More recent studies (Chang et al., 1995; Chang et al., 1999) have examined gonad histology and plasma sex steroids during sex differentiation in young-of-the-year striped mullet up to 12 months old, but these studies did not provide any detail on fish length during development and differentiation. Other studies have examined oocyte development and relative fecundity for the reproductive assessment of female striped mullet but did not examine reproductive development in males or take into consideration an independent confirmation of fish age (Greeley et al., 1987; Render et al., 1995). Few studies have described the process of spermatogenesis in striped mullet because most efforts on the propagation and enhancement of striped mullet reproduction have concentrated on female development because of their commercial value. Grier (1981) used striped mullet in describing the cellular organization of testes and spermatogenesis as a model for synchronously spawning fishes but did not describe size and age in relation to spermatogenesis.

Striped mullet are considered isochronal spawning fishes (Greeley et al., 1987; Render et al., 1995). There are only a few observations of offshore spawning activity (Arnold and Thompson, 1958), and eggs and larvae have rarely been collected offshore (Anderson, 1958; Finucane et al., 1978; Collins and Stender, 1989). Collins and Stender (1989) concluded that striped mullet spawn in and around the edge of the continental shelf off the coasts of North Carolina, South Carolina, Georgia, and the east coast of Florida (an area often referred to as the South Atlantic Bight), but may also spawn outside the South Atlantic Bight (SAB). They also indicated a protracted spawning season that extended from October to April. This contrasts with the estimated spawning season from previous studies (2–5 months from November through March) (Jacot, 1920; Broadhead, 1956; Anderson, 1958; Arnold and Thompson, 1958; Stenger, 1959; Dindo and MacGregor, 1981; Greeley et al., 1987; Render et al., 1995; Hettler et al., 1997). Female mullet were thought to mature at three years of age at a size of 230 to 350 mm standard length (Thomson, 1951, 1963; Greeley et al., 1987).

This study had three purposes: 1) to determine at what size and age striped mullet become fully sexually differentiated and to describe the morphological characteristics of sexual differentiation in both male and female striped mullet; 2) to determine the size and age at first maturity for each sex; and 3) to describe the timing and process of gametogenesis in relation to size and age in both males and females in order to provide a

histological baseline for the evaluation and reproductive staging of striped mullet.

Materials and methods

Sampling and data collection

Collections of striped mullet were conducted from October 1997 through December 2000. Collections were based on a protocol of monthly random stratified sampling conducted in the Cape Romain, Charleston Harbor, and the ACE Basin estuaries in South Carolina (Fig. 1). The Charleston Harbor estuarine system is made up of three river systems: the Ashley, Cooper, and Wando rivers. In addition, Charleston Harbor proper was sampled as a separate stratum. The ACE Basin estuary is formed by the confluence of the Ashepoo, Combahee, and Edisto rivers and was sampled as a single estuary. One of the problems initially encountered with sampling was the ability to sample striped mullet throughout their estuarine salinity range. The primary sampling gear used was a 184-meter trammel net with 356-mm stretch mesh outside panels and a 64-mm stretch mesh inner panel. Because striped mullet use the full range of estuarine habitats and freshwater, the use of alternate gear was necessary to obtain a representative sample of the population within all salinity regimes. Specimens collected with additional gear types in low salinity and freshwater habitats supplemented those specimens sampled with a trammel net. The additional gear types were an electroshock boat, cast nets, and gill nets. The electroshock boat samples were obtained from the South Carolina Department of Health and Environmental Control from the major coastal river basins in South Carolina, including freshwater portions of the Waccamaw, Black, Pee Dee, Santee, Cooper, Edisto, Ashepoo, Combahee, and Broad rivers (Fig. 1). Cast nets were used primarily in different portions of the Charleston Harbor estuary in tidal creeks and in areas where the trammel net could not be used effectively. The cast nets were 1.84 meters in diameter and had 10-mm mesh. The gill net was a 200-meter net with 64-mm stretch mesh that was used to test the efficiency of the trammel net sets.

Standard morphological measurements were total length (TL), fork length (FL), standard length (SL) in mm, and body weight (BW) in grams (g). Any subsequent mention of fish length in the remaining text will be total length unless otherwise noted. Sagittal otoliths were removed for estimating fish ages. A gross examination of the gonads was used for initial sex and maturity assessment. If the gonads were estimated to weigh more than 1 g they were also weighed. A small sample of gonad tissue was removed from the posterior portion of the gonad where the lobes were joined and was fixed in 10% neutral buffered formalin for histological examination. The tissue samples used for histological evaluation were taken from the posterior section of the gonad because earlier developmental stages and differentiation were more evident where the ductwork

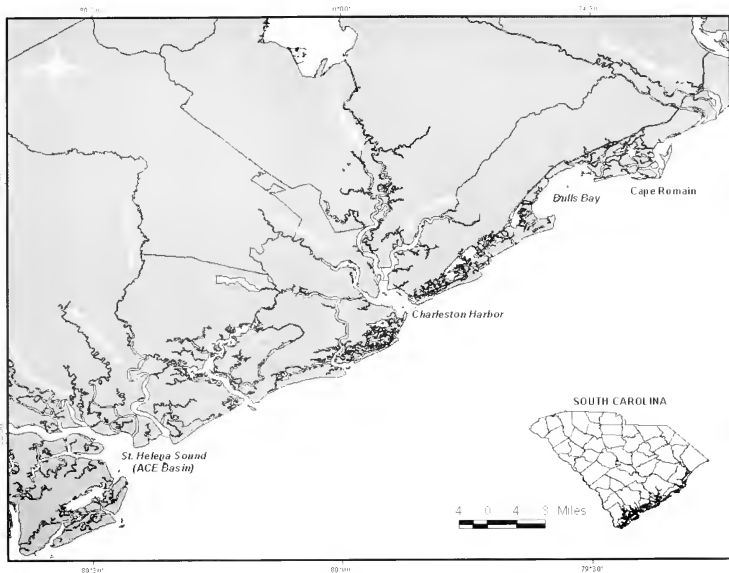


Figure 1

Map of coastal South Carolina with estuaries where trammel net collections were made: Cape Romain, Charleston Harbor, and Ashepoo River, Combahee River, Edisto River (ACE) Basin, as well as the coastal rivers where electroshock collections were made.

and gonad tissue joined in striped mullet (Chang et al., 1995). Comparisons of oocyte density from different sections of striped mullet ovary have also demonstrated uniform distribution throughout the ovary (Shehede et al., 1973; McDonough et al., 2003). A gonadosomatic index (GSI) was calculated for specimens according to the method of Render et al. (1995) where GSI was expressed as a percentage of gonad weight (GW) divided by body weight (BW) minus gonad weight, such that

$$GSI = (GW / (BW - GW)) \times 100.$$

Histological processing

The tissue samples were processed by using standard wax histology techniques (Humason, 1967). Tissues were embedded in paraffin and cut on a rotary microtome. The sections, which ranged from 5 to 7 μ m thick, were then placed on microscope slides and stained with standard haematoxylin and eosin-Y staining techniques (Humason, 1967). After staining, tissue sections were

sealed under a cover slip and evaluated for sex and maturity with a compound light microscope at 100 \times magnification. The sex of each specimen was determined to be male, female, or undifferentiated. Maturity was assessed according to a modified version of the schedule used by Wenner et al. (1986) that was adapted by the authors to work with isochronal spawning fish, as well as assessed with previous models of reproductive development (Stenger, 1959; Grier, 1981; Wallace and Selman, 1981) (Table 1). Ovarian atresia was divided into four distinct phases as described by Hunter and Macewicz (1985). For the sake of consistency, the same terminology was used to describe the four phases of ovarian atresia in striped mullet in this study: alpha, beta, gamma, and delta (see Table 2). These evaluation methods were based on identification of morphological characteristics evident in histological sections. Specimens were evaluated by two readers to avoid bias. Any discrepancies of maturity stage between readers were either mutually resolved or the specimen was excluded from further analysis.

Table 1

Histological criteria used to determine reproductive stage in striped mullet (*Mugil cephalus*) once sexual differentiation has occurred. Modified from Wenner et al. (1986).

Reproductive stage	Male	Female
1. Immature	Inactive testes; small transverse sections compared to those of resting male; spermatogonia and little or no spermatocytic development.	Inactive ovary with previtellogenic oocytes and no evidence of atresia. Oocytes are <80 μm , lamellae lack muscle, and connective tissue bundles are not as elongate as those in mature ovaries, ovary wall is very thin.
2. Developing	Development of cysts containing primary and secondary spermatocytes all the way through accumulation of spermatozoa in lobular lumina and ducts.	Developing ovary have enlarged oocytes generally greater than 120 μm in size. Cortical alveoli become present and actual vitellogenesis occurs after oocytes reach 180 μm in size and continue to increase in size. Abundant yolk globules with oocytes reach a size range of >600 μm .
3. Running, ripe	Predominance of spermatozoa in lobules and ducts and little occurrence of spermatogenesis.	Completion of yolk coalescence and hydration in most oocytes.
4. Atretic or spent	No spermatogenesis occurring but some residual spermatozoa in shrunken lobules and ducts.	More than 30% of developed oocytes undergoing the atretic process. See Table 2 for detailed description of the atretic process.
5. Inactive or resting	Larger transverse sections compared to those of immature males; little or no spermatocytic development; empty lobules with well-developed secondary ductwork and some residual spermatogonia.	Previtellogenic oocytes with only traces of atresia. In comparison to those of immature females, most oocytes are >80 μm , lamellae have some muscle and connective tissue bundles; lamellae are larger and more elongated than those of immature females and the ovarian wall is thicker.

Table 2

Histological criteria used to determine atretic stage in striped mullet (*Mugil cephalus*). Criteria based on ovarian atretic process described by Hunter and Macewicz (1985) and observational data of striped mullet ovaries from this study.

Atretic stage	Description
1. Alpha atresia α	Vitellogenic oocytes are present with distinct yolk globules, which are beginning to break down. The most developmentally advanced oocytes will undergo atresia first, followed by less developed oocytes. The oocyte will break down from the interior outward; the vitelline membrane and follicle layers are the last portion of the oocyte to decay. As the oocyte breaks down, a series of vacuoles of various sizes will appear within the oocyte.
2. Beta atresia β	The oocytes continue to become reduced in size as they decay. The vacuoles that began to form during the alpha stage are now coalescing together to form one large vacuole within the oocyte. This gives the lamellae a distinct hollow matrix and just the outer layers of the oocyte and follicle are now left. This appears to be the shortest atretic phase.
3. Gamma atresia γ	The oocytes that were left in the hollow matrix during the beta stage now begin to shrink in size and the outer layers fold in on themselves as the oocyte collapses. The areas in and around the collapsed oocytes and lamellae become highly vascularized during this stage in order to facilitate rapid resorption of decaying cellular material. There will still be some vacuoles present within the collapsed oocytes but they have become much smaller and there are far fewer of them. This stage continues until most of the remaining oocytes that developed for spawning are no longer recognizable as oocytes.
4. Delta atresia δ	The remnants of old oocytes at this stage are identifiable only as decaying cellular material and will stain a distinct yellow-brown color and are still present in (approximately) 30% or more of the material within the ovary. Undeveloped oocytes have a much more distinct and numerous presence within individual lamellae. The amount of vascularization seen in the gamma stage is reduced because most of the old material has been reabsorbed.

Aging techniques

Age was determined by using the left sagittal otolith, which was embedded in epoxy resin. A 0.5-mm transverse section encompassing the otolith core was cut with an Isomet low speed saw with diamond wafering blades. The thin section of otolith embedded in the epoxy was observed with a dissection microscope at 20 \times magnification, and age was recorded as the number of annular rings present. The otoliths were initially aged by one reader. A second reader then evaluated a subsample of specimens from 1998 and 2000 and all the otoliths from 1999. The two groups of ages were compared by the percentage of agreement between the different age determinations and by a paired *t*-test that allowed a comparison of the means and variances of the two groups (Campana et al., 1995). Ages were then validated by marginal increment analysis in order to establish the timing and periodicity of increment deposition (Campana, 2001). In addition, the precision of the ages was compared by using average percent error (APE) between the two sets of ages. "Precision" was defined as the reproducibility of age determinations (Beamish and Fournier, 1981; Chang, 1982). Using the Levenburg-Marquardt procedure (Zar, 1984), we determined the growth curve with a nonlinear least squares regression of total length on age.

Results

Age structure

We recorded the age of 3760 specimens and examined these specimens histologically to determine sex and maturity stage. An additional 2524 young-of-the-year (age 0) specimens were used for the nonlinear regression of total length on age, as well as the sex ratios by both size and age. The age range for striped mullet in this study was 0 to 10 years, and 1- and 2-year-olds dominated the age distribution (Fig. 2). There was 81.7% agreement for age data between the two readers, and 99.5% agreement within one year for both readers. A *t*-test indicated no significant difference between the two sets of age estimations ($t=2.898$, $df=1,233$, $P<0.05$). The average percent error (APE) (Beamish and Fournier, 1981) between the two sets of age estimations was 0.41%.

Marginal increment analysis indicated that growth increments were deposited during July (Fig. 3). The

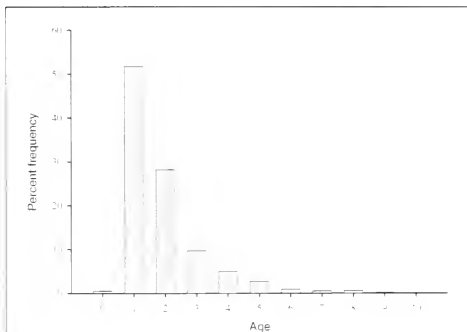


Figure 2

Age-frequency distribution (expressed as a percentage) for striped mullet (*Mugil cephalus* L.) from South Carolina estuaries October 1997 to December 2000. $n=3760$.

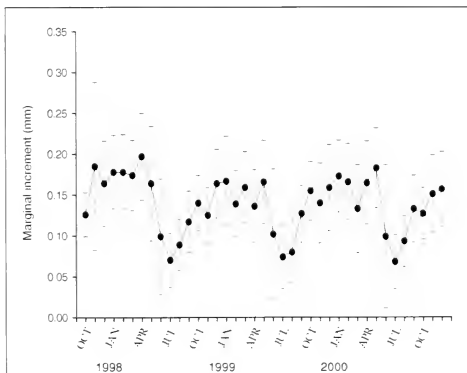


Figure 3

Mean marginal increment distance by month for striped mullet (*Mugil cephalus* L.) from South Carolina estuaries, October 1997 to December 2000. $n=3760$. Marginal increment equals the otolith section radius minus the distance from the core to the last annular increment.

total length at age regression demonstrated a strong relationship ($r^2=0.864$, $df=3759$, $F_{stat}=21.742$, $P<0.05$). Despite this strong relationship, there was a wide range of sizes among the 1-, 2-, and 3-year-olds (Fig. 4).

There was a lag period between the time of formation of the first annual growth mark and the actual one-year birthdate. The first annular mark was deposited between 15 and 19 months of age or at 1.25 to 1.6 years of age (Wenner and McDonough³).

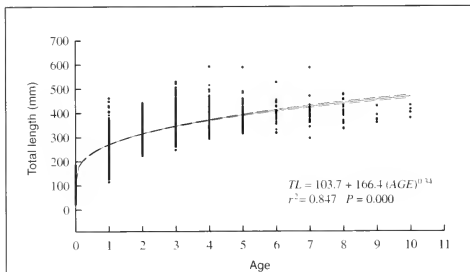


Figure 4

Nonlinear regression of total length on age for striped mullet (*Mugil cephalus* L.) from South Carolina estuaries, October 1997 to December 2000. $n=6284$.

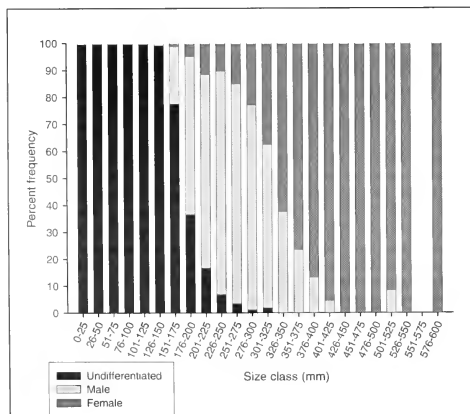


Figure 5

Sex by size class (25-mm size classes) for striped mullet (*Mugil cephalus* L.) from South Carolina estuaries, October 1997 to December 2000. $n=6284$.

Sexual differentiation

The smallest sexually differentiated male was 137 mm (Fig. 5). Male striped mullet 126 to 150 mm TL were eight to twelve months old (McDonough and Wenner, 2003). The first sexually differentiated female was 164 mm TL. Females 151 to 175 mm would have been approximately one year old (McDonough and Wenner, 2003). Specimens greater than 200 mm were at least 50% sexually differentiated. Only 1.5% of specimens over 300 mm remained undifferentiated. The largest sexually undifferentiated specimen was 325 mm. All fish >325 mm, although still possibly sexually immature, were fully sexually differentiated. The ratio of males to females was 2:1 until the fish were larger than 325 mm ($\chi^2_{\alpha=0.05}=2543.9$, $df=2$). The ratio of males to females was 1:3.8 for fish >325 mm ($\chi^2_{\alpha=0.05}=352.8$, $df=1$).

The sex ratio by age class showed 98.9% of the age-0 specimens were sexually undifferentiated (Fig. 6). The few age-0 fish that were differentiated were all males. At first annulus deposition, 91.9% of the specimens had differentiated. There were a few specimens (0.8%) that remained undifferentiated to 3 years old, but all striped mullet age 4 or older were completely differentiated. The sex ratio of males to females in the one-year-old age class was 1.0:0.25 ($\chi^2_{\alpha=0.05}=1065.4$, $df=2$). At age 2 the ratio was 1.0:0.68 ($\chi^2_{\alpha=0.05}=502.6$, $df=2$) and at age 3 the ratio had reversed to 0.32:1.0 ($\chi^2_{\alpha=0.05}=312.5$, $df=2$).

Size and age at maturity

The onset of spermatogenesis in males was first observed at 248 mm (Fig. 7A). The first running, ripe males occurred at 291 mm and this developmental stage was found in all larger sizes. Postspawning males were found only between November and March in mullets larger than 325 mm. Resting mature males were found in every month and occurred in most size classes greater than 251 mm. These resting males made up fewer than 50% of the specimens from any particular size class. A small percent-

³ Wenner, C. A., and C. J. McDonough. 2001. Cooperative research on the biology and assessment of nearshore and estuarine fishes along the southeast coast of the U.S.: Part IV: Striped mullet, *Mugil cephalus*, p. 17-23. Final Report, Grant no. NA77FF0550. Marine Resources Research Institute, South Carolina Dep. Natural Resources, P.O. Box 12559 Charleston, SC 29422-2559.

age (2.5%) of immature males were found in size classes greater than 325 mm. Male striped mullet showed 50% maturity at 275 mm, and 100% maturity by 350 mm.

Oogenesis began in specimens as small as 291 mm (Fig. 7B) and there were 15 females below 325 mm undergoing oogenesis (4.5% of all developing females). Ovaries were found in three small females (<300 mm). Immature females were not found larger than 400 mm or older than 3 years. All females greater than 400 mm were mature, regardless of their age. The majority of females over 425 mm (88.3%) were developing and found only in the fall. No ripe female striped mullet were found. Ovarian atresia was found from December through May. Female striped mullet showed that 50% maturity was reached at 325 mm, and 100% maturity occurred in specimens 400 mm.

Gametogenesis occurred in each sex between the first and second year (Fig. 8). However, the majority of specimens at age 1 (65%) were immature. Males and females showed 50% maturity at 2 years. Males showed 100% maturity at age 4 and females at age 5. Running, ripe males were first observed at age 1 but were found in much greater numbers at ages 4–6. Resting males occurred in every age class except age 6 (Fig. 8A). The abundance of males aged 3 and older was far lower (by at least an order of magnitude) than that of 1- and 2-year-olds (Fig. 8A). Atretic ovaries were found in all age classes, and resting females were found in every age class except age 0 (Fig. 8B).

Maturity stages by month showed immature and resting (but sexually mature) male and female striped mullet occurred in every month (Fig. 9). Developing males were found from August through February, and running, ripe males from October through February. Males (atretic) were found from November through March. Developing females occurred from August through April. Mean monthly GSI for males and females showed noticeably increased gonad size in November and December, and obviously enlarged gonads occurred from October through March (Fig. 10).

Histological descriptions: undifferentiated juveniles

The primordial gonad lobes were suspended by mesentery connected dorsally to the peritoneum and were attached ventrally to the intestines (Fig. 11A). Gonads from specimens <100 mm were identifiable only through histological examination of whole-body cross sections.

The gonads in specimens less than 50 mm had lobes ranging from 70 to 100 μ m in length (Fig. 11B). Lobes were made up of somatic cells and a peripheral germinal epithelium. The lobes were attached along their dorsomedial surface by loose fibrous connective tissue, known as stromal tissue. No defining male or female characteristics were present at this fish length.

In specimens ranging from 50 to 100 μ m gonad lobes had increased to 150 μ m and appeared more vascularized (Fig. 11C). The lobes were attached to the suspensory mesentery, which was attached to the peritoneum. A few deuteronia were visible along the lateral pe-

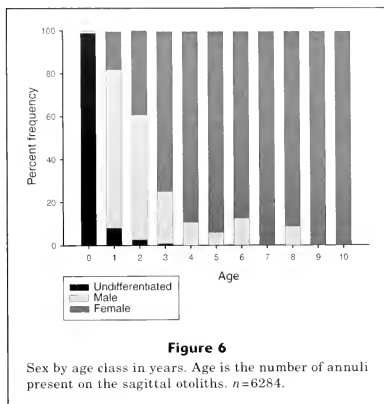


Figure 6

Sex by age class in years. Age is the number of annuli present on the sagittal otoliths. $n=6284$.

riphery of each lobe. The remainder of the lobes contained somatic tissue. The individual germ cells were approximately 5 μ m in size. In some specimens, somatic tissue was beginning to form bands that would later develop into ductwork.

In specimens ranging from 100 to 150 mm, the gonad lobes were obviously vascularized and had attained a size of 200 to 300 μ m (Fig. 11D). Early ductwork was beginning to become evident. Deuteronia were enlarging and forming nests along the lateral and distal portions of the lobes. Somatic cells made up a large portion of each lobe and the stromal tissue was now more stalklike, attaching each lobe to the suspensory tissue. There were only four specimens in this size range that had started to differentiate as males. Gonads destined to be males were identified by duct structures within the gonad lobe as well as by more elongated germ cell nests. These morphologically distinct features resulted in an early demonstration of the corradiating pattern of ducts and lobules seen in more advanced testes.

The 150 to 200 mm size class showed that 0.2% of females and 37.3% of males began initial differentiation, but the majority of all specimens (62.5%) remained undifferentiated. The undifferentiated gonads had become larger, and lobe size was 600 to 800 μ m (Fig. 11E). There was increased vascularization, particularly along the medial portion of the stroma. Germ-cell nests were now more organized, with 4 to 8 cells visible in each.

More than 83% of specimens >200 mm had become sexually differentiated. The undifferentiated gonads in specimens >200 mm were highly vascularized and had both the presence of ductwork, rounded germ cell nests, and lobule-like structures. In some cases, germ cell nests that were characteristic of female precursors

could also be found in the center portions of lobes adjacent to the characteristic male precursor lobe structures. The primary duct was now well formed; however there were still no definitive morphological characteristic that would enable sex determination.

Male differentiation

The initial differentiation of males was evident in the morphological features of the germ-cell tissue located along the peripheral portions of each lobe. The germ tissue began to form elongated bands perpendicular to the edge of the lobe, whereas the somatic tissue began to form fibrous bands originating along the edges of the

primary duct (Fig. 12A). The primary duct was defined structurally at this point. With continued increase in fish length, lobes increased in size and vascularization. The germ tissue continued to elongate medially within the lobe in a corradiating pattern (Fig. 12B). Somatic tissue continued to form bandlike structures that would eventually become secondary ductwork, and the germ-cell expanded to form lobules (Fig. 12C). As the lobules became more developed, spermatogonia began to line the lobules as part of the germinal epithelium (Fig. 12D). Sertoli cells were not visible because of the lack of resolution at this magnification (400 \times) level. Mitotic proliferation of spermatogonia caused lobular enlargement, although spermatogonia were very small at this stage (2–3 μ m). The overall male aspects of the physical structure of the lobes was clear at this point (Fig. 12E). Melanomacrophages were found in the lobes of some specimens (Fig. 12F). The melanomacrophages were found only in immature and differentiating males.

Female differentiation

The first sign of female sexual differentiation was the organization of germ-cell tissue into round nests of 8–10 cells each (Fig. 13A). The germ-cell nests, which eventually gave rise to oogonial nests, were first found along the lateral periphery of the lobe and were infrequently scattered within the gonad lobe. There was evidence of early ovarian wall development, which consisted of a single layer of cells forming the outer layer of the lobe, separate from the oogonial nests (Fig. 13B). Although some ductwork was present, there was no evidence of the formation of lamellae. Ductwork tended to become reduced as the germ-cell nests became more numerous. With continued development, individual cells within the nests became more visible and the ovary wall became more evident (Fig. 13B). Stalks or buds of tissue were observed growing out of the base of the stroma on the dorsolateral surface (Fig. 13C). As development progressed, the ovarian wall attached to these stalks or tissue buds appeared to grow over the dorsal surface of each ovarian lobe. This ovary-wall stalk bud was not necessarily an indicator of female differentiation because a small number of samples (0.6%) with definite male structure also had indications of these stalk buds. However, these tissue stalks were present in 68% of the differentiating females. The presence of both the ovary wall stalk buds and the rounded germ-cell nests located throughout the gonad lobe were diagnostic of female differentiation.

Primary growth oocytes increased in number and began to aggregate, forming distinct lamellae (Fig. 13D). The ovary wall continued to differentiate at this point but was only a few

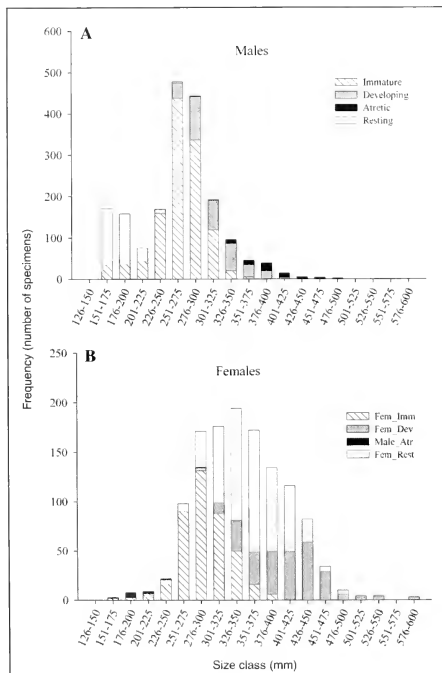


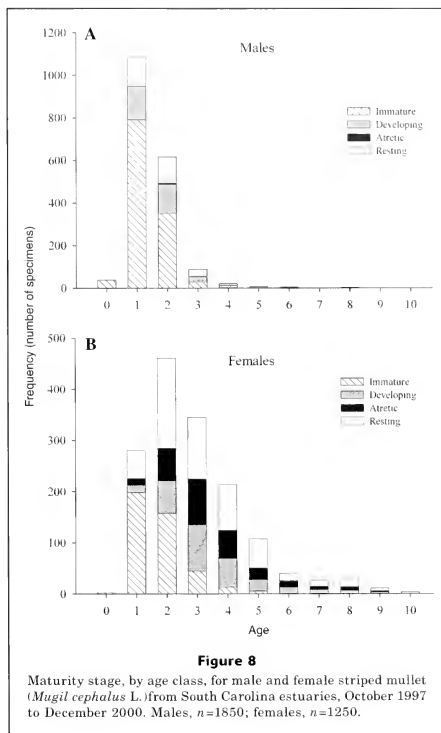
Figure 7

Maturity stage by size class for male and female striped mullet (*Mugil cephalus* L.) from South Carolina estuaries, October 1997 to December 2000. Males, $n=1850$; females, $n=1250$.

cell layers thick. There was still a great deal of stroma and somatic tissue left in the ovary, but it began to form bands of fibrous tissue, resulting from the regression of stroma and somatic tissue (where present) as the lamellae continued to develop. The primary duct was greatly reduced. Oogonia began proliferating and differentiating into primary growth oocytes as folliculogenesis commenced. The ovary wall, now becoming vascularized, began to separate from the lamellae, opening a space that would become the ovarian lumen (Fig. 13, D–F). The ovary wall was made up of squamous cells on the inside layers and collagen and elastic tissue on the outer layers. The stroma and somatic cells continued to be reduced until they were primarily fibrous tissue from which the lamellae were suspended. Histological ovarian cross-sections changed from the leaf or spade shape of the undifferentiated gonad to a more rounded one. Once ovarian differentiation was completed, the individual lamellae were seen to have oocytes within each and the stroma was reduced to suspensory tissue for the lamellae (Fig. 13F). The primary growth oocytes present in the lamellae remained small (80 to 100 μm) and relatively uniform in size. At the initiation of reproductive development, the oocytes started to grow from the arrested prophase of the first meiotic division (Stenger, 1959; Kuo et al., 1974).

Morphological features of atretic females

Females undergoing atresia were captured in all months except August–October, and 78% were seen January–March of each year. The first sign of alpha atresia was the breakdown of the most advanced residual oocytes. Vacuoles (of various sizes) began to appear (Fig. 14A), merging to form large spaces within the decaying oocyte. The overall diameter of oocytes decreased from 600 to 300–400 μm ; however oocytes retained their overall shape during alpha atresia and showed no signs of collapse (Fig. 14B). Beta atresia was the shortest phase. The oocytes had shrunk in size (<300 μm) but retained their previous overall structure and shape. A distinct hollow matrix retaining only the outer layers of the oocyte (follicle layers and the vitelline membrane) was the defining characteristic for beta atresia (Fig. 14C). The tissue retained this structure while the oocyte continued to decrease (150–180 μm). During gamma atresia the oocytes collapsed (Fig. 14D) or shrank. Some vacuoles remained in partially collapsed oocytes, but they were fewer in number and smaller in size (<150 μm) (Fig. 14E). The areas in and around the collapsed oocytes and ovarian lumen became more vascularized during this stage, and this helped facilitate rapid resorption of decaying cellular material (Fig. 14F). Undeveloped oocytes became more visible and numerous. Gamma atresia ended when only masses of broken-down



cellular material remained. Delta atresia was characterized by the presence and decay of nondescript cellular material from the previous spawning (Fig. 14G). Delta atresia was present in approximately 30% or more of the ovary. There was also a decrease in the amount of vascularization within the ovarian lamellae during this stage because most of the old oocyte material had been resorbed. The lamellae contained only undeveloped oocytes and all the remaining material from the previous spawn was concentrated medially in the lamellae.

In the resting stage, no reproductive activity occurred in the ovaries. Infrequently, resting ovaries showed some minor evidence of the previous spawning. The remaining undeveloped oocytes were previtellogenic and varied widely in size (80–120 μm). The ovary wall was relatively thick, particularly in comparison to the

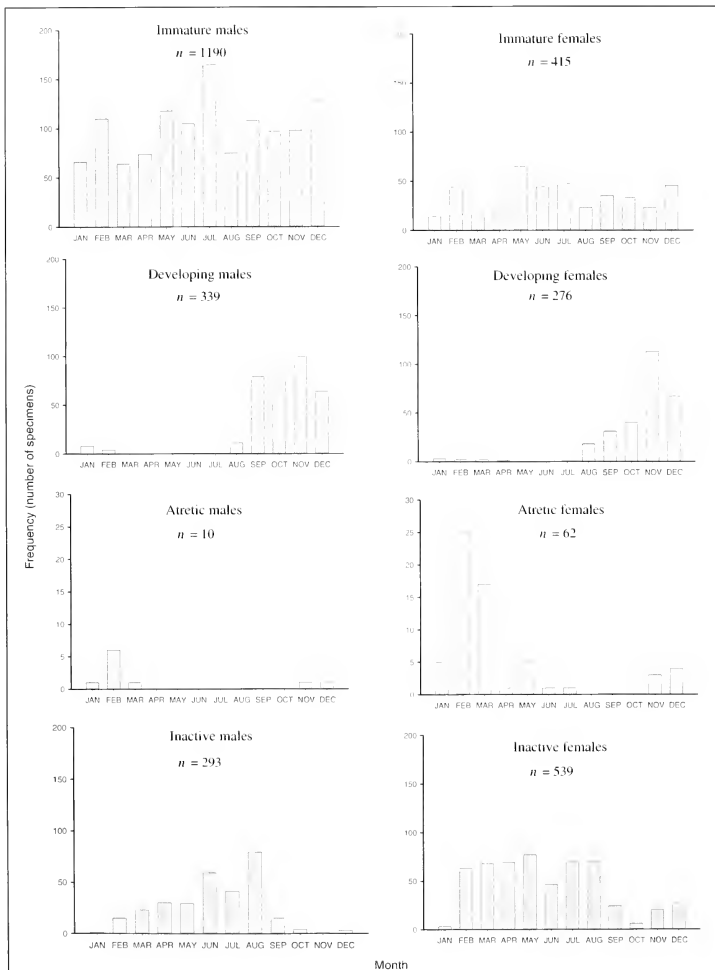


Figure 9

Frequency of occurrence of each maturity stage by month for male and female striped mullet (*Mugil cephalus* L.) from South Carolina estuaries, October 1997 to December 2000.

immature ovaries, and had distinct smooth muscle layers (Fig. 14H). Any stromal tissue left in the ovary at this point was also greatly reduced and was essentially the mesentery from which the lamellae were suspended.

Discussion

Age structure

The abundance of 1- and 2-year-old striped mullet in South Carolina indicated that immature fish dominate the estuarine population. The importance of proper age validation in order to make comparisons of age and sexual maturity cannot be understated. The most important aspect of age validation is to obtain a degree of precision that allows repeatability in age determinations (Campana, 2001). The periodicity of growth increment formation was validated by marginal increment analysis, and the precision of these age estimates was then tested by comparing age counts of two independent readers.

Marginal increment analysis showed that annual growth increments were deposited in striped mullet in July in the entire data set, as well as separately for ages 1–5. By validating increment periodicity separately for different age groups, a consistent pattern for the species can be determined (Campana et al., 1995; Campana, 2001). The percent agreement between the two readers and a *t*-test for independent age determinations allowed direct comparisons of the two groups of ages for consistency (Campana et al. 1995). However, these two methods were both independent of the age of the species. Therefore, average percent error (APE) was used to compare the different sets of ages because it is not independent of the age of a species (Beamish and Fournier, 1981). The low APE (0.41%) found between the two different age estimates indicated a high degree of precision, which allowed acceptance of these age determinations.

Sexual differentiation

Striped mullet are gonochoristic and sex is genetically determined. In contrast to mammals, gender of the mature germ cells of teleosts present in the gonad rather than the gender of the duct system forms the basis for classifying an individual as male or female (Shapiro, 1992). Early duct structures of the undifferentiated gonad characteristic of male development regress on female development. Initial duct development, along with germ tissue placement, takes on characteristics of the eventual sex once the process of differentiation begins (Asoh and Shapiro, 1997). Because of the plasticity of their gonad development, striped mullet retain some characteristics of the opposite sex (such as singular oogonia in males or

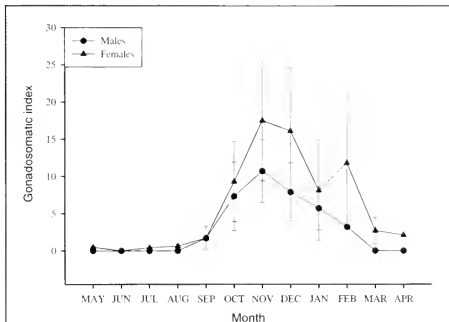


Figure 10

Mean gonadosomatic index value by month for male and female striped mullet (*Mugil cephalus* L.) from South Carolina estuaries from 1998 to 2000. $n=455$.

duct-work in females) during the initial stages of differentiation. The term that has been used to describe this phenomenon is "intersex" (Yamamoto, 1969) but this state could more accurately be defined as the hermaphroditic stage of some gonochoristic species. Numerous descriptions of intersex exist for teleosts (Atz, 1964). Previous studies have brought up the possibility of hermaphroditism in striped mullet (Stenger, 1959; Atz, 1964; Moe, 1966); however, there is only one example of a simultaneous hermaphroditic striped mullet in the literature (Franks et al., 1998). Once differentiation advances, these secondary characteristics atrophy, and the gonad develops toward the genetically determined sex.

We found that at first annual increment deposition (15–19 months), most (95%) immature striped mullet were sexually differentiated. Chang et al. (1995), using cultured striped mullet, found that differentiation began only after 12 months of age, and 70% to 90% of immature fish at 15 to 17 months had differentiated sexually. We found only a small percentage (1.2%) of differentiated specimens at 12 months of age. Chang et al. (1995) did not report fish sizes, and Stenger (1959) studied sizes at sexual differentiation without reporting age. Stenger (1959) concluded that striped mullet up to 150 mm generally were not differentiated sexually. We found four specimens in which differentiation had occurred in the 126–150 mm size range, which represented specimens 12 months or less in age. Once our specimens reached the 176–200 mm size range, just over 60% had sexually differentiated, which was also approximately the size range at which the first annulus appeared (Wenner and McDonough³).

Chang et al. (1995) found that females differentiated earlier than males; we, on the other hand, showed sex

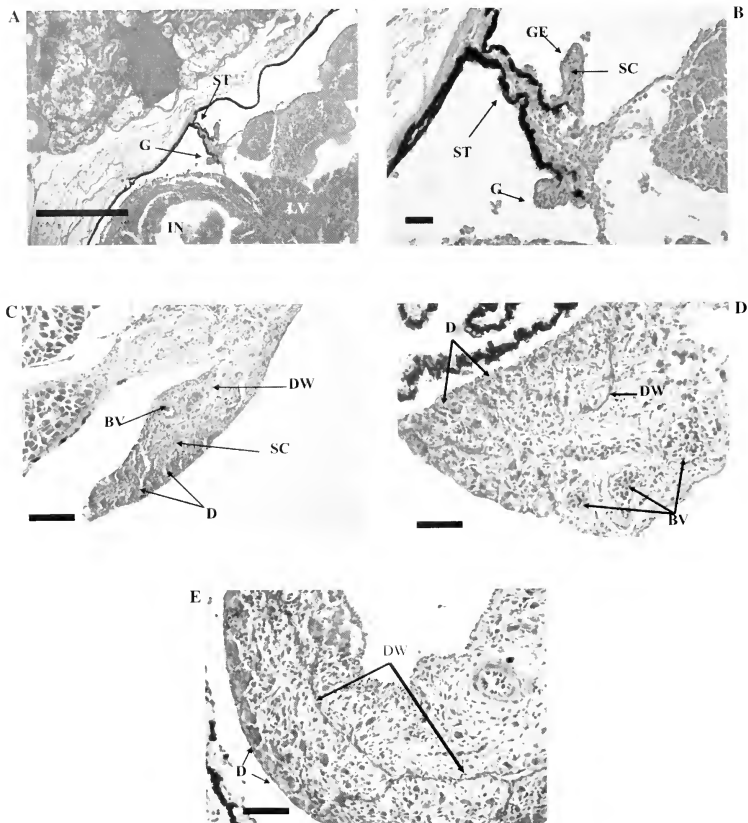
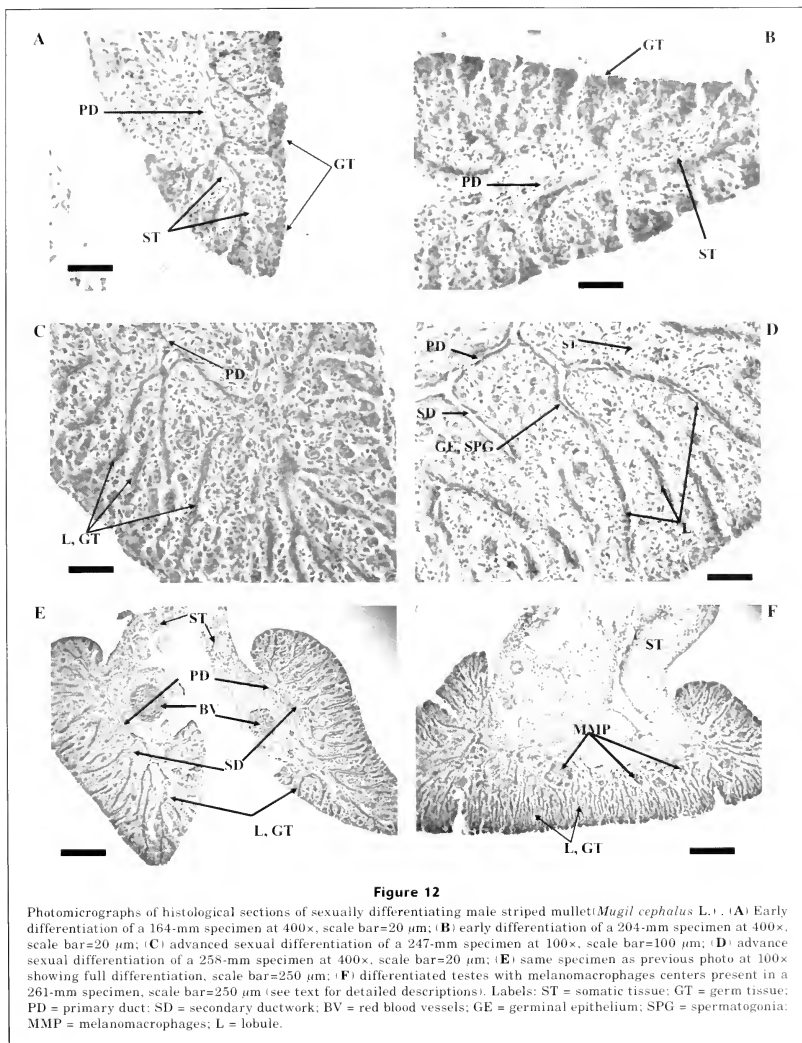


Figure 11

Photomicrographs of histological sections of undifferentiated juvenile striped mullet (*Mugil cephalus* L.): (A) 35-mm specimen at 100x (scale bar=50 μm) and (B) 600x (scale bar=10 μm) respectively; (C) 55-mm specimen at 400x, scale bar=20 μm; (D) 135-mm specimen at 400x, scale bar=20 μm; (E) 184-mm specimen at 400x, scale bar=20 μm (see text for detailed descriptions of each). Labels: G = primordial gonad; GE = germinal epithelium; SC = somatic cells; D = deuterogonia, DW = duct work; BV = blood vessel; ST = suspensory tissue; LV = liver; IN = intestine.



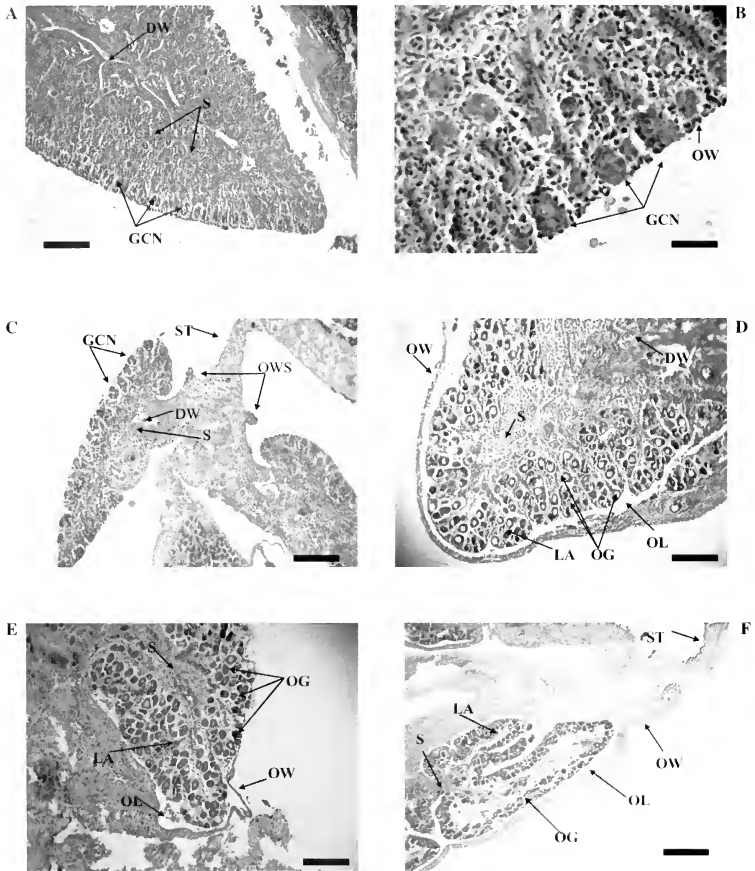


Figure 13

Photomicrographs of histological sections of sexually differentiating female striped mullet (*Mugil cephalus* L.). (A) Early differentiation of germ cell nests in a 239-mm specimen at 100 \times , scale bar=100 μ m; (B) early differentiation of germ cell nests in a 205-mm female at 400 \times , scale bar=20 μ m; (C) mid-differentiation in a 225-mm female at 100 \times , scale bar=100 μ m; (D) advanced sexual differentiation with developing lamellae and ovarian wall in a 279-mm female at 100 \times , scale bars=100 μ m; (E) advanced sexual differentiation in a 267-mm female at 100 \times , scale bar=100 μ m; (F) full differentiation of a 284-mm female, scale bar = 100 μ m. Labels: GCN = germ cell nests; OW = ovary wall; ST = suspensory tissue; OWS = ovary wall stalks; S = stroma; OG = oogonia; LA = lamellae; DW = ducts; OL = ovarian lumen.

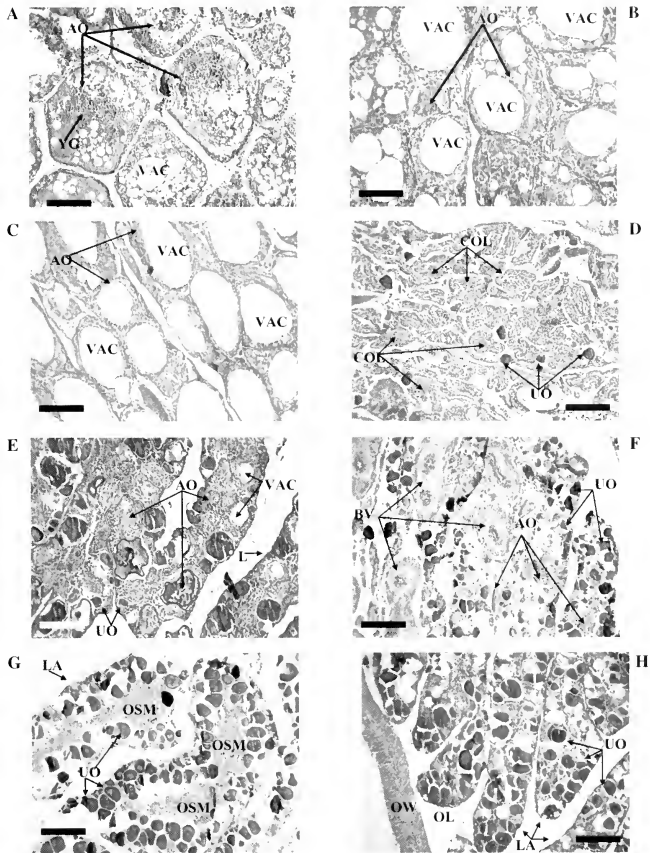


Figure 14

Photomicrographs of histological sections of ovarian atresia and the inactive reproductive stage in mature female striped mullet (*Mugil cephalus* L.). (A) Alpha-stage oocyte atresia, scale bar=100 μ m; (B) Late alpha-stage oocyte atresia, scale bar=100 μ m; (C) Beta-stage oocyte atresia, scale bar=100 μ m; (D) Early gamma-stage oocyte atresia, scale bar=100 μ m; (E) Gamma-stage oocyte atresia, scale bar=100 μ m; (F) Late gamma-stage and early delta-stage oocyte atresia, scale bar=100 μ m; (G) Delta-stage oocyte atresia, scale bar=100 μ m; (H) Reproductively inactive striped mullet ovary with degraded cellular material from previous spawning, scale bar=100 μ m. Labels: YG = yolk globules; VAC = vacuoles; AO = atretic oocytes; COL = collapsed outer cell layers; UO = undeveloped oocytes; BV = blood vessels; OSM = old spawn material; OW = ovary wall; OL = ovarian lumen; LA = lamellae.

ratios at size indicating that males differentiated first. This difference may be explained by the experimental methods because the differentiation process was likely similar between the cultured and wild fish. Chang et al. (1995) showed that female development occurred before male development based on levels of plasma sex steroids. However, this finding was later corrected to show that plasma sex steroid levels were the same for males and females throughout sexual differentiation (Chang et al., 1999).

The formation of lobules with the proliferation of germ tissue has been previously described as a male developmental pattern (Stenger, 1959; Grier, 1981; Grier and Taylor, 1998; Grier, 2000). The morphological progression seen in the present study was similar to that previously described in histological examinations of differentiation in striped mullet in conjunction with size (Stenger, 1959) and age (Chang et al., 1995). However, ours is the first study to examine sexual differentiation of both male and female striped mullet with changes in size and age and to describe these changes histologically.

The undifferentiated gonad appeared to have male morphological characteristics. The first morphological signs of female differentiation were the movement of deuteronial germ-cell nests from the periphery of the gonad. This pattern of development was similar to the ontogeny of differentiation described previously for striped mullet (Stenger, 1959). However, the presence of the tissue stalk at the base of the suspensory tissue, to which the ovary wall was attached, has not previously been described. The tissue stalk was present on the majority (68%) of differentiating ovaries and only a few (0.25%) of the differentiating testes. The presence of this stalk in differentiating testes indicated that this characteristic alone should not be used to determine genetic sex. However, the presence of the tissue stalk, in addition to the rounded oogonial nests throughout the gonad, strongly indicated that the specimen was female. There were no specimens observed to be developing an ovary wall that also had developing lobules or duct-work (male characters). Therefore, from a morphological standpoint, the initial definitive identification of the differentiating ovary was the formation of the ovary wall along with rounded germ cell nests throughout the lobe. A primary duct at the center of the developing ovary was present at this stage but any secondary duct-work had begun to atrophy. It was also observed that oogonial and oocyte proliferation could occur throughout the lobe without a definitive ovary wall, which would also be a strong indicator of the female sex.

Size and age at maturity

Once sexual differentiation had occurred, the earliest indication of spermatogenesis occurred at just under 250 mm (two specimens) and one year of age. However, the majority of the developing specimens (89.9%) did not show signs of spermatogenesis until they reached

300 mm and age 2. The greater abundance of immature males under 300 mm would also indicate that full maturity was reached by this length. Almost all the males over 325 mm were in some state of reproductive activity, either developing or running, ripe, because most of these larger males were captured only during the spawning season. October, November, and December were the only months when we saw these larger fish, except for some atretic-stage specimens taken from freshwater during the spring. The first signs of spermatogenesis for striped mullet, both from eastern Florida (Stenger, 1959) and South Carolina, were found in August.

Greeley et al. (1987) did not age female striped mullet but used the growth schedule of Thomson (1966) to conclude that striped mullet in eastern Florida reach sexual maturity at 2.25 to 2.5 years, which is 1 to 2 years earlier than that previously reported (Jacot, 1920; Broadhead, 1956; Anderson, 1958; Thomson, 1966). One problem in earlier studies was the use of scale-based age estimates (Jacot, 1920; Thomson, 1951, 1966; Timoshak, 1973). The otoliths used in our study showed more repeatability than would scales. Age schedules based on scales were likely to contain problems with the error terms and overestimation. Another factor may have been the lack of a proper age-validation protocol. The lag in time between the actual birthdate and the first increment formation was not incorporated into the age model. A fish with a single annular ring that appeared to be mature could actually have been up to 30 months old. Male striped mullet did not begin to mature until they were one year old, and almost 100% had reached sexual maturity by age 3. Ripe and atretic males were also found at age 1.

Size at maturity for female striped mullet was reported to be from 290 to 430 mm (Thomson, 1951, 1966; Broadhead, 1956; Chubb et al., 1981). This wide range in size at maturity depended on whether gonads were examined by gross morphological examination (Thomson, 1951, 1966; Broadhead, 1956) or histologically (Stenger, 1959; Chubb et al., 1981). Stenger (1959) found that oocyte development occurred in specimens as small as 270 mm fork length (300 mm TL). Greeley et al. (1987) reported the minimum size at maturity for female striped mullet in eastern Florida was 230 mm SL (290 mm TL). The minimum size at which a female was found to be undergoing active vitellogenesis in the present study was 291 mm. The first signs of female maturity were evident in small numbers (15) in the 2-year-olds. The first atretic females were also found at age 2. The age at maturity for female striped mullet in our study was similar to that found by Greeley et al. (1987) who used length-based predicted ages. Therefore, it appears that striped mullet in South Carolina have a similar maturity schedule to those found in eastern Florida.

Immature and inactive males and females were found every month of the year. The presence of ripe males from October through February and the presence of developing females from August through March support the idea of an extended spawning season from October through April.

The presence of developing females indicated reproductive activity through April; however numbers were small (McDonough et al. 2003). Most of the specimens collected in March and April were either immature or inactive. It has also been demonstrated that striped mullet in closed freshwater systems, such as impoundments, can begin reproductive development. However, unless artificially manipulated, spawning did not occur in freshwater and the fish resorbed the developed gametes (Shireman, 1975; Tamaru et al., 1994). The re-absorption of gametes would undoubtedly have a positive effect on growth rates and may contribute to some of the variation in size at age. Reproductively inactive (but mature) females present every month could indicate that mature mullet do not spawn every year or that fish that remain in the estuary do not migrate offshore to spawn. The most likely possibility would be that inactive females found in the early part of the spawning season may not spawn until much later. However, the presence of developing oocytes beginning in August would indicate that a few months were required for complete recrudescence. It has been shown that striped mullet undergoing the spawning migration between the Black Sea and the Sea of Azov required two months for full ovarian development (Apekin and Vilenkaya, 1978). Also, inactive females from the mid to late spawning season could have spawned early, returned to the estuary, and their ovaries could have regressed. We found no ripe female mullet in the estuaries during the entire study; their absence was likely due to their migration from coastal waters. Evidence of striped mullet spawning (through the back calculation of birthdates from daily growth increments from juveniles) has also shown that the spawning season extends from October through April (McDonough and Wenner, 2003).

Sexual development

It is not known what cue initiates gametogenesis in striped mullet, but it is generally accepted that changes in temperature and photoperiod help regulate the seasonal reproductive cycle (Anderson, 1958; Kuo et al., 1973; Greeley et al., 1987; Kelly et al., 1991; Render et al., 1995). It has been shown that although striped mullet can mature in a range of salinities, the best production is reached when their gonads develop in salinities of 13 to 35 ppt (Brusle, 1981; Tamaru et al., 1994). Previous studies of striped mullet (Kuo et al., 1974) and other fall spawning fishes that migrate offshore to spawn (de Vlaming, 1974; McQuarrie et al., 1978; Whitehead et al., 1978) have indicated that a shortening day length was the key stimulus for annual reproductive development and migration. Dindo and MacGregor (1981) demonstrated a high correlation between the levels of serum gonadal steroids and the gonadosomatic index in striped mullet during the reproductive cycle; a shortening photoperiod was suggested as the major factor in stimulating reproductive activity. In our study the most reproductively advanced specimens (late recr-

descence) in freshwater were captured in October and no other specimens of similar development were captured during the rest of the spawning season in freshwater. In contrast, the majority of the specimens undergoing vitellogenesis were captured in the lower portions of the estuaries during November and December in salinities greater than 15 ppt. This finding indicated movement of these developing fish from the freshwater portions of the estuary toward the ocean for the spawning migration. This migration time-period also coincided with a mean monthly temperature decrease in temperature (from 21.8° to 13.6°C) and in photoperiod in both the freshwater and brackish portions of the estuaries.

The ovarian atretic process in female striped mullet was characterized by four distinct stages that followed a very similar progression to that described for the northern anchovy (Hunter and Macewicz, 1985). Our study is the first to describe the atretic process in striped mullet ovaries in detail and to apply the classification system developed by Hunter and Macewicz (1985). Knowledge of ovarian atresia is useful for the timing of spawning. However, the lack of immediate atretic-stage fish, with indicators such as postovulatory follicles, prevented us from determining the temporal duration of the different atretic stages. The detailed morphological descriptions of ovarian atresia presented in our study would be of value for future studies to determine the specific timing of the atretic process.

The histological descriptions for male and female developmental stages in association with both size and age data provide a clear picture of these parameters at differentiation and maturity in South Carolina striped mullet. Previous studies of striped mullet reproduction concentrated on just one sex or used cultured fish extensively and may have considered size or age but not both in a single study. Because of the length of the undifferentiated gonad stage in juvenile striped mullet, previous studies have proposed the possibility of protandric hermaphroditism in this species. However, the results of our study indicated that striped mullet are gonochoristic but capable of nonfunctional hermaphroditic characteristics in differentiated mature gonads. It is hoped that the descriptions of developmental morphological features presented in the present study will be useful for future studies by providing a key to reproductive ontogeny that relates directly to somatic growth and age in striped mullet. In particular, the morphological characteristics of sexual differentiation could enable more precise determinations of sex in immature mullet, which, in turn, would indicate the sex ratio of males and females in a given population and allow the development of better management strategies.

Acknowledgments

This study would not have been possible without the assistance of everyone, past and present, at the Inshore Fisheries group at the Marine Resources Research Institute of the South Carolina Department of Natural

Resources—Myra Brouwer, John Archambault, Hayne Von Kolnitz, Will Hegler, Erin Levesque, Alice Palmer, Robin Freeman, Chad Johnson, Richie Eviatt, Larry Goss, and Katy Maynard. We especially thank Chad Altman of the South Carolina Department of Health and Environmental Control for collection of freshwater specimens. In addition, we thank Myra Brouwer and David Wyanski and the three anonymous reviewers for their careful review of and suggestions for this manuscript. This research was made possible by National Marine Fisheries Service MARFIN Grant no. NA77FF0550.

Literature Cited

- Anderson, W. W.
1958. Larval development, growth, and spawning of striped mullet (*Mugil cephalus*) along the south Atlantic coast of the United States. *Fish. Bull.* 58:501-519.
- Apekin, V. S., and N. L. Vilenskaya.
1978. A description of the sexual cycle and the state of the gonads during the spawning migration of the striped mullet, *Mugil cephalus*. *J. Ichthyol.* 58(3):446-456.
- Arnold, E. L. and J. R. Thompson.
1958. Offshore spawning of the striped mullet, *Mugil cephalus*, in the Gulf of Mexico. *Copeia* 1958:130-132.
- Asoh, K., and D. Y. Shapiro.
1997. Bisexual juvenile gonad and gonochorism in the fairy basslet. *Copeia* 1997:22-31.
- Atz, J. W.
1964. Intersexuality in fishes. In *Intersexuality in vertebrates, including man* (C. N. Armstrong and A. J. Marshall, eds.), p. 145-232. Academic Press, New York, NY.
- Beamish, R. J., and D. A. Fournier.
1981. A method for comparing the precision of a set of age determinations. *Can. J. Fish. Aquat. Sci.* 38: 982-983.
- Broadhead, G. C.
1956. Growth of the black mullet, *Mugil cephalus*, in west and northwest Florida. *Mar. Lab Tech. Series, Mar. Lab Tech. Serv.* 25:1-29.
- Brusle, J.
1981. Sexuality and biology of reproduction in grey mullets. In *Aquaculture of grey mullets* (O. H. Oren, ed.), p. 99-154. Cambridge Univ. Press, New York, NY.
- Campana, S. E.
2001. Accuracy, precision and quality control in age determination, including a review of the use and abuse of age validation methods. *J. Fish Biol.* 59: 197-242.
- Campana, S. E., M. C. Annand, and J. I. McMillan.
1995. Graphical and statistical methods for determining the consistency of age determinations. *Trans. Am. Fish. Soc.* 124:131-138.
- Chang, W. Y. B.
1982. A statistical method for evaluating the reproducibility of age determinations. *Can. J. Fish. Aquat. Sci.* 39:1208-1210.
- Chang, C. F., C. Y. Hung, M. C. Chiang, and S. C. Lan.
1999. The concentrations of plasma sex steroids and gonadal aromatase during controlled sex differentiation in grey mullet, *Mugil cephalus*. *Aquaculture* 177:37-45.
- Chang, C. F., S. C. Lin, and H. Y. Chou.
1995. Gonadal histology and plasma sex steroids during sex differentiation in grey mullet, *Mugil cephalus*. *J. Exp. Zool.* 272: 395-406.
- Chubb, C. F., I. C. Potter, C. J. Grant, R. C. J. Lenanton, and J. Wallace.
1981. Age, structure, growth rates, and movements of sea mullet, *Mugil cephalus* L., and yellow eye mullet, *Aldrichetta forsteri* (Valenciennes), in the Swan-Avon river system, Western Australia. *Aust. J. Mar. Freshw. Res.* 32:605-628.
- Collins, M. R., and B. W. Stender.
1989. Larval striped mullet (*Mugil cephalus*) and white mullet (*Mugil curema*) off the southeastern United States. *Bull. Mar. Sci.* 45(3):580-589.
- de Vlaming, V. L.
1974. Environmental and endocrine control of teleost reproduction. In *Control of sex in fish* (C. B. Schrek, ed.), p. 13-83. Sea Grant Publ. 74-101, Virginia Polytechnic Institute, Blacksburg, VA.
- Dindo, J. J., and R. MacGregor.
1981. Annual cycle of serum gonadal steroids and serum lipids in striped mullet. *Trans. Am. Fish. Soc.* 110:403-409.
- Finucane, J. H., L. A. Collins, and L. E. Barger.
1978. Spawning of the striped mullet, *Mugil cephalus*, in the northwestern Gulf of Mexico. *Northeast. Gul. Sci.* 2:148-150.
- Franks, J. S., N. J. Brown-Peterson, D. P. Wilson, R. J. Russell, and J. K. Welker.
1998. Occurrence of a synchronous hermaphroditic striped mullet, *Mugil cephalus*, from the northern Gulf of Mexico. *Gulf Res. Rept.* 10: 33-39.
- Greeley, M. S., D. R. Calder, and R. A. Wallace.
1987. Oocyte growth and development in the striped mullet, *Mugil cephalus*, during seasonal ovarian recrudescence: relationship to fecundity and size at maturity. *Fish. Bull.* 85:187-200.
- Grier, H. J.
1981. Cellular organization of the testes and spermatogenesis in fishes. *Am. Zool.* 21:345-357.
2000. Ovarian germinal epithelium and folliculogenesis in the common snook, *Centropomus undecimalis* (Teleostei: Centropomidae). *J. Morphol.* 243:265-281.
- Grier, H. J., and R. G. Taylor.
1998. Testicular maturation and regression in the common snook. *J. Fish Biol.* 53:521-542.
- Hettler, W. F., D. S. Peters, D. R. Colby, and E. H. Laban.
1997. Daily variability in abundance of larval fishes inside Beaufort Inlet. *Fish. Bull.* 95:477-493.
- Humason, G. L.
1967. Animal tissue techniques, 426 p. W. H. Freeman and Co., San Francisco, CA.
- Hunter, J. R., and B. J. Macewicz.
1985. Rates of atresia in the ovary of captive and wild northern anchovy, *Engraulis mordax*. *Fish. Bull.* 83:119-136.
- Jacot, A. P.
1920. Age, growth, and scale characters of the mullets, *Mugil cephalus* and *Mugil curema*. *Trans. Am. Fish. Soc.* 39(3):199-229.
- Kelly, C. D.
1990. Effects of photoperiod and temperature on ovarian maturation in the striped mullet, *Mugil cephalus*. *Pacific Sci.* 44(2):187-188.

- Kelly, C. D., C. S. Tamaru, C. S. Lee, A. Moriwake, and G. Miyamoto. 1991. Effects of photoperiod and temperature on the annual ovarian cycle of the striped mullet, *Mugil cephalus*. In Proceedings of the fourth international symposium on the reproductive physiology of fish (A. P. Scott, J. P. Sumpter, D. E. Kime, and M. S. Rolfe, eds.); Univ. East Anglia, Norwich, United Kingdom, 7-12 July 1991, p. 142-144.
- Kuo, C. M. 1995. Manipulation of ovarian development and spawning in grey mullet, *Mugil cephalus* L. Israel. J. Aquacult. Bamidegh 47(2):43-58.
- Kuo, C. M., C. E. Nash, and Z. H. Shehadeh. 1974. The effects of temperature and photoperiod on ovarian development in captive grey mullet (*Mugil cephalus* L.). Aquaculture 3:25-43.
- Kuo, C. M., Z. H. Shehadeh, and K. K. Milisen. 1973. A preliminary report on the development, growth and survival of laboratory reared larvae of the grey mullet, *Mugil cephalus* L. J. Fish Biol. 5:459-470.
- McDonough, C. J., W. A. Roumillat, and C. A. Wenner. 2003. Fecundity and spawning season of striped mullet (*Mugil cephalus* L.) in South Carolina estuaries. Fish. Bull. 101:822-834.
- McDonough, C. J., and C. A. Wenner. 2003. Growth, recruitment, and abundance of juvenile *Mugil cephalus* in South Carolina Estuaries. Fish. Bull. 101:343-357.
- McQuarrie, D. W., J. R. Markert, and W. E. Vanstone. 1978. Photoperiod induced off season spawning of coho salmon *Oncorhynchus kisutch*. Animal Biochem. Biophysiq. 18:1051-1058.
- Moe, M. A. 1966. Hermaphroditism in mullet, *Mugil cephalus*, Linnaeus. Quart. J. Florida Acad. Sci. 29:111-116.
- Pien, P. C., and J. C. Liao. 1975. Preliminary report of histological studies on the grey mullet gonad related to hormone treatment. Aquaculture 5:31-39.
- Render, J. H., B. A. Thompson, and R. L. Allen. 1995. Reproductive development of striped mullet in Louisiana estuarine waters with notes on the applicability of reproductive assessment methods for isochronal species. Trans. Am. Fish. Soc. 124(1):26-36.
- Rossi, A. R., M. Capula, D. Crosetti, D. E. Campton, and L. Sola. 1998. Genetic divergence and phylogenetic inferences in five species of Mugilidae (Pisces: Perciformes). Mar. Biol. 131:213-218.
- Shapiro, D. Y. 1992. Plasticity of gonadal development and protandry in fishes. J. Exp. Zool. 261: 194-203.
- Shehadeh, Z. H., C. M. Kuo, and K. K. Milisen. 1973. Validation of an *in vivo* method for monitoring ovarian development in the grey mullet (*Mugil cephalus* L.). J. Fish Biol. 1973(5):489-496.
- Shireman, J. V. 1975. Gonadal development of striped mullet (*Mugil cephalus*) in freshwater. Prog. Fish Cultur. 37(4): 205-208.
- Stenger, A. H. 1959. A study of the structure and development of certain reproductive tissues of *Mugil cephalus* Linnaeus. Zoologica 44(2):53-70.
- Tamaru, C. S., C. S. Lee, C. D. Kelley, G. Miyamoto, and A. Moriwake. 1994. Oocyte growth in the striped mullet, *Mugil cephalus* L., maturing at different salinities. J. World Aquacult. Soc. 25(1):109-115.
- Timoshek, N. G. 1973. The distribution and migration of mullet in the Black Sea. Tr. Vses. Nauchno-Issled. Inst. Morsk. Rybn. Khoz. 93:163-177. [In Russian; English summary.]
- Thomson, J. M. 1951. Growth and habits of the sea mullet, *Mugil dobula* Gunther, in Western Australia. Aust. J. Mar. Freshw. Res. 2:193-225.
1963. Mullet life history strategies. Aust. J. Sci. 25: 414-416.
1966. The grey mullets. Oceanogr. Mar. Biol. Ann. Rev. 4:301-335.
- Wallace, R. A. and K. Selman. 1981. Cellular and dynamic aspects of oocyte growth in teleosts. Am. Zool. 21: 325-343.
- Wenner, C. A., W. A. Roumillat, and C. W. Waltz. 1986. Contributions to the life history of black seabass, *Centropristis striata*, off the southeastern United States. Fish. Bull. 84:723-741.
- Whitehead, C., N. R. Bromage, R. M. Forster and A. J. Matty. 1978. The effects of alterations in photoperiod on ovarian development and spawning time in the rainbow trout *Salmo gairdneri*. Annales de Biologie Animale Biochimie Biophysique 18:1035-1043.
- Yamamoto, T. 1969. Sex differentiation. In Fish physiology, vol. 3 (W. S. Hoar and D. J. Randall, eds.), p. 117-175. Academic Press, New York, NY.
- Zar, J. H. 1984. Biostatistical analysis, 2nd ed., p. 292-305. Prentice Hall Inc. Englewood Cliffs, NJ.

Abstract—Large pelagic sharks are caught incidentally in the swordfish and tuna fisheries of the Mediterranean Sea. In our study, twelve shark species were documented as bycatch over three years from 1998 to 2000. Blue shark (*Prionace glauca*) was the predominant species in all gears and areas examined. Shortfin mako (*Isurus oxyrinchus*), common thresher shark (*Alopias vulpinus*), and tope shark (*Galeorhinus galeus*) were the next most abundant shark species—found in more than half of the areas sampled. Catch composition varied both in the areas and gears investigated. Sharks represented 34.3% in weight of total catches sampled in the Alboran Sea and 0.9% in the Straits of Sicily. Higher shark catches were observed in the swordfish longline fishery, where a nominal CPUE value reached 3.8 sharks/1000 hooks in the Alboran Sea. Size distribution by fishing gear varied significantly. Albacore longline catches consisted mainly of juveniles, whereas subadult and adult specimens were more frequent in the swordfish longline and drift-net fishery. The percentage of sharks brought onboard alive was exceptionally high; only 5.1% of the specimens died. Few discards (seven blue shark) were recorded in the Greek longline fleet during onboard sampling in the Aegean Sea.

Incidental catch and estimated discards of pelagic sharks from the swordfish and tuna fisheries in the Mediterranean Sea

Persefoni Megalofonou

Constantinos Yannopoulos

Dimitrios Damalas

Department of Biology
Section of Zoology-Marine Biology
University of Athens
Panepistimiopolis, Ilissia
Athens 15784, Greece
E-mail address (for P. Megalofonou) Pmegalo@biol.uoa.gr

Gregorio De Metro

Michele Defflorio

Department of Animal Health and Welfare
Faculty of Veterinary Medicine
University of Bari
Str. Prov. Per Casamassima
70010, Valenzano Bari, Italy

Jose M. de la Serna

David Macias

Instituto Espanol de Oceanografia
Malaga, Apartado 285
29640 Fuengirola, Malaga, Spain

The effect of fishing on shark stocks has become the focus of considerable international concern. The fishery-induced depletion of stocks is made worse by the slow growth, late maturity, and low fecundity of sharks, all of which make them extremely vulnerable even to modest levels of fishing. Although no pelagic shark-directed fishery exists in the Mediterranean Sea, other pelagic fisheries may be a great threat, because species with higher production rates, such as swordfish and tuna, continue to support the fishery while species with lower rebound potential are driven to stock collapse or extirpation (Musick et al., 2000). In recent years sharks, which were once considered bycatch (and discarded), have become a target species of the Spanish swordfish fleet because highly restrictive measures regulating swordfish catch have been established in the Atlantic Ocean,

coupled with the fact that the international market is now more open to pelagic sharks and their derivatives (Mejuto and de la Serna, 2000).

Most pelagic sharks are migratory species. Thus, effective management proposals require reliable data that reflect migratory patterns, and multilateral international agreements are needed between all Mediterranean countries involved. During the last 40-year period, Spanish, Italian, and Greek longline and driftnet fleets have operated throughout the Mediterranean, targeting mainly swordfish or albacore and bluefin tuna. Catches began to expand slowly after 1962, increased rapidly with the advent of monofilament driftnets, and peaked in the late 1980s (Anonymous, 1999). Until recent years sharks were the most abundant incidental catch (landed, but not specifically targeted, or discarded). But they may become

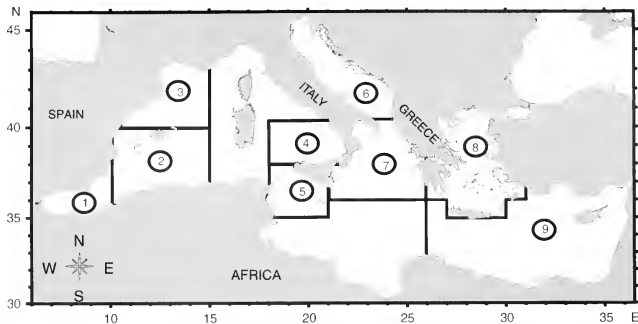


Figure 1

Map of the Mediterranean Sea, showing the nine study areas used for sampling sharks during 1998–2000. 1=Alboran Sea, 2=Balearic Islands area, 3=Catalonian Sea, 4=Tyrrhenian Sea, 5=Straits of Sicily, 6=Adriatic Sea, 7=Ionian Sea, 8=Aegean Sea, and 9=Levantine basin.

target species because their current low market value now appears to be increasing. Many of the data requirements of pelagic shark assessment are similar to those for assessing other highly migratory species; knowledge of stock structure, age and growth rates, natural mortality rates or fishery statistics. However, there is scant information about either the population biology or the catch levels of most incidental species. Primary literature on pelagic shark incidental catch in the Mediterranean Sea is rare and relates only to subareas that are not studied in a coordinated manner (De Metrio et al., 1984; Filanti et al., 1986; Buencuerpo et al., 1998; Di Natale, 1998; Mejuto et al., 2002). IC-CAT reports on pelagic shark catch show great annual variation in catch statistics and are fragmented because not all countries submit data for the entire time series. Catches of *Selachii* reported by FAO statistics for Spain, Italy, and Greece in the Mediterranean amount to 4209 metric tons in 2000, but include pelagic and benthic sharks, skates, rays, and chimaeras together.

Given the scarcity and heterogeneity of the available data, an international project was established (Megalofonou et al.¹) to collect fishing and biological data with standardized methods from all commercial fisheries of the European countries that catch pelagic sharks in the Mediterranean. This article presents the results of the

investigations carried out by observers at landing sites and onboard fishing vessels that target swordfish and tunas with longlines and driftnets. The main objective of this study was to analyze shark incidental catch and discards and to provide information on species composition, distribution, and abundance. The status of each shark brought on board (alive, dead, or damaged) and the disposition of sharks caught on some vessels (kept or discarded) were examined by using onboard observations to obtain essential data for effective fisheries management.

Materials and methods

Sampling areas

The Mediterranean Sea is a semi-enclosed area with pronounced oligotrophy in the surface waters due to small amounts of nutrient discharge from the land. The shallow and narrow Strait of Gibraltar connects it to the Atlantic. It consists of two nearly equal-sized basins, the eastern and the western basin, connected through the narrow and shallow Straits of Sicily. A network of sampling ports throughout the Mediterranean was established in order to cover a wide range of fishing grounds, fleets, and gears. The sampling areas, shown in Figure 1, were the following: the Alboran Sea (1), the Balearic Islands area (2), the Catalonian Sea (3), the Tyrrhenian Sea (4), the Straits of Sicily (5), the Adriatic Sea (6), the Ionian Sea (7), the Aegean Sea (8), and the Levantine basin (9). Researchers from Greece, Italy, and Spain were involved in data collection concerning incidental catch of pelagic sharks in the Mediterranean Sea.

¹ Megalofonou, P., D. Damalas, C. Yannopoulos, G. De Metrio, M. DeFlorio, J. M. de la Serna, and D. Macias. 2000. Bycatches and discards of sharks in the large pelagic fisheries in the Mediterranean Sea. European Union Project 97/50 Directorate General XIV/C1, 336 p. Directorate-General for Fisheries and Maritime Affairs, European Commission, Rue Joseph II, 99, B-1049 Brussels.

Description of gear

Fleets sampled by observers targeted swordfish (*Xiphias gladius*), albacore (*Thunnus alalunga*), or bluefin tuna (*Thunnus thynnus*). Five fishing gears were studied: swordfish longline (SWO-LL), "American type" swordfish longline (SWO-LL_A), albacore longline (ALB-LL), bluefin tuna longline (BFT-LL), and driftnet (DN).

The swordfish longline consists of a nylon monofilament main line, 2 to 3 mm in diameter, hung in a sagging curve between surface floats. Branch lines with a length of 5–18 m descend from the main line, each terminating in a single baited J-hook. The number of hooks ranges from 800 to 2800 and hook size varies from no. 0 to 5. The "American type" swordfish longline, a variation of the aforementioned gear and used mainly in Greece, was introduced in the Greek fishery in the mid 1980s. It consists of fewer hooks (350–700) of size 2, much longer branch lines (15–50 m), and a fish attractant light stick (Duralumes® Lindgren-Pitman Inc., Pompano Beach, FL) attached to each branch line, 1 m above the bait. The albacore longline is a more lightly constructed longline that has 800 to 4000 J-hooks, hook sizes 6–9, a main line from 1 mm to 1.6 mm in diameter, and shorter branch lines (3–6 m). The bluefin tuna longline is the most robust longline, having 1000 to 1200 J-hooks of size 0 or 1, a main line 5.0 mm in diameter, and branch lines 45 m long. Frozen mackerels (*Scomber scombrus*) or (*Scomber japonicus*) and frozen squids (*Illex* sp.) or (*Loligo* sp.) are used as baits, as in the swordfish and bluefin tuna fishery, whereas frozen sardines—*Sardina pilchardus* or *Sardinella* sp.—are the baits mainly used in the albacore fishery. Driftnets, ranging from 2.5–20 km in length and from 24–40 m in height and having a stretched mesh size of 380 mm, were used mainly in Italy by the swordfish and tuna fishery. Since 1998, after the enforcement of the regulatory measures for the driftnets, the traditional nets were rejected and the Italian fishermen introduced a smaller driftnet, called ferretara. This net has a length of 2.5 km, a depth from 18 to 25 m, and a mesh size of 180 mm. All gears targeting large pelagic fish, both longlines and nets, are shot (deployed) in the evening and their retrieval begins after midnight. Among the gears sampled, the swordfish longline is the main gear used in the Mediterranean Sea.

Data collection and statistical analyses

Sampling was carried out during a three-year period from 1998 to 2000. Catch and effort data were derived from records taken by observers stationed both at main fishing ports and onboard 11 commercial fishing vessels, from January 1998 to December 1999. Biological data, such as size and sex of sharks caught, were obtained from January 1998 to September 2000. Observers were present on fishing trips (702 fishing days) and at 17 landing sites, performing duties that included collecting fishing and operational data, identifying and measuring fish, as well as recording the exact location and date for

each fishing set. From each fishing vessel sampled at sea, these observers collected the following fishing and operational data series: name of fishing boat, gear used, duration of each trip in days, fishing effort per fishing day (number of hooks for longline gear, net length, and depth in meters for driftnet gear), number and weight of fish caught per fishing day by species, and number of sharks discarded. Because fishermen generally do not keep reliable logbooks to report their daily catch, sampling at landing sites was performed through interviews, as well as by direct observations and measurements. From each boat sampled at the landing site, observers, interviewing fishermen or skippers of the vessels, collected data on the duration of each trip in days, the number of fishing days, the fishing area, and the fishing effort per fishing day. The number and weight of fish landed were observed and measured directly during landing and recorded by species. Biological data for the specimens caught included total length (TL) in cm, fork length (FL) in cm, dressed weight (to the nearest 0.1 kg), and sex when possible.

To investigate trends in the abundance of sharks, we used the nominal catch per unit of effort (CPUE) expressed as the number of individuals per 1000 hooks for longlines, and per 1000 m of net for driftnets. Fishing duration was assumed to be constant because soak time was almost the same for all trips. Setting began at dusk and retrieving began after midnight. Each shark brought onboard vessels was assessed according to the following scale: 1) good—very high motility and active behavior; 2) fair—moderate motility; 3) poor—poor motility but having the ability to respond to external stimuli; 4) dead or showing no response to external stimuli.

Chi-square (χ^2) tests were performed to test variations in species composition by type of fishing gear, area sampled, and by sampling onboard or at landing sites. Catch data were classified in rows (species) and columns (gears, areas sampled, or sampling venue [fishing vessel or landing site]) to create contingency tables and were tested for significant association between rows and columns, assuming that row and column classifications are independent (null hypothesis). Nonparametric analysis of variance (Kruskal-Wallis test) was performed to compare the total length medians of the samples by fishing gear and per area. Nonparametric analysis of variance was used because our data sets did not meet the criteria needed to use the classical method of analysis of variance (ANOVA) e.g., normally distributed populations, equal variances.

Results

A total of 8733 sharks (153.6 t biomass) and 131,912 fish of other species (teleosts, rays, and skates) were documented from 5826 fishing days sampled, 5124 at landing sites and 702 onboard, during the two-year period 1998–99 (Tables 1–2). In all areas examined throughout the Mediterranean Sea, sharks represented

Table 1

Fishing sets by gear type and number of sharks caught (landed, plus discarded) throughout the Mediterranean areas studied during 1998–99 on selected vessels observed at-sea and recorded at landing sites. Area numbers: 1=Alboran Sea, 2=Balearic Islands area, 3=Catalonian Sea, 4=Tyrrhenian Sea, 5=Straits of Sicily, 6=Adriatic Sea, 7=Ionian Sea, 8=Aegean Sea, and 9=Levantine basin). Gear abbreviations: SWO-LL=swordfish longline, ABL-LL=albacore longline, BFT-LL=bluefin tuna longline, DN=driftnet, SO-LL_A=American-type swordfish longline, PG=*Prionace glauca*, IO=*Isurus oxyrinchus*, AV=*Alopias vulpinus*, GG=*Galeorhinus galeus*, LN=*Lamna nasus*, AS=*Alopias superciliosus*, SZ=*Sphyrna zygaena*, HG=*Hexanchus griseus*, CP=*Carcharhinus plumbeus*, SB=*Squalus blainvillet*, MM=*Mustelus mustelus*, CM=*Cetorhinus maximus*.

Area	Number of fishing sets				Number of sharks caught												
	SWO-LL	ALB-LL	BFT-LL	DN	SWO-LL _A	PG	IO	AV	GG	LN	AS	SZ	HG	CP	SB	CM	MM
1	1391	0	0	0	0	5057	268	11	10	0	6	1	0	0	0	0	0
2	1312	48	19	0	0	85	42	17	4	0	0	0	0	0	0	0	1
3	290	41	0	0	0	97	3	2	2	0	0	0	0	0	2	0	0
4	9	0	0	0	0	5	0	0	0	0	0	0	0	0	0	1	0
5	23	7	2	0	0	3	0	1	1	0	0	0	3	2	0	1	0
6	771	6	0	0	0	2053	0	8	0	1	0	2	0	0	0	0	0
7	594	239	0	715	0	938	0	21	0	14	0	1	0	0	0	0	0
8	0	99	0	0	42	28	0	1	1	0	0	0	0	0	0	0	0
9	7	0	0	0	211	29	8	1	1	0	1	0	0	0	0	0	0
Total	4397	440	21	715	253	8295	321	62	19	15	7	4	3	2	2	2	1

Table 2

Number of sharks discarded (by fishing gear and per area) from observations onboard fishing vessels and from interviews with fishermen at landing sites throughout the Mediterranean Sea during 1998–99. Area numbers: 1=Alboran Sea, 2=Balearic Islands area, 3=Catalonian Sea, 4=Tyrrhenian Sea, 5=Straits of Sicily, 6=Adriatic Sea, 7=Ionian Sea, 8=Aegean Sea, and 9=Levantine basin). Gear abbreviations: SWO-LL=swordfish longline, ABL-LL=albacore longline, BFT-LL=bluefin tuna longline, DN=driftnet, SO-LL_A=American-type swordfish longline.

Area	Sets observed onboard	Onboard sampling (693 sharks) Number of discarded sharks					Sets observed at landings	At landing sampling (8040 sharks) Number of discarded sharks reported				
		SWO-LL	ALB-LL	BFT-LL	DN	SWO-LL _A		SWO-LL	ALB-LL	BFT-LL	DN	SWO-LL _A
1	70	0	—	—	—	—	1321	0	—	—	—	—
2	192	0	0	0	—	—	1187	0	—	—	—	—
3	56	0	0	—	—	—	275	0	—	—	—	—
4	9	0	—	—	—	—	0	—	—	—	—	—
5	32	0	0	0	—	—	0	—	—	—	—	—
6	75	0	0	—	—	—	702	0	—	—	—	—
7	217	0	0	—	0	—	1331	0	0	—	0	—
8	39	0	—	—	—	7	102	0	0	—	—	0
9	12	0	—	—	—	0	206	0	—	—	—	0
Total	702	0	0	0	0	7	5124	0	0	—	0	0

6.2% in number and 13.5% in biomass of the catch sampled in swordfish and tuna fisheries. Sharks were rarely discarded from vessels and the rare instances were recorded only from areas off Greece. Out of 78 shark specimens caught by the Greek longline fishing vessels only seven blue sharks, killed onboard before they were unhooked, were thrown back to the sea. No

shark discarding at sea was reported by the skippers of the fishing boats, nor by the fishermen interviewed at landing sites (Table 2). Fishermen usually do not discard their shark catch because there is a market demand for sharks in the Mediterranean countries. Twelve shark species were identified—blue shark (*Prionace glauca*), being the most common in all areas and gears studied.

Table 3

Biomass (in kg) and percentage composition of species sampled on selected vessels observed at-sea and as reported at landing sites, by fishing gear in the large pelagic fisheries of the Mediterranean Sea during 1998–99. Gear abbreviations: SWO-LL=swordfish longline, SWO-LL_A=Albanian-type swordfish longline, ALB-LL=albacore longline, BFT-LL=bluefin tuna longline, DN=driftnet.

Species	SWO-LL		SWO-LL _A		ALB-LL		BFT-LL		DN		Total	
	kg	%	kg	%	kg	%	kg	%	kg	%	kg	%
At landing sites												
Sharks	139,056	19.01	1004	1.86	399	0.37	—	—	11,099	11.25	151,558	15.29
Swordfish	551,998	75.46	42,597	78.94	32,573	30.47	—	—	49,226	49.91	676,394	68.25
Bluefin tuna	17,511	2.39	9496	17.60	4500	4.21	—	—	31,224	31.66	62,731	6.33
Albacore	527	0.07	192	0.36	65,149	60.95	—	—	7085	7.18	72,953	7.36
Other	22,457	3.07	675	1.25	4266	3.99	—	—	— ¹	— ¹	27,398	2.76
Total	731,549		53,964		106,887		—	—	98,634		991,034	
On board												
Sharks	11,793	9.64	785	8.08	267	0.26	297	2.10	258	14.45	13,400	5.33
Swordfish	82,885	67.77	7146	73.57	5259	5.07	192	1.36	1486	83.22	96,969	38.54
Bluefin tuna	2981	2.44	1617	16.65	13,474	13.00	13,459	94.99	42	2.33	31,572	12.55
Albacore	55	0.05	23	0.24	79,107	76.32	0	0.00	0	0.00	79,185	31.47
Other	24,584	20.10	142	1.46	5546	5.35	221	1.56	— ¹	— ¹	30,493	12.12
Total	122,298		9713		103,653		14,169		1786		251,619	
All												
Sharks	150,849	17.67	1789	2.81	666	0.32	297	2.10	11,357	11.31	164,958	13.27
Swordfish	634,884	74.37	49,743	78.12	37,833	17.97	192	1.36	50,712	50.50	773,364	62.23
Bluefin tuna	20,492	2.40	11,113	17.45	17,974	8.54	13,459	94.99	31,266	31.13	94,303	7.59
Albacore	582	0.07	215	0.34	144,255	68.52	0	0.00	7085	7.06	152,138	12.24
Other	47,041	5.51	817	1.28	9812	4.66	221	1.56	— ¹	— ¹	57,891	4.66
Total	853,848		63,677		210,540		14,169		100,420		1,242,654	

¹ No weight data were available for other species.

Shortfin mako (*Isurus oxyrinchus*), common thresher shark (*Alopias vulpinus*), and tope shark (*Galeorhinus galeus*) were the next most abundant shark species and were found in more than half of the areas sampled. The rest of the shark species identified were the porbeagle (*Lamna nasus*), bigeye thresher shark (*Alopias superciliosus*), smooth hammerhead (*Sphyrna zygaena*), bluntnose sixgill shark (*Hexanchus griseus*), sandbar shark (*Carcharhinus plumbeus*), longnose spurdog (*Squalus blainvilliei*), smoothhound (*Mustelus mustelus*), and basking shark (*Cetorhinus maximus*).

The proportions of shark catches were significantly different among fishing gears ($\chi^2=15970.7$, $df=36$, $P=0.000<0.001$). Total shark catches in biomass represented 17.7% on swordfish longline gear, 11.3% on driftnet gear, and only 0.3% on albacore longline gear (Table 3). Comparisons of catch composition among the fishing gears in the same area showed similar results. In the Ionian Sea, shark percentage was higher in the swordfish longline catch than in the driftnet and albacore longline catch (Table 4). Catch composition also differed significantly by area ($\chi^2=494558.4$, $df=112$, $P=0.000<0.001$). The higher percentage of sharks, 34.3%, was found in the Alboran Sea and the lower

percentages, in the Straits of Sicily and the Catalanian Sea (Table 5). Statistically highly significant differences were detected in catch composition among types of sampling ($\chi^2=29760.41$, $df=17$, $P=0.000<0.001$). In all fishing gears and areas examined throughout the Mediterranean Sea, sharks represented 15.3% of the total catch in biomass at landings and only 5.3% on-board vessels. Among areas sampled, three areas (the Alboran Sea, Catalanian Sea, and Balearic Island area) revealed higher shark percentages at landing sites than on-board vessels (Table 5).

Relative shark abundance varied between fisheries. Higher shark catch rates were observed in swordfish fisheries both on-board vessels and at landing sites (Table 6 and 7). Overall CPUE reached 1.30 and 0.56 fish/1000 hooks in SWO-LL and SWO-LL_A, respectively (Table 8). Shark catch rates were higher in the Alboran Sea and the Adriatic Sea, where the average CPUEs were 3.80 fish/1000 hooks and 1 fish/1000 hooks, respectively in SWO-LL (Table 8). The driftnet fishery had a catch rate of only 0.04 fish/1000 m of nets. The comparison of catch rates (number of shark per set) among the different gear types in the same area (the Ionian Sea) revealed that the highest CPUE values were

Table 4

Biomass (in kg) and percentage composition of species by fishing gear sampled on selected vessels observed at-sea and as reported at landing sites in the Ionian Sea during 1998–99. Gear abbreviations: SWO-LL=swordfish longline, ABL-LL=albacore longline, DN=driftnet.

Species	SWO-LL		ALB-LL		DN		Total	
	kg	%	kg	%	kg	%	kg	%
Sharks	9787	13.4	568	0.5	11,357	11.3	21,711	7.5
Swordfish	43,395	59.5	35,122	30.6	50,713	50.5	129,229	44.9
Bluefin tuna	5838	8.0	5127	4.5	31,266	31.1	42,231	14.7
Albacore	0	0.0	67,594	58.9	7085	7.1	74,680	25.9
Other	13,921	19.1	6298	5.5	— ¹	— ¹	20,219	7.0
Total	72,941	100.0	114,709	100.0	100,421	100.0	288,070	100.0

¹ No available weight data were available for other species.

Table 5

Biomass (%) by species and area from data collected at landing sites and from selected longline vessels observed at-sea in the Mediterranean Sea during 1998–99. Area numbers: 1=Alboran Sea, 2=Balearic Islands area, 3=Catalonian Sea, 4=Tyrrhenian Sea, 5=Straits of Sicily, 6=Adriatic Sea, 7=Ionian Sea, 8=Aegean Sea, and 9=Levantine basin. Other = other species.

Species	Areas									Total
	1	2	3	4	5	6	7	8	9	
At landing sites										
Sharks	35.74	2.06	1.78	—	—	14.32	7.03	0.25	1.87	15.29
Swordfish	61.77	93.24	97.80	—	—	78.24	45.68	2.68	79.12	68.25
Bluefin tuna	1.83	1.89	0.28	—	—	2.62	16.12	3.39	17.42	6.33
Albacore	0.07	0.18	0.01	—	—	0.00	26.15	87.86	0.35	7.36
Other	0.59	2.62	0.13	—	—	4.82	5.02	5.82	1.24	2.76
Aboard longline vessels										
Sharks	7.82	1.14	0.78	5.63	0.89	19.57	10.69	11.18	2.89	5.33
Swordfish	81.04	38.15	12.91	42.66	31.73	44.40	39.73	81.31	60.60	38.54
Bluefin tuna	0.06	19.24	19.02	0.00	3.93	3.99	5.49	5.72	34.97	12.55
Albacore	0.00	33.91	67.06	0.00	44.44	4.34	24.53	0.28	0.17	31.47
Other	11.08	7.56	0.24	51.71	19.01	27.70	19.56	1.51	1.38	12.12
All										
Sharks	34.34	1.74	1.35	5.63	0.89	15.11	5.52	4.88	1.93	13.45
Swordfish	62.74	73.95	61.09	42.66	31.73	73.16	41.84	35.97	77.97	63.27
Bluefin tuna	1.74	7.97	8.38	0.00	3.93	2.83	5.84	4.38	18.52	5.52
Albacore	0.07	11.99	29.01	0.00	44.44	0.65	36.02	50.79	0.34	12.70
Other	1.11	4.35	0.18	51.71	19.01	8.25	10.77	3.99	1.25	5.07

found in the swordfish longline, about 1.02 fish/fishing set, followed by the driftnet and the albacore longline CPUE values (Table 9).

Seasonality in catch rates was evident in the swordfish longline fishery; shark CPUE peaked during late spring and summer, whereas swordfish CPUE peaked during fall and winter (Fig. 2). In the driftnet fishery, shark CPUE peaked during June and swordfish CPUEs were higher during June and July (Fig. 3).

Blue shark was the most abundant shark species in all areas and gears examined. It accounted for almost 95% of all sharks caught. Higher catch rates were observed in the swordfish fishery with an average value of 1.24 fish/1000 hooks in SWO-LL and 0.45 fish/1000 hooks in SWO-LL_A fishery. Analysis of catch rates by area showed that blue shark was caught more frequently in the Alboran and Adriatic Sea, reaching 3.59 fish/1000 hooks and 1.00 fish/1000 hooks, respectively (Table 8).

Table 6

Fishing sets, effort ($\times 1000$ hooks or 1000 m of net) and catch rates (number of fish/1000 hooks or number of fish/1000 m of net) of sharks and target species sampled on board in the large pelagic fisheries of the Mediterranean Sea during 1998–99. Gear abbreviations: SWO-LL=swordfish longline, SWO-LL_A=American-type swordfish longline, ABL-LL=albacore longline, BFT-LL=bluefin tuna longline, DN=driftnet. Abbreviations for species: PG=*Prionace glauca*, IO=*Isurus oxyrinchus*, AV=*Alopias vulpinus*, GG=*Galeorhinus galeus*. Target species for specific gears: *Xiphias gladius* for SWO-LL, SWO-LL_A and DN; *Thunnus alalunga* for ALB-LL; and *Thunnus thynnus* for BFT-LL.

Fishing gear	Area	Sets	Effort	Catch rate						
				PG	IO	AV	GG	Other sharks	Total sharks	Target species
SWO-LL	Ionian	140	267.4	0.759	0.000	0.000	0.000	0.004	0.763	3.152
	Adriatic	69	166.3	1.678	0.000	0.048	0.000	0.000	1.726	3.879
	Tyrrhenian	9	18.5	0.270	0.000	0.000	0.000	0.000	0.270	8.428
	Strait of Sicily	23	46.4	0.065	0.000	0.022	0.022	0.108	0.216	14.526
	Balearic	125	373.1	0.027	0.029	0.008	0.005	0.003	0.072	8.003
	Alboran	70	174.4	0.304	0.092	0.011	0.000	0.000	0.407	5.860
	Catalonian	15	43.5	0.299	0.023	0.023	0.023	0.046	0.414	6.989
Total	451	1089.6	0.519	0.026	0.014	0.004	0.008	0.571	6.085	
SWO-LL _A	Aegean	39	17.4	1.264	0.000	0.057	0.057	0.000	1.379	11.609
	Levantine	12	4.8	0.417	0.208	0.000	0.000	0.000	0.625	14.167
	Total	51	22.2	1.081	0.045	0.045	0.045	0.000	1.216	12.162
ALB-LL	Adriatic	6	15.3	0.000	0.000	0.000	0.000	0.000	0.000	22.222
	Ionian	47	112.9	0.168	0.000	0.000	0.000	0.000	0.168	13.853
	Strait of Sicily	7	17.5	0.000	0.000	0.000	0.000	0.000	0.000	127.143
	Balearic	48	158.7	0.000	0.006	0.000	0.000	0.006	0.013	23.732
	Catalonian	41	142.1	0.070	0.007	0.000	0.000	0.000	0.077	29.141
Total	149	446.5	0.065	0.004	0.000	0.000	0.000	0.069	26.957	
BFT-LL	Strait of Sicily	2	2.8	0.000	0.000	0.000	0.000	0.000	0.000	5.357
	Balearic	19	20.9	0.287	0.000	0.000	0.000	0.000	0.287	3.876
	Total	21	23.7	0.253	0.000	0.000	0.000	0.000	0.253	4.051
DN	Ionian	30	300.5	0.023	0.000	0.000	0.000	0.000	0.023	0.206

Of the 3771 blue sharks measured, individuals ranged from 40 to 368 cm TL (163.3 cm mean length and 37.7 cm SD). The overall length-frequency distribution is shown in Figure 4. The size distribution by fishing gear varied significantly (Kruskall-Wallis, test statistic=350.2, $P=0.000<0.05$); larger specimens were caught in the SWO-LL_A and DN fishery (Fig. 5). The Levantine basin had larger individuals whereas the Catalonian Sea had smaller ones (Fig. 6). Out of 564 blue sharks, 346 were determined to be males and 218 to be females. The sex ratio (males:female) favored males in almost all areas ranging from 1.29–2.50 males:1 female. The only exception was in the Alboran Sea where females were predominant (0.61 males:1 female). Relationships between TL and FL and dressed weight are given below:

$$TL = 4.1 + 1.176 FL \quad [r^2 = 0.99, n = 723]$$

$$TL = 74.6 DW^{0.307} \quad [r^2 = 0.95, n = 555].$$

The shortfin mako was reported in five out of nine areas examined and represented 3.7% of the

overall shark catches. This species was caught more often in the swordfish fishery with a mean CPUE of 0.07 fish/1000 hooks in SWO-LL_A and 0.05 fish/1000 hooks in SWO-LL. Shortfin makos were more abundant in the Alboran Sea and the Levantine basin (Table 8).

The total length-frequency distribution for the 257 specimens measured is shown in Figure 4. For shortfin makos collected, almost all were juvenile and ranged from 62.5 cm to 272 cm TL (mean length of 120.6 cm and 30.9 cm SD). Each fishing gear caught a statistically significant different average TL size (Kruskall-Wallis, test statistic=23.8, $P=0.000006<0.05$), and larger specimens were observed in the SWO-LL_A fishery (Fig. 5). As with the blue shark, larger makos came from the Levantine basin and smaller ones from the Catalonian Sea (Fig. 6). Out of 56 shortfin makos, 27 were determined to be males and 29 to be females. Sex ratio was almost equal (0.9 male:1 female). The relationship between FL and TL is given below:

$$TL = 1.136 FL - 2.5 \quad [r^2 = 0.98, n = 49].$$

Table 7

Fishing sets, effort ($\times 1000$ hooks or 1000 m of net) and catch rates (number of fish/1000 hooks or number of fish/1000 m of net) of sharks and target species sampled in the large pelagic fisheries of the Mediterranean Sea during 1998–99 as reported at landing sites. Gear abbreviations: SWO-LL=swordfish longline, SWO-LL_A=American-type swordfish longline, ABL-LL=albacore longline, DN=driftnet. Abbreviations for species: PG=*Prionace glauca*, IO=*Isurus oxyrinchus*, AV=*Alopias vulpinus*, GG=*Galeorhinus galeus*. The target species for specific gears: *Xiphias gladius* for SWO-LL, SWO-LL_A and DN; *Thunnus alalunga* for ALB-LL.

Fishing gear	Area	Sets	Effort	Catch rate						
				PG	IO	AV	GG	Other sharks	Total sharks	Target species
SWO-LL	Ionian	454	883.5	0.457	0.000	0.001	0.000	0.002	0.461	2.521
	Levantine	7	7.0	0.000	0.000	0.000	0.143	0.000	0.143	7.714
	Adriatic	702	1895.3	0.936	0.000	0.000	0.000	0.001	0.937	3.562
	Balearic	1187	795.7	0.087	0.038	0.018	0.003	0.000	0.145	15.474
	Alboran	1321	1232.3	4.061	0.204	0.007	0.008	0.005	4.285	11.259
	Catalonian	275	478.6	0.155	0.002	0.002	0.002	0.000	0.161	5.894
	Total	3946	5292.4	1.384	0.053	0.005	0.003	0.001	1.445	7.188
SWO-LL _A	Aegean	3	1.1	0.000	0.000	0.000	0.000	0.000	0.000	5.714
	Levantine	199	90.1	0.300	0.078	0.011	0.000	0.011	0.400	15.461
	Total	202	91.2	0.296	0.077	0.011	0.000	0.011	0.395	15.348
ALB-LL	Aegean	99	151.0	0.040	0.000	0.000	0.000	0.000	0.040	5.589
	Ionian	192	414.1	0.075	0.000	0.000	0.000	0.000	0.075	21.166
	Total	291	565.1	0.065	0.000	0.000	0.000	0.000	0.065	15.868
DN	Ionian	685	8035.8	0.034	0.000	0.002	0.000	0.001	0.038	0.215

Common thresher shark, the third most abundant shark reported in eight out of nine areas studied, accounted for 0.74% of the total shark catches. Catch rates per fishing gear were higher in the SWO-LL_A fishery with a mean CPUE of 0.02 fish/1000 hooks and per area sampled in the Aegean Sea, reaching 0.05 fish/1000 hooks (Table 8).

A total of 48 juvenile and adult common thresher sharks were measured. Length-frequency distribution was discontinuous and not very revealing because of the small number of sharks sampled (Fig. 4). Specimens ranged from 75 to 514 cm TL (mean value of 316.8 cm and SD 86.4 cm). No statistically significant differences were observed (Kruskal-Wallis, test statistic=0.638, $P=0.73>0.05$) in average size of specimens by fishing gear (Fig. 5). Larger specimens were reported from the Levantine basin area and a smaller one was reported from the Balearic Sea (Fig. 6). Out of 27 common thresher shark sexed, 15 were males and 12 females. Sex ratio was 1.25 male:1 female. The TL-FL and TL-dressed weight relationships are given below:

$$TL = 20.2 + 1.707 FL \quad [r^2 = 0.95, n = 24]$$

$$TL = 69.7 DW^{0.351} \quad [r^2 = 0.99, n = 18].$$

The remaining nine shark species observed accounted for only 0.87% of the total shark catches. In total, 26 tope sharks were measured (ranging from 35 to 190 cm),

15 porbeagles (ranging from 87 to 277 cm), 7 bigeye thresher sharks (ranging from 146 to 353 cm) and 4 smooth hammerheads (ranging from 277 to 300 cm TL). Only three bluntnose sixgill sharks (mean weight of 10.7 kg), two sandbar sharks (mean weight of 17 kg), two longnose spurdogs (mean weight of 1.7 kg), two basking sharks, and one smoothhound were reported, but no length measurements were available for these species.

A total of 571 specimens were examined for life condition on capture. The majority were very active following capture and their physical condition was especially good. Only 5.1% of the specimens brought onboard were dead (Table 10).

Discussion

Our results show that most of the sharks caught by the swordfish and tuna fisheries in the Mediterranean Sea are typically pelagic or coastal-pelagic species of widespread distribution in temperate and tropical waters throughout the world. However, some sporadic catches of poorly known, deepwater species of the families Hexanchidae and Alopiidae were also observed. The most plausible reason for these catches is that the deepwater species ascend close to the surface at night where they may be taken by longlines targeting swordfish (Castro et al., 1999).

Table 8

Fishing sets, effort ($\times 1000$ hooks or 1000 m of net), and catch rates (number of fish/1000 hooks or number of fish/1000 m of net) of sharks and target species sampled in the large pelagic fisheries of the Mediterranean Sea during 1998–99. Sampling conducted both at sea and at landing sites. PG=*Prionace glauca*, IO=*Isurus oxyrinchus*, AV=*Alopias vulpinus*, GG=*Galeorhinus galeus*. The target species for specific gears: *Xiphias gladius* for SWO-LL, SWO-LL_A and DN; *Thunnus alalunga* for ALB-LL; and *Thunnus thynnus* for BFT-LL.

Fishing gear	Area	Sets	Effort	Catch rate						
				PG	IO	AV	GG	Other sharks	Total sharks	Target species
SWO-LL	Ionian	594	1151.0	0.53	0.00	0.001	0.00	0.003	0.53	2.67
	Levantine	7	7.0	0.00	0.00	0.00	0.14	0.00	0.14	7.71
	Adriatic	771	2061.6	1.00	0.00	0.004	0.00	0.00	1.00	3.59
	Tyrrhenian	9	18.5	0.27	0.00	0.00	0.00	0.00	0.27	8.43
	Strait of Sicily	23	46.4	0.06	0.00	0.02	0.02	0.11	0.22	14.53
	Balearic	1312	1168.8	0.07	0.04	0.01	0.003	0.001	0.12	13.09
	Alboran	1391	1406.7	3.59	0.19	0.008	0.007	0.004	3.80	10.59
	Catalonian	290	522.1	0.17	0.004	0.004	0.004	0.004	0.18	5.99
Total	4397	6382.0	1.24	0.05	0.006	0.003	0.002	1.30	7.00	
SWO-LL _A	Aegean	42	18.5	1.19	0.00	0.05	0.05	0.00	1.30	11.27
	Levantine	211	94.9	0.31	0.08	0.01	0.00	0.01	0.41	15.40
	Total	253	113.4	0.45	0.07	0.02	0.01	0.01	0.56	14.72
ALB-LL	Aegean	99	151.0	0.04	0.00	0.00	0.00	0.00	0.04	5.59
	Adriatic	6	15.3	0.00	0.00	0.00	0.00	0.00	0.00	22.22
	Ionian	239	527.0	0.09	0.00	0.00	0.00	0.00	0.09	19.60
	Strait of Sicily	7	17.5	0.00	0.00	0.00	0.00	0.00	0.00	127.14
	Balearic	48	158.7	0.00	0.006	0.00	0.00	0.006	0.013	23.73
	Catalonian	41	142.1	0.07	0.007	0.00	0.00	0.00	0.08	29.14
Total	440	1011.6	0.07	0.002	0.00	0.00	0.00	0.07	20.76	
BFT-LL	Strait of Sicily	2	2.8	0.00	0.00	0.00	0.00	0.00	0.00	5.36
	Balearic	19	20.9	0.29	0.00	0.00	0.00	0.00	0.29	3.88
	Total	21	23.7	0.25	0.00	0.00	0.00	0.00	0.25	4.05
DN	Ionian	715	8336.3	0.03	0.00	0.002	0.00	0.001	0.04	0.21

Table 9

Fishing sets and catch rates (number of fish/fishing set) of sharks and target species in the three fishing gears studied in the Ionian Sea during 1998–99. PG=*Prionace glauca*, IO=*Isurus oxyrinchus*, AV=*Alopias vulpinus*, GG=*Galeorhinus galeus*. The target species for specific gears: *Xiphias gladius* for SWO-LL and DN; *Thunnus alalunga* for ALB-LL.

Fishing gear	Sets	Catch rate						
		PG	IO	AV	GG	Other sharks	Total sharks	Target species
SWO-LL	594	1.02	0.00	0.00	0.00	0.01	1.03	5.17
ALB-LL	239	0.21	0.00	0.00	0.00	0.00	0.21	43.22
DN	715	0.39	0.00	0.03	0.00	0.02	0.44	2.50

Onboard observations and interviews with fishermen at landing sites revealed that shark discarding is not a common practice in the large pelagic fisheries in the Mediterranean Sea. Very few shark discards were recorded and only from Greek vessels (seven blue sharks

out of 78 total). The fishermen usually retain their incidental catches because there is a market demand for sharks in Europe. However, wholesale shark flesh prices are quite variable, ranging from 2 to 8 euros. Moreover, the jaws and tails of some shark species are often sold

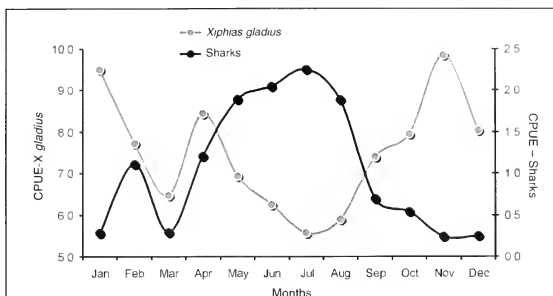


Figure 2

Monthly variation in sharks and swordfish longline CPUE (catch in numbers/1000 hooks) in the swordfish longline fishery of the Mediterranean Sea during 1998–99.

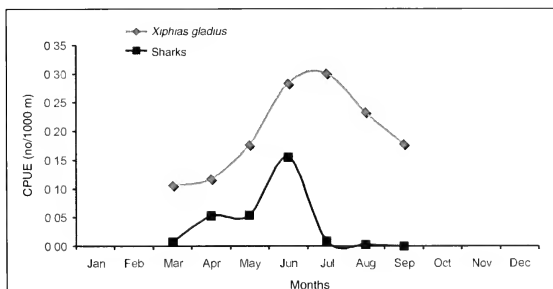


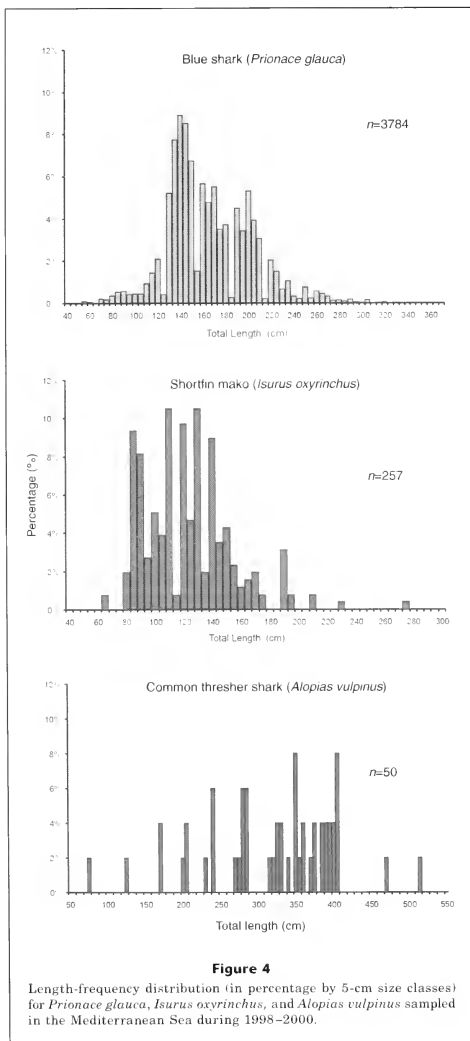
Figure 3

Monthly variation in sharks and swordfish CPUE (catch in numbers/1000 m net) in the driftnet fishery of the Mediterranean Sea during 1998–99.

in local markets. The very low discard rate of shark—about 1% of the sharks caught during onboard sampling was discarded—confirmed that sharks contribute to fishermen's income and may become target species with future increases in their market value. That discarding was observed only in the Greek swordfish fleets is probably due to the low market prices of shark meat compared to the high price of swordfish in this country. Sometimes during long trips fishermen are reluctant to retain them onboard and lose cool storage space for more valuable species such as swordfish or tuna.

The analysis of catch composition by gear and areas indicated that the various gears used in the swordfish

and tuna fisheries affect the shark populations differently and that the proportion of shark catches is related both to the type of fishing gear and the sampling area. This finding is consistent with previous findings for the Mediterranean Sea where incidental shark catch in the swordfish fisheries varied from insignificant to dominant, depending on the area studied (De Metrio et al., 1984; Di Natale, 1998; Filanti et al., 1986; Buencuerpo et al., 1998; Mejuto et al., 2002). The highest shark incidental catches were found in the Alboran Sea and were probably related to their location (Alboran Sea), adjacent to the Atlantic Ocean. Shark bycatch in the Atlantic swordfish fishery is one



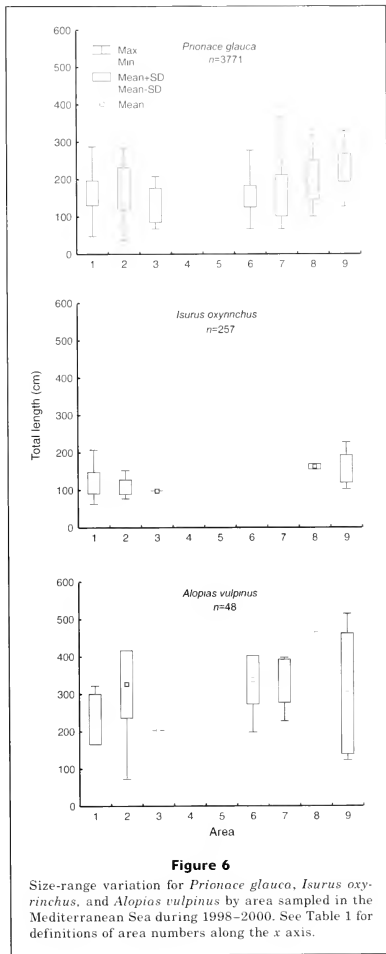
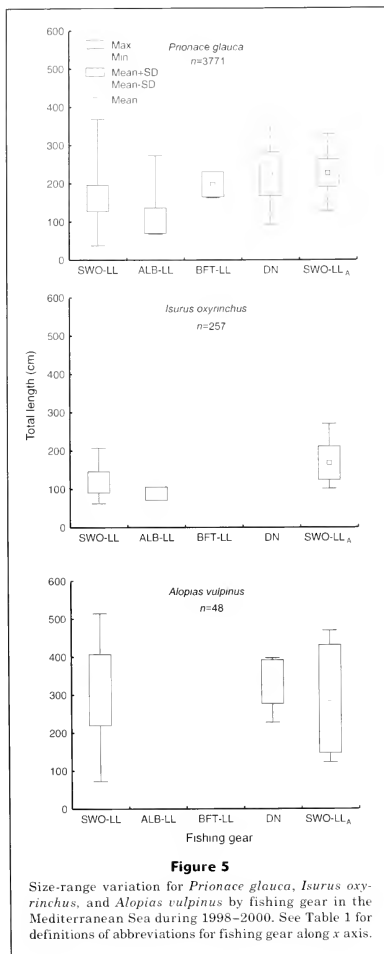
of the highest in the world, rarely dropping below 30% of the total catch in numbers of fish (Amorim et al., 1998; Buencuerpo et al., 1998; Hazin et al., 1998; Marin et al., 1998). The higher incidence of sharks in the Alboran Sea could also be due to the higher trophic potential of the western Mediterranean compared to the eastern part. The discrepancies in observed at-sea and at-landing data, especially in the western Mediterranean Sea catch composition, could be mainly due to the discarding of "other species." In addition, the discarding of undersize target species, such as swordfish and tunas, could be another reason for the discrepancies observed. It is reasonable that observers at landing sites were not able to record exactly the entire nonshark discards at sea from the information that fishermen provided; thus shark landings do not always reflect actual percentage of catch composition caught at sea.

The shark catch rates obtained in our study were lower than those reported in previous studies for various areas of the Mediterranean Sea (Table 1) probably because of the fishing pressure throughout the years.

A comparison of the shark catch rates in the Mediterranean and Atlantic indicated that the catch rates are generally lower throughout the Mediterranean (Table 1). Possible reasons could be either the lower productivity of the Mediterranean Sea, or, as alluded to above, lower availability of sharks in the Mediterranean due to regional depletion from historical fishing, or both. The configuration and effectiveness of fishing gears used could be another reason for the higher CPUE in the Atlantic Ocean. Hazin et al. (1998) and Kotas et al.² reported an increase in use of wire snoods in Atlantic swordfish fisheries to retain more sharks for the growing market for shark fins.

Monthly analysis of catches indicated that maximum catch rates occur during late spring and summer (May–August) in the swordfish longline (SWO-LL) fishery, and in June in the driftnet fishery. Monthly variations in catch rates were found also by Buencuerpo et al. (1998), who reported peaks of shark catch in April and Septem-

² Kotas, J. E., S. dos Santos, V. G. de Azevedo, J. H. de Lima, J. D. Neto, and C. F. Lin. 2000. Observations on shark by-catch in the monofilament longline fishery off southern Brazil and the National ban on finning. 8 p. IBAMA-REVIZEE research. [Copyright: www.wildaid.org.]



ber in the eastern N. Atlantic and Straits of Gibraltar. Probably, certain water temperature preferences of sharks during their biological cycle force them to shift to shallower and warmer water masses, especially in

summer. At these depths sharks are more vulnerable to surface gears and that is reflected in higher catches. Higher catch rates in late spring and summer could be also attributed to juvenile recruitment (Strasburg,

Table 10

Life-status condition of 571 sharks at time of capture, by species, and per fishing gear, observed onboard commercial fishing vessels in the Mediterranean Sea during 1998–2000. Gear abbreviations: SWO-LL=swordfish longline, SWO-LL_A=American-type swordfish longline, ALB-LL=albacore longline, DN=driftnet, BFT-LL=bluefin tuna longline.

Species	Good		Fair		Poor		Dead	
	Number	%	Number	%	Number	%	Number	%
<i>P. glauca</i>	364	71.0	69	13.5	57	11.1	23	4.5
<i>I. oxyrinchus</i>	7	22.6	10	32.3	9	29.0	5	16.1
<i>A. vulpinus</i>	3	18.8	4	25.0	8	50.0	1	6.3
<i>G. galeus</i>	4	80.0	1	20.0	0	0.0	0	0.0
<i>A. superciliosus</i>	1	100.0	0	0.0	0	0.0	0	0.0
<i>C. plumbeus</i>	0	0.0	2	100.0	0	0.0	0	0.0
<i>H. griseus</i>	3	100.0	0	0.0	0	0.0	0	0.0
Fishing gear								
SWO-LL	334	66.8	76	15.2	64	12.8	26	5.2
SWO-LL _A	34	97.1	0	0.0	0	0.0	1	2.9
ALB-LL	12	46.2	6	23.1	6	23.1	2	7.7
DN	2	40.0	2	40.0	1	20.0	0	0.0
BFT-LL	0	0.0	2	40.0	3	60.0	0	0.0
Total	382	66.9	86	15.1	74	13.0	29	5.1

1958; Carey and Scharold, 1990; Nakano, 1994; Bigelow et al., 1999).

The abundance and widespread distribution of blue sharks throughout the Mediterranean that we determined supports previous findings. However, our observed catch rates were lower than those reported earlier for the same areas (De Metro et al., 1984; Filanti et al., 1986; Buencuerpo et al., 1998; Di Natale, 1998; Relini-Orsi et al., 1999; De Zio et al., 2000). Variation in sex ratio and size distribution between different areas studied indicated sexual or size segregation, or both. Spatial and temporal segregation of pelagic sharks by sex and size was well documented by Strasburg (1958) and Nakano (1994) in the Pacific Ocean. Further analysis regarding distribution by latitude-longitude, time of year, and size classes of specimens is needed to establish a possible blue shark migratory pattern in the Mediterranean Sea. Pratt's estimates on the sexual maturity of blue shark (215 cm TL for males, 257 cm TL for females) from the North Atlantic Ocean (Pratt, 1979) indicate that in all areas studied in the Mediterranean Sea, albacore and swordfish longline fisheries generally capture immature to subadult specimens and driftnets and American type swordfish longlines capture adults. Of all blue sharks captured in the large pelagic fisheries of the Mediterranean during our study, 91.1% were under 215 cm TL and 96.3% under 257 cm TL. This observation, which indicates that the majority of Mediterranean blue sharks caught have not reached maturity, is of concern and reinforces the need for global assessments of this species. In the Atlantic and Pacific Ocean results based on a considerable time

series of data show a decrease in abundance (Cramer, 1996) and in average size (Holts et al., 1998) of blue sharks. Because blue sharks are an incidental catch in the large pelagic and highly migratory species fisheries in the Mediterranean, standardizing catch rates is very difficult. Average size may be a more sensitive indicator of shark stock status than catch rates when there is a long enough time-series of data.

We found a much lower incidental catch of shortfin mako than other authors have reported in the Mediterranean (Dai, 1997; Buencuerpo et al., 1998). This species seems more abundant in the Atlantic Ocean where in some areas it represents more than 10% of total catches (Buencuerpo et al., 1998; Stone et al., 2001). The almost equal sex ratio reflects the findings of Buencuerpo et al., (1998) and Moreno et al., (1992). As with blue sharks, larger makos were observed in the Levantine basin although in small numbers. Because males mature at 195 cm TL (Compagno, 1984) and females between 273 and 298 cm (Mollet et al., 2000), 98.4% of shortfin makos in our study were smaller than the size of first maturity. The absence of a consistent time series of abundance data did not allow us to estimate the trend in the status of the shortfin mako population in the Mediterranean Sea. Cramer (1996) outlined a steady decline in catch indices for this species from 11.86 fish/1000 hooks in 1985, to 3.52 in 1996 for the U.S. commercial Atlantic longline fishery in the Caribbean and the Gulf of Mexico. The Azorean fleet mako landings decreased by almost 50% in numbers from 1987 to 1994 (Castro et al., 1999). Together with the low catch rates in the Mediterranean Sea, short-

Table 11

Comparison of shark catch rates (CPUE in number of fish/1000 hooks) in longline fisheries during investigations in the Mediterranean Sea and the Atlantic Ocean. SWO-LL= swordfish longline; Tuna-LL=tuna longline gear.

Author	Area	Period	Gear	CPUE
De Metrio et al. (1984) ¹	Ionian Sea	1984	SWO-LL	0.9–2.2
Filanti et al. (1986)	Ionian Sea	1978–85	SWO-LL	1.5–3.0
De Zio et al. (2000)	Adriatic Sea	1984–98	SWO-LL	2.4
Di Natale (1998)	Tyrrhenian Sea, Strait of Sicily	1991–92	SWO-LL	0.4
Buencuerpo et al. (1998)	Gibraltar Strait	1991–92	SWO-LL	24.2
Present study	Ionian Sea	1998–99	SWO-LL	0.5
Present study	Adriatic Sea	1998–99	SWO-LL	1.0
Present study	Strait of Sicily	1998–99	SWO-LL	0.2
Present study	Alboran Sea	1998–99	SWO-LL	3.8
Buencuerpo et al. (1998)	E. Atlantic	1991–92	SWO-LL	9.9–37.8
Stone and Dixon (2001)	NW Atlantic	1999	SWO-LL	43.8
Hazin et al. (1998)	W. Atlantic	1983–97	Tuna-LL	16.8

¹ Blue shark catch rates only.

fin makos may be one of the most over-fished pelagic sharks in the Mediterranean Sea.

Our low catch rates for common thresher shark in the Mediterranean were almost identical with the findings of Buencuerpo et al. (1998) for the Gibraltar Strait region. However, the abundance of this species supports directed fisheries in some areas. Such a case occurred off California waters during 1977–85, when thresher shark CPUE in the driftnet fishery ranged from 0.13 to 1.92 fish/fishing set (Holts et al., 1998). In our study, one third of the specimens caught came from the Ionian driftnet fishery but the largest individual was captured in the Levantine basin (514 cm TL) with the swordfish longline. Pacific females mature at 315 cm TL (Strasburg, 1958) and males mature at about 333 cm TL (Cailliet and Bedford, 1983), and we calculated that 40% of the female common thresher sharks caught were below 315 cm and 50% of the males were below 333 cm. Although the above data indicate that most were caught as immature sharks, there are no data on the first maturity of common thresher sharks in the Mediterranean Sea. There is doubt, however, that females mature at a smaller size than males in the same region and we therefore deduced that fishing pressure was very intense on juvenile and subadult groups.

The low capture numbers for other shark species could be due either to the scarcity of these species in the Mediterranean Sea or to the "fished-down" condition of shark populations, or both could be causes. Another reason could be the low capture efficiency of the gears used.

The high proportion of sharks that were alive on capture agrees with Kotas et al.², who reported that 97% of blue sharks and 78% of shortfin makos were alive when landed on deck. These high survival rates are encouraging and could become the basis for conservation measures in the future, such as releasing immature fish or enforcing catch quotas.

Our study provides a reference point for the present status of pelagic sharks in the Mediterranean Sea, the effect of fisheries on them, and a baseline for future monitoring. Fishing for swordfish and tunas affects much of the pelagic ecosystem by taking predators of swordfish and tunas (large pelagic sharks), their prey (small tunas), and their competitors, such as other elasmobranchs, billfishes, and tunas. Up to now, there has been little documentation and understanding of fishing effects on the wider ecosystem. To strengthen management for large pelagic fishes such as sharks, a multi-species assessment with an ecosystem approach should be adopted. To achieve this goal, long-term monitoring programs should be established and exploitation strategies should be linked to conservation plans for shark species in the Mediterranean Sea.

Acknowledgments

We thank the Greek, Italian, and Spanish fishermen who collaborated during sampling procedures. We thank also the two anonymous reviewers who improved the manuscript with their valuable suggestions. This study was performed under the financial aid of the Commission of the European Communities (Project no. 97/50 DG XIV) and does not necessarily reflect the views of the European Commission and in no way anticipates the Commission's future policy in this area.

Literature cited

- Amorim de, A. F., C. A. Arfelli, and L. Fagundes.
1998. Pelagic elasmobranchs caught by longliners off southern Brazil during 1974–97: an overview. *Mar. Freshw. Res.* 49(7):621–632.

- Anonymous.
1999. Report of the Inter-sessional meeting of the ICCAT sub-committee on by-catch; Messina, Italy, May 11-14 1999. ICCAT Col. Vol. Sci. Pap. 51:1729-1775.
- Bigelow, K. A., C. H. Boggs, and X. He.
1999. Environmental effects on swordfish and blue shark catch rates in the US North Pacific longline fishery. *Fish. Oceanogr.* 8:178-198.
- Buencuerpo, V., S. Rios, and J. Moron.
1998. Pelagic sharks associated with the swordfish, *Xiphias gladius*, fishery in the eastern North Atlantic Ocean and the Strait of Gibraltar. *Fish. Bull.* 96:667-685.
- Cailliet, G. M., and D. W. Bedford.
1983. The biology of three pelagic sharks from California waters, and their emerging fisheries: a review. *CalCOFI Rep.* 24:57-69.
- Carey, F. G., and J. Scharold.
1990. Movements of blue sharks (*Prionace glauca*) in depth and course. *Mar. Biol.* 106:329-342.
- Castro, J. I., C. M. Woodley, and R. L. Brudek.
1999. A preliminary evaluation of the status of shark species. *FAO Fish. Tech. Pap.* 380:1-72. *FAO, Rome.*
- Compagno, L. J. V.
1984. *FAO species catalogue. Vol. 4: Sharks of the World: an annotated and illustrated catalogue of shark species known to date. Part 2: Carchariniformes.* *FAO Fish. Synop.* 125:251-655.
- Cramer, J.
1996. Recent trends in the catch of undersized swordfish by the U.S. pelagic longline fishery. *Mar. Fish. Rev.* 58:24-32.
- Dai, X.
1997. A preliminary analysis on the composition of catches obtained by longline fishing in the Mediterranean Sea. *J. Shanghai Fish. Univ.* 6:107-111.
- De Metrio, G., G. Petrosino, C. Montanaro, A. Matarrese, M. Lenti, and E. Cecere.
1984. Survey on summer-autumn population of *Prionace glauca* L. (PISCES, CHONDRICHTHYES) during the four-year period 1978-81 and its incidence on swordfish (*Xiphias gladius* L.) and albacore (*Thunnus alalunga* (Bonni)) fishing. *Oebalia* 10:105-116.
- De Zio, V., A. M. Pastorelli, and L. Rositani.
2000. Cature accessorie di *Prionace glauca* (L.) durante la pesca dei grandi pelagici nel basso Adriatico (1984-1998). *Biol. Mar. Mediterr.* 7:444-446.
- Di Natale, A.
1998. By-catch of shark species in surface gear used by the Italian fleet for large pelagic species. *ICCAT Col. Vol. Sci. Pap.* 48:138-140.
- Filanti, T., P. Megalofonou, G. Petrosino, and G. De Metrio.
1986. Incidenza dei Selaci nella pesca del Pesce Spada con longline nel golfo di Taranto. *Nova Thalassia* 8:667-669.
- Hazin, F. H. V., J. R. Zagaglia, M. K. Broadhurst, P. E. P. Travassos, and T. R. Q. Bezerra.
1998. Review of a small-scale pelagic longline fishery off Northeastern Brazil. *Mar. Fish. Rev.* 60:1-8.
- Holts, D. B., A. Julian, O. Sosa-Nishizaki, and N. W. Bartoo.
1998. Pelagic shark fisheries along the west coast of the United States and Baja California, Mexico. *Fish. Res.* 39:115-125.
- Marin, Y. H., F. Brum, L. C. Barea, and J. F. Chocca.
1998. Incidental catch associated with swordfish longline fisheries in the south-west Atlantic Ocean. *Mar. Freshw. Res.* 49(7):633-639.
- Mejuto, J., B. Garcia-Cortes, and J. M. de la Serna.
2002. Preliminary scientific estimations of by-catch landed by the Spanish surface longline fleet in 1999 in the Atlantic Ocean and Mediterranean Sea. *ICCAT Col. Vol. Sci. Pap.* 54:1150-1163.
- Mejuto, J., and J. M. de la Serna.
2000. Standardized catch rates by age and biomass, for the North Atlantic swordfish (*Xiphias gladius*) from the Spanish longline fleet for the period 1983-1998 and bias produced by changes in the fishing strategy. *ICCAT Col. Vol. Sci. Pap.* 51:1387-1411.
- Mollet, H. F., G. Cliff, H. L. Pratt Jr., and J. D. Stevens.
2000. Reproductive biology of the female shortfin mako, *Isurus oxyrinchus Rafinesque*, 1810, with comments on the embryonic development of lamnoids. *Fish. Bull.* 98:299-318.
- Moreno, J. A., and J. Moron.
1992. Comparative study of the genus *Isurus* (Rafinesque, 1810), and description of a form ("Marrajo Criollo") apparently endemic to Azores. *Aust. J. Mar. Freshw. Res.* 43:10-122.
- Musick, J. A., G. Burgess, G. Cailliet, M. Cambi, and S. Fordham.
2000. Management of sharks and their relatives (Elasmobranchii). *Fisheries* 3:9-13.
- Nakano, H.
1994. Age, reproduction and migration of blue shark in the North Pacific Ocean. *Bull. Natl. Res. Inst. Far Seas Fish./Enyosuikenho* 31:141-219.
- Relini-Orsi, L., G. Palandri, F. Garibaldi, and C. Cima.
1999. Longline swordfish fishery in the Ligurian Sea: eight years of observation on target and by catch species. *ICCAT Col. Vol. Sci. Pap.* 49:146-150.
- Pratt, H. L.
1979. Reproduction in the blue shark, *Prionace glauca*. *Fish. Bull.* 77:445-470.
- Stone, H., and L. Dixon.
2001. A comparison of catches of swordfish, *Xiphias gladius*, and other pelagic species from Canadian longline gear configured with alternating monofilament and multifilament nylon gangions. *Fish. Bull.* 99:210-216.
- Strasburg, D. W.
1958. Distribution, abundance and habits of pelagic sharks in the central Pacific Ocean. *Fish. Bull.* 58: 335-361.

Abstract—The annual ovarian cycle, mode of maturation, age at maturity, and potential fecundity of female Rikuzen sole (*Dexistes rikuzenius*) from the North Pacific Ocean off the coast of Japan were studied by 1) histological examination of the gonads, 2) measurement and observation of the oocytes, and 3) by otolith aging. The results indicated that ovulation occurs from September to December and peaks between September and October. Vitellogenesis began again soon after the end of the current season. Maturity was divided into eight phases on the basis of oocyte developmental stages. Mature ovaries contained developing oocytes and postovulatory follicles but no recruiting oocytes, indicating that this species has group-synchronous ovaries and is a multiple spawner. Almost all females matured first at an age of 1+ year and spawned every year until at least age 8+ years. Potential fecundity increased exponentially with body length and the most fecund fish had 15 times as many oocytes as the least fecund fish. Potential fecundity and relative fecundity were both positively correlated with age from 1 to 6+ years, but were negatively correlated, probably because of senescence, in fish over 7 years. These results emphasize that the total productivity of a *D. rikuzenius* population depends not only on the biomass of females older than 1+ but also on the age structure of the population.

Reproductive biology of female Rikuzen sole (*Dexistes rikuzenius*)*

Yoji Narimatsu

Daiji Kitagawa

Tsutomu Hattori

Tohoku National Fisheries Research Institute
Fisheries Research Agency
Hachinohe Branch, Same-machi
Hachinohe, Aomori, 031-0841 Japan
E-mail address (for Y. Narimatsu) nary@affrc.go.jp

Hirobuni Onodera

Iwate Fisheries Technology Center
Hirata, Kamaishi
Iwate, 026-0001 Japan

To understand fish population dynamics, reproductive information, such as the maturation of oocytes, the size and age at first maturity, and fecundity, is indispensable. Gonadal maturation is determined from the external appearance of the gonads, the gonadosomatic index, and oocyte size, or from observations of histologically prepared gonads (West, 1990). With the former two methods it is possible to measure samples in the field and to record data on numerous samples in a short period of time; however, the mode of oocyte development can only be clarified by using observations of histologically prepared gonads (Wallace and Selman, 1981). The methods used to determine if an individual has spawned and to measure the number of eggs spawned in the current reproductive season differ with the mode of oocyte development (West, 1990).

In fishery models, reproductive potentials are conventionally represented by spawning stock biomass (Ricker, 1954; Beverton and Holt, 1957; Trippel et al., 1997). However, at the population level spawning stock biomass does not always correlate with egg productivity. Length at first maturation, the frequency of occurrence of degenerated oocytes, and fecundity (that is, the total number of offspring produced in a reproductive season by an individual female)

are closely related to the age and energetic conditions of an individual (Hunter and Macewicz, 1985a; Horwood et al., 1986, 1989; Trippel et al., 1997; Sampson and Al-Jufaily, 1999; Kurita et al., 2003). Therefore, examination of age and body size in relation to fecundity is useful in determining the abundance of eggs laid in a population.

Oocyte development can be divided into three types (Wallace and Selman, 1981). In determinate fecundity, fecundity is fixed before spawning starts, such as in species which have synchronous or group-synchronous ovaries. In indeterminate fecundity (i.e., for those species whose ovaries develop asynchronously), unyolked oocytes grow to maturity after the onset of spawning (Hunter and Macewicz, 1985b; Hunter et al., 1992). In addition, the development of oocytes can vary even among populations of a single species (Sampson and Al-Jufaily, 1999) and some females classified as maturing or mature by external observation are often actually immature, and vice versa (Hunter et al., 1992; Zimmermann, 1997). Hence, with a species or a population for

Manuscript submitted 10 January 2004 to the Scientific Editor's Office.

Manuscript approved for publication 10 April 2005 by the Scientific Editor.
Fish. Bull. 103:635–647 (2005).

* Contribution B57 from Tohoku National Fisheries Research Institute, Fisheries Research Agency of Japan, Miyagi, Japan.

which little information is available, it is important to determine specific reproductive traits by using the most accurate methods and to compare the results with those of simpler methods.

Rikuzen sole (*Dexistes rikuzenius*) (also known as Rikuzen flounder, FAO) is a coastal flatfish that lives at depths of 100 to 360 m in the waters off the south coast of southern Hokkaido, Japan, and the southern Korean Peninsula (Sakamoto, 1984). It inhabits sandy bottoms and preys mainly on benthic invertebrates (Fujita et al., 1995). It is relatively abundant in the North Pacific off the coast of Japan and is an important fishery resource for bottom trawlers (Ishito, 1964; Ogasawara and Kawasaki, 1980). The commercial catch of flatfish such as the Rikuzen sole has fluctuated widely in this area over the past few decades (Anonymous, 2002), and therefore fisheries management is needed to maintain stable and appropriate fish-density levels.

In addition to fisheries, various internal and external conditions may affect the fluctuations in abundance of fish populations. Understanding reproductive traits, or survival in the early life stages, is a step toward revealing population dynamics. Although both sexes have indeterminate growth trajectories, conspicuous sexual dimorphism occurs during the growth and life span of Rikuzen sole. Females are larger at any given time after age 1+ and live longer than males (Ishito, 1964). The spawning period of the Sendai Bay population occurs from late October to late January and peaks from November to December (Ogasawara and Kawasaki, 1980). Using measurements of oocyte diameter and the appearance of the whole ovary, Ogasawara and Kawasaki (1980) revealed that females spawn several batches of eggs during one spawning season. However, because histological observations of the gonads have not been conducted, details of the reproductive biology, such as annual cycle of oocyte development, and body size and age at maturity, have not been determined. In addition, no information about fecundity has been reported.

We examined the oogenesis of Rikuzen sole caught in the North Pacific Ocean off the coast of Japan over a period of one year. The aim was to determine the mode of maturation, annual reproductive cycle, and age at first maturity based on histological examinations, age determinations from otolith growth increments, and gonadosomatic indices (GSIs). Using these results, we were able to estimate body size and age-related potential fecundity and were able to develop a simpler method for determining potential fecundity.

Materials and methods

From May 2000 to April 2001, except for July and August when commercial bottom trawl fishing was prohibited, Rikuzen sole samples were collected once or twice a month from the fisheries market in Hachinohe, Aomori Prefecture, Japan. All samples were caught by bottom trawl nets in the coastal waters off Shitsukari (41°22', 141°33'E) and Hachinohe (40°43'N, 144°44'E),

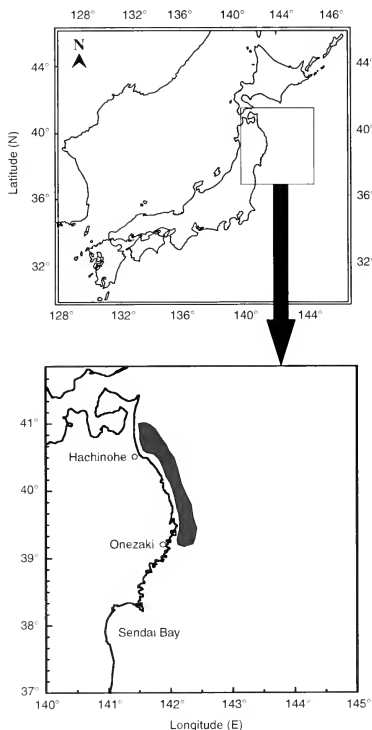
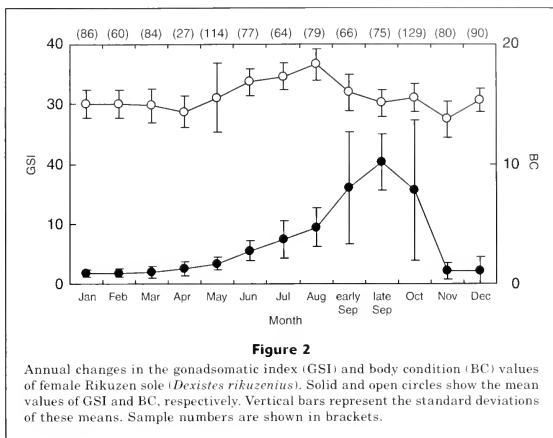


Figure 1
Catch area for Rikuzen sole (*Dexistes rikuzenius*) in the Northern Pacific Ocean off the northeast coast of Japan, 2000–2001.

from depths of 70–300 m (Fig. 1). During July and August, samples were collected with bottom long lines off the coast at Onezaki (39°12'N, 141°56'E) from a depth of 85–109 m.

A total of 1031 females were collected and their standard lengths (SL) to the nearest mm, total body weights, eviscerated body weights, and ovary weights to the nearest 0.1 g were measured. The GSI and body condition (BC) of each specimen were calculated with the following formulas: $GSI = (\text{gonad weight}/\text{eviscerated body weight}) \times 100$, and $BC = (\text{eviscerated body weight}/SL^3) \times 100$. Ovaries and sagittal otoliths were removed



within a day after each catch for histological observations and age determination, respectively. The otoliths were washed with distilled water and left to dry until preparation for age determination. Ovaries were fixed in 10% buffered formalin for 24 hours. The middle portions of eyed-side ovaries of 309 specimens were extracted, dehydrated, embedded in paraffin, sectioned at 8 μm , and stained with Mayer's hematoxylin and eosin (HE) and periodic acid Schiff (PAS).

Prepared sections were examined under a light microscope. The oocytes were then divided into eight stages according to the guidelines of Yamamoto (1956). Postovulatory follicles (POFs), which indicate spawning experience, were also examined. New POFs are easily identifiable, but those that have degenerated are difficult to distinguish from atretic follicles. In our study, only those that could be easily identified were defined as POFs. Atretic oocytes, namely advanced yolked oocytes that have been resorbed into the ovaries, were also determined; similarly, only those easily identifiable were defined as atretic oocytes. The percentage of advanced oocytes that were atretic was determined monthly for 10 randomly selected 2–7+ year-old fish (body size range: 143–210 mm SL).

Maturity was classified by the stage of the most advanced oocyte and the presence of POFs. By observing maturity and advanced oocyte diameter, we tested 15 ovaries for possible differences in oocyte development between anterior, middle, and posterior positions in the eyed-side ovary lobe, and between eyed-side and blind-side ovary lobes.

Oocyte diameter distributions in the late vitellogenic maturity phase were examined; the reason this maturity

phase was selected is described in the "Results" section. The diameters of 50 randomly selected oocytes, extracted from the middle portions of the ovaries, were measured under a dissecting microscope to the nearest 20 μm . Potential fecundity was estimated with the gravimetric method by using ovaries in the late vitellogenic maturity phase. Extracted ovaries were rinsed and then weighed to the nearest 0.0001 g, and only developing oocytes, whose size is also described in the "Results" section, were counted.

Age was determined for all fish samples. Blind-side otoliths were used for the analyses according to the methods of Ishito (1964). The lateral surfaces of the otoliths were polished with 1500-grit sand paper until the transparent zones were visible. Ishito (1964) revealed that one transparent zone is formed at the edge of the otolith each winter and suggested that this may be regarded as an annual mark. However, the most interior ring appears when fish are aged 0+ (Ishito, 1964); therefore the number of transparent zones minus the 0-year-old zone was the formula used for aging, and the relationship between age and potential fecundity was analyzed.

Results

Annual changes in gonadosomatic index and body condition

The annual changes in gonadosomatic index (GSI) and body condition (BC) are shown in Figure 2. The GSI was

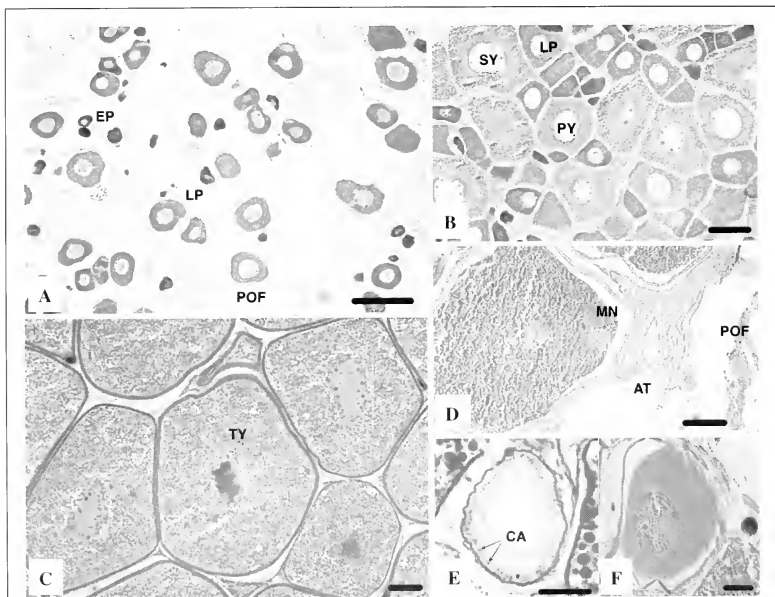


Figure 3

Histology of the ovarian maturity and oocyte developmental stages of Rikuzen sole (*Devistes rikuzentus*). (A) Spent phase. Bar: 200 μm . (B) Middle vitellogenic phase. Bar: 200 μm . (C) Late vitellogenic phase. Bar: 200 μm . (D) Maturity phase. Bar: 200 μm . (E) Oocyte at the cortical alveolus stage. Bar: 50 μm . (F) Oocyte at the premature stage. Bar: 50 μm . EP=early perinucleolus stage, LP=late perinucleolus stage, CA=cortical alveolus, PY=primary yolk stage, SY=secondary yolk stage, TY=tertiary yolk stage, MN=migratory nucleus stage, AT=atretic oocyte, POF=postovulatory follicle.

relatively low, less than 2.0, from January to March, increased steeply from April to August, and progressed to more than 15.0 during September to October. Values then rapidly decreased from October to November. The BC was low from January to April, increased to a maximum value of 18.3 in August, and then decreased to 13.7 in November.

Histological observations of oocyte development

Although oogenesis is continuous, in order to explain the developmental process, oocyte development was divided into eight stages, basically according to Yamamoto (1956) (Fig. 3). The characteristics of oocytes, cell and nuclear diameters, and time of occurrence of each stage of oocyte and POF are shown in Table 1.

Maturity

Ovary maturity did not differ among positions in the ovarian lobe or between eyed-side and blind-side lobes. In addition, the diameters of the largest oocytes did not vary significantly among positions (ANOVA, $F_{2,42} = 0.354$, $P = 0.704$) or between lobes (paired t -test, $f = 14$, $t = 0.058$, $P = 0.955$). Therefore, maturity was determined from observations of the middle portions of eyed-side ovaries.

Maturity was classified into eight phases, the characteristics of which are shown in Table 2. Because oocytes younger than the late perinucleolus stage occurred throughout the year, maturity was determined as occurring from this phase onwards. GSI values significantly varied among maturity phases (ANOVA, $F_{4,205}$,

Table 1

Characteristics, cell and nuclear diameters, and occurrence of oocytes and postovulatory follicles at each developmental stage. Developmental stage and measurements were determined by histological observations (EP=early perinucleolus, LP=late perinucleolus, CA=cortical alveoli, PY=primary yolk, SY=secondary yolk, TY=tertiary yolk, MN=migratory nucleus, PM=maturation, POF=postovulatory follicle). HE=hematoxylin and eosin; PAS=periodic acid Schiff.

Developmental stage	Characteristics	Cell diameter (μm)	Nuclear diameter (μm)	Occurrence
EP	The ooplasm is strongly stained by haematoxylin. Several basophilic nucleoli stained by hematoxylin are present inside the nuclear membrane.	20–70	10–35	year round
LP	The ooplasm increases in volume with growth of the oocyte and becomes less basophilic than that of the previous EP stage.	70–150	35–80	year round
CA	Cortical alveoli, which appear in the ooplasm, are seen as a small empty spherical structure with conventional HE preparations, and are stained reddish by PAS reagents.	160–200	80–120	Feb, Jun, Aug, Oct
PY	The yolk granule occurs at the periphery of the oocytes.	180–220	80–120	year round
SY	The yolk granule increases in number and occurs towards the nuclear membrane, and the ooplasm occurs slightly at the periphery of the nuclear membrane.	260–440	90–130	Jan to Oct
TY	The oocyte is characterized by occupancy of the total volume of the oocyte by a yolk granule. The nucleus of the oocyte is still located at the center of the oocyte.	420–680	120–170	May to Dec
MN	The germinal vesicle migrates to the periphery of the oocyte and becomes elongated and globular in shape.	600–740	130–190	Sep to Dec
PM	The germinal vesicle has broken down. Yolk granules fuse with each other, and are stained light pink by eosin.	620–800	—	Sep to Nov
POF	The POF, containing granular, is a convoluted folded shape.	—	—	Sep to Jan

$F=124.1$, $P<0.0001$) and became significantly higher in each successive stage of maturity (Fisher's PLSD test, $P<0.05$), except for the first two phases ($P=0.687$). The mature- and spent-phase ovaries were excluded from the test because their values fluctuated depending on spawning times or the degree of POF absorption.

Ovaries in the late vitellogenic maturity phase, which occurred from May to September, contained oocytes in the tertiary yolk stage, secondary yolk stage, cortical alveoli stage, and late and early perinucleolus stages, but not in the primary yolk stage (Table 3). Ovaries in the premature phase, which occurred from September to October, also revealed two peaks and a hiatus in oocyte developmental composition. As described before, ovaries with POFs also contained maturing oocytes. These results show that this species is a multiple-spawner and has group-synchronous ovaries (Wallace and Selman, 1981; Takano, 1989); therefore, fecundity is fixed before spawning starts.

On the other hand, ovaries in the mid-vitellogenic phase were observed from January to September and contained oocytes in the secondary and primary yolk

stages, and in the late perinucleolus stage. Cortical alveoli are very small and were present in only 10 of the 309 ovaries observed in our study. It is possible that the duration of this stage is very short. Therefore, in the ovaries oocytes do not divide into two groups, those that spawn in the next reproductive season and those that do not, until they have progressed to the late vitellogenic maturity phase.

Oocyte composition

Table 3 shows the annual changes in oocyte composition. One ovary observed in January contained POFs and perinucleolus stage oocytes, whereas the others contained oocytes in the primary and secondary yolk stages. Of those observed from February to April, none contained POFs. Frequency of occurrence of ovaries with secondary yolk-stage oocytes increased during the season. From May to August the most advanced oocyte observed was in the tertiary-yolk vitellogenic stage, and the frequency of this stage also increased in number throughout this season. Migratory-nucleus-stage and

Table 2

The characteristics, occurrence and gonadosomatic index values of each maturity phase. Developmental oocyte stages were abbreviated as follows: EP=early perinucleolus, LP=late perinucleolus, CA=cortical alveoli, PY=primary yolk, SY=secondary yolk, TY=tertiary yolk, MN=migratory nucleus, PM=prematuration, POF=postovulatory follicle. *n*=number of samples. PAS=periodic acid Schiff.

Maturity phase	Characteristics	The most advanced oocyte observed	Occurrence	GSI (mean±SD)	<i>n</i>
Immature	Ovaries contain only EPs and LPs, but not POFs.	LP	Jan to Apr	1.57 ±0.34	13
Previtellogenic	This phase can be discriminated by PAS staining. Specimens in this phase were scarce.	CA	Feb	1.67	1
Early vitellogenic	Ovaries consist of PY and unyolked oocytes, and occur prevalently from March to April.	PY	Jan to Oct	2.09 ±0.61	41
Mid-vitellogenic	Ovaries contain SY and all stages of oocytes younger than the SY stage.	SY	Jan to Oct	4.40 ±1.72	61
Late vitellogenic	Ovaries contain TY and all stage oocytes younger than TY, but not SY.	TY	May to Dec	12.98 ±5.74	67
Premature	Ovaries lack PY and SY, occurs prevalently during September.	MN or PM	Sep to Dec	17.56 ±5.00	28
Mature	Ovaries contain both empty follicles and oocytes that have advanced beyond the secondary yolk stage.	advanced more than SY	Sep to Dec	16.21 ±8.34	25
Spent	Ovaries contain empty follicles but oocytes that have advanced beyond the secondary yolk stage are absent.	LP	Sep to Jan	2.71 ±2.41	73

premature-stage oocytes and POFs began to occur in September. The composition of oocytes observed during this month was divided into three groups: premature, maturing, and postmature oocytes. In October, almost all ovaries (96.2%) contained POFs. Of these, 28.0% also contained oocytes at the tertiary yolk stage or migratory-nuclear stage (or at both stages) and the remaining 72.0% contained primary-yolk stage or less advanced stage oocytes (or both of these stages). From November to December, all ovaries contained POFs and only a few (3.7% in November and 5.3% in December) also contained vitellogenic oocytes. Therefore, almost all individuals had finished spawning by October, although a few continued to spawn until December.

Atretic oocytes were found in samples throughout the year, except February, in ovaries of various maturity phases. Frequency of occurrence was highest in May, and gradually decreased until the spawning season (Table 3). Oocytes that ovulated but remained in the ovigenous folds and were resorbed later were treated as atretic oocytes because it was difficult to distinguish between them and atretic oocytes if they were somewhat absorbed. Atretic oocytes did not always correspond to the most advanced oocytes in the ovaries. They occupied 0.3–1.8% (mean ±SD=1.0 ±0.5) of the yolked, advanced oocytes observed in the ovaries in May (the number of oocytes counted in 10 ovaries ranged from 117 to 615), and from 0.4 to 1.8% (1.0 ±0.4) of those observed in August (range: 108–383 oocytes in 10 ovaries).

Body length and age at first maturity

The relationship between SL or age and maturity of the fish caught between the prespawning month (August) and the late-spawning month (December) was examined. Otolith growth increments were counted for all specimens. Because the spawning season occurs from September to December, the birth dates of all fish were conveniently defined as 1 January; age was then determined accordingly. SL ranged from 114 to 237 mm ($n=189$, 170.6 ± 25.3) and age, from 1 to 8+ years (2.8 ± 1.4). Individuals grew steeply until 2 years and moderately until 6 years, after which time their growth was slow (Fig. 4). All females whose ages were estimated at more than 2+ years ($n=152$) were identified as maturing or spent-stage females. Only one 1+ year-old specimen (131 mm SL) was classified as immature, whereas the other 1+ specimens ($n=36$, 140.0 ± 11.8) were classified as maturing or postmaturation females (Fig. 4).

Potential fecundity

The diameters of oocytes in late vitellogenic maturity phase ovaries were measured because potential fecundity was determined as occurring before this maturity phase. Oocytes ranged in diameter from less than 100 to 950 μm and were separated into a small (less than 200 μm) or large group (larger than 300 μm , Fig. 5).

Table 3

Annual changes in the composition of female Rikuzen sole oocytes in each maturity phase. Some maturing and spent ovaries contained ovulated but not spawned oocytes. Such ovaries were included under "Number of samples with atretic oocytes." Developmental oocyte stages were abbreviated as follows: EP=early perinucleolus, LP=late perinucleolus, CA=cortical alveoli, PY=primary yolk, SY=secondary yolk, TY=tertiary yolk, MN=migratory nucleus, PM=prematurity, POF=postovulatory follicle.

Year	Month	EP	LP	CA	PY	SY	TY	MN	PM	POF	<i>n</i>	Maturity phase	Number of samples with atretic oocytes
2000	May	+	+		+						4	Early vitellogenic	4
		+	+		+	+					19	Mid vitellogenic	15
	Jun	+	+		+		+				1	Late vitellogenic	1
		+	+		+	+					18	Mid vitellogenic	10
	Jul	+	+		+	+		+			1	Mid vitellogenic	0
		+	+		+	+		+			3	Late vitellogenic	2
	Aug	+	+		+	+		+			7	Mid vitellogenic	2
		+	+		+	+		+			4	Late vitellogenic	1
	early Sep	+	+		+	+					1	Early vitellogenic	0
		+	+		+	+					1	Mid vitellogenic	0
		+	+		+	+					4	Mid vitellogenic	1
		+	+		+	+					33	Late vitellogenic	9
	late Sep	+	+		+	+		+			1	Late vitellogenic	0
		+	+		+	+		+			2	Mid vitellogenic	1
		+	+		+	+		+			4	Late vitellogenic	0
		+	+		+	+		+			6	Late vitellogenic	2
		+	+		+	+		+			1	Premature	0
		+	+		+	+		+			8	Premature	1
		+	+		+	+		+			2	Premature	1
		+	+		+	+		+			4	Spent	1
		+	+		+	+		+			3	Spent	1
		+	+		+	+		+			11	Mature	3
		+	+		+	+		+			2	Mature	0
		Oct	+	+		+	+		+			3	Late vitellogenic
	+		+		+	+		+			1	Late vitellogenic	0
	+		+		+	+		+			12	Late vitellogenic	2
	+		+		+	+		+			1	Premature	0
	+		+		+	+		+			12	Premature	1
	+		+		+	+		+			2	Premature	1
	Nov	+	+		+	+		+			3	Mature	2
		+	+		+	+		+			1	Premature	0
		+	+		+	+		+			10	Spent	4
		+	+		+	+		+			1	Spent	0
	Dec	+	+		+	+		+			7	Spent	4
		+	+		+	+		+			2	Mature	1
		+	+		+	+		+			5	Mature	3
		+	+		+	+		+			24	Spent	15
	Dec	+	+		+	+		+			2	Spent	1
		+	+		+	+		+			1	Mature	1
		+	+		+	+		+			13	Spent	5
											5	Spent	1
											1	Mature	0

continued

Those in the large-diameter group were regarded as advanced yolked oocytes that would be spawned in the next reproductive season and were used for estimations of potential fecundity. Potential fecundity varied widely among individuals from 24,765 (114 mm SL) to 393,212 (204 mm SL) eggs (an average of 161,340 ± 90,688 eggs (165 ± 25 mm SL)). Potential fecundity (PF) was posi-

tively correlated with body size and the relationship was expressed by the following equation:

$$PF = 0.000235SL^{3.96} \quad (\text{Fig. 6}).$$

Potential fecundity and relative fecundity (potential fecundity/eviscerated body weight) increased with

Table 3 (continued)

Year	Month	EP	LP	CA	PY	SY	TY	MN	PM	POF	n	Maturity phase	Number of samples with atretic oocytes	
2001	Jan	+	+								2	Immature	1	
		+	+								8	Early vitellogenic	0	
		+	+		+	+					2	Mid vitellogenic	0	
	Feb	+	+								+	1	Spent	0
		+	+									5	Immature	0
		+	+	+								1	Previtellogenic	0
		+	+		+							5	Early vitellogenic	0
		+	+			+	+					1	Middle vitellogenic	0
	Mar	+	+									3	Immature	0
		+	+			+						15	Early vitellogenic	2
		+	+			+	+					1	Mid vitellogenic	1
	Apr	+	+									3	Immature	0
		+	+			+						10	Early vitellogenic	3
		+	+			+	+					6	Mid vitellogenic	1
	Total										309		104	

growth at age $\leq 6+$ years and decreased at $\geq 7+$ years (Fig. 7). Comparisons of the relative fecundity among age groups (1-2+, 3-4+, 5-6+, and 7-8+) revealed significant differences with age (ANOVA, $F_{3,38}=7.431$, $P<0.0005$). In addition, *post hoc* tests (Fisher's PLSD, $P<0.05$) revealed significant differences between the following age groups: 1-2+ and 3-4+, 1-2+ and 5-6+, and 5-6+ and 7-8+. The GSI and BC values of individuals aged $\geq 7+$ years were also lower than those of individuals aged 5+ and 6+ years, but the differences were not significant (*aq*-test, $P>0.05$); however, the sample size was very small; therefore the tests have little power.

Discussion

Gonadal maturation

GSI and histological examinations showed that oocytes develop rapidly from May to August and that the reproductive season lasts from September to December; mainly from September to October in the study area. Mature females in the Sendai Bay area were also observed for four months, but the reproductive season in this area occurs from October to January and peaks in November (Ogasawara and Kawasaki, 1980), which was later than the peak documented in the present study for the area off the Hachinohe coast. The Sendai Bay catch area was located at a lower latitude (37°00'N-38°05'N; Ogasawara and Kawasaki, 1980) than that of the Hachinohe study area (Fig. 1); this difference is relevant because gonadal maturation is usually dependent on water temperature (Kruse and

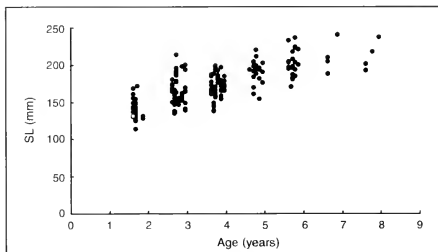
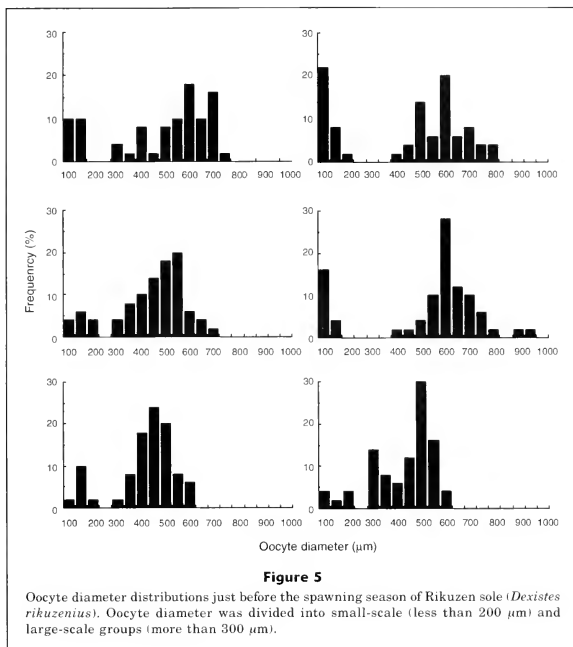


Figure 4

Relationship between age, including maturity, and the standard length of Rikuzen sole (*Dexistes rikuzenius*) caught between August and December. Solid circles represent maturing or spent individuals and the open circle at age 1+ represents an immature individual.

Tyler, 1983; Asahina and Hanyu, 1983; Conover, 1990). In 2000, the water temperature in the Hachinohe study area decreased faster than that of Sendai Bay in 1977 and 1978 when studied by Ogasawara and Kawasaki (TNFRI¹). These results indicate that gonadal maturation in Rikuzen sole also depends on water temperature.

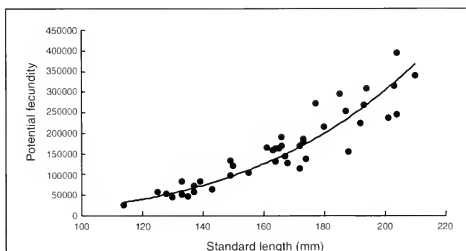
¹ TNFRI (Tohoku National Fisheries Research Institute). 2004. Unpubl. data. Water temperature data. Tohoku National Fisheries Research Institute, Fisheries Research Agency of Japan. Shiohama City, Miyagi Prefecture 985-0001 Japan.

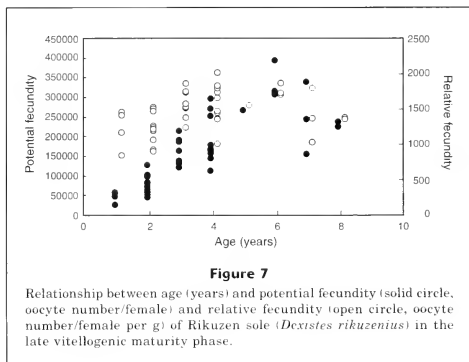


Rikuzen sole require a long period of time for vitellogenesis and therefore the reproductive cycle may differ among areas.

In some flatfishes, it has also been reported that oocytes in the cortical alveoli stage appear for only a short period of time because they develop rapidly into the primary yolk stage (Yamamoto, 1956; Janssen et al., 1995). In the present study, only a small percentage of individuals contained this stage of oocytes; however, cortical alveoli were present throughout various months from June to October and in February. These results are similar to results for other flatfish and may indicate that the absence of cortical alveoli oocytes in some ovaries does not represent an incontinuity of oocyte composition.

From October to December some females possessed primary yolk-stage oocytes,





although they had no other vitellogenic oocytes. There are three potential hypotheses to explain the fate of these primary yolk oocytes. One explanation is that the oocytes are spawned in the current reproductive season. Maddock and Burton (1999) showed that in American plaice (*Hippoglossoides platessoides*), a group-synchronous spawner, the size frequency of oocytes during the prereproductive season was not continuous, whereas during the reproductive season the size frequency was continuous. The reason for this difference was that during the reproductive season cortical alveoli stage oocytes are larger than those during the prereproductive season. It is unclear, however, whether these cortical alveoli oocytes will be spawned during the reproductive season (Maddock and Burton, 1999). Although similar to those of the American plaice, all Rikuzen sole ovaries with primary yolk-stage oocytes contained no secondary or more advanced stage oocytes. In addition, oocytes that would be spawned in the current reproductive season developed beyond the secondary yolk stage before the beginning of the reproductive season. Therefore, primary yolk-stage oocytes occurring late in the reproductive season might not be spawned that season.

Primary yolk-stage oocytes were found from October to August (the late reproductive to vitellogenic season) (Table 3). From October to December only a small percentage of individuals possessed oocytes in this stage, whereas their ratio increased from January to April. These results indicate that females begin vitellogenesis for the next reproductive season shortly after spawning. This hypothesis is supported by reports that the vitellogenesis of flatfishes takes a long time (Yamamoto, 1954, 1956; Ishida and Kitakata, 1982; Zamarro, 1992; Harmin et al., 1995).

Atretic oocytes were present in low proportions from March to April and in high proportions in May. The mature phase of ovaries with atretic oocytes did not

differ from that of ovaries without atretic oocytes. In addition, developmental stage did not differ between atretic and normal oocytes in any ovary. Therefore, it seems that the primary yolk-stage oocytes observed late in the reproductive season will not selectively degenerate, rather they will be spawned.

Decisions regarding maturity and age at maturity

POFs were present from September to January and all specimens caught during this period had either oocytes in the advanced yolk stage or POFs in their ovaries. All specimens caught between November and December contained ovaries with POFs, whereas they were observed only in a small percentage of the specimens caught in January. The spawning season lasted from September to December, but almost all spawning had finished by October. These results indicate that the duration until resorption of the POFs ranges from a few weeks to two months. For a few weeks immediately following spawning, the presence of POFs can be used as a criterion for the differences between post- and prespawning individuals. This feature is consistent with that of other flatfish in which POFs degenerate within one or two months (Barr, 1963; Janssen et al., 1995).

By noting the presence of POFs and advanced yolked oocytes, we were able to classify individuals as mature or immature. All but one individual caught during the reproductive period were maturing or had spawned. The body size of the mature females ranged from 114 to 237 mm SL, which corresponded to an age from 1 to 8+ years, respectively, whereas the immature female (131 mm SL) was age 1+. These results indicated that most female Rikuzen sole in this population mature at 2 years old, or at the latest at 3 years old, and spawn every year after maturation. Almost all (99.5%) fish caught commercially are adult individuals.

Fecundity

The potential fecundity of group-synchronous spawning fish can be determined prior to the spawning season (Takano, 1989). In Rikuzen sole, oocyte-stage composition became discontinuous beyond the late vitellogenic maturity phase, when a gap was found between secondary or tertiary yolk stages and the late perinucleolus stage. Oocyte diameter distributions in late vitellogenic maturity phase ovaries revealed that oocytes could be divided into small (less than 200 μm) and large (more than 300 μm) scale groups. Taking into account the oocyte diameters observed in the histological sections, small-scale group oocytes corresponded to cortical alveoli or less advanced stage oocytes, whereas larger oocytes corresponded to secondary yolk or more advanced stage oocytes.

The occurrence of atretic oocytes was highest in May and became lower as the season progressed until the end of the spawning season. These phenomena may correlate with both annual feeding cycles and maturation. Ogasawara and Kawasaki (1980) showed that in the Sendai Bay population, Rikuzen sole feed actively for a few months after spawning and then feed passively for the next few months. Gut-content weight began to increase again in June. In our study area, BC increased from about May, corresponding to the time when the oocytes begin to mature rapidly. As described before, vitellogenesis in this species takes a long time. Because oocytes are metabolically active in the season when the energetic condition of Rikuzen sole is still recovering, a higher proportion of atretic oocytes occur during this period.

Potential fecundity may not correspond to annual fecundity because of the presence of atretic and residual oocytes (Witthames and Greer Walker, 1995; Kurita et al., 2003). Therefore, we examined the potential fecundity of fish in the late vitellogenic maturity phase just before the spawning season. The frequency of occurrence of atretic oocytes may be underestimated because these oocytes have shrunk and are smaller than the maturing yolked oocytes. In addition, atretic oocytes may occur in the ovaries during the premature maturity phase. However, in our samples a low percentage of atretic oocytes were observed. Only a small percentage of premature ovaries were found on or before the reproductive season; this finding seems to indicate that the oocytes of this species take a short time to develop from the tertiary vitellogenic stage to maturation. These results make clear that potential fecundity differs from annual fecundity, but the extent of this difference was nevertheless relatively small in the samples. Moreover, ovulated, but not spawned oocytes were observed in the maturing and spent ovaries; these oocytes have the potential to cause an overestimation of annual fecundity. However, the frequency of ovaries with residual ovulated oocytes was small; therefore, such oocytes may not seriously influence annual fecundity, as with the case of Dover sole (*Microstomus pacificus*) (Hunter et al., 1992).

Vitellogenesis in American plaice was seen to begin soon after spawning (Zamarro, 1992), as with Rikuzen

sole. Separation of oocyte diameter in this species occurs approximately three months before the start of the spawning season. In Rikuzen sole, potential fecundity was determined as being much closer to the reproductive season. Reproduction occurred from early September, but occurrence of the maturity phase in August varied largely among individuals. The potential fecundity of almost all fish (85%) could be determined until August. These results indicate that certain conditions and measurements are necessary when examining potential fecundity without histological methods.

Potential fecundity became determinate for the first time at maturity during the late vitellogenic phase. Some of the maturity phase ovaries contained secondary yolk-stage oocytes and all contained tertiary yolk-stage oocytes. The secondary yolk-stage oocytes ranged in diameter from 260 to 440 μm —a range that does not overlap with the diameter range of primary yolk-stage oocytes (180–220 μm). Therefore, to measure potential fecundity without histological observations, it is first necessary to clarify the division of oocyte diameter into large- and small-scale groups in order to identify determinate fecundity. In ovaries that contain large- and small-scale oocytes, only oocytes greater than 260 μm in diameter but that do not experience ovulation between May and August are targets for potential fecundity measurements. This method will make it easier to measure the potential fecundity of this population in the future.

Potential fecundity increased curvilinearly with SL. The body size of the females continued to grow even after maturation; the most fecund individual had 15 times more maturing oocytes than the least fecund one. Potential fecundity also increased until age $\leq 6+$ years but decreased in individuals at $\geq 7+$ years. One reason that older fish have less potential fecundity is a lesser energetic condition with senescence. Fecundity has been also reported as declining with age in other fish. As American plaice in the tail of the Grand Bank Newfoundland become older, the number of eggs produced by females decreased (Horwood et al., 1986). Orange roughy, mature first at 25 years old and live for more than 100 years; their fecundity increases from an age of 25 to 60 years old, then decreases in individuals aged over 60 years old (Koslow et al., 1995). Fecundity is positively correlated with BC in the orange roughy. The oldest Rikuzen sole to appear in that study area was 10+ years (Ishito, 1964) and body growth almost finished by age 6+ years (Fig. 6). In addition, both the BC and relative fecundity of fish over 7+ years were lower than those of fish from 4 to 6+ years.

Spawning stock biomass (SSB) has been used to examine the relationship of spawning fish and recruitment; however, recent studies have indicated that SSB is not always linked to reproductive potential, mainly because age composition and nutrient conditions also affect fecundity (Hunter et al., 1985a; Trippel et al., 1997; Marshall et al., 1998). Our study shows that relative fecundity is positively correlated with body length. In addition, both relative and potential fecundity increase

with age, but decrease again in later years. These results support previous studies and emphasize the importance of understanding the demographic structure and reproductive biology of a population for the management of fish resources.

Acknowledgments

We are grateful to Hiroyuki Munehara for his valuable discussion and comments on the early version of this manuscript and to Yoshio Ishito for his support in collecting samples. This work was financially supported by the DEEP Program of the Ministry of Agriculture, Forestry, and Fisheries, Japan.

Literature citations

- Anonymous.
2002. Statistical catch record of fishes by bottom trawl net fisheries in northern Pacific coast of Japan (2001), edited by the Hachinohe Branch, 113 p. Tohoku Natl. Fish. Res. Inst., Fish. Agency, Japan.
- Asahina, K., and I. Hanyu.
1983. Role of temperature and photoperiod in annual reproductive cycle of the rose bitterling *Rhodeus ocellatus ocellatus*. Nippon Suisan Gakkaishi 49:61-67.
- Barr, W. A.
1963. The endocrine control of the sexual cycle in the plaice, *Pleuronectes platessa* (L.). I. Cyclical changes in the normal ovary. General Comp. Endocrinol. 3:197-204.
- Beverson, R. J. H., and S. J. Holt.
1957. On the dynamics of exploited fish populations. Fishery Invest. Series II 29, 553 p.
- Conover, D. O.
1990. The relation between capacity for growth and length of growing season: evidence for and implications of countergradient variation. Trans. Am. Fish. Soc. 119:416-430.
- Fujita, T., D. Kitagawa, Y. Okuyama, Y. Ishito, T. Inada, and Y. Jin.
1995. Diets of the demersal fishes on the shelf off Iwate, northern Japan. Mar. Biol. 123:219-233.
- Harmin, S. A., L. W. Crim, and M. D. Wiegand.
1995. Plasma sex steroid profiles and the seasonal reproductive cycle in male and female winter flounder, *Pleuronectes americanus*. Mar. Biol. 121:601-610.
- Horwood, J. W., R. C. A. Bannister, and G. J. Howlett.
1986. Comparative fecundity of North Sea plaice. Proc. R. Soc. Lond. B. 228:401-431.
- Horwood, J. W., M. G. Walker, and P. Witthames.
1989. The effect of feeding levels on the fecundity of plaice (*Pleuronectes platessa*). J. Mar. Biol. Assoc. U.K. 69: 81-92.
- Hunter, J. R. and B. J. Macewicz.
1985a. Rates of atresia in the ovary of captive and wild northern anchovy, *Engraulis mordax*. Fish. Bull. 83:119-136.
1985b. Measurement of spawning frequency in multiple spawning fishes. NOAA Tech. Rep. NMFS. 36: 79-94.
- Hunter, J. R., B. J. Macewicz, C. N. Lo, and C. A. Kimbrell.
1992. Fecundity, spawning, and maturity of female Dover sole, *Microstomus pacificus*, with an evaluation of assumptions and precision. Fish. Bull. 90:101-128.
- Ishida, R., and M. Kitakata.
1982. Studies on the maturity of the female flathead flounder, *Hippoglossoides dubius* (Schmidt). Bull. Tokai. Reg. Fish. Res. Lab. 107:61-105.
- Ishito, Y.
1964. Age and growth of the three flounder species, 'Sohachi', roundnose and 'Migigarei' flounders, in the fishing area off Hachinohe. Bull. Tohoku Reg. Fish. Res. Lab. 24:73-80.
- Janssen, P. A. H., G. D. Lambert, and H. J. Th. Goos.
1995. The annual ovarian cycle and the influence of pollution on vitellogenesis in the flounder, *Pleuronectes flesus*. J. Fish. Biol. 47:509-523.
- Koslow, J. A., J. Bell, P. Virtue, and D. C. Smith.
1995. Fecundity and its variability in orange roughy: effects of population density, condition, egg size, and senescence. J. Fish. Biol. 47:1063-1080.
- Kruse, G. H., and A. J. Tyler.
1983. Simulation of temperature and upwelling effects on the English sole (*Parophrys vetulus*) spawning season. Can. J. Fish. Aquat. Sci. 40:230-237.
- Kurita, Y., S. Meier, and O. S. Kjesbu.
2003. Oocyte growth and fecundity regulation by atresia of Atlantic herring (*Clupea harengus*) in relation to body condition throughout the maturation cycle. J. Sea Res. 49:203-219.
- Maddock, D. M., and M. P. M. Burton.
1999. Gross and histological observations of ovarian development and related condition changes in American plaice. J. Fish. Biol. 53 928-944.
- Marshall, C. T., O. S. Kjesbu, N. A. Yaragina, P. Solemdal, and Ø Ulltang.
1998. Is spawner biomass a sensitive measure of the reproductive and recruitment potential of Northeast Arctic cod? Can. J. Fish. Aquat. Sci. 55:1766-1783.
- Ogasawara, Y., and T. Kawasaki.
1980. Life history of Migigarei, *Dexistes rikuzenius* (Jordan et Starks), in Sendai Bay, with special reference to sexual dimorphism. Tohoku J. Agri. Res. 30: 163-182.
- Ricker, W. E.
1954. Stock and recruitment. J. Fish. Res. Board Can. 11:559-623.
- Sakamoto, K.
1984. *Dexistes rikuzenius*. In The fishes of the Japanese Archipelago (H. Masuda, K. Amaoka, C. Araga, T. Ueno, and T. Yoshino eds.), p. 338. Tokai Univ. Press, Tokyo. [In Japanese.]
- Sampson, D. B., and S. M. Al-Jufaily.
1999. Geographic variation in the maturity and growth schedules of English sole along the U.S. west coast. J. Fish. Biol. 54:1-17.
- Takano, K.
1989. Ovarian structure and gametogenesis. In Reproductive biology of fish and shellfish (F. Takahashi and I. Hanyu, eds.), p. 3-34. Midori-Shobo, Tokyo. [In Japanese.]
- Trippel, E., O. S. Kjesbu, and P. Solemdal.
1997. Effects of adult age and size structure on reproductive output in marine fishes. In Early life history and recruitment in fish populations (R. Chambers and

- E. Trippel, eds.), p. 31–62. Fish and Fisheries Series 21, Chapman and Hall, London.
- Wallace, R. A., and K. Selman.
1981. Cellular and dynamic aspects of oocyte growth in teleosts. *Am. Zool.* 21:325–343.
- West, G.
1990. Methods of assessing ovarian development in fishes: a review. *Aust. J. Mar. Freshw. Res.* 41:199–222.
- Witthames, P. R., and M. Greer Walker.
1995. Determinacy of fecundity and oocyte atresia in sole (*Solea solea*) from the Channel, the North Sea and the Irish Sea. *Aquat. Living Resour.* 8:91–109.
- Yamamoto, K.
1954. Studies on the maturity of marine fishes II. Maturity of the female fish in the flounder, *Liopsetta obscura*. *Bull. Hokkaido Reg. Fish. Res. Lab.* 11:68–77.
1956. Studies on the formation of fish eggs I. Annual cycle in the development of ovarian eggs in the flounder, *Liopsetta obscura*. *J. Fac. Fish. Hokkaido Univ.* 12: 362–373.
- Zamarro, J.
1992. Determination of fecundity in American plaice (*Hippoglossoides platessoides*) and its variation from 1987 to 1989 on the tail of the grand bank. *Neth. J. Sea Res.* 29:205–209.
- Zimmermann, M.
1997. Maturity and fecundity of arrowtooth flounder, *Atheresthes somias*, from the Gulf of Alaska. *Fish. Bull.* 95:598–611.

Abstract—Data from ichthyoplankton surveys conducted in 1972 and from 1977 to 1999 (no data were collected in 1980) by the Alaska Fisheries Science Center (NOAA, NMFS) in the western Gulf of Alaska were used to examine the timing of spawning, geographic distribution and abundance, and the vertical distribution of eggs and larvae of flathead sole (*Hippoglossoides elassodon*). In the western Gulf of Alaska, flathead sole spawning began in early April and peaked from early to mid-May on the continental shelf. It progressed in a southwesterly direction along the Alaska Peninsula where three main areas of flathead sole spawning were identified: near the Kenai Peninsula, in Shelikof Strait, and between the Shumagin Islands and Unimak Island. Flathead sole eggs are pelagic, and their depth distribution may be a function of their developmental stage. Data from MOCNESS tows indicated that eggs sink near time of hatching and the larvae rise to the surface to feed. The geographic distribution of larvae followed a pattern similar to the distribution of eggs, only it shifted about one month later. Larval abundance peaked from early to mid-June in the southern portion of Shelikof Strait. Biological and environmental factors may help to retain flathead sole larvae on the continental shelf near their juvenile nursery areas.

Temporal and spatial distribution and abundance of flathead sole (*Hippoglossoides elassodon*) eggs and larvae in the western Gulf of Alaska

Steven M. Porter

Alaska Fisheries Science Center
7600 Sand Point Way NE
Seattle, Washington 98115
Email address: steve.porter@noaa.gov

Flathead sole (*Hippoglossoides elassodon*) inhabit the continental shelf waters of the North Pacific Ocean from the northwest coast of North America to the Sea of Okhotsk in Asia (Alderice and Forrester, 1974). The western Gulf of Alaska is an important area for adult, juvenile, and larval flathead sole. The continental shelf from the entrance to Prince William Sound to Unimak Island contains the highest relative abundance of adult flathead sole (as expressed as kg/ha) off the west coast of North America (Fig. 1; Wolotira et al.¹). Adult flathead sole are most abundant between depths of 100 and 200 m in this area (Wolotira et al.¹). During the spring adult flathead sole move from wintering grounds on the upper continental slope onto the continental shelf (Rose, 1982). Spawning flathead sole are found from February to August, and the greatest proportion of spawning fish occurs in April and May at depths between 100 and 200 m (Hirschberger and Smith²). Flathead sole eggs range in size from 2.75 to 3.75 mm (Matarese et al., 1989), and under environmental conditions similar to those they could experience in the Gulf of Alaska (temperature=5.5°C and salinity=31 PSU) it takes them about 15 days to hatch (Alderice and Forrester, 1974). During the spring, flathead sole are the most abundant pleuronectid larvae in western Gulf of Alaska (Rugen³). Standard length at hatching is 6.89 ± 0.40 mm (95% ethanol-preserved size; S. Porter unpubl. data). Under conditions that flathead sole larvae could experience in the Gulf of Alaska, first feeding occurs about 1 week after hatching,

and in about 2 weeks the yolk is exhausted (Alderice and Forrester, 1974). Copepod nauplii 150–350 µm in size are their predominant prey (Watts, 1988). In Auke Bay, Alaska, flathead sole larvae undertake reverse diel vertical migrations; they are concentrated near 5 m depth during the day and then disperse over a wider range of depths at night (Halderson et al., 1993). The bays of the Alaska Peninsula and Kodiak Island provide nursery areas for juvenile flathead sole (Norcross et al., 1999).

Studies of the drift of walleye pollock (*Theragra chalcogramma*) larvae in Shelikof Strait have shown that there are physical processes that can slow the drift of these larvae out of Shelikof Strait and keep them near shore (Bailey et al., 1997). The pro-

¹ Wolotira, R. J., T. M. Sample, S. F. Noel, and C. R. Iten. 1993. Geographic and bathymetric distributions for many commercially important fishes and shellfishes off the west coast of North America, based on research survey and commercial catch data, 1912–84. NOAA Tech. Memo. NMFS-AFSC-6, 184 p. Alaska Fisheries Science Center, 7600 Sand Point Way NE, Seattle, WA 98115.

² Hirschberger, W. A., and G. B. Smith. 1983. Spawning of twelve groundfish species in the Alaska and Pacific coast regions, 1975–81. NOAA Tech. Memo. NMFS F/NWC-44, 50 p. Northwest and Alaska Fisheries Center, 2725 Montlake Boulevard East, Seattle, WA 98112.

³ Rugen, W. C. 1990. Spatial and temporal distribution of larval fish in the western Gulf of Alaska, with emphasis on the period of peak abundance of walleye pollock (*Theragra chalcogramma*) larvae. U.S. Dep. Commer., NWAFSC Processed Rep. 90-01, 162 p. Alaska Fisheries Science Center, 7600 Sand Point Way NE, Seattle, WA 98115.

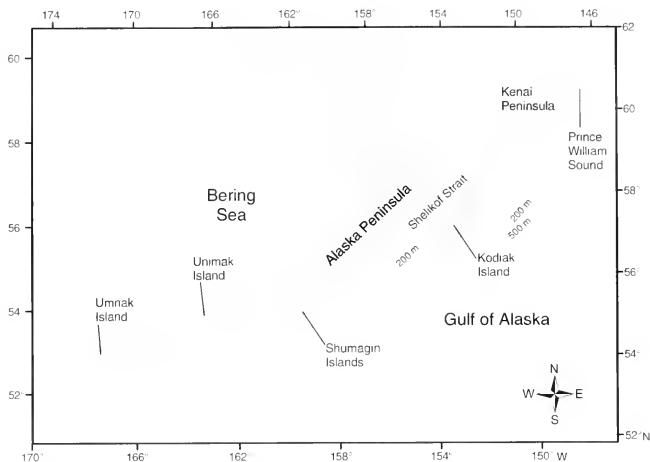


Figure 1

The western Gulf of Alaska where ichthyoplankton surveys were conducted in 1972 and from 1977 to 1999 by the Alaska Fisheries Science Center to examine the timing of spawning, geographic distribution and abundance, and vertical distribution of flathead sole (*Hippoglossoides elassodon*).

cesses that affect the drift of walleye pollock larvae may also affect the drift of flathead sole larvae in this area. For example, the drift of walleye pollock larvae in Shelikof Strait can be slowed if they become entrained in eddies that form there (Bailey et al., 1997). The Alaska Coastal Current flows southwest through Shelikof Strait and branches just south of it; one branch continues along the continental shelf, and the other heads seaward (Bailey et al., 1997). Whether larvae will stay near shore or move off shore is determined by one or other of these two branches of the current.

Information about the early life history of flathead sole in the Gulf of Alaska is lacking. Data from ichthyoplankton surveys conducted in the western Gulf of Alaska were used to examine the timing of spawning, geographic distribution and abundance, and the vertical distribution of flathead sole eggs and larvae. The purpose of this study was to give a general overview of flathead sole egg and larval distribution and abundance in the Gulf of Alaska during the calendar year.

Materials and methods

The study area covered the continental shelf (approximately 300 m depth and less) of the western Gulf of

Alaska from the Kenai Peninsula southwest along the Alaska Peninsula to Umnak Island (Fig. 1). Also covered was the east side of Kodiak Island out to the continental shelf break (Fig. 1). The Alaska Stream and the Alaska Coastal Current are two major surface currents that flow through the study area. Both currents flow southwesterly: the Alaska Stream along the shelf break and the Alaska Coastal Current through Shelikof Strait (Kendall et al., 1996).

A series of ichthyoplankton surveys were conducted in 1972 and from 1977 to 1999 (no data were collected in 1980) by the Alaska Fisheries Science Center (NOAA, NMFS) in the western Gulf of Alaska (Tables 1 and 2). Data were used from 75 surveys. Surveys were conducted from February to November; the most intensive sampling was in April and May. Not all months were sampled every year, and not all cruises surveyed the same area. A 60-cm diameter bongo sampler with a net mesh size of 333 or 505 μm was towed in a double oblique fashion (from the surface to near bottom and back to the surface) to collect samples used to examine the geographic distribution and abundance of eggs and larvae. Interannual variability in the abundance of eggs and larvae in the Shelikof Strait spawning area can vary as much as tenfold (S. Porter, unpubl. data), but to increase sampling coverage of the study area,

Table 1

The number of stations used each year to assess monthly flathead sole (*Hippoglossoides classodon*) egg distribution in the western Gulf of Alaska.

Cruise year	Feb	Mar	Apr 1-15	Apr 16-30	May 1-15	May 16-31	Jun 1-15	Jun 16-30	Jul	Aug	Sep	Oct	Nov
1972	— ¹	—	—	27	40	—	—	—	—	—	—	—	—
1977	—	—	—	—	—	—	—	—	—	—	—	11	48
1978	—	23	61	2	—	—	—	69	20	—	57	67	118
1979	48	40	—	—	—	58	—	—	—	—	18	—	—
1981	—	190	61	123	16	136	—	—	—	—	—	—	—
1982	—	—	55	28	—	62	—	—	—	—	—	—	—
1983	—	—	—	—	1	67	—	—	—	—	—	—	—
1984	—	2	63	66	28	—	—	—	—	—	—	—	—
1985	—	109	87	28	62	135	54	—	—	—	—	—	—
1986	—	11	185	34	89	19	—	—	—	—	—	—	—
1987	—	—	177	83	—	59	—	15	4	—	—	—	—
1988	—	102	228	64	13	4	1	—	—	—	—	—	—
1989	—	—	128	69	132	47	1	—	—	—	—	—	—
1990	—	—	107	—	88	70	78	—	—	—	6	—	—
1991	—	—	90	150	119	97	—	—	—	—	—	—	—
1992	—	—	94	—	158	136	—	—	—	—	—	—	—
1993	—	—	96	—	141	90	24	—	—	—	—	—	—
1994	—	10	9	—	88	133	6	—	—	—	—	—	—
1995	1	5	—	—	—	98	—	—	—	—	—	—	—
1996	—	—	—	59	269	130	—	—	—	—	—	—	—
1997	—	—	—	—	—	100	—	—	—	—	—	—	—
1998	—	—	—	—	72	128	—	26	—	—	—	—	—
1999	—	—	—	—	2	233	83	—	—	—	—	—	—
Total	49	492	1436	733	1320	1803	247	110	24	0	81	78	166

¹ No stations.

years were pooled for each month. Abundance did not appear to affect the spatial distribution of eggs or larvae; their distribution patterns were similar no matter whether abundance was high or low. Months of highest abundance (April, May, and June) were divided into early to mid-month (days 1-15) and mid- to late month (days 16-31). The area covered by the cruises was divided into 50×50 km grid cells. Mean catch per cell was calculated for each grid cell, averaging over all stations falling within the cell. For the areas other than Shelikof Strait, the number of stations per cell ranged from 1 to 10. The most intensive sampling was conducted in the Shelikof Strait area, south to approximately 56°N latitude. Cells in this area, depending on the month, could have more than 100 stations within them. To examine larval drift, the center and ellipse (centroid) of egg and larval abundance for early and late May 1994 and 1996 (two years with different flow regimes in Shelikof Strait) were calculated according to the methods described in Kendall and Picquelle (1989).

The vertical distribution of eggs and larvae was examined from samples from four 1-m² MOCNESS (multiple-

opening-closing-net and environmental sensing system) tows. For each tow, 6 to 8 depth intervals were sampled from near the sea floor to near the surface. The samples were collected during peak spawning in 1991 (one tow during day light), 1993 (one tow during day light), and 1996 (two tows: 1996A conducted during the night, and 1996B during day light). Eggs collected in each depth interval were categorized as early (stages 1-12), middle (stages 13-15), and late stage (stages 16-21) according to walleye pollock egg stages adapted from Blood et al. (1994). The late stage was divided into two categories: late A (stages 16-19) and late stage B (stages 20-21), to indicate which eggs were closest to time of hatching. Taking into account shrinkage in standard length due to collection and preservation (Theilacker and Porter, 1995), larvae were divided into three size categories based on development. Larvae <5 mm were classified as recently hatched, larvae 5-6 mm as prefeeding or first feeding, and larvae >6 mm as feeding, based not only on size but also on the amount of yolk present, and whether prey were visible in their gut. These categories were based on observations of flathead sole larvae

Table 2

The number of stations used each year to assess monthly flathead sole (*Hippoglossoides elassodon*) larval distribution in the western Gulf of Alaska.

Cruise year	Apr 1-15	Apr 16-30	May 1-15	May 16-31	Jun 1-15	Jun 16-30	Jul	Aug	Sep	Oct	Nov
1972	— ¹	27	40	—	—	—	—	—	—	—	—
1977	—	—	—	—	—	—	—	—	—	11	48
1978	60	2	—	—	—	69	20	—	—	67	118
1979	—	—	—	58	—	—	—	—	18	—	—
1981	61	123	16	136	—	—	—	—	—	—	—
1982	55	28	—	62	—	—	—	—	—	—	—
1983	—	—	1	63	—	—	—	—	—	—	—
1984	63	66	28	—	—	—	—	—	—	—	—
1985	87	28	62	135	54	—	—	—	—	—	—
1986	185	34	89	19	—	—	—	—	—	—	—
1987	177	83	—	58	—	15	4	—	—	—	—
1988	227	64	13	2	1	—	—	—	—	—	—
1989	128	69	132	34	1	—	—	—	—	—	—
1990	107	—	90	70	78	—	—	—	6	—	—
1991	90	150	119	97	—	—	—	—	—	—	—
1992	94	—	158	136	—	—	—	—	—	—	—
1993	96	—	141	90	24	—	—	—	—	—	—
1994	4	—	89	133	6	—	—	—	—	—	—
1995	—	—	—	98	—	—	—	—	—	—	—
1996	—	59	273	130	—	—	—	—	—	—	—
1997	—	—	—	100	—	—	—	—	—	—	—
1998	—	—	72	128	—	26	—	—	—	—	—
1999	—	—	6	233	83	—	—	—	—	—	—
Total	1434	733	1329	1782	247	110	24	0	81	78	166

¹ No stations.

reared in the laboratory (S. Porter, unpubl. data). In the laboratory, flathead sole larvae hatch with pigmented eyes, three tail pigment bands, and an open mouth (S. Porter, unpubl. data). Flathead sole larvae that were collected from MOCNESS tows and that did not have these features were classified as embryos (it was suspected that handling during collection may have caused some of the late stage eggs to prematurely hatch), and their lengths were not included in the weighted mean depth. For eggs and larvae, a weighted mean depth was calculated for each stage or size category, and depths were compared by using ANOVA and the Tukey HSD multiple comparison test.

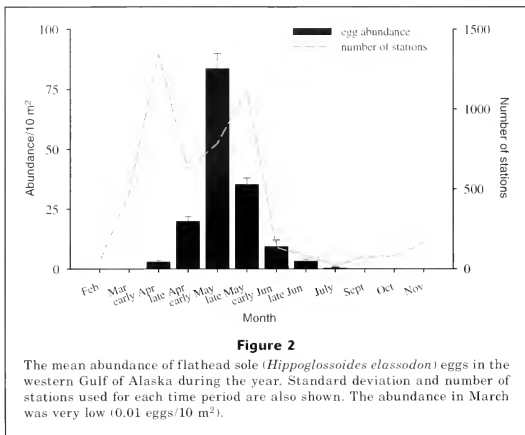
Results

Eggs

Geographic distribution and abundance Eggs were collected as early as March but in small numbers (Figs. 2 and 3A). Most spawning began from early to mid-April

(Fig. 3B) near the Kenai Peninsula and then progressed with time southwest into Shelikof Strait and along the Alaska Peninsula. There are two main areas where peak spawning (from early to mid-May) occurred: Shelikof Strait and between the Shumagin Islands and Unimak Island (Fig. 3C). In June, spawning generally declined in these areas and was most intense around Kodiak Island (3D). Eggs were collected as late as July (one station in 1978, on the eastern side of Kodiak Island).

Vertical distribution There were similar trends in the vertical distribution of eggs among tows (Fig. 4). Abundance peaked at about 20 to 35 m below the surface, decreased at greater depth, and then slightly increased below 125 m. Because the trend of the catches of the tows were similar, we were able to increase sample size in the depth intervals by pooling data from similar depth intervals for further analyses. Eggs were pelagic and most abundant near the surface (mean depth 43 ± 10 m) and at the deep sampling depths (mean depth 149 ± 6 m); abundance was low in mid-water (Fig. 4). Late-stage eggs (stages 16–21) dominated the depths of



high abundance. Early stage eggs were most abundant in mid-water; they accounted for 79% of the total number of eggs collected between 50 and 159 m depth. Sixty-six percent of all eggs collected above 66 m depth were middle- and late-stage A eggs. The largest numbers of late-stage B eggs were found below 124 m depth, where they accounted for 83% of all eggs collected. Mean egg stage depth showed that as the eggs developed from the early stages to the middle stages they rose toward the surface (mean depth of the eggs changed from 54 to 28 m); then in the later stages of development the eggs sank and hatched at depth. Late-stage B eggs were collected significantly deeper (mean depth 90 ± 37 m) than late-stage A eggs (mean depth 35 ± 7 m; ANOVA, $P=0.007$; Tukey HSD multiple comparison test, $P=0.006$).

Larvae

Geographic distribution and abundance Larvae were found from early April to October, but they were most abundant from mid-May to mid-June (Fig. 5). From mid- to late April, larvae were most abundant near the Kenai Peninsula (Fig. 6A), and as spring progressed their abundance increased southwest along the Alaska Peninsula (Fig. 6B). Peak abundance occurred during the first two weeks of June in the southern portion of Shelikof Strait (Fig. 6C). From mid- to late June larvae were most abundant on the east side of Kodiak Island (Fig. 6D). Although most of the surveys were conducted in this area, it is possible that larvae may have been abundant elsewhere in the study area during this time. From July through October, only the area east of Kodiak Island was surveyed, and larval abundance there was low.

Larval drift Satellite-tracked drifters released in May 1994 and drogued at 40 m indicated that the Alaska Coastal Current flow was strong and moving to the southwest—typical surface current flow for this area (Bailey⁴). In May 1996, drifters showed that flow was weak, disorganized and moving somewhat to the northeast (Bailey et al., 1999). In early May 1994, very few flathead sole larvae were collected; therefore the center point of the flathead sole egg distribution was used to infer the starting location of larval drift. Size-at-age data have shown that the growth rate for flathead sole larvae is 0.3 mm/day in Auke Bay, Alaska (Haldorson et al., 1989). Using this growth rate, we determined that larvae hatched in early May could have grown as much as 6 mm in the 21 days between surveys. The size class of larvae greater than 9 mm was assumed to include larvae that had hatched from the eggs present in early May. The location of the centers of distribution of the early May eggs and late May larvae indicated that the larvae had drifted southward over the continental shelf (Fig. 7). In 1996 all the larvae collected in early May were 7.1 mm and smaller (range 4.2 to 7.1 mm). The area was surveyed 26 days later, and growth of about 8 mm could have occurred between surveys. For larvae collected at the end of May, the size group longer than 12 mm was assumed to include the early May larval group. The location of the centers of distribution of the early May and late May larvae showed that the larvae were retained at nearly the same location (Fig. 8).

⁴ Bailey, K. M. 2002. Personal commun. NOAA, Alaska Fisheries Science Center, 7600 Sand Point Way NE, Seattle, WA 98115.

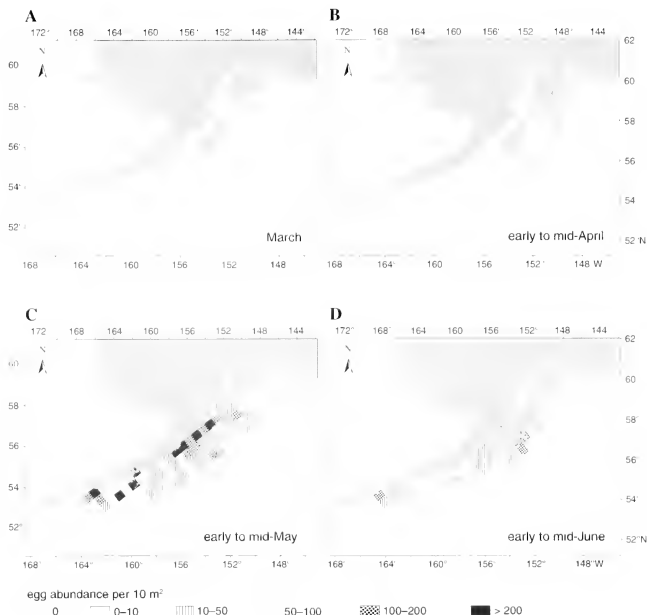


Figure 3

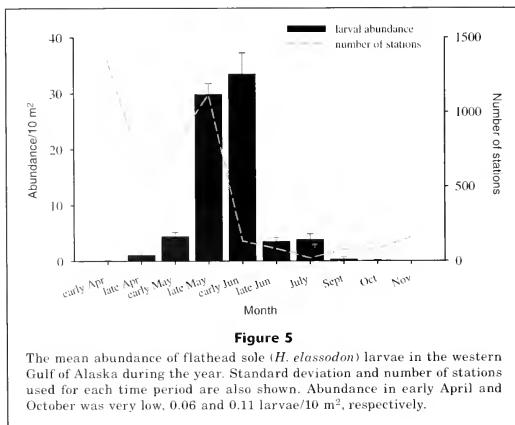
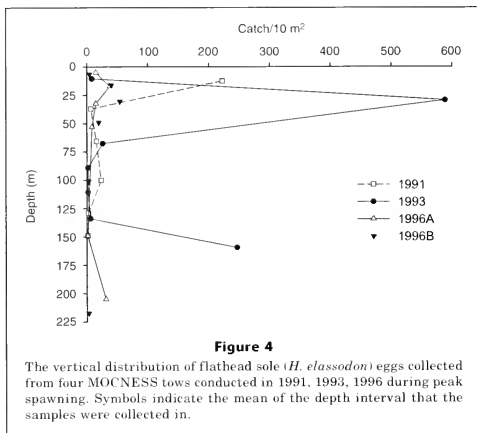
The geographic distribution of flathead sole (*H. elassodon*) eggs in the western Gulf of Alaska during the spawning season; (A) March, (B) early to mid-April, (C) early to mid-May, (D) early to mid-June.

Vertical distribution There were similar trends in the vertical distribution of larvae among tows (Fig. 9). Abundance peaked at about 15 to 30 m below the surface, then decreased, and larvae were collected from the deepest sampling depth interval from one tow (1996A; Fig. 9). Because the tows were alike, to increase sample size in the depth intervals, we pooled data from similar depth intervals but from different tows for further analyses. Larval abundance was highest near the surface and at the deepest depths sampled (Fig. 9). In Auke Bay, Alaska, flathead sole larvae migrated vertically at night no more than 15 m, ending at 20 m depth, and they were less aggregated (Halderson et al., 1993). This depth was much shallower than the depth at which larvae and late-stage eggs were collected in tow 1996A (sampling depth interval was 174–236 m). Therefore the deep concentration of larvae in 1996 was probably due to eggs hatching rather than to vertical

migration. The deepest sample comprised embryos and larvae (the larvae, however, were too damaged to determine whether they were prefeeding or feeding larvae), and samples collected above 100 m were a mixture of embryos and prefeeding larvae (29%), and feeding larvae (71%). The smallest larvae (<5 mm) were found in deepest water (mean depth 166 ± 32 m), and larger larvae (≥ 5 mm) were found in shallower water (above about 60 m depth; ANOVA, $P < 0.001$; Tukey HSD multiple comparison test, $P < 0.001$). The size distribution of the larvae indicated that soon after hatching they rise to the surface to feed.

Discussion

Flathead sole inhabit the continental shelf of the North Pacific Ocean, and the area used for the present study



contains the highest relative abundance of adult flathead sole off the west coast of North America (Wolotira et al.¹). Generally, outside the study area the abundance of adult flathead sole is low (Wolotira et al.¹); therefore these areas most likely had very little effect on the abundance of eggs and larvae collected from within the study area.

In the western Gulf of Alaska flathead sole spawn in three main areas during the spring: near the Kenai Peninsula, in Shelikof Strait, and in the area between the Shumagin Islands and Unimak Island. Spawning progresses in a southwesterly direction along the Alaska Peninsula. Flathead sole in spawning condition are abundant from March through May (Hirschberger and

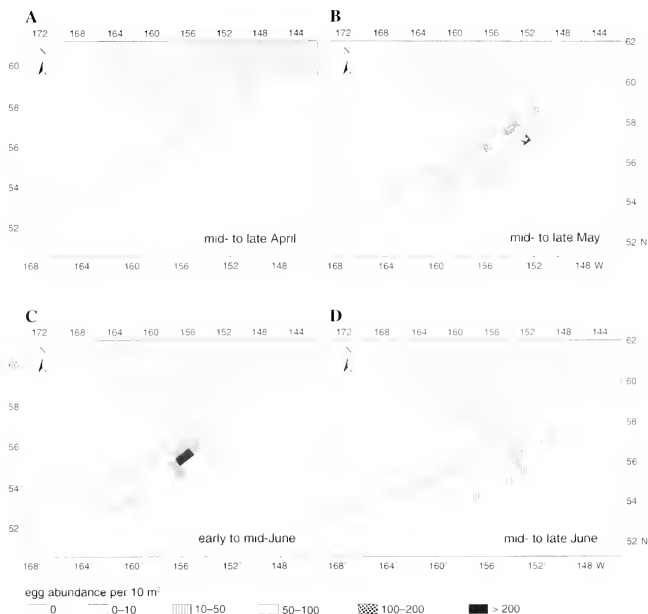


Figure 6

The geographic distribution of flathead sole (*H. elassodon*) larvae in the western Gulf of Alaska during months of the spawning season. (A) mid- to late April, (B) mid- to late May, (C) early to mid-June, (D) mid- to late June.

Smith²), which correlates with the period when eggs were collected in the present study. Peak spawning occurred from early to mid-May, and by the end of June spawning was nearing completion. Larval abundance peaked from early to mid-June in the southern portion of Shelikof Strait. In late July, late-stage flathead sole larvae were the most abundant of larval fish collected in the Gulf of Alaska between the Semidi Islands and Unimak Island (Brodeur et al., 1995). Flathead sole larvae have also been found on the east side of Kodiak Island during the summer (Kendall and Dunn, 1985).

Laboratory observations of the changes in density of flathead sole eggs during development are inconsistent. Results of one study showed that egg density decreased throughout development to hatching (Alderice and Forrester, 1974). Another study found that up to 24 hours before hatching the eggs floated at the surface of

a container and then sank to the bottom and hatched (Miller, 1969), indicating that density had increased late in development. A field study of the vertical distribution of Atlantic halibut (*Hippoglossus hippoglossus*) eggs in Norwegian fjords showed that later stage eggs had a higher density (and were found deeper) than earlier egg stages (Haug et al., 1986). Results from the present study support the findings of Miller (1969), in that the density of flathead sole eggs in the present study appeared to increase near the time of hatching. For the larvae of both the arrowtooth flounder (*Atheresthes stomas*) and Pacific halibut (*Hippoglossus stenolepis*), small larvae were found deep and larger sizes migrated towards the surface (Bailey and Picquelle, 2002). In the present study, flathead sole larvae had a similar vertical distribution pattern indicating that after hatching in deep water they rise to near the surface to feed.

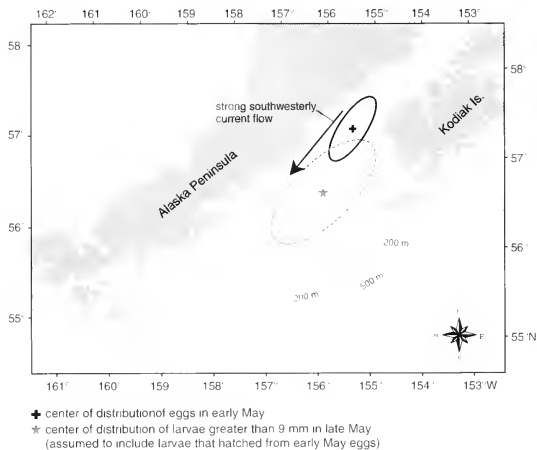


Figure 7

The drift of flathead sole (*H. classodon*) larvae in Shelikof Strait during May 1994. Surface current flow was strong and southwesterly.

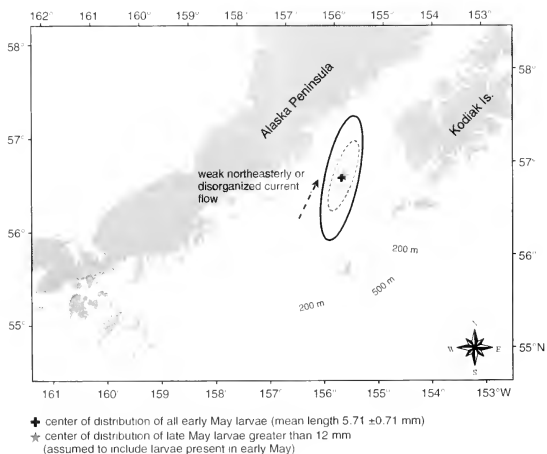


Figure 8

The drift of flathead sole (*H. classodon*) larvae in Shelikof Strait during May 1996. Surface current flow was disorganized, or weak, and to the northeast.

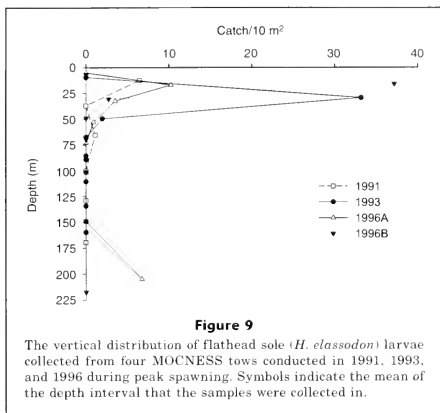


Figure 9

The vertical distribution of flathead sole (*H. elassodon*) larvae collected from four MOCNESS tows conducted in 1991, 1993, and 1996 during peak spawning. Symbols indicate the mean of the depth interval that the samples were collected in.

Some species of flatfish spawn offshore (e.g., arrowtooth flounder and Pacific halibut, Bailey and Picquello, 2002), but the present study has shown that flathead sole spawn on the continental shelf. Flathead sole nursery areas have been found to be in the bays of the Alaska Peninsula and Kodiak Island (Norcross et al., 1999), and it is crucial that the larvae remain on the shelf near their nursery areas. Changes in egg density may be a mechanism for retaining flathead sole larvae on the shelf. For arrowtooth flounder and Pacific halibut larvae in the western Gulf of Alaska, it has been suggested that deep water currents (100–400 m depth in sea valleys and in troughs in the continental shelf) transport these larvae from the offshore areas where they hatch to their nearshore nurseries (Bailey and Picquello, 2002). By sinking when they are nearing hatching, flathead sole eggs that have drifted southwestward (i.e. away from nursery areas) with the surface currents can be brought back (along with newly hatched larvae) toward inshore juvenile nursery areas. Alternatively, the act of sinking as they near hatching may be a way for newly hatched larvae to avoid predation by keeping them out of the surface waters where they are likely to encounter predators. The physical environmental conditions of Shelikof Strait may also serve to retain flathead sole larvae on the shelf. In May 1994 when the Alaska Coastal Current flow was strong and to the southwest, larvae drifted southward but remained on the continental shelf. In May 1996 when the flow was weak, disorganized, and moving somewhat to the northeast, the larvae remained at virtually the same location for the entire month because surface current flow in Shelikof Strait was weakened and reversed because of anomalous atmospheric con-

ditions. Under both flow regimes larvae remained on the continental shelf in southern Shelikof Strait. Eddies may also be an important retention mechanism for flathead sole larvae because entrainment in one of these could slow drift. Under typical conditions in Shelikof Strait (i.e., strong southwesterly current flow), eddies frequently occur and they drift slower than the water surrounding them (Kendall et al., 1996). They can also remain nearly stationary for two weeks (Schumacher et al., 1993). Both biological and environmental factors may work together to retain flathead sole larvae on the continental shelf and keep them near their nursery areas.

Acknowledgments

I would like to thank Debbie Blood and Angie Lind for determining developmental stages of flathead sole eggs, and Susan Picquello for assistance with egg and larval distribution charts. Kevin Bailey and Jeff Napp provided helpful comments on an early draft of this manuscript. Two anonymous reviewers offered improvements. This research is contribution FOCI-0475 to NOAA's Fisheries-Oceanography Coordinated Investigations.

Literature cited

- Alderdice, D. F., and C. R. Forrester.
1974. Early development and distribution of the flathead sole (*Hippoglossoides elassodon*). J. Fish. Res. Board Can. 31:1899–1918.

- Bailey, K. M., N. A. Bond, and P. J. Stabeno.
1999. Anomalous transport of walleye pollock larvae linked to ocean and atmospheric patterns in May 1996. *Fish. Oceanogr.* 8:264-273.
- Bailey, K. M., and S. J. Picquelle.
2002. Larval distribution of offshore spawning flatfish in the Gulf of Alaska: potential transport pathways and enhanced onshore transport during ENSO events. *Mar. Ecol. Prog. Ser.* 236:205-217.
- Bailey, K. M., P. J. Stabeno, and D. A. Powers.
1997. The role of larval retention and transport features in mortality and potential gene flow of walleye pollock. *J. Fish Biol.* 51 (suppl. A):135-154.
- Blood, D. M., A. C. Matarese, and M. M. Yoklavich.
1994. Embryonic development of walleye pollock, *Theragra chalcogramma*, from Shelikof Strait, Gulf of Alaska. *Fish. Bull.* 92:207-222.
- Brodeur, R. D., M. S. Busby, and M. T. Wilson.
1995. Summer distribution of early life stages of walleye pollock, *Theragra chalcogramma*, and associated species in the western Gulf of Alaska. *Fish. Bull.* 93:603-618.
- Haldorson, L., A. J. Paul, D. Serritt, and J. Watts.
1989. Annual and seasonal variation in growth of larval walleye pollock and flathead sole in a southeastern Alaska bay. *Rapp. P.-V. Reun. Cons. Int. Explor. Mer* 191:220-225.
- Haldorson, L., M. Prichett, A. J. Paul, and D. Ziemann.
1993. Vertical distribution and migration of fish larvae in a northeastern Pacific bay. *Mar. Ecol. Prog. Ser.* 101:67-80.
- Haug, T., E. Kjorsvik, and P. Solemdal.
1986. Influence of some physical and biological factors on the density and vertical distribution of Atlantic halibut *Hippoglossus hippoglossus* eggs. *Mar. Ecol. Prog. Ser.* 33:207-216.
- Kendall, A. W., Jr., and J. R. Dunn.
1985. Ichthyoplankton of the continental shelf near Kodiak Island Alaska. NOAA Tech. Rep. NMFS 20, 89 p.
- Kendall, A. W., Jr., and S. J. Picquelle.
1989. Egg and larval distributions of walleye pollock *Theragra chalcogramma* in Shelikof Strait, Gulf of Alaska. *Fish. Bull.* 88:133-154.
- Kendall, A. W., Jr., J. D. Schumacher, and S. Kim.
1996. Walleye pollock recruitment in Shelikof Strait: applied fisheries oceanography. *Fish. Oceanogr.* 5 (suppl. 1):4-18.
- Matarese, A. C., A. W. Kendall Jr., D. M. Blood, and B. M. Vinter.
1989. Laboratory guide to early life history stages of northeast Pacific fishes. NOAA Tech. Rep. NMFS 80, 652 p.
- Miller, B. S.
1969. Life history observations on normal and tumor-bearing flathead sole in East Sound, Orcas Island (Washington). Ph.D. diss., 131 p. Univ. Washington, Seattle, WA.
- Norcross, B. L., A. Blanchard, and B. A. Holladay.
1999. Comparison of models for defining nearshore flatfish nursery areas in Alaskan waters. *Fish. Oceanogr.* 8:50-67.
- Rose, C. S.
1982. A study of the distribution and growth of flathead sole (*Hippoglossoides classodon*). M.S. thesis, 59 p. Univ. Washington, Seattle, WA.
- Schumacher, J. D., P. J. Stabeno, and S. J. Bograd.
1993. Characteristics of an eddy over a continental shelf: Shelikof Strait, Alaska. *J. Geophys. Res.* 98: 8395-8404.
- Theilacker, G. H., and S. M. Porter.
1995. Condition of larval walleye pollock, *Theragra chalcogramma*, in the western Gulf of Alaska assessed with histological and shrinkage indices. *Fish. Bull.* 93:333-344.
- Watts, J. D.
1988. Diet and growth of first-year flathead sole (*Hippoglossoides classodon*) in Auke Bay, Alaska. M.S. thesis, 80 p. Univ. Alaska, Juneau, AK.

Abstract—With a focus on white marlin (*Tetrapturus albidus*), a concurrent electronic tagging and larval sampling effort was conducted in the vicinity of Mona Passage (off southeast Hispaniola), Dominican Republic, during April and May 2003. Objectives were 1) to characterize the horizontal and vertical movement of adults captured from the area by using pop-up satellite archival tags (PSATs); and 2) by means of larval sampling, to investigate whether fish were reproducing. Trolling from a sportfishing vessel yielded eight adult white marlin and one blue marlin (*Makaira nigricans*); PSAT tags were deployed on all but one of these individuals. The exception was a female white marlin that was unsuitable for tagging because of injury; the reproductive state of its ovaries was examined histologically. Seven of the PSATs reported data summaries for water depth, temperature, and light levels measured every minute for periods ranging from 28 to 40 days. Displacement of marlin from the location of release to the point of tag pop-up ranged from 31.6 to 267.7 nautical miles (nm) and a mean displacement was 3.4 nm per day for white marlin. White and blue marlin mean daily displacements appeared constrained compared to the results of other marlin PSAT tagging studies. White marlin ovarian sections contained postovulatory follicles and final maturation-stage oocytes, which indicated recent and imminent spawning. Neuston tows ($n=23$) yielded 18 istiophorid larvae: eight were white marlin, four were blue marlin, and six could not be identified to species. We speculate that the constrained movement patterns of adults may be linked to reproductive activity for both marlin species, and, if true, these movement patterns may have several implications for management. Protection of the potentially important white marlin spawning ground near Mona Passage seems warranted, at least until further studies can be conducted on the temporal and spatial extent of reproduction and associated adult movement.

Movements and spawning of white marlin (*Tetrapturus albidus*) and blue marlin (*Makaira nigricans*) off Punta Cana, Dominican Republic

Eric D. Prince¹

Robert K. Cowen²

Eric S. Orbesen¹

Stacy A. Luthy²

Joel K. Llopiz²

David E. Richardson²

Joseph E. Serafy¹

¹ Southwest Fisheries Science Center
National Marine Fisheries Service
75 Virginia Beach Drive
Miami, Florida 33149
E-mail address (for E. D. Prince): eric.prince@noaa.gov

² Rosenstiel School of Marine and Atmospheric Science
Division of Marine Biology and Fisheries
University of Miami
4600 Rickenbacker Causeway
Miami, Florida 33149

White marlin (*Tetrapturus albidus*) and blue marlin (*Makaira nigricans*) are widely distributed throughout the tropical and temperate waters of the Atlantic Ocean and adjacent seas; the former species is endemic only to the Atlantic Ocean (Mather et al., 1975). Genetic analyses and tag recapture data have indicated that each species has a single Atlantic-wide population (ICCAT, 1998). Several stock assessment indicators indicate that the white marlin population has been severely overfished for several decades (ICCAT, 2001, 2002). The Atlantic blue marlin stock is also heavily over-exploited, but to a lesser degree. The main source of adult mortality for both stocks is the multinational offshore longline fisheries that, in the process of targeting tunas (Scombridae) and swordfish (*Xiphias gladius*), land the marlins as bycatch (ICCAT, 2002, 2003).

Despite their economic and ecological value, little is known about the biology and ecology of Atlantic marlins (Prince and Brown, 1991). This is especially true regarding the repro-

ductive biology of white marlin and adult movement patterns in spawning areas (Baglin, 1979; Mather, 1975; White Marlin Status Review Team¹; SEFSC²). Long-term (i.e., >40 years) commercial (Goodyear, 2003) and recreational (i.e., Cabeza de Toro Billfish Tournament, Graves and McDowell, 1995; Casilla³) fishing records indicate that, every spring, white marlin are present in relatively high numbers off the southeastern coast of Hispaniola. This observation, coupled with

¹ White Marlin Status Review Team. 2002. Atlantic White Marlin Status Review Document, 49 p. Report to National Marine Fisheries Service, Southeast Regional Office, 263 13th Avenue, St. Petersburg, FL 33701-5511.

² SEFSC (Southeast Fisheries Science Center). 2004. Atlantic Billfish Research Plan. National Marine Fisheries Service, Southeast Fisheries Science Center, 75 Virginia Beach Drive, Miami, FL 33149-1003.

³ Casilla, W. 2003. Personal commun. Club Nautico de Santo Domingo, Calle Juan Baron Fajardo #2, Ensanche Iantini, Santo Domingo, Dominican Republic.

anecdotal information about gravid fish, prompted the present examination of adult movements in a potentially important, but as yet unconfirmed, spawning location.

The present study was conducted off Punta Cana, Dominican Republic, during April and May 2003. Objectives were 1) to characterize the horizontal and vertical movement of adult white marlin captured from the area using pop-up satellite archival tags (PSATs) and 2) to investigate by larval sampling, whether marlin were reproducing at this location.

Materials and methods

Deployment of PSAT tags on adult marlin was conducted from a 17-m charter fishing vessel by using standard trolling gear (9/0 long-shaft J hooks) and dead bait. Wildlife Computers Inc. (Redmond, WA) PAT 3 model tags were used. This tag allows the user to program pop-up date, sampling interval, criteria for premature release, bin demarcations for sampling temperature and pressure (depth), as well as transmission and memory priorities. These tags were programmed to sample depth (pressure), temperature, and light once every minute and the depth and temperature records were summarized into histograms at 3-hour intervals. A pressure-activated mechanical detachment device was also used which severs the monofilament tether at a depth of about 1500 m—well before the 2000 m depth at which the tag is crushed and disabled. This feature helps prevent data loss in the event of fish mortality.

All PSAT tags were rigged similarly according to methods described by Graves et al. (2002). Billfish handling and tagging procedures and associated devices reviewed by Prince et al. (2002a) were also used. The target area for tag placement was about 4 to 5 cm ventral to the dorsal midline, adjacent to the first several dorsal spines. An effort was made to insert the anchor through the dorsal midline, pterygiophores, and connective tissue to a depth just short of the anchor exiting the opposite side of the fish. In addition, a conventional streamer tag (series PS) was placed in the fish well posterior to the PSAT tag, according to standard procedures (Prince et al., 2002a).

Two devices were used during tagging which tend to reduce stress in captured fish and to aid in proper tag placement. The first was a "snooter" (a wire snare housed in a 1.5-m PVC tube), which secures to the upper bill and allows the tagger to maintain control of the fish while its head remains beneath the water during the tagging procedure (Prince et al., 2002a). The second was a small hook "gaff" (a long shaft 9/0 hook with point and barb removed) to manipulate the position of the fish in relation to the tagging vessel. Captured fish were resuscitated for 3 to 15 minutes, depending on their apparent state of exhaustion, by moving the vessel ahead at two to three knots while maintaining control of the fish with the snooter. State of exhaustion was inferred from coloration, fight time, and signs of sluggish movement.

One white marlin died during tagging and was retained for examination of its reproductive status. Whole or quarter transverse sections of ovarian tissue were preserved in 10% formalin. Preparation for histological analysis followed McBride et al. (2002). Histological determination of spawning activity was based on oocyte classification and the presence of postovulatory follicles (Wallace and Selman, 1981; Hunter and Macewicz, 1985; Hunter et al., 1992).

Once adult marlins were located for tagging, neuston sampling was conducted from the same fishing vessel with methods similar to those reported by Serafy et al. (2003). In the present study, ten-minute daytime tows were performed with two neuston nets. Both nets had 1000- μ m mesh and were attached to 1 m \times 0.5 m or 2 m \times 1 m rectangular aluminum frames. Water volume filtered was measured with a mechanical flow meter; station coordinates and water column depth measurements were obtained by using a hand-held geographical positioning system and depth sounder. Neuston collections were made along a series of transects that covered the general area of the recreational fishery for white marlin at this location (Fig. 1). The neuston samples were initially stored in 150 proof white rum. Upon returning to the laboratory (i.e., within 24–96 hours) they were transferred to 95% ethanol. Billfish larvae were sorted from the samples and measured by using Image Pro image analysis software (Image Pro Plus, version 4.5, Media Cybernetics, Inc. Silver Spring, MD). Larval identification was conducted by using restriction fragment length polymorphism analysis of the nuclear MN32-2 locus following the methods of McDowell and Graves (2002).

Results

Seven white marlin and one blue marlin were tagged with PSAT tags off Punta Cana, Dominican Republic, between April 23–24 and May 14–17 2003 (Table 1). All but two tags were programmed to pop-up after 30 days; the exceptions were 40-day deployments for one white marlin and one blue marlin. One of eight PSATs (deployed on a white marlin) failed to transmit data and one white marlin died prior to release (see below) from hook-related injuries. The displacements of the six white marlin from the original point of release ranged from 31.7 to 267.7 nmi (58.7 to 495.8 km), whereas the displacement for the blue marlin was 219.3 nmi (406.2 km, Table 1, Fig. 2). Displacements per day for white marlin ranged from 1.1 to 7.2 nmi (average of 3.4 nmi). Corresponding daily displacement for the one blue marlin was 5.48 nmi (Table 1).

The minimum and maximum depth and temperatures monitored for the seven PSAT-tagged marlin during the 30- and 40-day deployments showed that on most days, marlin visited depths \geq 100 m (Fig. 3). Minimum temperatures ranged from 16.8° to 20.6°C, whereas the maximum temperatures ranged from 28.2° to 30.0°C. In all cases, the minimum depths for each fish monitored

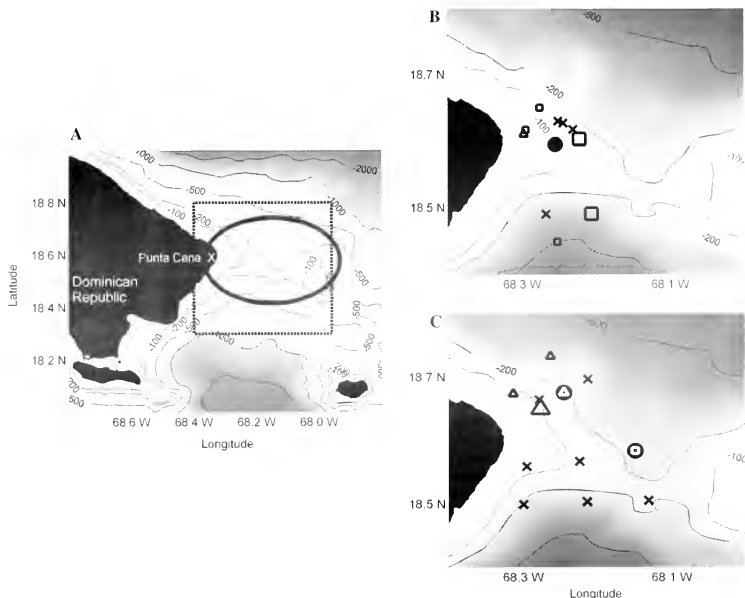


Figure 1

(A) Western part of Mona Passage off Punta Cana, Dominican Republic, showing the general area of the recreational fishery for white marlin (*Tetrapturus albidus*, rectangle) and larval sampling (oval); (B) April 23–24 sampling stations and (C) May 13–17 sampling stations. \times = stations with no billfish larvae. \square = stations with white marlin larvae, Δ = stations with blue marlin (*Makaira nigricans*) larvae. \bullet = stations with unidentified larval istiophorids. Larger markers indicate two billfish in sample; smaller markers indicate one billfish in sample. Depth contours are in meters.

during April and May were recorded at the surface, whereas maximum depths ranged from 184 to 368 m (Fig. 3). In one case (i.e., PC-WHM01), the minimum and maximum temperatures and depths converged at the surface, indicating constrained vertical movement for this individual. However, in the majority of tracks there was a clear separation of minimum and maximum temperature and depth (e.g., PC-WHM02, Table 1), indicating that active vertical movements were made each day. Only one of the transmitting tags appeared to pop-up prematurely (PC-WHM01, Fig. 3). This tag disengaged from its white marlin host during a deep dive (368 m) after 28 days at large (two days early). Although the fate of this fish cannot be determined, death is a distinct possibility. In general, all marlin spent a high proportion of the time in which they were monitored in the upper 25 m and at temperatures $\geq 28^{\circ}\text{C}$. For

example, marlin spent from 50% to 60% of the time in the first depth bin (0 to 25 m) and about 60% to 75% of their time in the 28° to 30°C temperature bin (Fig. 4). Both marlin species made dives down to 100–200 m or more on a fairly consistent basis but generally stayed at these depths less than 10% of the time (Fig. 4).

One female adult white marlin, measuring 157 cm lower jaw fork length, could not be resuscitated during pop-up satellite tagging, presumably because of damage caused by a hook that penetrated the stomach. Based on length-weight conversion equations (Prager et al., 1995), the estimated weight of this fish was 21.6 kg (47.2 pounds). The histologically examined ovaries contained distinct postovulatory follicles, indicating that spawning likely occurred within the previous 24 hours (Fig. 5, upper panel). In addition, imminent spawning (likely within the following 12 hours) was indicated by

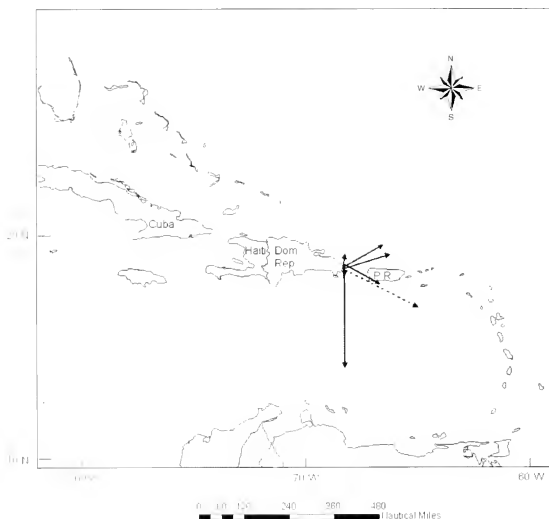


Figure 2

Displacement vectors (from point of tag release to point of tag pop-up in nautical miles, nmi) for six white marlin (*Tetrapturus albidus*) (solid lines, 31.7–268 nmi) and one blue marlin (*Makaira nigricans*) (dashed line, 219 nmi) released off Punta Cana, Dominican Republic, bearing pop-up satellite archival tags during April and May 2003. Tags were programmed for either 30- or 40-day deployments.

Table 1

Summary of pop-up satellite archival tag information for seven white marlin (*Tetrapturus albidus*, WHM) and one blue marlin (*Makaira nigricans*, BUM) released from recreational gear in the vicinity of Punta Cana, Dominican Republic, April and May 2003. Net displacements are given in nautical miles (nmi) and kilometers (km). Compass direction (in degrees) indicates the bearing from point of tag release to point of first transmission. Dashed line indicates that no value was available.

Tag number	Days monitored	Estimated weight (kg)	Location of release	Location of first transmission	Compass direction	Net displacement nmi (km)	Displacement per day nmi (km)
PC-WHM-01	28	40 (18.14)	18.49 N, 68.38 W	19.17 N, 68.26 W	9.52°	41.21 (76.32)	1.47 (2.72)
PC-WHM-02	31	40 (18.14)	18.60 N, 68.27 W	19.56 N, 66.58 W	58.87°	111.87 (207.18)	3.61 (6.69)
PC-WHM-03	31	50 (22.68)	18.49 N, 68.37 W	19.14 N, 66.25 W	71.81°	126.76 (234.76)	4.09 (7.57)
PC-WHM-04	30	35 (15.88)	18.69 N, 68.27 W	18.16 N, 68.28 W	181.03°	31.68 (58.67)	1.06 (1.96)
PC-WHM-05	30	50 (22.68)	18.70 N, 68.29 W	17.81 N, 66.70 W	120.11°	105.22 (194.87)	2.84 (5.26)
PC-WHM-06	0	50 (22.68)	18.29 N, 68.13 W	—	—	—	—
PC-WHM-07	37	60 (27.22)	18.60 N, 68.30 W	14.12 N, 68.38° W	181.00°	267.73 (495.84)	7.24 (13.41)
PC-BUM-01	40	130 (58.97)	18.49 N, 68.38° W	16.75 N, 65.01° W	117.78°	219.32 (406.18)	5.48 (10.51)

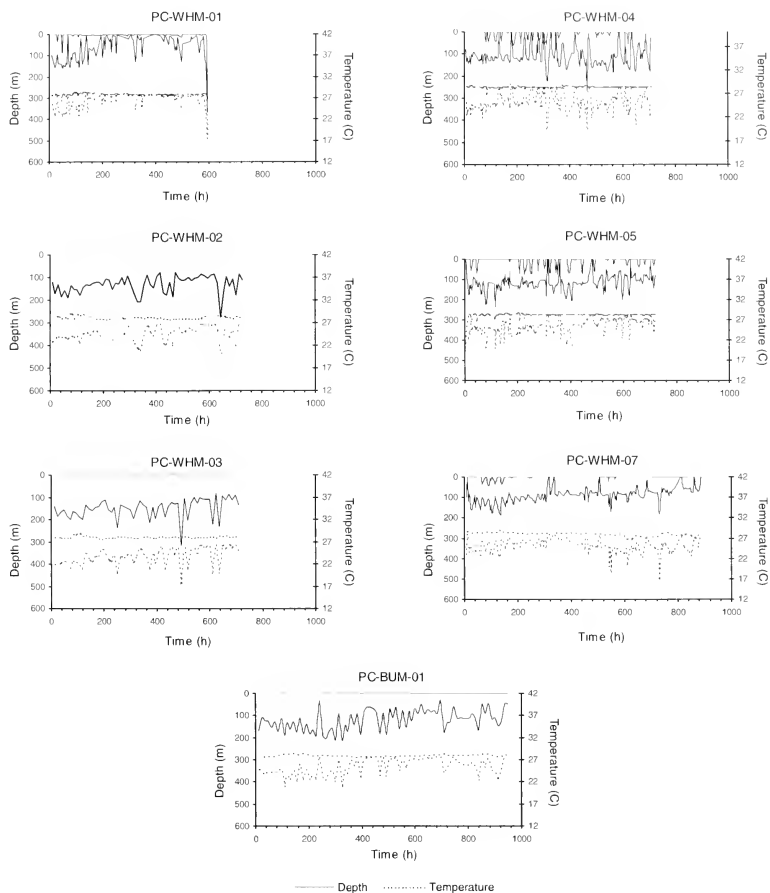
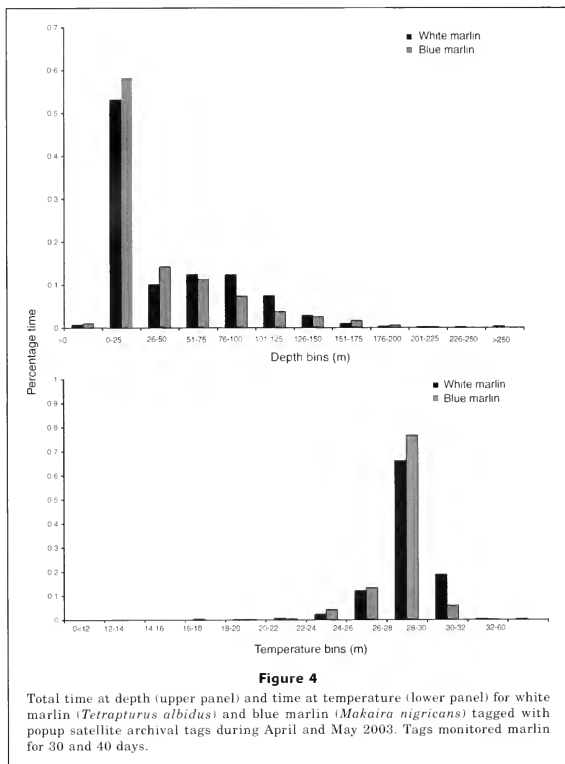


Figure 3

Minimum and maximum depth and temperature per 3-hour time intervals for six white marlin (*Tetrapturus albidus*) and one blue marlin (*Makaira nigricans*) monitored with pop-up satellite archival tags. Tags were programmed to deploy for either 30 or 40 days, April and May 2003, in the vicinity of Punta Cana, Dominican Republic. WHM=white marlin, BUM=blue marlin.



some oocytes exhibiting an early state of final oocyte maturation, including migration of the nucleus towards the oocyte periphery and yolk coalescence (Fig. 5, lower panel).

A total of 23 neuston net tows were made in the general area of the recreational fishery from 23 April to 17 May 2003 (Fig. 1). These tows yielded 18 larval billfishes. Molecular identification was successful for 12 larvae: 8 white marlin and 4 blue marlin (Table 2). Half of the white marlin larvae were 3–4 mm standard length (SL), two were 4–5 mm SL, one was 6.2 mm SL, and one was 12.1 mm SL (Fig. 6). The one positively identified blue marlin larva captured in April was 4.6 mm SL; the remainder taken in May were 3.5 mm SL,

5.1 mm SL, and 10.4 mm SL. Sizes of the six unidentified billfish larvae ranged from 3 to 6 mm SL (Fig. 6).

Discussion

Larval sampling with neuston tows and histological analyses of adult ovaries confirmed spawning activity of white marlin in the vicinity of Punta Cana during April and May (2003). Co-occurrence of larval blue marlin and white marlin in samples indicated that the two species share this spawning location. White and blue marlin spawning activity in the vicinity of Punta Cana, as indicated from the data presented in our study,

also coincided in time and space with the fishing activity of the recreational white marlin fishery that has operated each spring at this location for over 40 years. From PSAT tag data, adult white and blue marlin caught at this time and in this area appeared to exhibit similar vertical and horizontal movement patterns in terms of time at depth, time at temperature, average horizontal displacement per day, net horizontal displacement, and direction of dispersion (compass heading).

Movements

Average displacement per day is one possible measure to characterize daily horizontal movement activity. We examined this metric in other PSAT studies on marlin and compared them with our results (Fig. 7). Graves et al. (2002) monitored eight blue marlin with PSAT tags caught off Bermuda in July 2000 for periods of 5 days each and reported net displacement vectors ranging from 7.8 to 26.4 nmi/day (mean displacement for the eight fish was 17.5 nmi/day). Kerstetter et al. (2003) also monitored blue marlin during the summer months with PSAT tags in the northwest Atlantic (for 5 and 30 days) and found that displacements ranged from 15.1 to 39.2 nmi/day (mean for six fish was 22.9 nmi/day). Net displacement findings (17.5 and 22.9 nmi/day), presumably for blue marlin spawning times (summer months) from these two studies were roughly 5 to 6.5-fold higher than the average displacements for white marlin reported in our present study (about 3.3 nmi/day) and were 3 to 4-fold higher than the average displacement for the one blue marlin monitored in our study (Fig. 7). A recent report (Graves and Horodysky⁴) has provided displacement movements of white marlin monitored with PSAT tags for 5 to 10 day periods from three different areas in the Northwest Atlantic during May (Punta Cana, Dominican Republic), August–September (U.S. Mid-Atlantic waters), and November (La Guaira, Venezuela) 2002. Only the work in Punta Cana was conducted during the presumed spawning season for white marlin. Average displacements for these areas were 9.6

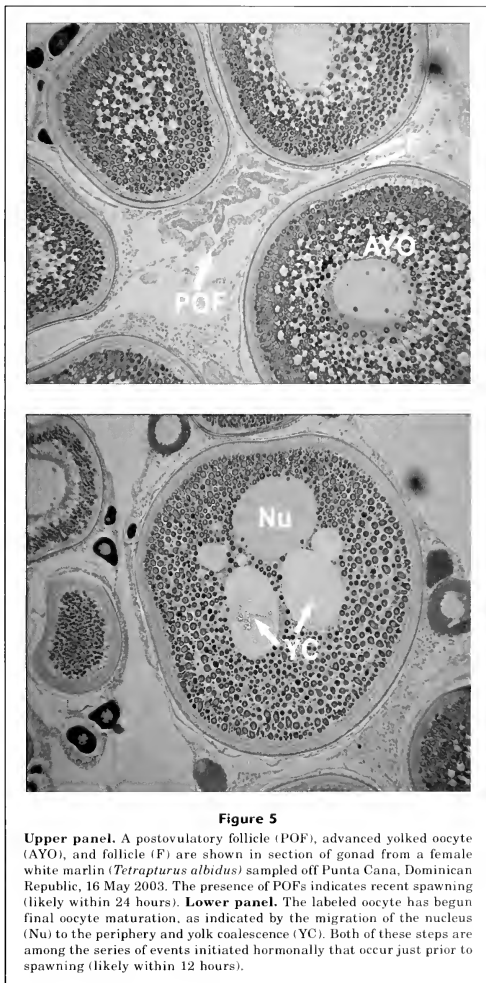


Figure 5

Upper panel. A postovulatory follicle (POF), advanced yolked oocyte (AYO), and follicle (F) are shown in section of gonad from a female white marlin (*Tetrapturus albidus*) sampled off Punta Cana, Dominican Republic, 16 May 2003. The presence of POFs indicates recent spawning (likely within 24 hours). **Lower panel.** The labeled oocyte has begun final oocyte maturation, as indicated by the migration of the nucleus (Nu) to the periphery and yolk coalescence (YC). Both of these steps are among the series of events initiated hormonally that occur just prior to spawning (likely within 12 hours).

⁴ Graves, G. E., and A. Z. Horodysky. 2002. Progress report. Use of pop-up satellite archival tags to study survival and habitat utilization of white marlin released from

the recreational fishery, 34 p. Virginia Institute of Marine Science, College of William and Mary, Gloucester Point, VA 23062-1346.

Table 2

Summary of neuston tow information for larval collections of istiophorids in the vicinity of Punta Cana, Dominican Republic, April and May 2003. "Unidentified istiophorids" refers to specimens for which molecular identification was unsuccessful.

2003 dates	Number of tows	Volume filtered (m ³)	Number of positive tows	Number (length range) of white marlin	Number (length range) of blue marlin	Number (length range) of unidentified istiophorids
23–24 April	11	9400	7	7 (3.45–12.16 mm)	1 (4.6 mm)	2 (3.98–5.28 mm)
13–17 May	12	8413	5	1 (6.20 mm)	3 (3.49–10.45 mm)	4 (3.25–4.4 mm)
Total	23	17,813	12	8	4	6

nmi/day for Punta Cana; 9.4 nmi/day for the U.S. Mid-Atlantic region; and 8.2 nmi/day for La Guaira Bank (Fig. 7). Thus, the average white marlin displacements found by Graves and Horodysky were 2 to 3-fold higher than those reported in the present study. Black marlin (*Makaira indica*, Gunn et al., 2003) and striped marlin (*Tetrapturus audax*, Domeier et al., 2003) monitored mostly outside of spawning times and areas had displacements per day 2 to 4-fold higher than those in the present study. Therefore, reproductively active white marlin and blue marlin monitored in our study (30- or 40-day deployments) appeared to have more constrained average displacements per day than those in other studies where similar PSAT technology was used to monitor marlin in and outside of their respective spawning seasons.

Further PSAT-based research, with extended monitoring durations (i.e. at least ≥3–4 months) on white marlin and other billfish species in their spawning areas, will be necessary to clarify the causative factors for these findings. Interpretation of our findings also needs to be tempered by the fact that the displacement vectors (minimum straight line distances) used to characterize movements in this study were limited to beginning and end points. In theory, daily estimates of light-based geolocation would provide improved resolution of small-scale movement patterns. However, there is little scientific agreement (Musyl et al., 2001; Hill and Braun, 2001) as to the methods and validity of daily tracks generated from highly variable light levels, particularly for wide ranging species near the equator.

Although we present no evidence that the horizontal movement patterns of blue marlin (other than possibly constrained displacements) reported in our study are directly related to spawning activity, the possibility that white marlin could show fidelity to a spawning area cannot be ruled out. For example, Pepperell (1990) examined conventional tagging results off eastern Australia and reported that the periodic peaks in return frequency were possibly indicative of black marlin returning to the spawning ground as part of their annual migration cycle. The multidirectional pattern of blue and white marlin displacements found in the

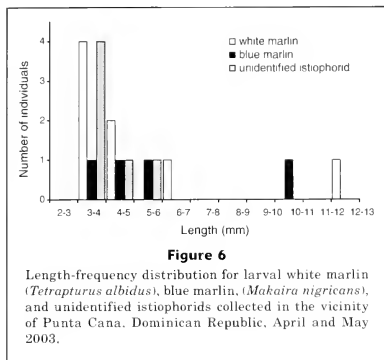
present study was very similar to the pattern reported by Graves et al. (2002) for blue marlin monitored with PSAT tags for five days off Bermuda. The relatively short-term duration of PSAT tags in both studies (5–40 days) generally precludes detection of directed seasonal horizontal movement patterns (including potential annual fidelity to a spawning area) as described by Mather et al. (1975), Pepperell (1990), and Ortiz et al. (2003).

Detailed accounts of temperature and depth preferences of electronically monitored white marlin have been rare and those that do exist are limited to very short (≤ten days) monitoring durations (Block et al., 1990; Horodysky et al., 2003; Graves and Horodysky⁴). We found that white marlin monitored with PSATs for periods of 28–40 days spent the majority of time in the upper 25 m of the water column at temperatures of 28–30°C. Similar findings were found for this species by Graves and Horodysky⁴ and Horodysky et al. (2003), as well as for blue marlin, black marlin, and striped marlin reported by Graves et al. (2002); Kerstetter et al. (2003); Gunn et al. (2003); and Domeier et al. (2003). However, we could not directly address the depth at which spawning occurs in our study from PSAT results, other than to note the preference of adults for, and capture of larvae in, surface waters. Empirical data on the depth of spawning for istiophorids are not available, although anecdotal evidence indicates that some species may spawn in surface waters (black marlin observations by Harvey, personal commun.⁵).

Spawning

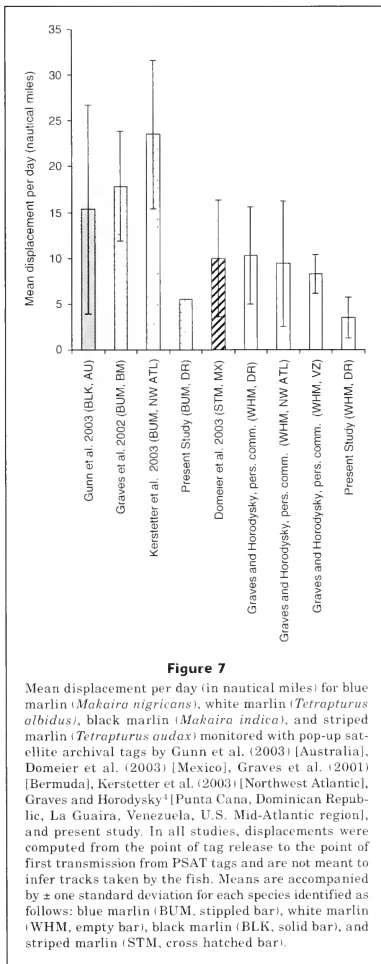
Prior studies of gonads have indicated that white marlin spawn in the northwest Atlantic during the spring (Baglin, 1977, 1979; de Silva and Breder, 1997). Spring aggregations of white marlin have been the target of the Cabeza de Toro billfish tournament off Punta Cana for over 40 years (Casilla³), and the sampling of larvae in

⁵ Harvey, G. C. McN. 2004. Personal commun. 102 Webster Drive, P.O. Box 10499 APO, Grand Cayman Island, Cayman Islands, British West Indies.



the present study is the first to provide direct evidence of springtime spawning activity in this area. Histological assessment of the captured female ovarian tissue is consistent with the premise that the adult white marlins in the aggregation that we located during fishing and PSAT tagging operations participated in spawning activity. This contention is strengthened by the presence of very small, presumably very young, white (and blue) marlin larvae in the same location.

The presence of larvae is the most direct way of documenting that a spawning event has actually occurred. This is particularly relevant to highly mobile species, such as billfishes, that can cover large distances in a short time (Prince and Brown, 1991). Serafy et al. (2003) used a similar approach to identify blue marlin spawning grounds in the area of Exuma Sound, Bahamas. In their neuston collections, 90 blue marlin, no white marlin, and three sailfish larvae were captured. Because Serafy et al., (2003) sampled during the entire month of July, it seems possible that larval sampling in Exuma Sound took place after the majority of white marlin spawning had already occurred. Subsequent neuston sampling of Bahamian waters yielded white marlin larvae in Exuma Sound in April and in the Old Bahama Channel and just east of Long Island in March, but no blue marlin during these months (D. E. Richardson and S. A. Luthy, unpubl. data). Extensive sampling of the Straits of Florida (SOF) over four years resulted in sporadic captures of white marlin larvae in May and June. Blue marlin was the more common larval marlin in the SOF and was captured from June to September (S. A. Luthy, unpubl. data). In the present study, white marlin larvae were twice as abundant in larval samples as blue marlin larvae (which had been captured earlier in Punta Cana) than in other areas where blue marlin larvae had been found. These results are consistent with reports that white marlin is primarily a spring-time spawner but



mark an expansion of the July to October spawning season reported for blue marlin in the North Atlantic by Erdman (1968) and de Sylva and Breder (1997).

For blue marlin larvae <6.2 mm SL, Serafy et al. (2003) found problems with estimating age from size with the larval growth equations reported by Prince et al. (1991). Serafy et al. (2003) suggested an exponential growth curve with an assumed size-at-hatching of 2.5 mm SL yielded more realistic larval age values for this growth stanza (<6.2 mm SL). Application of the Serafy et al. (2003) growth model to the larval blue marlin collected in the present study indicates that larvae 3 mm SL were 2 days old, 4-mm-SL larvae were 5 days old, and 5-mm-SL larvae were over 7 days old. It seems possible that blue and white marlin have similar size-at-hatching and growth rates at this early stage of development. Given this assumption, the fact that half of the white marlin larvae (4 out of 9) and a third of the blue marlin larvae sampled in this study were 3–4 mm long (i.e., only a few days old) indicates that spawning activity was taking place in the same general area where these larvae were captured and where the recreational fishery for these species was being pursued. This statement may not hold true for the larval marlin in our collections over 4 mm SL because increases in size and age add increased uncertainties concerning possible spawning locations. Providing a more precise estimate of spawning location was beyond the scope of our study, although we would expect that the upstream spawning locations (assuming minimal mobility of larvae) of both marlin species to be a function of the prevailing currents and oceanographic features in the Punta Cana area and the elapsed time between the spawning event and sample collection. Future research should focus on a more rigorous and comprehensive estimate of spawning location for all sizes and ages of larvae. This would require both a significant increase in the spatial and temporal larval sampling scheme, as well as direct aging methods for both species and sizes of marlin larvae collected.

Implications for management and future research

The current stock status of Atlantic white marlin indicates that biomass is only at about 12% of the level necessary to maintain maximum sustainable yield (MSY) and continues to decline (ICCAT, 2002). The stock has been estimated to be incurring fishing mortality at a rate about eight times higher than the population can sustain to produce MSY (ICCAT, 2002). Although the Atlantic blue marlin stock is also considered to be overexploited, its status is not as precarious as that of white marlin (ICCAT, 2001). The characterization of adult movements and larval distribution in a potentially important spawning area is seen as a necessary "first step" toward improved management and rebuilding of depressed Atlantic billfish stocks, possibly with gear restrictions (e.g., use of circle hooks, Prince et al., 2002b; Horodysky and Graves, 2005). Improved management seems particularly relevant in the area of Punta Cana because the target of the 40-year-old Cabeza de Toro tournament is, and probably always has been, a repro-

ductively active aggregation of white marlin. In light of the ICCAT recommendation to reduce mortality on the overexploited marlins from all Atlantic fisheries (ICCAT, 2002), a shift to catch-and-release requirements for the white marlin recreational fishery off Punta Cana, and the use of circle hooks during the spring months, may be suitable options. In terms of spawning, there is an obvious need for more detailed spatiotemporal information on the distribution of marlin reproduction and on the identification of nursery areas to help managers make informed decisions regarding conservation of the resource. In addition, more fine-scale data on adult movement patterns in relation to horizontal and vertical use of the water column, including identification of spawning depth, are necessary.

Acknowledgments

This work was made possible through Cooperative Research and Recover Protected Species Candidate Plus Program funds of the National Marine Fisheries Service and additional support from The Billfish Foundation and the University of Miami, Center for Sustainable Fisheries, Billfish Research Initiative. We thank Noretta Perry at the Florida Fish and Wildlife Commission's Fish and Wildlife Research Institute for histological slide preparations.

Literature cited

- Baglin, R. E., Jr.
1977. Maturity, fecundity and sex composition of white marlin (*Tetrapturus albidus*). Int. Comm. Cons. Atlantic Tunas, Madrid, Spain. Coll. Vol. Sci. Pap. 6:408–416.
1979. Sex composition, length-weight relationship, and reproduction of the white marlin, *Tetrapturus albidus*, in the western North Atlantic Ocean. Fish. Bull. 76:919–926.
- Block, B. A.
1990. Physiology and ecology of brain and eye heaters in billfishes. Planning the future of billfishes. In Proceedings of the international billfish symposium II; 1–5 August 1988, Kona, Hawaii, Part 2: Contributed papers (R. H. Stroud ed.), p. 123–136. National Coalition for Marine Conservation, Savannah, GA.
- de Sylva, D. P., and P. R. Breder.
1997. Reproduction, gonad histology, and spawning cycles of north Atlantic billfishes (Istiophoridae). Bull. Mar. Sci. 60:668–697.
- Domeier, M. L., H. Dewar, and N. Nasby-Lucas.
2003. Mortality of striped marlin (*Tetrapturus audax*) caught on recreational tackle. Mar. Fresh. Res. 54: 435–445.
- Erdman, D. S.
1968. Spawning cycle, sex ratio, and weights of blue marlin off Puerto Rico and the Virgin Islands. Trans. Am. Fish. Soc. 97:131–137.
- Goodyear, C. P.
2003. Spatiotemporal distributions of longline CPUE and sea surface temperatures for Atlantic marlins. Aust. J. Mar. Freshw. Res. 45:409–417.

- Graves, J. E., and J. R. McDowell.
1995. Inter-ocean genetic divergence of istiophorid billfishes. *Mar. Biol.* 122:193-203.
- Graves, J. E., B. E. Luckhurst, and E. D. Prince.
2002. An evaluation of pop-up satellite tags for estimating post release survival of blue marlin (*Makaira nigricans*) from a recreational fishery. *Fish. Bull.* 100:134-142.
- Gunn, J. S., T. A. Patterson, and J. G. Pepperell.
2003. Short term movement and behavior of black marlin *Makaira indica* in the Coral Sea as determined through a pop-up satellite archival tagging experiment. *Mar. Freshw. Res.* 54:515-525.
- Hill, R. D., and M. J. Braun.
2001. Geolocation by light level. In *Electronic tagging and tracking in marine fisheries* (J. R. Sibert and J. L. Nielsen, eds.), p. 317-330. Kluwer Academic Publishers, The Netherlands.
- Horodysky, A. Z., and J. E. Graves.
2005. Application of pop-up satellite archival tag technology to estimate post release survival of white marlin (*Tetrapturus albidus*) caught on circle and straight-shank "J" hooks in the western North Atlantic recreational fishery. *Fish. Bull.* 103:84-96.
- Horodysky, A. Z., D. W. Kerstetter, and J. E. Graves.
2003. Habitat preferences and diving behavior of white marlin (*Tetrapturus albidus*) released from the recreational rod-and-reel and commercial pelagic longline fisheries in the western North Atlantic Ocean: implications for habitat-based stock assessment models. *The Int. Comm. Cons. Atlantic Tunas*, Madrid, Spain. *Coll. Vol. Sci. Pap. SCRS/2003/033*, 13 p.
- Hunter, J. R., and B. J. Maciewicz.
1985. Measurement of spawning frequency in multiple spawning fishes. In *An egg production method for estimating spawning biomass of pelagic fish: application to the northern anchovy, *Engraulis mordax** (R. Lasker, ed.), p. 79-94. NOAA Tech. Rep. NMFS 36.
- Hunter, J. R., B. J. Maciewicz, N. C. H. Lo, and C. A. Kimbrell.
1992. Fecundity, spawning, and maturity of female Dover sole *Microstomus pacificus*, with an evaluation of assumptions and precision. *Fish. Bull.* 90:101-128.
- ICCAT (International Commission for the Conservation of Atlantic Tunas).
1998. Report of the third ICCAT billfish workshop. ICCAT, Madrid, Spain. *Coll. Vol. Sci. Pap.*, vol. XLVII, 352 p.
2001. Report of the fourth billfish workshop. ICCAT, Madrid, Spain. *Coll. Vol. Sci. Pap.*, vol. LIII, 375 p.
2002. Executive summary report for white marlin. ICCAT, Madrid, Spain. Report for biennial period, 2000-2001, part 2 (2001), vol. 2:76-82.
2003. Executive summary report for white marlin. ICCAT, Madrid, Spain. Report for biennial period 2002-2003, part 1 (2002), vol. 2: 97-103.
- Kerstetter, D. W., B. E. Luckhurst, E. D. Prince, and J. E. Graves.
2003. Use of pop-up satellite archival tags to demonstrate survival of blue marlin (*Makaira nigricans*) released from pelagic longline gear. *Fish. Bull.* 101:939-948.
- Mather, F. J. III, H. J. Clark, and J. M. Mason Jr.
1975. Synopsis of the biology of the white marlin, *Tetrapturus albidus* Poey (1861). In *Proceedings of the international billfish symposium: Kailua-Kona, Hawaii, 9-12 August 1972, Part 3: Species synopses* (R. S. Shomura and F. Williams, eds.), p. 55-94. NOAA Tech. Rep. NMFS SSRF-675.
- McBride, R. S., F. J. Stengard, and B. Mahmoudi.
2002. Maturation and diel reproductive periodicity of round scad (Carangidae: *Decapterus punctatus*). *Mar. Biol.* 140:713-722.
- McDowell, J. R., and J. E. Graves.
2002. Nuclear and mitochondria DNA markers for specific identification of istiophorid and xiphiid billfishes. *Fish. Bull.* 100:537-544.
- Musyl, M. K., R. W. Brill, D. S. Curran, J. S. Gunn, Jason R. Hartog, R. D. Hill, D. W. Welch, J. P. Eveson, C. H. Boogs, and R. E. Brainard.
2001. Ability of electronic archival tags to provide estimates of geographical position based on light intensity. In *Electronic tagging and tracking in marine fisheries* (J. R. Sibert and J. L. Nielsen, eds.), p. 343-367. Kluwer Academic Publishers, The Netherlands.
- Ortiz, M., E. D. Prince, J. E. Serafy, D. B. Holts, K. B. Davy, J. G. Pepperell, M. B. Lowry, and J. C. Holdsworth.
2003. Global overview of the major constituent-based billfish tagging programs and their results since 1954. *Mar. Freshw. Res.* 54:489-507.
- Pepperell, J. G.
1990. Movements and variations in early year class strength of black marlin *Makaira indica* off eastern Australia. Planning the future of billfishes. In *Proceedings of the international billfish symp. II: 1-5 August 1988, Kona, Hawaii, Part 2: Contributed papers* (R. H. Stroud, ed.), p. 51-66. National Coalition for Marine Conservation, Savannah, GA.
- Prager, M. H., E. D. Prince, and D. W. Lee.
1995. Empirical length and weight conversion equations for blue marlin, white marlin, and sailfin from the North Atlantic Ocean. *Bull. Mar. Sci.* 56:201-210.
- Prince, E. D., and B. E. Brown.
1991. Coordination of the ICCAT enhanced research program for billfish. In *Creel and angler surveys in fisheries management* (Guthrie et al., eds.), p. 13-18. Am. Fish. Soc. Symp. 12.
- Prince, E. D., D. W. Lee, J. R. Zweifel, and E. B. Brothers.
1991. Estimating age and growth of young Atlantic blue marlin, *Makaira nigricans*, from otolith microstructure. *Fish. Bull.* 89:441-459.
- Prince, E. D., M. Ortiz, A. Venizelos, and D. S. Rosenthal.
2002a. In-water conventional tagging techniques developed by the cooperative tagging center for large, highly migratory species. *Am. Fish. Soc. Symp.* 30:155-171.
- Prince, E. D., M. Ortiz, and A. Venizelos.
2002b. A comparison of circle hook and "J" hook performance in recreational catch-and-release fisheries for billfish. *Am. Fish. Soc. Symp.* 30:57-65.
- Serafy, J. E., R. K. Cowen, C. B. Paris, T. R. Capo, and S. A. Luthy.
2003. Evidence of blue marlin, *Makaira nigricans*, spawning in the vicinity of Exuma Sounds, Bahamas. *Mar. Freshw. Res.* 54:299-306.
- Wallace, R. A., and K. Selman.
1981. Cellular and dynamic aspects of oocyte growth in teleosts. *Am. Zool.* 21:325-343

Abstract—We summarize the life history characteristics of silvergray rockfish (*Sebastes brevispinis*) based on commercial fishery data and biological samples from British Columbia waters. Silvergray rockfish occupy bottom depths of 100–300 m near the edge of the continental shelf. Within that range, they appear to make a seasonal movement from 100–200 m in late summer to 180–280 m in late winter. Maximum observed age in the data set was 81 and 82 years for females and males, respectively. Maximum length and round weight was 73 cm and 5032 g for females and 70 cm and 3430 g for males. The peak period of mating lasted from December to February and parturition was concentrated from May to July. Both sexes are 50% mature by 9 or 10 years and 90% are mature by age 16 for females and age 13 years for males. Fecundity was estimated from one sample of 132 females and ranged from 181,000 to 1,917,000 oocytes and there was no evidence of batch spawning. Infection by the copepod parasite *Sarcotaces arcticus* appears to be associated with lower fecundity. Sexual maturation appears to precede recruitment to the trawl fishery; thus spawning stock biomass per recruit analysis (SSB/R) indicates that a $F_{50\%}$ harvest target would correspond to an F of 0.072, 20% greater than M (0.06). Fishery samples may bias estimates of age at maturity but a published meta-data analysis, in conjunction with fecundity data, independently supports an early age of maturity in relation to recruitment. Although delayed recruitment to the fishery may provide more resilience to exploitation, managers may wish to forego maximizing economic yield from this species. Silvergray rockfish are a relatively minor but unavoidable part of the multiple species trawl catch. Incorrectly “testing” the resilience of one species may cause it to be the weakest member of the species complex.

Manuscript submitted 6 April 2004
to the Scientific Editor's Office.

Manuscript approved for publication
31 March 2005 by the Scientific Editor.
Fish. Bull. 103:670–684 (2005).

Life history characteristics for silvergray rockfish (*Sebastes brevispinis*) in British Columbia waters and the implications for stock assessment and management

Richard D. Stanley

Allen R. Kronlund

Fisheries and Oceans, Canada
Pacific Biological Station
Nanaimo, British Columbia, Canada V9T 6N7
E-mail address (for R. D. Stanley) stanleyr@pac.dfo-mpo.gc.ca

Silvergray rockfish (*Sebastes brevispinis*) range from the Gulf of Alaska to central Baja California (Love et al., 2001) and are a minor part of the trawl and hook-and-line fisheries catch from northern Washington to the Gulf of Alaska (Alaska Fisheries Information Network,¹ Pacific Fisheries Information Network,² Pacific Biological Station³). Coastwide commercial landings averaged 2600 metric tons (t) from 1990 to 2000, and about two-thirds of these landings came from British Columbia (B.C.) waters, mostly from bottom trawling. Hook-and-line landings are the most common type in Alaskan waters (mostly from southeastern Alaska) and have averaged less than 20 t. Combined annual trawl landings from Washington and Oregon peaked at over 1000 t from 1977 to 1979, declined to an average of 210 t from 1990 to 1998, and since 1999 have further declined to negligible levels.

The B.C. bottom trawl fishery is currently managed through individual vessel quotas (IVQs) whereby a fixed proportion of the annual quota for each stock is allocated to each quota-holder. Because silvergray rockfish are currently assessed and managed as four separate stocks (Fig. 1: Pacific Marine Fisheries Commission areas 3CD, 5AB, 5CD, and 5E), a vessel may possess up to four area-specific quotas for silvergray rockfish. All bottom trawlers on the outer coastal waters of British Columbia are required to have an independent observer on the vessel. Once vessels have reached

their IVQ for one area and species, and have exhausted their limited opportunity to temporarily lease quota from other lease-holders, they must cease all bottom trawling even though they may still have IVQ remaining for other species in that area.

The quotas for silvergray rockfish are relatively small compared with those for other species in the fishery; thus fishermen can fully fill their silvergray rockfish IVQs as they target other species. However, if silvergray rockfish become difficult to avoid through increased abundance or availability, or if the silvergray rockfish quota is reduced, even though catch rates remain constant, they become a nuisance in that fishermen cannot fulfill their IVQs for other species without exceeding their silvergray rockfish IVQ. Therefore, the quotas for minor species, such as silvergray rockfish, now assume more importance than would be gained from their landed value. Finally, the enactment of species-at-risk legislation in Canada has led to the requirement

¹ Alaska Fisheries Information Network. 2000. AKFIN Support Center, 612 W Willoughby Ave. Suite B. Juneau, Alaska 99801.

² Pacific Fisheries Information Network. 2000. Pacific States Marine Fisheries Commission, 205 SE Spokane Street, Suite 100, Portland, Oregon 97202.

³ Pacific Biological Station. 2000. Unpubl. data. Fisheries and Oceans Canada. Nanaimo, British Columbia V9T 6N7, Canada.

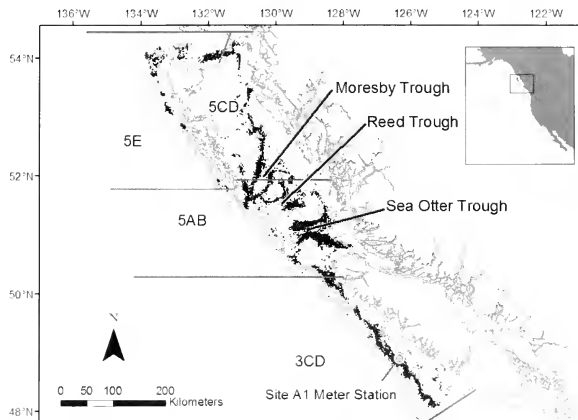


Figure 1

Coastal waters of British Columbia showing boundaries of silvergray rockfish (*Sebastes brevispinis*) stocks, trawl capture locations of silvergray rockfish (black dots) for 1996–2000, mooring site for the oceanographic metering of temperature at-depth (A1 meter station), and 500-, 1000-, and 1500-m depth contours.

to assess and protect the status of any species affected by fishing, regardless of its commercial value.

Research on silvergray rockfish is an example of an area that has been neglected owing to the lack of economic importance of this species in the commercial fisheries. Even the data that are available have been collected incidentally during fishing operations targeting other species or during generic sampling programs. Nevertheless, we show in the present article that these data, in conjunction with detailed commercial catch and effort data, can be used to provide insight into the biology, assessment, and management of silvergray rockfish. This article summarizes this information and provides estimates of the various life history parameters needed for stock assessment. Some of the estimates represent updates from previous work, but we also for the first time present estimates of fecundity and maturity at age and size. Using these values, we also derive a target reference point.

Materials and methods

Data sources

Data for silvergray rockfish were collected from B.C. waters during port sampling, at-sea observer programs, and research cruises from 1977 through 2000. These

data reside at the Pacific Biological Station, Nanaimo, B.C., Fisheries and Oceans, Canada. As of June 2000, the database contains information on over 40,000 specimens. Of these specimens, we aged 13,671 representing most of the specimens from which we obtained otoliths, in addition to documenting length, sex, and maturity stage. We also used catch observations from the commercial trawl observer program from 1996 through 2000.

Habitat

Preferred depth distributions of silvergray rockfish were inferred from analyzing catch rates in the commercial data. We used all bottom tows that contained silvergray rockfish and included tow duration. Bottom depth of the tows was determined as the midpoint between beginning and end depth of the tows. We applied a nonparametric locally weighted regression smoothing function (LOESS) (Cleveland, 1979) to log-CPUE observations grouped by 20-m intervals.

Depth of peak catch rates by month were compared with temperature-at-depth estimates based on data collected from the site A1 meter station on the west coast of Vancouver Island (Fig. 1: 48°32'N by 126°12'W). These data, collected from 1986 to 2000 (excluding El Niño years), were taken from 35-, 100-, 175-, and 400-m depths. The temperatures at fixed depths were then

Table 1

Field classification of gonad maturity stages for silvergray rockfish (*Sebastes brevispinis*) used by the Groundfish Section, Pacific Region Science Branch, Fisheries and Oceans, Canada.

	Female ovaries	Male testes
1	Immature (translucent, small, color can be clear, amber, yellow, or pink)	Immature (translucent, string-like)
2	Developing (small, opaque or translucent, can be yellow, usually light pink)	Developing (swelling, brown-white)
3	Developed (eggs usually white or cream white, can be yellow or orange-yellow)	Not used
4	Fertilized (large, cream or orange-yellow eggs, translucent)	Developed (large, white, easily broken)
5	Embryos or larvae present (includes eyed eggs)	Ripe (running sperm)
6	Spent (flaccid, red, a few larvae may be present)	Spent (flaccid, creamy-brown, some milt present but not free-flowing)
7	Resting (moderate size, firm, red-grey, red-grey, pink, or purple to almost black)	Resting (ribbon-like, small brown)

converted through interpolation to provide depth at specific temperatures (Hourston⁴).

Aging and growth determinations

Ages were determined by using the otolith burnt-section technique (MacLellan, 1997) with a minor modification. A survey directed at studying juvenile rockfish in 1991 captured two 17-cm silvergray rockfish. An examination of these otoliths indicated that the previous application of the method had incorrectly assigned the first annulus to the age count in specimens. Therefore, some previously aged specimens were probably under-estimated by one year (MacLellan⁵). A faint first annulus is consistent with the late spring to mid-summer parturition of silvergray rockfish that appears to preclude significant summer growth in its first year. The method was modified in August of 1992, and we added one year to all previously aged specimens in the data set.

Most (85%) of the otoliths were aged by one reader. The remaining 15% were aged by two readers to monitor consistency. If there was a disagreement, the two readers agreed on a "resolved" age.

Age and length data were fitted to a generalized growth model (Schnute, 1981) (Appendix 1). Growth dimorphism was calculated as the ratio of the mid-points of fork length (maximum observed length minus minimum observed length) between males and females (Lenarz and Wylie Echeverria, 1991).

Reproductive maturity

Maturity stage was classified macroscopically in the field (Table 1). We examined the annual reproductive cycle

by tracking the proportions in each maturity stage by month. Lacking histological confirmation for characterizing maturity, we followed the suggestion of Wylie Echeverria (1987) and used only those specimens collected from the reproductive or gestation period of March to August. Within this subset, we grouped female stages 1 and 2 as immature, and stages 3–7 as mature. Because most mature females exhibited fertilized eggs by March, we assumed that females with small, nondeveloped ovaries in March through August would not complete parturition in the same calendar year.

We assumed that stage 1, during which testes are translucent and string-like, was the only male immature stage. Subsequent stages 2 and 4–7 were grouped as mature (stage 3 was not used in the field). The proportion of stage-2 males (in relation to males in other mature stages) decreased rapidly during the mating season (September–January) indicating that many of the specimens classified as stage 2 would become mature within the same calendar year. We emphasize, however, that without histological support for these classifications, the assumptions of maturity-at-age or maturity-at-length remain tentative.

The estimated proportions of maturity at age were computed by fitting a generalized additive model (GAM) to the binomial maturity classes (0=immature, 1=mature) (Hastie and Tibshirani, 1990). A logistic link with a binomial error structure was applied, as well as a second-degree nonparametric LOESS smoother.

Fecundity

Fecundity was estimated from a single sample ($n=132$) of females captured by commercial bottom trawl in Sea Otter Trough in April 1989 (Fig. 1). The catch was stored in refrigerated seawater for four days prior to sampling. Sampling was stratified by length to obtain a range of ages, and from each fish we obtained measurements of fork length, gonad weight, and somatic weight. We also collected otoliths and counted the number of cysts con-

⁴ Hourston, R. 2003. Personal commun. Institute of Ocean Sciences, Fisheries and Oceans Canada, 9860 West Saanich Road, P.O. Box 6009, Sidney, British Columbia, V8L 4B2, Canada.

⁵ MacLellan S. 2000. Personal commun. Pacific Biological Station, Fisheries and Oceans Canada, Nanaimo, British Columbia, V9T 6N7, Canada.

taining the copepod parasite *Sarcotaces arcticus* in the coelomic cavity. All the oocytes of all the female gonads appeared to be in a prefertilized condition.

The ovaries that were used for fecundity estimation were fixed and stored in modified Gilson's solution (Leaman, 1988) and shaken weekly for one year. Fecundity estimates were derived gravimetrically (Leaman, 1988). Each ovary was drained and filtered through stacked sieves (100–750 μm); each clump was broken manually if possible. The ovarian membranes and connective tissue were teased away from eggs and discarded. The oocytes were transferred to millipore filters, vacuum-dried for 15 minutes, and the oocytes and filter were weighed to 0.01 g. Four subsamples of approximately 0.1 g and 1000 oocytes were weighed to 0.0001 g. Total fecundity was estimated for each fish by multiplying total vacuum-dried ovary weight by the mean density of the four samples. Fecundity relationships against age, weight, and length were examined with a generalized additive model (GAM) (Hastie and Tibshirani, 1990). An identity link with a Gaussian error structure was used in each case. Ovaries to be used for histological examination were fixed in Smith's formal dichromate solution and then stored in 3% formaldehyde. Histology samples were embedded, sectioned, mounted, stained with Harris' haematoxylin, and counterstained with alcoholic eosin (Gray, 1954).

Spawning stock biomass per recruit (SSB/R)

We combined estimates of instantaneous natural mortality rate (M) of 0.06 and partial recruitment from Stanley and Kronlund (2000) with our estimates of the proportion mature at age and predicted fecundity at age in order to derive estimates of the expected population fecundity of unfished populations (Appendix 2). The impact of fishing on spawning stock biomass per recruit (SSB/R) can then be explored by comparing the ratio of predicted cumulative fecundity of a cohort under exploitation to predicted cumulative fecundity under no fishing pressure (Gabriel et al., 1989; Clark, 1991).

Results

Habitat

The commercial data indicated that the highest catch rates and most of the landings of silvergray rockfish come from the edge of the continental shelf or along the edges of deep troughs (Fig. 1). These tows were typically conducted in bottom depths of 100 to 300 m, although silvergray rockfish have been reported from tows with mid-point bottom depths greater than 580 m. Monthly catch rates by depth indicate a seasonal trend wherein peak catch rates are highest in depths of 180–280 m in March and April, but highest in depths of 100–200 m in September and October (Fig. 2).

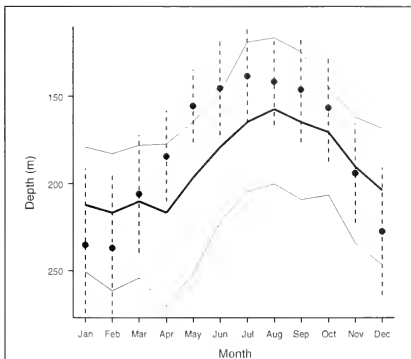


Figure 2

Silvergray rockfish (*Sebastes brevispinis*) seasonal depth distribution. The solid lines show the median (heavy line) and 25th and 75th percentiles (thin lines) for the number of silvergray rockfish catches observations (observed commercial trawl sets) at depth, between 1996 and 2003. The dots indicate the estimated depth at $7.2^\circ\text{C} \pm 1$ standard deviation (dotted line).

If the shift in catch rates correctly indicates seasonal movement, and the interpolated temperatures at site A1 characterize bottom temperatures on the coast, together they indicate that silvergray rockfish tend to maintain peak densities at bottom water temperatures centered around 7.2°C (Fig. 2). The move to shallower water in the late spring, however, seems to lag behind the cooling of shallower water that results from summer upwelling (Thomson⁶). The return to deeper water in the fall is coincident with the warming of water at greater depths.

The cohabitants of silvergray rockfish were also inferred from commercial trawl observations. For these data, we selected tows with at least 50 kg of silvergray rockfish. Silvergray rockfish represented 12.8% of the total catch of over 36,000 t (Table 2). The dominant species by weight in these tows were Pacific ocean perch (*Sebastes alutus*), arrowtooth flounder (*Atheresthes stomias*), yellowmouth rockfish (*S. reedi*), yellowtail rockfish (*S. flavidus*), redstripe rockfish (*S. proriger*), and canary rockfish (*S. pinniger*). The species most frequently co-occurring in the tows were arrowtooth flounder, lingcod (*Ophiodon elongatus*), spiny dogfish

⁶ Thomson, R. 2003. Personal commun. Institute of Oceans Sciences, Fisheries and Oceans Canada. 9860 West Saanich Road, P.O. Box 6000, Sidney, British Columbia V8L 4B2, Canada.

Table 2
Fish species captured in 1996–99 B.C. bottom trawl tows that contained silvergray rockfish (*Sebastes brevispinis*).

Common name	Species	% of total catch (36,489,773 kg)	% frequency (10,820 tows)
Silvergray rockfish	<i>Sebastes brevispinis</i>	12.8	100.0
Arrowtooth flounder	<i>Atheresthes stomias</i>	13.0	77.2
Lingcod	<i>Ophiodon elongatus</i>	2.8	65.1
Spiny dogfish	<i>Squalus acanthias</i>	2.5	58.4
Yellowtail rockfish	<i>Sebastes flavidus</i>	11.3	57.4
Canary rockfish	<i>Sebastes pinniger</i>	5.4	55.2
Redstripe rockfish	<i>Sebastes paucispinis</i>	1.3	54.0
Pacific cod	<i>Gadus macrocephalus</i>	1.1	53.7
Pacific halibut	<i>Hippoglossus stenolepis</i>	0.6	48.2
Redstripe rockfish	<i>Sebastes proriger</i>	7.2	47.3
Rex sole	<i>Errex zachirus</i>	0.8	46.6
Sablefish	<i>Anoplopoma fimbria</i>	0.6	46.2
Spotted ratfish	<i>Hydrolagus collieti</i>	0.6	43.7
Pacific ocean perch	<i>Sebastes alutus</i>	13.9	40.4
Yellowmouth rockfish	<i>Sebastes reedi</i>	12.7	39.2
Dover sole	<i>Microstomus pacificus</i>	1.1	36.0
Petrale sole	<i>Eopsetta jordani</i>	0.4	34.5
Redbanded rockfish	<i>Sebastes babcocki</i>	0.9	33.7
English sole	<i>Pleuronectes vetulus</i>	0.5	28.3
Widow rockfish	<i>Sebastes entomelas</i>	3.9	27.1
Greenstriped rockfish	<i>Sebastes elongatus</i>	0.3	27.0
Longnose skate	<i>Raja rhina</i>	0.3	26.0
Others		6.2	—

(*Squalus acanthias*), yellowtail rockfish, canary rockfish, redstripe rockfish, and Pacific cod (*Gadus macrocephalus*). All of these species were observed in more than 50% of the selected tows.

The cohabitants varied with depth. Tows conducted in depths less than 200 m tended to include lingcod, dogfish, canary rockfish, and yellowtail rockfish, whereas catches from greater than 200 m were dominated by arrowtooth flounder, Pacific ocean perch, redstripe rockfish, and yellowmouth rockfish. Fishermen report that silvergray rockfish are typically found over relatively "hard" bottom, often in proximity to bottom that was not trawlable because it was too rough. They are rarely caught in midwater tows.

Aging and growth estimates

The maximum ages observed in Canadian samples were 81 and 82 years for females and males, respectively. The corresponding ages at the 99.9% percentiles were 76 and 77 years.

Although we assumed that our aging methods for silvergray rockfish provided unbiased estimates of age, agreement between readers was poor. Agreement to ± 1

year was 60–80% for ages less than 20 years and then declined with age.

The standard errors of the growth parameter estimates show that there is a significant, albeit modest, difference in growth rates; females grow faster and to a larger size (Table 3, Fig. 3). Maximum observed length was 73 and 70 cm for females and males, respectively. We estimated the length-weight relationship for females and males separately and combined from 476 total specimens (Table 3, Fig. 3). The ratio of the mid-point lengths for males and females was 97.2 (Table 4), indicating little sexual dimorphism.

Maturation cycle

The field maturity observations were congruent for females and males (Fig. 4). Testes began developing (stage 2) in September and October and were large and swollen by November and December (stage 4) (Fig. 4). January and March testes were in the late stages of mating (stage 6), whereas from April through August testes appeared to be in a resting phase for males (stage 7). The few observations of large swollen testes with running sperm (stage 5) occurred from October through February. The

Table 3

Growth and fecundity parameter estimates and standard errors for silvergray rockfish (*Sebastes brevispinis*) (see Appendix 1 for parameter definitions).

Equation	Parameter	Females		Males		Combined	
		Estimate	SE	Estimate	SE	Estimate	SE
Length-at-age	y_1	48.985	0.048	47.887	0.041	48.468	0.034
	y_2	60.628	0.015	56.108	0.091	57.719	0.083
	a	0.0581	0.002	0.0708	0.002	0.0709	0.002
	b	1.0000		1.000		1.000	
	T_1	15.000		15.000		15.000	
	T_2	60.000		60.000		60.000	
Length/Weight (ln scale)	α	-4.000	0.137	-2.506	0.411	-3.634	0.157
	β	2.924	0.034	2.547	0.105	2.833	0.040
Fecundity/Somatic weight (ln scale)	α	3.014	0.572				
	β	1.367	0.073				
Fecundity/Length	α	-3.454	1.007				
	β	4.2833	0.251				

Table 4

Comparison of silvergray rockfish (*Sebastes brevispinis*) fork length ratio (group 1) with results from Lenarz and Echevarria (1991) (groups 2-4).

Species group		Deep (>125m)	Shallow (\leq 125 m)	All rockfish species combined
1	Silvergray rockfish (present study)	Fork length ratio	0.97	
2	Water-column species	Number of species	12	17
		Standard length ratio	0.88	0.91
3	Demersal species	Number of species	5	17
		Standard length ratio	0.95	0.98
4	All rockfish species combined	Number of species	17	34
		Standard length ratio	0.90	0.96

peak period of mating is presumably December to February. One sample of 109 males, collected in March 1988, was recorded entirely as maturing. This one sample accounted for all but two records of stage-4 males collected in March and, therefore, contradicted the results of 20 other March samples, totalling 364 specimens. Although we found no evidence of a recording error, we suggest that these specimens were misclassified and were probably recovering instead of developing males.

The developing ovaries (stages 2 and 3), observed from January to April, shifted to fertilized through to resting stages (stages 3-7) in April to June. Eyed larvae were commonly observed from May to July although a few individuals with eyed larvae were observed in February, August, and October.

We examined whether there was a relationship between the size of the female and the timing of parturition by categorizing July observations as either

"parturition not completed" (stages 3-5) or "parturition completed" (stages 6-7) (Fig. 5). The results indicated a dome-shaped relationship with length wherein it appears that a higher proportion of the smaller and larger females had not completed parturition. There were too few observations from June to examine the transition in more detail or to examine whether timing varied with latitude within B.C. waters.

Age observations from the commercial fishery indicate that both sexes are 50% mature at about 10 years of age and over 90% are mature at age 16 for females, and age 13 for males (Table 5, Fig. 6). However, the analysis was limited by the lack of young fish in the samples. For example, there were only five 8-year old and thirteen 9-year old females in the data set. Comparison of the age at maturity and partial recruitment at age indicates that silvergray rockfish mature prior to recruitment (Table 5, Fig. 7).

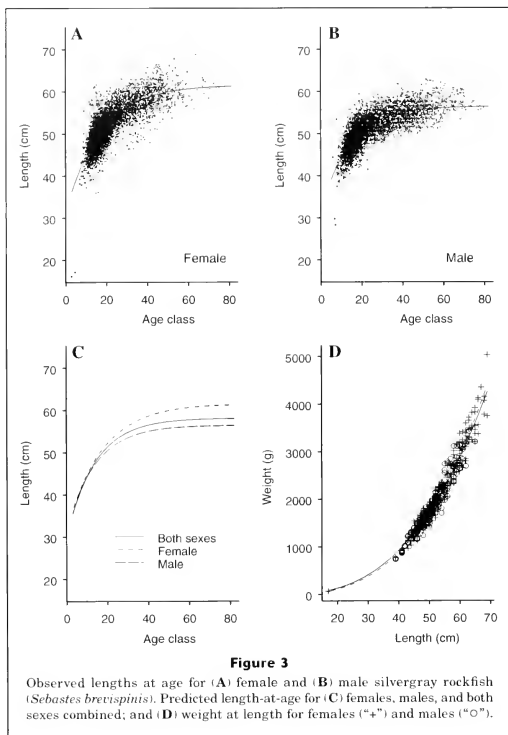


Figure 3

Observed lengths at age for (A) female and (B) male silvergray rockfish (*Sebastes brevispinis*). Predicted length-at-age for (C) females, males, and both sexes combined; and (D) weight at length for females ("+") and males ("o").

Fecundity and stock-assessment-parameter estimates

The total number of large oocytes ranged from 181,000 to 1,917,000 (Fig. 8). A general linear model (GLM) treatment of log fecundity against log somatic weight and age indicated that age was not a significant variable after accounting for somatic weight. Although size is a better predictor of fecundity than age, we also provide the predicted fecundity with age (Table 5) for subsequent calculation of SSB/R.

We examined histological cross-sections from 11 mature specimens in the sample. All appeared to be late in the process of vitellogenesis, the late stage 3 of Wylie Echeverria (1987) or stage V of Bowers (1992). The oocytes in each ovary were either large, with diameters ranging from 300 to 600 μm or smaller than 150 μm .

There was little variation within ovaries in the diameter of the larger eggs ($\pm 50 \mu\text{m}$) and thus no evidence of additional maturing batches.

The SSB/R analysis indicated that an instantaneous fishing mortality (F) that reduces the SSB/R to 50% of what could be expected with no fishing, ($F_{50\%}$) equates to an F of 0.072 (Fig. 9).

Discussion

Data sources

The opportunistic assemblage of samples collected from the commercial fishery and research cruises has two implications if one attempts to draw inference from these

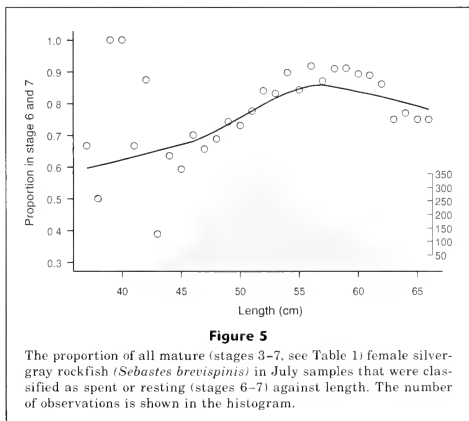
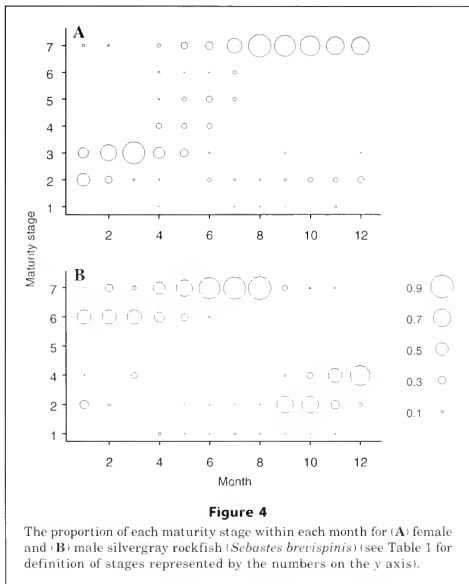
data. The first is that while the overall number of samples and specimens is large, they are not equally distributed over time and space. Thus, for example, we cannot examine whether larger or older males complete the mating earlier in the season because of the lack of winter samples. The second implication is that the results are influenced by the fishing practices. This is particularly the case for inferring depth distribution from trawl catches.

Habitat

Silvergray rockfish appeared to be concentrated in the 100–300 m depth interval. Their distribution tended to overlap the distribution of "slope" and "shelf" assemblages of Weinberg (1994) that were based on survey results from northern California to southern British Columbia. The distribution also agrees with observations from research surveys in B.C. waters (Nagtegaal, 1983). Peak catch rate at depth indicates an annual depth migration, noted by fishermen, of about 80 m. The timing and range of this movement is considered by fishermen to be typical for rockfish (Dickens⁷).

The movement appears correlated with temperature. Bottom temperature increases in winter owing to downwelling (Fig. 2) (Thomson⁶). Thus, the shift to shallower water in the summer means that peak catch rates throughout the year are found in waters centered at just over 7°C. The apparent seasonal movement has obvious implications for stock assessments. Surveys designed to track abundance among years need to be consistent with respect to their timing and depth. More importantly, those who attempt to use CPUE to monitor abundance must consider changes in the distribution of fishing effort by season among years.

There has been no research on the large-scale movements of silvergray rockfish. Barotrauma induced during traditional trawl or hook-and-line-fishing precludes tag-recapture studies, although recent work on other rockfish indicates there is potential for tagging *in situ* (Schrope, 2000; Starr et al., 2001). Nor do we know of any genetic studies on silvergray rockfish to determine stock structure, although the



⁷ Dickens, B. 2000. Personal commun. 1678 Admiral Tryon Boulevard, Qualicum Beach, British Columbia V0R 2T0, Canada.

Table 5

Summary of the predicted values of life history parameters at age for silvergray rockfish (NA: not applicable), partial recruitment values from Stanley and Kronlund (2000).

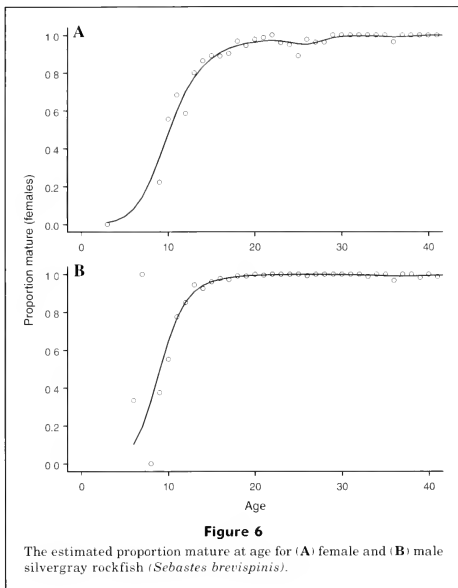
Age (years)	Both sexes		Females			Males		
	Partial recruitment	Length (cm)	Weight (g)	% mature	Fecundity (10^6)	Length (cm)	Weight (g)	% mature
1	0.000	NA	NA	0.000	NA	NA	NA	0.000
2	0.000	NA	NA	0.000	NA	NA	NA	0.000
3	0.000	NA	NA	0.010	NA	NA	NA	0.000
4	0.000	NA	NA	0.020	NA	NA	NA	0.000
5	0.000	NA	NA	0.041	NA	NA	NA	0.000
6	0.000	NA	NA	0.080	NA	NA	NA	0.103
7	0.000	NA	NA	0.143	NA	NA	NA	0.195
8	0.000	42.680	1158	0.235	NA	42.386	1138	0.330
9	0.000	44.750	1233	0.352	NA	43.348	1205	0.492
10	0.002	45.698	1307	0.479	NA	44.245	1270	0.647
11	0.151	46.593	1379	0.599	NA	45.080	1332	0.770
12	0.283	47.437	1448	0.700	0.496	45.858	1391	0.855
13	0.401	48.233	1516	0.776	0.536	46.583	1448	0.909
14	0.505	48.985	1582	0.833	0.576	47.258	1502	0.942
15	0.596	49.694	1645	0.875	0.616	47.887	1553	0.961
16	0.674	50.363	1707	0.906	0.656	48.473	1602	0.974
17	0.742	50.994	1766	0.928	0.696	49.019	1648	0.982
18	0.799	51.590	1823	0.944	0.736	49.528	1692	0.988
19	0.847	52.152	1877	0.955	0.776	50.002	1734	0.992
20	0.887	52.682	1930	0.962	0.817	50.444	1773	0.995
21	0.919	53.183	1980	0.968	0.857	50.855	1810	1.000
22	0.944	53.655	2029	0.971	0.898	51.238	1845	1.000
23	0.963	54.101	2075	0.967	0.939	51.595	1878	1.000
24	0.977	54.521	2119	0.962	0.981	51.928	1909	1.000
25	0.987	54.917	2161	0.953	1.022	52.238	1938	1.000
26	0.994	55.292	2201	0.949	1.057	52.527	1965	1.000
27	0.999	55.645	2240	0.960	1.087	52.796	1991	1.000
28	0.999	55.978	2276	0.972	1.117	53.046	2015	1.000
29	1.000	56.292	2311	0.985	1.145	53.280	2038	1.000
30	1.000	56.589	2345	0.992	1.166	53.497	2059	1.000
40	1.000	58.774	2598	1.000	1.252	55.002	2210	1.000
50	1.000	59.996	2747	1.000	1.228	55.743	2287	1.000
60	1.000	60.680	2832	1.000	1.069	56.108	2325	1.000
70	1.000	61.030	2881	1.000	NA	56.288	2344	1.000

relationship of silvergray rockfish to other rockfish species was examined by Gharrett et al. (2001).

Growth

Silvergray rockfish age estimates have not been validated as they have been for other rockfish (Bennett et al., 1982; Culver, 1987; Leaman and Nagtegaal, 1987; Andrews et al. 2002; Kerr et al. 2004); however, there is evidence of a modal progression in the year classes (Stanley and Kronlund, 2000).

Our estimated growth rates were similar to those reported by Archibald et al. (1981), who used a small subset of the current data. The maximum recorded size of 73 cm for silvergray rockfish is larger than that for most rockfish but smaller than that reported for the largest rockfishes, such as yelloweye rockfish (*S. ruberrimus*), cowcod (*S. levis*), shorttraker (*S. borealis*), and bocaccio (*S. paucispinis*), all of which can exceed 91 cm (Haldorson and Love, 1991). The growth rate of silvergray rockfish is similar to that of other rockfishes (Haldorson and Love, 1991), and weight at length was



similar between sexes as is common for most rockfishes (Love et al., 1990).

Lenarz and Wylie Echeverria's (1991) examination of growth dimorphism led them to categorize rockfish as demersal versus water column, and shallow (≤ 125 m) versus deepwater species (>125 m). Table 4 shows that silvergray rockfish are consistent with other demersal rockfish in that they show relatively little sexual dimorphism in growth. Lenarz and Wylie Echeverria (1991) suggested that the size dimorphism may result from trade-offs between fecundity and size; they suggest that among water-column species, males may optimize size solely for survival, whereas added size for a female may confer advantages in egg production.

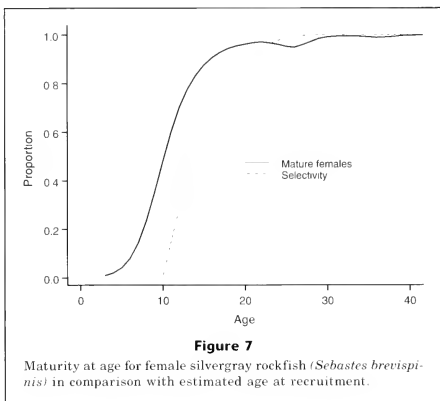
Seasonal maturation and age at maturity

The difficulties in the macroscopic staging of rockfish maturity have been widely discussed (Gunderson et al., 1980; Love and Westphal, 1981; Wylie Echeverria, 1987; Love et al., 1990; Nichol and Pritchard, 1994). These authors are consistent in suggesting that maturity stages should be verified by histological examination of samples collected through all seasons.

More problematic than the staging is the possibility that commercial fishery samples may not be representative of the overall population. If only the mature fraction of an age class recruits to the fishery, then age at maturity derived from commercial samples will underestimate actual age at maturity. For the trawl nets used in the rockfish fishery in British Columbia, size at 100% retention for rockfish is about 30 cm. Silvergray rockfish do not begin to recruit to the fishery until about 35 cm; thus age or size at recruitment is conditioned by behavior of the silvergray rockfish and not by mesh size.

Given the discussion above, our conclusions on age and length at maturity should be viewed as tentative. Nevertheless, the available observations indicate that most females are mature by age nine and most males by age nine or ten. Lenarz and Wylie Echeverria (1991) noted that in 21 of 31 rockfish species, females and males matured at similar ages.

Mating appears to take place from September through January and peaks from December through January. This time range differs from the range derived from observations for southeastern Alaska where ripe male silvergray rockfish were observed from January to March



(O'Connell⁸). Significant proportions of females with fertilized eggs began to appear 2–3 months later in March and peaked from April to May. This lag time does not differ noticeably from that for other rockfish. Wyllie Echeverria (1987) reported that fertilized eggs are usually found 1–3 months after mating. A few specimens with eyed larvae have been observed in February and March but significant proportions are not observed until April. Parturition lasts through July and peaks in June. Westrheim (1975) suggested that the principal month of parturition was later than June for Oregon–B.C. waters, and later than May for the Gulf of Alaska. Phillips (1964) suggested that the timing of rockfish reproduction could be classified into two broad seasons: early (winter) or late (spring–summer). Silvergray rockfish clearly fall within the latter category.

A mating period from December to January and parturition in June implies a 5–6 month process. This is longer than the average period reported for rockfish by Wyllie Echeverria (1987) but similar to those reported for greenstripe rockfish (*S. elongatus*) (Dec–Feb to June), redstripe rockfish (Nov–Jan to June) and sharpchin rockfish (*S. zacentrus*) (Oct–Jan to Apr–May) (Shaw, 1999). The longer periods may reflect that these species and samples were from higher latitudes than the California observations prevalent in Wyllie Echeverria's work. However, Shaw (1999) pointed out that

rosethorn rockfish (*S. helvomaculatus*) samples from the same latitudes indicated a maturation process of 1–2 months. Batch spawning has been reported by Moser (1967a, 1967b) for some rockfish species but our histological examination of 11 specimens taken from the April sample provided no indication of this in silvergray rockfish. Samples taken closer to parturition would be more conclusive.

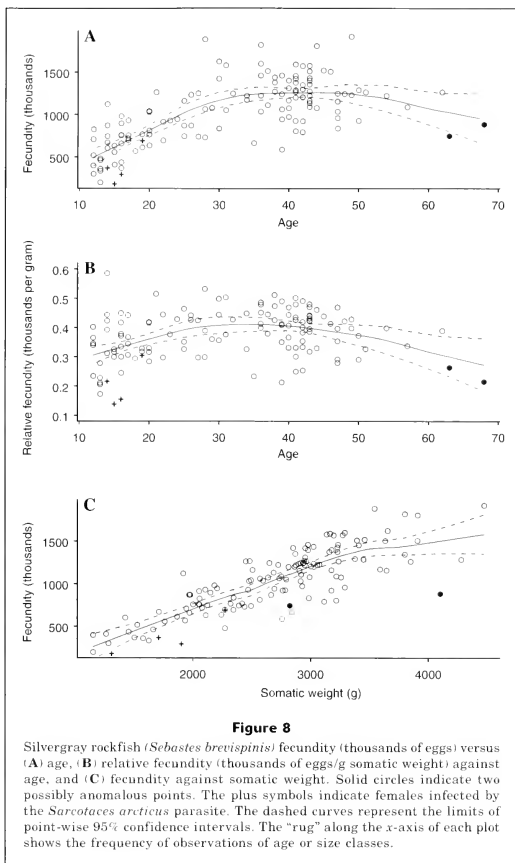
The July samples indicated a dome-shaped relationship in the timing of parturition. As reported for dark-blotched rockfish (Nichol and Pikitch, 1994) and yellowtail rockfish (Eldridge et al., 1991), we observed that the smaller females tended to complete parturition later. However, unlike the results from previous studies, our results indicate that the largest females also tended to complete parturition later.

Fecundity

Different authors have emphasized that actual fecundity at parturition may be lower than estimates derived prior to fertilization (MacGregor, 1970; Boehlert et al., 1982; Haldorson and Love, 1991; Gunderson, 1997), although this was not observed in yellowtail rockfish (Eldridge et al. 1991). Future studies could examine fecundity closer to parturition; however, it is difficult to capture specimens on the verge of parturition without inducing extrusion (Boehlert et al., 1982). We also caution that our estimates are from one sample and Guillemot et al. (1985) reported significant interannual variation in gonadal development among five species of northern California rockfish.

The presence of the *Sarcotaces arcticus* parasite, previously reported for silvergray rockfish (Sekerak, 1975),

⁸ O'Connell, V. 1986. Spawning seasons for some *Sebastes* species landed in the Southeast Alaska longline fishery for nearshore rockfishes (1982–1985). Unpublished report, 21 p. Alaska Department of Fish and Game, Division of Commercial Fisheries, 304 Lake St., No. 103, Sitka, AK 99835-7563.



appears to be associated with reduced fecundity, albeit this conclusion is based on three observations. This conclusion is consistent with qualitative observations by the senior author that the gonads of infected silvergray rockfish tend to be smaller.

Silvergray rockfish fecundity appears typical of the genus as summarized in the meta-data treatment by Haldorson and Love (1991). Predicted fecundity for a

40-year old female exceeds 1,250,000 oocytes, although the maximum observed fecundity in a small sample was almost 2,000,000. The slope of the relationship of log fecundity to log length from our study was 4.283, close to the mean of 4.10 reported for other rockfish (Haldorson and Love, 1991).

Haldorson and Love (1991) noted that the ratio of fecundity at the age of 50% maturity versus fecundity

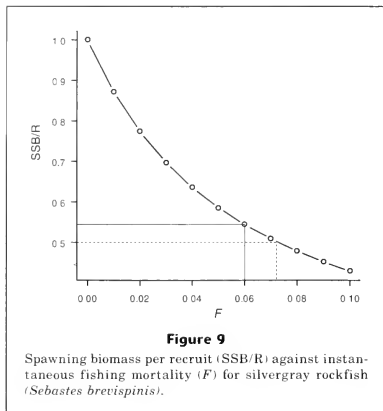


Figure 9

Spawning biomass per recruit (SSB/R) against instantaneous fishing mortality (F) for silvergray rockfish (*Sebastes brevispinis*).

at the age of maximum fecundity ranged from 0.01 to 0.25 for rockfish. Fecundity at 50% maturity could not be determined because we had no observations for females less than 12 years of age. However, if we use fecundity at age 12 (the youngest fish in our sample) and fecundity at age 40 (the predicted age of maximum fecundity), the ratio exceeds 0.40. This finding supports the contention that age at 50% maturity for silvergray rockfish is less than 12 years and adds credibility to the observation that the age of 50% maturity is lower than the age at 50% selectivity.

Estimates of specific fecundity (fecundity/somatic weight) were 356 and 482 ova/g for the 12-year-old and 40-year-old females, respectively. Given that the age at 50% maturity is probably less than 12 years; this range in "relative investment" in reproduction appears average for rockfish (Haldorsen and Love, 1991). As with other rockfish, specific fecundity increases with size, although it appears to reach an asymptote at age 40 for silvergray rockfish.

Age at maturity and SSB/R

An M of 0.06 places silvergray rockfish in the middle to lower end of the mortality range for rockfishes. It is higher than the estimates of 0.02–0.04 reported for yelloweye rockfish (O'Connell and Fujioka⁹; O'Connell et

al.¹⁰; Yamanaka and Lacko, 2001) but much less than 0.14 that has been used for yellowtail rockfish, or 0.28 used for black rockfish (*S. melanops*) (Dorn, 2002).

The analysis of SSB/R indicates that an $F_{50\%}$ corresponds to $F=0.072$ or $F=1.2M$. This F to M ratio represents a more aggressive harvest strategy than the range of 0.5–1.0 currently supported in the literature (Patterson, 1992; Walters, 1998). This result is caused by the special case of silvergray rockfish, anticipated by Clark (1991), wherein recruitment at age is delayed in comparison to maturity at age. If most females actually mature by age 11 or 12 years, but are still not 50% vulnerable at age 14 (Fig. 9), then even at a relatively high fishing mortality, most females can reproduce a few times prior to capture.

As stated above, recruitment to the fishery may be driven more by the stage of maturation than by size or age. Movement to areas and depths that are the source for most fishery samples may be governed by behavioral issues associated with maturation. If fish tend to recruit as they become mature, somewhat independent of size or age, then we may underestimate the age of 50% maturity. In this respect, it is interesting that the fecundity data, compared to other rockfish data, also indicate that the age of 50% maturity may be much less than 12 years.

Our suggestion to managers is that unless the non-recruited population can be sampled to verify maturity-at-age assumptions, then a more precautionary approach is warranted than is implied by an $F=1.2M$ logic for harvest strategy. This silvergray rockfish example emphasizes the sensitivity of an SSB/R harvest logic to estimating age at maturity, which in turn emphasizes the often neglected issues of field classification of maturity and the representativeness of samples. The task of estimating age at maturity is perhaps too often ignored at the expense of estimating other life history parameters.

Conclusion

Owing to the small role that silvergray rockfish has played in groundfish fisheries of the eastern North Pacific Ocean, this species has received little research attention. However, these less valuable stocks are beginning to attract more attention owing to their potential to disrupt precautionary management objectives within the context of a multispecies fishery. With the shift to a more precautionary paradigm, a lack of stock knowledge about the status of any of the incidental species, such as silvergray rockfish, can be a basis for restricting the overall fishery. Strategic allocation of resources by species or stock can no longer be predicated on landed value.

⁹ O'Connell, V., C. Brylinsky, and D. Carlile. 1991. Demersal shelf rockfish stock assessment and fishery evaluation report for 2004. Alaska Dep. Fish and Game Regional Information Report J03-39, 44 p. 304 Lake St. #103, Sitka, AK 99835-7563.

¹⁰ O'Connell, V., and J. Fujioka. 1991. Demersal shelf rockfish. In Status of living resources off Alaska as assessed in 1991, p. 46–47. NOAA Tech. Memo. NOAA-TM-NMFS-F/NWC-211. 304 Lake St. #103, Sitka, AK 99835-7563.

Finally, we note how a meta-data analysis such as that provided by Haldorson and Love (1991) can provide values for stock assessment parameters in the absence of direct estimation. By summarizing the basic life history characteristics for silvergray rockfish in B.C. waters, we add to the research on rockfish and improve the basis for effective management of at least one more minor, but potentially fishery-limiting, species in the eastern Pacific groundfish complex.

Acknowledgments

This summary of the biology of silvergray rockfish was much improved through discussions with four commercial trawl fishermen, Capt.'s Risk Benham, Brian Dickens, Ron Gorman, and Reg Richards. We also appreciated the derivation of temperature at depth provided by Roy Hourston and the help with the graphics from Norm Olsen. The document was much improved by review comments from Bruce Leaman and three anonymous reviewers.

Literature cited

- Andrews, A. H., G. M. Cailliet, K. H. Coale, K. M. Munk, M. M. Mahoney, and V. M. O'Connell.
2002. Radiometric age validation for the yelloweye rockfish (*Sebastes ruberrimus*) from southeastern Alaska. *Mar. Freshw. Res.* 53:139-146.
- Archibald, C. P., W. Shaw, and B. M. Leaman.
1981. Growth and mortality estimates of rockfishes (Scorpaenidae) from B.C. coastal waters, 1977-1979. *Can. Tech. Rep. Fish. Aquat. Sci.* 1048, 57 p.
- Bennett, J. T., G. W. Boehlert, and K. K. Turekian.
1982. Confirmation of longevity in *Sebastes diploproa* (Pisces: Scorpaenidae) from 210 Pb/226 Ra measurements on otoliths. *Mar. Biol.* 71:209-215.
- Boehlert, G. W., W. H. Barss, and P. B. Lamberson.
1982. Fecundity of the widow rockfish, *Sebastes entomelas*, off the coast of Oregon. *Fish. Bull.* 80:881-884.
- Bowers, M. J.
1992. Annual reproductive cycle of oocytes and embryos of yellowtail rockfish *Sebastes flavidus* (Family Scorpaenidae). *Fish. Bull.* 9:231-242.
- Clark, W. G.
1991. Groundfish exploitation rates based on life history parameters. *Can. J. Fish. Aquat. Sci.* 48:734-750.
- Cleveland, W. S.
1979. Robust locally weighted regression and smoothing scatterplots. *J. Am. Stat. Assoc.* 38:261-269.
- Culver, B.
1987. Results from tagging black rockfish (*Sebastes melanops*) off the Washington and northern Oregon coast. In Proceedings of the international rockfish symposium; Anchorage, Alaska, October 20-22, 1986, p. 155-170. Univ. Alaska, Alaska Sea Grant Report 87-2, Anchorage, Alaska.
- Dorn, M. W.
2002. Advice on west coast rockfish harvest rates from bayesian meta-analysis of stock-recruit relationships. *N. Am. J. Fish. Manag.* 22:280-300.
- Eldridge, M., J. A. Whipple, M. J. Bowers, B. Jarvis, and J. Gold.
1991. Reproductive performance of yellowtail rockfish, *Sebastes flavidus*. *Environ. Biol. Fishes* 30:91-102.
- Gabriel, W. L., M. P. Sissenwine, and W. J. Overholz.
1989. An analysis of spawning stock biomass per recruit: an example for Georges Bank haddock. *N. Am. J. Fish. Manag.* 9:383-391.
- Gharrett, A. J., A. K. Gray, and J. Heifetz.
2001. Identification of rockfish (*Sebastes* spp.) by restriction site analysis of the mitochondrial ND-3/ND-4 and 12S/16S rRNA gene regions. *Fish. Bull.* 99:49-62.
- Gray, P.
1954. The microtometist's formulary and guide, 794 p. Blakiston, New York, NY.
- Guillemot, P. J., R. J. Larson, and W. H. Lenarz.
1985. Seasonal cycles of fat and gonad volume in five species of northern California rockfish (Scorpaenidae: *Sebastes*). *Fish. Bull.* 83:299-311.
- Gunderson, D. R.
1997. Trade-off between reproductive effort and adult survival in oviparous and viviparous fishes. *Can. J. Fish. Aquat. Sci.* 54:990-998.
- Gunderson, D. R., P. Callahan, and B. Goiney.
1980. Maturation and fecundity of four species of *Sebastes*. *Mar. Fish. Rev.* 42:74-79.
- Haldorson, L., and M. Love.
1991. Maturity and fecundity in the rockfishes, *Sebastes* spp., a review. *Mar. Fish. Rev.* 53:25-31.
- Hastie, T. J., and R. J. Tibshirani.
1990. Generalized additive models, xv+335 p. Chapman and Hall, New York, NY.
- Kerr, L. A., A. H. Andrews, B. R. Frantz, K. H. Coale, T. A. Brown, and G. M. Cailliet.
2004. Radiocarbon in otoliths of yelloweye rockfish (*Sebastes ruberrimus*): a reference time series for the coastal waters of southeast Alaska. *Can. J. Fish. Aquat. Sci.* 61:443-451.
- Leaman, B. M.
1988. Reproductive and population biology of Pacific ocean perch (*Sebastes alutus* (Gilbert)). Ph.D. diss. 199 p. Univ. British Columbia, British Columbia, Canada.
- Leaman, B. M., and D. A. Nagtegaal.
1987. Age validation and revised natural mortality rate for yellowtail rockfish. *Trans. Am. Fish. Soc.* 116:171-175.
- Lenarz, W. H., and T. Wylie Echeverria.
1991. Sexual dimorphism in *Sebastes*. *Environ. Biol. Fishes* 30:71-80.
- Love, M. S., P. Morris, M. McCrae, and R. Collins.
1990. Life history aspects of 19 rockfish species (Scorpaenidae: *Sebastes*) from the Southern California Bight. NOAA Tech. Rep. NMFS 87, 38 p.
- Love, M. S., and W. V. Westphal.
1981. Growth, reproduction, and food habits of olive rockfish, *Sebastes serranoides*, off Central California. *Fish. Bull.* 79:533-545.
- Love, M. S., M. Yoklavich, and L. Thorsteinson.
2001. Rockfishes of the northeast Pacific, 406 p. Univ. Cal. Press, London.
- MacGregor, J. S.
1970. Fecundity, multiple spawning, and description of the gonads in *Sebastes*. *Mar. Fish. Rev.* 42:74-79.
- MacLellan, S. E.
1997. How to age rockfish (*Sebastes*) using *S. alutus* as

- an example—the otolith burnt section technique. Can. Tech. Rep. Aquat. Sci. 2146, 39 p.
- Moser, H. G.
1967a. Reproduction and development of *Sebastes paucispinus* and comparison with other rockfishes off southern California. *Copeia* 1967:773-797.
1967b. Seasonal histological changes in the gonads of *Sebastes paucispinus* Ayres, an ovoviparous teleost (Family Scorpaenidae). *J. Morph.* 123:329-354.
- Nagtegaal, D. A.
1983. Identification and description of assemblages of some commercially important rockfishes (*Sebastes* spp.) off British Columbia. Can. Tech. Rep. Fish. Aquat. Sci. no. 1183, 88 p.
- Nichol, D. G., and E. K. Pikitch.
1994. Reproduction of darkblotched rockfish off the Oregon coast. *Trans. Am. Fish. Soc.* 123:469-481.
- Patterson, K.
1992. Fisheries for small pelagic species: an empirical approach to management targets. *Rev. Fish. Biol. Fisheries* 2:321-338.
- Phillips, J. B.
1964. Life history studies on ten species of rockfish (genus *Sebastes*). Calif. Dep. Fish Game, Fish. Bull. 126, 70 p.
- Schnute, J.
1981. A versatile growth model with statistically stable parameters. *Can. J. Fish. Aquat. Sci.* 38:1128-1140.
- Schrope, M.
2000. Deep background. *New Scientist* 165:12.
- Sekerak, A. D.
1975. Parasites as indicators of populations and species of rockfishes (*Sebastes*: Scorpaenidae) of the Northeastern Pacific Ocean. Ph.D. diss, 251 p. Univ. Calgary, Alberta, Canada.
- Shaw, F. R.
1999. Life history traits of four species of rockfish (Genus *Sebastes*). M.Sc. thesis, 178 p. Univ. Washington, Seattle, WA.
- Stanley, R. D., and A. R. Kronlund.
2000. Silvergray rockfish (*Sebastes brevispinis*) assessment for 2000 and recommended yield options for 2001/2002. *Can. Stock Assess. Sec. Res. Doc.* 2000/173, 116 p.
- Starr, R. M., J. N. Heine, J. M. Felton, and G. M. Cailliet.
2001. Movements of bocaccio (*Sebastes paucispinus*) and greenspotted rockfishes (*Sebastes chlorostictus*) in a Monterey submarine canyon: implications for the design of marine reserves. *Fish. Bull.* 100:324-337.
- Walters, C.
1998. Evaluation of quota management policies for developing fisheries. *Can. J. Fish. Aquat. Sci.* 55:2691-2705.
- Weinberg, K. L.
1994. Rockfish assemblages of the middle shelf and upper slope off Oregon and Washington. *Fish. Bull.* 92:620-632.
- Westheim, S. J.
1975. Reproduction, maturation, and identification of larvae of some *Sebastes* (Scorpaenidae) species in the northeast Pacific Ocean. *J. Fish. Res. Board Can.* 32:2399-2411.
- Wyllie Echeverria, T.
1987. Thirty-four species of California rockfishes: maturity and seasonality of reproduction. *Fish. Bull.* 85:229-250.
- Yamanaka, K. L., and L. C. Lacko.
2001. Inshore rockfish (*Sebastes ruberrimus*, *S. maliger*, *S. caurinus*, *S. melanops*, *S. nigrocinctus*, and *S. nebulosus*) stock assessment for the west coast of Canada and recommendations for management. *Can. Stock Assess. Sec. Res. Doc.* 2002/139, 102 p.

Appendix 1—Growth formula from Schnute (1981)

$$Y(t) = \left[y_1^b + (y_2^b - y_1^b) \frac{1 - e^{-a(t-\tau_1)}}{1 - e^{-a(\tau_2-\tau_1)}} \right]^{1/b}$$

The model involves six parameters. $\Theta = (\tau_1, \tau_2, y_1, y_2, a, b)$, where τ_1 and τ_2 are two arbitrary ages in the life of a fish, such that $\tau_2 > \tau_1$. The parameter y_1 is the size of a fish at time τ_1 , and y_2 is the size of a fish at time τ_2 with $y_2 > y_1 > 0$. Parameters a and b determine the shape of the growth curve by controlling the acceleration (deceleration) in growth from times τ_1 to τ_2 . The parameter a has units (in time), and b is dimensionless. Although the mathematical expression of the model has four cases, these four cases actually represent the limiting forms of a single equation as a or b (or both) approach 0.

Appendix 2—Spawning stock biomass per recruit

If N_a is a vector of the numbers of females at each age under constant conditions, such that

$$N_{a+1} = N_a e^{-iFS_a + M_a}$$

where F = the instantaneous fishing mortality rate;
 S_a = the partial recruitment at age a ; and
 M = the instantaneous natural mortality rate;

then the cumulative spawning potential of a cohort of females over the lifetime of the cohort (under constant F and M and S_a) is

$$SSB/R = \sum_1^{\infty} N_a Fec_a Mat_a,$$

where Fec_a = fecundity at age a , and
 Mat_a = proportion mature at age a .

The spawning potential per recruit (SSB/R) can then be calculated under various estimates of F and compared with the unfished SSB/R ($F=0$) as shown in Figure 9.

Abstract—To assess the impact of California sea lions (*Zalophus californianus*) on salmon fisheries in the Monterey Bay region of California, the percentages of hooked fish taken by sea lions in commercial and recreational salmon fisheries were estimated from 1997 to 1999. Onboard surveys of sea lion interactions with the commercial and recreational fisheries and dockside interviews with fishermen after their return to port were conducted in the ports of Santa Cruz, Moss Landing, and Monterey. Approximately 1745 hours of onboard and dockside surveys were conducted—924 hours in the commercial fishery and 821 hours in the recreational fishery (commercial passenger fishing vessels [CPFVs] and personal skiffs combined). Adult male California sea lions were responsible for 98.4% of the observed depredations of hooked salmon in the commercial and recreational fisheries in Monterey Bay. Mean annual percentages of hooked salmon taken by sea lions ranged from 8.5% to 28.6% in the commercial fishery, 2.2% to 18.36% in the CPFVs, and 4.0% to 17.5% in the personal skiff fishery. Depredation levels in the commercial and recreational salmon fisheries were greatest in 1998—likely a result of the large El Niño Southern Oscillation (ENSO) event that occurred from 1997 to 1998 that reduced natural prey resources. Commercial fishermen lost an estimated \$18,031–\$60,570 of gear and \$225,833–\$498,076 worth of salmon as a result of interactions with sea lions. Approximately 1.4–6.2% of the available salmon population was removed from the system as a result of sea lion interactions with the fishery. Assessing the impact of a growing sea lion population on fisheries stocks is difficult, but may be necessary for effective fisheries management.

Impact of the California sea lion (*Zalophus californianus*) on salmon fisheries in Monterey Bay, California

Michael J. Weise

James T. Harvey

Moss Landing Marine Laboratories
8272 Moss Landing Road
Moss Landing, CA 95039-9647

Present address (for M. J. Weise): Department of Ecology and Evolutionary Biology
University of California Santa Cruz
Center for Ocean Health
100 Shaffer Rd.
Santa Cruz, California 95060

E-mail address (for M. J. Weise) weise@biology.ucsc.edu

California sea lions (*Zalophus californianus*) interact with almost all commercial and recreational fisheries along the California coast, causing entanglement and damage to fishing gear and loss of catch (Beeson and Hanan¹; NMFS²). The prey of these pinnipeds has been of interest for years because pinnipeds have been viewed as competitors with humans for a variety of fish species. Historically, this competition between pinnipeds and fishermen was of limited importance because fishes and pinnipeds were harvested. However, the increasing specialization within the fishing industry during the twentieth century and changing attitudes toward pinnipeds have intensified this competition (Harwood and Croxall, 1988). Since the passage of the Marine Mammal Protection Act (MMPA) in 1972, the population of California sea lions has increased along the West Coast of North America (NMFS²). This increase in pinniped populations has resulted in an increase in the number of reports of pinnipeds interacting with fishing boats and depredating the catch in fisheries along the West Coast (Beeson and Hanan¹; NMFS²).

The California sea lion population, found from offshore islands in Mexico north to Vancouver Island, British Columbia, has increased steadily throughout the latter part of the twentieth century (NMFS²). In the early 1900s, the over-riding management philosophy was to limit

the California sea lion population because of damage to commercial catches and competition for salmonid fishery resources (Everitt and Beach, 1982). Numbers of sea lions began to increase in the 1940s with curtailment of commercial harvests, but bounties were paid for seals and sea lions in Oregon and Washington until the early 1970s. Following passage of the MMPA in 1972, the California sea lion population increased at an annual average of 5.0–6.2% along the West Coast (Carretta et al.³). There are an estimated 204,000–214,000 sea lions in U.S. waters (Carretta et

¹ Beeson, M. J., and D. A. Hanan. 1996. An evaluation of pinniped-fisheries interactions in California. Report to the Pacific States Marine Fisheries Commission, 46 p. Pacific States Marine Fisheries Commission, 205 SE Spokane St., Portland, OR 97202.

² NMFS (National Marine Fisheries Service). 1997. Impacts of California sea lions and Pacific harbor seals on salmonids and the coastal ecosystems of Washington, Oregon, and California. NOAA Tech. Memo. NMFS-NWFSC-28, 150 p. Northwest Fisheries Science Center, 2725 Montlake Blvd. East, Seattle, WA 98112-2097.

³ Carretta, J. V., M. M. Muto, J. Barlow, J. Baker, K. A. Forney, and M. Lowry, editors. 2002. U.S. Pacific Marine Mammal Stock Assessments: 2002. NOAA/NMFS Tech. Memo., NOAA-TM-NMFS-SWFC-346, 290 p. Southwest Fisheries Science Center, 8604 La Jolla Shores Drive, La Jolla, California 92037-1508.

al.⁴), and an additional 45,000–54,000 animals along Baja, Mexico (Aurioles-Gamboa and Zavala-Gonzalez, 1994). In the Monterey Bay region, sea lions do not breed but several important resting sites exist with a range of 3000 to 7500 animals during the nonbreeding season (Weise, 2000). In contrast to increases in numbers of sea lions, serious declines in salmonid populations have occurred in recent years as a result of changes and degradation in riverine habitat, declines in water quality, overharvesting, changes in oceanic conditions, and the development of hydroelectric power systems that obstruct major riverine migration routes.

Chinook salmon (*Oncorhynchus tshawytscha*) stocks in the Central Valley of California probably represent 85% to 95% of the chinook salmon catches south of Pt. Arena and in Monterey Bay (PFMC⁴). Central Valley chinook originate in the Sacramento River and San Joaquin River and have four distinct runs (portion of a salmon stock that returns to their native streams to spawn during a specific season): fall, late-fall, winter, and spring. Fall and late-fall runs are relatively healthy, but winter and spring runs are listed as endangered under the Endangered Species Act (ESA). Salmon landed in Monterey Bay during the summer fishing season are predominantly fall and late-fall run Central Valley chinook salmon. Size limits and seasonal restrictions are set to reduce retention of listed winter run Central Valley chinook and Klamath River stocks (PFMC⁴). By taking hooked fish, sea lions can affect salmon stocks because commercial and recreational fishermen continue to fish for salmon to replace those taken by sea lion and this activity of predation and compensatory fishing leads to greater numbers of fish being removed from the population. In the ocean commercial troll and recreational salmon fishery, sea lions will swim near or follow fishing boats and will depredate fish once hooked.

Consumption of hooked salmon by sea lions may not only impact salmonid stocks but impact the economic viability of fisheries. Recreational and commercial salmon fishing is an important social and economic asset in California, representing \$28,856,000 in revenues in 1995 (PFMC⁵). Concern over declining salmonid stocks has resulted in adjustments of fishing regulations, such as allocation of harvest between ocean and inland user groups, harvest quotas, and time and area closures (Beeson and Hanan¹). Increasing losses of fish to California sea lions may produce further restrictions for the recreational and commercial salmon fisheries.

During the last several decades only a few researchers have attempted to quantify the impact of sea lions on fisheries in California waters and, more specifically, the Monterey Bay region. According to Beeson and Hanan,¹ the recreational ocean salmon landings in 1995 were greatest in Monterey Bay and San Francisco areas and experienced the greatest amount of sea lion predation (charter passenger fishing vessels and private skiff combined). In our study, we surveyed salmon fisheries in Monterey Bay because of the particularly high rates of interactions with sea lions (Beeson and Hanan¹) in an effort to better understand the nature and extent of these interactions in the commercial and recreational fisheries.

The purpose of this study was to estimate the percentage of salmon taken by California sea lions from commercial and recreational salmon fisheries in Monterey Bay from 1997 to 1999. We hypothesized that the percentages of fish taken by California sea lions in salmon fisheries would be greater than those taken in previous years and would be part of an increasing trend in sea lion and fisheries interactions paralleling the growth of the sea lion population. Further, we estimated the number of fish removed from the California Central Valley chinook stock from observed percentages of fish taken by sea lions in fisheries. Lastly, we estimated the monetary losses associated with sea lions interacting with commercial and recreational salmon fisheries in Monterey Bay from 1997 to 1999 by quantifying the value of fish lost and the type and amount of gear lost or damaged.

Methods

From 1997 to 1999, observations of interactions between pinnipeds and salmon fisheries were conducted onboard boats, and interviews with fishermen were performed at dockside at the three major ports in the Monterey Bay region: Santa Cruz, Moss Landing, and Monterey (Fig. 1). Salmon fishing operations included commercial troll fishery and recreational fisheries consisting of commercial passenger fishing vessels (CPFVs) and private skiffs. The timing of the commercial and recreational salmon fishery seasons varied each year of the study, and sampling was conducted from the beginning to the end of each season (Table 1). The commercial troll fishery included day boats (i.e., a one-day fishing trip) and multiple-day boats. Fishing areas included in our study ranged from Pt. Sur north to Año Nuevo Island. Data regarding fisheries interactions collected at the three different ports were pooled because fishermen from all three ports often fish as a fleet.

Dockside surveys were conducted to achieve a greater sampling effort than could be obtained from onboard observations alone. Onboard surveys were conducted to test reliability of dockside surveys and to ensure that investigators fully understood the nature of the interaction. Small biases have occurred when combining onboard and dockside surveys but were attributed to

⁴ PFMC (Pacific Fisheries Management Council). 1999. Review of 1998 ocean salmon fisheries. NOAA Award No. NA97FC0031, sections A1–A50 and B1–43. Pacific Fisheries Management Council, 7700 NE Ambassador Place, Suite 200, Portland, OR 97220-1384.

⁵ PFMC (Pacific Fisheries Management Council). 1995. Review of 1994 ocean salmon fisheries. NOAA No. NA57FC0007, sections A1–A50 and B1–B43. Pacific Fisheries Management Council, 7700 NE Ambassador Place, Suite 200, Portland, OR 97220-1384.

Table 1
Commercial and recreational salmon fishery seasons in the Monterey Bay region from 1997 to 1999.

	Commercial	Recreational
1997	1-31 May, 23 June-18 July, 1-30 September	15 March-19 October
1998	1-31 May, 16 June-30 September	14 March-7 September
1999	1 May - 21 August, 1-30 September	14 March-6 September

onboard sampling in areas where interaction was more prevalent (Miller et al.⁶). During this study, captains were requested during onboard observations to conduct normal fishing operations and not to intentionally seek out areas with greater or lesser rates of interaction between sea lions and fishery operations.

Sampling of commercial and recreational salmon fisheries was stratified by month and approximately equal numbers of onboard and dockside surveys were conducted monthly. Sampling days and ports were selected randomly for onboard and dockside surveys of commercial fishing operations, but onboard surveys were limited by crew cooperation and space availability. Each onboard survey in the commercial fishery took a full fishing day onboard one boat, and dockside interviews were conducted during four-hour periods in the middle to late afternoon during the peak time that vessels returned to port. For CPFVs, which operate virtually every day but have a greater number of boats and passengers on weekends, two-thirds of onboard and dockside sampling dates were selected randomly from possible weekend dates and one-third from all possible weekdays. Onboard surveys of CPFV took a full fishing day aboard one vessel, and dockside surveys took two to three hour periods in early afternoon during peak return times for CPFVs at a randomly selected port. The goal of CPFV dockside surveys was to sample (for the sampling day) all CPFVs targeting salmon and that had returned to port. In the skiff fishery, greater numbers of fishing trips occurred on weekends; therefore approximately three-quarters of sampling days occurred on weekends, and one-quarter occurred on weekdays. Onboard surveys in 1997 aboard one skiff took a full fishing day, and dockside surveys from 1997 to 1999 were conducted during two-hour sampling periods in late morning and early afternoon during the peak return time for private skiffs.

In 1997, four onboard surveys were conducted in the commercial and CPFV fishery, and five onboard private skiff surveys were conducted. Whereas in 1998 and 1999, in an effort to increase onboard sample size, survey effort was concentrated in the commercial and

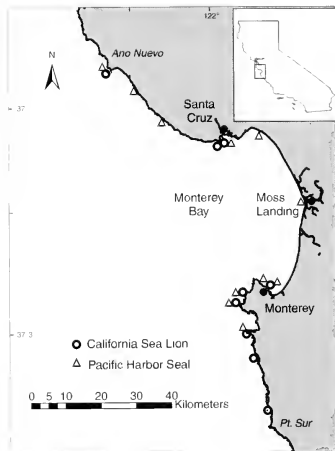


Figure 1

Primary fishing ports used by commercial and recreational salmon vessels, and pinniped haul-out sites in Monterey Bay, California.

CPFV fisheries; 22 surveys conducted each year in each fishery.

Information collected at dockside included port of call, number of fish landed, number of fish taken by pinnipeds at or below the surface, species and number of marine mammals involved in surface take, number of fish released, number of released fish taken by marine mammals, and type and amount of gear loss. Onboard surveys included the same information collected at dockside, as well as standard length of all fish landed.

Commercial troll and recreational salmon fisheries use different types of fishing gear, which can affect the nature and magnitude of their interactions with pinnipeds. Commercial salmon trolls are designed to catch fast-swimming fishes by using flashy lures that are trolled behind the moving vessel on heavily

⁶ Miller, D. J., M. J. Herder, and J. P. Scholl. 1983. California marine mammal-fishery interaction study, 1979-1981. NMFS Southwest Fish. Cent., Admin. Rep. LJ-83-13C, 233 p. Southwest Fisheries Science Center, 8604 La Jolla Shores Drive, La Jolla, CA 92037-1508.

weighted fishing lines. Multiple lines are mounted on outrigger poles to ensure separation of the lines and are controlled by small hydraulic winches (Starr et al., 1998). Depending on conditions, commercial fishermen use three to fifteen lures per line and two to six lines per boat, totaling six to ninety lures with hooks per boat. In recreational boats each fisherman traditionally uses one rod, reel, line, and hook with bait.

Surface takes, also termed "definite takes," were defined as takes when pinnipeds took a hooked salmon (and when the species and number of marine mammals involved could be determined). Surface takes were also recorded when fish were hooked and the action of the line indicated that a fish was no longer hooked, and a pinniped surfaced immediately with a fish in its mouth. Takes below the surface, or "probable takes," were defined as takes when fish were removed from the hook (and when the species and number of marine mammals involved could not be observed directly). Evidence that indicated the occurrence of below-surface takes was in the form of bent hooks, lost gear, or a sea lion surfacing within several minutes with a salmon, provided no other fishing boats were in close proximity. Two types of takes were designated because takes below surface were not witnessed, and other predators including sharks take fish from lines, or fish may have escaped. However, fishermen and researchers recognized that takes by pinnipeds, specifically by sea lions, differed from takes by sharks and other predators by the action of the line, effect on the hook or lure (or both), and type of bite on fish parts remaining on the hook.

Number of salmon and percentage of catch taken by pinnipeds were compared with the total catch and the legal catch in commercial and recreational fisheries. Total catch was defined as numbers of fish hooked, including all legal-size fish, fish taken by pinnipeds, and all undersize fish. Legal catch represented only fish of legal size landed by anglers. Our rationale for using total catch was that all fish, regardless of size, have an equal probability of being taken by pinnipeds; therefore, comparisons with total catch were a more accurate metric for quantifying the impact of pinnipeds on the salmon fishery. Comparisons with the legal catch inflated the percentage of fish taken by pinnipeds and exacerbated the perception of the problem of pinnipeds interacting with salmon fisheries. However, previous researchers have compared percentage takes by pinnipeds with legal catch; therefore we also made the comparison with legal catch to place our results in a historical context.

Mean percentages of fish taken by sea lions in relation to total catch (referred to as "mean percentage of fish taken by sea lions") for the commercial, CPFV, and skiff fisheries for onboard and dockside surveys from 1997 to 1999 were non-normal in distribution and were transformed by using the arcsine transformation for parametric statistical comparisons (Zar, 1996). Mean percentages of fish taken by sea lions in the three fisheries (commercial, CPFV, and skiff) were compared between onboard and dockside surveys, among years (1997 to 1999), between seasons (sea lion breeding and

nonbreeding seasons), and between takes (surface and below surface) using a Student's *t*-test and ANOVA or a Mann-Whitney *U*-test and Kruskal-Wallis test for data that were non-normal and heteroscedastic after transformation.

Sea lion breeding and nonbreeding seasons from 1997 to 1999 were determined by using aerial and ground counts from Weise (2000). The breeding season was designated as the time when a significant decline in the number of breeding adult males was recorded at haul-out sites in the Monterey Bay region, when animals were presumably heading for the breeding rookeries in southern California. Typically the breeding season is from June and July, and the nonbreeding season occurs during the months of March, April, May, August, and September.

Mean catch per unit of effort, or the numbers of fish hooked per day per boat, in commercial, CPFV, and skiff fisheries data were non-normal and heteroscedastic, therefore, they were transformed by using $\sqrt{\text{count} + 1}$ (Harvey, 1987; Zar, 1996). Mean catch per unit of effort for the three fisheries was compared among years with an ANOVA.

To estimate the impact of California sea lion depredation on salmon populations in Monterey Bay we compared estimated numbers of hooked salmon taken by sea lions and the Central California Valley index (CVI) for chinook salmon abundance. The CVI is the numbers of ocean- and inland-harvested Chinook salmon and the sum of all runs of chinook on the Sacramento Rivers (PFMC⁴) and represents presumably the population of salmon passing through the Monterey Bay region during the fishery season. The estimated number of salmon taken was calculated from the observed number of takes in the commercial and recreational fishery multiplied by the percentage of the total catch that was sampled. Percentage of the total catch sampled was estimated by dividing the number of observed legal-size fish landed by the total number of legal-size fish landed (CDF&G, unpubl. data⁷).

Monetary losses resulting from sea lion interactions with salmon fisheries were estimated by evaluating numbers of fish taken by sea lions and types and quantities of fishing gear damaged or lost during these interactions. Information for the analysis of monetary losses was collected during dockside and onboard surveys for commercial and recreational salmon fisheries.

Annual monetary losses resulting from fish taken by sea lions were calculated by using total numbers of estimated takes by sea lions, average dressed mass (mass of gutted and cleaned fish) of salmon landed in Monterey from 1997 to 1999, and average exvessel price (wholesale price per pound of fish paid to fishermen) for chinook salmon in California from 1997 to 1999 (PFMC⁴). Estimated numbers of takes by sea lions in Monterey Bay from 1997 to 1999 were a function of

⁷ CDF&G (California Department of Fish and Game). 2004. Ocean Salmon Project database. CDF&G Ocean Salmon Project, 475 Aviation Blvd., Suite 130, Santa Rosa, CA 95403.

numbers of observed takes (based on dockside samples) and proportions of the total catch sampled.

Estimates of lost and damaged gear were calculated by using average costs for each type of gear used in commercial and recreational salmon fishing operations. A survey of the seven local retail fishing tackle stores in Santa Cruz, Moss Landing, and Monterey was used to estimate mean value of each type of fishing gear used in the recreational (CPFV and skiff combined) salmon fishery. All charter-fishing companies in the three ports in Monterey Bay were surveyed to estimate mean cost of a "setup" sold by charter boat companies to customers. A "setup" was defined as a hook and leader, or a hook, leader, and a 4 oz. or 8 oz. lead sinker. Costs of commercial fishing gear were estimated by surveying 19 local fishermen from the three ports in Monterey Bay. Commercial fishermen buy the majority of their gear in bulk, and often by mail order to reduce costs.

Results

From 1997 to 1999, 1745 hours of onboard surveys and dockside interviews were conducted in the commercial and recreational salmon fisheries. In 1997, 337 hours of onboard and dockside surveys were conducted, 144 hours in the commercial fishery, 103 hours in the CPFV fishery, and 90 hours in the skiff fishery. In 1998, 704 hours of onboard and dockside surveys were conducted: 370 hours in the commercial fishery, 270 hours in the CPFV fishery, and 64 hours in the skiff fishery. During 1999, 704 hours of onboard and dockside surveys were conducted, 410 hours in the commercial fishery, 258 hours in the CPFV fishery, and 36 hours in the skiff fishery. Increased sampling effort in 1998 and 1999 were the result of increased onboard survey effort in the commercial and CPFV fisheries.

During this study 101 onboard surveys and 2780 dockside interviews (number of boats sampled) were conducted in the commercial and recreational salmon fisheries. There were no significant differences in mean percentages of fish taken by sea lions between onboard and dockside surveys in the commercial (1997, $P=0.329$; 1998, $P=0.623$; 1999, $P=0.653$), CPFV (1997, $P=0.276$; 1998, $P=0.660$; 1999, $P=0.327$) and skiff fisheries (1997, $P=0.052$; Fig. 2). We assumed, therefore, that dockside surveys provided a representative measure of pinniped takes in the salmon fisheries and onboard survey data were pooled with dockside interview data for subsequent analysis.

A total of 967 interviews with commercial fishermen and 1813 interviews with recreational fishermen were conducted at dockside in Monterey Bay, accounting for 41,895 and 15,115 hooked salmon, respectively (Table 2). In the commercial fishery a similar number of interviews were conducted in 1997 and 1998, whereas in 1999 approximately 21.2% greater numbers of interviews were conducted with the same effort. However, the number of fish landed in 1999 was significantly less than in 1997 and 1998. In the CPFV fishery, the trend

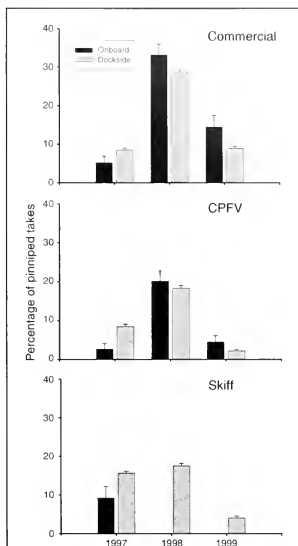


Figure 2
Percentage of pinniped takes in relation to the total number of salmon hooked as determined from dockside and onboard surveys for the commercial, commercial passenger fishing vessel (CPFV), and personal skiff fisheries in Monterey Bay, California, from 1997 to 1999. Onboard survey effort concentrated in CPFV and commercial fisheries during 1998 and 1999. Error bars indicate one standard error.

was similar to the commercial fishery, but the number of fish landed and the number of boats surveyed was significantly fewer overall. In the skiff fishery, there was a steady decline in the number of fishermen surveyed and the number of fish landed from 1997 to 1999.

Onboard observations combined with dockside interviews revealed that California sea lions were almost exclusively responsible for the depredation of hooked salmon in the commercial and recreational fisheries in Monterey Bay, taking 98.4% of the 1199 observed hooked salmon from 1997 to 1999. Of the estimated 2420 takes in 1997, 1072 were directly observed surface takes and sea lions were identified in 98.6% of the takes (Table 2). In 1998, approximately 501 of 5542 takes

Table 2

Yearly catch statistics and estimates of the number and percentage of salmon taken by pinnipeds in the commercial, commercial passenger fishing vessel (CPFV), and skiff salmon fisheries during dockside surveys in Monterey Bay in 1997, 1998, and 1999.

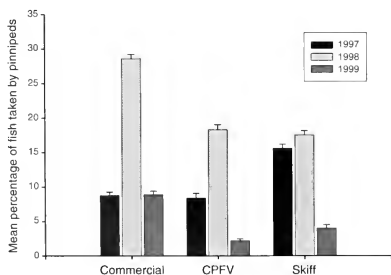
Fishery	Year	Number dockside interviews	Catch statistics			Number of takes		Percentage of takes	
			Total number of fish hooked	Number of legal-size fish landed	Number of under-size fish	Number of fish taken at surface	Number of fish taken below surface	Total % of total catch lost	Total % of total catch lost
Commercial	1997	297	17,943	12,288	4124	522	1009	12.5	8.5
	1998	293	15,446	6206	4829	97	4314	71.1	28.6
	1999	377	8506	6785	966	37	718	11.1	8.9
	Total	967	41,895	25,279	9919	656	6041	26.5	16.0
CPFV	1997	139	5168	3157	1577	247	187	13.7	8.4
	1998	179	4694	3267	569	305	553	26.3	18.3
	1999	58	362	319	35	6	2	2.5	2.2
	Total	376	10,224	6743	2181	558	742	19.3	12.7
Skiff	1997	723	2926	1643	828	303	152	27.7	15.6
	1998	538	1564	882	409	99	174	31.0	17.5
	1999	176	401	315	70	8	8	5.1	4.0
	Total	1437	4891	2840	1307	410	334	26.2	15.2

occurred at the surface, and sea lions were identified in 98.4% of those takes. In 1999, 51 of the 779 takes occurred at the surface, and sea lions were responsible for 96.1% of the takes. We assumed sea lions took similar percentages of fish below the surface. As evidence of takes below the surface, sea lions would come to the

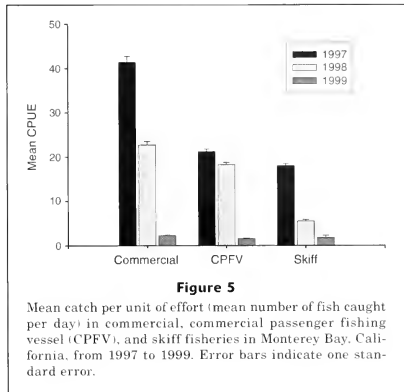
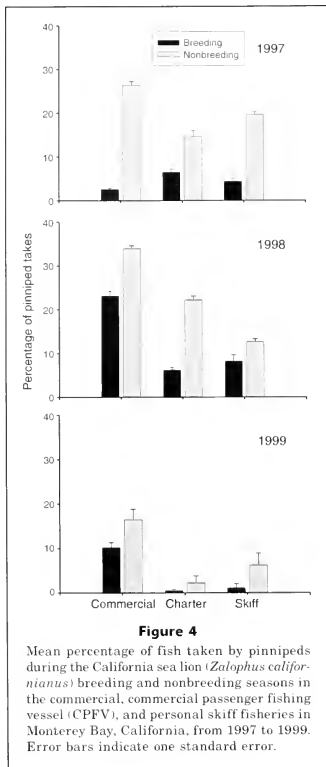
surface within minutes with a fish. Pacific harbor seal (*Phoca vitulina richardsi*) was responsible for other observed takes.

Percentages of the catch taken by sea lions, based on pooled dockside and onboard surveys, were significantly different among years in the commercial ($P < 0.000$), CPFV ($P < 0.000$), and skiff fishery ($P < 0.000$; Fig. 3). During 1998, significantly greater percentages of salmon were taken in the commercial (Tukey HSD multiple comparison, $P < 0.000$), CPFV (Tukey HSD multiple comparison, $P < 0.000$), and skiff fisheries (Tukey HSD multiple comparison, $P < 0.000$). Whereas during 1999, the CPFV (Tukey HSD multiple comparison, $P < 0.000$) and skiff fisheries (Tukey HSD multiple comparison, $P < 0.000$) experienced significantly smaller percentages of sea lion takes. In the commercial fishery there was no difference in the percentage of fish taken between 1997 and 1999.

Although the timing of the sea lion migration varied by year (Weise, 2000), the percentages of takes by sea lions were greater during the nonbreeding season than during the breeding season in all three years (Fig. 4). In the commercial fishery, those differences were significant for all three years (1997, $P < 0.000$; 1998, $P = 0.001$; 1999, $P = 0.041$). In the CPFV fishery, significantly more takes occurred during the nonbreeding season in 1997 ($P = 0.010$), and 1998 ($P < 0.000$); however, there was no significant difference in 1999 ($P = 0.358$). In the skiff fishery, significantly more takes by sea lions occurred during the non-

**Figure 3**

Mean percentage of salmon taken by California sea lion (*Zalophus californianus*) as determined from onboard and dockside surveys of the commercial, commercial passenger fishing vessel, and skiff fisheries in Monterey Bay, California, from 1997 to 1999. Error bars indicate one standard error.



surveys combined, percentages of takes by sea lions below the surface of the water varied throughout the season and were significantly greater than surface takes in 1997 ($P=0.001$), 1998 ($P<0.000$), and 1999 ($P<0.000$; Table 2). In contrast, in the recreational fishery the percentages of takes by sea lions occurred at the surface and at the surface varied by year. During 1997, greater percentages of takes by sea lions occurred at the surface than below the surface on CPFVs ($P=0.082$) and skiffs ($P=0.001$; Table 2). Whereas in 1998, significantly greater percentages of takes occurred below the surface in the CPFV ($P<0.000$) and skiff fisheries ($P<0.000$; Table 2). And in 1999, no differences between surface and below surface takes were detected for CPFV ($P<0.972$) or skiff fisheries ($P<0.310$); however this lack of significance was likely due to small sample sizes.

The catch per unit of effort (CPUE: number of fish landed per boat per day) was significantly less in 1998 than in 1997 for the commercial ($P<0.000$), CPFV ($P=0.011$), and skiff fisheries ($P<0.000$) in Monterey Bay (Fig. 5). In 1999, significantly fewer fish were caught than in 1998 and 1997 in the commercial ($P<0.000$) and CPFV ($P<0.000$) fisheries; however, there was no significant difference in the skiff fishery. The percentage of the CVI abundance for chinook salmon taken by sea lions from 1997 to 1999 ranged from 1.4% to 6.2% (Table 3).

From 1997 to 1999, commercial fishermen lost an estimated \$22,333–\$60,077 of gear, and \$224,011–\$504,548 worth of fish as a result of interactions with sea lions (Table 4). The recreational fisheries lost between \$172 and \$18,533 worth of gear as a result of sea lion interactions from 1997 to 1999. Estimates of gear and fish loss were extrapolated from observed losses to total losses based on percentages of the fisheries that were sampled. Gear types varied among commercial

breeding season of 1997 ($P<0.000$), whereas in 1998 ($P=0.158$) and 1999 ($P=0.358$) there was no significant difference. During all three years, surveys were conducted on commercial, CPFV, and skiff fisheries during August and September; however, there was little to no salmon fishing effort because of the perceived sea lion problem and because the remaining fishermen targeted albacore tuna or rockfishes (or both).

Because of the different styles of hook-and-line fishing in the commercial troll and recreational salmon fisheries, sea lions were more likely to take fish below the surface from commercial trollers but to take fish at and below the surface from recreational vessels. In the commercial fishery, according to dockside interviews and onboard

Table 3

Estimates of the pinniped predation index derived from estimates of observed takes of salmon by sea lions (*Zalophus californianus*) in Monterey Bay in relation to the California Central Valley chinook abundance index from 1997 to 1999. Data for Central Valley chinook abundance index were obtained from Pacific Fisheries Management Council, 1999.

Year	Estimated pinniped takes			Central Valley chinook abundance index (Ocean + river totals)	Pinniped predation index (%)
	Commercial	Recreational	Total		
1997	24,258	14,576	24,258	1,055,300	2.2
1998	40,585	9868	40,585	611,800	6.2
1999	8780	269	8780	636,500	1.4

Table 4

Estimates of monetary impact of California sea lion interactions with commercial and recreational salmon fisheries resulting in gear and fish loss in Monterey Bay from 1997 to 1999. Recreational fishery includes commercial passenger fishing vessels and private skiffs. Value of commercial fishery revenues were obtained from the California Department of Fish and Game ocean salmon database. n/a=not applicable.

Fishery	Year	Percentage fishery sampled	Value of gear loss	Value of fish loss	Commercial revenues	Equivalent percentage of commercial revenue lost
Commercial	1997	6.3	\$51,609	\$375,470	\$2,651,499	14.2
	1998	10.9	\$60,077	\$504,548	\$598,062	84.4
	1999	8.6	\$22,333	\$224,011	\$874,100	25.6
Recreational	1997	6.1	\$18,533	n/a	n/a	n/a
	1998	11.5	\$16,485	n/a	n/a	n/a
	1999	8.9	\$172	n/a	n/a	n/a

and recreational fisheries, and gear cost for each fishery varied greatly; therefore, an average estimate for each gear type was used to estimate gear loss for commercial and recreational fisheries. Total revenue losses as a result of fish taken by sea lions in the commercial fishery were equivalent to between 14.2% and 84.4% of the total salmon fishery revenues.

Discussion

Conflicts between pinnipeds and fisheries are well documented in California (Briggs and Davis, 1972; Fiscus, 1979; Ainley et al., 1982; Miller et al.⁶; Hanan et al., 1989; Beeson and Hanan¹; NMFS²). California sea lions have been the primary pinniped species involved in taking fish in ocean commercial and recreational salmon fisheries (Miller et al.⁶; Hanan et al., 1989; Beeson and Hanan¹). In comparing present results and past studies it is imperative to distinguish between the percentage of salmon taken by pinnipeds relative to the number of legal size fish landed (i.e. legal catch) and number of pinniped takes relative to total number of fish hooked (i.e., total catch). The former value inflates percentages by not including undersize fish caught, whereas the latter

includes all fish hooked in the calculation and assumes all fish, regardless of size, have an equal probability of being taken by sea lions.

Dockside surveys were representative of the magnitude of interactions between sea lions and salmon fisheries because there were no significant differences in mean percentages of takes by sea lions between onboard and dockside surveys. Onboard surveys alone would not provide sufficient samples to adequately assess levels of interactions between sea lions and salmon fisheries; conversely, the validity of dockside surveys alone would be questionable because of biases associated with dockside surveys. Biases included fishermen not providing truthful information, fishermen avoiding the survey, fishermen not answering all questions, and not all fishermen returning to the docks. Combining onboard and dockside surveys enabled us to verify dockside findings, obtain sufficient levels of sampling for comparisons, and directly observe and understand the nature of the interactions.

The percentage of hooked salmon taken by sea lions in the commercial salmon fishery in relation to the legal catch has increased by at least 8% since the 1970s and 1980s. Briggs and Davis (1972) reported that California sea lions took 4.1% of all salmon hooked during the

1969 commercial and sport salmon season, Miller et al.⁶ reported that in 1981 sea lions took 3.0% of the legal catch during commercial salmon activities, and Beeson and Hanan¹ found that sea lions took 15% of the legal catch in commercial fisheries in 1995. In Monterey Bay in 1997, 12.5% of the legal catch was taken by sea lions, 71.1% in 1998, and 11.1% in 1999.

Predation levels in the CPFV fishery have increased by at least 8% since 1983, and approximately 3% since 1995. Miller et al.⁶ reported predation rates of 5.2% for the CPFV legal catch in Monterey Bay, and Beeson and Hanan¹ reported predation rates of 10.5% of the legal catch for the recreational fishery in 1995 (CPFV and private skiff combined). In Monterey Bay, 13.7% of the legal catch was taken by sea lions in 1997, 26.3% in 1998, and 2.5% in 1999.

In the skiff portion of the recreational salmon fishery, predation of the legal catch has increased by at least 26% since 1983, and 17% since 1995. Miller et al.⁶ reported predation levels of 1.4% on the legal catch for skiff fisheries in Monterey Bay, and Beeson and Hanan¹ reported predation levels of 10.5% on the legal catch for the 1995 recreational fishery season (CPFV and private skiff combined). In Monterey Bay, predation on the legal catch was 27.7% in 1997, 31.0% in 1998, and 5.1% in 1999. Skiff fishermen typically fish in large groups called "the fleet." Sea lions had a greater probability of getting a hooked salmon when there were greater numbers of hooks in the water; therefore, sea lions most likely target a fleet of fishing boats. Skiff fishermen caught fewer fish than did commercial or CPFV fishermen, but lost a proportionally greater number of fish to sea lions.

The greatest levels of sea lion predation in commercial and recreational fisheries occurred in spring when the greatest numbers of adult male sea lions were migrating south to breeding rookeries in southern California and Baja California, Mexico. In 1997 and 1999, predation levels dropped significantly in June and July following a high level in May, corresponding to declines in numbers of sea lions in Monterey Bay as males headed southward to breeding colonies (Weise, 2000). In 1998, loss of catch to sea lions was greatest in May; slight decreases occurred in percentages of fish taken during June and July because the decline in numbers of adult male sea lions during the breeding season was far less and shorter in duration than in June and July of 1997 and 1999.

We concluded that adult male sea lions took the majority of hooked fish because animals identified taking fish during boat surveys were almost exclusively adult male sea lions and percentages of fish taken by sea lions were less during the sea lion breeding season. Briggs and Davis (1972), Miller et al.⁶, and Beeson and Hanan¹ also reported greater numbers of salmon taken in spring (the nonbreeding season) in the commercial and recreational salmon fisheries. Loss of catch to sea lions would most likely be greater during the northward migration of male sea lions because greater numbers of animals would be in the Monterey Bay re-

gion; however, fishing effort declined sharply and the commercial season was closed during a portion of that period in 1997.

Sea lions took most salmon below the water's surface in the commercial fishery and both at and below the surface in recreational fisheries. Commercial fishermen lost fish below the surface as a result of the large amount of trolling gear used, and the time required for pulling gear when fish were hooked. Commercial fishermen typically need five to 10 minutes, and as long as 20 minutes to pull hooked fish from the water, allowing ample time for sea lions to take fish. Before the 1994 amendments to the MMPA, sea lions were legally killed for endangering commercial catches, gear, and fishermen, and are still at risk for harassment for taking fish off hooks today. Consequently, most fish in the commercial fishery are taken below the surface and consumed at the surface some distance from the boat because of a combination of the time required to bring a fish to the surface and the threat of harassment. Less gear and perhaps different types of gear that can bring a fish to the surface faster may reduce the number of takes below the surface and overall predation levels. In recreational fisheries, fishermen typically used rod and reel, which allowed fish to be reeled in within minutes. It has been illegal for recreational fishermen to harass or kill sea lions since the passage of the MMPA in 1972; therefore it is not uncommon to see sea lions swimming next to recreational boats in close pursuit of fish that are pulled from the water or that are taken just before they are netted.

Increased depredation levels in the commercial and recreational salmon fisheries in 1998 were most likely the result of the large El Niño Southern Oscillation (ENSO) event that occurred during 1997-98. The 1997-98 ENSO event created large anomalies in physical and biological conditions in the coastal waters off California resulting in above average seasonal norms in sea surface temperatures and large displacements in the distribution of many fish species (Lynn et al., 1998). A combination of factors during the large ENSO event contributed to increased predation on salmon catches. These factors included shifts in sea lion prey composition, decreases in sea lion prey populations, increases in number of sea lions in the region, decreases in fishing effort by commercial and recreational salmon fishermen, and decreases in number of salmon landed. Intensified depredation of catch has been reported during past ENSO events by commercial gillnet fishermen (Beeson and Hanan¹).

Increased intensity in depredation of hooked fish by pinnipeds during ENSO events may be indicative of decreased foraging success resulting from shifts in prey availability and abundance. A significant shift in sea lion diet occurred between 1997 and 1998 from market squid, northern anchovy, and Pacific sardine to Pacific sardine and anchovy (Weise, 2000). Concurrently, commercial catches of squid, hake, and herring, common prey of sea lions, were low or virtually nonexistent from the fall of 1997 through the summer of 1998 (CalCOFI,

1999). In May 1998, the catch rate for pelagic-young-of-the-year rockfish was the lowest in the history of tri-annual rockfish surveys (Lynn et al., 1998). It is, therefore, reasonable to assume that sea lions were probably nutritionally stressed by the lack of prey and change in prey species and found a hooked salmon an attractive and easy meal.

Mean numbers of California sea lions recorded during the northward migration in summer and autumn of 1998 were approximately 2000 individuals greater than in the summer and autumn of 1997 and 1999, most likely in response to poor foraging conditions in southern California resulting from ENSO conditions (Weise, 2000). During the 1983 and 1992 ENSO events, numbers of sea lions increased along the central California coast owing to the enhancement of the normal northward migration of sea lions resulting from poor food availability in the Southern California Bight (Sydeman and Allen, 1999). During the 1983–84 ENSO, older juvenile sea lions migrated in greater than usual numbers from southern to central California (Trillmich et al., 1991). Greater numbers of female sea lions were counted on Año Nuevo Island in summer and fall 1998, presumably in response to poor foraging conditions in southern California (Morris, unpubl. data⁶). Increases in numbers of sea lions in Monterey Bay during 1998 were most likely due to increases in numbers of juveniles and adult females that moved northward because of the lack of schooling prey species in southern California resulting from the ENSO.

Presumably as a result of ENSO conditions, total landings of salmon and the catch per unit of effort in commercial and recreational fisheries were significantly less in 1998 than in 1997. During our sampling effort in 1998, approximately 2000 fewer fish were landed in commercial and recreational fisheries than in 1997, although approximately double the percentages of fisheries (total salmon landings) were sampled dockside. Numbers of salmon landed in Monterey Bay in 1998 decreased by 59.6% in the commercial fishery and 49.4% in the recreational fishery (PFMC⁴). In California during 1998, numbers of salmon landed in the commercial fishery were 55.7% less than in 1997, and 46.7% less in the recreational fishery. In 1998, CPUE of the commercial fishery declined proportionally more than in other fisheries, which corresponded to proportionally greater percentages of fish taken by sea lions. In Monterey Bay, numbers of angler trips in 1998 declined by 38.6% in the commercial fishery, and 39.9% in the recreational fishery (PFMC⁴). Therefore, there were fewer boats actively fishing, fewer fish being landed, and greater numbers of sea lions in the area, under these conditions, when a fish was hooked, it was more likely to be depredated.

Conversely, in 1999 the depredation levels in the commercial and recreational salmon fisheries in Monterey

Bay were significantly less as a result of cool and highly productive La Niña oceanographic conditions. Following one of the strongest ENSO events on record during 1997–98, there was a dramatic transition to highly productive cool-water La Niña conditions and anomalous, upwelling-favorable, wind forcing along the West Coast (Schwing et al., 2000). Upwelling anomalies off the central California coast during 1999 were the greatest in the 54-year record of the upwelling index (Schwing et al., 2000). Record harvest levels of Pacific sardines (CalCOFI, 2000) and greater frequency of occurrence of sardine in the diet of sea lions in central California during the 1999 La Niña (Weise, 2000) indicated that ample prey fishes were available for foraging California sea lions; therefore, depredation pressure on the salmon fisheries was reduced.

Monterey Bay was selected for the present study because it experienced the greatest levels of depredation during the 1995 commercial and recreational fisheries season (Beeson and Hanan¹). Although Monterey Bay experienced increased levels of pinniped predation in recreational fisheries in 1997 and commercial and recreational fisheries in 1998, these levels were probably not representative of the whole California coast but were more likely the worst-case scenario. Pinniped depredation may be increasing in other areas along the California coast as the sea lion population increases, but probably not to the degree that was observed in Monterey Bay. Pinniped predation of hooked fish in salmon fisheries is probably spatially and temporally variable. Whereas this variability complicates evaluating pinniped impacts on fisheries, it is important for fishery managers to take this variability into account.

Estimated levels of depredation reported for the commercial and recreational salmon fisheries in Monterey Bay may be affected by many assumptions. Lack of direct validation for information received during dockside surveys had unknown impacts on estimates of predation levels, but concurrent onboard sampling appeared to alleviate this bias. Commercial and private skiff salmon boats bypass the sampling docks when no fish are landed or they dock in a harbor slip. Boats that bypass sampling docks may have no fish because of predation by sea lions, and not sampling these boats would result in underestimates of predation levels, but the magnitude of this decrease was difficult to evaluate. Surveys of fishermen were limited by crew cooperation and therefore, not all fishing styles and locations were sampled. The lack of some data would have an impact on predation levels. Surveys of fishermen also were limited to boats fishing for one day because boats fishing for multiple days often fished outside the study area during the course of a trip; however, boats fishing for multiple days were surveyed at dockside so that any biases of onboard samples would have been detected in comparisons of dockside and onboard predation levels.

Depredation of salmon by California sea lions in Monterey Bay could negatively impact salmon populations along the Central California coast. Pinniped depredation of hooked salmon from the California Central

⁶ Morris, P. A. 1999. Abstract. 13th Biennial conference on the biology of marine mammals; Maui, HI, 131 p. The Society for Marine Mammalogy. <http://www.marinemammalogy.org/>

Valley chinook salmon population went from a low of approximately 1.4% during a non-ENSO year to an estimated 6.2% during an ENSO season. High harvest levels coupled with high natural depredation of salmon during an ENSO year could be devastating for the Central Valley Chinook salmon population. Further, when sea lions take fish in the fishery, fishermen continue to fish to replace depredated fish, further impacting the salmon population. Hooked salmon lost to sea lions are losses to the population and need to be considered when determining allotments, quotas, and area closures. To better estimate impacts of sea lion predation on the CVI, concurrent studies of sea lion and salmon fishery interactions and sea lion food habits need to be conducted along the entire Central California coast, including Half Moon Bay, San Francisco Bay, and the Farrallon Islands. Sea lions are only one of many natural predators of commercially important fish species. Identifying other natural predators and assessing their impact on prey populations is difficult but necessary for effective fisheries management.

It is likely that only a small proportion of the sea lion population, particularly adult males, were responsible for salmon taken off hooks in salmon fisheries. Percentages of fish taken off the hook declined in all years when adult males moved south during the breeding season in June and July. However, greater percentages of takes occurred in the fisheries in August and September when lesser numbers of adult male sea lions were present in the region. On any given fishing day peak numbers of sea lions were counted at haul-out sites from late-morning to early afternoon, which is also the period when most fishing occurred (Weise, 2000). Miller et al.⁶ suggested that the total damage to fisheries by California sea lions was not proportional to the number of sea lions in the area. It is likely that takes on a given day in Monterey Bay were repeat occurrences by the same animals. We agree with DeMaster et al. (1982) that a reduction in the number of animals or culling of the population would probably not reduce sea lion depredation levels unless the few animals responsible were identified and removed. Instead, there is a need for nonlethal deterrents to keep sea lions from taking hooked fish in open-ocean fisheries. A change in types of fishing gear, a limit in the amount of gear in the water, use of various harassment techniques, as well as area closures and a tolerance for sea lion predation most likely encompass other possible management options.

An increasing sea lion population and increased interactions with salmon fisheries resulting in salmon and gear losses will certainly affect individual fishermen negatively and possibly California's economy (Beeson and Hanan¹). Comparisons of economic losses between years and among studies must consider average fish weight, exvessel price per year, and definitions of fishing regions. For example, if greater numbers of fish were lost in a given year but exvessel prices were low, the overall economic impact would be less than during a year when fewer fish were taken but the exvessel prices were high.

In past studies, all ports in California were surveyed, and impacts were analyzed by port, but these studies encompassed different fishing areas under the same port names. For example, Miller et al.⁶ estimated annual losses resulting from sea lion interactions in 1980 at \$274,000 for California, and an estimated \$21,536 for Monterey Bay. It is unclear, however, if these figures included fishing areas south of Monterey, such as Morro Bay, and fishing areas north, such as Half Moon Bay. Beeson and Hanan¹ estimated 86,900 fish or \$1,734,000 was lost in 1995 because of sea lion interactions, and 48,000 fish were taken in Monterey, representing approximately \$960,000. Beeson and Hanan¹ included the Port of Princeton in Half Moon Bay in figures reported for Monterey. Therefore, it was not possible to make direct comparisons among studies, but it appears that economic losses per individual fisherman have increased since the 1980s and will probably continue to increase if the sea lion population and interactions with salmon fisheries increase. Assessment of economic impacts of salmon fisheries in Monterey Bay in the present study was limited to gear and fish loss; however impacts are most likely widespread. For example, during the salmon season when interactions with sea lions are great, CPFV operators report that customers will cancel or postpone trips, which decreases the amount of money infused into the local economy from trip expenditures, including hotel stays, restaurants meals, and gas. Estimating the economic impact of sea lion interactions on the local economy of Monterey Bay was beyond the scope of our study.

Discussions about the competition between sea lions and fisheries tend to arouse controversy because of the complex mix of biological, economic, social, political, and moral factors involved (Harwood and Crossall, 1988). Fishermen claim regularly that their activities are regulated, whereas predation by marine mammals is unrestricted (Harwood, 1992). Although losses in Monterey Bay in 1998 were most likely anomalously large because of ENSO conditions, this anomaly offered little reassurance to those fishermen whose livelihoods were threatened. Growing sea lion populations have undoubtedly intensified competition with fisheries, but greater fishing effort, more sophisticated fish equipment and fisheries methods, and less than rigorous fisheries management is equally responsible. Segments of the American public find marine mammals appealing and demand that populations be protected; whereas other segments demand protection from economic ruin resulting from marine mammal-fishery interactions. Clearly, demands from both segments of the public must be addressed (Everitt and Beach, 1982). Continued research to assess and refine our understanding of food habits of marine mammals is essential, and incorporating this information into fisheries management is equally important. When conflicts between fisheries and marine mammals are identified, population management strategies and nonlethal deterrent solutions need to be developed. Any management solutions need to consider not only the specific interactions but also the ecosystem as a whole and the viewpoints of all segments of the public.

Acknowledgments

This study could not have been completed without all the help from MLML students and Bird and Mammal Laboratory interns. We thank Tomoharu Eguchi, Tony Orr, Tony Alisea, Laird Henkel, Stori Oates, Jeff Field, Joe Bizarro, Julie Neer, Scott Benson, Denise Greig, Sarah Wilkin, Anu Kumar, Aviva Barsky, Meisha Key, Sean Lema, Lydia Neilson, Guido Parra, Mimi Reyes, Greg Cunningham, Sharon Uptide, Michelle Garcia, Inger-Marie Laursen, Cina Loarie, Judd Weiss, Kate Willis, and Wendy Cover for the countless hours spent undertaking dockside and onboard surveys. Scott Davis was instrumental in aerial photography for aerial surveys. We extend special thanks to the commercial, charter boat, and personal skiff fishermen, deckhands, and captains for their cooperation; this research would not have been possible without their help. This project was supported by funding from the Fishermen's Alliance of California, Monterey Bay Chapter, The David and Lucille Packard Foundation, and the National Marine Fisheries Service. We are grateful for constructive comments by Gregor Cailliet, Robert DeLong, and two anonymous reviewers.

Literature cited

- Ainley, D. G., H. R. Huber, and K. M. Bailey.
1982. Population fluctuations of California sea lions and the Pacific whiting fishery off Central California. *Fish. Bull.* 80:253-258.
- Aurioles-Gamboa, D., and A. Zavala-Gonzalez.
1994. Ecological factors that determine distribution and abundance of the California sea lion *Zalophus californianus* in the Gulf of California. *Ciencias Marinas* 20:535-553.
- Briggs, K. T., and C. W. Davis.
1972. Study of predation by sea lions on salmon in Monterey Bay. *Calif. Fish Game* 58(1):37-43.
- CalCOFI (California Cooperative Oceanic Fisheries Investigation).
1999. Review of some California fisheries for 1998: Pacific sardine, Pacific mackerel, Pacific herring, market squid, sea urchin, groundfishes, swordfish, sharks, nearshore finfishes, abalone, dungeness crab, prawn, ocean salmon, white seabass, and recreational fishery. *CalCOFI Rep.* 40:9-27.
2000. Review of some California fisheries for 1999: Market squid, dungeness crab, sea urchin, prawn, abalone, groundfish, swordfish and sharks, ocean salmon, nearshore finfishes, Pacific sardine, Pacific herring, Pacific mackerel, reduction, white seabass, and recreational. *CalCOFI Rep.* 41:8-25.
- DeMaster, P. D., D. J. Miller, D. Goodman, R. L. DeLong, B. S. Stewart.
1982. Assessment of California sea lions fishery interactions. *In* Marine mammals: conflicts with fisheries, other management problems, and research needs (D. G. Chapman, L. L. Eberhardt, eds.), p. 253-263. *Trans.* 47th North Am. Wildlife and Nat. Res. Conference. Wildlife Management Institute, Washington, D.C.
- Everitt, R. D., and R. J. Beach.
1982. Marine mammal-fisheries interactions in Oregon and Washington: an overview. *In* Marine mammals: conflicts with fisheries, other management problems, and research needs (D. G. Chapman and L. L. Eberhardt, eds.), p. 265-277. *Trans.* 47th North Am. Wildlife and Nat. Res. Conference. Wildlife Management Institute, Washington, D.C.
- Fiscus, C.
1979. Interactions of marine mammals and Pacific hake. *Mar. Fish. Rev.* 41(10):1-9.
- Hanan, D. A., L. M. Jones, and R. B. Read.
1989. California sea lion interaction and depredation rates with the commercial passenger fishing vessel fleet near San Diego. *CalCOFI Rep.* 30:122-126.
- Harvey, J. T.
1987. Population dynamics, annual food consumption, movements, and dive behavior of harbor seals, *Phoca vitulina*, in Oregon. Ph.D. diss., 177 p. Oregon State Univ., Corvallis, OR.
- Harwood, J.
1992. Assessing the competitive effects of marine mammal predation on commercial fisheries. *S. Afr. J. Mar. Sci.* 12:689-693.
- Harwood, J., and J. P. Croxall.
1988. The assessment of competition between seals and commercial fisheries in the North Sea and the Antarctic. *Mar. Mamm. Sci.* 4(1):13-33.
- Lynn, R. J., T. Baumgartner, J. Garcia, C. A. Collins, T. L. Hayward, K. D. Hyrenbach, A. W. Mantyla, T. Murphee, A. Shankle, F. B. Schwing, K. M. Sakuma, and M. J. Tegner.
1998. The state of the California Current, 1997-98: transition to El Niño conditions. *CalCOFI Rep.* 39:25-49.
- Schwing, F. B., C. S. Moore, S. Ralston, K. M. Sakuma.
2000. Record coastal upwelling in the California Current in 1999. *Cal. Coop. Ocean Fish* 41:148-160.
- Starr, R. M., K. A. Johnson, E. A. Laman, G. M. Cailliet.
1998. Fishery resources of the Monterey Bay National Marine Sanctuary. Publication No. T-042, 102 p. California Sea Grant College System, Univ. California, La Jolla, CA.
- Sydemann, W. J., and S. G. Allen.
1999. Pinniped population dynamics in central California: correlations with sea surface temperature and upwelling indices. *Mar. Mamm. Sci.* 15(2):446-461.
- Trillmich, F., K. A. Ono, D. P. Costa, R. L. DeLong, S. D. Feldkamp, J. M. Francis, R. L. Gentry, C. B. Heath, B. J. LeBoeuf, P. Majluf, and A. E. York.
1991. The effects of El Niño on pinniped populations in the eastern Pacific. *In* Pinnipeds and El Niño: responses to environmental stress (F. Trillmich and K. A. Ono, eds.), p. 247-270. Springer-Verlag, Berlin.
- Weise, M. J.
2000. Abundance, food habits, and annual fish consumption of California sea lion (*Zalophus californianus*) and its impact on salmonid fisheries in Monterey Bay, California. M.S. thesis, 103 p. San Jose State Univ., San Jose, CA.
- Zar, J. H.
1996. Biostatistical analysis, 3rd ed., 662 p. Prentice-Hall, Upper Saddle River, NJ.

Abstract—Growth of a temperate reef-associated fish, the purple wrasse (*Notolabrus fucicola*), was examined from two sites on the east coast of Tasmania by using age- and length-based models. Models based on the von Bertalanffy growth function, in the standard and a reparameterized form, were constructed by using otolith-derived age estimates. Growth trajectories from tag-recaptures were used to construct length-based growth models derived from the GROTAG model, in turn a reparameterization of the Fabens model. Likelihood ratio tests (LRTs) determined the optimal parameterization of the GROTAG model, including estimators of individual growth variability, seasonal growth, measurement error, and outliers for each data set. Growth models and parameter estimates were compared by bootstrap confidence intervals, LRTs, and randomization tests and plots of bootstrap parameter estimates. The relative merit of these methods for comparing models and parameters was evaluated; LRTs combined with bootstrapping and randomization tests provided the most insight into the relationships between parameter estimates. Significant differences in growth of purple wrasse were found between sites in both length- and age-based models. A significant difference in the peak growth season was found between sites, and a large difference in growth rate between sexes was found at one site with the use of length-based models.

Estimates of growth and comparisons of growth rates determined from length- and age-based models for populations of purple wrasse (*Notolabrus fucicola*)

Dirk C. Welsford

Jeremy M. Lyle

University of Tasmania
Tasmanian Aquaculture and Fisheries Institute
Marine Research Laboratories
Nubeena Crescent
Taroona, Tasmania 7053, Australia
E-mail address (for D. C. Welsford): Dirk.Welsford@utas.edu.au

Methods for estimating growth in wild fish stocks derive largely from two sources: 1) age-based models, such as the von Bertalanffy growth function (VBGF), from data for length-at-age, where fish ages are known or estimated from scales, otoliths, and other hard parts; and 2) length-based models, from recapture data from tagged fish to describe a growth trajectory over time at liberty (e.g., Fabens, 1965), or analysis of modal progressions in length-frequency data (e.g., MULTIFAN, Fournier, et al., 1990). Many of these models seek to characterize growth of the population in terms of the three standard von Bertalanffy parameters, *viz.* l_{∞} , the theoretical asymptotic mean length; k , the growth rate coefficient; and t_0 , the theoretical age at length zero.

Despite its wide use in descriptions of fish growth, the standard VBGF is often criticized because the function's parameters may represent unreasonable extrapolations beyond available data and hence lack biological relevance (e.g., Knight, 1968; Roff, 1980; Francis, 1988a; 1988b), estimates of l_{∞} produced by standard length- and age-based versions of the model lack mathematical equivalence (e.g., Francis, 1988b; 1992), the statistical properties of the parameters make comparisons between samples difficult (Ratkowsky, 1986; Cerrato, 1990; 1991), and individual variability introduces biases in parameter estimates (Wang, et al., 1995; Wang and Thomas, 1995; Wang, 1998; Wang and Ellis, 1998).

These criticisms have led to various reparameterizations of the VBGF (see Ratkowsky, 1986; Cerrato, 1991 for examples). Analyses of reparameterizations for age-based VBGFs indicate that the inclusion of parameters that are expected lengths-at-age, for age classes drawn from the data set, dramatically improve the statistical properties of the model (Cerrato, 1991) and also result in parameters that have direct biological interpretation. Reparameterizations that fit this criterion include the reparameterization of the Francis (1988b) model for length-at-age data, and GROTAG, a reparameterization of the Fabens model from tagging data with expected growth rates for length as parameters (Francis, 1988a). GROTAG in particular has the advantage of being readily parameterized to include seasonal growth terms, and, through the application of a likelihood function, can include estimators of measurement error, individual growth variability, and the proportion of outliers in a data set. It has been used to produce growth estimates for cartilaginous fishes (Francis and Francis, 1992; Francis, 1997; Francis and Mulligan, 1998; Sempendorfer, 2000; Sempendorfer, et al., 2000), bony fishes (Francis, 1988b; 1988c; Francis, et al., 1999), and bivalve mollusks (Cranfield, et al., 1996). Fitting of any growth model with maximum likelihood methods also permits straightforward application of LRTs in order to compare parameter estimates, and to deter-

mine optimal parameterization of models (Kimura, 1980; Francis, 1988a). Computationally intensive methods such as bootstrapping and randomization tests provide a nonparametric method for approximating probability distributions of growth parameter estimates (Haddon, 2001), for generating confidence intervals to test for differences between parameter estimates, and for visualizing relationships between parameters (Mooij, et al., 1999). Drawing together these methods, it is possible to fit growth models, to produce parameter estimates that are biologically interpretable, and to use tests that are robust for comparing populations.

The purple wrasse (*Notolabrus fucicola*) is a gonochoristic, site-attached, reef-associated fish, common on moderate to fully exposed coasts in southeastern Australia and New Zealand (Russell, 1988; Edgar, 1997). Both *Notolabrus fucicola* and its Australian congener, the blue-throated wrasse (*N. tetricus*), are large benthic carnivores that play a significant role in the trophic dynamics of temperate reef systems (Denny and Schiel, 2001; Shepherd and Clarkson, 2001).

The development of a live fishery for *N. fucicola* and *N. tetricus* in southeastern Australia has made temperate wrasses increasingly important economically (Lyle¹; Smith, et al.²).

Most previous attempts to describe the growth of *N. fucicola* (Barrett, 1995a; 1999; Smith, et al.²) have been compromised by small sample sizes, lack of age validation, and the use of unsuitable statistical models to compare length-at-age between populations. Ewing et al. (2003) recently validated an aging method and developed growth models for *N. fucicola*, combining samples from many sites from eastern and southeastern Tasmania. Our study describes site- and sex-specific age- and length-based models for this species. We also compare methods for examining differences in growth model parameter estimates, such as confidence intervals and randomization tests based on bootstrap estimates, plots of bootstrap estimates, and LRTs where comprehensive coverage of age and length data is unavailable—a situation commonly faced in fisheries.

Materials and methods

Field methods

Notolabrus fucicola were trapped and tagged at two sites on the east coast of Tasmania. Trapping was conducted

at 1–2 month intervals, between July 1999 and April 2001 at Lord's Bluff (42.53°S, 147.98°E), and between July 2000 and March 2001 at Point Bailey (42.36°S, 148.02°E). Standard T-bar tags were inserted between the pterygiophores in the rear portion of the dorsal fin. Total length of each fish was recorded prior to release. Because *N. fucicola* display no external sexual characters, sex of fish could only be determined by the presence of extruded gametes if fish were running ripe when captured, or by dissection at the conclusion of the study.

At the conclusion of the tag-recapture study, each site was fished intensively. Recaptured tagged fish were euthanized by immersion in an ice-slurry. Fish captured at Lord's Bluff were measured immediately after sacrifice; gonads were dissected to determine sex, and sagittal otoliths were collected. Untagged fish were returned immediately; therefore otoliths that were analyzed came from tagged fish only. All fish captured at Point Bailey were processed in a similar fashion but were stored frozen prior to examination.

Otolith preparation and interpretation

Sagittal otoliths were mounted in a polyester resin block, and transverse sections (250–300 µm thick) were cut through the primordium with a lapidary saw. Sections were mounted on a slide and examined under a binocular microscope at ×25 magnification. The primary author counted annuli and individuals were allocated to a year class, and fractional ages were assigned based on an arbitrary birthdate of 1 October, following the method of Ewing et al. (2003).

To determine if any significant differences existed within or between reader estimates, a random subsample of 55 otoliths, from both sites, was re-aged by the primary reader (DW) and another experienced otolith reader (GE). The frequency distribution of ages in each population was then compared with a Kolmogorov-Smirnov test. Consistency of age estimates was also compared by using age bias plots (Campana, et al., 1995) and the index of average percent error (IAPE *sensu* Beamish and Fournier, 1981).

Preliminary inspection of the length data for thawed individuals from Point Bailey revealed many negative growth increments when compared to length data collected from recaptures prior to the conclusion of field sampling. Repeated measurements of *N. fucicola*, conducted independently of our study, have shown length changes in the order of 8–9% in frozen and thawed individuals compared to measurements from individuals alive or freshly euthanized (G. P. Ewing, unpubl. data³). Consequently, measurements taken from frozen fish were deemed to be incompatible with measurements taken from fresh fish and were removed from the tagging and otolith data sets. Where data from

¹ Lyle, J. M. 2003. Tasmanian scalefish fishery—2002. Fishery Assessment Report, 70 p. Tasmanian Aquaculture and Fisheries Institute, Marine Research Laboratories, Univ. Tasmania, Nubeena Crescent, Tarooma, Tasmania 7053, Australia.

² Smith, D. C., I. Montgomery, K. P. Sivakumaran, K. Krusic-Golub, K. Smith, and R. Hodge. 2003. The fisheries biology of bluetooth wrasse (*Notolabrus tetricus*) in Victorian waters. Draft Final Report, Fisheries Research and Development Corporation No. 97/128, 88 p. Marine and Freshwater Resources Institute, 2a Bellarine Highway, Queenscliff, Victoria 3225, Australia.

³ Ewing, G. P. 2002. Unpubl. data. University of Tasmania, Tasmanian Aquaculture and Fisheries Institute, Marine Research Laboratories, Nubeena Crescent, Tarooma, Tasmania 7053, Australia.

multiple recaptures allowed, the initial length and penultimate length measurement and their corresponding dates were used in length-based analyses at this site. Individual length-at-age estimates were also adjusted according to the date of any previous reliable length record.

Age-based growth modeling

Data consisted of ages estimated from otoliths (T) and lengths at final recapture (or last reliable length measurement at Point Bailey) (L). Kolmogorov-Smirnov tests were conducted between sites and between sexes within sites to determine if there were differences between the proportional frequency distributions of fish lengths in length-at-age data sets. Growth was modeled by using the standard von Bertalanffy growth function (VBGF):

$$L = L_{\infty}[1 - e^{-k(T-t_0)}] \quad (1)$$

The VBGF for the two sites and sexes within sites were modeled separately (Table 1). Fish for which sex could not be determined were not included in the sex-specific models.

A reparameterized version of the VBGF was also estimated from Equation 4 in Francis (1988b):

$$L = L_{\tau} + \frac{[L_{\omega} - L_{\tau}][1 - r^{2\tau - \omega}]}{1 - r^2} \quad (2)$$

$$\text{where } r = \frac{L_{\tau} - L_{\omega}}{L_{\omega} - L_{\tau}} \quad (3)$$

and where L_{τ} , L_{ω} , and L_{∞} are the mean lengths at ages τ , ω , and $\omega = (\tau + v)/2$ —ages chosen from within the observed range within the data set. The values chosen for all the otolith-based models were $\tau = 4$, $\omega = 7$ and $v = 10$ years, encompassing the range of ages represented in the data sets for both sites. Estimates of these parameters have a direct biological meaning and have more statistically favorable properties than the standard VBGF parameters L_{∞} , k , and t_0 (Francis, 1988b; Cerrato, 1991).

Models were fitted by minimizing a likelihood function and assuming normally distributed residuals (Eq. 4):

$$-\lambda = -\sum_i \ln \left[\frac{1}{\sqrt{2\pi}\sigma} \exp \left\{ -\frac{(L_i - \mu_i)^2}{2\sigma^2} \right\} \right] \quad (4)$$

The measured length of the i th fish, L_i , has its corresponding expected mean length at age μ_i , as determined from Equation 1 or 2 above, where μ_i is normally distributed and has a standard deviation σ . The quality of the fits was gauged visually in the first instance by the lack of trends in plots of residuals against length-at-age.

To further investigate each model, each data set was bootstrapped 5000 times. The bootstrapping procedure involved randomly resampling, with replacement, from the original data set, and then fitting the VBGF to this new data set, thereby generating new estimates of all model parameters (Haddon, 2001).

Based on the percentile distribution of bootstrap parameter estimates, 95% confidence intervals (CIs) around the original sample estimates were calculated for each VBGF parameter. To account for any skew in the distribution of bootstrap parameter estimates, a first-order correction for bias of CIs was performed, where bootstrap percentiles used to estimate the CIs were adjusted on the basis of the proportion of bootstrap estimates less than the original estimate (Haddon, 2001).

To determine whether growth showed any site or sex-within-site (referred to as "sex-") differences, we plotted the overlap of first-order corrected CIs and plots of bootstrap estimates. Simple comparison of CI overlap as a test for parameter difference has been shown to be overly conservative (Schenker and Gentleman, 2001). Hence the null hypothesis of no difference was accepted in the first instance only in cases where the amount of overlap was obviously large. In cases where the extent of overlap was small, and the chance of incorrectly accepting the null hypothesis existed, a randomization test was performed. This test involved constructing the distribution of the difference between the estimates of the parameter of interest. Parameter estimates were randomly selected with replacement from each set of bootstrap estimates for the two populations, and the differences were determined for these 5000 random pairs. Then a 95% first-order corrected CI was constructed as above, and the null hypothesis was rejected only if the CI did not include zero. Likelihood ratio tests were also conducted on the VBGFs and individual parameters (Kimura, 1980).

Length-based growth modeling

Growth trajectories consisted of the initial length (L_1), time at first capture (T_1), time at final recapture (or penultimate recapture at Point Bailey) (T_2), change in length from the first to the final recapture (ΔL), and duration in years between capture and last recapture (ΔT). T_1 and T_2 were measured in years from an arbitrarily chosen point, 1 January 1999—the first day in the earliest year in which tagging was conducted. For individuals recaptured more than once, only information relating to the initial and final captures was used in the analyses. This approach maximized the time between recaptures for any fish, increasing the chance of detecting growth, and gave equal weight to each fish sampled.

Because the two sites were sampled over different time periods, only samples from Lord's Bluff that were taken at the same time as samples at Point Bailey were considered for the purposes of between-site growth comparisons (Table 1). The resulting data set, designated LB_{exp} , reduced potentially confounding effects of longer sampling durations at Lord's Bluff.

Table 1

Main model types (GROTAG and von Bertalanffy growth function [VBGF]), data sets, and sample sizes used to produce estimates of growth for *Notolabrus fucicola*. LB= Lord's Bluff, full data set; LB_{res} = Lord's Bluff, only fish captured over dates equivalent to the Point Bailey sample; PB=Point Bailey, full data set; ♀ =males only; ♂ = females only; n=sample size. The asterisk refers to one individual in this data set that was identified as an outlier during model parameterization and was excluded from bootstrapping.

Model type	Data set	Total n
GROTAG	LB _{res}	174
	PB	263
	LB ♀♂	103
	LB ♂♂	69
	PB ♀♂	96
VBGF	PB ♂♂	89
	LB	101
	PB	178
	LB ♀♂	47
	LB ♂♂	54
	PB ♀♂	68
	PB ♂♂	104

A Kolmogorov-Smirnov test was conducted to determine whether differences existed in the proportional frequency distributions of lengths of fish at first capture (L_1) between sites and between sexes within sites.

Growth was modeled by using GROTAG (Eqs. 2 and 4 in Francis [1988a]), a reparameterization and extension of the Fabens growth model for tag-recapture data that incorporates seasonal growth:

$$\Delta L = \left[\frac{\beta g_\alpha - \alpha g_\beta}{g_\alpha - g_\beta} - L_1 \right] \left[1 - \left(1 + \frac{g_\alpha - g_\beta}{\alpha - \beta} \right)^{3T + (\phi_2 - \phi_1)} \right], \quad (5)$$

where $\phi_i = u \frac{\sin[2\pi(T_i - w)]}{2\pi}$ for $i=1,2$. (6)

The parameters g_α and g_β are the estimated mean annual growth (cm/yr) of fish of initial lengths α cm and β cm, respectively, where $\alpha < \beta$. The reference lengths α and β were chosen such that the majority of values of L_1 in each data set fell between them (Francis, 1988a). For site-specific estimates of growth, α and β were set at 20 and 30 cm, respectively, whereas β was set at 28 cm for sex-specific models. Seasonal growth is parameterized as w (the portion of the year in relation to 1 January when growth is at its maximum) and u ($u=0$ indicat-

Table 2

Parameters estimated in the five GROTAG models fitted to each tag-recapture data set to evaluate optimal model parameterization.

GROTAG model	Parameters estimated
1	g_α, g_β, v, p
2	$g_\alpha, g_\beta, v, p, u, w$
3	$g_\alpha, g_\beta, v, p, s, m$
4	$g_\alpha, g_\beta, v, u, w, s, m$
5	$g_\alpha, g_\beta, v, p, u, w, s, m$

ing no seasonal growth through to $u=1$ indicating the maximum seasonal growth effect, i.e., where growth effectively ceases at some point each year).

The model was fitted by minimizing negative log-likelihood ($-\lambda$) function (Eq. 9 in Francis [1988a]). For each data set, made up of $i = 1$ to n growth increments:

$$\lambda = \sum_i \ln[(1-p)\lambda_i + p/R], \quad (7)$$

where $\lambda_i = \frac{\exp^{-1/2(\Delta L_i - \mu_i - m)^2 / (\sigma_i^2 + s^2)}}{[2\pi(\sigma_i^2 + s^2)]^{1/2}}$. (8)

The measured growth increment of the i^{th} fish, ΔL_i , has its corresponding expected mean growth increment, μ_i , as determined from Equation 5 above, where μ_i is normally distributed with standard deviation σ_i . In this study, σ_i was assumed to be a function of the expected growth increment μ_i (Eq. 5, Francis, 1988a):

$$\sigma_i = v\mu_i. \quad (9)$$

where v is estimated as a scaling factor of individual growth variability, assuming a monotonic increase in variability around the mean growth increment as the size of the increment increases.

In its fully parameterized form, the likelihood function estimates the population measurement error in ΔL as being normally distributed, and having a mean of m and standard deviation of s . To estimate the proportion of outliers, Francis (1988a) also included p , the probability that the growth increment for any individual could exist erroneously in the data set as any value, within the observed range of growth increments R . This enables the proportion of outliers to be identified. Francis (1988a) suggested that an estimate of $p > 0.05$ indicates a high level of outliers and therefore some caution would be required in interpreting the overall model fit.

The optimal model parameterization was determined by fitting five different models, comprising different

combinations of parameters (Table 2), with unfitted parameters held at zero. A LRT was used to determine the improvement in model fit with the different parameterizations (Francis, 1988a). For models with an equal number of parameters, the model producing the lowest negative log likelihood ($-\lambda$) was considered the best fit.

As with the otolith models, LRTs were conducted on the GROTAG models to compare between sites and sexes, and models were also bootstrapped 5000 times. First-order corrected 95% CIs were calculated for parameter estimates (Haddon, 2001), and pairwise comparisons of growth parameters, by using CIs and randomization tests, as described above for otolith-based models.

Results

Otolith interpretation

Kolmogorov-Smirnov tests showed no significant difference in age-frequency distributions generated by repeat readings of 55 otoliths by the primary reader ($D_{0.05}=0.259$, $D_{\max}=0.072$, not significant) or between readers ($D_{0.05}=0.259$, $D_{\max}=0.109$, not significant). The IAPE score for all three readings was calculated as 6.9%, and no systematic under- or over-estimation of ages was apparent in age bias plots within or between readers. Therefore age estimates derived from the first readings by the primary author were used for modeling.

Age-based growth modeling

Site comparisons No significant differences in length frequencies were detected in a Kolmogorov-Smirnov test between sites ($D_{0.05}=0.169$, $D_{\max}=0.097$, not significant).

Length-at-age estimates showed high variability among individuals, as evidenced by the spread of data points around the fitted models (Fig. 1), and estimates of σ ranged from 1.16 to 2.17 cm across all models (Table 3). However, mean lengths-at-age were adequately described by the VBGF across the ages represented by the samples from the two sites. The plots of the site-specific VBGFs indicated that mean length-at-age at Lord's Bluff was higher than at Point Bailey.

Because of the absence of young (0+ and 1+) fish in the samples from both sites, and fish >14+ at Lord's Bluff, the standard VBGF parameters were difficult to interpret biologically. Confidence intervals for the three standard VBGF parameters largely overlapped in comparisons between sites (Table 3). Plots of the bootstrap parameter estimates showed strong nonlinear correlations, particularly between l_{∞} and k , revealing minimal overlap between sites, most easily visualized with logarithmic axes (Fig. 2A). Nonlinear correlation between parameter estimates and minimal overlap between sites were also true to a lesser extent in estimates of l_{∞} versus t_0 (Fig. 2B). LRTs showed that differences between sites were highly significant overall

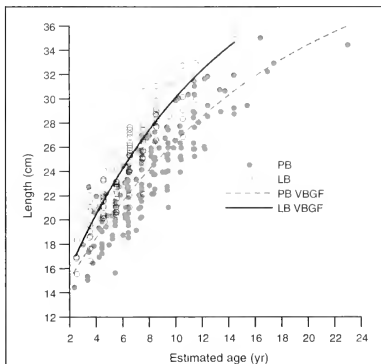


Figure 1

Length-at-age estimates for *Notolabrus fucicola*, derived from otoliths (symbols), and corresponding von Bertalanffy growth functions (VBGFs) fitted by least squares (lines). PB = Point Bailey, LB = Lord's Bluff.

but could not be attributed to significant differences in individual parameters (Table 4).

Confidence intervals for the Francis (1988b) reparameterized version of the VBGF clearly indicated significant differences in growth rates between sites in all three parameters, and no overlap between sites in the CIs of the estimates of mean length at 4, 7, or 10 years old (Table 3). These differences were also evident in plots of bootstrap parameter estimates, the two sites being clearly separated in the parameter space, and showed none of the high nonlinear correlations evident in the standard VBGF estimates (Fig. 3B). Randomization tests produced CIs of the difference between sites of 1.16–2.67, 2.48–3.50, and 2.82–4.44 cm for l_4 , l_7 , and l_{10} , respectively. Highly significant differences in all individual parameters growth parameters in the reparameterized model were also shown in LRTs between sites, but no significant difference in σ was detected (Table 4).

Sex comparisons Confidence intervals for the standard and reparameterized von Bertalanffy parameters significantly overlapped in all comparisons between sexes (Table 3). Likelihood ratio tests showed no significant differences between models of sexes within sites—a conclusion supported by considerable overlap in plots of bootstrap estimates (not shown).

Length-based growth modeling

Model parameterization Site-specific data sets were optimally parameterized under the most complex model,

Table 3

Von Bertalanffy growth function parameter estimates for *Notolabrus fucicola*. Numbers in bold text are parameter estimates from the original dataset. Numbers in parentheses are the proportion of parameter estimates from bootstrapped data sets that were less than the estimate from the original data set. Numbers in plain text are first-order corrected bootstrap 95% confidence intervals. LB = Lord's Bluff; PB = Point Bailey.

Dataset	Parameter estimate						
	L_{∞} (cm)	k (yr)	t_0 (yr)	l_4 (cm)	l_7 (cm)	l_{10} (cm)	σ (cm)
LB	44.7 (0.48)	0.085 (0.51)	-3.23 (0.50)	20.4 (0.51)	25.9 (0.50)	30.1 (0.51)	1.61 (0.57)
	35.4 to 68.4	0.036 to 0.152	-5.82 to -1.59	20.0 to 20.9	25.4 to 26.3	29.4 to 30.8	1.39 to 1.87
PB	43.3 (0.66)	0.065 (0.51)	-4.65 (0.50)	18.5 (0.52)	22.9 (0.53)	26.5 (0.58)	1.79 (0.32)
	37.9 to 86.7	0.021 to 0.096	-8.71 to -2.83	17.9 to 19.2	22.6 to 23.2	26.1 to 26.9	1.57 to 1.92
LB \ddagger	52.1 (0.51)	0.059 (0.49)	-4.46 (0.48)	20.3 (0.51)	25.5 (0.48)	29.7 (0.50)	1.38 (0.64)
	34.6 to 1210.1	0.001 to 0.157	-9.21 to -1.55	19.8 to 20.9	24.9 to 25.9	28.9 to 30.5	1.16 to 1.68
LB \ddagger	43.2 (0.47)	0.095 (0.51)	-2.80 (0.48)	20.5 (0.51)	26.1 (0.48)	30.4 (0.49)	1.74 (0.62)
	33.1 to 187.8	0.007 to 0.192	-7.42 to -0.98	19.9 to 21.3	25.5 to 26.7	29.2 to 31.7	1.45 to 2.17
PB \ddagger	43.3 (0.47)	0.060 (0.52)	-5.56 (0.51)	18.9 (0.54)	22.9 (0.53)	26.3 (0.55)	1.58 (0.60)
	33.3 to 163.3	0.007 to 0.138	-11.57 to -2.20	18.3 to 19.6	22.5 to 23.5	25.7 to 26.9	1.35 to 1.87
PB \ddagger	43.2 (0.48)	0.065 (0.43)	-4.60 (0.53)	18.5 (0.45)	22.9 (0.47)	26.5 (0.45)	1.91 (0.62)
	37.0 to 199.4	0.002 to 0.093	-10.61 to -2.35	17.6 to 19.3	22.5 to 23.3	25.9 to 27.0	1.73 to 2.16

incorporating seasonal growth and measurement error estimates (Table 5). Estimates of proportion of outliers in the data set (p) greater than zero were due to lack of fit and dropped to zero in model 5. Preliminary bootstrap-

ping showed that fitting p regularly produced spurious model fits. Because the full data sets were estimated to have no outliers, it was considered reasonable to fit model 4 (equivalent to model 5, but with p held equal to zero) to all bootstrapped data sets for site-specific growth estimates and comparisons.

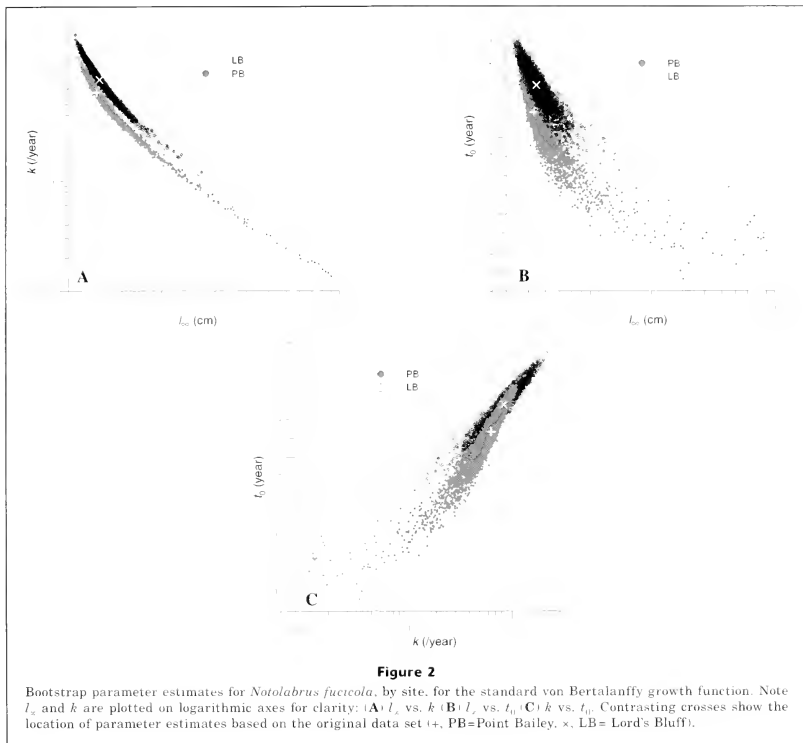
Estimates of p also dropped to zero in model 5 when this model was fitted to the sex-specific data sets, except for females at Lord's Bluff. Holding $p=0$ in model 4 for females at Lord's Bluff resulted in a less good fit compared to that of model 5 and also produced slightly different parameter estimates than those of model 5, namely increasing growth (g_{20} and g_{28}), growth variability (v), and measurement error (m) (Table 6). Visual inspection of residuals showed an obvious outlier in the data set. When this was removed and model 5 was refitted, p fell to zero and the other parameters estimates were very close to the values estimated from fitting model 5 to the original data set, and there was a large improvement in likelihood. Therefore the model for females at Lord's Bluff was based on the data set with the outlier excluded, and model 4 with p held at zero was fitted to all bootstrap data sets for sex-specific growth estimates and comparisons.

Site comparisons With the exception of s at Lord's Bluff, the proportion of bootstrap parameter estimates

Table 4

Likelihood ratio tests of site differences in the von Bertalanffy growth functions fitted to *Notolabrus fucicola* length-at-age data and individual VBGF parameters, both standard and reparameterized. $-\lambda$ = negative log-likelihood. The base case represents the summed likelihood for both curves fitted separately.

Hypothesis	$-\lambda$	χ^2	df	P
Base case	553.0	—	—	—
Coincident curves	617.8	129.75	3	<0.001
$= L_{\infty}$	553.0	0.03	1	0.870
$= k$	553.2	0.36	1	0.548
$= t_0$	553.4	0.78	1	0.376
$= l_4$	565.7	25.47	1	<0.001
$= l_7$	602.9	99.78	1	<0.001
$= l_{10}$	589.2	72.53	1	<0.001
$= \sigma$	554.2	2.49	1	0.114



were more or less evenly distributed around the original parameter estimates, resulting in approximately symmetrical first-order corrected 95% CIs (Table 7). Based on the lack of overlap of CIs, only g_{20} differed significantly between sites. A randomization test of the difference in g_{20} produced CIs of 0.75–2.85 cm/yr faster growth at Lord's Bluff.

Plots of bootstrap parameter estimates clearly indicate differences in growth rates between sites, and little overlap in the parameter clouds along the g_{30} axis when g_{20} is plotted against g_{30} (Fig. 4A). Plots of bootstrapped estimates of the seasonal growth parameters w and t_0 showed a high level of nonlinear correlation. A region of overlap between site estimates along the w axis is evident in Fig. 4B. However, the randomization test for

this parameter produced a CI of the difference between the two sites of 0.02–0.33 yr, corresponding to significantly different maximum in seasonal growth occurring at Lord's Bluff 8–120 days after Point Bailey. Estimates of w at Point Bailey ranged from –0.14 to 0.05 years in relation to 1 January (Table 7), corresponding to peak growth between austral mid-spring and mid-summer (early November through mid-January), contrasting with the Lord's Bluff estimate of –0.08 to 0.20 years and indicating peak growth from austral late spring to early autumn (mid-December through mid-March).

Site differences in growth were also indicated in the results of LRTs. The overall models were significantly different; the growth parameter g_{30} and the timing of maximum seasonal growth were significantly different

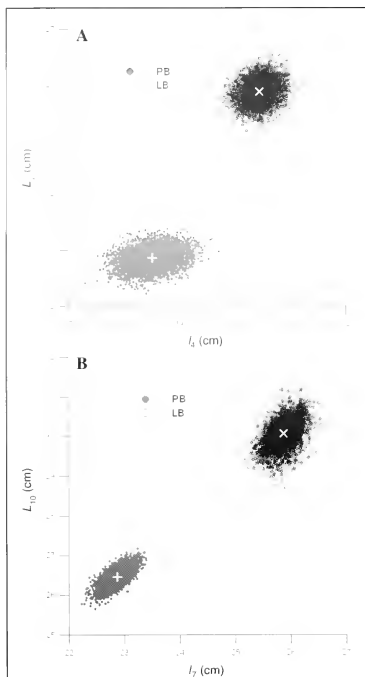


Figure 3

Bootstrap estimates of reparameterized von Bertalanffy growth function by mean lengths at age for *Notolabrus fucicola*, by site. (A) l_4 versus l_7 , (B) l_7 versus l_{10} mean length-at-ages at 7 and 10 years. Contrasting crosses show the location of parameter estimates based on the original data set (+, PB=Point Bailey, x, LB=Lord's Bluff).

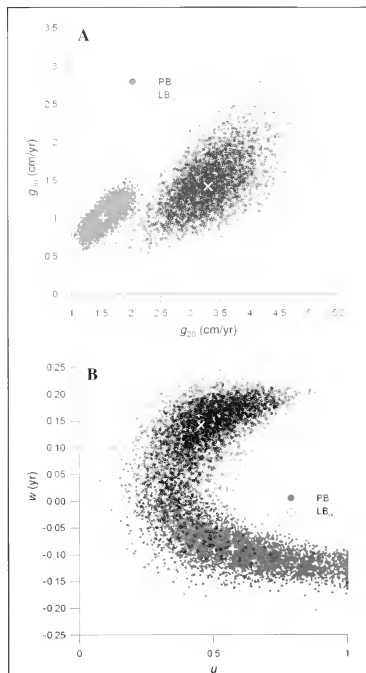


Figure 4

Bootstrap estimates of GROTAG parameters for *Notolabrus fucicola*, by site: (A) g_{20} versus g_{30} , mean annual growth at initial length 20 and 30 cm and (B) u versus w , magnitude and timing of seasonal growth. Contrasting crosses show the location of parameter estimates based on the original data set (+, PB = Point Bailey, x, LB_{res} =Lord's Bluff).

at $\alpha=0.05$ when tested individually (Table 8A), in agreement with the results of the randomization tests.

Sex comparisons Bootstrapped parameter estimates from sex-specific data sets were approximately symmetrical about the original estimates (Table 7). The largest divergence from 0.5 was evident in estimates of s for females at Lord's Bluff and males at Point Bailey. Bootstrap estimates of u for Lord's Bluff males occasionally extended into spurious negative values, lowering

confidence estimates of the extent of seasonal growth in this data set (Table 7).

Based on simple overlap of CIs, no single parameter differed significantly between sexes at either site (Table 7). Plots of the bootstrap estimates of the growth parameters g_{20} and g_{28} showed minimal overlap between males and females, and separation was most evident along the g_{20} axis (Fig. 5A). Plots of bootstrapped estimates of the seasonal growth parameters u and w (Fig. 5B), and the measurement error parameters m and s

Table 5

Parameter estimates and negative log-likelihoods ($-\lambda$) of models used in likelihood ratio tests to determine the optimal parameterization of GROTAG models for *Notolabrus fucicola* tagging data, by site. Bold text in $-\lambda$ column indicates the optimally parameterized model for each data set. Model 4 is equivalent to model 5 with $p = 0$ in these instances. LB_{res} = residents of Lord's Bluff; PB = Point Bailey.

Data set	Model	Parameter estimate							$-\lambda$	
		g_{20} (cm/yr)	g_{30} (cm/yr)	v	u	w (yr)	s (cm)	m (cm)		p
LB _{res}	1	1.84	1.07	0.88	—	—	—	—	0.07	57.06
	2	3.00	1.67	0.88	0.59	0.22	—	—	0.07	50.46
	3	2.60	1.12	0.29	—	—	0.22	-0.12	0.00	20.59
	4 and 5	3.30	1.42	0.26	0.45	0.14	0.22	-0.10	0.00	12.97
PB	1	1.50	1.01	0.73	—	—	—	—	0.16	87.82
	2	1.55	1.15	0.82	0.31	0.13	—	—	0.07	79.02
	3	1.87	1.18	0.36	—	—	0.19	-0.08	0.00	36.16
	4 and 5	1.53	1.01	0.35	0.57	0.91	0.18	-0.07	0.00	23.52

Table 6

Parameter estimates and negative log-likelihoods ($-\lambda$) of models used in likelihood ratio tests to determine the optimal parameterization of GROTAG models for *Notolabrus fucicola* tagging data, by sex within site. Bold text in $-\lambda$ column indicates the optimally parameterized model for each data set. † indicates the parameter estimates and likelihoods when GROTAG is fitted to the Lord's Bluff (LB) ‡ data set with a single outlier removed. Model 4 is equivalent to model 5 with $p = 0$ in all other instances. PB = Point Bailey.

Data set	Model	Parameter estimate							$-\lambda$	
		g_{20} (cm/yr)	g_{30} (cm/yr)	v	u	w (yr)	s (cm)	m (cm)		p
LB [†] ♂	1	1.98	1.49	0.52	—	—	—	—	0.00	43.07
	2	1.88	1.54	0.50	0.23	0.04	—	—	0.00	39.24
	3	2.09	1.62	0.27	—	—	0.21	-0.05	0.00	32.21
	4 and 5	2.04	1.67	0.27	0.23	0.19	0.20	-0.04	0.00	29.44
LB [†] ♀	1	2.05	1.40	0.52	—	—	—	—	0.16	60.58
	2	1.99	1.20	0.48	0.41	0.98	—	—	0.15	58.19
	3	2.88	1.87	0.26	—	—	0.25	-0.29	0.00	41.15
	4	2.75	1.75	0.25	0.32	0.96	0.24	-0.31	—	38.40
	5	2.66	1.48	0.22	0.47	0.94	0.22	-0.26	0.03	36.23
4 and 5†	2.66	1.48	0.22	0.48	0.94	0.23	-0.26	0.00	30.36	
PB [†] ♂	1	1.31	1.02	0.60	—	—	—	—	0.24	21.31
	2	1.15	0.96	0.61	0.41	0.90	—	—	0.19	19.93
	3	1.54	1.21	0.33	—	—	0.19	-0.03	0.00	6.43
	4 and 5	1.15	0.93	0.32	0.81	0.88	0.18	-0.04	0.00	2.49
PB [†] ♀	1	1.49	1.15	0.68	—	—	—	—	0.16	30.55
	2	1.43	1.16	0.90	0.33	0.12	—	—	0.00	28.85
	3	1.96	1.32	0.38	—	—	0.20	-0.11	0.00	19.06
	4 and 5	1.46	1.01	0.39	0.77	0.87	0.18	-0.12	0.00	15.78

(Fig. 5C) showed distinct relationships within the two sexes. Randomization tests confirmed significant differences in g_{20} , m , and w . The CIs of these differences were estimated to be 0.2–1.09 cm/yr faster for females

with an initial size of 20 cm, with an annual peak in female growth 3–152 days earlier than males, and with a measurement error that overestimated female length by 2–40 mm more than the measurement error for males.

Table 7

GROTAG parameter estimates derived from *Notolabrus fucicola* tag-recapture data. For all data sets, g_{1c} is the mean annual growth of individuals with an initial length of 20 cm. g_{2c} represents the estimated mean annual growth of individuals with an initial length of 30 cm for Lord's Bluff (LB_{res}) and Point Bailey (PB), or the estimate for 28-cm individuals for all other data sets. Numbers in bold text are the parameter estimates from the original data sets. Numbers in parentheses are the proportion of parameter estimates from bootstrap data sets less than the original estimate. Numbers in plain text are first-order corrected bootstrap 95% confidence intervals.

Data set	Parameters estimate						
	g_{1c} (cm/yr)	g_{2c} (cm/yr)	v	u	w (yr)	s (cm)	m (cm)
LB _{res}	3.30 (0.50)	1.42 (0.48)	0.26 (0.54)	0.45 (0.43)	0.14 (0.47)	0.22 (0.60)	-0.10 (0.48)
	2.32 to 4.34	0.80 to 2.19	0.14 to 0.40	0.23 to 0.68	-0.08 to 0.20	0.18 to 0.26	-0.18 to -0.03
PB	1.53 (0.51)	1.01 (0.51)	0.35 (0.50)	0.57 (0.46)	-0.09 (0.54)	0.18 (0.55)	-0.07 (0.56)
	1.21 to 1.94	0.76 to 1.31	0.27 to 0.44	0.25 to 1.00	-0.14 to 0.05	0.15 to 0.22	-0.12 to -0.01
LB [†]	2.04 (0.48)	1.68 (0.51)	0.27 (0.58)	0.23 (0.45)	0.19 (0.48)	0.20 (0.57)	-0.04 (0.49)
	1.77 to 2.31	1.32 to 2.01	0.20 to 0.40	-0.06 to 0.43	-0.02 to 0.29	0.12 to 0.28	-0.14 to 0.06
LB [‡]	2.66 (0.49)	1.48 (0.50)	0.22 (0.50)	0.48 (0.39)	-0.06 (0.52)	0.23 (0.62)	-0.26 (0.49)
	2.27 to 2.98	1.18 to 1.83	0.13 to 0.30	0.16 to 0.69	-0.16 to 0.12	0.14 to 0.34	-0.41 to -0.10
PB [†]	1.15 (0.41)	0.93 (0.43)	0.32 (0.57)	0.81 (0.51)	-0.12 (0.43)	0.18 (0.62)	-0.04 (0.53)
	0.83 to 1.69	0.61 to 1.41	0.17 to 0.47	0.18 to 1.00	-0.20 to 0.10	0.14 to 0.24	-0.14 to 0.06
PB [‡]	1.46 (0.50)	1.01 (0.47)	0.39 (0.56)	0.77 (0.46)	-0.13 (0.47)	0.18 (0.56)	-0.12 (0.51)
	1.08 to 2.33	0.70 to 1.01	0.23 to 0.74	0.14 to 1.00	-0.20 to 0.14	0.09 to 0.27	-0.22 to 0.00

Table 8

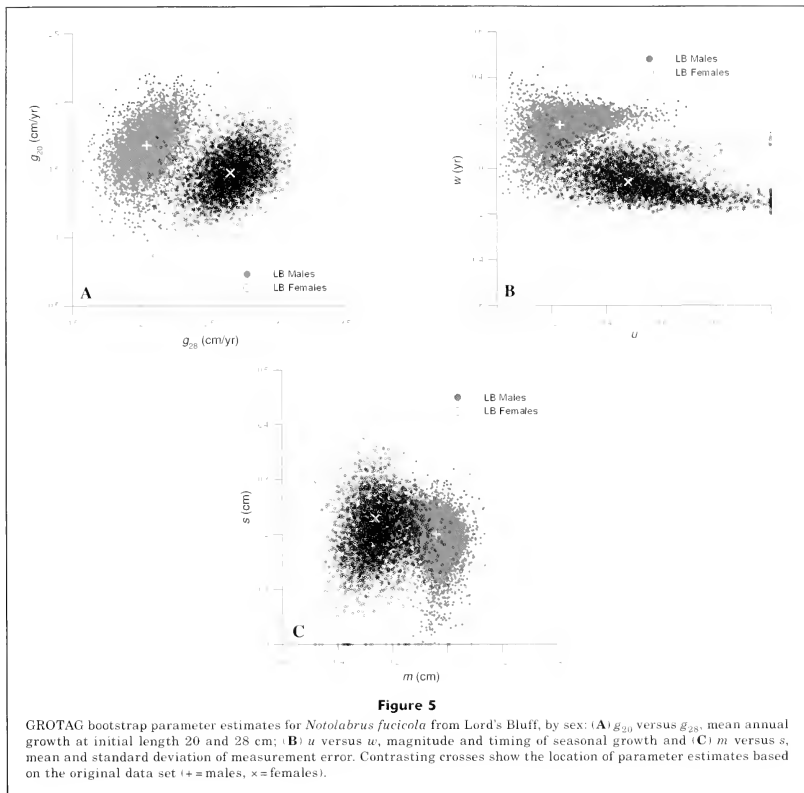
Likelihood ratio tests of the GROTAG models for which bootstrap parameter estimates were generated (Tables 5 and 6): (A) Point Bailey (PB) against Lord's Bluff (LB_{res}); (B) LB_{res} against LB[†]. $-\lambda$ = negative log-likelihoods. The base case is the negative log-likelihood of the data sets fitted with two wholly separate models. $^{\circ}$ = significant at $\alpha=0.05$.

A Hypothesis	$-\lambda$	χ^2	df	P	B Hypothesis	$-\lambda$	χ^2	df	P
Base case	36.49	—	—	—	Base case	59.80	—	—	—
Coincident curves	51.98	30.98	7	<0.001 [†]	Coincident curves	72.17	24.75	7	<0.001 [†]
$=g_{20}$	42.19	11.38	1	<0.001 [†]	$=g_{20}$	63.43	7.27	1	0.007 [†]
$=g_{30}$	37.36	1.72	1	0.189	$=g_{28}$	60.21	0.83	1	0.362
$=v$	37.35	1.72	1	0.190	$=v$	60.11	0.62	1	0.431
$=u$	36.62	0.12	1	0.623	$=u$	60.64	1.69	1	0.194
$=w$	38.91	4.84	1	0.028 [†]	$=w$	62.05	4.50	1	0.034
$=s$	37.64	2.28	1	0.130	$=s$	59.94	0.30	1	0.583
$=m$	36.66	0.33	1	0.565	$=m$	62.51	5.43	1	0.020 [†]

These conclusions agreed with the LRTs, which indicated highly significant differences between g_{20} between sexes at Lord's Bluff, and significant differences between m and w at $\alpha=0.05$ when tested individually (Table 8B). This contrasts with the results of age-based

modelling of sex-specific growth at Lord's Bluff, where no difference between the sexes was detected in any test.

Sex comparisons at Point Bailey revealed no sex-specific growth differences, and neither CIs (Table 7)



nor LRTs indicated significant difference in any of the model parameters, and bootstrap plots showed large regions of overlap (not shown).

Discussion

Comparisons of models

In this study, two methods, based on mathematically different concepts, produced similar conclusions, namely that growth in *N. fucicola* was faster at Lord's Bluff than

at Point Bailey. The results of length-based and age-based models also produced similar conclusions regarding the methods most suitable for robust comparisons of models and parameter estimates for different groups of fish. Confidence intervals were only reliable indicators of difference in cases where parameters showed low levels of correlation between estimates and where highly significant differences existed, such as in site comparisons of the reparameterized VBGF parameters, and hence were of limited utility.

Likelihood ratio tests provided a robust method of testing differences between models. However, we believe

that evidence from more than one source is required before conclusions can be drawn about differences between models designed to describe nonlinear processes such as growth. In the present study, bootstrapping techniques proved to be informative as a way of visualizing the behavior of the models used, and the distributions and correlations of parameter estimates that could not be determined readily from model likelihoods alone. They also provided a basis for estimating nonparametrically with randomization tests the differences, and CIs, of growth estimators between populations. Hence we recommend bootstrapping, plots of parameter estimates, and randomization tests to complement the "traditional" statistical tests such as the LRTs.

The standard VBGF has been criticized for the difficulty it causes in extracting biological meaning from parameters (Knight, 1968; Roff, 1980; Francis, 1988b; 1992). The problem is particularly acute where only a part of the size or age range (or both ranges) of animals is available—a situation regularly faced in analyses of fisheries data (Haddon, 2001). Data sets in our study were limited, particularly by the lack of fish in the lower age classes (cf. Ewing et al., 2003). Hence, any attempt to interpret or compare l_{∞} or t_0 as descriptors of the growth of *N. fucicola* would be spurious. Furthermore, because k and l_{∞} are highly correlated, comparisons of k cannot be independent of the effects of size or age selectivity on a data set. Because of the limitations of such parameters, and as l_{∞} and k are often inputs into population dynamics models and empirical models estimating parameters such as natural mortality (e.g., Pauly, 1979), extreme caution should be exercised when extrapolating these values from limited data. However, this instance exemplifies the utility of the reparameterization, because even with limited data, the useful parameters of mean lengths at age can be estimated and compared.

Variability in growth

Models of growth can be used to estimate length-dependent processes in fish populations, such as reproductive output, increases in biomass due to individual growth, selectivity of fishing gear, and the impact and appropriateness of size limits as management tools. The results of the present study demonstrate that growth varies significantly across individuals, seasons, sexes, and sites in *N. fucicola*.

Although the significance of estimating the variability in growth around the population mean (v) was not explicitly tested during model parameterization, values of v around 0.2 to 0.7 were estimated for all data sets modeled. Values in this range have been estimated with GROTAG from other species of bony fishes (Francis, 1988a; b; 1988c; 1992; Francis, et al., 1999) and cartilaginous fishes (Francis and Francis, 1992; Francis, 1997; Francis and Mulligan, 1998; Sempendorfer, 2000; Sempendorfer, et al., 2000), indicating that considerable individual variability in annual growth of size classes is common. The extent of variability in individual growth

is an important factor when quantifying growth because it may obscure other sources of growth variation, particularly in situations where data are limited. This effect may partially explain why age-based models failed to detect any significant effect of sex on growth rates in our study, whereas length-based modeling indicated that among smaller size classes, females grew faster than males at Lord's Bluff. On the basis of a large data set (>1000 individuals), Ewing et al. (2003) demonstrated that average length-at-age was significantly higher for females than males in *N. fucicola* although the magnitude of this difference was small. No growth differences between the sexes were evident at Point Bailey but given slower growth rates, the absolute magnitude of an expected growth differences related to sex would be relatively small and difficult to detect statistically.

Our study is the first to show that growth rates of *N. fucicola* vary significantly across small spatial scales; the two sites in our study were separated by less than 25 km. At Point Bailey, few individuals reach the minimum legal size limit of 30 cm until 10 years of age, whereas at Lord's Bluff they do so at least two years earlier (Fig. 1). An equivalent conclusion is evident from the GROTAG estimates, indicating that a 28-cm fish at Point Bailey will take nearly 2 years on average to exceed 30 cm, whereas fish of the same size are likely to reach legal size in just over a year at Lord's Bluff. Hence relative yields and rates of replacement of recruited size and age classes are likely to be lower at Point Bailey than at Lord's Bluff. However, because *N. fucicola* can be sexually mature at lengths of 12 cm (Patterson, 2000), some individuals are likely to have spawned for 6–8 years before recruitment to the fishery at Lord's Bluff (Fig. 1). This size at maturity suggests that the minimum legal size limit provides effective protection of the reproductive output of the prerecruit population of *N. fucicola* at both sites.

Using length-at-age estimated from whole otoliths, Barrett (1999) found no growth differences between several populations of *N. fucicola* in southeastern Tasmania and used these findings to support the hypothesis that populations are not resource limited. Our study did not specifically address any hypothesis about resource limitation but has clearly demonstrated that growth rates can vary between populations at the scale of individual reefs. *Notolabrus fucicola* are site-attached once they settle out of the plankton, rarely having an ambit of more than 500 m on contiguous reef, and rarely crossing soft bottom habitat if they are resident on smaller patch reef habitat (Barrett, 1995b). Intuitively, it follows that if productivity varies between reefs, then the potential for growth of individual site-attached reef fish may be limited. A variety of factors have been cited in other temperate reef species where spatial variability in length-at-age is evident, such as habitat type (Gillanders, 1997; Barrett, 1999), conspecific competition and variation in juvenile recruitment (Jones, 1980, 1984), and impacts of exploitation (Buxton, 1993). Further study is advocated to determine the factors that influence *N. fucicola* growth at this scale.

Parameterization of seasonal growth significantly improved the fit of the GROTAG models, indicating that seasonal variability in growth is significant for *N. fucicola*. The estimates of seasonal growth from our study constitute the first for this species. The LRTs indicated significant differences in the timing of maximum growth (w) between sites and between sexes at Lord's Bluff. This result was repeated in the randomization tests based on the outputs of bootstrapping. Peak growth in *N. fucicola* at both sites is estimated to occur over the austral spring–summer, during maximum water temperatures and increased productivity off the coast of Tasmania (e.g., Halpern, et al.⁴), and peak growth occurs significantly later in the season at Lord's Bluff than at Point Bailey. The mechanism affecting the timing of seasonal growth at this reef-by-reef scale is worthy of further investigation but is likely to include variability in seasonal cycles of oceanography, in availability of food (Denny and Schiel, 2001; Shepherd and Clarkson, 2001) and in temperature effects on metabolism, controlling the amount and timing of resources for allocation to growth throughout the year.

The estimate of the size of the difference in w between the sexes at Lord's Bluff had very broad CIs, and it is difficult to propose a hypothesis that could result in seasonal growth varying between the sexes by as much as five months, although resource allocation for reproduction could be involved. It may be that the particularly small size of the female data set at this site limited our ability to estimate seasonal growth accurately with GROTAG, and further study is required to more precisely determine how important seasonal growth differences between the sexes are in temperate reef fishes such as *N. fucicola*.

Sex-specific GROTAG analyses indicated a significant difference in measurement errors; females were under measured by a mean of 3 mm, compared to less than 1 mm for males at Lord's Bluff. Greater measurement errors for females have been detected in other studies with GROTAG (e.g., Sempendorfer, 2000), but a reason for greater difficulty in measuring females is difficult to determine. A possible explanation from our study is the high individual growth variability and small sample sizes. Both of these factors have been shown to affect accurate estimation of measurement error in GROTAG (Francis and Mulligan, 1998), and therefore the high estimate of m in our study may be an artifact of the data set.

⁴ Halpern, D., V. Zlotnicki, P. M. Woicheshyn, O. B. Brown, G. C. Feldman, M. H. Freilich, F. J. Wentz, and C. Gentemann. 2000. An atlas of monthly mean distributions of SSM/I surface wind speed, AVHRR sea surface temperature, TMI sea surface temperature, AMI surface wind velocity, SeaWiFS chlorophyll-*a*, and TOPEX/POSEIDON sea surface topography during 1998. Jet Propulsion Laboratory Publication 00-08, 102 p. National Aeronautics and Space Administration, Jet Propulsion Laboratory, California Institute of Technology, 4800 Oak Grove Drive, Pasadena, CA 91109.

A significant difference in growth between the sexes at Lord's Bluff indicates that under conditions of rapid growth, females may grow significantly faster than males. As discussed above, the current minimum legal size limit is effectively protecting the reproductive output of the prerecruit population of *N. fucicola*. However, any significant lowering of the legal minimum size is contraindicated where, in prerecruitment size classes, females grow more rapidly than males, because lowering the legal size may result in differences in sex-specific fishing mortality.

As demonstrated in the present study, the choice of growth model and the methods used to compare parameter estimates are critical to ensuring that growth is adequately described, differences in growth are detected, and if detected, are interpretable. In combination, the tests we employed are shown to be generally robust, even in situations where data sets are limited in sample size or by coverage across the full range of age and length classes. We recommend the use of a combination of approaches, including growth models with biologically interpretable parameters, statistical tests such as LRTs, plots of bootstrap parameters, and nonparametric randomization tests, to provide insight into the growth dynamics of fish species.

Acknowledgments

We wish to thank Malcolm Haddon, John Hoening, Craig Johnson, Paul Burch, and Philippe Ziegler for their constructive suggestions for the manuscript. Alan Jordan and Graeme Ewing made invaluable contributions to the field and laboratory analyses. This study was conducted as a part of a Ph.D. program by the primary author, through the Faculty of Science and Engineering at the University of Tasmania.

Literature cited

- Barrett, N. S.
1995a. Aspects of the biology and ecology of six temperate reef fishes (Families: Labridae and Monacanthidae). Ph.D. diss., 192 p. Univ. Tasmania, Hobart, Tasmania, Australia.
1995b. Short- and long-term movement patterns of six temperate reef fishes (Families Labridae and Monacanthidae). Mar. Freshw. Res. 46:853-860.
1999. Food availability is not a limiting factor in the growth of three Australian temperate reef fishes. Environ. Biol. Fish. 56:419-428.
- Beamish, R. J., and D. A. Fournier.
1981. A method for comparing the precision of a set of age determinations. Can. J. Fish. Aquat. Sci. 38:982-983.
- Buxton, C. D.
1993. Life-history changes in exploited reef fishes on the east coast of South Africa. Environ. Biol. Fish. 36:47-63.
- Campana, S. E., M. C. Annand, and J. I. McMillan.
1995. Graphical and statistical methods for determining

- the consistency of age determinations. *Trans. Am. Fish. Soc.* 124:131-138.
- Cerrato, R. M.
1990. Interpretable statistical tests for growth comparisons in the von Bertalanffy equation. *Can. J. Fish. Aquat. Sci.* 47:1416-1426.
1991. Analysis of nonlinearity effects in expected-value parameterizations of the von Bertalanffy equation. *Can. J. Fish. Aquat. Sci.* 48:2109-2117.
- Cranfield, H. J., K. P. Michael, and R. I. C. C. Francis.
1996. Growth rates of five species of subtidal clam on a beach in the South Island, New Zealand. *Mar. Freshw. Res.* 47:773-784.
- Denny, C. M., and D. R. Schiel.
2001. Feeding ecology of the banded wrasse *Notolabrus fucicola* (Labridae) in southern New Zealand: prey items, seasonal differences, and ontogenetic variation. *N. Z. J. Mar. Freshw. Res.* 35:925-933.
- Edgar, G. J.
1997. Australian marine life: the plants and animals of temperate waters, 544 p. Reed Books, Melbourne, Australia.
Ewing, G. P., D. C. Welsford, A. R. Jordan, and C. Buxton.
2003. Validation of age and growth estimates using thin otolith sections from the purple wrasse *Notolabrus fucicola*. *Mar. Freshw. Res.* 54:985-993.
- Fabens, A. J.
1965. Properties and fitting of the von Bertalanffy growth curve. *Growth* 29:265-289.
- Fournier, D. A., J. R. Sibert, J. Majkowski, and J. Hampton.
1990. MULTIFAN a likelihood-based method for estimating growth parameters and age composition from multiple length frequency data sets illustrated using data for southern bluefin tuna (*Thunnus maccoyii*). *Can. J. Fish. Aquat. Sci.* 47:301-317.
- Francis, M. P.
1997. Spatial and temporal variation in the growth rate of elephantfish (*Callorhynchus milii*). *N. Z. J. Mar. Freshw. Res.* 31:9-23.
- Francis, M. P., and R. I. C. C. Francis.
1992. Growth rate estimates for New Zealand rig (*Mustelus lenticulatus*). *Aust. J. Mar. Freshw. Res.* 43:1157-1176.
- Francis, M. P., and K. P. Mulligan.
1998. Age and growth of New Zealand school shark, *Galeorhinus galeus*. *N. Z. J. Mar. Freshw. Res.* 32:427-440.
- Francis, M. P., K. P. Mulligan, N. M. Davies, and M. P. Beentjes.
1999. Age and growth estimates for New Zealand hapuku, *Polyprion oxyenoides*. *Fish. Bull.* 97:227-242.
- Francis, R. I. C. C.
1988a. Maximum likelihood estimation of growth and growth variability from tagging data. *N. Z. J. Mar. Freshw. Res.* 22:42-51.
1988b. Are growth parameters from tagging and age-length data comparable? *Can. J. Fish. Aquat. Sci.* 45:936-942.
1988c. Recalculated growth rates for sand flounder, *Rhombosolea plebeia*, from tagging experiments in Canterbury, New Zealand. *N. Z. J. Mar. Freshw. Res.* 22: 53-56.
1992. L-infinity has no meaning for tagging data sets. In *The measurement of age and growth in fish and shellfish*. Australian Society for Fish Biology workshop, Lorne 22-23 August 1990 (D. A. Hancock, ed.), p. 182-184. Bureau of Rural Resources, Canberra, Australia.
- Gillanders, B. M.
1997. Comparison of growth rates between estuarine and coastal reef populations of *Achoerodus viridis* (Pisces: Labridae). *Mar. Ecol. Prog. Ser.* 146:283-287.
- Haddon, M.
2001. Modelling and quantitative methods in fisheries, 406 p. Chapman & Hall/CRC, Boca Raton, FL.
- Jones, G. P.
1980. Growth and reproduction in the protogynous hermaphrodite *Pseudolabrus celidotus* (Pisces: Labridae) in New Zealand. *Copeia* 1980:660-675.
1984. Population ecology of the temperate reef fish *Pseudolabrus celidotus* Bloch and Schneider (Pisces: Labridae) II. Factors influencing adult density. *J. Exp. Mar. Biol. Ecol.* 75:277-303.
- Kimura, D. K.
1980. Likelihood methods for the von Bertalanffy growth curve. *Fish. Bull.* 77:765-776.
- Knight, W.
1968. Asymptotic growth: an example of nonsense disguised as mathematics. *J. Fish Res. Board Can.* 25:1303-1307.
- Mooij, W. M., J. M. V. Rooij, and S. Winjhoven.
1999. Analysis and comparisons of fish growth from small samples of length-at-age data: detection of sexual dimorphism in Eurasian perch as an example. *Trans. Am. Fish. Soc.* 128: 483-490.
- Patterson, T.
2000. Fisheries models of the temperate wrasses *Notolabrus tetricus* and *Notolabrus fucicola*: implications of life history strategy for management. B.S. honours thesis, 111 p. Univ. Tasmania. Hobart, Tasmania, Australia.
- Pauly, D.
1979. On the interrelationships between natural mortality, growth parameters, and mean environmental temperature in 175 fish stocks. *J. Cons. CIEM* 39:175-192.
- Ratkowsky, D. A.
1986. Statistical properties of alternative parameterizations of the von Bertalanffy growth curve. *Can. J. Fish. Aquat. Sci.* 43:742-747.
- Roff, D. A.
1980. A motion for the retirement of the von Bertalanffy function. *Can. J. Fish. Aquat. Sci.* 37: 127-129.
- Russell, B. C.
1988. Revision of the labrid fish genus *Pseudolabrus* and allied genera. *Rec. Aust. Mus. Supplement* 9:1-76.
- Schenker, N., and J. F. Gentleman.
2001. On judging the significance of differences by examining overlap between confidence intervals. *Am. Statist.* 55:182-186.
- Shepherd, S. A., and P. S. Clarkson.
2001. Diet, feeding behaviour, activity and predation of the temperate blue-throated wrasse, *Notolabrus tetricus*. *Mar. Freshw. Res.* 52:311-322.
- Simpendorfer, C. A.
2000. Growth rates of juvenile dusky sharks, *Corcharrhinus obscurus* (Lesueur, 1818) from southwestern Australia estimated from tag-recapture data. *Fish. Bull.* 98:811-822.
- Simpendorfer, C. A., J. Chidlow, R. McAuley, and P. Unsworth.
2000. Age and growth of the whiskery shark, *Furgaleus macki*, from southwestern Australia. *Environ. Biol. Fish.* 58:335-343.

- Wang, Y. G., D. Thomas, and I. F. Somers.
1995. A maximum likelihood approach for estimating growth from tag-recapture data. *Can. J. Fish. Aquat. Sci.* 52:252-259.
- Wang, Y. G., and M. R. Thomas.
1995. Accounting for individual variability in the von Bertalanffy growth model. *Can. J. Fish. Aquat. Sci.* 52: 1368-1375.
- Wang, Y. G.
1998. An improved Fabens method for estimation of growth parameters in the von Bertalanffy model with individual asymptotes. *Can. J. Fish. Aquat. Sci.* 1998:397-400.
- Wang, Y. G., and N. Ellis.
1998. Effect of individual variability on estimation of population parameters from length-frequency data. *Can. J. Fish. Aquat. Sci.* 55:2393-2401.

Effects of harvesting methods on sustainability of a bay scallop fishery: dredging uproots seagrass and displaces recruits

Melanie J. Bishop

Charles H. Peterson

Henry C. Summerson

David Gaskill

University of North Carolina at Chapel Hill
Institute of Marine Sciences
3431 Arendell St.
Morehead City, North Carolina 28557

E-mail address (for M. J. Bishop, contact author): melanie.bishop-1@uts.edu.au

Present address (for M. J. Bishop): Department of Environmental science
University of Technology, Sydney
Corner of Westbourne St. and Pacific Highway
Gore Hill, New South Wales, Australia 2065

Fishing is widely recognized to have profound effects on estuarine and marine ecosystems (Hammer and Jansson, 1993; Dayton et al., 1995). Intense commercial and recreational harvest of valuable species can result in population collapses of target and nontarget species (Botsford et al., 1997; Pauly et al., 1998; Collie et al., 2000; Jackson et al., 2001). Fishing gear, such as trawls and dredges, that are dragged over the seafloor inflict damage to the benthic habitat (Dayton et al., 1995; Engel and Kvitek, 1995; Jennings and Kaiser, 1998; Watling and Norse, 1998). As the growing human population, over-capitalization, and increasing government subsidies of fishing place increasing pressures on marine resources (Myers, 1997), a clear understanding of the mechanisms by which fishing affects coastal systems is required to craft sustainable fisheries management.

Dredging, possibly the most destructive of common fishing methods (Collie et al., 2000), has been the subject of many recent ecological studies (Dayton et al., 1995; Jennings and Kaiser, 1998; Thrush et al., 1998). These studies indicate that dredge extraction and disturbance can have large direct effects on the abundance, biomass, and diversity of resident macrobenthic species (e.g., Caddy, 1973; Eleftheriou and Robert-

son, 1992). In addition, dredging can indirectly affect macrobenthic species through disturbance of benthic habitat (Ramsay et al., 1998; Lenihan and Peterson, 1998). Indirect impacts of dredging may be particularly serious where highly structured biogenic habitats, such as oyster reefs or seagrass beds, are affected (Peterson et al., 1987; Lenihan and Peterson, 1998; Collie et al., 2000; Lenihan and Peterson, 2004). These habitats may be considered essential habitat for many species of fish of commercial or recreational value (Thayer et al., 1975), providing refuges from predators (Orth et al., 1984; Castel et al., 1989) and abundant epibiotic food (Virnstein et al., 1984; Sánchez-Jerez et al., 1999).

Among fishery species dependent on biogenic habitat is the commercially and recreationally important bay scallop (*Argopecten irradians*). In the two reproductive seasons, spring and fall, bay scallop recruits settle onto hard substrates (Belding, 1910; Castagna, 1975) where they remain attached for the first few months of their lives. They then complete their 12–24 month life cycle on the estuary floor. In North Carolina, eelgrass is the only hard substrate of any abundance to which bay scallop recruits can attach themselves (Kirby-Smith, 1970).

Commercial harvest of bay scallops in North Carolina is achieved primarily by toothless epibenthic dredge (22.7 kg legal limit; NCMFC¹). Dredges have the advantage that, unlike rakes, they can be used from boats in deep as well as shallow waters. Their disadvantage is that they decrease the biomass and shoot density of seagrass in scallop beds (Fonseca et al., 1984). Early in the North Carolina scallop season, which extends from December through May (NCMFC¹), most of the juveniles from the previous fall spawning are still attached to seagrass blades (Spitsbergen²). If these juveniles are displaced by habitat destruction, reduced numbers of scallops may be available for harvest in the subsequent year (hypothesized by Thayer and Stuart, 1974). Although seagrasses can recover from small-scale disturbances to shoots by vegetative growth, large-scale disturbances to their subsurface root and rhizome system may permanently reduce the density of submerged aquatic vegetation (SAV) (Peterson et al., 1987) such that it may limit settlement of the following year's recruits or induce greater rates of predation on them (or bring about both). Although, in North Carolina, the bay scallop fishery management plan requires that the scallop season be opened after fall spawning is completed (Peterson, 1990); it fails to consider how methods of harvest may indirectly effect spawning stock biomass in years to come.

¹ NCMFC (North Carolina Marine Fisheries Commission). 2005. North Carolina fisheries rules for coastal waters, 210 p. North Carolina Department of Environment and Natural Resources, 1601 Mail Service Center, Raleigh, NC 27699.

² Spitsbergen, D. 1979. A study of the bay scallop (*Argopecten irradians*) in North Carolina waters. Report for Project 2-256-R, 44 p. North Carolina Division of Marine Fisheries, 3441 Arendell Street, Morehead City, NC 28557

Implementation of gear restrictions that allow only hand methods of harvesting scallops (i.e., hand, rake, dip nets) may minimize impacts of harvesting on scallop recruits by reducing damage to seagrass and the loss of juvenile bay scallops that comprise the year class that will be fished in the following year. Although such restrictions were introduced to Bogue Sound in 1992 in response to the 1987 red tide that decimated scallop populations in that water basin (Summerson and Peterson, 1990), this conservation-based measure was discontinued in 1998 because of social pressure from fishermen. In the present study, we ascertain the impacts of dredges and hand-harvesting methods on the biomass of seagrass, as compared to undisturbed controls, 1) by measuring the biomass of seagrass directly dislodged by each method, and 2) by ascertaining, through measurements of biomass one month later, whether this removal affects the standing stock of seagrass over a longer temporal scale. We also tested both direct and indirect effects of seagrass removal on bay scallop recruits by measuring their density before and one month after harvesting and by ascertaining whether any documented difference can be explained by the numbers directly removed by uprooting of seagrass during harvesting. Such an assessment of ecological impacts of dredging on bay scallop recruits is urgently required given that North Carolina landings of bay scallops have fallen to an historic low since the relaxation of gear restrictions (Burgess and Bianchi³).

Materials and methods

Nine adjacent experimental plots, 25 m × 8 m, were established as a research sanctuary, closed to commercial fishing activity, in western Bogue Sound, North Carolina (34°41.6'N, 76°59.1'W), prior to the opening of the scallop season in winter 2001–2002. Although this section of Bogue Sound has been closed to scallop dredging since at least 1998, its high-tide water depth of 1.5 m is well within the depth range for harvesting with this method. Plots contained continuous seagrass beds dominated by *Zostera marina* on a muddy-sand bottom. Three of the plots were randomly assigned to each of the experimental treatments: hand-harvested, dredge-harvested, and control (undisturbed). In order to ensure that our treatments were representative of harvesting methods and intensities used by the industry, they were performed with participation of an experienced commercial scallop fisherman (Ted Willis of Salter Path). Dredging was achieved with a standard 72-cm wide steel scallop dredge, at an intensity of five parallel tows, each running along the length of the plot within a 10-minute period. This method, which mimicked commercial fishing

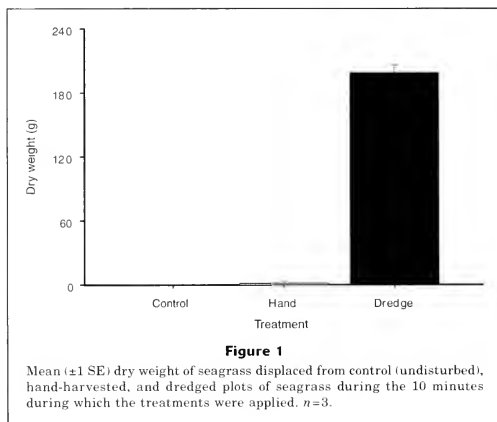
practices, minimized overlap between the dredge paths. Hand scalloping involved a single fisherman collecting scallops from the bottom by hand, also during 10-minute periods. Care was taken to ensure that the treatments were applied evenly over the entire plot to avoid creating large within-plot variance that might preclude detection of differences among plots.

Seagrass and scallops collected during harvesting were retained for measurements. The number of adult scallops (>40 mm shell height; Peterson et al., 1989) obtained with each of the methods of harvest was enumerated. The size (to the nearest 0.1 mm) and number of juvenile scallops collected as bycatch and the dry weight of seagrass removed during harvesting were quantified separately. Because not all seagrass and juvenile scallops displaced by harvesting are retained in the dredge or by a fisherman collecting scallops by hand methods, an 8-m long net with 5-mm mesh that extended from the bottom to the surface was set downstream from each plot and perpendicular to the flow of the current during harvest. The nets were strung between stakes marking the corners of the experimental plot. Dislodged juvenile scallops and seagrass collected by the nets were added to the amounts extracted from the dredge to compute displacement totals. Nets were also set downstream of controls to determine natural rates of transport of seagrass and juvenile scallops that could not be attributed to harvesting operations.

Each plot was sampled on 14 January 2002, immediately prior to harvesting on that same day to determine: 1) the density of bay scallop recruits (size ≤40 mm; Peterson et al., 1989); 2) the size distribution of the recruits; and 3) biomass per unit of area of seagrass. These variables were resampled on 25 February 2002, over one month later, to ascertain any lasting impact of harvest. Sampling of scallops was conducted with a 0.5-m² cylindrical quadrat, haphazardly positioned at nine locations within each plot. A 1.2-cm tall cylinder of 6-mm nylon mesh, attached to the quadrat and suspended by a buoyant plastic hoop that floated on the surface of the water, isolated the volume of water above each quadrat so that it could be sampled by suction with a Venturi suction device (according to Peterson et al., 1989). The suction device forced 600 mL of water per minute through a 3-mm collecting bag. Suction sampling was necessary because scallops, which typically recline on the bottom, can enter the water to swim when threatened by predators or otherwise disturbed (Peterson et al., 1982). The disturbance caused by suction sampling of only nine small areas was minimal compared to the scale of harvesting disturbance. Upon returning to the laboratory, seagrass was removed from samples for measurement of dry weight biomass and live scallops were counted, measured to the nearest 0.1 mm and categorized as adults (>40 mm) or recruits (≤40 mm) in the subsequent year class.

Seagrass was sampled in five replicate 0.25-m² areas within each plot by suction dredging inside a 0.56-m diameter circular quadrat to a sediment depth of 12 cm. Previous sampling has shown this method to be success-

³ Burgess, C. C., and A. J. Bianchi. 2004. An economic profile analysis of the commercial fishing industry of North Carolina including profiles for state-managed species, 243 p. North Carolina Division of Marine Fisheries, 3441 Arendell Street, Morehead City, NC 28557.



ful in removing both roots and shoots in their entirety (Peterson et al., 1983a). Shoots and roots, which were collected in a 3-mm nylon mesh bag, were dried at 60°C to constant weight to calculate total dry weight biomass of seagrass.

ANOVAs allowed us to test for a significant interaction between time (before versus after) and disturbance (dredge versus hand-harvest versus control) in the biomass of seagrass and recruit density of bay scallops (a basic BACI design; Green, 1979), indicative of an impact of harvest. The cause of any significant time \times disturbance interactions was explored by using Student-Newman-Keul (SNK) tests. Prior to each analysis, Cochran's (1951) C -test was done to test for heterogeneity of variances. Where variances were heterogeneous, data were $\ln(x+1)$ transformed to remove heteroscedasticity at $\alpha = 0.05$.

Results

Of the two methods used to harvest adult scallops, hand harvesting had by far the greater efficiency in these shallow waters (ANOVA, $P < 0.0001$). Over a period of 10 minutes, an average of 156 ± 12 (1 SE) scallops within each 25×8 m plot was harvested by hand as compared to 26 ± 1 scallops with the dredge.

The two methods of harvesting differed significantly in their impact on seagrass. Hand harvesting of scallops did not increase dislodgement of seagrass above the natural drift rate (Fig. 1). Dredging, in contrast, resulted in 127 times the export of seagrass. This extraction did not, however, result in detectable reductions in biomass per unit of area of seagrass within dredged

plots when sampled one month later. There was no significant temporal change in the biomass of seagrass in any of the three treatments from before to one month after harvesting (Table 1, Fig. 2).

Fewer than 2% of the estimated total number of juvenile scallops in a plot were directly removed by dredging and none was removed by hand-harvesting. Nevertheless, sampling one month after harvesting indicated depressed densities of juvenile bay scallops in dredged plots (Table 2; Fig. 3). This difference could not be attributed to natural change; small increases (16–55%) in numbers of juvenile bay scallops in the hand-harvested and control plots were documented over the same period (Fig. 3). A comparison of size-frequency histograms of juvenile bay scallops within each type of plot from before to after harvesting revealed that the decrease in juvenile scallop numbers in the dredged plots was primarily due to losses of scallops in the smallest size classes (< 14 mm; Fig. 4). In the dredged plots, mean (\pm SE) size of juveniles (≤ 40 mm in shell height) increased from 17.04 ± 0.83 in January to 20.43 ± 0.76 in February. Over the same time period, mean size changed little in the control (16.09 ± 0.85 to 16.75 ± 0.75 mm) or in the hand-harvested (18.19 ± 0.85 to 17.95 ± 0.65 mm) plots.

Discussion

Previous research indicates that the implementation of certain gear restrictions on estuarine bivalve fisheries can minimize habitat destruction without sacrificing harvesting efficiency (Peterson et al., 1983b; Lenihan and Peterson, 2004). In our study, which successfully mimicked the efficiency of commercial dredging and

Table 1

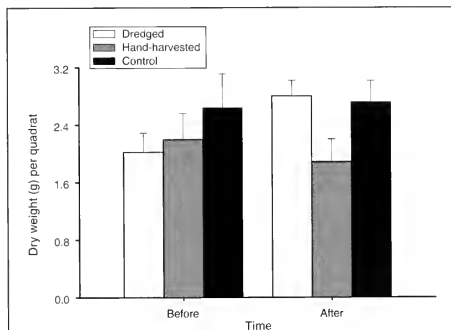
BACI (Green, 1979) analysis of variance that tests for an impact of scallop harvesting on biomass of seagrass. Nine plots of seagrass were randomly assigned to three treatments: undisturbed control, hand-harvested, dredged. Biomass of seagrass was determined immediately before (Jan 2002) and one month after (Feb 2002) application of treatments to plots. $n = 5$.

Source	df	MS	F	P
Before versus after treatment	1	0.14	0.78	0.41
Treatment	2	0.35	0.81	0.49
Plot (treatment)	6	0.43	3.50	0.00
Before vs. after \times treatment	2	0.26	1.41	0.31
Before vs. after \times plot (treatment)	6	0.18	1.49	0.19
Residual	72	0.12		
Transformation	ln(x+1)			
Cochran's test	C=0.16 (P>0.05)			

hand-harvesting of bay scallops (see Burgess and Bianchi³), hand-harvesting yielded six times the bay scallop harvest obtained per unit of time by dredging, while reducing deleterious environmental effects. Hand-harvesting did not result in uprooting of seagrass or displacing juvenile bay scallops, whereas dredging caused significant damage to seagrass. Ten minutes of dredging resulted in an average dry weight loss of 200 g of seagrass per plot—9 % of the estimated biomass of seagrass present prior to harvest. Despite this sizable removal of seagrass biomass, a persistent impact of dredging on seagrass biomass was not detected one month later. To the contrary, a 39% increase in seagrass biomass was seen across the dredged plots that was not replicated in the control plots. This result indicated that dredging had only a short-term negative impact on seagrass shoots (the necessary production of new leaves) and instead appeared to stimulate new production during the winter period that was more than sufficient to replace dredging damage.

Despite the rapid recovery of seagrass from dredging injury, a sustained negative impact of dredging on the density of juvenile bay scallops within plots was detected over the one-month period of our study. In contrast to the small increases in juvenile scallop density that occurred in hand-harvested and control plots over the course of the study, mean density of juveniles in dredged plots declined from 1.37 ± 0.33 (1 SE) to 0.89 ± 0.23 per 0.5 m^2 . This 40% reduction in juvenile scallops in dredged plots cannot be explained by the bycatch alone. Whereas total bycatch of juveniles was, on average, two scallops per dredged plot, the average reduction in the density of juvenile bay scallops was 0.5 per 0.5-m^2 quadrat or 200 per 200-m^2 plot.

Instead, the reduction in density of juvenile scallops in dredged plots is best explained by their migration

**Figure 2**

Mean (\pm SE) dry weight of seagrass per 0.25-m^2 quadrat in control (undisturbed), hand-harvested, and dredged plots immediately before and one month after the 10-minute treatments were applied. $n=15$.

after dredging injury to seagrass habitat into adjacent undisturbed control and hand-harvested plots. Abundances of juvenile bay scallops in hand-harvested and control plots increased over the one month of our study by an amount more than sufficient to compensate for losses of juveniles from dredged plots. These increases in abundances in control and hand-harvested plots cannot be attributed to the settlement of new recruits: fall recruitment of juvenile scallops to seagrass beds is typically completed by the end of December (Peterson et al., 1989), spring spawning does not commence until March (Peterson and Summerson, 1992), and scallops spawned during our experiment could not possibly have grown fast enough over one month to reach a size re-

Table 2

BACI analysis of variance testing for an impact of scallop harvesting on density of scallop recruits. Nine plots of seagrass were randomly assigned to three treatments: undisturbed control, hand-harvested, dredged. Density of scallop recruits was determined immediately before (Jan 2002) and one month after (Feb 2002) application of treatments to plots, $n=9$.

Source	df	MS	F	P
Before vs. after treatment	1	0.89	0.78	0.41
Treatment	2	5.57	2.74	0.14
Plot (treatment)	6	2.03	0.77	0.59
Before vs. after \times treatment	2	4.57	4.01	0.08
Before vs. after \times plot (treatment)	6	1.14	0.43	0.85
Residual	144			
Cochran's test	C = 0.13 ($P > 0.05$)			
SNK tests	Before vs. after \times treatment			
	Before: control = hand-harvested = dredged			
	After: control = hand-harvested > dredged			

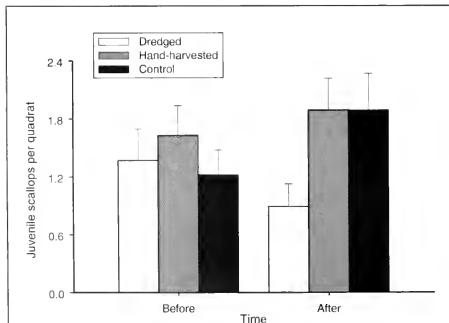
tained by sieves (see Irlandi et al., 1999 for growth rates). Scallops colonizing hand-harvested and control plots were of the right size and of sufficient abundance to be those missing from dredged plots. The migration appears to have included active swimming because tidal currents were perpendicular to the direction of scallop movement.

Although juvenile scallops are largely sessile, our interpretation that juveniles migrate in response to dredging is consistent with field and laboratory observations of juvenile bay scallop behavior. During seasonal sloughing of eelgrass blades, juvenile bay scallops break away

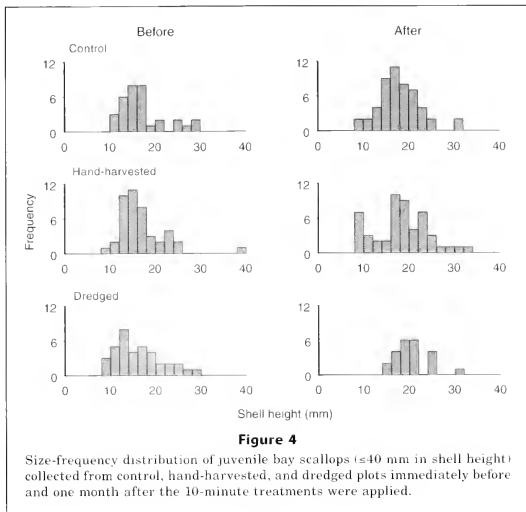
and re-establish byssal attachments to seagrass blades (Thayer et al., 1975). Mesocosm observations confirm that juveniles are capable of swimming distances of at least several meters when displaced (Bishop, personal observ.). Thus, our experimental restriction on dredging to small areas may have facilitated relocation of scallops to adjacent, undisturbed habitat, where they remained one month later even after seagrass had regrown in the dredged plots. In the case of the commercial fishery, however, juvenile scallops emigrating from disturbed habitat over the extensive fished areas would be far less likely to encounter undisturbed seagrass habitat for re-attachment. Indeed, transport to unfavorable unvegetated habitat where predation risk is enhanced would likely inflate mortality.

In our study, juvenile scallops lost from the dredged plots came primarily from the smallest size classes. Small juvenile scallops are more susceptible to benthic predators that forage within seagrass beds than larger juveniles (Pohle et al., 1991). Because the foraging efficiency of some predators increases with decreasing biomass of seagrass (Prescott, 1990), a decrease in seagrass biomass, even for a period of weeks, would likely increase predation on juvenile scallops. Thus, small juveniles probably are increasing their chances of survival by emigrating away from depleted and into denser seagrass. Larger juveniles, in contrast, experience a partial size refuge from predators (e.g., Pohle et al., 1991), and thus have less incentive to emigrate.

This study considered the impact of only a single bay scallop-harvesting event on seagrass biomass and abundance of juvenile bay scallops within small experimental plots. Fishing disturbances are, however, typically chronic, occurring multiple times within a given season, and over large spatial scales.

**Figure 3**

Mean (\pm SE) number of juvenile bay scallops (≤ 40 mm in shell height) per 0.5-m^2 quadrat in control (undisturbed), hand-harvested, and dredged plots immediately before and one month after the 10-minute treatments were applied. $n=15$.



In our study, just 10 minutes of dredging resulted in the removal of approximately 9% of the total biomass of seagrass in the experimental plot. Repeating this fishing disturbance over large spatial scales could, therefore, have substantial detrimental effects on seagrass habitat and, as an indirect result, the abundance of bay scallops that comprise the next generation. In addition, other habitat functions of seagrass are likely compromised until regrowth occurs. Peterson et al. (1987) demonstrated in this same system that a one-time reduction of 65% in seagrass biomass from gear disturbance during clam harvesting was not replaced over a subsequent 2-year period free of additional fishing.

The results of our study raise doubt about the sustainability of a bay scallop fishery in which the harvest method is dredging. Because this species, which lives only 12–24 months, is recruitment-limited (Peterson and Summerson, 1992; Peterson et al., 1996), reductions in densities of juvenile bay scallops by dredging will not only diminish that year's harvest but also presumably result in less spawning-stock biomass. Without restrictions on scallop dredging, impacts of dredging disturbance compounded across years may lead to the gradual collapse of the fishery. Re-imposing gear restrictions in shallow areas where hand harvest is practical may, therefore, pay big dividends. When use of the less destructive hand method carries little or no penalty of reduced fishing success, restricting scallop dredging from shallow SAV represents an appropriate ecosystem-based

management choice (Botsford et al., 1997) that may sustain SAV habitat and restore a bay scallop fishery now in serious decline (Burgess and Bianchi³).

Acknowledgments

We thank Ted Willis of Salter Path for advice and collaboration on harvesting methods and intensities. This work was funded by the North Carolina Fishery Resource Grant Program administered by North Carolina Sea-Grant (to C. H. Peterson). This manuscript benefitted from the comments of two anonymous reviewers.

Literature cited

- Belding, D. L.
1910. The scallop fishery of Massachusetts, 51 p. The Commonwealth of Massachusetts, Boston, MA.
- Botsford, L. W., J. C. Castilla, and C. H. Peterson.
1997. The management of fisheries and marine ecosystems. *Science* 277:509–515.
- Caddy, J. F.
1973. Underwater observations on tracks of dredges and trawls and some effects of dredging on a scallop ground. *J. Fish. Res. Board Can.* 30:173–80.
- Castagna, M.
1975. Culture of the bay scallop, *Argopecten irradians*, in Virginia. *Mar. Fish. Rev.* 37:19–24.

- Castel, J., P.-J. Labourg, V. Escaravage, I. Auby, and M. E. Garcia.
1989. Influence of seagrass beds and oyster parks on the abundance and biomass pattern of meio- and macrobenthos in tidal flats. *Estuar. Coastal Shelf Sci.* 28:71-85.
- Cochran, W. G.
1951. Testing a linear relationship among variances. *Biometrics* 7:17-32.
- Collie, J. S., S. J. Hall, M. J. Kaiser, and I. R. Poiner.
2000. A quantitative analysis of fishing impacts on shelf-sea benthos. *J. Anim. Ecol.* 69:785-798.
- Dayton, P. K., S. F. Thrush, M. T. Agardy, and R. J. Hoffman.
1995. Environmental effects of marine fishing. *Aquat. Conserv. Mar. Fresh. Ecosyst.* 5:205-232.
- Eleftheriou, A., and M. R. Robertson.
1992. The effects of experimental scallop dredging on the fauna and physical environment of a shallow sandy community. *Neth. J. Sea. Res.* 30:289-299.
- Engel, J., and R. G. Kvitck.
1995. Effects of otter trawling on a benthic community in Monterey Bay Marine Sanctuary. *Conserv. Biol.* 12:1204-1214.
- Fonseca, M. S., G. W. Thayer, A. J. Chester, and C. Foltz.
1984. Impact of scallop harvesting on eelgrass (*Zostera marina*) meadows: implications for management. *N. Am. J. Fish. Manag.* 4:286-293.
- Green, R. H.
1979. Sampling design and statistical methods for environmental biologists, 257 p. Wiley, New York, NY.
- Hammer, M. A., and A. J. B. Jansson.
1993. Diversity change and sustainability: implications for fisheries. *Ambio* 22:97-105.
- Irlandi, E. A., B. A. Orlando, and W.G. Ambrose Jr.
1999. Influence of seagrass habitat patch size on growth and survival of juvenile bay scallops, *Argopecten irradians concentricus* (Say). *J. Exp. Mar. Biol. Ecol.* 235:21-43.
- Jackson, J. B. C., M. X. Kirby, W. H. Berger, K. A. Bjorndal, L. W. Botsford, B. J. Bourque, R. H. Bradbury, R. Cooke, J. Erlanson, J. A. Estes, T. P. Hughes, S. Kidwell, C. B. Lange, H. S. Lenihan, J. M. Pandolfi, C. H. Peterson, R. S. Steneck, M. J. Tegner, and R. R. Warner.
2001. Historical overfishing and the recent collapse of coastal ecosystems. *Science* 293:629-638.
- Jennings, S., and M. J. Kaiser.
1998. The effects of fishing on marine ecosystems. *Adv. Mar. Biol.* 34:201-352.
- Kirby-Smith, W. W.
1970. Growth of the scallops, *Argopecten irradians concentricus* (Say) and *Argopecten gibbus* (Linné), as influenced by food and temperature. Ph.D. diss., 127 p. Duke Univ., Durham, NC.
- Lenihan, H. S., and C. H. Peterson.
1998. How habitat degradation through fishery disturbance enhances effects of hypoxia on oyster reefs. *Ecol. Appl.* 8:128-140.
2004. Conserving oyster reef habitat by switching from dredging and tonging to diver-harvesting. *Fish. Bull.* 102:298-305.
- Myers, N.
1997. Consumption: Challenge to sustainable development. *Science* 276:53-55.
- Orth, R. J., K. L. Heck Jr., and J. van Montfrans.
1984. Faunal communities in seagrass beds: a review of the influence of plant structure and prey characteristics on predator-prey relationships. *Estuaries* 7:339-50.
- Pauly, D., V. Christensen, J. Dalsgaard, R. Froese, and F. Torres Jr.
1998. Fishing down marine food webs. *Science* 279:860-63.
- Peterson, C. H.
1990. On the role of ecological experimentation in resource management: managing fisheries through mechanistic understanding of predator feeding behaviour. In *Behavioural mechanisms of food selection* (R. N. Hughes ed.) p. 821-846. Springer-Verlag, Berlin.
- Peterson, C. H., and H. C. Summerson.
1992. Basin-scale coherence of population dynamics of an exploited marine invertebrate, the bay scallop: implications of recruitment limitation. *Mar. Ecol. Prog. Ser.* 90:257-272.
- Peterson, C. H., W. G. Ambrose, and J. H. Hunt.
1982. A field-test of the swimming response of the bay scallop (*Argopecten irradians*) to changing biological factors. *Bull. Mar. Sci.* 32:939-944.
- Peterson, C. H., P. B. Duncan, H. C. Summerson, and G. W. Safrit.
1983a. A mark-recapture test of annual periodicity of internal growth bands of hard clams, *Mercenaria mercenaria*, along the southeastern United States. *Fish. Bull.* 81:765-779.
- Peterson, C. H., H. C. Summerson, and S. R. Fegley.
1983b. Relative efficiency of two clam rakes and their contrasting impacts on seagrass biomass. *Fish. Bull.* 81:429-434.
1987. Ecological consequences of mechanical harvesting of clams. *Fish. Bull.* 85:281-298.
- Peterson, C. H., H. C. Summerson, S. R. Fegley, and C. Prescott.
1989. Timing, intensity and sources of autumn mortality of adult bay scallops *Argopecten irradians concentricus* Say. *J. Exp. Mar. Biol. Ecol.* 127:121-140.
- Peterson, C. H., H. C. Summerson, and R. A. Luettich.
1996. Response of bay scallops to spawner transplants: a test of recruitment limitation. *Mar. Ecol. Prog. Ser.* 132:93-107.
- Pohle, D. G., V. M. Bricej, and Z. Garcia-Esquivel.
1991. The eelgrass canopy: an above-bottom refuge from benthic predators for juvenile bay scallops *Argopecten irradians*. *Mar. Ecol. Prog. Ser.* 74:47-59.
- Prescott, R.C.
1990. Sources of predatory mortality in the bay scallop *Argopecten irradians* (Lamarck): interactions with seagrass and epibiotic coverage. *J. Exp. Mar. Biol. Ecol.* 144:63-83.
- Ramsay, K. M., J. Kaiser, and R. N. Hughes.
1998. Responses of benthic scavengers to fishing disturbance by towed gears in different habitats. *J. Exp. Mar. Biol. Ecol.* 224:73-89.
- Sánchez-Jerez, P., C. B. Cebrián, and A. A. R. Esplá.
1999. Comparison of the epifaunal spatial distribution in *Posidonia oceanica*, *Cymodocea nodosa* and unvegetated bottoms: importance of meadow edges. *Acta Oecol.* 20:391-405.
- Summerson, H. C., and C. H. Peterson.
1990. Recruitment failure of the bay scallop, *Argopecten irradians concentricus*, during the first red tide *Ptychodiscus brevis* outbreak recorded in North Carolina. *Estuaries* 13:322-31.
- Thayer, G. W., and H. H. Stuart.
1974. The bay scallop makes its bed of seagrass. *Mar. Fish. Rev.* 36(7):27-30.

- Thayer, G. W., S. M. Adams, and M. W. LaCroix.
1975. Structural and functional aspects of a recently established *Zostera marina* community. In *Estuarine research* (L. E. Cronin ed.), p. 518-540. Academic Press, New York, NY.
- Thrush, S. F., J. E. Hewitt, V. J. Cummings, P. K. Dayton, M. Cryer, S. J. Turner, G. A. Funnell, R. G. Budd, C. J. Milburn, and M. R. Wilkinson.
1998. Disturbance of the marine benthic habitat by commercial fishing: impacts at the scale of the fishery. *Ecol. Appl.* 8:866-879.
- Virnstein, R. W., W. G. Nelson, F. G. Lewis, and R. K. Howard.
1984. Latitudinal patterns in seagrass epifauna: do patterns exist, and can they be explained? *Estuaries* 7A:310-330.
- Watling, L., and E. A. Norse.
1998. Disturbance of the seabed by mobile fishing gear: a comparison to forest clearcutting. *Cons. Biol.* 12:1180-1197.

Longline-caught blue shark (*Prionace glauca*): factors affecting the numbers available for live release*

Guillermo A. Diaz

Joseph E. Serafy

National Marine Fisheries Service
Southeast Fisheries Science Center
75 Virginia Beach Drive
Miami, Florida 33149

E-mail address (for G. A. Diaz) Guillermo.diaz@noaa.gov

The blue shark (*Prionace glauca*) is an oceanic species that occurs in temperate and tropical waters around the globe (Robins and Ray, 1986). This species is a major bycatch of pelagic longline fleets that operate to supply the world's growing demand for tunas and swordfish (*Xiphias gladius*) (Stevens, 1992; Bailey et al., 1996; Francis, 1998; Francis et al., 2001; Macias and de la Serna, 2002); numerically, the blue shark is the top nontarget species captured by the U.S. longline pelagic Atlantic fleet (Beerkircher et al.¹).

Ward et al. (2004) examined the effect of longline soak time (set duration) on the catch rate of several target and bycatch species, including the blue shark. However, they did not investigate the effects of fish size, set duration, and water temperature on shark survival, and, therefore, numbers potentially available for live release (Francis et al., 2001; Campana et al.²). Knowledge of such relationships may be of value: 1) for minimizing bycatch mortality on this and other highly vulnerable pelagic species through modification of fishing strategy; and 2) for blue shark stock assessments that are based on commercial longline catch data.

Materials and methods

Data analyses were conducted on a portion of the U.S. Atlantic Pelagic Observers Program (POP) database. The POP places trained observers aboard commercial fishing vessels

to record detailed information about each fishing set, the catch and the bycatch that would not otherwise be collected. Recorded information includes individual fish size (measured or estimated) and disposition (alive or dead), surface water temperature ($^{\circ}\text{C}$) at gear deployment and at haulback, and set location (latitude and longitude). The duration of each set (soak time, in hours) can be obtained because time at start of gear deployment and at end of gear retrieval is also recorded. In the present study, we restricted our analyses to observed sets made from 1992 to 2002 by U.S. flag vessels north of 35 $^{\circ}\text{N}$ latitude (Fig. 1). This area includes much of the U.S. exclusive economic zone north of Chesapeake Bay but also includes waters overlying the Grand Banks. Data resulting from experimental fishing conducted from 2001 to 2004 over the Grand Banks area (i.e., north of 35 $^{\circ}\text{N}$ latitude and west of 60 $^{\circ}\text{W}$ longitude) were not included because they did not reflect typical fishing operations.

For analysis purposes, blue shark were placed in 25-cm fork length (FL) size classes and water temperatures (means) and set durations into 2 C and 2-hour intervals, respectively.

Size intervals were set at 25 cm FL to increase the number of observations in each size category and to reduce the bias that results from estimating lengths versus actually measuring them (e.g., observed increase in the frequency of the estimated lengths in 5- or 10-cm intervals). For each combination of size,

temperature, set duration, season, and area (i.e., Grand Banks and U.S. Atlantic east coast), the proportion of blue shark released alive (P_{DA}) was calculated.

Only sharks explicitly recorded as "discarded alive" or "discarded dead" were used and only proportions derived from at least 20 observations (i.e., captured sharks) were analyzed. The influence of the fish size, water temperature, set duration, area, and season (and all possible interactions) on P_{DA} was assessed by using the linear model

$$P_i = \beta_0 + \beta_1 T_i + \beta_2 D_i + \beta_3 S_i + \beta_4 L_i + \beta_5 A_i + \epsilon_i,$$

where P_i = to the proportion of blue shark discarded alive;

T = the temperature;

D = set duration;

S = season;

L = length;

A = set area,

ϵ = the residual term of the i^{th} observation; and

$\beta_0 - \beta_5$ are model parameters.

Prior to regression, proportions were arcsine-transformed according to the methods of Sokal and Rohlf (1981). In

¹ Beerkircher, L. R., C. J. Brown, and D. W. Lee. 2002. SEFSC pelagic observer program data summary for 1992–2000. NOAA Tech. Memo. NMFS-SEFSC-486, 23 p. Southeast Fisheries Science Center, Miami, FL 33149.

² Campana S., P. Gonzalez, W. Joyce, and L. Marks. 2002. Catch, bycatch and landings of blue shark (*Prionace glauca*) in the Canadian Atlantic. Canadian Science Advisory Secretariat, Research Document 2002/101, 41 p. Marine Fish Division, Bedford Institute of Oceanography, Dartmouth, Nova Scotia, B2Y 4A2, Canada.

* Contribution number SFD-2005-030 from the Sustainable Fisheries Division, Southeast Fisheries Science Center, NMFS, 75 Virginia Beach Drive, Miami, FL 33149.

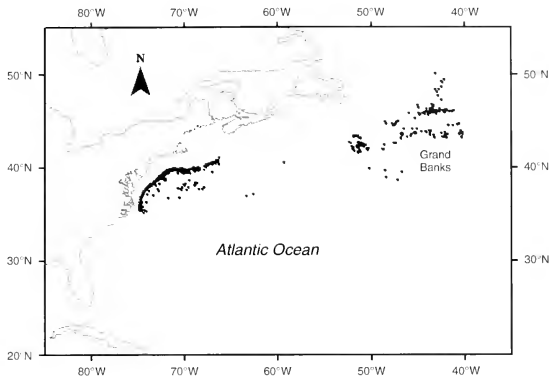


Figure 1

Locations of observed longline sets (1992–2002) recorded in the U.S. Pelagic Observers Program database and analyzed in the present study.

the event that a factor was found to be nonsignificant ($P > 0.05$), it was removed and a regression was rerun until all highest order model terms were significant (Hocking, 1976; Draper and Smith, 1981). We assumed maturity (both sexes) occurred at 185 cm FL (Pratt, 1979). The average P_{DA} and the ratio of immature-to-mature individuals discarded in each 0.5-degree cell were estimated and plotted in order to visually examine the spatial distribution of these two variables.

Results

Data from 702 longline sets were used in analyses and resulted in size and condition (i.e., live or dead) information on 4290 individual blue shark. From these data, a total of 37 proportions (i.e., P_{DA} values) were calculated and used in regression analyses.

Most of the sets targeted swordfish (39%) or swordfish and tuna (36%), or unspecified tuna species (14%). Bigeye tuna and yellowfin tuna were the target of 8% and 3% of the sets, respectively. About 88% of the sets included in the analysis were characterized as “night sets” and the remaining were “day sets.”

Overall, more blue shark were released alive (69%) than dead. Shark sizes, water temperatures, and set durations used in the multiple linear regression ranged from 75 to 300 cm FL (median=175 cm), 8 to 29°C (median=19°C), and 6 to 14 hours (median=12), respectively. About 68% of all released animals measured less than the size of sexual maturity (i.e., <185 cm FL).

Multiple linear regression indicated that no interaction terms were statistically significant and that only

Table 1

Regression coefficients and associated standard error values (SE) for the estimation of proportion of blue shark released alive (P_{DA}) ($n=37$), where β_0 corresponds to the intercept, and β_1 and β_2 are coefficients associated with blue shark fork length and set duration, respectively.

Parameters	Estimate	SE	$P > t $
β_0	0.967	0.0500	<0.0001
β_1	0.0021	0.0002	<0.0001
β_2	-0.0269	0.0037	<0.0001

shark size and set duration had significant effects on P_{DA} ($r^2=0.86$, $n=37$, $P < 0.00001$; Table 1). Plots of the observed proportions and the predicted response surface illustrate how the proportion of live releases increases with shark size and decreases with duration of set (Fig. 2, A and B). Whereas set duration has a moderate impact on the largest size classes, the proportion of live sharks <185 FL (i.e., immature stages) is considerably reduced even at relatively short set durations. For example, predicted P_{DA} for the smallest sharks (i.e., FL=75 cm) was 0.67 and 0.47 for set durations of 6 and 14 hours, respectively; for those animals measuring 250 cm FL, it was 0.94 and 0.80 for the same set durations. Maps of mean P_{DA} values and of the proportion of immature sharks caught indicated conspicuous differences off the U.S. east coast versus over the Grand Banks (Fig. 3, A and B). Specifically, the proportion of live releases

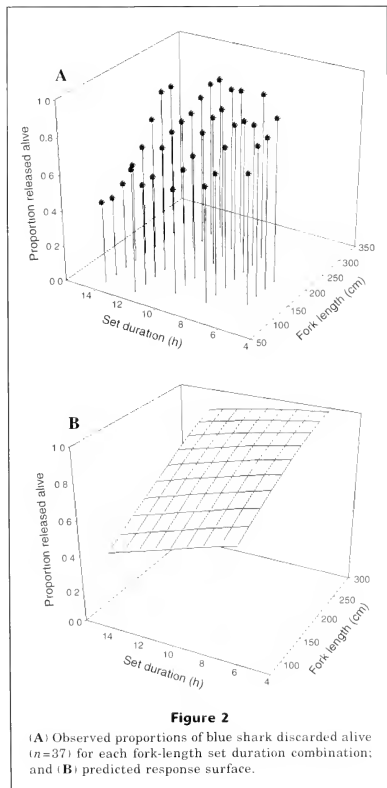
tended to be lower over the Grand Banks than off the U.S. east coast and the mean ratio of immature blue shark tended to be higher.

Discussion

Our results indicate that blue shark tolerance to the stresses associated with longline capture decreases with animal size at levels that vary with set duration. These results are consistent with the findings of Neilson et al. (1989) and Milliken et al. (1999) who observed greater discard mortality among the smallest sizes classes of

longline-caught Atlantic halibut (*Hippoglossus hippoglossus*) and cod (*Gadus morhua*), respectively. In our study, set duration represented the maximum possible time a given fish was "on-hook," and thus was only the coarsest of measures of the magnitude and duration of stress experienced by hooked fishes. Nevertheless, this crude measure appears to have captured enough of the cumulative stress effects on fish survival to emerge as a significant factor. In contrast, water temperature did not emerge as important in our analysis. However, we suspect this resulted because surface water temperatures (the only temperature measurements available) are poor indicators of the levels and changes in temperature actually experienced by captured sharks. Presumably, better predictions of condition at boat-side (and thus live discard quantities) could be made with knowledge of time-on-hook, depth, and temperature of capture, rate of gear retrieval, sea conditions, etc. Unfortunately, many of the measurements that are likely most relevant to recording shark condition at boat-side can only be made by distributing and retrieving large quantities of electronic instruments (i.e., temperature-depth recorders and hook-timers, see Boggs, 1992) near the hooks, and for each set. Such an approach is not only costly, but also difficult to implement without a research team dedicated for this purpose. Similarly, only by directed research can questions of postrelease mortality be addressed. Clearly, the proportions of living blue shark considered in our study are minimum estimates of fishing impacts because they do not account for delayed mortality of individuals released injured or otherwise impaired. For gauging postrelease mortality of longline-caught blue shark, tagging studies are warranted (Neilson et al., 1989; Kohler et al., 2002).

Evident in the maps is that the proportion of blue sharks available for live release was not homogeneous throughout the spatial range examined. Overall the proportion of blue shark released alive was higher (0.78) along the U.S. Atlantic east coast and decreased over the Grand Banks (0.67) (Fig. 3A). The maps also indicated that overall the proportion of immature blue sharks was highest over the Grand Banks (0.93) compared to the U.S. Atlantic east coast (0.63) (Fig. 3B). In their examination of U.S. Atlantic east coast longline catches south of the present study (i.e., between 35° and 22°N latitude), Beerkircher et al. (2004) found that 0.87 of blue shark caught were alive at boat-side. It seems likely, therefore, that contributing to the relatively higher survival observed by Beerkircher et al. (2004) was that only about half of the blue shark in their analysis were immature (as inferred from size). Blue shark interactions over the Grand Banks deserve special attention because most individuals discarded by the U.S. pelagic longline fleet are captured in that area. In 2002, for example, two thirds of the estimated 4335 blue shark mortalities attributed to U.S. Atlantic pelagic longline fleet were captured in this area (Diaz, unpubl. data³).



³ Diaz, G. A. 2005. NMFS Pelagic longline logbook program. NMFS/SEFSC Miami, FL 33149.

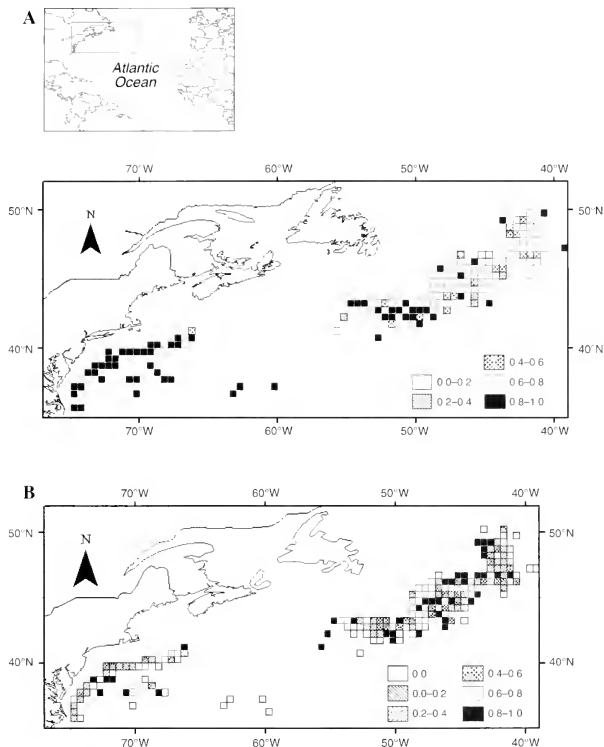


Figure 3

(A) Average proportion of blue shark released alive and (B) average proportion of immature blue shark released in pelagic longline sets. Proportions were estimated for 0.5-degree cells where at least one longline set was deployed in the period 1992–2002.

Ward et al. (2004) modeled the effect of set duration on pelagic longline catches and found that blue shark catch rates increased with set duration. According to our results, the increase in set durations also leads to increases in the number retrieved dead. In concept, a possible management measure to achieve reductions in blue shark mortality may include shortening longline set durations. However, a regulation of this nature would be difficult to implement (let alone enforce) be-

cause swordfish catch rates are also lowered when set durations are shortened (Ward et al., 2004) and therefore result in negative economic impacts that would likely be unacceptable to the industry.

Results of this analysis also have implications for blue shark stock assessment. Stock assessments based on longline fisheries data often use a hook selectivity function of a logistic form, whereby hook retention is 100% for fish larger than a certain size. In the particu-

lar case of blue shark, where most individuals caught are released (dead or alive), fishing mortality is best estimated from the number of animals released dead, rather than from all animals caught. Because larger animals have a higher probability of being released alive, a logistic selectivity function without size or age survival adjustment, could lead to overestimation of impacts on the stock. Thus, a dome-shaped selectivity function that incorporates the size-based survival information presented in the present study may represent an improvement over current techniques.

Acknowledgments

We thank L. Brooks, E. Cortes, S. Turner, and two anonymous reviewers for invaluable comments on the manuscript.

Literature cited

- Bailey, K., P. G. Williams, and D. Itano.
1996. By-catch and discards in Western Pacific tuna fisheries: a review of SPC data holdings and literature. Tech. Rep. Ocean Fish. Programme. S. Pac. Comm. no 34, 148 p.
- Beerkircher, L. R., E. Cortes, and M. Shivji.
2004. Characteristics of shark bycatch observed on pelagic longlines off the Southeastern United States, 1992-2000. Mar. Fish. Rev. 64(4):40-49.
- Boggs, C. H.
1992. Depth, capture time and hooked longevity of longline-caught pelagic fish: timing bites of fish with chips. Fish. Bull. 90:642-658.
- Draper, N., and H. Smith.
1981. Applied regression analysis, 709 p. Wiley Interscience, New York, NY.
- Francis, M. P.
1998. New Zealand shark fisheries: development, size and management. Mar. Freshw. Res. 49(7):579-591.
- Francis, M. P., L. M. Griggs, and S. J. Baird.
2001. Pelagic shark by-catch in the New Zealand tuna longline fishery. Mar. Freshw. Res. 52(2):165-178.
- Hocking R. R.
1976. The analysis and selection of variables in linear regression. Biometrics 32:1-50.
- Kohler, N. E., P. A. Turner, J. J. Hoey, L. J. Natanson, and R. Briggs.
2002. Tag and recapture data for three pelagic sharks species: blue shark (*Prionace glauca*), shortfin mako (*Isurus xyrinchus*), and porbeagle (*Lamna nasus*) in the North Atlantic ocean. International Commission for the Conservation of Atlantic Tuna (ICCAT) 54(4):1231-1260.
- Macias D., and J. M. de la Serna.
2002. By-catch composition in the Spanish Mediterranean longline fishery, 198 p. Proc. 4th meeting of the European Elasmobranch Association. Société Française d'Ichtyologie, Paris, France.
- Milliken, H. O., M. Farrington, H. A. Carr, and E. Lent.
1999. Survival of Atlantic cod (*Gadus morhua*) in the Northwest Atlantic longline fishery. Mar. Technol. Soc. J. 33:19-24.
- Neilson, D. J., K. G. Waiwood, and S. J. Smith.
1989. Survival of Atlantic halibut (*Hippoglossus hippoglossus*) caught by longline and otter trawl gear. Can. J. Fish. Aquat. Sci. 46:887-897.
- Pratt, H. L., Jr.
1979. Reproduction in the blue shark, *Prionace glauca*. Fish. Bull. 77:445-470.
- Robins, C. R., and G. C. Ray.
1986. A field guide to Atlantic coast fishes of North America. Peterson Field Guide Series, 354 p. Houghton Mifflin, Boston, MA.
- Stevens, J. D.
1992. Blue and mako shark by-catch in the Japanese longline fishery off south-eastern Australia. Sharks: biology and fisheries. Aust. J. Mar. Freshw. Res. 43(1):227-236.
- Sokal, R. R., and F. J. Rohlf.
1981. Biometry, 2nd ed., 859 p. W. H. Freeman, New York, NY.
- Ward, P., R. A. Myers, and W. Blanchard.
2004. Fish lost at sea: the effect of soak time on pelagic longline catches. Fish. Bull. 102:179-195.

Length correction for larval and early-juvenile Atlantic menhaden (*Brevoortia tyrannus*) after preservation in alcohol

Dariusz P. Fey

Sea Fisheries Institute
Dept. of Fisheries Oceanography and Marine Ecology
ul. Kollataja 1
81-332 Gdynia, Poland
E-mail address: dfey@mri.gdynia.pl

Jonathan A. Hare

NOAA National Ocean Service
Center for Coastal Fisheries and Habitat Research
101 Pivers Island Road
Beaufort, North Carolina 28516-9722

Body length measurement is an important part of growth, condition, and mortality analyses of larval and juvenile fish. If the measurements are not accurate (i.e., do not reflect real fish length), results of subsequent analyses may be affected considerably (McGurk, 1985; Fey, 1999; Porter et al., 2001). The primary cause of error in fish length measurement is shrinkage related to collection and preservation (Theilacker, 1980; Hay, 1981; Butler, 1992; Fey, 1999). The magnitude of shrinkage depends on many factors, namely the duration and speed of the collection tow, abundance of other planktonic organisms in the sample (Theilacker, 1980; Hay, 1981; Jennings, 1991), the type and strength of the preservative (Hay, 1982), and the species of fish (Jennings, 1991; Fey, 1999). Further, fish size affects shrinkage (Fowler and Smith, 1983; Fey, 1999, 2001), indicating that live length should be modeled as a function of preserved length (Pepin et al., 1998; Fey, 1999).

The goal of this study was to analyze the shrinkage of late-larval and early-juvenile Atlantic menhaden (*Brevoortia tyrannus*) during preservation in 95% alcohol. A length correction formula is presented that allows live standard length to be calculated from preserved standard length.

Materials and methods

Larval and early juvenile Atlantic menhaden were collected on three different occasions during January–March 2003 with a neuston net (2-m² opening and 947- μ m mesh) deployed for 2-minute durations from a bridge to Pivers Island, located about 2 km inside Beaufort Inlet, North Carolina. Samples were placed in a cooler and transported to the laboratory. Live Atlantic menhaden larvae were sorted from the samples ($n=100$) and their standard lengths (SL) were measured to the nearest 0.01 mm with a caliper. All specimens (19.1–31.4 mm SL) were placed in individual vials filled with 95% ethyl alcohol. The fish were remeasured 3, 20, and 90 days after preservation.

Repeated measures ANOVA and Tukey HSD tests were used to analyze the significance of length changes during 90 days of preservation. The preserved length after 90 days was then compared with live length to test whether a single correction factor is appropriate for a calculation of live length (t -test analysis for the slope difference from one). Additionally, the precision of measurements was evaluated by two replicate measurements of all larvae three days after preservation. Linear regression analysis was then used to describe the

relationship between the two length measurements. The possible deviation of intercept from zero and slope from one was estimated (t -test) to test for the possible significant differences between the two measurements.

Results

Time in preservative had a significant effect on measured length of Atlantic menhaden larvae (repeated measures ANOVA, $P<0.0001$). Fish were significantly larger prior to preservation compared to three days after preservation (Tukey HSD, $P<0.001$) and significantly larger three days after preservation compared to 20 and 90 days after preservation (Fig. 1) (Tukey HSD, $P<0.001$). When shrinkage is described as a relative value, the change in length that occurred during the first three days of preservation was 3.62%. Length decreased by an average of 0.22% during the following 17 days and by 0.073% during the remaining 70 days.

Although smaller fish shrank proportionally more than the larger ones (t -test for H_0 : slope=0, $P<0.001$) (Fig. 2A), no size effect was observed when shrinkage was analyzed as absolute length (regression slope=0.996, SE=0.008; H_0 : slope=1; t -test of regression slope, $P=0.605$). However, the y -intercept of the regression of preserved length at 90 days on live length was significantly different from zero (regression intercept=1.17; SE=0.21; H_0 : y -intercept=0; t -test of regression intercept, $P<0.001$) (Fig. 2B). Therefore, the significantly different from zero intercept can be used as a correction factor (i.e., $SL_{fresh}=SL_{preserved}+1.17$ mm). The shrinkage magnitude observed by Maillet and Checkley (1991) was compared to the results derived in our study (Fig. 2B). Their formula indicated shrinkage of about 2% compared to approximately 4% in our study.

Manuscript submitted 31 March 2004
to the Scientific Editor's Office.

Manuscript approved for publication
8 February 2005 by the Scientific Editor.
Fish. Bull. 103:725–727 (2005).

The two readings performed to estimate the measurement error were not statistically different as indicated by the parameters of the regression line fitted to the first measurement versus second measurement data ($SL_1 = 0.992 SL_2 + 0.21$, $r^2 = 0.998$). The slope was not statistically different from one (regression slope = 0.992, $SE = 0.005$; H_0 : slope = 1; t -test of regression slope, $P = 0.106$), and the intercept was not statistically different from zero (regression intercept = 0.21; $SE = 0.12$; H_0 :

y -intercept = 0; t -test of regression intercept, $P = 0.418$). Measurement precision, the absolute values of the difference between the two series of length measurements of the same specimens averaged 0.12 mm ($SD = 0.09$), which corresponded to an average of 0.47% of length ($SD = 0.35$). Thus, the error associated with measurement is an order of magnitude less than the change in length due to shrinkage within the first three days of preservation. Changes in length during following 87 days were below measurement error.

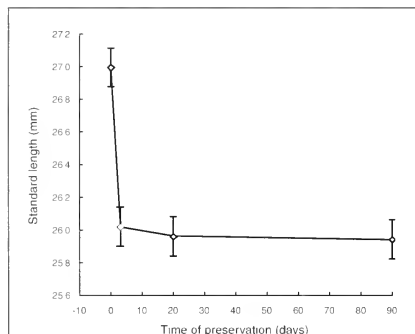


Figure 1

Change in standard length of Atlantic menhaden (*Brevoortia tyrannus*) ($n = 100$) during 90 days of preservation in 95% alcohol. Mean values and standard error of length measurements obtained from repeated measurements of 100 fish.

Discussion

This research on late-larval and early-juvenile Atlantic menhaden shrinkage is the first for this species. Maillet and Checkley (1991) used a shrinkage correction formula (cited as unpubl. data) in their study on larval menhaden growth but did not provide additional information (e.g., range of fish sizes) to accompany their formula. Their correction formula differs from ours, and the discrepancy may be related to differences in experimental procedure and different developmental stages. In the present study live fish were used, but in Maillet and Checkley's study (1991) it was not indicated whether larvae were alive or dead prior to preservation. Further Maillet and Checkley (1991) examined larval menhaden (17–24.5 mm SL), whereas we examined late-larval to early-juvenile menhaden (19.1–31.4 mm SL).

The shrinkage of larval and early-juvenile Atlantic menhaden after the first three days of preservation was significant, but small in magnitude. Beyond 20 days of preservation significant additional shrinkage did not occur. In fact, the length changes after day 3 were below the estimated measurement

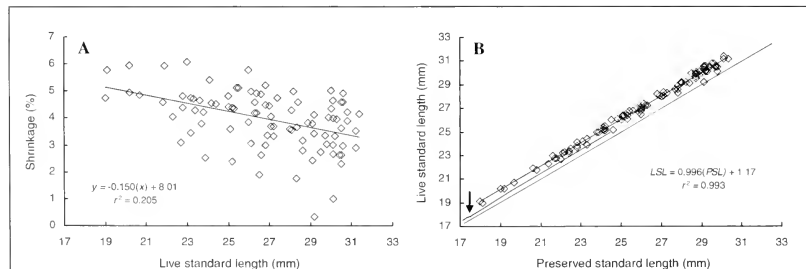


Figure 2

Length changes of Atlantic menhaden (*Brevoortia tyrannus*) during preservation for 90 days in 95% alcohol ($n = 100$). (A) The relationship between live standard length (LSL) and relative (%) shrinkage magnitude; (B) the relationship between live and preserved standard lengths described with linear regression. The solid line indicates the 1:1 ratio. The arrow points to the correction curve obtained from Maillet and Checkley (1991): $SL_{live} = 0.978(SL_{1e})^{1.285e^{-0.025N}}$.

error. Additionally, decreasing shrinkage as a function of increasing fish length was present when relative (%) shrinkage was analyzed. Similar results with regard to time and fish size effect were previously reported for other fish species preserved with formalin and alcohol (see Fey, 1999, for overview).

The effect of shrinkage on growth rate analysis was described by Fey (1999) for larval sprat. If growth rate is estimated by using a regression of length at age, the influence of shrinkage on growth estimates depends on the absolute value of length changes (i.e., expressed in mm) among small and large fish, and the error may be as high as 0.07 mm/d. However, if the absolute values of length decrease equally across fish lengths, even large shrinkage (on average) may have no effect on the results of growth rate analysis. In addition to length at age analysis, average growth rate (mm/d) may be calculated for individual fish. The potential error in growth estimates will then be directly proportional to both the relative and absolute magnitude of shrinkage. This potential bias in growth-rate calculations described by Fey (1999) for sprat emphasizes the importance of correcting for preservation. Although the relationship between otolith size and fish size may be used for length correction (Leak, 1986; Radtke, 1989), Fey (1999) showed that greater accuracy is provided when a fresh length-preserved length relationship is used. However, such a relationship may be supplemented by additional measurements (i.e., body depth and otolith size) to improve the accuracy of the correction model (Porter et al., 2001). In the current study, absolute changes in length (expressed in mm) of alcohol-preserved menhaden were not dependent on fish size and therefore a single correction factor was sufficient for a calculation of live length. The length correction factor provided in our study will benefit future studies on the ecology of early life stages of menhaden, similar to that conducted by Warlen et al. (2002), where preserved length measurements were used.

Acknowledgments

This research was performed while the first author held a National Research Council Research Associateship Award at NOAA Beaufort Laboratory. This note is also a contribution to the State Committee for Scientific Research (grant no. 2P04F 005 27).

Literature cited

Butler, J. L.
1992. Collection and preservation of materials for otolith analysis. In Otolith structure examination and analysis (D. K. Stevenson and S. E. Campana, eds.), p. 13-17. Can. Spec. Pub. Fish. Aquat. Sci. 117.

Fey, D. P.
1999. Effects of preservation technique on the length of larval fish: methods of correcting estimates and their implication for studying growth rates. Arch. Fish. Mar. Res. 47:17-29.
2001. Length correction of larval and early-juvenile herring (*Clupea harengus*) and smelt (*Osmerus eperlanus*) after preservation in formalin and alcohol. Bull. Sea Fish. Inst. 1155:47-51.
Fowler, G. M., and S. J. Smith.
1983. Length changes in silver hake (*Merluccius bilinearis*) larvae: effects of formalin, ethanol, and freezing. Can. J. Fish. Aquat. Sci. 40:866-870.
Hay, D. E.
1981. Effects of capture and fixation on gut contents and body size of Pacific herring larvae. Rapp. P.-V. Reun. Cons. Int. Explor. Mer 178:395-400.
1982. Fixation shrinkage of herring larvae: effects of salinity, formalin concentration, and other factors. Can. J. Fish. Aquat. Sci. 39:1138-1143.
Jennings, S.
1991. The effects of capture, net retention and preservation upon lengths of larval and juvenile bass, *Dicentrarchus labrax* (L.). J. Fish Biol. 38:349-357.
Leak, J. C.
1986. The relationship of standard length and otolith diameter in larval bay anchovy, *Anchoa mitchilli* (Val.). A shrinkage estimator. J. Exp. Mar. Biol. Ecol. 95:17-23.
Maillet, G. L., and D. M. Checkley Jr.
1981. Storm-related variation in the growth of otolith of larval Atlantic menhaden *Brevoortia tyrannus*: a time series analysis of biological and physical variables and implications for larva growth and mortality. Mar. Ecol. Prog. Ser. 79:1-16.
McGurk, M. D.
1985. Effect of net capture on the postpreservation morphology, dry weight, and condition factor of Pacific herring larvae. Trans. Am. Fish. Soc. 114:348-355.
Pepin, P., J. F. Dower, and W. C. Leggett.
1998. Changes in the probability density function of larval fish body length following preservation. Fish. Bull. 96:633-640.
Porter, S. M., A. L. Brown, and K. M. Bailey.
2001. Estimating live standard length of net-caught walleye Pollock (*Theragra chalcogramma*) larvae using measurements in addition to standard length. Fish. Bull. 101:384-404.
Radtke, R. L.
1989. Larval fish age, growth, and body shrinkage: information available from otoliths. Can. J. Fish. Aquat. Sci. 46:1884-1894.
Theilacker, G. H.
1980. Changes in body measurements of larval northern anchovy, *Engraulis mordax*, and other fishes due to handling and preservation. Fish. Bull. 78:685-692.
Warlen, S. M., K. W. Able, and E. H. Laban.
2002. Recruitment of larval Atlantic menhaden (*Brevoortia tyrannus*) to North Carolina and New Jersey estuaries: evidence for larval transport northward along the east coast of the United States. Fish. Bull. 100:609-623.

Comparison of average larval fish vertical distributions among species exhibiting different transport pathways on the southeast United States continental shelf

Jonathan A. Hare

John J. Govoni

Center for Coastal Fisheries and Habitat Research

101 Pivers Island Road

Beaufort, North Carolina 28516

Present address (for J. A. Hare): Narragansett Laboratory

Northeast Fisheries Science Center

28 Tarzwell Drive

Narragansett, Rhode Island 02882

E-mail address (for J. A. Hare): jon.hare@noaa.gov

Water currents are vertically structured in many marine systems and as a result, vertical movements by fish larvae and zooplankton affect horizontal transport (Power, 1984). In estuaries, the vertical movements of larvae with tidal periods can result in their retention or ingress (Fortier and Leggett, 1983; Rijnsdorp et al., 1985; Cronin and Forward, 1986; Forward et al., 1999). On the continental shelf, the vertical movements of organisms interact daily and ontogenetically with depth-varying currents to affect horizontal transport (Pillar et al., 1989; Barange and Pillar, 1992; Cowen et al., 1993, 2000; Batchelder et al., 2002).

A suite of fish species, which use estuaries during the juvenile stage, spawn during winter on the mid- and outer continental shelf of the southeast United States (Fig. 1A): *Brevoortia tyrannus* (Atlantic menhaden), *Leiostomus xanthurus* (spot), *Micropogonias undulatus* (Atlantic croaker), *Paralichthys albigutta* (Gulf flounder), *P. dentatus* (summer flounder), and *P. lethostigma* (southern flounder). Vertically structured flow is a major part of proposed larval transport mechanisms for these species from offshore spawning areas to estuarine nursery habitats (Govoni and Pietrafesa, 1994; Hare et al., 1999). *Brevoortia tyrannus*, however, is found higher in the water column on average than the other species that use estuaries

during their juvenile stage (Miller et al., 1984; Govoni and Pietrafesa, 1994; Govoni and Hoss, 2001). Further, larvae of *B. tyrannus* apparently exhibit a difference in horizontal transport compared to other winter-spawning species that use estuarine habitats as juveniles; *B. tyrannus* larvae spawned on the southeast U.S. shelf may be transported to estuarine nursery habitats along the northeast U.S. shelf (Warlen et al., 2002). The effects of differences in vertical larval distribution on cross-shelf larval transport are unknown, and the transport pathways from shelf spawning areas to estuarine nursery areas remain unclear.

Other species also spawn during winter on the southeast United States continental shelf. Some species settle to benthic habitats on the shelf (e.g., *Etropus cycloquamus* [shelf flounder], *E. microstomus* [smallmouth flounder], and *E. rimosus* [gray flounder], Leslie and Stewart, 1986) or remain on the shelf in pelagic habitats (e.g., *Etrumeus teres* [round herring], Crawford, 1981; Schwartz, 1989). However, some species are regularly advected offshore, entrained into the Gulf Stream, and exported northwards (e.g., *Bothus* spp. [peacock, eyed, and spotted flounders], *Pepilus triacanthus* [butterfish], *Syacium papillosum* [dusky flounder], *Xyrichtys novacula* [pearly razorfish]; Hare and Cowen, 1991; Cowen et al., 1993;

Rotunno and Cowen, 1997; Grothues and Cowen, 1999).

The purpose of our study was to examine associations between average larval fish vertical distributions and general larval transport pathways on the southeast United States continental shelf during winter. Our goal was to determine if larval vertical distributions differed among species that exhibit different outcomes of larval transport: export from the local shelf, arrival at local estuaries, and retention on the shelf. Our approach, however, was unconventional. Rather than couple detailed descriptions of the flow field with detailed descriptions of larval vertical distributions (including diel variation), we chose to compare average vertical distributions among species that exhibit overall differences in larval transport. Vertical distribution data were collected in three separate years, over periods of time ranging from 24 to 96 hours. If average larval vertical distributions are different among species, and these differences occur consistently among the various sampling times and in concordance with the general outcome of transport, then we conclude that larval vertical distributions are an important part of larval transport on the southeast U.S. shelf.

Our specific objectives were twofold: 1) to test the null hypothesis that there are no differences in larval fish vertical distributions between species, and 2) to evaluate significant differences in larval depth distribution in relation to the *a priori* classification of the outcome of transport. Vertically discrete data from six sampling times were analyzed, and owing to differences in protocols among sampling times, comparisons of larval vertical distributions were made within sampling times only. The results of these comparisons were then combined to evaluate whether there were consistent differences in larval vertical distributions among sampling times related to the outcome of larval transport.

Manuscript submitted 5 April 2004
to the Scientific Editor's Office.

Manuscript approved 30 March 2005
by the Scientific Editor.

Fish. Bull. 103:728-736 (2005).

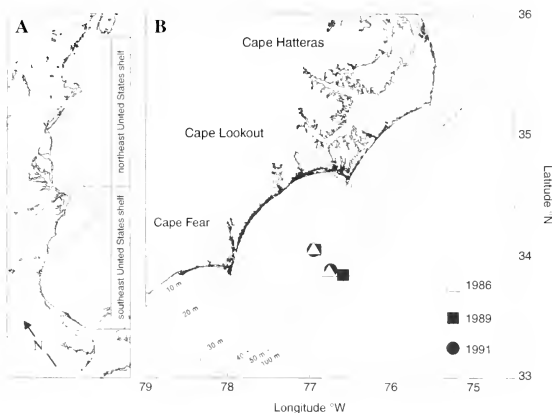


Figure 1

(A) Map of the east coast of the United States rotated 18° counter-clockwise. The spatial extent of the northeast and southeast United States continental shelves is indicated by each rectangle. The area of panel B is shown as a trapezoid. (B) The northern portion of the southeast United States continental shelf showing the coastline, the 10-m, 20-m, 30-m, 40-m, 50-m, and 100-m isobaths. The three prominent capes are identified and locations of stations sampled in this study are shown.

Material and methods

Data collection

Larval fish were collected every six hours (0600, 1200, 1800, and 2400) at an offshore and an inshore station during three winters: 21–26 February 1986, 26 January–1 February 1989, and 5–7 February 1991 (Fig. 1B). Offshore stations were located on approximately the 50-m isobath, and inshore stations were located on approximately the 35-m isobath. In 1986, offshore and onshore stations were occupied for 102 and 48 h, respectively. Collections were taken horizontally at 1, 18, and 32 m at the offshore station and 1, 13, and 25 m at the inshore station with a 60-cm opening-closing bongo net (Weibe and Benfield, 2003) with 333- μ m mesh and a 1-m² Tucker trawl (Weibe and Benfield, 2003) with 202- μ m mesh. In 1989, offshore and inshore stations were occupied for 78 and 72 hours, respectively. Collections were taken horizontally at 1, 22, and 45 m at the offshore station and 1, 13, and 30 m at the inshore station with a 1-m² Tucker trawl with 333- μ m mesh. In 1991, offshore and inshore stations were occupied for 24 and 30 h, respectively. Collections were made with 1-m² MOCNESS (Wiebe et al., 1976) with 333- μ m mesh. Oblique samples were collected within 5-m intervals from 35 m

to the surface at the offshore station and from 30 m to the surface at the inshore station. The mid-point of each depth stratum was used as the depth of the collection. In 1986 and 1989, volume of water filtered was measured with a flowmeter (General Oceanics model 2030, Miami, FL) with a standard rotor. In 1991, volume filtered was measured with a flowmeter provided with the MOCNESS (BESS, Falmouth, MA).

Larval fish were sorted from collections and identified to the lowest taxon possible. The larvae of selected taxa were counted: *Bothus* spp., *Etropus* spp. (not including *E. crossotus*), *E. teres*, *Paralichthys* spp., *P. triacanthus*, *S. papillosum* and *X. novaacula*. Counts of *B. tyrannus*, *L. xanthurus*, and *M. undulatus* were obtained from Govoni and Pietrafesa (1994) and Govoni and Spach (1999). Larval concentrations were calculated for each depth stratum (number of larvae/100 m³).

Comparisons of larval vertical distributions

Center of mass calculations are frequently used for comparison of fish larval depth distributions (e.g., Brodeur and Rugen, 1994), but Pearre (1979) raised valid criticisms of this approach; for example a uniform distribution still has a mean depth. To obviate these criticisms, larval depth distributions of each taxon were compared

by using a test of independence (Pearson chi-square, Sokal and Rohlf, 1981; McCleave et al. 1987). Depth distributions were averaged over each station. Comparisons were then made between all pairs of taxa within a station, and a Bonferoni correction was applied to assess the significance of the tests of independence. Comparisons were not made between stations, because sampling methods varied and depth distributions were not directly comparable. The following null hypothesis was evaluated: during each station occupation, average larval depth distributions were independent of species. Column and row variables were species and depth strata; cell values were the average proportion of the larvae captured in a depth stratum at a station. Comparisons of center of mass were also made and the results were very similar to the results of the test of independence reported in the present study.

The calculation of average proportion was made in two steps. First, the proportion of larvae (P) collected in each depth stratum (d) at each sampling time (i) during each station occupation (j) was calculated:

$$P_{dj} = \frac{C_{dj}}{\sum_i C_{di}}$$

where C = larval concentration 100/m³.

Then the average proportion of larvae (\bar{P}) for each depth stratum (d) was calculated for each station (j):

$$\bar{P}_{dj} = \frac{\sum_i P_{di}}{n_{ij}}$$

where n_{ij} = the number of sampling times (i) during station occupation (j).

Because the significance of a test of independence depends, in part, on the magnitude of the cell values (i.e., sample sizes), average larval concentration of each species during each station occupation (number of larvae/100 m³) was used as a weighting factor. The average proportion of larvae at depth during a station occupation (\bar{P}_{dj}) was multiplied by the weighting factor to derive the cell values for use in the test of independence. The weighting factor approximated the number of fish larvae collected, and incorporated the effect of variability in sampling volume.

Values of the standardized residuals, which are a result of the test of independence, were used to classify significant differences in depth distribution as follows: species A shallower (<) than species B, species A deeper (>) than species B, and species A distributed differently (< or >) than species B. This last category was assigned when one species was not clearly deeper or shallower than the other species, yet its depth distributions were significantly different.

To evaluate whether larval fish vertical distributions were associated with larval transport, the results of

the individual species comparisons were pooled across station by the *a priori* assigned outcome of transport. The number of significant differences found between species were then compared to the number of significant differences expected with a 5% error rate by using the G -statistic (Sokal and Rohlf 1981). For example, in a comparison of *B. tyrannus* to exported species, five pairwise comparisons of larval depth distributions were found to be significantly different and 12 were not significantly different. At $\alpha=0.05$, one significant and 16 nonsignificant differences are expected. The G -statistic demonstrates that more significant differences were found between *B. tyrannus* and exported species than expected by chance. The classifications of significant depth differences (shallower, deeper, different) were then examined to determine the relation between larval vertical distributions and the general outcome of larval transport.

Results

Comparison of larval vertical distributions indicated that *B. tyrannus* often had the shallowest larval vertical distribution. There were more significant differences than expected by chance between the vertical distributions of *B. tyrannus* and exported, estuarine, and shelf-resident taxa (Table 1). For all significant differences, the standard deviates from the test of independence indicated that *B. tyrannus* were found in shallower water than were other taxa (Appendix 1).

Exported taxa generally were higher in the water column than estuarine and shelf-resident taxa. There were more significant differences than expected by chance between the vertical distributions of exported taxa and estuarine and shelf-resident taxa (Table 1). Further, 9 of 12 significant differences between exported and estuarine taxa indicated that exported taxa were found in shallower water; 8 of 11 significant differences between exported and shelf resident taxa indicated that exported taxa were found in shallower water (Appendix 1).

The vertical distributions of estuarine and shelf-resident taxa were different more often than expected by chance, but taxa of neither group were consistently found in shallower water (Table 1). Significant differences in larval vertical distributions were distributed evenly among the three classifications of the direction of difference ($n=4$ shallower; $n=2$ deeper; $n=5$ different) (Appendix 1).

Discussion

The results indicate an overall hierarchy of larval vertical distributions; *B. tyrannus* was found in shallower water than were exported taxa, and exported taxa were shallower than estuarine and shelf-resident taxa. Although this general pattern emerged, considerable variability in larval vertical distributions was observed, which is a common result of many studies (e.g., Boehlert

Table 1

Summary of the pairwise comparisons of larval depth distributions between species classified by the *a priori* outcome of transport. In each table cell, the number to the left is the number of significant pairwise differences, the number to the right is the total number of comparisons across the six station occupations, and the number in parentheses is the *G*-statistic for evaluating the null hypothesis that the number of observed differences is as expected with a 5% error rate. The critical value at $\alpha=0.05$ is 5.99 and significant values are indicated in bold. Values greater than 5.99 indicate that there are more significant differences between species than expected by chance. Exported taxa are *Bothus* spp., *Peprilus triacanthus*, *Stacium papillosum*, *Xyrichtys novacula*. Estuarine taxa include *Leiostomus xanthurus*, *Micropogonias undulatus*, and *Paralichthys* spp. Shelf resident taxa include *Etropus* spp. and *Etrumeus teres*.

	<i>Brevoortia tyrannus</i>	<i>A priori</i> classification of the outcome of transport		
		Exported	Estuarine	Shelf resident
Exported	5 / 17 (10.29)	2 / 17 (1.17)		
Estuarine	12 / 15 (55.35)	12 / 43 (23.88)	5 / 13 (12.96)	
Shelf resident	9 / 12 (39.11)	11 / 34 (25.09)	11 / 30 (27.96)	2 / 6 (4.39)

and Mundy, 1994; Brodeur and Rugen, 1994). Variability in larval fish vertical distributions (and zooplankton) is related to processes that influence water column mixing (e.g., Heath et al., 1988; Incze et al., 2001) and to species-specific responses to diel cycles and gradients in turbulence, temperature, and salinity (DeVries et al. 1995; Olla et al., 1996; Gray and Kingsford, 2003). The approach used in the present study was to average over shorter-scale variability (hours) in larval vertical distributions to examine longer-time-scale patterns (days) in larval vertical distributions.

Average larval vertical distributions of exported, estuarine-dependent, and shelf-resident taxa and the implied outcomes of their larval transport are consistent with the results of physical oceanographic models and observations of shelf circulation in the southeast United States continental shelf. The model of Janowitz and Pietrafesa (1980) (see also Miller et al., 1984) indicated a three-layered, cross-shelf flow during winter: surface and near-bottom offshore flow, and intermediate onshore flow. Similarly, the model of Werner et al. (1999) indicated a two-layered, cross-shelf flow during winter: an offshore flow near the surface and onshore flow throughout the rest of the water column. Surface flow in the study area during winter is typically offshore (Govoni and Pietrafesa, 1994). On the inner and middle shelf (water depths <40 m), average bottom flow is onshore; on the outer shelf (water depth 40–75 m), average intermediate flow is onshore, whereas bottom flow is offshore (Fig. 5b in Lee et al., 1989). Modeled and observed flow fields may indicate that larvae in the surface water will move offshore (exported taxa), where the probability of entrainment into the Gulf Stream is higher. Larvae that are in the middle or lower portion of the water column will move onshore (i.e., estuarine-dependent and shelf-resident taxa). Thus, the average larval vertical distributions, the general outcome of larval transport, and the generalized observed and modeled vertical flow fields are consistent.

Differences between vertical distributions of larval *B. tyrannus* and the other estuarine-dependent taxa (Fig. 2; see also Govoni and Pietrafesa, 1994) imply differences in cross-shelf transport. There are several possibilities, none mutually exclusive. 1) Onshore transport of larval *B. tyrannus* occurs with northeast wind events and onshore transport of other estuarine-dependent larvae occurs with southwest or northwest wind events. This possibility is supported by the model simulations of Hare et al. (1999). 2) Cross-shelf transport of *B. tyrannus* larvae occurs in surface Gulf Stream intrusions (Checkley et al., 1988; Stegmann and Yoder, 1996), whereas cross-shelf transport of other estuarine-dependent larvae occurs by wind-driven mechanisms. This possibility has not been adequately evaluated. 3) All estuarine-dependent larvae are transported across the shelf by the same mechanisms, but the rate of their transport differs. For example, southwest wind events cause onshore transport rates to be greater for the other estuarine-dependent taxa because *B. tyrannus* larvae spend less time in the intermediate portion of the water column. This possibility is also supported by Hare et al. (1999), who found that in modeled larval vertical distributions, the outcome of larval transport was modified by circulation. From these alternative hypotheses, it is clear that our understanding of the cross-shelf transport of larval fishes remains incomplete and that the effective physical and biological mechanisms are complex.

One approach to resolving the affect of vertical distribution on cross-shelf larval transport is to develop a specific hypothesis regarding supply of larvae to inlets that is based on the above possibilities and then to test these hypotheses using the long time-series of larval ingress collected at Beaufort Inlet (see Warlen, 1994). Three alternative patterns in ingress, based on the three possibilities presented above, could be evaluated by using ingress data collected at Beaufort Inlet: 1) ingress of *B. tyrannus* occurs during northeast winds, and

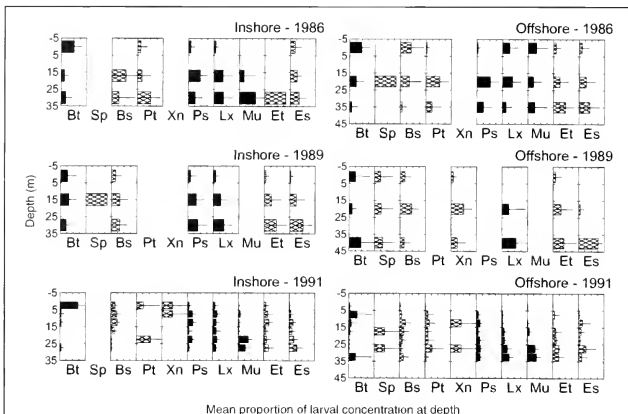


Figure 2

Mean proportions of larvae sampled at depths at six stations on the southeast United States shelf. Error bars indicate standard deviation of mean proportions calculated by using all the samples collected at a station. The x-axis of all panels is the same and ranges from 0 to 1.2. The species indicated in each figure is denoted by a two letter code (Bt=*Brevortia tyrannus*, Sp=*Syacium papillosum*, Bs=*Bothus* spp., Pt=*Peprilus triacanthus*, Xn=*Xyrichtys novacula*, Ps=*Paralichthys* spp., Lx=*Leiostomus xanthurus*, Mu=*Microponogonius undulatus*, Et=*Etrumeus teres*, and Es=*Etropus* spp.). Species are grouped by an *a priori* assignment of their general outcome of transport.

the ingress of other species occurs during northwest, west, and southwest winds; 2) ingress of *B. tyrannus* is not related to wind, and ingress of the other species is related to northwest, west, and southwest winds; 3) and ingress of all estuarine-dependent species occurs during similar wind forcing. Other studies have established similar *a priori* predictions for relations between wind forcing and ingress, yet results have been equivocal (e.g., Blanton et al., 1995). One explanation is that cross-shelf larval transport and larval ingress occur through multiple steps (Boehlert and Mundy, 1988; Hettler and Hare, 1998), effectively decoupling wind-driven, cross-shelf larval transport from larval ingress.

Similarities in vertical distributions of larval *B. tyrannus* and exported larval taxa indicate that a greater proportion of *B. tyrannus* larvae may be entrained into the Gulf Stream than larvae of other species that use southeast estuaries as juvenile nurseries. Once entrained into the Gulf Stream, larvae are transported northeastward and they either continue to move in the Gulf Stream or are returned to the shelf edge north of Cape Hatteras by warm-core ring streamers or in discharges of Gulf Stream water (Hare and Cowen 1991, 1996; Churchill et al., 1993; Cowen et al., 1993; Hare

et al., 2002). Govoni and Spach (1999) reported offshore exchange of *B. tyrannus* larvae into the Gulf Stream, and Warlen et al. (2002) concluded that some *B. tyrannus* larvae spawned south of Cape Hatteras do enter estuaries north of Cape Hatteras in the spring. The mechanisms of northward transport of *B. tyrannus* have yet to be studied, but transport to the northeast United States shelf edge by the same mechanisms as those that drive exported taxa is possible.

In marine systems, larval fish interact with vertically structured flow with vertical motions and thereby affect their horizontal transport (Cowen et al., 1993, 2000; Grioche et al., 2000). Apart from specific transport mechanisms, the present study demonstrates an overall link between larval vertical distributions and transport for multiple species. Species that moved inshore or remained on the shelf were found deeper in the water column than species that were exported from the shelf. Cowen et al. (1993) indicated that as larvae on the northeast U.S. shelf edge move deeper, they become more susceptible to onshore flows. Similarly, Cowen et al. (2000) argued that pomacentrid larvae are distributed at mid-depths off Barbados, and these mid-depth distributions resulted in larval retention

closer to the island. Peterson (1998) proposed that in upwelling systems, copepods can affect retention on the shelf through ontogenetic vertical migrations, whereby younger stages inhabit the upper offshore-flowing water and older stages inhabit the lower onshore-flowing water (see also Peterson et al., 1979). Similar models were developed by Pillar et al. (1989) and Barange and Pillar (1992) for euphausiids in the Benguela upwelling zone. Additionally, Batchelder et al. (2002) indicated that copepods can be retained nearshore in upwelling systems through diel vertical migrations between offshore-flowing surface waters and onshore-flowing bottom waters. From these studies and the results from the present study, a general hypothesis emerges that in many marine systems, fish larvae and zooplankton can affect onshore transport by moving deeper in the water column. Thus, similar to selective tidal stream transport whereby larvae use predictable tidal flows to either remain in estuaries or enter estuaries (Forward and Tankersley, 2001), general features in circulation may exist across physical oceanographic systems that allow larvae to influence their cross-shelf transport through basic changes in their vertical distribution.

Acknowledgments

We thank the participants of the South Atlantic Bight Recruitment Experiment for their constructive comments throughout this study. We also appreciate the contribution of those who assisted in the field and the officers and crews of the NOAA Ships *Oregon II* and *Chapman*. Dave Colby, Frank Hernandez, Patti Marraro, Allyn Powell, Larry Settle, Petra Stegmann, and six anonymous reviewers commented on earlier drafts of this manuscript. This study was completed while the senior author held a National Research Council Research Associateship at the NOAA Beaufort Laboratory.

Literature cited

- Barange, M., and S. C. Pillar.
1992. Cross-shelf circulation, zonation and maintenance mechanisms of *Nyctiphanes capensis* and *Euphausia hansenii* (Euphausiacea) in the northern Benguela upwelling system. *Cont. Shelf Res.* 12:1027-1042.
- Batchelder, H. P., C. A. Edwards, and T. M. Powell.
2002. Individual-based models of copepod populations in coastal upwelling regions: implications of physiologically and environmentally influenced diel vertical migration on demographic success and nearshore retention. *Prog. Oceanogr.* 53:307-333.
- Blanton, J., E. Wenner, F. Werner, and D. Knott.
1995. Effects of wind-generated coastal currents on the transport of blue crab megalopae on a shallow continental shelf. *Bull. Mar. Sci.* 57:739-752.
- Boehlert, G. W., and B. C. Mundy.
1988. Roles of behavior and physical factors in larval and juvenile fish recruitment to estuarine nursery areas. *Am. Fish. Soc. Symp.* 3:57-76.
1994. Vertical and onshore-offshore distributional patterns of tuna larvae in relation to physical habitat features. *Mar. Ecol. Prog. Ser.* 107:1-13.
- Brodeur, R. D., and W. C. Rugeley.
1994. Diel vertical distribution of ichthyoplankton in the northern Gulf of Alaska. *Fish. Bull.* 92:223-235.
- Checkley, D. M., S. Raman, G. L. Maillet, and K. M. Manson.
1988. Winter storm effects on the spawning and larval drift of a pelagic fish. *Nature* 335:346-348.
- Churchill, J. H., E. R. Levine, D. N. Connors, and P. C. Cornillon.
1993. Mixing of shelf, slope and Gulf Stream water over the continental slope of the Middle Atlantic Bight. *Deep-Sea Res.* 40:1063-1085.
- Cowen, R. K., J. A. Hare, and M. P. Fahay.
1993. Beyond hydrography: can physical processes explain larval fish assemblages within the Middle Atlantic Bight? *Bull. Mar. Sci.* 53:567-587.
- Cowen, R. K., K. M. M. Lwiza, S. Sponaugle, C. Paris, and D. Olson.
2000. Connectivity of marine populations: open or closed? *Science* 287:857-859.
- Crawford, R. J. M.
1981. Distribution, availability and movements of round herring *Etrumeus teres* off South Africa, 1964-1976. *Fish. Bull. South Africa* 14:141-181.
- Cronin, T. W., and R. B. Forward.
1986. Vertical migration cycles of crab larvae and their role in larval dispersal. *Bull. Mar. Sci.* 39:192-201.
- DeVries, M. C., R. B. Forward, and W. F. Hettler.
1995. Behavioral response of larval Atlantic menhaden *Brevoortia tyrannus* (Latrobe) and spot *Leiostomus xanthurus* (Lacepede) to rates of salinity change. *J. Exp. Mar. Biol. Ecol.* 185:93-108.
- Fortier, L., and W. C. Leggett.
1983. Vertical migrations and transport of larval fish in a partially mixed estuary. *Can. J. Fish. Aquat. Res.* 39:1150-1163.
- Forward, R. B., K. A. Reinsel, D. S. Peters, R. A. Tankersley, J. H. Churchill, L. B. Crowder, W. F. Hettler, S. M. Warlen, and M. D. Greene.
1999. Transport of fish larvae through a tidal inlet. *Fish. Oceanogr.* 8 (suppl. 2):153-172.
- Forward, R. B., and R. A. Tankersley.
2001. Selective tidal-stream transport of marine animals. *Oceanogr. Mar. Biol. Ann. Rev.* 39:305-353.
- Govoni, J. J., and D. E. Hoss.
2001. Comparison of the development and function of the swimbladder of *Brevoortia tyrannus* (Clupeidae) and *Leiostomus xanthurus* (Sciaenidae). *Copeia* 2001: 430-442.
- Govoni, J. J., and L. J. Pietrafesa.
1994. Eulerian views of layered water currents, vertical distribution of some larval fishes, and inferred advective transport over the continental shelf off North Carolina, USA, in winter. *Fish. Oceanogr.* 3:120-132.
- Govoni, J. J., and H. L. Spach.
1999. Exchange and flux of larval fishes across the western Gulf Stream front south of Cape Hatteras, USA, in winter. *Fish. Oceanogr.* 8 (suppl. 2):77-92.
- Gray, C. A., and M. J. Kingsford.
2003. Variability in thermocline depth and strength, and the relationships with vertical distributions of fish larvae and mesozooplankton in dynamic coastal waters. *Mar. Ecol. Prog. Ser.* 247:211-224.
- Grioche, A., X. Harlay, P. Koubbi, and L. Fraga Largo.
2000. Vertical migrations of fish larvae: Eulerian

- and Lagrangian observations in the Eastern English Channel. *J. Plankton Res.* 22:1813-1828.
- Grothues, T. M., and R. K. Cowen.
1999. Larval fish assemblages and water mass history in a major faunal transition zone. *Cont. Shelf Res.* 19:1171-1198.
- Hare, J. A., J. H. Churchill, R. K. Cowen, T. Berger, P. Cornillon, P. Dragos, S. Glenn, J. J. Govoni, and T. N. Lee.
2002. Routes and rates of larval fish transport from the southeastern to the mid-Atlantic North American continental shelf. *Limnol. Oceanogr.* 47:1774-1789.
- Hare, J. A., and R. K. Cowen.
1991. Expatriation of *Xyrichtys novacula* (Pisces: Labridae) larvae: evidence of rapid cross-slope exchange. *J. Mar. Res.* 49:801-823.
1996. Transport mechanisms of larval and pelagic juvenile bluefish (*Pomatomus saltatrix*) from South Atlantic Bight spawning grounds to Middle Atlantic Bight nursery habitats. *Limnol. Oceanogr.* 41:1264-1286.
- Hare, J. A., J. A. Quinlan, F. E. Werner, B. O. Blanton, J. J. Govoni, R. B. Forward, L. R. Settle, and D. E. Hoss.
1999. Larval transport during winter in the SABRE study area: results of a coupled vertical larval behavior-three-dimensional circulation model. *Fish. Oceanogr.* 8 (suppl. 2):57-76.
- Heath, M. R., E. W. Henderson, and D. L. Baird.
1988. Vertical distribution of herring larvae in relation to physical mixing and illumination. *Mar. Ecol. Prog. Ser.* 47:211-228.
- Hettler, W. F., and J. A. Hare.
1998. Abundance and size of larval fishes outside the entrance to Beaufort Inlet, North Carolina. *Estuar.* 21:476-499.
- Ince, L. S., D. Hebert, N. Wolff, N. Oakey, and D. Dye.
2001. Changes in copepod distributions associated with increased turbulence from wind stress. *Mar. Ecol. Prog. Ser.* 213:229-240.
- Janowitz, G. S., and L. J. Pietrafesa.
1980. A model and observation of time dependent upwelling over the mid-shelf and slope. *J. Phys. Oceanogr.* 10:1574-1583.
- Lee, T. N., E. Williams, J. Wang, R. Evans, and L. Atkinson.
1989. Response of South Carolina continental shelf waters to wind and Gulf Stream forcing during winter of 1986. *J. Geophys. Res.* 94:10715-10754.
- Leslie, A. J., and D. J. Stewart.
1986. Systematics and distributional ecology of *Etropus* (Pisces, Bothidae) on the Atlantic coast of the United States, with description of a new species. *Copeia* 1986:140-156.
- McCleave, J. D., J. M. Bédauz, P. G. Doucet, J. C. Jager, J. L. T. Jong, W. J. van der Steen, and B. Voorzanger.
1987. Statistical methods for analysis of plankton and nekton distribution, with application to selective tidal stream transport of juvenile American eels (*Anguilla rostrata*). *J. Cons. Int. Explor. Mer* 44:90-103.
- Miller, J. M., J. P. Reed, and L. J. Pietrafesa.
1984. Patterns, mechanisms and approaches to the study of estuarine dependent fish larvae and juveniles. *In* Mechanisms and migrations in fishes (J. D., McCleave, G. P. Arnold, J. J. Dodson, and W. H. Neill, eds.), p. 210-225. Plenum Press, New York, NY.
- Olla, B. L., M. W. Davis, C. H. Ryer, and S. M. Sogard.
1996. Behavioural determinants of distribution and survival in early stage walleye pollock, *Theragra chalcogramma*: a synthesis of experimental studies. *Fish. Oceanogr.* 5(suppl. 1):167-178.
- Pearre, S.
1979. Problems of detection and interpretation of vertical migration. *J. Plankton Res.* 1:29-44.
- Peterson, W. T.
1998. Life cycle strategies of copepods in upwelling zones. *J. Mar. Sys.* 15:313-326.
- Peterson, W. T., C. B. Miller, and A. Hutchinson.
1979. Zonation and maintenance of copepod populations in the Oregon upwelling zone. *Deep-Sea Res.* 26A:467-494.
- Pillar, S. C., D. A. Armstrong, and L. Hutchings.
1989. Vertical migration, dispersal and transport of *Euphausia lucens* in the southern Benguela Current. *Mar. Ecol. Prog. Ser.* 53:179-190.
- Power, J. H.
1984. Advection, diffusion, and drift migrations of fish larval fish. *In* Mechanisms and migrations in fishes (J. D., McCleave, G. P. Arnold, J. J. Dodson, and W. H. Neill, eds.), p. 27-37. Plenum Press, New York, NY.
- Rijnsdorp, A. D., M. van Stralen, and H. W. van der Veer.
1985. Selective tidal stream transport of North Sea plaice larvae *Pleuronectes platessa* in coastal nursery areas. *Trans. Am. Fish. Soc.* 114:416-470.
- Rotunno, T., and R. K. Cowen.
1997. Temporal and spatial spawning patterns of the Atlantic butterfish, *Peprilus triacanthus*, in the South and Middle Atlantic Bights. *Fish. Bull.* 95:785-799.
- Schwartz, F. J.
1989. Zoogeography and ecology of fishes inhabiting North Carolina's marine waters to depths of 600 meters. NOAA Nat. Undersea Res. Program Rep. 89-2335-374.
- Sokal, R. R., and F. J. Rohlf.
1981. Biometry, 2nd ed., 859 p. W. H. Freeman and Company, New York, NY.
- Stegmann, P. M., and J. A. Yoder.
1996. Variability of sea-surface temperature in the South Atlantic Bight as observed from satellite: implications for offshore spawning fishes. *Cont. Shelf Res.* 16:843-861.
- Warlen, S. M.
1994. Spawning time and recruitment dynamics of larval Atlantic menhaden, *Brevoortia tyrannus*, into a North Carolina estuary. *Fish. Bull.* 92:420-433.
- Warlen, S. M., K. W. Able, and E. H. Laban.
2002. Recruitment of larval Atlantic menhaden (*Brevoortia tyrannus*) to North Carolina and New Jersey estuaries: evidence for larval transport northward along the east coast of the United States. *Fish. Bull.* 100:609-623.
- Wiebe, P. H., K. H. Burt, S. H. Boyd, and A. W. Morton.
1976. A multiple opening/closing net and environmental sensing system for sampling zooplankton. *J. Mar. Res.* 34:313-326.
- Wiebe, P. H., and M. C. Benfield.
2003. From the Hensen net toward four-dimensional biological oceanography. *Prog. Oceanogr.* 56: 7-136.
- Werner, F. E., B. O. Blanton, J. A. Quinlan, and R. A. Luettich.
1999. Physical oceanography of the North Carolina continental shelf during the fall and winter seasons: implications for the transport of larval menhaden. *Fish. Oceanogr.* 8 (suppl. 2):7-21.

Appendix 1

Significant pairwise differences between the average larval vertical distributions of 10 species on the southeast United States continental shelf. A total of 187 comparisons were made and the 69 significant differences are listed below. Significant differences between average depth distributions were determined by using a test of independence with the cell values as average proportion of larvae at depth, averaged over a station occupation and weighted by the mean larval concentration at the station. A Bonferroni correction was applied to significance tests within each station occupation. The direction of significant differences (shallower [$<$], deeper [$>$], and different [$<>$]) was determined from the standardized residuals from the test of independence.

Year	Station	Species A		Species B
1986	Offshore	<i>Brevoortia tyrannus</i>	<	<i>Peprilus triacanthus</i>
1986	Offshore	<i>Brevoortia tyrannus</i>	<	<i>Paralichthys</i> spp.
1986	Offshore	<i>Brevoortia tyrannus</i>	<	<i>Leiostomus xanthurus</i>
1986	Offshore	<i>Brevoortia tyrannus</i>	<	<i>Etropus</i> spp.
1986	Offshore	<i>Brevoortia tyrannus</i>	<	<i>Etrumeus teres</i>
1986	Offshore	<i>Bothus</i> spp.	<	<i>Peprilus triacanthus</i>
1986	Offshore	<i>Bothus</i> spp.	<	<i>Paralichthys</i> spp.
1986	Offshore	<i>Bothus</i> spp.	<	<i>Etrumeus teres</i>
1986	Offshore	<i>Peprilus triacanthus</i>	>	<i>Leiostomus xanthurus</i>
1986	Offshore	<i>Peprilus triacanthus</i>	>	<i>Micropogonias undulatus</i>
1986	Offshore	<i>Peprilus triacanthus</i>	<>	<i>Etropus</i> spp.
1986	Offshore	<i>Peprilus triacanthus</i>	<>	<i>Etrumeus teres</i>
1986	Offshore	<i>Paralichthys</i> spp.	>	<i>Leiostomus xanthurus</i>
1986	Offshore	<i>Paralichthys</i> spp.	>	<i>Micropogonias undulatus</i>
1986	Offshore	<i>Paralichthys</i> spp.	<>	<i>Etropus</i> spp.
1986	Offshore	<i>Paralichthys</i> spp.	<>	<i>Etrumeus teres</i>
1986	Offshore	<i>Leiostomus xanthurus</i>	<	<i>Etropus</i> spp.
1986	Offshore	<i>Leiostomus xanthurus</i>	<	<i>Etrumeus teres</i>
1986	Inshore	<i>Brevoortia tyrannus</i>	<	<i>Peprilus triacanthus</i>
1986	Inshore	<i>Brevoortia tyrannus</i>	<	<i>Paralichthys</i> spp.
1986	Inshore	<i>Brevoortia tyrannus</i>	<	<i>Leiostomus xanthurus</i>
1986	Inshore	<i>Brevoortia tyrannus</i>	<	<i>Micropogonias undulatus</i>
1986	Inshore	<i>Brevoortia tyrannus</i>	>	<i>Etrumeus teres</i>
1986	Inshore	<i>Peprilus triacanthus</i>	>	<i>Paralichthys</i> spp.
1986	Inshore	<i>Paralichthys</i> spp.	<>	<i>Etropus</i> spp.
1989	Offshore	<i>Bothus</i> spp.	<	<i>Etropus</i> spp.
1989	Inshore	<i>Brevoortia tyrannus</i>	<	<i>Leiostomus xanthurus</i>
1989	Inshore	<i>Brevoortia tyrannus</i>	<	<i>Etropus</i> spp.
1989	Inshore	<i>Brevoortia tyrannus</i>	<	<i>Etrumeus teres</i>
1991	Offshore	<i>Brevoortia tyrannus</i>	<	<i>Bothus</i> spp.
1991	Offshore	<i>Brevoortia tyrannus</i>	<	<i>Peprilus triacanthus</i>
1991	Offshore	<i>Brevoortia tyrannus</i>	<	<i>Paralichthys</i> spp.
1991	Offshore	<i>Brevoortia tyrannus</i>	<	<i>Leiostomus xanthurus</i>
1991	Offshore	<i>Brevoortia tyrannus</i>	<	<i>Micropogonias undulatus</i>
1991	Offshore	<i>Brevoortia tyrannus</i>	<	<i>Etropus</i> spp.
1991	Offshore	<i>Brevoortia tyrannus</i>	<	<i>Etrumeus teres</i>
1991	Offshore	<i>Bothus</i> spp.	<	<i>Leiostomus xanthurus</i>
1991	Offshore	<i>Bothus</i> spp.	<	<i>Micropogonias undulatus</i>
1991	Offshore	<i>Bothus</i> spp.	<	<i>Etropus</i> spp.
1991	Offshore	<i>Bothus</i> spp.	<	<i>Etrumeus teres</i>
1991	Offshore	<i>Peprilus triacanthus</i>	<	<i>Leiostomus xanthurus</i>
1991	Offshore	<i>Peprilus triacanthus</i>	<	<i>Micropogonias undulatus</i>
1991	Offshore	<i>Peprilus triacanthus</i>	<	<i>Etrumeus teres</i>

continued

Appendix 1 (continued)

Year	Station	Species A		Species B
1991	Offshore	<i>Paralichthys</i> spp.	<	<i>Leiostomus xanthurus</i>
1991	Offshore	<i>Leiostomus xanthurus</i>	<>	<i>Etropus</i> spp.
1991	Offshore	<i>Leiostomus xanthurus</i>	<>	<i>Etrumeus teres</i>
1991	Offshore	<i>Etropus</i> spp.	<>	<i>Etrumeus teres</i>
1991	Inshore	<i>Brevoortia tyrannus</i>	<	<i>Bothus</i> spp.
1991	Inshore	<i>Brevoortia tyrannus</i>	<	<i>Paralichthys</i> spp.
1991	Inshore	<i>Brevoortia tyrannus</i>	<	<i>Leiostomus xanthurus</i>
1991	Inshore	<i>Brevoortia tyrannus</i>	<	<i>Micropogonias undulatus</i>
1991	Inshore	<i>Brevoortia tyrannus</i>	<	<i>Etropus</i> spp.
1991	Inshore	<i>Brevoortia tyrannus</i>	<	<i>Etrumeus teres</i>
1991	Inshore	<i>Bothus</i> spp.	<	<i>Peprilus triacanthus</i>
1991	Inshore	<i>Bothus</i> spp.	<	<i>Paralichthys</i> spp.
1991	Inshore	<i>Bothus</i> spp.	<	<i>Leiostomus xanthurus</i>
1991	Inshore	<i>Bothus</i> spp.	<	<i>Micropogonias undulatus</i>
1991	Inshore	<i>Bothus</i> spp.	<	<i>Etropus</i> spp.
1991	Inshore	<i>Bothus</i> spp.	<	<i>Etrumeus teres</i>
1991	Inshore	<i>Peprilus triacanthus</i>	<>	<i>Etropus</i> spp.
1991	Inshore	<i>Xyrichthys novacula</i>	<	<i>Micropogonias undulatus</i>
1991	Inshore	<i>Xyrichthys novacula</i>	<	<i>Etropus</i> spp.
1991	Inshore	<i>Paralichthys</i> spp.	<	<i>Micropogonias undulatus</i>
1991	Inshore	<i>Paralichthys</i> spp.	<	<i>Etropus</i> spp.
1991	Inshore	<i>Leiostomus xanthurus</i>	<	<i>Micropogonias undulatus</i>
1991	Inshore	<i>Leiostomus xanthurus</i>	<	<i>Etropus</i> spp.
1991	Inshore	<i>Micropogonias undulatus</i>	>	<i>Etropus</i> spp.
1991	Inshore	<i>Micropogonias undulatus</i>	>	<i>Etrumeus teres</i>
1991	Inshore	<i>Etropus</i> spp.	>	<i>Etrumeus teres</i>

Acknowledgment of reviewers

The editorial staff of Fishery Bulletin would like to acknowledge the scientists who reviewed articles published in 2004-2005. Their contributions have helped ensure the publication of quality science.

Dr. David A. Ambrose
Dr. Allen H. Andrews
Dr. John Arnould

Dr. Richard J. Beamish
Dr. James L. Bodkin
Dr. Richard W. Brill
Dr. Jon K.T. Brodziak
Dr. Nancy Brown-Peterson

Dr. John K. Carlson
Dr. Felicia Coleman
Dr. Michael Comeau
Dr. Bruce H. Comyns
Dr. Roy E. Crabtree

Mr. Andrew W. David
Dr. Michael W. Davis
Dr. Tim L.O. Davis
Ms. Allison DeLong
Dr. Edward E. DeMartini
Dr. P.J. Doherty
Dr. Michael L. Domeier
Dr. Miriam J. Doyle
Mr. Nick K. Dulvy

Dr. Anne-Marie Eklund
Dr. Alan R. Everson

Mr. John W. Forsythe
Dr. Clive Fox
Dr. Robert Foy
Mr. Michael Frick
Dr. Kevin D. Friedland
Dr. Stewart Frusher

Dr. Jacques Gagne
Dr. Francisco J. Garcia-Rodriguez
Dr. Lance P. Garrison
Dr. Anthony J. Gharrett
Dr. Chris W. Glass
Dr. Robert Grabowski
Dr. John E. Graves

Dr. Lewis J. Haldorson
Dr. Anne Hallowed
Dr. Jon Hare

Mr. Christopher W. Harnden
Dr. James X. Hartmann
Dr. Andrew J. Harwood
Dr. Kelly Hastings
Dr. Fabio H.V. Hazin
Dr. Thomas E. Helser
Dr. Steven W. Hewett
Mr. Peter B. Hood
Dr. Edward D. Houde
Dr. Harriet Huber

Dr. George D. Jackson
Dr. Stephen C. Jewett

Mr. Todd Kassler
Dr. John S. Kennelly
Dr. Mariano Koen-Alonso
Dr. Christopher C. Koenig
Dr. Robert G. Kope

Dr. Mary Labropoulou
Dr. Thomas E. Laidig
Ms. Kristen L. Laidre
Ms. Kathy L. Lang
Dr. Christopher M. Legault
Dr. Bruno Leroy
Dr. C.J. Limpus
Dr. Flavia M. Lucena
Mr. Sve-Gunnar Lunnerby
Dr. Molly E. Lutcavage
Dr. Joanne Lyczkowski-Schultz

Dr. Clyde L. Mackenzie
Dr. Niels Madsen
Dr. Francesc Maynou
Dr. John D. McEachron
Dr. M.J. Meekan
Dr. Richard L. Merrick
Dr. Russell B. Millar
Dr. Thomas J. Miller
Dr. Beatriz Morales-Nin
Dr. Debra J. Murie
Dr. Michael Musyl

Mr. Daniel G. Nichol
Dr. David L. Nieland

Dr. Victoria M. O'Connell

Dr. José G. Pajuelo
Dr. Donald E. Pearson
Dr. Pierre Pepin
Dr. R. Ian Perry
Dr. John S. Peters
Dr. William Peterson
Dr. Kenneth W. Pitcher
Dr. Dominique Ponton
Ms. Jennifer C. Potts

Dr. Terrance J. Quinn II

Dr. Robert J. Radke
Ms. Darlene Ramon
Dr. Christian Reiss
Dr. William J. Richards
Dr. Christopher N. Rooper

Dr. Susan E. Safford
Dr. Eric Saillant
Dr. Kurt M. Schaefer
Dr. Richard F. Shaw
Dr. Colin Simpfendorfer
Dr. G.B. Skomal
Dr. Peter J. Smith
Ms. Susan E. Smith
Dr. Roxanne Smolowitz
Mr. John Sneva
Dr. Derke Snodgrass
Dr. John D. Stevens
Dr. Iain M. Suthers

Mr. Jesus Tomas
Dr. Marc Trudel

Dr. Douglas S. Vaughan

Dr. Peter Ward
Dr. Christopher R. Weidman
Dr. Jerry A. Wetherall
Dr. Erik Williams
Dr. Dave T. Wilson

Ms. Tonya K. Zepplin
Dr. Christian E. Zimmerman

Fishery Bulletin Index

Volume 103(1-4), 2005

List of titles

-
- 103(1)
- 1 An assessment of scup (*Stenotomus chrysops*) and black sea bass (*Centropristis striata*) discards in the directed otter trawl fisheries in the Mid-Atlantic Bight, by Eleanor A. Bochenek, Eric N. Powell, Allison J. Bonner, and Sarah E. Banta
- 15 Fecundity of shortspine thornyhead (*Sebastes alascanus*) and longspine thornyhead (*S. altivelis*) (Scorpaenidae) from the northeastern Pacific Ocean, determined by stereological and gravimetric techniques, by Daniel W. Cooper, Katherine E. Pearson, and Donald R. Gunderson
- 23 Relative pleopod length as an indicator of size at sexual maturity in slipper (*Scyllarides squammosus*) and spiny Hawaiian (*Panulirus marginatus*) lobsters, by Edward E. DeMartini, Marti L. McCracken, Robert B. Moffitt, and Jerry A. Wetherall
- 34 Seasonal changes in growth of coho salmon (*Oncorhynchus kisutch*) off Oregon and Washington and concurrent changes in the spacing of scale circuli, by Joseph P. Fisher and William G. Pearcy
- 52 Escapement of the Cape rock lobster (*Jasus lalandii*) through the mesh and entrance of commercial traps, by Johan C. Groeneveld, Jimmy P. Khanyile, and David S. Schoeman
- 63 Quantification of drag and lift imposed by pop-up satellite archival tags and estimation of the metabolic cost to cownose rays (*Rhinoptera bonasus*), by Donna S. Grusha and Mark R. Patterson
- 71 Effects of El Niño events on energy demand and egg production of rockfish (Scorpaenidae: *Sebastes*): a bioenergetics approach, by Chris J. Harvey
- 84 Application of pop-up satellite archival tag technology to estimate postrelease survival of white marlin (*Tetrapturus albidus*) caught on circle and straight shank ("J") hooks in the western North Atlantic recreational fishery, by Andrij Z. Horodysky and John E. Graves
- 97 Age validation of quillback (*Sebastes maliger*) using bomb radiocarbon, by Lisa A. Kerr, Allen H. Andrews, Kristen Munk, Kenneth H. Coale, Brian R. Frantz, Gregor M. Cailliet, and Thomas A. Brown
- 108 Cross-shelf and seasonal variation in larval fish assemblages on the southeast United States continental shelf off the coast of Georgia, by Katrin E. Marancik, Lisa M. Clough, and Jonathan A. Hare
- 130 Year-class formation in Pacific herring (*Clupea pallasii*) estimated from spawning-date distributions of juveniles in San Francisco Bay, California, by Michael R. O'Farrell and Ralph J. Larson
- 142 Diet of oceanic loggerhead sea turtles (*Caretta caretta*) in the central North Pacific, by Denise M. Parker, William J. Cooke, and George H. Balazs
- 153 Indirect validation of the age-reading method for Pacific cod (*Gadus macrocephalus*) using otoliths from marked and recaptured fish, by Nancy E. Roberson, Daniel K. Kimura, Donald R. Gunderson, and Allen M. Shimada
- 161 Age and growth estimates of the thorny skate (*Amblyraja radiata*) in the western Gulf of Maine, by James A. Sulikowski, Jeff Kneebone, Scott Elzey, Joe Jurek, Patrick D. Danley, W. Hunting Howell, and Paul C. W. Tsang
- 169 Age-validation, growth modeling, and mortality estimates for striped trumpeter (*Latris lineata*) from southeastern Australia: making the most of patchy data, by Sean R. Tracey and Jeremy M. Lyle
- 183 Larval development of estuary perch (*Macquaria colonorum*) and Australian bass (*M. novemaculeata*) (Perciformes: Percichthyidae) and comments on their life history, by Thomas Trnksi, Amanda C. Hay, and D. Stewart Fielder
- 195 Early life history of the Argentine sandperch *Pseudoperca semifasciata* (Pinguipedidae) off northern Patagonia, by Leonardo A. Venerus, Laura Machinandiarena, Martin D. Ehrlich, and Ana M. Parma
- 207 Geographic variation among age-0 walleye pollock (*Theragra chalcogramma*): evidence of mesoscale variation in nursery quality?, by Matthew T. Wilson, Annette L. Brown, and Kathryn L. Mier
- 219 Tagging studies on the jumbo squid (*Dosidicus gigas*) in the Gulf of California, Mexico, by Unai Markaida, Joshua J. C. Rosenthal, and William F. Gilly
- 103(2)
- 229 Sex change rules, stock dynamics, and the performance of spawning-per-recruit measure in protogynous stocks, by Suzanne H. Alonzo and Marc Mangel

- 246 Neonatal growth of Steller sea lion (*Eumetopias jubatus*) pups in Alaska, by Elisif A. A. Brandon, Donald G. Calkins, Thomas R. Loughlin, and Randall W. Davis
- 258 Reproductive biology of carpenter seabream (*Argyrozona argyrozona*) (Pisces: Sparidae) in a marine protected area, by Stephen L. Brouwer and Marc H. Griffiths
- 270 Decline in sea otter (*Enhydra lutris*) populations along the Alaska Peninsula, 1986–2001, by Douglas M. Burn and Angela M. Doroff
- 280 Growth dynamics of the spinner shark (*Carcharhinus brevipinna*) off the United States southeast and Gulf of Mexico coasts: a comparison of methods, by John K. Carlson and Ivy E. Baremore
- 292 Tracking Pacific bluefin tuna (*Thunnus thynnus orientalis*) in the northeastern Pacific with an automated algorithm that estimates latitude by matching sea-surface-temperature data from satellites with temperature data from tags on fish, by Michael L. Domeier, Dale Kiefer, Nicole Nasby-Lucas, Adam Wagschal, and Frank O'Brien
- 307 Age, growth, mortality, and radiometric age validation of gray snapper (*Lutjanus griseus*) from Louisiana, by Andrew J. Fischer, M. Scott Baker Jr., Charles A. Wilson, and David L. Nieland
- 320 Estimating exploitable stock biomass for the Maine green sea urchin (*Strongylocentrotus droebachiensis*) fishery using a spatial statistics approach, by Robert C. Grabowski, Thomas Windholz, and Yong Chen
- 331 Abundance and distribution of California sea lions (*Zalophus californianus*) in central and northern California during 1998 and summer 1999, by Mark S. Lowry and Karin A. Forney
- 344 Variability in spawning frequency and reproductive development of the narrow-barred Spanish mackerel (*Scomberomorus commerson*) along the west coast of Australia, by Michael C. Mackie, Paul D. Lewis, Daniel J. Gaughan, and Stephen J. Newman
- 355 Seasonal marine growth of Bristol Bay sockeye salmon (*Oncorhynchus nerka*) in relation to competition with Asian pink salmon (*O. gorbuscha*) and the 1977 ocean regime shift, by Gregory T. Ruggerone, Ed Farley, Jennifer Nielsen, and Peter Hagen
- 371 Distribution, feeding condition, and growth of Japanese Spanish mackerel (*Scomberomorus niphonius*) larvae in the Seto Inland Sea, by Jun Shoji and Masaru Tanaka
- 380 Maximum likelihood estimation of mortality and growth with individual variability from multiple length-frequency data, by You-Gan Wang and Nick Ellis
- 392 Effects of fishing on growth traits: a simulation analysis, by Erik H. Williams and Kyle W. Shertzer
- 404 Preliminary evidence of increased spawning aggregations of mutton snapper (*Lutjanus analis*) at Riley's Hump two years after establishment of the Tortugas South Ecological Reserve, by Michael L. Burton, Kenneth J. Brennan, Roldan C. Muñoz, and Richard O. Parker Jr.
- 411 Feeding habits of European hake (*Merluccius merluccius*) in the central Mediterranean Sea, by Paolo Carpentieri, Francesco Colloca, Massimiliano Cardinale, Andrea Belluscio, and Giandomenico D. Ardizzone
- 417 Biology of queen snapper (*Etelis oculatus*: Lutjanidae) in the Caribbean, by Bertrand Gobert, Alain Guillou, Peter Murray, Patrick Berthou, Maria D. Oqueli Turcios, Ester Lopez, Pascal Lorange, Jérôme Huet, Nicolas Diaz, and Paul Gervain
- 426 Courtship and spawning behaviors of carangid species in Belize, by Rachel T. Graham and Daniel W. Castellanos
- 433 Comparison of two approaches for estimating natural mortality based on longevity, by David A. Hewitt and John M. Hoenig
- 438 Effects of current speed and turbidity on stationary light-trap catches of larval and juvenile fishes, by David C. Lindquist and Richard F. Shaw
- 445 Can a change in the spawning pattern of Argentine hake (*Merluccius hubbsi*) affect its recruitment?, by Gustavo J. Macchi, Marcelo Pájaro, and Adrián Madirolas
- 453 Feeding habits of the dwarf weakfish (*Cynoscion nannus*) off the coasts of Jalisco and Colima, Mexico, by Alma R. Raymundo-Huizar, Horacio Pérez-España, Maite Mascaró, and Xavier Chiappa-Carrara
- 461 Using bone measurements to estimate the original sizes of bluefish (*Pomatomus saltatrix*) from digested remains, by Anthony D. Wood
- 103(3)
- 469 Using poststratification to improve abundance estimates from multispecies surveys: a study of juvenile flatfishes, by Sherri C. Dressel and Brenda L. Norcross

- 489 Length at maturity in three pelagic sharks (*Lamna nasus*, *Isurus oxrinchus*, and *Prionace glauca*) from New Zealand, by Malcolm P. Francis and Clinton Duffy
- 501 Survey- and fishery-derived estimates of Pacific cod (*Gadus macrocephalus*) biomass: implications for strategies to reduce interactions between groundfish fisheries and Steller sea lions (*Eumetopias jubatus*), by Lowell W. Fritz and Eric S. Brown
- 516 Mitochondrial gene sequences useful for species identification of western North Atlantic Ocean sharks, by Thomas W. Greig, M. Katherine Moore, Cheryl M. Woodley, and Joseph M. Quattro
- 524 Genetic variation of rougheye rockfish (*Sebastes aleutonicus*) and shortraker rockfish (*S. borealis*) inferred from allozymes, by Sharon L. Hawkins, Jonathan Heifetz, Christine M. Kondzela, John E. Pohl, Richard L. Wilmot, Oleg N. Katugin, and Vladimir N. Tuponogov
- 536 The reproductive cycle of the thorny skate (*Amblyraja radiata*) in the western Gulf of Maine, by James A. Sulikowski, Jeff Kneebone, Scott Elzey, Joe Jurek, Patrick D. Danley, W. Hunting Howell, and Paul C. W. Tsang
- 544 Effect of type of otolith and preparation technique on age estimation of larval and juvenile spot (*Leiostomus xanthurus*), by Dariusz P. Fey, Gretchen E. Bath Martin, James A. Morris, and Jonathan A. Hare
- 553 Preliminary use of oxygen stable isotopes and the 1983 El Niño to assess the accuracy of aging black rockfish (*Sebastes melanops*), by Kevin R. Piner, Melissa A. Haltuch, and John R. Wallace
- 103(4)
- 561 Patterns of growth, mortality, and size of the tropical damselfish *Acanthochromis polyacanthus* across the continental shelf of the Great Barrier Reef, by Michael J. Kingsford and Julian M. Hughes
- 574 Variation in the distribution of walleye pollock (*Theragra chalcogramma*) with temperature and implications for seasonal migration, by Stan Kotwicki, Troy W. Buckley, Taina Honkalehto, and Gary Walters
- 588 Toward identification of larval sailfin (*Istiophorus platypterus*), white marlin (*Tetrapturus albidus*), and blue marlin (*Makaira nigricans*) in the western North Atlantic Ocean, by Stacy A. Luthy, Robert K. Cowen, Joseph E. Serafy, and Jan R. McDowell
- 601 Sexual differentiation and gonad development in striped mullet (*Mugil cephalus* L.) from South Carolina estuaries, by Christopher J. McDonough, William A. Roumillat, and Charles A. Wenner
- 620 Incidental catch and estimated discards of pelagic sharks from the swordfish and tuna fisheries in the Mediterranean Sea, by Persefoni Megalofonou, Constantinos Yannopoulos, Dimitrios Damalas, Gregorio De Metrio, Michel Deflorio, Jose M. de la Serna, and David Macias
- 635 Reproductive biology of female Rikuzen sole (*Dexistes rikuzenius*), by Yoji Narimatsu, Daiji Kitagawa, Tsutomu Hattori, and Hirobumi Onodera
- 648 Temporal and spatial distribution and abundance of flathead sole (*Hippoglossoides classodon*) eggs and larvae in the western Gulf of Alaska, by Steven M. Porter
- 659 Movements and spawning of white marlin (*Tetrapturus albidus*) and blue marlin (*Makaira nigricans*) off Punta Cana, Dominican Republic, by Eric D. Prince, Robert K. Cowen, Eric S. Orbesen, Stacy A. Luthy, Joel K. Llopiz, David E. Richardson, and Joseph E. Serafy
- 670 Life history characteristics for silvergray rockfish (*Sebastes brevispinis*) in British Columbia waters and the implications for stock assessment and management, by Richard D. Stanley and Allen R. Kronlund
- 685 Impact of the California sea lion (*Zalophus californianus*) on salmon fisheries in Monterey Bay, California, by Michael J. Weise and James T. Harvey
- 697 Estimates of growth and comparisons of growth rates determined from length- and age-based models for populations of purple wrasse (*Notolabrus fucicola*), by Dirk C. Welsford and Jeremy M. Lyle
- 712 Effects of harvesting methods on sustainability of a bay scallop fishery: dredging uproots seagrass and displaces recruits, by Melanie J. Bishop, Charles H. Peterson, Henry C. Summerson, and David Gaskill
- 720 Longline-caught blue shark (*Prionace glauca*): factors affecting the numbers available for live release, by Guillermo A. Diaz and Joseph E. Serafy
- 725 Length correction for larval and early-juvenile Atlantic menhaden (*Brevoortia tyrannus*) after preservation in alcohol, by Dariusz P. Fey and Jonathan A. Hare
- 728 Comparison of average larval fish vertical distributions among species exhibiting different transport pathways on the southeast United States continental shelf, by Jonathan A. Hare and John J. Govoni

Fishery Bulletin Index

Volume 103(1-4), 2005

List of authors

- Alonzo, Suzanne H. 229
 Andrews, Allen H. 97
 Ardizzone, Giandomenico D. 411
- Baker Jr., M. Scott 307
 Balazs, George H. 142
 Banta, Sarah E. 1
 Baremore, Ivy E. 280
 Bath Martin, Gretchen E. 544
 Belluscio, Andrea 411
 Berthou, Patrick 417
 Bishop, Melanie J. 712
 Bochenek, Eleanor A. 1
 Bonner, Allison J. 1
 Brandon, Elisif A. A. 246
 Brennan, Kenneth J. 404
 Brouwer, Stephen L. 258
 Brown, Annette L. 207
 Brown, Eric S. 501
 Brown, Thomas A. 97
 Buckley, Troy W. 574
 Burn, Douglas M. 270
 Burton, Michael L. 404
- Cailliet, Gregor M. 97
 Calkins, Donald G. 246
 Cardinale, Massimiliano 411
 Carlson, John K. 280
 Carpentieri, Paulo 411
 Castellanos, Daniel W. 426
 Chen, Yong 320
 Chiappa-Carrara, Xavier 453
 Clough, Lisa M. 108
 Coale, Kenneth H. 97
 Colloca, Francesco 411
 Cooke, William J. 142
 Cooper, Daniel W. 15
 Cowen, Robert K. 588, 659
- Damalas, Dimitrios 620
 Danley, Patrick D. 161, 536
 Davis, Randall W. 246
 De la Serna, Jose M. 620
 De Metrio, Gregorio 620
 Deflorio, Michel 620
 DeMartini, Edward E. 23
 Diaz, Guillermo A. 720
 Diaz, Nicolas 417
 Domeier, Michael L. 292
 Doroff, Angela M. 270
 Dressel, Sherri C. 469
 Duffy, Clinton 489
- Ehrlich, Martin D. 195
 Ellis, Nick 380
 Elzey, Scott 161, 536
- Farley, Ed 355
 Fey, Dariusz P. 544, 725
 Fielder, D. Stewart 183
 Fischer, Andrew J. 307
 Fisher, Joseph P. 34
 Forney, Karin A. 331
 Francis, Malcolm P. 489
 Frantz, Brian R. 97
 Fritz, Lowell W. 501
- Gaskill, David 712
 Gaughan, Daniel J. 344
 Gervain, Paul 417
 Gilly, William F. 219
 Gobert, Bertrand 417
 Govoni, John J. 728
 Grabowski, Robert C. 320
 Graham, Rachel T. 426
 Graves, John E. 84
 Grieg, Thomas W. 516
 Griffiths, Marc H. 258
 Groeneveld, Johan C. 52
 Grusha, Donna S. 63
 Guillou, Alain 417
 Gunderson, Donald R. 15, 153
- Hagen, Peter 355
 Haltuch, Melissa A. 553
 Hare, Jonathan A. 108, 544, 725, 728
 Harvey, Chris J. 71
 Harvey, James T. 685
 Hattori, Tsutomu 635
 Hawkins, Sharon L. 524
 Hay, Amanda C. 183
 Heifetz, Jonathan 524
 Hewitt, David A. 433
 Hoenig, John M. 433
 Honkalehto, Taina 574
 Horodysky, Andrij Z. 84
 Howell, W. Huntting 161, 536
 Huet, Jérôme 417
 Hughes, Julian M. 561
- Jurek, Joe 161, 536
- Katugin, Oleg N. 524
 Kerr, Lisa A. 97
 Khanyile, Jimmy P. 52
- Kiefer, Dale 292
 Kimura, Daniel K. 153
 Kingsford, Michael J. 561
 Kitagawa, Daiji 635
 Kneebone, Jeff 161, 536
 Kondzela, Christine M. 524
 Kotwicki, Stan 574
 Kronlund, Allen R. 670
- Larson, Ralph J. 130
 Lewis, Paul D. 344
 Lindquist, David C. 438
 Llopiz, Joel K. 659
 Lopez, Ester 417
 Lorange, Pascal 417
 Loughlin, Thomas R. 246
 Lowry, Mark S. 331
 Luthy, Stacy A. 588, 659
 Lyle, Jeremy M. 169, 697
- Macchi, Gustavo J. 445
 Machinandiarena, Laura 195
 Macias, David 620
 Mackie, Michael C. 344
 Madirolas, Adrián 445
 Mangel, Marc 229
 Marancik, Katrin E. 108
 Markaida, Unai 219
 Mascaró, Maite 453
 McCracken, Marti L. 23
 McDonough, Christopher J. 601
 McDowell, Jan R. 588
 Megalofonou, Persefoni 620
 Mier, Kathryn L. 207
 Moffitt, Robert B. 23
 Moore, M. Katherine 516
 Morris, James A. 544
 Munk, Kristen 97
 Muñoz, Roldan C. 404
 Murray, Peter 417
- Narimatsu, Yoji 635
 Nasby-Lucas, Nicole 292
 Newman, Stephen J. 344
 Nieland, David L. 307
 Nielsen, Jennifer 355
 Norcross, Brenda L. 469
- O'Brien, Frank 292
 O'Farrell, Michael R. 130
 Onodera, Hirobumi 635
 Oqueli Turcios, Maria D. 417
 Orbesen, Eric S. 659
- Pájaro, Marcelo 445
 Parker, Denise M. 142
 Parker Jr., Richard O. 404
 Parma, Ana M. 195
 Patterson, Mark R. 63
 Percy, William G. 34

- Pearson, Katherine E. 15
Pérez-España, Horacio 453
Peterson, Charles H. 712
Piner, Kevin R. 553
Pohl, John E. 524
Porter, Steven M. 648
Powell, Eric N. 1
Prince, Eric D. 659
- Quattro, Joseph M. 516
- Raymundo-Huizar, Alma R. 453
Richardson, David E. 659
Roberson, Nancy E. 153
Rosenthal, Joshua J. C. 219
Roumillat, William A. 601
Ruggerone, Gregory T. 355
- Schoeman, David S. 52
Serafy, Joseph E. 588, 659, 720
Shaw, Richard F. 438
Shertzer, Kyle W. 392
Shimada, Allen M. 153
Shoji, Jun 371
Stanley, Richard D. 670
Sulikowski, James A. 161, 536
Summerson, Henry C. 712
- Tanaka, Masaru 371
Tracey, Sean R. 169
Trnski, Thomas 183
Tsang, Paul C. W. 161, 536
Tuponogov, Vladimir N. 524
- Venerus, Leonardo A. 195
- Wagschal, Adam 292
Wallace, John R. 553
Walters, Gary 574
Wang, You-Gan 380
Weise, Michael J. 685
Welsford, Dirk C. 697
Wenner, Charles A. 601
Wetherall, Jerry A. 23
Williams Erik H. 392
Wilmot, Richard L. 524
Wilson, Charles A. 307
Wilson, Matthew T. 207
Windholz, Thomas 320
Wood, Anthony D. 461
Woodley, Cheryl M. 516
- Yannopoulos, Constantinos 620

Fishery Bulletin Index

Volume 103(1-4), 2005

List of subjects

- Abundance
- Argentine
 - hake 445
 - sandperch 195
 - California sea lion 331
 - flathead sole 648
 - sockeye salmon 355
- Acanthochromis polyacanthus* 561
- Acoustic survey 445
- Aerial survey 270, 331
- Age
- and growth
 - damsel fish 561
 - gray snapper 307
 - shark, spinner 280
 - silvergray rockfish 670
 - striped trumpeter 169
 - thorny skate 161
 - at maturity 635
 - determination
 - Rikuzen sole 635
 - striped mullet 601
 - estimates
 - accuracy 544
 - precision 544
 - validation
 - damsel fish 561
 - gray snapper 307
 - Pacific cod 153
 - rockfish
 - black 553
 - quillback 97
 - spot 544
 - striped trumpeter 169
- Age-0 207
- Aggregation 404
- Alaska 97, 207, 247, 270, 355, 469, 501, 524, 553, 574, 648
- Alaska Peninsula 270, 648
- Albacore 620
- Aleutian Islands 246, 501, 524
- Allozymes 524
- Alopias vulpinus* 620
- Amblyraja radiata* 161, 536
- ANOVA 685, 712, 725
- Archival tag 292
- Argentina 195
- Argopecten irradians* 712
- Argyrozoona argyrozoona* 258
- Atlantic Ocean 516, 536, 659
- southwest 445
 - northwest 161, 280, 553, 588, 720
 - western 404, 417
- Australia 169, 183, 344, 561
- Automated algorithm 292
- Back-calculation 130, 153, 461
- Bahamas 588
- Band count, vertebral section 161
- Bass
- Australian 183
 - black sea 1
 - batch fecundity 258
 - Batch spawner 15
 - Beaufort Inlet 725
 - Belize 426
 - Bering Sea 153, 501, 524, 574
 - Bioenergetics model 71
- Biomass
- Pacific cod 501
 - seagrass 712
 - sea urchin 320
 - walleye pollock 574
- Bluefish 461
- Body condition 635
- Bogue Sound 712
- Bone measurements 461
- Bottom trawl
 - fishery 670
 - nets 574
- Brevoortia tyrannus* 725, 728
- Bristol Bay 355
- British Columbia 670
- Bycatch mortality 574
- Callinectes sapidus* 433
- California 130, 331, 553, 685
- Canonical correspondence analysis (CCA) 108
- Canonical variates analysis (CVA) 588
- Cape rock lobster 52
- Carangidae 426
- Carapace base 52
- Carcharhinus brevipinna* 280
- Caretta caretta* 142
- Carinaria cithara* 142
- Caribbean 420, 516
- Catch efficiency 438
- Catch per unit of effort 438, 469, 501, 620, 670, 685
- Central California Valley Index (CVI) 685
- Centropristis striata* 1
- Chesapeake Bay 720
- Chiniak Bay 469
- Chi-square test 620
- Chondrophore 142
- Circulus spacing 34.
- Cirripedia 142
- Clupea pallasii* 130
- Cod, Pacific 153, 501
- Codends 1
- Colima coast 453
- Commercial harvest 712
- Commercial passenger fishing vessel 685
- Commercial traps 52
- Commercial troll fishery 685
- Conductivity-temperature-depth probe 108
- Copepod parasite 670
- Coral reef 561
- Courtship behavior 426
- CPUE 438, 469, 501, 620, 670, 685
- Crabs, blue 433
- Croaker
 - Atlantic 728
- Cross-shelf
 - transport 728
 - variation 108, 561
- Current 438
- Cynoscion nannus* 453
- Damsel fish 561
- Decapoda 142
- Deep snapper resources 417
- Demographic assessment 561
- Depredation 685
- Dexistes rikuzenius* 635
- Diet, loggerhead turtle 142
- Discard 620
 - mortality 1, 720
 - to-landings ratio 1
- Displacement 659
- Distribution
 - and abundance
 - Argentine sandperch 195
 - vertical larval 728
 - walleye pollock 574
- DNA 516, 588
- Dosidicus gigas* 219
- Drag and lift 63
- Dredging 712
- Egg
 - geographic distribution and abundance 648
 - mortality 130
 - production 445
- Elasmobranch 536
- El Niño 71, 553
- Southern Oscillation 685
- Endangered Species Act 270
- Energetic cost 63
- Energy consumption 71
- Enhydra lutris* 270

- Escapement, from lobster trap 52
 Essential fish habitat 659
 Estuarine bivalve fisheries 712
 Estuarine-dependent species 728
Etelis oculatus 417
Eumetopias jubatus 246, 501
 External body metric 23
- Fecundity**
 gravimetric estimates 15
 Rikuzen sole 635
 silvergray rockfish 670
 stereological estimates 15
 thornyhead 15
 thorny skate 536
- Feeding habits** 411, 453
First increment formation 544
Fisheries management 1, 229, 380,
 392, 469, 501
Fishery biology 417
Fishery interaction 685
Fishing gear 620, 712
Fishing mortality 720
Flatfishes 469
Flounder
 gulf 728
 southern 728
 summer 728
Flow, vertically structured 728
- G-statistic** 728
Gadus macrocephalus 153, 501
Galeorhinus galeus 620
 Gametogenesis 601
 Gas platforms 438
 Gastropoda 142
 Gene sequences 516
 Genetic identification 516, 588
 Genetic variation 524
Geographic
 distribution 648
 variation 207
Geolocation 292
 Georgia 108
 Gompertz model 280
 Gonadal maturation 635
 Gonad development 601
 Gonadosomatic index 536, 635
 Grand Banks 720
 Gravimetric technique 15
 Grapsidae 142
 Gray's Reef National Marine
 Sanctuary 108
 Great Barrier Reef 561
 Groundfish 469, 501
Growth 380, 392
 damselfish 561
 dimorphism 670
 effects of fishing on 392
- Pacific herring 130
 rate, daily 219
 salmon 34
 scale 355
 seasonal variation 34
 Steller sea lion 246
 striped trumpeter 169
 thorny skate 161
- Gulf**
 of Alaska 246, 524, 648
 of California 219
 of Maine 161, 536
 of Mexico 280, 438, 516
- Habitat**
 destruction 712
 flatfish 469
- Hake**
 Argentine 445
 European 411
 Halibut, Pacific 469
 Harvesting, effects of 712
 Hepatosomatic index 536
 Herring, Pacific 130
 Heteropoda 142
Hippoglossoides classodon 469,
 648
Hippoglossus stenolepis 469
 Hook type mortality estimates 91
 Horizontal transport 728
 Hydrodia 142
- Ichthyoplankton** 108, 195, 371,
 648
 Identification 516, 588
 Incidental catch 620
 Increment formation 544
 Indirect validation 153
 Individual-based model 392
 Individual variability 380
 Interannual variability 469
 Inverse distance-weighted 574
 Isochronal spawning fish 610
 Istiophoridae 588
Istiophorus platypterus 588
Isurus oxyrinchus 489, 620
- Jalisco coast** 453
Janthina spp. 142
 Japan 373, 635
Jasus lalandii 52
 Juvenile
 Argentine sandperch 195
 effects of turbidity on 438
 flatfish 469
 Pacific herring 130
 salmon 34
 scallops 712
 spot 544
 walleye pollock 207
- Kamchatka coast** 524
 Kruskal-Wallis test 620
 Kodiak Island 207, 648
- Lamna nasus* 489
Larval fish
 abundance 195, 648
 age estimation 544
 assemblages 108
 Atlantic menhaden 725
 billfish 588
 cross-shelf variation 108
 development 183, 195, 207
 diet 207
 distribution 371, 648
 effects of turbidity 438
 feeding conditions 371
 flathead sole 648
 geographic variation 207
 growth 207, 371
 mortality 130
 seasonal variation 108
 survival 130
 transport 728
Latris lineata 169
Leiostomus xanthurus 5 44, 728
 Length at maturity 489
 Length correction 720
 Length frequency 380
Lepas spp. 142
Lepidopsetta spp. 469
 Life history 183, 195, 229, 536, 670,
 392
 Light traps 438
 Linear regression analysis 725
 Linear regression model 433, 588
Lobster
 Hawaiian spiny 23
 slipper 23
 South African Cape rock 52
Logistic 280
 Longevity 433
 Longline 720
 Louisiana 307
 Lowrie Island rookery 246
 Lunar periodicity 426
 Lutjanidae 420
Lutjanus
analis 404
griseus 307
- Mackerel**
 Japanese Spanish 371
 narrow-barred Spanish 344
Macquaria
colonorum 183
novemaculeata 183
Makaira nigricans 588, 659
 Maine 320
 Marginal increment 161

- Marlin
 blue 588, 659
 white 84, 588, 659
- Marine mammal 331
- Marine protected areas 258
- Maturity
 lobster 23
 pelagic sharks 489
 Rikuzen sole 635
 silvergray rockfish 670
 striped mullet 601
- Maximum
 age 433
 likelihood 380
 sustainable yield 659
- Mediterranean Sea 411, 620
- Menhaden, Atlantic 725, 728
- Merluccius*
 hubbsi 445
 merluccius 411
- Mesh size 52
- Mesoscale variation 207
- Metabolic cost estimation 63
- Mexico 219, 453
- Micropogonias undulatus* 728
- Mid-Atlantic Bight 1
- Migration
 jumbo squid 219
 walleye pollock 574
- Mitochondrial DNA 516
- Models
 Bayesian 524
 bioenergetic 71
 generalized additive model (GAM) 670
 general linear model (GLM) 670
 growth 169, 380, 392, 670
 linear regression 433, 489
 Leslie 501
 Levenburg-Marquardt 601
 mortality 380, 433, 489
 Schnute growth model 670
 von Bertalanffy 380, 392
- Monte Carlo simulation 588
- Monterey Bay 685
- Morphological-based maturity 23, 601
- Morphometrics 588
- Mortality 380, 433
 blue shark 720
 damsel fish 561
 gray snapper 307
 hook type 84
 natural, estimation of 422
 release 720
 sea turtle 142
 striped trumpeter 169
- Moss Landing 685
- Movement
 patterns 659
 vertical 728
- Mugil cephalus* 601
- Multivariate analysis 108
- Natural mortality 433
- Neonatal growth 246
- Neustonic species 142
- New Hampshire 536
- New Zealand 489
- Nonparametric analysis of variance 620
- North Atlantic, western 84
- North Carolina 712, 725
- North Pacific, central 142
- Notolabrus fucicola* 697
- Nursery quality 207
- Ocean regime shift 355
- Oil platforms 438
- Oncorhynchus*
 gorbuscha 355
 kisutch 34
 nerka 355
 tshawytscha 685
- Ootogenesis 411
- Oocyte maturation 635
- Oogenesis 601, 635
- Opportunistic feeders 142
- Oregon 34
- Original prey size 461
- Otariidae 246
- Otolith 97, 130, 153, 169, 307, 373, 544, 553, 561, 601, 635, 670
- Otolith microchemistry 553
- Ovarian atresia 601
- Ovary 1, 23, 536
- Oxygen isotope 55
- Pacific Ocean
 eastern 71, 453, 685
 north 355, 635
 northeastern 15, 130, 292, 331, 648
- Panulirus marginatus* 23
- Paralichthys*
 albigata 728
 dentatus 728
 lethostigma 728
- Parasites 524
- Patagonia 195
- Patagonian stock 445
- Pelagic Observers Program, U.S. Atlantic 720
- Penaeus semisulcatus* 380
- Perch, estuary 183
- Percichthyidae 183
- Permit 426
- Phenotypic plasticity 229
- Phylogenetics 516
- Pigmentation patterns 588
- Pinguipedidae 195
- Pinniped 331, 685
- Pleopod measurement 23
- Pleuronectes asper* 469
- Pollock, walleye 207, 574
- Pomacentridae 561
- Pomotomus saltatrix* 461
- Population
 decline 270
 dynamics 229
- Pop-up satellite archival tags 63, 84, 292, 659
- Postrelease survival 84
- Postspawning morphology 601
- Poststratification 469
- Potential energetic costs 63
- Prawn, tiger 380
- Preservation shrinkage 725
- Prey size 461
- Prionace glauca* 489, 620, 720
- Protogynous sex change 229
- Pseudopercis semifasciata* 195
- Punta Cana 659
- Pup, sea lion 246
- Pyrosomas 142
- Radiocarbon 97, 307
- Rajidae 536
- Ray, cownose 63
- Recreational fishery 84
 salmon 685
- Recruitment
 Argentine hake 445
 gray snapper 307
 silvergray rockfish 670
- Reef fish 426, 369
- Reef promontory 426
- Regression analysis 34, 142
- Release mortality 720
- Reproductive development 344, 601
- Reproductive maturity 670
- Reproduction
 carpenter seabream 258
 marlin 659
 pelagic shark 489
 Rikuzen sole 635
 Spanish mackerel 344
 thorny skate 536
 striped mullet 601
- Restriction fragment length polymorphism analysis 588
- Rhinoptera bonasus* 63
- Riley's Hump 404
- Rockfish
 age validation 97
 black 553
 bioenergetics model 71
 quillback 97
 rougeye 524
 shortraker 524
 silvergray 670
 trophic ecology 71
 yelloweye 97

- Rookeries 246
 Russia 524
- Sailfish 588
- Salmon
 Asian pink 355
 coho 34
 chinook 685
 sockeye 355
- Sandperch, Argentine 195
- San Francisco Bay 130
- Sarcotaces arcticus* 670
- Santa Cruz 685
- Scale circuli 34, 355,
- Scallops, bay 712
- Scup 1
- Sciaenidae 453
- Scomberomorus*
 commerson 344
 niphonius 371
- Scombridae 371
- Scorpaenidae 15, 71
- Scyllarides squammosus* 23
- Sea bass, black 1
- Seabream, carpenter 258
- Seagrass 712
- Sea lion
 California 331, 685
 Steller 246, 501
- Sea of Hiuchi 373
- Sea otter, northern 270
- Sea-surface temperature 292
- Seasonal growth 34, 179, 355
- Seasonal migration 219
- Seasonal variation 108
- Sea turtles
 loggerhead 142
- Sea urchin, Maine green 320
- Sebastes* spp. 71
 aleuticus 524
 borealis 524
 brevispinis 670
 maliger 97
 mclanops 553
 mystinus 74
 ruberrimus 97
- Sebastolobus*
 alascanus 15
 altivelis 15
- Selection differentials 392
- Selectivity curves 52
- Senescence 635
- Semidemersal gadid 207
- Sequence 516
- Seto Inland Sea 371
- Sexual differentiation 601
- Sexual dimorphism 169, 635
- Sharks 516
 blue 489, 620 574
 coastal 280
 common thresher 620
 pelagic 489, 620
 porbeagle 489
 shortfin mako 489, 620
 spinner 280
 tope 620
- Size at maturity 258, 601
- Skate, thorny 161, 536
- Snapper
 gray 307
 mutton 404
 queen 417
- Sole
 flathead 469
 Rikuzen 635
 rock 469
 yellowfin 469
- South Africa 52, 258
- South America 183
- South Carolina 601
- Southeast United States continental shelf 108, 728
- Sparidae 258
- Spatial analysis 320
- Spatial distribution 574, 648
- Spatial variability 320
- Spawning
 aggregations 404, 426
 behavior 426
 date distribution 130
 flathead sole 648
 frequency 258, 344
 habitat 659
 marlin 659
 mutton snapper 404
 Pacific herring 130
 pattern change 445
 per-recruit 229
 season 258
- Spawning stock biomass per recruit analysis 670
- Species identification 516
- Spermatogenesis 536
- Spot 544, 728
- Squid, jumbo 219
- Starch gel electrophoresis 524
- Stenotomus chrysops* 1
- Stereological techniques 15
- Stock
 assessment 320, 433, 670
 dynamics 229
 management 670
- Straits of Florida 588
- Strip transect survey 270, 331
- Strongylocentrotus droebachiensis* 320
- Student-Newman-Keul test 685, 712
- Submerged aquatic vegetation 712
- Subtropical front 142
- Survival rate 620
- Swordfish 620
- Tagging
 jumbo squid 219
 pop-up satellite 63, 84, 292, 659
- Temperature 561, 574
- Temporal distribution 648
- Tetrapturus albidus* 84, 588, 648
- Theragra chalcogramma* 207, 574
- Thornyhead
 shortspine 15
 longspine 15
- Thunnus*
 alalunga 620
 thynnus 620
 thynnus orientalis 292
- Tortugas South Ecological Reserve 404
- Trachinotus falcatus* 426
- Trap selectivity 52
- Trawl survey 445, 501, 574
 echo integration 574
 groundfish 469
- Triangulated Irregular Networks 320
- Trophic breadth variation 453
- Trumpeter, striped 169
- Tsitsikamma National Park 258
- Tukey HSD test 725
- Tuna
 bluefin 620
 Pacific bluefin 292
- Turbidity 438
- U.S. Atlantic Pelagic Observers Program 720
- Variation
 genetic 524
 spawning frequency 344
- Velella velella* 142
- Vertebral band analysis 161
- Vertical distribution 728
- von Bertalanffy 380
 damsel fish 561
 gray snapper 307
 Pacific cod 153
 spinner shark 280
 striped trumpeter 169
 thorny skate 161
- Washington 34, 524
- Water column 728
- Wax histology technique 601
- Weakfish, dwarf 453
- Wrasse, purple 697
- Xiphias gladius* 620
- Year-class strength 130
- Zalophus californianus* 331, 685
- Zostera marina* 712

Fishery Bulletin

Guidelines for authors

Content of manuscripts

Contributions published in *Fishery Bulletin* describe original research in marine fisheries science, fishery engineering, and economics, as well as the art of marine environmental and ecological sciences including modeling. Although all contributions are subject to peer review, responsibility for the contents of papers rests upon the authors and not upon the editor or publisher. *Submission of an article implies that the article is original and is not being considered for publication elsewhere.* Manuscripts should be written in English. Authors whose native language is not English are strongly advised to have their manuscripts checked by English-speaking colleagues prior to submission. **Articles** may range from relatively short contributions (9–15 typed and double-spaced pages) to extensive contributions (20–30 typed pages). **Notes** are reports of 5 to 10 pages without an abstract and describe methods or results not supported by a large body of data.

Manuscript preparation

Title page should include authors' full names and mailing addresses and the senior author's telephone, fax number and e-mail address, and a list of key words to describe the contents of the manuscript. **Abstract** should be limited to 150 words (one-half page), state the main scope of the research, and emphasize the author's conclusions and relevant findings. Because abstracts are circulated by abstracting agencies, it is important that they represent the research clearly and concisely. **Text** must be typed in 12 point Times New Roman font throughout. A brief introduction should convey the broad significance of the paper; the remainder of the paper should be divided into the following sections: **Materials and methods**, **Results**, **Discussion (or Conclusions)**, and **Acknowledgments**. Headings within each section must be short, reflect a logical sequence, and follow the rules of multiple subdivision (i.e., there can be no subdivision without at least two items). The entire text should be intelligible to interdisciplinary readers; therefore, all acronyms, abbreviations, and technical terms should be written out in full the first time they are used. Include FAO common names for species in the list of keywords and in the opening statements. Regional common names may be used throughout the rest of the text if they are different. FAO common names can be found at <http://www.fishbase.org/search.html>. Follow the U.S. Government Printing Office Style Manual (1984 ed.) and the CBE Style Manual (6th ed.) for editorial style, and the most current issue of the American Fisheries Society's Common and Scientific Names of Fishes from the United States and Canada for fish nomenclature. Dates should be written as follows: 11 November 2000. Measurements should be expressed in metric units, e.g., 58 metric tons (t); if other units of measurement are used, please make this fact explicit to the reader. Write out the numbers zero through

nine unless they form part of measurement units (e.g., nine fish but 9 mm).

Text footnotes should be inserted in 9 point font at the bottom of the page that displays the first citation of the footnote. Footnotes should be formatted in the same manner as citations. Footnote all personal communications, unpublished data, and unpublished manuscripts with full address of the communicator or author, or, as in the case of unpublished data, where the data are on file. Authors are advised to avoid references to non-standard gray literature (such as internal project, processed, or administrative reports, ICES Council Minutes, IAWM Minutes or Working Papers, any "research" or "working" documents, laboratory or contract reports, Management Council reports, and manuscripts in review) wherever possible. If these references are used, present them as footnotes and list whether they are available from NTIS (National Technical Information Service) or from some other public depository. Cite all software and special equipment or solutions used in the study, not in a footnote but within parentheses in the text (e.g., SAS, vers 6.03; SAS Inst., Inc., Cary, NC).

Literature cited comprises published works and those accepted for publication in peer-reviewed literature (in press). Follow the name and year system for citation format. If there is a sequence of citations in the text, list chronologically (Smith, 1992; Green, 1947; Smith and Jones, 1985). Abbreviations of serials should conform to abbreviations given in the Serial Sources for the BIOSIS Previews Database. Authors are responsible for the accuracy and completeness of all citations. Literature citation format: Author (last name, followed by first-name initials). Year, Title of report or manuscript. Abbreviated title of the series to which it belongs. Always include number of pages. If there is a sequence of citations by the same first author, list the works alphabetically according to the last name of following authors (e.g., Smith G. P., L. C. Brown, 1982; Smith, G. P., and T. P. Stuart, 1982). If the authorship is identical, list works chronologically.

Tables and figures—general format

- Zeros should precede all decimal points for values less than one.
- Sample size, *n*, should be italicized.
- Capitalize the first letter of the first word in all labels within figures.
- Do not use overly large font sizes in maps and for units of measurements along axes in figures.
- Do not use bold fonts or bold lines in figures.
- Submit photographs on glossy paper.
- Do not place outline rules around graphs.
- Do not use horizontal lines in graphs to indicate measurement units on axes.
- Use a comma in numbers of five digits or more (e.g., 13,000 but 3000).
- Maps should have a North arrow and degrees latitude-longitude (e.g., 170 E).

Tables should not be excessively wide and not be cited in numerical order in the text. Headings should be short but ample enough to allow the table to be intelligible on its own. All numerical entries must be explained in the table level.

Other important content of a table should be footnoted with the footnote numbers. For instance, to indicate probability in statistical data. Do not type table legends into a separate page; place them on the same page as the table data.

Figures include film illustrations, photographs, slides, and computer-generated displays, and must be cited in numerical order in the text. The illustrations may be submitted as high quality laser prints. We require a hard copy of photographs in addition to an electronic copy. Figures are to be labeled with author's name and number of figure. Avoid placing labels vertically, except on axes. Figure legends should explain all symbols and abbreviations and should be double spaced on a separate page at the end of the manuscript. Please note that we do not print graphs in color.

FAILURE TO FOLLOW THESE GUIDELINES WILL DELAY PUBLICATION OF A MANUSCRIPT

Copyright law does not apply to *Fishery Bulletin*, which falls within the public domain. However, if an author reproduces any part of an article from *Fishery Bulletin* in his or her work, reference to source is considered correct form (e.g., Source: Fish Bull. 97:105).

Reprints are available free of charge to the senior author (50 copies) and to his or her laboratory (50 copies). Additional copies may be purchased in lots of 100 when the author receives page proofs.

Submission

The Scientific Editorial Office encourages authors to submit their manuscripts as a single PDF (preferred), Word (zipped), or WordPerfect (zipped) document by e-mail to fishbullet@noaa.gov. Please use the subject heading "Fishery Bulletin manuscript submission." Do not send encrypted files. For further details on electronic submission, please contact the Scientific Editorial Office directly (see address below). Or you may send your manuscript on compact disc in one of the above formats along with four printed copies (one original plus three copies); clipped, not stapled—to the Scientific Editor, at the address shown below. Send photocopies only of figures with initial submission of manuscript; do not send original figures. Original figures and electronic copies of figures will be requested later when the manuscript has been accepted for publication.

Until August 2005	Starting August 2005
Dr Norman Bartoo Scientific Editor, <i>Fishery Bulletin</i>	Dr Adam Miles Scientific Editor, <i>Fishery Bulletin</i>
NOAA/NMFS/SWFSC 8604 La Jolla Shores Dr La Jolla, CA 92038	11305 Glacier Hwy Juneau, AK 99801-8626

Once the manuscript has been accepted for publication, you will be asked to submit a final software copy of your manuscript. When requested, the text and tables should be submitted in Word or Word Rich Text Format. Figures should be sent as PDF files, Windows metafiles, or as EPS files. Send a copy of figures in original software if conversion yields a degraded version.

